



# Abstract Volume 11<sup>th</sup> Swiss Geoscience Meeting

Lausanne, 15<sup>th</sup> – 16<sup>th</sup> November 2013

## Cycles and Events in the Earth System

sc | nat 

Swiss Academy of Sciences  
Akademie der Naturwissenschaften  
Accademia di scienze naturali  
Académie des sciences naturelles

*Unil*

UNIL | Université de Lausanne

Faculté des géosciences  
et de l'environnement

*Large picture: View from the Tierbergli on the Steisee, the Sustenpass and the Titlis (BE)*

*Small picture: Warning sign along the Wyssa aqueduct (bisse/Suone) above Mund (VS) (Pictures: Pierre Dèzes, SCNAT)*

# 11<sup>th</sup> Swiss Geoscience Meeting, Lausanne 2013

## Table of contents

<b>Organisation</b>	<b>2</b>
<b>Abstracts</b>	
0. Plenary Session	4
1. Structural Geology, Tectonics and Geodynamics	10
2. Mineralogy, Petrology, Geochemistry	56
4. Cycles and Events in Earth History	110
5. Alpine Geology	136
6. Stratigraphy in Switzerland - new data and developments	154
7. + 8. Palaeontology + Fossils and plate tectonic events: Oceanic and continental gateways, landbridges and the dispersal of biota	166
9. Environmental Biogeosciences	194
10. + 15. Biogeochemical cycles in a changing environment + Greenhouse Gases: Linkages between Biosphere and Climate	230
11. Geophysics and Rockphysics	256
12. Shale-Gas, CO <sub>2</sub> Storage and Deep Geothermal Energy	290
13. Atmospheric predictability, phenology and seasonality	320
14. Cryospheric Sciences	334
17. Computational GIScience	362
18. Geoscience and Geoinformation - From data acquisition to modelling and visualisation	386
19. Earth System Science related Earth Observation	402
20. Quaternary environments: landscapes, climate, ecosystems, human activity during the past 2.6 million years	416
21. Scientific challenges for geoheritage conservation and promotion in Switzerland	446
23. Symposium in Human Geography	462
24. Sustainable Water Management – Scientific Findings from recent research	478
25. Limnological and hydro(geo)logical advances for mid-sized lakes as a water resource for the next century	502
26. Geomorphology	532
27. Fluxes of water, sediment and dissolved substances in geomorphologically active/changing environments	562

# Organisation

## Host Institution

Faculty of Geosciences and Environment of the University of Lausanne,  
Musée Cantonal de Géologie, Lausanne

## Patronnage

Platform Geosciences, Swiss Academy of Sciences

## Program Committee

Daniel Ariztegui	Alain Geiger	Eric Reusser
Rizlan Bernier-Latmani	Bernard Grobéty	Christoph Ritz
Gilles Borel	Irka Hajdas	Elias Samankassou
Hugo Bucher	Christian Klug	Bruno Schädler
Reto Burhalter	Olivier Lateltin	Michael Schaepman
Pierre Dèzes	Neil Mancktelow	Guido Schreurs
Hans-Rudolf Egli	Alain Morard	Dea Voegelin
Martin Engi	Thomas Nægler	Helmut Weissert
Werner Eugster	Nils Oesterling	Adrian Wiget
Charles Fierz	Jasquelin Peña	Saskia Willemse
Karl Föllmi	Adrian Pfiffner	

## Local Organizing Committee

Thierry Adatte	Jean-Paul Dutoit	Benita Putlitz
Gilles Borel	Karl Föllmi	Emmanuel Reynard
François Bussy	Stuart Lane	Eric Verrecchia

## Participating Societies and Organisations

Association for Geographical Education Switzerland (VGD-CH/AGD-CH)  
 Federal Office of Meteorology and Climatology (MeteoSwiss)  
 Federal Office of Topography (swisstopo)  
 Forum for Climate and Global Change (ProClim-)  
 International Geosphere-Biosphere Programme, Swiss Committee (IGBP)  
 International Union of Geodesy and Geophysics, Swiss Committee (IUGG)  
 International Union of Geological Sciences, Swiss Committee (IUGS)  
 Kommission der Schweizerischen Paläontologischen Abhandlungen (KSPA)  
 ProDoc project Leman21  
 Steering Committee NRP 61  
 Swiss Association of Energy Geoscientists (SASEG)  
 Swiss Association of Geologists (CHGEOL)  
 Swiss Commission on Atmospheric Chemistry and Physics (ACP)  
 Swiss Commission for Oceanography and Limnology (COL)  
 Swiss Commission for Phenology and Seasonality (CPS)  
 Swiss Commission for Remote Sensing (SCRS)  
 Swiss Committee for Stratigraphy (Platform Geosciences/SCNAT)  
 Swiss Geodetic Commission (SGC)  
 Swiss Geological Society (SGG/SGS)  
 Swiss Geological Survey (swisstopo)  
 Swiss Geomorphological Society (SGGm/SSGm)  
 Swiss Geophysical Commission (SGPK)  
 Swiss Geotechnical Commission (SGTK)  
 Swiss Geothermal Society (GEOTHERMIE.CH)  
 Swiss Hydrogeological Society (SGH)  
 Swiss Hydrological Commission (CHy)  
 Swiss Meteorological Society (SGM)  
 Swiss Paleontological Society (SPG/SPS)  
 Swiss Snow, Ice and Permafrost Society (SIP)  
 Swiss Society for Hydrology and Limnology (SGHL / SSSL)  
 Swiss Society for Quaternary Research (CH-QUAT)  
 Swiss Society of Mineralogy Petrography (SMPG / SSMP)  
 Swiss Tectonics Studies Group (Swiss Geological Society)  
 Verband Geographie Schweiz (ASG)  
 Working Group for Geotopes in Switzerland (Platform Geosciences/SCNAT)

# 0. Plenary Session

- 1 Yardley, B.: Fluids and Crustal Processes through Orogenic Cycles
- 2 Konhauser K.: Banded Iron Formation and the Rise of Oxygen
- 3 Coe A.: The impact of oceanic anoxic events on marine biota, ocean chemistry and Earth processes
- 4 Korup O.: Accounting for extreme events in Earth Surface Processes: the critical challenges
- 5 Kelemen P.: Carbonation of mantle peridotite: Natural systems, global carbon cycle, engineered capture & storage

## 1

# Fluids and Crustal Processes through Orogenic Cycles

Yardley, Bruce

*School of Earth and Environment, University of Leeds, Leeds LS2 9JT, UK*

There are some features of orogenic belts that have been repeated through time around the world, and almost certainly reflect fundamental properties of materials rather than coincidental repetition of plate movement patterns. One of the most basic observations in metamorphic terranes is that sedimentary sequences undergo pervasive ductile deformation while they are being buried and heated, beginning at very low temperatures, but when they subsequently cool through the same temperature range any deformation is more limited, and is strongly focussed. This universal cycle reflects the changing role of water through the orogenic cycle: during prograde metamorphism it is continuously released and allows extensive deformation by pressure solution at temperatures well below the notional brittle-ductile transition, whereas incipient retrograde reactions rapidly consume remaining pore water once cooling sets in, precluding deformation by mechanisms that require the presence of a water phase. Only where major structures such as shear zones allow water to penetrate deep crystalline crust does it show intense ductile deformation. The evidence of many years of accumulated geological observation is that rocks undergoing burial and heating are very weak, whereas those returning to the surface are strong and act as massive blocks, but this is simply the inevitable consequence of mineral equilibria dictating the fugacity of water in rock pores.

A second change between the burial and uplift stages of orogeny concerns rates of reactions. During burial and heating, rates of endothermic devolatilisation reactions are limited by heat supply, and so overall regional reactions proceed very slowly. During cooling and uplift, 2 types of reactions are possible, but both are subject to quite different constraints to prograde reactions. Retrograde reactions that reverse changes that took place during heating are limited by infiltration of volatiles; hydration reactions proceed very rapidly if water is present but the preservation of abundant high grade rocks demonstrates that this is very rarely the case. Rapid uplift and erosion leads to rapid decrease in pressure and under some metamorphic conditions, devolatilisation reactions can result. When this occurs, temperature becomes buffered by the mineral assemblage according to the prevailing pressure, and temperature drops as heat is consumed by endothermic reactions. These reactions can proceed more rapidly than those driven by heat input (Figure 1) and may be responsible for some orogenic gold deposits.

The direction of temperature change dictates whether crystalline rocks contain water, and thereby whether they are weak or and strong. These rheological differences in turn affect large scale crustal behaviour. While many aspects of orogenic belts do reflect the plate tectonic setting in which they originated, there are geochemical and petrological consequences of heating and cooling, burial and uplift, which also have a profound influence on their geological behaviour irrespective of external tectonic forces.

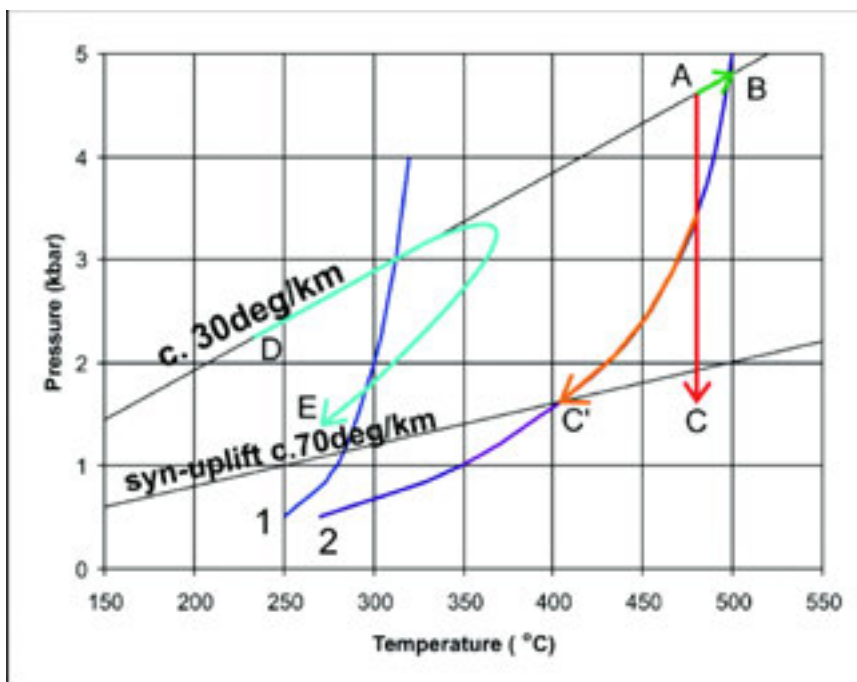


Figure 1: P-T diagram indicating possible P-T changes for a rock A sitting on an average crustal thermal gradient over a 4 Ma period. A-B denotes continued regional burial and heating. Path A-C is for rapid uplift without reaction, while A-C' shows the effect of uplift coupled to dehydration driven by the drop in pressure. For reference, path D-E shows heating followed by cooling with hydration reactions.

## 2

## Banded Iron Formation and the Rise of Oxygen

Kurt Konhauser

*Department of Earth and Atmospheric Sciences, University of Alberta, Edmonton, Alberta, T6G 2E3*

Iron formations (IF) are iron rich (~20-40% Fe) and siliceous (~40-50% SiO<sub>2</sub>) sedimentary deposits that precipitated throughout much of the Precambrian. Their trace element composition is now being used as a proxy for ancient seawater chemistry, with the view of better understanding the evolution of O<sub>2</sub>-producing cyanobacteria and subsequent aerobic metabolisms. Two related examples are provided here. First, it has been shown that the Ni content in IF has changed dramatically over time, and that a drop in Ni availability in the oceans around 2.7 billion years ago would have had profound consequences for microorganisms that depended on it, that being methane-producing bacteria called methanogens<sup>1</sup>. These bacteria have a unique Ni requirement for their methane-producing enzymes, and crucially, these bacteria have been implicated in controlling oxygen levels on the ancient Earth as the methane they produced was reactive with oxygen and kept atmospheric oxygen levels low. It is possible that a Ni famine eventually led to a cascade of events that began with reduced methane production, the expansion of cyanobacteria into shallow-water settings previously occupied by methanogens, and ultimately increased oxygenic photosynthesis that tipped the atmospheric balance in favour of oxygen, the so-called Great Oxidation Event (GOE) at around 2.5 Gyr. Second, a recent compilation of Cr enrichment in IF shows a profound enrichment coincident with the GOE<sup>2</sup>. Given the insolubility of Cr minerals, its mobilization and incorporation into IF indicates enhanced chemical weathering at that time, most likely associated with the evolution of aerobic continental pyrite oxidation. If we accept that IF can serve as useful proxies for the composition of ancient seawater, the question then becomes what do other trace elements in IF tell us about the ancient biosphere? In this regard, we have also been examining the temporal changes in U, Co and Zn concentrations in IF as a means of corroborating the oxidation trends observed via Ni and Cr. Prospectives for the future also include evaluating marine trace element evolution from other lithologies, such as black shales, cherts and/or carbonates, in an effort to better understand the paleo-nutrient landscape that, as today, should have varied along an ocean transect.

### REFERENCES

- Konhauser, K.O., Pecoits, E., Lalonde, S.V., Papineau, D., Nisbet, E.G., Barley, M.A., Arndt, N.T., Zahnle, K., and Kamber, B.S. Oceanic nickel depletion and a methanogen famine before the Great Oxidation Event. *Nature* 458, 750-753 (2009).
- Konhauser, K.O., Lalonde, S.V., Planavsky, N., Pecoits, E., Lyons, T., Mojzsis, S., Rouxel, O.J., Barley, M., Rosiere, C., Fralick, P.W., Kump, L.R., and Bekker, A.. Aerobic bacterial pyrite oxidation and acid rock drainage during the Great Oxidation Event. *Nature* 478, 369-374 (2011).

## 3

## The impact of oceanic anoxic events on marine biota, ocean chemistry and Earth processes

Angela L. Coe

*Department of Environment, Earth and Ecosystems, Centre for Earth, Planetary, Space and Astronomical Research, The Open University, Walton Hall, Milton Keynes, MK7 6AA, UK*

There have been at least four short periods in Earth history when significant amounts of marine organic matter were deposited and preserved globally. These periods have been termed oceanic anoxic events (OAEs) and almost all of them occurred during the greenhouse conditions of the Cretaceous. All of the OAEs are associated with severe environmental change including large perturbations to the carbon cycle, rapid global warming, major changes in ocean chemistry, an increase in the hydrological cycle and mass extinction. In addition, several putative oceanic anoxic events have been suggested including some in the Palaeozoic and a well-studied Cenozoic event, the Paleocene-Eocene thermal maximum (PETM), which occurred 56 million years ago.

The past decade has seen many advances in our understanding of these dramatic OAEs and seawater anoxia. These advances have been partially driven by advances in scientific techniques including the development of new isotopic tracers and refinement of the geological timescale using astronomical cycles. However, the other major driver has been the search for analogues of present day environmental change and the need to understand changes in the Earth system over millennial and decadal timescales.

One of the major impacts of global warming at present day is deoxygenation of the oceans. Areas with lower oxygen levels in the oceans have increased exponentially over the past 50 years and now cover 7% of ocean area and affect over 400 marine ecosystems. Putting this into context, the continental shelves cover 10% of the ocean area. The long-term biotic effects of deoxygenation of the oceans are likely to include changes in the marine food web, extinctions, smaller body size and reduced biodiversity. Similar to past events, the chemical and physical effects are likely to include a different chemical balance of many elements in seawater and changes in ocean circulation.

This talk will present some recent advances in our understanding of OAEs including:

- How both the micro- and macro-biota changed in response to the extreme conditions.
- The Mo-isotope proxy that can be used to determine the areal extent of deoxygenation.
- Proxies for the negative feedbacks that allowed the Earth to eventually recover from these extreme conditions.
- How astronomical cycles have been used to understand the duration and pacing of these events and their possible role in driving the events.

In particular, the only OAE that occurred during the Jurassic (Toarcian OAE, 183 Ma ago) will be discussed. This event occurred in four stages paced by Milankovitch cycles. It was associated with an area equivalent to approximately all of the continental shelves being deoxygenated periodically, a mass-extinction in marine biota and significant extinctions in the terrestrial realm. A recent study that collected data from 36,000 bivalve specimens shows that just two bivalve species were adapted to the conditions and suggests that the size of the bivalves were linked through primary productivity to changes in ocean chemistry.



## 4

# Accounting for extreme events in Earth Surface Processes: the critical challenges

Oliver Korup

*Institute of Earth and Environmental Sciences, University of Potsdam, D-14476 Golm, Germany,  
e-mail: oliver.korup@geo.uni-potsdam.de*

The steadily growing number of field and remote sensing data continues to underscore systematic inverse relationships between the magnitude and frequency of Earth surface processes, based on metrics such as mass-wasting volume, flood discharge, wildfire size, turbidite thickness, or sediment yield. Such frequency-magnitude relationships have turned out to be a useful tool, if not paradigm, for assessing the geomorphic efficacy of a given process, while serving as a quantitative basis for assessing concomitant natural hazards.

In the light of contemporary global warming and environmental change, however, current research interest has shifted towards quantifying potential changes to frequency-magnitude relationships in order to predict future consequences and regime shifts in Earth surface processes. This research focus raises a number of issues that have been partly disregarded in previous work mostly for reasons of mathematical convenience. Here I encapsulate and discuss some of these issues and highlight potential avenues of future research.

The most pertinent issues include (1) statistical means to distinguish reliably different frequency-magnitude relationships with a view towards the question of their particularity vs. universality; (2) the pitfall of confusing frequency with abundance; and (3) adequate choice of model fit, which eventually dictates our capability of meaningfully detecting changes to frequency-magnitude curves brought about by external changes. I outline possible solution pathways to resolving these issues by presenting several current examples from natural hazards research.

## 5

# Carbonation of mantle peridotite: Natural systems, global carbon cycle, engineered capture & storage

Peter B. Kelemen\*

*Dept. of Earth & Environmental Sciences, Columbia University, Lamont Doherty Earth Observatory, Palisades NY 10964,  
peterk@ldeo.columbia.edu*

Starting in 2007, my colleagues and I have been studying natural mineral carbonation systems in exposed mantle peridotite, part of a block of oceanic crust and upper mantle thrust onto the Arabian continental margin in Oman and the United Arab Emirates (the Samail ophiolite). There are two, distinct, well exposed examples. The low temperature system, continuing to the present day, occurs at 25 to 60°C [1-3], forming extensive travertine deposits on the surface, composed mainly of calcite, and complementary carbonate veins formed in the subsurface, at depths up to perhaps 3 km, composed mainly of magnesite and dolomite. Most of our samples from travertines and veins have <sup>14</sup>C ages less than 50 ka, with an average of ~ 20 ka for travertines and 30 ka for veins [1,2,4]. This low temperature process is well understood and modelled as the consequence of surficial weathering of the peridotite, forming Mg-HCO<sub>3</sub>-rich ground water, followed by subsurface reaction with extensive precipitation of Mg-carbonates + serpentine, and then by return of carbon-depleted water to the surface in alkaline spring waters (pH 11-12, Ca-OH-rich) which react with atmospheric CO<sub>2</sub> to form travertines [e.g., 5,6]. The rarity of veins older than 50 ka suggests that vein formation and erosion take place at the same rate. Abundance and ages of travertines and veins suggests uptake of 104 to 105 tons of CO<sub>2</sub> per year via peridotite carbonation in the ophiolite [1,2].

There was also a high temperature, peridotite carbonation system, in the hanging wall of the subduction zone that carried the Samail ophiolite over carbon-bearing metasediments during emplacement on the Arabian margin. Peridotites were completely replaced by listvenite (magnesite + quartz) and related lithologies, in bands up to 200 m thick formed within 0.5 km of the thrust, via reaction with CO<sub>2</sub>-rich aqueous fluids at ~ 100°C and 5 to 10 km depth. An Rb/Sr isochron yields 97 ± 27 Ma, consistent with the time of thrusting. Our data reveal unexpectedly large carbon fluxes at low temperature into the “leading edge of the mantle wedge” [7], where mineral decarbonation reactions are not predicted from metamorphic calculations [8]. Instead, carbon transport is via pore waters expelled from compacting sediments with ~ 250 ppm carbon, sufficient to explain the observed fluxes over the 10 to 20 Ma of emplacement.

Kinetic data on olivine carbonation indicate that reaction with CO<sub>2</sub>-rich fluids (e.g. CO<sub>2</sub> saturated water at ~ 100 bars), at pH ~ 6-7 and ~ 185°C, is ~ 106 times faster in the near surface conditions prevailing in the Samail ophiolite [reviews in 2,9; our new data in 10]. Thus, one proposed method of engineered, geological carbon storage is to inject CO<sub>2</sub>-rich fluid into subsurface peridotite at ~ 150-200°C, rapidly forming solid carbonate for permanent storage. Alternatively, we can emulate the active, natural system in the Samail ophiolite, which produces carbon-free fluids, by creating enhanced pathways for circulation of, e.g., seawater, through subsurface peridotite, and return carbon-depleted waters to the surface where they will draw down atmospheric CO<sub>2</sub> [1,2]. The latter method, for distributed carbon capture from natural waters, might cost ~ \$100/ton of CO<sub>2</sub> [2]. This may be a supplement or alternative to direct air capture, should it be necessary to reduce global, atmospheric CO<sub>2</sub>.

Natural mineral carbonation involves positive feedbacks between volume change – due to addition of CO<sub>2</sub> + H<sub>2</sub>O to the solid – together with decreased solid density. Stress due to volume change causes fractures, which maintain or enhance permeability and reactive surface area. In the case of the Cretaceous listvenites, this led to 100% carbonation, in which every Ca and Mg atom is in carbonate minerals. Elsewhere, carbonation and hydration involves negative feedbacks, destroying permeability and armouring surfaces. Thus, it is essential to understand the conditions favouring reaction driven cracking. Stress during peridotite carbonation and hydration is on the order of 100-300 MPa, based on independent but consistent estimates from (a) thermodynamic data and (b) fracture density plus mineral physics data [11]. Improved understanding of reaction driven cracking could be applied to geothermal power generation and extraction of tight oil and gas resources, as well as carbon storage [2].

Unexpectedly high fluxes of carbon from footwall sediment into the leading edge of the mantle wedge in the Samail ophiolite motivates review of the role of peridotite carbonation in the global carbon cycle. Peridotites sampled near the mid-ocean ridges have an average of ~ 0.5 wt% CO<sub>2</sub>. [2,12]. Combining this with seismic estimates of the extent of peridotite alteration in the oceanic mantle at the outer rise [13], just prior to subduction, yields an estimated flux of ~ 10<sup>10</sup> kg C/yr [14], comparable to the estimated flux in subducting oceanic crust. Carbonate solubility in aqueous fluids increases dramatically with increasing pressure at low temperature, yielding carbon concentrations of 1 wt% or more in aqueous fluids in subducting sediment and oceanic crust [15] and fluxes of ~ 10<sup>10</sup> kg carbon/yr into the cold nose of the mantle wedge at < 75 km depth [14]. At greater depth, subducting, buoyant marbles and calc-silicates with layer thicknesses greater than a few hundred meters could rise as diapirs into the mantle wedge beneath volcanic arcs, where they would react with high temperature peridotite [16], potentially producing carbon-rich fluids or melts, and increasing the carbon content of the upper mantle. These factors have not been incorporated in previous estimates of carbon transfer in subduction systems, and potentially represent globally important sources and sinks in the global carbon cycle.

## REFERENCES

- [1] Kelemen & Matter Proc Nat Acad Sci (US) 2008;
- [2] Kelemen et al. Ann Rev Earth Planet Sci 2011;
- [3] Streit et al. Contrib Mineral Petrol 2012;
- [4] Mervine et al. Geochim Cosmochim Acta submitted 2013;
- [5] Barnes & O'Neil GSA Bull 1969;
- [6] Paukert et al. Chem Geol 2012;
- [7] Streit PhD thesis 2013 and Streit et al. in prep.;
- [8] Gorman et al. G-cubed 2006;
- [9] Matter & Kelemen Nature Geosci 2009;
- [10] Gadikota et al. Energy Env Sci 2013;
- [11] Kelemen & Hirth Earth Planet Sci Lett 2012;
- [12] Früh-Green et al. AGU Monograph 2004;
- [13] Van Avendonk et al. G-cubed 2011;
- [14] Kelemen et al. in prep. 2013;
- [15] Manning Rev. Mineral Geochem 2013;
- [16] Behn et al. Nature Geosci. 2011

# 1. Structural Geology, Tectonics and Geodynamics

Neil Mancktelow, Guido Schreurs, Paul Tackley

*Swiss Tectonics Studies Group of the Swiss Geological Society*

## TALKS:

- 1.1 Houlié N., Stern T.: A comparison of GPS solutions for strain and SKS fast directions: implications for modes of shear in the mantle of a plate boundary zone
- 1.2 Hunziker D., Burg J.-P., Vonquadt A., Bouilhol P.: Jurassic extension in Northern Makran, SE Iran: Geochemistry, U/Pb ages and Sr-Nd isotopes
- 1.3 Kaczmarek M.-A., Grange M., Reddy S.M., Nemchin A.: Deformation mechanisms in Martian meteorites
- 1.4 Lourenço D. L. , Tackley P. J.: The effect of melting and crustal production on plate tectonics on terrestrial planets
- 1.5 Malz A., Madritsch H., Meier B., Navabpour P., Heuberger S., Kley J.: The Baden-Irchel-Herdern Lineament: An inherited normal fault controlling the front of the eastern Jura fold-and-thrust belt
- 1.6 Moulas E., Burg J.-P., Podladchikov Y.: Rheology-driven phase equilibria and the in-situ formation of high-pressure rocks
- 1.7 Nazari H., Ghorashi M., Kaveh Firouz A.: Probable Tsunami In The South Caspian Sea By A Large Earthquake!
- 1.8 Sala P., Pfiffner A.: The internal structure of the Säntis nappe: folds, thrusts and wrench faults
- 1.9 Schubert R., Herwegh M.: Kinematics and 3D pattern of ductile shear zones in the Gruebensee-Gelmersee transect (Hasli Valley, central Switzerland).
- 1.10 Simon-Labric T., Reiners P., Braun J.: Orographic precipitations need glaciers to control long-term erosion rates and topography of tectonically inactive mountain ranges
- 1.11 Strasser, M., Kodaira, S., Dinten, D.: Structural and morphological changes in the shallow plate boundary system and trench, triggered by rare subduction megathrust earthquakes
- 1.12 Valla P.G., Rahn M., Shuster D.L., van der Beek P.A.: Exhumation history, topographic relief evolution and geothermal activity in the Swiss Central Alps (Rhône valley): insights from low-temperature thermochronology
- 1.13 Wehrens P., Herwegh M., Berger A.: Fluid involved, high grade cataclasis during Alpine ductile deformation in basement rocks of the Aar massif

## POSTERS:

- P 1.1 Bagheri S., Sarani M.: On the origin of the Naybandan Arc-shaped structures, Tabas, Central Iran
- P 1.2 Bauville A., Schmalholz S.M.: 2D thermo-mechanical modeling of basement-cover deformation with application to the Western Alps
- P 1.3 Buchs D., Cukur D., Masago H.: Tectonosedimentary evolution of the Nankai forearc (Japan) constrained by detrital minerals in off-shore (IODP) drill sites and modern river beds
- P 1.4 Cioldi S., Moulas E., Burg J.P.: Geospeedometry of inverted metamorphic gradients of a crustal-scale thrust zone: first approach
- P 1.5 Collignon M., May D. A., Kaus B. J.P., Fernandez N.: Effects of surface processes on multilayer detachment folding: a numerical approach.
- P 1.6 Duretz T., Schmalholz S. M.: Thermo-mechanical feedback and modelling of crustal-scale shear zones
- P 1.7 Fischer R., Gerya T.: Was plate tectonics different in a hotter Earth? History and evolution of subduction in the Precambrium
- P 1.8 Frehner M.: 3D fold growth rates
- P 1.9 Golabek G., Jutzi M., Gerya T., Asphaug E.: Towards coupled giant impact and long term interior evolution models
- P 1.10 Gruber M., Sommaruga A., Mosar J.: 3D Modeling of the Fribourg Area - Western Swiss Molasse Basin, Switzerland
- P 1.11 Jaquet Y., Bauville A., Schmalholz S.: Viscous overthrusting versus folding: 2-D quantitative modeling and its application to the Helvetic and Jura fold and thrust belts
- P 1.12 Kelevitz K., Houlié N., Rothacher M., Giardini D.: Mapping Earth's interiors with GPS records: the first steps.
- P 1.13 Kilian R.: The role of phase distribution and reaction in an amphibolite facies ultramylonite
- P 1.14 Liao J., Gerya T.: Offsetting crustal and mantle neckings generates abandonment of continental rifts
- P 1.15 Lupi, M., Miller, S. A.: Deformation of the Sumatran, Chilean, and Japanese volcanic arcs after mega-thrust slips.
- P 1.16 Malz A., Jordan P., Meier B., Madritsch H., Navabpour P., Kley J.: Tectonic events predating the formation of the Jura fold-and-thrust belt: Constraints from cross section balancing
- P 1.17 Marti S., Heilbronner R., Stünitz H.: Semi-brittle deformation of fault rocks - an experimental study of the brittle-to-viscous transition in mafic rocks
- P 1.18 May D. A.: A scalable, parallel matrix-free Stokes solver for geodynamics applications

- P 1.19 Mohammadi A., Winkler W., Burg J.P., Ruh J., Von Quadt A.: Detrital zircon and provenance analysis on the onshore Makran accretionary wedge, SE Iran: implication for the geodynamic setting
- P 1.20 Moulas E., Burg J-P., Kostopoulos D., Schenker F., Chatzitheodoridis E.: Metamorphic conditions and exhumation of the Keshebir-Kardamos dome – Rhodope Metamorphic Complex (Greece-Bulgaria)
- P 1.21 Niane B., Moritz R., Guédron S., Poté J., Ngom P M., Pfeifer H.-R.: Assessment of mercury distribution in sediments, soil, fish and human hair sampled in gold mining areas in the Gambia River Basin at Kedougou, southeastern Senegal
- P 1.22 Philippe T.A., Frehner M., May D.A.: Single Viscous Layer Fold Interplay And Linkage: A 3d-Fem Modelling Approach
- P 1.23 Rabin M., Sue C., Champagnac J.D. & Eichenberger U.: Geomorphology approach in karstic domain: importance of underground water.
- P 1.24 Richter B., Kilian R., Stünitz H., Heilbronner R.: The effect of hot-pressing on the grain size distribution and microstructure of quartz gouge along the brittle-to-viscous transition in shear experiments
- P 1.25 Rozel A., Tackley P.J.: Convection and grain size evolution in mantle and lithosphere of the Earth
- P 1.26 Schmalholz S.M., Medvedev S., Lechmann S.M., Podladchikov Y.: Relationship between tectonic overpressure, deviatoric stress, driving force, isostasy and gravitational potential energy
- P 1.27 Valla P.G., Lowick S.E., Herman F., Champagnac J.-D., Guralnik B., Steer P., Chen J., Qin J.: Exploring feldspar IRSL-50 as a low-temperature thermochronometer: insights from field applications (Alaska, Norway and Pamir)
- P 1.28 Von Tscharner, M., Schmalholz, S.: 3D FEM modelling of geological structures caused by geometrical instabilities and contrasts in rock strength
- P 1.29 Von Tscharner, M., Duretz, T., Schmalholz, S.: Slab detachment – 3D versus 1D
- P 1.30 Zhu Y.F.: Baijiantan-Baikouquan ophiolitic mélanges: Implications for geology evolution of west Junggar, Xinjiang, NW China

## 1.1

### A comparison of GPS solutions for strain and SKS fast directions: implications for modes of shear in the mantle of a plate boundary zone

By Houlié N. and Stern, T.

*Institut für Geodäsie und Photogrammetrie, IGP, ETH Zürich*

The strain rate and vertical velocity fields for New Zealand are computed using GPS data from GEONET (NZ) collected during the past decade. Two domains for shear in the mantle are inferred by comparing the principal shortening direction with the fast direction of shear wave splitting. Beneath the central-southern part of the South Island the strains are low and it's unclear if irrotational strain is taking place or if the splitting here is dominated by anisotropy in the asthenosphere. In contrast, data for the central and northern South Island suggest simple shear is dominant and distributed over a zone ~ 200 km wide. An analysis of the major strike-slip faults confirms that the strike of the major South Island fault systems makes a  $60 \pm 15^\circ$  degree angle with the shortening direction. A map of the vertical component of GEONET GPS velocities shows regions of surface uplift > 5mm/y in both the central South and North Islands. While the pattern of uplift in central South Island is consistent with known geology, the rate of uplift in the central North Island is an order of magnitude higher than the geological rate estimated on a my time scale.

## 1.2

### Jurassic extension in Northern Makran, SE Iran: Geochemistry, U/Pb ages and Sr-Nd isotopes

Hunziker Daniela<sup>1</sup>, Burg Jean-Pierre<sup>1</sup>, Von Quadt Albrecht<sup>2</sup>, Bouilhol Pierre<sup>3</sup>

<sup>1</sup> *Strukturgeologie und Tektonik, Geologisches Institut, ETH Zürich, Sonneggstrasse 5, CH-8092 Zürich (daniela.hunziker@erdw.ethz.ch)*

<sup>2</sup> *Institut für Geochemie und Petrologie, Clausiusstrasse 25, 8092 Zürich*

<sup>3</sup> *Department of Earth Sciences, Durham University*

We present major and trace element analyses combined with U-Pb zircon crystallization ages from an intermediate to granitic intrusion sequence within the Dur Kan Complex, in the Iranian North Makran. The sampled granites – diorites – trondhjemites – plagiogranites and basaltic to andesitic lavas have tholeiitic and calc-alkaline chemical features. Field observations, petrographic relationships, trace element compositions and isotope chemistry indicate three different melt sources for granites, granitoids and the volcanic rocks. Granites yield 170-175Ma ages and represent the last crystallized melt of a continentally derived magma. The fractional crystallization dominated diorite-trondhjemite-plagiogranite sequence was crystallizing over 12Ma (165-153Ma) from the same source which has a mantle and minor continental component. East-west trending mafic dykes intruded the granitoids, which were eroded before being covered by lavas and their Cretaceous (Valangian) sedimentary cover. The source of dykes and lavas is mantle derived.

Temporal correlation with plutonites from the Sanandaj-Sirjan Zone suggests a narrow northwest-southeast striking belt of Jurassic granitoid intrusions that extends over nearly 2000km. Different than previous studies in the Sanandaj-Sirjan Zone, that interpreted these rocks as a magmatic arc and proof for Jurassic subduction of the Neotethys, we suggest extension, that separated the Sanandaj-Sirjan Zone and Central Iran. The increasing mantle influence in the magma source is explained by continuous thinning of continental crust and related mantle up-welling. This extensional phase resulted in the formation of the North Makran Ophiolites.

## 1.3

### Deformation mechanisms in Martian meteorites

Kaczmarek Mary-Alix<sup>1,2</sup>, Grange Marion<sup>2</sup>, Reddy Steve M.<sup>2</sup>, Nemchin Alexander<sup>2</sup>

<sup>1</sup> University of Lausanne, Institute of Earth Science, UNIL Mouline, Batiment Geopolis, CH-1016 Lausanne, Switzerland (mary-alix.kaczmarek@unil.ch)

<sup>2</sup> Department of Applied Geology, The Institute for Geoscience Research, Curtin University of Technology, GPO Box U1987, Perth, WA 6845, Australia

Martian meteorites are used to decipher the deformation mechanisms that have occurred on Mars before excavation of the rocks and during shock event(s). Quantitative microstructural analysis of minerals using Electron Backscatter Diffraction (EBSD), and geochemistry are combined to characterise processes recorded by sub-samples of both Nakhla and Zagami meteorites.

Nakhla and Zagami are clinopyroxene-rich basaltic meteorites, and Nakhla contains some Fe-rich olivine. Nakhla displays a granular texture, essentially composed of augite, fayalite, plagioclase and magnetite. The Zagami sample, essentially formed by clinopyroxene, plagioclase transformed in maskelynite, and whitlockite is part of the “coarse grained” portion of Normal Zagami texture (Stolper et al. 1979; McCoy et al. 1992). The sample shows long prisms of clinopyroxene underlying a weak preferential orientation. The chemical composition of clinopyroxenes reveals zoning from augite cores to pigeonite rims in both samples. However, chemical zoning in Zagami clinopyroxenes is more complex than in Nakhla and suggests melt interactions. In Nakhla the Mg# of olivine (between 0.30 and 0.32) is in equilibrium with Mg# of clinopyroxene rims (0.31) suggesting a late crystallization of olivine.

Crystallographic orientation data from whole thin section of both Zagami and Nakhla samples show a preferred orientation of clinopyroxene and CPOs displaying several point concentrations of <001> axes within a girdle. The relationship between the microstructure and CPOs inferred the possible activation of (100)[001] and (010)[100] slip systems in clinopyroxenes. Moreover, the crystallographic orientations of olivine grains in Nakhla are random and discordant to clinopyroxene. This is in accordance to a late crystallization of olivine in a cumulate texture. The several point concentrations on clinopyroxene <001> axis correspond to twinning along (100), (001) or (010) planes. Microstructural analysis of clinopyroxene single grains show that Nakhla clinopyroxenes have almost no internal deformation, whilst Zagami clinopyroxenes showing complicated microtextures with possible activation of several slip systems related to the shock.

Our results suggest a composite deformation related to magmatic deformation (preferred orientation and prismatic clinopyroxene) to impact event(s) (single grain internal deformation and twinning).

#### REFERENCES

- Stolper E. M. McSween H. Y. and Hays J. F., 1979. *Geochimica Cosmochimica Acta*. A petrogenetic model of the relationships among achondritic meteorites. 43: 589-602.
- McCoy T. J., Taylor G. J. and Keil K., 1992. *Geochimica Cosmochimica Acta*. Zagami: Product of a two-stage magmatic history. 56: 3571-3582.

## 1.4

# The effect of melting and crustal production on plate tectonics on terrestrial planets

Lourenço Diogo L.<sup>1</sup>, Tackley Paul J.<sup>1</sup>

<sup>1</sup> *Institute of Geophysics, ETH Zurich, Sonneggstrasse 5 (NO), CH-8092 Zurich, Switzerland (diogo.lourenco@erdw.ethz.ch)*

Within the Solar System, Earth is the only planet to be in a mobile-lid regime, whilst it is generally accepted that all the other terrestrial planets are currently in a stagnant-lid regime, showing little or no surface motion. A transitional regime between these two, showing episodic overturns of an unstable stagnant lid, is also possible and has been proposed for Venus.

Using plastic yielding to self-consistently generate plate tectonics on an Earth-like planet with strongly temperature-dependent viscosity is now well-established, but such models typically focus on purely thermal convection, whereas compositional variations in the lithosphere can alter the stress state and greatly influence the likelihood of plate tectonics. For example, Rolf and Tackley (2011) showed that the addition of a continent can reduce the critical yield stress for mobile-lid behaviour by a factor of around 2. Moreover, it has been shown that the final state of the system (stagnant- or mobile-lid) can depend on the initial condition (Tackley, 2000); Weller and Lenardic (2012) found that the parameter range in which two solutions are obtained increases with viscosity contrast.

We can also say that partial melting has a major role in the long-term evolution of rocky planets: (1) partial melting causes differentiation in both major elements (like Fe and Si) and trace elements, which are generally incompatible. Trace elements may contain heat-producing isotopes, which contribute to the heat loss from the interior; (2) melting and volcanism are an important heat loss mechanism at early times that act as a strong thermostat, buffering mantle temperatures and preventing it from getting too hot; (3) mantle melting dehydrates and hardens the shallow part of the mantle and introduces viscosity and compositional stratifications in the shallow mantle due to viscosity variations with the loss of hydrogen upon melting (Korenaga and Karato, 2008).

In this work we present a set of 2D spherical annulus simulations using StagYY (Tackley, 2008), which uses a finite-volume scheme for advection of temperature, a multigrid solver to obtain a velocity-pressure solution at each timestep, tracers to track composition, and a treatment of partial melting and crustal formation. We address the question whether melting-induced crustal production changes the critical yield stress needed to obtain mobile-lid behaviour as a function of governing parameters.

Our results show that melting and crustal production strongly influence plate tectonics on terrestrial planets, by making plate tectonics both easier and harder; i.e., for the same yield stress and reference viscosity the use or not of a treatment for melting and crustal production may result in a change from a stagnant-lid regime into an episodic-lid regime or a change from mobile-lid regime to an episodic-lid regime. Several factors can play a role on these, namely lateral heterogeneities and differences in the lid thickness induced by melting and crustal production, the maximum depth of melting, etc.

### REFERENCES

- Korenaga, J., & Karato, S. I. (2008): A new analysis of experimental data olivine rheology, *Journal of Geophysical Research*, 113(B02403).
- Rolf, T., & Tackley, P. J. (2011): Focussing of stress by continents in 3D spherical mantle convection with self-consistent plate tectonics, *Geophysical Research Letters*, 38(18).
- Tackley, P. J. (2000): Self-consistent generation of tectonic plates in time-dependent, three-dimensional mantle convection simulations, *Geochemistry, Geophysics, Geosystems*, 1(1).
- Tackley, P. J. (2008): Modelling compressible mantle convection with large viscosity contrasts in a three-dimensional spherical shell using the yin-yang grid, *Physics of the Earth and Planetary Interiors*, 171(1-4), 7-18.
- Weller, M. B., & Lenardic, A. (2012): Hysteresis in mantle convection: Plate tectonics systems, *Geophysical Research Letters*, 39(L10202).

## 1.5

# The Baden-Irchel-Herdern Lineament: An inherited normal fault controlling the front of the eastern Jura fold-and-thrust belt

Malz Alexander<sup>1</sup>, Madritsch Herfried<sup>2</sup>, Meier Beat<sup>3</sup>, Navabpour Payman<sup>1</sup>, Heuberger Stefan<sup>3,4</sup> & Kley Jonas<sup>5</sup>

<sup>1</sup> Institute of Geosciences, Friedrich-Schiller-University Jena, Burgweg 11, D-07749 Jena (alexander.malz@uni-jena.de)

<sup>2</sup> Nagra, Hardstraße 73, CH-5430 Wettingen

<sup>3</sup> Proseis AG Zürich, Schaffhauserstrasse 418, CH-8050 Zürich

<sup>4</sup> geosfer-ag, Büro für angewandte Geologie, Glockengasse 4. CH-9000 St.Gallen

<sup>5</sup> Georg-August-Universität Göttingen, Geowissenschaftliches Zentrum, Goldschmidtstr. 3, D-37077 Göttingen

Thin-skinned fold-and-thrust belts around the world are described as the outer thrust front of orogens located in their forelands. In these areas a tectonically weak layer acts as the basal décollement over which the sedimentary overburden detaches and moves towards the foreland. In general these fold-and-thrust belts are considered to obey the kinematics of critical accretionary wedges, where the outer toe of the fold belt acts as the frontal thrust.

The Late Miocene to Early Pliocene Jura fold-and-thrust belt, stretching across northern Switzerland and eastern France, is an example of such a foreland fold-and-thrust belt, which consists of a series of mainly E–W trending folds and thrusts often referred to as Folded Jura. In our study area, comprising the easternmost part of the thrust belt, the border between the Folded Jura and the non-detached autochthonous foreland (Tabular Jura) is not clearly defined. In most interpretations, the frontal thrust is however defined by the northernmost anticline of the Folded Jura visible at the surface, which is in our case the prominent Lägern Anticline. Based on newly reprocessed, depth migrated seismic sections across the front of the Folded Jura, we analyse the Baden-Irchel-Herdern Lineament (BIH), a regional structure located north of the Lägern Anticline. The ENE-WSW trending fault zone coincides with the southern border fault of a deep Palaeozoic trough system. This trough was extensionally reactivated in Miocene times during the subsidence of the North Alpine Foreland Basin. Along the eastern part of the BIH, this reactivation is documented by normal offsets of the Tertiary Molasse sediments in seismic sections, as well as in outcrops. In our study area, the Baden-Irchel-Herdern Lineament indicates an additional contractional deformation overprint.

We used classical cross section balancing methods of equal line lengths and areas through an iterative research process of validation and reinterpretation to verify the geometry of the BIH. Our results show that the best matching interpretation is to assume a complex triangle structure at the location where the basal décollement is ruptured by an inherited normal fault. The structure shows one major thrust emerging from the main décollement horizon in Middle Triassic strata and a back-thrust rooting in Jurassic strata. According to this interpretation, the Uppermost Jurassic and Tertiary units form a pop-up structure above the back-thrust. Next to this triangle structure, secondary high-angle thrusts and back-thrusts may indicate reverse reactivation of Tertiary normal faults during the contraction phase related with the formation of the Jura fold-and-thrust belt. Thereby, the BIH shows a very uniform amount of shortening over a relatively wide area. We interpret these equal shortening values as a kind of “structural saturation”, suggesting that the configuration of the structure has reached a maximum amount of deformation during an initial phase of Jura folding.

To the west of our study area the Baden-Irchel-Herdern Lineament merges with the frontal Jura thrust. At this location, the Lägern Anticline shows a conspicuous change in strike from an E-W to an ENE-WSW trend, the latter being parallel to the Baden-Irchel-Herdern Lineament. This strike change of the frontal thrust may imply that the BIH represents a kinematic “foreland stopper”, where the propagation of the thin-skinned frontal thrust ceased due to a disruption of the basal décollement along the inherited normal fault zone.

## 1.6

### Rheology-driven phase equilibria and the in-situ formation of high-pressure rocks

Moulas Evangelos<sup>1</sup>, Burg Jean-Pierre<sup>1</sup> & Podladchikov Yuri<sup>2</sup>

<sup>1</sup>Department of Earth Sciences, ETH-Zurich, Sonneggstrasse 05, CH-8092 Zurich (evangelos.moulas@erdw.ethz.ch)

<sup>2</sup>Faculty of Geosciences and Environment, University of Lausanne, CH-1015 Lausanne, Switzerland

Shear zones represent localised deformation in rocks, which directly depends on some weakening effect. Various processes such as viscous heating are responsible for decreasing the temperature-dependent viscosity in deforming shear zones that can be approximated as weak layers during deformation. Competent layers and boudins enhance the rheological heterogeneity where they are involved in the shear zones. Such heterogeneities cause perturbations in the pressure field if force balance is to be maintained.

The Kolosov-Muskhelishvili equations for elliptical bodies under slow viscous flow were employed to estimate the dynamic parameters (stress and pressure) and their relation to the far-field tectonic stress that generates deformation. Mohr-circle diagrams are used to illustrate the state-of-stress of deforming heterogeneities. The results show that pressure and stress perturbations depend strongly on the orientation of the far-field stresses with respect to the long axis of the elliptical heterogeneity. A viscosity ratio of 10 between the heterogeneity and the surrounding matrix is sufficient to produce pressure perturbations in with about the same magnitude as the far-field stress.

Comparison of the analytical solutions with thermo-mechanical models confirms such pressure perturbations and suggests that dynamic parameters such as pressure and temperature vary spatially and temporally in deforming zones. The dependence of metamorphic phase equilibrium on pressure and temperature implies that metamorphic rocks classified as high-pressure may form in-situ in collisional tectonic environments.

## 1.7

### Probable Tsunami in the south Caspian Sea by a large earthquake!

Nazari Hamid<sup>1</sup>, Ghorashi Manouchehr<sup>1</sup>, Kaveh Firouz Ameneh<sup>2</sup>

<sup>1</sup> Research Institute for Earth Sciences, Geological Survey of Iran, PO. Box: 13185-1494, Tehran- Iran. (h.nazari@gsi.ir)

<sup>2</sup> Geological Survey of Iran, PO. Box: 13185-1494, Tehran- Iran.

The South Caspian basin is surrounded by the Central Alborz mountain range in south and Talesh Mountain in its south western side (Allen et al., 2003). The Central Alborz corresponds to the E-W trending and Talesh is corresponding to the NS trending that both of them bounding the Caspian Sea to the south and south west, as an active terrain belonging to the Alpine-Himalayan seismic belt (Jackson et al., 2002). The Khazar (Caspian) fault, nearly 450 kilometres long, and Astara fault, 110km long appear as the northern border of the Central Alborz and eastern border of the Talesh chain where Mesozoic and paleogene rock units overridden on the young deposits of the South Caspian plain (Nazari 2006). Base on Morphotectonics and Paleoseismology studies, we suggest that a major part of the present shortening in Alborz is localized on the Northern face of the chain along the Khazar fault zone; it is however worth noting that this contact might be located further to the North under the sea (Nazari 2006; Ritz et al., 2006). This border can be interpreted as frontal contact between Alborz and the South-Caspian basin. A recent stratigraphic study on the Holocene –Pleistocene in East of the Haraz valley, suggests an incision rate of 1.25 mm/yr as calculated for the last 12 Kyr. If it is assumed that the incision is related to the vertical component along the Khazar fault, the horizontal N-S shortening along this fault would be 2.5 mm/yr (for a 35° S-dipping fault). This is only 1/10th of the total shortening of Alborz, estimated  $5 \pm 2$  mm/yr (Nazari 2006).

The Astara fault as major active fault system in south west of the SCB that regards to the seismic and geophysical observation propagated under the sea as well as the Khazar fault. Many earthquakes may have been caused by the activity of various branches of these fault systems in land or marine parts of the SCB.

regards to the basin geometry, propagated faults to north or east and its land slope, besides more than 20 km thickness of Neogene and Quaternary deposits in the south Caspian Basin in the scenario with the possibility of a seismic activity on the Khazar or the Astarra faults or one of their propagated branches to the north and east with magnitude  $M \geq 7$ , as the closest active faults to the great lake can trigger many large submarine earthquake ruptures or submarine landslides which is its potential for generating tsunamis in the steep southern coast. And if the tsunami wave height reaches to more than 5 meters, impact area could be estimated  $\sim 20$  km especially in south east of the Caspian beach.

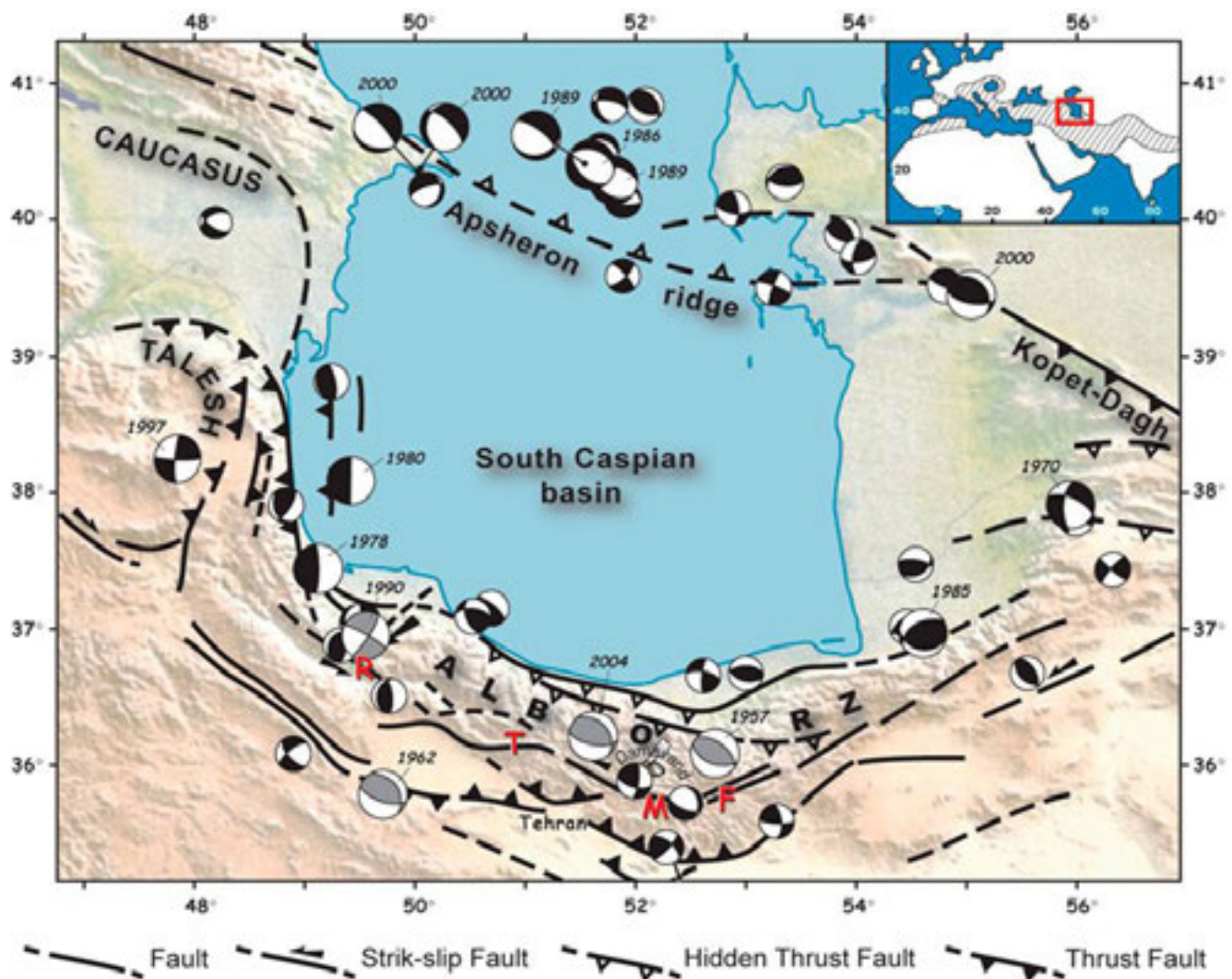


Figure 1. seismotectonic map of the South Caspian Basin (Ritz et al., 2006)

#### REFERENCES

- Allen, M. B., Vincent, S.J., Ian Alsop, G., Ismail Zadeh, A. & Flecker, R. 2003. Late Cenozoic deformation in south Caspian region : effects of a rigid basement block within a collision zone. *Tectonophysics* 366, 223-239.
- Jackson, J., Priestley, K., Allen, M. & Berberian, M., 2002. Active tectonics of the South Caspian Basin. *Geophys. J. Int.* 148, 214-245.
- Nazari, H., 2006. Analyse de la tectonique recente et active dans l'Alborz Central et la region de Teheran: Approche morphotectonique et paleoseismologique. *Science de la terre et de l'eau*. Montpellier, Montpellier II: 247.
- Ritz, J.-F., Nazari, H., Ghassemi, A., Salamati, R., Shafei, A., Solaymani, S. & Vernant, P., 2006. Active transtension inside Central Alborz: A new insight into the Northern Iran-Southern Caspian geodynamics, *Geology*, 34 (6), 477-480.

## 1.8

### The internal structure of the Säntis nappe: folds, thrusts and wrench faults

Sala Paola<sup>1</sup>, Pfiffner Adrian<sup>1</sup>

<sup>1</sup>Institut für Geologie, University of Bern, Baltzerstrasse 1, CH-3012 Bern (sala@geo.unibe.ch)

A 3D geological model (Sala et al. 2013) representative of an area of ca. 110 km<sup>2</sup> was constructed on the base of a series of cross-sections (Schlatter 1941, Funk et al. 2000, Pfiffner 2011) to determine how shortening within the Säntis nappe varies along strike. The cross-sections were constructed and validated using the technique of line-length balancing.

Minimum shortening estimates vary from West to East, from 50% to 30%. This pattern is similar to the observed decreases in shortening in the confining Helvetic nappes in Western Austria (Zerlauth et al. 2013).

Retrodeformation of the Säntis nappe using the top of a mechanical strong unit (Schrattenkalk Formation) was performed to restore the nappe internal thrust faults and folds to their original position. An independent deformation history is recognized in the Western part of the model, where the amount of shortening is higher than the eastern block and where an internal partitioning shows an increase of 10% shortening in the frontal part of the nappe.

#### REFERENCES

- Funk, H., Habicht, K. J., Hantke, R., & Pfiffner, O. 2000: Blatt 1115 Säntis. - Geol. Atlas Schweiz 1:25.000, erläut. 78. Bern: Bundesamt für Wasser und Geologie., pp. 61.
- Pfiffner, A. 2011: Structural map of the Helvetic Zone of the Swiss Alps including Vorarlberg (Austria) and Haute Savoie (France). Geological Special Map 1:100.000, Explanatory notes., Federal Office of Topography Swisstopo.
- Sala P., Pfiffner A., Frehner, M. 2013: The Alpstein in three dimensions: fold-and-thrust belt visualization in the Helvetic zone, Switzerland. Submitted to Swiss Journal of Geosciences.
- Schlatter, L. 1941: Neue Geologische Untersuchungen in Mittleren Säntisgebirge. Ph.D. thesis, St. Gallen, Zollikofer & co.
- Zerlauth, M., Ortner, H., Pomella, H., Pfiffner, A., & Fügenschuh, B. 2013: Inherited tectonic structures controlling the deformation style - an example from the Helvetic nappes between eastern Switzerland and Upper Allgäu (Bavaria). Swiss Journal of Geoscience, in press.

## 1.9

### Kinematics and 3D pattern of ductile shear zones in the Gruebensee-Gelmersee transect (Hasli Valley, central Switzerland).

Schubert Raphael<sup>1</sup> and Herwegh Marco<sup>1</sup>

<sup>1</sup>Geologisches Institut, University of Berne, Baltzerstrasse 3, CH-3012 (raphael.schubert@students.unibe.ch)

Within a master study, special emphasis has been paid to the evolution, the spatial distribution and the 3D geometry of ductile shear zones in the Central Aar granite (CAGr) and Mittagsfluh granite (MiGr) in the transect Gruebensee – Gelmersee (Hasli valley, central Switzerland). For this purpose, the shear zone pattern was mapped in detail at the surface as well as in several underground facilities. Based on the surface information (map and orientation measurements) the planes of the shear zones were projected to depth and a 3D model was built with the Move™, a Midland Valley software. The interpolation of the surface data and the underground data shows that all shear zones are steeply dipping. The building of the shear zones was done according to the dip azimuth and the dip measured on the surface and of a best-fit plane. The quality of the surface-based projections to depth of the 3D-model was evaluated by the misfit between the constructed planes of shear zones and those actually found in tunnels. An average misfit of 3.75% was estimated.

Basically, two major shear zone sets can be discriminated. The first set is NE-SW striking and subparallel to magmatic anisotropies, like magmatic foliations. It is characterized by steep south dipping lineations showing normal and reverse faulting. The second set is NW-SE striking and shows subhorizontal lineations representing strike slip faulting. Crosscutting relationships indicate that the NW-SE set is younger than the NE-SW one. While the first set is interpreted to reflect early thrust related shearing, the second set probably evolved due to transpression of an over-thickened continental crust. In this way, the max principal stress axis ( $\sigma_1$ ) remained constant over time, but  $\sigma_2$  and  $\sigma_3$  flipped. Consequently, ongoing compression induced lateral escape of material leading to the formation of the strike-slip shear zones. As a special feature, the NW-SE shear zones are turning into an E-W direction in the northern part of the working area, where the MiGr is located. This can be explained by ongoing compression, where the MiGr acted as a mechanically rigid body. In this way, inherited magmatic anisotropies control the style and evolution of the early Alpine shear zones, which are then brittly reactivated during a younger stage.

## 1.10

### Orographic precipitations need glaciers to control long-term erosion rates and topography of tectonically inactive mountain ranges

Thibaud Simon-Labric<sup>1</sup>, Peter W. Reiners<sup>2</sup>, Jean Braun<sup>3</sup>

<sup>1</sup> Institut des Sciences de la Terre (ISTE), Université de Lausanne (UNIL), 1015 Lausanne, Suisse.

<sup>2</sup> Geosciences, University of Arizona, Tucson, AZ, USA.

<sup>3</sup> Institut des Sciences de la Terre (Isterre), Université Joseph Fourier, BP53, 38041 Grenoble, France.

It is well known that mountain topography gives rise to some of the most pronounced climate gradients on Earth, the orographic precipitation, but his role on erosion pattern and interactions between the atmosphere and the rest of the Earth System remains poorly understood. The Washington Cascades is a mountain belt particularly sensitive to climate and offers correlations among modern orographic precipitation and erosion rates from 104 to 107 years. Here we use an extensive apatite (U-Th)/He thermochronology data set and thermal-kinematic modeling to reconstruct the erosional and topographic evolution of the range since 15 Myr and show that the forcing of the erosion pattern of the range by orographic precipitation do not start with the onset of orographic precipitation in the Middle-Late Miocene but around the time of the Plio-Quaternary transition. We find a five-time increase of the erosion on the humid side of the range producing a 10 km retreat of the main drainage divide in direction of the arid flank and conclude that the shift from fluvial to glacial-interglacial processes had been necessary to couple precipitation and erosion patterns.

## 1.11

# Structural and morphological changes in the shallow plate boundary system and trench, triggered by rare subduction megathrust earthquakes

Strasser Michael<sup>1</sup>, Kodaira Shuichi<sup>2</sup> Dinten Dominik<sup>1</sup>

<sup>1</sup>Geological Institute, ETH Zurich, Sonneggstrasse 5, CH-8092 Zurich (strasser@erdw.ethz.ch)

<sup>2</sup>Japan Agency of Marine-Earth Science and Technology (JAMSTEC), 2-15 Natsushima-Cho, Yokosuka-city, Kanagawa 237-0061, Japan

Topography and structures of frontal prisms in shallow plate boundary systems along subduction margins generally are assumed to reflect compressional tectonics in marine sediments. In contrast, also gravitational instability, prism collapses or submarine slumps can affect the shallow convergent plate boundary system, and often are hypothesized to be triggered by earthquakes. This study aims at (i) investigating this interplay between overall compressional vs. sporadic gravitational tectonics and subduction megathrust earthquakes; and at (ii) exploring rates and frequencies of processes and events governing the structural and morphological evolution of the frontal prism and trench system. The focus is on the Japan Trench subduction zone that ruptured in 2011 in the magnitude 9 Tohoku-oki earthquake off Japan.

We present bathymetric and reflection seismic data obtained before and after the 2011 earthquake, along with sediment cores, retrieved in 2012 from the >7km deep Japan Trench. Our data document significant seafloor- and subseafloor changes as tectonic and geomorphic expressions of this mega-earthquake. In particular, we present several lines of evidence for a large (> 27.7 km<sup>2</sup>) slump in the trench and interpret a causal link between earthquake slip to the trench and rotational slumping above a subducting horst structure, which significantly impacted the geometry and evolution of the shallow plate boundary system by emerging a new submarine fold-and-thrust. This implies that earthquake-triggered slumps can be leading agents for accretion of trench sediments into the forearc and that forward growth of the prism and seaward advance of the deformation front by several kilometres can occur, punctuated, during a single-event large mega-thrust earthquake.

We further use numerical frontal prism stability models which include transient stresses due to seismic ground motion and scenarios for a complete stress drop along the décollement to constrain our conceptual interpretation based on the seafloor and sub-seafloor data and samples. Model results reproduce deep-seated rotational gravitational instability in the frontal prism, but also indicated that slip-to-the trench and >M.8.5 earthquakes are needed to trigger the observed instability and deformation. This suggests that only rare mega-events, such as the 2011 Tohoku-oki earthquake, which may have recurrence patterns in the order of 1000 years, can impart sudden structural and morphological changes in the shallow plate boundary system and trench.

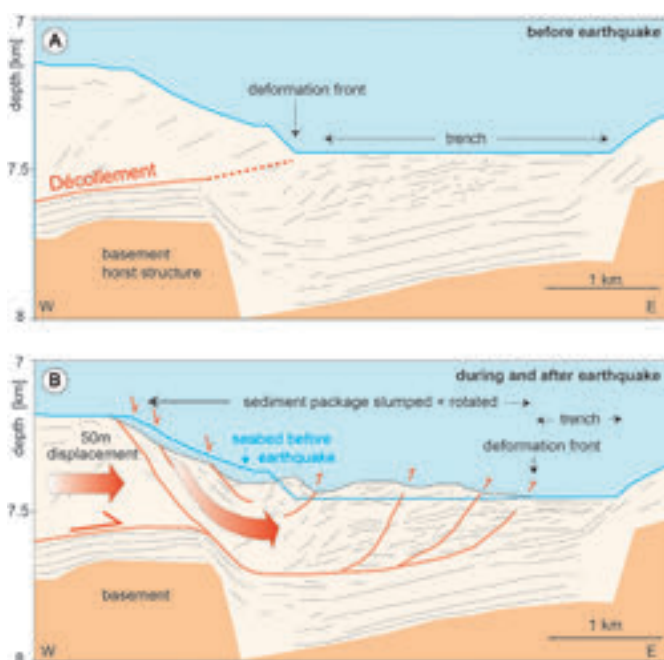


Figure 1. Conceptual sketch modified after Strasser et al., 2013 proposing a causal link between (1) earthquake rupture to the trench, (2) rotational slumping induced by co-seismic displacement of the sedimentary block above the horst structure over the graben, and (3) compressional effects resulting in forward imbrication and accretion of trench material into a 2–3-km-wide emerging submarine fold-and-thrust belt. Deformation front advances seaward by 2–3 km, establishing a new frontal thrust/décollement system in Japan Trench after the earthquake.

## REFERENCES

Strasser M., et al., 2013: A Slump in the Trench: Tracking the impact of the 2011 Tohoku-Oki earthquake, *Geology*, 41, 935-938.

## 1.12

## Exhumation history, topographic relief evolution and geothermal activity in the Swiss Central Alps (Rhône valley): insights from low-temperature thermochronology

Pierre G. Valla<sup>1,2</sup>, Meinert Rahn<sup>3,4</sup>, David L. Shuster<sup>5,6</sup> & Peter A. van der Beek<sup>7</sup>

<sup>1</sup> Geological Institute, ETH Zürich, Sonneggstrasse 5, CH-8092 Zürich (pierre.valla@erdw.ethz.ch)

<sup>2</sup> Institute of Earth Sciences, University of Lausanne, Géopolis, CH-1015 Lausanne

<sup>3</sup> Swiss Federal Nuclear Safety Inspectorate, Industriestrasse 19, CH-5200 Brugg

<sup>4</sup> Department of Mineralogy and Geochemistry, Albert-Ludwigs-Universität, Albertstrasse 23b, D-79104 Freiburg

<sup>5</sup> Department of Earth & Planetary Science, University of California, 479 McCone Hall, USA-94720 Berkeley

<sup>6</sup> Berkeley Geochronology Center, 2455 Ridge Road, USA-94707 Berkeley

<sup>7</sup> Institute of Earth Sciences, University of Grenoble, 1381 Rue de la Piscine, F-38041 Grenoble

The Neogene evolution of the European Alps and potential climatic and/or tectonic controls on denudation rates and relief development during the late-stage exhumation remain subjects of scientific debate (e.g. Willett, 2010). Late Cenozoic to Plio-Quaternary increases in both *in-situ* denudation rates and sediment flux to surrounding basins are suggested to have been caused by climatically-induced relief amplification (Kuhlemann et al., 2002; Vernon et al., 2008). However, even though geomorphologic and sedimentologic studies both suggest topographic relief change and transition from fluvial to oscillations between glacial/fluvial conditions (Muttoni et al., 2003; Norton et al., 2011), precise quantifications on both the timing and magnitude of this transition are only sparse (Häuselmann et al., 2007).

In this study, we focus on the upper Rhône valley (Swiss Central Alps) within the Visp-Brig area (Aar massif, Valais). This area shows among the highest late Neogene exhumation rates within the Western-Central European Alps (Vernon et al., 2008), influenced by tectonic activity along the major Simplon-Rhône extensional fault system (e.g. Mancktelow, 1985; Campani et al., 2010). Moreover, the upper Rhône valley has experienced enhanced glacial erosion associated with strong relief development during the Pliocene-Quaternary period (Norton et al., 2011; Valla et al., 2011). Finally, structural inheritance, late-stage tectonics and rapid exhumation may have promoted recent hydrothermal activity in this region (Sonney and Vuataz, 2008).

We have addressed these aspects and their potential interaction on the cooling history by using different low-temperature thermochronometers along a pseudo-vertical bedrock profile with additional samples from a geothermal well (Brigerbad). Bedrock samples come from elevations between 600 and 2900 m and were combined with samples from a 500-m depth drilling well, resulting in a total ~3 km elevation difference. Apatite fission-track (AFT) dating, as well as track-length data, have been added to previously published (Valla et al., 2011) and new apatite (U-Th-Sm)/He (AHe) and <sup>4</sup>He/<sup>3</sup>He data.

Our AFT and AHe results reveal high-exhumation rates (~1 km/Myr) within late-Cenozoic to Pliocene times, while <sup>4</sup>He/<sup>3</sup>He data confirm this exhumation pulse (Valla et al., 2011). <sup>4</sup>He/<sup>3</sup>He data from valley bottom samples, confirmed by AHe data from the drilling well, show a rapid increase in late-stage exhumation associated to the onset of major Alpine glaciation triggering valley carving. Apatite track length measurements suggest that well samples have been affected by recent hydrothermal activity.

### REFERENCES

- Campani, M., Herman, F. & Mancktelow, N. 2010. Two- and threedimensional thermal modeling of a low-angle detachment: Exhumation history of the Simplon Fault Zone, central Alps. *Journal of Geophysical Research*, 115, B10420.
- Häuselmann, P., Granger, D.E., Jeannin, P.-Y. & Lauritzen, S.-E. 2007. Abrupt glacial valley incision at 0.8 Ma dated from cave deposits in Switzerland. *Geology*, 35, 143-146.
- Kuhlemann, J., Frisch, W., Szekely, B., Dunkl, I. & Kazmer, M. 2002. Post-collisional sediment budget history of the Alps: Tectonic versus climatic Control. *International Journal of Earth Sciences*, 91, 818-837.
- Mancktelow, N. 1985. The Simplon Line: A major displacement zone in the Western Lepontine Alps. *Eclogae Geologicae Helveticae*, 78, 73-96.
- Muttoni, G., Carcano, C., Garzanti, E., Ghielmi, M., Piccin, A., Pini, R., Rogledi, S. & Sciunnach, D. 2003. Onset of major Pleistocene glaciations in the Alps. *Geology*, 31, 989-992.
- Norton, K.P., Abbühl, L.M. & Schlunegger, F. 2010. Glacial conditioning as an erosional driving force in the central Alps. *Geology*, 38, 655-658.

- Sonney, R. & Vuattaz, F.-D. 2008. Properties of geothermal fluids in Switzerland: A new interactive database. *Geothermics*, 37, 496-509.
- Valla, P. G., Shuster, D.L. & van der Beek, P.A. 2011. Major increase in relief of the European Alps during mid-Pleistocene glaciations recorded by apatite  $4\text{He}/3\text{He}$  thermochronometry. *Nature Geoscience*, 4, 688-692.
- Vernon, A.J., van der Beek, P.A., Sinclair, H.D. & Rahn, M.K. 2008. Increase in late Neogene denudation of the European Alps confirmed by analysis of a fission track thermochronology database. *Earth and Planetary Science Letters*, 270, 316-329.
- Willett, S.D. 2010. Late Neogene Erosion of the Alps: A Climate Driver? *Annual Review of Earth and Planetary Sciences*, 38, 411-437.

## 1.13

### Fluid involved, high grade cataclasis during Alpine ductile deformation in basement rocks of the Aar massif

Wehrens Philip<sup>1</sup>, Herwegh Marco<sup>1</sup>, Berger Alfons<sup>1</sup>

<sup>1</sup>Institute of Geological Sciences, University of Bern, Baltzerstrasse 1+3, 3012 Bern ([philip.wehrens@geo.unibe.ch](mailto:philip.wehrens@geo.unibe.ch))

The Aar massif belongs to the external massifs of the Alps and is mainly composed of granitoids and gneisses. Post-Variscan granitoid rocks have intruded old gneisses (Altkristallin) belonging to the pre-Variscan basement. Despite numerous detailed studies in the past decades, the overall exhumation history and the associated massif internal deformation (internal strain distribution and its evolution in time) is largely unknown at present. Here we aim to provide insides into the relation between strain, fluid, rheology and their role in shear zone initiation, progression and localization.

Shear zone initiation and evolution is studied at a variety of scales along shear zones located at the southern margin of the Aar massif (from Rättrichsbodensee to Grimselpasshöhe). Detailed field mapping combined with microscopic analysis along strain gradients has been carried out.

During the Alpine orogeny, strain localized and re-activated along the following pre-existing mechanical anisotropies: i) Lithological variations between Post-Variscan intrusives and Pre-Variscan basement as well as between primary magmatic features (i.e., varying mica content in the Post-Variscan intrusive), ii) pre-existing Pre-Variscan and Variscan brittle and ductile faults.

During the Alpine orogeny alternations of ductile and brittle deformation have affected the host rocks. In domains weakly affected by Alpine deformation, dynamically recrystallized quartz grains indicate ductile deformation by subgrain rotation followed by a static overprint. Despite this ductile background strain, several microstructures indicate a coeval activity of hydrofracking. (i) Overprinting of the aforementioned ductile structures, by fractures along which biotite and epidote have precipitated and (ii) ultracataclasites overgrown by biotite. The fact that both fracture infill and mineral overgrowths consist of biotite suggest formation temperatures above 400°C, i.e. metamorphic conditions under which quartz deforms in a ductile manner. The only explanation for the simultaneous occurrence of brittle and ductile deformation structures at these elevated temperatures is a fast strain rate, which typically occurs during seismic events. We therefore postulate that our structures document seismic cycles characterized by fast brittle deformation followed by subsequent aseismic periods of ductile creep.

White mica and chlorite overgrowth of biotite on the previously described ductile shear zones indicate continuous shearing during retrograde metamorphic cooling. The retrograde decay of feldspars in form of fine-grained reaction products combined with a decrease in crystal plastic deformation of quartz, forced deformation to localize in these ultrafine-grained and thin high strain zones. With ongoing uplift and exhumation these late ductile shear zones are replaced by different generations of cataclasites which cut and/or reactivate the aforementioned precursor structures during the subsequent late stage deformation.

Altogether, this sequence shows the complex history of strain localization and the involvement of both brittle and ductile processes under the presence of fluids at elevated temperatures (>400°C). These conditions fit excellently with the base of the recent seismogenic zone underneath the Aar massif. We therefore suggest that the structural relations nowadays exposed in the Grimsel area give insights on the origin of today's earthquake activity at depths of about 12-15km.

## P 1.1

# On the origin of the Naybandan Arc-shaped structures, Tabas, Central Iran

Bagheri Sasan<sup>1</sup> & Sarani Maryam<sup>1</sup>

<sup>1</sup>Department of geology, University of Sistan and Baluchestan, 98135 Zahedan, Iran

The Tabas Block, a lens shaped continental tectonic sliver, which is surrounded by the Lut and Yazd Blocks in central Iran, and bordered by the two fault systems of Nayband and Kalmard-Kuhbanan, is the host of at least three arc-shaped structures which extend through the width of the block along the lens's short diameter. The presence of such EW-trending structures among the NS-trending ones is the main theme of this research. Each arc has a NE curvature at its eastern termination where it is separated from the Nayband fault, but gradually changes to an EW smooth trend at the middle and abruptly breaks into a NS trend where it joins the Western Tabas fold belt. The northeastern sloping part of each arc is characterized by south-westward-dipping thrusts which brought up the deeper rock of the crust onto the younger sedimentary rocks.

Inside of each arc, structures similar to the dome and basin interference fold pattern can be observed, which may have occurred either as a result of two separate deformational events or during a long progressive deformation; the pattern which cannot be addressed outside of the arcs. Because the youngest sediment, such as the Paleocene Kerman Conglomerate south of the Tabas Block, has been affected by the aforementioned deformations, whereas the Oligocene pyroclastic rock covers the arc-shape structures with a pronounced angular nonconformity, the age of arc formation must be late Paleogene.

On a large-scale view, the Naybandan arc-shaped structures can be viewed as a portion of the large Tabas sigmoidal structure which closely follows the style of the Shotori Mountains (Figure 1), but with a difference of about 90° when we rotate anticlockwisely the sigmoidal around a vertical axis. We propose that the Tabas sigmoidal is a large deflection which appeared during the anticlockwise rotation of the Lut block. The essential role of the right-lateral strike-slip faults around the Tabas Block during the Paleogene period cannot be denied. The interference fold pattern mentioned above can be interpreted as the structures which originated during the distortion of the first set of folds formed at the primary stage of block rotation. Subsequently, the appearance of the NE-trending, right-lateral, strike-slip faults which dissected this sigmoid probably has been developed in continuation of the deflection. These faults are different from the NE-trending left-lateral strike-slip faults which have been activated since the Neogene time by another mechanism, such as the Doruneh fault.

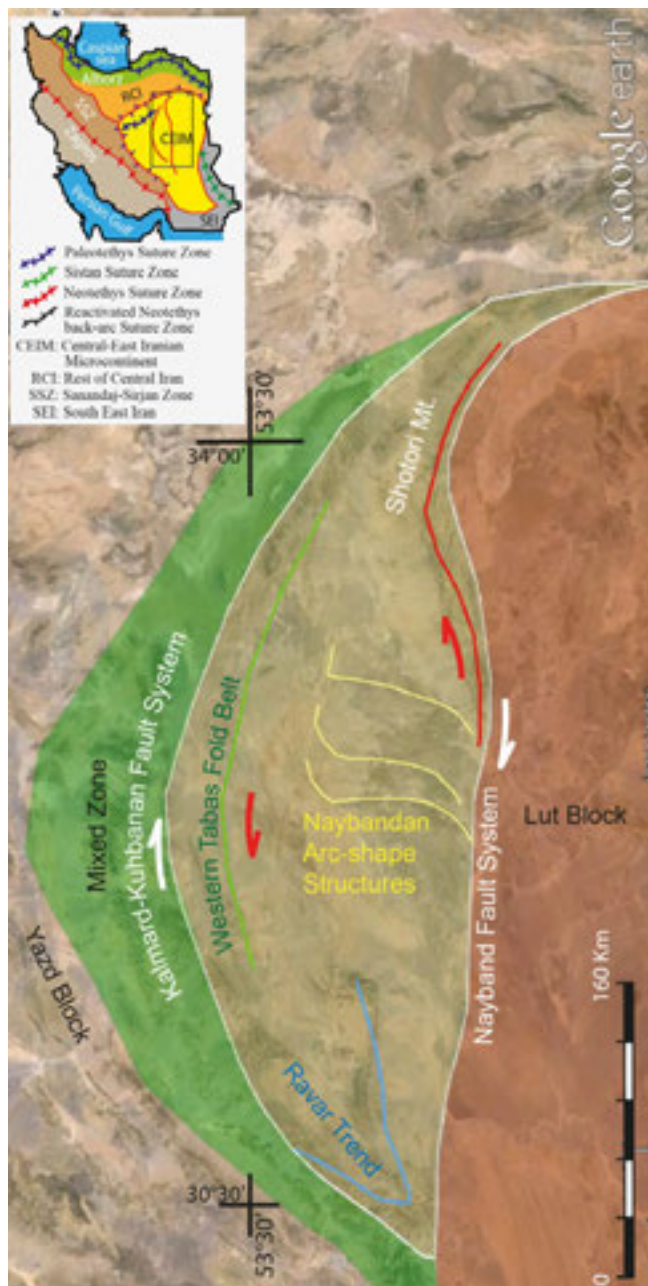


Figure 1: Location of the Tabas Block in the simplified tectonic map of central Iran

## P 1.2

### 2D thermo-mechanical modeling of basement-cover deformation with application to the Western Alps

Arthur Bauville<sup>1</sup> & Stefan M. Schmalholz<sup>1</sup>

<sup>1</sup>ISTE, University of Lausanne, CH-1015 Lausanne (Arthur.bauville@unil.ch)

The external crystalline massifs of Western Alps and the Helvetic sedimentary nappe stack result from the deformation of the European passive margin during the Alpine collision. This area has been studied extensively for the past hundred years. However although the geometry and tectonic structures are well documented, the mechanical behavior of the rocks during nappe stacking and basin inversion is still highly debated. The aim of this study is to reproduce the first order tectonic structures of the Western external Alps. We use a 2-D thermo-mechanical finite element model with visco-elasto-plastic rheology formulation to simulate the deformation of half-graben structures during collision. We systematically investigate the control of (1) the rheology, i.e. ductile vs brittle; linear vs power-law viscous rheology, and (2) the boundary condition, i.e. pure shear vs simple shear. Geometry and finite deformation patterns in both basement and sediments are then compared to cross-sections, finite strain ellipses and cleavage orientation from published field data. Orientation and distribution of plastic shear bands in the model are compared to fault distribution from field data and sand box analogue models.

## P 1.3

### Tectonosedimentary evolution of the Nankai forearc (Japan) constrained by detrital minerals in off-shore (IODP) drill sites and modern river beds

Buchs David<sup>1</sup>, Cukur Deniz<sup>2</sup>, Masago Hideki<sup>3</sup>

<sup>1</sup> School of Earth and Ocean Sciences, Cardiff University, Main Building, Cardiff CF10 3AT, UK (buchsd@cf.ac.uk)

<sup>2</sup> GEOMAR Helmholtz Centre for Ocean Research Kiel, Wischhofstraße 1-3, D-24148 Kiel

<sup>3</sup> CDEX-JAMSTEC, 3173-25 Kanazawa-ku, Yokohama, 2360001, Japan

The evolution of the Nankai forearc (central and SW Japan, Fig. 1) since the Pliocene has been primarily controlled by subduction of the Philippine Sea Plate under the Eurasian Plate, collision of the Izu-Bonin volcanic arc with Japan, and construction of a large accretionary prism by successive sediment stacking. Characterising the evolution of the forearc is central to the Nankai Trough Seismogenic Zone Experiment (NanTroSEIZE) of the Integrated Ocean Drilling Program (IODP), which aims at improving our understanding of processes ultimately leading to the formation of large earthquakes.

Seismic profiles and drilling in the framework of the NanTroSEIZE have shown that the forearc in SW Japan (Kumano transect, Fig. 1) includes contrasted structural domains, with, from NW to SE, a forearc basin, a megasplay fault zone, and imbricate and frontal thrust zones (Moore et al. 2009; Fig. 2).

Sedimentary and tectonic processes in the forearc together with the supply of detrital material to the Nankai Trough have played an important role in the recent evolution of the margin (Underwood and Moore 2013). Our study investigates the tectonosedimentary evolution of the upper forearc slope and Kumano forearc basin since the Pliocene using a sediment provenance analysis with samples collected in 8 major Japanese rivers and 3 drill sites (Figs 1 and 2). Our results show that cuttings samples, collected for the first time by the IODP during the NanTroSEIZE, can be successfully used to characterise the composition of sediments recovered by destructive drilling mode (i.e., without core recovery). In addition, the composition of detrital pyroxenes and amphiboles from our samples allow to identify the main sources of turbiditic deposits in the upper forearc, and provide new constraints on sedimentary patterns prior and during the development of the Kumano Basin. Integration of these data with a regional seismic profile along the Kumano transect provides new insights into the mode and timing of development of the Kumano Basin and its relationship with the development of the megasplay fault in underlying accretionary complex. A reconstruction of the evolution of the upper slope and Kumano Basin enlightens tectonosedimentary processes at tectonically-active subduction zones and provides a model for similar areas elsewhere.

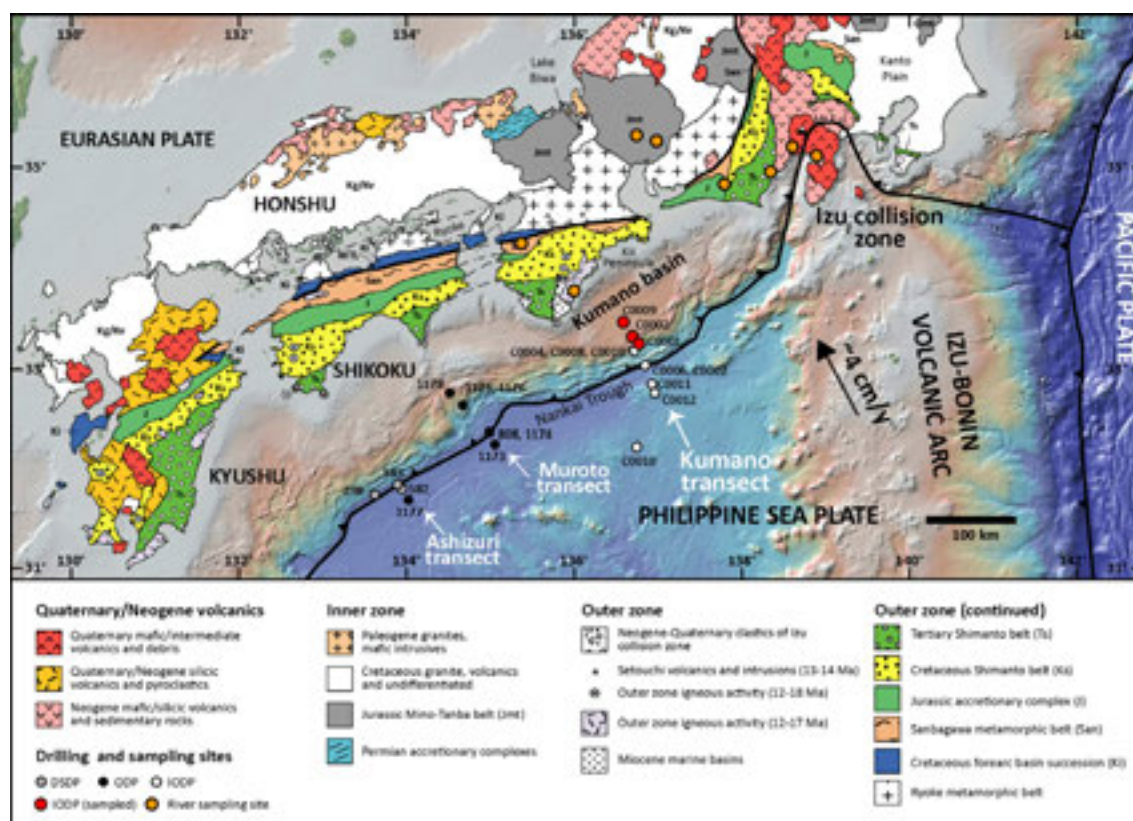


Figure 1. Simplified geological map of SW and central Japan (modified after Fergusson 2003), with location of off-shore (IODP) and on-land (river beds) samples used in this study.

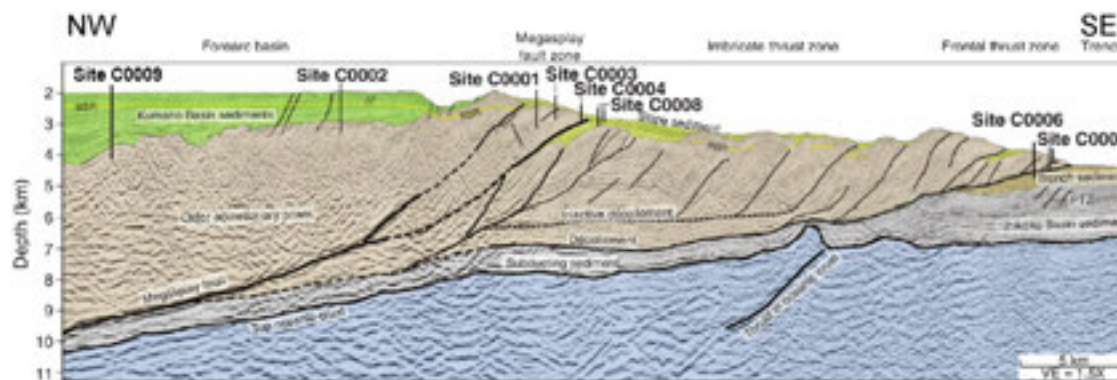


Figure 2. Main structures of the forearc along the Kumano transect (after Moore et al. 2009). Drill sites used in this study include C0001, C0002 and C0009 in the upper forearc slope and Kumano Basin.

## REFERENCES

- Fergusson, C.L., 2003. Provenance of Miocene–Pleistocene turbidite sands and sandstones, Nankai Trough, Ocean Drilling Program Leg 190. In Mikada, H., Moore, G.F., Taira, A., Becker, K., Moore, J.C., and Klaus, A. (Eds.), *Proceedings of the ODP, Scientific Results, 190/196*, 1–28.
- Moore, G.F., Park, J.-O., Bangs, N.L., Gulick, S.P., Tobin, H.J., Nakamura, Y., Sato, S., Tsuji, T., Yoro, T., Tanaka, H., Uraki, S., Kido, Y., Sanada, Y., Kuramoto, S., and Taira, A., 2009. Structural and seismic stratigraphic framework of the NanTroSEIZE Stage 1 transect. In Kinoshita, M., Tobin, H., Ashi, J., Kimura, G., Lallement, S., Screamon, E.J., Curewitz, D., Masago, H., Moe, K.T., and the Expedition 314/315/316 Scientists, *Proceedings of the IODP, 314/315/316*, 1–46.
- Underwood, M.B., Moore, G.F., 2012. Evolution of Sedimentary Environments in the Subduction Zone v of Southwest Japan: Recent Results from the NanTroSEIZE Kumano Transect, in: Busby, C., Azor, A. (Eds.), *Tectonics of Sedimentary Basins: Recent Advances*. John Wiley & Sons, Ltd, 310–328.

## P 1.4

# Geospeedometry of inverted metamorphic gradients of a crustal-scale thrust zone: first approach

Cioldi Stefania, Moulas Evangelos & Burg Jean-Pierre

*Geological Institute, ETH Zurich, Sonneggstrasse 5, CH-8092 Zurich*

*(stefania.cioldi@erdw.ethz.ch, evangelos.moulas@erdw.ethz.ch, jean-pierre.burg@erdw.ethz.ch)*

Thrust tectonics and inverted metamorphic gradients are major consequences of large and likely fast movements in compressional environments. These zones reportedly preserve high-grade metamorphic rocks in the hanging wall and inverted isograds in the footwall of the major thrust zone and occur in tectonic settings ranging from continent-continent collision to subduction zones.

The purpose of this study is to investigate the tectonic setting and the timescale of inverted metamorphic zonation due to crustal-scale thrusting. The aim is to contribute to understand the link between mechanical and thermal evolution of major thrust zones and to clarify the nature and the origin of orogenic heat. Chemical zoning profiles in garnet combined with mineral chemistry from the other minerals in the assemblage are useful indicators of pressure and temperature history of metamorphic rocks. In order to constrain the duration of the thermal event,  $^{40}\text{Ar}/^{39}\text{Ar}$  geochronology offers a temporal resolution with the potential to characterized shear zone movement.

The first case-study is the Nestos thrust in the Rhodope metamorphic complex (Greece). The Rhodope massif is interpreted to be a deformed segment of the Alpine-Himalaya suture and represents a collisional system with an association of structures of both large-scale thrusting and pervasive exhumation tectonics. The study area is divided into three sections across the Nestos Shear Zone (NSZ): Drama, Xanthi and Komotini regions. The inverted metamorphic zonation starts from chlorite-muscovite grade and reaches locally the kyanite-sillimanite grades with migmatites in the highest tectonic levels. The high temperature metamorphic overprint replaces the relics of an earlier high-pressure metamorphic event and constrains the anatexis to have occurred at crustal levels. An overview of the geology and the methods used in this project are presented.

## P 1.5

### Effects of surface processes on multilayer detachment folding: a numerical approach.

Collignon Marine <sup>1</sup>, May Dave A. <sup>2</sup>, Kaus Boris J.P. <sup>3</sup>, and Fernandez Naiara <sup>3</sup>

<sup>1</sup> Geological Institute ETH Zurich, Sonneggstrasse 5, 8092 Zurich, ([marine.collignon@erdw.ethz.ch](mailto:marine.collignon@erdw.ethz.ch))

<sup>2</sup> Institute of Geophysics, ETH Zurich, Switzerland.

<sup>3</sup> Institut für Geowissenschaften, Johannes Gutenberg-Universität, Mainz, Germany.

Over the past decades, the interaction between surface processes and development of mountain belts has been extensively studied. While syntectonic sedimentation appears to control the external development of the fold-and-thrust belts, erosion strongly influences the evolution of internal regions within mountain belts.

The effects of surface processes on brittle deformation have been thoroughly studied using analogue and numerical models of accretionary wedges, however, most of the numerical studies used a 2D model of deformation and/or a simple formulation for the surface processes, where both sedimentation and erosion are rarely present together. Coupled analogue models of deformation and surface processes are challenging, due to material and scaling issues, and often only reproduce two end-member cases (no erosion vs very strong erosion, where all the material is removed), but fail to investigate the transitional cases.

In contrast, interactions between surface processes and ductile deformation (e.g. multilayer detachment folding) have been poorly investigated.

Thin-skinned fold and thrust belts are seen as the result of compressional deformation of a sediment pile over a weak layer acting as a décollement level. The resulting surface expression has often been interpreted, based on geometrical criteria in terms of fault bend folds, propagation folds and/or detachment folds. A few analogue studies have demonstrated that fold morphology can be influenced by erosion rates or preferential localization of sedimentation, and additionally, that the fold growth can be stopped by increasing the supply of sediments.

Here we aim to numerically investigate the effects of surface processes and multilayer folding in three dimensions. For this purpose, we have developed a finite-element based landscape evolution model (both erosion and sedimentation) using PETSc, and coupled it to the 3D mechanical code LaMEM. The landscape evolution model uses a non-linear diffusion formulation (Simpson and Schlunegger, 2003), taking into account both hillslope and channel processes. We present here preliminary results of the coupling between sediment loading and folding.

## P 1.6

# Thermo-mechanical feedback and modelling of crustal-scale shear zones.

Thibault Duretz<sup>1</sup>, Stefan M. Schmalholz<sup>1</sup>

<sup>1</sup> *Institut des Sciences de la Terre, University of Lausanne, UNIL Geopolis, CH-1015 Lausanne (thibault.duretz@unil.ch)*

The collision between continental plates results in the development of orogenic belts. It is well known that the development of crustal-scale shear zone is a common feature of orogenic structures. Ductile shear zones may develop at various structural levels and can be characterised by their metamorphic grade, which is quantified by petrological analysis. Ductile shear zones are often invoked as mechanism for the exhumation of high-pressure (HP) rocks, however their role in the formation of HP units is often debated.

State of the art geodynamic modelling of continental collision is usually used to model the genesis and exhumation of HP rocks. Nevertheless, it is a common approach to model continental collision by predefining shear zones and/or by employing constitutive models that introduce mesh dependency (e.g. strain softening). Mesh size dependency leads to difficult comparison between physical models and natural data since pressure and temperature cannot be accurately computed within modelled shear zones.

In this study, we employ thermo-mechanical modelling to model the self-consistent development of crustal-scale shear zones. Our approach allows for full coupling between momentum and energy equations by including viscous dissipation. We show that this methodology allows for the spontaneous development of shear zones around a cylindrical weak inclusion. Systematic numerical simulations are performed and the results suggest that shear zone dimensions are independent on the mesh resolution. Moreover, we demonstrate that these results can be achieved by using two different numerical methods, which are both popular methods in the geodynamic modelling community (Lagrangian finite elements and Eulerian-Lagrangian finite differences). These results show that thermo-mechanical feedback allows for the development of finite-width shear zones. Such models can therefore be reliably used to quantify stresses, pressure and strain rates in shear zones, and for the modelling of continental collision. Further developments will include comparison with natural data, with a particular focus on the Alpine orogeny.

## P 1.7

## Was plate tectonics different in a hotter Earth? History and evolution of subduction in the Precambrium

Fischer Ria<sup>1</sup>, Gerya Taras<sup>1</sup>

<sup>1</sup> Institute of Geophysics, ETH Zürich, Sonneggstrasse 5, CH-8092 Zürich (ria.fischer@erdw.ethz.ch)

Plate tectonics is a global self-organising process driven by negative buoyancy at thermal boundary layers. Phanerozoic plate tectonics with its typical subduction and orogeny is relatively well understood and can be traced back in the geological records of the continents. Interpretations of geological, petrological and geochemical observations from Proterozoic and Archean orogenic belts however (e.g., Brown, 2006; Taylor and McLennan, 1995), suggest a different tectonic regime in the Precambrian. The lithosphere shows very low internal strength and is strongly weakened by percolating melts and increased temperature due to higher radioactive heating rates and secular cooling. The fundamental difference between Precambrian and Phanerozoic subduction is therefore the upper-mantle temperature, which determines the strength of the upper mantle and hence further subduction history.

3D petrological-thermomechanical numerical modelling experiments of oceanic subduction at an active plate margin done with the finite difference multigrid solver I3ELVIS (Gerya and Yuen, 2007) at increased upper-mantle temperature have been performed to model subduction under Precambrian conditions. Results show (1) an increased importance of small-scale convection with plume shaped cold downwellings replacing the large-scale cold downwelling at temperatures of +150 K to +200 K above present day upper mantle temperature. (2) Thickening of oceanic plates and thinning of continental plates leads to a tectonic style which does not distinct between oceanic and continental plates anymore but merely between two types of terrains, mafic and felsic, of the same thickness. (3) Fracture zones are rendered ineffective at high temperatures which, together with the thickening of oceanic crust, chokes the subduction zone and does not allow any subduction for temperatures above +200 K.

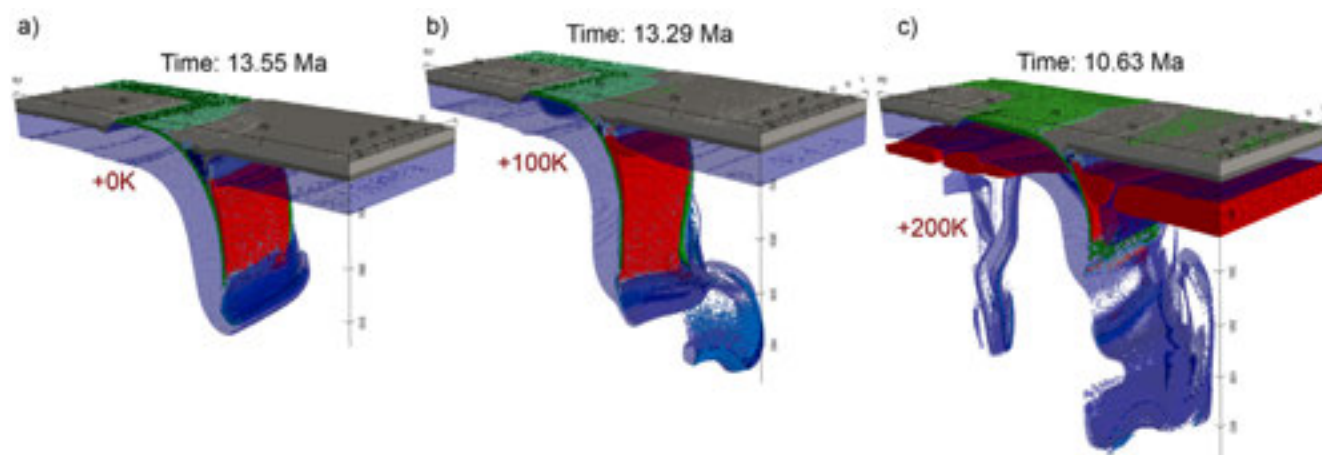


Figure 1. Subduction style depends strongly on upper mantle temperature. (a) Modern subduction with present day temperature gradients in upper-mantle and lithosphere. (b) Increase of temperature by 100 K at the lithosphere-asthenosphere boundary (LAB) leads to melting and drip-off of the of the slab-tip. (c) A temperature increase of 200 K leads Rayleigh-Taylor instabilities and delamination of the whole lithosphere.

### REFERENCES:

- Brown, M., 2006. Duality of thermal regimes is the distinctive characteristic of plate tectonics since the neoproterozoic. *Geology* 34, 961–964.
- Gerya, T.V., Yuen, D.A., 2007. Robust characteristics method for modelling multiphase visco-elasto-plastic thermo-mechanical problems. *Physics of the Earth and Planetary Interiors* 163, 83–105.
- Taylor, S.R., McLennan, S.M., 1995. The geochemical evolution of the continental crust. *Reviews of Geophysics* 33, 241–265. Taylor.

## P 1.8

### 3D fold growth rates

Frehner Marcel

Geological Institute, ETH Zurich, Sonneggstrasse 5, CH-8092 Zurich (marcel.frehner@erdw.ethz.ch)

Geological folds are inherently 3D structures. Therefore, a fold also grows in three dimensions (Bretis et al., 2011; Grasmann and Schmalholz, 2012). In this study, fold growth in all three dimensions is studied and quantified numerically using a finite-element algorithm for simulating 3D deformation of Newtonian materials. Upright symmetrical single-layer folds are considered. The higher-viscous layer exhibits a 2D Gaussian initial perturbation. Horizontal compression in x-direction leads to a folding instability, which grows from this perturbation in all three dimensions (1). Fold amplification in 3D setups has been described analytically by Fletcher (1991) for low limb dips, but fold growth in all three dimensions has not been quantified. It is described by:

#### Fold amplification (growth in z-direction):

Fold amplification describes the growth from a low-limb-dip fold to a higher-limb-dip fold.

#### Fold elongation (growth in y-direction):

Fold elongation is parallel to the fold axis. It describes the growth from a dome-shaped structure to a more cylindrical fold.

#### Sequential fold growth (growth in x-direction):

Sequential fold growth is parallel to the shortening direction and describes the growth of secondary (and further) folds adjacent to the initial isolated fold.

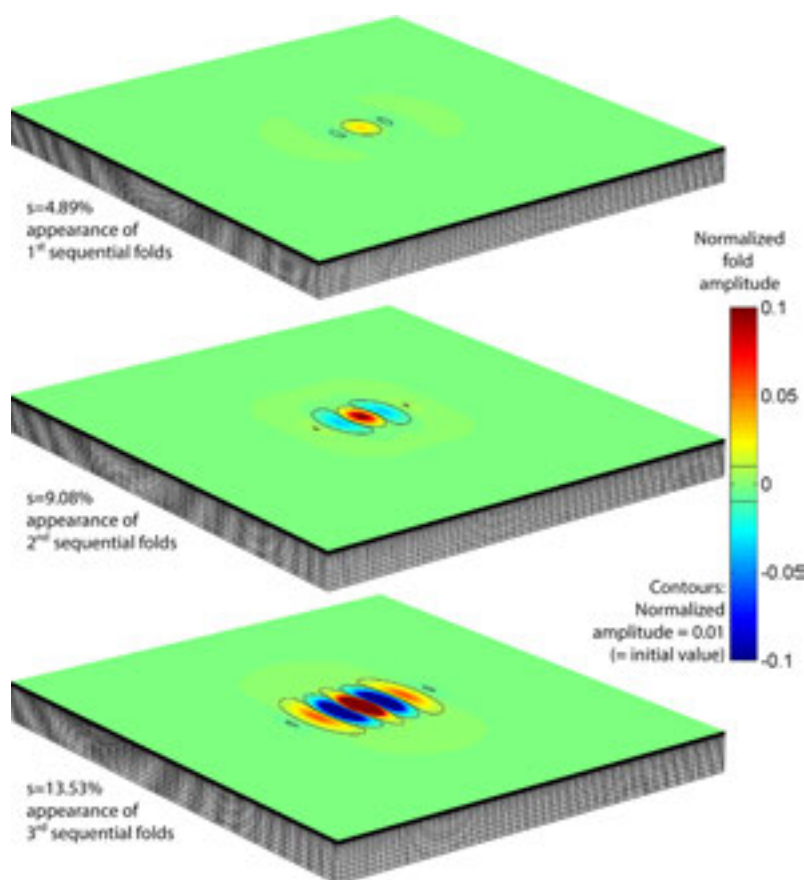


Figure 1: Growth of a 3D fold from a 2D Gaussian initial perturbation in all three dimensions.

Both fold elongation and sequential fold growth have previously been referred to as lateral fold growth, which is here used as an umbrella term for both.

The numerical results demonstrate that the two lateral directions generally show a very similar averaged growth (Figure 2). However, the fold elongation is smooth and continuous, while the sequential fold growth exhibits jumps in its evolution. These jumps occur whenever a secondary or further fold appears for the first time (1) and the entire fold structure therefore suddenly occupies more space in x-direction. For a given initial perturbation, the jumps occur earlier in the folding history for larger viscosity ratios.

Compared to the fold amplification, the two lateral directions grow slower (i.e., values  $<1$  in Figure 2). Exceptions only occur for the sequential fold growth direction in early folding stages in the case of very narrow initial perturbations (Figure 2a). In these cases, the fold amplification is particularly slow and the sequential fold growth rate can therefore be larger. Generally, all three normalized fold amplitudes are of the same order (Figure 2), particularly at the early folding stages.

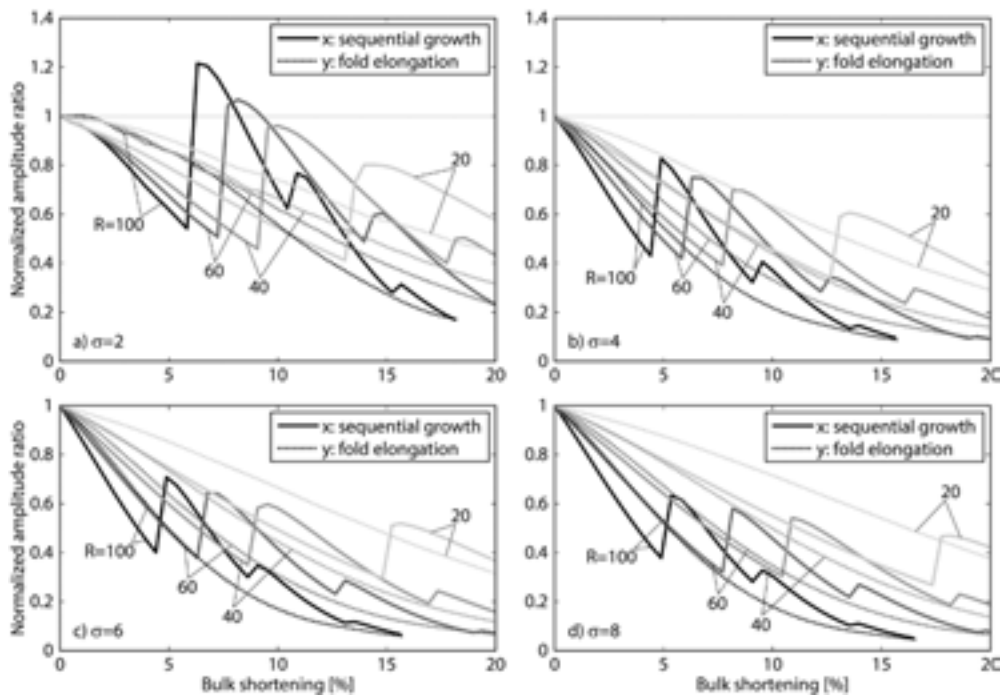


Figure 2. Ratios of normalized amplitudes  $A_x/A_z$  (sequential growth/amplification, bold line) and  $A_y/A_z$  (elongation/amplification, dotted line) for different initial perturbation widths ( $\sigma=2$ : narrow initial perturbation;  $\sigma=8$ : narrow initial perturbation) and different viscosity ratios  $R=\eta_{\text{layer}}/\eta_{\text{matrix}}$ . Values below 1 mean that the corresponding normalized lateral fold amplitude is smaller than the normalized vertical amplitude.

## REFERENCES

- Bretis, B., Bartl, N. and Grasemann, B. 2011. Lateral fold growth and linkage in the Zagros fold and thrust belt (Kurdistan, NE Iraq). *Basin Research*, 23, 615–630.
- Grasemann, B. and Schmalholz, S. M. 2012. Lateral fold growth and fold linkage. *Geology*, 40, 1039–1042.

## P 1.9

# Towards coupled giant impact and long term interior evolution models

Golabek Gregor<sup>1</sup>, Jutzi Martin<sup>2</sup>, Gerya Taras<sup>1</sup> & Asphaug Erik<sup>3</sup>

<sup>1</sup> Institut für Geophysik, ETH Zürich, Sonneggstrasse 5, CH-8092 Zürich (gregor.golabek@erdw.ethz.ch)

<sup>2</sup> Physikalisches Institut, Universität Bern, Sidlerstrasse 5, CH-3012 Bern

<sup>3</sup> School of Earth and Space Exploration, Arizona State University, 550 East Tyler Mall, AZ 85287, Tempe, USA

The crustal dichotomy (McCauley et al., 1972) is the dominant geological feature on planet Mars. The exogenic approach to the origin of the crustal dichotomy (Wilhelms and Squyres, 1984; Frey and Schultz, 1988; Andrews-Hanna et al., 2008; Marinova et al., 2008; Nimmo et al., 2008) assumes that the northern lowlands correspond to a giant impact basin formed after primordial crust formation. However these simulations only consider the impact phase without studying the long-term repercussions of such a collision.

The endogenic approach (e.g. Weinstein, 1995), suggesting a degree-1 mantle upwelling underneath the southern highlands (Zhong and Zuber, 2001; Roberts and Zhong, 2006; Zhong, 2009; Keller and Tackley, 2009), relies on a high Rayleigh number and a particular viscosity profile to form a low degree convective pattern within the geological constraints for the dichotomy formation. Such vigorous convection, however, results in continuous magmatic resurfacing, destroying the initially dichotomous crustal structure in the long-term.

A further option is a hybrid exogenic–endogenic approach (Reese and Solomatov, 2006, 2010; Reese et al., 2010; Golabek et al., 2011), which proposes an impact-induced magma ocean and subsequent superplume in the southern hemisphere. However these models rely on simple scaling laws to impose the thermal effects of the collision.

Here we present the first results of impact simulations performed with a SPH code (Benz and Asphaug 1995, Jutzi et al., 2013) serially coupled with geodynamical computations performed using the code I3VIS (Gerya and Yuen, 2007) to improve the latter approach and test it against observations. We are exploring collisions varying the impactor velocities, impact angles and target body properties, and are gauging the sensitivity to the handoff from SPH to I3VIS.

As expected, our first results indicate the formation of a transient hemispherical magma ocean in the impacted hemisphere, and the merging of the cores. We also find that impact angle and velocity have a strong effect on the post-impact temperature field (e.g. Marinova et al., 2008) and on the timescale and nature of core merger.

## REFERENCES

- Andrews-Hanna J.C., Zuber M.T. and Banerdt W.B. 2008: *Nature* 453, 1212-1215.  
 Benz W. and Asphaug E. 1995: *Computer Physics Communications* 87, 253–265.  
 Gerya T.V. and Yuen D. A. 2007: *Phys. Earth Planet. Int.* 163, 83-105.  
 Golabek G.J., Keller, T., Gerya, T.V., Zhu G., Tackley P.J. and Connolly J.A.D. 2011: *Icarus* 215, 346-357.  
 Frey H. and Schultz R.A. 1988: *Geophys. Res. Lett.* 15, 229-232.  
 Jutzi M., Asphaug E., Gillet P., Barrat J-A. and Benz W. 2013: *Nature* 494, 207–210.  
 Keller T. and Tackley P.J. 2009: *Icarus* 202, 429-443.  
 Marinova M.M., Aharonson O. and Asphaug E. 2008: *Nature* 453, 1216-1219.  
 McCauley J.F., Carr M.H., Cutts J. A., Hartmann W.K., Masursky H., Milton D.J., Sharp R.P. and Wilhelms D.E. 1972: *Icarus* 17, 289-327.  
 Nimmo F., Hart S.D., Korycansky D.G. and Agnor C.B. 2008: *Nature* 453, 1220-1223.  
 Reese C.C. and Solomatov V.S. 2006: *Icarus* 184, 102-120.  
 Reese C.C. and Solomatov V.S. 2010: *Icarus* 207, 82-97.  
 Reese C.C., Orth C. P. and Solomatov V.S. 2010: *J. Geophys. Res.* 115, E05004.  
 Roberts J.H. and Zhong S. 2006: *J. Geophys. Res.* 111, E06013.  
 Weinstein S.A. 1995: *J. Geophys. Res.* 100, 11719-11728.  
 Wilhelms D.E. and Squyres S. W. 1984: *Nature* 309, 138-140.  
 Zhong S. 2009: *Nature Geosci.* 2, 19–23.  
 Zhong S. and Zuber M.T. 2001: *Earth Planet. Sci. Lett.* 189, 75-84.

## P 1.10

# 3D Modeling of the Fribourg Area - Western Swiss Molasse Basin, Switzerland

GRUBER Marius<sup>1</sup>, SOMMARUGA Anna<sup>1</sup>, MOSAR Jon<sup>1</sup>

<sup>1</sup> University of Fribourg, Departement of Geosciences, Earth Sciences, Chemin du Musée 6, CH-1700 Fribourg, Switzerland  
(marius.gruber@unifr.ch, anna.sommaruga@unifr.ch, jon.mosar@unifr.ch)

This study focusses on the structural style of the western Swiss Molasse Basin (WSMB) near Fribourg (west of Bern, Switzerland). We are elaborating a 3D geological model with Move Software (Midland Valley) covering an area of 1700 km<sup>2</sup> around the city of Fribourg. Based on 2D seismic line interpretations and deep borehole data (Sommaruga et al., 2012) three dimensional seismic horizons are built. Horizons correspond to the following stratigraphic boundaries: Near Base Tertiary, near Top Late Malm, near Top Early Malm, near Top Dogger, near Top Lias, near Top Trias, near Top Muschelkalk and near Base Mesozoic. Surface bed dip data from the Geological Atlas 1:25'000 (swisstopo) are included so as to improve orientations of geological strata. Fault surfaces in Tertiary and Mesozoic cover as well as in Pre-Mesozoic basement rocks are constructed based on seismic interpretations (Sommaruga et al. 2012), geological cross-sections (Geological Atlas 1:25:000, swisstopo) and hypocenter positions (Vouillamoz & Abednego, in prep.). Due to the lack of continuous seismic reflectors in Tertiary Molasse sediments, an appropriate mapping of fault structures in the latter is difficult. As a consequence Mesozoic fault surfaces are extrapolated through Tertiary Molasse sediments based on mapped surface fault structures (Geological Atlas 1:25'000, swisstopo; Ibele, 2011). 3D seismic horizons are depth converted based on a 3D heterogeneous P-velocity model of the Fribourg area (Abednego, in prep.).

The model shows a kinematic decoupling of Tertiary and Mesozoic units along a detachment horizon in Triassic evaporites. A second decoupling can be observed along the base Tertiary horizon in the south of the study area, probably linked to the thrust front of Subalpine Molasse as described in Ibele 2011. East of the city of Fribourg several N-S-striking, en echelon type normal faults in Mesozoic and Tertiary units can be observed. Faults form a zone of 20 km length. The zone is called the "Fribourg zone". Faults root in listric bends within middle Triassic evaporites forming a graben or half-graben structure. Triassic evaporites show an important thickening beneath the Fribourg zone. The location of fault traces between 2D seismic lines is speculative in the central part of the Fribourg zone due to a gap of seismic data. Recent studies on present earthquake activity show an enhanced recurrence of low magnitude earthquakes along the Fribourg zone. It is therefore proposed, that the Fribourg zone is formed by an assemblage of multiple small scale fault surfaces rather than a few large scale faults. The Fribourg zone forms the eastern border of a N-S striking, low amplitude syncline, called the "Fribourg structure". The N-S-alignment of the Fribourg structure deviates from the overall NE-SW trend of fold axis in the region. Triassic evaporites show a thinning beneath the Fribourg structure.

## REFERENCES

- IBELE, T. (2011). Tectonics of the Western Swiss Molasse Basin during Cenozoic Time, PhDThesis, University of Fribourg, 166 p.
- SOMMARUGA, A., EICHENBERGER, U. and MARILLIER, F. (2012). Seismic Atlas of the Swiss Molasse Basin, Edited by the Swiss Geophysical Commission. Matér. Géol. Suisse, Géophys. 44.

## P 1.11

## Viscous overthrusting versus folding: 2-D quantitative modeling and its application to the Helvetic and Jura fold and thrust belts

Jaquet Yoann<sup>1</sup>, Bauville Arthur<sup>1</sup>, Schmalholz Stefan<sup>1</sup>

<sup>1</sup>Institute of Earth Science, University of Lausanne, Bâtiment Geopolis, CH-1015 Lausanne (yoann.jaquet@unil.ch)

This paper presents two-dimensional (2-D) numerical simulations of the shortening of a stiff viscous layer with pre-existing weak zones that is embedded in a weaker viscous matrix above a rigid detachment. Four deformation styles are observed that depend on the ratio of the layer and matrix viscosities,  $\mu_L/\mu_M$ ; the ratio of the distance between the layer and the detachment to the layer thickness,  $H_M/H_L$ ; and the power-law stress exponent of the matrix,  $n_M$ . The results show that (1) pure shear-dominated deformation occurs for  $\mu_L/\mu_M < \sim 50$  and  $n_M = 1$  (i.e., linear viscous); (2) overthrusting-dominated deformation occurs for  $n_M > 1$  (i.e., power-law viscous fluid),  $\mu_L/\mu_M > \sim 50$  and  $H_M/H_L < \sim 0.5$ ; (3) folding-dominated deformation occurs for  $n_M = 1$ ,  $\mu_L/\mu_M > \sim 50$ , and  $H_M/H_L > \sim 1$ ; and (4) folding and overthrusting occur for  $n_M > 1$  and  $\sim 0.5 < H_M/H_L < \sim 2$ . The power-law stress exponent of the stiff layer has a minor effect on deformation style. Simulations with layers that contain two weak zones show the formation of a nappe stack. The change in deformation style as a function of  $H_M/H_L$  corroborates field observations from the Helvetic nappe system. The agreement of the results with first-order observations from the Helvetic fold and thrust belt suggest that ductile deformation dominated this fold and thrust belt.

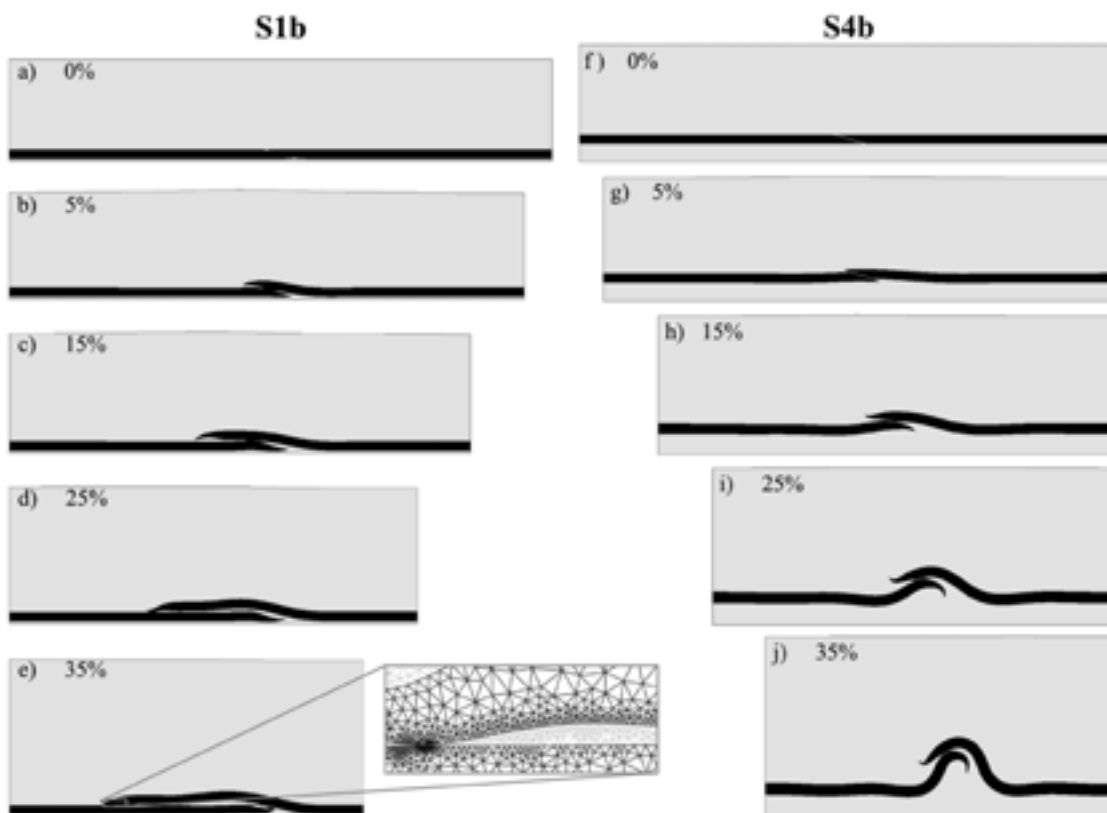


Figure 1: The development of the model geometry with increasing shortening. The layer (black) is linear viscous, whereas the matrix (gray) is power-law viscous ( $n_M=5$ ). a-e) The model has a viscosity ratio ( $\mu_L/\mu_M$ ) of 200 and a thickness ratio ( $H_M/H_L$ ) of 0.25. During shortening, the layer deforms by essentially overthrusting. f-j) The model has a viscosity ratio ( $\mu_L/\mu_M$ ) of 100 and a thickness ratio ( $H_M/H_L$ ) of 1. During shortening, the layer deforms by simultaneously overthrusting and folding. The detail of the numerical mesh is shown in e).

## P 1.12

### Mapping Earth's interiors with GPS records: the first steps.

Kelevitz Krisztina<sup>1,2</sup>, Houlié Nicolas<sup>1,2</sup>, Rothacher Markus<sup>2</sup>, Giardini Domenico<sup>1</sup>

<sup>1</sup> Institute of Geophysics, ETH Zurich, Switzerland

<sup>2</sup> Institute of Geodesy and Photogrammetry, ETH Zurich, Switzerland

Nowadays, GPS networks are expanding faster than the global network of broadband seismometers (STS-1 or STS-2). Indeed, almost 10.000 GPS receivers are recording data at 1 Hz with 100+ stations are streaming data in Real-Time (RT). The reasons for this quick expansion are the price of receivers, their low maintenance, and the wide range of activities they can be used for (transport, science, public apps, etc.).

Many authors proposed then that GPS could help studying not only the long-term continuous continental deformation (earthquake sources [Cervelli, et al., 2001; Langbein et al., 2006], volcanoes [Houlié, et al., 2006a], post seismic deformation [Langbein et al., 2006]) but also transient (less than one hour) ground deformation [Houlié et al., 2011]. Potential applications are numerous including seismic wave propagation at the regional or global scale and earthquake source studies.

In this poster we are presenting work completed on the GPS records of the Hokkaido earthquake (2003 September 25th, Mw=8.3). 1Hz GPS waveforms have been recomputed by improving the inversion of the ground motion displacement history. GPS are computed in the range of frequencies 0.02-0.033 Hz and 0.002-0.033 Hz; the latter frequency band matching the frequency range recorded by a very-broadband STS-1 seismometer (up to 300s with flat response).

At co-located sites (STS-1 and GPS located within 10km) the agreement is good for the vertical component. We show that 1) horizontal components are dependent on the distribution of the satellites visible in the sky at the moment of the seismic wave front propagation while 2) the new inversion algorithm improves the accuracy of the east component of the GPS data.

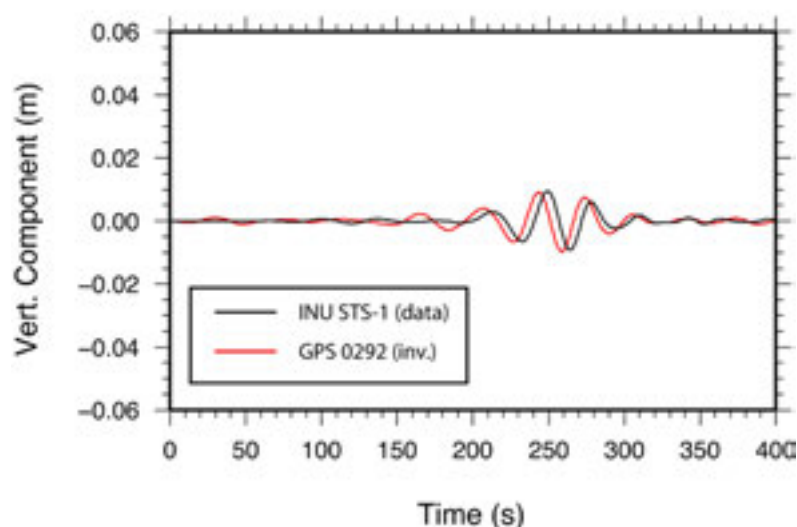


Figure 1: We compare the time-series of GPS displacement (in red) with the seismograms recorded at the GEOSCOPE site INU (in black). We note that while the agreement between the two sets of waveforms is reasonable for vertical component. Instrument responses have been provided by GEOSCOPE. Both datasets have been band-pass filtered between 30 and 50 seconds (20 and 35 mHz) according to the periodogram presented in Figure 5. From Houlié et al., 2011

#### REFERENCES

- Cervelli, P. et al. 2001: Estimating source parameters from deformation data, with an application to the March 1997 earthquake swarm off the Izu Peninsula, Japan
- Houlié, N., et al. 2006a: Large scale ground deformation of Etna observed by GPS between 1994 and 2001
- Houlié, N., et al. 2011: New approach to detect seismic surface waves in 1Hz-sampled GPS time series
- Langbein, J., et al. 2006: Coseismic and initial postseismic deformation from the 2004 Parkfield, California, earthquake, observed by global positioning system, electronic distance meter, creepmeters, and borehole strainmeters

## P 1.13

# The role of phase distribution and reaction in an amphibolite facies ultramylonite

Kilian Rüdiger

*Geological Institute, Basel University, Switzerland, Bernoullistr. 32, 4056 Basel, (ruediger.kilian@unibas.ch)*

Rocks deforming by diffusion creep are usually characterized by a small grain size, an anti-correlated phase distribution and the lack of a crystallographic preferred orientation. The present study focuses on the role of bulk material transfer and reaction during homogeneous flow of an amphibolite facies ultramylonite.

The analyzed samples are from the Nordmannvik Nappe, Upper Allochthon of the Norwegian Caledonides. The shear zone separates a marble unit from a garnet amphibolite with enclosed relict mafic granulite lenses. Contacts with the wallrock are very sharp and no intermediately strained zone is present.

The ultramylonite matrix is composed of quartz, biotite, white mica, oligoclase and ilmenite with grain sizes below 10  $\mu\text{m}$  (eq. diameter) and has an extremely homogeneous microstructure. Grains have slightly lobate, interlocking boundaries. Aligned grain and phase boundaries are absent and shear bands are very rare.

Garnet, white mica and plagioclase-quartz aggregates form porphyroclasts. Towards the center of the shear zone, porphyroclasts disappear subsequently while garnet porphyroclasts are the last being present. The increase in matrix percentage from 80 to 98% is interpreted to result from increasing strain. White mica and plagioclase-quartz porphyroclasts attain aspect ratios of 2-3 while garnet remains at low aspect ratios. White mica porphyroclasts have monoclinic shapes and a stable orientation of the clast long axis at 5° with respect to the lineation, which is independent on strain and clast size. Plagioclase porphyroclasts have orthorhombic shapes and reach a stable orientation less frequently.

The matrix shows a strong anti-correlation of quartz clusters and biotite and white mica. Quartz clusters are separated by biotite stacks parallel to the foliation and by white mica perpendicular to the foliation. Those quartz clusters have a long axis at 50 -70° to the foliation, inclined against the sense of shear. Occasionally thin Fe-Ca-rich seams decorate quartz grain boundaries which are oriented at a low angle to the foliation.

Adjacent to porphyroclasts, the matrix homogeneity is locally disturbed. In the sector of instantaneous shortening around porphyroclasts, matrix biotite and plagioclase are depleted and garnet shows newly grown seams. In the sectors of instantaneous stretching, biotite and plagioclase grow and occasionally garnet porphyroclasts show signs of dissolution. Within less than 1mm, the homogeneity of the matrix is reestablished. Foliation parallel biotite is replaced by white mica during thinning of the mica aggregates and concurrently biotite grows adjacent to quartz grains in stacks perpendicular to the foliation. The anti-correlation of oblique quartz clusters and mica is the result of both processes.

The microstructures suggest that dissolution, replacement, nucleation and growth of matrix phases occur synkinematically and simultaneously. A cyclic reaction of garnet + white mica = plagioclase + biotite, driven by local gradients, can explain the observations.

## P 1.14

# Offsetting crustal and mantle neckings generates abandonment of continental rifts

Liao Jie<sup>1</sup>, & Gerya Taras<sup>1</sup>

<sup>1</sup> *Geophysical Fluid Dynamics, Institute of Geophysics, ETH Zurich, Zurich, Switzerland (jie.liao@erdw.ethz.ch)*

During continental extension, localized deformation can redistribute, and as a consequence, a new continental rift is generated offsetting from the previously formed rift that is abandoning. This phenomenon is called continental rifts jump, and the natural examples of continental rifts jump are globally distributed (Wood, 1983, Armitage et al., 2010, Yamasaki and Gernigon, 2010). The reasons why continental rifts jump remain elusive. Once deformation initiates in a pre-existing weakness (Dunbar J. A., 1988), whether deformation will concentrate in this area or migrate to a new location is determined by the competition between thermal diffusion (lithosphere strengthening) and thermal advection (lithosphere weakening) (Buck et al., 1999, Yamasaki and Gernigon, 2010). Slow extension corresponds to slow thermal advection and fast thermal diffusion, which favors lithosphere strengthening (England, 1983), and may generate the abandonment of intracratonic rifts (White, 1999). Numerical models suggest that the multi-phase rifting history [Armitage et al., 2010], migration of plume or thermal event (such as magma intrusion) (Yamasaki and Gernigon, 2010) are possible mechanisms that leads to the redistribution of deformation during extension.

Here, based on three-dimensional thermo-mechanical numerical models, we demonstrate that the formation of offsetting crustal and mantle neckings leads to the abandonment of continental rifts. Offsetting crustal and mantle neckings are naturally formed in the model employing crust-mantle-decoupled rheology and a crustal weak zone. Crustal weak zone controls the formation of the crustal necking and the initial continental rift in the early extension stage. Decoupled rheology determines the formation of mantle necking after a certain extension, which is offsetting from the crustal necking. The offsetting mantle necking becomes dominate and therefore governs a new continental rift development (from rifting, breakup to seafloor spreading), and as a consequence, the initial continental rift is abandoned.

## REFERENCES

- Armitage, J. J., Collier, J. S., & Minshull, T. A. 2010: The importance of rift history for volcanic margin formation. *Nature* 465, 913–917.
- Buck, W. R., Lavier, L. L., & Poliakov, A. N. B. 1999: How to make a rift wide. *Phil. Trans. R. Soc. Lond. A* 357, 671–693.
- Dunbar, J. A., & Sawyer, D. S. 1988: Continental rifting at pre-existing lithospheric weaknesses. *Nature* 333, 450–452.
- England, P. 1983: Constraints on extension of continental lithosphere. *J. Geophys. Res.* 88(B2), 1145–1152.
- White, R. S. 1999: The lithosphere under stress. *Phil. Trans. R. Soc. Lond. A* 357, 901–915.
- Wood, C. A. 1983: Continental rift jumps. *Tectonophysics* 94, 529–540.
- Yamasaki, T., & Gernigon, L. 2010: Redistribution of the lithosphere deformation by the emplacement of underplated mafic bodies: implications for microcontinent formation. *Journal of the Geological Society, London* 167, 961–971.

## P 1.15

## Deformation of the Sumatran, Chilean, and Japanese volcanic arcs after mega-thrust slips

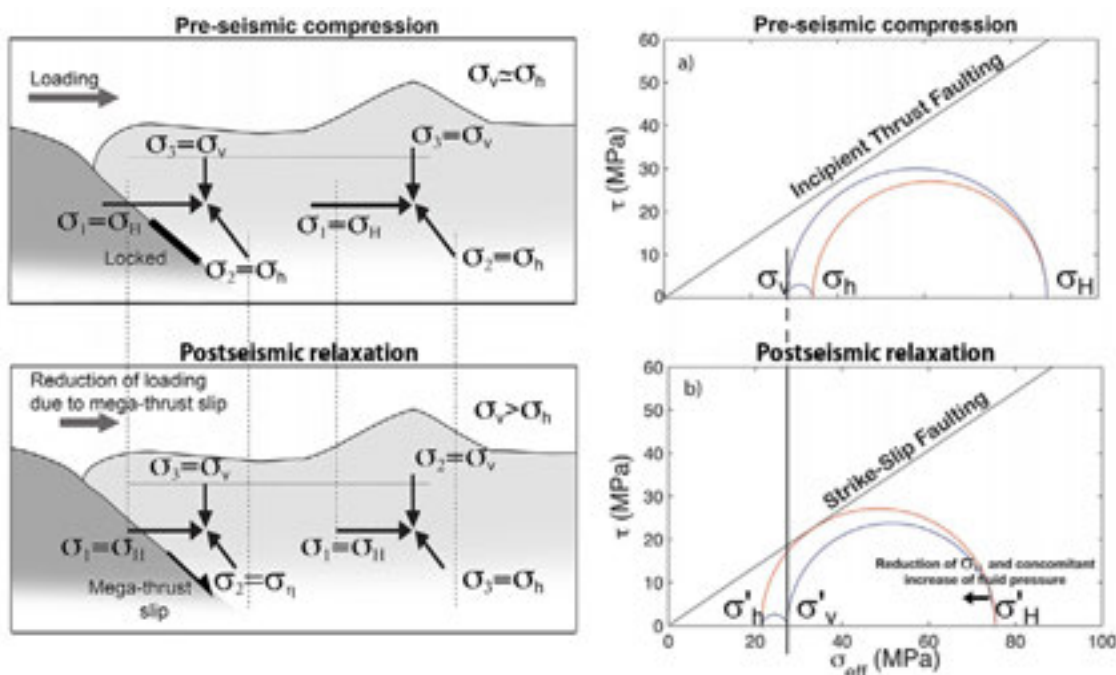
Lupi, M.<sup>1</sup>, Saenger, E.H.<sup>1</sup>, Fuchs, F.<sup>2</sup>, Miller, S.A.<sup>2</sup>

<sup>1</sup> ETH Zurich, Geological Institute, Sonneggstrasse 5, 8092, Zurich, CH

<sup>2</sup> Steinmann Institute, University of Bonn, Meckenheimer Allee 173, Bonn, DE

Eruptive rates in volcanic arcs increase significantly after subduction zone mega-thrust earthquakes. Over short time periods the response of the volcanic arc is attributed to the passage of seismic waves and almost-instantaneous subsidence of the volcanic system. A second peak of activity also occurs over decadal timescales but a kinematic mechanism that controls long-term pulses has yet to be proposed.

We conducted Coulomb stress transfer analyses to investigate the stress perturbations induced by five recent mega-thrust earthquakes (2005 M8.6, 2007 M8.5, and 2007 M7.9 Sumatra earthquakes; the 2010 M8.8 Maule, Chile earthquake; and the 2011 M9.0 Tohoku, Japan earthquake) and compared them with (large magnitude) shallow seismic activity occurring in the years that followed the mega-thrust slip. We use geomechanical, geological, and geophysical arguments to suggest that increased volcanic activity over longer timescales is due to a change of the local kinematics in the arc. More specifically, our study highlights a relaxation of the compressional regime that accompanies mega-thrust subduction zone earthquakes, which in turn promotes the reduction of the horizontal stress  $\sigma_h$ . This causes the occurrence of short-lived strike-slip kinematics and facilitates magma mobilization. Our results show that all, but one, the shallow earthquakes that occurred in the arcs of Sumatra, Chile and Japan have a marked lateral component. We suggest that the long-term volcanic response of the Sumatran, Chilean, and Japanese volcanic arcs will be manifested as predominantly strike-slip seismic events, that will be followed closely by seismic swarms, inflation, and other indications of a rising magma source.



## P 1.16

## Tectonic events predating the formation of the Jura fold-and-thrust belt: Constraints from cross section balancing

Malz Alexander<sup>1</sup>, Jordan Peter<sup>2</sup>, Meier Beat<sup>3</sup>, Madritsch Herfried<sup>4</sup>, Navabpour Payman<sup>1</sup> & Kley Jonas<sup>5</sup>

<sup>1</sup> Institute of Geosciences, Friedrich-Schiller-University Jena, Burgweg 11, D-07749 Jena (alexander.malz@uni-jena.de)

<sup>2</sup> Böhlinger AG, Mühlegasse 10, CH-4104 Oberwil

<sup>3</sup> Proseis AG Zürich, Schaffhauserstrasse 418, CH-8050 Zürich

<sup>4</sup> Nagra, Hardstraße 73, CH-5430 Wettingen

<sup>5</sup> Georg-August-Universität Göttingen, Geowissenschaftliches Zentrum, Goldschmidtstr. 3, D-37077 Göttingen

The deformation of the Jura fold-thrust-belt in the foreland of the Western Alps is widely accepted to be of a thin-skinned type (Laubscher 1961). Most folds and thrusts are considered to have been formed above a subhorizontal basal detachment (décollement) located in Middle to Upper Triassic evaporites. Especially, in the easternmost part of the Jura Mountains this décollement and the underlying pre-Mesozoic basement is locally dissected by Palaeozoic normal faults that were reactivated during the Tertiary subsidence of the Molasse basin (Diebold & Noack 1997). During the Mesozoic, the area of the future Jura fold-thrust-belt is widely considered to have witnessed a time of relative tectonic quiescence. This general view contrasts with sedimentological indications for differential subsidence (Allenbach 2002) and large scale analyses of the North-Alpine foreland (Ziegler 1990). The latter suggest extensional deformation during Jurassic up to Cretaceous times and a phase of transtension and compression during the Upper Cretaceous and Early Cenozoic.

Here we present a new interpretation of a recently reprocessed and depth migrated seismic reflection profile across the eastern Jura, which incorporates all available geological field and subsurface data and was verified by classical cross section balancing methods of equal bed length and constant area. Beside the restoration of the thin-skinned thrust stack we also explore the probable pre-thrusting tectonic evolution along the section.

Our results reveal thickness changes of Jurassic strata that could point toward a Middle Jurassic extensional deformation event. Moreover, thickness variations between the base of the Upper Jurassic and the discordance of the base of the Tertiary may suggest a second, contractional deformation event during Cretaceous-Palaeocene times, coinciding with a phase of transpression in the North Alpine foreland (Ziegler 1987) and erosion of up to 700 m of Cretaceous strata prior to the Molasse sedimentation (Mazurek et al. 2006).

### REFERENCES

- Allenbach, R.P. 2002: The ups and downs of "Tectonic Quiescence" - recognizing differential subsidence in the epicontinental sea of the Oxfordian in the Swiss Jura Mountains. *Sedimentary Geology*, 150, 323-342
- Diebold, P. & Noack, T. 1997: Late Paleozoic troughs and Tertiary structures in the eastern Jura. In: Heitzmann, P. & Lehner, P. (eds.): *Deep structures of the Swiss Alps*. Birkhäuser Verlag, Basel.
- Laubscher, H. 1961: Die Fernschubhypothese der Jurafaltung, *Eclogae Geol. Helv.*, 54, 222 – 282.
- Mazurek, M., Hurford, A.J. & Leu, W. 2006: Unravelling the multi-stage burial history of the Swiss Molasse Basin: Integration of apatite fission track, vitrinite reflectance and biomarker isomerisation analysis, *Basin Research*, 18, 27-50.
- Ziegler, P.A. 1987: Late Cretaceous and Cenozoic intra-plate compressional deformation in the Alpine Foreland – a geodynamic model, *Tectonophysics*, 137, 389-420.
- Ziegler, P.A. 1990: *Geological Atlas of Western and Central Europe*. Shell Internationale Petroleum Maatschappij, Den Haag.

## P 1.17

# Semi-brittle deformation of fault rocks - an experimental study of the brittle-to-viscous transition in mafic rocks

Sina Marti<sup>1</sup>, Renée Heilbronner<sup>1</sup>, Holger Stünitz<sup>2</sup>

<sup>1</sup> Department of environmental sciences, Geological institute, University of Basel, Bernoullistr. 32, 4056 Basel (sina.marti@unibas.ch)

<sup>2</sup> Department of Geology, University of Tromsø, Dramsveien 201, Tromsø Norway

In order to investigate the brittle-viscous transition in mafic rocks, a series of rock deformation experiments is carried out – here we report the first results.

The experiments are performed using a modified Griggs-type solid-medium apparatus at confining pressures of  $P_c = \sim 0.5$  GPa and  $\sim 1.0$  GPa, temperatures,  $T$ , between  $300^\circ\text{C}$  and  $700^\circ\text{C}$  and shear displacement rates of  $\dot{d} = \sim 10^{-8}$   $\text{ms}^{-1}$  and  $\sim 10^{-7}$   $\text{ms}^{-1}$  along the  $45^\circ$  precut (inducing shear strain rates of  $\dot{\gamma} = \sim 10^{-5}$   $\text{s}^{-1}$  and  $\sim 10^{-4}$   $\text{s}^{-1}$  in the fault rock). The starting material is crushed Maryland diabase sieved to a grain size  $< 125$   $\mu\text{m}$ , with a composition of  $\sim 57\%$  Plg,  $33\%$  Cpx,  $8\%$  Opx, and  $2\%$  accessories (apatite, Kfs, Qtz, ilmenite, magnetite and biotite).

The peak stress,  $\tau_{\text{max}}$ , and the steady state shear stress,  $\tau_{\text{flow}}$  of the fault rock show both a temperature and a pressure dependence:

- At confining pressures, of  $\sim 1$  GPa and  $T=300^\circ\text{C}$ ,  $\tau_{\text{max}} \approx 1.4$  GPa and  $\tau_{\text{flow}} \approx 1.2$  GPa; at  $T=700^\circ\text{C}$ ,  $\tau_{\text{max}} \approx 0.7$  GPa and  $\tau_{\text{flow}} \approx 0.6$  GPa.
- At confining pressures, of  $\sim 0.5$  GPa and  $T=300^\circ\text{C}$ ,  $\tau_{\text{max}} \approx 1.1$  GPa and  $\tau_{\text{flow}} \approx 1.05$  GPa; at  $T=700^\circ\text{C}$ ,  $\tau_{\text{max}} \approx 0.5$  GPa and  $\tau_{\text{flow}} \approx 0.25$  GPa.

At  $P_c = \sim 0.5$  GPa and  $\dot{d} = \sim 10^{-8}$   $\text{ms}^{-1}$ , the stress-strain curves show the same initial slope for all  $T$ . With increasing shear stress,  $\tau$ , the curves start to deviate from the initial slope indicating the beginning of yielding with a lower slope until peak stress values,  $\tau_{\text{max}}$ , are reached. After the  $\tau_{\text{max}}$ , the rocks weaken to a steady state shear stress,  $\tau_{\text{flow}}$ . Despite the initial congruency of the stress-strain curves at all temperatures, the shear stresses at yielding and the peak stresses decrease with increasing  $T$ .

Microstructural observations show that at  $T=300^\circ\text{C}$ , a strong foliation develops due to the formation of pervasive micro shear-fractures in Riedel shear orientation. Prominent slip-zones of approx.  $10$  to  $20$   $\mu\text{m}$  in thickness form; they contain highly comminuted material and display flow structures and small scale folding. With increasing  $T$ , micro-fracturing decreases and the slip-zones become less prominent. At  $T > 500^\circ\text{C}$ , solution and precipitation microstructures are observed, like the dissolution of Ca-depleted exsolution lamellae in pyroxene and healing of fractures in plagioclase and more Ca-rich pyroxene.

So far we conclude that the dominating processes that accumulate strain are fracturing and granular flow. The pressure dependence of strength is interpreted to indicate the influence of friction on deformation. The strong sensitivity to temperature is not yet well understood and needs further investigations.

## P 1.18

# A scalable, parallel matrix-free Stokes solver for geodynamics applications

Dave A. May<sup>1</sup>

<sup>1</sup> Institute of Geophysics, ETH Zurich, Sonneggstrasse 5, CH-8092 Zurich ([dave.may@erdw.ethz.ch](mailto:dave.may@erdw.ethz.ch))

Here I describe a numerical method suitable for studying non-linear, large deformation processes in crustal and lithospheric dynamics. The method utilizes a hybrid spatial discretisation which consists of mixed finite elements for the Stokes flow problem, coupled to a Lagrangian marker based discretisation to represent the material properties (viscosity and density). This approach is akin to the classical Marker-And-Cell (MAC) scheme of Harlow and the subsequently developed Material Point Method (MPM) of Sulsky and co-workers. The geometric flexibility and ease of modelling large deformation processes afforded by such mesh-particle methods has been exploited by the lithospheric dynamics community over the last 20 years.

The strength of the Stokes preconditioner fundamentally controls the scientific throughput achievable and represents the largest bottleneck in the development of our understanding of geodynamic processes.

The possibility to develop a “cheap” and efficient preconditioning methodology which is suitable for the mixed Q2-P1 element is explored here. I describe a flexible strategy, which aims to address the Stokes preconditioning issue using an upper block triangular preconditioner, together with a geometric multi-grid preconditioner for the viscous block. The key to the approach is to utilize algorithms and data-structures that exploit current multi-core hardware and avoid the need for excessive global reductions. In order to develop a scalable method, special consideration is given to; the definition of the coarse grid operator, the smoother and the coarse grid solver.

The performance characteristics of this hybrid matrix-free / partially assembled multi-level preconditioning strategy is examined. The robustness of the preconditioner with respect to the viscosity contrast and the topology of the viscosity field, together with the parallel scalability is demonstrated.

## P 1.19

# Detrital zircon and provenance analysis on the onshore Makran accretionary wedge, SE Iran: implication for the geodynamic setting

Mohammadi Ali<sup>1</sup>, Winkler Wilfried<sup>1</sup>, Burg Jean-Pierre<sup>1</sup>, Ruh Jonas<sup>1</sup>, Von Quadt Albrecht<sup>1</sup>

<sup>1</sup> Geological Institute, ETH-Zurich, Sonneggstrasse 5, CH- 8092 Zürich

The Makran, located in Southeast Iran and South Pakistan, is one of the largest accretionary wedges on Earth. In Iran it comprises turbiditic sediments ranging in age from Late Cretaceous to Holocene. We present a provenance analysis on sandstones, which is aimed at reconstructing the assemblages of source rocks and the tectonic setting from which the clastic material was derived. Sandstone samples collected from different units span the regional stratigraphy from Late Cretaceous to Miocene.

Laser ablation ICP-MS resulted in ca 2800 new U-Pb ages of individual detrital zircons from 18 samples collected in onshore Makran. 101 detrital zircons from a Late Cretaceous fine grained sandstone range from 180 to 160 Ma (Middle Jurassic). 478 detrital zircons from mid- to late Eocene sandstones allow differentiating a NE and NW sector of the Makran Basin. Zircon grains in the NE basin belong to two populations peaking at 180 to 160 Ma (late Early to Middle Jurassic) and 50 to 40 Ma (Mid-Eocene), with the noticeable absence of Cretaceous grains. In the NW basin, detrital zircons are 120 to 40 Ma (late Early Cretaceous to Lutetian, Eocene). 587 detrital zircon grains from fine to medium grained Oligocene sandstones collected over the whole area also range from 120 to 40 Ma (late Early Cretaceous to Eocene, Lutetian). 1611 detrital zircons from early Miocene sandstones show again distinctly different ages in the eastern and western parts of the basin. They range from 120 to 40 Ma (late Early Cretaceous to Eocene) in the eastern and from 80 to 40 Ma (Late Cretaceous to Eocene) in the western basin.

Hf isotopes analyses were performed on 120 zircon grains from 6 samples. Negative values (-2 to -15) in Middle Jurassic and late Early Cretaceous zircons indicate minor or no influence of mantle reservoirs which implies a rifting setting during crystallization of the zircons. Low negative to positive (-5 to +10) values in Late Cretaceous and Eocene zircons indicate mixed crustal and juvenile magma sources, which are common in continental arc environments.

Point counts of 32 sandstone thin sections were performed following the Gazzi-Dikinson method. 300-400 points were counted in each thin section. The sandstones are feldspathic litharenites and litharenites. Feldspar is dominantly plagioclase (> 90%) with minor amounts of K-feldspar. Most quartz grains (75%) are mono-crystalline but poly-crystalline ones (maximum 25%) occur. Rock fragments are represented by sedimentary, volcanic and metamorphic grains. Volcanic rock-fragments mostly are andesites and volcanic chert. Sedimentary lithic grains comprise mostly sandstone, siltstone, limestone and dolomite. Metamorphic lithic grains generally are low-grade schists and phyllites. In various compositional ternary diagrams, the sources of the sandstones plot in the transitional to dissected arc and recycled orogenic fields.

We selected 26 samples for heavy mineral study. 200-300 grain were identified and counted in each sample. Heavy mineral suites show a highly variable composition including (1) a group of ultra-stable minerals (zircon, monazite, tourmaline, rutile, brookite, anatase and sphene) derived from a granitic continental crust sources, (2) metastable minerals delivered from variable metamorphic-grade source rocks (epidote group, garnet, staurolite, chloritoid, kyanite, andalusite, glaucophane), (3) chromian spinel from ultrabasic rocks, (4) common hornblende either supplied from metamorphic or basic igneous series, and (5) a local pyroxene-rich source in the pyroclastic sandstone formation overlying pillow lavas. Glauco-phane (5-20%) occurs in several samples, which indicates high-pressure/low-temperature metamorphic rocks in the detrital source areas for Eocene and Miocene sandstones.

Earlier work in the Pakistani Makran suggested that pre-Miocene sediments were supplied from the Himalaya, whereas Miocene to Recent deposits were reworked older sediments of the accretionary wedge. Our data do not support this conclusion. Instead, we identified rifting-related detrital sources from Middle Jurassic to late Early Cretaceous (175 - 100 Ma) and the establishment of a continental volcanic arc from Late Cretaceous to Eocene (80 to 40 Ma). In addition, paleocurrent directions in Makran sandstone show general sediment transport from North to South; Cr-spinel as well as high-P/low-T heavy minerals most likely have been derived from the blueschist-bearing Makran ophiolitic and igneous belt to the North.

**P 1.20****Metamorphic conditions and exhumation of the Keshebir-Kardamos dome – Rhodope Metamorphic Complex (Greece-Bulgaria)**Moulas Evangelos<sup>1</sup>, Burg Jean-Pierre<sup>1</sup>, Kostopoulos Dimitrios<sup>2</sup>, Schenker Filippo<sup>1</sup> & Chatzitheodoridis Elias<sup>3</sup><sup>1</sup> Department of Earth Sciences, ETH-Zurich, Sonneggstrasse 05, CH-8092 Zurich (evangelos.moulas@erdw.ethz.ch)<sup>2</sup> Department of Mineralogy and Petrology, University of Athens, Panepistimioupoli Zographou, 15784, Athens, Greece<sup>3</sup> School of Mining and Metallurgical Engineering, National Technical University of Athens, Heroon Polytechniou 9, 15780, Athens, Greece

The Rhodope Metamorphic Complex (RMC) in northern Greece and southern Bulgaria is a synmetamorphic nappe pile that developed during the Alpine-Himalayan orogen. The nappe system is deformed and forms dome-and-basin structures that indicate syn- to post-convergent exhumation. High-pressure rocks showing variable degrees of retrogression occur in the intermediate imbricate units including eclogites and micro-diamond-bearing paragneisses. We document the deformation style and present new thermobarometric and geochronological constraints for the Keshebir-Kardamos dome in the eastern RMC in an attempt to comprehend the major mechanisms involved in the exhumation of high-pressure (HP) and high-temperature (HT) rocks.

The studied high-grade metamorphic rocks from the intermediate thrust sheets of the core of the Kardamos dome are broadly subdivided into two compositional groups: a) typical Ca-poor pelites and b) calcsilicate lithologies. For the Ca-poor compositions, thermodynamic modelling using phase diagram sections in the NCKFMMnASHT (Na<sub>2</sub>O-CaO-K<sub>2</sub>O-FeO-MgO-MnO-Al<sub>2</sub>O<sub>3</sub>-SiO<sub>2</sub>-H<sub>2</sub>O-TiO<sub>2</sub>) model system suggests peak conditions at 1.2 GPa and ca. 750°C. Garnet-clinopyroxene thermometry combined with Raman barometry applied on quartz inclusions in garnets from the calcsilicate lithologies corroborate the above calculations within 0.1GPa (i.e. 1.3 GPa and ca. 750°C). Thin chlorite and biotite selvage replacing garnets along cracks and minor albite replacing more calcic plagioclase document minor greenschist-facies retrogression. U-Pb SHRIMP dating of zircons from the metapelites reveals Early Cretaceous (144 Ma) as the time of the major metamorphic overprint whereas some zircon rims yield reset ages at Eocene times (53 and 44 Ma).

Kinematic indicators from the imbricate units suggest a continuum from ductile to brittle conditions during exhumation. The exhumed high-grade rocks were covered by marine sediments soon after their exhumation (Lutetian-Priambronian?). Slumps in sediments suggest that sedimentation took place in a tectonically active environment. Our new structural, petrological and geochronological data suggest that the major shear zone in the core of the Keshebir-Kardamos dome is equivalent to the Nestos-Chepelare suture zone.

**P 1.21****Assessment of mercury distribution in sediments, soil, fish and human hair sampled in gold mining areas in the Gambia River Basin at Kedougou, southeastern Senegal**Niane Birane<sup>1</sup>, Moritz Robert<sup>1</sup>, Guédron Stéphane<sup>2</sup>, Poté John<sup>1</sup>, Ngom Papa Malick<sup>3</sup>, Pfeifer Hans Ruedi<sup>4</sup><sup>1</sup> Section des sciences de la Terre et de l'Environnement, Université de Genève, Rue des Maraîchers 13, 1205 Genève<sup>2</sup> Institut des sciences de la Terre Université Joseph Fourier, F-38041, Grenoble, France<sup>3</sup> Département de géologie, Université de Cheikh Anta DIOP, Dakar, Sénégal<sup>4</sup> Institut des sciences de la Terre, Université de Lausanne, Géopolis 3871, Lausanne

Little information is available on the impact of mercury (Hg) from artisanal small-scale gold mining (ASGM) in environmental compartments, and neither is there much information regarding the assessment and potential impact of Hg in biota and human health in Sub-Saharan Africa, especially in the Kedougou region, southeastern Senegal.

The Kedougou inlier is interpreted as an accretion of north-easterly trending Birimian age volcanic terrains. There are two types of gold mineralization: alluvial gold and gold-bearing quartz veins hosted by shear zones. Approximately 30,000-60,000 persons are involved since about 1995 in ASGM activities spread across several villages. This study has been under-

taken to assess the impact of ASGM in different sites of the Kedougou region. The assessment was based on the determination of Hg contents in sediment and soil profiles, in various fish species and human hairs collected in the region.

The total Hg (THg) concentration from different samples was obtained using an AMA-254 mercury analyzer (Atomic Absorption Spectrometry). The accuracy of measurements was checked by analyzing the reference material MESS- 3 (National Water Research Institute, Canada) in between every third sample. Enrichment factors were used to classify the sampling sites according to their degree of contamination.

The results indicate that sediments and soils from the active ASGM sites have high levels of THg in contrast to reference sites. The comparison of THg sediment concentrations at different sites with the values of sediment quality guideline shows that the main active ASGM sites present concentrations of Hg higher than standard recommended values. The THg concentrations range from 0.14 to 1.6 mg/kg in fish species, exceeding WHO standard recommendations of 0.5 mg/kg in piscivorous fish. THg concentrations in hair range between 0.10 and 7.67 mg/kg, with 5 mg/kg being the maximum concentration recommended by WHO. The results of this study demonstrate that ASGM in the Kedougou region are potential environmental and human hazards.

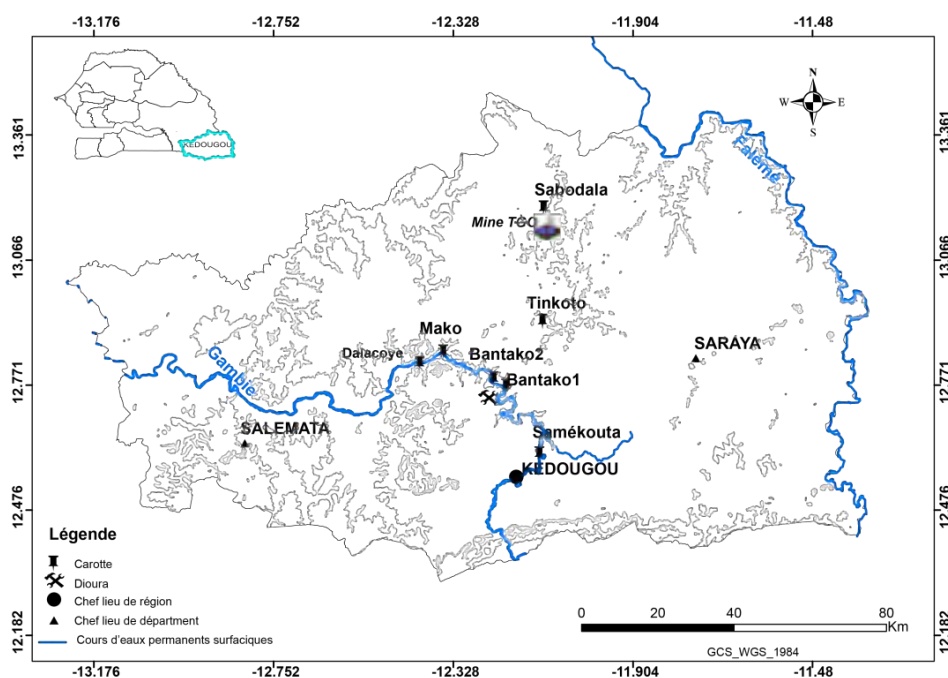


Figure 1: Sampling locations in the Kedougou study area eastern Senegal

## REFERENCES

- Bassot, J. P. (1997). Albitisations dans le Paléoprotérozoïque de l'Est du Sénégal: relations avec les minéralisations ferrifères de la rive gauche de la Falémé. *Journal of African Earth Sciences* 25: 353-367.
- Donkor, A. K. et al. (2006). Mercury in different environmental compartments of the Pra River Basin, Ghana. *Science of The Total Environment* 368: 164-176.
- Kainz, M. and M. Lucotte (2002). Can flooded organic matter from sediments predict mercury concentrations in zooplankton of a perturbed lake? *Science of The Total Environment* 293: 151-161.
- Katner, A., et al. (2010). An evaluation of mercury levels in Louisiana fish: Trends and public health issues. *Science of The Total Environment* 408: 5707-5714.
- MacDonald, D. D. et al. (2000). Development and Evaluation of Consensus-Based Sediment Quality Guidelines for Freshwater Ecosystems. *Archives of Environmental Contamination and Toxicology* 39: 20-31.
- van Straaten, P. (2000). Mercury contamination associated with small-scale gold mining in Tanzania and Zimbabwe. *The Science of The Total Environment* 259: 105-113.

## P 1.22

# Single Viscous Layer Fold Interplay And Linkage: A 3d-Fem Modelling Approach

Philippe Thomas A.<sup>1</sup>, Frehner Marcel<sup>2</sup>, May Dave A.<sup>1</sup>

<sup>1</sup>Institute of Geophysics, ETH Zurich, Sonneggstrasse 5 CH - 8092 Zurich (thomas.philippe.74@gmail.com)

<sup>2</sup>Geological Institute, ETH Zurich, Sonneggstrasse 5 CH - 8092 Zurich

Recent fieldwork observations and numerical experiments have demonstrated that large fold-belt systems do not necessarily grow uniformly in a cylindrical manner but arise from the lateral connection (parallel to the fold axis) of smaller embryonic folds (Bretis et al., 2011). The mechanical feasibility of the linkage of two isolated embryonic folds has already been studied (Grasemann and Schmalholz 2012). In this context, the mechanical feasibility of the fork-linkage or more generally the triple-linkage (three isolated embryonic folds linking laterally together, Figure 1) is studied using the pTatin3d code<sup>1</sup> (May et al., 2013). To address this issue, a template for modelling the triple-linkage is introduced, which consists of a solitary embryonic fold opposite to a binary perturbation.

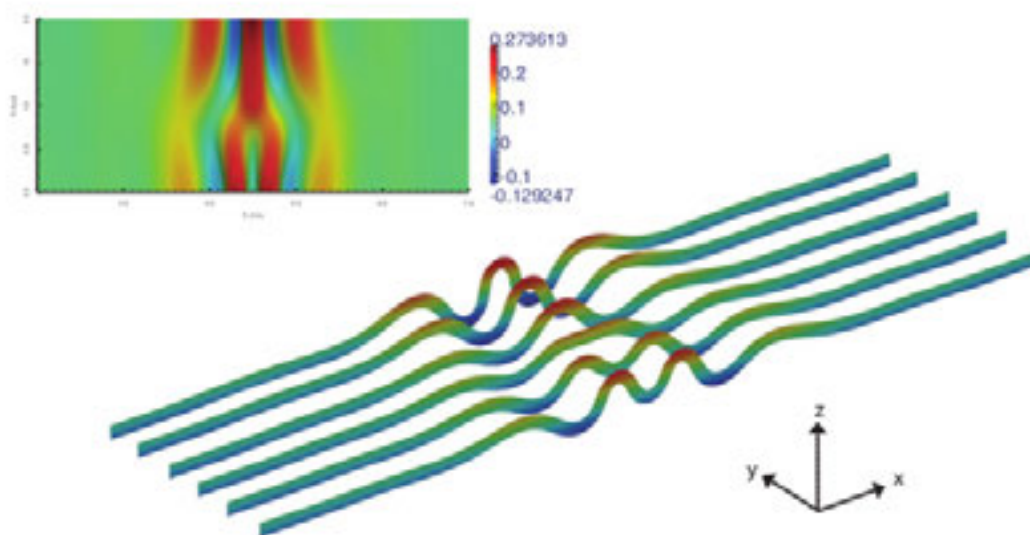


Figure 1: Triple-linkage: slices of a fork-structure. At the junction, we observe clearly a double hinge fold section with a flat topography. The colours indicate the relative topography.

A new terminology stemming from the observed patterns is introduced and a phase diagram highlighting the various linkage structures as a function of the geometric parameters is presented.

The folding and linkage process is tackled considering the vorticity field

$$\omega = \frac{1}{2} \nabla \times u,$$

where  $u$  is the velocity field. It turns out to be a very interesting and fruitful framework that makes the linkage patterns and embryonic fold interplays simple to understand. Based on the 3D analytical solution for the finite amplitude folding of a single viscous layer embedded in a matrix (Fletcher 1991), the planar-vorticity dominant wavelength (in the viscous layer plane) is computed numerically. This planar-vorticity dominant wavelength turns out to be distinct from the dominant amplification wavelength and it appears to be the characteristic length controlling the linkage process. In the light of these observations, a new interpretation and explanation is given for the simple-linkage previously studied and the perspectives for the general case are proposed.

<sup>1</sup>The pTatin3d code has been developed by D.A. May to model 3D-multiphase Stokes flows for geodynamical applications.

## REFERENCES

- Bretis, B., Bartl, N., and Grasemann, B. 2011. Lateral fold growth and linkage in the Zagros fold and thrust belt (Kurdistan, NE Iraq). *Basin Research*, 23(6), 615-630.
- Fletcher, R. C. 1991. Three-dimensional folding of an embedded viscous layer in pure shear. *Journal of Structural Geology*, 13(1), 87-96.
- Grasemann, B. and Schmalholz, S. M. 2012. Lateral fold growth and fold linkage. *Geology*, 40(11), 1039-1042.
- May, D. A., Brown, J. and Le Pourhiet, L. 2013. A scalable, matrix-free Stokes discretisation for geodynamic applications, to be submitted to *Computational Methods in Applied Mechanics and Engineering*.

## P 1.23

## Geomorphology approach in karstic domain: importance of underground water.

Rabin Mickaël<sup>1</sup>, Sue Christian<sup>1</sup>, Champagnac Jean-Daniel<sup>2</sup> & Eichenberger Urs<sup>3</sup>

<sup>1</sup> Chrono-environnement Laboratory, UMR 6249. University of Franche-Comté, 16 route de Gray 25000 Besançon. France (mickael.rabin@univ-fcomte.fr) (christian.sue@univ-fcomte.fr)

<sup>2</sup> Geologisches Institut. ETH-Zürich Sonneggstrasse 5 8092 Zürich. Switzerland (jean-daniel.champagnac@erdw.ethz.ch)

<sup>3</sup> ISSKA, 68 rue de la Serre CH-2301 La Chaux-de-Fonds. Switzerland (urs.eichenberger@isska.ch)

The Jura mountain belt is the westernmost and one of the most recent expressions of the Alpine orogeny. The Jura has been well studied from a structural point of view, but still remains the source of scientific debates, especially regarding its current and recent tectonic activity [Laubscher, 1992; Burkhard et Sommaruga, 1998]. It is deemed to be always in a shortening state, according to old leveling data [Jouanne et al., 1998] and neotectonic observations on paleo-meanders of the Doubs river [Madritsch et al., 2010]. However, the few GPS data available on the Jura don't show evidence of shortening, but a small extension parallel to the arc [Walpersdorf et al., 2006]. Moreover, the traditionally accepted assumption of a collisional activity of the Jura raises the question of its geodynamic origin. The Western Alps are themselves in a post-collisional regime and characterized by a noticeable isostatic-related extension, due to the interaction between buoyancy forces and external dynamics [Sue et al., 2007].

Quantitative morphotectonic approaches are increasingly used in active mountain belt to infer relationship between climate and tectonics [Whipple, 2009]. In this study we propose to apply these tools to calcareous bedrock, in a slowly deformed mountain belt. We have used, in particular, watersheds analysis and associated rivers profiles which allow quantifying the degree and the nature of the equilibrium between the tectonic forcing and the fluvial erosional agent [Kirby and Whipple, 2001]. Slope profiles of rivers are controlled by climatic and tectonic forcing through the expression [Whipple and Tucker, 1999]:

$$S = (U / K)^{1/n} A^{m/n}$$

(with U: uplift rate, K: empirical erodibility factor, function of hydrological and geological settings; A: drained area, m, n: empirical parameters).

We present here a systematic study of these profiles applied to most of the Jura rivers. First results show several abnormal signals along main rivers; for the Ain river for example, anthropogenic dams aren't always pointed, or, for the Loue river, water flow are strongly under-estimated because its spring is a karstic one. These problems are due to several factors; 1) the chemical erosion process of limestone which is, combined with classical mechanical process, more efficient and faster than erosion processes on granitic or metamorphosed bedrock, and 2) karstic losses and outlets which strongly modify water flow. The complexity of the karst system doesn't allow us to properly quantify the flow.

This study highlights the importance of underground water and the rapid chemical erosion process in a karstic domain. For further study, now we work in speleology and karstology with a structural point of view. This structural study is coupled with a morphological study of oxbows and watergap, in order to characterize the recent tectonic evolution of the Jurassic arc.

## REFERENCES:

- Burkhard, M. and Sommaruga, A., 1998. Evolution of the western Swiss Molasse basin: structural relations with the Alps and the Jura belt. In: Cenozoic Foreland Basins of Western Europe. (A. Mascle, C. Puidgefabregas, H. P. Luterbacher and M. Fernandez eds), Geol.Soc. Spec. Publ. 134, 279-298.
- Jouanne, F., Genaudeau, N., Menard, G., Darmendrail, X., 1998. Estimating present-day displacement fields and tectonic deformation in active mountain belts: an example from the Chartreuse Massif and the southern Jura Mountains, western Alps. *Tectonophysics* 296, 403–419.
- Kirby, E., Whipple, K., 2001. Quantifying differential rock-uplift rates via stream profile analysis. *Geology* 29, 415–418.
- Laubscher, HP., 1992. Jura kinematics and the Molasse basin, *Eclogae Geol. Helv.* (85), 287-303
- Madritsch, H., Fabbri, O., Hagedorn, E.-M., Preusser, F., Schmid, S.M., Ziegler, P.A., 2010. Feedback between erosion and active deformation: geomorphic constraints from the frontal Jura fold-and-thrust belt (eastern France). *INTERNATIONAL JOURNAL OF EARTH SCIENCES* 99, S103–S122.
- Sue, C., Delacou, B., Champagnac, J.-D., Allanic, C., Tricart, P., Burkhard, M., 2007. Extensional neotectonics around the bend of the Western/Central Alps: an overview. *International Journal of Earth Sciences* 96, 1101–1129.
- Walpersdorf, A., Baize, S., Calais, E., Tregoning, P., Nocquet, J.-M., 2006. Deformation in the Jura Mountains (France): First results from semi-permanent GPS measurements. *Earth and Planetary Science Letters* 245, 365–372.
- Whipple, K.X., Tucker, G.E., 1999. Dynamics of the stream-power river incision model: Implications for height limits of mountain ranges, landscape response timescales, and research needs. *J. Geophys. Res.-Solid Earth* 104, 17661–17674.

**P 1.24****The effect of hot-pressing on the grain size distribution and microstructure of quartz gouge along the brittle-to-viscous transition in shear experiments**

Bettina Richter<sup>1</sup>, Rüdiger Kilian<sup>1</sup>, Holger Stünitz<sup>2</sup> & Renée Heilbronner<sup>1</sup>

<sup>1</sup> Geological Institute, University of Basel, Bernoullistrasse 32, CH-4056 Basel (bettina.richter@unibas.ch)

<sup>2</sup> Department of Geology, University of Tromsø, Dramsveien 201, N-9037 Tromsø

We conducted a series of shear experiments on quartz gouge in a Griggs-type solid medium deformation apparatus to investigate the brittle to viscous transition. The samples were deformed at high confining pressures of ~1.5 GPa at temperatures between 500 °C and 1000 °C at constant shear strain rates of ~5×10<sup>-5</sup> s<sup>-1</sup>. The starting material is produced by crushing a quartz single crystal (resulting grain size <100 μm) and adding 0.2 wt% water.

First results show a decrease of the strength of the sample with increasing temperatures. Continued deformation indicates steady-state stress for the high-temperature experiments and strain hardening for lower temperatures. The grain sizes distribution of the low-temperature experiments is similar to the initial grain size distribution before deformation. With increasing temperatures the size and volume portion of the larger grains decreases while the portion of recrystallized grains increases. The crystallographic preferred orientation (CPO) of the c-axis evolves with increasing temperature from a random distribution towards (1) two elongated maxima rotated antithetically with respect to the shear sense or (2) a single y-maximum. With increasing shear strain the elongated maxima rotate with shear direction.

Some of the experiments included a hot-pressing stage (20 h at 1000 °C/~1.5 GPa) in the apparatus before the temperature was decreased to the conditions of deformation. The resulting maximum shear stresses of those experiments are significantly lower (~50 %) than those without the hot-pressing stage. In contrast, the CPO of the hot-pressed samples is similar to the samples without hot pressing at the same deformation temperature. The grain size distribution of the hot-pressed and deformed samples covers a smaller range compared to that without hot-pressing. Obviously, a size reduction of the larger grains as well as the growth of the smaller grains during the hot-pressing results in a narrower grain size distribution.

We conclude that the material with the narrower grain size distribution has a more quartzite-like behaviour, whereas the material without hot pressing behaves more like a heterogeneous fault gouge of clasts and matrix with different material properties. Thus, a fault gouge may evolve towards a homogeneous quartzite at moderate temperatures in natural rocks over extended periods of time (hot-pressing may simulate normal healing or fluid-rock interaction in nature). In addition, dynamic recrystallisation of cataclastic material or quartzite produces the same finite microstructures and we conclude that former brittle deformation can merge into plastic flow and recrystallisation.

## P 1.25

### Convection and grain size evolution in mantle and lithosphere of the Earth

Rozel Antoine, Tackley Paul

*Institut für Geophysik, Geophysical Fluid Dynamics, ETH Zurich, Sonneggstrasse 5, 8092 Zurich*

The physical mechanisms responsible for localisation of deformation in the lithosphere of the Earth remains largely misunderstood. Since very reduced grain sizes are often observed in faults and large scale shear zones, grain size is largely suspected to have an important influence on the generation of plate tectonics. Most of the grain size evolution laws derived up to now have failed to generate mature and self-sustained lithospheric shear zones in numerical computations of mantle convection. Yet, recent developments of a new physical approach of grain size reduction have shown that self-consistent plate tectonics is at hand if two-phase grain size distributions are considered instead of a single average grain size.

We present a set of numerical simulations of mantle convection including this new physical approach of two phase grain size evolution. We consider a composite rheology mixing diffusion, dislocation and grain-boundary sliding creep. This approach involving a large set of poorly constrained parameters, we only investigate the impact of grain size-dependent quantities in a reference model kept constant. Preliminary results are discussed.

## P 1.26

### Relationship between tectonic overpressure, deviatoric stress, driving force, isostasy and gravitational potential energy

Schmalholz Stefan<sup>1</sup>, Medvedev Sergei<sup>2</sup>, Lechmann Sarah<sup>3</sup> & Podladchikov Yuri<sup>1</sup>

<sup>1</sup> *Institut of Earth Sciences, University of Lausanne, Switzerland (stefan.schmalholz@unil.ch)*

<sup>2</sup> *Centre for Earth Evolution and Dynamics, University of Oslo, Norway*

<sup>3</sup> *Geological Institute, ETH Zurich, Switzerland; now at: armasuisse, Federal Department of Defence, Civil Protection and Sport, Switzerland*

We present analytical derivations and two-dimensional numerical simulations that quantify magnitudes of deviatoric stress and tectonic overpressure (i.e. difference between the pressure, or mean stress, and the lithostatic pressure) which arise due to variations in the gravitational potential energy (GPE). We consider a simple situation with lowlands and mountains (plateau), and a model lithosphere consisting of a crust with higher linear viscosity than the mantle. Our results (1) explain why estimates for the magnitude of stresses in Tibet, previously published by different authors, vary by a factor of two, (2) are applied to test the validity of the thin-sheet approximation, (3) show that the magnitude of the depth integrated tectonic overpressure is equal to the magnitude of the depth integrated deviatoric stress if depth integrated shear stresses within the lithosphere are negligible, and (4) show that tectonic overpressure is required to build and support continental plateaus such as in Tibet or in the Andes. The prediction of tectonic overpressure associated with GPE differences is independent of rock rheology (e.g. viscous or elastic) and rock strength. We also discuss the mechanical conditions that are necessary to achieve isostasy (i.e. the lithostatic pressure is constant) at a certain depth. The results show that tectonic overpressure can exist at a certain compensation depth although all deviatoric stresses are zero at this depth, because this tectonic overpressure is related to horizontal gradients in a force per unit length resulting from shear stresses integrated vertically across the entire lithosphere. The existence of tectonic overpressure implies that the pressure estimated from observed mineral assemblages is likely not equal to the lithostatic pressure, and pressure is not directly related to depth. However, lithostatic pressure-depth conversions, neglecting overpressure, are frequently applied in the reconstruction of the tectonic evolution of mountain ranges.

## P 1.27

# Exploring feldspar IRSL-50 as a low-temperature thermochronometer: insights from field applications (Alaska, Norway and Pamir)

Pierre G. Valla<sup>1,2</sup>, Sally E. Lowick<sup>3</sup>, Frédéric Herman<sup>2</sup>, Jean-Daniel Champagnac<sup>1</sup>, Benny Guralnik<sup>1</sup>, Philippe Steer<sup>4</sup>, Jie Chen<sup>5</sup> & Jintang Qin<sup>5</sup>

<sup>1</sup>. Geological Institute, ETH Zürich, Sonneggstrasse 5, CH-8092 Zürich  
([pierre.valla@erdw.ethz.ch](mailto:pierre.valla@erdw.ethz.ch))

<sup>2</sup>. Institute of Earth Sciences, University of Lausanne, Géopolis, CH-1015 Lausanne

<sup>3</sup>. Institute of Geology, University of Bern, Baltzerstrasse 1+3, CH-3012 Bern

<sup>4</sup>. Géosciences Rennes, Université de Rennes 1, 263 Avenue du Général Leclerc, F-35700 Rennes

<sup>5</sup>. State Key Laboratory of Earthquake Dynamics, China Earthquake Administration, C-100029 Beijing

Quartz luminescence dating has shown great potential in low-temperature thermochronometry (e.g. Herman et al., 2010) and has opened a new spatial and temporal “window” to study late stages of rock exhumation. Even though quartz OSL dating appears a suitable candidate (e.g. Li and Li, 2012), quartz separates from bedrock often show measurement complications (IR contamination, dim signals, no dateable fast component). Here, we explore feldspar IRSL-50 as an alternative signal with similar thermal characteristics, this mineral usually showing brighter signals in separates derived from bedrock. We collected samples in various mountain ranges, covering a wide range of lithologies and exhumation histories: western Norway (<0.1 mm/yr exhumation), southern Alaska (0.1-5 mm/yr exhumation), and eastern Pamir (>5 mm/yr exhumation). This offers a unique dataset to assess the potential of feldspar IRSL as a low-temperature thermochronometer.

Feldspar separates extracted from bedrock were dated using the conventional IRSL-50 protocol, which exhibits good reproducibility and dose recovery across different lithologies (although some samples may suffer from minor thermal transfer). We study fading variability in bedrock samples (using different protocols), and explore the apparent correlation between fading rate and apparent saturation ratio (e.g. Huntley and Lian, 2006). Our results show that almost all studied samples appear in field saturation (Kars et al., 2008). Indeed, feldspar saturation may limit the applicability of IRSL-50 thermochronometer to only rapidly-cooling settings (>300°C/Myr), as confirmed by isothermal holding experiments and calibration in the KTB borehole (Guralnik et al., 2010). Nonetheless, some samples from the Pamir and southern Alaska fault zones show deviation from field saturation, allowing to infer either cooling rates within rapidly-exhuming areas or localized rock reheating (through fault shearing or geothermal fluids circulation). Extending the applicability of luminescence dating in thermochronometry will require exploring lower-energy traps and/or targeting different minerals with later saturation.

## REFERENCES

- Herman, F., Rhodes, E.J., Braun, J. & Heiniger, L. 2010. Uniform erosion rates and relief amplitude during glacial cycles in the Southern Alps of New Zealand, as revealed from OSL-thermochronology, *Earth and Planetary Science Letters*, 297, 183-189.
- Li, B. & Li, S.-H. 2012. Determining the cooling age using luminescence-thermochronology, *Tectonophysics*, 580, 242-248.
- Huntley, D.J. & Lian, O.L. 2006. Some observations on tunnelling of trapped electrons in feldspars and their implications for optical dating. *Quaternary Science Reviews*, 25, 2503-2512.
- Guralnik, B., Herman, F., Preusser, F., Rhodes, E.J., and Lowick, S.E. 2010. Preliminary constraints on the kinetics of OSL thermochronology. American Geophysical Union (AGU) Fall Meeting, San Francisco, December 2010.

## P 1.28

# 3D FEM modelling of geological structures caused by geometrical instabilities and contrasts in rock strength

von Tscharner Marina & Schmalholz Stefan

*Université de Lausanne, Institut des sciences de la Terre, Quartier UNIL-Mouline, Bâtiment Géopolis, CH-1015 Lausanne, (marina.vontscharner@unil.ch)*

Many three-dimensional (3D) structures in rock, which formed during the deformation of the Earth's crust and lithosphere, are controlled by a difference in mechanical strength between rock units and are often the result of a geometrical instability. Such structures are, for example, folds, pinch-and-swell structures (due to necking) or cusped-lobate structures (mullions).

These structures occur from the centimeter to the kilometer scale and the related deformation processes control the formation of, for example, fold-and-thrust belts and extensional sedimentary basins or the deformation of the basement-cover interface. The 2D deformation processes causing these structures are relatively well studied, however, several processes during large-strain 3D deformation are still incompletely understood. One of these 3D processes is the lateral propagation of these structures, such as cusp propagation in a direction orthogonal to the shortening direction or neck propagation in a direction orthogonal to the extension direction.

We study the 3D evolution of geometrical instabilities with numerical simulations based on the finite element method (FEM). Simulating geometrical instabilities caused by sharp variations of mechanical strength between rock units requires a numerical algorithm that can accurately resolve material interfaces for large differences in material properties (e.g. between limestone and shale) and for large deformations. Therefore, our FEM code combines a numerical contour-line technique and a deformable Lagrangian mesh with re-meshing. With this combined method it is possible to accurately follow the initial material contours with the FEM mesh and to accurately resolve the geometrical instabilities.

The algorithm can simulate 3D deformation for a visco-elasto-plastic rheology. Stresses are limited by a yield stress using a visco-plastic formulation and the viscous rheology is described by a power-law flow law. The 3D FEM code is applied to model 3D power-law folding and power-law Rayleigh-Taylor instabilities (diapirs) with different re-meshing scenarios. The results are tested with the analytical solution for small amplitudes and with 2D numerical results for large amplitudes.

Thereby, the small initial geometrical perturbations for folding and necking are exactly followed by the FEM mesh. In order to test and measure the numerical properties for an Eulerian mesh we use the analytical solution for a two-dimensional viscous inclusion in pure shear.

## P 1.29

### Slab detachment – 3D versus 1D

von Tschärner Marina, Duretz Thibault & Schmalholz Stefan

Université de Lausanne, Institut des sciences de la Terre, Quartier UNIL-Mouline, Bâtiment Géopolis, CH-1015 Lausanne, (marina.vontschärner@unil.ch)

Slab detachment is a geodynamic mechanism that may affect subduction zones on Earth. The model is characterized by the detachment of a subducting slab fragment and results in a dramatic decrease of the slab pull force magnitude. As a result, slab detachment has many potential consequences for the dynamics of convergent zones such as orogens.

We study three-dimensional (3D) lateral propagation of slab detachment with a laterally varying initial slab length with numerical simulations based on the finite element method (FEM). The slab detachment is simulated by buoyancy-driven necking in a layer of power-law fluid embedded in a linear viscous medium. Our 3D FEM code combines a numerical contour-line technique and a deformable Lagrangian mesh with re-meshing. With this combined method it is possible to accurately follow the initial material contours with the FEM mesh and to accurately resolve the geometrical instabilities. We are able to follow the material contour and therefore, to study the accurate slab geometry at any time.

We provide a detailed description of the evolution of the slab morphology and evaluate the rates of lateral propagation of slab detachment.

We compare the 3D results with the one-dimensional (1D) necking analytical solution by Schmalholz (2011). The numerical results give reasonably good agreement with the analytical prediction, despite the fact that 3D detachment may occur on a much longer timescale.

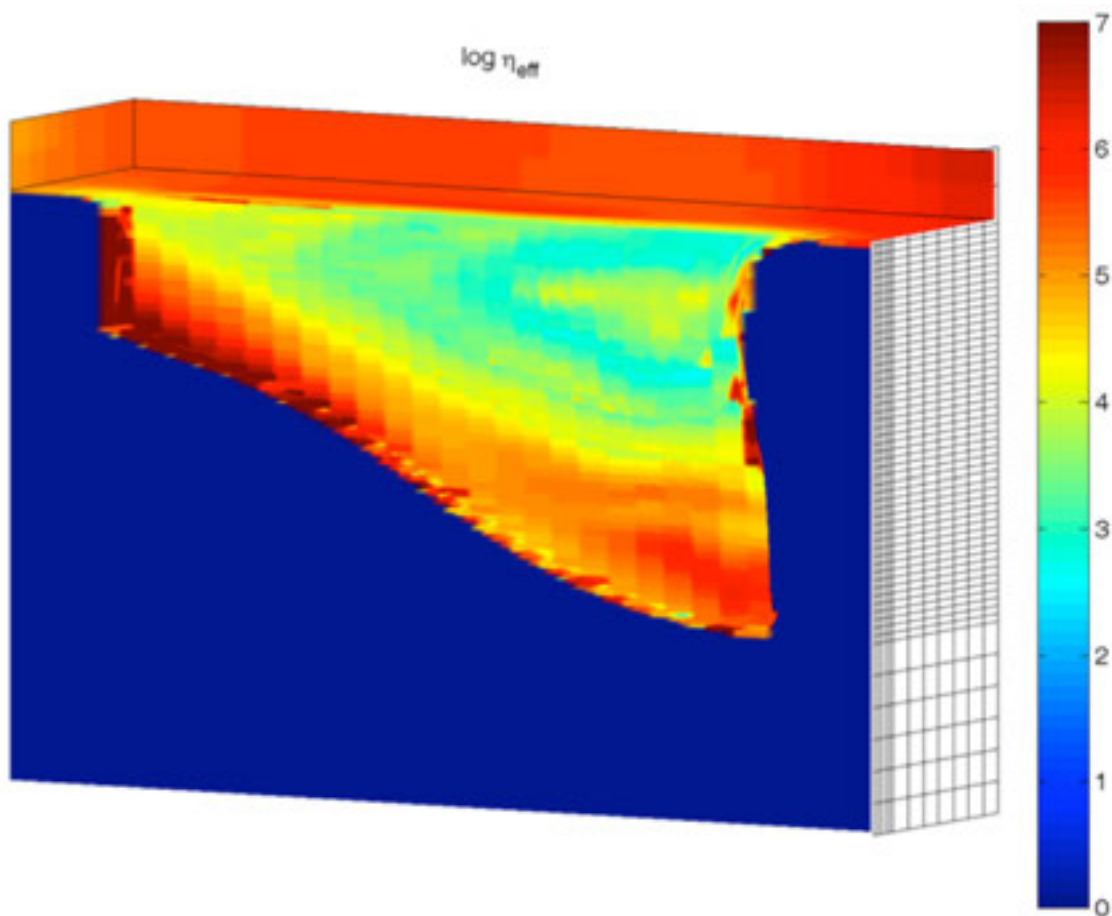


Figure 1: color plot of effective viscosity on the slab contour.

#### REFERENCES

Schmalholz, S., 2011, A simple analytical solution for slab detachment, Earth and Planetary Science Letters 304, 45-54

## P 1.30

# Baijiantan-Baikouquan ophiolitic mélanges: Implications for geology evolution of west Junggar, Xinjiang, NW China

Zhu Y.F.

*The Key Laboratory of Orogenic Belts and Crustal Evolution, Ministry of Education, China; School of Earth and Space Science, Peking University, Beijing 100871, China*

The west Junggar, as a major component of the core part of the central Asian Orogenic Belt, is considered to be a Paleozoic orogenic belt resulting from the convergence of the Siberian and Kazakhstan-Junggar plates. Three ophiolite belts occur in this region (Fig. 1): the Tangbale ophiolite mélange in west; the Darbut-Sartohay ophiolite mélanges in northeast, and the newly discovered Baijiantan-Baikouquan ophiolitic mélanges in southeast (Feng, 1986; Zhang, 1997; Chen & Zhu, 2011; Zhu et al. 2011). This paper focuses on petrology and geochemistry of the Baijiantan-Baikouquan ophiolite mélanges. We provide the comprehensive geologic, petrographic, and geochemical data-set, discuss the P-T conditions for the metamorphic evolution of the ophiolitic mélanges based on thermodynamically calculated P-T pseudosections for garnet amphibolite, and interpret the lithological characteristics of the west Junggar in a subduction-accretion scheme.

Lherzolite consists mainly of olivine, orthopyroxene, clinopyroxene, spinel and serpentine. Brown spinel with homogeneous composition were replaced by ilmenite along rim. Metagabbro consists of clinopyroxene, plagioclase pseudomorph, amphibole, and other second mineral phases. Plagioclase occurs as pseudomorph consisting mainly of zoisite and albite. Clinopyroxene, as a mineral phase crystallized from magma, was replaced by amphibole along rim. Garnet occurs along the rim of plagioclase pseudomorph. This suggests a transformation from plagioclase to garnet, which was accompanied with chlorite and ilmenite. Garnet amphibolite contains various amounts of garnet and amphibole with minor amounts of zoisite, epidote, chlorite, clinopyroxene, ilmenite, biotite, and sphene. Garnet contains various kinds of mineral inclusions including clinopyroxene, rutile, apatite, ilmenite, biotite, and quartz. All garnet analyses fall in the field corresponding to the garnet in eclogite coexisting with blueschist.

Zircon SHRIMP analyses give a weighted average U-Pb age of  $385.0 \pm 3.3$ Ma for metagabbro and  $363.3 \pm 3.1$ Ma for amphibolite. We consider the U-Pb age of  $\sim 385$ Ma could most probably represent the magma intrusion time, while the younger age might be affected by metamorphism.

Two Ordovician ophiolitic belts could be identified in west Junggar: the TTKH locating on the south boundary of the Chingiz-Tarbahatai arc, and the TBB locating on the south of west Junggar (Fig. 1). The Darbut-Sartohay ophiolitic belt, occurring between the above two Ordovician ophiolitic belts, was formed during Devonian. The TTKH represents an accretionary terrane added on the south edge of Chingiz-Tarbahatai arc, which was intruded by Silurian granitic rocks. The TBB represents an accretionary terrane added on the Junggar plate. The Darbut-Sartohay ophiolitic belt represents the relics of the Paleo-Ocean floor. The lithologic units of the TBB and Darbut-Sartohay ophiolitic mélanges were intruded by Carboniferous granite.

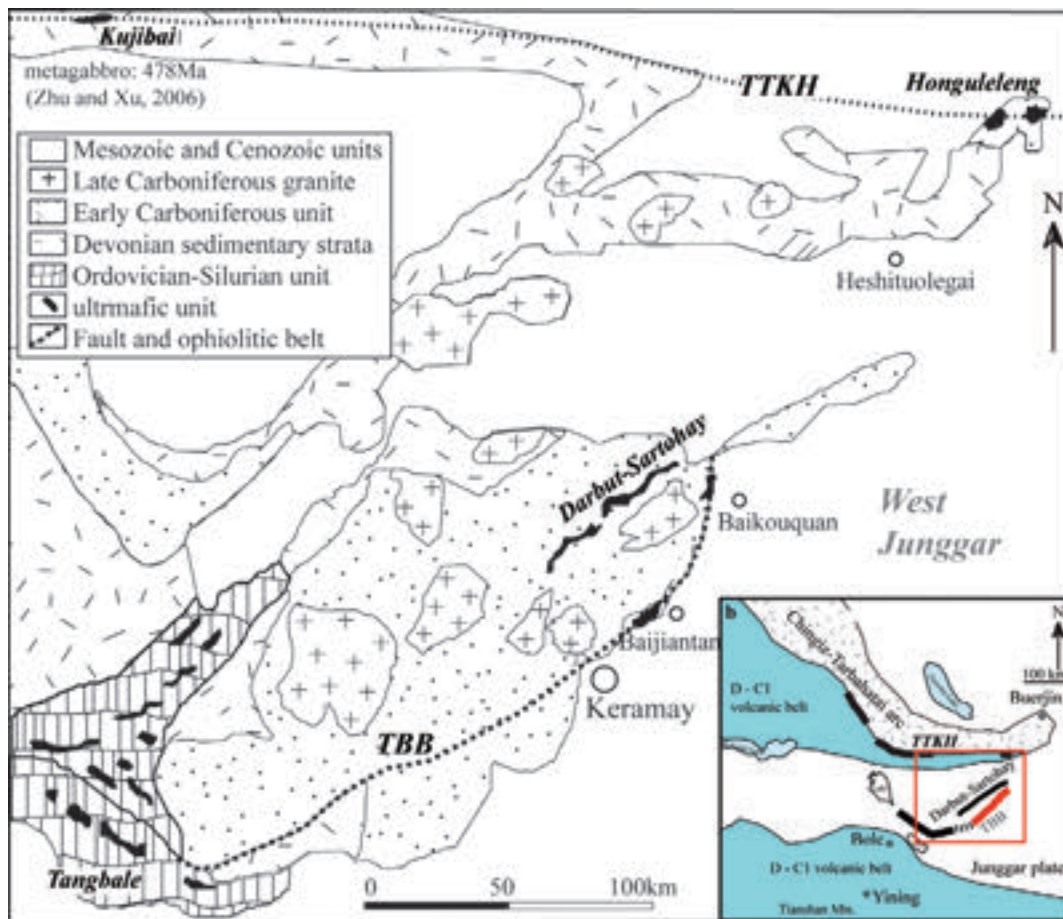


Figure 1. Simplified geological map showing the major geological units and the distribution of ophiolite belts in west Junggar.

#### REFERENCES

- Chen, B. & Zhu, Y.F. 2011: Petrology, geochemistry and zircon U-Pb chronology of gabbro in Darbut ophiolitic melange, Xinjiang. *Acta Petrologica Sinica*, 27, 1746-1758.
- Feng, Y. M. 1986: Genetic environments and original types of ophiolites in west Junggar. *Bull. Xi'an Inst. Geol. Min. Res., Chinese Acad. Geol. Sci.*, 13, 37-45.
- Zhang, L.F. 1997:  $^{40}\text{Ar}/^{39}\text{Ar}$  age of blueschists in Tangbale, western Junggar, Xinjiang, and its significance. *Chinese Science Bulletin*, 42, 2178-2181.
- Zhu, Y.F. & Xu, X. 2006: The discovery of Early Ordovician ophiolite mélangé in Tarbagatai Mts., Xinjiang, NW China. *Acta Petrologica Sinica*, 22, 2833-2842.
- Zhu, Y.F., Yan, Q.M., Ma, H.D. & Lehmann, B. 2011: Recent advances in geology and exploration in the Balkash-western Junggar region (Kazakhstan and Xinjiang, China): Report on the "International workshop on the large Balkash-western Junggar copper-gold province", Karamay, Xinjiang, China, 22-27 August, 2011. *Episodes*, 34, 208-211.



## 2. Mineralogy, Petrology, Geochemistry

Eric Reusser, Bernard Grobéty, Sébastien Pilet

*Swiss Society of Mineralogy and Petrology (SSMP)*

### TALKS:

- 2.1 Bosshard-Stadlin S.A., Stewart C., Mattsson, H.B.: Leaching of natrocarbonatitic ash and consequences for drinking water: The 2007/2008 explosive eruption of Oldoinyo Lengai, northern Tanzania
- 2.2 Bretscher A., Pettke T.: The mineral and fluid chemistry of high-P serpentinite dehydration
- 2.3 Burn M., Giuntoli F., Regis D., Lanari P., Engi M.: Mobile Fragments in a Subduction Channel: Correlation of P-T-D-t stages
- 2.4 El Korh, A.: Ablation behaviour and matrix effects during U–Th–Pb geochronology of allanite by LA-ICP-MS
- 2.5 Ewing T., Müntener O.: Formation and geochemistry of rutile from the roots of island arcs: an example from the Jijal Complex, Kohistan
- 2.6 Ferreiro Mählmann R.: Standardisation, calibration and correlation of the Kübler-Index and the vitrinite/bituminite reflectance: an inter-laboratory and field related study
- 2.7 Floess D., Baumgartner L.: Constraining magmatic fluxes through thermal models for contact metamorphism
- 2.8 Fomin I., Dubinina E., Avdeenko A., Ariskin A.: Oxygen isotopes in Ioko-Dovyren layered intrusion rocks
- 2.9 Gilgen S. A., Diamond L. W., Mercogli I.: Volcanostratigraphic Controls on the Occurrence of Massive Sulfide (VMS) Deposits in the Semail Ophiolite, Oman
- 2.10 Leuthold J., Blundy J., Holness M.: Quantification of successive reactive melt flow episodes in a layered intrusion (Unit 9, Rum Eastern Series, Scotland)
- 2.11 Pretet C., Nägler T. F., Reynaud S., Böttcher M. E., Samankassou E.: Barium isotope fractionation in coral skeleton: Tracking anthropogenic contaminations?
- 2.12 Rottier B., Kouzmanov K., Fontboté L.: Ore-forming fluids associated with the early mineralization at Cerro de Pasco, Peru
- 2.13 Schenker F. L., Burg J.-P., Kostopoulos D.: Distinguishing metacarbonatites from marbles – Challenge from the carbonate-amphibolite-epidotite rock association in the Pelagonian zone (Greece)
- 2.14 Schlatter D.M., Stensgaard B.M.: Evaluation of the mineral potential in the Bjørnesund greenstone belt, southern West Greenland, combining multivariate studies, field work and geochemistry
- 2.15 Thien B., Kosakowski G., Kulik D.: Modeling water-rock interactions in Icelandic hydrothermal systems
- 2.16 Tomé C., Kouzmanov K., Fontboté L., Bendejú A., Wälle M.: Magmatic-hydrothermal fluid evolution of a multiphase porphyry-centered system: the Miocene Morococha district, central Peru
- 2.17 Tripoli B. A., Cordonnier B., Ulmer P.: Effects of crystallization and bubble nucleation on the seismic properties of magmas
- 2.18 Vils F., Elliott T., Willbold M., Teagle D.: Molybdenum isotopes: the new tracer to identify subducted material? Hints from the altered oceanic crust and oceanic eclogites.

## POSTERS:

- P 2.1 Bouvier A.-S., Manzini M., Baumgartner L.: Cl isotopes in melt inclusions
- P 2.2 Siron G., Baumgartner L. P., Bouvier A. S.: Development of  $\delta^{18}\text{O}$  and  $\delta^{37}\text{Cl}$  SIMS analysis on biotites
- P 2.3 Siron G., Baumgartner L., Bodner R., Putlitz B., Müntener O.: High chloride concentration in biotites of host rocks documents infiltration of fluids exsolved from the Torres del Paine granites
- P 2.4 Baumgartner L., Bouvier A.-S., Putlitz B.: Development of a quartz oxygen isotope standard for the SwissSIMS
- P 2.5 Ulianov A., Müntener O., Schaltegger U.: Uncertainties of the laser ablation ICPMS analysis: how do they arise and how do we calculate them?
- P 2.6 Honisch M., Ulianov A., Ulmer P., Müntener O.: Stress and strain in olivine - a RAMAN-mapping approach
- P 2.7 Giuntoli F., Engi M., Regis D., El Korh A., Lanari P.: Recognizing metamorphic stages and tectonic slices in HP-terraces: Case study in the Sesia Zone (NW-Alps, Italy)
- P 2.8 Franz L., De Capitani C., Romer R.L.: Whiteschists - protoliths and phase petrology
- P 2.9 May E., Vennemann T., Meisser N.: Geochemical study of mineral paragenesis from Alpine-type veins in the western Swiss Alps.
- P 2.10 Seitz S., Putlitz B., Baumgartner L.P., Leresche S., Nescher P.: Oxygen isotope and trace element behaviour in rhyolites from the contact-aureole of the Chaltén Plutonic Complex (Mt. Fitz Roy, Patagonia, Argentina)
- P 2.11 Axelsson E., Mezger K., Villa I.M.: Biotite Rb-Sr and Rutile U-Pb age data confirming an extensive Neoproterozoic overprint in the Eastern Ghats Belt (India)
- P 2.12 Galster F., Müntener O., Ewing T.: Nb/Ta, Zr/Hf and HREE to Understand Accessory Mineral Thermometers at High and Ultra-High Temperatures
- P 2.13 Tene Djoukam J., Moritz R., Tchouankoue J.:  $\text{CO}_2$ -rich fluid inclusion in upper mantle xenoliths from Nyos and Barombi-Mbo lakes: Cameroon Volcanic Line
- P 2.14 Caricchi L., Annen C., Blundy, J., Simpson G.: Control of magma recharge and buoyancy on the frequency and magnitude of volcanic eruptions
- P 2.15 Ernst K., Franz L., Decapitani C., Harlow G., Krzemnicki M., Kouznetsov N.: A new occurrence of kosmochlor in Cr-jadeite rocks from Kenterlau-Itmurundy (Lake Balkhash, Kazakhstan)
- P 2.16 Schweinar K., Franz L., De Capitani C., Hänni H.A., Thyesun T.: Kosmochlor from Myanmar - Investigations on a possible miscibility gap in the solid solution jadeite-kosmochlor
- P 2.17 Casanova V., Kouzmanov K., Fontboté L., Bendezú R.: Multiple quartz generations associated with polymetallic mineralization at Colquijirca, central Peru: a fluid inclusion and SEM-CL study
- P 2.18 Lambiel F., Dold B., Fontboté L., Vennemann T., Spangenberg J.E.: Neoformation of «exotic» copper minerals from gel-like precursors at the Exotica deposit (northern Chile)
- P 2.19 Buret Y., Kouzmanov K., Spikings R., Gerdjikov Y.: Timing of polymetallic Pb-Zn mineralisation in the Laki district, southern Bulgaria - constraints from  $^{40}\text{Ar}/^{39}\text{Ar}$  dates
- P 2.20 Large S., Bakker E., Weis P., Wälle M., Heinrich C., Ressel M.: A magmatic origin of ore-forming fluids in Carlin-type deposits? Fluid inclusion studies on Carlin-type deposits and a Au-Cu porphyry deposit on the Carlin and Battle Mountain-Eureka trends, Nevada
- P 2.21 Davoudi A., Lak R., Bahramabadi B.: Estimation of environmental contaminations value of heavy metals in the sediments of Sari area with using geochemical parameter of Enrichment Factor (EF)
- P 2.22 Franz L., Wetzel A., Doerner E.: Petrographic and sedimentologic investigation of boulders in the riverbed of the 'Hauensteiner Murg'
- P 2.23 Bauer, K., Adatte, T., Vennemann, T.: Oxygen and hydrogen stable isotopes in waters and soils from the Visp catchment, Valais, Switzerland

## 2.1

# Leaching of natrocarbonatitic ash and consequences for drinking water: The 2007/2008 explosive eruption of Oldoinyo Lengai, northern Tanzania

Sonja A. Bosshard-Stadlin<sup>1</sup>, Carol Stewart<sup>2</sup>, Hannes B. Mattsson<sup>1</sup>

<sup>1</sup>*Institute for Geochemistry and Petrology, ETH Zürich, Clausiusstrasse 25, 8092 Zürich (sonja.stadlin@erdw.ethz.ch)*

<sup>2</sup>*Joint Centre for Disaster Research, Massey University, Wellington, New Zealand*

Oldoinyo Lengai, a stratovolcano located in the East African Rift System, is best known for its unique natrocarbonatitic activity, which alternates with highly explosive nephelinitic eruptions. Since 1883, five major ash eruptions have been reported, with natrocarbonatitic lava flows in the time between the ash eruptions (Dawson, 2008). The most recent explosive eruption of Oldoinyo Lengai started during the night from the 3<sup>rd</sup> to 4<sup>th</sup> September 2007 and lasted until April 2008. Volcanic ash fall has significant impacts on the chemistry of surface waters (e.g. Stewart et al., 2006). During volcanic eruptions, a variety of gases (such as H<sub>2</sub>O, CO<sub>2</sub>, H<sub>2</sub>, HS, HF, CO and Cl<sub>2</sub>), are released into the atmosphere.

The surface coating of fresh volcanic ash is highly acidic; it originates from interaction of ash with aerosols such as H<sub>2</sub>SO<sub>4</sub>, HCl and HF in the plume. Therefore, the contact of such ash with surface water lowers the pH of the water significantly below acceptable limits for drinking water (e.g. 7-8.5 for New Zealand, Stewart et al., 2006). The pH is often in the range of 6.5-9.5, but no health-based guideline value is proposed for pH by the World Health Organization, WHO (WHO, 1996). Over 55 soluble components have been reported in volcanic ash leachates, and Witham et al. (2005) described fluoride (F) as the main toxic element adsorbed on ash, although F is beneficial in small amounts in drinking water. However, long-time consumption of waters with elevated fluoride concentrations can result in seriously health effects such as dental and skeletal fluorosis. Elevated fluoride concentrations in drinking waters are a major problem in most parts of the East African Rift System, where high fluoride concentrations are a direct result of water-rock interaction and leaching of fluoride-bearing minerals.

The amount of adsorption and the composition of the salts and volatiles depend on different factors such as magma composition, explosivity of the eruption, gas-pyroclast dispersion immediately after fragmentation, concentration of aerosols in the plume, particle size-fraction and ratio of particles to gas (Witham et al., 2005).

The ash is leached in distilled water following the protocol of the International Volcanic Health Hazard Network (IVHHN). This protocol has been set up in order to have all ash leaching experiments conducted in the same way, enabling a direct comparison between different data sets.

The experiments are carried out on four ash samples which never touched the ground, collected three days and three weeks after the onset of the eruption. These samples never came in contact with rain water and were always kept in a desiccator and are thus suitable for such experiments.

We show, which elements are leached out of the ash, and compare the values with the guidelines of the World Health Organization (WHO) for health standard concentrations. To understand the amount of leaching into the drinking water is of great importance to the ~300'000 Maasai people and their cattle living in close vicinity to Oldoinyo Lengai.

## REFERENCES

- Dawson, J.B., 2008. The Gregory Rift Valley and Neogene-Recent Volcanoes of Northern Tanzania. Geological Society, London, Memoirs, 33(1), 102.
- Stewart, C., Johnston, D.M., Leonard, G.S., Horwell, C.J., Thordarson, T. and Cronin, S.J., 2006. Contamination of water supplies by volcanic ashfall: A literature review and simple impact modelling. *Journal of Volcanology and Geothermal Research*, 158(3-4), 296-306.
- WHO, 1996. pH in Drinking-water, Background document for development of WHO Guidelines for Drinking-water Quality. Guidelines for drinking-water quality, World Health Organization, 2(2).
- Witham, C.S., Oppenheimer, C. and Horwell, C.J., 2005. Volcanic ash-leachates: a review and recommendations for sampling methods. *Journal of Volcanology and Geothermal Research*, 141(3-4), 299-326.

## 2.2

### The mineral and fluid chemistry of high-P serpentinite dehydration

Bretscher Annette<sup>1</sup>, Pettke Thomas<sup>1</sup>

<sup>1</sup>Institute of Geological Sciences, University of Bern, Baltzerstrasse 1+3, CH-3012 Bern ([annette.bretscher@geo.unibe.ch](mailto:annette.bretscher@geo.unibe.ch))

Serpentinites play a key role in the fluid mediated chemical cycling in subduction zones. Subduction of oceanic plates (including serpentinitized/hydrated peridotites) refertilizes the Earth's mantle with crustal components and influences the chemistry of magma sources beneath volcanic arcs. Recent research on ocean floor serpentinites and their eclogite facies equivalents has revealed their role as a carrier for fluid mobile elements (e.g. As, Sb, Cl, B, Li, Cs, Pb, U, Rb, Ba, halogens and noble gases). It was found that these elements partially partition into the fluid upon dehydration reactions during subduction metamorphism. These reactions include the transition from lizardite/chrysotile to antigorite, breakdown of brucite, antigorite and chlorite (in the order of increasing P-T during subduction). Quantitative constraints on the chemical composition of fluids released during two major (in terms of water liberated) serpentinite dehydration reactions (brucite-out and antigorite-out) as well as the chemical inventory of the residual rocks have remained scarce to date. Which and how much of the soluble element inventory of arc magmas interpreted to originate from slab dehydration actually originates from subducted serpentinites as opposed to subducted sediments or altered oceanic crust has thus remained largely speculative.

The ultramafic massif at the Cerro del Almirez (Betic Cordillera, southern Spain) is a unique field occurrence to study eclogite facies antigorite dehydration to form chlorite harzburgite (Trommsdorff et al., 1998; Scambelluri et al., 2001a, Padrón-Navarta et al., 2011). Small amounts of the fluid released upon antigorite breakdown are stored as fluid inclusions in olivine of the chlorite harzburgite. Our project aims at obtaining the chemical inventory (major to trace elements of minerals and fluid inclusions) of the antigorite breakdown reaction recorded in the Cerro del Almirez ultramafic massif in order to contribute to a better understanding of the fluid mediated mass transfer during subduction of oceanic lithosphere. The analytical techniques chosen for this approach are optical microscopy and in-situ analytical techniques, most importantly EPMA, LA-ICP-MS and SIMS (in future).

In outcrop we have identified 5 different rock types across the antigorite serpentinite to chlorite harzburgite transition: (1) Antigorite serpentinite (atg-serpentinite): an antigorite schist that contains variable amounts of olivine, clinopyroxene, tremolite, minor chlorite, Ti-clinohumite and opaques, embedded in a fine-grained matrix of oriented antigorite; (2) Transitional lithology 1 (TL1): A foliated rock similar to the atg-serpentinite but its antigorite content is dramatically reduced and the olivine content increased. It contains talc and a second generation of large, unoriented antigorite flakes. This new antigorite generation contains chlorite cores and overgrows the atg-serpentinite assemblage (Figure 1); (3) Transitional lithology 2 (TL2): This rock differs from TL1 only by a further decrease of modal antigorite and increase of olivine, accompanied by first appearance of orthopyroxene. Chlorite harzburgite (chl-harzburgite, a massive ol-opx-chl-rock) is characterized by two textural types, a (4) granofels and a (5) spinifex-like type, the latter being the dominant mass. Both types consist of olivine, orthopyroxene, flaky chlorite, minor tremolite, opaques and  $\pm$ talc. The spinifex-like textured chl-harzburgite (Figure 2) contains 3 generations of olivine. A first clear granular olivine (ol1, interpreted to be relics of the serpentinite stage) that is overgrown by arborescent olivine with a strong brownish color as well as numerous fluid inclusions (ol2), rimmed by clear olivine (ol3).

The mineral major element chemistry confirms the texturally distinct occurrences of each mineral phase. As an example, chlorite which is present in all 5 rock types shows the following evolution: from atg-serpentinite over TL1 and TL2 its Al<sub>2</sub>O<sub>3</sub>-content decreases continuously (from 14 to 12 wt%). The Al<sub>2</sub>O<sub>3</sub>-content of chlorite of the granofelsic harzburgite overlaps with both chlorite in atg-serpentinite and transitional lithologies. Chlorite in the spinifex-like harzburgite on the other hand is clearly Al<sub>2</sub>O<sub>3</sub>-richer (13.5 to 16 wt%).

Bulk rock chemical analysis is planned as a basis for mass balance estimations to constrain whether element input or loss via fluid migration is associated with the antigorite-out reaction. LA-ICP-MS trace element analysis will be carried out to investigate the trace element transfers that accompany the reactions involved in the continuous antigorite dehydration.

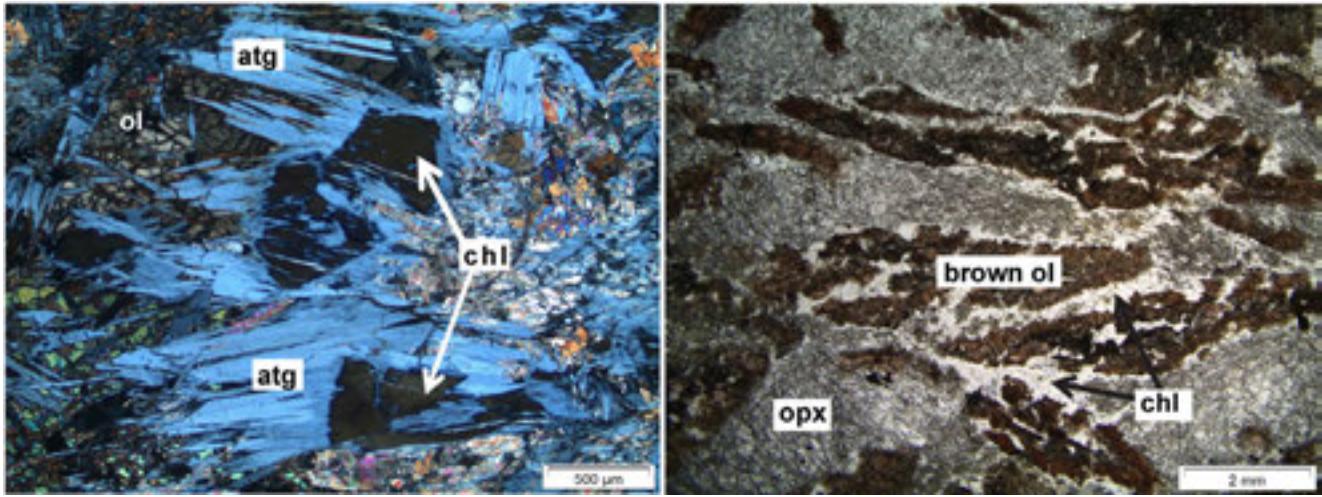


Figure 1: Transitional lithology 1 (TL1). Large unoriented antigorite flakes with chlorite cores. This is the first metamorphic chlorite appearing in the antigorite bearing rock. Crossed polarizers.

Figure 2: Spinifex-like textured chlorite harzburgite. The antigorite assemblage is replaced by brown spinifex-textured olivine, orthopyroxene and chlorite. Single polarizer.

## REFERENCES

- Padrón-Navarta, J.A., et al., 2011. *J. Petrol.* 52, 2047-2078.  
 Scambelluri, M., et al., 2001. *Earth Planet. Sci. Lett.* 192, 457-470.  
 Trommsdorff, V., et al., 1998. *Contrib. Mineral. Petrol.* 132, 139-148.

## 2.3

### Mobile Fragments in a Subduction Channel: Correlation of P-T-D-t stages

Marco Burn<sup>1</sup>, Francesco Giuntoli<sup>1</sup>, Daniele Regis<sup>1,2</sup>, Pierre Lanari<sup>1</sup>, Martin Engi<sup>1</sup>

<sup>1</sup> Universität Bern, Institut für Geologie, Baltzerstrasse 3, CH-3012 Bern, Switzerland

<sup>2</sup> Open University, Dept. of Environment, Earth & Ecosystem, Milton Keynes, MK7 6AA, UK

Some numerical models of subduction channels indicate that tectonic mixing may be an important process. Opinions diverge with regards to possible origins of fragments, amplitudes of internal mobility, and temporal scales of such mixing processes. Recent work in the Sesia Zone of the Western Alps shows that the HP-evolution was substantially more long-lived and complex than previously established (e.g. Rubatto et al., 2011). Significantly different HP-stages have been identified in different slices of the Eclogitic Micaschists Complex (EMC; Regis et al. 2013), providing evidence of differential movements of HP-fragments, with subduction- and exhumation-related stages being recorded. The size, geometry, and ultimate provenance of fragments are in the focus of our present research, the main emphasis being on the various klippen units thought to derive from the NW-Adriatic margin.

We report on methods refined to relate petrochronology to structural data. Detailed analysis of local phase equilibria using X-ray images (XMapTools software, Lanari et al. 2011) yields local P-T equilibrium conditions; these are combined with *in situ* U-Th-Pb dating for growth zones in allanite and zircon. Careful microstructural details (e.g. on deformation fabrics, mineral inclusions) and REE-distribution data are used to document an integrated HP-record for single samples. Where corresponding time intervals have been recorded in several tectonic units, it thus appears possible to correlate stages of HP-metamorphism and deformation.

Results are shown for HP-fragments from several tectonic units in the internal Western Alps, with examples ranging from the eastern parts of the Sesia Zone right across to the Austroalpine klippen units now resting atop Piemonte-Liguria oceanic units:

- In eastern parts of the EMC (Mombarone area) HP-micaschist equilibrated at 1.9-2.0 GPa and 540-550 °C contains allanite dated at 85.8±1.0 Ma; zircon shows rims at ~75 Ma and 70-60 Ma, these reflect growth during decompression, but still at pressures >1.4 GPa.
- Further west (Val de Lys), micaschists from the EMC show a HP foliation (ECL-BLS facies) and weak (GRS facies) retrogression. Successive generations of phengite, garnet, glaucophane (±early omphacite) and allanite are distinguished, plus quartz, epidote, chlorite, and titanite (rimming rutile). Growth zones in garnet and allanite correspond to distinct HP stages. Preliminary Th-Pb age data for allanite from *in situ* LA-ICP-MS analysis show 80-74 Ma for cores and 68-62 Ma for rims. These ages compare well with the two HP stages (HP1: ~75 Ma; HP2: ~65 Ma) Regis et al. (2013) found in several samples of the Fondo slice of the Sesia Zone, from which pressure cycling was inferred.
- Leucocratic gneiss from the Glacier-Rafray klippe shows assemblages including actinolite-phengite-epidote-albite-titanite-quartz. Complex growth zoning patterns in phengite allow us to establish a relative, but detailed P-t path. Replacement of phengite by chlorite adds late-stage information. When combined with published P-T data, an absolute P-T path can be constructed. Dating of the HP-stage(s) is underway.

Analysis of the fossil continental margin between the Sesia Zone, the Piemonte Zone and the external klippen is likely to have significant tectonic implications. Several stages and scenarios for the evolution of this margin are being considered, from pre-collisional rifting and formation of an OCT zone, through polyphase subductive processes to the juxtaposition of fragments during collision or exhumation.

#### REFERENCES

- Lanari et al. (in press) XMapTools: a MATLAB©-based program for electron microprobe X-ray image processing and geothermobarometry. Computers and Geosciences doi:10.1016/j.cageo.2013.08.010
- Regis et al. 2013: Deciphering metamorphic dynamics in an eclogite-facies terrane (Sesia Zone, Western Alps) using U/Th-Pb petrochronology (in progress at J. Petrology)
- Rubatto et al. 2011: Yo-yo subduction recorded by accessory minerals in the Italian Western Alps. Nature Geoscience 4, 338-342.

## 2.4

# Ablation behaviour and matrix effects during U–Th–Pb geochronology of allanite by LA-ICP-MS

El Korh Afifé<sup>1</sup>

<sup>1</sup> Institut für Geologie, Universität Bern, Baltzerstrasse 1+3, CH-3012 Bern (afife.elkorh@geo.unibe.ch)  
Centre de Recherches Pétrographiques et Géochimiques (CRPG), 54500 Vandœuvre-lès-Nancy, France

Allanite is a common mineral in magmatic and metamorphic rocks. It has a large range of composition through the substitution reaction  $\text{Ca}^{2+} + \text{Fe}^{3+} \rightleftharpoons \text{REE}^{3+} + \text{Fe}^{2+}$ , and may host a high amount of Th and U. In-situ U–Th–Pb geochronology of allanite by LA-ICP-MS has become a promising method. Allanite often contains a significant amount of common Pb ( $\text{Pb}_c$ ), which must be determined with highest accuracy to minimise age uncertainties. Age accuracy depends strongly on protocol adopted for the analyses, including ablation mode (spot or raster), ablation rate and on-sample fluence. As only few suitable allanite reference materials are available, the possibility of using non matrix-matched standards (e.g. zircon) is still in debate.

In this study, ablation experiments were carried out in spot mode using a 193 nm excimer laser coupled to a quadrupole ICP-MS, in order to characterise the ablation behaviour of allanite. The ratio-of-the-mean intensities method (see Ulianov et al. 2012) was used for data reduction, and  $\text{Pb}_c$  was corrected using the  $^{207}\text{Pb}$  method. Three allanite reference materials are compared: Tara (417 Ma; Gregory et al. 2007), AVC ( $276.3 \pm 2.2$  Ma; Barth et al. 1994), and Bona ( $30.1 \pm 0.3$  Ma; von Blankenburg 1992). They have different chemical composition:  $\text{Pb}_c$ -poor Tara ( $^{208}\text{Pb}_c < 2.4\%$ ;  $\text{FeO}_{\text{total}}$ : 11.5–13.9%; REE + Th of 0.76–0.84 apfu),  $\text{Pb}_c$ -poor AVC ( $^{208}\text{Pb}_c < 5.0\%$ ;  $\text{FeO}_{\text{total}}$ : 15.1–16.1%; REE + Th of 0.86–0.90 apfu) and  $\text{Pb}_c$ -rich Bona ( $^{208}\text{Pb}_c < 33\%$ ;  $\text{FeO}_{\text{total}}$ : 11.6–12.8%; REE + Th of 0.52–0.73 apfu). The U–Th–Pb data were also compared to the Plešovice reference zircon in order to investigate the matrix effects that may occur between the different matrices.

The temporal change of the intensity ratios for allanites indicates that Ca, Ce, U and Th share a similar behaviour to each other. Similarly, Pb, Si and, to a lesser extent, Fe do not show any time-dependant fractionation. This effect increases with time and with increasing fluence and ablation rate conditions, but only weakly with decreasing the spot size from 44  $\mu\text{m}$  to 32  $\mu\text{m}$ .

Elemental fractionation of the  $^{206}\text{Pb}/^{238}\text{U}$  and  $^{208}\text{Pb}/^{232}\text{Th}$  ratios is low and linear at 4 Hz and 4.5  $\text{J}/\text{cm}^2$  for the  $\text{Pb}_c$ -poor Tara and AVC allanites. With increasing fluence and ablation rate, the intensity ratio pattern displays a parabolic shape at the beginning of the signal, resulting from a decrease of the rate of change of the intensity ratio with time. The fractionation for the  $\text{Pb}_c$ -rich allanite displays a parabolic shape at the beginning of the signal already at 4 Hz and 4.5  $\text{J}/\text{cm}^2$ .

The  $\text{Pb}_c$  corrected mass bias values (know ratio/measured ratio) calculated for the  $^{206}\text{Pb}/^{238}\text{U}$  and  $^{208}\text{Pb}/^{232}\text{Th}$  ratios for the  $\text{Pb}_c$ -poor Tara and AVC allanites are similar and slightly lower than those calculated for the Plešovice zircon. They decrease with increasing the fluence and ablation rate and with decreasing the spot size. The mass bias values calculated for the  $\text{Pb}_c$ -rich Bona allanite are lower than those calculated for the  $\text{Pb}_c$ -poor allanites at 4 Hz and 4.5  $\text{J}/\text{cm}^2$ , and remain relatively constant with increasing the ablation rate and fluence conditions.

The mass bias values display a negative correlation with the Fe/Si ratio suggesting that Fe-correlated matrix effects may occur during allanite analysis (El Korh, submitted). Fe/Si ratios increase with increasing the fluence and ablation rate conditions, i.e. with increasing the mass load to the plasma. A poor correlation is also observed with the Ce/Si ratio. This suggests that Ce-correlated, and by extension LREE-correlated matrix effects, are less liable to occur.

$^{206}\text{Pb}/^{238}\text{U}$  and  $^{208}\text{Pb}/^{232}\text{Th}$  ages of AVC and Bona allanites were calculated using both Tara allanite and Plešovice zircon as external standards, with varying ablation conditions. The weighted ages obtained using Tara allanite as standard are within uncertainty with the reference ages, using 4 Hz and 4.5  $\text{J}/\text{cm}^2$  for both 32  $\mu\text{m}$  and 44  $\mu\text{m}$ . Using Plešovice zircon as external standard, the weighted average  $^{206}\text{Pb}/^{238}\text{U}$  and  $^{208}\text{Pb}/^{232}\text{Th}$  ages for allanites are higher than the reference ages, even if they remain within uncertainty with the reference ages for  $\text{Pb}_c$ -poor AVC allanite. In all cases, allanite weighted average ages are shifted away from the reference value with increasing ablation rate up to 12 Hz and with increasing fluence up to 12  $\text{J}/\text{cm}^2$ .

Analyses in spot mode at low frequency and on-sample fluence provide accurate and precise allanite  $^{206}\text{Pb}/^{238}\text{U}$  and  $^{208}\text{Pb}/^{232}\text{Th}$  ages, using matrix-matched calibration (El Korh, submitted). Matrix effects between allanites with different  $\text{Pb}_c$ ,  $\text{FeO}_{\text{total}}$  and REE + Th composition are sources of random errors and larger uncertainties, but do not significantly affect the age accuracy. However, matrix effects between allanites and zircon may often be responsible for systematic errors on ages.

## REFERENCES

- Barth, S., Oberli, F. & Meier, M. 1994: Th-Pb versus U-Pb isotope systematics in allanite. *Earth and Planetary Science Letters* 124, 149-159.
- El Korh, A. (submitted): Ablation behaviour of allanites during U–Th–Pb dating using a quadrupole ICP-MS coupled to a 193 nm excimer laser. Submitted to *Chemical Geology*.
- Gregory, C.J., Rubatto, D., Allen, C.M., Williams, I.S., Hermann, J. & Ireland, T. 2007: Allanite micro-geochronology: A LA-ICP-MS and SHRIMP U-Th-Pb study. *Chemical Geology* 245, 162–182.
- Sláma, J., Košler, J., Condon, D.J., Crowley, J.L., Gerdes, A., Hanchar, J.M., Horstwood, M.S.A., Morris, G.A., Nasdala, L., Norberg, N., Schaltegger, U., Schoene, B., Tubrett, M.N. & Whitehouse, M.J. 2008: Plesovice zircon – a new natural reference material for U–Pb and Hf isotopic microanalysis. *Chemical Geology* 249, 1–35.
- Ulianov, A., Müntener, O., Schaltegger, U. & Bussy, F. 2012: The data treatment dependent variability of U-Pb zircon ages obtained using mono-collector, sector field, laser ablation ICP-MS. *Journal of Analytical Atomic Spectrometry* 27, 663–676.
- von Blanckenburg, F. 1992: Combined high-precision chronometry and geochemical tracing using accessory minerals: applied to the Central-Alpine Bergell intrusion (central Europe). *Chemical Geology* 100, 19–40.

## 2.5

# Formation and geochemistry of rutile from the roots of island arcs: an example from the Jijal Complex, Kohistan

Ewing Tanya<sup>1</sup> & Müntener Othmar<sup>1</sup>

<sup>1</sup>Institut de Sciences de la Terre, Université de Lausanne, CH-1015 Lausanne (tanya.ewing@unil.ch)

The Kohistan complex crops out in northeastern Pakistan, and presents a ~50 km thick cross-section through a Jurassic–Cretaceous island arc. It is renowned as one of the best exposed and most complete sections through an exhumed island arc, and has therefore been the subject of intensive study over the past several decades. Nonetheless, some aspects of the evolution of the arc complex remain enigmatic.

The Jijal Complex represents the root of the Kohistan arc, and preserves the uppermost sub-arc mantle, the paleo-Moho, and the lowermost arc crust. It is subdivided into an ultramafic section and a mafic section. The mafic section is dominated by garnet gabbros, the origin of which is controversial. Formation of garnet in these rocks has been variously attributed to prograde metamorphic reactions (Yamamoto and Yoshino, 1998), dehydration melting of hornblende-bearing precursors (Garrido et al., 2006), or magmatic crystallisation at high pressures followed by isobaric cooling (Ringuette et al. 1999). A range of rock types contain accessory rutile (TiO<sub>2</sub>), including garnet gabbros, epidote-bearing pegmatites, paragonite-bearing gabbros, pyroxenites and garnetites. Geochemical and isotopic analysis of rutile may provide insight into processes that have affected these lithologies, and thus help understand the evolution of the lowermost part of this classic exhumed island arc section.

In most Jijal Complex lithologies, petrographic evidence indicates early commencement of rutile crystallisation, with ongoing rutile formation throughout a protracted period. This is consistent with approximately isobaric cooling, as rutile remains stable during lowering temperatures at constant relatively high pressures. In a pyroxenite from the ultramafic section, rutile is observed to have formed after ulvöspinel, which is also consistent with isobaric cooling. Zr-in-rutile temperatures record a spread of temperatures dominantly between ~650–700 °C. There is no relationship between Zr-in-rutile temperature and depth in the crustal section, in spite of the samples spanning ~5 km former depth. Instead there is a tendency towards lower, more scattered Zr-in-rutile temperatures in samples that show evidence for the most extensive interaction with residual melt. In spite of the textural evidence for early formation of rutile, Zr-in-rutile temperatures are significantly lower than Fe–Mg temperatures for garnet–clinopyroxene cores, which range between 800 °C (paragonite-bearing gabbro) and >1000 °C (pyroxenite). The Zr-in-rutile temperatures are interpreted to record ongoing re-equilibration of rutile with melt. Where cores and rims of the same rutile have been analysed they generally show no difference in Zr content, arguing against diffusive re-equilibration. Recrystallisation (e.g. by dissolution–precipitation) is favoured instead. The 650–700 °C Zr-in-rutile temperatures agree well with ~650 °C temperatures determined by Ti-in-quartz and epidote–quartz oxygen isotope thermometry (Dessimoz, 2012). They are also close to the water-saturated solidus for the Jijal Complex lithologies at relevant pressures. This is consistent with the Zr-in-rutile temperatures recording ongoing re-equilibration with residual melt, which would cease with final crystallisation of melt at the solidus.

Rutile hosts 20–40% of bulk rock Zr and 20–30% of bulk rock Hf in Jijal Complex lithologies. This rutile has generally subchondritic Zr/Hf ratios. Differences in the Zr/Hf of rutile from the Kohistan arc and from the Ivrea–Verbano Zone lower continental crustal section suggest different controls on the Zr/Hf ratio in these diverse settings.

### REFERENCES

- Dessimoz, M. 2012: Epidote in hydrous magmas: near solidus phase relations in the lower crust. PhD thesis, Université de Lausanne.
- Garrido, C.J. et al. 2006: Petrogenesis of Mafic Garnet Granulite in the Lower Crust of the Kohistan Paleo-arc Complex (Northern Pakistan): Implications for Intra-crustal Differentiation of Island Arcs and Generation of Continental Crust, *Journal of Petrology*, 47, 1873–1914.
- Ringuette, L., Martignole, J. & Windley, B.F. 1999: Magmatic crystallization, isobaric cooling, and decompression of the garnet-bearing assemblages of the Jijal sequence (Kohistan terrane, western Himalayas), *Geology*, 27, 139–142.
- Yamamoto, H. & Yoshino, T. 1998: Superposition of replacements in the mafic granulites of the Jijal complex of the Kohistan arc, northern Pakistan: dehydration and rehydration within deep arc crust, *Lithos*, 43, 219–234.

## 2.6

# Standardisation, calibration and correlation of the Kübler-Index and the vitrinite/bituminite reflectance: an inter-laboratory and field related study

Rafael Ferreiro Mählmann<sup>1, 2</sup>

<sup>1</sup> *Technical and Low Temperature Petrology, Institut für Angewandte Geowissenschaften, Technische Universität Darmstadt, Schnittspahnstraße 9, D 64287 Darmstadt*

<sup>2</sup> *Mineralogisch-Petrographisches Institut, Universität Basel, Bernoullistrasse 30, CH-4056 Basel*

A multiple inter-laboratory calibration with illite Kübler-Frey-Kisch „crystallinity“ index and related standards is presented and compared with CIS standards used in the last two decades in very low-grade metamorphic studies. Comparing CIS values with KI standards the CIS values show a higher full width at half-high maximum peak intensity. In all cases due to broadening effects on the Kübler-Index, zone-limits, specifically the diagenetic zone/anchizone boundary, a shift is produced in geographical dimensions in a metamorphic map-view. Combining standardised Kübler-Index and vitrinite-bituminite reflectance measurements a coherent data set for compilation studies can be generated from the data of different research groups.

This attempt to establish a unified database of independent measures to determine diagenetic/metamorphic zones with different analytical instrumental methods are indispensable to present metamorphic maps at very low-grade conditions. Given that the Kübler-Frey-Kisch standards are difficult to preserve for the future and presumably they will be replaced with ongoing time by the CIS standards, a rescue of the laboratory settings from Frey, Kübler and others is done.

After having compiled the Kübler-Index–vitrinite reflectance zones in the Alps for the „New Metamorphic Map of the Alps“, the presented calibration and inter-laboratory correlation gives a chance to save the KI values obtained by very different preparation procedures applied. This is an important step for further studies in an area like the Central Alps with a very high data grid. This correlation study will also make it possible that nearly the 90% of Kübler-Index data from Switzerland can be compared in future work.

Using the same calibration and preparation technique no fundamental problem in data comparison is achieved for the vitrinite/bituminite reflectance data operation. The main problem arises when rock maturity is compared with CIS calibrated Kübler-Index values. Kübler-Index values obtained by the so-called CIS calibration are not compatible with Kübler-Frey-Kisch (Árkai, Aprahamian, Brime, Ferreiro Mählmann, H. Krumm, Leoni, Petschick) calibrated Kübler-Indices. Applying both standardisation approaches for field studies, partially different results are obtained.

Unfortunately, after the retirement or death of the researchers, the rock collections, but also stored rock standards are more and more neglected at Swiss and German Universities, due to financial and space reasons. The excellence status of a university should be visible also in the potential to further re-investigate and use of published data. Refusing this responsibility will complicate research in many geo-science fields.

## 2.7

## Constraining magmatic fluxes through thermal models for contact metamorphism

Floess David<sup>1,2</sup> & Lukas Baumgartner<sup>1</sup>

<sup>1</sup> ISTE, University of Lausanne

<sup>2</sup> University of Geneva (david.floess@unige.ch)

The rate, at which magma ascents (flux) and its manner of accumulation control whether the emplaced increments form a pluton with a low melt fraction, or alternatively, a large mass of eruptible magma (eg. Bachmann & Bergantz, 2008). It is difficult to estimate magma fluxes of ancient systems using geochronology and volumetric estimates. While recent advances permit to date some intrusions with the necessary precision of a few tens of kyrs, it is impossible to estimate the volume accurately. Significant amounts of the pluton might have been eroded or erupted. Here we present a different approach to estimate magma fluxes based on metamorphic isogrades and thermal modeling in the Tertiary Adamello batholith, Northern Italian Alps.

Field, geochronological, geochemical, and structural data suggest that the marginal parts of the Western Adamello Tonalite represent a feeder conduit, through which magma was transported towards shallower levels. The magma flux caused significant heating of the adjacent host rock. Temperature estimates from the host rocks are based on phase petrology modeling of observed (or absent) isogrades. These are (1) the absence of orthopyroxene at a distance of 50m from the intrusive contact ( $T < 815^\circ\text{C}$ ), (2) partial melting occurring at 350m ( $T > 675$ ), and (3) the appearance of andalusite at 1700m ( $T \sim 525$ ). A 1D model was used to study the heat conduction perpendicular to the contact. Magma flow in the conduit was modeled in increments assuming different conduit widths, flow times (active time), for each increment, as well as quiescence (repose time) intervals. We simulated magma flow to occur at the contact, while cooled increments displaced towards the inside of the pluton. Integrated conduit size was taken to be the 500m based on field and structural work. We show that only a small set of variables match the aureole temperature constraints. For example, the thermal profile is well modeled by an active to repose time ratio of 110 years to 3000 years, repeated in 50 cycles of 10m thick feeder zones.

Finally, the minimum amount of magma flowing through this conduit can be calculated using a tabular dyke model (Delaney and Pollard, 1981). The above-cited parameters require a minimum total magma volume of  $30 \text{ km}^3$  to be transported through the feeder towards shallower levels and potentially fed eruptions at the surface. The equivalent time-averaged flux is  $0.17 \text{ m}^3/\text{s}$ . A comparison with time-averaged fluxes of recent volcanoes and the presence of re-worked volcanic sediments in the surroundings of the Adamello batholith (Sciunnach and Borsato, 1994) indicate that the calculated rates and volumes are plausible.

### REFERENCES:

- Bachmann, O., Bergantz, G. 2008: The Magma Reservoirs That Feed Supereruptions. *Elements* 4, 17–21.
- Delaney, P.T., Pollard, D.D. 1981: Deformation of host rocks and flow of magma during growth of Minette dikes and breccia-bearing intrusions near Ship Rock, New Mexico. *Geological Survey Professional Paper* 1–59.
- Sciunnach, D., Borsato, A. 1994: Plagioclase-arenites in the Molveno Lake area (Trento): record of an Eocene volcanic arc. *Studi Trentini di Scienze Naturali - Acta Geologica* 69, 81–92.

## 2.8

### Oxygen isotopes in Ioko-Dovyren layered intrusion rocks

Fomin Ilya<sup>1</sup>, Dubinina Elena<sup>2</sup>, Avdeenko Anna<sup>2</sup> & Ariskin Alexey<sup>3</sup>

<sup>1</sup> Institute of Geophysics, ETH Zürich, Sonneggstrasse 5, CH-8092 Zürich (ilya.fomin@erdw.ethz.ch)

<sup>2</sup> Institute of Geology of Ore Deposits, Petrography, Mineralogy and Geochemistry (IGEM RAS), Russian Academy of Sciences, Staromonetnyy 35, RU-125009 Moscow

<sup>3</sup> Vernadsky Institute of Geochemistry and Analytical Chemistry (GEOKHI RAS), Russian Academy of Sciences, Kosygina 19, RU-119991 Moscow

Ioko-Dovyren layered intrusion is located in the Northern Transbaikalia (Southern Siberia). This intrusion forms 26×3 km mountain ridge, with full layer sequence exposed on the earth surface. Lower part of intrusion contains dunites, lherzolites and troctolites, and the upper one includes gabbroid rocks. Almost all rocks are nearly unaltered. Magma source, influence of surrounding rocks, and Cu-Ni ores formation are still under discussion [Ariskin et al., 2009].

Two profiles in flank parts (Ioko and Shkolnyi) and one profile in central part (Central) of intrusion were sampled. Ioko profile (73÷2005 m from the bottom, flank of the intrusion) is the most unaltered, so it was studied as a reference profile. Central part of the intrusion (138÷1227 m from the bottom) contain zone with high amount of carbonate xenoliths up to 100 meters in size. Shkolnyi profile (162÷784 m from the bottom, another flank of the intrusion) is quiet altered; rocks contain more pyroxene, than other parts of intrusive body.

Olivine (33 samples) and plagioclase (21 samples) were separated from rocks. Analysis was performed in IGEM RAS (laser fluorination technique using BrF<sub>5</sub> with dual inlet measurements by DELTAplus mass-spectrometer). Accuracy is within ±0.1‰. Bulk rock oxygen isotope composition was calculated, for the case than the sum of normative plagioclase and olivine was more than 95%.

Mean δ<sup>18</sup>O values for olivine from Ioko and Shkolnyi profiles is +5.9±0.1‰, and lower part's olivines from Central part has the δ<sup>18</sup>O values +5.8±0.2‰. Olivines near xenoliths in the central part have increased δ<sup>18</sup>O values (up to 7.0).

Almost all plagioclase samples were separated from the Ioko profile rocks. In Central and Shkolnyi profile samples plagioclase is a rare phase. Average δ<sup>18</sup>O value for plagioclase is 7.4±0.2‰.

A previous oxygen isotope data (overviewed in [Kislov, 1998]) have shown huge variations of δ<sup>18</sup>O for olivine (from +2.6‰ to +19‰). We suppose that these values are the result of technical disadvantages of the old fluorination methods. Recent studies of [Orsoev, 2010] for narrow zone of Ioko-Dovyren intrusion have shown similar results to our data. Our study gave the first systematic data on δ<sup>18</sup>O for minerals and rocks of Ioko-Dovyren layered intrusion.

Almost constant values of olivine δ<sup>18</sup>O in Ioko (flank) profile for the first 2000 m of intrusion allow us to suppose nor frame rocks, nor xenoliths could not affect on magma composition significantly. Dispersion of δ<sup>18</sup>O values in other parts of intrusion could be caused by intrachamber processes.

The δ<sup>18</sup>O values for olivine and bulk rock represents frame-rocks influence only near xenolith-rich zones. Interval of the influence is about 200-250 meters (fig. 1), and it is located above xenolith zones. Probably, it is the result of anatectic melt and fluid upwards migration [Mollo et al., 2010].

Values of δ<sup>18</sup>O in olivine and bulk rocks conform to slab melting products [Bindeman et al., 2005]. It is important result, because magma origin and history are still under discussion.

#### REFERENCES

- Ariskin, A.A., Konnikov, E.G., Danyushevsky, L.V., et al. 2009: The Dovyren intrusive complex: problems of petrology and ni sulfide mineralization. *Geochemistry International*, 47, 425-453.
- Bindeman, I. N., Eiler, J. M., Yogodzinski, G. M., et al., 2005: Oxygen isotope evidence for slab melting in modern and ancient subduction zones. *Earth and Planetary Science Letters*, 235, 480-496.
- Kislov, E.V., 1998: Ioko-Dovyren layered massif (in Russian). Published by BNTs SO RAN, 1998, 265.
- Mollo, S., Gaeta, M., Freda, C., et al., 2010: Carbonate assimilation in magmas: A reappraisal based on experimental petrology. *Lithos*, 114, 503-514
- Orsoev, D.A., 2010: Distribution of Oxygen Isotopes in Rocks and Minerals from the Critical Zone of the Ioko-Dovyren Pluton. *Geology of Ore Deposits*, 52, 543-550

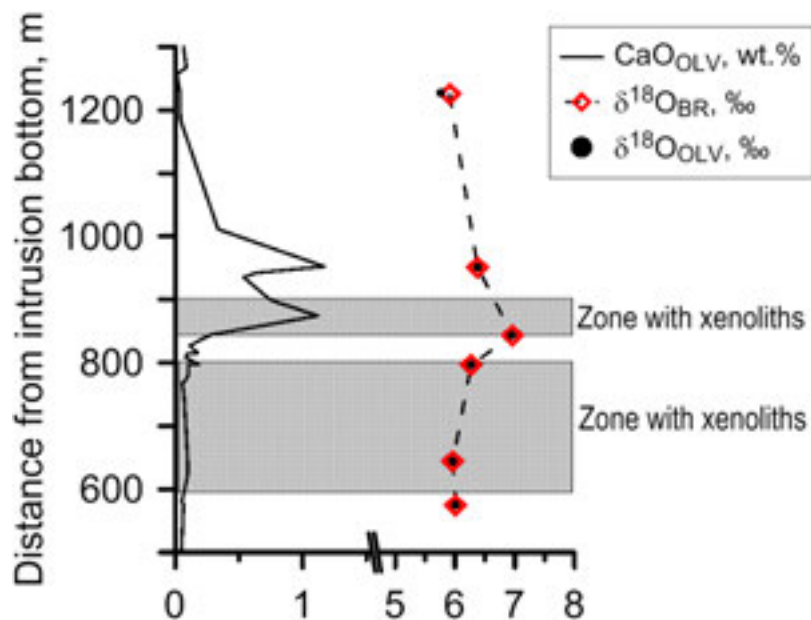


Figure 1. Zones with xenoliths caused increased level of CaO in olivine and values of  $\delta^{18}\text{O}$ .

## 2.9

### Volcanostratigraphic Controls on the Occurrence of Massive Sulfide (VMS) Deposits in the Semail ophiolite, Oman

Gilgen Samuel Andreas<sup>1</sup>, Diamond Larryn William<sup>1</sup>, Ivan Mercolli<sup>1</sup>

<sup>1</sup>Institute of Geological Sciences, University of Bern, Baltzerstrasse 1+3, CH-3012 Bern ([samuel.gilgen@geo.unibe.ch](mailto:samuel.gilgen@geo.unibe.ch))

The Semail ophiolite in northern Oman is capped by up to 2 km of basaltic–andesitic lavas that host copper-dominant, Cyprus-type, volcanogenic massive sulfide (VMS) deposits. This study identifies the multiple volcanostratigraphic horizons on which the deposits are situated, based on characterization of footwall and hanging-wall lavas from 16 deposits or deposit clusters. Comparison of their field and petrographic features, compositions of igneous clinopyroxenes and whole-rock geochemical signatures permits their classification within a modified version of the established regional volcanostratigraphy.

Four extrusive units host VMS deposits: Geotimes (earliest), Lasail, Alley and Boninitic Alley (latest). The latter was known only at a few localities but the present study reveals its regional extent and significance as a host for VMS deposits. The new results show that VMS deposits sit on or near the Geotimes/Lasail and Geotimes/Alley contacts as well as entirely within the Lasail, Alley and Boninitic Alley Units. The Geotimes and Lasail Units represent Late Cretaceous, ocean spreading ridge and related off-axis volcanic environments respectively. Highest Cu grades tend to occur in deposits lying on or within the Geotimes. The Alley and Boninitic Alley Units represent younger, subduction-related volcanism prior to Coniacian–Santonian obduction of the ophiolite. Highest Au grades occur in deposits within the Boninitic Alley.

In contrast to earlier studies, the new results show that essentially every horizon that marks a hiatus in lava deposition in the Semail ophiolite, i.e. contacts between the four major eruptive units, and umbers and sedimentary chert layers within the units, has exploration potential for Cu–Au VMS deposits.

## 2.10

# Quantification of successive reactive melt flow episodes in a layered intrusion (Unit 9, Rum Eastern Series, Scotland)

Leuthold Julien<sup>1,2</sup>, Blundy Jonathan<sup>1</sup>, Holness Marian<sup>1</sup>

<sup>1</sup>School of Earth Sciences, University of Bristol, Bristol, BS8 1RJ, United Kingdom (julien.leuthold@bristol.ac.uk)

<sup>2</sup>Department of Earth Sciences, University of Cambridge, Cambridge, CB2 3EQ, United Kingdom

In plutonic rocks formed by the accumulation of crystals, reactive melt flow (or infiltration metasomatism) modifies the composition and geochemistry of the percolating liquid and the crystal mush through which it migrates. Displacing the liquid line of descent from that of a simple, closed-system differentiation trend changes the mineral saturation temperature, geochemistry and texture, resulting in the formation a texturally and chemically different rock. Here we present a detailed multidisciplinary study of Unit 9 of the Rum Eastern Layered Intrusion, Scotland, to identify and quantify the importance of such processes in the development of these cumulate rocks. Unit 9 is composed of Plg wehrlite with poikilitic Plg and Cpx, troctolite with interstitial Cpx, and equigranular gabbro (Figure 1). Gabbro enclaves occur within troctolite. Cpx rims are poorly developed in layered Plg wehrlite and troctolite and bulk rock analyses display distinct Eu positive anomalies, evidencing loss of interstitial liquid. Cpx rims are Cr-poor, REE-rich and display low La/Sm ratio relative to associated cores. Troctolite is overlain by gabbro, separated by a wavy horizon. Gabbro Cpx show discrete reverse Cr and REE zoning and a constant high La/Sm ratio. Interstitial Cpx in troctolite and equigranular Cpx in gabbro become progressively oikocrystic towards the northern edge of an intrusive Plg wehrlite sill, forming poikilitic gabbro with Cpx oikocrysts. Oikocrysts consist of Cr-rich (~1.1 wt% Cr<sub>2</sub>O<sub>3</sub>), moderate REE, and high La/Sm anhedral cores (core1) that enclose randomly oriented small (up to 0.5 mm) Ol and Plg inclusions (Figure 2). Cores are overgrown by a moderate-Cr (~0.7 wt% Cr<sub>2</sub>O<sub>3</sub>), REE-poor, high La/Sm anhedral zone (core2). Oikocryst rims are Cr-poor (~0.2 wt% Cr<sub>2</sub>O<sub>3</sub>), REE-rich and display lower La/Sm ratio. They enclose large (1 mm) oriented Plg and Ol crystals. The rim thickness increases from the base of Unit 9 to the top. Cpx rim crystallization is synchronous with cumulate pile compaction.

Equilibrium liquids responsible for Cpx precipitation were calculated using partition coefficients. The liquids parental to the Plg wehrlite, troctolite and poikilitic gabbro Cpx cores display a higher La/Sm ratio and higher REE content than the corresponding rims and associated picritic dykes. The REE pattern of the liquids in equilibrium with the Cpx cores is interpreted as a signature of partial melting, compatible with the resorption texture. Cpx core1 of all lithologies crystallized from the parental Rum picritic liquid. Cpx core2 are best explained by 59% partial fractional melting of a gabbroic assemblage (Rum interstitial crystals or bulk gabbro), mixed with 70% picritic liquid, with subsequent Rayleigh fractional crystallization ( $F = 1-0.6$ ). Gabbro enclaves within troctolite are relics after partial melting. The multiple generations of Cpx are witness to successive melting episodes resulting from repeated incursions of picritic melt. Cpx rims are best explained by partial melting (34%) of a Cpx-poor gabbroic assemblage, mixed with picritic liquid (70%) and subsequent Rayleigh fractional crystallization ( $F = 1-0.3$ ).

Subsequent intrusions of Plg wehrlite sills induced partial melting of the Unit 9 gabbro. Once porosity was sufficient, differentiating liquids from the Plg wehrlite percolated throughout the crystal mush pile, mixing with interstitial liquid and crystallizing the interstitial crystals. Thus, through reactive melt flow, the composition of the percolating liquid and the cumulate rocks differ from simple fractionation products along the Rum liquid line of descent.

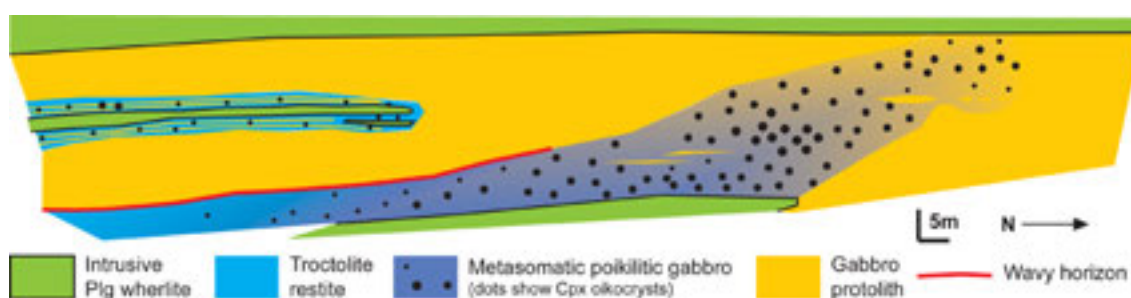


Figure 1. Vertical sketch of the Rum Eastern Layered Intrusion (Unit 9), showing the Plg wehrlite - troctolite - gabbro succession. Troctolite and gabbro are separated by a sharp wavy horizon. Troctolite grades into poikilitic gabbro towards the Plg wehrlite northern extremity, with large Cpx oikocrystic. The poikilitic gabbro forms an oblique channel throughout the overlying gabbro. Gabbro enclaves occur within poikilitic gabbro.

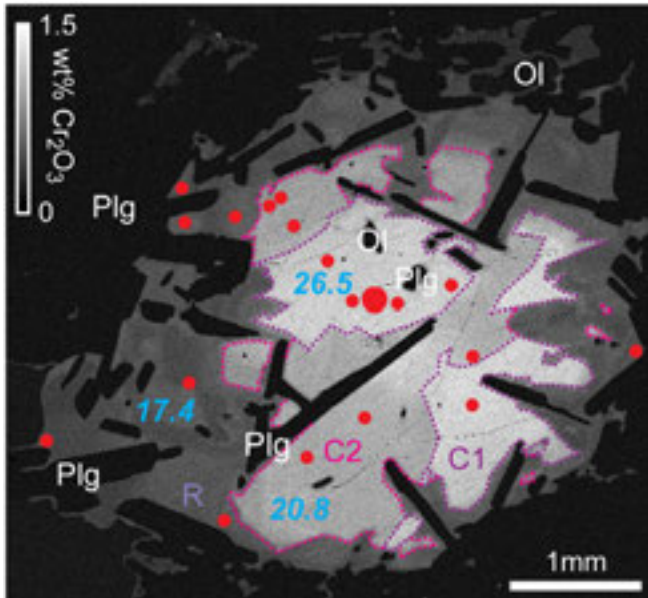


Figure 2: Rum poikilitic gabbro Cpx EMPA Cr map. Blue italic values are calculated equilibrium melt La/Lu ratios (using DREE of Wood & Blundy, 1997). Note the two successive episodes of Cpx partial melting, overgrown by a Cr-poor, LREE-depleted rim. Red dots show LA-ICP-MS analyses. C1=Core1, C2=Core2, R=Rim.

## 2.11

### Barium isotope fractionation in coral skeleton: Tracking anthropogenic contaminations?

Pretet Chloé<sup>1,2</sup>, Nägler Thomas F.<sup>3</sup>, Reynaud Stéphanie<sup>4</sup>, Böttcher Michael E<sup>5</sup>, Samankassou Elias<sup>1</sup>

<sup>1</sup>Section of Earth and Environmental Sciences, University of Geneva, Switzerland

<sup>2</sup>Present address: Department of Environmental Geosciences, University of Vienna, Austria

<sup>3</sup>Institut für Geologie, University of Bern, Switzerland

<sup>4</sup>Centre Scientifique de Monaco, Monaco

<sup>5</sup>Geochemistry & Isotope Geochemistry Group, Leibniz Institute for Baltic Sea Research (IOW), Warnemünde, Germany

We plan to gain a first order view of the marine Barium (Ba) isotope cycle by measuring the Ba isotopic composition of carbonates and seawater. Ba in ocean water originates from two major natural sources, i.e. terrestrial weathering and hydrothermal precipitates. Further, an additional Ba source is coming from the use of diagenetic barite in drilling mud for oil and gas exploration. Barium with an exploration/production origin is found in modern sediments and is a potential source of stress for scleractinian corals (e.g. Lepland and Mortensen, 2008). A special focus, therefore, is the question whether the different Ba sources are reflected in Ba isotope ratios of carbonate archives.

The present sample set is composed of modern scleractinian coral skeletons. Some corals were cultured in monitored aquaria (CSM, Monaco) others originate from natural environments (warm water corals: the Bahamas/Florida, cold water corals: the Norwegian shelf). The analytical procedure includes the application of a <sup>130</sup>Ba/<sup>135</sup>Ba double spike, a cation exchange column followed by isotope measurements on a Nu Instruments Multicollector ICP-MS. The Ba fractionation of the samples is compared to a Ba nitrate standard solution, IAEA BaCO<sub>3</sub> and BaSO<sub>4</sub> standards, and a natural limestone standard (BSC-CRM 393).

Coral skeletons show a significant positive fractionation (mean = 0.4 ± 0.05 ‰, 2 SEM) compared to the Ba nitrate standard solution (± 0.1 ‰, 2SD, N=270). This signature is significantly different from barites from a massive Cambrian deposit (-0.5‰) and a further diagenetic barite (von Allmen et al. 2010) as well as from experimental orthorhombic Ba carbonate (von Allmen et al., 2010, unpublished data).

Thus, corals from different environments bear the potential to serve as an archive of environmental influence on the Ba cycle (e.g. upwelling regions or influenced by terrestrial or industrial input). Given that the most important economic occurrences of barite are stratabound massive beds, it appears reasonable to test the hypothesis that potential Ba pollution from drilling fluid are detectable in corals, based on Ba isotopes. Thus, our results clearly encourage a further investigation of the Ba cycle by means of Ba isotope analyses on different natural materials and settings. The more the Ba cycle is constrained in detail, the better the anthropogenic influence can be deciphered from the natural signal, for instance in the vicinity of drilling sites, where barium-enriched drilling muds are in use.

#### REFERENCES

- Lepland, A. & Mortensen, P.B. 2008: Barite and barium in sediments and coral skeletons around the hydrocarbon exploration drilling site in the Traena Deep, Norwegian Sea. *Environ. Geol.*, 56, 119-129
- von Allmen, K., Böttcher, M.E., Samankassou, E., Nägler, Th. F. 2010: Barium isotope fractionation in the global barium cycle: First evidence from barium minerals and precipitation experiments. *Chem. Geo.* 277, 70-77

## 2.12

### Ore-forming fluids associated with the early mineralization at Cerro de Pasco, Peru

Rottier Bertrand, Kouzmanov Kalin, Fontboté Lluís

*Earth and Environmental Sciences, University of Geneva, rue des Maraîchers 13, CH-1205 Geneva, Switzerland  
(Bertrand.Rottier@unige.ch)*

Cerro de Pasco, central Peru, is a large Cordilleran base metal deposit formed along the eastern margin of a diatreme-dome complex, as part of the Miocene metallogenic belt of central and northern Peru. It was formed during two stages of mineralization by fluids with contrasting  $f_{S_2}$ ,  $f_{O_2}$  and pH (figure 1). Recent work (Rottier et al., 2013) has shown that stage-1 consists of a number of pyrrhotite pipes that grade outwards into massive Fe-rich sphalerite and galena rims; they are structurally controlled by major N-S faults. Their inner parts contain minor arsenopyrite and Fe-rich sphalerite, as well as traces of chalcopyrite, galena and stannite (Baumgartner et al, 2007). During stage-2, a massive body consisting mainly of pyrite and quartz was emplaced. It is associated with a pervasive sericite-pyrite alteration affecting the diatreme-dome complex. Subsequent to the emplacement of the pyrite-quartz body, high-sulfidation mineralization was formed. It is expressed in the western part of the deposit, as a set of E-W-trending Cu-Ag-(Au-Zn-Pb) enargite-pyrite veins hosted by the diatreme-dome complex, and, in the eastern part, as large well-zoned Zn-Pb-(Bi-Ag-Cu) carbonate replacement ore bodies (figure 1).

A systematic microthermometry study on primary and pseudo-secondary fluid inclusions assemblages (FIAs) in quartz and Fe-rich sphalerite from the pyrrhotite pipes and their rims, and in quartz from the pyrite-quartz body, has been performed for the first time. All the fluid inclusions are aqueous, liquid-rich, with 20-30 vol% vapor phase.

Quartz- and sphalerite-hosted fluid inclusions from the pyrrhotite pipes show a systematic center-to-rim decrease of homogenization temperature ( $T_h$ ), from 355° to 205°C, and salinity, from 15.2 to 3.23 wt% NaCl equiv. (figure 2A). This pattern results from mixing between a hot and saline magmatic fluid with dilute meteoric waters.

FIAs hosted in quartz from the pyrite-quartz body show a complex pattern. The large majority homogenize at 270-220°C (figure 2B). A few FIAs have lower  $T_h$ , between 220° and 175°C. These FIAs are always hosted by the last growth band of crystals or are from samples from the upper part of the pyrite-quartz body, thus recording the cooling of the system. Fluid salinity varies from 16.13 to 2.4 wt% NaCl equiv; in most of the studied quartz crystals salinity decreases towards the crystal border without correlation with  $T_h$ . This implies a progressive fluid dilution at roughly constant temperature, related to mixing with a less saline magmatic fluid or with a heated meteoric fluid. One FIA presents higher salinity (~23 wt% NaCl equiv.) and low eutectic temperatures (<-50°C), indicating presence of  $CaCl_2$ -dominated fluids (figure 2B), possibly due to local input of basinal brine-type fluids or formation waters.

$CO_2$  has been detected by Raman microspectroscopy in all FIAs from the pyrrhotite pipes and their outer sphalerite-bearing rims. In FIAs from the pyrite-quartz body,  $CO_2$  has been detected only in samples taken from depths <200 m from the present day surface. Such a vertical zoning is indicative of phase immiscibility between  $CO_2$  and  $H_2O$ .

These preliminary results are consistent with the new field and textural findings (Rottier et al, 2013) indicating that pyrrhotite pipes constitute the earliest mineralizing events at Cerro de Pasco. Further, the results suggest complex mixing of magmatic fluids with others coming from different sources. LA-ICP-MS analyses of fluid inclusions will contribute to a better understanding of the fluid evolution within the studied sequence.

#### ACKNOWLEDGEMENTS

This research is supported by the Swiss National Science Foundation (grant 200020\_134872).

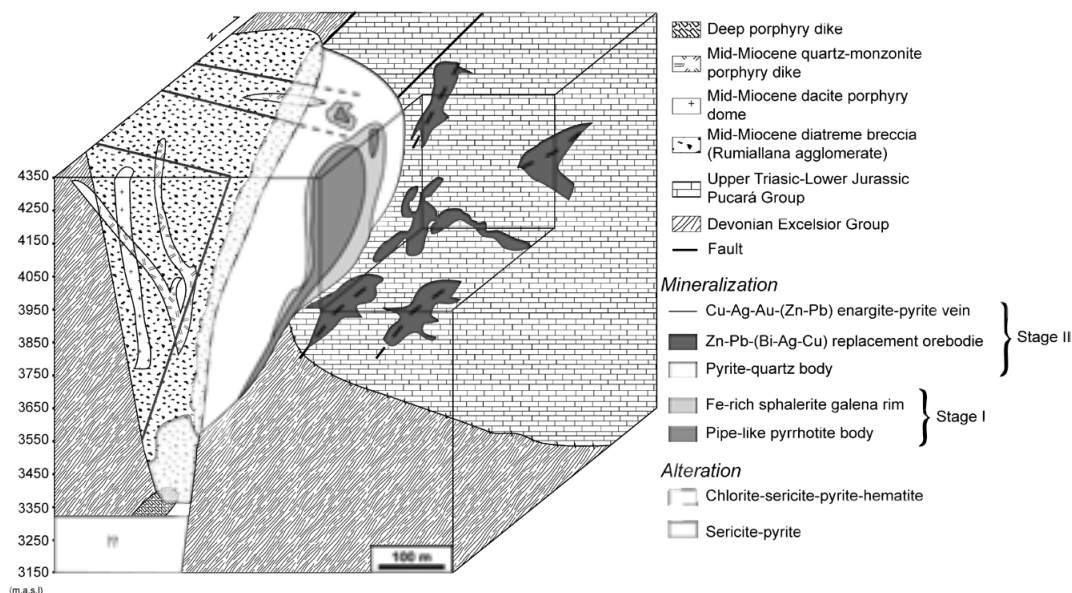


Figure 1. Block diagram showing the two stages of mineralization (modified from Baumgartner, 2007).

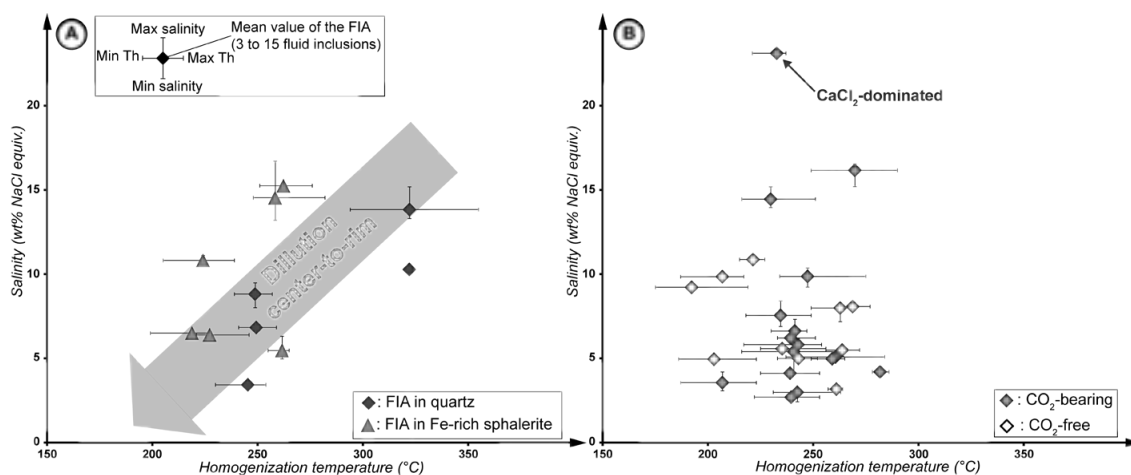


Figure 2. Microthermometry results: A. Pyrrhotite pipes and their rims, B. Pyrite-quartz body (quartz-hosted FIAs).  $\text{CO}_2$  presence detected by Raman microspectroscopy. Salinity values not yet corrected for  $\text{CO}_2$  content.

## REFERENCES

- Baumgartner, R., Fontboté, L., Vennemann, T. 2008: Mineral zoning and geochemistry of epithermal polymetallic Zn-Pb-Ag-Cu-Bi mineralization at Cerro de Pasco, Peru. *Economic Geology* 103, 493-537.
- Rottier, B., Casanova, V., Fontboté, L., Kouzmanov, K., Alvarez, H., Bendejú, R. 2013: Early mineralization at Cerro de Pasco (central Peru) revisited. *Proceedings of the 12th Biennial SGA Meeting, 12–15 August 2013, Uppsala, Sweden*, ISBN 978-91-7403-207-9, 864–868.

## 2.13

### Distinguishing metacarbonatites from marbles – Challenge from the carbonate-amphibolite-epidotite rock association in the Pelagonian zone (Greece)

Filippo Luca Schenker<sup>1</sup>, Jean-Pierre Burg<sup>1</sup>, Dimitrios Kostopoulos<sup>2</sup>

<sup>1</sup> Geological Institute, ETH Zurich, Sonneggstrasse 5, 8092 Zürich, Switzerland ([filippo.schenker@erdw.ethz.ch](mailto:filippo.schenker@erdw.ethz.ch))

<sup>2</sup> National and Kapodistrian University of Athens School of Science, Zographou Athens 157 84, Greece

Carbonate rocks were found in association with amphibolites and epidotites in the greenschist- to amphibolite-facies metamorphic basement of the Pelagonian zone (Greece). The mafic rocks both include and are truncated by the carbonates, hinting to a cogenesis of siliceous and carbonatic magmas/fluids. The carbonates have an isotopic signature of  $\delta^{13}\text{C}$  ranging from -5.18 to -5.56 (‰ vs. PDB) and of  $\delta^{18}\text{O}$  from 10.68 to 11.59 (‰ vs. SMOW) giving them the geochemical characteristic of carbonatites (magmatic carbonates). Mafic rocks have high Nb and Ta concentrations, typical for alkaline basalts. Therefore, textural relationships and geochemical signals in both the silicate and carbonate rocks hint at a cogenetic, mantle origin. SHRIMP U-Pb zircon ages from a carbonate bearing amphibolite date the intrusion at 278 Ma (magmatic zircon cores), well before the metamorphic event at 118 Ma (metamorphic zircon rims).

However, the concentration of rare earth elements (REE) in the carbonates, amphibolites and apatites is lower than in typical carbonatites, probably because of the interaction with metamorphic fluids during the Cretaceous metamorphism. Since these low REE concentrations raise doubts regarding the carbonatitic origin, other processes altering the  $\delta^{13}\text{C}$  have to be considered. Skarn metasomatism can fractionate the  $\delta^{13}\text{C}$  in the carbonates to carbonatitic values, but the absence of a Cretaceous contact metamorphism speaks against that possibility leaving the suggestion that the carbonatite rock association sign the Permian opening of the Tethys Ocean in the eastern Mediterranean.

## 2.14

### Evaluation of the mineral potential in the Bjørnesund greenstone belt, southern West Greenland, combining multivariate studies, field work and geochemistry

Denis Martin Schlatter<sup>1</sup> & Bo Møller Stensgaard<sup>2</sup>

<sup>1</sup> Helvetica Exploration Services GmbH, Carl-Spitteler-Strasse 100, CH-8053 Zürich ([denis.schlatter@helvetica-exploration.ch](mailto:denis.schlatter@helvetica-exploration.ch))

<sup>2</sup> De Nationale Geologiske Undersøgelser for Danmark og Grønland - GEUS, Ø. Voldgade 10, DK-1350 Kbh. K

The Bjørnesund area is dominated by amphibolites containing bodies and slivers of ultramafic to mafic rocks and gneiss whereas granitic rocks and anorthosite are minor (Fig. 1). Based on regional qualitative and quantitative mineral potential mapping for gold the Bjørnesund West and East areas were selected for field work with the aim to provide new detailed information, sampling and mapping from the area in order to characterise the geological environment, follow up on results from the mineral potential mapping and processed remote sensing data and evaluate the possibilities for gold mineralisations in the areas. A newly compiled, detailed and geo-referenced digital geological map, a new gold discovery and recognition of areas potential to host Ni and platinum group element (PGE) resulted from this work. The most interesting gold occurrences were found in a hydrothermally altered shear zone. This several tens-of-metre wide shear zone is located in the Bjørnesund West area (Fig. 1). The shear zone trends northeast-southwest and dips 80 degrees towards the southeast. It can be followed over several hundreds of metres along strike. This shear zone contains a 50 cm yellow-brownish, rusty stained amphibolite, which hosts parallel quartz-carbonate-feldspar veinlets. Chip samples over 50 cm, within the amphibolite hosted quartz-carbonate-feldspar veined shear zone yield 569 ppb Au, and alteration related to this Au-mineralization is of the Grt, Bt, Iron oxide-hydroxide type (Kolb et al. 2013).

Artificial neural network analysis has been used for mineral potential mapping and this analysis has predicted the area where the gold was found as being favourable. Elevated Ni/Mg ratios from analyzed stream sediment samples have also indicated the same area as being favourable. Lithogeochemistry was applied and based on immobile-element-ratio classification seven types of amphibolites were discriminated and the gold horizon was found to be located at the contact of basalt A and basalt E (Schlatter & Stensgaard 2012). Interpretation of ASTER remote sensing data have identified anomalous levels of  $Fe^{3+}$  and the follow up field work has shown that several of these anomalous areas correspond to extensive rust zones which in term were caused by surface weathering of ultramafic dunitic and pyroxenitic rocks. Chemical analysis of samples from these rust zones have revealed elevated Ni, Cr, Co and PGE contents, and pentlandite, which was identified using an electron microprobe.

These findings indicate that the Bjørnesund anorthosite-greenstone belt has the potential to host economic mineral deposits: gold and possibly Ni-PGE deposits. Field work has confirmed that the area is highly prospective, as outlined prior to field work. The spatial association of gold and Ni-PGE occurrences in the Bjørnesund area is intriguing and possibly is related to a deep seated crustal structure which has brought ultramafic dunitic and pyroxenitic rocks from deeper parts of the crust to higher levels as well as fluids associated with gold. The results presented here show that the multidisciplinary approach using qualitative conceptual and quantitative mineral potential multivariable studies, geological maps and lithogeochemistry can be applied to generate targets previous to field work. Field work on the ground should then subsequently be carried out in order to successfully confirm that such predicted areas are indeed host to mineral resources.

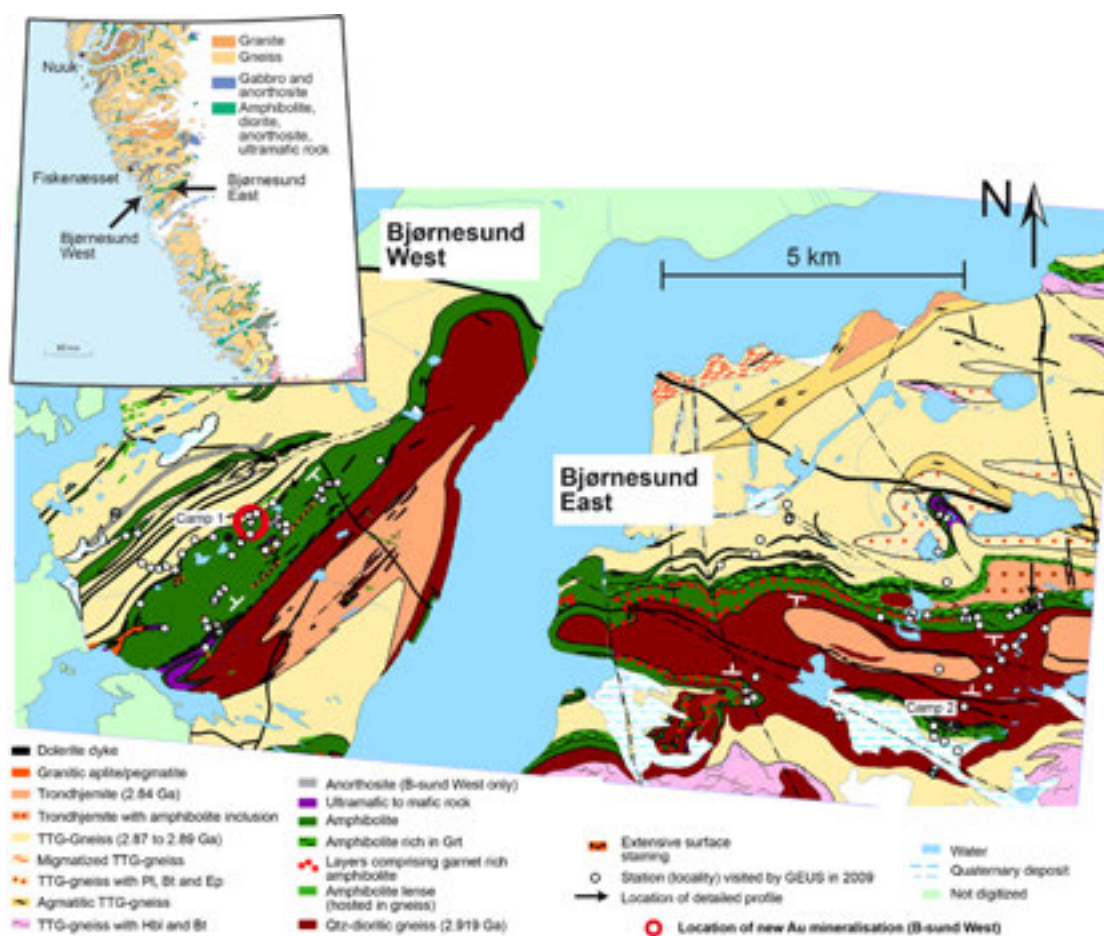


Figure 1. A newly compiled, detailed and geo-referenced digital geological map (modified from Escher & Pulvertaft 1976) showing the Bjørnesund West and East areas, as well as the location where gold was discovered in 2009 by using mineral potential mapping.

## REFERENCES

- Escher, J.C., & Pulvertaft, T.C.R. 1995: Geological map of Greenland, 1:2 500 000. Copenhagen: Geological Survey of Greenland.
- Kolb J, Dziggel A, & Schlatter, D.M. 2013: Gold occurrences of the Archean North Atlantic craton, Southern West and South West Greenland: A review and first approach to a comprehensive genetic model. *Ore Geology Reviews* 54: 29-58.
- Schlatter, D.M., & Stensgaard, B.M. 2012: Evaluation of the mineral potential in the Bjørnesund Greenstone Belt combining mineral potential mapping, field work and lithogeochemistry. *Danmarks og Grønlands Geologiske Undersøgelse Rapport 2012/60*, 60 pp.

## 2.15

**Modeling water-rock interactions in Icelandic hydrothermal systems**

Thien Bruno<sup>1</sup>, Kosakowski Georg, Kulik Dmitrii

*Laboratory for Waste Management, Nuclear Energy and Safety Research Department, Paul Scherrer Institut, CH-5232 Villigen*

<sup>1</sup>*bruno.thien@psi.ch*

We present first results of a modeling study on the mineralogical and porosity evolution of Icelandic hydrothermal systems. The study is part of the COTHERM project (COMbined hydrological, geochemical and geophysical modeling of geot-THERMal systems) that is an integrative research project to advance our understanding of the sub-surface processes of magmatically-driven natural geothermal systems.

The geothermal systems of interest are typically high enthalpy systems where a pluton located at few km depth increases the geothermal gradient and triggers a hydrothermal circulation. The bedrock is expected to interact and equilibrate with circulating fluids. The spatial and temporal variable mineralogical evolution typically depends on the composition, temperature (and pressure) of the circulating fluid, the composition of the rock and the character of the fluid pathways (fractured or porous medium).

We investigate two hydrothermal systems: Krafla, for which the water recharge consists of meteoritic water; and Reykjanes, for which the water recharge mainly consists of seawater.

In a first attempt, we model only one fluid path with a 1D porous media approach with the OpenGeoSys-GEM code. The open source code OpenGeoSys for modeling multi-physics problems is based on Finite Elements (Kolditz et al. 2012) and is used to calculate fluid flow and heat and mass transport. The code is coupled with the numerical kernel of the GEM-Selektor geochemical modeling package (Kulik et al. 2013). The GEM approach minimizes the total Gibbs energy of the system computed from species amounts and primal chemical potentials. The kinetic control of mineral dissolution/precipitation reaction constraints on the mass balance can be enforced for any chemical species based on various kinetic equations (e.g. Palandri & Kharaka, 2004; Pham et al., 2011).

We consider a fluid pathway from the surface to 3 km depth, and back to the ground surface. Initially at each grid node we attribute specific P and T conditions. The composition of the injected fluid is, depending on the case, meteoric water, sea water, or a mixture of both. In a first attempt we set a constant temperature along the fluid path based on an enhanced geothermal gradient. More realistic models will be based on results from another COTHERM subprojects which concentrates on the realistic simulation of fluid and heat transport including phase changes and multi-phase flow.

The initial rock composition is a fresh basalt. We considered basalt minerals dissolution kinetics according to Palandri & Kharaka (2004). Reactive surface areas are supposed to be geometric surface areas, and are corrected using a spherical-particle dissolution model. For secondary minerals, we consider that they reach partial equilibrium, assuming that primary mineral dissolution is slow, whereas secondary mineral precipitation is rather fast. Our first modeling results evidenced that such a concept is not able to satisfactorily describe mineralogical assemblages as observed in the field by Gudmundsson & Arnorsson (2005) and by Icelandic partners of the COTHERM project. Currently we work on implementing kinetic controls also for secondary minerals.

Proper account for mineral precipitation kinetics in reactive transport modeling is a challenge, because:

1. Available experimental kinetic parameters are relatively sparse in the literature; when exist, they are often inconsistent;
2. The experimentally determined mineral surface area is not necessarily the same as the reactive mineral surface area;
3. Since secondary phases do not exist initially, their nucleation rates must be included in the kinetic model. It is then not completely clear how the reactive surface area evolves in time because it is related to nucleation mechanisms, which are poorly known.

## REFERENCES

- Gudmundsson B.T., Arnorsson S., 2005. Secondary mineral-fluid equilibria in the Krafla and Namafjall geothermal systems, Iceland. *Applied Geochemistry* 20, 1607-1625.
- Kolditz, O., Bauer, S., Bilke, L., Boettcher, N., Delfs, J.O., Fischer, T., Goerke, U.J., Kalbacher, T., Kosakowski, G., McDermott, C.I., Park, C.H., Radu, F., Rink, K., Shao, H., Shao, H.B., Sun, F., Sun, Y.Y., Singh, A.K., Taron, J., Walther, M., Wang, W., Watanabe, N., Wu, Y., Xie, M., Zehner, B., 2012. OpenGeoSys: An open source initiative for numerical simulation of thermo-hydro mechanical/chemical (THM/C) processes in porous media. *Environmental Earth Sciences* in press, 1-13. <http://www.opengeosys.net>
- Kulik D.A., Wagner T., Dmytrieva S.V., Kosakowski G., Hingerl F.F., Chudnenko K.V., Berner U., 2013. GEM-Selektor geochemical modeling package: revised algorithm and GEMS3K numerical kernel for coupled simulation codes. *Computational Geosciences* 17, 1-24. <http://gems.web.psi.ch>
- Palandri, J.L., Kharaka, Y.K., 2004. A compilation of rate parameters of water-mineral interaction kinetics for application to geochemical modelling. U.S. Geological Survey, Menlo Park, CA, pp. 1-64.
- Pham V.T.H., Lu P., Aagaard P., Zhu C., Hellevang H., 2011. On the potential of CO<sub>2</sub>-water-rock interactions for CO<sub>2</sub> storage using a modified kinetic model. *International Journal of Greenhouse Gas Control* 5, 1002-1015.

## 2.16

## Magmatic-hydrothermal fluid evolution of a multiphase porphyry-centered system: the Miocene Morococha district, central Peru

Tomé Cristina<sup>1</sup>, Kouzmanov Kalin<sup>1</sup>, Fontboté Lluís<sup>1</sup>, Bendejú Aldo<sup>1</sup> & Wälle Markus<sup>2</sup>

<sup>1</sup>Department of Earth Sciences, University of Geneva, Rue des Maraîchers, CH-1205 Geneva ([cristina.tome@unige.ch](mailto:cristina.tome@unige.ch))

<sup>2</sup>Institute of Isotope Geochemistry and Mineral Resources, ETH Zentrum, CH-8092, Zurich

The world-class Miocene Morococha mining district in central Peru represents one of the best examples of multiphase porphyry-centered systems, overprinted by a late-stage Cordilleran polymetallic vein and replacement type mineralization (Bendejú et al., 2008; Kouzmanov et al., 2008). Detailed geological, geochronological and structural studies on both porphyry and polymetallic ore-bodies in Morococha have been recently reported (Bendejú et al., 2008; Catchpole et al., 2011). In this contribution we present new data on the magmatic-hydrothermal fluid evolution at Morococha, combining fluid inclusion microthermometry, LA-ICP-MS, SEM-CL, and Raman microspectrometry analyses on the high-T-P porphyry style mineralization.

The recently identified centers that represent this porphyry style mineralization include the following three that are studied in this work (Fig. 1): i) Codiciada Cu-Mo center (9.3 – 8.8 Ma); ii) Ticlio Cu-Au center (8.3 – 8.05 Ma), and iii) Toromocho porphyry Cu-Mo center (7.7 – 7.2 Ma). Codiciada and Toromocho consist of composite stocks, while Ticlio represents essentially a single intrusion. In order to constrain temperature and pressures of ore formation, we have applied microthermometry on vapor-liquid “boiling” assemblages in early quartz (+/- sulfides) stockwork veins. Results give temperatures and pressures ranging from 533° to 450 °C / 380 - 400 bar in Codiciada, 460° to 350 °C / 230 to 255 bar in Ticlio and 350° to 300 °C / 120 to 150 bar in Toromocho. These estimations are supported by the titanium-in-quartz geothermometer (Wark and Watson, 2006), using trace-element LA-ICP-MS data for the host quartz crystals. Pressure estimates are indicative of magmatic and hydrothermal activity in the area and are in good correlation with available data on the erosion / uplift history of the system as a whole. The Codiciada center was formed at higher pressure and depth, compared to the 0.5 my younger Ticlio center and the still 0.3 Ma younger and shallower Toromocho center (Fig. 2). Such a scenario is typical for telescoped systems worldwide (Sillitoe, 1994, 2010) and may have important implications for exploration strategies in multiple porphyry-centered districts.

On respect to the fluid composition studied by LA-ICP-MS, presence of high concentrations of Cu, Mo as well as S has been observed in each center, among other elements. Ongoing study will elucidate if the three mineralized centers share the same magmatic source or are fed by independent pulses of magma. Especially interesting is the presence of significant concentrations of elements commonly considered as “immobile”, such as Ti, Y, La, Ce, and V in the intermediate-density high-temperature fluid inclusions, regarded as analogues of the pristine magmatic fluid, as well as in the hypersaline liquid inclusions resulting from phase separation.

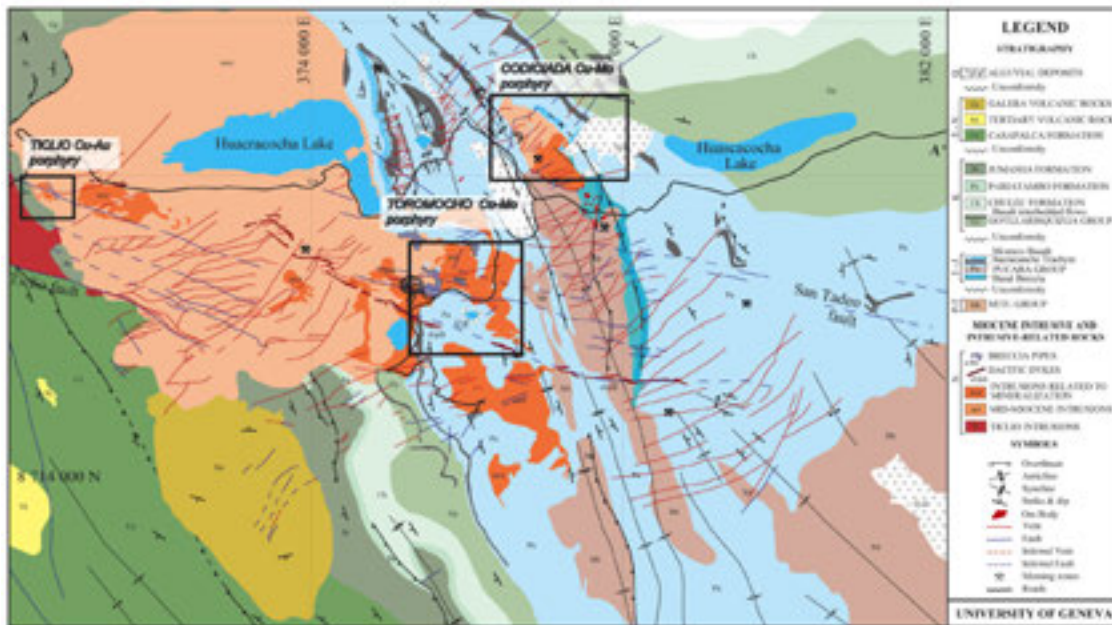


Figure 1. Geologic map of the Morococha mining district, modified after Bendezú et al. (2008).

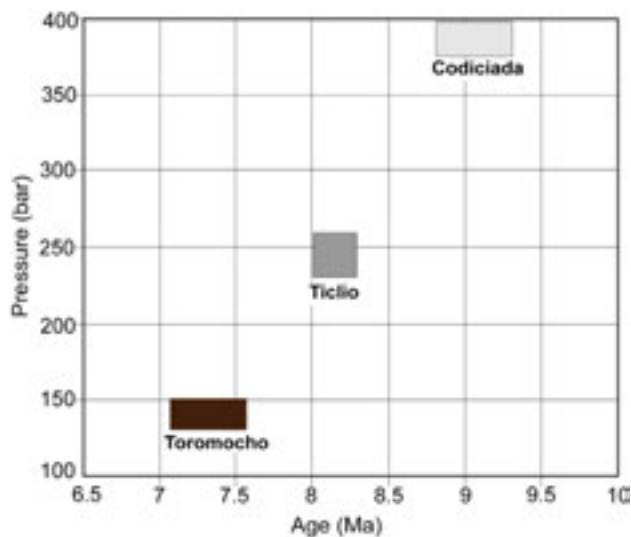


Figure 2. Age vs. pressure diagram showing the ranges for the three studied porphyry centers.

## REFERENCES

- Bendezú, A., Catchpole, H., Kouzmanov, K., Fontboté, L. & Astorga, C. 2008: Miocene magmatism and related porphyry and polymetallic mineralization in the Morococha district, central Peru. XIII Geological Congress of Peru, Lima.
- Catchpole, H., Kouzmanov, H., Fontboté, L., Guillong, M. & Heinrich, C.A. 2011: Fluid evolution in zoned Cordilleran polymetallic veins-insights from microthermometry and LA-ICP-MS of fluid inclusions. *Chemical Geology*, 281, 293-304.
- Sillitoe, R.H. 1994: Erosion and collapse of volcanoes: Causes of telescoping in intrusion-centered ore deposits. *Geology*, 22, 945-948.
- Sillitoe, R.H. 2010: Porphyry Copper Systems. *Economic Geology*, 105, 3-41.
- Wark, D.A. & Watson, E.B. 2006: TitaniQ: a titanium-in-quartz geothermometer. *Contributions to Mineralogy and Petrology*, 52, 743-754.

## 2.17

### Effects of crystallization and bubble nucleation on the seismic properties of magmas

Tripoli Barbara Andrea<sup>1</sup>, Cordonnier Benoit<sup>1</sup>, Ulmer Peter<sup>1</sup>

<sup>1</sup>Institute of Geochemistry and Petrology, ETH Zürich, Clausiusstrasse 25, 8092 Zürich (barbara.tripoli@erdw.ethz.ch).

Seismic tomography of potentially hazardous volcanoes is a prime tool to assess the physical state of magma reservoirs. Processes occurring in the conduit or in the chamber, such as crystallization and bubble exsolution, control the magma rheology, hence the style of volcanic eruption. Elastic parameters of vapor-saturated, partially molten systems are thus providing fundamental information for the identification of such reservoirs under active and seemingly dormant volcanoes.

We investigated a chemically simplified melt analogous to andesite and trachyte, in the system  $\text{CaO-Na}_2\text{O-Al}_2\text{O}_3\text{-SiO}_2\text{-H}_2\text{O-CO}_2$  (Picard et al, 2011), which undergoes plagioclase crystallization and bubble exsolution. Using a Paterson-type internally-heated gas pressure apparatus, we measured the ultrasonic velocities at a constant pressure of 250 MPa and at a frequency of 0.1 MHz. Samples have been first heated at 850 °C for 30 minutes. Subsequently, the temperature has been decreased to 650°C at a rate of 0.5 or 0.1°C/min and velocities were recorded each 45 minutes. The Paterson apparatus doesn't permit a fast quench. Consequently, a serie of cold-seal experiments at identical pressure conditions but with rapid-quenching at various temperature have been undertaken.

Seismic velocities are strongly affected by bubble nucleation and crystallization (Carrichi et al, 2009). We will thus present new experimntal results that clarify the dependence of the seismic velocities on the evolution of microstructures (bubble- and crystal-size distribution) as well as the evolution of composition (melt and crystals).

#### REFERENCES

- Carricchi, L., Burlini, L., and Ulmer, P. (2009) Propagation of P and S-waves in magmas with different crystal contents: insights into the crystallinity of magmatic reservoirs. *Journal of Volcanology and Geothermal Research*, 178, 740-750.
- Picard D., Arbaret L., Pichavant M., Champallier R. and Launeau P. (2011). Rheology and microstructure of experimentally deformed plagioclase suspensions, *Geology*, 39, 747-750.

## 2.18

### Molybdenum isotopes: the new tracer to identify subducted material? Hints from the altered oceanic crust and oceanic eclogites.

Vils Flurin<sup>1,4</sup>, Elliott Tim<sup>1</sup>, Willbold Matthias<sup>2</sup>, Teagle Damon<sup>3</sup>

<sup>1</sup> University of Bristol, BS8 1RJ Bristol, United Kingdom (correspondence: flurin.vils@gmail.com)

<sup>2</sup> Imperial College London, SW7 2AZ London, United Kingdom

<sup>3</sup> National Oceanography Centre, SO14 3ZH Southampton, United Kingdom

(<sup>4</sup> now at Wanner AG Solothurn, 4500 Solothurn)

During movements of the oceanic crust away from mid-ocean ridges, hydrothermal alteration of the oceanic crust imparts distinct elemental and isotopic signals. The change in isotopic composition of the altered oceanic crust compared to unaltered MORB provides important tracers to identify the involvement of fluids/melts released from the subducted slab in the formation of volcanic arc basalts and ultimately of deep recycling of subducted material. Over the last decade, many studies demonstrated the great potential of Mo isotopes in the understanding of ocean processes and continental weathering. These studies showed that Mo is a redox-sensitive tracer. Although recent studies suggest that diffusion can play an important role in isotope fractionation, the heavy element Mo, forming large oxyanion complexes, is unlikely to be substantially isotopically fractionated by diffusion.

In the first part of the project, samples from the deepest drill hole into the Pacific Oceanic crust (IODP Site1256) were analysed for Mo isotopes and Mo concentrations. A profile through the complete upper altered oceanic crust (passing pillow basalts, sheeted dyke complex, and gabbros) at ODP Site 1256D has been sampled and Mo isotopes and Mo concentrations have been measured. The studied samples show high variability down-hole (over 1.5‰  $\delta^{98/95}\text{Mo}$ ), with a tendency to increase with depth. The heterogeneous dehydration of the oceanic crust might lead to extraction of the heavier isotopic ratio in the source of arc volcanoes, while the lighter isotopic ratio might be the source for the light isotope ratio found in some ocean islands basalts. In general, it seems that the altered oceanic crust has an isotopic ratio slightly heavier than average continental crust and mantle, highlighting the potential of Mo to fingerprint recycling of subducted material, depending on the consequences of processing beneath the arc.

Eclogites are the high temperature/ high pressure dehydrated equivalent of the altered oceanic crust, thus are the indication of the isotopic composition of material transported into the deep mantle after a full range of subduction zone processes have acted upon it. In additions, some subduction related metasediments were analyzed. The samples studied come from Syros and the Alps, both identified as exhumed fragments of subducted oceanic crust. The samples show that there is a significant change in  $\delta^{98/95}\text{Mo}$  as lithologies change from hydrated blueschists to anhydrous eclogites. The changes in isotopic compositions indicate that heavy Mo leaves the subducted slab, resulting in an isotopically light residue.

## P 2.1

### Cl isotopes in melt inclusions

Bouvier Anne-Sophie<sup>1</sup>, Manzini Mélina<sup>1</sup>, Baumgartner Lukas<sup>1</sup>

<sup>1</sup> ISTE, University of Lausanne, Lausanne, Switzerland (anne-sophie.bouvier@unil.ch)

Chlorine is an important volatile element. Its two stable isotopes are used to track the global halogen cycle and to determine fluid sources. Chlorine isotopes are fractionated by fluid/rock interaction, degassing, diffusion and mineralogical transformations. However, the range of Cl isotopes in terrestrial rocks has been shown to be relatively limited ( $\sim$ -2.0 to +2.0‰, e.g., Barnes et al., 2008), requiring precise measurements of  $\delta^{37}\text{Cl}$ . Usually Cl isotopes are measured by TIMS or IRMS, and only a few measurements have been performed so far by ion probe. Previous SIMS studies reported a reproducibility of 0.8 to 1.5‰ (2 Standard Deviation (SD)) for glasses with > 200 ppm Cl (e.g., John et al., 2010; Straub and Layne, 2007). Using the SwissSIMS, a CAMECA IMS 1280-HR, we have been able to obtain a precision as good as 0.4‰ (2SD), with a beam size of 10 microns, in glasses containing only 100 ppm Cl. With such a precision, it is now possible to study the Cl isotopic composition of melt inclusions trapped in olivines.

In this study, we will analyze melt inclusions representing both primary (in high Fo olivines) and more evolved (at least partly degassed) melts. This dataset will allow us to better understand the behavior of Cl in the mantle and to bring new clues on the behavior of Cl isotopes during shallow magma degassing.

#### REFERENCES

- Barnes, J.D., Sharp, Z.D., Fischer, T.P., 2008. Chlorine isotope variations across the Izu-Bonin-Mariana arc. *Geology* 36, 883-886.
- John, T., Layne, G.D., Haase, K.M., Barnes, J.D., 2010. Chlorine isotope evidence for crustal recycling into the Earth's mantle. *Earth and Planetary Science Letters* 298, 175-182.
- Straub, S.M., Layne, G., 2007. Chlorine Isotope Ratios of Volcanic Glasses from Arc, Back-Arc and Mid-Ocean Ridges Settings - First Results of an Ion Microprobe Study. American Geophysical Union Fall Meeting 2007, abstract #V41B-0610.

## P 2.2

### Development of $\delta^{18}\text{O}$ and $\delta^{37}\text{Cl}$ SIMS analysis on biotites

Siron Guillaume<sup>1</sup>, Baumgartner Lukas<sup>1</sup> & Bouvier Anne-Sophie<sup>1</sup>

<sup>1</sup> Institut des Sciences de la Terre, Université de Lausanne, CH-1015 Lausanne (guillaume.siron@unil.ch)

Fluids are a major driving force in many geologic processes. They lower the melting temperature, are behind many ore forming processes and facilitate mineral reactions, for example. C-O-H fluids are the most common fluids and chlorine is thought to be the main anion in those fluids. Stable isotopes of C-O-H-Cl carry information on source, pathways, and mechanisms of fluid-rock interaction. Advances in stable isotopes analysis by Secondary Ion Mass Spectroscopy (SIMS) permit isotopic analysis in minerals with high spatial resolution. SIMS analyses are typically rapid (4-10 minutes/analysis), so that today we can obtain large amount of in-situ data with a spatial resolution of 5-20mm, at relatively low cost and high speed.

SIMS analyses are hampered by large matrix effects; in some cases more than 10‰ absolute (Eiler et al. 1997; Riciputi et al. 1998). To correct for instrumental mass bias and matrix effects it is crucial to have reliable standard materials of the same structure and composition. We present  $\delta^{18}\text{O}$  and  $\delta^{37}\text{Cl}$  analysis obtained with the new SwissSIMS facility in Lausanne on biotites spanning the annite-phlogopite solid solution. So far we have identified 2 potential standards, in which the reproducibility ( $2\sigma$ ) of  $\delta^{37}\text{Cl}$  analysis are ca 0.3‰, that of  $\delta^{18}\text{O}$  better than 0.3‰. Considering that magmatic fluids have a  $\delta^{37}\text{Cl}$  signature of -0.5 to 2‰, whereas marine pore waters are comprised between -8 and 0‰ (Banks et al. 2000; Barnes et al. 2008), this reproducibility is good enough to discriminate between fluid sources

#### REFERENCES

- Banks, D., Green R., Cliff, R. A. & Yardley, B. W. D. 2000: Chlorine isotopes in fluid inclusions: Determination of the origin of salinity in magmatic fluids. *Geochimica et Cosmochimica Acta*, 64, 1785-1789.
- Barnes, J. D., Sharp, Z. D. & Fischer, T. P. 2008: Chlorine isotope variations across the Izu-Bonin-Mariana arc. *Geology*, 36, 883-886.
- Eiler, J. M., Graham, C., & Valley, J. W. 1997: SIMS analysis of oxygen isotopes: matrix effects in complex minerals and glasses. *Chemical Geology*, 138, 221-244.
- Riciputi, L. R., Paterson, B. A. & Ripperdan, R. L. 1998: Measurement of light stable isotope ratios by SIMS: Matrix effects for oxygen, carbon, and sulfur isotopes in minerals. *International Journal of Mass Spectroscopy*, 178, 81-112.

## P 2.3

# High chloride concentration in biotites of host rocks documents infiltration of fluids exsolved from the Torres del Paine granites

Siron Guillaume<sup>1</sup>, Baumgartner Lukas P.<sup>1</sup>, Bodner Robert<sup>1</sup>, Putlitz Benita<sup>1</sup>, Müntener Othmar<sup>1</sup>

<sup>1</sup> Institut des Sciences de la Terre, Université de Lausanne, CH-1015 Lausanne (guillaume.siron@unil.ch)

The Torres del Paine intrusive complex (TPIC) is located in southern Patagonia east of the Patagonian batholith. It intruded between 12.6-12.45 Ma (Leuthold et al 2012, Michel et al. 2008), and was constructed by three major granites laccolith intrusions and by underplating of a mafic sill complex, which formed again in 3 major batches (Leuthold et al. 2012). The TPIC intruded the Cretaceous Punta Barossa and Cerro Toro Formations at a depth of ca. 3 km, creating a small, well-exposed contact aureole. The previous study by (Bodner 2013) determined that the temperature in the contact aureole never exceed 550°C. The chlorine content of biotites increases in the vicinity (1-20m from contact) of the intrusion from 50-500ppm to over 1500 ppm. Most samples in the far-field have less than 300 ppm.

Samples with high chloride concentrations in biotite contain biotite, k-feldspar, and cordierite, with no or very minor retrogression. We interpret this to be the result of Cl-rich, igneous fluids infiltrating these samples at peak metamorphic temperatures. Stable isotope compositions of hydrogen in biotites also reflect an igneous source for these fluids. The fact that only 3 out of 16 samples located within 30 meters of the contact show high chlorine concentrations reflects channelized, limited infiltration of fluids.

Preliminary calculation based on Zhu and Sverjensky (1991) give a predicted total dissolve chlorine content 5 mol in the fluids, while non-infiltrated rocks have fluids with total chlorine concentrations as low as <0.1 m. The high chlorine concentrations are typical for Cl-enriched fluids exsolving from a crystallizing magma attaining fluid saturation. Fluid saturation of magmas is also documented by the presence of abundant miarolitic cavities in the granites. Further work is planned using  $\delta D$ ,  $\delta^{18}O$  and especially  $\delta^{37}Cl$  of biotites, since chlorine isotopes and the other isotopes aqueous fluids exsolved from magmas carry characteristic signatures, allowing them to be identified.

### REFERENCES

- Bodner, R., 2013: Metamorphism and Kinetics in the Torres del Paine Contact Aureole. PhD Thesis, University of Lausanne.
- Leuthold, J., Müntener, O., Baumgartner, L.P., Putlitz, B., Ovtcharova, M. & Schaltegger, U. 2002: Time resolved construction of a bimodal laccolith (Torres del Paine, Patagonia). *Earth and Planetary Science Letters*, 325, 85-92.
- Michel, J., Baumgartner, L.P., Putlitz, B., Schaltegger, U. & Ovtcharova, M. 2008: Incremental growth of the Patagonian Torres del Paine laccolith over 90 k.y. *Geology*, 36, 459-462.
- Zhu, C. & Sverjensky, D.A. 1991: Partitioning of F-Cl-OH Between Minerals and Hydrothermal Fluids. *Geochimica et Cosmochimica Acta*, 55, 1837-1858.

## P 2.4

### Development of a quartz oxygen isotope standard for the SwissSIMS

Lukas Baumgartner<sup>1</sup>, Anne-Sophie Bouvier<sup>1</sup>, Benita Putlitz<sup>1</sup>

<sup>1</sup>Institute of Earth Sciences, University of Lausanne, CH-1015 Lausanne (Lukas.Baumgartner@unil.ch)

The SwissSIMS facility is built around a dynamic secondary ion mass spectrometer (SIMS), the CAMECA 1280HR. The facility became operational in January, 2013. It was acquired by the universities of Bern, Geneva and Lausanne, the ETHZ, and the Swiss National Science foundation. It is housed by the University of Lausanne in its new Geosciences building. The 1280HR is optimized for high mass resolution analysis (>20K), has a dual primary ion beam (oxygen and Cesium), and can reach a spatial resolution (Ce-source) of ca. 2-5µm). Its use is for stable isotope geochemical analysis in solids, and in-situ dating of accessory minerals, for example.

Since January, we have been involved in developing our proper standards for analysis of different isotopic systems. SIMS instruments are plagued by large instrumental mass fractionation (IMF), which depends on instrument settings, the matrix analyzed and sample preparation. As a consequence, a standard grain of at least a few 100µm size, with known composition, matching structure and major element composition of the mineral or glasses to be analyzed needs to be mounted on each SIMS sample block.

A quartz standard has been developed for oxygen isotope analysis using the central part of a 15cm long quartz crystal from a pegmatite in the Torres del Paine, Chile. Laser fluorination analysis produced a  $\delta^{18}\text{O}$  value of  $9.8 \pm 0.24\text{‰}$  ( $2\sigma$ ,  $n=5$ ), using quartz NBS-28 as reference. SIMS analysis resulted in uncorrected values between 3-24‰  $\delta^{18}\text{O}$ . Instrumental drift was corrected by using one grain as a reference (e.g. assigning it the value of 9.8‰). It was analyzed 4 times every 10-15 analysis of any other grain of the Paine 1 quartz. Drift corrected data of ca. 100 analysis on 10 grains had a reproducibility of 0.37‰ ( $2\sigma$ ). Within single grain variability of 0.18-0.47‰ was obtained. We are currently testing if this standard for oxygen isotopes can be used for trace elements like Ti, Na, Al.

## P 2.5

### Uncertainties of the laser ablation ICPMS analysis: how do they arise and how do we calculate them?

Ulianov Alex<sup>1</sup>, Müntener Othmar<sup>1</sup> & Schaltegger Urs<sup>2</sup>

<sup>1</sup>Institute of Earth Sciences, University of Lausanne, Géopolis, CH-1015 Lausanne (alexey.ulyanov@unil.ch)

<sup>2</sup>Section of Earth and Environmental Sciences, University of Geneva, Rue des Maraîchers 13, CH-1205 Geneva

Inductively coupled plasma mass spectrometry (ICPMS) is a major branch of modern mass spectrometry with important applications in Earth Sciences. In combination with the laser ablation (LA) sample probing, it is widely used for the in-situ determination of trace element abundances and isotope ratios in solids. Some of such determinations require the calculation of concentration or concentration ratio uncertainties as a compulsory part of the analytical result. Curiously, neither the fundamental sources of noise in the ICPMS nor methods used for the practical uncertainty calculation are thoroughly discussed in the literature. Regarding the fundamental sources of noise, it is declared without explanation that the Poisson process is involved in the generation of ICPMS signals. Regarding the uncertainty calculation methods used in practice, they are often buried in computers programs used for LA-ICPMS data reduction without a detailed analysis of their properties and limitations.

To explain the appearance of the Poisson process in the distribution of ICPMS count numbers, we consider this distribution as a limiting case of the binomial distribution constrained by inefficient ion transmission from the ICP to the detector. The ICP is an atmospheric pressure ion source. The extraction of ions from the ICP into the spectrometer ion channel, kept under vacuum, is a technical challenge: most ions generated in the ICP are lost during the extraction. Thus, if a large number ( $M$ ) of ions face the sampler cone per time interval, but the probability ( $p$ ) for each individual ion to reach the

detector and be registered is low, the numbers ( $N$ ) of actually registered ions per time interval (per analysis) are Poisson distributed with a mean and variance equal to  $\mu$ . This formalism is valid if the number  $M$  of ions subject to extraction per time interval is constant. However, due to turbulences in the torch and instabilities of the sample introduction system,  $M$  fluctuates with time. This is the case of the so-called doubly stochastic, or mixed, Poisson process. It could be imagined that a subset of  $N$  values is acquired at one  $M$ , another subset – at another  $M$ , etc., after which all subsets are mixed in proportions corresponding to the probability of occurrence of a given  $M$  value. The mixing results in the appearance of an excess variance in the distribution of count numbers compared to the variance of an ordinary Poisson process (constant  $M$ ). The excess variance shows a quadratic dependence on the signal intensity. In weak signals, it is insignificant. Such signals can be approximated by an ordinary Poisson process with a variance equal to the mean count number. In strong signals, it increases. The excess variance in the uncertainty of ICPMS signals is otherwise known as flicker noise, although it is an integral part of the doubly stochastic Poisson process, not an individual noise component. We review mathematical formalisms existing to describe it using correlation properties of the signal, and show how to use the conditional intensity (autocovariance) function of the signal to derive the entire uncertainty.

Although the Poisson description of uncertainty in ICPMS is a causal model describing the sources of fluctuations and not only their extent, it requires estimating the autocovariance function above and invokes a complex mathematical formalism, especially in the case of transient signals typical of LA-ICPMS analyses. Therefore, descriptive approaches based on the individual sweep intensities or their ratios are widely used and still remain the only practical solution for the uncertainty estimation of strong ICPMS signals with a significant excess variance due to double stochasticity. These approaches can be divided in three large groups: (1) ratio of the mean intensities; (2) mean of the intensity ratios, (3) intercept, or regression-based, approach. We showed in a recent work that using approaches (2) and (3) can yield indefinite results in terms of the both intensity ratio value and its uncertainty; these results are influenced by the extent of the signal fluctuation and averaging for the standard and the sample (Ulianov et al., 2012). Approach (1) is devoid of these deficiencies and can be recommended, but requires developing methods to calculate the mean intensity uncertainty for a transient signal. We suggest two such methods: differencing and signal segmentation. The differencing method invokes transforming the original series of sweep intensities into a series of intensity differences obtained from each two consecutive sweeps. This series is not transient, even if the original signal is transient. The standard deviation of the mean for this series is easy to compute, which allows to immediately calculate the uncertainty for the original transient signal. For a single collector ICPMS, this method shows excellent performance on tests, including comparisons with uncertainties calculated from a number of replicate analyses of the same material. We recommend this method. The segmentation method is based on the uncertainty computation for the individual signal segments, each of them being considered as non-transient. The total uncertainty is then obtained by error propagation. This very straightforward method is, however, limited to signal showing little transience, where it can also be recommended.

Estimating the uncertainty of the individual isotope intensity (intensity ratio) is a pre-requisite for the calculation of the concentration and concentration ratio uncertainties. It is, however, not the only component necessary to obtain them. Another important component is the uncertainty of the mass bias. In the current LA-ICPMS practice, especially in the practice of high-precision isotope ratio analysis, the mass bias is obtained by (repetitively) analysing one single standard. This results in a small mass bias uncertainty further decreasing with increasing the number of replicates. At the same time, repetitively analysing a second standard does not ensure that the mean mass bias value from the first standard is reproduced because, for example, the two standards can show different laser induced fractionation patterns. The solution is to use a multi-standard regression based calibration of the mass bias, which potentially increases the concentration ratio uncertainty, but reduces its inaccuracy.

## REFERENCES

- Ulianov, A., Müntener, O., Schaltegger, U. & Bussy, F. 2012: The data treatment dependent variability of U–Pb zircon ages obtained using mono-collector, sector field, laser ablation ICPMS. *J. Anal. At. Spectrom.* 27, 663-676.

## P 2.6

### Stress and strain in olivine – a RAMAN–mapping approach

Honisch Maria<sup>1</sup>, Ulianov Alexey<sup>1</sup>, Ulmer Peter<sup>2</sup>, Müntener Othmar<sup>1</sup>

<sup>1</sup>Institute of Earth Sciences, University of Lausanne, Géopolis, CH-1015 Lausanne (Maria.Honisch@unil.ch)

<sup>2</sup>Institute of Geochemistry and Petrology, ETH Zürich, Clausiusstrasse 25 / NW E77, CH-8092 Zürich

The shift in Raman-peak position of the 823/855  $\text{cm}^{-1}$  olivine doublet, caused by stress and strain, was studied for several olivine compositions with a LabRAM HR High Resolution Raman spectrometer from Horiba Scientific with a focal length of 800mm. A spectral resolution of approximately 0.33  $\text{cm}^{-1}$  and a peak position uncertainty after peak fitting of approximately 0.1  $\text{cm}^{-1}$  were achieved using a 2400 grating. The individual olivine crystals were mapped by Raman- and electron microprobe before and after annealing at 1350°C and slow cooling down to 500°C during 30 hours. The use of a 2400 grating necessitates recording both a reference peak (Rayleigh line zero position) and the doublet olivine peak at circa 823  $\text{cm}^{-1}$  and 855  $\text{cm}^{-1}$  respectively. The peak positions of the doublet depend on the chemical composition of the olivine grains, Mg-rich olivines showing higher wavenumbers than the Fe-rich ones (Kuebler et al. 2006). Raman maps were acquired to show both the peak positions and the FWHM (full width half maximum) of the doublet before and after annealing the sample. FWHM maps (Figure 1) are especially useful to visualize progressive changes in crystallographic orientations within a grain (Ishibashi et al. 2008). The peak positions of stress- and strain-free olivine crystals can be plotted against the associated olivine compositions (Fo-values). The resulting diagram can further be used to quantify the amount of stressed olivine crystals in selected kimberlite samples, for which conventional methods (e.g. polarized microscopy and EBSD) are inoperable.

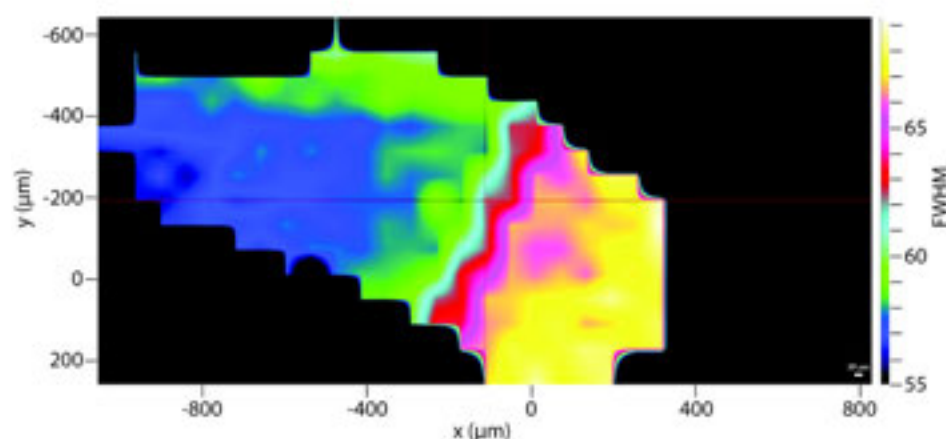


Figure 1. Raman map visualizing the FWHM (full width half maximum) of the first peak of the olivine doublet at circa 823  $\text{cm}^{-1}$ , revealing a gradual change in relative peak intensities of the doublet and thereby a progressive change in crystallographic orientation within the grain.

#### REFERENCES

- Ishibashi, H., Arakawa, M., Ohi, S., Yamamoto, J., Miyake, A., Kagi, H. 2008: Relationship between Raman spectral pattern and crystallographic orientation of a rock-forming mineral: a case study of Fo<sub>89</sub>Fa<sub>11</sub> olivine. *Journal of Raman Spectroscopy*, 39, 1653-1659.
- Kuebler, K. E., Jolliff, B. L., Wang, A., Haskin, L. A. 2006: Extracting olivine (Fo-Fa) compositions from Raman spectral peak positions. *Geochimica et Cosmochimica Acta*, 70, 6201-6222

## P 2.7

# Recognizing metamorphic stages and tectonic slices in HP-terrane: Case study in the Sesia Zone (NW-Alps, Italy)

Giuntoli Francesco<sup>1</sup>, Engi Martin<sup>1</sup>, Regis Daniele<sup>1,2</sup> El Korh Afifé<sup>1,3</sup> & Lanari Pierre<sup>1</sup>

<sup>1</sup> Institut für Geologie, University of Bern, Baltzerstrasse 1+3, CH-3012 Bern, Switzerland, francesco.giuntoli@geo.unibe.ch, engi@geo.unibe.ch, pierre.lanari@geo.unibe.ch

<sup>2</sup> Department of Environment, Earth and Ecosystem, The Open University, Walton Hall, Milton Keynes, MK7 6AA, UK, daniele.regis@open.ac.uk

<sup>3</sup> Université de Lorraine Faculté des Sciences et Technologies Département des Géosciences, Boulevard des Aiguillettes 54506, Vandœuvre-Lès-Nancy, France afife.elkorh@geo.unibe.ch

The dynamics of assembly of HP-terrane is of major geotectonic significance. We report on a field-based study in the Sesia Zone, a HP-terrane that formed during Alpine convergence. Traditionally, three main parts of the Sesia Zone have been recognized, all of them deriving from the rifted NW-margin of the Adriatic continent. Our work is examining internal tectonometamorphic limits, both spatial and temporal, within the Sesia terrane. Here, the focus is on the main body, traditionally called the Eclogitic Micaschist Complex (EMC).

By combining structurally controlled sampling, based on existing tectonic studies, with petrological analysis and mineral chronometry (allanite, zircon), we show that the EMC is non-uniform and comprises discrete tectonic slices. These show substantially different PTdt-paths and thus represent mobile fragments during the convergent history. An internal fragment (called Druer slice) experienced eclogite facies as early as 85 Ma (allanite Th/Pb SHRIMP age at 2 GPa, 560°C), followed by decompression at ~74 Ma (zircon age at ~1.6 GPa, ~570°C). By contrast, a more external fragment (Fondo slice) shows evidence of pressure cycling (Rubatto et al. 2011), with an eclogite facies peak at 75 Ma (allanite Th/Pb age at 1.7 GPa, ~550°C), a decompression stage at ~68 Ma (allanite Th/Pb age, lower Si-contents of phengites) and a second HP stage between 65-60 Ma (allanite Th/Pb age, P between 2.0 and 1.4 GPa, ~550°C). Recently, we started investigating the Lillianes area, some 16 km far away along strike from the Fondo slice. This area comprises micaschists with a HP foliation (composite D1/D2, eclogite to blueschist facies) and weak (greenschist facies) retrogression. Assemblages include multiple generations of phengite, garnet, glaucophane (±early omphacite) and allanite, plus quartz, epidote, chlorite, and titanite rimming rutile. Microstructural and mineral-chemical data indicate that growth zones in garnet and allanite correspond to distinct HP stages. In some cases, these can be related to discrete phases of deformation (D1/D2, D3).

Garnet cores are strongly porphyroclastic (mm-size), with two or more rims. Allanite composite grains have a LREE-rich metamorphic core believed to be stable with early grt plus first generation phe (Si-rich), gln, and rutile. Allanite rims (one or more) show lower LREE and seem to be stable with second generation phe, gln and probably grt. Preliminary Th-Pb age data, obtained by in situ LA-ICP-MS, span from 80 to 74 Ma for allanite cores, and 68-62 Ma for allanite rims.

Thermobarometry for each stage is in progress, but so far these ages compare well with the two HP stages of the Fondo slice (Regis et al. 2013).

Field-based research is being continued to define the size and geometry of tectonic slices that constitute the Sesia HP terrane. Kinematic constraints quantifying the relative mobility of such fragments are sorely needed, as the scale of mixing within subduction channels is poorly known. Understanding the overall processes in subduction channels will benefit from field data in order to test results from numerical models.

## REFERENCES

- Regis et al. 2013: Deciphering metamorphic dynamics in an eclogite-facies terrane (Sesia Zone, Western Alps) using U/Th-Pb petrochronology (in progress at J. Petrology)
- Rubatto et al. 2011: Yo-yo subduction recorded by accessory minerals in the Italian Western Alps. *Nature Geoscience* 4, 338-342.

## P 2.8

# Whiteschists - protoliths and phase petrology

Franz Leander<sup>1</sup>, De Capitani Christian<sup>1</sup>, Romer Rolf L.<sup>2</sup>

<sup>1</sup>Mineralogisch-Petrographisches Institut, University of Basel, Bernoullistrasse 30, CH-4056 Basel

<sup>2</sup>Deutsches GeoForschungsZentrum, Telegrafenberg, D-14473 Potsdam

Whiteschists appear in numerous high- and ultrahigh-pressure rock suites and are characterized by the mineral assemblage kyanite + talc (+ quartz or coesite; cf. Schreyer 1973). Thermodynamic modelling using the THERIAK-DOMINO program of De Capitani & Brown (1987) demonstrates that whiteschist mineral assemblages are well stable up to pressures of more than 4 GPa but may already form at pressures of 0.5 GPa (Franz et al. 2013). The formation of whiteschists is rather depending on the composition of the protolith, which requires elevated contents of Al and Mg as well as low Fe, Ca, and Na contents, as otherwise chloritoid, amphibole, feldspar, or omphacite are formed instead of kyanite or talc. Furthermore, the stability field of the whiteschist mineral assemblage strongly depends on  $X(\text{CO}_2)$  and  $f(\text{O}_2)$ ; already at low values of  $X(\text{CO}_2)$ ,  $\text{CO}_2$  binds Mg to carbonates strongly reducing the whiteschist stability field whereas high  $f(\text{O}_2)$  enlarges the stability field and stabilizes yoderite. Similarly, elevated amounts of sulfur may extract iron from the system fixing it to phases like pyrite or pyrrhotite and thus extend the whiteschist stability field. We conclude that the scarcity of whiteschist is not necessarily due to unusual P–T conditions, but to the restricted range of suitable protolith compositions and the spatial distribution of these protoliths:

1.) Continental sedimentary rocks, which typically have been deposited under arid climatic conditions in closed evaporitic basins. These rocks are usually restricted to relatively low latitudes and often contain large amounts of the clay minerals palygorskite and sepiolite (Figs. 1A & B). Marine sediments generally do not yield whiteschist mineral assemblages as marine shales commonly have too high iron contents. Sabkha deposits may have too high  $\text{CO}_2$  contents.

2.) Hydrothermally and metasomatically altered felsic to mafic rocks, e.g. metasomatic gneisses, hydrothermally altered volcanic rocks or mafic rocks with hydrothermal palygorskite veins. Furthermore, eclogite facies quartz veins also yield whiteschist mineral assemblages. Ultramafic rocks, which often yield elevated contents of Mg and Al, contain far too little  $\text{SiO}_2$  and therefore generate the mineral assemblage olivine + spinel instead of talc + kyanite at the appropriate metamorphic P–T conditions.

Although thorough pre- or syn-metamorphic metasomatism with removal of alkali elements, Ca and Fe may well lead to suitable protoliths for whiteschists (see Chopin 1991, John et al. 2004, Ferrando et al. 2009 and citations within), our calculations demonstrate that whiteschists can also form by closed-system metamorphism, which implies that the chemical and isotopic composition of these rocks provide constraints on the development of the protoliths.

Sedimentary protoliths of appropriate geochemical composition occur in and on continental crust. Therefore, whiteschist assemblages typically are only found in settings of continental collision or where continental fragments were involved in subduction.

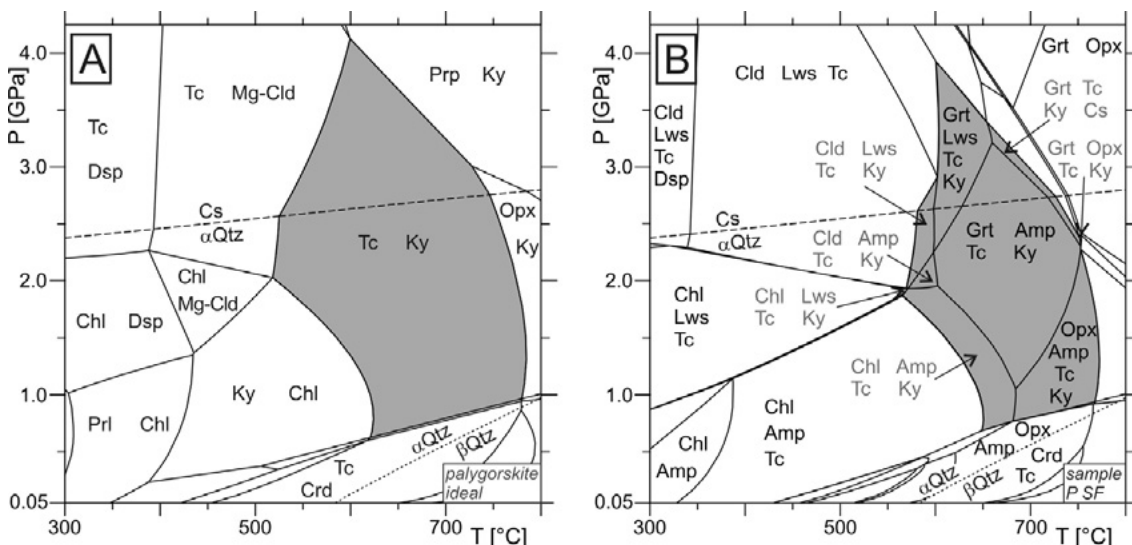


Figure 1. (A) Equilibrium phase diagram of palygorskite (ideal formula) and (B) of a continental, palygorskite-rich pelite from Springbok Flats (RSA; cf. Heystek & Schmidt 1953). Whiteschist stability fields are marked grey.

## REFERENCES

- Chopin, C., Henry, C., & Michard, A. 1991: Geology and petrology of the coesite-bearing terrain, Dora Maira massif, Western Alps. *European Journal of Mineralogy*, 3, 263–291.
- De Capitani, C., & Brown, T.H. 1987: The computation of chemical equilibrium in complex systems containing non-ideal solutions. *Geochimica et Cosmochimica Acta*, 51, 2639–2652.
- Franz, L. Romer, R.L., & De Capitani, C. 2013: Protoliths and phase petrology of whiteschists. *Contributions to Mineralogy and Petrology*, 166, 255–274.
- Ferrando, S., Frezzotti, M.L., Petrelli, M., & Compagnoni, R. 2009: Metasomatism of continental crust during subduction: the UHP whiteschists from the Southern Dora-Maira Massif (Italian Western Alps). *Journal of Metamorphic Geology*, 27, 739–756.
- Heystek, H., & Schmidt, E.R. 1953: The mineralogy of the attapulgite-montmorillonite deposit in the Springbok Flats, Transvaal. *Geological Society of South Africa Transactions*, 56, 99–119.
- John, T., Schenk, V., Mezger, K., & Tembo, F. 2004: Timing and P–T evolution of whiteschist metamorphism in the Lufilian Arc–Zambesi Belt orogen (Zambia) implications for the assembly of Gondwana. *Journal of Geology*, 112, 71–90.
- Schreyer, W. 1973: Whiteschist: a high-pressure rock and its geologic significance. *Journal of Geology*, 81, 735–739.

## P 2.9

## Geochemical study of mineral paragenesis from Alpine-type veins in the western Swiss Alps.

May Eric<sup>1</sup>, Vennemann Torsten<sup>1</sup> and Meisser Nicolas<sup>2</sup>

<sup>1</sup>*Institute of Earth Sciences, University of Lausanne, Geopolis building, CH-1015 Lausanne*

<sup>2</sup>*Musée cantonale de géologie, University of Lausanne, Anthropole building, CH-1015*

The minerals in Alpine-type veins bear witness to fluid circulation in the crust. The veins are part of the porosity and permeability of the rocks and allow for the transfer of elements in an open or closed system. By studying the geochemistry and structures of such veins formed during the tectonism of the Alps an insight into the origin, composition, and evolution of fluids during retrograde Alpine metamorphism can be gained (e.g., Mullis, 1996) These extensive veins have been well studied for the central Swiss Alps (e.g., Sharp et al. 2005, and references therein) but for the western Swiss Alps, apart from the Mont-Blanc massif (e.g., Rossi, 2005), less is known about their age, conditions of formation, and origin.

The purpose of the present study is to use various bulk (CO<sub>2</sub>-laser assisted fluorination extraction technique) and in-situ techniques (EMPA, LA-ICPMS, SIMS) to analyze the isotopic and major and trace element composition of the vein minerals in the Western Alps. In addition, fluid inclusion microthermometry and Raman spectroscopy provide information on the composition and variability of fluids from which the minerals precipitated for the different and contrasted growth environments. Oxygen isotopic composition of quartz together with co-existing phases (chlorite, calcite, epidote, hematite, titanite, monazite) are studied to help constrain the conditions of formation of the veins sampled from the western part of the Swiss Alps.

A number of sites have been sampled (Fig. 1), including contrasting host-rock types and representing rocks formed at different metamorphic conditions. Early macroscopic and SEM-CL investigations (Fig. 2) on quartz showed that growth conditions and P-T-X evolution influence the habitus considerably. As previously noted (Ramseyer and Mullis, 1990), growth mode (rapid vs. slow and discontinuous vs. continuous) influences the luminescence and trace element incorporation in quartz.

The bulk oxygen isotope compositions measured so far vary by up to 1‰ in different growth zones of the crystals. δ<sup>18</sup>O values measured on quartz from the Central Alps previously showed variable zonation depending on the conditions of growth (Jourdan et al. 2009a). Ongoing in-situ analyses with the new Swiss SIMS on a larger array of natural hydrothermal quartz will provide high-resolution data to link growth processes with trace element and oxygen isotope zoning.



Figure 1: Tectonic map of the area studied and giving the sampling sites.

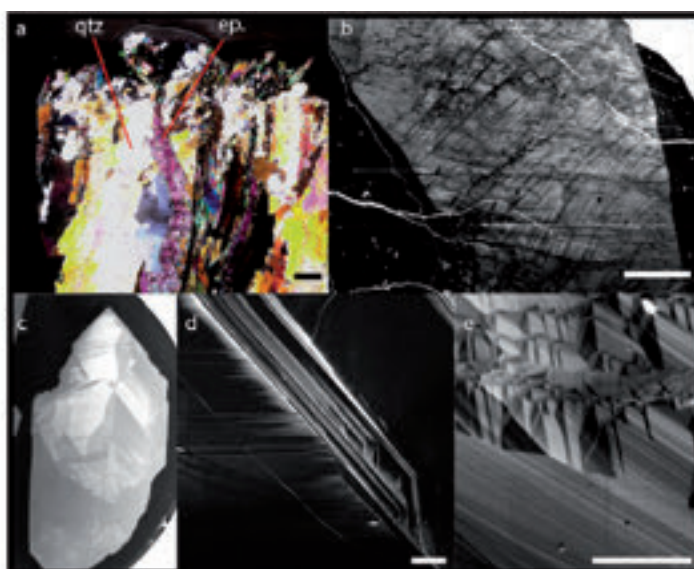


Figure 2 a. Syntectic extensional vein with co- the area studied and giving genetic quartz and epidote (scale bar 1 mm). b. Quartz vein with complex fluid history (scale bar 250 microns). c. Amethyst crystal (2 cm) with brazilian twinning and cyclic growth. d. (enlargement of c.) typical layering of amethyst generation with clear variable luminescence (scale 250 microns). e. Complex and disturbed growth of a skeletal quartz from Val d'Illeiez. Note the arrangement of growth sectors (scale 250 microns). (a: thick section in polarized light; b, d and e: SEM-CL images; c: SEM-BSE image).

## REFERENCES

- Jourdan A.-L., Vennemann T.W., Mullis J., and Ramseyer K., 2009. Oxygen Isotope Sector Zoning in Natural Hydrothermal Quartz. *Mineral. Mag.* 73, 615-632.
- Mullis J. 1996: P-T-t path of quartz formation in extensional veins of the Central Alps. *Schweiz. Minerl. Petrogr. Mitt.* 76, 159-164.
- Ramseyer K., Mullis J. 1990: Factors influencing short-lived blue cathodoluminescence of  $\alpha$ -quartz. *American Mineralogist*, 75, 791-800.
- Rossi M. 2005: Déformations, transferts de matière et de fluide dans la croûte continentale: application aux massifs cristallins externes des Alpes. PhD thesis, University of Grenoble.
- Sharp Z., Masson H., Lucchini R. 2005: Stable isotope geochemistry and formation mechanisms of quartz veins; extreme paleoaltitudes of the Central Alps in the Neogene. *American Journal of Science*, 305, 3, 187-219.

## P 2.10

# Oxygen isotope and trace element behavior in rhyolites from the contact-aureole of the Chaltén Plutonic Complex (Mt. Fitz Roy, Patagonia, Argentina)

Susanne Seitz<sup>1</sup>, Benita Putlitz<sup>1</sup>, Lukas P. Baumgartner<sup>1</sup>, Stéphane Leresche<sup>1</sup> & Peter Nescher<sup>1</sup>

<sup>1</sup>*Institut des Sciences de la Terre, Université de Lausanne, CH-1015 Lausanne (susanne.seitz@unil.ch)*

The Chaltén Plutonic Complex (CHPC) is located near the village of Chaltén at the frontier between Chile and Argentina in southern Patagonia. It consists of a suite of calc-alkaline mafic and granitic rocks emplaced in several successive batches. High-precision U/Pb zircon dating yield ages between  $16.90 \pm 0.05$  Ma and  $16.37 \pm 0.02$  Ma (Ramirez et al. 2012). The host-rocks include a Paleozoic clastic sequence (Bahia de la Lancia Formation), Jurassic rhyolites and volcanoclastic rocks (El Quemado Complex), and a Cretaceous pelitic sequence (Rio Mayer Formation). The intrusion of the CHPC post-dates the major regional deformation cycle.

The rhyolite and volcanoclastic rocks are the most common host-rocks in the contact-aureole of the CHPC. The simple mineralogy of those rocks provides the opportunity to use the contact-aureole as a well-constrained natural laboratory to investigate trace-element thermometry (e.g. Ti in quartz) and stable-isotope exchange kinetics for some key minerals (mainly quartz and zircon). We use conventional and ion-probe data (SwissSIMS) in order to decipher the effect of deformation and partial melting on trace-element and isotope exchange. Understanding these mechanisms will in turn help to further constrain intrusion mechanism.

Partial melting in the Chaltén contact aureole is limited to small zones at gabbro and tonalite contacts with rhyolites, but no partial melts have been found along granite-host-rock contacts. An anastomosing network of veins of quartz, feldspar and almandine-rich garnet characterizes the rhyolitic migmatites. This network is most prominent at 10m to 15m from the contact. Some cm-scale shear zones concentrated partial melt. On a microstructural scale partial melt is segregated along quartz-feldspar grain boundaries. They show typically cusped grain boundaries with melt penetrating along the edges.

Petrologic investigations show that melting is the result of biotite breakdown to cordierite and garnet. Thermodynamic calculation for these peraluminous rhyolites indicate that first melt occurs at 650-700°C and pressures around 3kbar. Simple thermal calculations yield maximum temperatures of about 550°C at the mafic-rhyolite contact, which is 100-150°C lower than the required temperature for partial melting. More complex thermal models (multiple pulses of intrusion, fluid flow) will be needed to obtain temperatures this high.

Melting in the rhyolitic migmatites was intense enough to partially reset U/Pb ages as indicated by a younging of zircon ages (obtained by laser ablation). Non-metamorphosed rhyolite samples show undisturbed Jurassic ages consistent with the previous stratigraphic characterization.

The Jurassic rhyolites show quartz phenocrysts of several millimeter-size. Pre- and syn-intrusive deformation has produced textures in these phenocrysts varying from undeformed to undulose quartz up to heavily recrystallized. Cathodoluminescence (CL) images suggest that quartz phenocrysts from weakly deformed samples (from the low-grade aureole) preserved the magmatic zonation with a bright CL core. CL images of recrystallized quartz (from the high grade aureole) show a complex pattern of dark CL bands, which partly mimics the shape of subgrains.

Oxygen isotope values obtained by laser fluorination show relatively high  $\delta^{18}\text{O}$  values between 11-13 ‰ for both whole rocks and quartz phenocrysts. Quartz-phenocrysts and their whole rocks seem to be in (near) magmatic equilibrium outside the contact aureole i.e., show small high-temperature fractionations. Approaching the contact the fractionation between quartz phenocrysts and their whole rocks increases.

Ion-probe data by SwissSIMS from phenocrysts of the low-grade aureole confirms the high  $\delta^{18}\text{O}$ -value obtained by laser fluorination. The  $\delta^{18}\text{O}$  composition of individual phenocrysts is relatively homogenous, and shows no indication of isotope exchange along cracks. This is in contrast to the observations of King et al. (1997), and suggests that these quartz phenocrysts preserved their magmatic values.

Oxygen isotope profiles across two deformed and partially recrystallized quartz crystals from the high-grade aureole show a more complex pattern. Both profiles show sharp, local changes in the oxygen isotope value of more than 1‰. Based on the textural observations we assume that these spikes are correlated to the small, low luminescence zones separating different subgrains. However, this has to be further verified by more SEM and CL work and further ion-probe analyses.

We assume that oxygen isotope fractionation is the result of partial equilibration during heating, followed by sluggish, diffusion driven re-equilibration during cooling, as predicted by the FGB model of Eiler et al. (1993). Diffusion is enhanced due to deformation-induced formation of domain- and subgrain boundaries, as seen in CL images as a network of narrow dark CL bands. Those fast diffusion pathways reduce diffusion distances for stable isotopes and trace elements.

## REFERENCES

- Eiler et al. (1993), *Geochim. Cosmochim. Acta*, 57/11, 2571-2583.  
 King EM, Barrie CT, Valley JW (1997), *Geology* 25:1079–1082  
 Ramírez de Arellano et al. (2012), *Tectonics*, 31, 1-18.

## P 2.11

### **Biotite Rb-Sr and Rutile U-Pb age data confirming an extensive Neoproterozoic overprint in the Eastern Ghats Belt (India)**

Axelsson Emelie, Mezger Klaus, Villa Igor M.

*Institute of Geological Sciences, University of Bern, Balzerstrasse 3, CH-2012 Bern (axelsson@geo.unibe.ch)*

The Eastern Ghats Belt (EGB) is a granulite facies metamorphic belt along the East coast of India, and is a patchwork of discrete crustal segments with distinct geological histories. It records the formation and destruction of at least two earlier supercontinents, namely Columbia (ca. 2.1 – 1.8 Ga) and Rodinia (ca. 1.0 – 0.9 Ga); as a part of the amalgamation of India and East Antarctica, and Australia into the SWEAT (SW United States and East Antarctica) terrane.

Four crustal domains with unique isotopic signatures and ages can be distinguished within the EGB (Rickers et al., 2001). The highest-grade metamorphism was attained during the regional metamorphism at ca. 950 Ma.

To reconstruct the post-peak evolution after the 950 Ma metamorphic imprints, biotite Rb-Sr and rutile U-Pb ages were determined for biotite-rich metapelitic gneisses. These ages range from 437 – 615Ma for the biotites with a general trend of a younging towards the Northwest. Rutile U-Pb ages range from 480 – 531Ma and record ages slightly younger than the biotite Rb-Sr ages, in samples where mineral pairs could be dated. The biotites have high Mg content, and the general mineral assemblage for all samples is that typical of high temperature granulites: plag + phl + sil + grt and, depending on the protolith, kfs, crn or crd. Common accessory mineral phases are: rt, zrc, spl, ap, spr.

Very young biotite and rutile ages like these are unlikely to be the result of slow cooling from the granulite facies conditions at ca 950 Ma. Instead they record a low-grade static thermal overprint of the orogenic belt. This overprint coincides with high-grade metamorphism in southern India and Sri Lanka (ca. 580-550 Ma), during the Pan-African orogeny. The young ages on a regional scale extend the known area of the pan-African overprint in India significantly.

## REFERENCES

- Rickers, K., Mezger, K., Raith, M. (2001), *Precambrian Research*, 112:28.

## P 2.12

# Nb/Ta, Zr/Hf and HREE to Understand Accessory Mineral Thermometers at High and Ultra-High Temperatures.

Federico Galster, Othmar Müntener & Tanya Ewing

*Institut of Earth Sciences, University of Lausanne. Géopolis, 1015 Lausanne.*

Zr-in-Rutile is a newly established thermometer calibrated both empirically and experimentally (e.g. Zack et al., 2004a; Ferry & Watson, 2007). Its validity and precision as thermometer at intermediate temperatures (400-650°C) has been shown in various geologic settings. However, the application of this thermometer to high and ultra-high temperatures (700-1100°C) is more problematic since investigations on small terranes or even single samples result in a large set of temperatures. Moreover, the application of Zr-in-Rutile and Ti-in-Zircon to single samples results in contrasting temperatures. With the aim to explain these contrasting temperatures, we study the systematics of these thermometers at high and ultrahigh temperature using the lower crustal section of the Ivrea-Verbano Zone (IVZ) as an example.

The IVZ consists of a metamorphic heterogeneous formation (the so-called kinzigite formation, mostly composed by paragneiss whose metamorphic grade ranges from amphibolite in the southeast to granulite conditions in the northwest) intruded by a Mafic Complex. The Mafic Complex consists essentially of gabbros and diorites with minor pyroxenites and ultramafic intercalations. The lower (northwestern) and the central part of the mafic complex are rich in metric to hectometric paragneiss septa (host-rock) originated from the kinzigite formation. We collect rutile and zircon from these highly metamorphic paragneiss septa.

Zircons and rutiles are investigated by LA-ICP-MS. For Zr-in-Rutile we apply the thermometer of Tomkins et al. (2007) assuming 8 kbar, for Ti-in-Zircon we apply the thermometer of Ferry and Watson (2007).

Temperatures (T) obtained by both thermometers in single samples are contrasting: samples showing ultrahigh Zr-in-Rutile T (950-1000°C) show a second population of “rutile” T close to 750-800°C and, if present, one population of Ti-in-Zircon T close to 850°C. Samples showing ultrahigh Ti-in-Zircon T (~970°C) show a second population of “zircon” T close to 850°C and one population of Zr-in-Rutile T close to 750-800°C. No sample shows ultrahigh temperatures (UHT) recorded by both Ti-in-Zircon and Zr-in-Rutile thermometers. Ti-in-Quartz thermometer records UHT in all rutile-bearing samples.

The geochemistry of zircon and rutile coupled with their textural context can help in the interpretation of these contrasting results. Particularly useful are the Nb/Ta ratio and the HREE profiles in zircon, and the Zr/Hf ratio in rutile. The apparently contrasting results can be explained as a consequence of 1) two generations of rutile, one of UHT and one of lower T, 2) subsequent recrystallization at lower T of part of the UHT generation, 3) protracted zircon growth and 4) heterogeneous and evolving zircon solubility and aTiO<sub>2</sub> in the rocks.

In the IVZ rutile grew mainly as a consequence of biotite breakdown. Rutile growth can dramatically fractionate Ta from Nb, thus the topology of the Nb/Ta vs Ta line for a zircon population helps us to understand which zircon rim precedes rutile growth, and which rim grows during or after rutile.

The HREE profiles in zircon yield important information concerning the competition of zircon with other phases with high HREE partition coefficient (e.g. garnet). Zircon with steep HREE profiles are interpreted as grown in garnet free domains or in open system, zircon with flat HREE profile are interpreted as grown in garnet bearing domains and in a closed system.

Our zircons rim with high Ta and low Nb/Ta (i.e grown before rutile growth) have steep HREE profiles and yield lower T compared to rims with low Ta and medium to high Nb/Ta (i.e grown during or after rutile growth). The UHT zircons with low Ta and medium to high Nb/Ta ratio are split in two populations: one with higher Ta, lower Nb/Ta and steeper HREE profiles and one with lower Ta, higher Nb/Ta and flat HREE profiles.

Hf in rutile shows a strong correlation with T obtained by Zr-in-Rutile, but the preference of rutile for Hf compared to Zr increases with decreasing T. Thus, theoretically, rutile recording UHT should have higher Zr/Hf compared to low T rutile. Some samples show exclusively this trend, but some samples additionally show some low T rutile with high Zr/Hf. We interpret this signature as evidence for two generations of rutile: (1) one growing at UHT (High Zr/Hf and high Zr-in-rutile T°C, high W), some of these rutile grains recrystallize at lower T (low Zr/Hf ratios, but still high W), and (2) one group, which grew at lower T in a domain controlled by zircon dissolution (high Zr/Hf, low Zr-in-Rutile T, low W). The presence of both generations in a single sample is found in a highly depleted mostly zircon-free paragneiss septa. The UHT generation is confined to the restitic part of the septa (gr+sill+cor+ru+sp), the low T generation is confined to the melt (pl+ru±q).

A model making the link between the obtained temperatures, the geochemistry of zircons and rutile and the geological evolution of the rocks will be presented.

## REFERENCES

- Ferry, J., Watson, E., 2007: New thermodynamic models and revised calibration for Ti-in Zircon and Zr-in-Rutile thermometers. *Contrib Min Petrol* 154, 429-437
- Tomkins, H.S., Powell, R., Ellis, D.J., 2007: The pressure dependence of Zr-in-rutile thermometer. *J. Metamorph Geol* 25, 703-713
- Zack, T., Moraes, R., Kronz, A., 2004. Temperature dependence of Zr in rutile: empirical calibration of a rutile thermometer. *Contrib Min Petrol* 148, 471-488

## P 2.13

# CO<sub>2</sub>-rich fluid inclusion in upper mantle xenoliths from Nyos and Barombi-Mbo lakes: Cameroon Volcanic Line

Tene Djoukam Joëlle Flore<sup>1,2</sup>, Moritz Robert<sup>2</sup>, Tchouankoue Jean Pierre<sup>1</sup>

<sup>1</sup> Département des sciences de la Terre, Université de Yaoundé I, BP: 812, Yaoundé-Cameroun. [Joeflora2003@yahoo.fr](mailto:Joeflora2003@yahoo.fr)

<sup>2</sup> Section des sciences de la Terre et de l'environnement, Université de Genève, Rue des Maraîchers 13, 1205 Genève.

The western part of Cameroon displays an alignment of Tertiary to Recent alkaline volcanoes, plutons and grabens over a distance of more than 1600 km, which is known as the Cameroon Volcanic Line (CVL). The CVL stretches from the island of Palagu through the Gulf of Guinea to Lake Chad within the African continent. Recently, the CVL has been considered as a major lithospheric structure tapping a hot deep asthenospheric zone. Nyos and Barombi-Mbo alkali basalts are between 1.5 and 0.2 my old (Déruelle *et al.*, 2007), and their pyroclastic deposits include a large number of ultramafic xenoliths (Temdjim *et al.*, 2004; Teichou *et al.*, 2007).

The studied xenoliths are spinel lherzolites, mostly composed of olivine, orthopyroxene (commonly enstatite), and clinopyroxene (diopside) with granular and porphyroclastic textures. CO<sub>2</sub>-bearing fluid inclusions have been studied by petrography, microthermometry and Raman spectroscopy. Based on fluid inclusions petrography, the Barombi and Nyos xenoliths contain abundant CO<sub>2</sub>-rich inclusions, trapped in orthopyroxene, clinopyroxene and olivine.

In Barombi xenoliths, fluid inclusions are mostly hosted by orthopyroxene and clinopyroxene and have negative-crystal, elongated, round, sub-round and irregular shapes with sizes varying between 2 and 48 μm. They contain either only one phase (liquid) or two phases (liquid and vapor) at room temperature. All inclusions are generally grouped along healed fractures.

By contrast, in Nyos xenoliths, fluid inclusions are mostly hosted by orthopyroxene and olivine, they are randomly distributed and isolated and are generally located along healed fractures. We can distinguish two well-defined fluid inclusion types. Type 1 is negative crystal shaped, irregular, sub-angular and round inclusions hosted by orthopyroxene, with sizes between 7 and 27 μm, containing two to three phases at room temperature. Type 2 are hosted by olivine, have negative crystal and sub-round shapes, contain one to two phases at room temperature, and have sizes ranging between 4 and 14 μm.

In Barombi xenoliths, CO<sub>2</sub> melting temperature range between -58.0 and -56.6 °C, whereas, in the Nyos samples, there is a wider range between -68.0 and -56.8 °C. These data suggest that in most cases, the fluid phase is pure CO<sub>2</sub>. Homogenization temperatures into the liquid and vapor phases are between -48.1 and +31.1 °C in the Barombi-Mbo xenoliths, and between -38.1 and +31.1 in the Nyos xenoliths.

The calculated density of CO<sub>2</sub> based on our microthermometric data yields a range of 0.20 to 1.15 g/cm<sup>3</sup> for the Barombi-Mbo inclusions, whereas those of Nyos have densities between 0.77 and 1.06 g/cm<sup>3</sup>. Microthermometry suggests the presence of other dissolved gas phase(s) in the fluid inclusions trapped in the xenoliths, which show values of melting temperatures below the one of pure CO<sub>2</sub> (<-56.6 °C). Raman microspectroscopy confirms that such fluid inclusions contain H<sub>2</sub>S besides CO<sub>2</sub> in Barombi xenoliths.

### REFERENCES :

- Déruelle, B., Ngounouno, I and Demaiffe, D. (2007). The Cameroon Hot Line (CHL): A unique example of active alkaline intraplate structure in both oceanic and continental lithospheres. *Comptes Rendus Géosciences* 339, pp. 589-600.
- Teichou, M.I., Grégoire, M., Dantas, C. et Tchoua, F.M. (2007). Le manteau supérieur à l'aplomb de la plaine de Kumba (Ligne du Cameroun), d'après les enclaves de péridotites à spinelles dans les laves basaltiques. *Comptes Rendus Géosciences* 339, pp. 101-109.
- Temdjim, R., Boivin, P., Chazot, G., Robin, C., et Rouleau, E. (2004). L'hétérogénéité du manteau supérieur à l'aplomb du volcan de Nyos (Cameroun) révélé par les enclaves ultrabasiques. *Comptes Rendus Géosciences* 336, 1239-1244.

## P 2.14

### Control of magma recharge and buoyancy on the frequency and magnitude of volcanic eruptions

Luca Caricchi<sup>1</sup>, Catherine Annen<sup>2</sup>, Jon Blundy<sup>2</sup>, Guy Simpson<sup>1</sup>

<sup>1</sup> Section of Earth and Environmental Sciences, University of Geneva, Rue des Maraîchers 13, CH-1205 Geneva, CH

<sup>2</sup> Department of Earth Sciences, University of Bristol, Wills Memorial Building, Queen's Road, BS8 1RJ, Bristol, UK

The frequency at which volcanic eruptions occur is inversely proportional to the volume of magma released in a single event. The basic requirements for a volcanic eruption to occur are that enough heat is supplied to the crust to assemble a body of eruptible magma and that overpressure is sufficient for the magma to reach the surface without solidifying. Starting from these basic principles we used thermo-mechanical calculations and Monte Carlo simulations to quantify the relative contribution of magma fluxes and the physical properties of the crust on likelihood and volume of volcanic eruptions. The calculations were performed considering the periodic input of magma in pulses of different size and shape injected at various frequencies. The average rate of magma supplied to the upper crust over hundreds of thousands of years appears to control the volume of magma that can potentially be released during a single eruption, whereas the time interval between short-lived pulses of magmatism, affects the total duration of magma injection preceding an eruption. Our calculations reconcile the relationship between erupted volume and upper crustal magma residence times, and replicate the correlation between erupted volumes and caldera dimensions. Our modelling shows that relatively small and frequent eruptions are triggered by magma injection while buoyancy is important to trigger large eruptions. These calculations permit to identify the physical processes controlling the relationship between frequency and magnitude of volcanic eruptions and increase our capability of determining the temporal evolution of volcanic activity in different volcanic systems.

## P 2.15

### A new occurrence of kosmochlor in Cr-jadeite rocks from Kenterlau-Itmurundy (Lake Balkhash, Kazakhstan)

Ernst Kristina<sup>1</sup>, Franz Leander<sup>1</sup>, Krzemnicki Michael S.<sup>2</sup>, Harlow George E.<sup>3</sup>, De Capitani Christian<sup>1</sup>  
& Kouznetsov Nikolai<sup>4</sup>

<sup>1</sup>Geologisch-Paläontologisches Institut, University of Basel, Bernoullistrasse 32, CH-4056 Basel (kristina.ernst@stud.unibas.ch)

<sup>2</sup>Schweizerisches Gemmologisches Institut SSEF, Falknerstrasse 9, CH-4001 Basel (gemlab@ssef.ch)

<sup>3</sup>American Museum of Natural History, New York

<sup>4</sup>Jade Resources, LTD, Hong Kong

Petrographic, petrologic and geochemical investigations on Cr-jadeite rocks from Kenterlau-Itmurundy near Lake Balkhash (Kazakhstan) reveal five different rock groups. *Jadeitites* show irregular, medium-grained white sections made up of decussate jadeite crystals and fine-grained sections made up of aligned Cr-jadeite. *Omphacite jadeitites* show a homogeneous, pale green color with randomly oriented jadeite crystals, which are overgrown by omphacite on their rims and along fractures.

*Phlogopite-analcime jadeitites* show decussate, white sections made up of jadeite and foliated, partially microfolded green layers and spots consisting of Cr-jadeite. Analcime and phlogopite formed late in fractures in the jadeite-rich sections. *Phlogopite-omphacite jadeitites* reveal an inhomogeneous mineral distribution with a dark-green matrix made up of sheaf-like aggregates of Cr-omphacite and white spots of decussate prismatic jadeite crystals. Post-crystallization deformation is evident by bent and twisted pyroxenes while phlogopite formed post-tectonically on fractures and grain boundaries.

Due to the extreme textural inhomogeneity, transitions between these four groups are blurred. *Kosmochlor-analcime-albite-omphacite jadeitites* reveal an inhomogeneous fabric with decussate, white sections, pale-green shear bands, and dark green layers. Again, white jadeite-rich sections formed pre-tectonically while shear bands display aligned Cr-omphacite and Cr-jadeite. In rare cases, these bands contain small aggregates of kosmochlor.

The main occurrence of kosmochlor is in the dark green layers, where it mantles strongly corroded chromite grains. Microprobe investigations of two kosmochlor-bearing rocks and one phlogopite omphacite jadeitite reveal extreme mineral compositional variability. Pyroxene zoning with jadeite cores and rim sections of omphacite or Cr-omphacite are wide spread. Similarly, kosmochlor aggregates are very inhomogeneous covering a wide range in the pyroxene plots (Figs. 1 A&B). Similar textures have been observed by other investigations (e.g. Shi et al. 2005) and are due to pre-, syn- and post-tectonic crystallization processes. Distinct inhomogeneities are also revealed by ED-XRF spot analyses, which show a strong compositional variability from section to section.

As evident from these investigations, nearly pure jadeite formed pre-tectonically. During subsequent deformation, Ca- and Cr-rich fluids led to the formation of omphacite, Cr-omphacite, Cr-jadeite and eventually to kosmochlor. The largest modal amount of kosmochlor formed pre- and syn-tectonically in chromite-bearing layers of the rocks. Analcime, albite and phlogopite formed post-tectonically and during late brittle deformation.

Until now, terrestrial kosmochlor has been described from Burma (Ou Yang 1984), New Zealand (Ikehata & Arai 2004), Japan (Anthony et al. 1995), Kola peninsula and Lake Baikal, Russia (Zozulya et al. 2003; Reznitskii et al. 1999). Similar to these occurrences, the presence of kosmochlor in Cr-rich jadeitites from Kenterlau-Itmurundy, is explained by appropriate rock composition, pervasive HP/LT conditions (i.e. 600°C at 1.2 GPa; Dobretsov & Ponomareva 2009). According to their rock fabrics and to the geology of the area we interpret the Kazakhstan jadeitites as P-types as defined by Tsujimori & Harlow (2012).

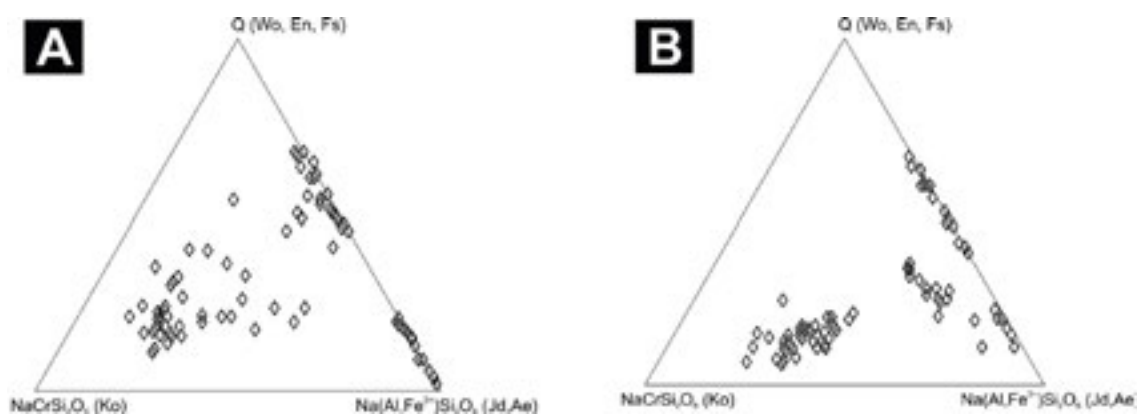


Figure 1. Microprobe analyses from the kosmochlor-bearing samples 104276 (A) and 104277 (B) reveal the great compositional variability of pyroxene in these rocks.

## REFERENCES

- Anthony, J.W., Bideaux, R.A., Bladh, K.W. & Nichols, M.C. 1995: Handbook of Mineralogy. Volume 2: Silica, silicates. Part one, 430.
- Dobretsov, N.L. & Ponomareva, L.G. 2009: Comparative characteristics of jadeite and associated rocks from Polar Ural and Prebalkhash region. *International Geology Review* 10, 221-242.
- Ikehata, K. & Arai, S. 2004: Metasomatic formation of kosmochlor-bearing diopside in peridotite xenoliths from North Island, New Zealand. *American Mineralogist*, 89, 1396-1404.
- Ou Yang, C.M. 1984: Terrestrial source of ureyite. *American Mineralogist*, 69, 1180-1183.
- Zozulya, D.R., Gavrilenko, B.V. & Savchenko, Y.E. 2003: Kosmochlor from coastal sediments of Tersky coast in the White Sea, Kola Peninsula. *Zapiski Vserossijskogo Mineralogicheskogo Obshchestva*, 132, 101-108.
- Reznitskii, L.S., Sklyarov, E.V., Karmanov, N.S. (1999): The first find of kosmochlor (ureyite) in metasedimentary rocks. *Doklady Akademii Nauk*, 363, 1049-1053.
- Shi, G.H., W., Stöckhert, B. & Cui, W.Y. 2005: Composition and texture of kosmochlor and chromium clinopyroxenes in rocks from the Myanmar jadeitite area. *Mineralogical Magazine*, 69, 1059-1075.
- Tsujimori, T. & Harlow, G.E. (2012): Petrogenetic relationships between jadeitite and associated high-pressure and low-temperature metamorphic rocks in worldwide jadeitite localities: a review. *European Journal of Mineralogy*, 24, 371-390.

## P 2.16

## Kosmochlor from Myanmar – Investigations on a possible miscibility gap in the solid solution jadeite-kosmochlor

Schweinar Kevin<sup>1</sup>, Franz Leander<sup>1</sup>, De Capitani Christian<sup>1</sup>, Hänni Henry A.<sup>2</sup> & Thyesson Tay<sup>3</sup>

<sup>1</sup>Mineralogisch-Petrographisches Institut, University of Basel, Bernoullistrasse 30, CH-4056 Basel (k.schweinar@stud.unibas.ch; leander.franz@unibas.ch; christian.decapitani@unibas.ch)

<sup>2</sup>SSEF Schweizerisches Gemmologisches Institut, Basel, Falknerstrasse 9, CH-4001 Basel (h.a.haenni@gmail.com)

<sup>3</sup>Far East Gemological Laboratory, 360 Orchard Road, Singapore

Petrographic, petrologic and geochemical investigations on kosmochlor-bearing rocks from the so-called Jade Mine Tract, near Hpakan, Kachin State (Myanmar) reveal five different lithologies. *Kosmochlor(-bearing)-clinoamphibole-jadeite rocks and schists* show aggregates of radiating dark green kosmochlor formed around strongly corroded chromite grains. Kosmochlor is partly replaced by a light green rim of Cr-jadeite or Cr-omphacite, which in turn shows diffuse grain boundaries towards jadeite. Post-crystallisation folding is evident by partly aligned matrix minerals. *Albite-glaucophane-kosmochlor-Cr-jadeites* reveal an inhomogeneous fabric consisting of lenses made up of kosmochlor and Cr-jadeite. Again, kosmochlor aggregates are intergrown with tiny fragments of chromite. Foliated sections mainly consisting of albite and glaucophane cut through these structures. *Kosmochlor-bearing jadeite clinoamphibolites* also show an inhomogeneous mineral distribution with richterite-rich sections and sections made up of Cr-jadeite and Cr-omphacite. The occurrence of kosmochlor, which is mainly enclosed in Cr-jadeite and richterite, is restricted to small spots. The last rock types are *kosmochlor-bearing clinoamphibole phlogopite jadeite schists* and *kosmochlor-analcime-microcline jadeites*, which bear kosmochlor and Cr-jadeite in microfractures formed by post-crystallisation deformation. Eventually, dynamic recrystallisation may be observed. Along these fractures, Cr-rich fluids percolated leading to the formation of Cr-pyroxenes.

All investigated rocks are boulders, which formed as dikes in serpentinitised, ultramafic bodies. The growth of kosmochlor, Cr-jadeite, Cr-omphacite as well as sodic and sodic-calcic amphiboles was due to metasomatic reactions between jadeite and depleted peridotite at HP/LT-conditions ( $T \sim 450^\circ$ ,  $P = 10-15$  kbar; cf. Shi et al., 2005; Harlow et al. 2007).

Microprobe investigations on one probe of each lithology reveal massive mineral chemical inhomogeneities especially in the case of kosmochlor. Strongly zoned minerals with increasing Cr content towards the rims are common. Furthermore, jadeite, Cr-jadeite and Cr-omphacite also show extremely complex internal structures (i.e. irregular zoning, exsolution textures and microcrystalline intergrowth). Q-Ko-(Jd+Ae) plots show clusters of data points at distinct compositions on the join Ko-(Jd+Ae) (Fig. 1 A). An apparent lack of data points between 25-40 mol-% Ko and 62-71 mol-% Ko might be a hint at a possible miscibility gap in this system. This tendency becomes more indistinct with plotting all results in one diagram (Fig. 1 B), which may be due to microcrystalline intergrowth beyond the resolution of the microprobe or local geochemical inhomogeneities of the rock. Additionally, the well-known miscibility gap in the system (Jd+Ae)-Omp (Davidson & Burton 1987) can be observed in every sample.

The existence of a miscibility gap has been discussed by several authors (e.g. Abs-Wurmbach & Neuhaus 1976, Yang 1984, Mével & Kiénast 1986). As evident from these investigations, even two or three gaps seem possible. However, to prove these hypothetical gaps, transmission electron microscope (TEM) investigations as well as further experimental and thermodynamic data are needed.

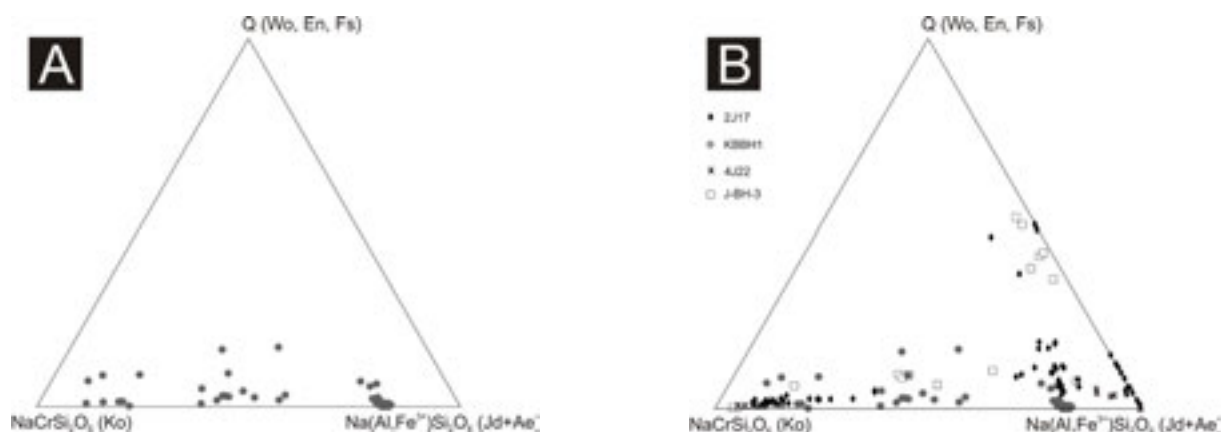


Figure 1. Microprobe analyses from the sample KBBH1 (A) and all samples (B) reveal possible miscibility gaps along the join Ko-(Jd+Ae).

## REFERENCES

- Abs-Wurmbach, I. & Neuhaus, A. 1976: Das System NaAlSi<sub>2</sub>O<sub>6</sub> (Jadeit) – NaCrSi<sub>2</sub>O<sub>6</sub> (Kosmochlor) im Druckbereich von 1 bar bis 25 kb bei 800°C. *Neues Jahrbuch für Mineralogie*, 127, 213-241.
- Davidson, P.M. & Burton, B.P. 1987: Order-disorder in omphacitic pyroxenes: A model for coupled substitution in the point approximation. *American Mineralogist*, 72, 337-344.
- Mével, C., & Kinéast, J.R. 1986: Jadeite-kosmochlor solid solution and chromian sodic amphiboles in jadeitites and associated rocks from Tawmaw (Burma). *Bulletin de Minéralogie*, 109, 617-633.
- Harlow, G.E., Sorensen, S.S. & Sisson, V.B. 2007: Jade. In: *Geology of Gem Deposits*. Mineralogical Association of Canada, 207-253.
- Shi, G.H., Stöckhert, B. & Cui, W.Y. 2005: Kosmochlor and chromian jadeite aggregates from the Myanmar jadeite area. *Mineralogical Magazine*, 69, 1059-1075.
- Yang, C.M.O. 1984: A terrestrial source of ureyite. *American Mineralogist*, 69, 1180-1183.

## P 2.17

## Multiple quartz generations associated with polymetallic mineralization at Colquijirca, central Peru: a fluid inclusion and SEM-CL study

Casanova Vincent<sup>1</sup>, Kouzmanov Kalin<sup>1</sup>, Fontboté Lluís & BendeZú Ronner<sup>2</sup>

<sup>1</sup>*Earth and Environmental Sciences, University of Geneva, Rue de Maraîchers 13, CH-1205 Geneva, Switzerland  
(vincent.casanova@unige.ch)*

<sup>2</sup>*Terra Pristina S.A.C., Calle Bilbao 295, San Isidro, Peru*

The Colquijirca district in central Peru is an 8 km-long mineralized N-S corridor centered onto the dacitic diatreme-dome complex of Marcapunta, and comprises two distinct mineralization styles BendeZú and Fontboté (2009). A first high-sulfidation disseminated Au-Ag mineralization event/stage was emplaced within the diatreme-dome complex. A later sulfide-rich polymetallic epithermal event/stage, exhibiting zonal metal distribution, mostly replaces favorable carbonate rocks of Late Triassic-Lower Jurassic and Early Cenozoic age. Zonation consists of enargite-luzonite in the core of the system grading into intermediate-sulfidation assemblage of chalcopyrite-sphalerite-galena and eventually Zn-bearing carbonates towards the periphery. Preliminary fluid inclusion data were reported by BendeZú (2007). This work focuses on mineral textures and relationships and presents results of the subsequent fluid inclusion study.

Applying the scanning electron microscopy-cathodoluminescence (SEM-CL) technique on representative samples from Colquijirca, five different generations – Q1 to Q5 – have been distinguished (Figure 1). Q1 is associated with pyrite and replaces the carbonate host rocks. Pyrite-free banded colloform quartz precipitation followed (Q2). These two early quartz generations precede mineralization and are devoid of fluid inclusions. They are later brecciated and fine-grained quartz (Q3) with numerous liquid-vapor (L-V) fluid inclusions is deposited. Q3 is associated with fine-grained pyrite and contains barite-celestite and anhydrite inclusions. Coarser-grained quartz (Q4), with sphalerite, hematite, pyrite, and rare enargite inclusions, overgrows Q3. Inclusions are often associated to one of Q4 outermost growth bands. In places, Q4 is overgrown by Q5 containing inclusions of aluminum phosphate-sulfate (APS) minerals, most likely woodhouseite. Q3 and Q4 are present throughout the deposit and contain fluid inclusion assemblages that can be classified as primary L-V using the CL textures of quartz; secondary L-V and boiling assemblages are also observed in certain Q4 grains.

Preliminary study of quartz- and sphalerite-hosted fluid inclusions and available isotope data suggest mixing between a hot (300°C), moderately saline (6-7 wt% NaCl eq.), magmatic-derived fluid and cooler meteoric waters. This study also shows that homogenization temperatures (Th) are strongly controlled by the distance of a given sample to the assumed center of the magmatic-hydrothermal system – Th decreases outward from 300°C, next to the diatreme-dome complex to 190°C 3.5 km northward (BendeZú 2007).

The present study was performed on quartz-hosted primary fluid inclusion assemblages (FIA); all of which contain aqueous, liquid-rich fluid inclusions having a vapor phase of 15-25% vol.%. Relative timing was established based on SEM-CL study (Figure 1) and mineral inclusions associated with individual growth bands.

FIA's hosted in the inner part of Q4, devoid of any mineral inclusions have salinities and Th decreasing outward from 11 to 3.3 wt% NaCl eq. and 264° to 220°C, respectively. Subsequent growth zones are associated with 5 to 20 µm-large pyrite inclusions. They contain FIA's with salinities ranging from 3.15 to 9.2 wt% NaCl eq. while Th ranges between 204° and 240°C. Salinities in these FIA's may however be overestimated as CO<sub>2</sub> has been detected in some inclusions using Raman spectroscopy. This pyrite zone is often overgrown by a zone containing 5 to 10 µm-large hematite and scarce 20 µm-large sphalerite crystals. FIA's associated with the hematite zone have lower salinities 2.8-3.2 wt% NaCl eq. and homogenize between 270° and 290°C. Such a fluid evolution requires several pulses of a moderately saline (around 11 wt% NaCl eq.) magmatic fluid mixing to various degrees with heated meteoric waters.

The ongoing work unravels a complex fluid history. It shows that the polymetallic mineralization at Colquijirca is the result of several distinct pulses of magmatic fluids. Further well constrained FIA's study performed in both gangue and ore minerals coupled with LA-ICP-MS analyses of individual fluid inclusions, and in situ δ<sup>18</sup>O analysis of hydrothermal quartz are planned in order to support this hypothesis.

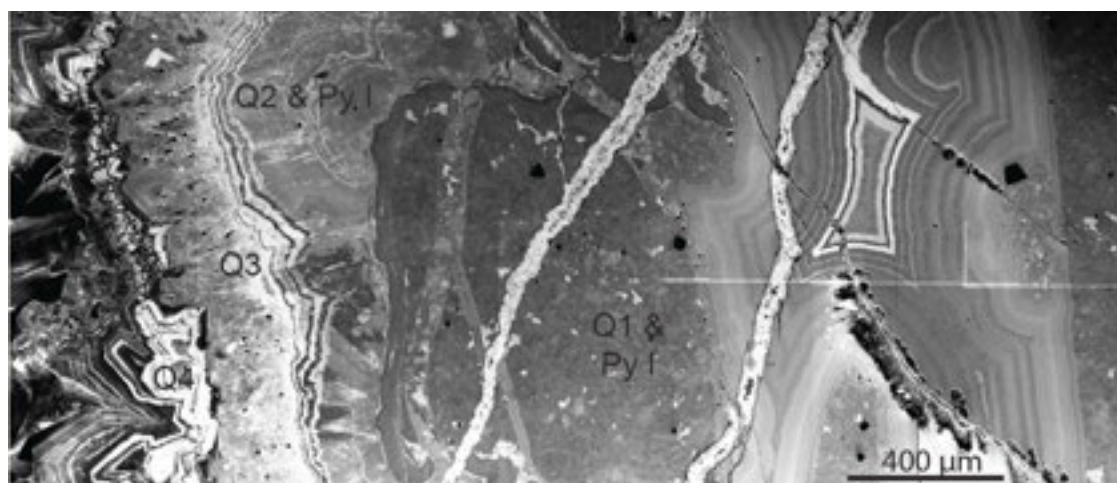


Figure 1: Multiple quartz generations replacing the carbonate host rock (Q1 & Q2) and associated with polymetallic mineralization (Q3 & Q4); a composite SEM-CL image.

#### ACKNOWLEDGMENTS

This study is supported by the Swiss National Science Foundation (grant 200020\_134872). The El Brocal SAA is gratefully acknowledged for logistic support and access to the mine site.

#### REFERENCES

- Bendezú, R. 2007: Shallow polymetallic and precious metal mineralization associated with a Miocene diatreme-dome complex: the Colquijirca district in the peruvian andes, *Terre & Environnement*, 64, 221p.
- Bendezú, R. & Fontboté, L. 2009: Cordilleran epithermal Cu-Zn-Pb-(Au-Ag) mineralization in the Colquijirca district, central Peru. *Economic Geology*, 104, 905-944.

## P 2.18

# Neof ormation of “exotic” copper minerals from gel-like precursors at the Exotica deposit (northern Chile)

Lambiel Frédéric<sup>1</sup>, Dold Bernhard<sup>2</sup>, Fontboté Lluís<sup>3</sup>, Vennemann Torsten<sup>1</sup> & Spangenberg Jorge E.<sup>1</sup>

<sup>1</sup> Institute of Earth Sciences (ISTE), University of Lausanne, CH-1015 Lausanne (frederic.lambiel@unil.ch)

<sup>2</sup> SUMIRCO (Sustainable Mining Research & Consult.EIRL), San Pedro de la Paz, Chile

<sup>3</sup> Earth and Environmental Sciences, University of Geneva, CH-1205 Genève

Cu-rich solutions seep out presently at several parts of Mina Sur (Lambiel 2012, 2013), the exotic mineralization south of the giant porphyry Cu-deposit of Chuquicamata (Atacama Desert, northern Chile; Pinget 2011, 2012). At the places where these solutions outflow, they give rise to the formation of blue and green Cu-bearing gel-like precipitates (Fig. 1a). Within these gels, typical exotic Cu-minerals such as atacamite, brochantite and other less common Cu-sulfates such as devilline, spangolite, schulenbergite have been determined using XRD, SEM, ESEM, and FTIR (Fig.1b), some present only in trace amount. Malachite crusts underneath gels were recognized. Chrysocolla, the main copper mineral of the exotic mineralization, was never identified in the copper gels.

The Cl/SO<sub>4</sub> ratio of water-gel solutions dominated by Cu-sulfates is < 0.25 and about 2.38 in water-gel solutions dominated by Cu-chloride. The Cu-hydroxide-chloride atacamite is associated with solutions with a pH slightly below 6. Most Cu-sulfates (e.g. brochantite, spangolite) are associated with slightly acidic water (pH 6.0 to 6.5) whereas the Cu-sulfate devilline is stable in gel associated with near neutral to slightly alkaline water (pH 7.2 to 7.8). Gels kept in sealed bottles developed within months textures similar to those seen in exotic veins. Similarities in terms of mineralogy, chemistry and/or texture suggest that these gel-like materials are a normal and major step in the formation of exotic Cu-mineralization. Several authors have proposed elsewhere that chrysocolla is formed by the solidification of a hydrogel of Cu-silica. The findings of the present work suggest that other copper minerals such as atacamite also develop within gel-like materials. Gel and neof ormed Cu-minerals within gels in Mina Sur may mirror past ore formation processes of porphyry Cu-deposits in northern Chile.

A total of 27 water samples were analyzed for their chemical composition (major and trace elements), stable isotope compositions of water ( $\delta^{18}\text{O}$  and  $\delta^2\text{H}$ , Fig. 1c) and sulfate ( $\delta^{34}\text{S}$  and  $\delta^{18}\text{O}$ , Fig. 1d). The results suggest that in the northeast side of the Mina Sur pit, gels are derived from industrial waters that have leached copper oxide zones located north of Mina Sur. On the southern part of the pit, the outflow of high Cl and NO<sub>3</sub><sup>-</sup> rich waters suggest that the lower, saline aquifer of the Loa basin is involved and crops out. The  $\delta^{34}\text{S}$  and  $\delta^{18}\text{O}$  values of the dissolved sulfate in these waters suggest its derivation from Oligocene to Pleistocene evaporites of the Loa basin. These saline outflows give rise in places to Cu-rich gels partly containing atacamite. The most plausible source of Cu contained in these outflows of saline waters is an unknown supergene enriched zone buried below the southern part of the pit. The continuous gel formation (since 2005) and the abundance suggest that the Cu-source may be important.

### Acknowledgements

The project is carried out with funding of the Swiss National Science Foundation (grant 129988) and of the Fondation A. Lombard, and with the support of the Geology Department of the Chuquicamata mine (CODELCO).

### REFERENCES<sup>1</sup>

- Pinget, M.C., Fontboté, L., Dold, B., Ramirez, F., Vergara, M. 2011: The supergene enrichment at Chuquicamata revisited. Proceedings 11th SGA Biennial Meeting, Antofagasta, Chile, 823-825.
- Pinget, M.-C., Dold, B., Fontboté, L., Vergara, M., Rojas de la Rivera, J. 2012: Mineralogía de la mineralización exótica en Chuquicamata: nuevos avances. Proceedings 13th Congreso Geológico Chileno, Antofagasta, Chile, 37-39.
- Lambiel, F., Dold, B.S., and Fontboté, L. 2012: Present copper-rich “gel” formation in the giant porphyry copper deposit of Chuquicamata (northern Chile), in 10th Swiss Geoscience Meeting, p. 122-123.
- Lambiel, F. 2013: New insights into the ore genesis of the Exotica deposit at Chuquicamata (Northern Chile) through the neof ormation of Cu-oxide minerals from gel-like precursors, Master Thesis, 92 p.

<sup>1</sup>Other references in Lambiel, F. 2013

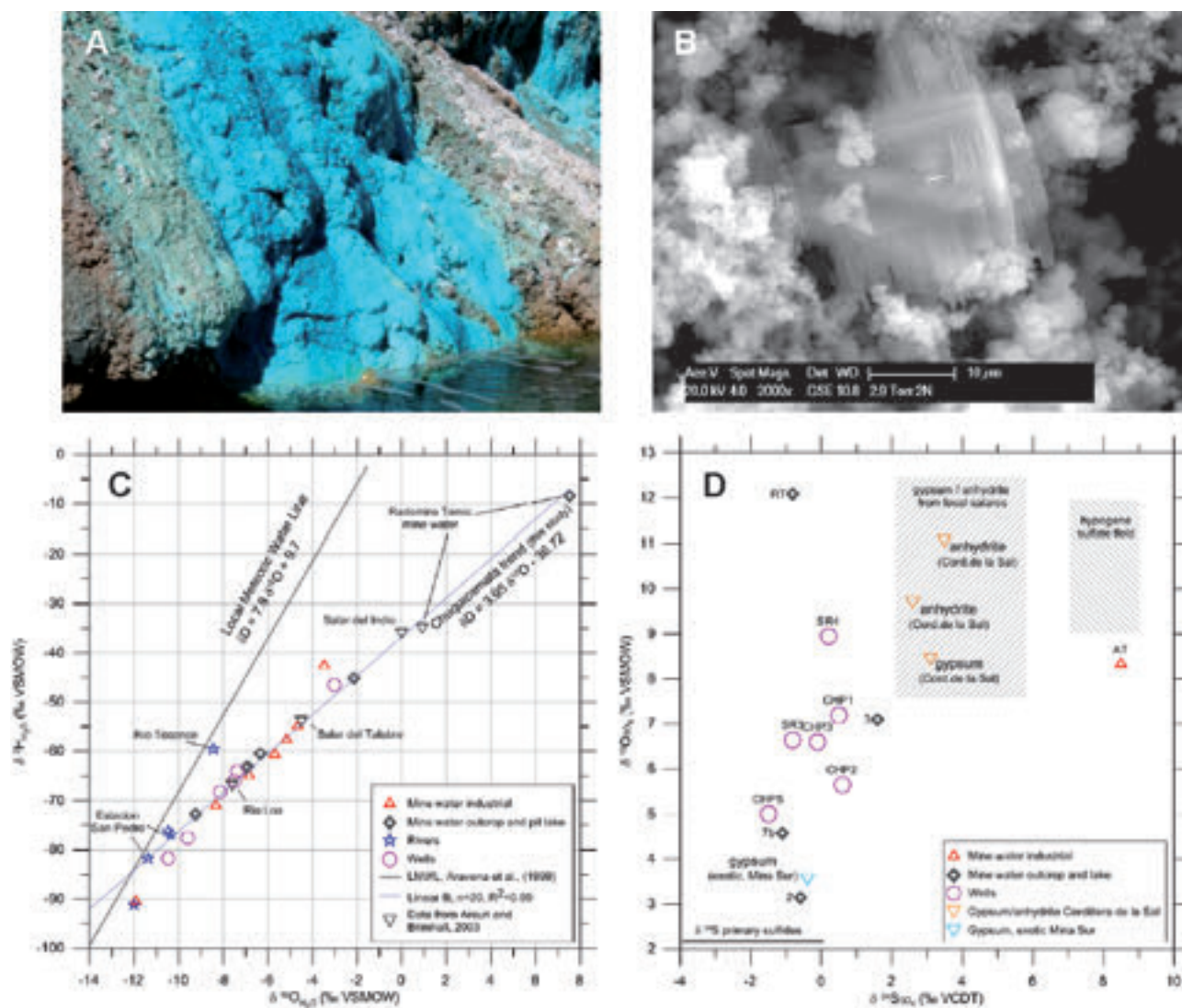


Figure 1 A) Occurrence of copper rich gel in the southernmost part of Mina Sur. B) Cu-sulfate (devilline?) in a gel precipitate north of Mina Sur (ESEM micrograph, sample 2N) C) Oxygen and hydrogen isotope analyses of water samples from Chuquicamata and the Calama region. D) Sulfur and oxygen isotope composition of dissolved sulfates and gypsum/anhydrite from Chuquicamata and the Calama region ( $\delta^{34}\text{S}$  of Chuquicamata primary sulfides from Zentilli et al., 1994 and Smuda, 2008; isotope composition of sulfate from local salares (hatched area) from Rech et al., 2003)

## P 2.19

# Timing of polymetallic Pb-Zn mineralisation in the Laki district, southern Bulgaria – constraints from $^{40}\text{Ar}/^{39}\text{Ar}$ dates

Buret Yannick<sup>1</sup>, Kouzmanov Kalin<sup>1</sup>, Spikings Richard<sup>1</sup>, Gerdjikov Yanko<sup>2</sup>

<sup>1</sup>Earth and Environmental Sciences, University of Geneva, Rue de Maraichers 13, CH-1205 Geneva (burety@tcd.ie)

<sup>2</sup>Department of Geology, Sofia University, 1000-Sofia, Bulgaria

The Central Rhodopean Dome (CRD), in southern Bulgaria and northern Greece, is composed of high-T, low-P gneisses and marbles which were exhumed along detachment faults during post-collisional extension, resulting in widespread migmatization and local anatexis. Peak metamorphic temperatures are recorded at  $35.9 \pm 0.2$  Ma (Ovtcharova et al., 2003), whereas cooling below  $\sim 300^\circ\text{C}$  occurred between 36 and 34 Ma (Kaiser-Rohrmeier et al., 2013). Regional acid magmatism ( $\sim 33 - 30$  Ma; Ovtcharova et al. 2001), occurring throughout the CRD as dykes and sub-volcanic bodies, cross-cuts detachment faults and sedimentary basins, and is commonly spatially associated with polymetallic Pb-Zn veins and metasomatic replacement bodies.

The CRD hosts six Oligocene Pb-Zn mining districts: Laki, Davidkovo, Ardino, Enyovche, Madan and Thermes (from north to south), all of which display similar mineralisation styles (polymetallic veins and metasomatic replacement bodies) and are all located proximal to the Middle Rhodopean detachment fault. Fluid inclusion studies from the Madan (Kostova et al., 2004; Kotzeva et al., 2011) and Laki (Buret, 2012) districts reveal similar temperatures and salinities of the mineralising fluids ( $\sim 300 - 350^\circ\text{C}$ ;  $\sim 1 - 10$  wt % NaCl eq) for both districts. However, previous studies, based on  $^{40}\text{Ar}-^{39}\text{Ar}$  dating of sericite indicate a significant age difference between the Laki ( $\sim 29.5$  Ma) and the Madan ( $\sim 30 - 30.5$  Ma) districts, which suggests an overall younging of mineralisation towards the north (Kaiser-Rohrmeier et al., 2004).

This study applies high-precision  $^{40}\text{Ar}/^{39}\text{Ar}$  thermochronology to hydrothermal and metamorphic K-feldspar from the Laki mining district. In order to better constrain the timing of mineralisation, K-feldspar separates were dated from vein selvages and a mineralised polymictic volcanic breccia containing intergrown hydrothermal K-feldspar and sulfides. Hydrothermal K-feldspar from non-mineralised sub-volcanic bodies were also dated to establish the extent of the hydrothermal activity in the Laki district, while metamorphic K-feldspar from gneiss spatially unrelated to mineralisation was dated to constrain the upper age limit of metamorphic K-feldspar in the vein selvages.

Our data obtained from hydrothermal and metamorphic K-feldspar reveal three stages: (1)  $\sim 33 - 33.5$  Ma, pre-mineralisation metamorphic K-feldspar; (2)  $\sim 32 - 30$  Ma, K-feldspar from vein selvages and mineralised polymictic breccia; and (3)  $\sim 27 - 29.5$  Ma, post-mineralisation hydrothermal K-feldspar from non-mineralised sub-volcanic bodies.

$^{40}\text{Ar}/^{39}\text{Ar}$  dates from stage (1) closely match U-Pb zircon dates from sub-volcanic bodies in the Laki district, which form part of the Borovitsa volcanic zone ( $\sim 33$  Ma; Ovtcharova et al., 2001), and therefore can be interpreted as being thermally reset by magmatism.

The range of  $^{40}\text{Ar}/^{39}\text{Ar}$  dates displayed during stage (2) is indicative of partial to complete resetting of metamorphic K-feldspar by the hydrothermal, mineralising fluid. Consistent minimum dates of  $\sim 30$  Ma from the vein selvages and corresponding hydrothermal K-feldspar dates obtained from a mineralised polymictic breccia from the Chetroka mine, as well as fluid temperatures of  $300-350^\circ\text{C}$  recorded during the main stage of mineralisation in the Djurkovo mine, suggest that mineralisation in the Laki district ceased at  $\sim 30$  Ma, and was coeval with hydrothermal activity in the Madan district to the south.

Post-mineralisation hydrothermal fluid circulation (at temperatures  $<200^\circ\text{C}$ ) during stage (3) resulted in the precipitation of hydrothermal K-feldspar within the previously altered sub-volcanic bodies from  $27 - 29.5$  Ma, possibly corresponding to previously published  $^{40}\text{Ar}/^{39}\text{Ar}$  sericite dates from the Laki district.

## REFERENCES

- Buret, Y. 2012: Polymetallic mineralization of the Djurkovo deposit, Laki mining district, Southern Bulgaria: Paragenesis and fluid evolution. Unpubl.MSc. thesis, University of Geneva, 151 p.
- Kaiser-Rohrmeier, M., Handler, R., von Quadt, A., & Heinrich, C. 2004: Hydrothermal Pb-Zn ore formation in the Central Rhodopean Dome, south Bulgaria: review and new time constraints from Ar-Ar geochronology. *Swiss Bulletin of Mineralogy and Petrology*, 84, 37-58.
- Kaiser-Rohrmeier, M., von Quadt, A., Driesner, T., Heinrich, C., Handler, R., Ovtcharova, M., Ivanov, Z., Petrov, P., Sarov, St., & Peytcheva, I. 2013: Post-orogenic extension and hydrothermal ore formation: High-precision geochronology of the Central Rhodopian metamorphic core complex (Bulgaria-Greece). *Economic Geology*, 108, 691-718.
- Kostova, B., Pettke, T., Driesner, T., Petrov, P. & Heinrich, C. 2004: LA ICP-MS study of fluid inclusions in quartz from the Yuzhna Petrovitsa deposit, Madan ore field, Bulgaria. *Swiss Bulletin of Mineralogy and Petrology*, 84, 25-36.

- Kotzeva, B., Guillong, M., Stefanova, E., & Piperov, N. 2011: LA-ICP-MS analysis of single fluid inclusions in a quartz crystal (Madan ore district, Bulgaria). *Journal of Geochemical Exploration*, 108, 163-175.
- Ovtcharova, M., von Quadt, A., Heinrich, C.A., Frank, M., Rohrmeier, M., Peycheva I., & Neubauer, F. 2001: Late Alpine Extensional Stage of the Central Rhodopian Core Complex and Related Acid Magmatism (Madan Dome, Bulgaria) - Isotope and Geochronological Data. In: Piestrzyński et al. (eds.) *Mineral Deposits at the Beginning of the 21st century* (Balkema), 551–553.
- Ovtcharova, M., von Quadt, A., Heinrich, C., Frank, M., Kaiser-Rohrmeier, M., Peytcheva, I., & Cherneva, Z. 2003: Triggering of hydrothermal ore mineralization in the Central Rhodopean Core Complex (Bulgaria) – Insight from isotope and geochronological studies on Tertiary magmatism and migmatization. In: Eliopoulos et al. (eds.) *Mineral Exploration and Sustainable Development* (Balkema), 367-370.

## P 2.20

### **A magmatic origin of ore-forming fluids in Carlin-type deposits? Fluid inclusion studies on Carlin-type deposits and a Au-Cu porphyry deposit on the Carlin and Battle Mountain-Eureka trends, Nevada**

Simon J. E. Large, Edine Y. N. Bakker, Philipp Weis, Markus Wälle, Christoph A. Heinrich, Michael W. Ressel

Eocene ore deposits of the Great Basin in north-central Nevada are collectively the US' largest producer of gold. They resulted from an ideal combination of early tectonics making the determining structures for later events, and several phases of metamorphism and magmatism, causing fertile fluids and melts to rise in the crust into a stratigraphy of reactive, carbonate rocks covered by non-reactive, siliceous cap rock (e.g. Dickinson, 2006). The majority of deposits are aligned in three main trends: the Carlin, Getchell and Battle Mountain-Eureka trends. While many studies have identified similarities between the individual structurally-controlled, sediment-hosted deposits, the source and evolution of the mineralizing fluid remain debated. Recent studies favour a conceptual model including a deep magmatic fluid source (e.g. Muntean et al., 2011) rather than a sedimentary or metamorphic fluid source. This magmatic-hydrothermal hypothesis implies that Carlin-type Au-deposits are distal products of gold transported in fluids derived from a large, deep-seated intrusive body. On the Carlin trend itself, there is only indirect evidence for the existence of Eocene plutons at depth. However, in the Battle Mountain-Eureka trend, gold mineralization that formed at relatively higher P-T is found in proximity to Eocene granodioritic intrusions. Under the conditions prevailing in the Carlin area, transport of gold via similar magmatically-derived fluids over large distances would be feasible (Heinrich, 2005). Two joint fluid inclusion studies on both of these sub-parallel trends were performed aiming to determine the major- and trace-element composition of the ore forming fluids.

Here, we present results from petrographic observations, fluid inclusion microthermometry and laser ablation ICP-MS analyses on fluid inclusions from the Copper Canyon Cu-Au porphyry, located at the northwest end of the Battle Mountain-Eureka trend and from the Gold Quarry and Chukar Underground Carlin type deposits located on the central Carlin-trend. An Eocene granodioritic porphyry is central to the deposits at Copper Canyon and is thought to be the cupola of a larger intrusion that acted as the source of fluids and metals (Cu, Au, Ag, Mo, Pb, Zn) for the deposits. It is hypothesized that the granodiorite cupola and its associated ore fluids could represent the highest P-T part of gold-producing hydrothermal systems, which formed the proximal skarn-hosted Au-Cu mineralization at Copper Canyon, whereas Carlin-type Au mineralisation may have been formed as more distal products of similar systems, at lower temperature and preserved in areas that were eroded less deeply.

Copper Canyon contains abundant fluid inclusion assemblages of vapour, intermediate-density, aqueous and hypersaline fluids in quartz veins and garnets. We present evidence for phase separation of a moderately saline intermediate density supercritical fluid splitting into a vapour and a brine under relatively high pressures. Subsequent small variations in pressure upon cooling of the vapour, caused parts of the vapour to contract to a liquid. Fluid inclusions in quartz and barite from the Carlin trend deposits have a very similar appearance to the contracted vapour liquid. Similarities in the chemical composition of fluid inclusions of the different sources indicate chemically similar source.

#### REFERENCES

- Dickinson, W. R., 2006, Geotectonic evolution of the Great Basin: *Geosphere*, v. 2, p. 353-368.
- Heinrich, C. A., 2005, The physical and chemical evolution of low-salinity magmatic fluids at the porphyry to epithermal transition: a thermodynamic study.: *Mineralium Deposita*, v. 39, p. 864-889.
- Muntean, J. L., Cline, J. S., Simon, A. C., and Longo, A. A., 2011, Magmatic-hydrothermal origin of Nevada's Carlin-type gold deposits: *Nature Geoscience*, v. 4, p. 122-127.

## P 2.21

# Estimation of environmental contaminations value of heavy metals in the sediments of Sari area with using geochemical parameter of Enrichment Factor (EF)

Davoudi Azam <sup>1</sup>, Lak Razyeh <sup>2</sup>, Bahramabadi Behruz <sup>3</sup>

<sup>1</sup>M.A. Sedimentology and sedimentary petrology, Tarbiat Moallem University, Iran.

Corresponding author. E-mail: Davoudi242@Gmail.com.

<sup>2</sup>Assistant professor, Research Institute for Earth Sciences, Geological Survey of Irane, E-mail: Lak\_ir@yahoo.com.

<sup>3</sup>M. A in Geomorphology, University of Tehran and Faculty Member of Imam Ali University, E-mail: Bahramabadi.b@ Gmail.com.

Sedimentary samples can provide comprehensive pieces of information such as sedimentation rates, changes of weather conditions during the different periods and the concentration of heavy metals in their deposition environments. Aimed at assessing heavy metal contamination, this study focused on 11 sediment samples from two regions (i.e., Larym and FarahAbad in Sari area); which 9 samples were selected through trenching at depths between 0 to 70 cm and two others from surface sediment. The samples were transferred to laboratories of geological survey of Iran for ICP analysis. The sediment of the Caspian coastal plains is the combination of the batch and sediments deposited especially in the southern Caspian Sea by the effect of waves and different currents; which from sedimentology perspective and environment are characterized by changes of genus and granulometry in the southern part from the western regions to the east coast. Fine grain particles, because of their high adsorption capacity, is a factor in the absorption and potential accumulation of toxic elements in sediments. Figure 1 shows position of study area and sampling stations.

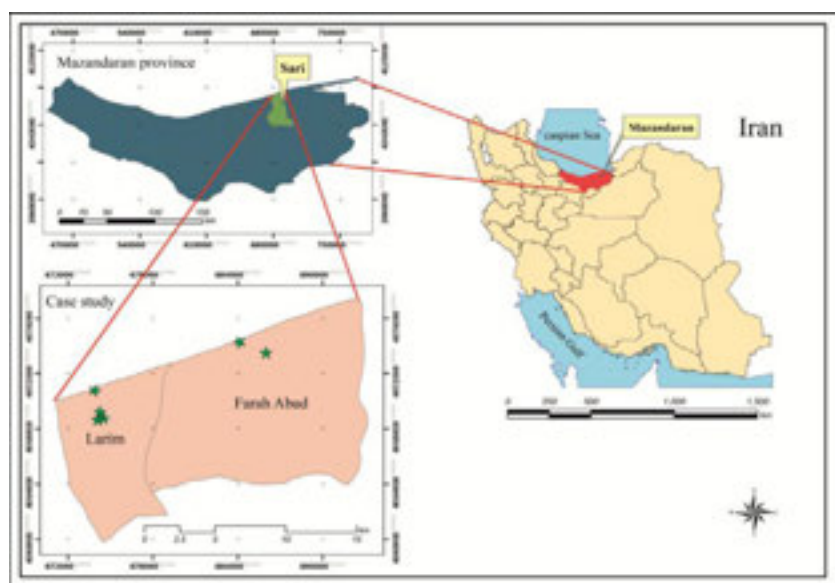


Fig.1 Shows Position Map of Sampling Stations Marked with Green color

Comparison of mean of the concentration of heavy metals with the mean of the global sediments and the crustal mean indicates that the cobalt element concentration (15.08 ppm) is between the mean scores of the global sediments and crustal. Mean scores of concentrations of chromium, copper, and manganese (respectively 88.700, 22 and 688.92 ppm) are lower than those of the Global sediments and crustal mean. While the means of lead and zinc concentration (20.75 ppm and 102.70 ppm) are higher than those of the global sediments and crustal and the mean of nickel concentration (52.50 ppm) is approximately equal to that of the global sediments; the concentration less than that of the crustal average. Obviously, differences between the concentration means of the elements in the study area and the global sediment and earth's crust are due to Geological and different climatic conditions in various parts of the Earth (Table 1).

Table 1. Concentrations of heavy metals in the studied sediment samples

Sample No.	ppm							%	
	Co	Cr	Cu	Zn	Pb	Mn	Ni	Fe(Fe <sub>2</sub> O <sub>3</sub> )	Ca (CaO)
L1-1	20.2	58.0	33.3	125.5	40.6	766.2	76.6	8.3	6.5
L1-2	13.9	125.7	20.1	96.1	24.5	540.5	56.1	5.9	13.3
L1-3	17.8	132.0	11.2	95.2	12.2	738.7	49.4	7.1	19.2
L2-1	21.6	44.6	38.7	121.3	33.6	725.5	75.8	6.9	12.1
L2-2	9.7	69.5	6.9	51.9	13.2	616.9	32.3	3.9	16.4
L3-1	11.0	150.2	7.1	57.6	9.7	741.1	36.5	4.9	18.6
L4	10.1	71.7	38.8	222.0	18.2	692.2	33.3	3.7	16.6
F2-1	12.5	112.7	12.2	79.6	12.1	763.1	38.8	5.1	15.5
F2-2	18.5	71.1	33.6	118.6	26.8	594.3	74.6	6.1	11.5
F2-3	20.8	108.6	34.0	111.0	31.9	807.2	73.8	6.7	14.8
F-1(reference sample)	9.8	31.6	6.1	51.0	5.5	592.5	30.3	3.5	15.7
Earth crust <sup>1</sup>	20.0	100.0	50.0	75.0	14.0	850.0	80.0	4.1	4.1
Global sediments <sup>1</sup>	14.0	90.0	33.0	95.0	19.0	770.0	52.0	4.6	6.6

<sup>1</sup>(Ref. Bowen 1979)

For the evaluation of the pollution of heavy metals, geochemical parameter of Enrichment Factor (EF) was used. EF is used to compare inter-region geochemical trends, and also to identify anthropogenic pollution. Heavy metal enrichment factors (EF) were estimated. Their EF means are also as follows: Pb> Cu> Cr> Zn> Ni> Co> Mn. On the basis of the EF mean of each element, the sediments were classified from moderate enrichment with lead and copper, deficient enrichment with nickel and cobalt, and to mineral enrichment with chromium and zinc. Also EF indicating that 1) cobalt and nickel have a geogenic origin; 2) zinc, copper and lead have both geogenic origin and an anthropogenic origin; 3) chromium element has source of biogenic and partly anthropogenic origins.

## REFERENCES

- Bowen, H.J.M. 1979: Environmental geochemistry of the elements. Academic press, London, England. P333.
- Koshrahan H (2000) Morphological zonation of south Caspian Sea. The Department of Energy, Water Resources. P123.
- Forstner, U. 2004; Sediment dynamics and pollutant mobility in river: An interdisciplinary approach, lake and reservoirs: Research and management. 9, 25-40.
- Hernandez, L. Probst, A. Probst, J.L. Ulrich E. 2003: Heavy metal distribution in some French forest soils: evidence for atmospheric contamination. Sci Total Environ. 312,195–219.
- Yu K, C. Tsal L. J. Chen, S.H. Ho, S.T. 2001: Chemical binding of heavy metals in anionic river sediments. Water Research. 35(17), 4086-4096.

## P 2.22

### Petrographic and sedimentologic investigation of boulders in the riverbed of the 'Hauensteiner Murg'

Dörner Eva Lisa<sup>1</sup>, Franz Leander<sup>1</sup>, Wetzel Andreas<sup>2</sup> & de Capitani Christian<sup>1</sup>

<sup>1</sup>*Institute of Mineralogy and Petrography, University of Basel, Bernoullistrasse 32, CH-4056 Basel (eva.doerner@stud.unibas.ch)*

<sup>2</sup>*Institute of Geology and Paleontology, University of Basel, Bernoullistrasse 32, CH-4056 Basel*

In the framework of a comprehensive petrologic and sedimentological study of gravels delivered by the tributaries of the Rhine River performed at the geoscience institutes of the University of Basel, pebbles carried by the 'Hauensteiner Murg' were investigated. This small river, which has a length of 22.4 km, is located in the Hotzenwald area of the Black Forest (southern Baden-Wuerttemberg, Germany).

Pebbles were sampled at six different locations along the whole river course, from the spring southwest of 'Lochhäuser' and to the mouth in the village Murg, where the river merges with the Rhine. Based on hand specimens and thin sections of the pebbles the mineral phases and their modal amount were identified and the rock fabric evaluated to draw conclusions on the formation of the rock. In case of metamorphic rocks, a rough estimate of the metamorphic PT conditions and evolution was possible. In addition, the frequency of boulder-types occurring at specific sampling points has been recorded and their sphericity and roundness have been measured for a sedimentologic analysis. By comparing the pebble petrography with geological maps (Metz & Rein, 1958) and literature data (Pfannenstiel & Rahm, 1963; Günther, 2010; Geyer & Gwinner, 2011) the boulders found in the 'Hauensteiner Murg' could be assigned to their parent rocks. To confirm the preliminary results the petrographic findings were linked to the sedimentologic data to get an insight into the transportation processes and their energy levels over the transport distance. The combination of both, petrographic and sedimentologic results were useful to decipher where the boulders originate from.

Very important is that the sampling points (1) and (6) were within the reach of a former glacier. Sampling point (1) was influenced by the Black Forest glaciation and sampling point (6) by the Alpine glaciation, both during the Riss glacial period. Point (6) is close to the Rhine River, which very likely transported some gravel during high-flood stages into the mouth of the 'Hauensteiner Murg'. Rocks originating from the center of the Black Forest glaciation around the 'Feldberg' have also been found.

The southern Black Forest is mainly build up by the Variscan basement rocks. It is divided from north to south into several domains: Baden-Baden-Zone, North and Middle Black-Forest crystalline complex, Badenweiler-Lenzkirch-Zone and Southern Black Forest crystalline complex. The latter is passed by the the 'Hauensteiner Murg'. Although sampling point (1) is located in the Albatal granite, lots of gneiss pebbles have be found. These rocks are assigned to the gneiss-anatexite complex of Todtmoos and have been transport by the Feldberg glacier. Towards the sampling point (2) the 'Hauensteiner Murg' crosses some porphyry granites and quartz veins, which then enrich the pebble inventory. A similar origin is assumed for lamprophyre pebbles at sampling point (5). Sampling point (3) is also located in the Albatal granite, but also boulders originating from north of the spring, like a gabbro from Ehrsberg and a 'Bärhalde'-granite have been encountered. Due to the proximity to the gneiss complex of the Wiese-Wehra valley the number of gneiss pebbles increased. Sampling point (4) is located within the gneiss complex of the Wiese-Wehra valley, which results in a further distinct increase of the abundance of gneiss pebbles. Furthermore, two amphibolite pebbles may orginate from the Gisiboden area close to Todtnau. Orthogneiss pebbles were taken from sampling point (5). Their provenance area is also situated north of the river head. At sampling point (6) the pebble spectrum markedly differs from others because of the numerous sedimentary-rock pebbles. Red sandstone from the Buntsandstein formation outcropping northwest and northeast of sampling point (5) are quite frequent. The presence of pebbles consisting of Melser sandstone and limestone pebbles could clearly ascribe to the Helvetic realm of the Alps.

The marked difference of sphericity between sampling points (1) and (2) (Fig. 1) is due to the input by the Feldberg-glacier at (2). The sandstones at the mouth of the 'Hauensteiner Murg' also have a high sphericity, which resulted from the long-distance transport out of the Alpine region.

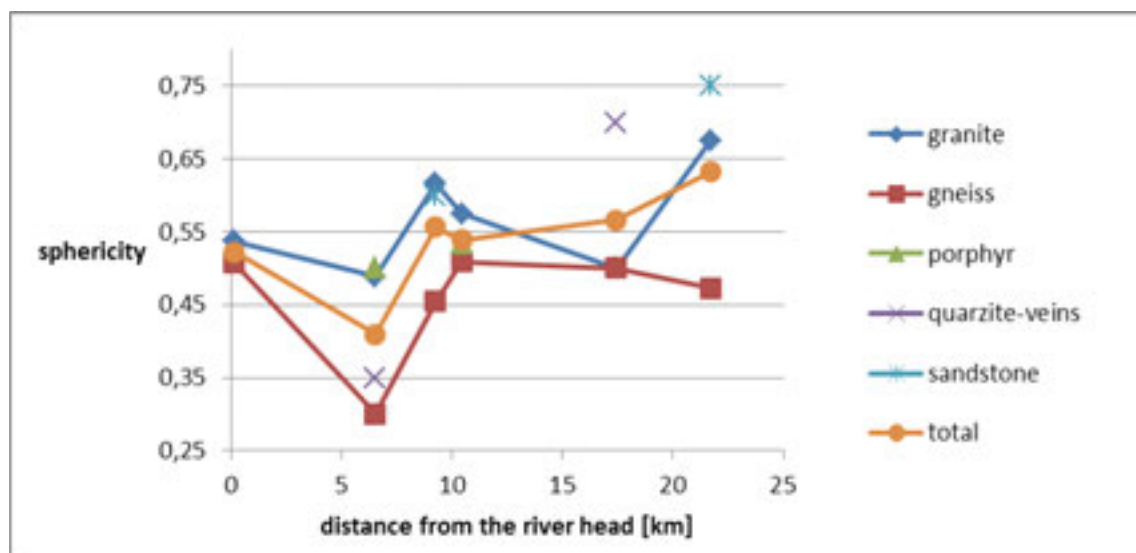


Figure 1: The general trend of increasing sphericity with transport distance is interrupted at sampling location (2) by the input of glacier-carried pebbles.

#### REFERENCES

- Geyer, O. & Gwinner, M. 2011: Geologie von Baden-Württemberg. Stuttgart, E. Schweizerbart'sche Verlagshandlung (Nägele und Obermiller), 627 p.
- Günther, D. 2010: Sammlung geologischer Führer Band 102. Der Schwarzwald und seine Umgebung. Stuttgart, Gebrüder Borntraeger.
- Pfannenstiel, M. & Rahm, G. 1963: Die Vergletscherung des Wutachtals während der Rißeiszeit. Freiburg, Ber. D. Naturf. Ges. Freiburg 53, 5-62.
- Metz, R. & Rein, G. 1958: Geologisch-petrographische Übersichtskarte des Südschwarzwaldes. Massstab 1:50'000.

## P 2.23

# Oxygen and hydrogen stable isotopes in waters and soils from the Visp catchment, Valais, Switzerland

Bauer Kerstin K.<sup>1</sup>, Adatte, Thierry<sup>1</sup>, Vennemann, Torsten W.<sup>1</sup>

<sup>1</sup>*Institut des Sciences de la Terre, Université de Lausanne, Géopolis, CH-1015 Lausanne (kbauer@unil.ch)*

Samples of soil and surface water were collected along a transect of 30 km with 1600 m of difference in altitude in the valleys of Saas Fee and Visp in the Swiss Alps. Mineralogical, chemical, and isotopic (O and H) compositions as well as physical parameters were determined in order to study water-rock interactions, first stages of clay mineral formation, and a possible influence of altitude on the isotopic composition of soils during weathering of the parent rock. Further data from GIS based modeling of the total watershed as well as sub-catchments allows to study elevation profiles, distribution of precipitation and the occurring host rock lithologies.

The background of this work is to explore the usability of hydrous minerals in foreland sediments derived from Alpine weathering for paleoelevation studies, based on the altitude effect in stable O and H isotopes.

Waters have a range of  $\delta^{18}\text{O}$  and  $\delta\text{D}$  values typical for precipitation and snow and glacier melt water in high-Alpine regions. The major ions are characterized by the dissolution of host rock minerals, leading to an enrichment of Ca, sulphate, K, and Mg ions along the stream. Mixing with side streams and the artificial input of waters derived from high elevations due to hydropower utilization can be observed in both the isotope and ion composition.

The mineralogical composition of the soils corresponds to the occurrence of ophiolitic material in higher elevations and granitic gneisses and mica schists in lower regions. Phyllosilicates from early-stage weathering and transformation of illite and chlorite to interstratified minerals (vermiculite, illite-vermiculite, chlorite-vermiculite and illite-smectite) are present already in high altitudes but their abundance is higher in lower altitudes as well as in the fine grained separates. This is also supported by higher water contents, lower  $\delta\text{D}$  values and a shift to a more illitic character of mica minerals in the  $<2\ \mu\text{m}$  material.

The overall isotopic composition of the soil samples however is still similar to values of the host rock material and in  $\delta^{18}\text{O}$  no significant change is noticeable between the different size fractions.

This suggests that the present climate and this environment do not allow for the neoformation of larger quantities of clay minerals in contact with ambient water.

## 4. Cycles and Events in Earth History

Karl Föllmi, Urs Schaltegger, Thierry Adatte

### TALKS:

- 4.1 Adatte T., Fantasia A., Samant B., Mohabey D., Keller G., Khozyem H., Gertsch B.: Deccan Volcanism: a main trigger of environmental changes leading to the KTB mass extinction?
- 4.2 Baresel B., Bucher H., Schaltegger U.: High precision time calibration of the Permo-Triassic boundary mass extinction event by U-Pb geochronology
- 4.3 Bonvallet L., Godet A., Adatte T., Spangenberg J.E., Arnaud-Vanneau A., Föllmi K.B.: Depositional geometries in the Tierwis and Schrattenkalk Formations: a geochemical and sequence stratigraphic correlation
- 4.4 Brack, P.: Latemar - What dictates the rhythm?
- 4.5 Charbonnier G., Duchamp-Alphonse S., Adatte T., Spangenberg J.E., Colin C., Gardin S., Boulila S., Galbrun B., Föllmi K.B.: Detrital and nutrients influxes in the Northwestern Tethyan margin during the Valanginian: new insights from weathering changes during the Weissert episode
- 4.6 Deconinck J.-F., Ghirardi J., Martinez M., Bruneau L., Pellenard P., Pucéat E.: Orbital chronology of the Lower-Middle Aptian: Palaeoenvironmental implications (Serre Chaitieu section, Vocontian Basin, France)
- 4.7 Freeman, R.: Cyclic Sedimentation in the Drusberg Beds, Wägital region, Helvetic Alps, Switzerland
- 4.8 Gertsch B., Keller G., Adatte T., Spangenberg J.E., Berner Z.: Environmental and climatic changes on the Brazilian shelf during the Campanian-Maastrichtian
- 4.9 Greber N.D., Nägler T.F., Mäder U.: Experimental investigation of molybdenum solubility under low atmospheric O<sub>2</sub> concentrations: Implications for pre GOE conditions
- 4.10 Hosseini S., Kindler P., Conrad A.M.: Valanginian Weissert event in a shallow-platform setting, Zagros fold-thrust belt, southern Tethys
- 4.11 Khozyem H., Adatte T., Spangenberg J.E., Keller G., Sament B.: Response of terrestrial environment to the Paleocene Eocene Thermal Maximum (PETM)
- 4.12 Kocsis L., Ozsvárt P., Becker D., Ziegler R., Scherler L., Codrea V.: Continental climate reconstruction during late Eocene–early Oligocene in Europe
- 4.13 Sanson-Barrera A., Hochuli P. A., Bucher H., Meier M., Schneebeli-Hermann E., Weissert H., Bernasconi S.M. : Latest Permian to Early Triassic high-resolution stable carbon isotope record from North-east Greenland
- 4.14 Sell B., Schaltegger U., Ovtcharova M., Bartolini A., Jourdan F., Guex J.: Evaluating the causal link between the Karoo LIP and climatic-biologic events of the Toarcian Stage with high-precision geochronology
- 4.15 Wotzlaw J.-F., Guex J., Bartolini A., Gallet Y., Krystyn L., McRoberts C., Taylor D., Schoene B., Schaltegger U.: Towards accurate numerical calibration of the Late Triassic: High-precision U-Pb constraints on the duration of the Rhaetian

## POSTERS:

- P 4.1 Corminboeuf F., Adatte T., Spangenberg, J.E.: Origin of Devonian conical mud mounds of Hamar Lakhdad Ridge, Anti-Atlas, Morocco: hydrothermal or hydrocarbon venting ?
- P 4.2 Fantasia A., Adatte T., Samant B., Mohabey D., Keller G.: Sedimentological, mineralogical and geochemical study of sediments associated with the Deccan Traps in the Nagpur area, India
- P 4.3 Gnos E., Hofmann B.A., Al-Wagdani K., Mahjub A., Abdullah Al-Solami A., Habibullah S.N., Matter A., Halawani M.A.: The Jabal Rayah meteorite impact crater, Saudi Arabia
- P 4.4 Ovtcharova M., Goudemand N., Galfetti T., Brayard A., Hammer O., Bucher H., Schaltegger U.: Early-Middle Triassic boundary – precision and accuracy achieved by combining U-Pb zircon geochronology and biochronology
- P 4.5 Wohlwend S., Celestino R., Weissert H.: Sea level and current controlled sedimentary successions in the Hawasina Basin (Oman) during the Late Jurassic to Early Cretaceous time

## 4.1

# Deccan Volcanism: a main trigger of environmental changes leading to the KTB mass extinction?

Thierry Adatte<sup>1</sup>, Alicia Fantasia<sup>1</sup>, Bandana Samant<sup>2</sup>, Dhananjay Mohabey<sup>2</sup>, Gerta Keller<sup>3</sup>, Hassan Khozyem<sup>1</sup> & Brian Gertsch<sup>1</sup>

<sup>1</sup>ISTE, Lausanne University, 1015 Lausanne, Switzerland (thierry.adatte@unil.ch)

<sup>2</sup>Department of Geology, Nagpur University, Nagpur 440 001, India

<sup>3</sup>Department of Geosciences, Princeton University, Princeton NJ 08540, USA

Model results predict that Deccan Traps emplacement was responsible for a strong increase in atmospheric pCO<sub>2</sub> accompanied by rapid warming of 4°C (Dessert et al., 2001) that was followed by global cooling. During the warming phase, increased continental weathering of silicates associated with consumption of atmospheric CO<sub>2</sub> likely resulted in the draw-down of greenhouse gases that reversed the warming trend leading to global cooling at the end of the Maastrichtian.

Massive CO<sub>2</sub> input together with massive release of SO<sub>2</sub> may thus have triggered the mass extinctions in the marine realm as a result of ocean acidification leading to a carbon crisis and in the terrestrial realms due to acid rains (Fig. 1). Global stress conditions related to these climatic changes are well known and documented in planktic foraminifera by a diversity decrease, species dwarfing, dominance of opportunistic species and near disappearance of specialized species. Recent studies indicate that the bulk (80%) of Deccan trap eruptions (phase-2) occurred over a relatively short time interval in magnetic polarity C29r (Chenet et al., 2007). Multiproxy studies from central and southeastern India place the Cretaceous-Tertiary (KT) mass extinction near the end of this main phase of Deccan volcanism suggesting a cause-and-effect relationship (Keller et al., 2012).

In India a strong floral response is observed as a direct response to Deccan volcanic phase-2. In Lameta (infra-trappean) sediments preceding the volcanic eruptions, palynoflora are dominated by gymnosperms and angiosperms with a rich canopy of gymnosperms (Conifers and Podocarpaceae) and an understory of palms and herbs (Samant and Mohabey, 2009). Immediately after the onset of Deccan phase-2, this floral association was decimated leading to dominance by angiosperms and pteridophytes at the expense of gymnosperms. In subsequent intertrappean sediments a sharp decrease in pollen and spores coupled with the appearance of fungi mark increasing stress conditions apparently as a direct result of volcanic activity. The inter-trappean sediments corresponding to Phase-2 (80% of Deccan basalt emissions, latest Maastrichtian) are characterized by the highest Chemical Index of Alteration (CIA) values. This can be explained by increased acid rains due to SO<sub>2</sub> emissions rather than a global climatic shift, because clay minerals from the corresponding sediments do not reflect a significant climate change. The increased weathering is coeval with the sharp decline in pollen and an increase in fungal spores observed by Samant and Mohabey (2009) and corresponds to the main phase-2 of Deccan activity.

Beyond India, multiproxy studies also place the main Deccan phase in the uppermost Maastrichtian C29r below the KTB (planktic foraminiferal zones CF2-CF1 spanning 120ky and 160ky respectively), as indicated by a rapid shift in <sup>187</sup>Os/<sup>188</sup>Os ratios in deep-sea sections from the Atlantic, Pacific and Indian Oceans (Robinson et al, 2009), coincident with rapid climate warming, coeval increase in weathering, a significant decrease in bulk carbonate indicative of acidification due to volcanic SO<sub>2</sub>, and major biotic stress conditions expressed in species dwarfing and decreased abundance in calcareous microfossils (planktic foraminifera and nannofossils). These observations indicate that Deccan volcanism played a key role in increasing atmospheric CO<sub>2</sub> and SO<sub>2</sub> levels that resulted in global warming and acidified oceans, which led to increased biotic stress that predisposed faunas to eventual extinction at the KTB.

## REFERENCES

- Chenet, A-L., Quidelleur, X., Fluteau, F., Courtillot, V. (2007). 40K/40Ar dating of the main Deccan large igneous province: further evidence of KTB age and short duration. *Earth, Planet. Sci. Lett.* V. 263, pp. 1-15.
- Dessert, C., Dupré, B., François, L.M., Schott, J., Gaillardet, J., Chakrapani, G.J., Bajpai, S. (2001). Erosion of Deccan Traps determined by river geochemistry: impact on the global climate and the 87Sr/86Sr ratio of seawater. *Earth Planet. Sci. Lett.*, v. 188, pp. 459– 474.
- Keller, G., Adatte, T., Bhowmick, P.K., Upadhyay, H., Dave, A., Reddy, A.N., Jaiprakash, B.C. (2012). Nature and timing of extinctions in Cretaceous-Tertiary planktic foraminifera preserved in Deccan intertrappean sediments of the Krishna-Godavari Basin, India. *Earth, Planet. Sci Lett.*, v. 344, p. 211-221.
- Robinson, N, Ravizza, G, Coccioni, R, Peucker-Ehrenbrink, B And Norris, R. (2009) A high-resolution marine 187Os/188Os record for the late Maastrichtian: Distinguishing the chemical fingerprints of Deccan volcanism and the KP impact event. *Earth and Planetary Science Letters*, v. 281, pp. 159-168.
- Samant, B., And Mohabey, D. M. (2009). Palynoflora from Deccan volcano-sedimentary sequence (Cretaceous-Palaeogene transition) of Central India: implications for spatio-temporal correlation. *J. Biosciences* 34 (5), pp.811-823

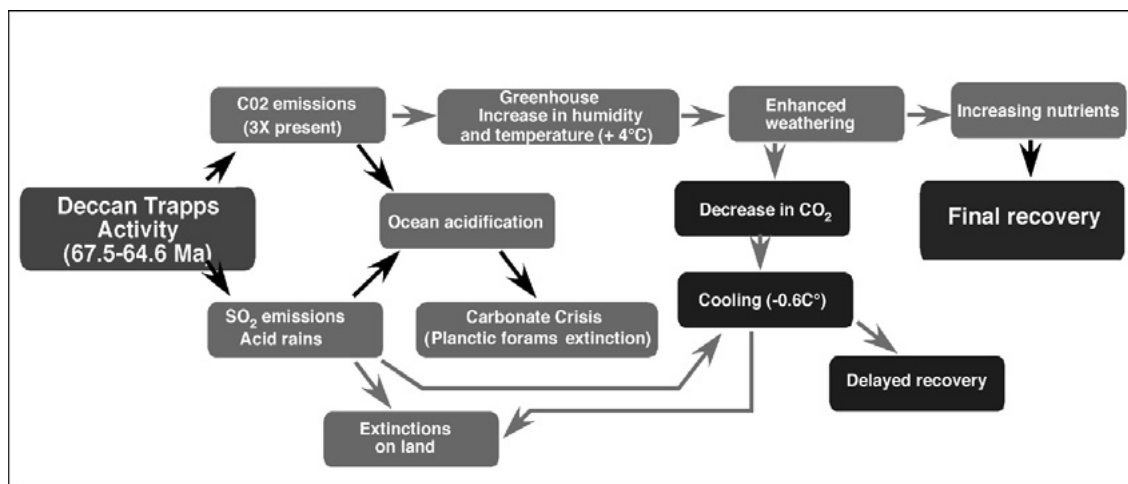


Figure 1: Flow chart for the model of massive Deccan volcanism as a main trigger of environmental changes leading to the KTB mass extinction.

## 4.2

### High precision time calibration of the Permo-Triassic boundary mass extinction event by U-Pb geochronology

Baresel Björn<sup>1</sup>, Bucher Hugo<sup>2</sup>, Schaltegger Urs<sup>1</sup>

<sup>1</sup>Département des sciences de la Terre, University of Geneva, Rue des Maraîchers 13, CH-1205 Genève (bjorn.baresel@unige.ch)

<sup>2</sup>Paläontologisches Institut und Museum, University of Zürich, Karl-Schmid-Strasse 4, CH-8006 Zürich

Thermal Ionization Mass Spectrometry (TIMS) has and continues to be the principal analytical method for geochronologists, allowing high sensitivity and high time resolution analyses of single grain samples. For zircon geochronology, the advent of multicollector instruments, the development of double spike methodologies coinciding with the reassessment of the uranium decay constants and further improvements in ion counting technology led to nowadays precision better than 0.1% for single grain and 0.05% for population ages, respectively. These analytical innovations now allow to calibrate the record of biological evolution at a resolution relevant to magmatic and biological timescales.

To construct a revised and high resolution calibrated time scale for the Permian-Triassic boundary (PTB) we use U-Pb zircon geochronology from ash layers in the marine Nanpajiang Basin (South China) in combination with quantitative biostratigraphic methods and carbon isotope variations across the PTB. Establishing stratigraphic tie points between the Late Permian to the Early Jurassic allows globally valid intercalibration of biochronological, chemostratigraphic, and astrochronological time-series with radio-isotopic ages for quantifying extinction and recovery rates.

## 4.3

### Depositional geometries in the Tierwis and Schrattekalk Formations: a geochemical and sequence stratigraphic correlation

Bonvallet Lucie<sup>1</sup>, Godet Alexis<sup>2</sup>, Adatte Thierry<sup>1</sup>, Spangenberg Jorge E<sup>1</sup>., Arnaud Vanneau Annie<sup>3</sup>, Föllmi Karl B.<sup>1</sup>

<sup>1</sup> Institute of Earth Sciences, University of Lausanne, Geopolis, CH-1015 Lausanne (lucie.bonvallet@unil.ch)

<sup>2</sup> Department of Geological Sciences, The University of Texas at San Antonio, One UTSA Circle, San Antonio, TX 78249, USA

<sup>3</sup> Association Dolomieu, 6 chemin des Grenouilles, 38700 Grenoble France

Urgonian platform carbonates are a common feature of subtropical and tropical shallow-water environments of late Early Cretaceous age. They include the remains of rudists, corals, chaetetids and stromatoporoids, which are interpreted as indicators of a predominantly photozoan, oligotrophic carbonate-producing ecosystem. The late Early Cretaceous is also marked by the occurrence of several oceanic anoxic episodes, such as the latest Hauterivian Faraoni and the early Aptian Selli Events, which are both interpreted as the consequence of generalized eutrophic conditions. These observations imply that the late Early Cretaceous underwent larger fluctuations in nutrient supply, which may have interfered with the evolution of the widespread Urgonian platforms.

Our goal is to study the interactions between paleoceanographic and paleoclimatic change, and Urgonian carbonate buildup in the northern, Helvetic Alps. This unit remains understudied relative to its counterparts in eastern and central France. We specifically intend to compare the Urgonian units of late Barremian age and early Aptian age, which are separated by the so-called “Lower Orbitolina Beds”. The late Barremian was less affected by anoxia, whereas the early Aptian witnessed progressive change in paleoceanographic conditions, which led up to the Selli Event.

The preliminary results of a selection of representative sections from the Helvetic Alps will be shown. They were analyzed both for their phosphorus and stable-isotope (C, O) contents, as well as for their microfacies in order to develop a sequence stratigraphic framework. One of the key features is the total disappearance of a late Barremian depositional sequence in proximal areas, and the progressive morphological change of the platform, from a ramp-like (early Barremian) to a distally-steepened platform (late Barremian and early Aptian).

## 4.4

### Latemar - What dictates the rhythm?

Brack Peter<sup>1</sup>

<sup>1</sup> Departement Erdwissenschaften, ETH Zürich, Sonneggstrasse 5, 8092 Zürich (peter.brack@erdw.ethz.ch)

Around two decades ago the ca. 600 sedimentary cycles identified in the Middle Triassic platform interior at Latemar in the Dolomites (northeastern Italy) became a reference example for Mesozoic shallow water carbonates that were considered to record Milankovitch-type sedimentary rhythms. By 1987 L.A. Hardie, R.K. Goldhammer and co-workers had established a solid cyclostratigraphy based mainly on visual analysis and „Fischer plots“ of bedding patterns. Support for the then “in vogue” interpretation came from sophisticated mathematical analysis (Goldhammer & Hinnov 1991; Preto et al., 2001) and available age constraints were largely neglected or discredited. However, the Milankovitch interpretation of the Latemar cycles was soon challenged by new paleontological evidence and later by U-Pb-zircon age constraints for the cyclic interval. The contradicting results triggered a heated debate known in the literature as the „Latemar controversy“. Another, probably related consequence was that the then state-of-the-art radio-isotope data were not considered in the International Geological Time Scale until 2011, i.e. almost 15 years after they had been published!

Meanwhile a precise calibration of the Latemar stratigraphy has been established on the basis of elements observed in both, platform carbonates and corresponding basinal successions: i) macrofossils (mainly ammonoids), ii) physical stratigraphy (tracing of sedimentary layers and intervals between platforms and basinal successions), iii) different generations of U-Pb zircon age data of tephra layers, iv) patterns of magnetic reversals and data series on magnetic susceptibilities. The result is one of the arguably best calibrated Mesozoic platform-basin settings with a short duration in the order of 1 myr.

The ca. 450 m thick “cyclic” succession at Latemar corresponds to only a small interval of basinal sediments at short distance (< 4 km) from the toes of actively growing platforms (Fig. 1). The short-term carbonate production in the Middle Triassic was evidently high and probably compares to recent figures. Unlike many modern settings only little sediment was available for far travelled off-platform transport.

The age calibration of the “cyclic” portion at Latemar results in an average duration in the order of 1-2 kyr for the 600+ shortest “beats” (Kent et al., 2004; Spahn et al., 2013). These are considered to reflect small amplitude fluctuations of sea level. Frequencies of the Milankovitch band seem to be superimposed on this basic signal (e.g., Meyers 2008). The driver of such a short rhythm remains unknown but Pleistocene examples suggest that short low amplitude (< 10 m) sea level fluctuations may also be preserved in modern environments.

## Carbonate platform

## Basinal succession

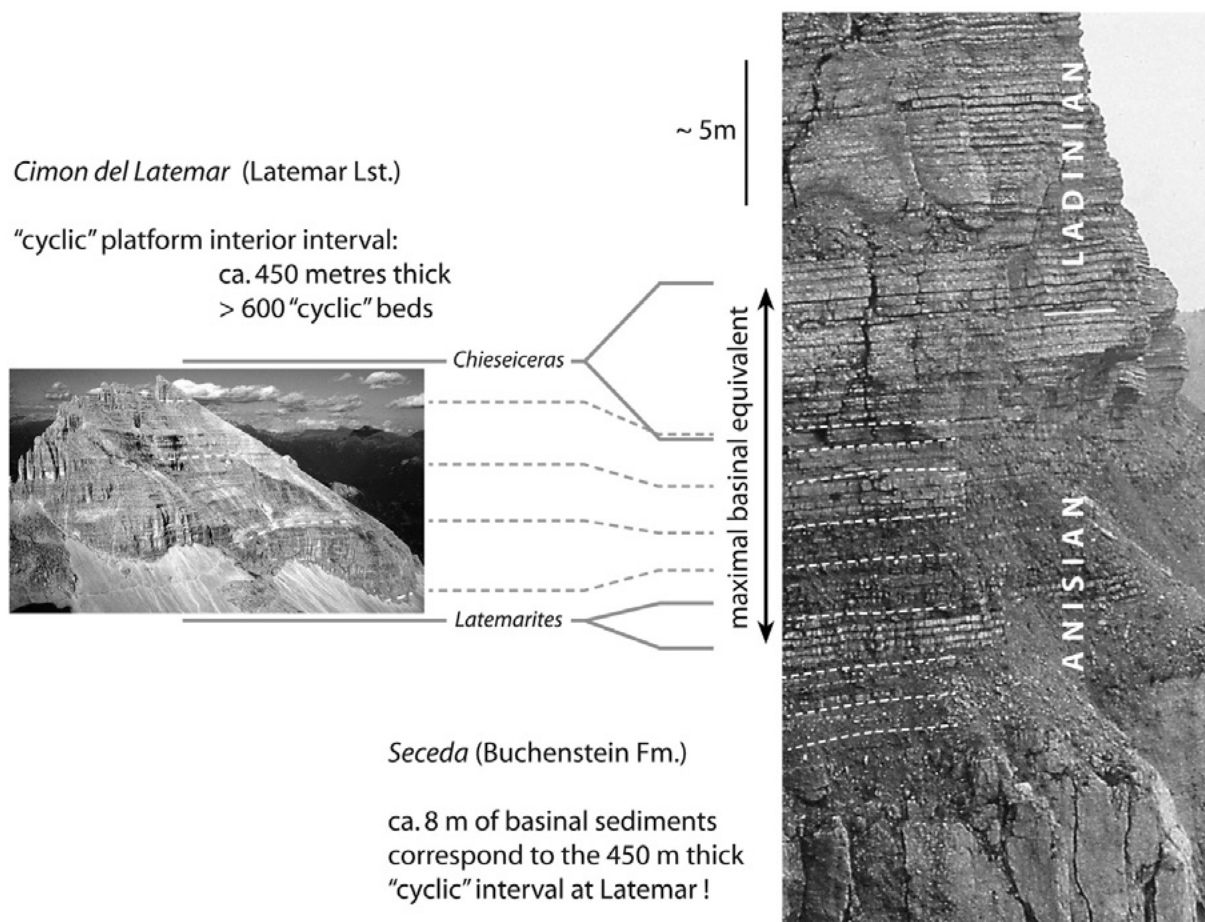


Figure 1. Comparison of the Latemar stratigraphy and the basinal succession at Seceda. The thickness of the basinal carbonates corresponding to the “cyclic” interval at Latemar is almost two orders of magnitude smaller!

Full lines indicate the distributions of the oldest and youngest ammonoid genera used for correlation. Dotted lines mark possibly corresponding tephra layers. The time span represented by the Latemar as shown is < 2 myr and possibly as small as 1 myr or even less.

## REFERENCES

- Goldhammer, R.K., Dunn, P.A. & Hardie, L.A. 1987: *American Journal of Science*, 287, 853-892.
- Hinnov L.A. & Goldhammer, R.K. 1991: *Journal of Sedimentary Petrology*, 61, 1173-1193.
- Kent, D.V., Muttoni, G. & Brack, P. 2004: *Earth and Planetary Science Letters*, 228, 369-377.
- Meyers, S.R. 2008: *Geology*, 36, 319-322.
- Spahn, Z.P., Kodama, K.P. & Preto, N. 2013: *Geochemistry Geophysics Geosystems*, 14, 1245-1257.

## 4.5

# Detrital and nutrients influxes in the Northwestern Tethyan margin during the Valanginian: new insights from weathering changes during the Weissert episode

Charbonnier Guillaume<sup>1</sup>, Duchamp-Alphonse Stéphanie<sup>1</sup>, Adatte Thierry<sup>2</sup>, Spangenberg Jorge.E<sup>2</sup>, Colin Christophe<sup>1</sup>, Gardin Silvia<sup>3</sup>, Boulila Slah<sup>4</sup>, Galbrun Bruno<sup>4</sup> & Föllmi Karl.B<sup>2</sup>.

<sup>1</sup> UMR CNRS 8148 IDES, *Interactions et Dynamique des Environnements de Surface, University Paris Sud XI, Bâtiment 504, 91405 Orsay, France (guillaume.charbonnier@u-psud.fr).*

<sup>2</sup> *Institut des Sciences de la Terre, Quartier UNIL-Mouline, Bâtiment Géopolis, 1015 Lausanne, Switzerland.*

<sup>3</sup> UMR-CNRS 7072 CR2P, *Centre de Recherche sur la Paléobiodiversité et les Paléoenvironnements, University Pierre et Marie Curie, 4 place Jussieu, 75252 Paris CEDEX 5, France.*

<sup>4</sup> UMR-CNRS 7193 ISTeP, *Institut des Sciences de la Terre-Paris, Université Pierre et Marie Curie, 4 place Jussieu, 75252 Paris CEDEX 5, France.*

The Valanginian stage is characterized by a positive carbon isotope excursion (CIE, 1.5‰), the so-called « Weissert Event » (Erba et al., 2004). This event coincides with a widespread crisis of carbonate producing biota associated with important platform drowning events (Föllmi et al., 1994). The formation of the Parana-Etendeka large igneous province (LIP) (ca. 134 Ma) (Janasi et al., 2011) has been widely assumed to be responsible for an increase of CO<sub>2</sub>, triggering long-term greenhouse conditions, increased weathering and elevated nutrient transfer rates from continents to oceans. However, many aspects of this model have recently been questioned. Climate is the fundamental parameter of the model proposed in the previous studies as it is linked to both geodynamic and stratigraphic events. However, despite the ongoing importance of the debate on Valanginian climate variations, there are relatively few studies that detail high-resolution climatic changes during the positive C-isotope shift.

The aim of the study is to assess the changes in terrigenous and nutrients influxes in the Vocontian Basin associated to fluctuations in weathering processes. The used herein multiproxies approach is focused on high-resolution mineralogical (clay assemblages) and geochemical (major elements, CaCO<sub>3</sub> and phosphorus contents) analyses performed on the marl-limestones alternations of the Upper Berriasian–Valanginian Orpierre section (SE France). This section consists of a continuous sedimentation, well-time calibrated by biostratigraphy and cyclostratigraphy (Charbonnier et al., 2013).

At Orpierre, it appears that mineralogical and geochemical trends reflect a primary signal driven by palaeoenvironmental changes. Based upon the previous cyclostratigraphic study, performed at Orpierre, terrigenous, nutrients and clay influxes are calculated for the first time during the Valanginian.

The fluctuations of the terrigenous, phosphorus and clay influxes reflect changes in terrigenous inputs and nutrients levels linked to changed in the weathering regime in the source areas. At Orpierre it appears that during the Valanginian time interval, the weathering pattern results mainly from climate variations. Three major climate episodes have been highlighted: (i) at the Late Berriasian–Valanginian boundary : the Berriasian–Valanginian Episode (BVE) with a duration of ~576 kyr ; (ii) at the Early–Late Valanginian transition that includes the positive carbon isotope excursion : the Weissert episode (WE) with a duration of ~653 kyr ; and (iii) in the Late Valanginian : the Late Valanginian–Hauterivian Episode (VHE) with a duration of ~516 kyr. These episodes are marked by higher terrigenous and nutrient influxes related to enhanced humid conditions. They coincide with major platform demises in the northwestern tethyan margin. Over the full record, they closely follow the variations in the insolation induces by Earth orbital parameters. Particularly, maxima eccentricity are recorded when the wetter conditions and the higher terrigenous inputs are recorded in the Vocontian basin. The orbital forcing is probably the major driving force behind the palaeoenvironmental changes that prevailed in the northwestern margin during the Berriasian–Valanginian interval.

## REFERENCES

- Charbonnier, G., Boulila, S., Gardin, S., Duchamp-Alphonse, S., Adatte, T., Spangenberg, J.E., Föllmi, K.B., Colin, C., & Galbrun, B. 2013: Astronomical calibration of the Valanginian “Weissert” episode: the Orpierre marl-limestone succession (Vocontian Basin, southeastern France). *Cretaceous research*. 45, 25–42.
- Erba, E., Bartolini, A.C., & Larson, R.L. 2004 : Valanginian Weissert oceanic anoxic event. *Geology* 32, 149–152.
- Föllmi, K.B., Weissert, H., Bisping, M., & Funk, H. 1994: Phosphogenesis, carbon-isotope stratigraphy, and carbonate-platform evolution along the Lower Cretaceous northern Tethyan margin. *Geological Society of American Bulletin* 106, 729–746.
- Janasi, V.D., de Freitas, V.A., & Heaman, L.H. 2011 : The onset of flood basalt volcanism, Northern Parana Basin, Brazil: a precise U–Pb baddeleyite/zircon age for a Chapeco-type dacite. *Earth and Planetary Science Letters* 302, 147–153.

## 4.6

## Orbital chronology of the Lower-Middle Aptian: Palaeoenvironmental implications (Serre Chaitieu section, Vocontian Basin, France)

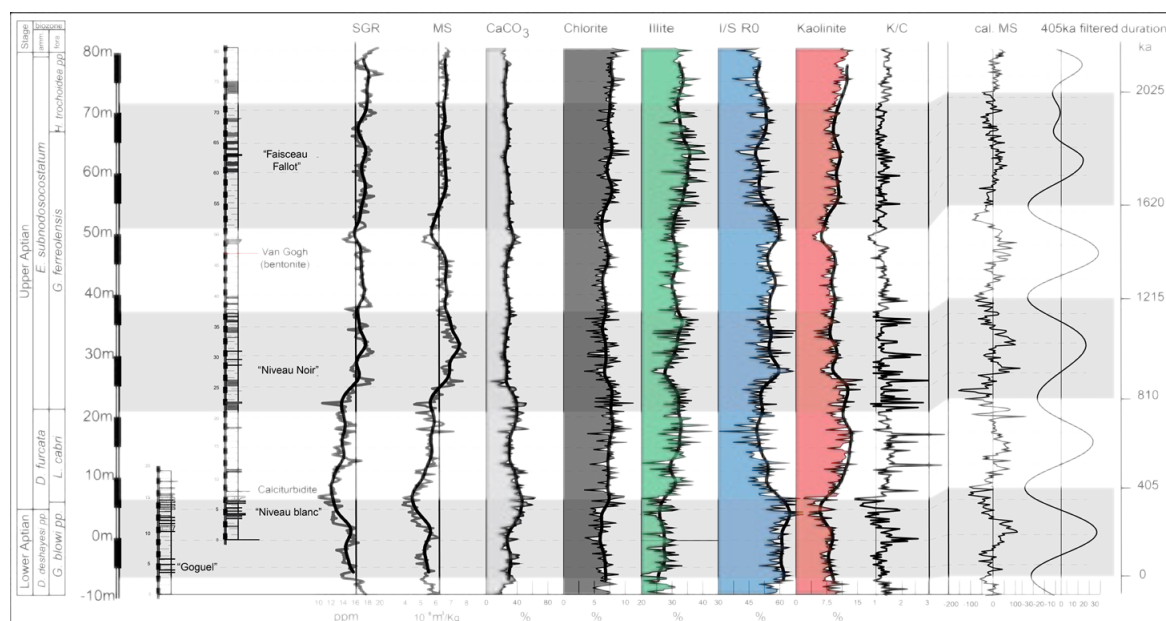
Deconinck Jean-François<sup>1</sup>, Ghirardi Julie<sup>2</sup>, Martinez Mathieu<sup>1</sup>, Bruneau Ludovic<sup>1</sup>, Pellenard Pierre<sup>1</sup>, Pucéat Emmanuelle<sup>1</sup>

<sup>1</sup> UMR CNRS 6282 Biogéosciences, Université de Bourgogne, 6 Bd Gabriel, 21000 Dijon, France (jean-francois.deconinck@u-bourgogne.fr)

<sup>2</sup> Univ d'Orléans, CNRS - ISTO, UMR 7327, 45071, Orléans, France

In the early Aptian, the OAE 1a is well defined by a negative  $\delta^{13}\text{C}$  excursion followed by a positive  $\delta^{13}\text{C}$  excursion, covering the *Deshayesites deshayesi* and *Dufrenoya furcata ammonite* zones (Menegatti *et al.*, 1998). To estimate the time required for the carbon cycle recovery following the major disruption due to anoxia after OAE1a and to provide durations of ammonites biozones, a cyclostratigraphic approach was performed in the Aptian of the Vocontian Basin (VB). The sedimentary succession mainly consists of hemipelagic blue-grey marl with frequent slumping and turbidites controlled by syn-sedimentary faulting, but in the Serre Chaitieu (SC) section located close to Lesches-en-Diois, resedimented material represents less than 10% of the succession (Friès & Parize, 2003) making this section a reference for cyclostratigraphy.

At the base of the SC section, above the OAE1a called "Niveau Goguel", marls become clearer and the carbonate content increases up to the "Niveau blanc", a limestone bed considered as a reliable marker throughout the VB (Fig). Above this bed, the continuous hemipelagic sedimentation is interrupted by a centimetric calciturbidite, which may have induced the erosion of some meters of marls (Bréhéret, 1997). The section studied encompasses the *Deshayesites deshayesi* Zone to the end of the *Epicheloniceras martini* Zone (Dutour 2005). Using a field Spectral Gamma Ray (SGR), 450 measurements were performed with a sample step of 20 cm. Each measured point was sampled for calcimetry, clay mineralogy and magnetic susceptibility (MS). Spectral analyses were then performed on all proxies. The lower part of the section (0 to 25 m) shows relatively low SGR and MS values while from 25 m to the top of the section, these values increase. These two parameters show a good correlation ( $r = 0.79$ ), while carbonate content and MS show an inverse correlation, which confirms that the MS reflects mainly the clay content. Clay mineral assemblages consist of illite, illite/smectite mixed-layers (I/S), kaolinite and chlorite. The proportions of illite and kaolinite covary and fluctuate in opposition with I/S. Cyclic fluctuations of relative proportions of clay minerals are particularly well expressed by the kaolinite/chlorite ratio. Spectral analyses, using the multi-taper and the amplitude spectrogram methods, were performed on SGR, MS,  $\text{CaCO}_3$  and K/C signals to detect sedimentary cycles related to an orbital forcing throughout the series. The geochronometer 405-kyr eccentricity cycle well expressed and significant (up to 99% confidence level) is used to provide a robust temporal framework. More than five 405-kyr eccentricity cycles are recognized (Fig.), allowing a total duration of at least 2.33 myr for the whole sedimentary succession to be proposed. The minimum duration of the *D. furcata* Zone is assessed at 0.46 myr, the duration of the *E. martini* Zone at 1.45 myr. Amplitude spectrograms show a strengthening signal of obliquity during the *D. furcata* Zone, which would confirm the global cooling characterising this interval, probably leading to the development of low-extension polar ice and the lowering of the sea level. Finally, the return to equilibrium in the carbon cycle in the aftermath of OAE1a covering the *G. ferreolensis* foraminifer Zone occurred in more than 1 myr.



## REFERENCES

- Boullila, S., Galbrun, B., Hinnov, L. A. & Collin, P.-Y. 2008: High-resolution cyclostratigraphic analysis from magnetic susceptibility in a Lower Kimmeridgian (Upper Jurassic) marl-limestone succession (La Méouge, Vocontian Basin, France). *Sed. Geol.* 203 (1-2), 54-63.
- Bréhéret, J.-G. 1997 : L'Aptien et l'Albien de la Fosse vocontienne (des bordures au bassin). Evolution de la sédimentation et enseignements sur les événements anoxiques. Thèse Univ. Tours. Publ. Soc. Géol. Nord 25, 614 p.
- Dutour, Y. 2005 : Biostratigraphie, évolution et renouvellements des ammonites de l'Aptien supérieur (Gargasien) du bassin vocontien (Sud-Est de la France). Thèse Univ. Aix-Marseille (unpublished), 302 p.
- Friès, G. & Parize, O. 2003: Anatomy of ancient passive margin slope systems: Aptian gravity-driven deposition on the Vocontian palaeomargin, western Alps, south-east France. *Sedimentology* 50 (6), 1231-1270.
- Hochuli, P. A., Menegatti, A. P., Weissert, H., Riva, A., Erba, E. and Premoli Silva, I. 1999: Episodes of high productivity and cooling in the early Aptian Alpine Tethys. *Geology*, 27, 7, 657-660.
- Laskar, J., Fienga, A., Gastineau, M. & Manche, H. 2011: La2010: a new orbital solution for the long-term motion of the Earth. *Astron.Astrophys.* 532, A89.
- Menegatti, A. P., Weissert, H., Brown, R. S., Tyson, R. V., Farromond, P., Strasser, A. & Caron, M. 1998: High resolution  $\delta^{13}\text{C}$  stratigraphy through the early Aptian « Livello Selli » of the Alpine Tethys. *Paleoceanography* 13 (5), 530-545.

## 4.7

## Cyclic Sedimentation in the Drusberg Beds, Wägital region, Helvetic Alps, Switzerland

Freeman Roy

*Thorenbergmatte 8, 6014 Lucerne. Email: roywfreeman@gmail.com*

The Lower Cretaceous limestones of the Drusberg Beds in the Wägital region of the central Helvetic Alps (Switzerland) exhibit three orders of rhythmic (cyclic sedimentation) in several well-exposed outcrops, (Fig. 1):

1. small scale laminations (.1mm to 1mm thick),
2. alternating limestone and marl beds (10 to 20 m thick), and
3. rhythmic units (2 to 6 m thick).

The clear interrelationships of the rhythms, excellent correlativity along strike, and the record of unbroken sedimentation lend good bases for discussing variations in bedding and facies, climate control of the depositional record, and of periodicities relating to rhythmic sedimentation. The marine basinal environment of deposition did not itself change, but the Drusberg sediments were affected by terrigenous detritus in suspension, variations in current regimes, and changes in nutrient supply, ocean anoxic events, temperature, and salinity of the surrounding water. Clearly, most of these may be interrelated in complex ways.

The first order (mm) cycles appear to be modes of deposition influenced primarily by variations in autochthonous sedimentation and local current regimes, perhaps even storm tempestites. These rhythms are clearly sedimentary-spatial and time-irregular. The wavy appearance of the bedding surfaces is most probably due to diagenetic transfer of calcium carbonate. The second cyclic order (cm) may have been influenced by local basin paleotopography as the controlling factor of facies variations. Shoals could have provided local detritus and shielded seaward basins from terrigenous influxes. Anoxic conditions may have alternated with more oxidizing environments (Föllmi, 2012).

The third order of cyclic sedimentation, (m-scale), may mirror real periodic cyclic fluctuations on a planetary-global scale. Global climate during the Quaternary exhibits periodicities and variations in the calcium carbonate content similar to those of the rhythmic units. The only true regular time cycles are related to planetary motions, the orbital eccentricity, obliquity, and precession of Earth's movements. Combining these periodicities give the well-known Milankovitch cycles of ca. 110,000 years. Using the biostratigraphy of Föllmi & Godet (2013, Fig. 6), the Drusberg Beds were deposited over a time period of ca. 1-2 Ma. Many of the third order (m-scale) cycles between the underlying Altmann Beds and the overlying Schratteknalk formation can be correlated, but the total number varies along strike due to the diachronous inception of

the younger Schrattenkalk. The number of m-scale cycles in the Wägital area range from 7-15. The number of Milankovitch cycles in the bracketed 1-2 Ma time period range from 9-18 and certainly occurred during the Lower Cretaceous. Thus it is possible that global climatic variations caused by planetary motions and may be reflected in the m-scale rhythmic sedimentation of the Drusberg Beds.



Figure 1. Brünnelistock, Wägital, Schwyz (view looking SW from Oberseetal). Middle: Drusberg Beds, below, dark marly Altmann Beds, top of image, thick banks of the light gray Schrattenkalk Formation (photo R. Freeman).

#### REFERENCES

- Föllmi, K. 2012: Early Cretaceous life, climate, and anoxia, *Cretaceous Research*, 35, 230-257.
- Föllmi, K. & Godet, A. 2013: Palaeoceanography of Lower Cretaceous Alpine carbonates, *Sedimentology*, 60, 131-151.
- Hays, J. D., Imbrie, J. & Shackleton, N. J. 1976: Variations in the Earth's orbit: pacemaker of the Ice Ages, *Science*, 194 (4270), 1121-1132.

## 4.8

# Environmental and climatic changes on the Brazilian shelf during the Campanian-Maastrichtian

Gertsch Brian<sup>1</sup>, Keller Gerta<sup>2</sup>, Adatte Thierry<sup>1</sup>, Spangenberg Jorge<sup>1</sup> & Berner Zsolt<sup>3</sup>

<sup>1</sup> *Institut des Sciences de la Terre, Quartier Unil-Mouline, Bâtiment Géopolis, CH-1015 Lausanne (brian.gertsch@unil.ch)*

<sup>2</sup> *Geoscience Department, Princeton University, Guyot Hall, 08544 Princeton, NJ, USA*

<sup>3</sup> *Karlsruhe Institute of Technology, University, 76131 Karlsruhe, Germany*

The upper Campanian to upper Maastrichtian interval was examined in the Olinda sub-basin near Recife, Brazil, to determine the response of inner to outer shelf environments in the equatorial Atlantic realm to global environmental and climatic changes of the late Campanian – Maastrichtian time. A multi-proxy approach involving sedimentological observations, carbon and oxygen isotopes, organic matter quantification and evaluation, bulk-rock mineralogy and planktic foraminifera biostratigraphy was carried out on three cores (Olinda, Poty and Itamaraca) drilled in 2005.

Sediments consist of phosphatic marly limestone topped by bioturbated light to dark gray marly limestone/marls. Although planktic foraminifera preservation is relatively poor, integrated planktic foraminifera and isotopic stratigraphy reveals that Poty and Itamaraca cores span the entire Maastrichtian, whereas the Olinda core is truncated with a major hiatus between the late Campanian and the late Maastrichtian (planktic foraminifera biozones CF8 to CF3). Each core shows a disconformity at the Cretaceous-Tertiary (KT) boundary similar to the short hiatus (280 kyr) observed by Gertsch et al. (2013). Bulk-rock mineralogy suggests a secondary dolomitization of the phosphatic marly limestone interval with the absence of calcite and the prevalence of dolomite, ankerite and Ca-apatite. Calcite (50-90%) and phyllosilicates (20-30%) are dominant in the bioturbated marly limestone/marl interval. Organic carbon is abundant (up to 4%) and of mixed origin (terrestrial and marine) indicative of both marine productivity and input of terrestrial organic matter from continents on the Brazilian shelf.

Isotopic measurements on bulk sediment suggest that oxygen isotopes are strongly affected by dolomitization. Minor diagenetic effect leads to negative values (up to -4.6‰) in the marly limestone/marl interval, but climatic trends are well-preserved with characteristic negative excursions in the terminal Maastrichtian indicative of warming events associated with Deccan volcanic activity. Carbon isotopes are more reliable with overall positive values (0 - 2‰). A negative shift in the terminal Campanian correlates well with global carbon isotope records (Wendler, 2013). In the Maastrichtian, carbon isotope trends show a plateau in the early Maastrichtian (up to CF4) followed by a regular increase up to the KT disconformity. This contrasts with global carbon isotope curves that record a positive excursion in the late Maastrichtian and suggests a local influence.

### REFERENCES

- Gertsch, B., Keller, G., Adatte, T. & Berner, Z. 2013: The Cretaceous-Tertiary (K-T) transition in NE Brazil, *Journal of Geological Society, London*, 170, 249-262.
- Wender, I. 2013. A critical evaluation of carbon isotope stratigraphy and biostratigraphic implications for Late Cretaceous global correlation, *Earth Science Reviews*, in press.

## 4.9

# Experimental investigation of molybdenum solubility under low atmospheric O<sub>2</sub> concentrations: Implications for pre GOE conditions

Nicolas D. Greber<sup>1</sup>, Thomas F. Nägler<sup>1</sup> and Urs Mäder<sup>1</sup>

<sup>1</sup> *Institut für Geologie, Universität Bern, Balzerstrasse 3, CH-3012 (greber@geo.unibe.ch)*

The history of the rise of atmospheric oxygen in the late Archean is a matter of considerable debate. Mass independent sulfur isotope fractionation in marine sediments before the great oxidation event (GOE; ~2.4 Ga ago), is generally considered to be the best indication of an anoxic early atmosphere (Farquhar et al. 2000). Model calculations performed by Pavlov et al. (2002) suggest that the O<sub>2</sub> level prior to the GOE was not higher than 10<sup>-5</sup> in respect to the present atmospheric level (PAL). However, this model result is not yet confirmed by experimental findings. New trace elemental isotope proxies as e.g. molybdenum (Wille et al. 2007) or chromium (Frei et al. 2009) suggest a mild increase in O<sub>2</sub> before the GOE, starting at around 2.7 Ga. These elements are redox sensitive and exhibit isotope fractionation, when oxidized to in water-soluble oxyanions.

The relation of Mo isotope fractionation to atmospheric O<sub>2</sub> levels is not yet quantified. To improve on this parameter, we conducted laboratory experiments on molybdenite (MoS<sub>2</sub>) using a glove box set up. The oxygen concentration in the N<sub>2</sub> atmosphere of the glove box has been controlled with platinum scrubbers and logged with an external computer. Pulverized molybdenite samples, pre-treated in a several weeklong process to reduce and wash out impurities and oxidized surfaces, have been put in water at different atmospheric oxygen concentrations ranging from 0 to 320 ppm. The O<sub>2</sub> concentration needed to oxidize and partially dissolve the molybdenite has been found to be around 3·10<sup>-4</sup> PAL and therefore slightly higher than the proposed value of Pavlov et al. (2002). The laboratory conditions used in our setup probably results in a maximum value of the needed oxygen. In any case, these results indicate that prior to the GOE the atmosphere has already seen a whiff of oxygen with concentrations probably slightly higher than suggested until now.

## REFERENCES

- Farquhar, J., Bao, H., and Thiemens, M.H. 2000: Atmospheric Influence of Earth's Earliest Sulfur Cycle. *Science*, 289, p. 756.
- Frei, R., Gaucher, C., Poulton, S.W., and Canfield, D.E. 2009: Fluctuations in Precambrian atmospheric oxygenation recorded by chromium isotopes. *Nature*, 461, p. 250–253.
- Pavlov, A.A., and Kasting, J.F. 2002: Mass-independent fractionation of sulfur isotopes in Archean sediments: strong evidence for an anoxic Archean atmosphere. *Astrobiology*, 2, p. 27–41.
- Wille, M., Kramers, J.D., Nägler, T.F., Beukes, N.J., Schröder, S., Meisel, T., Lacassie, J.P., and Voegelin, A.R. 2007: Evidence for a gradual rise of oxygen between 2.6 and 2.5 Ga from Mo isotopes and Re-PGE signatures in shales. *Geochimica et Cosmochimica Acta*, 71, p. 2417.

## 4.10

# Valanginian Weissert event in a shallow-platform setting, Zagros fold-thrust belt, southern Tethys

Hosseini Seyedabolfazl<sup>1,2</sup>, Kindler Pascal<sup>1</sup>, Conrad A. Marc<sup>3</sup>

<sup>1</sup> University of Geneva, Section of Earth and Environmental Sciences, 1205, Geneva, Switzerland (Seyedabolfazl.Hosseini@unige.ch)

<sup>2</sup> Exploration Directorate, National Iranian Oil Company (NIOC), 1st Dead End, Sheikh Bahai' Sq., Seoul Ave., P. O. Box: 19395 – 6669, Tehran, Iran

<sup>3</sup> 71 chemin de Planta, 1223 Cologny Switzerland

A well-defined, positive carbon isotope excursion (2.03‰ in  $\delta^{13}\text{C}$ ) was recognized in a shallow platform carbonate succession, the Fahliyan Fm. Location is in the Zagros fold-thrust belt of SW Iran, corresponding to the northeastern part of the Arabian Platform. This significant perturbation and change in the carbon cycle, is reported for the first time from the Southern Tethyan realm. It is interpreted as corresponding to the “Weissert Event”, dated late Early Valanginian-early Late Valanginian (135 Ma). The excursion may be related to (1) a rise of  $\text{CO}_2$  in the atmosphere-ocean system, (2) an increase in the amount and preservation of buried organic carbon and/or (3) the growth of extended photozoan platforms which operated as a sink for dissolved inorganic carbon of continental origin.

In the Zagros fold-thrust belt, an important phase of carbonate-platform growth started in the Late Triassic, and continued until the Early Cretaceous along the northeastern passive margin of the Arabian Plate (Alavi 2007). Platform margins are rather stable, reflecting different settings in the Zagros region: neritic conditions prevailed in the Fars and Khuzestan areas, while pelagic facies were deposited in the Lurestan area during the Early Cretaceous.

The dataset used for this study includes two outcrops respectively located in the Fars and Izeh zone, that were studied in details for biostratigraphy and facies analysis, essentially based on benthic foraminifera and dasycladacean algae. The dating was calibrated using the Sr-isotope method following the LOWESS version 4:08/04 (Howarth and McArthur 1997, McArthur et al. 2001). The benthic foraminifera and calcareous green algae found in shallow-platform deposits were identified and, relying on sequence stratigraphy and platform-basin transects, indirectly dated by assemblages of planktonic foraminifera, dinoflagellates and calpionellids occurring in interbedded deeper marine intervals. A portable gamma-ray spectrometer (GRS) was used to measure the in-situ total gamma values, and to quantify three major naturally radioactive elements, potassium (K), uranium (U) and thorium (Th) in the studied outcrops. Results were used to correlate the amount of clay content and siliciclastic input, considered a proxy for organic matter.

Seventy measurements of stable carbon and oxygen isotopes of sedimentary carbonates were carried out on 200-300  $\mu\text{g}$  of powdered bulk samples, derived from the sediment matrix alone. In order to avoid lithology and diagenetic-related side effects, rock samples were first slabbed to avoid calcite veins, then washed with normal and pure waters, dried at 110°C in an oven, and finally crushed and homogenized in an agate mortar.

Besides the positive carbon isotope excursion, in the studied sections the interval assigned to the Weissert Event is characterized by the highest amount of uranium (up to 9.0 ppm), tentatively explained by the precipitation of authigenic uranium under oxygen-depleted conditions. Preliminary interpretation consequently calls for the signature of a short-lived anoxic event which, new for the record, is identified in the shallow-platform setting of the study area. Based on oxygen-isotope analyses carried out so far, such an anoxia was likely accompanied by global warming and greenhouse conditions.

In the same intermission, a biotic crisis occurred in the marine realm, with the extinction of approximately 50% of the genera of benthic foraminifera and 75% of the genera of dasycladacean algae. Only opportunistic photozoan communities, presumably tolerant to oxygen-poor conditions, are found within the corresponding interval. Moreover, the average size of some dasycladacean algae was affected by anoxia. Specimens from the Berriasian and Early Valanginian are large, whereas those from the Late Valanginian and Early Hauterivian are dwarfed (Hosseini et al. 2013). The same is true for benthic foraminifera, only low spiral and basal-inflated trocholinids being present within this interval.

*We are thankful to the Exploration Directorate of the National Iranian Oil Company (NIOC) and also to the Department of Geology and Paleontology, University of Geneva for permission, under a co-operation agreement, to publish this abstract as a part of an ongoing Ph.D. thesis of the first author. This research was partly supported by a grant from the Société de Physique et d'Histoire naturelle de Genève (SPHN, “Bourse Lombard”).*

## REFERENCES

- Alavi, M., 2007, Structures of the Zagros fold-thrust belt in Iran. *Am. J. Sci.*, v. 307, p. 1064-1095.
- Hosseini, S.A, Conrad, M.A, & Kindler, P., 2013: *Iranella inopinata* Gollestaneh 1965, a puzzling dasycladalean alga from the Lower Cretaceous shallow carbonate shelf deposits of the Zagros fold- thrust belt, SW Iran. *Facies*: v. 59, p. 231-245.
- Howarth, R.J., & McArthur, J.M., 1997: Statistics for strontium isotope stratigraphy: a robust LOWESS fit to the marine strontium isotope curve for the period 0 to 206 Ma, with look-up table for derivation of numerical age. *Journal of Geology*, v. 105, p. 441-456.
- McArthur, J.M., Howarth, R.J., & Bailey, T.R., 2001: Strontium isotope stratigraphy: LOWESS version 3: best fit to the marine Sr-isotope curve for 0-509 Ma and accompanying look-up table for deriving numerical age. *Journal of Geology*, v. 109, p. 155-17

## 4.11

## Response of terrestrial environment to the Paleocene Eocene Thermal Maximum (PETM).

Hassan Khozyem<sup>1</sup>, Thierry Adate<sup>1</sup>, Jorge. E. Spangenberg<sup>1</sup>, Gerta Keller<sup>2</sup>, and Bandana Sament<sup>3</sup>

<sup>1</sup> Institut de Science de la Terre et de l'Environnement (ISTE), Université de Lausanne, Lausanne, Switzerland (Hassanmohamed.saleh@unil.ch).

<sup>2</sup> Department of Geosciences, Princeton University, Guyot Hall, Princeton, NJ 08544, USA

<sup>3</sup> Postgraduate Department of Geology, RTM Nagpur University, Nagpur, 440001, India.

The late Paleocene Early Eocene transition (56Ma) is marked by the warmest climate period of the Cenozoic, known as the Paleocene Eocene Thermal Maximum (PETM). The importance of the PETM studies is linked to the fact that the PETM bears some striking resemblances to the human-caused climate change unfolding today (Zachos et al. 2001; 2005 and Norris et al 2013). Most notably, the culprit behind it was a massive injection of heat-trapping greenhouse gases into the atmosphere and oceans, comparable in volume to what our persistent burning of fossil fuels could deliver in coming centuries. Knowledge of exactly what went on during the PETM could help us foresee what our future will be like. The response of the oceanic and continental environments to the PETM is different. Many factors might control the response of the environments to the PETM such as paleogeography, paleotopography, paleoenvironment, and paleodepth. Herein, we present two different examples from terrestrial environment and their response to the PETM warming.

In northwestern India, the establishment of wetland conditions and related thick lignite accumulations reflects the response of the continental environments to the PETM. This continental climatic shift towards more humid conditions led to migration modern mammals northward following the migration of the climatic belts. What remains uncertain is the timing and tempo of this mammal migration event and whether it originated in Asia or more specifically out of India.

Biostratigraphy and carbon isotope analyses in three lignite mines located in NW India reveal the presence of both PETM and ETM2 organic carbon isotope negative excursions and demonstrate that modern mammals appeared in India after the PETM. Relative ages of this mammal event based bio-chemo- and paleomagnetic stratigraphy support a migration path originating from Asia into Europe and North America, followed by later migration from Asia into India. The delayed appearance of modern mammals in India suggests a barrier to migration that is likely linked to the timing of the India-Asia collision.

In contrast, at Esplugafreda, north-eastern Spain, the terrestrial environment reacted differently; increased weathering due to enhanced runoff led to the formation thick paleosol accumulation enriched with carbonate nodules (Microcodium like) suggesting a coeval semi-arid climate (Retallack 2001, Calvet et al., 1999).  $\delta^{18}\text{O}/\delta^{16}\text{O}$  analyses performed on these soil nodules formed during the PETM provide important clues to better constrain the temperatures, intensity of warming and  $\text{PCO}_2$  fluctuations through the PETM. Preliminary data shows: 1) two significant  $\delta^{13}\text{C}$  shifts with the lower one linked to the PETM and the upper corresponding to the Early Eocene Thermal Maximum (ETM2); 2)  $\delta^{18}\text{O}/\delta^{16}\text{O}$  analyses of two different carbonate nodule types (microsparitic and micritic) reveal a temperature increase of around 10°C during the PETM; 3) This warming corresponds to a significant increase in  $\text{PCO}_2$  values; 4) a prominent increase in kaolinite content within the PETM linked to increased runoff and/or weathering of adjacent and coeval soils. These preliminary results demonstrate that the PETM coincides globally with extreme climatic fluctuations and that terrestrial environments are very likely to record such climatic changes.

### REFERENCES

- Zachos, J., Pagani, M., Sloan, L., Thomas, E. And Billups, K. (2001). Trends, rhythms, and aberrations in global climate 65 Ma to present. *Science*, v. 292, pp. 686–693.
- Zachos, J.C., Röhl, U., Schellenberg, S.A., Sluijs, A., Hodell, D.A., Kelly, D.C., Thomas, E., Nicolo, M., Raffi, I., Lourens, L.J., McCarren, H. & Kroon, D., 2005. Rapid acidification of the ocean during the Paleocene–Eocene Thermal Maximum. *Science*, V. 308, Pp.161–1611.
- Norris, R. D., Turner S. Kirtland, Hull, P. M., and Ridgwell, A., (2013), Marine Ecosystem Responses to Cenozoic Global Change. DOI: 10.1126/science.1240543 *Science* V. 341, p.492.
- Retallack, G. J. 2001. *Soils of the past*. Blackwell, Oxford, 600 pp.
- Calvet, J. C and Coauthors, 1999: MUREX: A land-surface field experiment to study the annual cycle of the energy and water bud- gets. *Ann. Geophys.*17, 838–854.

## 4.12

# Continental climate reconstruction during late Eocene–early Oligocene in Europe

Kocsis László<sup>1</sup>, Ozsvárt Péter<sup>2</sup>, Becker Damien<sup>3</sup>, Ziegler Reinhard<sup>4</sup>, Scherler Laureline<sup>5</sup> & Codrea Vlad<sup>6</sup>

<sup>1</sup> Institute of Earth Sciences, University of Lausanne, (laszlo.kocsis@unil.ch)

<sup>2</sup> Geologisch Research Group for Paleontology, MTA-MTM-ELTE, Hungary

<sup>3</sup> Musée jurassien des Sciences naturelles, Porrentruy, Switzerland

<sup>4</sup> Staatliches Museum für Naturkunde Stuttgart, Germany

<sup>5</sup> Institut des Sciences de l'Evolution, University of Montpellier 2, France

<sup>6</sup> Department of Geology, Babes-Bolyai University, Cluj-Napoca, Romania

The most recent shift between greenhouse and icehouse climate modes is placed at the Eocene–Oligocene transition (EOT, ~34 million years ago–Ma), where the marine record reveals stepwise cooling and increased ice accumulation at high latitudes. The terrestrial responses to the EOT climate change, however, show strong spatial heterogeneity and the reported palaeo-climate records are often contradictory (Kohn et al., 2004; Grimes et al., 2005; Zanazzi et al., 2007; Hooker et al., 2009; Hren et al., 2013). Here, we present stable isotope data for tooth enamel of large, herbivorous terrestrial mammals from Europe's mid-latitudes (N 40–50) to better comprehend the continental environment during the late Eocene–early Oligocene between 40 and 27 million years ago.

Our isotope data show general decrease in average  $\delta^{18}\text{O}_{\text{PO}_4}$  and  $\delta^{13}\text{C}$  values during the studied period, but strong spatial heterogeneity is apparent as well. Southern maritime localities have high and steady isotope values indicating warm and dry climate till 32 Ma. Northern sites, yielded lower isotopic values with an average offset of -2.4 ‰ in  $\delta^{18}\text{O}_{\text{PO}_4}$  from the southern localities. These data indicate different moisture sources (Atlantic vs. Tethys Ocean) in these regions and point to the existence of an already moderately high Alpine chain at this time. Further on, variation in the isotope values in the north reveals a minimum of  $1.3 \pm 0.7^\circ\text{C}$  drop in mean annual temperature at the EOT, confirming this cooling event in the terrestrial realm of Europe.

After 30 Ma, we find more fractionated meteoric water in Central Europe, which we explain by sudden relative altitude changes of at least 1100 meters based on modern relationship between altitude and isotopic composition of precipitation in the Alps. Considering that the proto-Alps acted already as a climatic barrier before 30 Ma, average palaeo-altitude could have been as high as 2000 meters in the Alps by the end of the Early Oligocene.

## REFERENCES

- Grimes, S.T., Hooker, J.J., Collinson, M.E., & Matthey, D.P., 2005: Summer temperatures of late Eocene to early Oligocene freshwaters. *Geology* 33, 189–192.
- Hooker, J.J., Grimes, S.T., Matthey, D.P., Collinson, M.E. & Sheldon, N.D. 2009: Refined correlation of the UK Late Eocene–Early Oligocene Solent Group and timing of its climate history. *The Geological Society of America, Special Paper* 452, 179–195.
- Hren, M.T., Sheldon, N.D., Grimes, S.T., Collinson, M.E., Hooker, J.J., Melanie Bugler, M. & Lohmann, K.C. 2013: Terrestrial cooling in Northern Europe during the Eocene–Oligocene transition. *PNAS*, 110 (19), 7562–7567.
- Kohn, M.J., Josef, J.A., Madden, R., Kay, R., Vucetich, G. & Carlini, A.A. 2004: Climate stability across the Eocene–Oligocene transition, southern Argentina. *Geology*, 32; 621–624.
- Zanazzi, A. Kohn, M.J. MacFadden, B.J. & Terry Jr, D.O. 2007: Large temperature drop across the Eocene–Oligocene transition in central North America. *Nature*, 445, 639–642.

## 4.13

### Latest Permian to Early Triassic high-resolution stable carbon isotope record from North-east Greenland

Sanson-Barrera, A.<sup>1</sup>; Hochuli, P. A.<sup>1</sup>; Bucher, H.<sup>1</sup>; Meier, M.<sup>1</sup>; Schneebeili-Hermann, E.<sup>1</sup>; Weissert, H.<sup>2</sup> and Bernasconi, S. M.<sup>2</sup>

<sup>1</sup> Paleontological Institute and Museum, University of Zurich, Karl Schmid-Strasse 4, 8006 Zurich, Switzerland  
(anna.sanson@pim.uzh.ch)

<sup>2</sup> Department of Earth Sciences, ETH Zurich, Sonneggstrasse 5, 8092 Zurich, Switzerland

Large and rapid fluctuations of the global carbon cycle during the Late Permian and Early Triassic left a global imprint in the organic carbon isotope record observed in numerous Permian–Triassic sections (Payne et al., 2004; Galfetti et al., 2007). Expanded and well preserved successions, i.e. Norway and NE Greenland covering the lower part of the Lower Triassic (Griesbachian/Dienerian), are crucial for assessing the evolution of the carbon cycle in detail. Sections of this interval are rare, and often incomplete or condensed. Expanded sections also allow the construction of a reliable biostratigraphic zonation, and therefore a better assessment of the temporal patterns of recovery after the end Permian mass extinction events, in both marine and terrestrial ecosystems.

At the north-western margin of Pangea, the rifting system between Greenland and Norway led to the accommodation of thick sedimentary sequences of earliest Triassic age. In East Greenland this interval is represented by a succession of deltaic sediments reflecting a general regressive trend. They are an excellent archive to study the evolution of terrestrial and marine ecosystems during this time. At Hold with Hope (East Greenland, 74°N) a 700m thick fossiliferous succession of the Wordie Creek Formation has been logged and sampled.

Here we present a high resolution lithostratigraphic and organic carbon isotope record of a composite section, covering the uppermost Permian and the lower part of the Lower Triassic (Dienerian). Palynofacies data are used to assess the composition of the organic matter.

Measurements of about 580 samples show several distinct trends and major shifts in the organic carbon isotope record. The following major excursions can be recognised (from 1 to 8): 1. a first negative shift of ca. -6‰ corresponds to the unconformity between the Late Permian Ravnefjeld Fm. and earliest Triassic Wordie Creek Fm., regionally known as the lithological Permian–Triassic boundary; 2. after a short interval with stable carbon isotope values around -28‰ a second negative shift of -4‰ (to values of ca. -32‰) follows. This correlates with the negative carbon isotope shift recorded in numerous globally distributed Permian–Triassic successions. 3. This shift is followed by a steady trend to more positive carbon isotope values. 4. This trend culminates in a distinct positive shift reaching values of ca. -22‰, comparable to the values of the Ravnefjeld Fm.; 5. Another negative shift of ca. 7‰ leads again to negative values of around -31‰; 6. This interval of low carbon isotope values is followed by a steady positive trend reaching values around -26‰. 7. At around 350m a step-like negative shift follows with a minimum at around -32‰, its most negative values are observed close to the *Bukkenites rosenkrantzi*-bearing layers, possibly corresponding to the Griesbachian–Dienerian boundary (Bjerager et al., 2006). 8. The last part of the curve shows fluctuating but progressively more positive values, reaching ca. -23‰ at the top of the section. Palynofacies data reflect alternating marine and terrestrial conditions in the lower part of the section changing to predominant terrestrial conditions near the top.

At basinal scale our isotope data are closely comparable with the coeval section from the Trøndelag platform in Mid-Norway (Hermann et al., 2010). At global scale similar trends can be observed in organic carbon isotope records from Pakistan (Hermann et al., 2012). In NE Greenland the distinct negative shift (7) tentatively interpreted to be close to the Griesbachian–Dienerian boundary can be compared and correlated to the shifts in the carbonate carbon isotope records from the Arabian Peninsula (Clarkson et al., 2013) and from China (Galfetti et al., 2007; Korte & Kozur, 2010). Thus our data from NE Greenland reflect multiple and major changes in the global carbon cycle, which occurred at the onset of the Triassic within less than one million years.

#### REFERENCES

- Bjerager, M., Seidler, L., Stemmerik, L., & Surlyk, F. (2006). Ammonoid stratigraphy and sedimentary evolution across the Permian – Triassic boundary in East Greenland, 143, 635–656. doi:10.1017/S0016756806002020
- Clarkson, M. O., Richoz, S., Wood, R. A., Maurer, F., Krystyn, L., McGurty, D. J., & Astratti, D. (2013). A new high-resolution  $\delta^{13}\text{C}$  record for the Early Triassic : Insights from the Arabian Platform. *Gondwana Research*, 24(1), 233–242. doi:10.1016/j.gr.2012.10.002
- Galfetti, T., Bucher, H., Brayard, A., Hochuli, P. A., Weissert, H., Guodun, K., Atudorei, V., et al. (2007). Late Early Triassic climate change : Insights from carbonate carbon isotopes , sedimentary evolution and ammonoid paleobiogeography,

243, 394–411. doi:10.1016/j.palaeo.2006.08.014

- Galfetti, T., Bucher, H., Ovtcharova, M., Schaltegger, U., Brayard, A., Brühwiler, T., Goudehand, N., et al. (2007). Timing of the Early Triassic carbon cycle perturbations inferred from new U – Pb ages and ammonoid biochronozones. *Earth and Planetary Science Letters*, 258, 593–604. doi:10.1016/j.epsl.2007.04.023
- Hermann, E., Hochuli, P. A., Bucher, H., Vigran, J. O., Weissert, H., & Bernasconi, S. M. (2010). A close-up view of the Permian – Triassic boundary based on expanded organic carbon isotope records from Norway ( Trøndelag and Finnmark Platform ). *Global and Planetary Change*, 74, 156–167. doi:10.1016/j.gloplacha.2010.10.007
- Hermann, E., Hochuli, P. A., Bucher, H., Ware, D., Weissert, H., Roohi, G., & Yaseen, A. (2012). Climatic oscillations at the onset of the Mesozoic inferred from palynological records from the North Indian Margin. *Journal of the Geological Society*, 169, 227–237.
- Korte, C., & Kozur, H. W. (2010). Carbon-isotope stratigraphy across the Permian – Triassic boundary : A review. *Journal of Asian Earth Sciences*, 39(4), 215–235. doi:10.1016/j.jseaes.2010.01.005
- Payne, J. L., Lehrmann, D. J., Wei, J., Orchard, M. J., Schrag, D. P., & Knoll, A. H. (2004). Large Perturbations of the Carbon Cycle During Recovery from the End-Permian Extinction. *Science*, 305(July), 506–509.

## 4.14

### Evaluating the causal link between the Karoo LIP and climatic-biologic events of the Toarcian Stage with high-precision geochronology

Sell Bryan<sup>1,2</sup>, Schaltegger Urs<sup>2</sup>, Ovtcharova Maria<sup>3</sup>, Bartolini Annachiara<sup>3</sup>, Jourdan Fred<sup>4</sup>, Guex Jean<sup>5</sup>

<sup>1</sup> *Earth and Environmental Sciences, University of Michigan, 1100 N University Avenue, Ann Arbor, MI 48109-1005*

<sup>2</sup> *Section des sciences de la Terre et de l'environnement, Université de Genève, Rue des Maraîchers 13, CH-1205 Genève (urs.schaltegger@unige.ch; presenting author)*

<sup>3</sup> *Museum d'Histoire Naturelle, Paris*

<sup>4</sup> *Western Australian Argon Isotope Facility, Curtin University of Technology, GPO Box U1987, Perth, WA 6845*

<sup>5</sup> *Institut des sciences de la Terre, Université de Lausanne, Géopolis, 1015 Lausanne*

The emplacement of the Karoo Large Igneous Province (LIP) has been previously invoked as a causal mechanism for Lower Toarcian ocean anoxia, climate change, and marine biotic turnover. This causal relationship has been questioned because of a general lack of precise geochronologic constraints. One narrow time interval in the Early Toarcian in particular, approximately at the level of the *H. falciferum* ammonite zone, has received much attention because it contains a prominent negative carbon isotope excursion (CIE) of global importance, as well as other geochemical and biological perturbations. Potential links to igneous activity have been proposed as causal mechanisms, one of them being the release of massive amounts of carbon to the atmosphere via rapid sill emplacement in the sedimentary Karoo basin. Here we test some of these hypotheses with new high-precision U-Pb zircon and baddeleyite dates from both the Toarcian sedimentary record in southern Peru, as well as of volcanic rocks and sills from the Karoo volcanic province.

The U-Pb zircon dates come from tephra interstratified with ammonites in marine sedimentary rocks in southern Peru (Palquilla section near Tacna). We also present new U-Pb zircon and baddeleyite dates from three sills and one rhyolite of the Karoo LIP. The duration of *falciferum* Zone negative CIE is now constrained by U-Pb zircon ages to be between 1.4 and 0.75 myr and is likely of shorter duration on the basis of stratigraphic relationships. The age of the *falciferum* Zone is between  $182.097 \pm 0.085$  Ma and  $183.17 \pm 0.24$  Ma ( $2\sigma$  analytical uncertainty), thus the Pliensbachian-Toarcian boundary must be somewhat older than 183 Ma. The onset of the *falciferum* Zone CIE appears to correlate in time with the onset Karoo LIP dike emplacement. Sill emplacement, however is recorded by our data to take place over a time span of some 2 million years. It is therefore substantially longer than the duration of the *falciferum* zone CIE and cannot be considered as one catastrophic event that caused global ocean anoxia, instantaneous carbon gas release, global warming, and biotic perturbation. Volcanic activity in the Karoo persisted at least until 179 Ma.

Our new U-Pb results support the interpretation made on the basis of published <sup>40</sup>Ar-<sup>39</sup>Ar data that Karoo LIP magmatism had a duration of more than 4 myr from approximately 183 to 179 Ma, and therefore do not support global extinction or anoxia hypotheses that require rapid magmatism of Karoo LIP.

## 4.15

### Towards accurate numerical calibration of the Late Triassic: High-precision U-Pb constraints on the duration of the Rhaetian

Wotzlaw Jörn-Frederik<sup>1</sup>, Guex, Jean<sup>2</sup>, Bartolini Annachiara<sup>3</sup>, Gallet Yves<sup>4</sup>, Krystyn Leopold<sup>5</sup>, McRoberts Christopher<sup>6</sup>, Taylor David<sup>7</sup>, Schoene Blair<sup>8</sup> & Schaltegger Urs<sup>1</sup>

<sup>1</sup> Department of Earth Sciences, University of Geneva, Geneva, Switzerland (joern.wotzlaw@unige.ch)

<sup>2</sup> Institute of Earth Sciences, University of Lausanne, Lausanne, Switzerland

<sup>3</sup> Muséum d'Histoire Naturelle, Paris, France

<sup>4</sup> Equipe de Paléomagnétisme, IPGP, Paris, France

<sup>5</sup> Institute of Paleontology, University of Vienna, Vienna, Austria

<sup>6</sup> Geology Department, SUNY Cortland, Cortland, NY, USA

<sup>7</sup> North West Museum, Lowell, Portland, OR, USA

<sup>8</sup> Department of Geosciences, Princeton University, Princeton, NJ, USA

Numerical calibration of the Late Triassic stages is arguably the most controversial issue in Mesozoic stratigraphy despite their importance for assessing mechanisms of environmental perturbations and associated biologic consequences preceding the end-Triassic mass extinction. Here we report new CA-TIMS zircon U-Pb dates for volcanic ash beds within the Aramachay Formation of the Pucara Group in Northern Peru that place precise constraints on the maximum age of the Norian-Rhaetian boundary. Previous estimates for the age of this boundary and the duration of the Rhaetian stage were primarily derived from magnetostratigraphic correlations of biochronologically well constrained Tethyan sections and the astrochronologic record of the Newark basin. Different correlation schemes lead to the concept of a short (4 m.y.) versus long Rhaetian (up to 10 m.y.; for a synthesis see Ogg, 2012). Sampled ash beds are closely associated with a characteristic uppermost Norian bivalve assemblages comprising the last occurrence of large flat clam *Monotis subcircularis* as well as thin shelled *Otapiria* aff. *O. norica* and *Oxytoma* cf. *O. inaequalvis*. Zircon U-Pb dates of sampled ash beds constrain the deposition age of this interval to be between 205.70 Ma and 205.30 Ma. We further recalibrate previously published zircon U-Pb dates for ash beds bracketing the Triassic-Jurassic boundary in the same basin (Schoene et al., 2010; Guex et al., 2012) employing the most recent calibration of the EARTHTIME tracer solution. These dates constrain the duration of the Rhaetian to be <4.5 m.y., thus strongly supporting the concept of a short Rhaetian. This ends a prolonged controversy about the duration of this stage and has fundamental implications for the rates of paleoenvironmental deterioration inferred for the Late Triassic, culminating in the end-Triassic mass extinction and provides an absolute tie-point for magnetostratigraphic and cyclostratigraphic correlations of marine and continental Late Triassic sedimentary sections.

#### REFERENCES

- Guex, J., Schoene, B., Bartolini, A., Spangenberg, J., Schaltegger, U., O'Dogherty, L., Taylor, D., Bucher, H., and Atudorei, V., 2012: Geochronological constraints on post-extinction recovery of the ammonoids and carbon cycle perturbations during the Early Jurassic. *Palaeogeography, Palaeoclimatology, Palaeoecology*, 346-347, 1–11.
- Ogg, J.G., 2012: Triassic, in Gradstein, F.M., Ogg, J.G., Schmitz, M.D., and Ogg, G.M., eds., *The Geologic Time Scale 2012*. Elsevier, Oxford-Amsterdam-Waltham, 681–730.
- Schoene, B., Guex, J., Bartolini, A., Schaltegger, U., and Blackburn, T.J., 2010: Correlating the end-Triassic mass extinction and flood basalt volcanism at the 100 ka level. *Geology*, 38, 387–390.

## P 4.1

# Origin of Devonian conical mud mounds of Hamar Lakhdad Ridge, Anti-Atlas, Morocco: hydrothermal or hydrocarbon venting ?

Frank Corminboeuf<sup>1</sup>, Thierry Adatte<sup>1</sup> and Jorge Spangenberg<sup>1</sup>

<sup>1</sup> ISTE, Geopolis, quartier Mouline Lausanne University, 1015 Lausanne, Switzerland (frank.corminboeuf@unil.ch)

In the Eastern Anti Atlas desert of Morocco, 8 km S-E of Erfoud stands the Hamar Laghdad ridge. An E-W orientated monoclinical ridge of 8 km length for 1.5 km width, which exposes a Devonian sedimentary succession crossed by important senestral N-E to S-W transforming faults. The western part of the ridge overlies directly the Silurian shales succession, whereas the eastern part spreads over 100 m thick pillow basalts of early Devonian age. This particularity produced a significant difference in the sedimentation patterns. The western part of the ridge consists of marine outer shelf sediments dominated by shales and marls intercalated with scarce fossiliferous limestones enriched in cephalopods (orthoceratids) deposited during the Pragian and early Emsian. However, the eastern part experienced shallower deposition characterized by crinoidal limestones.

The most interesting features consist of a constellation of 48 calcareous cones emerging from the sediment surface, the Kess-kess; they are 30 to 60 m in diameter and 30 to 50 m high. They correspond to thick limestone layers organized around a central funnel. The mound walls, as the inter mounds layers, are enriched in fossil especially crinoids, but the mounds seem to have been colonized from time to time by communities of organisms such as bivalves et corals. Some of these mud mounds have been formed during the early Devonian (Kess-Kess) and others (Hollard mound) later in the middle Devonian. Some neptunian dykes and up to 0.5 m large cemented fractures postdate the Kess Kess, but predate the formation the Hollard mound.

Two different interpretations mainly based on stable isotopes analyses have been proposed for the origin of these peculiar carbonate mounds: (1) accretion of the material driven by hydrothermal venting linked to volcanism (Mounji et al, 1998), (2) hydrocarbon venting (Peckman et al., 1999). The sediment micrite of the Kess Kess is characterized by very negative  $\delta^{18}\text{O}$  values, ranging from -10 to -6‰ VPDB and positive  $\delta^{13}\text{C}$  values, between 0 and 2‰ (Fig.1), which suggest a precipitation from hydrothermal waters derived from underlying volcanic intrusives.

The mounds also contain cemented cavities (stromatactis). The latter are filled by three different generations of cement with  $\delta^{18}\text{O}$  6-8‰ higher than the host rock, in or near the field of early Devonian seawater. Some fully recrystallized corals (Auloporids) have also been observed in the limestone layers and in the mound flanks indicating that at least some of the stromatactis are in fact relicts of dissolved organisms fossils recrystallized later in isotopic equilibrium with sea-water.

A younger mud mound framework of middle Devonian age (Peckmann et al., 1999) is present in the western part of the ridge. They are characterized by very low  $\delta^{13}\text{C}$  values (-22‰ to -10‰ VPDB) derived from degradative oxidation of methane or higher hydrocarbon. The neptunian dykes and associated fractures are more variable fluctuating between very low  $\delta^{13}\text{C}$  and  $\delta^{18}\text{O}$ , and normal Devonian values (-22‰ to -10‰ and 0‰ to 4‰ VPDB, respectively), indicating a precipitation of the earliest cement influenced by both hydrothermal circulations and hydrocarbon venting (Fig.1, phase A) followed by normal marine carbonate cement precipitation (Fig.1, phase B)

In addition, the distribution of the saturated hydrocarbons (analyzed by GC-MS) in both Hollard mound, neptunian dyke and associated fractures samples indicates a similar origin for the petroleum staining these rocks (Silurian graptolith shales). The generation/expulsion of this petroleum was most probably accelerated by exceptionally high geothermal gradient linked to regional volcanism. For the first time, a model integrating both Kess-Kess and Hollard mound formation is proposed. To sum up, the younger mudmounds (Hollard mound) originated in an environment influenced by hydrocarbon venting, contrary to the older Kess-Kess, which are related to hydrothermal venting

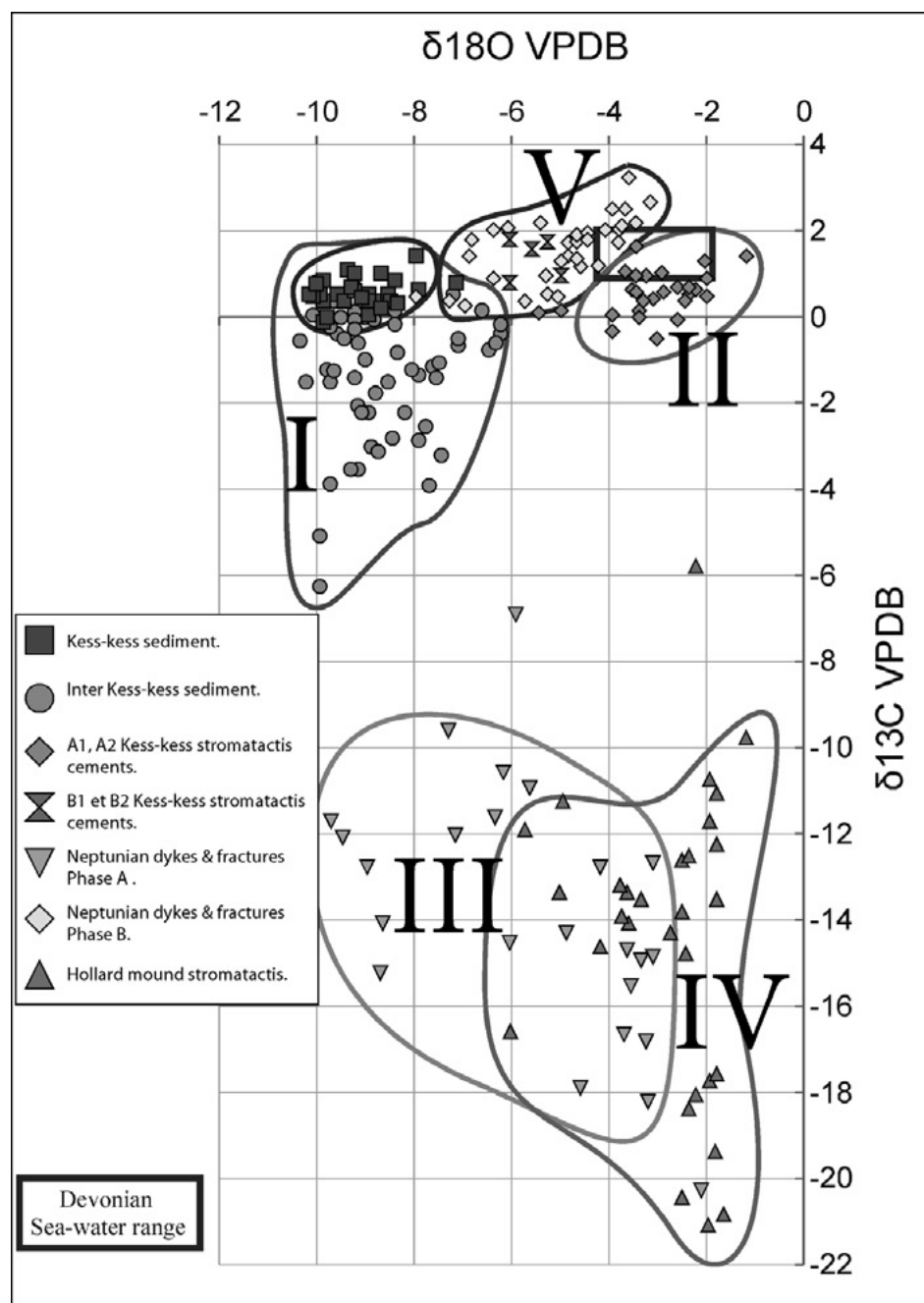


Figure 1. Cross plot of  $\delta^{18}\text{O}$  versus  $\delta^{13}\text{C}$  for the Kess-Kess sediment, Kess-Kess stromatactis, neptunian dykes and associated fractures, Hollard mound stromatactis

## REFERENCES

- Mounji, D., Bourque, P.A. and savard, M. M., (1998) Hydrothermal origin of Devonian conical mounds (kess-kess) of Hamar Lakhdad Ridge, Anti-Atlas, Morocco. *Geology*, 26, 1123–1126
- Peckmann, J., Walliser, O. R., Riegel, W., Reitner, J. (1999) Signatures of Hydrocarbon Venting in a Middle Devonian Carbonate Mound (Hollard Mound) at the Hamar Laghdad (Antiatlas, Morocco). *Facies*, 40, 281-286.

## P 4.2

# Sedimentological, mineralogical and geochemical study of sediments associated with the Deccan Traps in the Nagpur area, India

Alicia Fantasia<sup>1</sup>, Thierry Adatte<sup>1</sup>, Bandana Samant<sup>2</sup>, Dhananjay Mohabey<sup>2</sup>, Gerta Keller<sup>3</sup>

<sup>1</sup> ISTE, Lausanne University, 1015 Lausanne, Switzerland (thierry.adatte@unil.ch)

<sup>2</sup> Department of Geology, Nagpur University, Nagpur 440 001, India

<sup>3</sup> Department of Geosciences, Princeton University, Princeton NJ 08540, USA

The sedimentary beds (infra- and inter-trappeans) associated with Deccan volcanism in India are located in the eastern part (Madhya Pradesh and Maharashtra States) of the Traps, in the Nagpur, Chandrapur and Chhindwara districts. These sediments were deposited in terrestrial environments during periods of quiescence of the volcanic activity, mainly in alluvial-limnic to lacustrine environments.

A sedimentological, mineralogical and geochemical approach has been achieved to evaluate the changes triggered by the Deccan volcanism in central part India. The results have been compared with the existing palynological data (Samant and Mohabey, 2009). Bulk rock, clay minerals, phosphorus, organic matter and major/trace elements analyses indicated that the inter-trappean sediments deposited during the Deccan volcanism do not reflect the same characteristics than the infra-trappeans sediments preceding the volcanic eruptions.

Sedimentological and mineralogical observations indicate alluvial-limnic environment under arid climate for the deposition of the infra-trappean sediments. Moreover, palynoflora are dominated by gymnosperms and angiosperms with a rich canopy of gymnosperms (Conifers and Podocarpaceae) and an understory of palms and herbs. The low content in organic matter could be related to excessive desiccation and/or oxidation under arid conditions (Samant and Mohabey, 2009).

The eruption of Deccan volcanic flows severely affected the environment. Inter-trappean sediments associated with volcanic phase-1 and phase-2 were deposited in terrestrial to lacustrine environments under arid seasonal climate alternating long dry and short humid cycles. Moreover, clay minerals indicate a predominance of smectites resulting from the basalts alteration. Dinoflagellates, diatoms and ostracods blooms in the sediments preceding phase-2 could be related increased micronutrients availability. Organic matter is well preserved in the sediments deposited before the onset of the main volcanism phase consists of a mixed source with low oxidized lacustrine organic matter and terrestrial inputs. Trace elements (Ba, Cu, Ni, Zn, U and V) revealed a high productivity under low oxygenated conditions.

A strong floral response is observed with the onset of the main volcanism phase leading to dominance by angiosperms and pteridophytes at the expense of gymnosperms. In subsequent inter-trappean sediments a sharp decrease in pollen and spores coupled with the appearance of fungi mark increasing stress conditions apparently as a direct result of intensified volcanic activity. The organic matter analyses indicate a strong degradation suggesting that the biomass was oxidized because of strong volcanic activity and resulting acidic conditions. The chemical index of alteration (CIA) shows a gradual increase culminating within the main phase of volcanism reflecting increased acid rains. Ti/Al and K/(Fe+Mg) ratios are high and close to Deccan average basalt values indicating a strong influence from the basalts.

Mineralogical and geochemical observations indicate more contrasted sources for the sediments deposited after the main phase of volcanism and paleontological observations indicate a floral and fauna recovery.

## REFERENCES

Samant, B., And Mohabey, D. M. (2009). Palynoflora from Deccan volcano-sedimentary sequence (Cretaceous-Palaeogene transition) of Central India: implications for spatio-temporal correlation. *J. Biosciences* 34 (5), pp.811-823

## P 4.3

### The Jabal Rayah meteorite impact crater, Saudi Arabia

Edwin Gnos<sup>1</sup>, Beda A. Hofmann<sup>2</sup>, Khalid Al-Wagdani<sup>3</sup>, Ayman Mahjub<sup>3</sup>, Abdulaziz Abdullah Al-Solami<sup>3</sup>, Siddiq N. Habibullah<sup>3</sup>, Albert Matter<sup>4</sup> & Mohammed A. Halawani<sup>3</sup>

<sup>1</sup> Natural History Museum of Geneva, route de Malagnou 1, CH-1208 Geneva (edwin.gnos@ville-ge.ch)

<sup>2</sup> Natural History Museum Bern, Bernastrasse 15, CH-3005 Bern

<sup>3</sup> Saudi Geological Survey, P.O. Box 54141, Jeddah 21514, Saudi Arabia

<sup>4</sup> Institute of Geological Sciences, University of Bern, Baltzerstrasse 1+3, CH-3012 Bern

Only two certain and two likely meteorite impact sites are so far known on the Arabian Peninsula (Fig. 1): 1) The Wabar impact crater cluster in Saudi Arabia (e.g., Philby, 1933; Wynn and Shoemaker, 1998; Gnos et al., in review), 2) the Jebel Waqf as Suwwan impact structure in Jordania (e.g., Kenkmann et al., 2010), 3) the As Shutbah impact crater in Saudi Arabia (e.g., Gnos et al., 2011) and 4) the obscured Albian Murshid impact crater in Oman (Levell et al., 2002). Only in the Wabar case impact melts and fragments from the iron meteorite impactor were found. Shocked material and shatter cones have also been found at Jebel Waqf as Suwwan and at Ash Shutbah.

The ~5.5 km sized Jabal Rayah ring structure (Fig. 1) is the fifth impact crater on the Arabian Peninsula. It is a strongly eroded, complex impact crater located in Saudi Arabia, 68 km NE of Tabuk at 28°39'N and 37°12'E (Fig. 1). It is well visible on aerial and satellite photographs (e.g., Garvin and Blodget, 1986) and was mapped by Janjou et al. (1997). Erosional processes led to a relief inversion. A ring depression consisting of displaced blocks of Silurian to Early Devonian strata is now forming a topographically outstanding, up to 150 m high ring crest. The displaced blocks show internal folding and faulting and some of the sediment packages were thrust over others. The drainage towards the centre of the structure is controlled by a set of radial faults. The central uplift part of the structure consists of strongly folded, graptolite- and orthocone-bearing micaceous sandstones of the Qusaiba Formation of Early Silurian age. This part is eroded to the level of the surrounding plateau and partially covered with gravel.

Despite the fact that the sampled sediments are devoid of shock features, outward plunging fold axes of the central uplift and folded and displaced blocks forming the ring crest clearly indicate an impact origin of the ring structure. Based on the crater diameter it can be estimated that the rocks forming the central uplift come from a depth of ~400 m.



Figure 1. Overview map of the Arabian Peninsula showing known impact craters and the Jabal Rayah ring structure located NE of Tabuk.

## REFERENCES

- Garvin, J.B. & Blodget, H.W. (1987). Suspected impact crater near Al Madafi, Saudi Arabia. *Lunar and Planetary Science Conference*, 38,314-315.
- Gnos, E., Al-Wagdani, A., Mahjub, A., Al-Solami, A.A., Allah, S.H., Matter, A., Hofmann, B.A., Schmieder, M. & Buchner, E. (2011) Ash Shutbah: A new impact crater in Saudi Arabia. *Abstract Annual Meteoritical Society Meeting*., 5108.pdf.
- Gnos, E., Hofmann, B.A., Tarabulsi, Y., Al Halawani, M., Hakeem, M., Al Shanti, M., Greber, N., Holm, S., Greenwood, R.C. & Ramseyer, K. (in review). The Wabar impact craters, Saudi Arabia, revisited. *Meteoritics & Planetary Science*.
- Janjou, D., Halawani, M.A., Brosse, J.-J., Al-Muallem, M.S., Becq-Giraudon, J.-F., Dagain, J. Genna, A. Razin, P. Robool, J., Shorbaji, H. & Wyns, R. 1997. Geological map of the Al Qualibah quadrangle, Kingdom of Saudi Arabia, Geoscience map GM-135, scale 1:250'000, sheet 28C. Jeddah, Saudi Geological Survey.
- Kenkmann, T., Reimold, W.U., Khirfan, M., Salameh, E., Khoury, H. & Konsul, K. 2010. The complex impact crater Jebel Waqf as Suwwan in Jordan: Effects of Target heterogeneity and impact obliquity on central uplift formation. *Geological Society of America, Special Papers*, 465, 471-487.
- Levell, B., Richard, P. & Hoogendijk, F. 2002. A possible Albian impact crater at Murshid, Southern Oman. *GeoArabia*, 7, 721-730.
- Philby, H.S.J. 1933. Rub' al Khali: An account of exploration in the Great South Desert of Arabia under the auspices and patronage of his majesty 'Abdul 'Aziz ibn Sa'ud, King of Hejaz and Nejd and its dependencies. *The Geographical Journal*, 81, 1-21.
- Wynn, J. C. & Shoemaker, E. M. 1998. The day the sands caught fire. *Scientific American*, 279/5, 36-45.

## P 4.4

# Early-Middle Triassic boundary – precision and accuracy achieved by combining U-Pb zircon geochronology and biochronology

Ovtcharova Maria<sup>1</sup>, Goudemand Nicolas<sup>2</sup>, Galfetti Thomas<sup>3</sup>, Brayard Arnaud<sup>4</sup>, Hammer Oyvind<sup>5</sup>, Bucher Hugo<sup>2</sup> & Schaltegger Urs<sup>1</sup>

<sup>1</sup> *Section des sciences de la Terre et de l'environnement, Université de Genève, rue des Maraîchers, 13, CH-1205 Geneva (maria.ovtcharova@unige.ch)*

<sup>2</sup> *Paleontological Institute and Museum, University of Zurich, Karl Schmid-Strasse 4 8006 Zurich & Department of Geological and Environmental Sciences, Stanford University, 4550 Serra Mall, Stanford, CA 94305, USA*

<sup>3</sup> *Holcim Group Support Ltd, Materials Technology, CH-5113 Holderbank*

<sup>4</sup> *UMR-CNRS 6282 Biogéosciences, Dijon, France*

<sup>5</sup> *Museum of Natural History, University of Oslo, P.O.Box, 1172 Blindern, Oslo, N-0318, Norway*

The importance of the Early-Middle Triassic boundary (EMTB) lies in the fact that this boundary marks the end of the time interval characterized by the biotic recovery after the end-Permian mass extinction. Therefore, to gain highest possible time accuracy and precision for quantification of biotic processes, we undertook a detailed calibration of the EMTB with high-precision CA-ID-TIMS U-Pb age determinations on zircons from volcanic ash beds interbedded with biostratigraphically well dated marine sedimentary sections. These dates have been used to quantify and calibrate different stratigraphic schemes across the EMTB in the Nanpanjiang basin in South China. Despite an optimal control on the continuity of the studied stratigraphic record and on the accuracy of analytical procedures, we recognized that some single ash-beds yielded ages that are too old and contradict the stratigraphic succession. We therefore try to tackle questions such as: How can we improve the confidence in the interpretation of zircon dates as proxies for the age of deposition of these ash beds? How can we define more precisely and accurately EMT boundary?

We sampled 14 volcanic ash beds within a 15m stratigraphic section bracketing the EMTB in the Monggan-WanTuo section (Luolou Fm., NW Guangxi) in the Nanpanjiang basin, South China. The section is biostratigraphically well calibrated with conodonts (Goudemand et al., 2012). Our ash bed data start with the so called “green-bean rock” (GBR), which is a composite volcanoclastic greywacke, customarily used as a mapping unit to separate Lower from Middle Triassic marine rocks in the Nanpanjiang Basin (Lehrmann et al., 2006).

In 9 out of 14 ash beds zircon dates are following the stratigraphic succession within analytical uncertainty (from the late Early Triassic Luolou Formation –  $247.41 \pm 0.12$  Ma to the Middle Anisian “Transition Beds” –  $246.44 \pm 0.14$  Ma). The studied sequence shows four samples with reworked zircons, indicating that the zircons in this magma batches were crystallizing over a long period of time or remobilized from deeper levels within the same magmatic system. Another four samples show clear residual lead loss (mainly the lower part of the section represented by GBR). If such Pb loss is combined with the presence of antecrystic material, no information can be reliably derived from such material. This study exemplifies that in such complex cases the number of analysed samples to build up a robust dataset that agrees with the stratigraphic sequence can be substantial. Through analysis of an insufficient number of samples, not recognizing reworked greywacke type layers, missing lead loss effects and magmatic reworking effects, one could arrive at highly inaccurate numbers for rates of sedimentation and biotic change.

Spline interpolation age model for the eight selected radiometric ages yields an EMTB boundary age of  $247.11 \pm 0.08$  Ma. This result is well within the uncertainty interval of the previous  $247.2 \pm 0.4$  Ma age of Lehrmann et al. (2006), which was obtained by linear interpolation between two U-Pb ages. The new EMTB age interval is significantly more accurate and precise and is based on the robust residual maximal associations of conodonts, avoiding biostratigraphical discrepancies.

## REFERENCES

- Goudemand, N., Orchard, M., Bucher, H. & Jenks, J. 2012: The elusive origin of *Chiosella timorensis* (Conodont Triassic). *Geobios*, Volume 45, Issue 2, March–April 2012, Pages 199–207.
- Lehrman, D., Ramezani, J., Bowring, S., Martin, M., Montgomery, P., Enos, P., & Payne, J. 2006. Timing of recovery from the end-Permian extinction: Geochronologic and biostratigraphic constraints from south China. *Geology*, 34(12), 1053.

## P 4.5

# Sea level and current controlled sedimentary successions in the Hawasina Basin (Oman) during the Late Jurassic to Early Cretaceous time

Wohlwend Stephan<sup>1</sup>, Celestino Ricardo<sup>1</sup>, Weissert Helmut<sup>1</sup>

<sup>1</sup> *Geologisches Institut, ETH Zürich, Sonneggstrasse 5, CH-8052 Zürich (stephan.wohlwend@erdw.ethz.ch)*

The Oman mountains preserve a Late Jurassic to Cretaceous continental margin transect with the Arabian carbonate shelf and the adjacent deep Hawasina Basin. The whole nappe pile containing the continental margin transect is today outcropping in the Central Oman Mountains. The sediment successions of the Hawasina Basin (Sumeini, Hamrat Duru and Kawr Group) provide the opportunity to investigate the response of an eastern Tethyan equatorial ocean system to multiple perturbations of the carbon cycle in the Cretaceous.

The Hawasina Basin and also the easternmost Arabian Platform was affected by the Late Jurassic sea level rise and by regional tectonic (Rousseau et al. 2005). The widespread change “to a “Maiolica Facies” of the Rayda, the Lower Sid'r and also the Nadan Fm documents this transition in oceanography.

Chemo- and biostratigraphy serve for correlation of the pelagic facies across the Hawasina Basin. Pelagic to hemipelagic conditions existed until the time of the Valanginian carbon isotope excursion. With the onset of this excursion chert and silicification features in the pelagic sediments disappeared for a while. On the seamounts (Kawr Group) the top of the Nadan Formation (Maiolica facies) is marked by a hardground spanning the Valanginian to the Early Cenomanian time. The hardground documents intensification of an erosive deep current. Chemostratigraphic work combined with radiolarian biostratigraphy from Blechschmidt et al. (2004) shows a reduced sedimentation rate with a strong silicification during the mid-cretaceous time in the Hamrat Duru Group. The hardground and the reduced sedimentation reflect the current pattern as simulated by Hotinski and Toggweiler (2003).

Because of the equatorial position of the Arabian Platform and the offshore Hawasina Basin, the wind driven equatorial current produced an upwelling current bringing nutrient rich water masses to the surface of the Hawasina Basin. This may explain the chert pulse during the onset of the OAE1a. Until now the data suggest that the Hawasina Basin was not affected by major anoxia during the OAE 1 and 2.

## REFERENCES

- Blechschmidt, I., Dumitrica, P., Matter, A., Krystyn, L., & Peters, T. 2004: Stratigraphic architecture of the northern Oman continental margin - Mesozoic Hamrat Duru Group Hawasina complex, Oman, *GeoArabia*, 9, 81-124.
- Hotinski, R.M., & Toggweiler, J.R. 2003: Impact of a Tethyan circumglobal passage on ocean heat transport and “equable” climates, *Paleoceanography*, 18.
- Rousseau, M., Dromart, G., Garcia, J.P., Atrops, F. & Guillocheau, F. 2005: Jurassic evolution of the Arabian carbonate platform edge in the central Oman Mountains, *Journal of the Geological Society*, 162, 349-36.

## 5. Alpine Geology

Lukas Baumgartner, Jean-Luc Epard, Fritz Schlunegger

*Swiss Society of Mineralogy and Petrology (SSMP)*

### TALKS:

- 5.1 De Meyer Caroline M. C., Baumgartner Lukas P., Beard Brian L., Johnson Clark M.: Rb-Sr isochron ages from phengite inclusions in garnets from eclogite facies metasediments of the Zermatt-Saas Fee Zone (Western Alps)
- 5.2 Gnos E., Berger A., Janots E., Whitehouse M., Soom, M., Frei, Waight T.E.: Constraining Alpine brittle deformation with hydrothermal monazite
- 5.3 Kunz B., Von Niederhäusern B., Manzotti P., Lanari P., Engi M.: Tracing Permian lower continental crust through rifting and orogeny
- 5.4 Lanari P., Loury C., Burn M., Riel N., Rolland Y., Schwartz S., Guillot S., Vidal O., Engi M.: Tracing the continuous P-T path by combining thermobarometry with a micro-mapping approach
- 5.5 Letsch D., Winkler W., Gallhofer D., Von Quadt A.: The volcano-sedimentary evolution of a Late-Variscan intermontane basin in the Swiss Alps (Glarus Verrucano) as revealed by zircon U-Pb age dating
- 5.6 Masson H., Steck A.: New tectonic limits in the Central Alps: the case of the «Simano nape»
- 5.7 Mullis J., Wolf M.: Retrograde evolution of paleo- to recent fluids and their impact on mineral precipitation in the Gotthard base tunnel between Amsteg and Sedrun, Switzerland.
- 5.8 Ragusa J., Ospina-Ostios L-M., Kindler, P.: Provenance analysis of the Voirons Flysch (Gurnigel nappe, Haute-Savoie, France): highlighting two major sources

### POSTERS:

- P 5.1 Cavargna-Sani M., Epard J.-L.: Structure and kinematics of the northern Adula nappe (Central Alps, Switzerland) and its emplacement in the Lower Penninic nappe stack.
- P 5.2 Marger K., Mueller T.: Fluid-infiltration driven formation of reaction rims between carbonates and silica-rich sediments during contact metamorphism of the Buchenstein formation in the Southern Adamello contact aureole, Italy
- P 5.3 Proce M., Mullis J.: Fluid investigation on prograde, T-max and retrograde inclusions in quartz from the southern part of the NEAT Gotthard base tunnel, Central Alps: preliminary results.
- P 5.4 Skora S., Baumgartner L., Johnson C.: Lu-Hf ages from the Zermatt-Saas Fee ophiolite
- P 5.5 Youcef Brahim E., Chadi M.: Drowning history of Jurassic carbonate platform, Northern Atlasic fringe (NE ALGERIAN)
- P 5.6 Fiebich E., Müller T., Foster C.T. Jr.: Diffusion-controlled garnet growth in silicious marbles of the Adamello contact aureole, N-Italy

## 5.1

### Rb-Sr isochron ages from phengite inclusions in garnets from eclogite facies metasediments of the Zermatt-Saas Fee Zone (Western Alps)

de Meyer Caroline M. C.<sup>1</sup>, Baumgartner Lukas P.<sup>1</sup>, Beard Brian L.<sup>2</sup>, Johnson Clark M.<sup>2</sup>

<sup>1</sup>*Institut des Sciences de la Terre, Université de Lausanne, CH-1015 Lausanne, Suisse*

<sup>2</sup>*Department of Geosciences, University of Wisconsin, 1215 W. Dayton, Madison 53706, WI, USA*

The ultramafic, mafic and metasedimentary units of the Zermatt-Saas Fee Zone (ZSZ) (Western Alps) were subducted to eclogite-facies conditions, reaching peak pressures and temperatures of 20-28 kbar and 500-600 °C. The rocks were partially retrogressed to greenschist-facies conditions during exhumation. Published Rb-Sr isochron ages obtained on matrix phengites in metasediments of the ZSZ are believed to date cooling to below the closure temperature of phengite of ca. 500 °C. Here we present Rb-Sr isochrons of phengite fully included in garnets to date garnet growth. We show that garnet acted as a shield for the completely included phengites, preventing Rb and Sr isotopic exchange with the matrix.

Garnets were separated from two metasedimentary samples from Triftji, using the Selfrag apparatus. Phengites included in garnet were manually recovered from abraded garnet separates. The Rb and Sr isotopic compositions of the phengite inclusion separates and of matrix minerals were analysed using the TIMS at the University of Wisconsin. Phengite inclusion ages for the samples are  $44.25 \pm 0.48$  Ma and  $43.19 \pm 0.32$  Ma. They are ~4 m.y. older than the corresponding matrix mica ages of  $40.02 \pm 0.13$  Ma and  $39.55 \pm 0.25$  Ma, respectively. To explain the 4 Ma difference in age for the phengites included in the garnet and the phengites in the matrix we suggest that: (a) phengites were included during prograde garnet growth; (b) inclusion of phengite in the garnet allowed for total isolation of the inclusions for isotopic exchange with the matrix, and hence the micas were protected against re-equilibration during the further prograde and subsequent retrograde path, even though the metamorphic peak exceeded the closure T of the Rb/Sr system in phengite-; and (c) the 44 Ma inclusion age is a mixed age for the incorporation of phengite in garnet, weighted towards the later part of the garnet growth; hence towards the peak of the prograde metamorphism. The results are consistent with previous Sm-Nd and Lu-Hf geochronology on the ZSZ. They confirm that at least parts of the ZSZ underwent peak metamorphic HP conditions younger than 43 m.y. ago, followed by rapid exhumation to upper greenschist-facies conditions at  $39.9 \pm 0.5$  Ma.

## 5.2

### Constraining Alpine brittle deformation with hydrothermal monazite

Edwin Gnos<sup>1</sup>, Alfons Berger<sup>2</sup>, Emilie Janots<sup>3</sup>, Martin Whitehouse<sup>3</sup>, Michael Soom<sup>4</sup> Robert Frei<sup>5</sup> & Tod Earle Waight<sup>5</sup>

<sup>1</sup>Natural History Museum, Route de Malagnou 1, CH-1208 Geneva (edwin.gnos@ville-ge.ch)

<sup>2</sup>Institute of Geological Sciences, University of Bern, Baltzerstrasse 1 + 3, CH-3012 Bern

<sup>3</sup>ISTerre, 1381 rue de la piscine, F-38041 Grenoble

<sup>4</sup>Swedish Museum of Natural History, Box 50007, SE104-05 Stockholm, Sweden

<sup>5</sup>Department of Geosciences and Natural Resource Management, Section of Geology Øster Voldgade 10 1350 København K, Denmark

Two millimeter-sized hydrothermal monazites from an open fissure (cleft) that developed late during a dextral transpressional deformation event in the Baltschieder valley, Aar Massif, Switzerland, have been investigated using electron microprobe and ion probe. The monazites are characterised by high Th/U ratios typical of other hydrothermal monazites. Deformation events in the area have been subdivided into three phases: (D<sub>1</sub>) main thrusting including formation of a new schistosity; (D<sub>2</sub>) dextral transpression; and (D<sub>3</sub>) local crenulation including development of a new schistosity. The two younger deformational structures are related to a subvertically-oriented intermediate stress axis, which is characteristic for strike slip deformation. The inferred stress environment is consistent with observed kinematics and the opening of such clefts. Therefore, the investigated monazite-bearing cleft formed at the end of D<sub>2</sub> and/or D<sub>3</sub>, and during dextral movements along NNW dipping planes.

Interaction of cleft-filling hydrothermal fluid with wall-rock results in REE mineral formation and alteration of the wall-rock. The main newly-formed REE-minerals are Y-Si, Y-Nb-Ti-minerals and monazite. Despite these mineralogical changes, the bulk chemistry of the system remains constant and thus these mineralogical changes require redistribution of elements via a fluid over short distances (cm). Low-grade alteration enables local redistribution of REE, related to the stability of the accessory phases. This allows high precision isotope dating of cleft monazite. <sup>232</sup>Th/<sup>208</sup>Pb ages are not affected by excess Pb (Janots et al., 2012) and yield growth domain ages between 8.03 ± 0.22 Ma and 6.25 ± 0.60 Ma.

The monazite crystallization is coeval or younger than 8 Ma zircon fission track data (Michalski and Soom 1990) and hence occurred below 280°C.

#### REFERENCES

- Janots, E., Berger, A. Gnos, E., Whitehouse, M., Lewin, E. & Pettke, T. 2012: Constraints on fluid evolution during metamorphism from U–Th–Pb systematics in Alpine hydrothermal monazite. *Chemical Geology*, 326-327, 61–71.
- Michalski, I. & Soom, M.A. 1990: The Alpine thermo-tectonic evolution of the Aar and Gotthard massifs, central Switzerland: Fission track ages on zircon and apatite and K/Ar mica ages, *Schweizerische Mineralogische und Petrographische Mitteilungen*, 70, 373–387.

## 5.3

### Tracing Permian lower continental crust through rifting and orogeny

Barbara E. Kunz<sup>1</sup>, Brigitte von Niederhäusern<sup>1</sup>, Paola Manzotti<sup>2</sup>, Pierre Lanari<sup>1</sup> & Martin Engi<sup>1</sup>

<sup>1</sup> Institute of Geological Sciences, University of Bern, Baltzerstrasse 1+3, CH-3012 Bern, Switzerland (barbara.kunz@geo.unibe.ch)

<sup>2</sup> Géosciences Rennes, UMR-CNRS 6118, Université de Rennes 1, 35042 Rennes Cedex, France

In the Western Alps crustal fragments of the Austroalpine domain, once belonging to the northwest margin of Adria, are widely distributed. The IIDK in the Sesia Zone and the Valpelline in the Dent Blanche show numerous similarities to the Kinzigite Formation of the Ivrea Zone. The IIDK and Valpelline show a large variability in Alpine overprint, therefore correlation of these units to their origin in the Adriatic margin is often difficult. Marginally overprinted mineral assemblages indicate amphibolite to granulite facies metamorphic conditions. However sometimes only mineral relics, pseudomorphs and zircon crystals preserve the high-T history of the rocks. Zircons are known to be very robust to resetting under severe geological conditions and are thus used as archives.

To be able to compare and link the lower crustal fragments in the Western Alps to the Ivrea Zone, it is necessary to understand the variability of ages and textures in zircons related to metamorphic grade. Recent high precision geochronology in the Ivrea Zone (e.g., Ewing *et al.*, 2013, Peressini *et al.*, 2007) has resolved three relatively short-lived (metamorphic) events during Carboniferous/Permian time. Ewing *et al.* (2013) showed that the Ivrea Zone was affected first by a regional metamorphic event at ca. 316 Ma, a second contact metamorphic event around 276 Ma and a third event most likely related to fluid flow at ~258 Ma. Samples for the present study were collected in two valleys along two metamorphic field gradients within the Kinzigite Formation.

(1) In **Val Strona di Omegna** (N-Italy) a regional field gradient is exposed, with *P–T* conditions ranging from 650°C at 3–6 kbar to >900°C at 10–12 kbar (Ewing *et al.*, 2013; Luvizotto & Zack, 2009; Redler *et al.*, 2012). Zircon crystals in the lowest grade samples (mid amphibolite facies) show no datable overgrowth rims. Detrital cores have variable textures (igneous and metamorphic clasts), with ages clustering into three groups: the oldest one is Grenvillian (950–1000 Ma), the second and dominant group clusters around the Cadomian orogeny (530–650 Ma), and a third group preserves Variscan ages (~350 Ma). Towards higher metamorphic grade (*T*~750°C), zircon crystals are rich in inclusions (mostly sillimanite, minor feldspar and quartz) and have detrital cores; these show the same age distribution as the lowest grade samples (Grenvillian, Cadomian, Variscan). The Carboniferous/Permian metamorphic overgrowth rims show three age groups (315 Ma, 290 Ma and 270 Ma). At highest grade (≥900°C) few very small detrital cores are present. Zircons crystals in leucosomes show less complex textures, and the rim morphologies indicate growth in the presence of the anatectic melt. In melanosome domains zircon rims are more heterogeneous and have textures typical of high-grade metamorphism, such as planar growth banding, radial sector zoning and fir-tree sector zoning. Zircon ages show a similar distribution as the other samples (304 Ma, 273 Ma, 261 Ma); however, absolute ages are shifted towards younger ages.

(2) In **Val Sesia** (N-Italy) the metamorphic field gradient is dominated by contact metamorphism. The metamorphic conditions range from 680–940°C and 4–7 kbar (Redler *et al.*, 2012). Zircons show detrital cores with complex resorption and overgrowth textures. The detrital cores have Cadomian ages of ~570 Ma and Caledonian ages of ~430 Ma. Zircon mantles have ages of ca. 310 Ma, and rims ages cluster around 290–280 Ma.

Zircon ages obtained from the IIDK and Valpelline units show similar patterns in their overall Carboniferous/Permian age distribution as in the Ivrea Zone. However absolute ages for the individual slices deviate from those the Ivrea Zone; preliminary data indicate the following pattern:

Ivrea	IIDK	Valpelline
315 / 290 / 260	302 / 285 / 271	287 / 274 / 264 Ma
304 / 273 / 261		

So far it remains ambiguous whether these differences are due to partial preservation or indicate real differences in the original crustal positions within the Adriatic margin; additional work is underway.

These observations are promising as a help in correlating slices of continental crust, exposed now as tectonic blocks scattered across the Western Alps. Indeed, their approximate crustal position prior the Alpine rifting, subduction and uplift may be related to the Ivrea Zone, where continuous metamorphic field gradients are established, especially when the *P–T*-data of the Carboniferous / Permian metamorphic imprint in each tectonic fragment is also incorporated in the analysis.

## REFERENCES

- Ewing, T.A., Hermann, J. & Rubatto, D. 2013: The robustness of the Zr-in-rutile and Ti-in-zircon thermometers during high-temperature metamorphism (Ivrea-Verbano Zone, northern Italy). *CMP* 165, 757–779.
- Luvizotto, G. & Zack, T. 2009: Nb and Zr behavior in rutile during high-grade metamorphism and retrogression: An example from the Ivrea-Verbano Zone. *Chem. Geol.* 261, 303–317.
- Peressini, G., Quick, J.E., Sinigoi, S., Hofmann, A.W. & Fanning, M. 2007: Duration of a Large Mafic Intrusion and Heat Transfer in the Lower Crust: a SHRIMP U-Pb Zircon Study in the Ivrea-Verbano Zone (Western Alps, Italy). *J. Petrol.* 48, 1185–1218.
- Redler, C., Johnson, T.E., White, R.W. & Kunz, B.E. 2012: Phase equilibrium constraints on a deep crustal metamorphic field gradient: metapelitic rocks from the Ivrea Zone (NW Italy). *J. Met. Geol.* 30, 235–254.

## 5.4

## Tracing the continuous P-T path in metamorphic rocks by combining thermobarometry with a micro-mapping approach

Lanari Pierre<sup>1</sup>, Loury Chloé<sup>2</sup>, Burn Marco<sup>1</sup>, Riel Nicolas<sup>3</sup>, Rolland Yan<sup>2</sup>, Schwartz Stéphane<sup>3</sup>, Guillot Stéphane<sup>3</sup>, Vidal Olivier<sup>3</sup>, Engi Martin<sup>1</sup>

<sup>1</sup> Institute of Geological Sciences, University of Bern, Baltzerstrasse 1+3, CH-3012 Bern, Switzerland ([pierre.lanari@geo.unibe.ch](mailto:pierre.lanari@geo.unibe.ch)).

<sup>2</sup> Géoazur, UMR7329-CNRS, UNS, 250 rue Albert Einstein, Sophia Antipolis, 06560 Valbonne France.

<sup>3</sup> ISTerre, University of Grenoble 1, CNRS, 1381 rue de la Piscine, 38041 Grenoble, France.

Our understanding of geodynamic and processes in subduction zones critically relies on estimates of the pressure-temperature (P-T) conditions of crystallization of metamorphic mineral assemblages. In subduction-collision mountain belts, eclogitic rocks have witnessed burial to LT-HP conditions followed by rapid exhumation. In favorable cases a series of assemblages remains, preserved in the same sample, with metamorphic minerals that grew at different times and under a range of equilibrium conditions of P, T, pH and fO<sub>2</sub>. Such distinct assemblages provide the opportunity to calculate the preserved local equilibrium condition and to construct a detailed P-T path from a single thin section. Ideally, P-T estimates can be correlated with deformational microstructures observed at micrometer scale. The identification of relationships between microstructures, chemical variations and metamorphic conditions demands contiguous compositional data in at least two dimensions, i.e. compositional maps.

To explore links between microstructure and P-T equilibrium conditions X-ray images acquired using the electron microprobe are very useful. The X-ray data processing involves several steps such as (i) analytical standardization, (ii) classification, (iii) structural formulae and (iv) estimation of P-T conditions. These tasks are achieved using a MATLAB®-based graphical user interface program XMapTools (Lanari et al. in press, freely available at <http://www.xmaptools.com>). To estimate P-T conditions of crystallization at the micrometer scale, XMapTools include a set of ~50 empirical and semi-empirical thermobarometry functions and can easily be coupled with forward (i.e. Gibbs free energy minimization) and inverse (i.e. multi-equilibrium) modeling calculations.

In this contribution we present some select examples of application of XMapTools to rocks from NW Himalaya, from the Atbashi Range and from the Alps. In the Himalayas, an extensively retrogressed eclogite sample from the Stak massif, northern Pakistan was investigated (Lanari et al. 2013, in press). A continuous P-T path and P-T maps (Fig. 1) were calculated from the eclogite stage to amphibolite-facies retrogression. In the Atbashi Range (southern Tien-Shan, Kyrgyzstan) a large massif (10 x 100 km) of continental HP rocks was investigated to reconstruct the geodynamic evolution of the northern rim of the Tarim basin (Loury et al. 2012). In the Alps (Glacier-Rafray Klippe, Aosta valley), phengite in leucocratic dyke was analyzed to link P-T conditions to the timing of the HP metamorphism. These examples will illustrate how X-ray data can be used to decipher P-T paths. In such case, P-T estimates have been estimated using both inverse modeling multi-equilibrium and equilibrium phase diagrams computed for a specific rock composition using forward modeling software (Theriak-Domino).

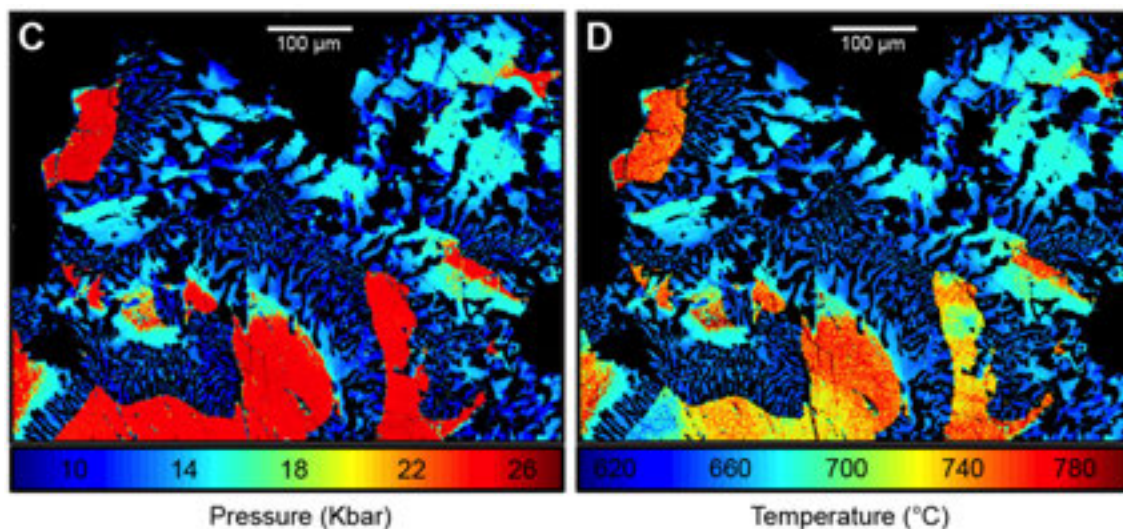


Figure 1. Pressure and Temperature maps of clinopyroxene modified from Lanari et al. (2013, in press). This eclogite sample comes from the Stak massif in Himalaya (N Pakistan). HP omphacite grains are destabilized into symplectite of clinopyroxene + amphibole + plagioclase.

#### REFERENCES

- Lanari, P., Riel, N., Guillot, S., Vidal, O., Schwartz, S., Pêcher, A., Hattori, K. (2013). Deciphering High-Pressure metamorphism in collisional context using microprobe-mapping methods : application to the Stak eclogitic massif (NW Himalaya). *Geology*, 41, 111-114.
- Lanari, P., Vidal, O., De Andrade, V., Dubacq, B., Lewin, E., Grosch, E., Schwartz, S. (in press) XMapTools: a MATLAB®-based program for electron microprobe X-ray image processing and geothermobarometry. *Computers and Geosciences*.
- Loury, C., Rolland, Y., Guillot, S., Alexeiev, D. Mikolaichuk, A. (2012) Geodynamic significance of HP metamorphism in Atbashi Range (South Tianshan, Kyrgyzstan) and inferences on crustal-scale structure of north Tarim-Tibet orogenic system, *Journal of the Nepal Geological Society*, 45, P. 29.

## 5.5

### The volcano-sedimentary evolution of a Late-Variscan intermontane basin in the Swiss Alps (Glarus Verrucano) as revealed by zircon U-Pb age dating

Dominik Letsch<sup>1</sup>, Wilfried Winkler<sup>1</sup>, Daniela Gallhofer<sup>2</sup>, Albrecht von Quadt<sup>2</sup>

<sup>1</sup>Geological Institute, ETH Zentrum, Sonneggstrasse 5, CH-8092 Zurich, Switzerland

<sup>2</sup>Institute of Geochemistry and Petrology, ETH Zentrum, Clausiusstrasse 25, CH-8092 Zurich, Switzerland

The Late Palaeozoic Glarus Verrucano basin formed in an intermontane graben in the aftermath of the Variscan orogeny. Its entirely continental fill, the Glarus Verrucano, mainly consists of immature alluvial fan and playa deposits with intercalated bimodal volcanics (basalts and rhyolites, see Figure 1). It can attain a maximum thickness of 1600 m. Despite its importance for local and regional geology, no modern sedimentologic or stratigraphic studies on the GVB exist.

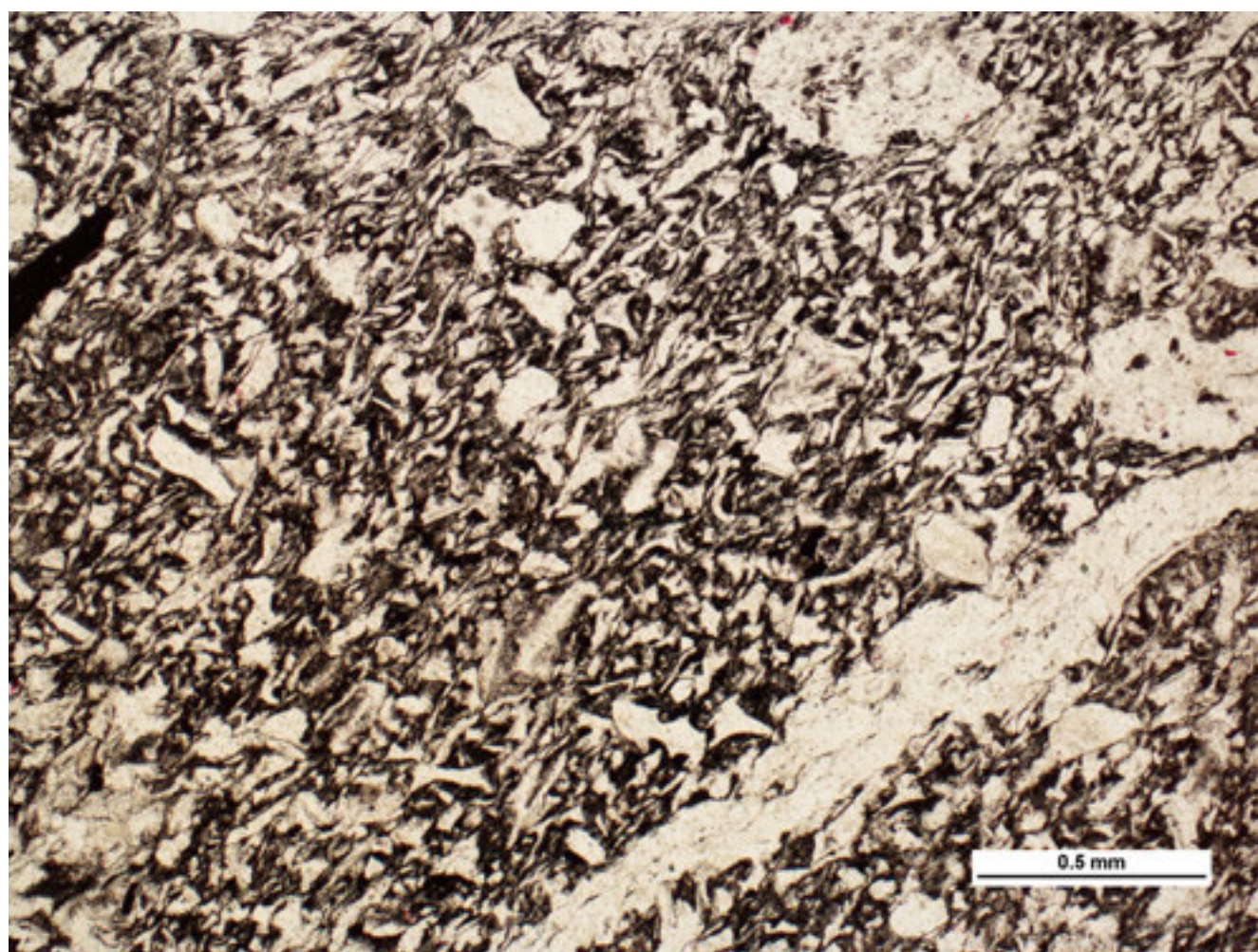


Figure 1. The youngest volcanic rocks in the Glarus Verrucano: ignimbritic rhyolites (“Schönbüel quartzites”, Upper Chrauchtal, Canton Glarus). In thin sections the characteristic recrystallized glass shards can easily be recognized. Age: 268 Ma. From Letsch et al. 2013.

For the present project we sampled volcanic rocks (rhyolitic tuffs) for high-precision zircon U-Pb dating (CA-TIMS) and clastic sediments for detrital zircon U-Pb dating (LA-ICP-MS). In the Glarus Verrucano we distinguish two volcanic episodes (Figure 2). A first phase (Mären Formation) was of bimodal character with basaltic lava flows and rhyolitic flows (mainly ignimbrites). The lowest rhyolitic tuff (Sample DL V5) yielded a zircon U-Pb age (CA-TIMS) of 285 Ma. A second phase (“Schönbüel quartzites”, Schönbüel formation, Figure 1) was exclusively of rhyolitic (ignimbritic) character. One ignimbrite layer (sample DL V7) yielded an U-Pb age (CA-TIMS) of 268 Ma. Thus, the lifespan of the Glarus Verrucano basin can be estimated as at least 17 Ma.

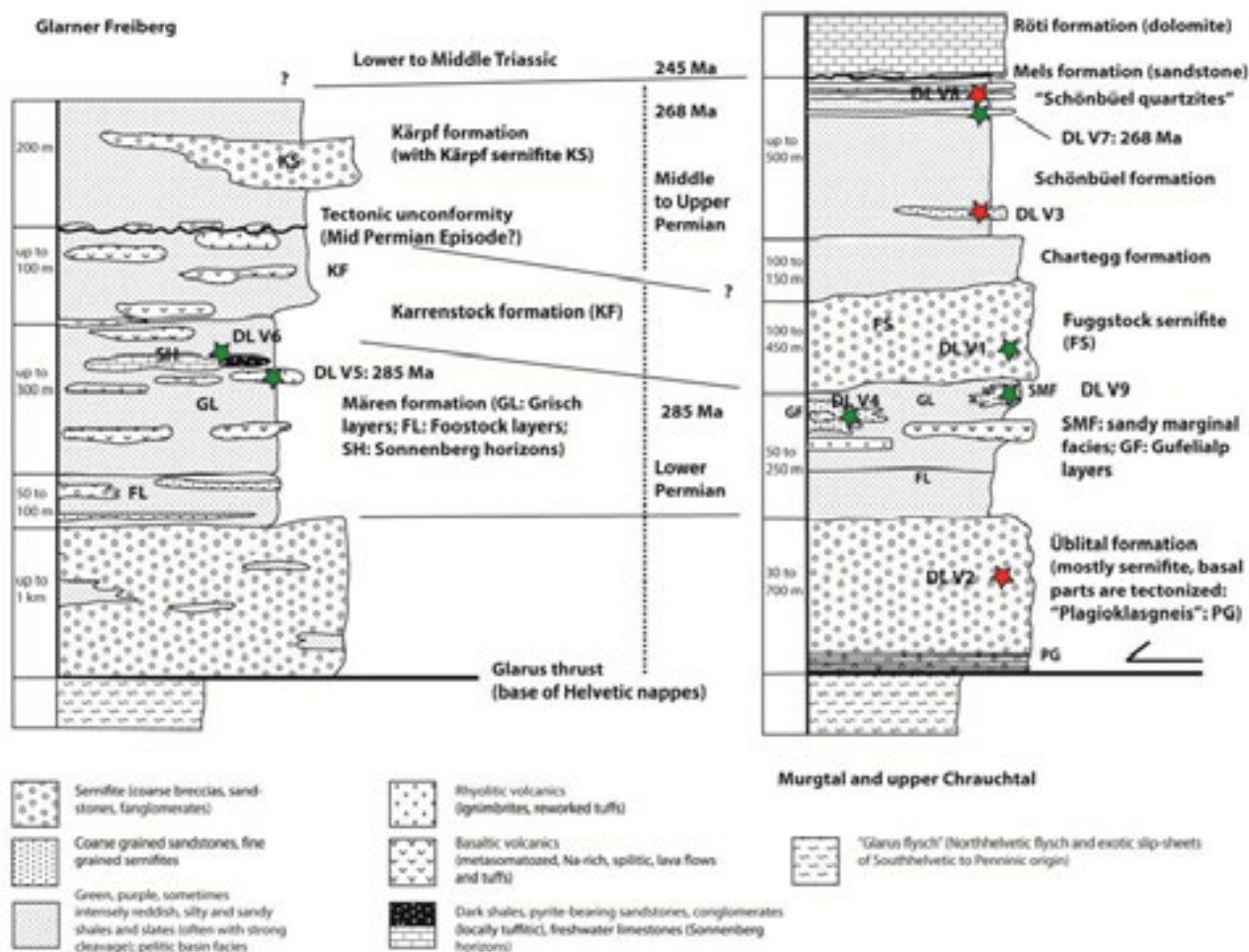


Figure 2. Schematic stratigraphic sections through the Verrucano in the Freiberg (left) and Murgtal/upper Chrauchtal area (right). Asterisks indicate sampling sites (green/red: sample yielded enough/not enough zircons for analysis). Stratigraphy mainly after unpublished PhD theses summarized by Trümpy and Dössegger (1972). From Letsch et al. 2013.

The detrital zircon ages from four samples (DL V1, V4, V6, V9) yielded mostly unimodal to slightly bimodal age distribution patterns with dominantly late Variscan ages (296 to 298 Ma) and subordinate older ages (with a maximum at 458 Ma, Ordovician). Synsedimentary zircons were present in each sample. Thus, the Glarus Verrucano records fast erosion and exhumation of the surrounding source areas, which were mainly composed of rather young intrusive rocks. Synsedimentary volcanism culminated in the Early Permian but continued into the early Late Permian.

## REFERENCES

- Letsch D., Winkler W., von Quadt A. & Gallhofer D. 2013: The volcano-sedimentary evolution of a Late-Variscan intermountain basin in the Swiss Alps (Glarus Verrucano) as revealed by zircon U-Pb age dating. Submitted to International Journal of Earth Sciences.
- Trümpy and Dössegger 1972: Permian of Switzerland. In: Falke H (ed.): Rotliegend – Essays on European Lower Permian, International Sedimentary Petrographical Series.

## 5.6

### New tectonic limits in the Central Alps : the case of the “Simano nappe”

Masson Henri<sup>1</sup>, Steck Albrecht<sup>1</sup>

<sup>1</sup>*Institut des Sciences de la Terre, Université de Lausanne, Geopolis, CH-1015 Lausanne*

The “Simano nappe” is a classical tectonic element of the Lower Penninic nappes in the Central Alps. It consists in a large, mainly gneissic body, situated geographically between the Maggia-Sambuco and the Adula nappes. Our researches reveal that it is a composite body made of at least two tectonic units of completely different origin, separated by a major Alpine thrust.

1.- The lower unit, the *Verzasca* nappe, lost most of its sedimentary cover, probably by early syn-tectonic erosion. Remnants of its Mesozoic cover are preserved as boudinaged lenses which discontinuously materialize the axial trace of a deep isoclinal recumbent syncline. Its Triassic is similar to rocks of same age in the Teggiolo zone, on the other side of the Maggia synform.

2.- The upper unit, the *Campo Tencia* nappe, has a very different constitution. The Triassic of its sedimentary cover (called the Campo Lungo zone) is similar to the Triassic of several units that belong to the middle part of the Lower Penninic nappes (e.g. Monte Leone, Adula, Valser Schuppen, etc). Recent researches provide hints that this Triassic is a reduced, littoral equivalent of the Briançonnais Triassic platform.

The differences in the petrographic composition of the gneissic basements of these two parts (orthogneisses abundant in Verzasca, scarce in Campo Tencia, etc) had been noticed long ago by previous authors who already considered the possibility of a subdivision of the “Simano nappe” into two or more “Lappen” (a distinction generally abandoned on modern tectonic maps). However our proposition is different as it is also based on significant differences of their Mesozoic cover series: these reveal different geological evolutions and different paleogeographical positions before their coupling during an early stage of Alpine tectonics. The presence in the “Simano” gneissic body of a few remnants of the Triassic cover of the Verzasca nappe confirms this interpretation. Consequently the origin of the Campo Tencia nappe is internal with respect to the Verzasca nappe.

We will discuss several consequences of these new observations.

## 5.7

# Retrograde evolution of paleo- to recent fluids and their impact on mineral precipitation in the Gotthard base tunnel between Amsteg and Sedrun, Switzerland

Mullis Josef<sup>1</sup> & Wolf Mathias<sup>1</sup>

<sup>1</sup>Mineralogisch-Petrographisches Institut, University of Basel, Bernoullistrasse 30, CH-4056 Basel (josef.mullis@unibas.ch)

The present study is focused on eight selected Alpine fissures situated in different crystalline units of the Aar massif along the Gotthard railway base tunnel. Preliminary results of the fluid evolution from paleo- to the recent fluids are presented and preliminarily interpreted.

Due to compressional tectonics, the investigated Alpine fissures opened at PT-conditions of 350 - 410 °C and 3.5 - 4 kbar (Mullis et al., 2001; Mullis, 2011). Episodic tectonic activity affected these fissure systems. According to such tectonic events, already formed fissure minerals like quartz were systematically sheared, broken and rehealed, trapping fluids during retrograde conditions.

Salinity of the trapped fluids evolved from 10 wt % in the earliest fluid inclusion population to  $\leq 2$  wt % NaCl equivalents in the latest detected fluid inclusion population. Comparing fluid compositions of paleofluids with recent fluids (Bergwässer; Bucher, 2011; Seelig & Bucher, 2010), bulk salinities decrease to values between 0.27 to 0.035 wt %.

Due to the episodic tectonic events, several paleofluid populations and at least 3 mineral assemblages formed. One mineral assemblage within the Central Aar granite (Alpine fissure 42 W) is characterized by precipitation of anhydrite, baryte and pyrite, showing  $\delta^{34}\text{S}$  of anhydrite of 25.6 ‰.

Preliminary interpretation:

1. The decrease in salinity within paleofluids during retrograde conditions along a geotraverse through the Central Alps is well known (Mullis et al., 1994). Dilution of salt-enriched metamorphic fluids is interpreted predominantly by infiltration of meteoric water due to enhanced tectonic activity.
2. Sulfur infiltration during retrograde conditions is interpreted to originate from overlying Triassic evaporites (above the crystalline rocks of the Aar massif), due to strong tectonic events.
3. The decrease in salinity from the youngest paleofluids (within fluid inclusions of fissure minerals) to recent waters (Bergwässer) of up to 100 times is controlled by meteoric waters, the neotectonic fault networks, the actual orography of the Alpine body, and in consequence, the deep lying discharge systems along the concerned valleys.

To improve the presented preliminary results, more stable isotope and ICP-MS investigations are planned.

## REFERENCES

- Bucher, K. 2011: Bergwässer. In: P. Amacher und T. Schüpbach, NEAT-Mineralien, Kristallschätze tief im Berg; 176-193. Verlag: GEO-Uri GmbH, Amsteg.
- Mullis, J. 2011: Entstehung alpiner Zerrklüfte und Kluftminerale im Gotthard-Basistunnel, Abschnitt Amsteg-Sedrun und im Zugangs- und Kabelstollen von Amsteg. In: P. Amacher und T. Schüpbach, NEAT-Mineralien, Kristallschätze tief im Berg; 194-229. Verlag: GEO-Uri GmbH, Amsteg.
- Mullis, J., Dubessy, J., Poty, B. & O'Neil, J. 1994: Fluid regimes during late stages of a continental collision: Physical, chemical, and stable isotope measurements of fluid inclusions in fissure quartz from a geotraverse through the Central Alps, Switzerland, *Geochim. Cosmochim. Acta*, 58, 2239-2267.
- Mullis, J., Overstolz, M., Wyder, R., Rahn, M., Peretti, A. & Amacher, P. 2001: Fluid inclusion investigations of fissure minerals from NEAT transects (Gotthard and Lötschberg base tunnels) through the Central Alps: Preliminary results. EUG XI, Strasbourg, April 8th - 12th, 2001, *Journal of Conference, Abstracts*, 6/1, 258.
- Seelig, U. & Bucher, K. (2010): Halogens in water from the crystalline basement of the Gotthard rail base tunnel (Central Alps). *Geochim. Cosmochim. Acta* 74, 2581-2595.

## 5.8

### Provenance analysis of the Voiron Flysch (Gurnigel nappe, Haute-Savoie, France): highlighting two major sources

Ragusa Jérémy<sup>1</sup>, Ospina-Ostios Lina Maria<sup>1</sup> and Kindler Pascal<sup>1</sup>

<sup>1</sup> University of Geneva, Section des Sciences de la Terre et de l'environnement, 1205 Genève (jeremy.ragusa@unige.ch)

Our provenance analysis has identified two major sources for the Voiron Flysch. The first one supplied most of the members of this flysch and is similar to that of the Gurnigel Flyschs. It is characterized by a high content in quartz and sedimentary clasts. The second one is specific to the Vouan Conglomerates and is localized in basement rocks. Next steps will be to provide a sedimentary model and the paleogeographic location of the Voiron Flysch basin.

In the Chablais Prealps, the Gurnigel nappe is represented by the Voiron Flysch which is exposed in the Voiron and Vouan massifs and in some minor reliefs. This flysch is subdivided into three units: (1) the Voiron Sandstones (VS) basically constituted by a thick-bedded sandstone series, punctuated with some conglomeratic layers; (2) the Vouan Conglomerates (VC) formed of m-thick beds of matrix-supported conglomerates with subordinate sandstones; and (3) the Saxel Marls (SM) represented by a series of m-thick marl layers separated by thinly bedded sandstones. Finally to the NE, the Allinges Sandstones (AS) is considered as the lateral equivalent of VC or the VS, according to previous works. This succession is interpreted as a sequence from intermediate (VS) to proximal (VC and AS) turbidites, topped by distal turbiditic/contouritic facies (SM).

Biostratigraphic investigations (Ospina-Ostios et al., 2013) have rejuvenated this flysch from the Middle Eocene to the Late Eocene - Early Oligocene, which is in discrepancy with most palaeogeographic models where the Gurnigel nappe is subducted earlier (up to the Middle Eocene) while the North Penninic flyschs go up to the Oligocene. Additionally few sedimentological studies have been made and provenance interpretation of this flysch is mainly based upon the other Gurnigel Flyschs studies.

More than 250 thin sections have been elaborated from the three members of the Voiron Flysch. Each thin section has been stained in order to differentiate alkaline feldspars, plagioclases and quartz. Counting of 300 points per section was made following the Gazzi-Dickinson method. Quartz and feldspars enclosed in lithoclasts have been counted in a dedicated class. Other constituents have also been taken into account as extra-counting.

All samples have been classified as quartzo-feldspathic sandstones with variable composition. They are depleted in lithoclasts. Most of them plot into the Continental Block field in Qm-F-Lt ternary diagrams (Dickinson and Suczek, 1979) and are organized into two clusters. The first one regroups the VS, SM and AS in the Transitional continental to Mixed area, while the second group is located in the Basement uplift field. This separation between the former group and the VC is confirmed by the relative content in lithoclasts (mainly sedimentary in the former and metamorphic to volcanic in VC). Additionally heavy-mineral analysis reveals a rich content in garnet for the VC, whereas the other members are characterized by a more important ZTR content.

Compared to the other Gurnigel Flyschs (Winkler, 1984; Winkler et al., 1985), VS, SM and AS members present similarities and seem to have same provenance than the former: Continental block to clastic wedge provenance according to Garzanti et al. (2007). However, there is some difference as, for example, the lack of tourmaline. The VC is, in contrast, not related to the Gurnigel provenance. Its source is more influenced by basement, with high content in feldspars and relative richness in metamorphic rocks. These characteristics imply an Axial Belt provenance (Garzanti et al., 2007) with some inputs from a Magmatic Arc.

#### REFERENCES

- Dickinson, W. R. & Suczek, C. A. 1979: Plate tectonics and sandstone compositions. *American Association of Petroleum Geologists Bulletin*, 63, 2164-2182.
- Garzanti, E., Doglioni, C., Vezzoli, G. & Andò, S. 2007: Orogenic belts and orogenic sediment provenance. *The Journal of Geology*, 115, 315-334.
- Winkler, W. 1984: Palaeocurrents and petrography of the Gurnigel-Schlieren flysch: A basin analysis. *Sedimentary Geology*, 40, 169-189.
- Ospina-Ostios, L.M., Ragusa, J., Wernli, R. & Kindler, P. 2013: Planktonic foraminifer biostratigraphy as a tool in constraining the timing of flysch deposition: Gurnigel flysch, Voiron massif (Haute-Savoie, France). *Sedimentology*, 60, 225-238.
- Winkler, W.; Wildi, W.; van Stuijvenberg, J. & Caron, C.: 1985. Wägital-Flysch et autres flyschs pennique en Suisse Centrale. Stratigraphie, sédimentologie et comparaisons. *Eclogae Geologicae Helveticae*, 78, 1-22.

## P 5.1

# Structure and kinematics of the northern Adula nappe (Central Alps, Switzerland) and its emplacement in the Lower Penninic nappe stack.

Cavargna-Sani<sup>1</sup>, M. & Epard, J.-L.<sup>1</sup>

<sup>1</sup> *Institut des sciences de la Terre, Université de Lausanne, Bâtiment Géopolis, CH-1015 Lausanne, mattia.cavargna-sani@unil.ch*

The Adula nappe belongs to the Lower Penninic domain of the Central Alps. It consists mostly of pre-Triassic basement rocks containing also numerous eclogites. The Adula nappe has the peculiarity to comprise several cover occurrences within the basement. The nature of the deformation experienced by the nappe reveals a complex history with several deformation phases.

The purpose of our study is a better understanding of the Alpine kinematics of the northern Adula nappe with a special focus on the early deformation phases responsible for the nappe emplacement. This study is mainly based on a detailed geologic mapping of several representative key-areas in the Northern Adula nappe. It has been also extended to a multi-scale structural analysis of the nappe at a broader scale.

We recognized that the nappe emplacement is associated with two phases of deformation. The early Ursprung ductile deformation phase is characterized by folds that are compatible with a top-to-the-south shearing. The Zapport phase, partially contemporaneous with the Ursprung phase, produces the main structural features of the nappe by ductile north directed shear and forms two generations of isoclinal nappe-scale folds. These folds are revealed by a detailed mapping in areas preserved by later deformation. The Zapport phase folds are complex synclines cored by the sedimentary cover at the front of the nappe.

In the Eastern transect of the Central Alps, the Adula nappe and the nappes derived from paleogeographic domains located south of the Adula domain (hyper-extended margin) are mostly emplaced by detachment and basal accretion in the Alpine accretionary prism. In contrast, the Adula nappe and the other nappes located northward in the paleogeography are derived from a coherent European slab and form fold-nappes. The specific paleogeographic position of the Adula domain at the leading edge of a coherent European slab explains why this unit was subducted to depth sufficient to form eclogites. This leads the Adula nappe to act as a major shear zone during the nappe emplacement.

Two later deformation phases postdate mainly the nappe emplacement. The Leis and the Carassino deformation phases are principally characterized by NW-vergent folds. These deformations affect the nappe front formed during the previous nappe emplacement phases.

## P 5.2

# Fluid-infiltration driven formation of reaction rims between carbonates and silica-rich sediments during contact metamorphism of the Buchenstein formation in the Southern Adamello contact aureole, Italy.

Katharina Marger, Thomas Mueller

*Institut für Geologie, Mineralogie und Geophysik, Ruhr-Universität Bochum, Universitätsstr. 150, D-44801 Bochum, Germany  
katharina.marger@rub.de, thomas.mueller-1@rub.de*

Contact aureoles provide a unique natural laboratory to study rates and mechanisms of mineral reactions. Metamorphic reactions in contact aureoles are often driven by fluid-infiltration leading to large element fluxes and metasomatism between adjacent lithologies with different bulk composition. Intrusion of southern Adamello batholith into mainly dolomitic and calcareous sequences of lower to middle Triassic sediments produced a variety of metamorphic reactions and metasomatic textures. In this study, we present a detailed petrographic and geochemical characterization of the evolving reaction rims in the Buchenstein formation. The latter consists of well bedded pure limestones with nodular chert layers and some volcanoclastic, shale and sandstone intercalations. We collected a total of 12 samples with different grade of metasomatic overprint. Most samples locations are on the southern slope of Monte Frerone, ~ 50 m below the peak near the contact with the intrusion. Samples with lower grade metamorphism are collected about 400 m below the peak and one almost non-metamorphic sample was collected in Valle del Gaver south of the Monte Blumone.

Four zones with different mineral assemblages can be distinguished in the investigated samples. Progressing from marl to hornfels layer the zones are as follows: (1) calcite + clinopyroxene, (2) wollastonite, (3) quartz + plagioclase + clinopyroxene, and (4) plagioclase + quartz + biotite. Layer (1) is mostly homogeneous and dominated by coarse-grained (up to 800  $\mu\text{m}$  in diameter) calcite with some fine-grained (50  $\mu\text{m}$ ) rounded clinopyroxene. Layer (2) consists almost entirely of wollastonite with a few xenomorphic clinopyroxene crystals. Here, two different textures of wollastonite can be recognized: a) grey elongate radiating aggregates and b) short prismatic grains of brightly yellow color showing lamellar twinning. The grain size of both occurrences is strongly variable ranging from 20 to 750  $\mu\text{m}$  in diameter. A continuous increase in size of the clinopyroxenes is observed in layer (3) towards the silica-rich hornfels layer. On the opposite side, i.e. at the contact to the wollastonite-rich layer, the typical grain size does not exceed 20  $\mu\text{m}$  and clinopyroxene forms small roundly grains, which overgrow plagioclase in a quartz dominated matrix. Clinopyroxene is already up to 300  $\mu\text{m}$  and forms xenomorphic poikilitic grains near the hornfels contact. In this zone, plagioclase is the dominating phase in the matrix. Plagioclase crystals are strongly xenomorphic with many inclusions of quartz. In contrast, idiomorphic twinned plagioclase (up to 200  $\mu\text{m}$ ) can be observed beneath fine-grained clinopyroxene in the zone near the contact to the wollastonite layer. A few up to one millimeter broad veins dominated by coarse-grained clinopyroxene and some plagioclase occur in layer (3). Layer (4) is a hornfels with a mostly homogeneous fine-grained plagioclase-quartz-matrix. Here, biotite occurs as small (up to 20  $\mu\text{m}$ ) flaky grains, but are also rarely found as aggregates as large as 200  $\mu\text{m}$  in diameter. A preferred orientation of biotite parallel to the overall layer structure can be observed. Some idiomorphic titanite crystals are found, mostly in contact with clinopyroxene within the transition zone between layers (3) and (4). The whole sequence described above is about 5 cm in length and repeats itself on hand specimen scale, whereas the exact width of different layers can vary between samples.

Element X-ray maps measured by electron microprobe show a general decrease of Al and Si from the hornfels towards the calcite-dominated layer. Reverse, observed Ca-concentration decreases from carbonate to the hornfels layer. Taken together, these gradients represent the major element fluxes of Ca, Al, and Si during fluid-infiltration at elevated temperatures.

## P 5.3

# Fluid investigation on prograde, T-max and retrograde inclusions in quartz from the southern part of the NEAT Gotthard base tunnel, Central Alps: preliminary results.

Proce Medea<sup>1</sup>, Mullis Josef<sup>1</sup>

<sup>1</sup>Mineralogisch-Petrographisches Institut, University of Basel, Bernoullistrasse 30, CH-4056 Basel (medea.proce@stud.unibas.ch)

The present study is focused on fluid inclusions in quartz, which are formed during increasing, maximum and decreasing temperature conditions.

The main topics to investigate are:

1. the evolution of fluid composition during prograde, T-max and retrograde conditions
2. the evolution of fluid composition and pressure at 400 °C from Biasca to the North of the Piora valley
3. the fluid evolution from the metasedimentary rocks of the Piora valley toward the crystalline units situated North and South of them
4. the difference between surface and NEAT base tunnel fluids.

Quartz samples were collected especially from Alpine fissures within the NEAT Gotthard base tunnel between the southern Gotthard massif and Biasca, situated in the Penninic Leventina nappe. In addition samples were also collected in quartz segregates (QS) and in Alpine fissures of the Piora valley.

All fluid inclusions are investigated by microthermometry. Prograde fluid inclusions are systematically found in the QS. They are stretched or decrepitated and contain the highest amount of CO<sub>2</sub>. Tessin habit quartz (THQ) that were formed close to the T-max contain CO<sub>2</sub>-enriched fluids in ± idiomorphic inclusions. Late retrograde H<sub>2</sub>O-enriched fluid inclusions are common in both, QS and THQ.

Results:

1. The evolution from prograde (in QS) over ≤ T-max (in early THQ) to younger retrograde (in THQ) fluid inclusions display a characteristic decrease in CO<sub>2</sub>-content, from ≥ 65 to ≤ 5 % CO<sub>2</sub> at pressures from ~3 to ≤ 2 kbar.
2. Prograde fluids show a decrease of CO<sub>2</sub> from the Piora valley toward the Lucomagno nappe in the South and the Gotthard massif in the North.
3. T-max fluids in the base tunnel show an increase of CO<sub>2</sub> and fluid pressure from South (Leventina nappe) to North (Piora valley).

Discussion and preliminary conclusions:

1. The source of CO<sub>2</sub> are metasedimentary rocks of the Piora valley and metasediments situated under the Leventina nappe. This is supported by fluid inclusions containing the highest CO<sub>2</sub>-content located on prograde overprinted QS. Thus CO<sub>2</sub> was predominantly produced by decarbonatisation of metasedimentary rocks (Mullis et al. 1994).
2. Decrease of CO<sub>2</sub> within the given locality is probably controlled by meteoric water contribution and carbonate precipitation during retrograde conditions, what has to be proved by stable isotope investigations.
3. Fluid migration decreases from the Piora valley toward the crystalline Gotthard massif and the Lucomagno nappe.

## REFERENCES

- Bonanomi, Y., Dietler, T. & Etter, U. 1992: Querschnitt zwischen dem südlichsten Aar-Massiv und der Lucomagno-Decke im Bereich des Gotthard-Basistunnel, *Eclogae Geologicae Helveticae* 85/1, 257-266.
- Mullis, J., Dubessy, J., Poty, B. & O'Neil, J., 1994: Fluid regimes during late stages of a continental collision: Physical, chemical, and stable isotope measurements of fluid inclusions in fissure quartz from a geotraverse through the Central Alps, Switzerland, *Geochimica et Cosmochimica Acta* 58, 2239-2267.
- Mullis, J., Overstolz, M., Wyder, R., Rahn, M., Peretti, A. & Amacher, P. 2001: Fluid inclusion investigations of fissure minerals from NEAT transects (Gotthard and Lötschberg base tunnels) through the Central Alps: Preliminary results. EUG XI, Strasbourg, April 8th - 12th, 2001, *Journal of Conference, Abstracts* 6/1, 258.

## P 5.4

### Lu-Hf ages form the Zermatt-Saas Fee ophiolite

Susanne Skora<sup>1,2</sup>, Lukas Baumgartner<sup>1</sup>, Clark Johnson<sup>3</sup>

<sup>1</sup> Institute of Mineralogy and Geochemistry, University of Lausanne, Geopolis, CH-1015 Lausanne (Susanne.Skora@erdw.ethz.ch)

<sup>2</sup> Institute of Geochemistry and Petrology, ETHZ, Clausiusstr. 25NW, CH-8092 Zürich

<sup>3</sup> Department of Geosciences, University of Wisconsin-Madison, 1215 W Dayton Street, Madison, WI-53706, USA

The Alpine chain is a classic continent-continent collisional orogen that formed by the collision of Apulia/Africa with the Europe, after the closure of the Liguro-Piemont oceanic trough. Today, the remnants are exposed in the Western Alps as eclogite facies rocks of the Zermatt-Saas Fee (ZSF) unit. The eclogites have been the focus of many geochronological studies aiming at constraining the Alpine high-pressure event. Garnets are particularly useful, because they clearly belong to the HP paragenesis. There is a large spread in garnet-isochron ages throughout the ZSF unit, depending on the location and/or decay system. This spread can either have a petrologic and/or a geologic origin. For example, it was shown that due to differences in prograde Lu (enriched in early grown garnet cores) and Sm (enriched in late-grown garnet rims) zoning, Lu-Hf ages can be skewed towards the onset of garnet growth, whereas Sm-Nd most closely dates peak metamorphism (Skora et al. 2009). Conversely, it is well possibly that the ZSF unit was subducted diachronously. This study aims to shed light on garnet age differences found in the ZSF unit.

We have combined trace-element zoning in garnets with new Lu-Hf garnet geochron ages in order to extract information on its prograde growth. In total, 4 new Lu-Hf ages from Pfulwe ( $49.9 \pm 3.3$ ;  $51.9 \pm 2.7$ ;  $46.9 \pm 3.6$ ; and  $47.0 \pm 2.3$  Ma) and one from Chamois, Valtournenche ( $52.7 \pm 2.7$ ) are very similar to the Lu-Hf age from Lago di Cignana, Valtournenche ( $48.8 \pm 2.1$ , Lapen et al. 2003). The similarity of Lu-Hf ages and Lu zoning suggest that all these localities have shared a similar prograde tectonic history. In fact, we have suggested that the Lago di Cignana garnets have grown over 20 m.y., peaking at around 40 Ma (Skora et al. 2009). Two Saas-Fee and one Val d'AYas samples, however, produced much younger Lu-Hf ages ( $40.7 \pm 2.3$ ;  $38.1 \pm 4.5$ ; and  $39.2 \pm 2.2$ , respectively), which are close to exhumation ages of the Zermatt-Saas Fee zone. Neither differences in whole rock geochemistry, nor differences in rare earth element zoning can be held responsible for this discrepancy. This suggests a much later prograde history for these samples, and growth times that were much shorter (<10 m.y.) when compared to the other locations.

Combined, the new Lu-Hf ages suggest that the ZSF was subducted diachronously. Areas that have oldest Lu/Hf ages (~50 Ma) are structurally located highest in the obducted ZSFO. Their inferred prograde garnet growth interval results in initial subduction ages which are close to what is permitted by other geological constraints. We conclude, that these areas must have originated at the southernmost realm of the Liguro-Piemont ocean, being subducted first. On the other hand, samples dated from the Saas Fee area yield young Lu/Hf ages (~40 Ma age). Here the eclogite are structurally just above the Monte Rosa unit (Briançonnais/Europe), at the structural base of the ZSF. Hence their paleoposition was likely the northernmost realm of the Liguro-Piemont ocean, subducting last. We interpret the first group to have had significantly longer prograde garnet growth times compared to the second group, which is well reconciled with the fact that, initially, the ZSFO was subducted oblique, turning into a near-perpendicular subduction zone towards the end.

#### REFERENCES

- Skora, S., Lapen, T.J., Baumgartner, L.P., Johnson, C.M., Hellebrand, E. & Mahlen, N.J. (2009) The duration of prograde garnet crystallization in the UHP eclogites at Lago di Cignana, Italy. *Earth and Planetary Sciences Letters*, 287, 402-411.
- Lapen, T.J., Johnson, C.M., Baumgartner, L.P., Mahlen, N.J., Beard, B.L. & Amato, J.M. (2003) Burial rates during prograde metamorphism of an ultra-high-pressure terrane: an example from Lago di Cignana, western Alps, Italy. *Earth and Planetary Sciences Letters*, 215, 57-72.

## P 5.5

# Drowning history of Jurassic carbonate platform, Northern Atlasic fringe (NE ALGERIAN)

El Hadj Youcef Brahim<sup>1</sup> & Mohamed Chadi<sup>2</sup>

<sup>1</sup> University of Batna (wahidyb@yahoo.fr), BP 25, Merouana-Batna, zip:05013

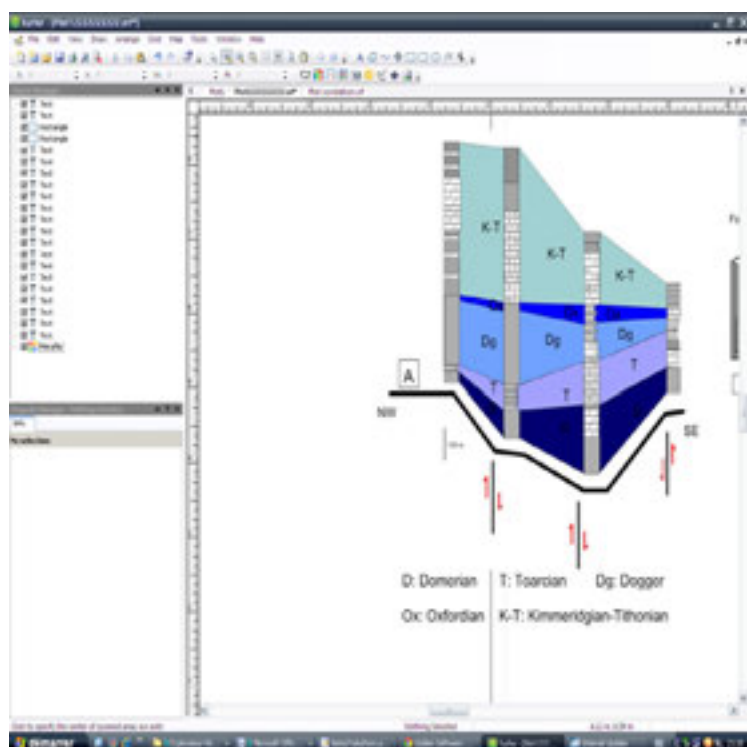
<sup>2</sup> Normal superior school, zouaghi faculty, Constantine zip:25000

This study focuses on an area located at the convergence of the allochthonous and the Atlasic forelands of the Northern Algerian Alpine Belt. The objective of this work is to reconstruct the drowning history of the Jurassic carbonate platform, and discuss its relationship with the geodynamic evolution of the Southern Tethysian margin.

The identification and interpretation of drowning events in the platforms can help significantly to the reconstruction of the depositional, tectonics and eustatic history of these platforms.

The drowning of carbonate platforms was the subject of several stratigraphic and sedimentological researches in different places on the planet, at different periods of Phanerozoic times (Read, 1980, 1982, 1985, Kendall & Schlager, 1981, Schlager, 1981, 1989, Santantonio 1993).

The stratigraphic interpretation and correlation of the study area Jurassic series from a few cross-sections, have allowed the highlighting of the platform physiography during this geological period and individualizing three stratigraphic units. The synthesis of bio-sedimentological data reveals diversified facies, involving various deposits environments ranging from supratidal to deep pelagic paleoenvironments. These facies have evolved within subsiding carbonate ramp. Thereof has experienced drowning (Toarcian) and filling (Tithonian, Berriasian) phases, in relation with the eustatic sea level changes at the global scale and regional tectonics.



D : Domesian T : Toarcian Dg : Dogger Ox : Oxfordian K-T : Kimmeridgian-Tithonian

Figure 1. Correlation of the Jurassic series

## REFERENCES

- Kendall, C. G. ST. G., & Schlager, W. 1981: Carbonates and relative changes in sea level. *Marine Geology* 44, 181–212.
- Read, J. F. 1985: Carbonate platform facies models. *American Association of Petroleum Geologists, Bulletin*, 69, 1–21.
- Santantonio, M. 1993: Facies associations and evolution of pelagic carbonate platform / basin systems: examples from the Italian Jurassic. *Sedimentology*, 40, 155–181.
- Schlager, W. 1981: The paradox of drowned reefs and carbonate platforms. *Geological Society of America, Bulletin*, 92, 197–211.
- Schlager, W. 1989: Drowning unconformities on carbonate platforms. In *Controls on carbonate platform and basin development* (eds Crevello, P. D. et al.), Society of Economic Paleontologists and Mineralogists, Special Publication, 44, 15–25.

## P 5.6

# Diffusion-controlled garnet growth in silicious marbles of the Adamello contact aureole, N-Italy

Elena Fiebich<sup>1</sup>, Thomas Müller<sup>1</sup>, C. Tom Foster, Jr.<sup>2</sup>

<sup>1</sup> Institut für Geologie, Mineralogie und Geophysik, Ruhr-Universität Bochum, Universitätsstraße 150, D-44801 Bochum (elena.fiebich@rub.de)

<sup>2</sup> Department of Geoscience, University of Iowa, 121 Trowbridge Hall, IA 52245 USA, Iowa

Metamorphic textures and spatial variations of chemical and isotopic composition are direct records of the temporal evolution, i.e. mineral reactions and mass transport of elements/isotopes in a rock and its mineral phases. More specifically, metamorphic mineral growth can be described by a combination of interface controlled and diffusion controlled processes. In this study, we present petrological and geochemical data combined with textural modeling to constrain the conditions and the reaction mechanism during contact metamorphic garnet growth in the southern Adamello Massif, Italy.

A petrological study was conducted on a contact metamorphic siliceous carbonates from the Adamello Massif, Italy. The sample contains garnet porphyroblasts ( $\text{Grs}_{87}\text{And}_7\text{Alm}_3\text{Pyr}_1\text{CaTi}_2$ ), sitting in a fine-grained matrix of calcite+diopside+wollastonite+anorthite. The porphyroblasts are idiomorphic and poikiloblastic, ranging between 0.3-1 cm in diameter with small inclusions being uniquely diopside. In the hand specimen garnets are surrounded by concentric coronas of about 0.6-1.2 cm, indicating a diffusion-limited reaction mechanism to be responsible for the garnet formation.

In course of this study samples have been characterized regarding their mineralogical composition and textures using polarization microscopy, EMPA and cathodoluminescence microscopy. Additionally, the stable isotopic composition of carbon and oxygen of matrix calcite has been determined.

X-ray maps of garnets show distinct growth zoning, with Al decreasing from core to rim and Fe showing the inverse zoning pattern, whereas the distribution of Ca is homogenous. Stable isotopic compositions of carbonates from halos and matrix do not show any significant variation. However, measured values are in perfect agreement with previous results indicating the infiltration and equilibration of the carbonates with a light magmatic fluid phase. (Gerdes, et. al. 1999, Mueller, et. al. 2009).

Pseudosections have been calculated using the software package PerpleX (Connolly, 2005) based on the bulk rock composition of collected samples to constrain the garnet forming reaction history. Results indicate that garnet was produced by the breakdown of wollastonite, calcite and anorthite at water-rich conditions ( $X_{\text{CO}_2} = 0.3$ ) and temperatures around 630°C. Limited transport of reacting species led to a depletion of wollastonite and anorthite surrounding the garnet porphyroblasts, representing the concentric halos seen in the hand specimen. The spatial relation of garnet and halo radius indicate a transport limited reaction mechanism.

The observed textures can successfully be reproduced using the SEG program (Foster, 1993), which has also been applied to decipher the relative phenomenological diffusion coefficients of Mg, Al, Ca and Si. Assuming no chemical potential gradient for Ca and a pore fluid being undersaturated in  $\text{CO}_2$  (which can be justified by fluid infiltration during contact metamorphism), the wollastonite free zone is about the same size as the anorthite halo. Textures corresponding to the sample can be reproduced, assuming the wollastonite concentration being higher than the anorthite concentration and the transport of Al being about two orders of magnitude faster compared to Si. However, the modeled halo sizes strongly depend on the modal abundances and thus inverted concentrations for wollastonite and anorthite in the starting rock would result in inverted halo distributions.

## REFERENCES

- Connolly, J.A.D., 2005, Computation of phase equilibria by linear programming: A tool for geodynamic modeling and its application to subduction zone decarbonation. *EPSL*, 236 : p. 524-541.
- Foster, C.T., 1993, SEG93: A program to model metamorphic textures: *Geological Society of America Abstracts with Programs*, v. 25, no. 6, p. A264.
- Gerdes, M., Baumgartner, L.P. and Valley, J.W., 1999: Stable isotopic evidence for limited fluid flow through dolomitic marble in the Adamello contact aureole, Cima Uzza, Italy. *Journal of Petrology*, v. 40, no. 6, p. 853-872.
- Müller, T., Baumgartner, L.P., Foster, C.T. and Bowman, J.R. 2009: Crystal size distribution of periclase in contact metamorphic dolomite marbles from the southern Adamello massif, Italy. *Journal of Petrology*, v. 50, no. 3, p. 451-465.



## 6. Stratigraphy in Switzerland - new data and developments

Alain Morard, Reto Burkhalter, Oliver Kempf & Ursula Menkveld-Gfeller

*Comité Suisse de Stratigraphie – Schweizerisches Komitee für Stratigraphie (SCNAT)*

### TALKS:

- 6.1 Deplazes G., Bläsi H., Jordan P., Meier B., Traber D., Schnellmann M.: Tracing the extent and formation of the Oxfordian limestone-marl successions of the Effingen Member
- 6.2 Hostettler B.: Die Rolle der Biostratigraphie für die Korrelation lithostratigraphischer Einheiten
- 6.3 Jordan P.: Neugliederung der Trias in der Nordschweiz – ein Arbeitsbericht
- 6.4 Morard A.: Stratigraphic scaling and correlations - mind the gaps!
- 6.5 Reisdorf A., Hostettler B., Waltschew A., Jaeggi D., Menkveld-Gfeller U.: Chrono- and Biostratigraphy of the Opalinus Clay of the Mont Terri Rock Laboratory, Canton Jura, Switzerland

### POSTERS:

- P 6.1 Dall'Agnolo S., Plancherel R.: Lithostratigraphy in the Prealps: proposed units in the area of Château-d'Oex
- P 6.2 Kempf O., Dall'Agnolo S., Funk H.-P.: New lithostratigraphic formations of the middle penninic Klippen nappe (late Triassic – early Jurassic)
- P 6.3 Rebetez D., Ramseyer K.: The Middle Triassic (Anisian) marine transgression in central Switzerland, comparisons with the Jura Mountain and the Brescian Prealps

## 6.1

# Tracing the extent and formation of the Oxfordian limestone-marl successions of the Effingen Member

Deplazes Gaudenz<sup>1</sup>, Bläsi Hansruedi<sup>2</sup>, Jordan Peter<sup>3</sup>, Meier Beat<sup>4</sup>, Traber Daniel<sup>1</sup> & Schnellmann Michael<sup>1</sup>

<sup>1</sup>Nagra, Hardstrasse 73, CH-5430 Wettingen (gaudenz.deplazes@nagra.ch)

<sup>2</sup>Institute of Geological Sciences, University of Bern, Baltzerstrasse 1 + 3, CH-3012 Bern

<sup>3</sup>Böhringer AG, Mühlegasse 10, CH-4104 Oberwil

<sup>4</sup>Proseis AG, Schaffhauserstrasse 418, CH-8050 Zürich

The Effingen Member consists of an up to 240 m thick intercalation of limestones and marls in northeastern Switzerland. Individual limestone beds are mostly bundled in 3 - 12 m thick successions which are surrounded by calcareous marl successions. The sediments were deposited in an epicontinental sea during the lower to middle Oxfordian (Late Jurassic) in about 2 Myr with a depositional centre between Brugg and Olten ("Argovian" realm, Wetzel et al. 2003). Towards the west the epicontinental basin was limited by a carbonate reef and platform ("Celtic" realm), which prograded to the southeast during the Oxfordian. Previous studies have focused mostly on the correlation of basinal and shallow marine sediments or individual limestone-marl successions using outcrops.

In this study, facies, extent and stratigraphic correlation of the limestone and calcareous marl successions within the Effingen Member are studied using morphological mapping, geophysical borehole analysis, macro- and microfacies analysis and seismic facies analysis. Whereas it is postulated that the most characteristic of the limestone successions, referred to as Gerstenhübel Beds, can be followed on a large scale (Gygi & Persoz 1986), the extent of the other successions was not known so far. Our study shows that the limestone successions can form morphological elements in the field that can be followed over up to 500 m based on high resolution LiDAR mapping. Clay mineral content records derived from geophysical logging represent a powerful tool to correlate boreholes on a previously unprecedented resolution. Based on this analysis certain limestone successions especially in the upper Effingen Member can be followed over at least 20 km, which is consistent with seismic facies analysis. The Gerstenhübel Beds can also be followed over several kilometers but towards the west they seem to thin and change their characteristics. Limestone successions consist mostly of micrite which is presumably transported from the northwestern platform or from local shallow marine swells in the east. A detailed analysis of the clay mineral content suggests a diachronous transition of the top of the Effingen Member to the overlying more calcareous sediments from the central Argovian basin both towards east and west. It is postulated that the intercalation of limestone and calcareous marl successions was forced by climate cycles in combination with sea level changes in a differentially subsiding basin.

## REFERENCES

- Gygi, R.A. & Persoz, F. 1986: Mineralostratigraphy, litho- and biostratigraphy combined in correlation of the Oxfordian (Late Jurassic) formations of the Swiss Jura range. *Eclogae Geol. Helv.* 79/2, 385-454.
- Wetzel, A., Allenbach, R. & Allia, V. 2003: Reactivated basement structures affecting the sedimentary facies in a tectonically "quiescent" epicontinental basin: an example from NW Switzerland. *Sedimentary Geology* 157/1, 153-172.

## 6.2

# Die Rolle der Biostratigraphie für die Korrelation lithostratigraphischer Einheiten

Hostettler Bernhard

*Naturhistorisches Museum der Burgergemeinde Bern, Bernastrasse 15, 3005 Bern und Institut für Geologie, Universität Bern, Baltzerstrasse 1+3, 3012 Bern. bern61@bluewin.ch*

Die Definition lithostratigraphischer sedimentärer Gesteinskörper basiert auf rein lithologischen Kriterien wie Fazies, Ablagerungsraum, Sedimentstrukturen, Partikel, Porosität, Farbe, u.s.w., wobei Unter- und Obergrenze generell nicht isochron sein müssen.

Wird aber die räumliche Entwicklung eines solchen Sedimentkörpers in der Zeit betrachtet, ist es am einfachsten die Biostratigraphie zu verwenden. Neben der zeitlichen Abgrenzung des Gesteinskörpers können so gleichzeitig auch Schichtlücken und deren Dauer ermittelt werden.

Zur biostratigraphischen Datierung können unterschiedlichste Organismengruppen herangezogen werden. Für die Jura-Zeit erreicht man mittels Ammoniten die beste zeitliche Auflösung. Die zeitliche Auflösung ist aber abhängig vom Ablagerungsraum und von der Sedimentationsgeschwindigkeit.

Wie Figur 1 zeigt, ist die biostratigraphische Auflösung in der koenigi-Zone relativ schlecht: Dies kann damit erklärt werden, dass während dieser Periode die Karbonatplattform vorrückt und der Lebensraum deshalb immer seichter wird. Solche Bedingungen sind für Ammoniten ungünstig. Gleichzeitig wird hier im Callovien die grösste Sedimentmenge abgelagert.

Die beste zeitliche Auflösung weist das Renggeri-Member auf: Hier beträgt die Meerestiefe deutlich mehr als 50 Meter, was zu diversen Ammonitenfaunen führt. Eine gleichzeitig hohe Sedimentationsrate erlaubt eine gute Abgrenzung der sich in der Zeit folgenden Ammonitenpopulationen.



## 6.3

# Neugliederung der Trias in der Nordschweiz – ein Arbeitsbericht

Peter Jordan<sup>1</sup>

<sup>1</sup> Geologisch-Paläontologisches Institut, Universität Basel, Bernoullistrasse 32, CH-4056 Basel  
(peter.jordan@unibas.ch; peter.jordan@boe-ag.ch) /  
Arbeitsgruppe „Jura-Ost“ des Schweizerischen Komitees für Stratigraphie SKS

Die Arbeitsgruppe „Jura Ost“ des Schweizerischen Komitees für Stratigraphie SKS (Burkhalter & Heckendorn 2009) hat im Herbst 2012 vorgeschlagen, die Trias des Ostjura aufgrund von Literaturdaten entsprechend den Vorgaben von Remane et al. (2005) neu zu gliedern (Jordan 2012). Der Vorschlag wurde vom Komitee wohlwollend aufgenommen und wird von der Schweizerischen Landesgeologie im Rahmen von Harmos unterstützt.

Im Vordergrund stehen dabei die Ansprache in Gelände und Bohrungen sowie die Kartierbarkeit. Entsprechend ergeben sich insgesamt sechs Formationen. Um die Korrelation mit den bis anhin verwendeten stratigraphischen Einheiten zu erleichtern, werden 18 Member bezeichnet.

Für verschiedene Formationen finden sich auf Schweizer Boden keine Typusprofile, die den Anforderungen von Remane et al. (2005) entsprechen. So wird hier jeweils eine Kombination von Typlokalität (namengebende Örtlichkeit mit rudimentären Aufschlüssen) und Paratypusprofil (vollständiges Referenzprofil in Bohrung) vorgeschlagen.

Eine Übernahme der in Deutschland verwendeten Formationen mitsamt ihrer Typusprofile wurde geprüft und verworfen. Die im Zentrum des Germanischen Beckens oft mehrere Dutzend Meter mächtige Formationen keilen in der hier betrachteten Randzone so stark aus, dass sie, um der Anforderung der Kartierbarkeit zu genügen, zusammengefasst werden müssen. Ferner entspricht die randliche Ausprägung in einigen Fällen kaum mehr der im Beckeninnern vorherrschenden Fazies.

Die vorgeschlagene Gliederung ist rein lithofaziell. Jüngere Untersuchungen im Germanischen Becken haben gezeigt, dass die Formationsgrenzen oft diachron sind (z.B. Franz et al. 2013). Wie weit dies auch in der Nordschweiz nachweisbar ist, bleibt abzuklären. Die vorgeschlagene Gliederung ist so ausgelegt, dass sie durch zukünftige Erkenntnisse zwar verfeinert und präzisiert aber wohl kaum in Frage gestellt werden kann.

### REFERENZEN

- Burkhalter, R. & Heckendorn, W. 2009: Das Stratigraphische Komitee der Schweiz (SKS). *Swiss Bull. angew. Geol.* Vol. 14/1+2, p. 159-162
- Franz, M., Henniger, M., Barnasch, J. 2013: The strong diachronous Muschelkalk/Keuper facies shift in the Central European Basin from the type-section of the Erfurt Formation (Lower Keuper, Triassic) and basin-wide correlations. *Int J Earth Sci*, 102: 761 - 780.
- Jordan, P., AG Jura-OST SKS 2012: Neugliederung der Trias in der Nordschweiz – ein Diskussionsvorschlag. Abstract, SGM 2012.
- Remane, J., Adatte, T., Berger, J.-P., Burkhalter, R., Dall'Agnolo, S., Decrouez, D., Fischer, H., Funk, H., Furrer, H., Graf, H.-R., Gouffon, Y., Heckendorn, W., & Winkler, W. 2005: Richtlinien zur stratigraphischen Nomenklatur. *Eclogae Geol. Helv.*, 98(3)

## 6.4

### Stratigraphic scaling and correlations – mind the gaps !

Morard Alain<sup>1</sup>

<sup>1</sup> Swiss Geological Survey (SGS), Federal Office of Topography swisstopo, Seftigenstrasse 264, CH-3084 Wabern

For the harmonisation of the legend of the Geological Atlas of Switzerland 1:25'000, a revised lithostratigraphic scheme is under development [Morard et al. 2012]. The present contribution is a first personal reflection about some fundamental options for the graphical presentation of the results of this project, to be further discussed by the stratigraphic community.

From field logging to basin analysis and further correlations, different kinds of stratigraphic representations are used. These mainly differ in the choice of the parameter used as vertical scale, whereas the horizontal axis usually represents lateral variation:

(a) In a first step, individual profiles are measured and drawn proportionally to their original thickness. The identification of marker beds is the most basic (though not always straightforward and univocal) method to correlate one profile to the next.

(b) In order to consistently “map” the stratigraphic succession in a given region, a first lithostratigraphic synthesis is established as a working legend. Observed discontinuities at formation boundaries can be integrated at this point.

(c) With some chance, a relative age can already be assessed in the field, e.g. based on fossil finds. Careful analysis may later provide a more detailed relative datation (stage, biozone, isotopic event, ...). This step is nowadays often simultaneous to – if not preceded by – the next one.

(d) Ultimately an interpretation in terms of absolute ages and durations can be tentatively proposed. This involves critical assumptions concerning both the specific case under study and the reference chart used.

As can readily be seen from the virtual example illustrated in Fig. 1a–d, each scaling technique has its own strengths and limitations. The most problematical pitfalls concern the (non-)representation of hiatuses and diachronism, as well as the pervasive distortion of either spatial proportions or time (or both). All these shortcomings ultimately result from the non-linear and fragmentary nature of the stratigraphic record.

For our harmonisation project, a compromise has to be found between scientific correctness (spatial pattern and temporal succession), ease of reading (deliberate symbolism vs. pseudo-realism), but also stability relative to future age revisions. In this respect, and keeping in mind that the project is aimed at the elaboration of a legend for field geological mapping, the representation scheme should primarily highlight the geometrical relationships of the elemental lithostratigraphic units – i.e. formations, including the nature of their contacts. Our challenge is thus to try and develop a “scaling method” somewhat intermediate between Fig. 1b and 1c.

#### REFERENCES

Morard, A., Burkhalter, R., Möri, A. & Strasky, S. 2012: Lithostratigraphy of Switzerland: options and challenges for a harmonisation, Abstract Volume 10th Swiss Geosciences Meeting, p.173.

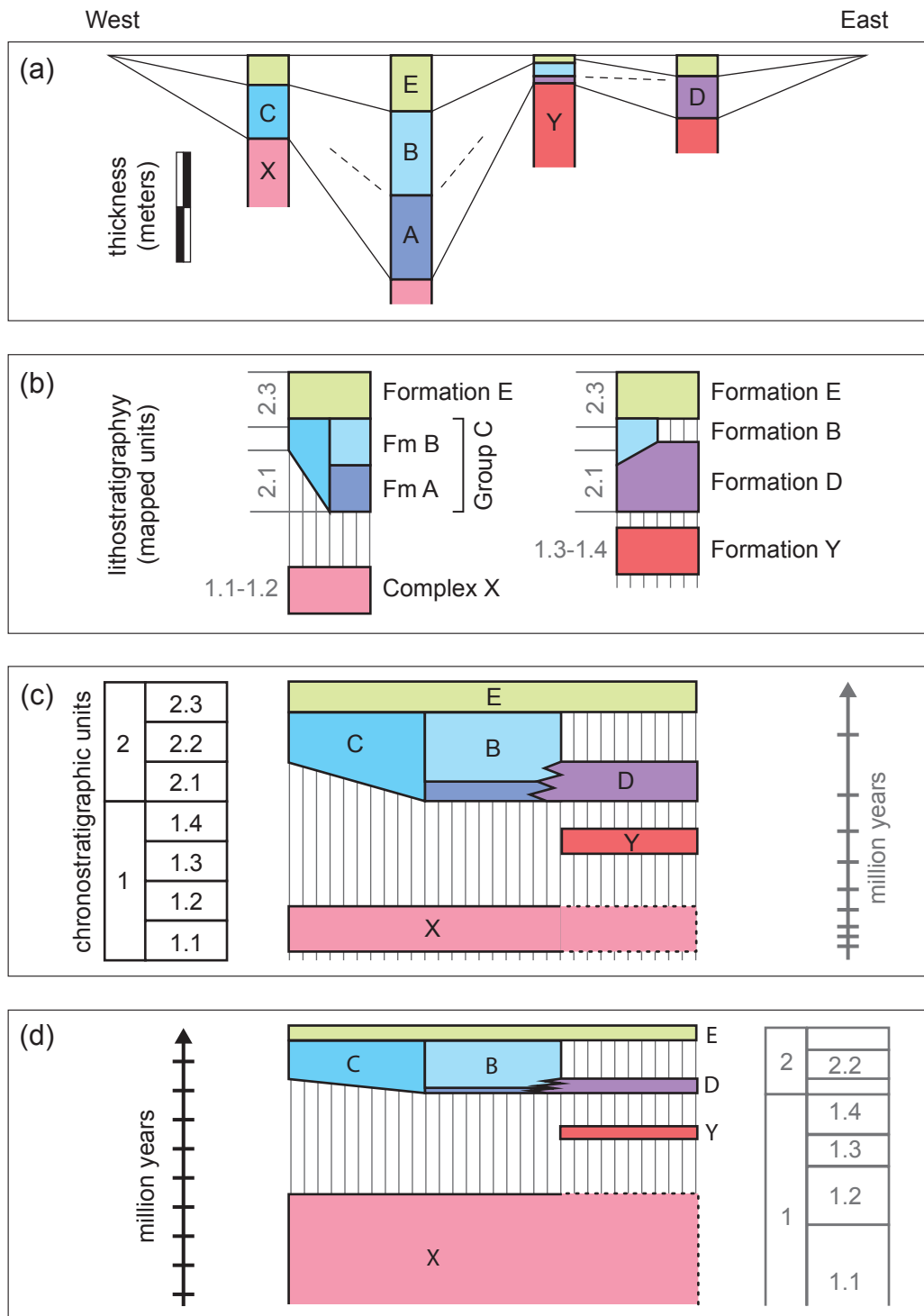


Figure 1. Alternative representation schemes with differing vertical stratigraphic scaling for a simple virtual geological situation (discussion in the text).

## 6.5

### Chrono- and Biostratigraphy of the Opalinus Clay of the Mont Terri Rock Laboratory, Canton Jura, Switzerland

Reisdorf Achim<sup>1,2</sup>, Hostettler Bernhard<sup>2</sup>, Waltschew Anton<sup>3</sup>, Jaeggi David<sup>4</sup> & Menkveld-Gfeller Ursula<sup>2</sup>

<sup>1</sup> Geologisch-Paläontologisches Institut, University of Basel, Bernoullistrasse 32, CH-4056 Basel (achim.reisdorf@unibas.ch)

<sup>2</sup> Naturhistorisches Museum der Burgergemeinde, Bernastrasse 15, CH-3005 Bern

<sup>3</sup> Nürnberg, Germany

<sup>4</sup> Mont Terri Consortium, Swisstopo, Fabrique de Chaux, Rue de la gare 63, CH-2882 St-Ursanne

Since the existence of the Mont Terri Project, for the first time, the Opalinus Clay has been subjected to a macropaleontological study. Ammonites were extracted from bedrock from a number of small exposures and a drill core at the Mont Terri Rock Laboratory. In addition, ammonites were obtained from excavated material of a particular stretch of drifting.

From the faunal spectrum, it was possible to make a biostratigraphical subdivision of the basal strata of the Opalinus Clay. *Pleydellia aalensis* s.l., *P. fluitans*, *P. subcompta*?, *P. leura* and *P. costula* were found in the >10-meter-thick basal strata of the Opalinus Clay. The stratigraphical occurrence of these ammonites is evidence that a significant part of the Opalinus Clay of the Mont Terri Rock Laboratory belongs most certainly to the latest Toarcian (aalensis Subzone, Aalensis Zone). Furthermore, there is evidence in the exposed section that the Late Toarcian ammonite fauna was succeeded without significant facies change by an Early Aalenian faunal assemblage that included *Leioceras opalinum*. These macropaleontological and lithological facts corroborate our micropaleontological data set.

The basal strata of the Opalinus Clay of the Mont Terri Rock Laboratory are lithofacially significantly different from the deposits of the same age of the Tabular Jura and the eastern Folded Jura, which appear in a mostly phosphoritic marly facies (= Gross Wolf Member after Reisdorf et al. 2011, "Jurensis-Schichten" *sensu* Jordan 1983, "Jurensismergel" *sensu* Müller 1984). When considering the facies and the thickness relationships of the latest Toarcian in the Mont Terri area, however, there exists a strong affinity with the strata south of Freiburg i.Br., Germany (cf. for example Etter 1990; Geologisches Landesamt Baden-Württemberg 1996; Wetzel & Allia 2003).

#### REFERENCES

- Etter, W. 1990: Paläontologische Untersuchungen im Unteren Opalinuston der Nordschweiz. Inaugural-Dissertation Universität Zürich, 151 pp., Zürich.
- Geologisches Landesamt Baden-Württemberg 1996, ed.: Die Grenzziehung Unter-/Mitteljura (Toarcium/Aalenium) bei Wittnau und Fuentelsaz. – Beispiele interdisziplinärer geowissenschaftlicher Zusammenarbeit. Informationen Geologisches Landesamt Baden-Württemberg, 8: 52 pp., Freiburg i. Br.
- Jordan, P. 1983: Zur Stratigraphie des Lias zwischen Unterem Hauenstein und Schinznach (Solothurner und Aargauer Faltenjura). *Eclogae geologicae Helveticae*, 76, 355-379.
- Müller, W.H., Huber, M., Isler, A. & Kleboth, P. 1984: Erläuterungen zur Geologischen Spezialkarte Nr. 121 der zentralen Nordschweiz 1: 100 000 mit angrenzenden Gebieten von Baden-Württemberg. Nationale Genossenschaft für die Lagerung radioaktiver Abfälle (NAGRA) und Schweizerische Geologische Kommission, 234 pp., Baden.
- Reisdorf, A.G., Wetzel, A., Schlatter, R. & Jordan, P. 2011: The Stafflegg Formation: a new stratigraphic scheme for the Early Jurassic of northern Switzerland. *Swiss Journal of Geosciences*, 104, 97-146.
- Wetzel, A. & Allia, V. 2003: Der Opalinuston in der Nordschweiz: Lithologie und Ablagerungsgeschichte. *Eclogae geologicae Helveticae*, 96(3), 451-469.

## P 6.1

# Lithostratigraphy in the Prealps: proposed units in the area of Château-d'Oex

Dall'Agnolo Stephan<sup>1</sup>, Plancherel Raymond<sup>2</sup>

<sup>1</sup> swisstopo, Swiss Geological Survey, Seftigenstrasse 264, CH-3084 Wabern (stephan.dallagnolo@swisstopo.ch)

<sup>2</sup> CH-1822 Chernex

The edition of map sheet 144 Châteaux-d'Oex (Plancherel & Dall'Agnolo in prep.) of the Geological Atlas of Switzerland 1:25000 showed the necessity of proposing several lithostratigraphic units for formal definition. Many of them are derived from established names and are officialised by using the term of «Formation» or «Member» instead of «Couches» and will not be discussed here. Other units are new or replace informal names. A novelty is that melanges are treated and described like formations (or groups).

In the Préalpes médianes, the Formation des Erpilles (Carnian) is proposed as formal substitute for the «formation bréchique» (Baud 1972). The best profile is found at the rock face close to Erpilles.

The Combe du Pissot Formation, of early Toarcian age is proposed following the classic profile described by Jeannet (1913) in the Tinière valley. This formation consists of bituminous shales (Couches du Creux de l'Ours) and glauconitic marls (Couches des Chevalets) as a lateral facies variation.

Within the Staldengraben Formation (Septfontaine 1983) of middle Jurassic age the Soladier, Verdy, Vanil Carré and Col de Lys Members are proposed as replacement of the subunits A, B, C, D.

The Torrent de Lessoc Formation (Oxfordian) is proposed to replace the «calcaires noduleux». A good profile is described by Weiss (1949) in the gorges de Mury near Lessoc.

The «Calcaires massifs» (Kimmeridgian-early Berriasian) are now formally subdivided into two formations. These are the medium to thick bedded limestone of the Moléson Formation and the massif limestone of the Dorfflüe Formation. Very comprehensive descriptions can be found in Heinz & Isenschmid (1988).

The Sciernes d'Albeuve Formation (Berriasian-Barremian) replaces the «calcaires plaquetés formation» (Spicher 1966). Excellent profile descriptions can be found in Boller (1963).

The Cuvigne-Derrey Formation stands for the so called «Flysch des Préalpes médianes» described by Favre (1952).

The Coulaytes Melange (late Eocene-early Oligocene) is proposed as a formal unit representing the «Flysch à lentilles de Couches Rouges» (Badoux 1962) on top of the Préalpes médianes.

A similar but not identical unit is called Melange des Mattes and represents the «Flysch à lentilles de Couches Rouges» on top of the Breccia nappe.

## REFERENCES

- Badoux, H. 1962: Géologie des Préalpes valaisannes (rive gauche du Rhône). Matér. Carte géol. Suisse, [n.s.] 113.
- Baud, A. 1972: Observations et hypothèses sur la géologie de la partie radicale des Préalpes médianes. *Eclogae geol. Helv.*, 65/1, 43-55.
- Boller, K. 1963: Stratigraphische und mikropaläontologische Untersuchungen im Neocom der Klippendecke (östlich der Rhone). *Eclogae geol. Helv.*, 56/1, 15-102.
- Favre, G. 1952: Les Préalpes médianes entre l'Hongrin inférieur et la Sarine. Région de la Dent de Corjon. *Bull. Soc. Fribourg. Sci. Nat.*, 41, 41-119.
- Heinz, R. & Isenschmid, C. 1988: Mikrofazielle und stratigraphische Untersuchungen im Massivkalk (Malm) der Préalpes médianes. *Eclogae geol. Helv.*, 81/1, 1-63.
- Jeannet, A. 1913: Monographie géologique des Tours d'AI et des régions avoisinantes (Préalpes vaudoises). 1. Stratigraphie de la nappe rhétique, du Trias et du Lias des Préalpes médianes et de la zone interne. Matér. Carte géol. Suisse, [n.s.] 34.
- Mettraux, M. 1989: Sédimentologie, paléotectonique et paléocéanographie des Préalpes médianes (Suisse romande) du Rhétien au Toarcien. Thèse Univ. Fribourg.
- Plancherel, R. & Dall'Agnolo, S. (in prep) : Feuille 1245 Château-d'Oex. Atlas géologique de la Suisse 1:25000, carte et notice 144.
- Septfontaine, M. 1983: Le Dogger des Préalpes médianes suisses et françaises. *Mém. Soc. Helv. Sci. Nat.*, 97.
- Spicher, J.P. 1966: Géologie des Préalpes médianes dans le massif des Bruns, partie occidentale (Préalpes fribourgeoises). *Eclogae geol. Helv.*, 58/2, 591-742.
- Weiss, H. 1949: Stratigraphie und Microfauna des Klippenmalm. Diss. Univ. Zürich.

## P 6.2

# New lithostratigraphic formations of the middle penninic Klippen nappe (late Triassic – early Jurassic)

Kempf Oliver<sup>1</sup>, Dall'Agnolo Stephan<sup>1</sup>, Funk Hanspeter<sup>2</sup>

<sup>1</sup> swisstopo, Swiss Geological Survey, Seftigenstrasse 264, CH-3084 Wabern (oliver.kempf@swisstopo.ch)

<sup>2</sup> Seminarstrasse 26, CH-5400 Baden

In the course of editing a new map sheet of the Geological Atlas of Switzerland 1:25'000 (map sheet Alpnach; Funk et al. in prep.) the formal definition of four lithostratigraphic units is proposed. The investigated units are part of the middle penninic Klippen nappe and are of late Triassic (Rhaetian) to early Jurassic (Hettangian – Pliensbachian) age. The proposed formations are based on stratigraphic profiles that were originally described in great detail by Christ (1920) in the Stanserhorn region.

### Late Triassic

1. Lückengraben-Formation, Rhaetian: Christ (1920, p. 9 ff.) describes a detailed profile in the Lückengraben near Wiesenberg on the southern flank of the Stanserhorn (Swiss coordinates: 670.110/197.725). The profile is composed of ca. 45 m micritic, sparitic, dolomitic and sandy limestone beds with occasional marl intervals.

### Early Jurassic

2. Horngraben-Formation, Hettangian: The Jurassic profiles were originally described by Christ (1920, p. 19 ff.) at the locality «Brandgraben», which is today named «Horngraben» (667.875/197.175) southwest of the Stanserhorn summit. The profile of the Horngraben-Formation is composed of ca. 70 m micritic, sparitic, oolitic and sandy limestone beds.

3. Brand-Formation, Sinemurian: A ca. 37.5 m thick profile follows up-section of the Horngraben-Formation. The profile consists of dark gray sparitic limestone beds (echinoid-breccia) and a siliceous micritic limestone at the top of this unit.

4. Obflue-Formation, Pliensbachian: The profile follows on top of the Brand-Formation in the Horngraben and is composed of ca. 27 m gray siliceous micritic limestone beds interbedded with thin layers of brown marl.

### REFERENCES

Christ, P. 1920: Geologische Beschreibung des Klippengebietes Stanserhorn-Aravigrat am Vierwaldstättersee, Beitr. geol. Karte Schweiz [N.F.], 22.

Funk, H. et al. (in prep.): Blatt 1170 Alpnach. Geol. Atlas Schweiz 1:25'000, Karte und Erläut. 165.

## P 6.3

# The Middle Triassic (Anisian) marine transgression in central Switzerland, comparisons with the Jura Mountain and the Brescian Prealps

Rebetez Daniel<sup>1</sup>, Ramseyer Karl<sup>1</sup>

<sup>1</sup> Institut für Geologie, Universität Bern, Baltzerstrasse 1+3, CH-3012 Bern

During the basal Triassic, a shallow sea flooded the crystalline basement in central Switzerland. The knowledge on this transgression, i.e., stratigraphic allocation, depositional environment and paleogeographic setting, has been refined by numerous geologists since the end of the 18th century (e.g., Brunnschweiler, 1948; Widmer, 1949). Still, chronology, dynamics and direction(s) of this transgression remain unclear. First efforts based on palynological data (Gisler et al., 2007) indicated a marine transgression direction from the Tethys towards the Jura Mountains at lowermost Anisian time.

This study focuses on different stratigraphic sections in central Switzerland, i.e., Scheidnössli, Limmernsee, Val Punteglias, Obersand, Schwandi and Hüfihütte, where lack of vegetation, well-exposed rocks and little tectonic deformation allowed detailed logging. The first sediments deposited on the weathered crystalline basement consist of conglomerates and sandstones. Numerous sedimentary structures such as ripple marks or channels can be observed in this siliciclastic unit.

Following-up section, the clastic beds become thinner and dolomite layers appear randomly until they dominate. In the uppermost 20 m of the sequence, dolomite beds become massive and show a well-developed stacking pattern. The tops of the Triassic sections are erosive surfaces followed by black shales of Lias to Dogger in age. The thickness of these sedimentary deposits vary from one section to another with an West to east decreasing trend. The Val Punteglias section is the thickest (54 m), and the Schwandi section the thinnest (9 m).

Facies and microfacies determinations, sedimentary structure analyses as well as stable isotope analyses ( $\delta^{13}\text{C}$ ,  $\delta^{18}\text{O}$ ) have been carried out. Preliminary results show that the sedimentary record displays several depositional sequences implying that high-frequency relative sea-level fluctuations were superimposed onto the general transgressive trend. These observations allow to correlate the six locations and to give indications about the depositional system and paleotopography.

This data have been compared with a borehole from the Jura mountains (Weiach) and with two well-documented sections of the Brescian Prealps (Northern Italy) i.e. Dosso Alto and Bagolino (Brack & Rieber, 1986; Brack et al., 2005) where isotopic analyses have been carried out. This allows getting a better understanding on the Alpine realm at middle Triassic times.

## REFERENCES

- Brack, P., Rieber, H., Nicora, A., Mundil, R. 2005: The global boundary stratotype section and point (GSSP) of the Ladinian Stage (Middle Triassic) at Bagolino (southern Alps, northern Italy) and its implications for the Triassic time scale. *Episodes*, 28 pp. 233–244.
- Brack, P., and Rieber, H. 1986: Stratigraphy and ammonoids from the lower Buchenstein Beds in the Brescian Prealps and Giudicarie and their significance for the Anisian/Ladinian boundary. *Eclogae geol. Helv.*, 79, v. pp. 181-225.
- Brunnschweiler, R.O. 1948: Beiträge zur Kenntnis der Helvetischen Trias östlich des Klausenpass. Mitteilung aus dem Geologischen Institut der Eidgenössischen Technischen Hochschule und der Universität Zürich, Serie C, 33.
- Gisler, Ch., Hochuli, P.A., Ramseyer, K., Bläsi, H.R. & Schlunegger, F. 2007: Sedimentological, and palynological constraints on the basal Triassic sequence in Central Switzerland. *Swiss Journal of Geosciences* 100, 263-272.
- Widmer, H. 1949: Zur Geologie der Tödigruppe. A.-G. Buchdruckerei Wetzikon und Rüti, 98.



## 7. Palaeontology +

# 8. Fossils and plate tectonic events: Oceanic and continental gateways, landbridges and the dispersal of biota

Lionel Cavin, Damien Becker, Christian Klug ,  
+ P.O. Baumgartner, Laureline Scherler

*Swiss Palaeontological Society*  
*Kommission des Schweizerischen Paläontologischen Abhandlungen (KSPA),*  
*Schweizerisches Komitee für Stratigraphie (SCNAT)*

### TALKS:

- 7.1 Andjic G., Baumgartner-Mora C., Baumgartner P.O.: Shallow-water events in the Sandino Forearc Basin, Nicaragua - Costa Rica, evidence for subduction of seamounts ?
- 7.2 Baumgartner P.O., Sandoval M.I., Escuder-Viruete J.: Radiolarians and radiolarites, Pangea breakup and the plate tectonic evolution of the Caribbean region
- 7.3 Brosse M., Goudemand N., Frisk Å.M., Baud A., Bagherpour B., Bucher H.: New conodonts from the Griesbachian microbialite in South China: implications for an improved definition of the base of the Triassic
- 7.4 Costeur L.: The ruminant inner ear: evolutionary perspectives
- 7.5 Forasiepi A.M., Carrillo J.D.: Geographic isolation, land connection, and evolution of the terrestrial mammalian associations during the Cenozoic in South America: the carnivorous zone
- 7.6 Hiard F.: Eocene migrations of European mammals
- 7.7 Klug C., De Baets K., Kröger B., Bell M.A., Korn D.: Latitudinal shifts of Palaeozoic marine invertebrate gigantism and global change
- 7.8 Martini P., Costeur L., Le Tensorer J.-M., Schmid P.: The evolution of Pleistocene camelids from El Kowm, Syria
- 7.9 Neenan J.M., Li C., Rieppel O., Bernardini F., Tuniz C., Muscio G., Scheyer T.M.: Unique method of tooth replacement in Placodontia (Diapsida, Sauropterygia), with new data on the dentition of Chinese taxa
- 7.10 Pictet A., Föllmi K.B., Linder P., Spangenberg J.: Ammonite biostratigraphy ... what utility? Example of the Aptian Grüntes Member and Lutere Bed in the Alpine Helvetic domain
- 7.11 Sandoval M.I., Baumgartner P.O., Scientific Party of IODP (Integrated Ocean Drilling Program 344 Expedition): Radiolarian biostratigraphy and Miocene to Recent Cocos Plate motion in the frame of the tropical, E-Pacific palaeoceanographic setting (IODP Exp. 344, off Costa Rica)

## POSTERS:

- P 7.1 Baldessin E., Kindler P., Fischer G., Godefroid F.: Upper Cenozoic dolostones from the Mayaguana Bank, SE Bahamas: new insights from a core study
- P 7.2 Baumgartner-Mora C., Baumgartner P.O., Andjic G., Barat F.: Mid Cretaceous to Oligocene rise of the Middle American landbridge – documented by south-eastwards younging Larger Foraminifera in shallow water carbonates (Nicaragua – Costa Rica – Panama)
- P 7.3 Bôle M., Baumgartner P.O.: Geochemistry and  $^{30}\text{Si}$  of Radiolaria and Mesozoic Radiolarites of Panthalassa and Tethys
- P 7.4 Fischer G., Kindler P., Godefroid, F., Baldessin E.: The Mayaguana Bank (SE Bahamas) from the Late Oligocene to the present: A delicate equilibrium between tectonics and sedimentation
- P 7.5 Marchegiano M., Gliozzi E., Buratti N., Ariztegui D., Cirilli S.: Middle Pleistocene ostracod assemblages from Lake Trasimeno, Perugia, (Italy)
- P 7.6 Scherler L., Mennecart B., Hiard F., Becker D.: The «*Microbunodon* Event», or the European evolution of ungulates during the Oligocene-Miocene transition
- P 7.7 Székely S. E., Spezzaferri S., Stalder C., Filipescu S.: Paleoenvironmental reconstruction based on foraminiferal assemblages and the sedimentary phosphorus record in the Oligocene of Romania (Transylvanian Basin)

## 7.1

# Shallow-water events in the Sandino Forearc Basin, Nicaragua – Costa Rica, evidence for subduction of seamounts?

Andjic Goran<sup>1</sup>, Baumgartner-Mora Claudia<sup>1</sup> & Baumgartner Peter O.<sup>1</sup>

<sup>1</sup>Institut des Sciences de la Terre, Université de Lausanne, Bâtiment Géopolis, CH-1015 Lausanne (goran.andjic@unil.ch)

The Sandino Basin corresponds to a latest Cretaceous – Neogene forearc basin that is exposed today in the southwestern Nicaraguan Pacific coastal plain and in the northwestern corner of Costa Rica (Astorga 1987, fig.1). It consists of an elongated, slightly-folded belt of approximately 160 km long and 30 km wide. The basin developed between the Campanian and the Pliocene and includes essentially deep-water detrital sequences and basinal to platform carbonates in minor proportions (Astorga 1987; Hodgson 1998). The latter deposited at different steps of the basin evolution. The initial stage of basin development is only observed in the Santa Elena Peninsula (Costa Rica), where the basement of the southern part of the basin crops out. The basement consists of a tectonic stack of a serpentinite massif (Santa Elena Ultramafic nappe) on a mid-Cretaceous accretionary complex (Santa Rosa Accretionary Complex; Baumgartner & Denyer 2006). The stacking of these two units is believed to have taken place when their intraoceanic arc collided with the pre-existing margin. This thrust uplifted parts of the tectonic pile to shallow-water environments, as it is deduced from the mid-Campanian El Viejo Fm. (Baumgartner et al. 1984). This formation exhibits rudist-rich platform limestones in its proximal parts and slope deposits in its distal parts, both containing reworked clasts of the serpentinitic basement (Baumgartner et al. 1984). Shallow-water environments were rapidly drowned as the tectonic pile subsided in the forearc setting of the Mid-American Trench. A discordance (~ 20°) is observed between the slope sediments and the subsequent deposit of pelagic limestones (Piedras Blancas Fm., mid-Campanian – Up. Maastrichtian).

Basin evolution is then dominated by detrital sedimentation through Paleocene-Miocene times (Hodgson 1998). The detrital sediments range from thin-bedded distal turbidites to plurimetric proximal debris-flow and rarely record shallow-water conditions. However, Tertiary shallow-water limestones have been observed in several places, in Nicaragua and Costa Rica. They always appear as isolated outcrops which do not present stratigraphic contacts with the neighboring detrital sequences. The presence of these short-lived platforms could be attributed to localized uplifts in the forearc area, as the possible consequence of seamount subduction. The best-preserved exposure of platform limestones is located on the small, undescribed Isla Juanilla (0.15 km<sup>2</sup>). The whole island is made of reef carbonates, displaying corals in growth position associated with coralline red algae. A small outcrop of a wackestone containing abundant *Lepidocyclina* ssp. of the *L. undosafavosa* group permits to attribute an Oligocene age to this reef.

Finally, the Pliocene El Salto Fm. (Hodgson 1998; Nicaragua, fig.1) represents shallow-water, untilted terraces that deposited after the Miocene folding of the forearc basin (NW-SE fold axes).

### REFERENCES

- Astorga, A. 1987: El Cretácico Superior y el Paleógeno de la vertiente pacífica de Nicaragua meridional y Costa Rica septentrional: Origen, evolución y dinámica de las cuencas profundas relacionadas al margen convergente de Centroamérica. Lic. Thesis, University of Costa Rica, 1- 115.
- Baumgartner, P.O. & Denyer, P. 2006: Evidence for middle Cretaceous accretion at Santa Elena Peninsula (Santa Rosa Accretionary Complex), Costa Rica. *Geologica Acta*, 4 (1/2), 179–191.
- Baumgartner, P.O., Mora, C.R., Butterlin, J., Sigal, J., Glacon, G., Azéma, J. & Bourgeois, J. 1984 : Sedimentación y paleogeografía del Cretácico y Cenozoico del litoral pacífico de Costa Rica. *Revista Geológica de América Central*, 1, 57-136.
- Darce Rivera, M. & Duarte Morales, M. 2002 : Mapa geológico de la cuenca Sandino, Pacífico de Nicaragua, 1:175'000. Instituto Nicaragüense de Energía, Managua.
- Hodgson, G. 1998: Resumen de la geología en el perfil geotransversal Nicaragüense – Estado del conocimiento 1984. In : Investigación geocientífica en Nicaragua 1981 - 1991 (Ed. By Elming, S.A., Widenfalk, L. & Rodríguez, D.). Universidad Tecnológica de Lulea, Suecia, 1- 340.



Figure 1. Geology of the Sandino Basin. Based on Darce & Duarte (2002), Astorga (1987), Hodgson (1998) and Baumgartner & Denyer (2006).

## 7.2

# Radiolarians and radiolarites, Pangea breakup and the plate tectonic evolution of the Caribbean region

Baumgartner Peter O.<sup>1</sup>, & Sandoval, Maria Isabel<sup>1</sup> & Escuder-Viruete, Javier<sup>2</sup>

<sup>1</sup> *Institut des Sciences de la Terre, Université de Lausanne, Bâtiment Géopolis, CH-1015 Lausanne (peter.baumgartner@unil.ch)*

<sup>2</sup> *Instituto Geológico y Minero de España, 28760 Tres Cantos, Madrid, Spain.*

The now well-known Mesozoic radiolarian record yields several hundred morpho-species for any time interval. Most species have a global distribution either in a low latitude belt and/or in a still poorly defined, bipolar high palaeolatitude region (Figure 1).

While an intermittent marine connection through Pangea via the western Tethys-Central Atlantic – and the Proto-Caribbean rift area may have existed since the late Early Jurassic, low latitude cosmopolitan radiolarian assemblages are known only since the middle Bathonian from the Central Atlantic (DSDP Ste 534, UAZ95:6, Baumgartner & Matsuoka 1995). While a Toarcian (late Early Jurassic) breakup is well constrained for the Central Atlantic, the place and timing of initial ocean crust formation between the Americas (Gulf of Mexico or Proto-Caribbean?) is still poorly constrained. Although oceanic crust seemingly started to form in the early Late Jurassic (158 my), recent plate tectonic reconstructions show important obstructions throughout the Late Jurassic and early Cretaceous between the Central Atlantic, the Proto-Caribbean, and the Colombian back-arc basin, which in turn was separated from the Pacific by a mature arc.

Ribbon-bedded radiolarites are the most common oceanic sediment in Circum-Pacific remnants of Panthalassa. They range in age from Middle Palaeozoic to Late Cretaceous. Remnants of Palaeotethys also yield radiolarites of Late Palaeozoic to Early Triassic age. Remnants of Neotethyan ocean basins are characterized by Middle Triassic to Late Jurassic, sometimes early Cretaceous radiolarites. Although low latitude radiolarian assemblages spread into the early Central Atlantic, their productivity was too low to produce radiolarites. Middle to early Late Jurassic radiolarite facies can still be found in the Subbetic realm of SW-Spain and in the Rif on N-Morocco, but are absent from Jurassic sections of the Central Atlantic, such as exposed in Fuerteventura (Canary Islands) or drilled at DSDP Site 534 (Blake Bahama Basin). The radiolarite facies is also absent from pelagic realms related to the Proto-Caribbean (e.g. Guaniguanico Terrane of NW-Cuba) and the Gulf of Mexico (e.g. Taman Formation of East-Central Mexico). Detrital sediments dominate in the Middle Jurassic and pelagic carbonates characterise the late Jurassic-early Cretaceous in these “intra-Pangean” realms.

We interpret Jurassic-Early Cretaceous pelagic carbonates in the Central Atlantic and the Proto-Caribbean realms as the consequence of more oligotrophic surface waters than those of the adjacent Tethys and Panthalassa (Baumgartner 2013). The Central Atlantic was a ‘Mediterranean-type’ ocean basin, such as the Modern Red Sea. It was (and still is) a carbonate ocean, characterised by an anti-estuarine circulation.

What about the radiolarite occurrences in the Antilles and Cuba? Ribbon radiolarites in these areas are systematically related to oceanic seafloor basalts of various (within plate, primitive island arc, or rarely MORB) origins. Many occur as blocks in serpentinite-matrix mélanges (Cuba, Puerto Rico) that are reminiscent of Franciscan-type, subduction-related mélanges of the Pacific façade of Central and N-America. Radiolarian biochronology indicates an age range from Aalenian to Cenomanian (Bandini et al. 2011). Pre-Late Jurassic radiolarites (e.g. Bermeja Complex, Puerto Rico) cannot be Proto-Caribbean in origin (Montgomery et al. 1994), because they would be coeval with syn-rift detrital and evaporitic sediments known from Proto-Caribbean margins. The Aguacate Chert resting on the MORB-type Loma La Monja volcano-plutonic sequence has been considered as Late Jurassic in age and of Proto-Caribbean origin. Our recent findings indicate that at least part of the Aguacate Chert is Middle Jurassic in age, hence cannot be of Proto-Caribbean origin.

Our conclusion is that the Jurassic-Early Cretaceous ribbon radiolarites of the Antilles belong to exotic terranes of Pacific origin, which were emplaced into the Caribbean area in front of the Caribbean Large Igneous Province. These radiolarites are a major augment for the allochthony of the Modern Caribbean Plate.

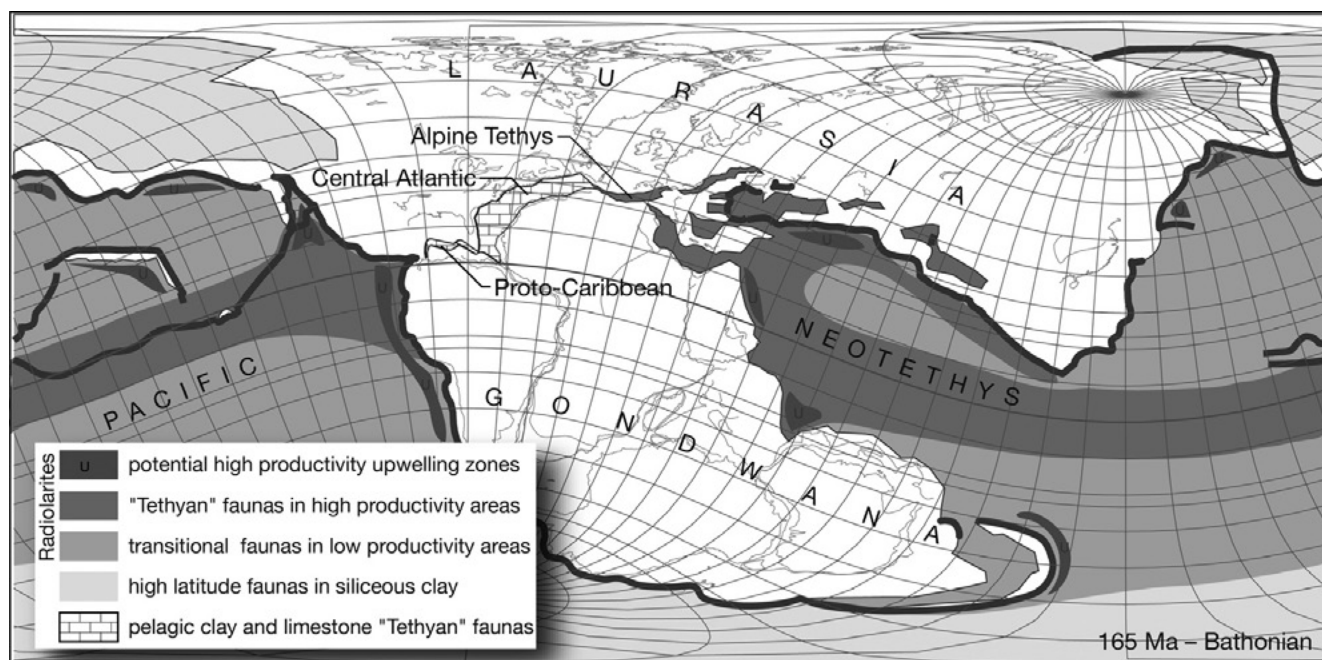


Figure 1. Palaeogeographic map for 165 Ma (Bathonian) adapted from Bandini et al. (2011) showing major oceanic radiolarian bio-provinces and low/high accumulation radiolarites.

## REFERENCES

- Bandini, A., Baumgartner, P.O., Flores, K., Dumitrica, P., Hochard, C., Stampfli, G. M. & Jackett, S.-J. 2011: Aalenian to Cenomanian Radiolaria of the Bermeja Complex (Puerto Rico) and Pacific origin of radiolarites on the Caribbean Plate. *Swiss Journal of Geosciences*, 104 : 367-408.
- Baumgartner, P. O. 2013: Mesozoic radiolarites – Accumulation as a function of sea surface fertility on Tethyan margins and in ocean basins. *Sedimentology*, 60 (1): 292-318.
- Baumgartner, P. O., & Matsuoka, A. 1995: New radiolarian data from DSDP Site 534, Blake Bahama Basin, Central Northern Atlantic. In: "Middle Jurassic to Lower Cretaceous Radiolaria of Tethys: Occurrence, Systematics, Biochronology" (Ed. by Baumgartner, P.O. et al.). *Mém. de Géol. Lausanne* 23, 709-715.
- Mongomery, H., Pessagno, E.A., & Pindell, J. 1994: A 195Ma terrane in a 165Ma ocean: Pacific origin of the Caribbean Plate. *GSA Today*, 4: 1, 3-6.

## 7.3

## New conodonts from the Griesbachian microbialite in South China: implications for an improved definition of the base of the Triassic

Morgane Brosse<sup>1</sup>, Nicolas Goudemand<sup>1,2</sup>, Åsa M. Frisk<sup>1</sup>, Aymon Baud<sup>3</sup>, Borhan Bagherpour<sup>1</sup>, Hugo Bucher<sup>1</sup>

<sup>1</sup> Paleontological Institute and Museum, Zurich, Switzerland;

<sup>2</sup> Paleobiology Group, Stanford University, USA;

<sup>3</sup> Parc de la Rouvraie 28, Lausanne, Switzerland.

\* presenting author: morgane.brosse@pim.uzh.ch

A new sampling of Early Triassic (Griesbachian) conodonts is obtained from the microbialite overlying the latest Permian peri-reefal shallow water limestone in Wuzhuan section (Nanpanjiang Basin, Guangxi, South China). High resolution sampling in the lower twelve meters of the Luolou Formation provides rather diversified conodont faunas and allows constructing a well resolved conodont distribution for this crucial earliest Triassic interval. In the Wuzhuan section, the nine meters thick microbialite is bracketed by two calcarenite beds and contains several fossiliferous lenses. The co-occurrence of typical Permian foraminifera such as *Paraglobivalvulina mira* (Reitlinger) and *Dagmarita chanakchiensis* (Reitlinger) in the calcarenite underlying the microbialite indicates a late Permian age. Our preliminary results indicate the presence of one residual maximal horizon (RMH) based on conodont faunas in the microbialite and of a second one in the overlying calcarenite. The lowest RMH occurs four meters above the base of the microbialite and is defined by *Neogondolella taylorae* (Orchard) and *Neogondolella n. sp. A*. The second RMH from the calcarenite that caps the microbialite is defined by the co-occurrence of *Isarcicella staeschei* (Dai and Zhang) and *Isarcicella isarcica* (Huckriede). The lowest RMH including *N. taylorae* partly overlaps with the *N. taylorae* interval zone established in sections without microbialite such as Meishan and Shangsi. However, the *N. taylorae* RMH is here reported for the first time from section with microbialite in the Yangtze platform or the Nanpanjiang basin. The second RMH partly overlaps with the *Isarcicella isarcica* interval zone recorded above the microbialite in other sections. Although *H. parvus* is dominant in Wuzhuan and in other microbialite-bearing sections, its first occurrence has been documented as diachronous. In Wuzhuan, the most appropriate conodont association for constraining the base of the microbialite is the RMH with *N. taylorae* and *N. n. sp. A*.

### Funding:

M.B., B.B and H.B are funded by the Swiss SNF project 135446 (to H.B.). N.G. is funded by the Swiss SNF fellowship PA00P1-145314. Å. M. F. is funded by the Swedish Research Council, The Royal Swedish Academy of Sciences and the Lars Hierta Memorial Foundation.

## 7.4

### The ruminant inner ear: evolutionary perspectives

Loïc Costeur<sup>1</sup>

<sup>1</sup> *Naturhistorisches Museum Basel, Augustinergasse 2, CH-4001 Basel (loic.costeur@bs.ch)*

The inner ear or bony labyrinth contains the organs of hearing and balance. It's housed inside the petrosal bone which has historically been a source of phylogenetic information for mammals and for cetartiodactyls in particular (e.g., Luo and Gingerich, 1999; O'Leary, 2010; Theodor, 2010). After the seminal work of Gray (1907), several studies focused on the inner ear itself in primates, rodents, "insectivores" or marsupials to investigate functional signals (Schwarz, 2012), phylogenetic patterns (e.g., Gunz et al., 2012; Ekdale, 2013) or developmental issues (Sánchez-Villagra & Schmelzle, 2007). But its use remains very limited in ruminants. The morphology of the inner ear in basal artiodactyls has been described only recently (Theodor, 2010; Orliac, 2012) and very few is known on morphological variability, ontogenetic changes or relevance of potentially significant phylogenetic characters. The inner ear being a strongly functional structure, the relevance of characters has to be taken with caution. However, recent works successfully started to tackle this issue (Jeffery et al., 2008).

I will review the use of the inner ear in ruminant research and show how this structure can be useful. The more and more widespread use of high resolution X-ray computer tomography has made it possible to reconstruct relatively easily the inner ear in extant and extinct taxa without destruction of the skull. Studying the bony labyrinth involves looking at variability, a time-consuming but feasible task. I will show examples taken from extant taxa in different ruminant families (Tragulidae, Bovidae, Cervidae and Moschidae) to illustrate ontogenetic changes or morphological differences. I will also incorporate extinct taxa from the same families (especially the musk-deer family, i.e., Moschidae) for which I could investigate morphological variability and possibly discriminate species of the same genus.

Comparative morphological descriptions of the inner ear yield interesting insights, but quantitative data are needed for statistically sound comparisons. I will then emphasize this need and show what future works, especially involving geometric morphometrics, could bring to the understanding of the shape signal born by the ruminant inner ear.

#### REFERENCES

- Ekdale, E.G. 2013: Comparative Anatomy of the Bony Labyrinth (Inner Ear) of Placental Mammals, *PlosOne* 8(6), e66624.
- Jeffery, N., Ryan T.M. & Spoor, F. 2008: The primate subarcuate fossa and its relationship to the semicircular canals part II: Adult interspecific variation, *Journal of Human Evolution* 55, 326-339.
- Gray, A.A. 1907: The labyrinth of animals: including mammals, birds, reptiles and amphibians, Volume 1, London, J. & A. Churchill, 98 pp.
- Gunz, P., Ramsier, M., Kuhrig, M., Hublin, J.-J. & Spoor, F. 2012: The mammalian bony labyrinth reconsidered, introducing a comprehensive geometric morphometric approach, *Journal of Anatomy*, 220, 529-543.
- Luo, Z. & Gingerich, P.D. 1999: Terrestrial mesonychia to aquatic cetacea: transformation of the basicranium and evolution of hearing in whales." *University of Michigan papers on Palaeontology*, 31, 1-98.
- O'Leary, M.A. 2010: An anatomical and phylogenetic study of the osteology of the petrosal of extant and extinct artiodactylans (Mammalia) and relatives, *Bulletin of the American Museum of Natural History*, 335, 1-206.
- Orliac, M., Benoît, J. & O'Leary, M.A. 2012: The inner ear of *Diacodexis*, the oldest artiodactyl mammal, *Journal of Anatomy*, 221(5), 417-426.
- Sánchez-Villagra, M.R. & Schmelzle, T. 2007: Anatomy and development of the bony inner ear in the woolly opossum, *Caluromys philander* (Didelphimorphia, Marsupiala), *Mastozoología Neotropical*, 14(1), 53-60.
- Theodor, J.M. 2010: Micro-computed tomographic scanning of the ear region of *Cainotherium*: character analysis and implications, *Journal of Vertebrate Paleontology*, 30(1), 236-243.
- Schwarz, C. 2012: Phylogenetische und funktionsmorphologische Untersuchungen der Ohrregion bei *Sciuromorpha* (Rodentia, Mammalia), Ph.D. Dissertation, Rheinischen Friedrich-Wilhelms-Universität Bonn, 350 p.

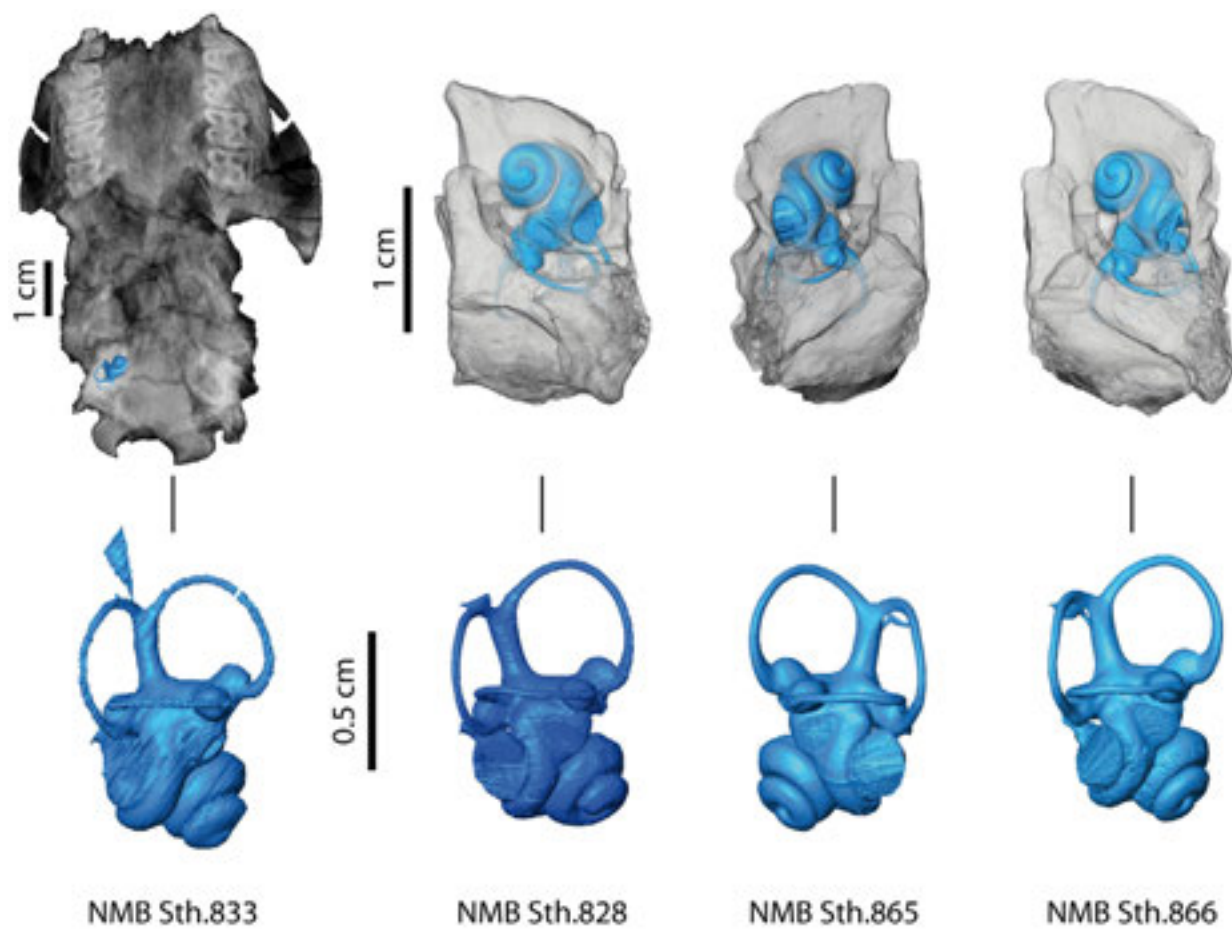


Figure 1. Four inner ears of the fossil musk deer *Micromeryx* (Mammalia, Moschidae), reconstructed from high resolution CT-scans of a skull and three isolated petrosals from the Middle Miocene German locality of Steinheim. Note the variability in the number of cochlear whorls for instance.

## 7.5

# Geographic isolation, land connection, and evolution of the terrestrial mammalian associations during the Cenozoic in South America: the carnivorous zone

Forasiepi, Analia Marta<sup>1,2</sup> & Carrillo, Juan David<sup>2</sup>

<sup>1</sup> Instituto Argentino de Nivología, Glaciología y Ciencias Ambientales, CCT-Mendoza, CONICET, Av. Ruiz Leal s/nº, Mendoza 5500, Argentina (borhyaena@hotmail.com)

<sup>2</sup> Palaeontological Institute and Museum, University of Zürich, Karl Schmid-Strasse 4, CH- 8006 Zürich (juanchorrillo@gmail.com)

The physical isolation of the South American continent during most of the Cenozoic resulted in an endemic fauna. The eutherians and metatherians were the major components of the mammalian associations with the carnivorous adaptive zone occupied by metatherian sparassodonts. The Sparassodonta has been registered from the Paleocene to the Pliocene. They were predominantly hypercarnivores and with a broad range of body sizes, locomotory capabilities, and morphologies, including some extreme specializations, such as the sabre-tooth thylacosmilids.

Placental Carnivora started to occupy the carnivorous adaptive zone since the Late Miocene in South America. However, after the complete formation of the Panama Bridge, during the Pleistocene, the richness of the placental carnivores massively increased. There was temporal overlap of Sparassodonta and Carnivora during the Late Miocene–Early Pliocene but no ecological superposition. This suggests an opportunistic ecological replacement, as part of a larger faunistic turnover, in contrast to a competitive displacement.

The oldest placental carnivores in South America currently found are in Argentina, in the south tip of the continent. Recent discoveries in northern South America provide further information about the interchange with North America.

Fossil and present day distribution of mammals in South America highlight the importance of the tropics and the Andes during the interchange. The diversity of northern immigrants in South America abruptly increased since the Late Miocene, reaching in the Quaternary about half of the total mammalian fauna. In fossil and current terrestrial ecosystems from South America, mammals with North American origin dominate in temperate and high altitude zones, whereas mammals with South American origin dominate in the tropics.

## REFERENCES

- Forasiepi, A.M. 2009: Osteology of *Arctodictis sinclairi* (Mammalia, Metatheria, Sparassodonta) and phylogeny of Cenozoic metatherian carnivores from South America. *Monografías del Museo Argentino de Ciencias Naturales* ns, 6, 1-174.
- Prevosti, F.J., Forasiepi, A.M., & Zimicz, N. 2013: The Evolution of the Cenozoic Terrestrial Mammalian Predator Guild in South America: Competition or Replacement?. *Journal of Mammalian Evolution*, 20, 3-21.

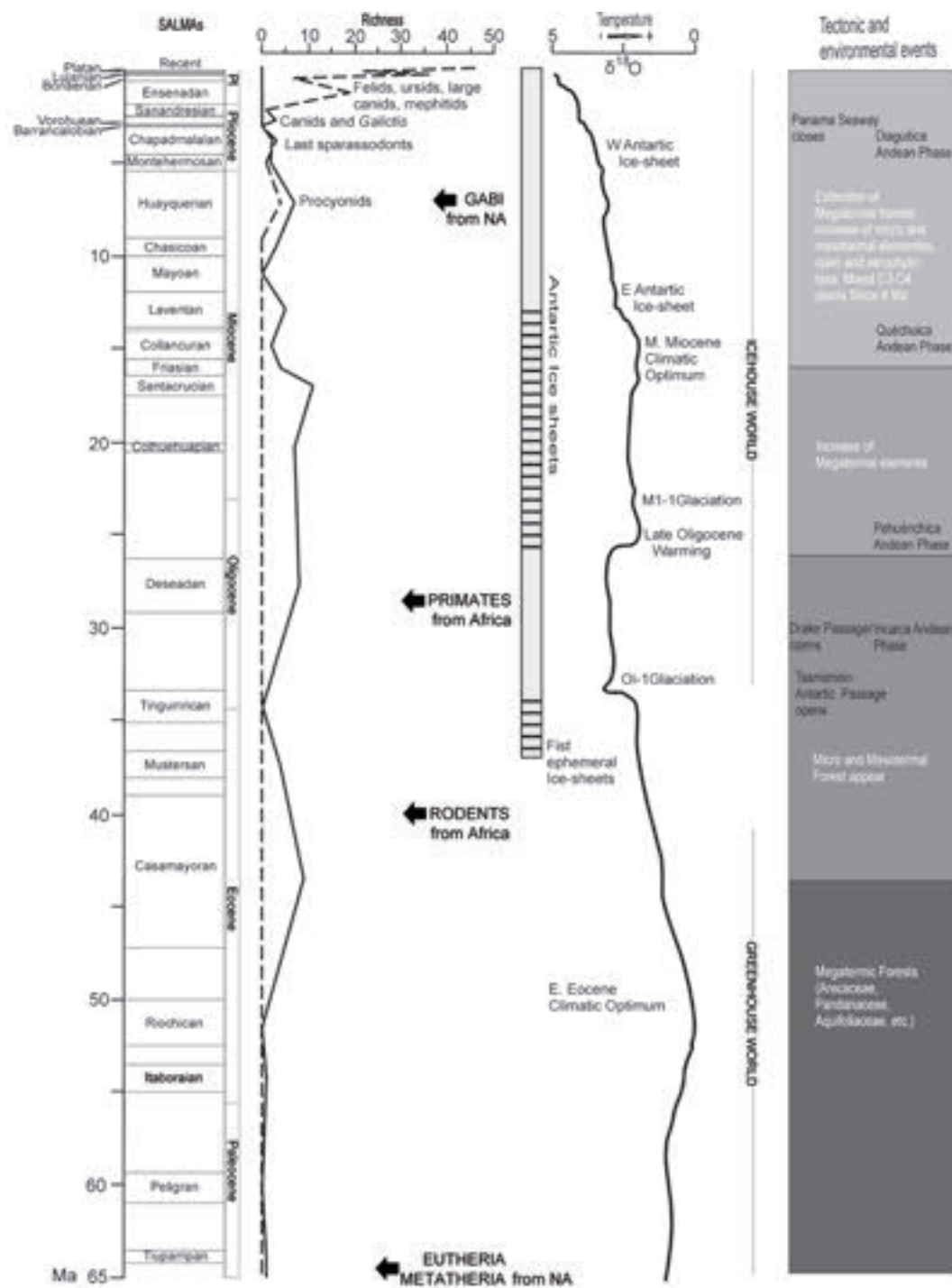


Figure 1. South American Land Mammals Ages (SALMAs), sparassodont and carnivoran richness line, major faunistic events, temperature line, environments, and major tectonic events in the Cenozoic of South America (modified from Prevosti et al. 2013).

## 7.6

### Eocene migrations of European mammals

Hiard Florent<sup>1</sup>

<sup>1</sup> *Department of Geosciences\_Earth Sciences, University of Fribourg, Chemin du Musée 6, CH-1700 Fribourg (florent.hiard@unifr.ch)*

During the Eocene, Europe was an isolated archipelago, separated to Africa by the Tethys, to Asia by the Turgai strait and, since the late early Eocene, to North America by the opening of the Atlantic Ocean (e.g. Brinkhuis et al 2006, MacFadden 1992). During this epoch, the mammalian fauna of Europe was characterised by a high level of endemism, such as in the terrestrial cetartiodactyls (e.g. Erfurt and Métais 2007).

However, the biostratigraphy and of the evolution of European mammals suggest several arrivals of migrants from other continents. Two main questions remain: Where they came from and which ways did they use. Asia and North America are the two main possibilities of their origin. From America, the mammals could cross the North Atlantic by the DeGeer dispersal route. Mammals could also come from Asia, crossing the Turgai strait or following a corridor made by central Asia and Anatolia. Arguments in favor or at the contrary in the detriment of those different possibilities will be discussed. Furthermore, an overview of the Eocene mammals from other parts of the world will highlight the difficulties to answer to those different questions.



Figure 1. Eocene paleogeography with potential origins and migratory ways of European mammals (Modified from Scotese 2001).

#### REFERENCES

- Blakey, R. C., 2010: Paleogeographic maps.
- Brinkhuis, H., Schouten, S., Collinson, M. E., Sluijs, A., Sinninghe Damsté, J. S., Dickens, G. R., Huber, M., Cronin, T. M., Onodera, J., Takahashi, K., Bujak, J. P., Stein, R., van der Burgh, J., Eldrett, J. S., Harding, I. C., Lotter, A. F., Sangiorni, F., van Konijnenburg-van Cittert, H., de Leeuw, J. W., Matthiessen, J., Backman, J., Moran, K. & the Expedition 302 Scientists. 2006 : Episodic fresh surface waters in the Eocene Arctic Ocean, *Nature*, 441, 606-609.
- Erfurt, J., & Métais, G. 2007: Endemic European Paleogene artiodactyls. In: *The Evolution of artiodactyls* (Ed. by Prothero, D.R., and Foss, S.E.). The Johns Hopkins University Press, Baltimore, p. 59-84.
- MacFadden, B. J. 1992: *Fossil Horses: systematics, paleobiology, and evolution of the family Equidae*. Cambridge University Press, New-York, 369pp.
- Scotese, R. C., 2001: *Atlas of Earth History: Volume 1, Paleogeographic Maps*. PALEOMAP project, Arlington, 52pp.

## 7.7

# Latitudinal shifts of Palaeozoic marine invertebrate gigantism and global change

Christian Klug<sup>1</sup>, Kenneth De Baets<sup>2</sup>, Björn Kröger<sup>3</sup>, Mark A. Bell<sup>4</sup> and Dieter Korn<sup>3</sup>

<sup>1</sup> *Paläontologisches Institut und Museum, Universität Zürich, Karl Schmid-Strasse 4, CH-8006 Zürich*

<sup>2</sup> *Universität Erlangen, Loewenichstr. 28, D-91054 Erlangen, Germany*

<sup>3</sup> *Museum für Naturkunde, Humboldt-Universität zu Berlin, Invalidenstraße 43, D-10115 Berlin, Germany*

<sup>4</sup> *Department of Earth Sciences, University College London, Gower Street, London, WC1E 6BT, UK*

Since the Cambrian Explosion, giant marine invertebrate species have evolved iteratively in several groups. In the Palaeozoic, marine invertebrate gigantism was heterogeneously distributed through time and space; changes in maximum sizes show no clear relationship with atmospheric or oceanic oxygen and other environmental factors. Although gigantism has found an explanation for Carboniferous land invertebrates in the atmospheric oxygen peak, marine gigantism has not been studied empirically and explained comprehensively.

By quantifying the spatiotemporal distribution of the largest representatives of some major marine invertebrate clades, we assessed links between ecological parameters and giant growth. These occurrence data suggest that temperature and latitude in combination with oxygen played important roles. Marine invertebrate gigantism developed in certain phases and regions with a greater number of extremely large species and their occurrences shifted independently from middle towards low latitudes during the Palaeozoic in all examined groups. This trend roughly coincides with the Late Devonian to Carboniferous cooling and regression as well as with a rise in atmospheric oxygen. This shows how global environmental changes can control the geographical distribution of organisms and that the optimal ecological requirements might differ depending on body size: extremely large organisms might react less flexibly to ecological changes.

## 7.8

### The evolution of Pleistocene camelids from El Kowm, Syria

Pietro Martini<sup>1,2</sup>, Loïc Costeur<sup>2</sup>, Jean-Marie Le Tensorer<sup>1</sup>, Peter Schmid<sup>1,3</sup>

<sup>1</sup> Institut für Prähistorische und Naturwissenschaftliche Archäologie, University of Basel, Spalenring 145, CH-4055 Basel CH (pietro.martini@unibas.ch)

<sup>2</sup> Naturhistorisches Museum Basel, Augustinergasse 2, CH-4001 Basel

<sup>3</sup> Evolutionary Science Institute, University of the Witwatersrand, Private Bag 3, Wits 2050, South Africa.

The Camelidae (Artiodactyla) originated in North America during the middle Eocene (~45 Ma). In the Miocene they became very successful, and diversified into at least 20 genera (Honey *et al.* 1998). The first genus in the Old World was *Paracamelus*, which is recorded since the latest Miocene (MN13, ~7 Ma). It was likely ancestral to modern *Camelus* (Pickford *et al.* 1995). However, the evolution of Eurasian camelids is poorly known. Several species are recognized, but most are based on scarce material or have been described only superficially.

A good opportunity to study the diversity and evolutionary trends of Eurasian camelids is provided by the fauna of the El Kowm Basin (central Syria). This region is rich in Palaeolithic archaeological sites with abundant mammalian fossils. The complete sequence spans the early to late Pleistocene, from 1.5-1.8 Ma to 50 ka (Jagher and Le Tensorer 2011). Camelids are the most frequent faunal elements in all layers. Here we present preliminary results from the analysis of this camelid succession. The material studied was excavated in three sites (Ain al Fil, Hummal and Nadaouiyeh Ain Askar) within few km from each other.

The oldest remains from Ain al Fil (Early Palaeolithic, Early Pleistocene, between 1.8 and 1.5 Ma) suggest the coexistence of two species, one dromedary-sized and one much larger. Later forms from the lower section of Hummal are also larger than modern camels, with long limbs and small heads. A size reduction is seen from the Early to the Late Pleistocene. A Middle Pleistocene skull from the rich sample of Nadaouiyeh Ain Askar (Acheulean layers, about 400 Ka) has a unique morphology. Fossils that are similar and somehow intermediate between the two modern species are frequent only in the Late Pleistocene of Hummal (Mousterian layers, 150 to 50 Ka). During this period they coexisted with a highly distinctive giant species, which is the most recent example of the formerly common giant camels.

The study of Pliocene and Pleistocene fossil camelids is hampered by the lack of knowledge about the comparative morphology of the recent camel species, the dromedary *C. dromedarius* L. and the Bactrian camel *C. bactrianus* L. (Peters & von den Driesch 1997). Our project begins with a morphometric analysis of the modern species that will allow the identification and description of the several species found in the El Kowm sequence.

#### REFERENCES

- Honey, J. J., J. A. Harrison, Prothero, D. R., Stevens, M. S. 1998: Camelidae. Evolution of Tertiary Mammals of North America: Terrestrial Carnivores, Ungulates, and Ungulatelike Mammals. C. M. Janis, K. Scott and L. L. Jacobs. Cambridge, Cambridge University Press. 1: 439-462.
- Pickford, M., J. Morales, Soria, D. 1995: Fossil camels from the Upper Miocene of Europe: implications for biogeography and faunal change. *Geobios* 28(5): 641-650.
- Jagher, R. & Le Tensorer, J.-M. 2011: El Kowm, a key area for the palaeolithic of the Levant in Central Syria. The Lower and Middle Palaeolithic in the Middle East and Neighbouring Regions. J. M. Le Tensorer, R. Jagher and M. Otte. Liège, Etudes et Recherches Archéologiques de l'Université de Liège (ERAUL). 126.
- Peters, J. & von den Driesch, A. 1997: The two-humped camel (*Camelus bactrianus*): new light on its distribution, management and medical treatment in the past. *Journal of Zoology* 242: 651-679

## 7.9

## Unique method of tooth replacement in Placodontia (Diapsida, Sauropterygia), with new data on the dentition of Chinese taxa

Neenan James M.<sup>1</sup>, Li Chun<sup>2</sup>, Rieppel Olivier<sup>3</sup>, Bernardini Federico<sup>4</sup>, Tuniz Claudio<sup>4</sup>, Muscio Giuseppe<sup>5</sup>, Scheyer Torsten M.<sup>1</sup>

<sup>1</sup> Paläontologisches Institut und Museum der Universität Zürich, Zürich, Switzerland, (james.neenan@pim.uzh.ch)

<sup>2</sup> Institute of Vertebrate Paleontology and Paleoanthropology, Chinese Academy of Sciences, Beijing, P. R. China.

<sup>3</sup> The Field Museum, Chicago, IL, USA

<sup>4</sup> The 'Abdus Salam' International Centre for Theoretical Physics, Multidisciplinary Laboratory, Trieste, Italy.

<sup>5</sup> Museo Friulano di Storia Naturale, Udine, Italy.

The placodonts of the Triassic period (~251–201 mya) represent one of the earliest and most extreme specializations to a durophagous diet of any known reptile group (e.g. Rieppel 2000). Exceptionally enlarged crushing tooth plates on the maxilla, dentary and palatine cooperated to form 'crushing areas' in the buccal cavity (Mazin & Pinna 1993). However, the extreme size of these teeth, combined with the unusual way they occluded, constrained how replacement occurred (Rieppel 2001). Using an extensive  $\mu$ CT dataset of 11 specimens that span all geographic regions and placodont morphotypes, tooth replacement patterns were investigated. In addition, the previously unknown dental morphology and formulae of three Chinese taxa is described for the first time.

Placodonts have a unique tooth replacement method and results appear to follow a phylogenetic trend (Fig. 1). The plesiomorphic *Placodus* species show many replacement teeth at various stages of growth, with little or no discernable pattern. On the other hand, the more derived cyamodontoids tend to have fewer replacement teeth growing at any one time, replacing functional teeth diagonally across the palate and/or in functional units. *Cyamodus*, *Sinocyamodus* and *Macroplacus* in particular show strong modularity, with unilateral replacement of teeth that form functional units. The highly nested placocheilids *Psephoderma* and *Psephochelys* have fewer teeth and, as a result, only have one or two replacements in the upper jaw, and supports previous suggestions that these taxa had an alternative diet to other placodonts (Rieppel 2002). Importantly, all specimens show at least one replacement tooth growing at the most posterior palatine tooth plates, indicating increased wear at this point and supporting previous suggestions that this was the main site of crushing (Rieppel 2002).

*P. inexpectatus* has a very similar dentition to the European *P. gigas*, although there is one extra anterior dentary tooth plate and the anterior dentary teeth as well as premaxillary teeth are much shorter and bulbous in the former (Fig. 2A). The teeth of *Sinocyamodus* are numerous and small (Fig. 2B), similar to the condition seen in a sub-adult *Cyamodus hildegardis* (Kuhn-Schnyder 1959), evidence that this is also a sub-adult. *Psephochelys* has fewer teeth and an edentulous rostrum (Fig. 2C) and is very similar to that of the European *Psephoderma*, indicating a comparable diet and feeding strategy.

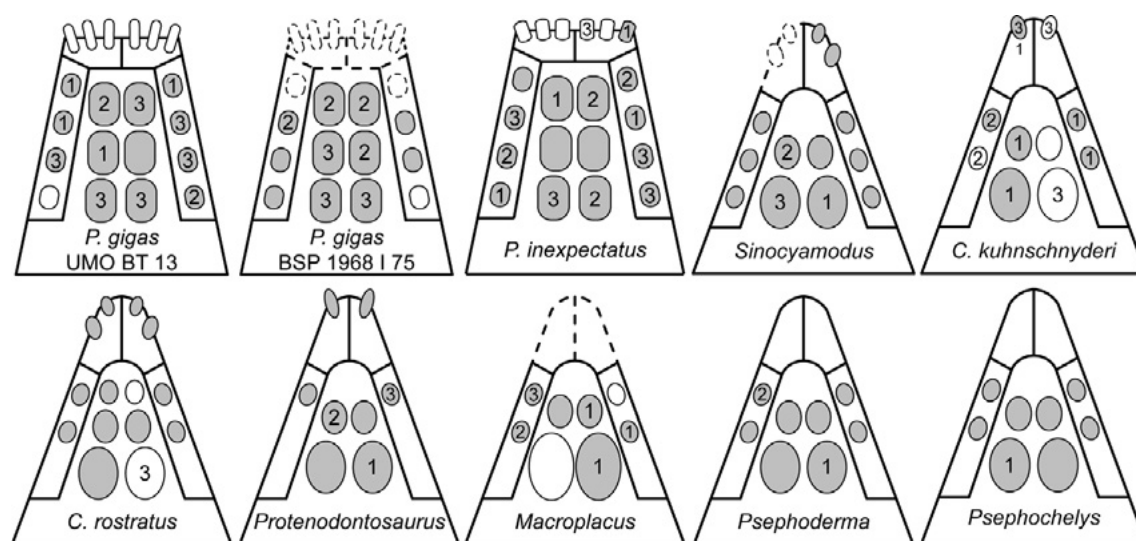


Figure 1. Schematic representations of placodont skulls in palatal view showing tooth replacement stages. Grey teeth indicate presence of a functional tooth, whereas white represents absence. Stage 1, the replacement tooth is a thin layer of enamel and does not resemble a functional tooth. Stage 2, the replacement tooth begins to resemble a functional tooth, but has not reached full size. Stage 3, the replacement tooth has reached approximately full size.

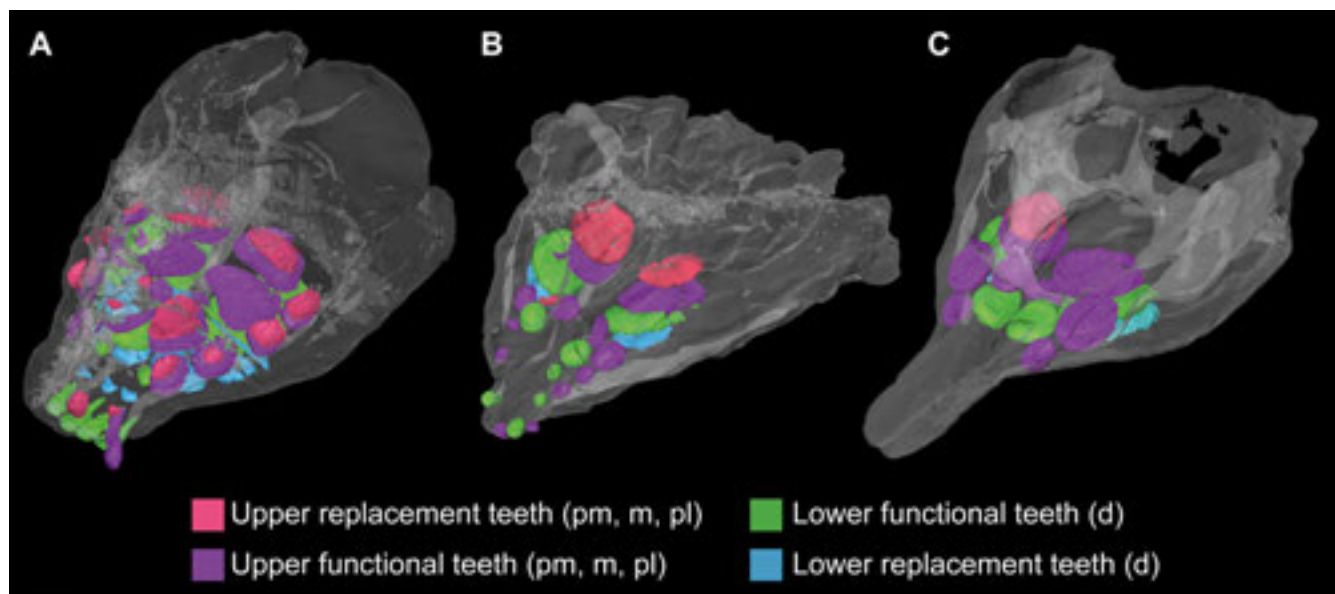


Figure 2. The dentitions of the Chinese placodonts *Placodus inexpectatus* (A), *Sinocyamodus* (B) and *Psephochelys* (C). Abbreviations: d, dentary; m, maxilla; pl, palatine; pm, premaxilla.

## REFERENCES

- Kuhn-Schnyder, E. 1959: Über das Gebiss von *Cyamodus*. Mitteilungen aus dem Paläontologischen Institut der Universität Zürich, 1, 174-188.
- Mazin J.-M. & Pinna G. 1993: Palaeoecology of the armoured placodonts. *Paleontologia Lombarda N. S.*, 2, 83-91.
- Rieppel, O. 2000: Sauropterygia I - Placodontia, Pachypleurosauria, Nothosauroida, Pistosauroida. *Handbook of Paleoherpertology*, 1-134.
- Rieppel, O. 2001: Tooth implantation and replacement in Sauropterygia. *Paläontologische Zeitschrift*, 75, 207-217.
- Rieppel, O. 2002: Feeding mechanics in Triassic stem-group sauropterygians: the anatomy of a successful invasion of Mesozoic seas. *Zoological Journal of the Linnean Society*, 135, 33-63.

## 7.10

### Ammonite biostratigraphy ... what utility? Example of the Aptian Grünten Member and Luitere Bed in the Alpine Helvetic domain.

Pictet Antoine<sup>1</sup>, Föllmi Karl B.<sup>1</sup>, Linder Pascal<sup>2</sup>, Spangenberg, Jorge<sup>1</sup>

<sup>1</sup> Institut of Earth Sciences, University of Lausanne, Géopolis – CH-1015 Lausanne; antoine.pictet@unil.ch.

<sup>2</sup> Petit Pontarlier 15, 2000 Neuchâtel

A first model for the stratigraphy of the Aptian sedimentary succession in the northern Alps originated early in the twentieth century (Jacob & Tobler 1906; Heim 1913; Fichter 1934) with the following age attribution to the lithological succession: the Upper Urgonian Member (*Deshayesites oglanlensis* to *D. deshayesi* ammonite zones), the Grünten Member (*Dufrenoyia furcata* zone), the Luitere phosphatic Bed (*Epicheloniceras martini* and *Parahoplites melchioris* zones), Gams Beds (*Parahoplites melchioris* zone), and the Brisi Sandstone and Limestone Beds (*Acanthoplites nolani* zone). In the early XXth, more precise studies based on sedimentological, geochemical, mineralogical and biostratigraphic analyses, allow to assign more precise ages to these units (Linder et al. 2006; Föllmi & Gainon 2008; Föllmi 2009) with an age corresponding to the *D. oglanlensis* and *D. forbesi* zones for the Upper Urgonian Member, *D. deshayesi* and *D. furcata* zones for the Grünten Member, and *E. martini* and *P. melchioris* zones for the Luitere bed.

Recent results, based on comparisons with the Chabert Formation on the Ardèche Platform (SE France), and geochemical analyses and numerous new ammonite findings including Deshayesitidae and Cheloniceratinae from the Helvetic Alps, allow for a new and more precise stratigraphic and biostratigraphic subdivision of the Grünten member and the Luitere Bed, resulting in a new interpretation of the age of the Luitere bed and some important modifications in the ammonite biozonal attributions.

A correlation with the Ardèche Platform allows to date the basal Rohrbachstein interval to the late early *D. forbesi* zone based on the discovery of the last *Procheloniceras* accompanied by classical *Deshayesites* from this zone. The lower Grünten Member is dated as the *Roloboceras hambrovi* subzone and the *D. deshayesi* zone thanks to the index fossil from the *R. hambrovi* and *D. grandis* sub-zones, and also by comparison of the carbon isotope curves. The Plaine Morte Bed is dated as the late *D. grandis* subzone – early *D. furcata* zone by the discovery of the index forms. The Upper Grünten Member is dated as the *D. furcata* zone by the observation of the index fossil. The alpine ammonite fauna composing the Luitere Bed allows the recognition of three distinctive phosphatic fauna (Luitere 1 to 3), which may separate two third-order sequences belonging to the *D. furcata* zone and to the *E. martini* zones. For the moment, only the first sequence was observed in the Rawil (Swiss Alps) outcrop (Föllmi & Gainon 2008), separated by two distinct phosphatic layers, the Plaine Morte and Luitere Beds, which meet laterally.

Inversely, these new stratigraphic scheme allows for a better understanding of the ammonite species created by the past on these beds of reworking (e.g. Jacob & Tobler 1906) and of their age attribution, species used as indexes in the past or present biostratigraphy by ammonites (e.g. *Colombiceras tobleri*, *Epicheloniceras buxtorfi*).

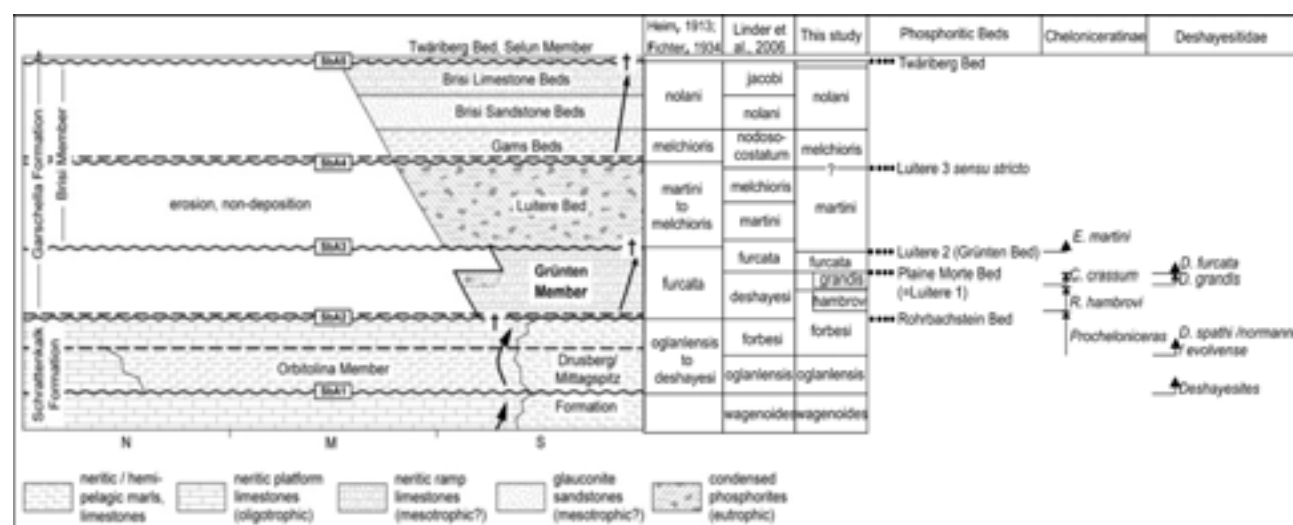


Figure 1. Schematic plot of lithostratigraphic units in the Helvetic Realm from Linder et al. (2006) with on the right the different ages assigned, the position of the phosphatic beds, and the FAD / LAD of Deshayesitidae and Cheloniceratinae ammonite families and subfamilies.

## REFERENCES

- Fichter, H.J. 1934: Geologie der Bauen-Brisen-Kette am Vierwaldstättersee und die zyklische Gliederung der Kreide und des Malm der helvetischen Decken. Beiträge zur geologischen Karte der Schweiz NF 69, 129 pp.
- Föllmi K.B. 2009: Neubenennungen lithostratigraphischer Einheiten in der helvetischen Kreide (Schweizerisches Komitee für Stratigraphie, Swiss Journal of Geosciences, 102/2). *Swiss Journal of Geosciences* 102, pp. 515-518.
- Föllmi, K.B. & Gainon, F. 2008: Demise of the Tethysian Urganian carbonate platform and subsequent transition towards pelagic conditions: The sedimentary record of the Col de la Plaine Morte area, central Switzerland. *Sed. Geol.* 205, 142-159.
- Heim Arnold 1913: Monographie der Churfürsten-Mattstock-Gruppe. Beiträge zur Geologischen Karte der Schweiz, Neue Folge, 20.Lieferung, 1. Teil 1910, 2. Teil 1913, 3. Teil 1916.
- Jacob & Tobler 1906: Etude stratigraphique et paléontologique du gault de la Vallée de la Engelberger AA (Alpes calcaires suisses, environs du Lac des quatre cantons). *Mém. Soc. Paléont. Suisse*, vol. 33.
- Linder, P., Gigandet, J., Hüsser, J.-L., Gainon, F., Föllmi, K.B. 2006: The Early Aptian Grünten Member: description of a new lithostratigraphic unit of the Helvetic Garschella Formation. *Eclogae geologicae Helvetiae* 99, 327-341.

## 7.11

### Radiolarian biostratigraphy and Miocene to Recent Cocos Plate motion in the frame of the tropical, E-Pacific palaeoceanographic setting (IODP Exp. 344, off Costa Rica).

Sandoval María Isabel<sup>1</sup>, Baumgartner Peter O,<sup>1</sup> Scientific Party of IODP (Integrated Ocean Drilling Program 344 Expedition)

<sup>1</sup> *Institute of Earth Sciences, Géopolis, University of Lausanne, CH-1015 Lausanne*

The IODP Expedition 344 (the “Costa Rica Seismogenesis Project” CRISP 2) drilled a transect across the convergent margin off Costa Rica (Figures 1, 2).

Five sites were drilled during seven weeks of expedition: **Site U1381** (8°25.7027'N, 84°9.4800'W, 2064.6 m water depth) is ~4.5 km seaward of the deformation front on the incoming (Cocos) plate, offshore Osa Peninsula and Caño Island, Costa Rica. Recovery was 103.8 mbsf. **Site U1414** (8°30.2304'N, 84°13.5298'W, 2459 m water depth), also located on the incoming plate, recovered 375.2 mbsf of sediments and basalt. The following sites were drilled in the Neogene slope apron of the upper (Caribbean) plate. **Site U1380** (8°35.9879'N, 84°4.3918'W, 502.7 m water depth). The coring reached 800 mbsf. **Site U1412** (8°29.1599'N, 84°7.7512'W, 1965 m water depth), involved drilling four holes with a maximum depth of 350.4 mbsf. Overall core recovery at this site was moderate (average of 59%), but became poor toward the bottom. **Site U1413** (8°44.4593'N, 84°6.8095'W, 540 m water depth), recovered sediments to 582.2 mbsf.

Micropaleontological samples were collected at all sites. Two sites from the Cocos plate were selected to obtain a detailed biostratigraphy of the middle Miocene to Recent oceanic sequence deposited on the incoming plate. At both localities radiolarian assemblages are well preserved and abundant. The sediments recovered from the two sites consist mainly of calcareous nannofossil ooze with foraminifers, diatoms and radiolarians. 295 samples were prepared with the standard method for Neogene Radiolarians. It consisted of extracting the radiolarians by washing the sample first with HCl 10% in order to digest carbonate and then washing it with H<sub>2</sub>O<sub>2</sub> 10% to destroy organic matter. Residues were collected with a 60µm mesh sieve.

The objectives of this study are: 1. detailed radiolarian biostratigraphy of the early-middle Miocene to Recent sequence of the incoming plate (Site U1381C, U1414A) and 2. a taxon-quantitative analysis aimed at tracing faunal changes related to the northward movement of the sites and to palaeoceanographic changes in context of the final closure of the Middle American Isthmus.

According to the modern plate motion vector, (7.3 cm/year, Mann 2007). Site U1414 A and U1381 C were located slightly south of Equator during the middle Miocene. Radiolarian assemblages of that age should therefore reflect the influence of the cold tongue generated by the South Equatorial Current. In contrast, today the sites are located in the influence of the warm North Equatorial Countercurrent (Fig. 2).

To achieve these objectives, 300 specimens will be counted per sample to obtain a representative faunal spectrum. An age model will be based on the radiolarian zonation for the tropics (Riedel et al 1978), the nannofossil zonation and paleomagnetic data that will be analyzed by others scientists of the expedition.

#### REFERENCES

- Riedel, W.R., Sanfilippo, A., Westberg-Smith, M.J. 1978: Cenozoic Radiolaria. Stratigraphy and Evolution of Tropical Cenozoic Radiolarians *Micropaleontology*, Vol. 24, No. 1, pp. 61-96.
- Mann, P, Rogers, R & Gahagma, L . 2007: Overview of plate tectonic history and its unresolved tectonic problems. In: *Central America Geology, Resources and Hazards* (Eds. Jochen Bundschuh and Guillermo E . Alvarado)

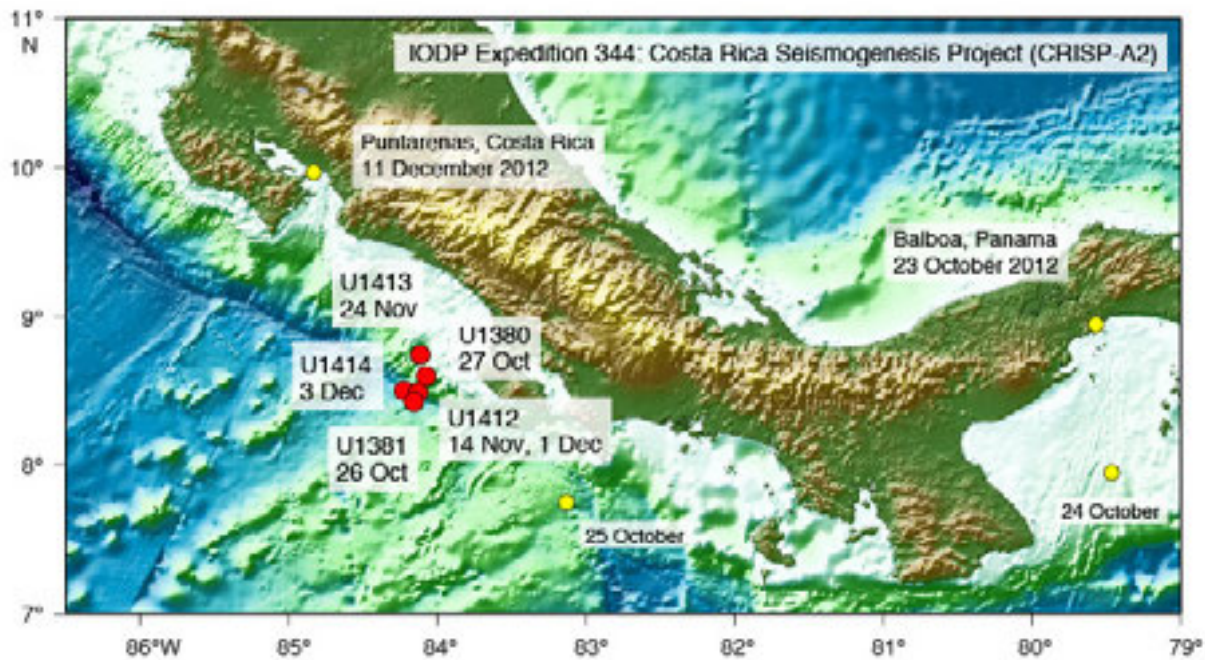


Figure 1: Location of the drilled sites of IODP 344 Expedition off Costa Rica

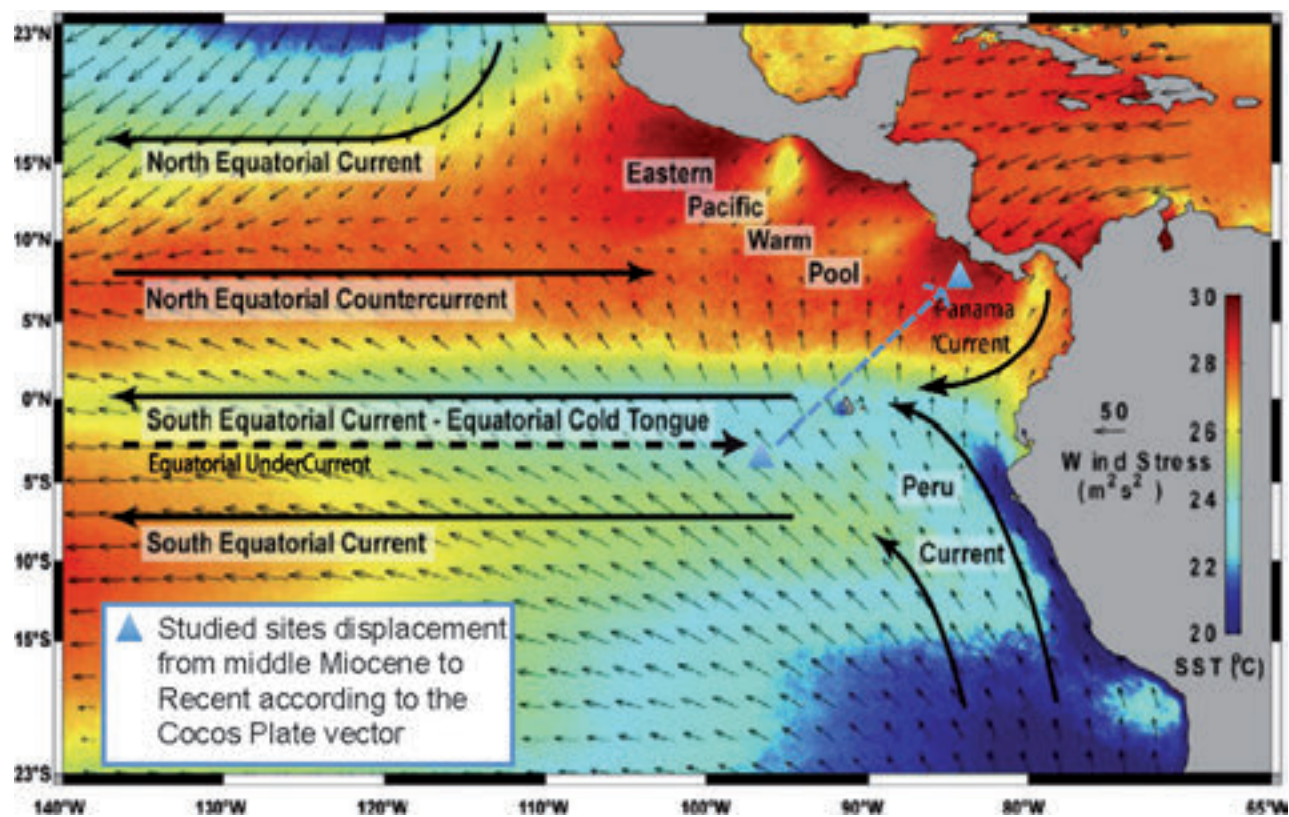


Figure 2: Oceanography of the tropical E-Pacific and projected displacement of the studied sites since middle Miocene. Taken from Baldessin *et al* (in preparation)

## P 7.1

# Upper Cenozoic dolostones from the Mayaguana Bank, SE Bahamas: new insights from a core study

Erika Baldessin<sup>1</sup>, Pascal Kindler<sup>1</sup>, Gyöngyvér Fischer<sup>1</sup> and Fabienne Godefroid<sup>1</sup>

<sup>1</sup> Section of Earth and Environmental Sciences, University of Geneva, 13 rue des Maraîchers, CH-1205 Geneva (Erika.Baldessin@unige.ch)

Preliminary study of a core retrieved from the Mayaguana Bank (SE Bahamas) reveals the occurrence of two distinctive dolomitization episodes in Cenozoic limestones. One of them only affects karst infills without influencing the encasing limestone, whereas the other is pervasive and completely replaces the parent carbonate facies.

Massive, pervasive dolomites have been described in the subsurface of the Bahamas for decades (Supko, 1970; Dawans, 1988), but the precise dolomitization mechanism remains uncertain (Machel, 2004). One core drilled on the north coast of Mayaguana contains intervals of both “karstic” and massive dolomite, and offers an opportunity to better constrain the dolomitization processes at the origin of these rocks.

Mayaguana is a small, elongated (57 x 13 km) carbonate island lying between latitudes N 22°15' - N 22°30' and longitudes W 72°40' - W 73°10' (Pierson, 1982) in the SE part of the Bahamas archipelago. Godefroid (2012) described several lithostratigraphic units exposed on the island, including the Mayaguana and the Little Bay Formations. The Mayaguana Formation consists of a Lower Miocene (18.4-18.7 Ma), fine-grained, hard limestone with numerous larger benthic foraminifers, whereas the Little Bay Formation is an Upper Miocene (5.59-6.81 Ma), solid, fine-grained, fabric-destroying dolostone, made of a dense network of microsucrosic dolomite.

A 43 m-long core was drilled at Little Bay with a CME 750X rubber-tired core drill by Martin Marietta Materials Company. Back in Geneva, the core was cut in half, logged and sampled for analyses.

Different findings were made during the preliminary examination of the core. First, the core spans a time interval from the Oligocene (Rupelian-Chattian according to the occurrence of the porcelaneous benthic foraminifer *Praerhapydionina delicata*) to the Early Miocene, with the Mayaguana Formation forming its top. This formation presents small karstic cavities and fissures filled with white, laminated, hard dolomite (Fig. 1) which is tentatively correlated to the Little Bay Formation. A pervasive dolomite occurs more deeply in the core (Fig. 2) and completely replaces the parent bioclastic limestone. These two types of dolomite likely result from distinctive and diachronous diagenetic events, and reflect different conditions of dolomitization during the Neogene on Mayaguana.

## REFERENCES

- Dawans, J.M.L., 1988: Distribution and petrography of Late Cenozoic dolomites beneath San Salvador and New Providence Islands, The Bahamas. Unpublished PhD Thesis, University of Miami, Florida, USA, 91 pages.
- Godefroid, F., 2012: Géologie de Mayaguana, SE de l'archipel des Bahamas. *Terre et Environnement*, Vol. 108, 230 pages. ISBN 978-2-940472-08-6.
- Machel, H.G., 2004: Concepts and models of dolomitization: a critical reappraisal. In: Braithwaite, C.J.R., Rizzi, G., and Darke, G. (eds), *The geometry and petrogenesis of dolomite hydrocarbon reservoirs*. Geological Society, London, Special Publications, v. 235, p. 7-63.
- Pierson, B.J., 1982: Cyclic sedimentation, limestone diagenesis and dolomitization in upper Cenozoic carbonates of the southeastern Bahamas. Unpublished PhD Thesis, University of Miami, Florida, USA, 286 pages.
- Supko, P.R., 1970: Subsurface dolomites, San Salvador, Bahamas. *Journal of Sedimentary Petrology*, vol. 47, n° 3, p. 1063-1077.

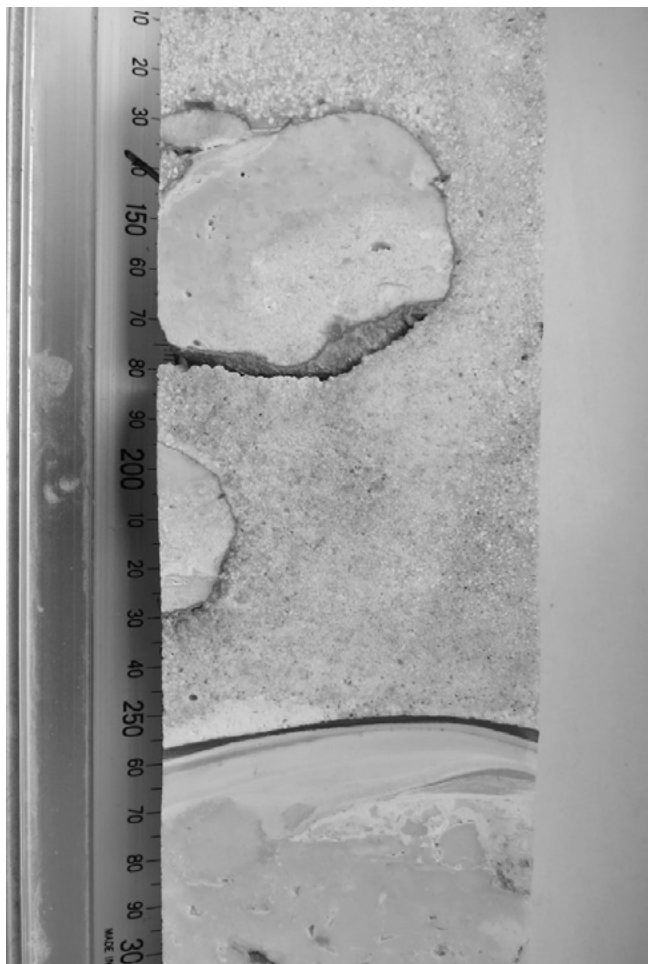


Figure 1 - Karstic dolomite

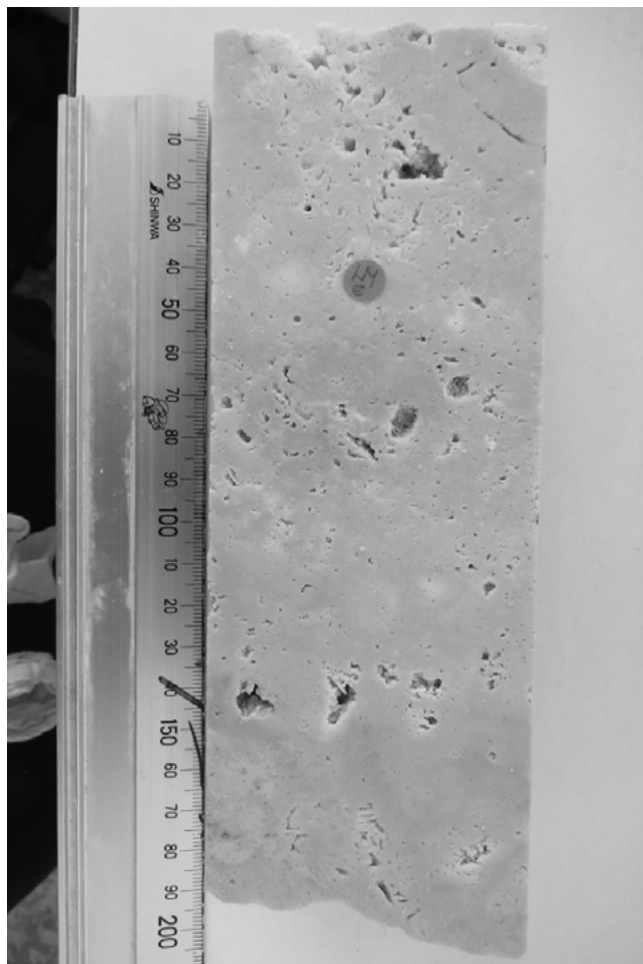


Figure 2 - Pervasive dolomite

## P 7.2

# Mid Cretaceous to Oligocene rise of the Middle American landbridge – documented by south-eastwards younging Larger Foraminifera in shallow water carbonates (Nicaragua – Costa Rica – Panama)

Baumgartner-Mora Claudia<sup>1</sup>, Baumgartner Peter O.<sup>1</sup>, Andjic Goran<sup>1</sup> & Barat, Flore<sup>2</sup>

<sup>1</sup> Institut des Sciences de la Terre, Université de Lausanne, Bâtiment Géopolis, CH-1015 Lausanne (claudia.baumgartner@unil.ch)

<sup>2</sup> Université de Nice-Sophia Antipolis, Laboratoire Géoazur, 06560 Valbonne, France

Basements of Southern Central America are oceanic in origin, including the southern half of the classical “Chortis Block” formed by subduction/accretion mélanges named Mesquito Composite Oceanic Terrane (MCOT, Baumgartner et al., 2008). The rise of these oceanic basements into the photic zone and their occasional emergence was controlled by convergent, collision tectonics, and/or arc development. In this context, shallow carbonate palaeo-environments were short-lived and formed on uplifted basements and arcs, and also on (now accreted) volcanic edifices of Pacific oceanic seamounts.

From Northern Nicaragua (NW) to Eastern Panama (SE) we observe a systematic younging of the **first** shallow water carbonate facies encroaching on basements and/or older deep-water formations: In the Siuna area (NE-Nicaragua) Aptian-Albian shallow water limestones dated by rudists and *Orbitolina texana* (Figure 1) rest unconformably on the Jurassic/Early Cretaceous Siuna Serpentinite Mélange, part of the MCOT. In N-Costa Rica, the assembly of several terranes (Santa Elena Ultramafic Unit, Nicoya Complex s. s., Matambu and Manzanillo Terranes) is overlapped by Late Campanian-Maastrichtian shallow water facies dated by rudists and Larger Foraminifera, such as *Pseudorbitoides rutteni*, *Pseudorbitoides israelski*, *Sulcoperculina* sp. and *Sulcoperculina globosa* (Baumgartner-Mora & Denyer, 2002). Reworked Campanian-Maastrichtian shallow water material including Larger Foraminifera was found in the Herradura Promontory (central Pacific coast of Costa Rica). It could be derived from an accreted seamount. No shallow carbonates are known so far from the early Palaeocene.

The Tempisque Basin (N-Costa Rica) hosts the Barra Honda carbonate platform (originally >900 km<sup>2</sup>) dated as late Palaeocene (Thanetian) by planktonic Foraminifera, <sup>87</sup>Sr / <sup>86</sup>Sr ratios and *Ranikothalia* spp. (Jaccard et al., 2001). Other late Palaeocene shallow carbonates documented in S-Costa Rica/W-Panama (Quepos, Burica) are interpreted as insular carbonate shoals (atolls?) on now accreted seamounts.

To the SE of the S-Nicoya fault line (Central Costa Rica) Late Cretaceous oceanic plateaus may represent actual outcrops of the trailing edge of the Caribbean Large Igneous Province (CLIP). These include the SE corner of the Herradura Promontory (Costa Rica) and the Azuero Plateau cropping out in Coiba, Sona and Azuero (Panama). CLIP formation triggered a new, E-dipping subduction zone and Campanian-Maastrichtian arc initiation on the CLIP edge (Buchs et al. 2011). By middle to late Eocene times this Middle American Arc and forearc areas reached the photic zone leading to widespread formation of carbonate banks/ramps. They are dated by many Larger Foraminifera of the genera *Amphistegina*, *Asterocyclina*, *Discocyclina*, *Euconoloides*, *Eofabiania*, *Fabiania*, *Gypsina*, *Helicolepidina*, *Heterostegina*, *Lepidocyclina*, *Linderina*, *Neodiscocyclina*, *Nummulites*, *Operculina*, *Orthophragmina*, *Polylepidina*, *Proporocyclina*, and *Sphareogypsina*.

The first shallow carbonates that encroach on arc/forearc basements in Panama are dated as Late Eocene in Azuero and the Canal Basin and as Oligocene, dated by *Lepidocyclina miraflorensis*, *L. giraudi*, *L. canellei* around the Chucunaque Basin of Eastern Panama.

Progressive shallowing of the trailing edge of the Caribbean plate from NW (middle/Late Cretaceous) to SE (Late Eocene-Oligocene) implies a growing restriction of the Atlantic – Caribbean – Pacific seaway that must have affected global circulation patterns, to be considered in palaeo-oceanographic/palaeo-climatic models of the Late Cretaceous –Tertiary.

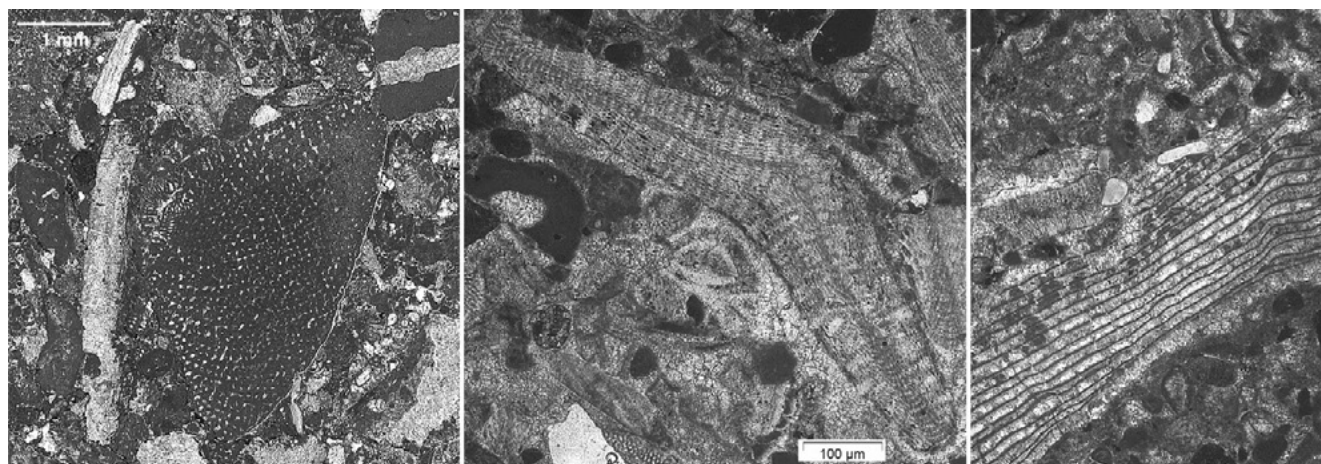


Figure 1. left: *Orbitolina texana* in a Aptian-Albian bioclastic shallow water limestone from the Siuna area (NE-Nicaragua). Center & right: Campanian bioclastic shallow water facies from Rio Nisperal, Santa Elena peninsula, N-Costa Rica. microsperic form of *Pseudorbitoides israeli* (center), rudistid fragment (right).

## REFERENCES

- Baumgartner, P. O., Flores, K., Bandini, A. N., Girault, F., & Cruz, D. (2008) Late Triassic to Cretaceous Radiolaria from Nicaragua and Northern Costa Rica - The Mesquito Oceanic Terrane.- *Ofioliti*, 33(1): 1-19.
- Baumgartner-Mora, C., Baumgartner, P. O., & Tschudin, P. (2008) Late Oligocene Larger Foraminifera from Nosara, Nicoya Península (Costa Rica) and Windward, Carriacou (Lesser Antilles), calibrated by  $^{87}\text{Sr} / ^{86}\text{Sr}$  isotope stratigraphy, *Rev. Geológica de America Central*, 38: 33-52.
- Baumgartner-Mora, C. And Denyer, P. (2002) Upper Cretaceous (Campanian-Maastrichtian) limestone with Larger Foraminifera from Pena Bruja Rock (Santa Elena Peninsula), *Revista Geologica de America Central*. 26 : 85-89.
- Buchs, D.M., Baumgartner, P.O., Baumgartner-Mora, C., Flores, K., and Bandini, A.N. (2011) Upper Cretaceous to Miocene tectonostratigraphy of the Azuero area (Panama) and the discontinuous accretion and subduction erosion along the Middle American margin: *Tectonophysics*, v. 512, p. 31-46.
- Jaccard, S., Münster, M., Baumgartner, P.O., Baumgartner-Mora, C. and Denyer, P. (2001) Barra Honda (upper Paleocene-lower Eocene) and El Viejo (Campanian- Maastrichtian) carbonate platforms in the Tempisque area (Guanacaste, Costa Rica). *Revista Geologica de America Central*, 24 : 9-28.

## P 7.3

# Geochemistry and $\delta^{30}\text{Si}$ of Radiolaria and Mesozoic Radiolarites of Panthalassa and Tethys

Bôle Maximilien<sup>1</sup> & Baumgartner Peter Oliver

<sup>1</sup>*Institut des Sciences de la Terre, University of Lausanne, Geopolis, CH-1015 Lausanne (maximilien.bole@unil.ch)*

Radiolarians, diatoms and sponges are currently the main consumers of silica in ocean. Until the Cenozoic explosion of diatoms, radiolarians had dominated the oceanic silicon cycle. Despite their important role in the past, only scarce geochemical data exists on radiolarites. In the frame of a SNF project, we are planning to compare radiolarites from the Mesozoic Panthalassa and Tethys Oceans.

Geochemical and mineralogical investigations are carried out to constrain the depositional conditions of radiolarians. For example, trace elements will be used to determine paleo-productivity and paleo-oxygenation of the water column (Tribovillard, 2006). In the Tethys, which was surrounded by continents, a stronger detrital influence is expected and will be verified by analysing the clay mineralogy and abundance.

The measurement of precise accumulation rates of biogenic silica is affected by the presence of non-biogenic silica in clays and detrital (aeolian) quartz. We are developing analytical methods to determine the biogenic silica fraction.

Concurrently, we are studying silicon isotopes of Jurassic to Recent radiolarians and in Mesozoic radiolarites, as very few data are currently available. Most data on silicon isotopes of biogenic silica were carried on diatoms and sponges. De La Rocha et al. (1998) have inferred a positive correlation for diatoms between primary productivity ( $\delta^{13}\text{C}_{\text{Org}}$ ) and  $\delta^{30}\text{Si}$ , considered to be a proxy for silicic acid consumption in the water column. We expect to examine such relationships on a global scale based on measurements in Mesozoic open ocean radiolarites.  $\delta^{30}\text{Si}$  should show similar but a little smoother trends than  $\delta^{13}\text{C}$  due to a longer residence time in sea water. Based on the result of Wu et al. (1997), radiolarians seem to have a lower fractionation factor than diatoms ( $\Delta^{30}\text{Si}_{\text{seawater-diatoms}} = -1.1\text{‰}$ ) but more work as to be done. In the modern ocean, De la Rocha et al. (1998) and Fripiat et al. (2011) demonstrated that  $\delta^{30}\text{Si}$  is influenced by currents. This is of particular interest in the search for understanding paleocurrents and oceanic changes during the Pangea break-up.

There are several challenges in this project. 1) Radiolarians produce their skeleton as biogenic opal that is recrystallized during diagenesis as microcrystalline chalcedony. We do not know if the silicon isotope signal is preserved in this process. 2) The radiolarian silicon isotope signal, present in chalcedony, needs to be distinguished from that of interstitial clays and oxides. However, many new insights will be obtained on the long-term silicon cycle and on the radiolarite dispersal trough time coupled with the Pangea break-up.

## REFERENCES

- De La Rocha C.L., Brzezinski M.A., DeNiro M.J. & Shemesh A. 1998: Silicon-isotope composition of diatoms as an indicator of past oceanic change. *Nature*, 395, 680-683
- Fripiat F., Leblanc K., Cavagna A.-J., Elskens M., Armand L. & Cardinal D. 2011: Efficient silicon recycling in summer in both Polar Frontal and Subantarctic Zones, southern Ocean. *Marine Ecology Progress Series*, 435, 47-61.
- Tribovillard N., Algeo T.J., Lyons T. Riboulleau A. 2006: Trace metals as paleoredox and paleoproductivity proxies: An update. *Chemical Geology*, 232, 12-32
- Wu S., Ding T., Meng X. & Bai L. 1997: Determination and geological implication of O-Si isotope of sediment core in the CC area, the Pacific Ocean. *Chinese Science Bulletin*, 42, 1462-1465

## P 7.4

# The Mayaguana Bank (SE Bahamas) from the Late Oligocene to the present: A delicate equilibrium between tectonics and sedimentation

Gyöngyvér Fischer<sup>1</sup>, Pascal Kindler<sup>1</sup>, Fabienne Godefroid<sup>1</sup> & Erika Baldessin<sup>1</sup>

<sup>1</sup> Département des Sciences de la Terre, University of Geneva, Rue des Maraîchers 13, CH-1205 Genève (Gyongyver.Fischer@unige.ch)

Four drill cores from the north and south coasts of Mayaguana (SE Bahamas), combined with a literature review on the surface geology of the island (Kindler et al., 2011; Godefroid, 2012), reveal that its stratigraphic units are distributed asymmetrically. This implies an initial ramp morphology of the bank with a northward dip in the Late Oligocene/Early Miocene, followed by a southward tilt of the platform during the Pleistocene.

The Mayaguana Bank is a small, rectangular carbonate platform (57x13 km) located in the south-eastern portion of the Bahamas archipelago in close proximity to the convergent margins of the North American and Caribbean plates (Dolan et al., 1998). A low relief island (maximum +30 m) covers most of the bank area (Pierson, 1982). An industrial drilling campaign, conducted in 2011, led to the recovery of several cores from the south-western part and from the north-western coast of Mayaguana. This paper presents the preliminary results obtained from four cores along a south-north transect in relation with outcrop data from the northern shoreline (Godefroid, 2012).

Petrographic, micropaleontological and geochemical (<sup>87</sup>Sr/<sup>86</sup>Sr) analyses enabled us to define four lithostratigraphic units briefly described below (from the top to the bottom):

- Poorly lithified reefal to peri-reefal limestones of Pleistocene age. This unit is characterized by the presence of corals of the genera *Acropora*, *Montastrea* and *Diploria*;
- Partly dolomitized, well-lithified reefal limestones of Middle Pliocene age. This unit contains corals of the genus *Stylophora* and encrusting algae;
- Microsugrosic, laminated dolostones yielding a Messinian age, essentially based on Sr-isotope data;
- Well-lithified and locally dolomitized bioclastic limestones (grainstone to rudstone). This unit is rich in hyaline and/or porcelaneous benthic foraminifers (Miogypsiniidae, *Praerhapydionina delicata*) with an age ranging from the Chattian to the Burdigalian (Eames et al., 1968; Godefroid, 2012).

These units form a 12 m-thick exposure along the north coast representing a condensed succession from the Early Miocene to the Middle Pleistocene (Godefroid, 2012). The Plio-Pleistocene boundary is exposed at up to +4 m above sea level (Godefroid, 2012). In the south, the Pliocene reefal carbonates and the Messinian dolostones are missing, leaving a discontinuity surface between the Pleistocene and the Lower Miocene strata found between -8.75 and -17 m below the present-day sea level.

The asymmetrical distribution of these stratigraphic units suggests a northward-dipping ramp configuration of the Mayaguana Platform, at least in the Middle Miocene. The positive accommodation in the north resulted in the deposition of the Messinian dolostones and of the Pliocene reefal carbonates, while in the south karstification and erosion of Upper Oligocene/Lower Miocene bioclastic limestones took place. The bank was likely tilted towards the south in the Middle Pleistocene, exposing the Lower Miocene to Lower Pleistocene succession on the north coast of Mayaguana.

The Mayaguana Platform represents a unique example of the behavior of a carbonate bank in the close proximity of an active tectonic margin.

## REFERENCES

- Dolan, J. F., Mullins, H. T., & Wald, D. J., 1998, Active tectonics of the north-central Caribbean: Oblique collision, strain partitioning, and opposing subducted slabs, in Dolan, J. F., and Mann, P., eds, Active strike-slip and collisional tectonics of the northern Caribbean plate boundary zone: Geological Society of America, Special Paper, 326, 1-61.
- Eames, F. E., Clarke, W. J., Banner, F. T., Smout, A. H., & Blow, W. H., 1968, Some larger foraminifera from the Tertiary of Central America: *Palaeontology*, 11, 49-59.
- Godefroid, F., 2012, Géologie de Mayaguana, SE de l'archipel des Bahamas : Terre & Environnement, 108, 1-230.
- Kindler, P., Godefroid, F., Chiaradia, M., Ehlert, C., Eisenhauer, A., Frank, M., Hasler, C.-A., & Samankassou, E., 2011, Discovery of Miocene to early Pleistocene deposits on Mayaguana, Bahamas: Evidence for recent active tectonism on the North American margin: *Geology*, 39, 523-526.
- Pierson, B. J., 1982, Cyclic sedimentation, limestone diagenesis and dolomitisation in upper Cenozoic carbonates of the southeastern Bahamas: Unpublished PhD thesis. University of Miami, Florida, USA, 1- 286.

## P 7.5

# Middle Pleistocene ostracod assemblages from Lake Trasimeno, Perugia, (Italy)

Marchegiano Marta<sup>1</sup>, Gliozzi Elsa<sup>2</sup>, Buratti Nicoletta<sup>3</sup>, Ariztegui Daniel<sup>1</sup> & Cirilli Simonetta<sup>3</sup>

<sup>1</sup> Section of Earth & Environmental Sciences, University of Geneva, 13 rue de Maraichers, 1205 Geneva, Switzerland, (marta.marchegiano@unige.ch, daniel.ariztegui@unige.ch)

<sup>2</sup> Department of Science, University Roma Tre, Largo S. Leonardo Murialdo, 1, 00146 Roma, Italy (elsa.gliozzi@uniroma3.it)

<sup>3</sup> Department of Geological Sciences, University of Perugia, Piazza Università 1, 06100 Perugia, Italy (stradott@unipg.it, simocir@unipg.it)

Lake Trasimeno is a meso-eutrophic, shallow (<6 m deep) and large lake (~120km<sup>2</sup>) located in central Italy, at 259 m above sea level. As it is common in shallow-water ecosystems, climate change plays a fundamental role in the Lake Trasimeno evolution and its history is signed by a strong dependence of the water balance on meteorological conditions (Dragoni, 2004; Ludovisi & Gaino, 2010). Recent geophysical data reveals that the Lake Trasimeno evolution was accompanied by a constant subsidence rate driven by normal faults. The extensional tectonic regime does not show substantial changes since the lake formation and it is probably responsible for its long-term preservation against sediment infill (Gasperini et al., 2010).

A 175 m long sedimentary core was retrieved by the Geological Survey of the Umbria Region along the present southern shore of the lake (north of Panicarola town). A multidisciplinary study of the core (i.e. palynology, paleontology, geochemical analyses, magnetic susceptibility, paleomagnetism) is now in progress and a preliminary age model based on pollen data suggests that the record may be as old as Middle Pleistocene. The investigation of the first 30 meters of the Panicarola core revealed its great potential as archive of palaeoclimatic/palaeoenvironmental changes in the region.

As widely recognized, ostracod assemblages in lacustrine sediments represent a main tool for palaeoenvironmental reconstructions (von Grafenstein, 2002; Decrouy et al., 2012). The absence or presence of different species, their possible polymorphism, and the geochemical composition of the valves are strongly controlled by the prevailing environmental parameters (i.e. water and/or air temperature, oxygen content, isotopic composition of the host waters, water quality, water chemistry, salinity) during their moulds (Horne et al., 2012; Viehberg & Mesquita-Joanes, 2012).

A first inspection of the Panicarola core reveals a constant presence of ostracod assemblages along the uppermost part (from 30 m to 5 m). On the whole, 13 species referable to 10 genera were collected (*Ilyocypris gibba*, *Candona neglecta*, *Candona angulata*, *Cypridopsis vidua*, *Heterocypris salina*, *Limnocythere sp1*, *Limnocythere stationis*, *Darwinula stevensoni*, *Cyprideis sp.*, *Leptocythere spp.*, *Fabaeformiscandona fabaeformis*, *Cyclocypris ovum*). Some changes in the frequency and composition of the ostracod assemblages have been detected along the sediment core, allowing to recognize different environmental variations. In particular, two intervals are significative for the palaeoenvironmental reconstruction of the sedimentary successions: 1) the interval from 25.60 m to 23.50 m is characterized by a rich ostracod fauna (dominated by *Cyprideis sp.*, *Candona angulata* and *Leptocythere spp.*). This assemblages is possibly indicating an increase in salinity; 2) the interval from 21.05 m to 17.60 m contains *Ilyocypris gibba*, *Candona neglecta*, *Cypridopsis vidua*, *Heterocypris salina*, *Limnocythere sp1*, *Limnocythere stationis* and *Darwinula stevensoni*. *Limnocythere stationis* is, a central European species, until now only signaled in Italy at the Panicarola core (this study) and in the Holocene of Sicily (Curry et al., 2013) probably suggesting a period of cool waters.

Further ostracod identifications as well as geochemical analyses on their valves will provide a more detailed reconstruction of the timing and magnitude of palaeoclimate changes in the Lake Trasimeno area

## REFERENCES

- Curry, B., Mesquita-Joanes, F., Fanta, S., Sterner, D., Calò C. & Tinner W., 2013 : Two coastal sinkhole lakes in SW Sicily (Italy) reveal low-salinity excursion during Greek and Roman occupation. 17th International Symposium on Ostracoda, Rome July 23-26, 2013, Il Naturalista Siciliano, Abstract Book, 93-95.
- Decrouy, L., Vennemann, T. & Ariztegui, D., 2012: Sediment penetration depths of epi- and infaunal ostracods from Lake Geneva (Switzerland). *Hydrobiologia* 688/1, 5-23
- Dragoni W. 2004 : Il Lago Trasimeno e le Variazioni Climatiche. Progetto informativo dell'assessorato all'Ambiente della Provincia di Perugia, Servizio Gestione e Difesa Idraulica, 1-60, Perugia
- Gasperini L., Barchi M.R., Bellucci L.G., Bortoluzzi G., Ligi M. & Pauselli C. 2010 : Tectonostratigraphy of Lake Trasimeno (Italy) and the geological evolution of the Northern Apennines. *Tectonophysics* 492, 164-174.
- Horne, D.J., Holmes, J.A., Rodriguez-Lazaro, J. & Viehberg, F. (Eds.) 2012 : Ostracoda as Proxies for Quaternary Climate

- Change. *Developments in Quaternary Sciences* 17, 1-373, Elsevier.
- Ludovisi A. & Gaino E. 2010 : Meteorological and water quality changes in Lake Trasimeno (Umbria, Italy) during the last fifty years. *J. Limnol.* 69 (1), 174-188.
- Viehberg, F.A., Mesquita-Joanes, F. 2012: Quantitative Transfer Function Approaches in Palaeoclimatic Reconstruction Using Quaternary Ostracods. In: Horne, D.J., Holmes, J.A, Rodriguez-Lazaro, J., Viehberg, F.A. (Eds.), *Ostracoda, as Proxies for Quaternary Climate Change. Developments in Quaternary Sciences*, 17: 47-64
- von Grafenstein, U., 2002 : Oxygen-isotope studies of ostracods from deep lakes. In Holmes, J. A. & A. R. Chivas (Eds.), *The Ostracoda: Applications in Quaternary Research*, AGU Geophysical Monograph, 131, 249–266

## P 7.6

### The “*Microbunodon* Event”, or the European evolution of ungulates during the Oligocene–Miocene transition

Scherler Laureline<sup>1</sup>, Mennecart Bastien<sup>2</sup>, Hiard Florent<sup>2</sup> & Becker Damien<sup>3</sup>

<sup>1</sup> Institut des Sciences de l'Evolution, Place Eugène Bataillon, Université de Montpellier 2, F-34095 Montpellier (laureline.scherler@net2000.ch)

<sup>2</sup> Département des Géosciences, Université de Fribourg, Chemin du Musée 6, 1700 Fribourg

<sup>3</sup> Musée jurassien des sciences naturelles, Route de Fontenais 21, 2900 Porrentruy

The biostratigraphy and diversity patterns of terrestrial, hoofed mammals help to understand the transition between the Palaeogene and the Neogene in Western Europe. Three phases are highlighted: 1) the beginning of the Arvernian (Late Oligocene, MP25-27) was characterised by a “stable” faunal composition including the last occurrences of taxa inherited from the Grande Coupure and of newly emerged ones; 2) the latest Arvernian (Late Oligocene, MP28-30) and the Agenian (Early Miocene, MN1-2) saw gradual immigrations leading to progressive replacement of the Arvernian, hoofed mammals towards the establishment of the “classical” Agenian fauna; 3) the beginning of the Orleanian (Early Miocene, MN3-4) coincided with the African-Eurasian faunal interchanges of the Proboscidean Datum Events and led to complete renewal of the Agenian taxa and total disappearance of the last Oligocene survivors. Faunal balances, poly-cohorts and particularly cluster analyses emphasise these three periods and define a temporally well-framed Oligocene-Miocene transition between MP28 and MN2. This transition started in MP28 with a major immigration event, linked to the arrival in Europe of new ungulate taxa, notably a stem group of “Eupecora” and the small anthracothere *Microbunodon*. Due to its high significance in the reorganisation of European ungulate communities, we propose to name it the *Microbunodon* Event. This first step was followed by a phase of extinctions (MP29-30) and later by a phase of regional speciation and diversification (MN1-2). The Oligocene-Miocene faunal transition ended right before the two-phased turnover linked to the Proboscidean Datum Events (MN3-4). Locomotion types of rhinocerotids and ruminants provide new data on the evolution of environments during the Oligocene-Miocene transition and help understand the factors controlling these different phases. Indeed, it appears that the faunal turnovers were primarily directed by migrations, whereas the Agenian transitional phase mainly witnessed speciations.

## P 7.7

# Paleoenvironmental reconstruction based on foraminiferal assemblages and the sedimentary phosphorus record in the Oligocene of Romania (Transylvanian Basin)

Székely Szabolcs-Flavius<sup>1,2</sup>, Spezzaferri Silvia<sup>2</sup>, Stalder Claudio<sup>2</sup>, Filipescu Sorin<sup>1</sup>

<sup>1</sup> Babeş-Bolyai University, Faculty of Biology and Geology, Geology Department, Str. M. Kogălniceanu 1, 400084 Cluj Napoca, Romania (szekely\_szabolcs\_flavius@yahoo.com)

<sup>2</sup> Department of Geosciences, University of Fribourg, Chemin du Musée 6, Perolles, 1700 Fribourg, Switzerland.

Oligocene deposits from Romania outcrop in the Vima Formation along the northwestern border of the Transylvanian Basin. Three outcrops in the Fântânele section were sampled for this study. The lithology is characterized by alternations of, clay, silty-clay, sandy-clay and sandstone. More than one hundred samples are analyzed for their benthic and planktonic foraminiferal content.

The presence of the species *Chiloguembelina cubensis* and *Paragloborotalia opima* places the assemblages of the first outcrop in the P21a Zone (04 Zone, Wade et al., 2011), while the younger sediments in the last two outcrops were probably deposited in the “Late Oligocene”. Other planktonic foraminifera such as *Globigerina lentiana*, *Globigerina praebulloides*, *Globigerinella obesa* are also present together with small sized tenuitellids e.g., *Tenuitella clemenciae*, *Tenuitella munda*, *Tenuitella angustiumbilocata*.

Paleoecological interpretations of the depositional environment are based on benthic calcareous and agglutinated forms. Benthic specimens are divided into three groups: epifaunal, shallow infaunal and deep infaunal. Epifaunal species such as *Heterolepa praecineta*, *Cibicidoides ungerianus filicosta* suggest higher oxygenation in the bottom water, while infaunal species indicate lower oxygen content (*Bulimina schischkinskayae*, *Bolivina dilatata dilatata*, *Fursenkoina* spp.). The assemblages are sometimes dominated by agglutinated foraminifera represented by *Haplophragmoides carinatus*, *Recurvoides* spp., *Karreriella* spp. and tubular forms (*Rhabdammina* spp., *Bathysiphon* spp.).

Phosphorus is extracted from the bulk sediment samples using the five-step SEDEX method (Ruttenberg et al., 2009). The distinguished sedimentary phosphorus phases (Loosely-bound P, Iron-bound P, Authigenic P, Detrital P and Organic-bound P) together with the distribution of the foraminiferal assemblages give a better view of the paleoenvironmental conditions during the Oligocene.

## REFERENCES

- Ruttenberg, K.C., Ogawa N.O., Tamburini F., Briggs R.A., Colasacco N.D., Joyce E., 2009: Improved, high-throughput approach for phosphorus speciation in natural sediments via the SEDEX sequential extraction method, *Limnol. Oceanogr.*: Methods 7, 319–333.
- Wade, B. S., Pearson, P. N., Berggren, W. A., Pälike, H., 2011: Review and revision of Cenozoic tropical planktonic foraminiferal biostratigraphy and calibration to the geomagnetic polarity and astronomical scale, *Earth-Science Reviews* 104, 111-142.

## 9. Environmental Biogeosciences

Jasquelin Peña, Rizlan Bernier-Latmani

### TALKS:

- 9.1 Bagnoud A., Schwyn B., Leupin O., Bernier-Latmani R.: *In situ* microbial oxidation of H<sub>2</sub> in the deep subsurface
- 9.2 Brauchli M., Bontognali T.R.R., McKenzie J. A., Vasconcelos C.: Evaluating the importance of microbial mats for dolomite formation in the Dohat Faishakh sabkha, Qatar
- 9.3 Dumas N., Peña J.: Impact of microbial surfaces on biogenic birnessite reactivity
- 9.4 Eglinton T., Shah S., Pearson A., Griffith D., Slater G., White H., Reddy C.: Utilizing natural abundance variations in radiocarbon to probe microbial metabolism in the environment
- 9.5 Jassey V.E.J., Lamentowicz M., Payne R., Mitchell E.A.D., Gilbert D., Robroek B.J.M., Mills R.T.E., Fournier B., Bragazza L., & Buttler A.: Use of a trait-based framework for predicting where microbial adaptation to climate change will affect peatland functioning
- 9.6 Kluepfel L., Piepenbrock A., Kappler A., Sander M.: Natural organic matter as a fully regenerable terminal electron acceptor for anaerobic microbial respiration in temporarily anoxic systems
- 9.7 Lacroix E., Brovelli A., Barry D. A. , Holliger C.: Utilization of Silicate Minerals for pH Control during *In Situ* Bioremediation of Chlorinated Solvents
- 9.8 Le Faucheur S., Portilla Castillo E., Slaveykova V.: Toxicity of mercury towards *Chlamydomonas reinhardtii* in presence of perfluorooctane sulphonate
- 9.9 Lloyd J.R.: Hot topics in environmental biogeosciences; the microbiology of the nuclear fuel cycle
- 9.10 Monteux S., Tisato N., Bontognali T.R.R., Torriani S., Tavagna M.-L., Chailloux D., Renda M., Eglinton T.: Hints towards a biogenic origin of Asperge Cave concretions
- 9.11 Senn A.-C., Kaegi R., Hug S., Hering J., Voegelin A.: Composition and structure of fresh and aged Fe oxidation products
- 9.12 Simanova A.A., Peña J.: Time-resolved *in situ* investigation of metal sorption mechanisms in layer-type manganese oxides
- 9.13 Spangenberg J. E., Ferrer M., Jacomet S., Bleicher N. & Schibler J.: Plant oils used to maintain bone and antler tools in the Neolithic lakeshore settlement, Zurich Opera Parking
- 9.14 Wang Y., Fruttschi M., Suvorova E., Phrommavanh V., Descostes M., Osman A., Geipel G., Bernier-Latmani R.: Uranium(IV) mobility in a mining-impacted wetland
- 9.15 Wrighton K.C., Castelle C.J., Wilkins M.J., Hug L.A., Sharon I., Thomas B.C., Lipton M.S., Long P.E., Williams K.H., Banfield J.F.: Metabolic interdependencies between phylogenetically novel fermenters and respiratory organisms in an unconfined aquifer

## POSTERS:

- P 9.1 Cailleau G., Pons S., Bindschedler S., Junier P., Verrecchia E.: When a century is enough to invert a million years' pedogenesis: the oxalate carbonate pathway in tropical agro-ecosystems
- P 9.2 Koishi A., Bragazza L., Maltas A., Sinaj S., Albrecht R., Pfeifer HR.: Long-term Organic Management Induced Changes in Soil Organic Matter Stability and Enzyme Activities
- P 9.3 Marafatto F.F., Pena J.: Mineralogical and chemical controls on the photoreductive dissolution of birnessite minerals
- P 9.4 Martignier A., Jaquet J.-M., Nirel P.: Typology of alkaline-earth metal precipitates in meso-oligotrophic lake (Léman, Switzerland)
- P 9.5 Pestrinaux C., Le Faucheur S., Mortimer M., Bernardi Aubry F., Botter M., Zonta R., Slaveykova V.: Effects of salinity on TiO<sub>2</sub> nanoparticles behavior and toxicity towards natural plankton. A case study: the Venice Lagoon, Italy
- P 9.6 Reinsch, B., Descostes, M., Bernier-Latmani, R., Rossi, P.: The impacts of acidic in-situ recovery of uranium in southern Kazakhstan on geochemistry and microbial community structure
- P 9.7 Pinard G., Spangenberg J. E., Adatte T., Verrecchia E.P.: Distribution and dynamics of SOM on carbonate rocks (Jura Mountains): a geochemical approach
- P 9.8 Tavagna M.L., Eglinton T.: Building a global database on organic geochemical characteristics of surface marine sediments: design & call for input
- P 9.9 Thomas C., Ariztegui D.: Archaeal 16S rRNA gene sequences in the deep extreme Dead Sea sediments: determining who is there and why?
- P 9.10 Wildi M., Le Faucheur S.: Structure of biofilm communities and their sensitivity to metals. A case study of the Lagoon of Venice
- P 9.11 Feldmann M.: The influence of the biological nitrogen cycle on stromatolite formation

## 9.1

### *In situ* microbial oxidation of H<sub>2</sub> in the deep subsurface

Bagnoud Alexandre<sup>1</sup>, Schwyn Bernhard<sup>2</sup>, Leupin Olivier<sup>2</sup> & Bernier-Latmani Rizlan<sup>1</sup>

<sup>1</sup> Environmental Microbiology Laboratory, Ecole Polytechnique Fédérale de Lausanne (EPFL), CH-1015 Lausanne (alexandre.bagnoud@epfl.ch)

<sup>2</sup> NAGRA, CH-5430 Wettingen, Switzerland

Autotrophic growth is metabolic strategy that is well described but for which there are few studies, particularly in the deep subsurface. The ability of microorganisms to carry out this type of metabolism is of importance due to their independence from sunlight-driven biogeochemical cycling. We performed an *in situ* experiment in which we amended a 25m long borehole, 300 meters deep in a Clay Rock formation in Western Switzerland with hydrogen. The goal of the experiment was to characterize the response of the microbial community to this amendment and to document the succession or parallel metabolisms that ensue.

Within a month of the start of the amendment, Fe(II) and sulfide appeared in the porewater, suggesting microbial Fe(III) reduction and sulfate reduction. Repeated H<sub>2</sub> amendments supported these findings. Isotopic fractionation of S, H, C and O was also evaluated and generally supported the dominance of microbial processes. We evaluated the rate of the microbial sulfate reduction using S isotope fractionation. Additionally, we monitored geochemical changes such as the depletion of sulfate in this low conductivity rock, the rapid consumption of H<sub>2</sub> and resumption of sulfate reduction after a few days of amendment interruption.

Community changes were monitored using 16S rRNA pyrosequencing as well as metagenomic and metatranscriptomic approaches. Pyrosequencing results to date confirm the rapid establishment of sulfate-reducing conditions and the predominance of one or several representative(s) of the family Desulfobulbaceae, Gram-negative sulfate reducing bacteria (SRB) with known genera able to grow on Fe(III), sulfate as well as autotrophic representatives. In fact, analysis of the porewater as a function of time (3 days, 48 days and 101 days after the start of H<sub>2</sub> amendment) shows a steady progression towards an increased contribution of this subset of microorganisms with time. This result is striking in light of the dominance of Gram-positive SRB in anoxic boreholes sampled at the same site. This works suggests that H<sub>2</sub> supports an active microbial community and strongly selects for a subset of SRB. The absence of H<sub>2</sub> at other boreholes precludes the growth of these autotrophic Gram-negative SRB. Current investigations focus on metagenomic analysis of the community to further describe the metabolic diversity within this family as well as to understand the biochemical basis for autotrophic growth. H<sub>2</sub> amendment has been ongoing for approximately 200 days and will continue with the aim to reach methanogenic conditions in the borehole and to further characterize the Archaeal community able to thrive *in situ*. This study is unique due to the unfettered access to the subsurface provided by the Mont Terri facility in Switzerland and the ability to monitor the processes as they unfold and to correlate concurrent geochemical and microbial changes.

## 9.2

# Evaluating the importance of microbial mats for dolomite formation in the Dohat Faishakh sabkha, Qatar

Marisa Brauchli<sup>1</sup>, Tomaso R. R. Bontognali<sup>2</sup> Judith A. McKenzie<sup>2</sup>, Crisogono Vasconcelos<sup>2</sup>

<sup>1</sup>*Institute of Evolutionary Biology and Environmental Studies, University of Zürich, Switzerland*

<sup>2</sup>*ETH Zürich, Geologisches Institut, Zürich, Switzerland*

Research conducted in recent years has demonstrated that microbes can induce dolomite formation at low temperature, providing a possible solution for the long-standing enigma surrounding the origin of sedimentary dolomite. The goal of this study was to evaluate the relationship between microbial activity and dolomite precipitation in the Dohat Faishakh sabkha, Qatar. This hypersaline coastal area was one of the first settings recognized as a rare modern geological environment where dolomite formation occurs (Illing et al., 1965). In previous studies, dolomite formation in this area was considered to be the result of a penecontemporaneous replacement of aragonite. However, no conclusive evidence confirms this hypothesis. To evaluate whether a “microbial factor” is important in this evaporitic environment, we collected core samples and microbial mats along a transect from the lower intertidal to the supratidal zone of the sabkha. X-ray diffraction analysis and measurements of total organic carbon (TOC) revealed the existence of a direct correlation between portions of the cores rich in buried organic material (likely the biomass of partially degraded mats) and dolomite. Oxygen and carbon stable isotope analysis of bulk carbonate samples indicates a strong positive co-variation, suggesting precipitation in isotopic equilibrium within a closed evaporative hydrologic system. Moreover, scanning electron microscopy (SEM) investigations showed that dolomite is not exclusively forming in the supratidal zone, but also in the lower intertidal zone, nucleating within the extracellular polymeric substances (EPS) of living microbial mats. EPS are recognized as an important component for the formation of Mg-rich carbonates. We, therefore, hypothesize that the main factor controlling the occurrence of dolomite within the sediments of the Dohat Faishakh sakha is the presence of EPS (constituting living and buried microbial mats) and not a replacement process transforming primary aragonite into dolomite, as proposed in earlier studies.

### REFERENCES

Illing et al., 1965, SEPM Spec. Publication 13, p. 89-111.

## 9.3

### Impact of microbial surfaces on biogenic birnessite reactivity

Dumas Naomi<sup>1</sup>, Jasquelin Peña<sup>1</sup>

<sup>1</sup>University of Lausanne, Switzerland, [naomi.dumas@unil.ch](mailto:naomi.dumas@unil.ch), [jasquelin.pena@unil.ch](mailto:jasquelin.pena@unil.ch)

Birnessite minerals (layer-type MnO<sub>2</sub>) are known for their ability to adsorb heavy metals in the environment. They are found in different soil compartments and can be precipitated by a wide range of microorganisms. When produced by bacteria, biogenic birnessite particles are typically deposited in a biofilm matrix comprised by bacteria, extracellular polymeric substances and mineral particles. However, the impact of the biofilm on the sorption behavior of heavy metals by biogenic birnessite is poorly understood. For example, Zhu et al., (2010) showed that heavy metals adsorbed preferentially to biomass when the mineral fraction was small relative to the biomass fraction (<4%). Other researchers using a biomass-mineral assemblage containing 10-20% birnessite by mass found that birnessite significantly enhanced Zn and Ni sorption relative to biomass alone, with trace metals adsorbing preferentially to birnessite cation vacancy sites (Peña et al., 2011; Peña et al., 2010; Toner et al., 2005). Based on these studies we hypothesize that changing the mineral-biomass ratio may cause birnessite-organic interactions that modify the mineral structure and/or the total number of surface sites that can bind metals.

The goal of this study is to evaluate the impact of the biofilm on the reactivity of biogenic birnessite at varying MnO<sub>2</sub>:biomass ratios. The experiments were performed with cultures of *Pseudomonas putida* strain GB-1, known for its ability to oxidize Mn. The birnessite-biomass sorbents were produced using bacterial cultures containing different concentrations of Mn to obtain sorbents with 0 to 14.5 % (on a mass basis) birnessite. We combined adsorption experiments for Ni at pH 6 with electron microscopy and X-ray absorption spectroscopy to better understand the molecular-scale reactivity of biogenic birnessite.

Our results indicate a difference in the adsorption reactivity of the composite biomass-birnessite assemblage depending on the mineral to organic ratio. Larger Ni uptake (molNi.mol<sup>-1</sup>Mn) was observed at low birnessite:biomass ratios than when birnessite is present in greater quantity. Our results suggest that the biomass fraction (bacteria and EPS) of the sorbent and the bacterial growth conditions play an important role in governing Ni removal. The impact of bacterial growth conditions on the composition of the biomass, mineral structure (e.g., vacancy content) and the interaction between mineral and organic matter should be accounted for in predicting the sorption behavior of complex microbe-mineral assemblages.

#### REFERENCES

- Peña, J., Bargar, J.R., Sposito, G., 2011. Role of Bacterial Biomass in the Sorption of Ni by Biomass-Birnessite Assemblages. *Environmental Science & Technology* 45, 7338-7344.
- Peña, J., Kwon, K.D., Refson, K., Bargar, J.R., Sposito, G., 2010. Mechanisms of nickel sorption by a bacteriogenic birnessite. *Geochimica et Cosmochimica Acta* 74, 3076-3089.
- Toner, B., Fakra, S., Villalobos, M., Warwick, T., Sposito, G., 2005. Spatially resolved characterization of biogenic manganese oxide production within a bacterial biofilm. *Applied and Environmental Microbiology* 71, 1300-1310.
- Zhu, M., Ginder-Vogel, M., Sparks, D.L., 2010. Ni(II) Sorption on Biogenic Mn-Oxides with Varying Mn Octahedral Layer Structure. *Environmental Science & Technology* 44, 4472-4478.

## 9.4

# Utilizing natural abundance variations in radiocarbon to probe microbial metabolism in the environment

EGLINTON Timothy I.<sup>1</sup>, SHAH Sunita<sup>2</sup>, PEARSON Ann<sup>3</sup>, GRIFFITH David R.<sup>2</sup>, SLATER Greg F.<sup>2,4</sup>, WHITE Helen K.<sup>2,5</sup>, REDDY Christopher M.<sup>2</sup>

<sup>1</sup> Geological Institute, ETH Zurich, Sonneggstrasse 5, CH-8092 Zurich (timothy.eglinton@erdw.ethz.ch)

<sup>2</sup> Woods Hole Oceanographic Institution, Woods Hole, MA 02543 USA

<sup>3</sup> Harvard University, Cambridge MA 02138 USA

<sup>4</sup> McMaster University, Hamilton, Ontario L8S 2G4, Canada

<sup>5</sup> Haverford College, Haverford, PA 19041, USA

Recent studies have revealed a remarkable diversity of microorganisms in the environment, as well as surprisingly diverse environmental conditions that appear conducive to sustain microbial life. A key challenge related to such findings concerns the elucidation of microbial metabolisms associated with specific environmental conditions and biogeochemical processes. The natural abundance of radiocarbon, with its half-life of approximately 5730 years, provides a powerful tool to probe metabolism of carbon-containing compounds in systems where distinct age contrasts exist in potential carbon sources available to microbial communities. With emerging methods that enable radiocarbon measurements on microgram quantities of carbon, it is now feasible to target an increasingly broad range of environmental systems, and to examine radiocarbon signals associated with individual organic compounds that may be characteristic of specific members of a microbial community. This presentation will provide an overview that seeks to highlight the manner in which natural-abundance radiocarbon measurements can help to shed light on carbon sources and processes associated with microbial communities in terrestrial and marine environments. Examples will be provided both for natural environment systems as well as those impacted by anthropogenic activity.

## 9.5

## Use of a trait-based framework for predicting where microbial adaptation to climate change will affect peatland functioning

Jassey Vincent EJ<sup>1,2</sup>, Lamentowicz Mariusz<sup>3,4</sup>, Payne Richard<sup>5</sup>, Mitchell Edward AD<sup>6</sup>, Gilbert Daniel<sup>7</sup>, Robroek Bjorn JM<sup>8</sup>, Mills Robert TE<sup>1,2</sup>, Fournier Bertrand<sup>6</sup>, Bragazza Luca<sup>1,2,9</sup>, & Buttler Alexandre<sup>1,2</sup>

<sup>1</sup> *École Polytechnique Fédérale de Lausanne (EPFL), School of Architecture, Civil and Environmental Engineering (ENAC), Laboratory of Ecological Systems (ECOS), Lausanne, Switzerland (vincent.jassey@epfl.ch; alexandre.buttler@epfl.ch; luca.bragazza@epfl.ch)*

<sup>2</sup> *WSL - Swiss Federal Institute for Forest, Snow and Landscape Research, Research Unit Community Ecology, Lausanne, Switzerland*

<sup>3</sup> *Department of Biogeography and Palaeoecology, Adam Mickiewicz University in Poznań, Dziegiełowa 27, 61-680 Poznań, Poland (mariuszl@amu.edu.pl)*

<sup>4</sup> *Laboratory of Wetland Ecology and Management, Adam Mickiewicz University in Poznań, Dziegiełowa 27, 61-680 Poznań, Poland*

<sup>5</sup> *Biological and Environmental Science, University of Stirling, Stirling FK94ND, Scotland, UK (r.j.payne@stir.ac.uk)*

<sup>6</sup> *Laboratory of Soil Biology, University of Neuchâtel, Neuchâtel, Switzerland (edward.mitchell@unine.ch; bertrand.fournier@unine.ch)*

<sup>7</sup> *Université de Franche-Comté – Laboratoire Chrono-Environnement, UMR CNRS/UFC 6249, F-25211 Montbéliard cedex, (daniel.gilbert@univ-fcomte.fr)*

<sup>8</sup> *Ecology and Biodiversity Group, Institute of Environmental Biology, Utrecht University, Utrecht, The Netherlands (b.j.m.robroek@uu.nl; bjorn.robroek@epfl.ch)*

<sup>9</sup> *University of Ferrara, Department of Life Science and Biotechnologies, Ferrara, Italy.*

As the earth system changes in response to human activities, a critical objective is to predict how biogeochemical process rates (e.g. carbon cycling) and ecosystem function (e.g. microbial decomposition) will change under future conditions. An important question within this context is the effect of warming on the microbial communities which control carbon cycling (Wallenstein & Hall 2012). Understanding linkages between microbial diversity and function is then essential if we are to increase our knowledge of the control mechanisms involved in biogeochemical cycling in ecosystems. Although microbial communities can adapt to changes in temperature and precipitation regimes, they are typically not optimally adapted to their local environment. Here we addressed the above by examining the effect of climate warming on the microbial food web and belowground functioning in temperate peatlands using a trait-based framework.

We conducted two different climate experiments in peatlands situated in the Jura and Alps mountains (France and Switzerland): a warming manipulation experiment by Open Top Chambers (OTCs) and an altitudinal experiment. The complex interplay between temperature increase, microbial community structure, microbial traits, microbial food web structure and ecosystem processes such as carbon cycling was studied in both studies. We focus our work on main microbial consumers within the microbial food web in peatlands: the testate amoebae, a diverse group of common soil protozoa. Samples of water were collected to determine the concentrations of dissolved organic carbon (DOC) - a sensitive indicator of changes in C cycling (Neff and Asner 2001).

We show that the community could be separated into two main categories, high vs. low trophic position taxa based on their shell-aperture size/body size ratio. This approach combined with the Community Size Spectrum (CSS) approach show that warming by OTCs reduced the size structure of testate amoebae. We found warming by OTCs excludes specialist microbial taxa such as top-predators (-70%) over two warming years. This, in turn, increased the functional redundancy of the main microbial consumer community. Similar tendencies were found along the altitudinal gradient, where the abundance of high trophic level testate amoeba species as well as the CSS increased from lowest to highest elevation (respectively by 3.7x and 6x). We further found in both experiments that changes in CSS of testate amoebae were concomitant to increases in DOC (Fig. 1), suggesting that decreased testate amoeba size structure enhance microbial decomposition and thus increase C turnover within the food web. These findings suggest that climate-induced changes in microbial community structure represent a mechanism controlling the carbon balance of peatlands.

### REFERENCES

- Wallenstein MD, Hall EK (2012) A trait-based framework for predicting when and where microbial adaptation to climate change will affect ecosystem functioning. *Biogeochemistry* 109(1-3): 35-47.
- Neff JC, Asner GP (2001) Dissolved organic carbon in terrestrial ecosystems: Synthesis and a model. *Ecosystems* 4(1): 29-48.

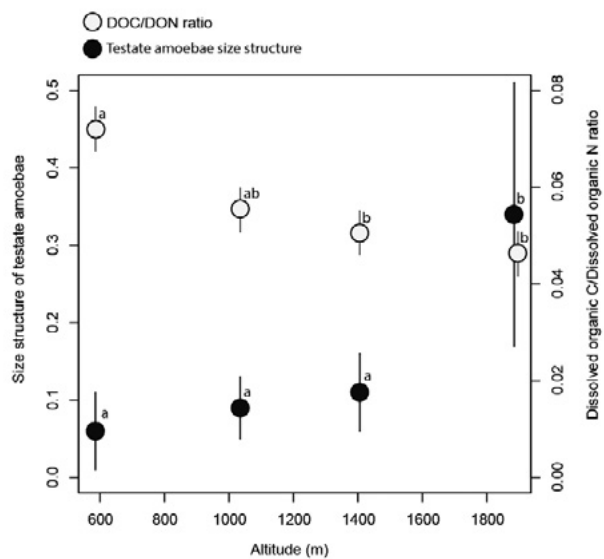


FIGURE 1: Size structure of testate amoebae and ratio of dissolved organic carbon over dissolved organic nitrogen in pore water at different altitude. Different superscripts indicate significant differences between sites for each variable ( $P < 0.05$ ,  $n = 77$ ).

## 9.6

# Natural organic matter as a fully regenerable terminal electron acceptor for anaerobic microbial respiration in temporarily anoxic systems

L.Klöpffel<sup>1</sup>, A.Piepenbrock<sup>2</sup>, A.Kappler<sup>2</sup>, M.Sander<sup>1</sup>

<sup>1</sup>Institute for Biogeochemistry and Pollutant Dynamics, Swiss Federal Institute of Technology Zurich (ETHZ)

<sup>2</sup>Geomicrobiology Group, Applied Geosciences, Eberhard Karls University, Tübingen, Germany

### Introduction

Natural organic matter (NOM) plays a key role in electron transfer reactions in many element cycles, including the carbon cycle. NOM is particularly important in temporarily anoxic environments with a high NOM content, such as wetlands and peats. In these system, NOM may serve as terminal electron acceptor (TEA) in anaerobic microbial respiration under anoxic conditions. Reduction of NOM may competitively suppress electron transfer to other TEAs, including CO<sub>2</sub>, and hence suppress hydrogenotrophic methanogenesis. Upon re-aeration, reduced NOM moieties may be re-oxidized by the transfer of electrons to O<sub>2</sub>. Despite the overall importance of NOM redox cycling to the biogeochemistry of temporarily anoxic environments, the changes in NOM redox state over successive microbial reduction and O<sub>2</sub> re-oxidation cycles have not been explicitly investigated. In previous studies, such changes in NOM redox states were difficult to quantify due to the lack of appropriate methods.

In this study we applied a novel electrochemical method, to (i) assess the reversibility of electron transfer to/from NOM over microbial reduction and O<sub>2</sub>-re-oxidation cycles (ii) to determine the sustainability of electron transfer over repeated redox cycles and (iii) to elucidate the thermodynamics of microbial NOM reduction.

### Method

We recently introduced mediated electrochemical analysis as a novel approach to quantify the redox states of dissolved NOM (Aeschbacher et al. 2010). This method employs electron transfer mediators to facilitate electron transfer between NOM and the working electrode of an electrochemical cell. The redox states of NOM are characterized by mediated reduction and oxidation towards defined reductive and oxidative potentials. The number of transferred electrons is measured directly as reductive and oxidative current responses which, upon integration, yield the electron accepting (EAC) and electron donating capacities (EDC). The EAC and EDC measurements are complemented by mediated potentiometric redox potential ( $E_h$ ) measurements in which small amounts of the mediators are used to facilitate  $E_h$  equilibration.

For this study; we conducted laboratory incubation experiments with four humic acids (HAs), which were both from aquatic and terrestrial sources and were chosen to represent a broad range of NOM. The HAs were inoculated with the facultative anaerobe *Shewanella oneidensis* MR-1 and lactate as electron donor. Using the electrochemical approach described above, we quantified the changes in redox states of the HAs over successive cycle of microbial reduction under anoxic conditions, followed by O<sub>2</sub> re-oxidation (Klöpffel et al, 2013, submitted).

### Results & Discussion

Anoxic incubations of HAs with *S. oneidensis* resulted in extensive microbial HA reduction, as evidenced by decreasing EAC and increasing EDC values. No changes in the redox states of the HAs were observed in sterile controls incubated under the same conditions. Introduction of O<sub>2</sub> resulted in re-oxidation of the microbially reduced NOM, as shown by increasing EAC and decreasing EDC values. The sum of EAC and EDC (=electron exchange capacity, EEC) in the inoculated samples stayed constant over the time course of the experiment (3 months) and was statistically indistinguishable from the EEC of the HAs in the sterile control samples. A constant EEC and hence number of redox active moieties in HAs implies that no redox active groups in the HA were being destroyed or created during the redox cycling. In addition, the constant EEC demonstrate reversible electron transfer to and from HA in single redox cycles and sustainable redox buffering by the HAs over consecutive redox cycles.

The use of mediated  $E_h$ -measurements revealed that the extents of microbial reduction of the different HAs was limited by system thermodynamics: Even though the four HAs used in the experiment exhibited very differing redox properties (e.g., EACs), they were reduced by *S. oneidensis* to comparable redox potentials,  $E_h$ , between -0.18 V and -0.2 V (pH 7; reported against the Standard Hydrogen Electrode). These potentials were much lower than the potentials of the unreduced HAs (0 V <  $E_h$  < +0.1 V). This implies that the tested HAs accepted electrons over wide  $E_h$  ranges, including iron reducing, sulfur reducing and methanogenic conditions.

### Implications

To assess the importance of NOM redox cycling for carbon cycling in temporarily anoxic environments, we compared methane fluxes reported for northern peatlands with the number of electrons that can be transferred to NOM under anoxic conditions and subsequently to O<sub>2</sub> under oxic conditions. For this calculation, we assumed 20 cm of annual water table fluctuation, which was reported in literature for peatlands, and EAC values for dissolved organic matter (from this work) and particulate organic matter (Roden et al. 2010). This estimation showed that NOM redox cycling may lead to a suppression of methane fluxes of 190'000 mol CH<sub>4</sub> per km<sup>2</sup> a<sup>-1</sup>, which corresponds to between 10 and 166% of reported average CH<sub>4</sub> fluxes from northern peatlands.

### REFERENCES

- Aeschbacher M., Sander M., Schwarzenbach R. 2010: Novel Electrochemical Approach to Assess the Redox Properties of Humic Substances. *Environmental Science & Technology*, 44(1), 87-93.
- Klöpfel L., Piepenbrock P., Kappler A., Sander M. Humics as fully regenerable terminal electron acceptors in recurrently anoxic environments. Under revision in *nature geoscience*
- Roden E., Kappler A., Bauer I., Jiang J., Paul A., Stoesser R., Knoishi H., Xu H. 2010: Extracellular electron transfer through microbial reduction of solid-phase humic substances. *nature geoscience*, 3, 417-421.

## 9.7

## Utilization of Silicate Minerals for pH Control during *In Situ* Bioremediation of Chlorinated Solvents

Lacroix Elsa<sup>1,2</sup>, Brovelli Alessandro<sup>2</sup>, Barry David Andrew<sup>2</sup> & Holliger Christof<sup>1</sup>

<sup>1</sup> Laboratory for Environmental Biotechnology, EPFL, Lausanne, Switzerland (elsa.lacroix@epfl.ch)

<sup>2</sup> Ecological Engineering Laboratory, EPFL, Lausanne, Switzerland

Chloroethenes such as tetrachloroethene (PCE) and trichloroethene (TCE) are among the most prevalent contaminants in groundwater due to their extensive use in industrial processes. *In situ* bioremediation (ISB) is an attractive technology for the removal of these compounds. This technology has been widely used for treatment of chloroethene plumes and recent studies have shown promising results for removal source zones containing dense non-aqueous phase liquids (DNAPLs). However, application of source zone ISB is still a significant technical challenge. One of the main issues is groundwater acidification due to organohalide respiration and fermentation processes, which can inhibit the activity of dehalogenating micro-organisms. The main objective of this work was to develop an efficient pH control strategy for chloroethene ISB by using the acid-neutralizing potential of silicate minerals. These minerals are of particular interest as their dissolution rate and their solubility is pH-dependent with faster kinetics and higher solubility in the acidic range. In addition, they persist in the subsurface and are long term alkalinity sources. Their usage therefore potentially reduces the frequency of injection of buffering solution.

To assess the potential of this technology, modeling and experimental approaches were combined. A geochemical model, implemented within PHREEQC, was developed to select appropriate buffer candidates and to help determine main parameters influencing mineral buffering capacity. The model included microbial degradation kinetics, mineral dissolution kinetics and chemical speciation. Anaerobic microcosm experiments were conducted to compare the buffering capacity of five silicate minerals in presence of organohalide-respiring bacteria (OHRB). Finally the long-term buffering capacities of three minerals (forsterite, fayalite and diopside) in porous media were investigated in flow-through column experiments. The columns were bioaugmented with an organohalide-respiring consortium containing *Dehalococcoides* and were operated at close to saturation concentrations to reproduce the conditions found in the contamination source zone. The distribution of the microbial communities at the end of the experiment was evaluated by molecular biology analyses.

The results of model simulations confirmed that silicate minerals are promising candidates for pH control of groundwater undergoing ISB. The efficiency of the system is dependent on mineral dissolution kinetics, equilibrium constants, temperature, and reactive surface area. The developed model allows the estimation of the amount of mineral needed to maintain the pH in the neutral range for specified site characteristics. Results of microcosm experiments with silicate minerals demonstrated that, under the selected conditions, diopside, fayalite, forsterite and andradite were able to maintain the pH in the appropriate range for PCE degradation, i.e., between 5.5 and 7.5. However, minerals containing iron III such as andradite had inhibitory effect on organohalide respiration due to their influence on the redox potential.

The results the column experiment showed that olivine minerals (such as fayalite and forsterite) are suitable agents for long-term pH control. They successfully maintained the pH in the neutral range (7.5 for forsterite and 6.5 for fayalite) and sustained the activity of OHRB. In contrast, the buffering potential of diopside rapidly decreased due to the formation of a less-reactive cation-depleted leached layer at the mineral surface. This study demonstrated the potential of silicate minerals to act as a long-term source of alkalinity release for groundwater pH control. This technology was applied here to the particular case of chlorinated solvent ISB but can be extended to any groundwater remediation technology requiring near neutral pH conditions.

## 9.8

# Toxicity of mercury towards *Chlamydomonas reinhardtii* in presence of perfluorooctane sulphonate

Le Faucheur Séverine<sup>1</sup>, Portilla Castillo Enrique C.<sup>1</sup> & Slaveykova Vera<sup>1</sup>

<sup>1</sup> *Aquatic Biogeochemistry and Ecotoxicology, University of Geneva, Institute F.A. Forel, 10 route de Suisse, CP 416, CH-1290 Versoix (severine.lefaucheur@unige.ch)*

In natural waters, aquatic organisms are exposed to cocktails of numerous inorganic and organic micropollutants. However, if algal response to one toxicant at a time is now better known, their sensitivity to mixture of pollutants is still poorly understood. The present study aims to fill this gap and examines the effect of mercury (Hg) and perfluorooctane sulphonate (PFOS) mixtures towards the unicellular green algae, *Chlamydomonas reinhardtii*. PFOS is a synthetic surface-active compound, which, such as Hg, is environmentally persistent and accumulates in wildlife around the globe (Giesy & Kannan 2002; Houde *et al* 2006). PFOS is also known to increase algal membrane permeability (Liu *et al* 2008). Our working hypothesis is thus that the presence of PFOS will modify algal Hg accumulation and as such increases its toxicity.

To that end, *C. reinhardtii* is exposed for 48 h to increasing concentrations of Hg (0.1  $\mu\text{M}$  to 1  $\mu\text{M}$  – 92% under  $\text{HgCl}_2^0$  form) and three concentrations of PFOS (0.01  $\mu\text{M}$ , 1  $\mu\text{M}$  and 100  $\mu\text{M}$ ), alone and in combination. Algal growth as well as pollutant impact on its physiology is determined using flow cytometry and fluorescence microscopy. Cell dying with propidium iodide is used to assess modifications of algal membrane permeability. Additionally, intracellular Hg concentrations are measured with an Advanced Mercury Analyser after washing algal cells with cysteine.

Algal growth remains optimal up to 0.2  $\mu\text{M}$  Hg, whereas higher Hg concentrations (0.4  $\mu\text{M}$ ) lead to 27 % of growth inhibition. No additional physiological effects such as modifications of cell size, granularity or chlorophyll *a* content are measured at the studied Hg concentrations. PFOS alone does not affect algal growth or the studied physiological parameters up to 100  $\mu\text{M}$  whereas no effect on algal membrane permeability is observed. Mixtures of 0.2  $\mu\text{M}$  Hg or 0.4  $\mu\text{M}$  Hg with 0.01  $\mu\text{M}$  PFOS and 1  $\mu\text{M}$  PFOS induce similar growth inhibition as exposure to Hg alone. However, exposure to 0.4  $\mu\text{M}$  Hg or 0.6  $\mu\text{M}$  Hg with 100  $\mu\text{M}$  PFOS leads to about 2.5 times higher toxicity towards algae than exposure to Hg alone. This result could be partly explained by a 1.5-time increase of intracellular Hg concentration in these conditions. The present study demonstrates that Hg can be more toxic to algae when exposed in combination with other pollutants (here PFOS) than alone and that aquatic organisms may not be fully protected by established legislation due to mixture effects.

## REFERENCES

- Giesy, J.P. & Kannan K. 2002: Perfluorochemical surfactants in the environment. *Environmental Science and Technology*, 36, 146A-152A.
- Houde, M., Martin, J.W., Letcher, R.J., Solomon, K.R. & Muir, D.C.G. 2006: Biological monitoring of polyfluoroalkyl substances: a review. *Environmental Science and Technology*, 40, 3463-3473.
- Liu, W., Chen, S., Quan, X. & Jin, Y.-H. 2008: Toxic effect of serial perfluorosulfonic and perfluorocarboxylic acids on the membrane system of a freshwater alga measured by flow cytometry. *Environmental Toxicology and Chemistry*, 27, 1597-1604.

## 9.9

# Hot topics in environmental biogeosciences; the microbiology of the nuclear fuel cycle

Jonathan R. Lloyd

*University of Manchester, UK*

Microorganisms are able to colonise some of the most extreme environments on Earth, including highly radioactive environments associated with the nuclear fuel cycle. In nuclear facilities, their proliferation as biofilms or planktonic “blooms” can cause operational challenges and concerns regarding the long-term stability of stored nuclear waste. However, in contaminated land they can have a controlling influence on the solubility of actinides and fission products, and here microbial activity can be harnessed for non-invasive bioremediation applications. In the “far field” deep geosphere surrounding underground nuclear repositories, microorganisms can also immobilise redox active radionuclides via respiratory processes that either change directly the oxidation state of the element, or produce new biogenic phases for enhanced sorption. In the “near field” of the repository, where higher level wastes are located, the direct and indirect impacts of microbial metabolism are less well characterised but have the potential to have a significant impact on waste-form evolution and radionuclide mobility, and must be incorporated into the safety case of the repository.

Recent work on the molecular ecology of a range of nuclear facilities will be discussed, and the impact of microbial metabolism on various steps of the nuclear fuel cycle discussed. Focusing on contaminated land and geodisposal scenarios, this talk will also discuss the biogeochemistry and redox cycling of priority radionuclides including U, Np, Pu and Tc in the subsurface, including both reduction and oxidation reactions and their impact on soluble and insoluble radionuclide inventories. The roles of proteins, secreted electron shuttles and other microbial products will be discussed alongside additional controls coupled to bulk element cycles e.g. the production of new mineral phases or significant changes in the geochemical environment such as pH. Studies from a range of contrasting natural and engineered systems will highlight how microbial communities can respond to the radioactive inventory and the extreme (radio)chemistry of some disposed wastefoms, and ultimately control the biogeochemical fate of key radioactive elements, including new studies on microbial gas metabolism, metal chelate (ISA) biodegradation and radionuclide biotransformations mediated via direct and indirect interactions with microbial systems.

## 9.10

### Hints towards a biogenic origin of Asperge Cave speleothems

MONTEUX Sylvain<sup>1</sup>, TISATO Nicola<sup>2</sup>, BONTOGNALI Tomaso Renzo Renzio<sup>2</sup>, TORRIANI Stefano<sup>3</sup>, TAVAGNA Maria Luisa<sup>2</sup>, CHAILLOUX Daniel<sup>4</sup>, RENDA Michel<sup>5</sup> & EGLINTON Timothy Ian<sup>2</sup>

<sup>1</sup> University Montpellier 2, 34095 Montpellier Cedex 5 (FR) (Monteux.s@gmail.com)

<sup>2</sup> ETH Zürich, Geologisches Institut, 8092 Zürich (CH)

<sup>3</sup> ETH Zürich, Institut für Integrative Biologie, 8092 Zürich (CH)

<sup>4</sup> Association de Recherche et d'Etude du Milieu Souterrain, 91830 Le Coudray-Montceaux (FR)

<sup>5</sup> Commission scientifique Fédération française de spéléologie, 69002 Lyon (FR)

Asperge Cave (Hérault, FR) is 7 km long, 126 m deep, and opens at the contact between schist and marble (Alabouvette et al., 1982). Limited zones of the cave present acicular-, coralloid-, and bulb-shaped aragonitic speleothems, as well as beaded aragonite which formation is still unexplained (Davis, 2012), (Fig. 1). The presence of blue aragonite is related to the important copper and uranium concentrations in the ceiling schists, as revealed by XRF analyses. Atypical morphologies such as U-loops, as well as field observations of mycelium-like filaments and microbial biofilms (Fig. 2) suggest that the speleothems could be biogenic. In addition, SEM analyses (Fig. 2C) showed that the coralloid concretions present extracellular polymeric substances (EPS) on the inner and outer parts, suggesting that calcite precipitation could be mediated by these EPS.

In order to investigate the microbial diversity, environmental DNA was sampled in portions of the cave presenting the speleothems. The bacterial diversity was proven different from other European caves diversity and consisted in 30 to 60% of putative new species, genera or higher clades. Cultivable bacteria isolated from the biofilms were checked for their ability to induce carbonate precipitation. Strains belonging to the phylum Actinobacteria were able to induce carbonate precipitation, in agreement with similar cave studies (Diaz-Herraiz et al., 2013).

Due to the high concentrations of copper in the ceiling schists, copper tolerance was assessed for the cultivable bacteria isolated from the biofilms. Most of the strains were tolerant to high concentrations of cupric ion, with some strains resisting up to 1g Cu<sup>2+</sup>.L<sup>-1</sup>. Uranium tolerance has not yet been assessed, but genetic analyses showed that a third of the strains from the concretions room were closely related with strains sequenced in highly radioactive environments.

We hypothesize that the heavy metal tolerances could be linked to detoxification via co-precipitation of calcite and heavy metals. This precipitation could be mediated by biofilms' EPS as it has been shown in other studies (Decho, 2010).

Further investigations would allow to (1) inventory new diversity; (2) understand these speleothems' genesis and mineralization mechanisms; (3) search for bioremediation processes for heavy-metal and radioactive polluted environments.

#### REFERENCES

- Alabouvette, B., Arthaud, F., Bambier, A., Freytet, P., Paloc, H. 1982: Carte et notice explicative de la feuille de Saint-Chinian à 1/50,000. BRGM Map no. 1014, scale 1:50,000.
- Davis, D.G. 2012: Helictites and Related Speleothems. In *Encyclopedia of Caves* (Second Edition), William B. White, and David C. Culver, eds. (Amsterdam: Academic Press), 379–383.
- Decho, A.W. 2010: Overview of biopolymer-induced mineralization: What goes on in biofilms? *Ecological Engineering* 36, 137–144.
- Diaz-Herraiz, M., Jurado, V., Cuezva, S., Laiz, L., Pallecchi, P., Tiano, P., Sanchez-Moral, S., and Saiz-Jimenez, C. 2013: The actinobacterial colonization of Etruscan paintings. *Sci Rep* 3, 1440.

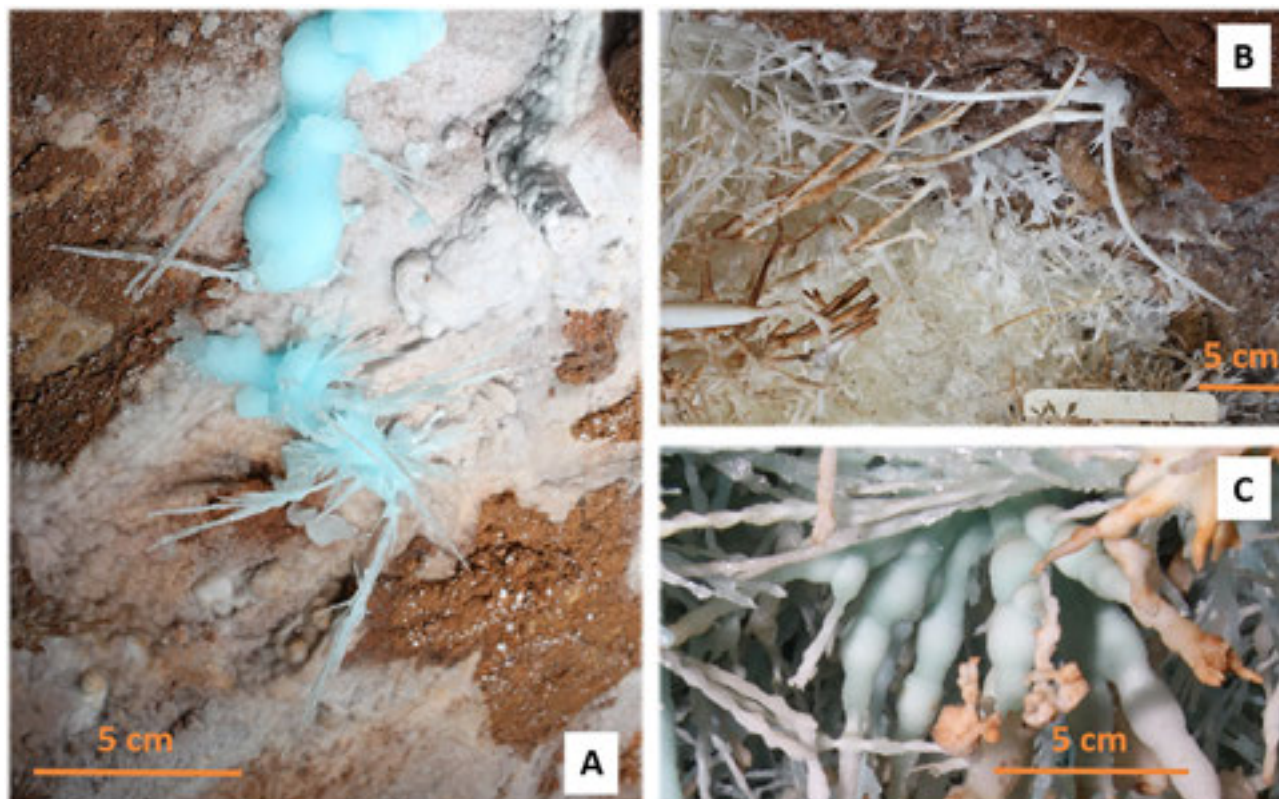


Figure 1. Various aragonite morphologies. A) Acicular and bulb-shaped aragonite; B) Coralloid aragonite; C) Beaded and acicular aragonite. Credits: Nicola Tisato

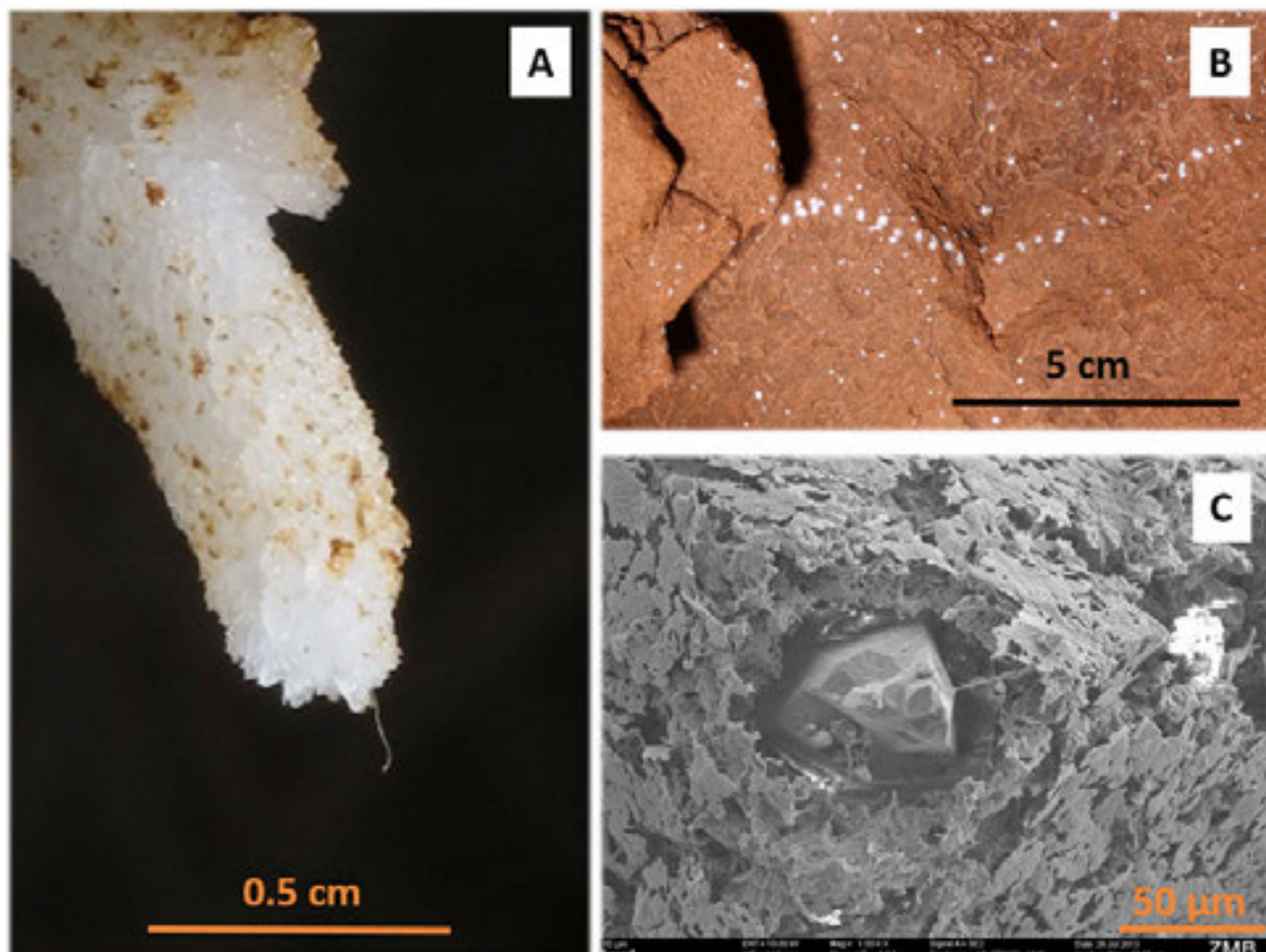


Figure 2. Hints towards a biogenic origin. A) Mycelium-like filament at the tip of a coralloid concretion; B) Microbial biofilms in the vicinity of the concretions; C) Calcite crystal of a coralloid concretion surrounded by extracellular polymeric substances. Credits: Nicola Tisato

## 9.11

### Composition and structure of fresh and aged Fe oxidation products

Senn Anna-Caterina, Kaegi Ralf, Hug Stephan, Hering Janet, Voegelin Andreas

*Eawag, Swiss Federal Institute of Aquatic Science and Technology, Überlandstrasse 133, CH-8600 Dübendorf  
(anna-caterina.senn@eawag.ch)*

The oxidation of dissolved Fe(II) by O<sub>2</sub> leads to the formation of amorphous to poorly crystalline Fe(III)-precipitates. These precipitates control the fate of major and trace elements at redox-interfaces and play an important role in many natural and technical systems. Dissolved phosphate (P), silicate and Ca are major factors controlling composition and structure of fresh Fe(III)-precipitates [1, 2, 3]. In this study, we therefore investigated (i) the interdependent effects of P/Fe ratio, Si and Ca on the composition and structure of fresh Fe(III)-precipitates formed by oxidation of 0.5 mM Fe(II) in bicarbonate-buffered solution at pH 7.0 and (ii) changes in precipitate composition and structure during aging for 30 days at 40 °C.

During Fe(II) oxidation, mostly lepidocrocite (Lp) formed at initial P/Fe ratios below ~0.1. Phosphate was nearly completely co-precipitated with Fe(III) up to an initial molar P/Fe ratio of ~0.55 in the absence of Ca and ~0.75 in the presence of dissolved Ca. Above these P/Fe ratios, only amorphous Fe(III)-phosphate formed and phosphate removal was incomplete. Enhanced co-precipitation of phosphate and Ca with Fe(III) was attributed to electrostatic effects and to the formation of mixed Ca-Fe(III)-phosphates, with a fraction of Fe(III)-octahedra exhibiting mitridatite-like corner- and edge-sharing linkage. Silicate did not interfere with the initial phosphate uptake but inhibited Lp formation at low P/Fe ratios, instead promoting the formation of hydrous ferric oxide (HFO; ferrihydrite-like polymers with limited corner-sharing linkage of Fe(III)-octahedra). Continuing Fe(III) polymerization during aging led to the remobilization of phosphate, especially in the absence of Ca and silicate. Phosphate remobilization was limited in the presence of Ca, which stabilizes mixed Ca-Fe(III)-phosphate, and especially silicate, which inhibits Fe(III) polymerization into crystalline Fe(III)-precipitates.

The results from this study form the basis for an improved mechanistic and quantitative understanding of Fe(III)-precipitate formation and trace element co-sequestration at aquatic redox-interfaces and in technical systems, for example drinking water treatment for As removal.

#### REFERENCES

- Voegelin, A., Senn, A.-C., Kaegi, R., Hug, S. J., Mangold, S. 2013: Dynamic Fe-precipitate formation induced by Fe(II) oxidation in aerated phosphate-containing water. *Geochim. Cosmochim. Acta* 117, 216-231.
- Voegelin, A., Kaegi, R., Frommer, J., Vantelon, D. & Hug, S. J. 2010: Effect of phosphate, silicate, and Ca on Fe(III)-precipitates formed in aerated Fe(II)- and As(III)-containing water studied by X-ray absorption spectroscopy. *Geochim. Cosmochim. Acta* 74, 164-186.
- Kaegi, R., Voegelin, A., Folini, D. & Hug, S. J. 2010: Effect of phosphate, silicate, and Ca on the morphology, structure and elemental composition of Fe(III)-precipitates formed in aerated Fe(II) and As(III) containing water. *Geochim. Cosmochim. Acta* 74, 5798-5816.

## 9.12

## Time-resolved *in situ* investigation of metal sorption mechanisms in layer-type manganese oxides

Simanova Anna<sup>1</sup>, Peña Jasquelin<sup>2</sup>

<sup>1</sup> Institute of Earth Sciences (ISTE), Faculté des géosciences et de l'environnement, University of Lausanne, Batiment Geopolis, CH-1015 Lausanne (anna.simanova@unil.ch)

<sup>2</sup> Institute of Earth Sciences (ISTE), Faculté des géosciences et de l'environnement, University of Lausanne, Batiment Geopolis, CH-1015 Lausanne (jasquelin.pena@unil.ch)

Manganese oxides are minerals commonly found in aquifers, soils, and sediments and are thought to originate mostly from microbially catalyzed Mn(II) oxidation. They are characterized by a layer-type crystal structure with hexagonal sheet symmetry and abundant vacant Mn(IV) sites. Due to their high sorption capacity for metals, these minerals strongly influence the distribution, mobility and bioavailability of the metals in the environment.

Traditionally, the mechanisms of trace metal sorption on mineral surfaces are studied on pre-equilibrated samples by bulk X-ray absorption spectroscopy (XAS). In general, metals have been shown to sorb via the following mechanisms: 1) sorption at the vacancy sites via triple-corner sharing (TCS) coordination; 2) incorporation into the vacancy site (Inc); 3) sorption at the particle edges via double-corner or double-edge sharing coordination (DCS or DES). The coordination geometry of adsorbed metals varies with pH, mineral structure, and nature of a metal. For example, at the surface of both biotic and abiotic birnessite Co(II) is sorbed as a TCS complex, which can be oxidized to Co(III) and incorporated into the MnO<sub>2</sub> sheet resulting in a mixture of TCS and Inc (Manceau et al, 1997). In contrast, the bonding environment of Ni highly depends on the type of birnessite and pH. At pH 6 at the surface of biogenic birnessite Ni(II) can sorb as TCS complex, while at pH 8 it occurs as a mixture of Inc and TCS species (Peña et al, 2010). In the case of abiotic birnessite ( $\delta$ -MnO<sub>2</sub>), the surface speciation of Ni significantly differs at pH 6 where Ni is found as a mixture of TCS, DCS and DES, while at pH 8 the bonding mechanism closely resembles that observed at the biogenic birnessite (Simanova et al 2013).

Detailed knowledge of trace metal sorption mechanisms is crucial for predicting the mobility, bioavailability and thus environmental fate of heavy metals. However, for more complete understanding we also need to acquire knowledge about the time scale over which different surface species are formed. Previously, the sorption speciation has been probed using the bulk XAS measurements of samples pre-equilibrated for hours to days, while evolution of different surface species may lie in second-to-minute time scale. In this study, we apply quick X-ray absorption spectroscopy (QXAS) to gather time-resolved *in situ* XAS spectra of Co or Ni sorbed at the birnessite particles at different surface loadings and pH values. We collected Co and Ni K-edge QXAS spectra to follow the changes in the bonding environment and Mn K-edge QXAS spectra to monitor any changes in Mn oxidation states and birnessite structure. Information on time-resolved evolution of different surface complexes will help us better understand the reactivity of different surface sites (e.g., vacancy sites, particle edges) towards metal sorption.

### REFERENCES

- Manceau, A., Drits, V.A., Silvester, E., Bartoli, C., Lanson, B. 1997: Structural mechanism of Co<sup>2+</sup> oxidation by the phyllosulfate buserite. *American Mineralogist* 82, 1150-1175.
- Peña, J., Kwon, K.D., Refson, K., Bargar, J.R., Sposito, G., 2010: Mechanisms of nickel sorption by a bacteriogenic birnessite. *Geochim. Cosmochim. Acta* 74, 3076-3089.
- Simanova A.; Bone S.; Bargar J.; Sposito G.; Peña, J. 2013: Ni sorption at the particle edges of synthetic and biogenic birnessites (in preparation)

## 9.13

## Plant oils used to maintain bone and antler tools in the Neolithic lakeshore settlement, Zurich Opera Parking

Spangenberg Jorge E.<sup>1</sup>, Ferrer Montserrat<sup>1</sup>, Jacomet Stefanie<sup>2</sup>, Bleicher Niels<sup>3</sup> & Schibler Jörg<sup>2</sup>

<sup>1</sup> Institute of Earth Sciences, University of Lausanne, Geopolis, 1015 Lausanne (Jorge.Spangenberg@unil.ch)

<sup>2</sup> Institute for Prehistory and Archaeological Science, University of Basel, Spalenring 145, 4055 Basel

<sup>3</sup> Dendrochronological Laboratory, Department of the City of Zurich, Office for Urbanism, 8008 Zurich

A not rare and still unclear observation in Neolithic Alpine lakeshore settlements is that a large number of archaeological bone and antler tools with clearly different functions like massive chisels made of bones from cattle or red deer (used for processing wood or antler), small points made of sheep or goat bones and bigger points made of bones from cattle or red deer (for processing leather or textiles), combs made of ribs from cattle or deer (for processing plant fibres), scrapers made of red deer antler and even sockets or sleeves (used to connect axes with the wooden handles) made of red deer antler show clear shiny and apparently polished surfaces (e.g. Schibler 2013). The so different materials that were worked with a variety of tools could not have produced these brightness areas, and other explanations must be sought.

We explore the origin of such shiny surfaces by molecular and isotopic analyses of the lipids staining freshly unearthed and not conserved bone and antler artifacts from the recent excavation at the underground parking garage for the Zurich opera house dating to about 3230 to 2729 BC. A set of 10 artifacts, covering distinct osteological and typological features was selected for this study. Most of the artifacts are made of bones or antler from red deer (*Cervus elaphus*) or bones from large ruminants, such as cattle (*Bos taurus*) or red deer. One artifact is made of a metatarsus from roe deer (*Capreolus capreolus*). For each tool the lipids were extracted separately from the tapered thinner working part and the wider handling part. The saponifiable and unsaponifiable lipids were analysed by GC-MS and GC-C-IRMS. The overall extractable lipid distribution is characterized by an important amount of animal sterols (cholesterol, cholestanol, coprostanol, epicholestanol), waxy *n*-alkanes, *n*-alkan-1-ol and phytosterols ( $\beta$ -sitosterol, sitostanol), and abundant saturated, mono- and polyunsaturated fatty acids in the C<sub>14</sub>-C<sub>24</sub> range. The high concentrations of C<sub>18</sub> polyunsaturated acids, linoleic (18:2) and linolenic (18:3) acids, clearly indicate that oil plants are overprinting the indigenous animal lipid signature. The  $\delta^{13}\text{C}$  values of the main fatty acids confirm that the archaeological samples were stained with C<sub>3</sub> plant oils. C<sub>3</sub> vegetable oils rich in 18:2 and/or 18:3 may be obtained from seeds of poppy (*Papaver somniferum*; 50-75% 18:2), flax (*Linum usitatissimum*; 15-30% 18:2, 45-50% 18:3), rape (Brassicaceae; 8-30% 18:2, 0.1-3% 18:3), sunflower (*Helianthus annuus*; 48-74% 18:2), safflower (*Carthamus tinctorius*; 83% 18:2), *Sesamum indicum* (sesame; 48% 18:2), and hazelnut (*Corylus avellana*; 55% 18:2) (Gunstone and Harwood, 2007). Flax and poppy seeds are extremely frequent in important amounts in the Neolithic lakeshore settlements in central Europe (Jacomet 2007). Both, flax and poppy were domestic oil and/or fiber plants. Seeds from the wild oil plant turnip (*Brassica rapa*) and also hazelnut shells are common in the Neolithic lakeshore settlements, whereas the other above-mentioned 18:2 rich oil plants were not present in Neolithic Europe (*Helianthus annuus*, *Sesamum indicum*) or extremely rare (*Carthamus tinctorius*) (e.g. Jacomet 2007). The fatty acid concentrations, fatty acid and sterols concentration ratios, and  $\delta^{13}\text{C}$  values of individual fatty acids show significant correlations. Principal component analysis was used to define the chemical associations characterizing the indigenous animal lipid signature, the exogenous staining lipids, and (bacterial) alteration of the primary lipids at the archaeological site.

The results indicate that most of the shiny and polished surfaces of the bone and antler artifacts is not the result of the use but is due to a combination of preserved indigenous animal lipids and plant oils staining the tools.

Now we have archaeological and chemical evidence that the Neolithic craftsmen of the late 4<sup>th</sup> and early 3<sup>rd</sup> millennium BC, used specific tools deliberately fashioned, pre-treated and maintained with a preservative material based on plant oils most likely obtained from seeds of *Linum usitatissimum* and *Papaver somniferum*, with probably some minor contribution of *Brassica rapa*.

### REFERENCES

- Gunstone, F.D., Harwood, J.L., 2007. Occurrence and characterisation of oils and fats. In: Gunstone, F.F., Harwood, J.L., Dijkstra, A.J. (Eds.), *The Lipid Handbook*. CRC/Taylor & Francis, Boca Raton, pp. 37-141.
- Jacomet, S., 2007. Neolithic plant economies in the northern alpine foreland from 5500-3500 BC cal. In: Colledge, S. und Conolly, J. (Eds.) *The origins and spread of domestic plants in southwest Asia and Europe*. Walnut Creek CA, 221-258.
- Schibler, J., 2013. Bone and antler artifacts in wetland sites. In F. Menotti and A. O'Sullivan (eds.) *The Oxford Handbook of Wetland Archaeology*. Oxford: Oxford University Press.

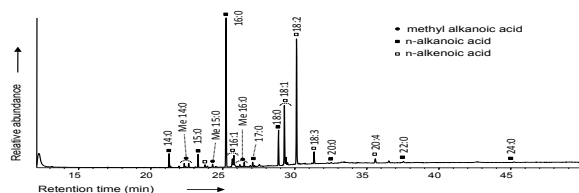


Figure 1. Representative GC-MS total ion chromatogram of the fatty acid methyl esters in the lipids extracted from the bone or antler artifacts recovered at Zurich opera parking.

## 9.14

### Uranium(IV) mobility in a mining-impacted wetland

Wang Yuheng<sup>1</sup>, Frutschi Manon<sup>1</sup>, Suvorova Elena<sup>1</sup>, Phrommavanh Vannapha<sup>2</sup>, Descostes Michael<sup>2</sup>, Osman Alfatih<sup>3</sup>, Geipel Gerhard<sup>3</sup> & Bernier-Latmani Rizlan<sup>1</sup>

<sup>1</sup> Ecole Polytechnique Fédérale de Lausanne (EPFL), Environmental Microbiology Laboratory, Lausanne, Switzerland  
(<sup>1</sup>presenting author: yuheng.wang@epfl.ch)

<sup>2</sup> AREVA - Business Group Mines, Direction R&D, BAL 0414C-2, Tour AREVA, Paris, France

<sup>3</sup> Helmholtz Center Dresden Rossendorf (HZDR), Institute of Resource Ecology, Dresden, Germany

Wetland soils are known to accumulate uranium and other heavy elements. The sorption of U(VI) onto solid phases in soil and precipitation of sparingly soluble U(IV) minerals under reducing conditions are thought to be the main processes of U immobilization within wetlands. We studied a wetland, located near a former U mine in central France (Limousin), which was impacted by mining activity and exhibited a few U hotspots (~4,000 ppm). We observed U release into a stream flowing through the wetland, as evidenced by a steady increase in the concentration of U in the stream as a function of distance from the entry point into the wetland. To elucidate U speciation and the U release mechanism, soil and porewater samples were collected from two selected U hotspots in the wetland as a function of depth and season and in such a way as to preserve the redox state. High porewater Fe(II) concentrations and decreasing  $\text{SO}_4^{2-}$  concentrations with depth were indicative of the onset of Fe(III) and  $\text{SO}_4^{2-}$  reduction, respectively. Microbial analysis showed sulfate-reducing bacteria (i.e., Desulfobacteraceae and Thermodesulfobionaceae) and microorganisms potentially capable of iron and uranium reduction (e.g., Clostridiales), supporting the microbial origin of  $\text{SO}_4^{2-}$  and Fe reduction. Surprisingly given the prevailing reducing conditions, high U concentrations (~1  $\mu\text{M}$ ) were observed throughout the porewater profiles while high soil U content was restricted to the top 30 cm. Using laser fluorescence spectroscopy (LFS) and X-ray absorption spectroscopy (XAS) at low temperature, we showed that tetravalent U is predominant in both porewater and soil, and U in the soil occurs primarily as a non-crystalline U(IV) species: U(IV) adsorbed onto amorphous Fe-Al-P-Si aggregates. Transmission electron microscopy (TEM) and ultrafiltration analysis demonstrated U association with colloidal  $\text{Fe}(\text{OH})_2$ -organic matter assemblages in porewater, which could lead to the observed U(IV) mobility. Hence, U(IV) species in the porewater are distinct from those present in the soil, suggesting the release of a labile form U(IV) from soil. Moreover, U(IV) association with mobile colloids ultimately results in its release into the stream, despite the reducing conditions and the low solubility of U(IV) phases. The unexpected mobility of U(IV) in this system brings into question the often assumed immobilization of U through (bio)reduction, particularly in high organic matter environments such as wetlands.

## 9.15

### Metabolic interdependencies between phylogenetically novel fermenters and respiratory organisms in an unconfined aquifer

Wrighton K.C.<sup>1</sup>, Castelle C.J.<sup>2</sup>, Wilkins M.J.<sup>1</sup>, Hug L.A.<sup>2</sup>, Sharon I.<sup>2</sup>, Thomas B.C.<sup>2</sup>, Lipton M.S.<sup>3</sup>, Long P.E.<sup>4</sup>, Williams K.H.<sup>4</sup>, Banfield J.F.<sup>1,4</sup>

<sup>1</sup> The Ohio State University, Department of Microbiology, Columbus, OH, 43214

<sup>2</sup> University of California Berkeley, Department of Earth and Planetary Science, Berkeley, CA 94720

<sup>3</sup> Pacific Northwest National Laboratory, Department of Energy, Biological Sciences Department, Richland, WA 99352

<sup>4</sup> Lawrence Berkeley National Laboratory, Department of Energy, Berkeley, CA 94720

Fermentation-based metabolism is an important ecosystem function often associated with environments rich in organic carbon, such as wetlands, sewage sludge, and the mammalian gut. The diversity of microorganisms and pathways involved in carbon and hydrogen cycling in sediments and aquifers and the impacts of these processes on other biogeochemical cycles remain poorly understood. Here we used metagenomics and proteomics to characterize microbial communities sampled from an aquifer adjacent to the Colorado River at Rifle, Colorado, USA, and document interlinked microbial roles in geochemical cycling. The organic carbon content in the aquifer was elevated *via* two acetate-based biostimulation treatments. Samples were collected at three time points, with the objective of extensive genome recovery to enable metabolic reconstruction of the community. Fermentative community members include genomes from a new phylum (ACD20), phylogenetically novel members of the Chloroflexi and Bacteroidetes, as well as candidate phyla genomes (OD1, BD1-5, SR1, WWE3, ACD58, TM6, PER, and OP11). These organisms have the capacity to produce hydrogen, acetate, formate, ethanol, butyrate, and lactate, activities supported by proteomic data. The diversity and expression of hydrogenases suggests the importance of hydrogen currency in the subsurface. Our proteogenomic data further indicate the consumption of fermentation intermediates by Proteobacteria can be coupled to nitrate, sulfate, and iron reduction. Thus, fermentation carried out by previously unstudied members of sediment microbial communities may be an important driver of diverse subsurface biogeochemical cycles.

## P 9.1

# When a century is enough to invert a million years' pedogenesis: the oxalate carbonate pathway in tropical agro-ecosystems

Cailleau Guillaume<sup>1</sup>, Pons Sophie<sup>1</sup>, Bindschedler Saskia<sup>2,3</sup>, Junier Pilar<sup>2</sup> & Verrecchia Eric<sup>1</sup>

<sup>1</sup> ISTE, University of Lausanne, Geopolis, CH-1015 Lausanne (guillaume.cailleau@unil.ch)

<sup>2</sup> Lamun, University of Neuchatel, Emile argand 11, CH-2001 Neuchatel

<sup>3</sup> Department of Environmental Microbiology, Helmholtz Centre for Environmental Research – UFZ, Leipzig, Germany

Ferralsols are intertropical soils that spread over ca. 750 millions of ha on three continents (WRB, 2006) and develop over long time span, up to million years. A relative geomorphological stability combined with warm-humid conditions and a very weak relief allow ferralitization to take place. Ferralitization involves intense weathering processes that concentrate Al, Si, and Fe in the soil in comparison to other cations such as Na, Mg, K, and Ca, which are eliminated from the solum by leaching. These soils are consequently highly acidic with a low nutrient availability. However, a yet overlooked pedogenic process is able, in less than a century, to mitigate the effect of ferralitization. This process, called the oxalate-carbonate pathway, can be described as the transformation of the sunlight energy into pedogenic carbonate. Briefly, the oxalate produced by primary producers is oxidized by soil oxalotrophic bacteria, leading to a local increase of soil pH, which can further induce carbonate precipitation (Braissant et al., 2004; Verrecchia et al., 2006; Cailleau et al., 2011).

In a coffee plantation from the Western Province of Cameroon, the influence of a ca. 150 yrs old Iroko tree (*Milicia excelsa*) has been studied along a 30 m long transect. Five soil pits, and for each, three surrounding coffee plants (*Coffea arabica* L.), were collected in order to compare their elemental content.

Oxalotrophy leads to an increase of up to 2.2 pH units close to the Iroko tree (pH: 7.4) compared to a control soil at 45 m (pH: 5.2). The total amount of Ca, Mg, K, and P in the soil close to the Iroko tree is more important than at distance. A similar trend is observed for exchangeable cations like Ca<sup>2+</sup>, Mg<sup>2+</sup>, and K<sup>+</sup>. Furthermore, other trends have been noted in coffee plants tissues. At a distance of 0.5 to 2.5 m from the Iroko tree, Ca, and K contents are higher than at a distance of 8 to 30 m, while at 45 m Ca content increases up to the level close to the iroko whereas K continues to decrease. This suggests a slight Ca impoverishment between both ends of the transect (in the 8 to 30 m interval). Finally, while P does not show any trend in the coffee plant transect, N/P ratio increases, indicating P deficiency for plants all along the transect from the Iroko tree. These results suggest that the Iroko tree ecosystem tends to be less dependent from the organic matter turnover, by constituting a more resilient nutrient's storage in the soil.

This study emphasizes drastic changes in biogeochemical soil characteristics in the relationship with the oxalate carbonate pathway induced by an iroko tree. Beyond the importance of understanding nutrient cycling in such ecosystems, a question arises if these iroko ecosystems could constitute a soil improving system, which could be used in a context of agroforestry.

## REFERENCES

- Braissant, O., Cailleau, G., Aragno, M., Verrecchia, E.P., 2004. Biologically induced mineralization in the iroko *Milicia excelsa* (Moraceae): its causes and consequences to the environment. *Geobiology* 2, 59-66.
- Cailleau, G., Braissant, O., Verrecchia, E.P. 2011. Turning sunlight into stone: the oxalate-carbonate pathway in a tropical tree ecosystem. *Biogeosciences* 8, 1755-1767.
- IUSS Working Group WRB. 2006. World reference base for soil resources 2006. 2nd edition. World Soil Resources Reports No. 103. FAO, Rome.
- Verrecchia, E.P., Braissant, O., Cailleau, G., 2006. The oxalate-carbonate pathway in soil carbon storage: the role of fungi and oxalotrophic bacteria. In: Gadd, G.M., (Ed.) *Fungi in the biogeochemical cycles*, Cambridge University Press, pp. 289-310.

## P 9.2

# Long-term Organic Management Induced Changes in Soil Organic Matter Stability and Enzyme Activities

Koishi Ayumi<sup>1</sup>, Bragazza Luca<sup>2</sup>, Maltas Alexandra<sup>3</sup>, Sinaj Sokrat<sup>3</sup>, Albrecht Remy<sup>1</sup> & Pfeifer Hans-Rudolf<sup>1</sup>

<sup>1</sup> Institute of Earth Science, University of Lausanne, CH-1015 Lausanne  
(ayumi.koishi@unil.ch)

<sup>2</sup> Swiss Federal Institute for Forest, Snow and Landscape Research, Site Lausanne, Station 2, CH-1015 Lausanne; Laboratory of Ecological Systems, School of Architecture, Civil and Environmental Engineering, École Polytechnique Fédérale de Lausanne, Station 2, CH-1015 Lausanne; Department of Life Science and Biotechnologies, University of Ferrara, Corso Ercole I d'Este 32, I-44121 Ferrara

<sup>3</sup> The Swiss Research Station Agroscope ACW – Changins, CH-1260 Nyon 1

Launched in 1976 by the Swiss Research Station Agroscope ACW - Changins, Nyon (VD), a long-term experiment investigates the capacities of different organic fertilizers to maintain soil fertilities and improve crop yield, in particular in relation to soil organic matter “SOM” (Maltas et al., 2012a, 2012b). The experiment consists of 6 treatments: “control” with only PK fertilizers, mineral NPK fertilizers “Min”, cereal straw “Str” + NPK fertilizers, green manure “GM” (mustard applied every 2 years) + NPK fertilizers, solid farmyard manure “Ma” (35t ha<sup>-1</sup> applied every 3 years)+ NPK fertilizers, and liquid farmyard manure “Slu” (60m<sup>3</sup> ha<sup>-1</sup> applied every 3 years) + NPK fertilizers. The main objective of this study is to evaluate the effect of the replacement of farmyard manures by mineral fertilizers and/or fresh organic matter (straw and green manure) on SOM quality and soil biological activity.

Organic fertilizers and SOM quality were analyzed by infrared spectroscopy (FTIR). For soils, humic acids (HA) were extracted by sodium pyrophosphate. FTIR signatures (Fig. 1) indicate that green manure is rich in carboxylic acids, which may increase its solubility in the soil solution. Cereal straw seems to be enriched in aliphatic compounds (fats, wax, or lipids), contributing to its water-repellent property. Solid (Ma) and liquid (Slu) farmyard manures, in contrast, contain more aromatic compounds, indicating an advanced stage of humification. Soil treated with green manure, “GM” soil, had the most degraded HA due to its lowest aromatic and carboxylic contents, while HA of “Min” soil seems to be the most stabilized with its highest carboxylic content. HA of “Str”, “Ma” and “Slu” soils demonstrated an intermediate degree of stabilization between “GM” soil and “Min” soil.

To better understand the mechanisms by which the organic fertilizations contribute to the SOM stability, C-, N- and P-degrading enzyme activities ( $\beta$ -1,4-glucosidase (BG), phenol-oxidase (PO);  $\beta$ -1,4-N-acetylglucosaminidase (NAG), leucine aminopeptidase (LAP); phosphatase (AP)) were also assayed. Relatively high BG, NAG (Fig. 2) and AP (data not shown) activities were observed in “GM” soil as well as “Str” soil. Green manure being easily decomposable, its application probably stimulated these enzymes, resulting in the most unstable SOM. Water-repellent straw, in contrast, may have helped the SOM stabilization despite of the enzyme activity. In addition, enzymatic activity seems to increase due to a lower availability of nitrogen and phosphorus compared to carbon in straw. Therefore, our study demonstrates the effect of organic inputs on SOM quality, closely mediated by hydrolytic enzymes. It is to note that the enzyme activity seems to be strongly influenced by the decomposability and the nutrient balance of organic inputs.

## REFERENCES

- Maltas, A., Oberholzer, H., Charles, R., Bovet, V., and Sinaj, S. 2012a: Effet à long terme des engrais organiques sur les propriétés du sol. *Rech. Agron. Suisse* 3, 148–155.
- Maltas, A., Charles, R., Bovet, V., and Sinaj, S. 2012b: Effet à long terme des engrais organiques sur le rendement et la fertilisation azotés des cultures. *Rech. Agron. Suisse* 3, 156–163.

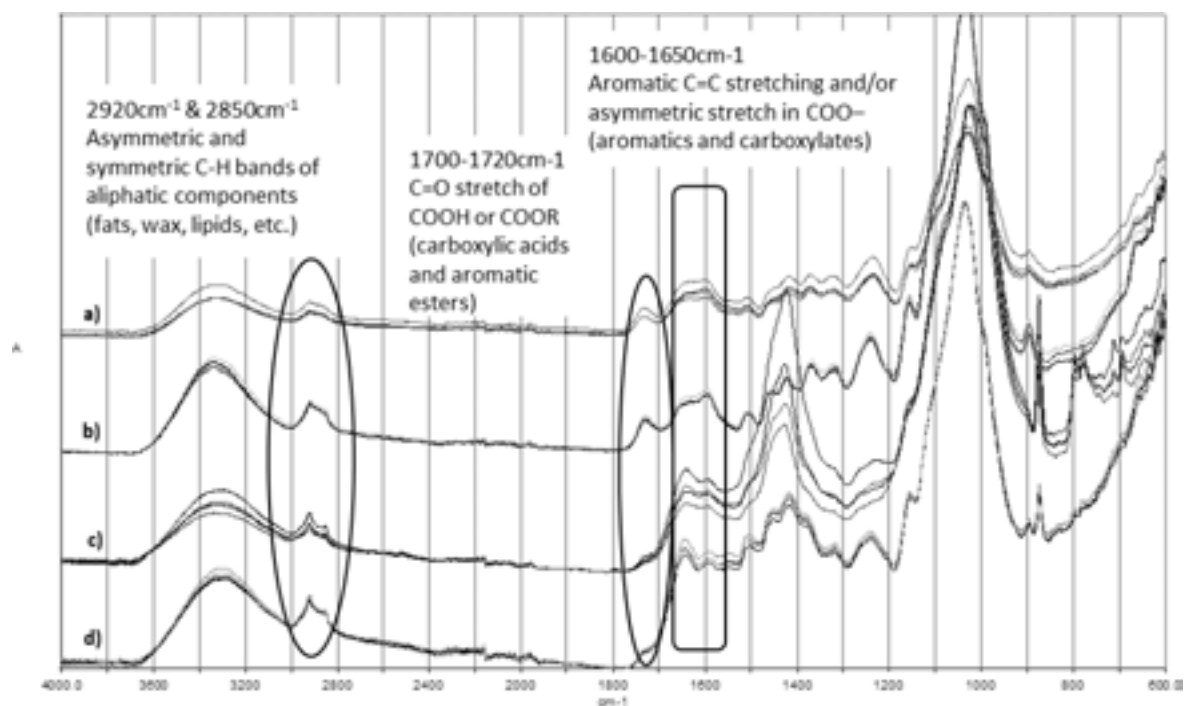


Figure 1. FTIR major signatures of organic fertilizers: a) green manure, b) cereal straw, c) solid farmyard manure and d) liquid farmyard manure.

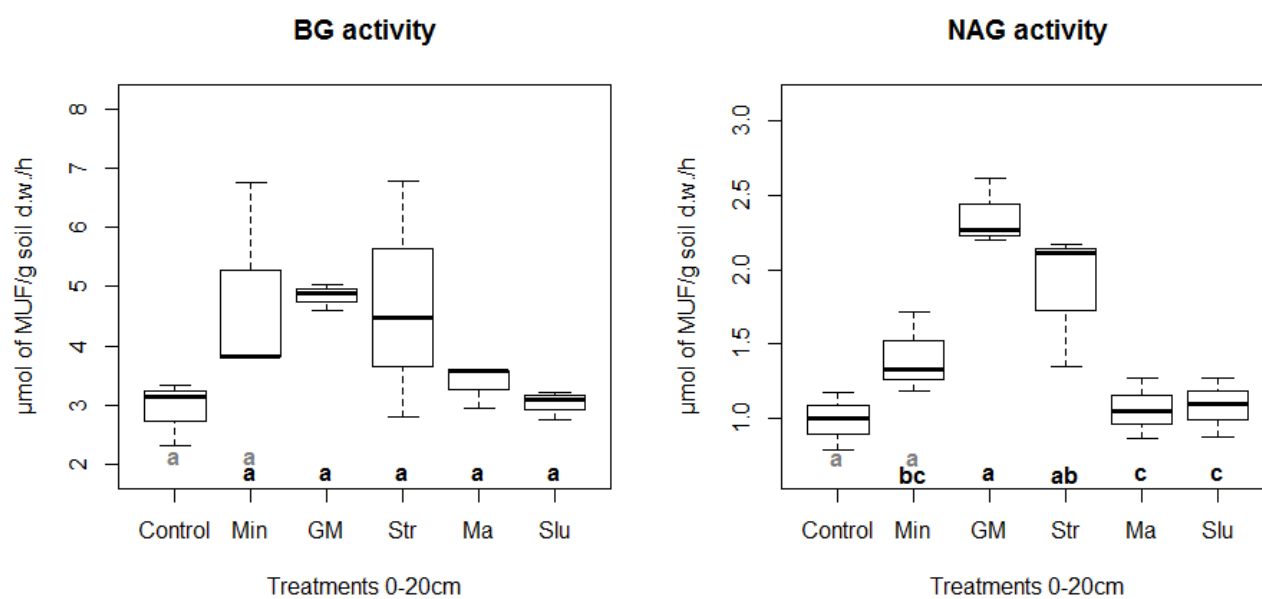


Figure 2. Enzyme study in soils: C-degrading BG and N-degrading NAG activity in Control: no N fertilization, Min: mineral fertilizer, GM: green manure, Str: cereal straw, Ma: solid farmyard manure and Slu: liquid farmyard manure, n = 4.

## P 9.3

# Mineralogical and chemical controls on the photoreductive dissolution of birnessite minerals

Marafatto Francesco Femi<sup>1</sup>, Peña Jasquelin<sup>2</sup>

<sup>1</sup> Institute of Earth Sciences (ISTE), Faculté des géosciences et de l'environnement, University of Lausanne, Batiment Geopolis, CH-1015 Lausanne (francesco.marafatto@unil.ch)

<sup>2</sup> Institute of Earth Sciences (ISTE), Faculté des géosciences et de l'environnement, University of Lausanne, Batiment Geopolis, CH-1015 Lausanne (jasquelin.pena@unil.ch)

Of the different known manganese oxides, layered-type Mn(IV) oxide phases (birnessites) are amongst the most environmentally significant. Birnessite minerals play a key role in elemental cycles due to their high sorption reactivity, oxidizing potential and important role in microbial metabolisms. Furthermore, birnessite minerals are commonly produced by the enzymatic oxidation of Mn(II) to form Mn(IV) oxides. Manganese oxides are also known to have semiconducting properties. Spectroscopic and computational studies (Sherman, 2005; Kwon et al., 2009) have shown that the band gap – the energetic separation between valence band and conduction band of birnessites – is in an energy range that allows electronic excitation by visible light. Upon excitation by light, electrons may be injected into the mineral structure and cause re-equilibration through valence change (i.e., Mn reduction) if the excited state has a long enough lifetime (Gilbert, 2005). Furthermore, metal impurities, structural defects and organic matter – all of which are characteristic of birnessite minerals in natural environments – can enhance the photoreactivity of semiconductors.

The goal of this research is to evaluate the fate of birnessite minerals and metal contaminants in sunlit aquatic environments. We are studying the effect of structural defects (Mn(IV) vacancy sites), particle size and adsorbed trace metals on the photoreductive dissolution of birnessites by comparing the dissolution rates obtained for three chemically-synthesized birnessites: microcrystalline K-birnessite, characterized by Mn(IV) layers with approximately 12% vacancies and Mn(III) in the interlayer; nanocrystalline triclinic birnessite characterized by layers of alternating Mn(IV) and Mn(III) and low to no vacancy content; and nanocrystalline  $\delta$ -MnO<sub>2</sub>, with Mn(IV) rich layers and approximately 6% structural vacancies. By doping the minerals with various metals (Ni, Co, Zn) we plan to probe the effect of chemical impurities on the dissolution rates.

Preliminary experiments carried out under a custom-built fluorescent light setup suggest possible competition between reductive dissolution and sorption of produced Mn(III) or Mn(II), as inferred from wet chemical measurements (ICP-OES, potentiometric titrations). The role of metal impurities suggest an increase of mineral reactivity towards metal sorption under the effect of light. This research furthers our knowledge of the Mn cycle, with important implications for the mobility and availability of metal contaminants associated with mineral surfaces.

## REFERENCES

- Gilbert, B., 2005. Molecular-Scale Processes Involving Nanoparticulate Minerals in Biogeochemical Systems. *Reviews in Mineralogy and Geochemistry* 59, 109-155.
- Kwon, K.D., Refson, K., Sposito, G., 2009. On the role of Mn (IV) vacancies in the photoreductive dissolution of hexagonal birnessite. *Geochimica et Cosmochimica Acta* 73, 4142-4150.
- Sherman, D.M., 2005. Electronic structures of iron(III) and manganese(IV) (hydr)oxide minerals: Thermodynamics of photochemical reductive dissolution in aquatic environments. *Geochimica Et Cosmochimica Acta* 69, 3249-3255.

## P 9.4

# Typology of alkaline-earth metal precipitates in meso-oligotrophic lake (Léman, Switzerland)

Agathe Martignier <sup>1</sup>, Jean-Michel Jaquet <sup>1</sup> and Pascale Nirel <sup>2</sup>

<sup>1</sup> Section des Sciences de la terre et de l'Environnement, Laboratoire de Géomicrobiologie, Université de Genève, 13 rue des Maraîchers, CH-1205 Genève, Suisse

<sup>2</sup> Service de l'Ecologie de l'Eau, DIME, 23 avenue Ste Clotilde, CH-1211, Genève 8, Suisse

In the course of a routine water-quality survey in meso-oligotrophic Lake Léman (Switzerland), suspended matter was collected by filtration on 0.2 µm membranes between July 2012 and August 2013, mostly at the depth of maximal Chla concentration. In spring and summer samples, scanning electron microscopy revealed the presence of numerous dark and gelatinous patches occluding the pores of the membranes, containing high numbers of picoplanktonic cells and, in places, clusters of smooth microspheres 0.5-2 µm in diameter (fig. 1).

Their chemical composition, determined by semi-quantitative, energy-dispersive X ray spectroscopy (EDS) shows Mg, Ca, Sr and Ba (alkaline earth metals) to be the dominant cations. Carbon (as carbonate) and phosphorus (presumably as phospho-carbonate) are present as anions. The carbonate microspheres have been subdivided into four types represented in a Ca-Sr-Ba ternary space. All types are confined within a domain bound by Ca > 40, Sr < 10 and Ba < 50 (in mole %). Type I, the most frequent, displays a broad variability in Ba/Ca, even within a given cluster. Types II and III are devoid of Ba, but may incorporate P and S. Type IV contains only Ca. In contrast to the other types, phosphorus-rich microspheres are smaller and occur as isolated individuals or loose aggregates. The Type I composition resembles that of benstonite, a Group IIA carbonate that was recently found as intracellular granules in a cyanobacterium from alkaline Lake Alchichica (Mexico).

Lake Léman microspheres are solid, featureless and presumably amorphous. They are embedded in a mucilage-looking substance in the vicinity of picoplanktonic cells (Fig. 1), morphologically similar to small eukaryotes (*Chlorella* sp) or cyanobacteria (*Synechococcus* sp). In summer 2012, the macroscopic physico-chemical conditions in Lake Léman epilimnion were such as to allow precipitation of calcite, but not strontium and barium carbonates. For these, favorable conditions did exist, though, in the micro-environment provided by the combination of active picoplankton and a mucilaginous envelope.

A multidisciplinary research program is ongoing to gain a proper understanding of this intriguing process of alkaline-earth metals sequestration. By means of techniques such as SEM/EDX/TEM, epifluorescence microscopy, flow cytometry and genomics, the following questions will be addressed: the spatio-temporal distribution of the precipitates, their exact mineralogical composition, and the taxonomy and role of picoplankton in the precipitation processes.

## REFERENCES

- Callieri C. & Stockner J.G. 2002: Freshwater autotrophic picoplankton: a review. *J. Limnol.*, 61(1): 1-14.
- Couradeau, E. et al. 2012: An Early-Branching Microbialite Cyanobacterium Forms Intracellular Carbonates. *Science*, 336:459-462.
- Dupraz C. et al. 2009: Processes of carbonate precipitation in modern microbial mats. *Earth-Science Reviews*, 96(3): 141-162.
- Jaquet, J.-M. Et al. 2013: Preliminary investigations on picoplankton-related precipitation of alkaline-earth metal carbonates in meso-oligotrophic Lake Geneva (Switzerland). Accepted for publication in *Journal of Limnology*.
- Plée K. et al. 2008: Unravelling the microbial role in ooid formation – results of an in situ experiment in modern freshwater Lake Geneva in Switzerland. *Geobiology*, 6: 341-350.

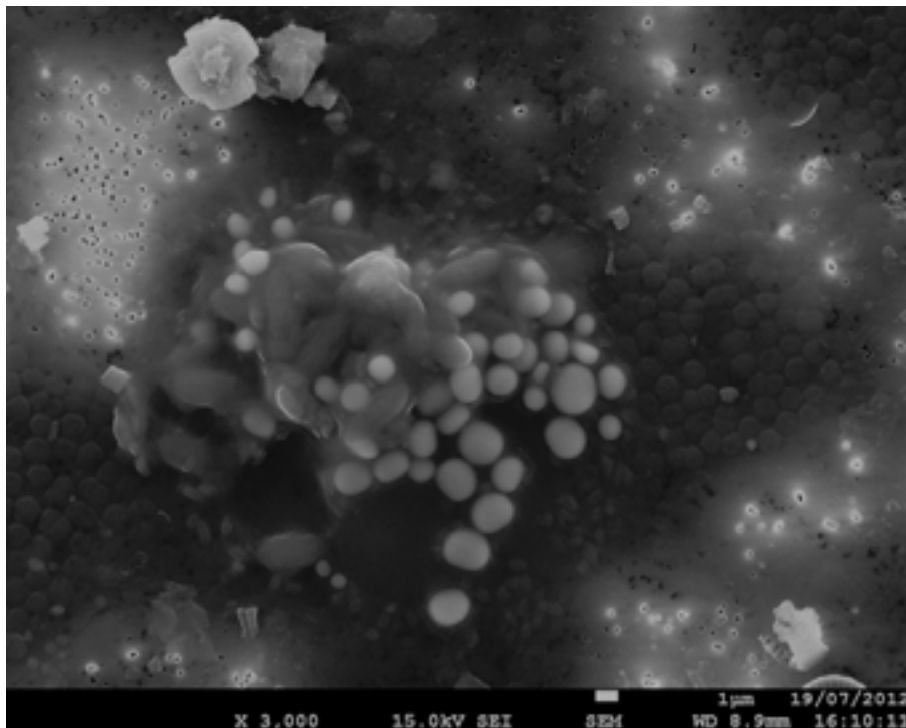


Figure 1. Cluster of smooth microspheres [Ca (approx. 50 mole %) / Ba (>45%) / Sr (>4%)], surrounded by picoplanktonic cells. Sample taken at 6 m under the water surface of lake Léman in July 2012. Photograph: Department of Earth Sciences, University of Geneva.

## P 9.5

## Effects of salinity on TiO<sub>2</sub> nanoparticles behavior and toxicity towards natural plankton. A case study: the Venice Lagoon, Italy

Pestrimaux Clémentine<sup>1</sup>, Le Faucheur Séverine<sup>1</sup>, Mortimer Monika<sup>1</sup>, Bernardi Aubry Fabrizio<sup>2</sup>, Botter Margherita<sup>2</sup>, Zonta Roberto<sup>2</sup>, Slaveykova Vera<sup>1</sup>

<sup>1</sup> Aquatic Biogeochemistry and Ecotoxicology, University of Geneva, Institute F.A. Forel, 10 route de Suisse, CP 416, CH-1290 Versoix

<sup>2</sup> Istituto di Scienze Marine, Arsenale-Tesa 104, Castello 2737/F, 30122 Venezia

Manufactured TiO<sub>2</sub> nanoparticles are widely used in many commercially available products (food, cosmetics, clothes...). This massive consumption could lead to their large input into the environment and to their potential impact on aquatic life. The physico-chemical composition of ambient waters determines the behavior of nanoparticles in aquatic systems as well as their interactions with organisms (Battin et al., 2009; Scown et al., 2010). The presence of salts can for example modifies the zeta potential of nanoparticles in making them more neutral, and as such promoting their aggregation (Brunelli et al., 2013). The aim of the present study was thus to examine the toxicity of manufactured TiO<sub>2</sub> toward natural plankton. Our working hypothesis was that the negative effects of TiO<sub>2</sub> towards plankton would decrease when salinity will increase due to the increase of nanoparticles aggregation.

To that end, the aggregation and zeta potential of TiO<sub>2</sub> nanoparticles were analyzed in artificial and natural seawaters with a Zetasizer Nano ZS (Malvern). The effects of TiO<sub>2</sub> on a model organism, the protozoa *Tetrahymena thermophila* exposed to three concentrations (1, 10, 100 mg / L) were examined using flow cytometry and the fluorescent dye propidium iodide as a marker of cell viability. Finally two fractions of natural plankton (one lower than 45 μm and one higher than 45 μm,) were collected in the lagoon of Venice at five different salinities and exposed to three concentrations of TiO<sub>2</sub> (1, 10 and 100 mg/L). The two planktonic fractions were also analyzed for their viability using propidium iodide but with fluorescence microscopy.

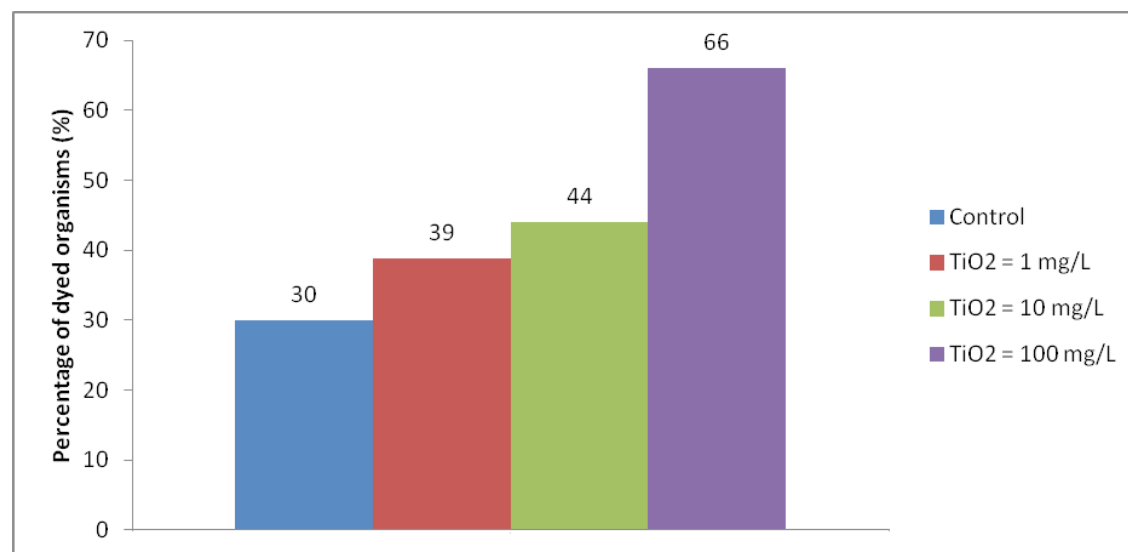


Figure 1 : Percentage of dyed organisms with propidium iodide after 24 hours of exposure to TiO<sub>2</sub> nanoparticles. Test performed with natural plankton of Venice lagoon (fraction higher than 45 μm, salinity = 12 ‰).

The fluorescent dye propidium iodide was successful to assess the toxicity of TiO<sub>2</sub> nanoparticles in natural plankton (Figure 1). In the control, about 30 % of the population was dyed, possibly due to a stress experienced during the sampling. Increase of TiO<sub>2</sub> nanoparticles concentration up to 100 mg/L in the ambient water of planktonic organisms doubled the number of stressed organisms. This method was further used to evaluate the effects of nanoparticles along a salinity gradient.

### REFERENCES

- Battin, T. J., et al., 2009. Nanostructured TiO<sub>2</sub>: Transport Behavior and Effects on Aquatic Microbial Communities under Environmental Conditions. *Environmental Science & Technology*. 43.
- Brunelli, A., et al., 2013. Agglomeration and sedimentation of titanium dioxide nanoparticles (n-TiO<sub>2</sub>) in synthetic and real waters. *Journal of Nanoparticle Research*. 15.
- Scown, T. M., et al., 2010. Review: Do engineered nanoparticles pose a significant threat to the aquatic environment? *Critical Reviews in Toxicology*. 40.

## P 9.6

### The impacts of acidic in-situ recovery of uranium in southern Kazakhstan on geochemistry and microbial community structure

Reinsch Brian<sup>1</sup>, Descostes Michael<sup>2</sup>, Bernier-Latmani Rizlan<sup>1</sup>, & Rossi Pierre<sup>1</sup>

<sup>1</sup> Central Environmental Laboratory (GR-CEL), 1<sup>ère</sup> École Polytechnique Fédérale de Lausanne, CH A1 374, CH-1015 Lausanne (brian.reinsch@epfl.ch)

<sup>2</sup> AREVA Mines, Tour AREVA - 1, Place Jen Millier, 92084 Paris

Acidic *in situ* recovery (ISR) of uranium is one of the major mining processes utilized worldwide (Kazakhstan, USA, Australia, South Africa...) for low ore grade deposits. ISR is suited for deposits typically located in porous rock, and confined in impermeable rock layers. Among the main advantages of this technology, compared to traditional physical mining techniques, are: the reduction of hazards for the employees from accidents, dust, and radiation, the absence of mill tailings and its low cost. ISR circulates acid below the surface of the Earth within a closed loop recovery system within a mineralized aquifer. Once mining operations cease, some mines practice natural attenuation. Hence, in order to recover the initial physico-chemical conditions of the aquifer, clay minerals are expected to sorb metals and buffer the acidic pH while the native Fe and SO<sub>4</sub><sup>2-</sup> reducing bacteria will also raise the pH and generate reduced conditions favorable for uranium precipitation. The main risks of ISR coupled with natural attenuation are groundwater contamination and a long timeframe of pH recovery. In order to evaluate the rate of such 'natural processes', first the effect of the acid on both geochemistry and the native microbial communities must be understood. The initial sampling mission from this collaboration revealed that the acid not only liberates metals and salts, as predicted, but also has an affect on the indigenous microbes. These results will be presented along with future plans to compare natural attenuation vs. biostimulation *in situ*.

## P 9.7

### Distribution and dynamics of SOM on carbonate rocks (Jura Mountains): a geochemical approach

Pinard Gladys<sup>1</sup>, Spangenberg Jorge E.<sup>1</sup>, Adatte Thierry<sup>1</sup> & Verrecchia Eric P.<sup>1</sup>

<sup>1</sup> Institute of Earth Sciences, University of Lausanne, Geopolis, 1015 Lausanne (jorge.spangenberg@unil.ch)

Soil organic matter (SOM) is considered as a key factor in ecosystem dynamics. Its degradation state depends on several interactive factors, including bedrock lithology, vegetation, litter, temperature, and humidity. The geochemistry of SOM on carbonate substrata is little studied (e.g. Grünewald et al 2006). An on-going multi-proxy geochemical study of soil profiles on two carbonate lithologies in the Swiss Jura Mountains (Ballens) aims to fill this gap. The bedrocks include Kimeridgian limestone and calcareous moraine and a C<sub>3</sub> vegetation as a mixed forest (Abieti-Fagetum association) with beeches and conifers as the dominant trees. In order to evaluate the potential combined influence of litter and carbonate bedrock lithology on SOM, four bedrock-vegetation combinations ("soil groups") were considered: limestone-beech (L/B), limestone-conifer (L/C), moraine-beech (M/B) and moraine-conifer (M/C). Twelve soil profiles (triplicates for each combination) were described and systematically sampled. Soil geochemical analyses include mineralogical composition (XRD), major and trace element contents (XRFA), SOM characterization by Rock-Eval pyrolysis, bulk C and N isotope analyses, distribution of the soil lipids and compound specific C isotope analysis of the main fatty acids.

Soils are referenced as mollic Umbrisols, calcaric Cambisols, and hypereutric Cambisols, and have similar texture (silty) and pH (~6). Major element concentrations reflect soil mineralogy defined mainly by the quartz and calcite contents. The TOC for L/B and L/C soil decreases with depth from 37 wt.% (holorganic horizons) to 25 wt.% (mineral horizons), and for M/B and M/C from 16 to 0.07 wt.%. Rock-Eval HI and OI indexes (214 to 371 mg HC/g TOC and 92 to 151 mg CO<sub>2</sub>/g TOC, respectively) show small but still significant differences between the different soil groups. The δ<sup>13</sup>C<sub>org</sub> and δ<sup>15</sup>N<sub>org</sub> values increase from holorganic horizons to mineral horizons, with a clear separation between both horizon types (Figure 1). The holorganic horizons have the more negative values (δ<sup>13</sup>C<sub>org</sub>: -32 to -27‰, δ<sup>15</sup>N<sub>org</sub>: -7.6 to -3.5‰). The discriminant role of

either litter or lithology remains unclear. The mineral horizons have a slightly different  $\delta^{13}\text{C}_{\text{org}}$  values according to bedrock lithology (-27 to -25.2‰ for SOM on calcareous moraine, -25.4‰ to -24.5‰ for SOM on Kimmeridgian limestones). Similar  $^{15}\text{N}$  enrichment was also measured for the SOM on Kimmeridgian limestone. There were two controls of SOM isotopic compositions: new litter inputs and overall isotopic fractionation during decomposition on different lithologies. Decomposition increased the  $\delta^{15}\text{N}$  and  $\delta^{13}\text{C}$  values: surface SOM (high litter contribution) with low  $\delta^{13}\text{C}_{\text{org}}$  and  $\delta^{15}\text{N}_{\text{org}}$  values and mineral soils with high  $\delta^{13}\text{C}_{\text{org}}$  and  $\delta^{15}\text{N}_{\text{org}}$  values. The distribution of fatty acids (FA, carboxylic acids abbreviated as x:y, where "x" is the number of carbon atoms and "y" the number of double C-C bonds in the chain) are characterized by straight chains in the  $\text{C}_{12}$  to  $\text{C}_{32}$  range, with clear even-over-odd C number preference, maximizing at 16:0 for the beech forest soils and at 22:0 for the conifer forest soils (Figure 2). The relative concentration ratios of the FA decrease severely with depth. All samples contain small to trace amount of odd chain acids in the  $\text{C}_{13}$  to  $\text{C}_{33}$  range (maxima at 23:0) and terminally branched iso and anteiso methyl alkanolic chains in the  $\text{C}_{12}$  to  $\text{C}_{18}$  range. These acids are abundant in lipids from soil microbial communities. The molecular concentration ratios and the  $\delta^{13}\text{C}_{\text{org}}$  and  $\delta^{15}\text{N}_{\text{org}}$  values show differences between the SOM on moraine and on limestone, suggesting different edaphic conditions, development and decomposition pathways of SOM on the Kimmeridgian limestone and calcareous moraine. On-going compound specific C isotope analyses combined with the information from neutral lipids (*n*-alkanes, *n*-alcohols, sterols) will provide further information on SOM transformations with depth in both lithological contexts.

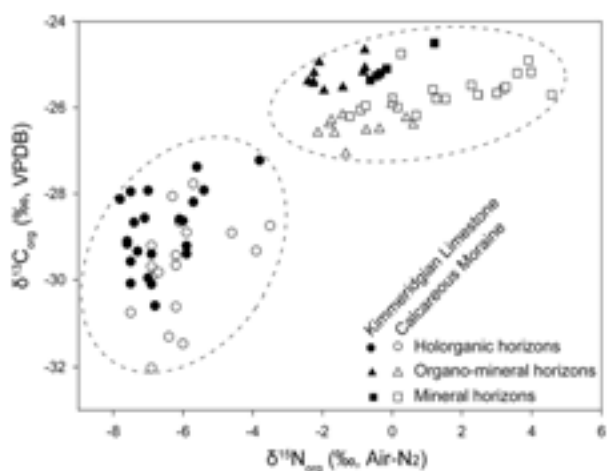


Figure 1.  $\delta^{13}\text{C}_{\text{org}}$  vs.  $\delta^{15}\text{N}_{\text{org}}$  of SOM on carbonate rocks of the Jura Mountains.

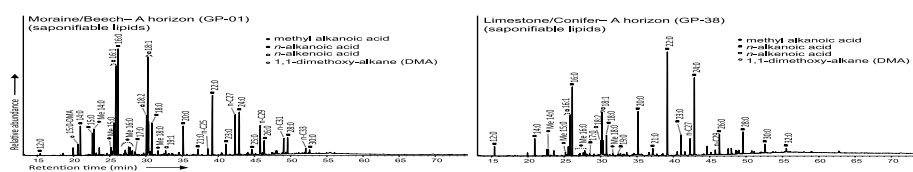


Figure 2. Distribution of saponifiable lipids extracted from surficial M/B and L/C soils.

## REFERENCE

Grünewald, G., Kaiser, K., Jahn, R., Guggenberger, G. 2006: Organic matter stabilization in young calcareous soils as revealed by density fractionation and analysis of lignin-derived constituents. *Organic Geochemistry* 37, 1573-1589.

## P 9.8

# Building a global database on organic geochemical characteristics of surface marine sediments: design & call for input

Tavagna Maria Luisa<sup>1</sup> and Eglinton Timothy<sup>1</sup>

<sup>1</sup> *Geology Institute, ETH Zürich, Sonneggstrasse 5, CH-8092 (maria.tavagna@erdw.ethz.ch)*

A growing and more diverse community is focused on studying the organic geochemical characteristics of marine sediments. The results of such studies are increasingly rich both in terms of data density and also in the variety of the parameters measured. At present, however, most of the resulting data remains disseminated in the literature and is not readily accessible for broader scale assessments. In particular, the fact that the data are not available in a single public source renders global-scale evaluations of composition and distribution of the sedimentary organic matter impractical. For this reason we have initiated a project to build a global database as a free instrument to be utilized by the whole international community. The database, called MOSAIC (Modern Ocean Sediment Archive and Inventory of Carbon), will be a resource for detailed organic geochemical and related information on marine sediments. MOSAIC will incorporate geospatial analysis tools in order to provide regional to global scale views on organic matter content and composition.

Key characteristics of MOSAIC include:

- Greatest emphasis is given on continental margin sediments since they represent the major loci of carbon burial, represent the interface between the terrestrial and oceanic realm, and are spatially highly heterogeneous;
- Organic geochemical parameters include concentrations and isotopic compositions at the bulk and molecular level and associated properties;
- The database will incorporate extensive contextual data regarding the depositional setting, and in particular, incorporating sedimentological properties;
- MOSAIC will be online and freely consultable.

The database is structured in a way that users will be able to provide and recover data and contextual parameters. The procedure will involve data incorporation into pre-configured spreadsheets (tables) available on the MOSAIC website. Completed tables will be imported via the Structural Query Language (SQL) into MOSAIC. The database is written in PostgreSQL, an open-source database management system. In order to visualize the data geographically, each element/datum must be associated to a latitude, longitude and altitude, enabling PostGIS (the spatial extension for PostgreSQL) to create a spatial database in a manner that can be interfaced to a Geographic Information System (GIS). In order to make the database broadly accessible, a HTML-PHP language-based website will ultimately be created and connected directly to the database. From the website it will be possible to both visualize and save data (in txt format) for utilization using common software (e.g. Excel, Word, PPT, Illustrator, ODV).

This contribution will outline the structure of the database, solicit feedback on desirable features, request data for inclusion in MOSAIC, and provide examples of data output.

## REFERENCES

- Griffith D.R., Martin W.R. & Eglinton T.I. 2010: The radiocarbon age of organic carbon in marine surface sediments. *Geochim. Cosmochim. Acta.* 74, 6788-6800.
- Sherman G. 2012, *The geospatial desktop*, Local Press.

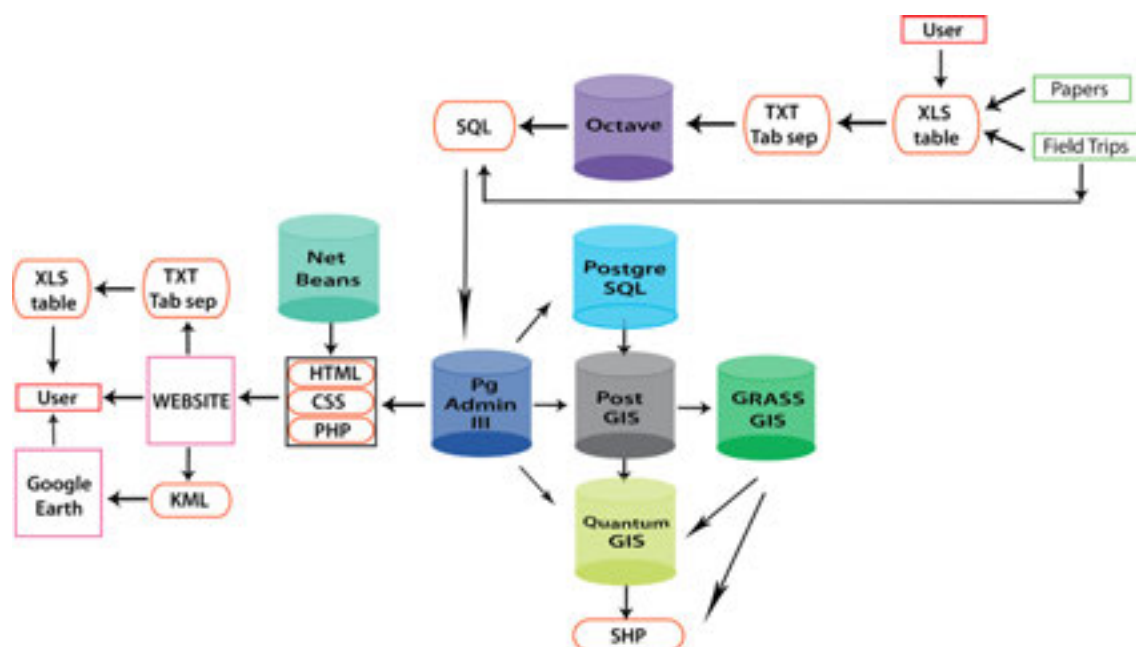


Figure 1. Architecture of MOSAIC database

## P 9.9

### Archaeal 16S rRNA gene sequences in the deep extreme Dead Sea sediments: determining who is there and why?

Camille Thomas<sup>1</sup>, Daniel Ariztegui<sup>1</sup> and the DSDDP Scientific Team<sup>o</sup>

<sup>1</sup> Department of Earth Sciences, University of Geneva

<sup>o</sup> Complete list of DSDDP scientists at [www.icdp-online.org](http://www.icdp-online.org)

The ICDP Dead Sea Deep Drilling Project (DSDDP) is an internationally funded initiative aiming to reconstruct the paleo-environmental and paleoseismicity histories of the Dead Sea Basin, in the Levantine region. Here we present preliminary results of the first geomicrobiological investigation in this extreme environment based on 16S rRNA gene sequences. We aim to obtain a comprehensive view of the Dead Sea sediment subsurface biosphere to identify and better understand the interaction between sediment and microbes and its imprint in the sedimentary record.

A 454m long sedimentary core retrieved from the center of the present Dead Sea displays distinctive facies that can be correlated to different lake regimes under contrasting climatic conditions that induced the preferential precipitation of evaporitic minerals. During rather dry periods as today in the Levant, the lake is holomictic and halite deposits as the main evaporitic phase. The lacustrine basin displays maximum salinities under such conditions. During more humid intervals, like those experienced in the late glacial period, or punctually during the Holocene, the lake becomes stratified, and aragonite precipitates forming varve-like laminae alternating with detritus laminae (aad facies) brought by incoming freshwater. Transitional periods of increasing aridity are further characterized by massive gypsum precipitation. We investigated the 16S rRNA gene sequences in several samples from key lithologies. Knowing the prevalent environmental conditions and the state of the lake when it happens we can propose some hypothesis to explain the presence of the identified archaeal sequences down to 200m below today's lake floor.

We have attempted to characterize as largely and completely as possible the microbial subsurface biosphere using DNA extractions and amplifications. We present here libraries of archaeal 16S rRNA sequences from two halite samples of 0.2 and 204m depth below lake floor (blf), one from a gypsum sample of 96 m blf, and one from an aad facies at 2.35 m blf. In order to give a good insight into the specific archaeal assemblages of the Dead Sea, we also compare the identified microbial assemblages with those of a microbial mat found in the saline shores of the present Dead Sea.

Our results show a microbial population largely dominated by obligate halophiles of the *Euryarcheota* family. Sequences retrieved from the halite and gypsum samples show very strong similarities with each other, with maximum richness found in the shallowest sediments. They also share their main phylotypes with those identified in the modern microbial mat, and previously described in the modern Dead Sea water column (Bodaker et al., 2010). While those populations show relatively little variation between each other, the aad sample, deposited in a completely different setting, under stratified lake conditions display a completely different population. It is almost exclusively composed of members of the MSBL1 candidate division first described in the Mediterranean deep brine basins (Van der Wielen et al., 2005). They are potential candidates for the production of methane found in high quantities in those environments. The Dead Sea water during aragonite precipitation shares with these sites extremely high salinity and high divalent cation concentrations, forming sharp gradients against less saline water, together with anoxic conditions.

The identified assemblages do not show major variations in the archaeal communities of the Dead Sea and lake ancestors sediments. The similarity between sequences found in the oldest and present day halite and gypsum point towards very low activity within the sediments. Thus, it is actually more likely that most of the microbial diversity and metabolic changes occur in the water column and the most recent sediments. Once buried, *Archaea* may have very low metabolic rates, and probably do not influence much their environments when deposited in halite and gypsum sediments of a holomictic lake.

On the other hand, the aad facies shows a unique archaeal assemblage with very specific phylotypes. The MSBL1 Candidate Division is here identified for the first time in a continental setting. Its unique recovery in this specific lithology advocates for the importance of specific sedimentary conditions and pore water chemistry for their development. It appears that the prevalence of sharp salinity gradients and anoxic conditions in the lake water at the moment of sedimentation are the prerequisites for their presence. Their activity and potential metabolism is nevertheless still to be expressed.

Finally, although primarily controlled by the salinity, it seems that physico-chemical conditions found in the (paleo)lake water, which are originally driven by climatic variations, are responsible for the development and preservation of specific archaeal assemblages recovered in the Dead Sea Basin sediments.

## REFERENCES

- Bodaker, I., Sharon, I., Suzuki, M. T., Feingersch, R., Shmoish, M., Andreishcheva, E., Sogin, M. L., et al. (2010). Comparative community genomics in the Dead Sea: an increasingly extreme environment. *The ISME journal*, 4(3), 399–407.
- Van der Wielen, P. W. J. J., Bolhuis, H., Borin, S., Daffonchio, D., Corselli, C., Giuliano, L., D'Auria, G., et al. (2005). The enigma of prokaryotic life in deep hypersaline anoxic basins. *Science*, 307(5706), 121–3.

## P 9.10

# Structure of biofilm communities and their sensitivity to metals. A case study of the Lagoon of Venice

Wildi Michel<sup>1</sup>, Le Faucheur Séverine<sup>1</sup>, Bernardi Aubry Fabrizio<sup>2</sup>, Botter Margherita<sup>2</sup>, Zonta Roberto<sup>2</sup>, Slaveykova Vera<sup>1</sup>.

<sup>1</sup> Aquatic Biogeochemistry and Ecotoxicology, University of Geneva, Institute F.A. Forel, 10 route de Suisse, CP 416, CH-1290 Versoix

<sup>2</sup> Istituto di Scienze Marine, Arsenale-Tesa 104, Castello 2737/F, 30122 Venezia

Biofilms are communities of microorganisms, which colonize the bottom of aquatic systems such as rivers, lakes and lagoons. They are mainly composed of algae, bacteria, fungi and viruses, which are wrapped in a matrix of exopolymeric substances (Paul S. Giller, 1998). As primary producers, they form the basis of aquatic food chains and represent a major source of carbon for grazers and fish. Moreover, biofilms are known to be very sensitive to environmental changes and as such could be used as biomarkers of metal contamination (Barranguet, et al., 2000). The present study aims to further evaluate the use of biofilms as a biomarker of water quality.

The biofilms growing in the Lagoon of Venice have been chosen for this study because the site provides a set of different environmental conditions. First, the lagoon is subject to a salinity gradient due to the mixing of freshwaters coming from twelve main rivers with seawater (Collavini, et al., 2005, Zonta, et al., 2005). In addition, a large variety of pollutants (trace metals, organic pollutants, fertilizers) occur in the Lagoon as a result of the proximity of the city (transport, wastewater), industrial activities situated in Porto Marghera (petrochemical, metallurgy, refinery) and agricultural activities which take place on 70 % of the watershed of the Lagoon (Collavini, et al., 2005). Our working hypothesis is that (i) the structure of biofilm communities will change according to metal concentrations and environmental conditions in the Venice lagoon (ii) their sensitivity to metals will depend on the composition of the biofilm i.e. EPS quantity and (iii) their metal content is directly proportional to the concentration of metals in ambient waters.

Colonisation boxes containing 32 microscope slides were immersed in water between 60 to 110 cm deep in five different sites representing various sources of pollution, i.e. a less-impacted site, which was considered as a control station (Santa Maria del Mare), an industrial site (Porto Marghera), an urban site (in a channel of Venice city) and two agricultural sites (in the Dese River). Two weeks later, slides colonized with biofilms were collected and kept undisturbed until treatment with fluorescent dyes for microscopy analysis. A combination of DAPI for biotic quantification and Concaviline A Texas Red for EPS quantification (Battin, et al., 2003) was used to determine biofilm structures whereas the algal autofluorescence was used to assess algal fraction. At least ten images per parameter were processed with Image J and the color thresholding method. Chlorophyll *a* was also measured in the samples after extraction with acetone. Total and intracellular metal concentrations (after washing with EDTA) were measured by ICP-MS after acidic digestion. Finally, biofilms were exposed to 100 µM of cadmium for 24 hours using microcosms and analysed for their concentration of bioaccumulated cadmium. Their sensitivity to cadmium was assessed using a fluorescent marker of lipid peroxidation.

Structural differences between communities were successfully assessed using fluorescent microscopy (Figure 1). Biofilms grown in Santa Maria del Mare (control site) were observed to be essentially composed of a biotic fraction (91 %) whereas a lower percentage (7 %) was found in biofilms collected in the Dese river in which abiotic fractions were predominant. The percentage of EPS was 7 times higher in the biofilms collected in the Dese River than in the one collected on the control site. Further analysis will be performed to relate water quality with the structure of biofilm communities.

## REFERENCES

- Barranguet, C., E. Charantoni, M. Plans, and W. Admiraal. 'Short-Term Response of Monospecific and Natural Algal Biofilms to Copper Exposure', *European Journal of Phycology* Vol. 35, No. 4, 397-406, 2000.
- Battin, T. J., L. A. Kaplan, J. D. Newbold, X. H. Cheng, and C. Hansen. 'Effects of Current Velocity on the Nascent Architecture of Stream Microbial Biofilms', *Applied and Environmental Microbiology* Vol. 69, No. 9, 2003.
- Collavini, F., C. Bettiol, L. Zaggia, and R. Zonta. 'Pollutant Loads from the Drainage Basin to the Venice Lagoon (Italy)', *Environment International* Vol. 31, No. 7, 939-947, 2005.
- Paul S. Giller, B. Malmqvist. *The Biology of Streams and River*, Oxford University Press, 1998.
- Zonta, R., F. Costa, F. Collavini, and L. Zaggia. 'Objectives and Structure of the Drain Project: An Extensive Study of the Delivery from the Drainage Basin of the Venice Lagoon (Italy)', *Environment International* Vol. 31, No. 7, 2005.

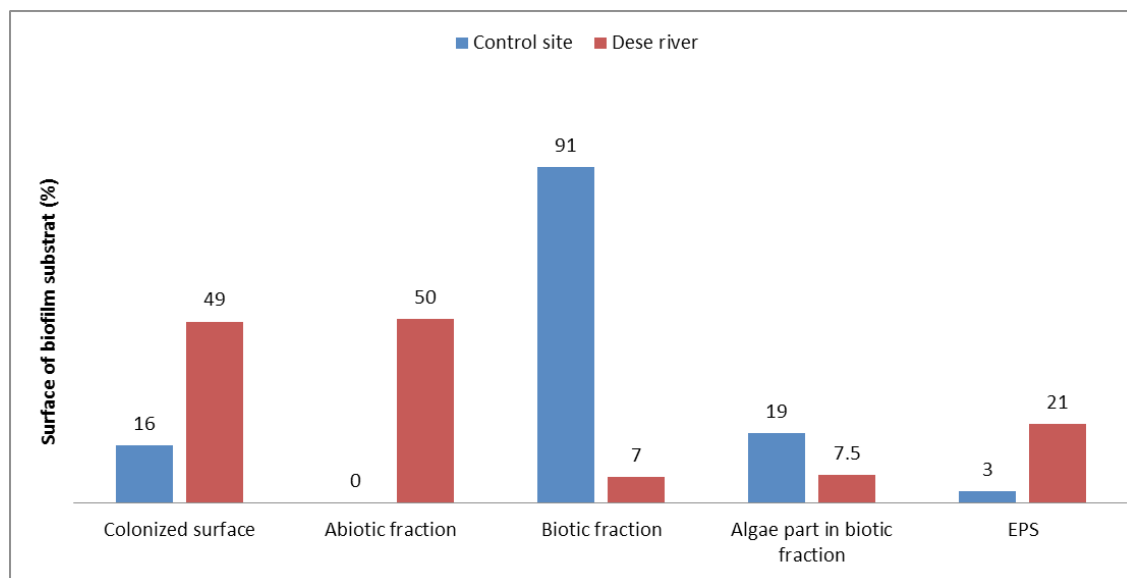


Figure 1: Structure of biofilm communities collected at the control site and at the Dese river site in the Venice Lagoon.

## P 9.11

# The influence of the biological nitrogen cycle on stromatolite formation

Feldmann M.

*geo-life, Buchholzstrasse 58, 8750 Glarus (mark@geo-life.ch)*

Comparative studies of different shaped stromatolites that were built through geologic times, from the early Precambrian to the present in varying environments, and studies of stromatolite forming organisms and satellite images of recent stromatolite locations, indicate that the biologic nitrogen cycle plays a key role for an explanation and the understanding of stromatolite formation.

Nitrogen is a key element in biological cycles, particularly for the creation of proteins. However, nitrogen has to be present in a biologically available form such as nitrogen oxide or ammonia. Abiotic nitrogen oxide occurs in volcanoes, in black smokers and other blowouts. Biological nitrogen fixation occurs when atmospheric nitrogen is converted to ammonia.

The characteristic layers of stromatolites arise when procaryotes form microbial mats with biofilms in which minerals precipitate. Biofilms are exclusively a product of photosynthesis. Since many procaryotes use protons for their metabolism it was an evolutionary pressure to develop a strategy to ensure a proton source. The result was the invention of photosynthesis by which protons became separated either from hydrogen sulfide ( $H_2S$ ) or water ( $H_2O$ ). Early shallow marine basins near blowouts containing nitrogen oxide may have been composed of solutions of  $H_2S$ . Under such circumstances the early sulfur photosynthesis evolved. Extracellular polymer substances (EPS) formed the first biofilms in which minerals precipitated, building the first dense stromatolitic layers. Progressively, condensing water filled the ocean basins and began to cover the landmasses of the early cratons. Around the blowouts the necessary nitrogen oxide was still abundantly available, the sunlight, however, reached only the water covered areas of the landmasses. For an autotrophic life it became necessary to invent a new form of photosynthesis, the oxygen photosynthesis, by which not only protons were separated from oxygen but also a new global energy currency was formed, ATP – adenosinetriphosphate, produced by cyanobacteria.

The increasing distance of the shallow water areas from the energy rich blowouts became problematic for the early prokaryotes. A new nitrogen source was necessary, and found in the atmosphere – elemental nitrogen. However, with a huge amount of ATP production cyanobacteria changed the elemental nitrogen into the biological available form of ammonia. Consequently, life explosively developed at the water-atmosphere boundary in intertidal areas. Cyanobacteria formed biofilms and microbial mats that subsequently led to the formation of stromatolitic layers.

For the next two billion years cyanobacteria changed the world not only with their production of oxygen but also with the conversion of elemental nitrogen into ammonia.

Because nitrogen fixation is very energy-consuming it is strongly regulated by organisms and only processed if there is no other possibility for a biologically available nitrogen supply. Thus, cyanobacteria, too, use ammonia if existent. As a consequence, with increasing concentration of ammonia in the open ocean stromatolites developed in deeper waters. The occurrence of conophyton stromatolites towards the end of the Precambrian is an indicator of such circumstances. They formed at slopes in a deeper marine environment and their shapes point towards the sunlight.

As a requirement for the evolution of eucaryotes ammonia was distributed in the seas by oceanic currents subsequently, leading to an explosion of life, and announcing the descent of the stromatolites.

In modern reefs cyanobacteria are as abundant as in microbial mats of Precambrian stromatolites, but they are accompanied by eucaryotes. This new assemblage led to new reef structures beginning with thrombolites and ending in fascinating coral reefs. Undisturbed biofilms that form stromatolitic microbial mats only occur if there is a need for nitrogen fixation under conditions of depleted biologically available nitrogen. A co-existence of stromatolites and evolved reef types under similar conditions is impossible. Thus, there are only two marine environments known today in which stromatolites grow, Shark Bay in Western Australia and the Exuma Cays in the Bahamas.



## 10. Biogeochemical cycles in a changing environment

## 15. Greenhouse Gases: Linkages between Biosphere and Climate

Ansgar Kahmen, Werner Eugster (session 10) ,  
& Werner Eugster, Christoph Ammann, Christoph Ritz (session 15)

*ACP – Commission on Atmospheric Chemistry and Physics,  
ProClim – Forum for Climate and Global Change,  
IGBP- Swiss Committee*

### TALKS:

- 10.1 Aemisegger, F., Pfahl, S., Spiegel, J., Eugster, W., Sodemann, H., Wernli, H.: Importance of evapotranspiration and rainfall reevaporation for the  $\delta^2\text{H}$  and  $\delta^{18}\text{O}$  signature of precipitation and boundary layer water vapour: a case study
- 10.2 Dietrich F., Cailleau G., Golay A., Junier P., Verrecchia E.: The Ca biogeochemical cycle in soils during a tropical tree lifetime
- 10.3 Gavazov K., Mills R., Bahn M.: Winter climate extremes and their role in biogeochemical processes under the snow
- 10.4 Lehmann M.M., Rinne K.T., Blessing C., Siegwolf R., Buchmann N., Werner R.A.: Carbon isotopic signatures in leaf dark-respired  $\text{CO}_2$  under different environments in potato
- 10.5 Mills R.T.E., Robroek B.J.M., Buttler A., Jassey V., Gatenby P., Gavazov K.S., Fujii K.: Altitude effects on soil function in forest and grassland systems of the Swiss Jura.
- 10.6 Mystakidis S., Davin E.L., Gruber N., Seneviratne S.I.: Constraining future climate-land carbon cycle projections using observationally-based carbon flux estimates
- 10.7 Rehmus A., Bigalke M., Valarezo C., Wilcke W.: Aluminum toxicity in tropical montane forest soils
- 10.8 Robroek B.J.M., Mills R.T.E., Jassey V.E.J., Signarbieux C., Refine M.-A., Vitali S., Bragazza L., Buttler A., Dorrepaal E.: SnowMan: peatland carbon and nitrogen cycling under changing snow conditions
- 10.9 Schwarz M.T., Bischoff S., Blaser S., Schmitt B., Thieme L., Boch S., Fischer M., Michalzik B., Schulze E.-D., Siemens J., Wilcke W.: Woody plant diversity drives retention of nitrogen in Central European forest canopies
- 10.10 Tomlinson G., Buchmann N., Schleppi R., Siegwolf R., Waldner P., Weber P.: The mobility of nitrogen between tree-rings of Norway spruce (*Picea abies* L.) and the effect of extraction on tree-ring  $\delta^{15}\text{N}$  and  $\delta^{13}\text{C}$
- 15.1 Bamberger I., Stieger J., Eugster W., Buchmann N.: Spatial variability of atmospheric methane: Attributing measured concentrations to emissions
- 15.2 Brunner, D., Henne, S., Oney, B., Bamberger, I., Buchmann, N., Davin, E., Mystakidis, S., Seneviratne, S., Gruber, N., Liu, Y., Leuenberger, M., Roches, A., Bey, I.: Understanding and quantifying  $\text{CO}_2$  and  $\text{CH}_4$  greenhouse gas fluxes on the regional scale: The project CarboCount CH
- 15.3 Felber R., Neftel A., Munger A., Ammann C.: Discerning cows from pasture – Contribution of grazing animals to eddy covariance greenhouse gas fluxes
- 15.4 Skinner, C., Gattinger, A., Muller, A., Mader, P., Fliebach, A., Stolze, M., Ruser, R., Niggli, U.: Greenhouse gas fluxes from agricultural soils under organic and non-organic management – a global meta-analysis

## POSTERS:

- P 10.1 Bamberger I., Hörtnagl L., Walser M., Hansel A., Wohlfahrt G.: Gap-filling Strategies for Annual VOC Flux Data Sets
- P 10.2 Bao R., Eglinton T.: Hydrodynamic controls on the age and composition of sedimentary organic matter on continental shelves: a case study from Chinese marginal seas
- P 10.3 Krüger J.P., Leifeld J., Alewell C.: Uplifting of hummocks in palsa peatlands in northern Sweden identified by stable carbon isotope profiles
- P 10.4 Schomburg A., Krüger J.P., Conen F., Alewell C.: Soil respiration rates of degrading palsa mires in northern Sweden

## 10.1

# Importance of evapotranspiration and rainfall reevaporation for the $\delta^2\text{H}$ and $\delta^{18}\text{O}$ signature of precipitation and boundary layer water vapour: a case study

Aemisegger Franziska<sup>1</sup>, Pfahl Stephan<sup>1</sup>, Spiegel Johanna<sup>2,3</sup>, Eugster Werner<sup>2</sup>, Sodemann Harald<sup>1</sup>, Wernli Heini<sup>1</sup>

<sup>1</sup> Institute for Atmospheric and Climate Sciences, ETH Zurich, Universitätstrasse 16, 8092 Zürich (franziska.aemisegger@usys.ethz.ch)

<sup>2</sup> Institute of Agricultural Sciences, ETH Zurich, Universitätstrasse 2, 8092 Zürich

<sup>3</sup> Swiss Federal Institute of Metrology, METAS, Lindenweg 50, 3003 Bern-Wabern

Atmospheric circulation patterns and precipitation determine local meteorological conditions and water availability and thus have a strong impact on plant ecosystems. In turn, local ecohydrology feeds back on the regional atmospheric water cycle through evapotranspiration. Studying evapotranspiration and its link to atmospheric circulation is thus central for a better understanding of the coupling between the land surface vegetation and the atmosphere. In this context, stable water isotopes, which are naturally available tracers of water phase changes, serve as a powerful and instructive research tool.

Here we present a case study, which aims at gaining a better understanding of the respective role of plant transpiration, soil evaporation and below-cloud rainfall reevaporation for the isotope signature of rain and boundary layer water vapour. We performed collocated rain and vapour isotope measurements in Zürich during a week in July 2011 with frequent but moderate rainfall intensities. Precipitation samples were collected hourly for isotope analysis with IRMS and the water vapour isotope signature was measured continuously at a 5 s temporal resolution using a commercial laser spectrometer (Aemisegger, et al. 2012).

An isotope-enabled, limited-area weather prediction model (Pfahl, et al. 2012) has been used to simulate the measurement period and perform sensitivity experiments. The isotope fractionation effects during plant transpiration, soil evaporation and rainfall reevaporation have been alternately suppressed during these experiments to investigate the relative importance of these processes for the isotope signature of low-level water vapour and precipitation. We found that the precipitation isotope signal is controlled to a large extent by cloud and below cloud interaction processes between the rain drops and ambient water vapour. The low-level water vapour isotope signal, however, is strongly influenced by evapotranspiration. By combining our isotope measurements with the results from numerical model simulations we illustrate the use of water isotopes in atmospheric moisture as a constraint for validation of the model representation of processes like evapotranspiration and below-cloud interaction of rain with low-level water vapour.

## REFERENCES

- Aemisegger, F., Sturm, P., Graf, P., Sodemann, H., Pfahl, S., Knohl, A. & Wernli, H. 2012: . Measuring variations of  $\delta^{18}\text{O}$  and  $\delta^2\text{H}$  in atmospheric water vapour using two commercial laser-based spectrometers: an instrument characterisation study, *Atmos. Meas. Tech.*, 5, 1491-1511, doi:10.5194/amt-5-1491-2012.
- Pfahl, S., Wernli, H., & Yoshimura, K. 2012: The isotopic composition of precipitation from a winter storm – a case study with the limited-area model COSMO<sub>ISO</sub>, *Atmos. Chem. Phys.*, 12, 1629-1648, doi:10.5194/acp-12-1629-2012.

## 10.2

### The Ca biogeochemical cycle in soils during a tropical tree lifetime

Dietrich Fabienne<sup>1</sup>, Cailleau Guillaume<sup>1</sup>, Golay Anne<sup>1</sup>, Pilar Junier<sup>2</sup> & Verrecchia Eric<sup>1</sup>

<sup>1</sup> Institut des sciences de la Terre, University of Lausanne, Geopolis-Mouline, CH-1015 Lausanne

<sup>2</sup> Laboratory of Microbiology, University of Neuchâtel, Emile-Argand 11, CH-2000 Neuchâtel

The study of calcium (Ca) biogeochemical cycle has always been neglected compared to those of other elements, such as carbon or nitrogen. Nevertheless, Ca supply is a key question in the context of the oxalate carbonate pathway (OCP). OCP is a process leading to the conversion of atmospheric CO<sub>2</sub> into pedogenic carbonate through the formation of plant oxalate (Cailleau et al., 2011). Ca is involved all along the OCP. This pathway comprises an oxalogenic tree, i.e. an iroko (*Milicia excelsa*), which leads to the formation of an oxalate-rich forest ground. When accessible in the soil, oxalate is consumed by soil oxalotrophic bacteria. Oxalotrophy induces the release of carbonate ions in the soil solution and thus, allows a local soil pH increase. When stability pH of calcite is reached, in presence of Ca, Ca-carbonate precipitates (Verrecchia et al., 2006). As tropical ferralitic soils are known to be very poor in alkaline elements (Leneuf, 1959), understanding the Ca cycle, and its dynamics, is instrumental in the context of oxalogenic-oxalotrophic ecosystems.

The aim of this study is to provide a snapshot of an OCP system in order to propose a dynamical model focused on Ca during an oxalogenic tree lifetime. A quantification of the Ca cycle in an iroko tree ecosystem is presented and compared to those of a secondary tropical forest (OCP-free ecosystem). This Ca balance between the two systems shows that the Ca amount in the iroko soil is at least one order of magnitude higher than the one in an OCP-free setting. The massive amount of Ca, required to support carbonate accumulation, raises the question of substantial Ca supply in such tropical soils. Thus, figure 1 proposes a sketch of OCP emphasizing the Ca cycle.

In these tropical ecosystems, the Ca reservoir is the vegetation and the high turnover of the organic matter allows Ca recycling (Jordan, 1985) to support phytomass production. During the seedling stage, oxalotrophy starts to influence the initial soil acidic pH, but this process might still be weak. At the juvenile stage, the pH increase is sufficient enough to allow Ca<sup>2+</sup> storage into soil. In addition, increasing Ca concentration starts to catalyze oxalogenesis (Franceschi and Nakata, 2005), leading to a positive feedback. At the mature stage, the stability pH for calcite is reached and pedogenic carbonate accumulates. Finally, the initial positive feedback is generalized to the entire OCP ecosystem. In conclusion, OCP ecosystems are able to trigger the formation of a long-term pedogenic carbonate reservoir in tropical settings.

#### REFERENCES

- Cailleau G., Braissant O. & Verrecchia E.P. 2011: Turning sunlight into stone: the oxalate-carbonate pathway in a tropical tree ecosystem. *Biogeosciences*, 8, 1755–1767.
- Franceschi V.R. & Nakata P.A. 2005: Calcium Oxalate in Plants: Formation and Function. *Annual Review of Plant and Biology*, 56, 41-71.
- Jordan C.F. 1985: Nutrient cycling in tropical forest ecosystems. John Wiley and sons, New York, 189 p.
- Leneuf N. 1959: L'altération des granites calco-alcalins en Côte d'Ivoire forestière et les sols qui en sont dérivés. O.R.S.T.O.M., Paris, 210 p.
- Verrecchia E.P., Braissant O., & Cailleau G. 2006: The oxalate-carbonate pathway in soil carbon storage: the role of fungi and oxalotrophic bacteria. *Fungi in Biogeochemical Cycles*, ed. G. M. Gadd, Published by Cambridge University Press.

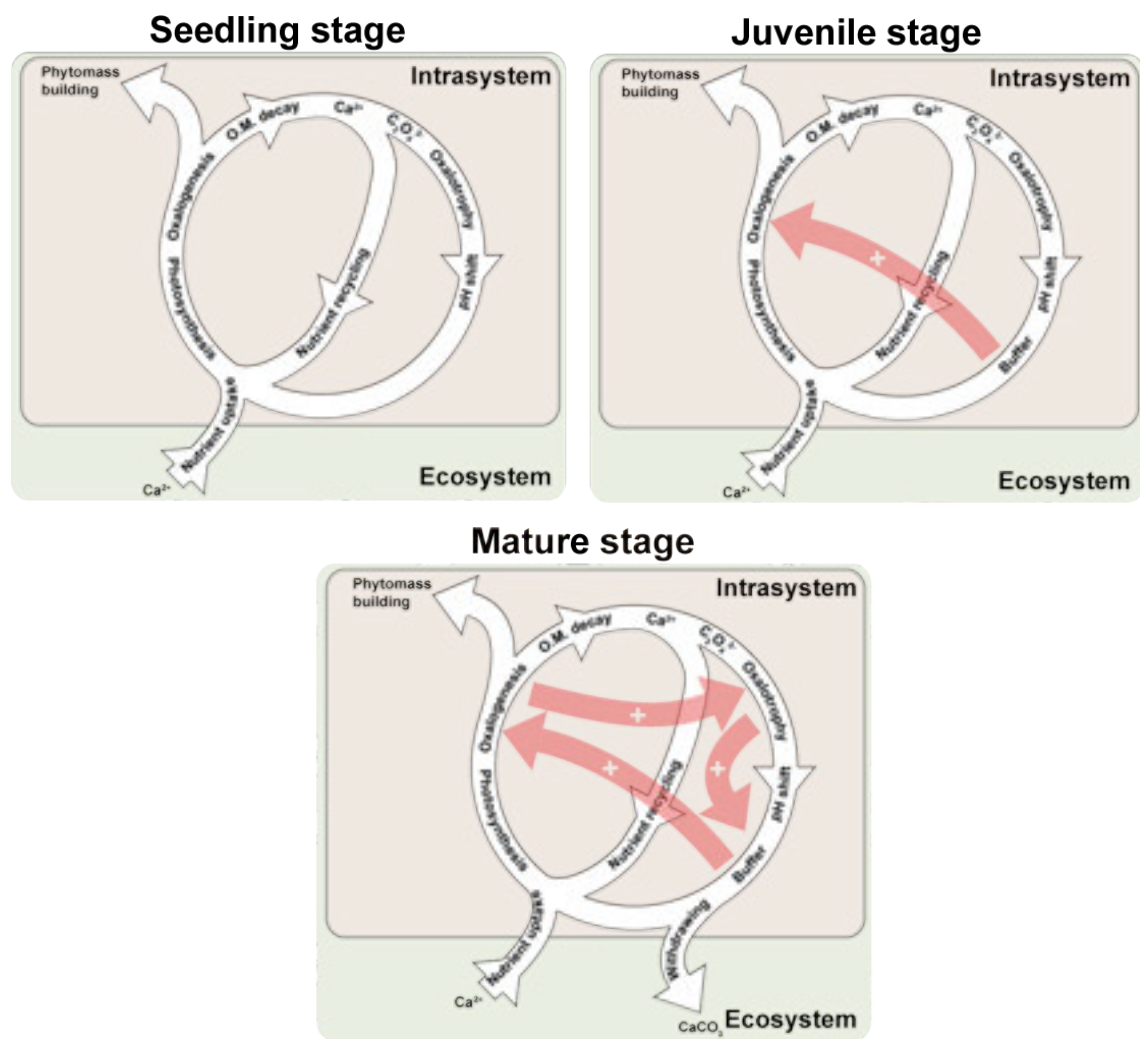


Figure 1. Sketch showing the model for the positive feedback of Ca on the OCP ecosystems.

## 10.3

# Winter climate extremes and their role in biogeochemical processes under the snow

Gavazov Konstantin<sup>1,2</sup>, Mills Robert<sup>1,2</sup>, Bahn Michael<sup>3</sup>

<sup>1</sup> Ecole Polytechnique Fédérale de Lausanne EPFL, School of Architecture, Civil and Environmental Engineering ENAC, Laboratory of ecological systems ECOS, Station 2, CH-1015 Lausanne (konstantin.gavazov@epfl.ch)

<sup>2</sup> Swiss Federal Institute for Forest, Snow and Landscape Research WSL, Site Lausanne, Station 2, CH-1015 Lausanne

<sup>3</sup> University of Innsbruck, Institute of Ecology, Ecophysiology and Ecosystem Processes Research Group, A-6020 Innsbruck

The central research question of this project is how soil respiration and soil microbial community composition and activity of subalpine grasslands are affected by extreme winter climate events, such as advanced snowmelt date. Continuous winter season data on source and fate of CO<sub>2</sub> produced in soil under ambient and reduced snowpack will be presented, testing hypotheses on the underlying mechanisms.

In the scope of this talk, focus will be laid on the assumptions that (1) under ambient snow regime with a consistent snow cover, temporal variations in soil respiration rates are independent from fluctuations in soil temperature and moisture, but are determined by DOC concentration in the soil solution. In contrast, (2) reduced snow cover due to advanced snowmelt leads to intensive freeze-thaw cycles in the soil with larger amplitudes of microbial biomass, DOC and soil CO<sub>2</sub> production and efflux over the course of winter. Expected (3) shift in microbial community composition towards decreased fungal / bacterial ratios due to snow removal will further result in (4) a stronger incorporation of labile C in microbial biomass and more pronounced priming effects of soil organic matter turnover.

As a perspective, adequate carbon budgets for temperate mountain ecosystems could be constructed, relating snow insulation capacities to soil carbon availability, to microbial diversity and activity, and ultimately to the production and efflux of CO<sub>2</sub> from soils under various snow conditions. We hope to contribute some further understanding on the process of temperature decoupling of soil respiration in winter, which should feed into the development of more accurate global carbon circulation models.

## 10.4

### Carbon isotopic signatures in leaf dark-respired CO<sub>2</sub> under different environments in potato

Lehmann Marco M.<sup>1</sup>, Rinne Katja T.<sup>2</sup>, Blessing Carola<sup>1</sup>, Siegwolf Rolf<sup>2</sup>, Buchmann Nina<sup>1</sup>, Werner Roland A.<sup>1</sup>

<sup>1</sup> Institute of Agricultural Sciences, ETH Zurich, Universitaetsstr. 2, CH-8092 Zurich (malehman@ethz.ch)

<sup>2</sup> Laboratory of Atmospheric Chemistry, Paul Scherrer Institute (PSI), CH-5232 Villigen

Plants permanently respire various carbon sources to gain energy and intermediates for many essential plants processes. Thereby, CO<sub>2</sub> is produced during the Krebs cycle and connected anabolic reactions. Typically, the carbon isotope ratio of leaf dark-respired CO<sub>2</sub> ( $\delta^{13}\text{C}_r$ ) shows a diel cycle with a <sup>13</sup>C-enrichment during illumination and a <sup>13</sup>C-depletion during darkness.  $\delta^{13}\text{C}_r$  can be enriched by 10‰ relative to the isotopic composition of the respiratory compounds ( $\delta^{13}\text{C}_{RC}$ ) such as sugars or organic acids. The reasons for this isotopic offset between  $\delta^{13}\text{C}_r$  and  $\delta^{13}\text{C}_{RC}$  are not fully understood, since we lack knowledge about the  $\delta^{13}\text{C}$  values of single respiratory compounds. Moreover, the diel cycle of  $\delta^{13}\text{C}_r$  and  $\delta^{13}\text{C}_{RC}$  can also vary due to species and environmental factors such as temperature and water status. For example,  $\delta^{13}\text{C}_r$  and  $\delta^{13}\text{C}_{RC}$  were shown to be more positive under drought, but less is known about the influence of higher temperature.

We carried out climate chamber experiments with potato plants grown under two different temperature and two water regimes. Using the in-tube incubation technique, we assessed the diel cycle of  $\delta^{13}\text{C}_r$ . In parallel, we measured  $\delta^{13}\text{C}$  and concentrations of several carbohydrates (soluble mono- and disaccharides; starch) as well as organic acids (malate and citrate) using EA- and HPLC-IRMS.

At higher temperatures,  $\delta^{13}\text{C}_r$  and  $\delta^{13}\text{C}_{RC}$  values were significantly more negative, whereas under drought  $\delta^{13}\text{C}_r$  and  $\delta^{13}\text{C}_{RC}$  values were significantly more positive. The combined treatment of higher temperature and drought showed intermediate  $\delta^{13}\text{C}_r$  and  $\delta^{13}\text{C}_{RC}$ , seeming that both impacts partially compensate each other. The diel course of  $\delta^{13}\text{C}_r$  cannot be explained by  $\delta^{13}\text{C}$  of soluble sugars and starch, but we suggest malate as a key carbon source of  $\delta^{13}\text{C}_r$ .

## 10.5

### Altitude effects on soil function in forest and grassland systems of the Swiss Jura.

Robert Mills<sup>1,2</sup>, Bjorn Robroek<sup>4,2</sup>, Alexandre Buttler<sup>1,2,3</sup>, Vincent Jasse<sup>1,2</sup>, Peter Gatenby<sup>2</sup>, Konstantin Gavazov<sup>2</sup>, Kazumichi Fujii<sup>5</sup>.

<sup>1</sup> WSL Swiss Federal Research Institute for Forest, Snow and Landscape Research, Site Lausanne, Station 2, CH-1015 Lausanne, Switzerland

<sup>2</sup> École Polytechnique Fédérale de Lausanne (EPFL), School of Architecture, Civil and Environmental Engineering (ENAC), Laboratory of Ecological Systems (ECOS), Station 2, CH-1015 Lausanne, Switzerland

<sup>3</sup> Laboratoire de Chrono-environnement, UMR CNRS 6249, UFR des Sciences et Techniques, 16 route de Gray, Université de Franche-Comté, F-25030 Besançon, France

<sup>4</sup> Ecology and Biodiversity, Utrecht University, Padualaan 8, 3584 CH Utrecht, The Netherlands

<sup>5</sup> Forestry and Forest Products Research Institute, Tsukuba 305-8687, Japan

We investigated the role of altitude as a proxy for climate along a ~800m transect in the Swiss Jura, as a driver of soil function in forest and grassland systems. We used radiocarbon-labelled substrates to mimic soil solution concentrations of low molecular weight compounds and measured potential enzymatic activity as two broad measures of soil function. Functional measures are variably sensitive to altitude, with strong response in mineralisation kinetics of sugars, amino acids and organic acids, but not all enzyme activities showed a response. Grasslands showed a much greater altitude response than forests, suggesting a decoupling of decomposition processes with climate under forests, and a role for ground-cover vegetation. Our results also highlighted the exceptional soil functional capacity of dry grassland systems, which in the current study had metrics of function twice that of other grassland systems. These findings suggest a disconnect between some metrics of soil function, but reinforce the strong link between function and organic matter content in soils. This underpins the need to elucidate ecosystem effects on soil function, and encourages further safeguarding of SOM as a significant reservoir of functional capacity.

## 10.6

## Constraining future climate-land carbon cycle projections using observationally-based carbon flux estimates

Mystakidis Stefanos<sup>1,3</sup>, Davin Edouard Léopold<sup>1,3</sup>, Gruber Nicolas<sup>2,3</sup> & Seneviratne Sonia Isabelle<sup>1,3</sup>

<sup>1</sup> Institute for Atmospheric and Climate Science, Universitaetstrasse 16, ETH Zürich, CH-8092 Zürich (stefanos.mystakidis@env.ethz.ch)

<sup>2</sup> Environmental Physics, Institute of Biogeochemistry and Pollutant Dynamics, Universitaetstrasse 16, ETH Zürich, CH-8092 Zürich

<sup>3</sup> Center for Climate Systems Modeling, Universitaetstrasse 16, ETH Zürich, CH-8092 Zürich

The increase in atmospheric CO<sub>2</sub> concentration as a result of the human perturbation of the carbon cycle is mainly driven by fossil fuel and cement emissions, and land-use associated emissions and partially compensated by ocean and land carbon uptake. It is well known that the terrestrial biosphere response to climate change is not well understood. The need to better understand the behaviour of the land biosphere has been driving the development of terrestrial biogeochemistry models (Prentice et al., 1989). The ability of these models to reproduce the observed features of the terrestrial carbon cycle increases the confidence in future projections but the sensitivity of carbon cycle models to different environmental factors is possibly just a result of the particular parameterization chosen by the model developer.

Here, we first evaluate the land carbon fluxes from coupled carbon-climate models used in the framework the CMIP5 project (Coupled Model Intercomparison Project-phase 5, Taylor et al., 2011) for the historical period and then use the fit of the different models to better constrain the modeled sensitivity of the land carbon cycle in these models to future climate change. The overall aim of the study is to find an emergent constraint linking the future change in the land carbon sink to observationally-based carbon flux estimates. To this end, we compare monthly mean Gross Primary Production (GPP) estimates for the period 1989–2005 from the CMIP5 models with the MPI FLUXNET-based upscaled GPP (Jung et al., 2009, 2011) for 26 different regions in the world based on the definition of the IPCC's SREX Report (Seneviratne et al., 2012) by means of quantile-quantile (q-q) diagrams showing model against observations. We find that the CMIP5 models tend to underestimate (overestimate) the low (high) quantiles of GPP. Depending on the regions these biases in GPP can be related to biases in other variables such as evapotranspiration, temperature and precipitation.

The identified biases in present-day GPP are then used to constrain future change in climate-carbon cycle projections. A strong relationship ( $r > 0.8$ ) is found between the future changes in the land carbon sink (NEE) and GPP biases in CMIP5 models. Preliminary results suggest that the use of this emergent constraint decreases the future land carbon uptake by photosynthesis and the net land carbon sink by more than 30% in the Tropics (30°N–30°S). The use of a second constraint based on atmospheric CO<sub>2</sub> inversions of the Transcom 3 project (Baker et al., 2006, Gurney et al., 2004) will also be discussed.

### REFERENCES

- Baker, D. F., & Coauthors 2006: Transcom 3 inversion intercomparison: Impact of transport model errors on the interannual variability of regional CO<sub>2</sub> fluxes, 1988–2003. *Global Biogeochem. Cycles*, 20, GB1002, doi:10.1029/2004GB002439.
- Gurney, K. R., & Coauthors 2004: Transcom 3 inversion intercomparison: model mean results for the estimation of seasonal carbon sources and sinks. *Global Biogeochem. Cycles*, 18, GB1010, 1320 doi:10.1029/2003GB002111.
- Jung, M., M. Reichstein, & A. Bondeau 2009: Towards global empirical upscaling of FLUXNET eddy covariance observations: Validation of a model tree ensemble approach using a biosphere model. *Biogeosciences*, 6, 2001–2013.
- Jung, M., & Coauthors 2011: Global patterns of land-atmosphere fluxes of carbon dioxide, latent heat, and sensible heat derived from eddy covariance, satellite, and meteorological observations. *J. Geophys. Res.*, 116, G00J07, doi:10.1029/2010JG001566.
- Prentice IC, Webb RS, Ter-Mikhaelian MT et al. 1989: Developing a global vegetation dynamics model: results of an IASA summer workshop. *IASA Research Reports*, 89(7). International Institute for Applied Systems Analysis.
- Seneviratne, S., et al. 2012: Changes in climate extremes and their impacts on the natural physical environment. In: *Managing the Risks of Extreme Events and Disasters to Advance Climate Change Adaptation* [Field, C.B., V. Barros, T.F. Stocker, D. Qin, D.J. Dokken, K.L. Ebi, M.D. Mastrandrea, K.J. Mach, G.-K. Plattner, S.K. Allen, M. Tignor, and P.M. Midgley (eds.)]. A Special Report of Working Groups I and II of the Intergovernmental Panel on Climate Change, (IPCC SREX Report), pp. 109–230.
- Taylor, K. E., R. J. Stouffer & G. Meehl 2011: An Overview of CMIP5 and the Experiment Design. *Bull. Am. Meteorol. Soc.*, 93, 485–498.

## 10.7

## Aluminum toxicity in tropical montane forest soils

Rehmus Agnes<sup>1</sup>, Moritz Bigalke<sup>1</sup>, Carlos Valarezo<sup>2</sup>, Wolfgang Wilcke<sup>1</sup>

<sup>1</sup> Institute of Geography, University of Berne, Hallerstrasse 12, 3012 Bern, Switzerland

<sup>2</sup> National University of Loja, Loja, Ecuador

Aluminum is a major cation in the tropical element cycle on acid soils. In the literature, it is therefore frequently stated that Al phytotoxicity might inhibit plant growth on acid tropical soils (Alleoni et al. 2010; Delhaize and Ryan 1995; Schaedle et al. 1989). Possible Al toxicity is indicated by a wide distribution of Al-accumulating plant species (> 1000 mg kg<sup>-1</sup> in leaves), mostly pertaining to the families Rubiaceae and Melastomataceae which is usually interpreted as adaptation to Al toxicity (Jansen et al. 2002). A further adaptation is a shallow rooting mainly in the organic horizons, where Al toxicity can be avoided, because of low Al concentrations and organo-complexation of Al (Wullaert et al. 2013).

Environmental changes, such as elevated H and N deposition because of Amazonian forest fires acidify the ecosystem and could result in increased Al availability and thus, increased phytotoxicity to Al-sensitive plants.

To explore the role of Al in a tropical montane rain forest in south Ecuador, we determined Al fluxes through the forest canopy (Boy et al. 2008) and conducted an hydroponic experiment for selected tropical montane forest trees – which were no Al accumulators. To determine dose-response functions of Al, seedlings of *Cedrela odorata* Moritz ex Turcz., *Heliocarpus americanus* L., and *Tabebuia chrysantha* (Jacq.) G. Nicholson were incubated with a Hoagland nutrient solution containing 0, 300, 600, 1200, and 2400  $\mu$ M Al. In an additional treatment, we grew the same tree species in native litter leachate from the study area. Nutrient solutions were sampled and replaced weekly. After six weeks, plants were harvested. Roots and leaves were scanned and parameters like root length and diameter and leaf area were determined with the software WinRhizo™. Furthermore, we determined macro and micro nutrient concentrations in nutrient solutions before and after incubation and in plant tissue with AAS, ICP-MS, and TOC and CNS analyzer.

Total Al deposition (bulk and dry) from the atmosphere was low (2 kg ha<sup>-1</sup> yr<sup>-1</sup>) and increased strongly in throughfall (10) and litterfall (7.5) indicating substantial Al uptake into the plant. Increasing Al concentrations reduced biomass production, healthy leaf area, and number of root tips. Root diameter, root-to-shoot biomass ratio, and diseased leaf area increased (Figure 1). Yet, Al toxicity occurred at Al concentrations between 300 and 600  $\mu$ M, which is far above usual total Al concentrations (< 60  $\mu$ M, even mostly as non-toxic organo-Al complex) in native litter leachate which can be considered as the plant-available Al pool. Biomass production was lowest if plants grew in litter leachate indicating limitation of plant growth by other factors than Al toxicity. We conclude that Al toxicity in the studied ecosystem is unlikely and that considerable Al is cycled through the plants without damage.

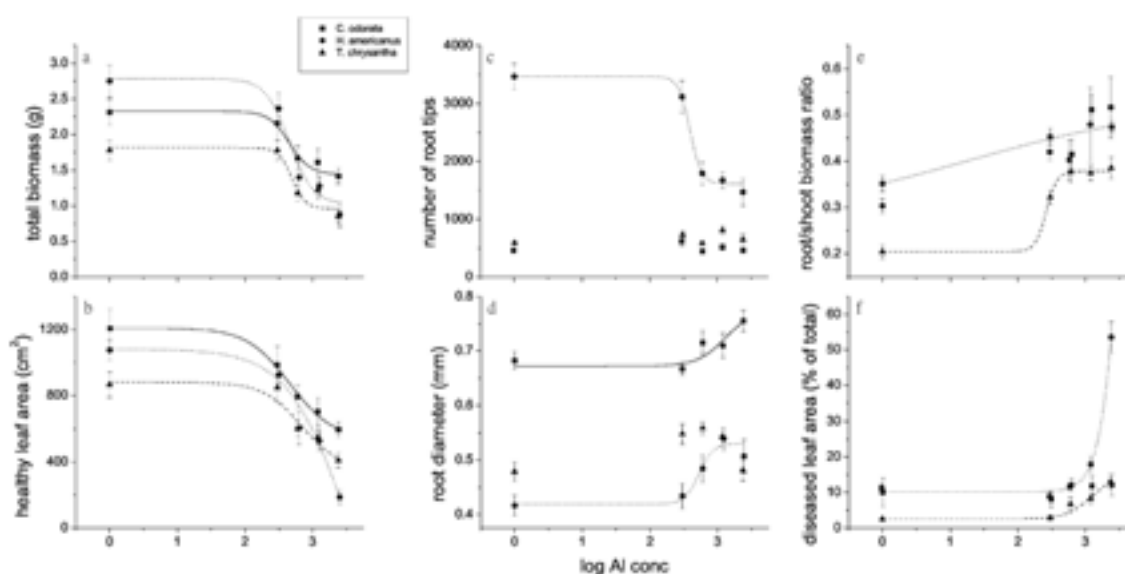


Figure 1. Dose response functions for total biomass (a), healthy leaf area cm<sup>2</sup> (b), number of root tips (c), root diameter (mm) (d), root-to-shoot biomass ratio (e), and diseased leaf area (% of total) (f), for *C. odorata* (N=9), *H. americanus* (N=8), and *T. chrysantha* (N=8). Error bars represent SE of means. Lines are fitted sigmoid growth functions

## REFERENCES

- Alleoni, L.R.F., Cambri, M.A., Caires, E.F., Garbuio, F.J. 2010. Acidity and aluminium speciation as affected by surface liming in tropical no-till soils. *Soil Sci. Soc. Am. J.* 74, 1010–1017.
- Boy, J., Valarezo, C., Wilcke, W. 2008. Water flow paths in soil control element exports in an Andean tropical montane forest. *Eur. J. Soil Sci.* 59, 1209-1227.
- Delhaize, E., Ryan, P.R. 1995: Aluminum toxicity and tolerance in plants. *Plant Physiol.* 107, 315–321, DOI 10.1104/pp.107.2.315.
- Jansen, S., Watanabe, T., Smets, E. 2002: Aluminium accumulation in leaves of 127 species in Melastomataceae, with comments on the order Myrtales, *Ann. Bot.*, 90, 53-64.
- Schaedle, M., Thornton, F., Raynal, D., Tepper, H. 1989. Response of tree seedlings to aluminum. *Tree Physiol.* 5, 337–356.
- Wullaert, H., Bigalke, M., Homeier, J., Cumbicus, N.L., Valarezo, C., Wilcke, W. 2013. Short-term response of the Ca cycle of a montane forest in Ecuador to low experimental CaCl<sub>2</sub> additions. *J. Plant Nutr. Soil Sci.*, published online on 19/08/2013, DOI 10.1002/jpln.2012300146.

## 10.8

## SnowMan: peatland carbon and nitrogen cycling under changing snow conditions

Bjorn JM Robroek<sup>1</sup>, Robert TE Mills<sup>2,3</sup>, Vincent EJ Jassey<sup>2,3</sup>, Constant Signarbieux<sup>2</sup>, Marine-Anaïs Refine<sup>2</sup>, Sylvain Vitali<sup>2</sup>, Luca Bragazza<sup>2,3,4</sup>, Alexandre Buttler<sup>2,3</sup> & Ellen Dorrepaal<sup>5</sup>

<sup>1</sup> Ecology and Biodiversity Group, Utrecht University, The Netherlands (b.j.m.robroek@uu.nl; bjorn.robroek@epfl.ch).

<sup>2</sup> École Polytechnique Fédérale de Lausanne (EPFL), Laboratory of Ecological Systems (ECOS), Switzerland.

<sup>3</sup> WSL - Swiss Federal Institute for Forest, Snow and Landscape Research, Lausanne, Switzerland.

<sup>4</sup> University of Ferrara, Dept. of Life Science and Biotechnologies, Italy.

<sup>5</sup> Ecology and Environmental Sciences, Umeå University, Sweden.

Most of the studies on climate change effects on ecosystem processes have mainly focused on the effects of temperature and precipitation during the plant growing season, but recently awareness of the importance of altered environmental conditions during winter has increased (Groffman *et al.*, 2011). Global warming has caused the snow free period (*i.e.* earlier spring melt) to advance by 3-5 days per decade (Dye, 2002). As snow has an insulating effect on soil and vegetation, a reduction in depth and duration of the snow cover can alter the structure and function of microbial and plant community (Brooks *et al.*, 2011; Robroek *et al.*, 2013), with cascade effects on biogeochemical cycles (Groffman *et al.*, 2011).

In a Swiss Jura peatland, we performed a snow manipulation experiment to understand the complex interplay between snow cover and soil freezing dynamics on enzymatic activities (roots and mosses), carbon and nitrogen cycling and plant ecophysiology. We studied 15 plots in *Sphagnum* dominated lawns, equally divided in control (no manipulation), snow removal, and snow addition plots (Fig. 1).



Figure 1. Snow removal plot (left) and control and addition plots (right) in the Swiss Jura peatland.

Soil C fluxes were measured from all plots on a weekly basis from December 2012 to September 2013. All plots were inoculated with <sup>15</sup>N four times over the experimental period (under peak snow conditions, just before and after melt-out and during summer period) while making sure not to disturb the physical character of the snow (control and addition plots). Before each inoculation, we collected peat soil samples from which all roots were sorted for background <sup>15</sup>N analyses and root enzymatic activity analyses. One week after inoculation, additional peat soil samples were taken and roots were sorted according to the corresponding plant functional type (ericoids and graminoids), whereas all vascular plants and *Sphagnum* mosses were sorted to species level and analysed for <sup>15</sup>N. Enzymatic activities from *Sphagnum* mosses were measured at above-mentioned periods as well as some ecophysiological parameters (*i.e.* photosynthesis, chlorophyll content, chlorophyll fluorescence) on a representative graminoid and moss species.

In this presentation we will present the results of this extensive snow manipulation experiment. Initial data exploration shows no discernable trend in a treatment effect regarding C fluxes, indicating resilience of respiration processes under changing snow conditions. Soil respiration peaks in all treatments just after melt-out (Fig. 2). Under the snowpack (control and addition), maximum efficiency of PSII (health indicator for the plant) of the grass and moss species was close to the maximum, while in the removal plot PSII of both species was strongly reduced. After full melt-out, PSII of both species in the removal plots recovered and their photosynthetic performance was higher as compared to the control and addition. Similar patterns were recorded for enzymatic activities in *Sphagnum* mosses, especially for  $\beta$ -glucosidase activity.

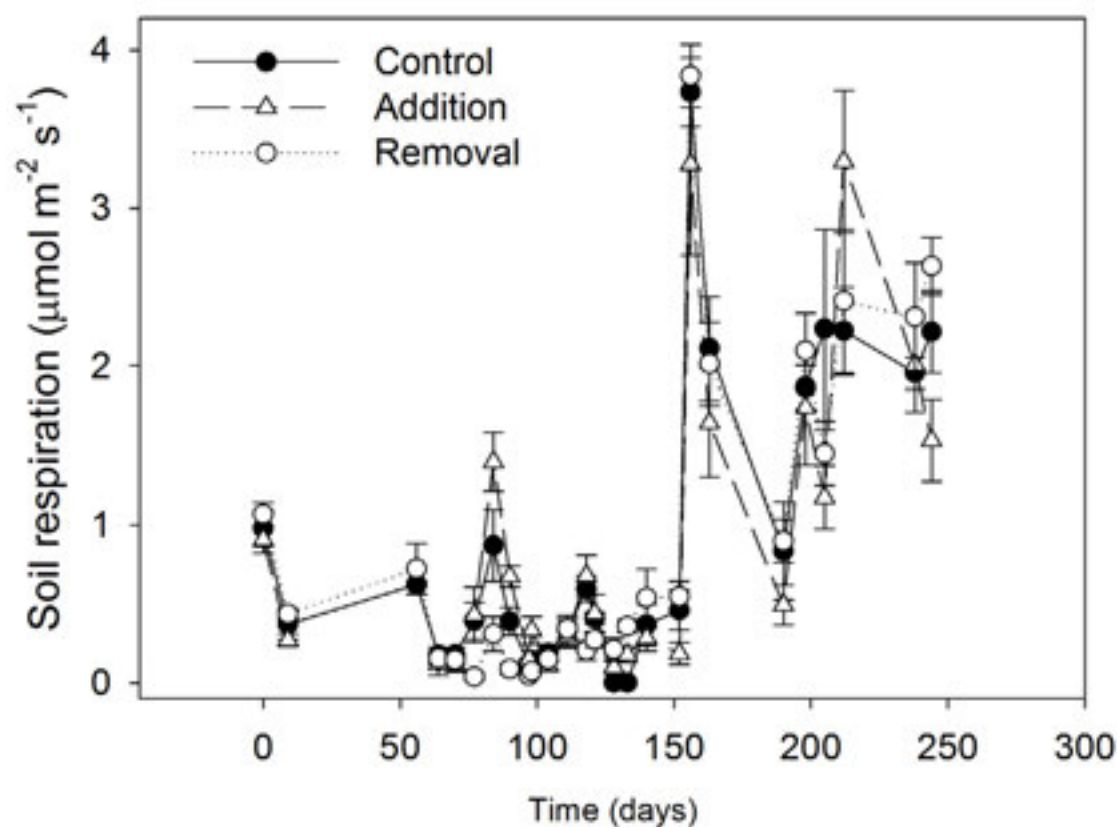


Figure 2. Soil respiration over the experimental period.

#### REFERENCES

- Brooks P.D., Grogan P., Templer P.H., Groffman P., Öquist MG, Schimel J 2011: Carbon and nitrogen cycling in snow-covered environments. *Geography Compass*, 5, 682–699.
- Dye D.G. 2002: Variability and trends in the annual snow-cover cycle in Northern Hemisphere land areas, 1972–2000. *Hydrological Processes*, 16, 3065–3077.
- Groffman P.M., Hardy J.P., Fashu-Kanu S., Driscoll C.T., Cleavitt N.L., Fahey T.J., Fisk M.C. 2011: Snow depth, soil freezing and nitrogen cycling in a northern hardwood forest landscape. *Biogeochemistry*, 102, 223–238.
- Robroek B.J.M., Heijboer A., Jassey V.E.J., Hefting M.M., Rouwenhorst T.G., Buttler A., Bragazza L. 2013: Snow cover manipulation effects on microbial community structure and soil chemistry in a mountain bog. *Plant and Soil*, 369, 151–164.

## 10.9

## Woody plant diversity drives retention of nitrogen in Central European forest canopies

Martin T. Schwarz<sup>1</sup>, Sebastian Bischoff<sup>2</sup>, Stefan Blaser<sup>3</sup>, Barbara Schmitt<sup>3</sup>, Lisa Thieme<sup>4</sup>, Steffen Boch<sup>3</sup>, Markus Fischer<sup>3</sup>, Beate Michalzik<sup>2</sup>, Ernst-Detlef Schulze<sup>5</sup>, Jan Siemens<sup>4</sup> & Wolfgang Wilcke<sup>1</sup>

<sup>1</sup> Geographisches Institut, Universität Bern, Hallerstrasse 12, CH-3012 Berne (martin.schwarz@giub.unibe.ch)

<sup>2</sup> Institut für Geographie, Universität Jena, Löbdergraben 32, D-07743 Jena

<sup>3</sup> Institut für Pflanzenwissenschaften und Botanischer Garten, Universität Bern, Altenbergrain 21, CH-3013 Berne

<sup>4</sup> Institut für Nutzpflanzenwissenschaften und Ressourcenschutz, Universität Bonn, Nussallee 9, D-53115 Bonn

<sup>5</sup> Max-Planck-Institut für Biogeochemie, Hans-Knoell-Strasse 10, D-07745 Jena

Studies in experimental grassland showed that ecosystem processes and services such as nitrogen (N) use are related with plant diversity but evidence is scarce for real-world ecosystems like managed forests. We assessed the effect of shrub and tree diversity (Shannon index based on species cover values) in forests on the retention of bulk (wet and coarse particles) and dry deposited N (fine particles) in a range of forest canopies in three distinct research areas in Germany that are representative for large parts of the Central European landscape and represent the most common cultivated tree species.

Deposited N was retained in 25 out of 27 studied forest canopies. Canopy N retention differed by region (Table 1) which we attributed to differences in soil fertility and nutrient availability in soils. However, N concentrations in soil solution were not directly related with canopy N retention indicating that there were other biogeochemical controls of soil N availability to plants. Total deposition of N differed between deciduous and coniferous forests because of higher dry deposition resulting from higher aerosol scavenging of conifers. Furthermore, canopy N retention increased with total deposition ( $P < 0.001$ ). This pointed at a higher foliar uptake because of the larger canopy surface area. Alternatively, foliar N uptake could be favored by an adaptation of the plant N-use strategies at higher N deposition rates. However, the effect of forest type was not uniform among regions (as indicated by the interaction term in Table 1) suggesting that foliar N uptake was co-determined by regional site conditions.

After accounting for regional and forest type effects, shrub and tree diversity explained 14% of the variance in canopy N retention (Table 1) and increased canopy N retention (Fig. 1). We attributed the biodiversity effect to spatial (resulting from canopy stratification), temporal (resulting from temporal variability in phenological and nutritional N demands), and functional complementarity (resulting from variation in preferential use of various N forms) in complex plant assemblages. However, strength and direction of the biodiversity effect varied by region and forest type highlighting the need for large-scale studies that include variation among regions and habitats within landscapes to test general relationships between biodiversity and ecosystem services and processes.

Our results are the first evidence for complementary N use in real-world forests and also for complementarity in aboveground N acquisition. We therefore conclude that the theory of belowground complementary N use can be extended to aboveground N use.

Table 1: Analysis of (Co-)Variance of the canopy budget of total dissolved nitrogen based on linear modeling.

	Df	Sum Sq	Mean Sq	F value	P (>F)	
region	2	254.4	127.2	65.4	<0.001	***
forest type	1	56.4	56.4	29.0	<0.001	***
basal area	1	6.15	6.15	3.16	0.099	
Shannon index	1	70.3	70.3	36.1	<0.001	***
region x forest type	2	19.2	9.58	4.92	0.026	*
region x Shannon index	2	26.6	13.3	6.83	0.009	**
forest type x basal area	1	17.8	17.8	9.13	0.010	*
forest type x Shannon index	1	11.9	11.9	6.14	0.028	*
Residuals	13	25.3	1.95			

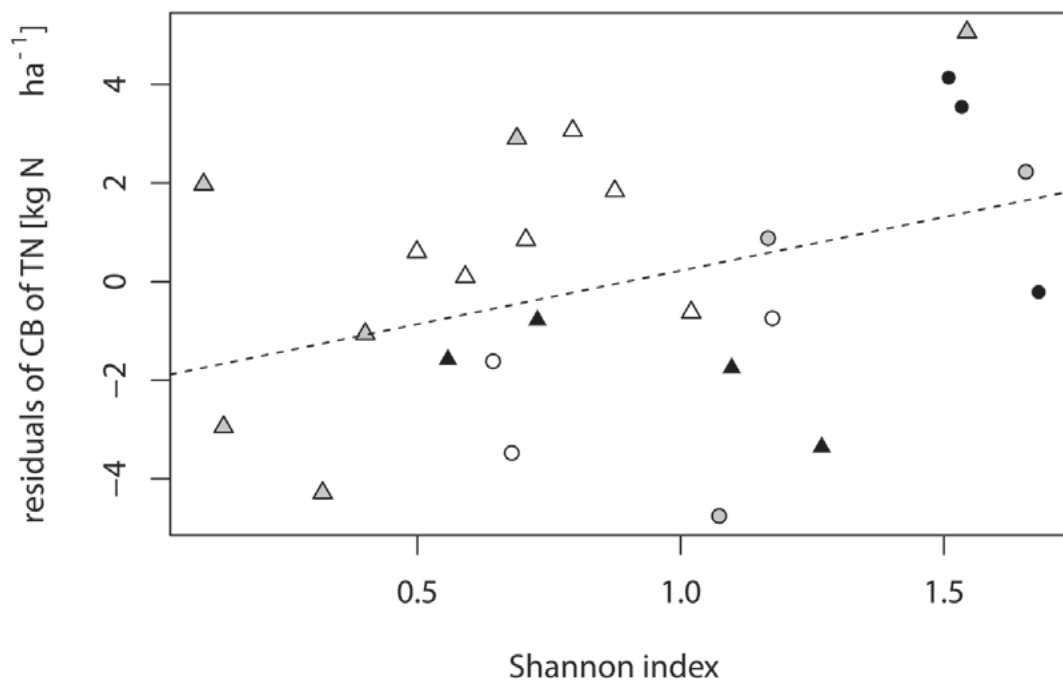


Figure 1. Relationship of the Shannon index of shrubs and tree species versus the residuals of the canopy budget of total dissolved N of a linear model using region, forest type, and basal area as explanatory variables.

## 10.10

## The mobility of nitrogen between tree-rings of Norway spruce (*Picea abies* L.) and the effect of extraction on tree-ring $\delta^{15}\text{N}$ and $\delta^{13}\text{C}$

Tomlinson Greg<sup>1</sup>, Buchmann Nina<sup>2</sup>, Schleppei Patrick<sup>1</sup>, Siegwolf Rolf<sup>3</sup>, Waldner Peter<sup>1</sup> & Weber Pascale<sup>1</sup>

<sup>1</sup> WSL Swiss Federal Research Institute, Zücherstrasse 111, CH-8903 Birmensdorf, (gregory.tomlinson@wsl.ch)

<sup>2</sup> Institute of Agricultural Sciences, Universitätstrasse 2, CH-8092 Zurich

<sup>3</sup> Paul Scherrer Institute, CH-5232 Villigen PSI,

Studies utilising stable isotopes of nitrogen ( $\delta^{15}\text{N}$ ) in tree-rings are rare in comparison to those using carbon ( $\delta^{13}\text{C}$ ) and oxygen ( $\delta^{18}\text{O}$ ). This is mainly due to the potential distortion of environmental signals by the translocation of mobile N compounds between tree-rings (Hart & Classen, 2003). Thus, pre-treatment extraction procedures have been used to remove these mobile N compounds prior to isotope analysis. Studies in the recent past, however, have begun to question the necessity of this extraction procedure (Doucet et al., 2011).

We studied the magnitude of the mobility of tree-ring nitrogen by comparing five Norway spruce (*Picea abies* L.) trees from a plot labelled with  $^{15}\text{N}$  in 1995/6, and under experimentally elevated N deposition (Schleppei et al. 1999), with five control trees. We also investigated the effect of the extraction of mobile N compounds on the tree-ring  $\delta^{15}\text{N}$  and N concentration, as well as the tree-ring  $\delta^{13}\text{C}$  and C concentration.

The  $^{15}\text{N}$  label was found in all tree-rings between 1951-2009 at the labelling plot, suggesting a high radial redistribution of N within the tree stem sapwood. The extraction procedure had no significant effect on either the  $\delta^{15}\text{N}$  or  $\delta^{13}\text{C}$  in either the labelled or control trees. Similarly the N concentrations from both plots were also unaffected by the extraction procedure. These results imply that the pre-treatment removal of mobile N compounds is not necessary prior of using  $\delta^{15}\text{N}$  and  $\delta^{13}\text{C}$  in dendrological studies. However, the use of Norway spruce tree-ring  $\delta^{15}\text{N}$  to understand tree response to changing environmental conditions must be carried out with extreme care due to the high radial mobility of N within the tree stem.

### REFERENCES

- Doucet, A., Savard, M. M., Begin, C., & Smirnoff, A. 2011: Is wood pre-treatment essential for tree-ring nitrogen concentration and isotope analysis? *Rapid Communications in Mass Spectrometry*, 25(4), 469-475.
- Hart, S. C., & Classen, A. T. 2003: Potential for assessing long-term dynamics in soil nitrogen availability from variations in  $\delta^{15}\text{N}$  of tree rings. *Isotopes in Environmental and Health Studies*, 39(1), 15-28.
- Schleppei, P., Bucher-Wallin, L., Siegwolf, R., Saurer, M., Muller, N., & Bucher, J. B. 1999: Simulation of increased nitrogen deposition to a montane forest ecosystem: partitioning of the added  $^{15}\text{N}$ . *Water, Air, & Soil Pollution*, 116(1), 129-134.

## 15.1

### Spatial variability of atmospheric methane: Attributing measured concentrations to emissions

Bamberger Ines<sup>1</sup>, Stieger Jacqueline<sup>1</sup>, Eugster Werner<sup>1</sup> & Buchmann Nina<sup>1</sup>

<sup>1</sup>*Institute of Agricultural Sciences, ETH Zürich, Universitätstrasse 2, CH-8092 Zürich (Ines.Bamberger@usys.ethz.ch)*

Regional variations of methane concentrations are poorly understood, although methane is known to be a highly abundant trace gas and very potent greenhouse gas. Atmospheric methane concentrations are typically only measured at sites close to methane emitters or at remote areas to quantify atmospheric background levels. But at the same time, the density of measurement stations is not sufficient to resolve small-scale regional variations in methane concentration levels.

In this study, we measured diurnal and regional variations of methane concentrations in a valley located in the Alpine foreland in Switzerland and compared the data to a spatially explicit emission inventory. Methane measurements were carried out in July 2012 using a Fast Methane Analyzer (Los Gatos Research, USA), installed in the luggage compartment of a car. The measurement tracks extended over 87.5 km alongside the valley floor as well as the eastern and western hillsides. The measurement area is mainly used for agriculture and livestock farming, representing a major source of methane.

Methane concentrations showed high spatio-temporal variability, with concentrations ranging from 1.88 ppm in remote areas to 7.66 ppm close to local sources. Peak concentrations were observed during the night within the valley; average daytime methane concentrations were typically below 2.1 ppm. Nighttime vertical profiles of temperature and methane concentrations showed a clear temperature inversion, suppressing vertical mixing. Thus, methane was trapped at the valley bottom below the nocturnal boundary layer inversion. In contrast, diel patterns of methane concentrations at the hill sides were mainly affected by topography and local transport processes. Although we did not observe strong diurnal patterns at the eastern hillside, we measured elevated methane concentrations in the morning at the western slopes. An autocorrelation analysis of the spatial measurements indicated that point sources had expanded (for areas up to 64 km<sup>2</sup>) influence on regional patterns of methane concentrations close to the valley bottom during nighttime. In contrast, daytime methane concentrations were only increased very close (< 200 m) to local sources as a consequence of the efficient turbulent mixing. Comparing our measurement data with a spatially explicit, high resolution (500 m x 500 m) methane emission inventory we found a significant positive correlation for the relationship between the lowest flux percentiles and concentrations. Thus the source distribution for the lower methane sources in the emission inventory was reproducible by ambient concentration measurements.

## 15.2

## Understanding and quantifying CO<sub>2</sub> and CH<sub>4</sub> greenhouse gas fluxes on the regional scale: The project CarboCount CH

Dominik Brunner<sup>1</sup>, Stephan Henne<sup>1</sup>, Brian Oney<sup>1</sup>, Ines Bamberger<sup>2</sup>, Nina Buchmann<sup>2</sup>, Edouard Davin<sup>3</sup>, Stefanos Mystakidis<sup>3</sup>, Sonia Seneviratne<sup>3</sup>, Nicolas Gruber<sup>4</sup>, Yu Liu<sup>4</sup>, Markus Leuenberger<sup>5</sup>, Anne Roches<sup>6</sup> and Isabelle Bey<sup>6</sup>

<sup>1</sup> EMPA, Laboratory for Air Pollution/Environmental Technology, Empa, Dübendorf, Switzerland

<sup>2</sup> Institute for Agricultural Sciences, ETH Zurich, Switzerland

<sup>3</sup> Institute for Atmospheric and Climate Science, ETH Zurich, Switzerland

<sup>4</sup> Institute of Biogeochemistry and Pollutant Dynamics, ETH Zurich, Switzerland

<sup>5</sup> Physics Institute, University of Berne, Switzerland

<sup>6</sup> Center for Climate Systems Modeling, ETH Zurich, Switzerland

The project CarboCount CH investigates human-related emissions and natural exchange between atmosphere and biosphere of the two most important long-lived greenhouse gases carbon dioxide (CO<sub>2</sub>) and methane (CH<sub>4</sub>) in Europe and especially in Switzerland. In addition to performing long-term simulations of CO<sub>2</sub> exchange fluxes and their response to climate variations in Europe during the past 30 years, the project combines measured and simulated concentrations in an inverse modelling framework to better quantify CO<sub>2</sub> and CH<sub>4</sub> fluxes at the regional scale. For this purpose, four new measurement sites have been established in Switzerland including the tall tower (210 m) at Beromünster, all equipped with Picarro instruments for continuous measurements of CO<sub>2</sub>, CH<sub>4</sub>, and partially CO. Bi-weekly <sup>14</sup>CO<sub>2</sub> samples at the tall tower site will provide valuable insights into the contributions from fossil fuel emissions. Two separate atmospheric transport and inverse modelling frameworks are being developed within the project. The first one uses the new tracer transport module of the regional numerical weather prediction model COSMO together with the CarbonTracker inversion scheme (Peters et al. 2010). The second framework is based on backward simulations with the Lagrangian transport model FLEXPART-COSMO and a Kalman filter (Brunner et al. 2012). Anthropogenic a priori emissions are taken from newly developed high-resolution (500 m x 500 m) inventories of CH<sub>4</sub> (Hiller et al. 2013) and CO<sub>2</sub> emissions in Switzerland. Atmosphere-biosphere exchange fluxes of CO<sub>2</sub> are simulated with the coupled system COSMO-CLM2, i.e. COSMO coupled to the Community Land Model.

Here we will present a general outline of the project, the setup of the measurement network and of the different modeling components and inverse methods. By the time of the meeting, a complete year of measurements will be available for most sites. These data are analysed for their diurnal and seasonal components and for their dependence on meteorology. Correlations between the measured trace gases provide a first indication of their relative emission strengths and for the variation of sources and sinks with season. First simulations and an analysis of model performance in comparison with observations will also be demonstrated.

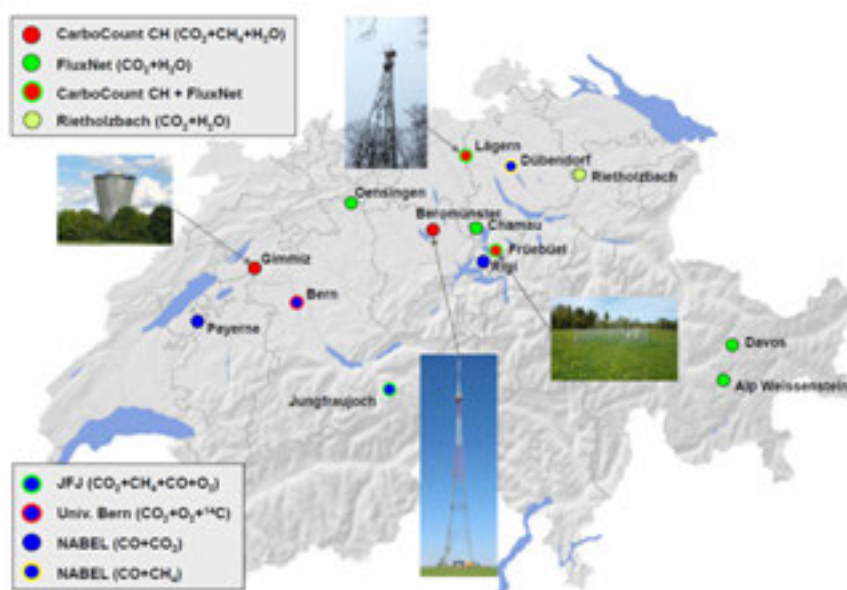


Figure 1. The CarboCount CH observation network. The filled red circles denote the 4 new sites. Blue and green circles are measurements from complementary networks including Swiss Fluxnet with Eddy covariance sites and further sites with continuous CO<sub>2</sub> and CH<sub>4</sub> measurements including Jungfrauoch.

## REFERENCES

- Brunner, D., S. Henne, C. A. Keller, S. Reimann, M. K. Vollmer, S. O'Doherty, & M. Maione, 2012: An extended Kalman-filter for regional scale inverse emission estimation, *Atmos. Chem. Phys.*, 12, 3455-3478, doi:10.5194/acp-12-3455-2012.
- Hiller, R., D. Bretscher, T. DelSontro, T. Diem, W. Eugster, R. Henneberger, S. Hobi, E. Hodson, D. Imer, M. Kreuzer, T. Künzle, L. Merbold, P. A. Niklaus, B. Rihm, A. Schellenberger, M. H. Schroth, C. J. Schubert, H. Siegrist, J. Stieger, N. Buchmann, and D. Brunner, 2013: Anthropogenic and natural methane fluxes in Switzerland synthesized within a spatially-explicit inventory, *Biogeosciences Discuss.*, in press.
- Peters W., A. R. Jacobson, C. Sweeney et al., 2007: An atmospheric perspective on North American carbon dioxide exchange: CarbonTracker. *Proceedings of the National Academy of Sciences*, 104, 18925–18930.

## 15.3

# Discerning cows from pasture – Contribution of grazing animals to eddy covariance greenhouse gas fluxes

Felber Raphael<sup>1,2</sup>, Neftel Albrecht<sup>1</sup>, Munger Andreas<sup>3</sup> & Ammann Christof<sup>1</sup>

<sup>1</sup> Air Pollution and Climate Group, Agroscope Reckenholz, Reckenholzstrasse 191, CH-8046 Zurich (raphael.felber@agroscope.admin.ch)

<sup>2</sup> Institute of Agricultural Science, ETH Zurich, Universitatstrasse 2, CH-8092 Zurich

<sup>3</sup> Dairy Cow Nutrition Group, Agroscope Posieux, Rte de la Tioleyre 4, CH-1725 Posieux

Grasslands act as sinks and sources for greenhouse gases (GHG) and are, in conjunction with the animals utilizing these feed resources, responsible for a large share of agricultural GHG emissions. Ecosystem scale flux measurements (by eddy covariance; EC) have been extensively used to investigate CO<sub>2</sub>, CH<sub>4</sub>, and N<sub>2</sub>O exchange over different ecosystems and are becoming state-of-the-art for animal grazing systems, too (e.g. Dengel et al., 2013). Direct GHG emissions from ruminants in agriculture are usually investigated on the scale of individual animals by respiration chambers (Munger & Kreuzer, 2008) or by the SF<sub>6</sub> method (Pinares-Patino et al., 2007). The advantage of EC flux measurements is the possibility of emission monitoring under real grazing conditions on the pasture with a high time resolution (about 30 min). However, EC measurements do not provide individual animal data and represent a spatially integrated flux over an upwind area (the so-called footprint) in the order of 1000 m<sup>2</sup> containing a variable number of grazing animals. Thus a careful analysis of the location and extension of the flux footprint is necessary. In addition, data on the position of the animals relative to the flux footprint is very important but usually lacking (Baldocchi et al., 2012).

In our experiment we investigate the ability of EC flux measurements to reliably quantify the contribution of the grazing animals to the net exchange of CO<sub>2</sub> and CH<sub>4</sub> over pasture systems. For this purpose, a field experiment with a herd of twenty dairy cows in a full-day rotational grazing system has been established in Posieux near Fribourg. Net CO<sub>2</sub> and CH<sub>4</sub> exchange of the grazing system are measured continuously by the eddy covariance technique (Sonic Anemometer HS-50, Gill Instruments Ltd; FGGA, Los Gatos Research Inc. and LI-7500, LI-COR Biosciences). In order to quantify the contribution of the animals to the net flux, the position, movement and grazing/rumination activity of the individual cows is recorded using GPS (5 s time resolution) and mastication sensors on each animal. In combination with a detailed footprint analysis of the eddy covariance fluxes, the animal related CO<sub>2</sub> and CH<sub>4</sub> emissions are derived and compared to calculated animal emission rates based on animal energy expenditure factors.

First results show, that the accuracy of the GPS derived cow position is better than 4 m and thus clearly sufficient for the localization of grazing animals within the EC flux footprint (see example in Fig. 1). Observed eddy covariance fluxes indicate a good detectability of the grazing animals especially for CH<sub>4</sub>, which has a very low background flux. For CO<sub>2</sub> a partitioning of the net flux is necessary to separate contributions of vegetation and soil (assimilation and respiration) from the animal respiration flux.

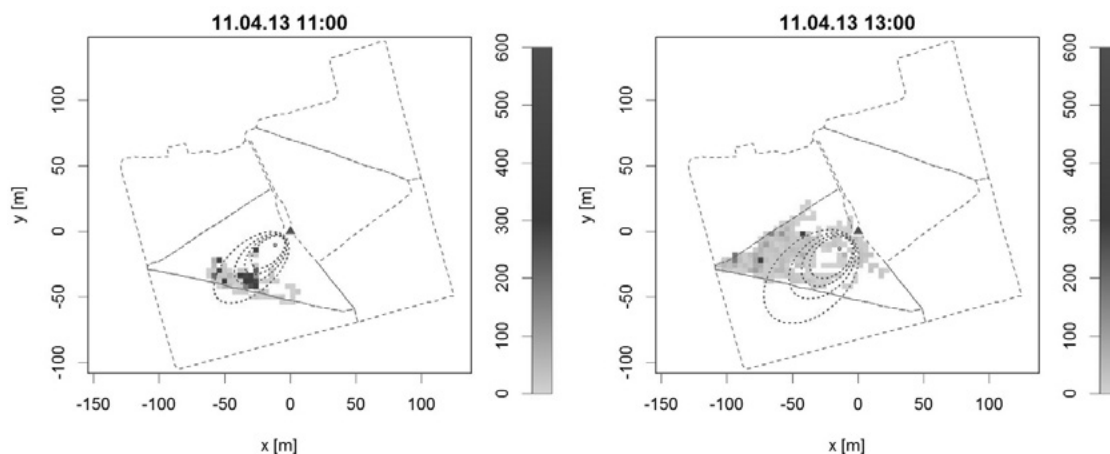


Figure 1. Cow distribution (colored pixels in a.u.; 4 x 4 m) and footprint extension (dashed lines) during two 30 minutes measurement intervals. The lines comprising 80%, 60%, 40%, and 20% of the flux footprint. The triangle indicates the measurement tower. According to the animal density in the footprint, a decreasing methane flux of 0.99 and 0.24  $\mu\text{mol m}^{-2} \text{s}^{-1}$  was observed for 11:00 and 13:00, respectively.

We gratefully acknowledge the funding from the Swiss National Science Foundation SNSF (Grant No. 205321\_138300). We also thank Hubert Bollhalder, Roman Gubler, Andreas Rohner, Manuel Schuler, Lukas Eggerschwiler and Bernard Papaux for support with sensors and in the field experiment.

## REFERENCES

- Baldocchi, D., Detto, M., Sonnentag, O., Verfaillie, J., Teh, Y.A., Silver W. & Kelly N.M. 2012: The challenges of measuring methane fluxes and concentrations over a peatland pasture. *Agricultural and Forest Meteorology*, 153, 177-187.
- Dengel, S., Levy, P.E., Grace, J., Jones, S.K. & Skiba, U.M. 2011: Methane emissions from sheep pasture, measured with an open-path eddy covariance system. *Global Change Biology*, 17, 3524-3533.
- Münger, A. & Kreuzer, M. 2008: Absence of persistent methane emission differences in three breeds of dairy cows. *Australian Journal of Experimental Agriculture*, 48, 77-82.
- Pinares-Patino, C.S., D'Hour, P., Jouany, J.P. & Martin, C. 2007: Effects of stocking rate on methane and carbon dioxide emissions from grazing cattle. *Agriculture Ecosystems & Environment*, 121, 30-46.

## 15.4

### Greenhouse gas fluxes from agricultural soils under organic and non-organic management – a global meta-analysis

Skinner Colin<sup>1</sup>, Gattinger Andreas<sup>2</sup>, Muller Adrian<sup>2</sup>, Mäder Paul<sup>2</sup>, Fließbach Andreas<sup>2</sup>, Stolze Matthias<sup>2</sup>, Ruser Reiner<sup>3</sup>, Niggli Urs<sup>2</sup>

<sup>1</sup> Research Institute of Organic Agriculture (FiBL), Ackerstrasse 113, CH-5070 Frick ([colin.skinner@fibl.org](mailto:colin.skinner@fibl.org))

<sup>2</sup> Research Institute of Organic Agriculture (FiBL), Ackerstrasse 113, CH-5070 Frick

<sup>3</sup> Fertilisation and Soil Matter Dynamics (340i), Institute of Crop Science, University of Hohenheim, Fruwirthstraße 20, 70599 D-Stuttgart

Agricultural soil management induces nitrous oxide and methane emissions that account for around 40% of the sector's direct greenhouse gas (GHG) emissions globally (Smith et al., 2007). The reduction of these emissions thus constitutes an important part of agriculture's mitigation potential concerning climate change.

Thirty seven Mio hectares of agricultural land (= 0.9% of total agricultural land) are currently farmed organically. It is anticipated that these systems provide environmental benefits, particularly with regard to soil conservation and climate protection. A literature search, the first of its kind, on measured soil-derived greenhouse gas (GHG) (nitrous oxide and methane) fluxes under organic and non-organic management from farming system comparisons was conducted and followed by a meta-analysis. This review showed that paired field measurement data of soil GHG emissions is scarce. Up to date only 19 studies based on field measurements could be retrieved, all conducted in the Northern hemisphere under temperate climate. Among them is only one comparative study on rice paddies.

Based on 12 studies that cover annual measurements, it appeared with a high significance that area-scaled nitrous oxide emissions from organically managed soils are  $492 \pm 160$  kg CO<sub>2</sub> eq. ha<sup>-1</sup> a<sup>-1</sup> lower than from non-organically managed soils. For arable soils the difference amounts to  $497 \pm 162$  kg CO<sub>2</sub> eq. ha<sup>-1</sup> a<sup>-1</sup>. Furthermore, a higher methane uptake of  $3.2 \pm 2.5$  kg CO<sub>2</sub> eq. ha<sup>-1</sup> a<sup>-1</sup> for arable soils under organic management can be observed. However, yield-scaled nitrous oxide emissions are higher by  $41 \pm 34$  kg CO<sub>2</sub> eq. t<sup>-1</sup> dry matter (arable land use). This is due to 26% lower crop yields under organic management. To equalize this mean difference in yield-scaled nitrous oxide emissions between both farming systems, the yield gap has to be less than 17%.

Nitrous oxide emissions from conventionally managed soils seemed to be influenced mainly by total N inputs, whereas for organically managed soils other variables such as soil characteristics seemed to be more important. This can be explained by the higher bioavailability of the synthetic N fertilisers in non-organic farming systems while the necessary mineralisation of the N sources under organic management leads to lower and retarded availability. This might also be the reason for the large variation of the corresponding nitrous oxide emission factors ranging from 0.3 to 36% of the applied N (Fig. 1), whereas most of the calculated emission factors for soils under non-organic management were within the uncertainty range of 0.3 – 3% attributed to the 1% standard emission factor for N fertiliser also used in the IPCC Guidelines for National GHG Inventories (De Klein et al., 2006). Thus, it seems quite likely that due to the retarded release of mineral N from organic sources a substantial part of the resulting nitrous oxide emissions will become effective later than the vegetation period under study.

Further GHG flux measurements in farming system comparisons are required to confirm the results and close the existing knowledge gaps.

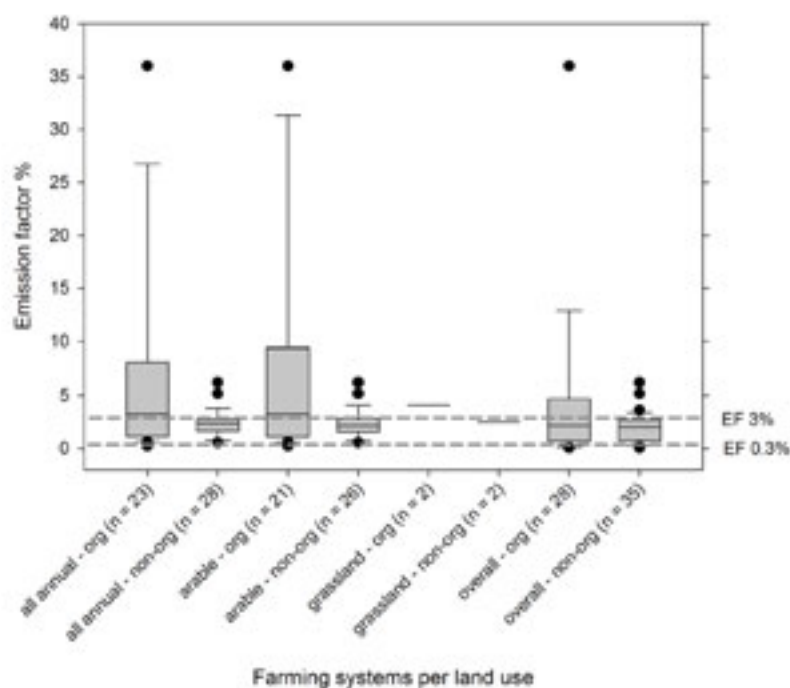


Fig.1. Emission factors for the organic and non-organic farming system of the different land uses.

Box plots illustrate the distribution of the emission factors from the treatments of the respective farming systems and land use category. The boxes denote the 25 to 75% quartiles including the median (= 50% quartile). The error bars denote the non-outlier range and black dots are outliers. The dashed grey lines indicate the uncertainty range (0.3% - 3%) of the 2006 IPCC guidelines standard emission factor for N fertiliser that is 1% (De Klein et al., 2006).

## REFERENCES

- De Klein, C., Novoa, R.S.A., Ogle, S., Smith K.A., Rochette, P., Wirth, T.C. 2006: Chapter 4: Agriculture, Forestry and Other Land Use. In: National Greenhouse Gas Inventory Guidelines. (Ed. by IPCC).
- Smith, P., Martino, D., Cai, Z., Gwary, D., Janzen, H., Kumar, P., et al. 2007: Agriculture in Climate Change: Mitigation In: Fourth Assessment Report of the Intergovernmental Panel on Climate Change (Ed. by IPCC).

## P 10.1

### Gap-filling Strategies for Annual VOC Flux Data Sets

Bamberger Ines<sup>1,3</sup>, Hörtnagl Lukas<sup>2</sup>, Walser Mario<sup>1</sup>, Hansel Armin<sup>1</sup> & Wohlfahrt Georg<sup>2</sup>

<sup>1</sup> Institute of Ion Physics and Applied Physics, University of Innsbruck, Technikerstrasse 25, A-6020 Innsbruck  
(Ines.Bamberger@usys.ethz.ch)

<sup>2</sup> Institute of Ecology, University of Innsbruck, Sternwartestrasse 15, A-6020 Innsbruck

<sup>3</sup> now at: Institute of Agricultural Sciences, ETH Zürich, Universitätstrasse 2, CH 8092 Zürich

Chemical degradations of volatile organic compounds (VOCs) in the atmosphere facilitate tropospheric ozone production and secondary organic aerosol formation and thus VOCs are influencing air quality and climate. Flux data sets which quantify the exchange of volatile organic compounds at the interface between biosphere and atmosphere, however, are sparse and often measurements are performed for several weeks to some months only. To make an important step towards a better understanding of the VOC ecosystem-atmosphere exchange on longer time scales complete annual data sets are required and a gap-filling of missing VOC data is inevitable.

Flux measurements of several VOCs were conducted above a mountain meadow in Austria during the complete snow-free period of the years 2009 and 2011. The performance of four different gap-filling routines, mean diurnal variation (MDV), mean gliding window (MGW), look up tables (LUT) and linear interpolation (LIP), in missing data replacement was tested using the measured VOC flux data set. The MDV routine yielded to the lowest gap-filling errors for both years and all quantified VOCs. The other gap-filling routines, which performed gap-filling on 24h average values, introduced considerably larger uncertainties. The gap-filling error scaled linearly with the number of data gaps for each gap-filling routine. Measured VOC fluxes during times of complete snow cover were close to zero but also highly variable. Consequently the missing data replacement for the winter period introduced considerably higher uncertainties than the gap-filling during the measurement period.

The compound which contributed most to the cumulative non-methane VOC carbon emissions was with annual sums of 381.5 mg C m<sup>-2</sup> (2009) and 449.9 mg C m<sup>-2</sup> (2011) methanol during both years. As opposed to the year 2011, when monoterpene cumulative fluxes were quite low, we observed considerable deposition fluxes of monoterpenes to the grassland (-327.3 mg C m<sup>-2</sup>) in 2009. The monoterpene uptake in 2009 was a consequence of a severe hailstorm in June 2009. The influence of the other quantified VOCs on the annual patterns was considerably lower.

## P 10.2

# Hydrodynamic controls on the age and composition of sedimentary organic matter on continental shelves: a case study from Chinese marginal seas

Bao Rui<sup>1</sup>, Eglinton Timothy<sup>1</sup>

<sup>1</sup> Geological Institute, ETH Zürich, Sonneggstrasse 5, CH-8092 Zürich (rui.bao@erdw.ethz.ch)

As a crucial interface between the land and the ocean, continental shelves receive organic carbon inputs from both reservoirs. Although these systems account for ~90% of global organic carbon in the modern oceans (Hedges and Keil, 1995), considerable uncertainty remains concerning the source and fate of organic carbon delivered to and produced over continental shelves. In particular, controls on spatial variability in the content and composition of sedimentary organic matter on continental shelves remain the focus of on-going investigations (e.g., Schmidt et al., 2010; Vonk et al., 2012).

In addition to the magnitude and nature of organic matter supply from terrestrial sources and from surface water productivity, there is strong evidence that hydrodynamic processes and physical protection mechanisms play a critical role in influencing dispersal redistribution and eventual burial of organic matter on the continental shelf (Keil et al., 1994).

This study explores these processes in a large marginal sea system: Chinese marginal seas. We are examining spatial variations in grain-size, mineral surface area, bulk elemental, and isotopic compositions of organic matter in surface sediments. Preliminary measurements of organic carbon contents and isotopic compositions coupled with grain size measurements suggest that pre-aged organic matter accumulates on the outer shelf and in low energy regions where clay-rich sediments accumulate. Further geochemical investigations are underway on surface sediment fractions separated by grain size in order to examine variations in organic matter content and isotopic composition between different fractions as well as within the same fractions from different regions within the Chinese marginal seas. Observations are discussed in the context of both hydrodynamic and mineralogical control on sedimentary organic matter distribution and composition.

We discuss the implications of our findings for the application of organic geochemical proxies and for budgets of organic carbon burial in this and other continental shelf sea systems.

## REFERENCES

- Hedges, J.I. & Keil, R.G. 1995: Sedimentary organic matter preservation: an assessment and speculative synthesis. *Marine Chemistry* 49, 81–115.
- Keil, R.G., Montluçon, D.B., Prahl, F.G. & Hedges, J.I. 1994: Sorptive preservation of labile organic matter in marine sediments. *Nature* 370, 549–552.
- Schmidt F., Hinrichs K.U. & Elver T. M. 2010: Sources, transport, and partitioning of organic matter at a highly dynamic continental margin. *Marine Chemistry* 118, 37–55.
- Vonk J. E., Sánchez-García L., van Dongen B. E., Alling V. , Kosmach D., Charkin A., Semiletov I. P., Dudarev O. V., Shakhova N., Roos P., Eglinton T. I., Andersson A. & Gustafsson Ö. 2012: Activation of old carbon by erosion of coastal and subsea permafrost in Arctic Siberia *Nature* 489, 137–140.

## P 10.3

# Uplifting of hummocks in palsa peatlands in northern Sweden identified by stable carbon isotope profiles

Krüger Jan Paul<sup>1</sup>, Leifeld Jens<sup>2</sup> & Alewell Christine<sup>1</sup>

<sup>1</sup> *Environmental Geosciences, University of Basel, Bernoullistrasse 30, CH-4056 Basel (janpaul.krueger@unibas.ch)*

<sup>2</sup> *Agroscope Reckenholz-Tänikon ART, Reckenholzstrasse 191, CH-8046 Zürich*

The carbon pool of palsa peatlands is an important component in the global carbon cycle and is projected to change in the 21<sup>st</sup> century. It is predicted, that the area suitable for palsa development will be lost until 2100. Uplifting of the hummocks above the surrounding wetter areas is a process which starts at the beginning of palsa formation. The degradation of palsa peatlands with cracks and erosion on the edges can be a natural process after the palsa reached his mature status but is now accelerated by permafrost thawing under climate change regime.

We took samples from uplifted peat material down to the permafrost in three palsa peatlands in the Abisko valley, northern Sweden, and analyzed them for <sup>13</sup>C, C and N contents. In the profile  $\delta^{13}\text{C}$  values change from increasing to decreasing values; the highest values are found at the so-called turning point (Alewell et al. 2011). The turning point indicates a change from anaerobic to aerobic conditions due to the uplifting of the peat material by permafrost and is indicative for the time of uplifting of the palsa. The stable isotope depth pattern is supported by the C/N ratio of the peat material. Above the turning point C/N ratios are high, indicating oligotrophic decomposition, whereas C/N ratios are lower below the turning point, corresponding to minerotrophic conditions. We calculated palsa formation in this peatlands at about 120 to 600 years BP based on <sup>14</sup>C dated peat layers (Alewell et al. 2011). Kokfelt et al. (2010) detected a similar time period of palsa formation and a change from minerotrophic to oligotrophic conditions at a similar depth. Hence, stable carbon isotopes indicators for the depth and thus the time when uplift of hummocks in palsa peatlands by permafrost commenced.

## REFERENCES

- Alewell, C., Giesler, R., Klaminder, J., Leifeld, J. & Rollog, M. (2011): Stable carbon isotopes as indicators for environmental change in palsa peats. *Biogeosciences* 8: 1769-1778.
- Kokfelt, U., Reuss, N., Struyf, E., Sonesson, M., Rundgren, M., Skog, G., Rosén, P. & Hammarlund, D. (2010): Wetland development, permafrost history and nutrient cycling inferred from late Holocene peat and lake sediment records in subarctic Sweden, *J. Paleolimnol* 44: 327-342.

## P 10.4

### Soil respiration rates of degrading palsa mires in northern Sweden

Schomburg Andreas<sup>1</sup>, Krüger Jan Paul<sup>1</sup>, Conen Franz<sup>1</sup>, Alewell Christine<sup>1</sup>

<sup>1</sup>*Environmental Geosciences, University of Basel, Bernoullistrasse 30, CH-4056 Basel (andreas.schomburg@stud.unibas.ch)*

Quantifying carbon decomposition rates in soils is a key approach to estimate potential CO<sub>2</sub> emissions that lead to climate warming and permafrost thawing. High emission rates are predicted especially in northern peatlands storing 280 Pg C. Palsa mires are common peatlands in the discontinuous permafrost region characterized by dry mounds or plateaus, which have been raised up by permafrost out of the wetter parts. In palsa mires, rapid changes in environmental conditions may accelerate peat degradation and alter hydrological and biogeochemical processes. (Bäckstrand et al. 2010; Olefeldt et al. 2012). The magnitude of the resulting shift in CO<sub>2</sub> emission rates has not been well investigated yet. We measured respiration rates from degraded and non-degraded palsa sites under laboratory conditions. Soil samples were taken from the Stordalen and the Storflaket mires in the Abisko region, northern Sweden. The samples were separated in two vertical depth layers (5 – 10 and 15 – 20 cm) and incubated at 4 and 12°C for one month. We sampled the headspace for analysis of CO<sub>2</sub> by gas chromatography. The emission rates ranged between 0 and 7.638 µg CO<sub>2</sub> g<sup>-2</sup> h<sup>-1</sup> over the whole experiment. Respiration rates at 12°C were almost twice as large as at 4°C. In the vertical soil profile, the upper peat layer respired in average 34 % more CO<sub>2</sub> than the lower one. CO<sub>2</sub> emissions were 25 % higher on degraded than on non-degraded sites. Higher respiration rates of the upper soil layer are most likely due to stronger microbial activity and less recalcitrant organic compounds. Our results confirm the general assumptions that carbon decomposition rates increase with increasing temperature. Furthermore, the difference between degraded and non-degraded sites indicates that disturbance of peat layers due to thawing also leads to higher CO<sub>2</sub> release.

#### REFERENCES

- Bäckstrand, K. et al. (2010): Annual carbon gas budget for a subarctic peatland, Northern Sweden. In: *Biogeoscience*, 7, 95-108.
- Olefeldt, D. et al. (2012): Net carbon accumulation of a high-latitude permafrost palsa mire similar to permafrost-free peatlands. In: *Geophysical Research Letters*, 39, L03501.

# 11. Geophysics and Rockphysics

Marcel Frehner, Klaus Holliger

*Swiss Geophysical Commission*

## TALKS:

- 11.1 Bakker R.R., Benson P.M.: Tensile fracturing and dyking in volcano-tectonic settings, a laboratory approach
- 11.2 Dafflon B., Hubbard S.S., Ulrich C., Peterson J.E., Wainwright H., Wu Y.: Investigating arctic permafrost behaviors using geophysical, point-scale and remote sensing data
- 11.3 Favero V., Ferrari A., Laloui L.: Shales retention properties and permeability through laboratory testing
- 11.4 Hunfeld U., Brenner O., Orłowsky D.: High-resolution CMP-refraction seismics in combination with refraction tomography, reflection seismics and surface wave analysis
- 11.5 Jougnot D., Rubino J.G., Rosas Carbajal M., Linde N., Holliger K.: Seismoelectric effects due to mesoscopic heterogeneities: numerical study for a fractured rock
- 11.6 Lupi, M., Saenger, E.H., Fuchs, F., Miller, S.A.: Focusing of seismic energy at LUSI mud volcano, Indonesia
- 11.7 Thüring M., Sayah S.M.: Assessment of the complex rock mass conditions for tunnels and underground caverns of the Hydropower Project Cerro del Águila (Peru)
- 11.8 Vouillamoz N., Abednego M., Deichmann N., Wust- Bloch H.G., Mosar J.: Lowering microseismic detection threshold by sonogram analysis for Fribourg area (Switzerland)

## POSTERS:

- P 11.1 Correia Demand J., Marillier F., Kremer K., Girardclos S.: Large mass wasting deposits in Lake Geneva off the city of Lausanne revealed by detailed reflection seismic data
- P 11.2 Demirel S., Roubinet D., Irving J.: Modeling electric current flow in 3D fractured media
- P 11.3 Koepke C., Irving J., Roubinet D.: Exploring the issue of model error in stochastic solutions to hydrogeophysical inverse problems
- P 11.4 Kuhn P., Abdelfettah Y., Mauri G., Schill E., Vuataz F.: Improvement of the regional 3D modeling of deep geological structures with gravity: A case study in the Neuchatel Jura Mountains
- P 11.5 Mo Y.K., Greenhalgh S.A., Karaman H., Robertsson J.: Laboratory seismic scale model study of reflection imaging beneath a distorting near surface zone
- P 11.6 Peters, M., Poulet, T., Karrech, A., Regenauer- Lieb, K., Herwegh, M.: Material softening as a potential cause for the development of boudinage - an elasto-visco-plastic numerical modeling approach
- P 11.7 Rosas Carbajal M., Linde N., Kalscheuer T., Vrugt J.: Two-dimensional probabilistic inversion of plane-wave electromagnetic data
- P 11.8 Roubinet D., Irving J.: Discrete dual porosity modeling of electrical current flow in fractured media
- P 11.9 Rubino J.G., Müller T.M., Guarracino L., Holliger K.: Seismic energy dissipation in fractured rocks
- P 11.10 Shih P.J.R., Frehner M.: Numerical modeling and laboratory measurements of seismic properties in fractured fluid reservoirs
- P 11.11 Subramaniyan S., Madonna C., Tisato N., Saenger E.H., Quintal B.: Seismic attenuation: Laboratory measurements in fluid saturated rocks
- P 11.12 Tisato N., Quintal B., Podladchikov Y.: How much seismic energy is “stolen” by bubbles?
- P 11.13 Wei Wu: Some new observations on dynamically induced fault slip
- P 11.14 Zhang Y., Song S., Dalguer L., Clinton J.: Effect of network density and geometric distribution on non-linear kinematic source inversion models

## 11.1

### Tensile fracturing and dyking in volcano-tectonic settings, a laboratory approach.

Bakker Richard R.<sup>1</sup>, Benson Philip M.<sup>2</sup>

<sup>1</sup> ETH Zürich, Department Erdwissenschaften, Structural Geology and Tectonics, Rock Deformation Laboratory, NO E 17, Sonneggstrasse 5, CH-8092

<sup>2</sup> University of Portsmouth, School of Earth and Environment, Burnaby Building, Burnaby Road, UK-P01 3QL

It is well known that magma ascends through the crust by the process of dyking. During dyke movement crustal rocks, specifically the volcano's basement rocks, fracture due to the stress imposed by the ascending magma, thus providing conduits for magma transport. Dykes are frequently seen in the field and have been reproduced via numerical and analogue studies. However, a number of assumptions regarding rock mechanical behaviour frequently has to be made as such data are very hard to directly measure at the pressure/temperature conditions of interest: high temperatures at relatively shallow depths. Such data are key to simulating the magma intrusion dynamics through the lithologies that underlie the volcanic edifice.

Studies on the mechanical properties in a compressive regime have been successful. Volcanic rocks and basement rocks have been deformed at temperatures up to 1000 °C at relatively shallow pressures. However in the tensile regime, it remains a significant technical challenge to precisely reproduce the conditions of dyking in the lab. As a starting point, we are now testing an analogue material to replace the magma to avoid such high temperatures, relying on maintaining similar temperature/viscosity ratios between magma/country rock in the laboratory and the field. We chose PMMA (commonly known as plexiglass) for this task as it displays a large range in viscosities ( $\log(\text{visc})\text{range} = 10 - 1$ ) with temperatures between 100 and 300 °C, making it an excellent analogue material. In addition PMMA solidifies after the sample cools to permit post-test analysis of the pseudo dyke.

We have modified a traditional compression test / tri-axial test assembly setup to be able to use a Paterson High Pressure, High Temperature deformation apparatus. Sample setup consists of cylindrical rock samples with a 22mm diameter and a 8mm bore at their centre, filled with a PMMA cylinder. The top and lower parts of the rock sample are fitted with plugs, sealing in the PMMA. The assembly is then placed between ceramic pistons to ensure there are no thermal gradients across the sample. The assembly is jacketed to ensure the confining medium (Ar) cannot enter the assembly. When the assembly is brought to the desired PT conditions, a piston is driven up which pressurizes the conduit and the filler material. The filler material is "squeezed out" and thus transfers little to no stress on to the sample.

With the inner PMMA conduit pressurized, a sufficient pressure gradient between the inner and outer surfaces eventually cause the sample to deform and fail in the tensile regime. Tensile fractures can occur when the hoop stress exerted on the outer shell exceeds its tensile strength. The PMMA is then likely to flow into the newly formed fracture, depending on its viscosity and the fracture dimensions, allowing comparisons to be made between the temperature and intrusions dynamics of the simulated dyke process.

Ultimately this method will be extended to higher temperatures using NIST standard glasses and collected volcanic glasses for comparison to the analogue setup.



Figure 1, Schematic setup of the assembly

## 11.2

# Investigating Arctic Permafrost Behaviors Using Geophysical, Point-Scale and Remote Sensing Data

Baptiste Dafflon<sup>1</sup>, Susan S. Hubbard<sup>1</sup>, Craig Ulrich<sup>1</sup>, John E. Peterson<sup>1</sup>, Haruko Wainwright<sup>1</sup> & Yuxin Wu<sup>1</sup>

<sup>1</sup>Lawrence Berkeley National Laboratory (LBNL), Berkeley (CA), USA, (bdafflon@lbl.gov)

The trajectory of arctic tundra ecosystem feedbacks to climate is recognized as a significant source of uncertainty in climate projections (e.g., Friedlingstein et al., 2006, Chapin et al., 2000). The uncertainty is associated with our inability to predict the behavior of components of the system as well as their interactions, including ecosystem energy balance, vegetation dynamics, and microbial soil organic carbon degradation associated with permafrost thaw, which could lead to significant CO<sub>2</sub> and CH<sub>4</sub> production (e.g., Schuur et al., 2009, Zimov et al., 2006). Improving understanding of arctic ecosystem functioning and parameterizing process-rich models that simulate feedbacks to a changing climate require advances in estimating the spatial and temporal variations in active layer, ice-wedge and permafrost soil properties.

As part of the DOE Next-Generation Ecosystem Experiments (NGEE-Arctic), we are developing advanced geophysical strategies to improve arctic subsurface imaging, and using the data to quantify land and subsurface co-variability and dynamics (e.g., Hubbard et al., 2013). Some specific objectives involve (i) developing advanced geophysical approaches for characterizing subsurface compartments and associated properties, including active layer, ice-wedges, ground-ice, saline layers, and permafrost with variable ice-content, (ii) quantifying relations between geomorphology, soil hydrological and geochemical properties, and geophysical properties, and (iii) integration of multi-scale and -resolution remote sensing, surface geophysical and point measurements to estimate properties (e.g., thaw depth, soil moisture, ice content and geochemical properties) and their uncertainty over scales that are relevant for modeling.

These objectives are pursued through various numerical developments, laboratory experiments, and field investigations. Field investigations have been performed at the NGEE site located in the Barrow Environmental Observatory (BEO) near the coastal village of Barrow (AK). This site shows a significant range of hydrological and geomorphological conditions; including low- to high- centered polygons and drained thaw lake basins (e.g., Sellmann et al., 1975). The data involved in this study includes point- scale (TDR, core analysis), surface-based geophysical (galvanic-coupled electrical resistance tomography (ERT), capacitively-coupled resistivity (CCR), electromagnetic induction (EMI), and Ground Penetrating Radar (GPR)), and remote sensing (LiDAR, Kite-based low-altitude aerial imaging) datasets.

In this presentation, we will describe several recent advances, including: (i) a novel parameter-estimation approach adapted to explore the solution non-uniqueness inherent to EMI and CCR data, which facilitates estimation of electrical conductivity variations in the active layer as well as trends in permafrost distribution over large areas (Dafflon et al., in press) (ii) high-resolution imaging of ice-wedges, permafrost and active layer using multi 2D electrical resistance tomography (ERT) at a high-spatial resolution, which enables identification of properties that vary substantially over length scales of less than a meter, (iii) understanding the complex resistivity electrical signature of arctic soils during freeze-thaw transitions at the laboratory and field scale, (iv) quantification of land-surface properties (using remote sensing data) and their co-variability with the subsurface properties.

Overall, the above advances enable improvements in estimating the i) thaw layer electrical conductivity distribution, which informs on soil water content distribution that strongly influences microbial activity, ii) soil ice-content distribution showing a variability from below one meter length scales to large trends over more than a kilometer, which is crucial to assess spatial variations in arctic permafrost dynamics, iii) distribution of low freezing-point saline layers that implies different compartment to temperature variations than surrounding permafrost, and iv) permafrost characteristics that correspond with changes in hydrogeomorphological surface expressions which is important to guide permafrost behavior zonation at larger spatial scale. Together, these advances are critical to guide investigations of carbon cycling processes and for improving the understanding of Arctic terrestrial environment characteristics and dynamics, in high resolution and over modeling-relevant spatial extents.

### REFERENCES

- Brown, J., 1969, Ionic Concentration Gradients in Permafrost Barrow, Alaska: Hanover, New Hampshire, Cold Regions Research and Engineering Laboratory, Corps of Engineers, US Army.
- Chapin, F.S., McGuire, A.D., Randerson, J., Pielke, R., Baldocchi, D., et al., 2000, Arctic and boreal ecosystems of western North America as components of the climate system, *Global Change Biology*, 6, 211-223.
- Dafflon B., Hubbard S.S., Ulrich, C., and Peterson J.E., Electrical conductivity imaging of active layer and permafrost in Arctic ecosystem, through advanced inversion of electromagnetic induction data, *Vadose Zone Journal*, in press,

- doi:10.2136/vzj2012.0161.
- Friedlingstein, P., Cox, P., Betts, R., Bopp, L., Von Bloh, W., et al., 2006, Climate-carbon cycle feedback analysis: Results from the C(4)MIP model intercomparison, *Journal of Climate*, 19(14), 3337-3353.
- Hubbard, S.S., Gangodagamage, C., Dafflon, B., Wainwright, H., Peterson, J., et al., 2013, Quantifying and relating land-surface and subsurface variability in permafrost environments using LiDAR and surface geophysical datasets, *Hydrogeology Journal*, 21(1), 149-169.
- Schuur, E.A.G., Vogel, J.G., Crummer, K.G., Lee, H., Sickman, J.O., et al., 2009, The effect of permafrost thaw on old carbon release and net carbon exchange from tundra, *Nature*, 459(7246), 556-559.
- Sellmann, P.V., Brown, J., Lewellen, R.I., McKim, H., and Merry, C., 1975, The Classification And Geomorphic Implication of Thaw Lakes on the Arctic Coastal Plain, Alaska, US Army CRREL, Volume Research Report 344.
- Zimov, S.A., Davydov, S.P., Zimova, G.M., Davydova, A.I., Schuur, E.A.G., et al., 2006, Permafrost carbon: Stock and decomposability of a globally significant carbon pool, *Geophysical Research Letters*, 33(20).

## 11.3

### Shales retention properties and permeability through laboratory testing

Favero Valentina, Ferrari Alessio & Laloui Lyesse

*Laboratory for Soil Mechanics, École Polytechnique Fédérale de Lausanne (EPFL), EPFL-ENAC-LMS, Station 18, CH-1015 Lausanne. (valentina.favero@epfl.ch; alessio.ferrari@epfl.ch; lyesse.laloui@epfl.ch)*

The development of engineering activities involving shales such as the extraction of shale gas and shale oil, and the sequestration of CO<sub>2</sub>, has led to an increasing need to understand the geomechanical behaviour of shales. The water retention mechanisms play a major role in fluid trapping due to the capillary forces present in low permeability formations as in the case of shale gas reservoir; moreover the variations in the degree of saturation (or suction) affect the swelling/shrinkage behaviour and the permeability of shales. Different techniques for the assessment of the retention properties are discussed. The first technique involves the direct control of the water content and the subsequent measurement of the suction at equilibrium by a psychrometer; a fluid displacement technique is used to detect the volume changes in order to allow the computation of the degree of saturation. The second procedure consists in progressive wetting and drying paths applied on a single shale sample and in the execution of psychrometric readings in order to highlight hysteretical and scanning features in the retention behaviour.

Shale permeability and its relation to shale porosity are investigated by means of oedometric tests and direct permeability measurements.

Selected results are presented for three shales from Switzerland: the Opalinus Clay from the Mont Terri Underground Research Laboratory (URL), the “Brown Dogger” shale formation (depth of 766.67 - 807.44 m) and the Opalinus Clay formation (depth of 837.44 - 891.25 m), from a deep geothermal well near the village of Schlattingen in the Molasse Basin.

The water retention behaviour of the Opalinus Clay from Mont Terri is reported in Figure 1. The material has an initial degree of saturation close to one, which is in agreement with the fact that it was reported to be saturated in situ. The initial state was found along the main drying paths as a consequence of the coring process and the exposure to atmosphere before preservation. The main drying and wetting paths are well distinguished, and hysteresis zones can be observed. The evolution of the void ratios with the total suction showed that the porosity changes are more significant for the lowest range suction variations. The void ratios of the lowest measured suctions were in very good agreement with the results of the free swelling tests carried out with the same synthetic waters used for determining the water retention curves.

Shale permeability is assessed by means of laboratory testing: an advanced oedometric cell has been designed to investigate the volume change behaviour of shales at high vertical stresses and the permeability as a function of the vertical effective stress and porosity is computed by the back-analysis of the consolidation process. The previous results are compared to direct permeability measurements which are performed by means of an advanced triaxial system. High pressure gradients and high confining stresses are required in order to produce measurable flows. The good agreement of the obtained results can be highlighted and a clear decrease of shale permeability with decreasing porosity can be observed. The agreement of the obtained results shows that, when the end-of-primary consolidation and the coefficient of consolidation are properly computed, high-pressure oedometric tests can be used to gather information on the permeability of the tested shales within a significant range of porosity (Ferrari and Laloui, 2012).

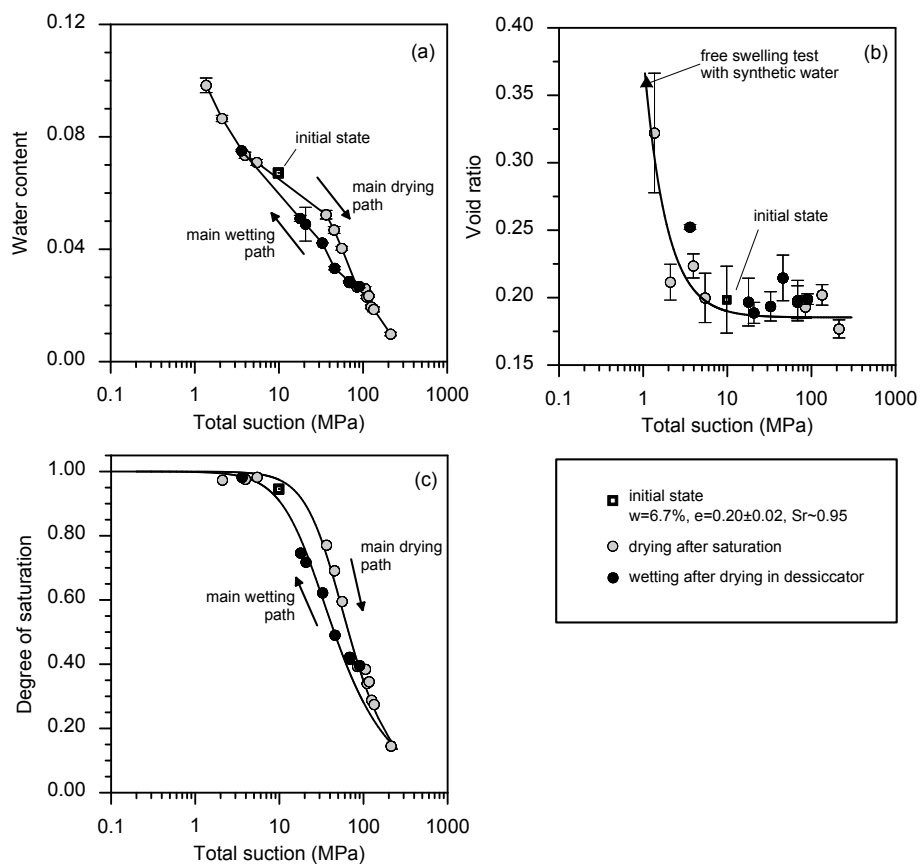


Figure 1. Water retention behaviour of the Opalinus Clay core sample: the water content (a), the void ratio (b) and the degree of saturation (c) as a function of the total suction.

## REFERENCES

- Ferrari, A. and Laloui, L. 2012: Advances in the testing of the hydro-mechanical behaviour of shales. In L. Laloui and A. Ferrari editors. *Multiphysical Testing of Soils and Shales*, pages 57-68, Springer.

## 11.4

# High-resolution CMP-refraction seismics in combination with refraction tomography, reflection seismics and surface wave analysis

Hunfeld Ulrich<sup>1</sup>, Brenner Olaf<sup>2</sup> & Orlowsky Dirk<sup>2</sup>

<sup>1</sup> Wili 3, CH-6222 Gunzwil (Ulrich.Hunfeld@bluewin.ch)

<sup>2</sup> DMT GmbH & Co. KG, Exploration & Geosurvey, Am Technologiepark 1, D-45307 Essen

### Motivation

High-resolution seismic measurements were carried out in spring 2009 to evaluate the subsoil of a construction site. The results were used for the design of the tunnel system of a motorway in an urban area.

### Aims

The aim of the study was to determine the exact position of the second refractor. There was a geological fault zone suspected in the second refractor and the location should be determined by the measurement.

### Methods used

The data acquisition was carried out with three different seismic sources: The three sources were an accelerated drop weight (type Mjöltnir), a sledgehammer of 8 kg and a vibroseismic air source. The signal quality of the different sources are compared. The receiver layout was a fixed spread layout with a geophone spacing of one meter and a source point spacing of two meters. This spread was chosen to fit each requirements of the selected data processing methods.

The seismic data was analysed with the methods of CMP-refraction, refraction tomography and reflection seismics. An analysis of the surface waves was also performed. Like the results of the reflection seismics, the results of the CMP-refraction seismics is also a stacked section with time to depth converted layer boundaries. In opposite to a standard refraction or a refraction tomography, the phase information of the seismic wave is also taken into account in the stacked section. Together with the wave velocity distribution in the refraction tomography section, the analysis of the surface waves and the deeper layer boundaries derived from the seismic reflection section, all information within the seismic data can be used in optimally manner.

### Results

The results of each data processing methods are presented and compared. Figure 1 shows the interpreted section of the refraction tomography and Figure 2 the geological interpreted combined stacked section of the CMP-refraction and reflection seismics. Based on these results, the main focus of the discussion will be lying on the advantages of the common interpretation of the different methods.

### Acknowledgement

The activities were carried out by DMT GmbH & Co. KG in spring 2009.

I would like to express my gratitude for using the results in this presentation.

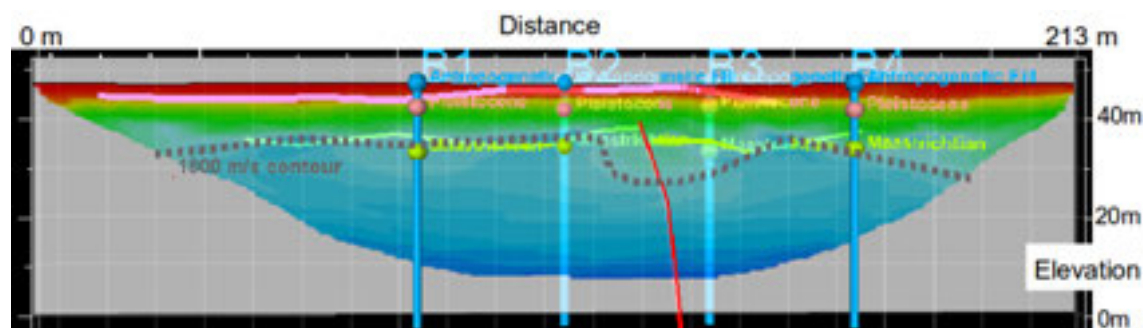


Figure 1. Interpreted section of the refraction tomography

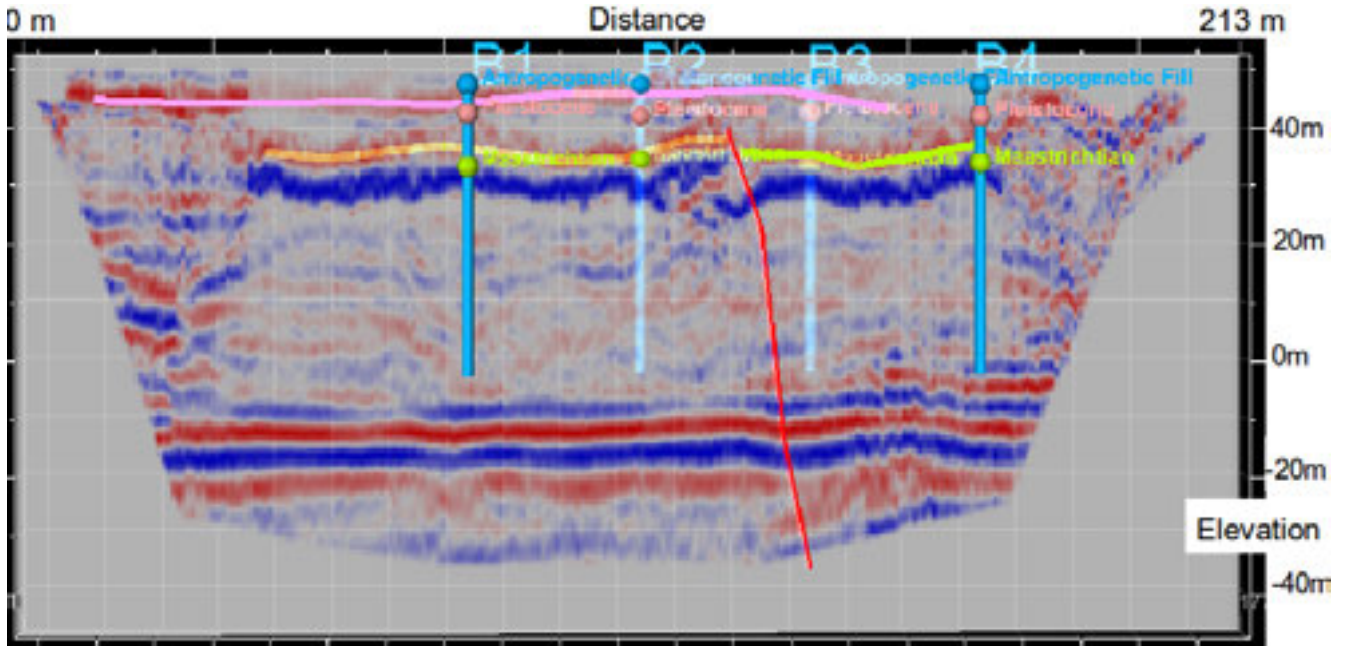


Figure 2. Geological interpreted combined stacked section of the CMP-refraction and reflection seismics

## 11.5

# Seismoelectric effects due to mesoscopic heterogeneities: numerical study for a fractured rock

Jougnot Damien, Rubino J. German, Rosas Carbajal Marina, Linde Niklas, and Holliger Klaus

*Applied and Environmental Geophysics Group, University of Lausanne, CH-1015 Lausanne, Switzerland.*

When a seismic wave propagates through a fluid saturated porous medium, it produces a relative motion between the fluid phase and the rock matrix. In the presence of an electric double layer at the fluid-solid interface, this movement introduces a separation of electrical charges which in turn generates a time-varying electrical source current and a resulting distribution of electrical potential (Pride, 1994). The presence of mesoscopic heterogeneities, that is, heterogeneities having sizes larger than the typical pore size but smaller than the prevailing wavelength, can induce a significant oscillatory fluid flow in response to the propagation of seismic waves (Müller et al., 2010). Indeed, the energy dissipation related to this phenomenon is considered to be one of the most common and important seismic attenuation mechanisms operating in the shallow part of the crust. Given that the amount of fluid flow produced by this phenomenon can be significant, a potentially important seismoelectric signal is also expected in such media. However, to the best of the authors' knowledge, the role played by mesoscopic wave-induced fluid flow on seismoelectric phenomenon is so far largely unexplored.

In this work, we propose a numerical approach for computing seismoelectric signals related to the presence of mesoscopic heterogeneities such as fractures. To this end, we consider a two-dimensional homogeneous sandstone sample containing three fractures with a small aperture. We apply an oscillatory compression on its top boundary considering a frequency range from 1Hz to 10kHz and an amplitude of 1kPa (Rubino et al., 2011). The solid phase is neither allowed to move on the bottom boundary nor to have horizontal displacements on the lateral boundaries and the fluid is not allowed to flow into or out of the sample. The fluid velocity field is determined by solving the quasi-static poroelastic equations in the space-frequency domain under the governing boundary conditions (Rubino et al., 2009). Next, the seismoelectric conversion is calculated using the so-called effective electrical excess charge approach, which has been recently developed in streaming potential studies (Revil et Leroy, 2004).

For the particular material properties and geometries considered in this analysis, the results clearly show a frequency-dependent response of the seismoelectric signal that is caused by the mesoscopic heterogeneities (Fig. 1). The magnitude tends to be negligible at frequencies below 100Hz. Conversely, at higher frequencies the induced fluid flow between the fractures and the embedding rock matrix becomes fairly important, thus yielding a measurable seismoelectric signal of a few mV. Our results therefore suggest that seismoelectric signals caused by mesoscopic heterogeneities should be explored in more detail. Such efforts should not only include further numerical analysis to better understand the role played by different types of heterogeneities, but also well-controlled laboratory investigations.

### REFERENCES

- Jougnot, D., Rubino, J. G., Rosas Carbajal, M., Linde, N., & Holliger, K., 2013: Seismoelectric effects due to mesoscopic heterogeneities, *Geoph. Res. Lett.*, 40, 2033–2037.
- Müller, T., Gurevich, B., & Lebedev, M., 2010: Seismic wave attenuation and dispersion resulting from wave-induced flow in porous rocks – A review, *Geophysics*, 75, A147–A164.
- Pride, S., 1994: Governing equations for the coupled electromagnetics and acoustics of porous media, *Phys. Rev. B*, 50, 15,678–15,696.
- Revil, A. & Leroy, P., 2004: Constitutive equations for ionic transport in porous shales, *J. Geoph. Res.*, 109, B03208.
- Rubino, J. G., Ravazzoli, C., & Santos, J., 2009: Equivalent viscoelastic solids for heterogeneous fluid-saturated porous rocks, *Geophysics*, 74, N1–N13.
- Rubino, J. G., Guarracino, L., Müller, T. M., & Holliger, K., 2013: Do seismic waves sense fracture connectivity? *Geophys. Res. Lett.*, 40, 692–696.

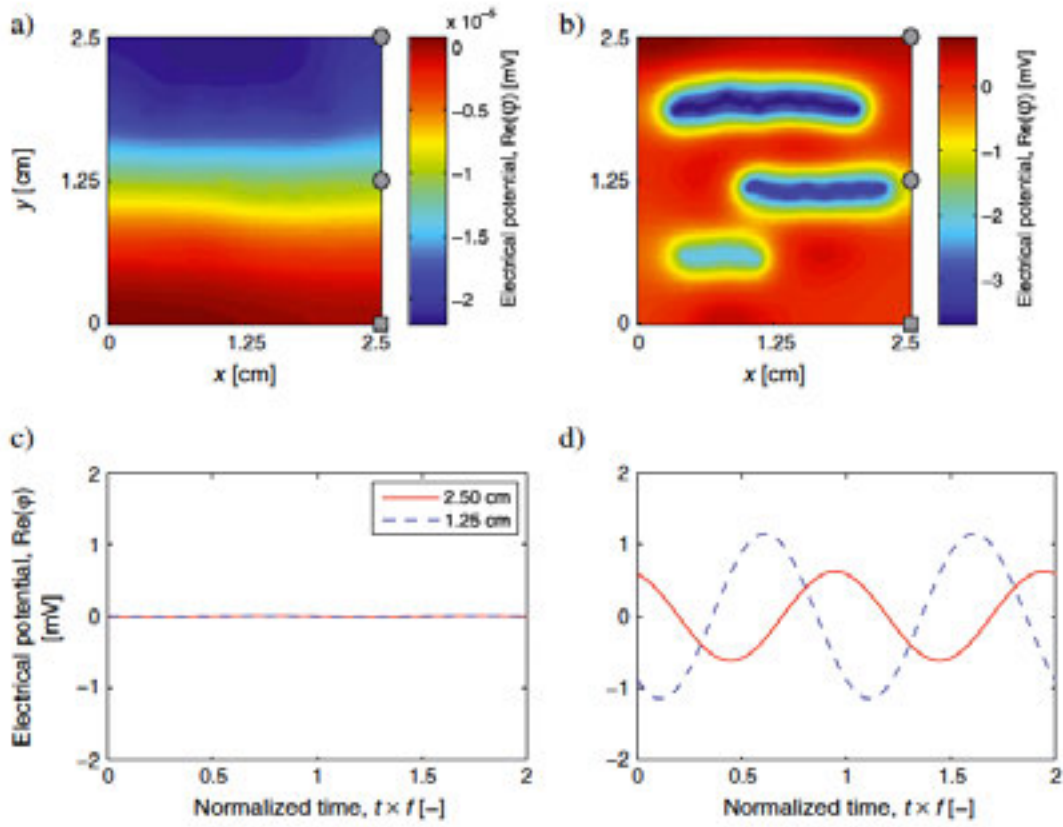


Figure 1. Seismoelectric potential response to the oscillatory compression test on a fractured sandstone for 1 Hz (a. & c.) and 10 kHz (b. & d.) (modified from Jougnot et al., 2013)

## 11.6

## Focusing of seismic energy at LUSI mud volcano, Indonesia

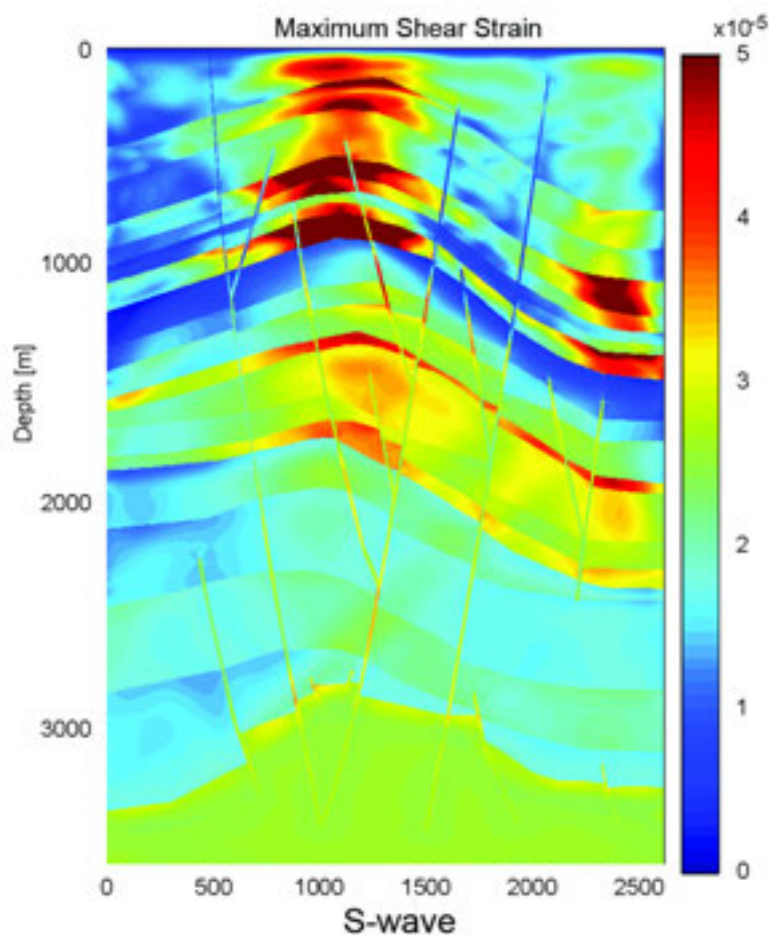
Lupi, M., Saenger, E. H., Fuchs, F., Miller, S. A

1 ETH Zurich, Geological Institute, Sonneggstrasse 5, 8092, Zurich, CH

2 Steinmann Institute, University of Bonn, Meckenheimer Allee 173, Bonn, DE

The M6.3 Yogyakarta earthquake occurred offshore of Central Java on May 27<sup>th</sup>, 2006. Forty seven hours later, hot mud erupted approximately 250 km from the earthquake epicenter near Sidoarjo, Java. The continuous, and still on-going, eruption of mud originated the LUSI mud volcano, which is the youngest mud volcanic system on earth. The causes that initiated the eruption are still debated and are based on different geological observations. The earthquake-triggering hypothesis is supported by the evidence that at the time of the earthquake ongoing drilling operations experienced a loss of the drilling mud down-hole. In addition, the eruption of the mud began only 47 hours after the Yogyakarta earthquake and the mud reached the surface at different locations aligned along the Watukosek fault, a strike-slip faults upon which LUSI resides. Moreover, the Yogyakarta earthquake also affected the volcanic activity of Mt. Semeru, located as far as Lusi from the epicentre of the earthquake. However, the drilling-triggering hypothesis points out that the earthquake was too far from LUSI for inducing relevant stress changes at depth and highlight how upwelling fluids that reached the surface first emerged only 200 m far from the drilling rig that was operative at the time. Hence, was LUSI triggered by the earthquake or by drilling operations?

A recent study suggests that a high-velocity seismic reflector located above the low-velocity formations that fed the mud eruption may have enhanced and focused seismic energy from the Yogyakarta earthquake and initiated the mud eruption. However, the occurrence of such a high-velocity formation at approximately 1000 m deep as well as the velocity model used to characterize the numerical study have been highly debated. To investigate effects of such a high-velocity layer and the sensitivity of the numerical analysis to the velocity model we conducted further simulations and found that the overall geological structure characterized by alternating and contrasting impedances, not the single high-velocity layer, is key to understand the response of the system and the resulting wave field.



## 11.7

# Assessment of the complex rock mass conditions for tunnels and underground caverns of the Hydropower Project Cerro del Águila (Peru)

Thüring Manfred & Sayah Selim M.

Lombardi Engineering Ltd., Via R. Simen 19, CH-6648 Minusio, Switzerland  
(manfred.thuering@lombardi.ch, selim.sayah@lombardi.ch)

### The project

The 510 MW hydropower project Cerro del Águila is currently under construction by Lombardi Ltd. as the designer, the consortium AGyM (Astaldi SA, Italy and Graña y Montero, Peru) as the constructor and KALLPA as the client. It is located in the external Peruvian Andes (Amazonian watershed) and exploits the water of Rio Mantaro. The plant consists of a 80 m high gravity dam, a roughly 5.7 km long headrace tunnel and 1.9 km long tailrace tunnel with a 93 m<sup>2</sup> simplified horseshoe section, a powerhouse cavern of 40x86x18 m (height/length/width) located 350 m underground and various surge, access and adit tunnels. All underground excavations are carried out using the conventional drill and blast method.

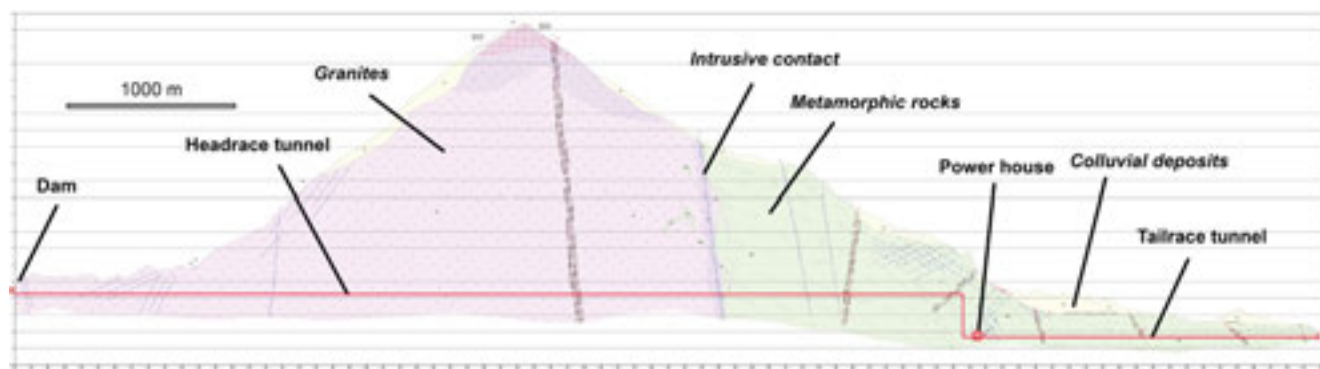


Figure 1: Geological profile along the 7.6 km long headrace-tailrace tunnel system.

### Geological challenges

The project has several exceptional and challenging features (Figure 1):

The 7.6 km long headrace-tailrace tunnel of more than 10 m section height runs under a maximum overburden exceeding 1600 m in a mixed geological environment of highly metamorphic paragneisses intruded by granites, introducing the probable threat of rock burst and convergences. Particularly challenging will be the crossing of the intrusive contact under an overburden of 900 m.

Recent tectonics and uplift have created more than 125 m thick colluvial/landslide deposits, fracture patterns and a spectacular topography particularly at the powerhouse area, putting challenges for the construction of access roads and the condition of the rock mass for the excavation of the power house cavern and the tailrace tunnel.

The power house cavern is situated under a strongly inclined slope, 350 m below surface, demanding a special focus on the rock mass conditions and water tightening of the pressure shaft and alignment of the caverns with in-situ stresses and joints orientation. For this reason extensive hydrojacking tests were carried out in order to verify the initial geological assumptions related to the rock quality of the cavern system and the unlined pressure shaft.

### Work progress

In order to better understand the underground conditions the geological model of the feasibility study has been completed by an investigation campaign, consisting of boreholes with field tests, seismics and laboratory tests for the key project structures. Together with geological field surveys the scheme was optimized.



Figure 2: Progress of excavation of more than 10 m high headrace tunnel, performed by drill and blast.

This presentation illustrates how the various geological and design related challenges concerning the rock mass condition have been addressed and resolved, using boreholes, field tests, seismic campaigns, hydrojacking tests, and computer modeling. A particular focus is put on the underground structures (tunnels and powerhouse cavern). The presentation also shows the current progress of the project (Figure 2).

## 11.8

# Lowering microseismic detection threshold by sonogram analysis for Fribourg area (Switzerland)

Vouillamoz Naomi<sup>1</sup>, Abednego Martinus<sup>1</sup>, Deichmann Nicolas<sup>2</sup>, Wust-Bloch Hillel Gilles<sup>3</sup>, Mosar Jon<sup>1</sup>,

<sup>1</sup> University of Fribourg, Department of Geosciences, Earth Sciences, Chemin du Musée 6, CH-1700 Fribourg, Switzerland (martinussatiapurwadi.abednego@unifr.ch, naomi.vouillamoz@unifr.ch, jon.mosar@unifr.ch).

<sup>2</sup> Schweiz. Erdbebendienst (SED), Sonneggstrasse 5, CH-8092 Zürich, Switzerland

<sup>3</sup> Tel Aviv University, Department of Geophysics and Planetary Sciences, P.O.B. 39040, Tel Aviv, 69978, Israel

This study investigates low-magnitude seismicity generated within the Fribourg area (Western Molasse Basin – Switzerland (Fig 1)). It focuses on the Fribourg Lineament (FL), a North-South trending cluster of weak earthquakes that were generated East of the city of Fribourg and may be associated to the lineament described by Kastrup et al. (2007). Visual event screening by sonogram analysis (Sick et al. 2012) is carried out on 50 months of continuous data recorded by the Swiss Earthquake Service (SED), between 2001 and 2013.

Earthquake detection is carried out with the NanoseismicSuite software package (Institute for Geophysics-Stuttgart: Joswig 2008; Sick et al. 2012), which uses sonograms, a type of power spectral density (PSD) matrix. These PSD, which are noise adapted, muted and pre-whitened, allow for the detection of signal energy near to 0 dB signal to noise ratio (SNR).

This analysis uses continuous data recorded between October 2001 and April 2013 by three SED permanent stations: SCOU, STAF and TORNY (Figure 1). SCOU and STAF are two accelerometers installed in 2008 at some 5 and 10 kilometers away from the FL. TORNY is a broadband sensor located 20 kilometers west of the FL (Figure 1), whose continuous data is available since 2001.

The ECOS-09 catalog (Earthquake Catalog of Switzerland) reports about 40 events recorded between 2001 and 2012, within a radius of 20 km around the city of Fribourg. Our sonogram-based analysis of SED continuous data for the same period and same area, identified more than 200 previously undetected events.

Among these 200 events, 60 can be reliably located with the NanoseismicSuite software, using SED waveforms recorded near the FL as well as data acquired by two mini-arrays deployed near the FL (Abednego & Vouillamoz, 2011). The remaining micro-earthquakes do not present enough phase information to be located. Since most of these weaker events show excellent signal correlation (>90%) with higher magnitude events, they have been used for further earthquake spatio-temporal analysis. Our new catalog shows how most of the 200 events can be associated to specific event clusters along the FL.

Our analysis suggests that most events, which were newly detected, are indeed located on the FL and seem to be related to stronger earthquakes that were previously detected (Kastrup et al., 2007). However, our new catalog shows that additional events, previously undetected, cluster under the city Fribourg. Since these events are not located near substructures that were detected and interpreted by existing subsurface imaging surveys (Interoil 2010), our investigations show the potential of sonogram analysis for active fault mapping and seismic hazard assessment.

## REFERENCES

- Abednego, M. & Vouillamoz, N., Wust-Bloch H. G., Mosar J., 2011. Nano-seismology on the Fribourg Lineament - Switzerland. Poster presented at the Swiss Geoscience Meeting 2011, Zürich.
- Interoil, 2010. 2D Seismik Interpretation in den Gebieten Payerne, Fribourg und Berner Seeland. Bericht vorbereitet von Interoil E&P Switzerland AG für die Resun AG, Zürich, September 2010.
- Joswig, M., 2008. Nanoseismic monitoring fills the gap between microseismic networks and passive seismic, First Break, 26, 2008.
- Kastrup, U., Deichmann, N., Fröhlich, A., Giardini, D., 2007. Evidence for an active fault below the northwestern Alpine foreland of Switzerland, Geophys. J. Int. (2007) 169, 1273-1288.
- Sick, B., Walter, M., Joswig, M., 2012. Visual Event Screening of Continuous Seismic Data by Supersonograms, Pure Appl. Geophys., 2012.

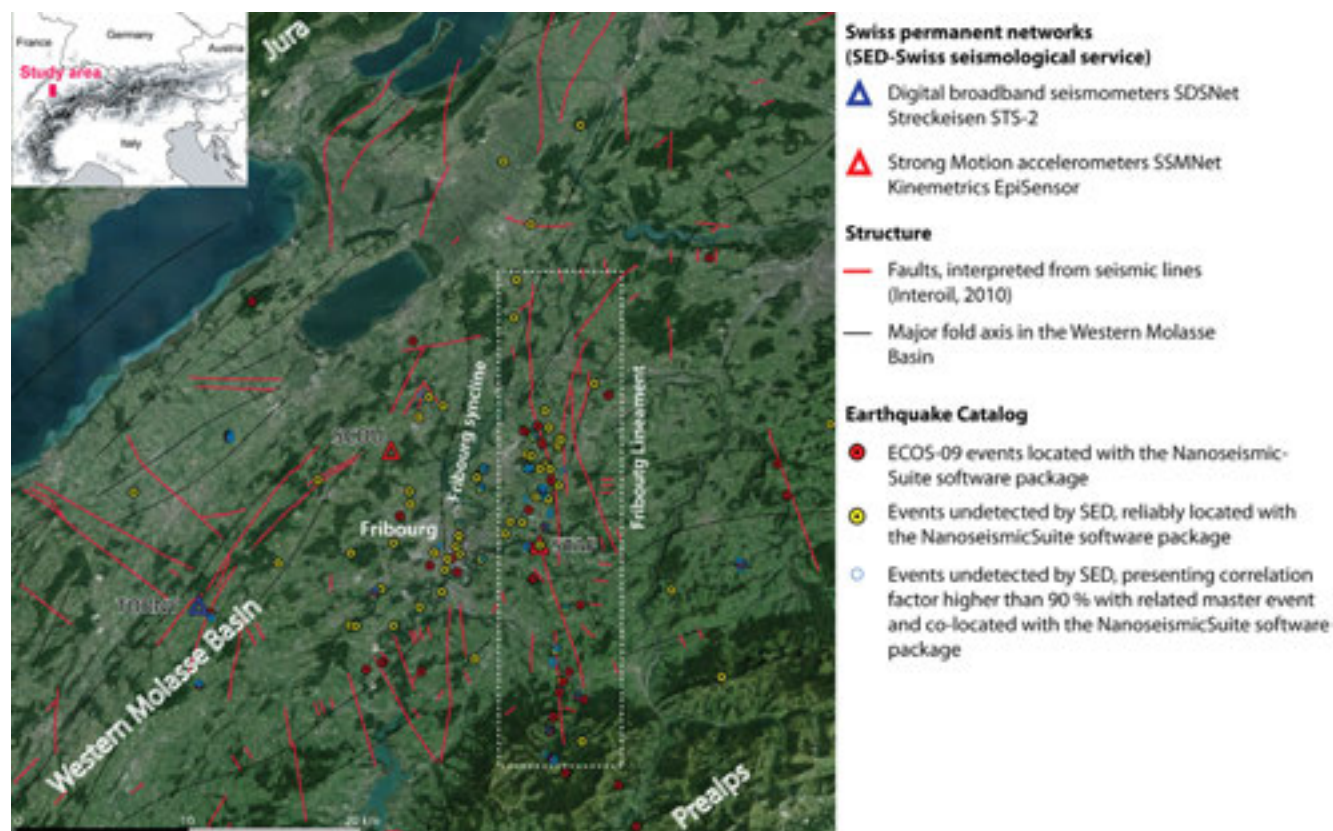


Figure 1: Google Earth view of study area with location of SED permanent stations used for earthquake detection, principal tectonic structures and earthquake catalog.

## P 11.1

# Large mass wasting deposits in Lake Geneva off the city of Lausanne revealed by detailed reflection seismic data

Correia-Demand Jehanne<sup>1</sup>, Marillier François<sup>1</sup>, Kremer Katrina<sup>2,3</sup> & Girardclos Stéphanie<sup>2,3</sup>

<sup>1</sup> Center for Research on Terrestrial Environment (CRET), University of Lausanne, Geopolis, CH-1015 Lausanne (jehanne.correia-demand@unil.ch)

<sup>2</sup> Department of Earth Sciences, University of Geneva, Rue des Maraîchers 13, CH-1205 Genève

<sup>3</sup> Environmental Sciences Institute (ISE), University of Geneva, Site Batelle, Route de Drize 7, CH-1227 Carouge

Seismic studies in the central part of Lake Geneva (“Grand-Lac”) have revealed the occurrence of several mass wasting deposits (MWD) within Holocene sedimentary layers. While some of them are small, a large MWD (MWD A) is observed off the city of Lausanne. The depth of the associated failure scars (100 m water depth), its volume (~ 13 km<sup>3</sup>), and the occurrence of other smaller MWD’s that were possibly co-deposited with MWD A point to a major event in the lake, most likely associated with an earthquake. Numerical simulations indicate that it could have generated a tsunami with local wave heights of up to 6 m near Lausanne. This earthquake-triggered event may be responsible for a gap in lake-dweller occupation in this region revealed by dendrochronological dating of remaining piles at palafitte sites (Kremer et al, in review).

To resolve the details of the MWD offshore Lausanne and to better understand its geological context different seismic systems were used. These were a 3.5 KHz pinger with a theoretical vertical resolution of 0.15 m and a multichannel system with either a water gun or an air gun seismic source with vertical resolution of 0.6 m and 1.1 m, respectively. After a first pass processing, the water gun data were reprocessed in order to take into account the shape of the streamer in the water. Examples of the different seismic resolutions as well as the enhanced data quality through reprocessing are shown in Figs. 1 to 4.

In addition to typical seismic images of MWDs often observed in other alpine lakes, intriguing features within the Holocene sediments with apparent sub-vertical offsets are shown in both the water-gun and pinger seismic data (Figs. 2 to 4). They are located above large faults zones in the Tertiary Molasse. The question whether these features and the large MWD off Lausanne were caused by the activity of these faults must be further investigated.

## REFERENCE

Kremer, K., Marillier, F., Hilbe, M., Simpson, G., Dupuy, D., Yrro, B., Rachoud-Schneider, A-M., Corboud, P., Bellwald, B., Wildi, W. & Girardclos, S. Pile dwellers occupation gap in Lake Geneva (France-Switzerland) possibly explained by an earthquake – slide – tsunami event during Early Bronze Age. In review at Earth and Planetary Science Letters.

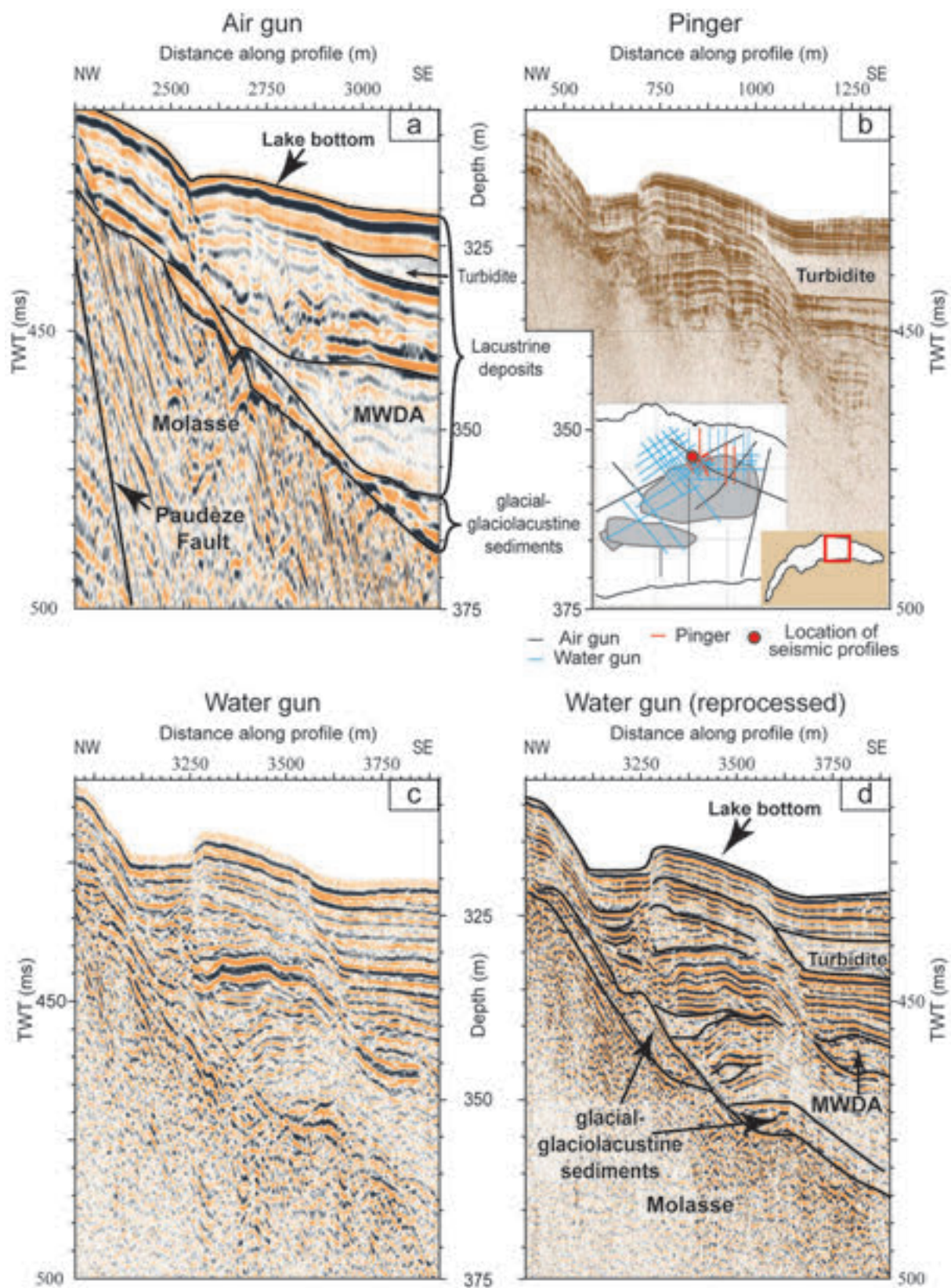


Figure 1. Comparison of seismic profiles with different seismic sources or processing. b), c) and d) show profiles with identical locations. a) Profile with orientation slightly different from the other ones, but sampling the same geological structures. Simplified geological interpretation shown on a) and d). MWDA : Mass-wasting deposit off the city of Lausanne.

## P 11.2

### Modeling Electric Current Flow in 3D Fractured Media

Serdar Demirel, Delphine Roubinet, and James Irving

*Applied and Environmental Geophysics Group, Center for Research of the Terrestrial Environment, University of Lausanne, Switzerland*

The study of fractured rocks is highly important in a variety of research fields and applications such as hydrogeology, geothermal energy, hydrocarbon extraction, and the long-term storage of toxic waste. Fractured media are characterized by a large contrast in permeability between the fractures and the rock matrix. For hydrocarbon extraction, the presence of highly conductive fractures is an advantage as they allow for quick and easy access to the resource. For toxic waste storage, however, the fractures represent a significant drawback, as there is an increased risk of leakage and migration of pollutants deep into the subsurface. In both cases, the identification of fracture network characteristics is a critical, challenging, and required step.

Recently, we have utilized the discrete fracture network (DFN) approach to model electric current flow in 2D fractured media. Our approach is based on a discrete dual-porosity model where fractures are represented explicitly, the matrix is coarsely discretized into blocks, and current flow exchange between the fracture and matrix is analytically evaluated at the fracture scale and integrated at the block scale. This approach is promising and has proven its efficiency for 2D simulations. However, its extension to 3D fractured media is a challenge that remains to be addressed. Assuming that fractures can be represented by two-dimensional finite planes embedded in a surrounding matrix, the principal difficulties are (i) expressing current flow conservation at fracture intersections that are represented by lines in 3D, instead of by nodes in 2D; (ii) evaluating the impact of fracture-matrix exchange at the fracture scale on the electric potential in a fracture; and (iii) integrating the fracture-matrix exchange from the fracture scale to the matrix-block scale in order to evaluate its impact on the electric potential in the porous domain.

We are working on developing an efficient model for electric current flow in 3D fractured rock with the following main application objectives: (i) studying the impact of heterogeneous fracture orientations, as existing 3D solutions are analytical and deal only with horizontal and vertical fractures; and (ii) applying our model to large-scale fracture networks that provide major pathways for electric current, as existing 3D numerical methods would underestimate these effects by integrating fracture electrical conductivity to a block-scale equivalent conductivity. The overarching goal of our work is to test how geoelectrical surveys may help with localizing and characterizing fractures in natural environments through a low-computational-cost modeling method.

## P 11.3

# Exploring the Issue of Model Error in Stochastic Solutions to Hydrogeophysical Inverse Problems

Corinna Koepke, James Irving, and Delphine Roubinet

*Applied and Environmental Geophysics Group, Center for Research of the Terrestrial Environment, University of Lausanne, Switzerland*

Geophysical methods have gained much interest in hydrology over the past two decades because of their ability to provide, in a minimally invasive manner, estimates of the spatial distribution of subsurface properties at a scale that is often relevant to key hydrological processes. Because of an increased desire to quantify uncertainty in hydrological predictions, many hydrogeophysical inverse problems have recently been posed within a Bayesian framework, such that estimates of hydrological properties and their corresponding uncertainties can be obtained. With the Bayesian approach, it is often necessary to make significant approximations to the associated hydrological and geophysical forward models such that stochastic sampling from the posterior distribution, for example using Markov-chain-Monte-Carlo (MCMC) methods, is computationally feasible. These approximations lead to model structural errors in the inverse problem which, if not properly accounted for through the Bayesian likelihood function, have the potential to influence posterior parameter estimates and uncertainties to the extent that subsequent hydrological predictions become meaningless. So far, however, the characterization and proper treatment of model errors in hydrogeophysical inverse problems has not been investigated.

Here, we present initial work in this domain with reference to the inverse problem of estimating unsaturated hydraulic properties, namely the van Genuchten – Mualem parameters, in a series of subsurface layers from time-lapse, zero-offset-profile (ZOP), ground penetrating radar (GPR) data collected over the course of an infiltration experiment. In particular, we investigate stochastically the effect of a variety of assumptions, commonly made for the sake of computational tractability during the stochastic inversion of these data, on the errors produced in the modeled results as a function of depth and time. These assumptions include (i) that infiltration is purely vertical and can thus be modeled by the one dimensional Richards' equation; (ii) that the subsurface layers are internally homogeneous; and (iii) that the infiltration rate of water into the subsurface is exactly known. Results so far indicate that model errors for this problem are far from being normal and independently identically distributed, which has been the common assumption in all previous stochastic inversion efforts in this domain. As a result, posterior uncertainties obtained through these efforts will likely be strongly biased. Future work will involve developing more appropriate likelihood functions to be used in Bayesian-MCMC inversions, with the goal of obtaining more meaningful posterior parameter estimates and uncertainties.

## P 11.4

# Improvement of the regional 3D modeling of deep geological structures with gravity: A case study in the Neuchatel Jura Mountains.

Kuhn Pascal<sup>1</sup>, Abdelfettah Yassine<sup>2</sup>, Mauri Guillaume<sup>3</sup>, Schill Eva<sup>4,5</sup> & Vuataz Francois-David<sup>2</sup>

<sup>1</sup> Eidgenössisches Departement für Verteidigung, Bevölkerungsschutz und Sport VBS, armasuisse, Bundesamt für Landestopografie swisstopo, Landesgeologie, Seftigenstrasse 264, CH-3084 Wabern (pascal.kuhn@swisstopo.ch)

<sup>2</sup> Centre for Hydrogeology and Geothermics (CHYN), University of Neuchâtel, Emile-Argand 11, CH-2000 Neuchâtel (yassine.abdelfettah@unine.ch)

<sup>3</sup> Geo2X SA, Oulens-sous-Echallens, CH-1377

<sup>4</sup> EEIG «Heat Mining», Route de Soutz - BP 40038, F-67250 Kutzenhausen, France

<sup>5</sup> Steinbeis-Transfer Centre «Geoenergy and Reservoir Technology» D-79807 Lottstetten-Nack, Germany

Pioneer work on the Atlas of gravimetry (Klingelé & Olivier, 1980) has allowed the scientific community to discover that the underground structure of Switzerland was affected by significant gravity variation within the Molasse basin, the Rhine graben and the Jura Mountains. While some of the gravity decreases are clearly associated to sedimentary deposit during the post-Mesozoic period, source of decrease of gravity in other parts cannot be explained using the existent knowledge on current geophysical and geological information. Post processing of the Bouguer anomaly allows an interpretation of the density anomalies correlating with the deep Paleozoic structures (Abdelfettah et al., in preparation). Permo-Carboniferous basins has been identified in seismic studies (Sommaruga et al., 2012) as well as in former gravity explorations (Klingelé & Schwendener, 1984).

A gravity data set from the BRGM was also used to cover the French area. Special considerations were taken in account to merge both Swiss and the French database. Two techniques were used to validate this compilation; i) using a geostatistical approach, and ii) using the means value of the neighboring measurements within a specified radius. In the end, a complete Bouguer anomaly computed at the same ellipsoid is obtained for the whole studied area. As this Bouguer anomaly is strongly dominated by the regional trend, caused by the sedimentary layer and by the deepening of the crystalline basement, a Betterworth filter (Abdelfettah and Schill, 2012) using different wavelengths was applied to get residual anomalies which are ready to be interpreted.

This study investigates the occurrence of Permo-Carboniferous basins underneath the Jura Mountains in the north-west part of Canton of Neuchâtel. The investigated area reaches from Pontarlier (F) in the west to Biel/Bienne in the east as well as Estevayer-le-Lac in the south to Orasans (F) in the north resulting in a geological 3D model of ~65x50 km. Due to the regional scale and the low data-density (geological profiles, seismics, drillholes) the model was set up using 13 geological profiles (Charrue unpubl.; Pfiffner, 2009; Sommaruga et al., 2012) and 3 deep drillholes. The obtained 3D geological model has then been used to calculate the theoretical gravity response by doing a 3D forward modeling. By try and error the modeled structures must fit the real gravity data as close as possible.

A comparison of the observed gravity data with the gravity model response reveals that to reduce the misfit, a density variation of the Permo-Carboniferous basins in the Paleozoic basement must be considered.

## REFERENCES

- Abdelfettah Y., Schill E., Kuhn P., in preparation. Characterization of geothermally relevant inhomogeneities in crystalline basement using filters and gravity forward modeling: an example from to Permo-Carboniferous grabens in Switzerland.
- Abdelfettah Y. & Schill E., 2012. Delineation of geothermally relevant Paleozoic graben structures in the crystalline basement of Switzerland using gravity. Submitted to Society of Exploration Geophysics meeting, Istanbul, 2012.
- Klingelé, E. and Olivier, R., 1980. Die neue Schwere-Karte der Schweiz (Bouguer- Anomalien), Bern.
- Klingelé, E. & Schwendener H., 1984. Geophysikalisches Untersuchungsprogramm Nordschweiz: Gravimetrische Messungen 81/82, Nagra, Baden.
- Sommaruga, A., 1997. Geology of the central Jura and the molasse basin: New insight into an evaporite-based foreland fold and thrust belt. Dissertation. Univ. Neuchâtel.
- Sommaruga A., Eichenberger U. & Marillier F., 2012. Seismic Atlas of the Swiss Molasse Basin. 24 Tafeln. ISBN 978-3-302-40064-8.

## P 11.5

# Laboratory seismic scale model study of reflection imaging beneath a distorting near surface zone

Yike Mo & Hakki Karaman

<sup>1</sup>*Institute of Geophysics, ETH Zürich, Sonneggstrasse 5, CH-8092 Zürich (yimo@student.ethz.ch)*

The near-surface weathered layer has a profound impact on surface seismic reflection data (Yilmaz, 2001). Surface waves, guided and refracted waves often obscure the reflection record, especially when near surface layering is present and the velocity contrasts are strong. Unfortunately, our understanding of the physics of wave propagation in the near surface is limited and the techniques available to invert for near-surface properties have not been developed to a stage where they can be applied to solve many relevant problems.

To tackle the challenges and imaging problems referred to above, several two – dimensional scale models built out of 2 mm thick plastic and metal sheets (cut and bonded together) were assembled in the Wave Propagation Lab at ETH Zurich. The models were used, in full recognition of the similitude relations (Pant et al., 1988), to investigate reflections from beneath a complex overburden. The plate models are rather thin relative to a wavelength, so that the only longitudinal and shear waves which propagate in the plate are the fundamental mode symmetric non-dispersive vibrations which travel at the plate velocity  $V_p$  and the extended medium shear velocity  $\beta$ , respectively (Redwood, 1960). Dipping layers, anomalous block inserts were simulated. The experiment entails the use of a piezoelectric source driven by a pulse amplifier at ultrasonic frequencies (20 – 300 kHz) to generate waves in the plate, which are detected by piezoelectric receivers and recorded digitally on a 32 channel National Instruments recording system, under SignalExpress software control.

In the experiment, a single cycle sinusoidal pulse with a negative onset (5  $\mu$ s pulse width and 600 V pulse voltage) was selected as the optimized source. Reflection and transmission data were initially collected over a homogenous model for calibration purposes. For the heterogeneous models, different recording configurations and processing techniques, such as deconvolution, normal move-out and migration, were applied. The experiments are continuing but preliminary results clearly show the difficulties of imaging beneath an irregular overburden.

### REFERENCES

- Pant, D.R., Greenhalgh S. A. & Watson, S. 1988: Seismic reflection scale model facility. *Exploration Geophysics*. 19, 499–512.
- Redwood, M. 1960: *Mechanical Waveguides: The Propagation of Acoustic and Ultrasonic Waves in Fluids and Solids with Boundaries*. 300 pp, Pergamon Press.
- Yilmaz, Oz. 2001: *Seismic Data Analysis: Processing, Inversion and Interpretation*. Society of Exploration Geophysicists.

## P 11.6

# Material softening as a potential cause for the development of boudinage - an elasto-visco-plastic numerical modeling approach

Peters Max<sup>1</sup>, Poulet Thomas<sup>2</sup>, Karrech Ali<sup>3</sup>, Regenauer-Lieb Klaus<sup>4</sup> & Herwegh Marco<sup>1</sup>

<sup>1</sup> *Institute of Geological Sciences, University of Bern, Switzerland*

<sup>2</sup> *CSIRO Earth Science and Resource Engineering, Kensington, Western Australia*

<sup>3</sup> *School of Civil and Resource Engineering, The University of Western Australia*

<sup>4</sup> *School of Earth and Environment, The University of Western Australia*

Layered rocks deformed under viscous deformation frequently show boudinage, a process which results from differences in effective viscosity between the layers involved (Goscombe et al., 2004 and references therein). Information on the deformation processes, physical conditions (T, stress, strain rate) and effective viscosities are crucial to obtain rheological constraints directly from nature. In the past, various numerical modeling studies of boudinage in layers under going power-law creep attempted to describe the development of pinch-and-swell structures under different physical deformation conditions (low to high T; e.g. Schmalholz and Maeder, 2012). However, there exists rather limited knowledge about both the origin of necking instabilities as well as the relation between boudinage and the involved flow regimes.

The finite element modeling software ABAQUS in combination with user-defined subroutines UMAT (Karrrech et al., 2011a) was applied to investigate aforementioned problems. We implemented thermo-mechanical coupling between elastic, viscous and plastic deformation of pure calcite (Cc) or quartz (Qtz) aggregates or Qtz+Cc mixtures. Finite elements, each representing a population density function of a number of individual grains, undergo layer-parallel extension, which resembles co-axial plane strain. In terms of geometry, a simulated pure-shear box is built up by 3 layers, consisting of a central layer of coarse-grained populations, surrounded by finer grained populations on bottom and top. In contrast to previous studies, the rheology evolves with increasing shear strain starting with initial elastic behavior, adding then the transient Ramberg-Osgood strain hardening on the way to composite viscous flow (Herwegh et al., in review). Composite flow on the base of dislocation and diffusion creep for both mineral phases is involved.

Compared to nature, this model setup corresponds to a secondary phase-controlled polymineralic host rock (pinned and fine-grained matrix grains) around a coarse-grained monomineralic vein, in which grains can dominantly deform in a plastic manner involving dynamic recrystallization. While the small grain sizes in top and bottom layers are strain invariant, they are allowed to adapt to the physical deformation conditions in the central layer by grain growth or grain size reduction following an energy optimization procedure based on the Paleowattmeter approach of Austin and Evans (2007) and the thermodynamic approach of Regenauer-Lieb and Yuen (XYZ2004).

Note that the chosen model set up corresponds to situations in natural high strain shear zones such as thrust and detachment faults, where highly strained and fine grained polymineralic (ultra-) mylonites are subjected to synkinematic veining. We use natural examples of the Helvetic Alps and the Penninic front to check and discuss the relevance of our numerical results.

## REFERENCES

- Austin, N. and Evans, B. (2007). Paleowattmeters: A scaling relation for dynamically recrystallized grain size. *Geology*, 35.
- Goscombe, B.D., Passchier, C.W. and Hand, M. (2004). Boudinage classification: End-member boudin types and modified boudin structures, *Journal of Structural Geology*, 26.
- Herwegh, M., Poulet, T., Karrech, A. and Regenauer-Lieb, K. (in review). From transient to steady state deformation and grain size: A thermodynamic approach using elasto-visco-plastic numerical modeling. *Journal of Geophysical Research*.
- Karrrech, A., Regenauer-Lieb, K. and Poulet, T. (2011a). A Damaged visco-plasticity model for pressure and temperature sensitive geomaterials. *Journal of Engineering Science* 49.
- Regenauer-Lieb, K. and Yuen, D. (2004). Positive feedback of interacting ductile faults from coupling of equation of state, rheology and thermal-mechanics. *Physics of the Earth and Planetary Interiors*, 142.
- Schmalholz, S.M. and Maeder, X. (2012). Pinch-and-swell structure and shear zones in viscoplastic layers. *Journal of Structural Geology*, 34.

## P 11.7

# Two-dimensional probabilistic inversion of plane-wave electromagnetic data

M. Rosas Carbajal<sup>1</sup>, N. Linde<sup>1</sup>, T. Kalscheuer<sup>2</sup>, J. Vrugt<sup>3,4</sup>

<sup>1</sup> *Applied and Environmental Geophysics Group, University of Lausanne (marina.rosas@unil.ch).*

<sup>2</sup> *Institute of Geophysics, ETH Zurich.*

<sup>3</sup> *Department of Civil and Environmental Engineering, University of California Irvine, 4130 Engineering Gateway, Irvine, CA 92697-2175, USA.*

<sup>4</sup> *Institute for Biodiversity and Ecosystems Dynamics, University of Amsterdam, Amsterdam, The Netherlands.*

Probabilistic inversions based on Markov chain Monte Carlo (MCMC) methods help to characterize the inherent non-uniqueness of non-linear inverse problems. By stating the inverse problem as an inference problem, the emphasis is placed on sampling the posterior probability density function (pdf) of the model parameters, which provides direct information about the model parameters' uncertainty. Unfortunately, for non-linear problems involving many model parameters, MCMC algorithms may take great time to converge. This is why most geophysical applications based on MCMC rely on 1D assumptions. We present here the first fully two-dimensional pixel-based MCMC inversion of radio magnetotelluric (RMT) and electrical resistivity tomography (ERT) data, using up to 300 model parameters. Using synthetic data, we demonstrate that stochastic inversion of high-dimensional problems necessitates prior constraints on the model structure to yield meaningful results. We investigate how model parameter uncertainty depends on model structure constraints using different norms of the likelihood function and on the model constraints. In particular, we focus on two popular types of regularization: smoothly varying model parameters and compact anomalies. We invert not only for the pdf of the model parameters, but also for two hyper-parameters: the variance of the data errors and a trade-off between data fit and model structure. The derived model uncertainties are compared with deterministic most-squares inversions and we analyze how these uncertainties change when jointly inverting RMT and ERT data. Finally, we present a field application to characterize the geometry of an aquifer in Sweden. The numerical examples illustrate that model regularization not only decreases the uncertainty of the model parameters, but also accelerates the convergence of the MCMC algorithm. A drawback is that the regularization may lead to posterior pdfs that do not contain features in the true model that are insensitive to data. This problem can be partly mitigated if the plane-wave EM data is augmented with ERT observations. The hierarchical Bayesian inverse formulation used is able to recover the probabilistic properties of the measurement data errors and a model regularization weight. Application of the proposed inversion methodology to field data from an aquifer demonstrates that the posterior mean model realization is very similar to that derived from a deterministic inversion with similar model constraints.

## P 11.8

# Discrete Dual Porosity Modeling of Electrical Current Flow in Fractured Media

Roubinet Delphine & Irving James

*Center for Research of the Terrestrial Environment, University of Lausanne, Switzerland*

The study of fractured rocks is highly important in a variety of research fields and applications such as hydrogeology, geothermal energy, hydrocarbon extraction, and the long-term storage of toxic waste. Fractured media are characterized by a large contrast in permeability between the fractures and the rock matrix. For hydrocarbon extraction, the presence of highly conductive fractures is an advantage as they allow for quick and easy access to the resource. For toxic waste storage, however, the fractures represent a significant drawback, as there is an increased risk of leakage and migration of pollutants deep into the subsurface. In both cases, the identification of fracture network characteristics is a critical, challenging, and required step.

A number of previous studies have indicated that the presence of fractures in geological materials can have a significant impact on geophysical electrical resistivity measurements. It thus appears that, in some cases, geoelectrical surveys might be used to obtain useful information regarding fracture network characteristics. However, existing geoelectrical modeling tools and inversion methods are not properly adapted to deal with the specific challenges of fractured media. This prevents us from fully exploring the potential of the method to characterize fracture network properties. We thus require, as a first step, the development of accurate and efficient numerical modeling tools specifically designed for fractured domains.

Building on the discrete fracture network (DFN) approach that has been widely used for modeling groundwater flow in fractured rocks, we have developed a discrete dual-porosity model for electrical current flow in fractured media. Our novel approach combines an explicit representation of the fractures with fracture-matrix electrical flow exchange at the block-scale. Tests in two dimensions show the ability of our method to deal with highly heterogeneous fracture networks in a highly computationally efficient manner, which permits us to study the impact of fractures and their properties on the electrical response of the domain. With additional development, the method will be extended to three dimensions and used in the context of geoelectrical field investigations.

## P 11.9

## Seismic energy dissipation in fractured rocks

J. Germán Rubino<sup>1</sup>, Tobias M. Müller<sup>2</sup>, Luis Guarracino<sup>3</sup> & Klaus Holliger<sup>1</sup>

<sup>1</sup> Applied and Environmental Geophysics Group, University of Lausanne, CH-1015 Lausanne (German.Rubino@unil.ch)

<sup>2</sup> Earth Science & Resource Engineering Division, Commonwealth Scientific and Industrial Research Organization, Perth, Australia

<sup>3</sup> CONICET – Facultad de Ciencias Astronómicas y Geofísicas, Universidad Nacional de La Plata, Argentina.

Up until now, the enhanced energy dissipation observed in fractured rocks has been considered to be mainly produced by wave-induced fluid flow (WIFF) between fractures and the pore space of the embedding matrix (e.g., Brajanovski et al., 2005). Since this process is strongly controlled by the hydraulic characteristics of the heterogeneous sample, it is expected that seismic attenuation also contains information on fracture connectivity.

Extending a recent pilot study of this topic (Rubino et al., 2013a), we explore here the effects of fracture connectivity on seismic attenuation. We represent fractures as highly compliant and permeable heterogeneities embedded in a stiffer porous matrix (e.g., Brajanovski et al., 2005) and employ a numerical upscaling procedure similar to that presented by Rubino et al. (2013b). That is, we apply an oscillatory compression at the top boundary of a square rock sample containing mesoscopic fractures. The solid phase is allowed neither to move on the bottom boundary nor to have horizontal displacements on the lateral boundaries. The fluid is not allowed to flow into or out of the sample. The equivalent undrained, complex plane-wave modulus, which contains the information on seismic attenuation for vertically propagating P waves, is expressed in terms of the applied compression and the oscillatory volume change. The latter is obtained by numerically solving the Biot's (1941) consolidation equations.

We consider two models corresponding to homogeneous water-saturated sandstones permeated by two quasi-orthogonal fractures without and with intersection (Figure 1). In both cases, the rock sample is a square of side length 3.33 cm, and the mean aperture of the fractures is 0.033 cm. The red curve in Figure 1 shows that the presence of fractures perpendicular to the direction of wave propagation produces strong attenuation over a wide frequency range. This is expected, because the strong compressibility contrast between the quasi-horizontal fracture and background material produces a large amount of fluid flow between these two regions and, consequently, energy dissipation. By comparing the blue and red curves we see that when the fractures intersect significant changes in the overall attenuation arise. In particular, the attenuation levels corresponding to WIFF between fractures and background material decrease and a second peak arises at higher frequencies. Corresponding spatial distributions of energy dissipation allow us to observe that in absence of fracture connectivity energy dissipation takes place in the vicinity of the quasi-horizontal fracture. In presence of fracture connectivity, dissipation takes place in the vicinity of the two fractures for the frequency of the first attenuation peak. However, the pressure gradient between fractures and background is reduced, and therefore the total energy dissipation is less significant (blue curve in Figure 1). For the frequency of the second attenuation peak, 98% of the energy dissipation takes place inside the connected fractures, thus demonstrating that this additional peak is due to WIFF within the fractures. That is, the applied compression at the top boundary of the sample induces a strong fluid pressure increase in the quasi-horizontal fracture. This, in turn, generates fluid injection from the horizontal fracture into the vertical one. Therefore, significant fluid flow within the two fractures takes place, thus producing energy dissipation.

Additional simulations allowed us to verify that in presence of fracture connectivity seismic attenuation is sensitive to valuable characteristics of the probed rock, namely permeabilities, lengths, intersection angles and aperture of the fractures, as well as connectivity degree of the fracture network. This indicates that a deeper understanding of this topic will reveal promising perspectives for characterization of fractured rocks.

## REFERENCES

- Biot, M. 1941: General theory of three-dimensional consolidation, *Journal of Applied Physics*, 12, 155-164.
- Brajanovski, M., B. Gurevich & M. Schoenberg 2005: A model for P-wave attenuation and dispersion in a porous medium permeated by aligned fractures, *Geophysical Journal International*, 163, 372-384.
- Rubino, J., L. Guarracino, T. Müller & K. Holliger 2013a: Do seismic waves sense fracture connectivity?, *Geophysical Research Letters*, 40, 692-696.
- Rubino, J., L. Monachesi, T. Müller, L. Guarracino & K. Holliger 2013b: Seismic wave attenuation and dispersion due to wave-induced fluid flow in rocks with strong permeability fluctuations, *Journal of the Acoustical Society of America*, in press.

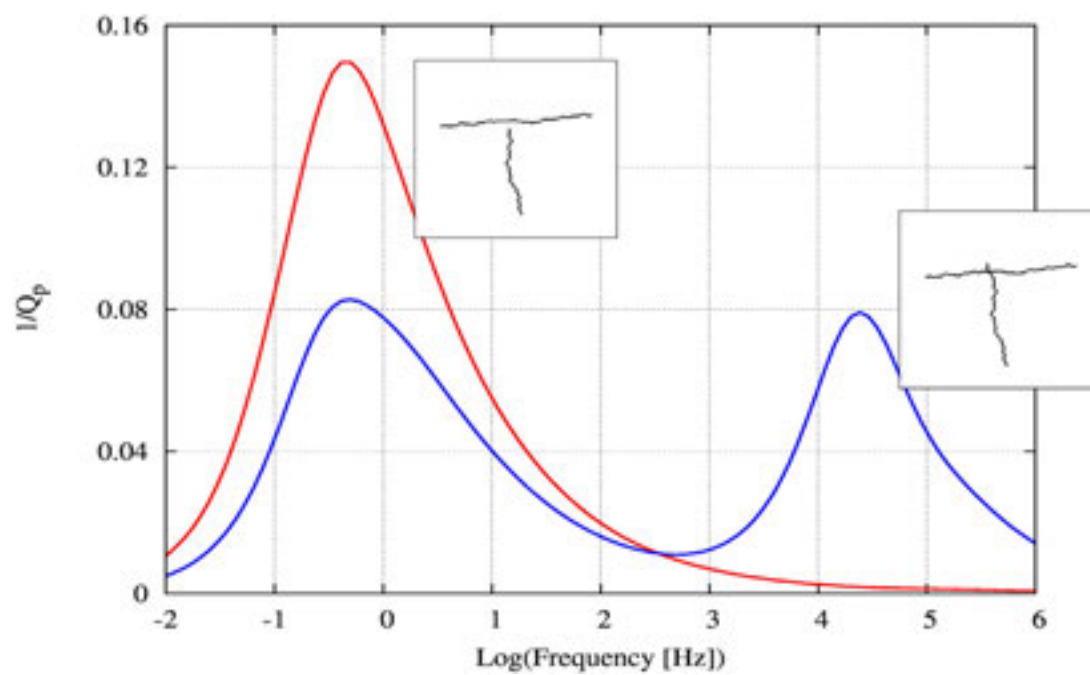


Figure 1. Inverse quality factor as a function of frequency for a rock sample containing two quasi-orthogonal fractures without (red curve) and with (blue curve) intersection.

## P 11.10

# Numerical modeling and laboratory measurements of seismic properties in fractured fluid reservoirs

Pei-Ju Rita Shih<sup>1</sup>, Marcel Frehner<sup>1</sup>

<sup>1</sup> Geological Institute, ETH Zurich, Sonneggstrasse 5, CH-8092 Zurich  
(pei-ju.shih@erdw.ethz.ch, marcel.frehner@erdw.ethz.ch)

Understanding fluid-saturated reservoir rocks is essential for the applications of, for example, CO<sub>2</sub> sequestration, hydrocarbon exploration, or underground nuclear waste disposal. Seismic waves are influenced by the fluids in reservoir rocks, leading to dispersion and frequency-dependent attenuation (Biot, 1962). A reliable rock characterization can be obtained if the effects of fluids filling the pore and fracture space on the seismic response are well understood.

The Krauklis wave is a unique seismic waveform, which is bound to fluid-filled fractures and propagates along fractures. It can resonate and emit seismic signals with a signature frequency. This resonant behavior should lead to a strong frequency dependence, enabling their identification in the coda (Korneev, 2008). The characteristics of Krauklis waves might be one of the keys to reveal fracture-related petrophysical parameters of reservoirs.

Several theoretical studies have demonstrated analytically the dispersion behavior of Krauklis waves in infinitely long and straight fractures (e.g., Korneev, 2008). However, purely analytical methods cannot reveal the realistic fracture geometries or finite-length fractures. Therefore, we combine numerical modeling results with laboratory experiments to visualize fracture-related effects on seismic wave propagation in reservoir rocks. Frehner and Schmalholz (2010) demonstrated that the Krauklis wave can be detected as a converted body wave as a result of scattering at the crack tip. The study also shows that the reflection behavior of the Krauklis wave depends significantly on different crack geometries and different fluids in the crack. For laboratory studies, we simulate similar conditions for a homogenous media (e.g., Plexiglas) as in the numerical experiments. We record the signatures obtained from the propagation of ultrasonic waves along samples with and without a crack, with different crack geometries and different fluids filling the crack. The design of the experiment setup thus allows us to observe and compare the effects of fluids in fractures. The comparison of numerical modeling and preliminary experimental results will be presented.

## REFERENCES

- Biot, M.A. 1962: Mechanics of deformation and acoustic propagation in porous media, *Journal of Applied Physics*, 1482-1498.
- Frehner, M. & Schmalholz, S.M. 2010: Finite-element simulations of Stoneley guided-wave reflection and scattering at the tips of fluid-filled fractures, *Geophysics*, 75, T23-T36.
- Korneev, V. 2008: Slow waves in fractures filled with viscous fluid, *Geophysics*, 73, N1-N7.

## P 11.11

### Seismic attenuation: Laboratory measurements in fluid saturated rocks

Subramaniyan Shankar<sup>1</sup>, Madonna Claudio<sup>1</sup>, Tisato Nicola<sup>1</sup>, Saenger Erik<sup>1</sup>, & Quintal Beatriz<sup>2</sup>

<sup>1</sup> ETH Zurich, Department of Earth Sciences, Sonneggstrasse 5, CH-8092 Zurich

(shankar.subramaniyan@erdw.ethz.ch, claudio.madonna@erdw.ethz.ch, nicola.tisato@erdw.ethz.ch, erik.saenger@erdw.ethz.ch)

<sup>2</sup> University of Lausanne, Applied and Environmental Geophysics Group, Quartier UNIL-Mouline, Géopolis, CH-1015 Lausanne

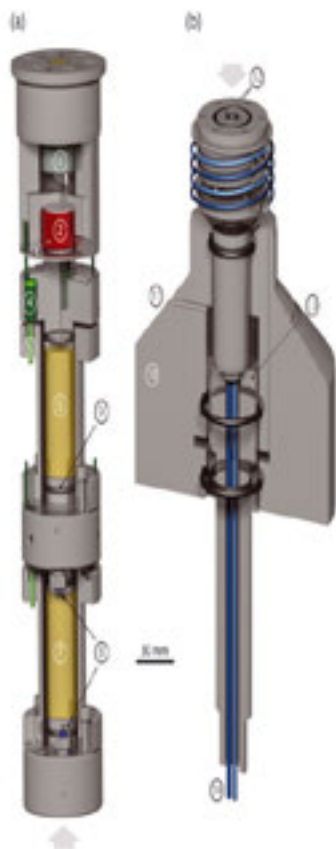
(beatriz.quintal@unil.ch)

Seismic wave attenuation could be used as an indicator of reservoir fluids due to its dependence on rock and fluid properties. Over the past 30 years, many laboratory methodologies to study attenuation in rocks have been employed, such as ultrasonic (MHz), resonant bar (kHz) and quasi-static methods in the low frequency range (0.1-100Hz) (Tisato & Madonna 2012; Madonna & Tisato 2013). Quasi-static methods have gained prominence over time as the frequency range of measurements correspond to that of field seismic data acquired for oil/gas exploration. These quasi-static experiments measure attenuation as the phase shift between the applied stress (sinusoidal) and measured strain. Since the magnitudes of measured phase shifts are quite low ( $Q^{-1} \sim 0.01-0.1$ ) and the amplitudes of strain applied to the rock samples are of the order  $\sim 10^{-6}$  (i.e., similar orders of magnitude to seismic waves), it is challenging. A comparison of such quasi-static setups will be presented to provide an overview of the various possibilities of design and implementation for future setups.

Several theories have been proposed in the process of identifying mechanisms causing frequency dependent attenuation in fluid saturated rocks. Wave-induced fluid flow has surfaced as the dominant mechanism and various models account for it in different ways, such as squirt flow, double porosity and patchy saturation (Pride et al. 2004). Only recently, Tisato & Quintal (2013) verified that patchy saturation can explain the frequency-dependent component of seismic attenuation measured in the laboratory for partially saturated Berea sandstone at room pressure and temperature. However, in general, there is a lack of laboratory data to test the proposed mechanisms. For example, most of the published data are for sandstones. As squirt-flow should be significant only at higher frequencies and sandstones are homogeneous in structure on the mesoscopic scale, it is relatively straightforward to attribute the observed frequency-dependent seismic attenuation to patchy saturation. Carbonates are more complicated in structure and not only patchy saturation, but also double porosity could induce significant frequency-dependent attenuation because of the heterogeneities in the solid matrix. Adam et al. (2009) observed frequency dependence in one among the five fluid saturated carbonates upon which quasi-static experiments were conducted. Currently, attenuation measurements are being carried out on samples drilled from deep carbonate reservoirs. We employ the Seismic Wave Attenuation Module (SWAM, Figure 1, Madonna & Tisato 2013) to measure seismic attenuation in these samples for different saturation degrees (90% and 100% water) and under three different confining pressures (5, 10, and 15 MPa). Preliminary results from these investigations will be discussed.

#### REFERENCES

- Adam, L., Batzle, M., Lewallen, K. T. & van Wijk, K. 2009: Seismic wave attenuation in carbonates. *Journal of Geophysical Research*, doi: 10.1029/2008JB005890.
- Madonna, C. & Tisato, N. 2013: A new seismic wave attenuation module to experimentally measure low-frequency attenuation in extensional mode. *Geophysical Prospecting*, doi: 10.1111/1365-2478.12015.
- Pride, S. R., Berryman, J. G. & Harris, J. M. 2004: Seismic attenuation due to wave-induced flow. *Journal of Geophysical Research*, 109, B01201.
- Tisato, N. & Madonna, C. 2012: Attenuation at low seismic frequencies in partially saturated rocks: Measurements and description of a new apparatus. *Journal of Applied Geophysics*, 86, 44-53.
- Tisato, N., & Quintal, B. 2013: Measurements of seismic attenuation and transient fluid pressure in partially saturated Berea sandstone: evidence of fluid flow on the mesoscopic scale. *Geophysical Journal International*, doi: 10.1093/gji/ggt259.



1) top plug, 2) Piezo Electric Actuator (PZA), 3) bending lamella, 4) LVDT, 5) core of the LVDT 6) reference sample (Al-Zn-Mg-Cu alloy), 7) sample 8) inlet and outlet of the pore pressure system, 9) o'ring, 10) bottom plug, 11) vent 12) inlet and outlet holes for the pore fluid, 13) pressure compensating piston, 14) inlet/outlet pipes for the pore fluid. The big grey arrows designate where part a) is connected to part b).

Figure 1. Sketch of the SWAM (after Madonna & Tisato 2013).

## P 11.12

### How much seismic energy is “stolen” by bubbles?

Tisato Nicola<sup>1</sup>, Quintal Beatriz<sup>2</sup>, and Podladchikov Yuri<sup>2</sup>

<sup>1</sup>ETH Zurich, Zurich, Switzerland. Email: nicola.tisato@erdw.ethz.ch

<sup>2</sup>University of Lausanne, Lausanne, Switzerland.

Wave induced fluid flow causes large attenuation and is governed by diffusion of fluids into a porous media (e.g. White, 1975). Regardless the scale at which the diffusion occurs, the fluid flow is a function of diffusivity [ $\text{m}^2 \text{s}^{-1}$ ] and a pressure gradient [ $\text{Pa m}^{-1}$ ]. Pressure gradient is responsible for the fluid flow. In a similar way Fick's law can be used to model gas diffusion in liquids.

Micro bubbles (e.g. 20  $\mu\text{m}$  in diameter) might be present in the pore space of rocks (Madonna et al., 2013). In an almost fully saturated porous media the strain caused by a seismic wave increases the fluid pressure and preferentially deform these bubbles. Assuming equilibrium between gas and liquid phase prior to the seismic wave propagation, variation of fluid pressure will change that. In fact, by increasing and decreasing the fluid pressure, the seismic wave will cause gas dissolution and exsolution, respectively.

Utilizing a kinetic model of gas bubble dissolution, we were able to explain attenuation measurements at tele-seismic to seismic frequencies which cannot be explained with wave induced fluid flow theories (i.e. squirt flow or patchy saturation) (Figure 1; Tisato, 2013).

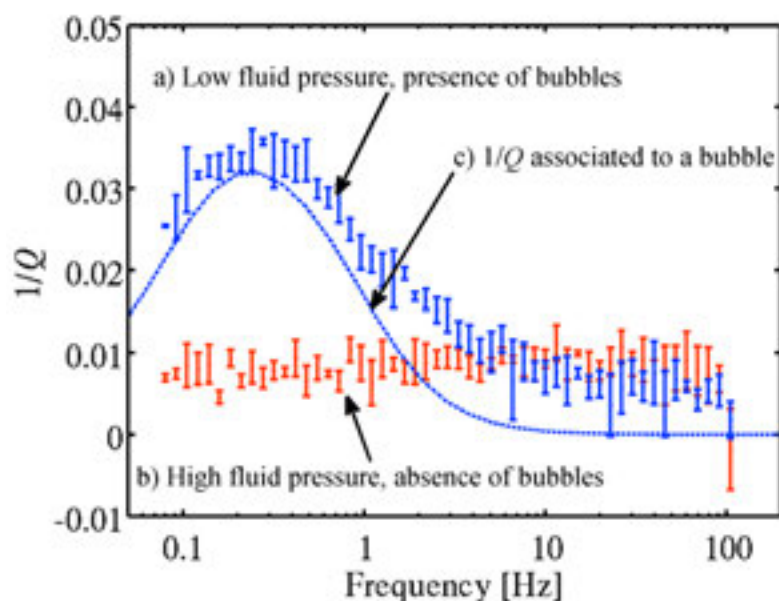


Figure 1. a) Attenuation ( $1/Q$ ) for a  $\sim 100\%$  water-glycerin saturated sample. State of stress was set to promote the formation of bubbles in the pores. b) Attenuation ( $1/Q$ ) for a  $\sim 100\%$  water-glycerin saturated sample. State of stress was set to promote the dissolution of gas in the liquid. c) Example of attenuation ( $1/Q$ ) associated to a 20 mm diameter nitrogen bubble surrounded by water stressed with a sinusoidal pressure of 1 kPa.

We believe that the present contribution is of major impact for geophysics because it reports a new attenuation mechanism for partially saturated rocks operating at seismic and tele-seismic frequencies (Figure 2).

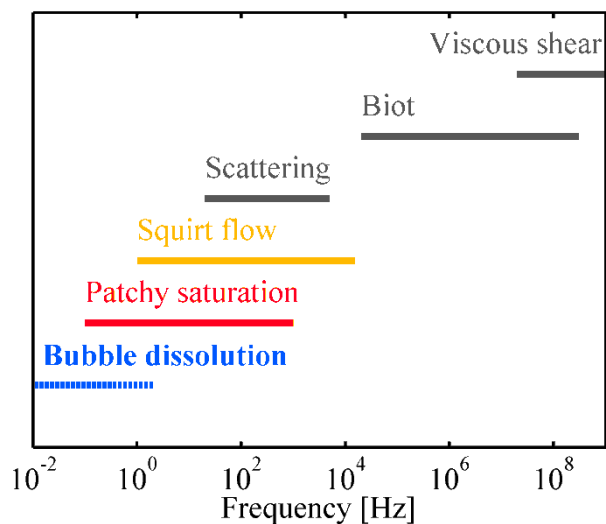


Figure 2. Attenuation mechanisms at different frequency ranges from Mavko et al. (2009) modified to include the new mechanism here proposed: Bubble Dissolution. Frequency limits for the mechanism related to Bubble Dissolution have not been yet clearly defined.

## REFERENCES

- Madonna, C., B. Quintal, M. Frehner, B. S. G. Almqvist, N. Tisato, M. Pistone, F. Marone, and E. H. Saenger 2013: Synchrotron-based X-ray tomographic microscopy for rock physics investigations, *Geophysics*, 78(1), D53–D64, doi:10.1190/geo2012-0113.1.
- Mavko, G., T. Mukerji, and J. Dvorkin 2009: *The rock physics handbook: tools for seismic analysis of porous media*, 2nd ed., Cambridge University Press.
- Tisato, N. 2013: *Experimental characterization of reservoir rocks and geotechnical materials. Low frequency attenuation, ultrasonic velocities and local pore pressure effects*, PhD Thesis (Diss. Nr. 21106) ETH Zurich, Switzerland.
- White, J. E. 1975: Computed seismic speeds and attenuation in rocks with partial gas saturation, *Geophysics*, 40(2), 224–232, doi:10.1190/1.1440520.

## P 11.13

### Some new observations on dynamically induced fault slip

Wei Wu<sup>1</sup>

<sup>1</sup> *Ecole Polytechnique Fédérale de Lausanne (EPFL), School of Architecture, Civil and Environmental Engineering, Laboratory of Rock Mechanics (LMR), CH-1015 Lausanne (wei.wu@epfl.ch)*

A series of dynamic-induced direct-shear tests is conducted on a simulated granular fault zone. The direct-shear configuration consists of an incident norite plate (1000 × 120 × 30 mm) and a transverse norite plate (500 × 80 × 30 mm). A quartz sand layer (80 × 30 × 2 mm) is sandwiched between the incident and transverse plates to simulate a granular fault zone. A dynamic loading system containing two identical parallel compressed springs instantaneously launches a striker norite plate (100 × 120 × 30 mm) to impact the front end of the incident plate and to induce an incident P-wave (a half-wavelength of 750 mm). The P-wave propagates in the incident plate and causes the fault slip. The dynamically induced fault slip is designed to be solely induced by the P-wave before wave reflection at the plate end. It is found that the dynamic triggering induce non-uniform shear stress distribution along the fault zone. There is a shear stress at the trailing edge, which controls the fault slip, and a rebound stress at the leading edge, which is caused by a small torque (Rubinstein et al., 2004). The fault slip is triggered when the maximum shear stress reaches a critical value at the trailing edge and is accompanied by shear stress drop. By comparing with the statically induced fault slip, which is induced by a servo-controlled static loading system, it is observed that:

- The statically induced fault slip is unrecoverable and includes a main slip and a few short slips before and after the main slip, while the dynamically induced fault slip can be partially recovered after the P-wave and consists of a few unrecovered slips.
- Fault strengthening takes a long time owing to the static compaction of fault gouges (Marone, 1998). However, seismic waves successively induce fault slip and restrict fault self-healing.
- Seismic wave radiated from fault slip can reduce frictional resistance of a fault zone, which depends on local released strain energy.
- The duration of the dynamically induced fault slip is a few microseconds, while the duration of the statically induced fault slip may last from a few seconds to many years.

#### REFERENCES

- Marone, C. 1998: The effect of loading rate on quasi-static friction and the rate of fault healing during the earthquake cycle, *Nature*, 391, 69-72.
- Rubinstein, S.M., Cohen, C. & Fineburg, J. 2004: Detachment fronts and the onset of dynamic friction, *Nature*, 430, 1005-1009.

## P 11.14

# Effect of network density and geometric distribution on non-linear kinematic source inversion models

Youbing Zhang; Luis Dalguer; Seok Goo Song; John Clinton

*Swiss Seismological Services. ETH Zurich, Switzerland*

Detailed source imaging of the spatial and temporal slip distribution of earthquakes is a main research goal for seismology. In this study we investigate how the number and geometrical distribution of seismic stations affect finite kinematic source inversion results by inverting ground motions derived from a known synthetic dynamic earthquake rupture model, which is governed by the slip weakening friction law with heterogeneous stress distribution.

The target dynamic rupture model is a buried strike-slip event (Mw 6.5) in a layered half space (Dalguer & Mai, 2011) with broadband synthetic ground motions created at 168 near-field stations. A dynamic consistent regularized Yoffe function (Tinti, et al. 2005) was applied as a single window slip velocity function. And the Tikhonov regularization was used to smooth final slip. In the inversion, we modeled low frequency (under 1Hz) waveforms using a genetic algorithm in a Bayesian framework (Moneli et al. 2008) to retrieve peak slip velocity, rupture time, and rise time of the source. Three station network geometry cases were tested: (a) single station, in which we inverted 3 component waveforms from a single station varying azimuth and epicentral distance; (b) multi-station configurations with similar numbers of stations all at similar distances from, but regularly spaced around the fault; (c) irregular multi-station configurations using different numbers of stations. For analysis, waveform misfits are calculated using all 168 stations.

Our preliminary results show: 1) single station tests suggest that it may be possible to obtain a relatively good source model even using one station, with a waveform misfit comparable to that obtained with the best source model. The best single station performance occurs with stations in which amplitude ratios between the three components are not large, indicating that P and S waves are all present. We infer that both body wave radiation pattern and distance play an important role in the selection of optimal station. 2) Multi-station tests indicate irregular distribution of stations with different azimuths and distances around the fault provides the best source models. The minimum waveform misfit is obtained using the all-168 stations, but source model is not significantly improved by using denser network. It suggests the best source model is not necessarily derived from the model with minimum waveform misfit. 3) Number of stations affects the estimated source image, but a surprisingly small number of well-spaced stations appear sufficient to obtain acceptable solutions in our study.



# 12. Shale-Gas, CO<sub>2</sub> Storage and Deep Geothermal Energy

Paul Bossart, Lyesse Laloui, Larryn Diamond

*Swiss Geothermal Society,  
Swiss Association of Energy Geoscientists (SASEG)*

## TALKS:

- 12.1 Abdelfettah Y., Schill E., Kuhn P.: Delimitation and characterization of geothermally relevant Permo-Carboniferous graben in the Swiss Crystalline basement
- 12.2 Alt-Epping P., Diamond L. W.: Numerical simulation of fluid-rock interaction upon CO<sub>2</sub> injection into the Muschelkalk aquifer in N-Switzerland
- 12.3 Aschwanden L., Diamond L.D., Ramseyer K., Mazurek M., Fallick T., Donnelly T.: Development of porosity in the Upper Muschelkalk carbonate aquifer, NE-Switzerland: relevance for geothermal energy and gas storage
- 12.4 Badoux V., Mégel T.: Cartographic representation of a geomechanical criterion for site-screening of sub-surface projects in the energy sector
- 12.5 Burri P., keynote speaker: Unconventional Hydrocarbons - The Revolution in Exploration (Chances and Risks) (Keynote)
- 12.6 Diamond L. W., Alt-Epping, P.: Simulation of water-rock interaction and porosity evolution in a granitoid-hosted, enhanced geothermal system (Basel, Switzerland)
- 12.7 Fabbri S., Zappone A., Madonna C., Mazzotti M.: The effects of CO<sub>2</sub> injection in Muschelkalk: first laboratory results
- 12.8 Gawenda P.: Unconventional plays along the East European Craton – a review of E & P activities in Poland
- 12.9 Herwegh M., Baumberger R., Wehrens P., Schubert R., Mock S., Berger A., Mäder U., Spillmann T.: Internal structure of the Aar Massif: What can we learn in terms of exploration for deep geothermal energy?
- 12.10 Li C., Laloui L.: Hydromechanical coupling in carbon dioxide injection into a deep aquifer
- 12.11 Manceau Jc., Claret F., Tremosa J., Audigane P., Nussbaum C.: Field experiment in an underground rock laboratory to study the well integrity in the context of CO<sub>2</sub> geological storage
- 12.12 Moscariello A., Mondino F., Vinard P.: The geothermal site of Eclépens: new geological insights from an integrated seismic and satellite study.
- 12.13 Paolacci S., Gorin G., Moscariello A.: The subsurface geology of the Western Swiss Plateau and its French extension: state of the art and implications for geo-resources exploration.
- 12.14 Schilke S., Probert T., Bradford I., Özbek A., Robertsson J. O. A.: Use of surface patches for hydraulic fracture monitoring
- 12.15 Tomin P., Lunati I.: Multiphysics methods: a link between pore-scale and Darcy-scale models
- 12.16 Wyss R.: Deep geothermal Energy in Switzerland – actual developments and perspectives for the future (Keynote)

## POSTERS:

- P 12.1 Jain C., Clauser C., Vogt C.: Optimized layout of engineered geothermal systems and potential in Germany
- P 12.2 Räss L., Omlin S., Podladchikov Y. Y., Simon N. S. C.: Solving three-dimensional non-linearly coupled hydro-mechanical two-phase flow on GPUs
- P 12.3 Soma L., Ambrosi C., Bernoulli D., Bonini L., Pera S. & Seno S.: Geochemical and structural data for the evaluation of the geothermal potential

## 12.1

# Delimitation and characterization of geothermally relevant Permo-Carboniferous graben in the Swiss Crystalline basement

Abdelfettah Yassine<sup>1</sup>, Schill Eva<sup>2,3</sup> & Kuhn Pascal<sup>4</sup>

<sup>1</sup>Centre of hydrogeology and geothermics – CHYN, University of Neuchâtel, Emile-Argand 11 - CH-2000 (yassine.abdelfettah@unine.ch)

<sup>2</sup>EEIG “Heat Mining”, Route de Soultz - BP 40038, F-67250 Kutzenhausen, France

<sup>3</sup>Steinbeis-Transfer Centre “Geoenergy and Reservoir Technology” D-79807 Lottstetten-Nack, Germany

<sup>4</sup>Eidgenössisches Departement für Verteidigung, Bevölkerungsschutz und Sport VBS armasuisse Bundesamt für Landestopografie swisstopo Landesgeologie Seftigenstrasse 264 CH-3084 Wabern

We have investigated the application of 3D geology for gravity forward modeling as well as the application of Butterworth filters of different wavelength. Real application was conducted in the northern part of Switzerland under the Molasse basin in order to systematically assess the potential of the gravity data to detect and characterize the horizontal and vertical extension of the Permo-Carboniferous (PC) troughs in the Crystalline basement.

Synthetic gravity data sets were generated for these geological models using basement’s homogeneous density. Gravity forward modeling is carried out using developed and unpublished finite element code. The finite element mesh allows approaching the geological geometry using tetrahedrons shape. To simulate the real conditions, the gravity stations are located on the real topography. After computing a gravity effect of the 3D geological model, we get a complete Bouguer anomaly. Since, and as expected from the geology, the Bouguer anomaly is strongly dominated by the gravity effect of the Molasse sediments, where the slightly bended Mesozoic sediments are inclined by about 2-5 ° towards the Alps and the Tertiary filling of the molasses basin is deepening following this geometry. A code using Butterworth filter was developed and so applied on the computed anomaly as well as on the observed Bouguer anomaly to eliminate this regional trend, and characterize a probable presence of PC grabens.

The result reveals high potential in the delimitation of the PC-troughs by the combination of the seismic and gravity interpretation. Assuming a similar geometry for these graben structures, gravity data post-processing traces these structures at different depth using a Butterworth filter with different wavelength, in order to calculate a residual gravity anomalies. Filtered Bouguer anomaly with different wavelengths is an essential tool to detect and characterize the horizontal and vertical extensions of the PC-troughs. The different wavelengths provide insight into different vertical levels of the trough and thus, allow describing 3D geometry of the graben structures in depth and give us a pseudo-tomography image.

Finally, the application of the filters to real measurements reveals the distribution of the PC-grabens in the northern west part of Switzerland. The results is an agreement with the informations provided in different deep boreholes exit in the studied area. Roughly speaking, the negative residual anomalies agree with the PC-trough whereas the lack of these end, agree generally with a positive residual anomalies. The geophysical and geological interpretations allow also to confirm the geological concept of intracontinental alternation of transpression and transtension resulting in wrench-faulting, which was also observed in analogue shear faulting dual-layer models, where a complex pull-apart basins as observed in the northern studied area, southern Basel.

## 12.2

# Numerical simulation of fluid-rock interaction upon CO<sub>2</sub> injection into the Muschelkalk aquifer in N-Switzerland

Alt-Epping Peter<sup>1</sup>, Diamond Larryn W.<sup>1</sup>

<sup>1</sup>Rock–Water Interaction Group, Institute of Geological Sciences, University of Bern, Baltzerstrasse 3, CH-3012 Bern, Switzerland (alt-epping@geo.unibe.ch)

A recent study (Chevalier et al., 2010) has identified several deep saline aquifers in the Swiss Molasse Basin, which may potentially be useful as reservoirs to store industrial CO<sub>2</sub>. Of these aquifers, the Trigonodus Dolomite of the Upper Muschelkalk appears to be the most promising. To further evaluate its potential of storage capacity, injectivity and the long-term isolation performance, predictive numerical simulations constrained by experimental and observational data have been carried out. These simulations assess the implications of the dynamics of the CO<sub>2</sub> plume and the ensuing fluid-fluid and fluid-rock reactions for the safe, long-term storage of CO<sub>2</sub> in the aquifer.

The numerical simulation of processes during and after the injection of CO<sub>2</sub> into deep saline aquifers is a challenging task because of the complexity and the coupled nature of the physical and chemical phenomena. During and shortly after injection, the immiscible CO<sub>2</sub> displaces the brine in a drainage-like process and migrates laterally away from the injection wells and to the top of the injection aquifer due to buoyancy forces. Once injection stops, CO<sub>2</sub> continues to migrate upward and displace water at the leading edge of the plume, while at the trailing edge water displaces CO<sub>2</sub> in an imbibition-like process. A trail of residual, immobile CO<sub>2</sub> is left behind the plume. The residual CO<sub>2</sub> and the CO<sub>2</sub> at the plume/brine interface slowly dissolves into the formation water, altering its chemical composition and density. Over longer time scales the fluid may then be involved in reactions with the rock and under favourable conditions dissolved CO<sub>2</sub> may precipitate and be permanently trapped as carbonate minerals.

Critical aquifer properties and their spatial variability are known only from core samples but for realistic simulations these properties need to be specified for regional-scale domains. The most important of these properties are the porosity and the permeability of the rock. The porosity of the rock determines the overall CO<sub>2</sub> storage capacity and it affects the permeability of the reservoir rock. The permeability controls the injectivity of CO<sub>2</sub>, the dynamics of the CO<sub>2</sub> plume and its size and shape (Fig. 1). The porosity/permeability distribution determines the contact area between the plume and the brine and thus the dissolution rate of CO<sub>2</sub> into the aqueous phase. Laboratory measurements on core samples of the Trigonodus Dolomite indicate a strongly heterogeneous distribution of porosity (values in the range of 3 - 24%) and permeability (1.6e-18 m<sup>2</sup> – 5.6e-15 m<sup>2</sup>).

Preliminary simulations suggest that in carbonate-hosted aquifers such as the Trigonodus Dolomite, CO<sub>2</sub> can be trapped as a residual phase in the pore space, by dissolution into the aqueous phase or by the physical containment of the CO<sub>2</sub> plume in structural traps such as anticlines. Unlike in silicate aquifers, the storage in carbonate minerals is not possible. This emphasizes the need to ensure the long-term integrity of the seal to prevent the leakage of CO<sub>2</sub> into overlying freshwater aquifers. Potential leakage pathways include existing faults/fractures or those created as a consequence of pressure build-up in the aquifer during injection, concrete-plugged abandoned wells or the corrosion of the seal due to the influx of CO<sub>2</sub> and acidity from the underlying aquifer.

We are conducting numerical simulations with the code PFLOTRAN (Hammond & Lichtner, 2010 and Hammond et al. 2011). The code permits fully coupled simulations involving multiphase fluid flow, solute transport, heat transport and chemical reactions. We present preliminary results of numerical simulations carried out for domains with heterogeneous, correlated porosity/permeability fields (Fig. 1) and for smaller-scale, simplified systems at high spatial resolution (Fig.2) to address some of the above issues.

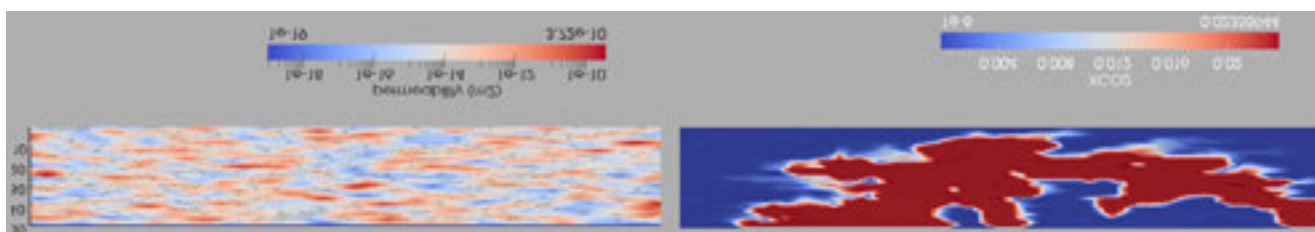


Figure 1: A generic (and extreme) example of how the extent and shape of the CO<sub>2</sub> plume is controlled by the permeability distribution. Correlated random permeability field and the CO<sub>2</sub> plume after 25 years. Total injected CO<sub>2</sub> is 315 t.

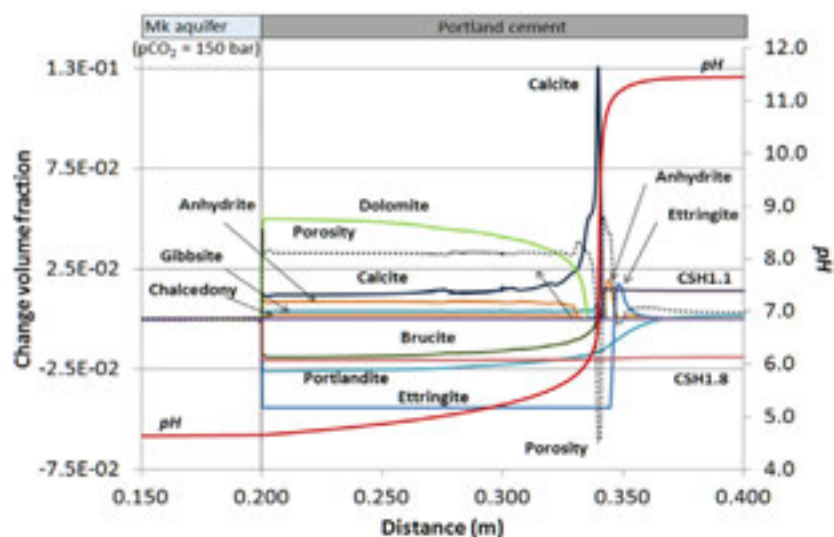


Figure 2: Reactions at the contact between the aquifer and a cement plug in a well. High  $p\text{CO}_2$  conditions in the aquifer induce carbonatization and mechanical weakening (porosity increase) of the cement. Shown are mineral volume changes after 25 years (<0: dissolution, >0 precipitation) and pH.

#### REFERENCES

- Chevalier, G., Diamond, L. W. & Leu, W., 2010: Potential for deep geological sequestration of  $\text{CO}_2$  in Switzerland: a first appraisal. *Swiss Journal of Geosciences* 103 (3)
- Hammond GE, PC Lichtner, and ML Rockhold. 2011. "Stochastic Simulation of Uranium Migration at the Hanford 300 Area." *Journal of Contaminant Hydrology* 120-121:115-128
- Hammond GE, and PC Lichtner. 2010. "Field-Scale Model for the Natural Attenuation of Uranium at the Hanford 300 Area using High Performance Computing." *Water Resources Research* 46:Paper No. W09527

## 12.3

### Development of porosity in the Upper Muschelkalk carbonate aquifer, NE-Switzerland: relevance for geothermal energy and gas storage

Aschwanden Lukas<sup>1</sup>, Diamond Larryn William<sup>1</sup>, Ramseyer Karl<sup>1</sup>, Mazurek Martin<sup>1</sup>, Fallick Tony<sup>2</sup>, Donnelly Terry<sup>2</sup>

<sup>1</sup> University of Bern, Institute of Geological Sciences, Baltzerstrasse 1+3, CH-3012 Bern (l.aschwanden@students.unibe.ch)

<sup>2</sup> SUERC, Scottish Enterprise Technology Park, Rankine Avenue, G75 0QF East Kilbride

In the Swiss Molasse Basin, deeply buried Middle Triassic carbonate rocks of the Upper Muschelkalk aquifer show potential for geothermal energy exploitation and for geological storage of gas – whether permanent storage of waste CO<sub>2</sub> or seasonal storage of imported methane (Chevalier et al., 2010). Particularly the Trigonodus Dolomite, the top of the Upper Muschelkalk aquifer, regionally shows elevated porosities and permeabilities. However, owing to the low spatial density of wells with available core in the region of interest, there is currently only a rudimentary understanding of the 3D distribution of porosity and permeability throughout the basin. One way to better characterize the reservoir is to develop a genetic understanding of how porosity and permeability developed over time. This understanding could then be used to interpolate the distribution and magnitudes of the rock properties between boreholes and to extrapolate their values outside the region sampled by wells.

This study takes a first step in this direction by focusing on the genesis of porosity in the Trigonodus Dolomite at one specific drill site, Benken, which is situated 5 km south of Schaffhausen at the northeastern margin of the Swiss Molasse Basin. The investigated drill core was extracted by the Swiss National Cooperative for the Disposal of Radioactive Waste (Nagra). This study presents a detailed reconstruction of the formation, diagenesis, burial history and water-rock interactions of the Trigonodus Dolomite at Benken with emphasis on processes that generated or clogged porosity. The reconstruction is based on new petrographic observations by standard optical, UV-fluorescence and scanning-electron microscopy, and on analyses of stable and radiogenic isotopes (i.e.  $\delta D$ ,  $\delta^{13}C$ ,  $\delta^{18}O$ ,  $\delta^{34}S$  and  $^{87}Sr/^{86}Sr$ ) in bulk samples of rock-forming and pore-filling minerals. Literature data on fluid inclusions and on the regional geological and hydrological evolution are integrated into the interpretations. No new insight is provided on porosity provided by fracture networks, as no evidence for these was found in the drill core.

The results show that the present-day 2-22% bulk porosity (Chevalier et al., 2010) in the Trigonodus Dolomite is the combination of (1) micropores (< 10  $\mu m$  diam.) formed during dolomitization of the precursor calcareous sediment, (2) intergrain pores formed during its deposition, (3) moldic pores formed by the selective dissolution of bivalve shell fragments and (4) cavernous pores formed by the dissolution of anhydrite nodules. The formation of intergrain pores is closely associated with the deposition of shore-parallel oolite shoal bodies in the in the back-bank environment of the Upper Muschelkalk carbonate ramp. Following deposition of the initially calcareous sediment, eogenetic dolomitization affected the still unlithified sediment. The dolomitization process is characterized by three different stages. The earliest corresponds to an evaporation-related, replacement dolomitization entailing formation of microporosity between the individual dolomite crystals, the selective dissolution of bivalve shell fragments (formation of moldic porosity) and the precipitation of anhydrite as nodules. The two later stages correspond to burial related precipitation of primary dolomite cement in the available pore space, thereby reducing porosity. The latest stages of dolomite cementation are at least partially contemporaneous with the early stages of dissolution of the anhydrite nodules and thus the formation of cavernous porosity. The dissolution of the anhydrite nodules was accompanied by the replacement of the anhydrite by quartz, which co-precipitated with pyrite and probably sphalerite from diagenetically modified pore waters. Most likely the dissolution was caused by an event of pervasive infiltration of highly saline water into the Mesozoic sediment stack of the Zürcher Weinland. Neither the timing of infiltration nor the origin of the brine is exactly known but the appearance of primary, high-salinity fluid inclusions in the Dogger  $\beta$  limits its maximum age to late Dogger/Malm (Bläsi et al., 2002), whereas its minimum age is the Eocene. Later pore space reduction by the precipitation of pore-filling kaolinite and calcite is related to the Paleocene–late Neogene doming of the Schwarzwald area and associated infiltration of meteoric water into crystalline rocks, which recharged into the Upper Muschelkalk aquifer. The exact timing of mineral formation cannot be determined but it must have occurred before the recent ground water infiltrated the rock during the last glacial period at around 12–14 ka.

This study shows that the porosity of the Trigonodus Dolomite at Benken is highly influenced by the depositional environment and by early diagenetic processes. It has been shown that the volumetrically dominant cavernous porosity formed before the late Neogene establishment of the current hydrogeological system at Benken. Consequently, there is presently no reason to rule out the presence of similar porosity in the central and southern parts of the Swiss Molasse Basin. In contrast, porosity reduction by precipitation of pore-filling calcite and kaolinite was clearly related to the doming of the Schwarzwald area and to the establishment of the Recent hydrogeological system. Therefore, these pore-filling minerals are likely restricted to the northern margin of the basin. Overall, these findings are a positive indication for the potential of the Trigonodus Dolomite aquifer in other parts of the basin for geothermal energy and gas storage.

## REFERENCES

- Bläsi, H.R., Ramseyer, K., Haas, H. und Matter, A., 2002: Die Paläofluid-Entwicklung in mesozoischen Formationen der Bohrungen Benken, Weiach und Siblingen aufgrund von Porenraum-, Ader- und Drusen-Mineralen. Nagra Interner Bericht. Nagra, Wettingen, unveröffentlicht.
- Chevalier, G., Diamond, L. W. & Leu, W., 2010: Potential for deep geological sequestration of CO<sub>2</sub> in Switzerland: a first appraisal. *Swiss Journal of Geosciences*, 103 (3), 427-455.

## 12.4

# Cartographic representation of a geomechanical criterion for site-screening of sub-surface projects in the energy sector

BADOUX Vincent<sup>1</sup> and MEGEL Thomas<sup>1</sup>,

<sup>1</sup> GEOWATT AG, Dohlenweg 28, CH-8006 Zürich ([badoux@geowatt.ch](mailto:badoux@geowatt.ch))

The knowledge of the geomechanical behaviour of the deep underground is of prior importance for sub-surface projects related to the energy sector (shale-gas, CO<sub>2</sub> storage and EGS or hydrothermal projects,...). Experience from past and present projects has shown that a modification of the stress conditions in the reservoir could induce seismicity. The understanding of the geomechanical conditions of the underground should be addressed in an early phase of any sub-surface project in order to reduce collateral risk in a later phase of the project such as induced seismicity or groundwater pollution, for instance.

A new methodology is presented here to allow using a criterion derived from the classical geomechanical theory for site screening of sub-surface project. The proposed methodology consists in a cartographic representation of this criterion at the depth of a target horizon. Depending on the project, the target horizon could be a geological layer or an isotherm surface. The resulting map could then be used for site-screening of sub-surface projects complementary to other site screening criteria. A generic example of the cartographic representation of the geomechanical criterion is presented in Figure 2.

The geomechanical criterion is derived from the classical Mohr-Coulomb rock-failure approach, which allows estimating the additional fluid pressure required in the reservoir to reach the failure. Prerequisite is the knowledge of the stress-field magnitudes, the geomechanical properties of the rocks and the depth of the target horizons (Figure 1). The resulting geomechanical criterion in MPa is presented in Figure 2.

For reservoirs where the productivity is known to be naturally good enough to make the project economically viable (e.g. hydrothermal projects), no hydraulic stimulation is required. The site of such projects should thus be located in areas where the geomechanical criterion is high. This would reduce the risk of induced seismicity while testing the well or while reinjecting the water in the reservoir during the exploitation phase. In contrary, for reservoirs where the natural productivity is expected to be too low to make the project economically viable, engineering techniques are then required to increase artificially the reservoir productivity (EGS or petrothermal projects). The site of these projects would thus be located in areas where the geomechanical criterion is low enough to make the engineering techniques applicable (over-pressure reachable by normal injection pumps). The map could also be used to delineate areas where the stress-field is subcritical.

The presented methodology has been developed using generic case datasets. The methodology is ready to be applied with real datasets as an additional criterion for site selection of sub-surface projects in the energy sector.

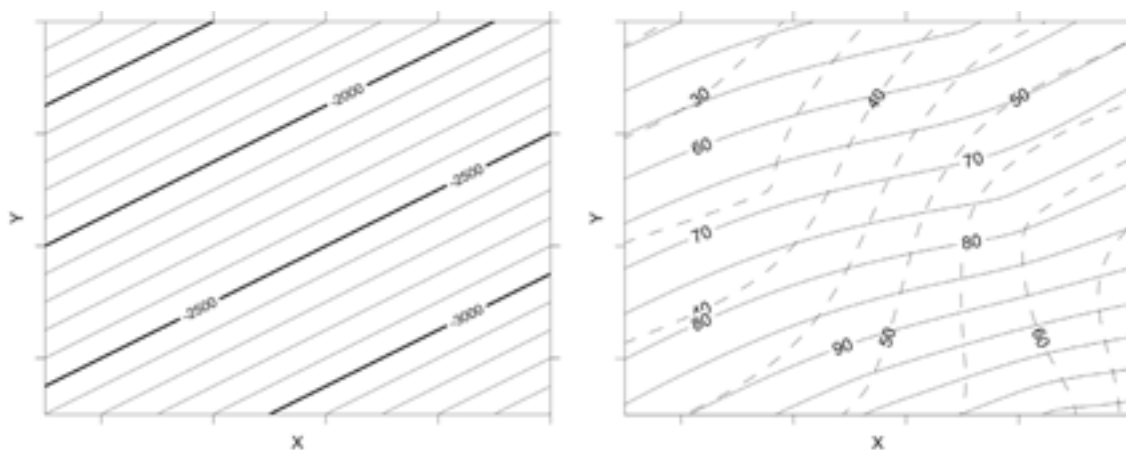


Figure 1. (left) Depth of the target horizon (m BGL) and (right) principal stress field components in MPa along the target horizon (S1 in plain lines; S3 in dashed lines).

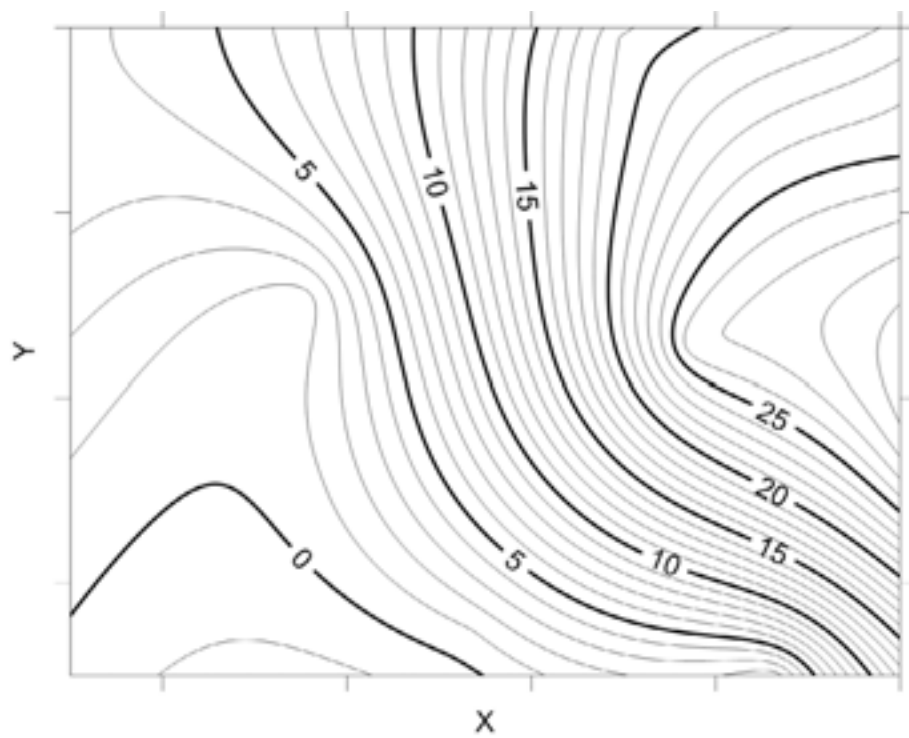


Figure 2. Cartographic representation of the geomechanical criteria (MPa) along a target horizon.

## 12.5

# Unconventional Hydrocarbons - The Revolution in Exploration (Chances and Risks)

Burri Peter

*Swiss Association of Energy Geoscientists, SASEG*

Contrary to common belief the recent, dramatic development in the unconventional hydrocarbon exploration is not primarily a question of operational technology but has its roots much more in revolutionary new insights into the geological and geochemical aspects of hydrocarbon generation, migration and accumulation. Key new insights are: that probably the larger part of the generated hydrocarbons remain in the source rocks and that the porosity of the source rocks is created by the hydrocarbon generation itself. The latter is the explanation for the phenomenon that even nano-porosity can be economically produced, something considered impossible only a few years ago.

The methods of hydraulic fracturing and horizontal drilling are routine technologies that have been used in the industry safely for many decades. Nevertheless unconventional hydrocarbon production has led in the US locally to unacceptable cases of water and surface pollution. This is mainly due to human error, poor execution of wells and unprofessional operating practices. The methods have, however, evolved very considerably. Best practice examples show that safe and environmentally responsible operations (through cluster drilling, recycling of fluids and the use of only non-toxic additives) are today not only possible but also economic.

Unconventional gas has fundamentally changed the energy outlook of the world, and the scenarios that were used until the last decade have no longer any validity. The very large new gas reserves give the world the possibility to replace coal, the fastest growing and by far dirtiest fossil energy and partially diesel and can thus help to significantly curtail the output of CO<sub>2</sub> and of air pollutants. In this role natural gas can provide an ideal bridge to a predominantly renewable energy future.

## 12.6

# Simulation of water-rock interaction and porosity evolution in a granitoid-hosted, enhanced geothermal system (Basel, Switzerland)

Diamond Larryn W.<sup>1</sup>, Alt-Epping, Peter<sup>1</sup>

<sup>1</sup>Rock–Water Interaction Group, Institute of Geological Sciences, University of Bern, Baltzerstrasse 3, CH-3012 Bern, Switzerland (diamond@geo.unibe.ch)

From 2003 to 2006 a 5 km well was drilled into basement granitoids below the city of Basel as a step towards establishing a geothermal doublet circulation system to produce electricity and space heating. To enhance the permeability of the granitoids, river water was injected into the base of the well. Unfortunately, this hydraulic stimulation induced seismic events strong enough to be felt at the surface, leading to the project being permanently abandoned. Nevertheless, there is still interest in Switzerland to pursue this approach to geothermal energy exploitation. To aid planning of future projects, the present study uses numerical simulations based on the specifications of the Basel project to address some of the open geochemical questions associated with such deep enhanced geothermal systems (EGS).

The important geochemical issues regarding the sustainability of EGS are (1) whether mineral precipitation due to water–rock reactions will eventually lead to clogging of flow paths in the reservoir, wells and surface installations and thereby reduce or even completely block fluid throughput; and (2) whether the well casing will be significantly corroded by the production fluid. Using the computer code FLOTRAN (Hammond et al., 2011), we have constructed a reactive transport model that allows the main chemical reactions to be predicted and the resulting evolution of porosity to be tracked over the expected 30-year operational lifetime of the system.

The simulations show that injection of surface water to stimulate fracture permeability in the monzogranite reservoir at 190 °C and 5000 m depth induces redox reactions between the oxidized surface water and the reduced wall rock. Although new calcite, chlorite, hematite and other minerals precipitate near the injection well, their volumes are low and more than compensated by those of the dissolving wall-rock minerals. Thus, during stimulation, reduction of injectivity by mineral precipitation is unlikely.

During the simulated long-term, closed-system operation of the system (Fig. 1), the main mineral reactions are the hydration and albitization of plagioclase, the alteration of hornblende to an assemblage of smectites and chlorites and of primary K-feldspar to muscovite and microcline. Within a closed-system doublet, the composition of the circulated fluid changes only slightly during its repeated passage through the reservoir, as the wall rock essentially undergoes isochemical recrystallization. Even after 30 years of circulation, the calculations show that porosity is reduced by only ~0.2%, well below the expected fracture porosity induced by stimulation. This result suggests that permeability reduction owing to water–rock interaction is unlikely to jeopardize the long-term operation of deep, granitoid-hosted EGS systems.

A peculiarity at Basel is the presence of anhydrite as fracture coatings at ~5000 m depth. Simulated exposure of the circulating fluid to anhydrite induces a stronger redox disequilibrium in the reservoir, driving dissolution of ferrous minerals and precipitation of ferric smectites, hematite and pyrite. However, even in this scenario the porosity reduction is at most 0.5%, a value which is unproblematic for sustainable fluid circulation through the reservoir.

Owing to the low ligand content of the circulating fluid in the closed-system doublet, mass transfer and scaling in the wells and surface installations is predicted to be very limited. While this closed-system simulation represents an interesting end-member case, in reality the inevitable loss of water at depth would require the circulation to be periodically topped-up with fresh river water. This could result in slightly higher levels of scaling. Assuming kinetic inhibition of quartz and chalcedony precipitation (as observed in comparable natural geothermal systems), the model shows that scaling due to precipitation of amorphous silica can be avoided completely by keeping the reinjection temperature of the fluid above 58 °C.

## REFERENCES

Hammond GE, PC Lichtner, and ML Rockhold. 2011. “Stochastic Simulation of Uranium Migration at the Hanford 300 Area.” *Journal of Contaminant Hydrology* 120-121:115-128

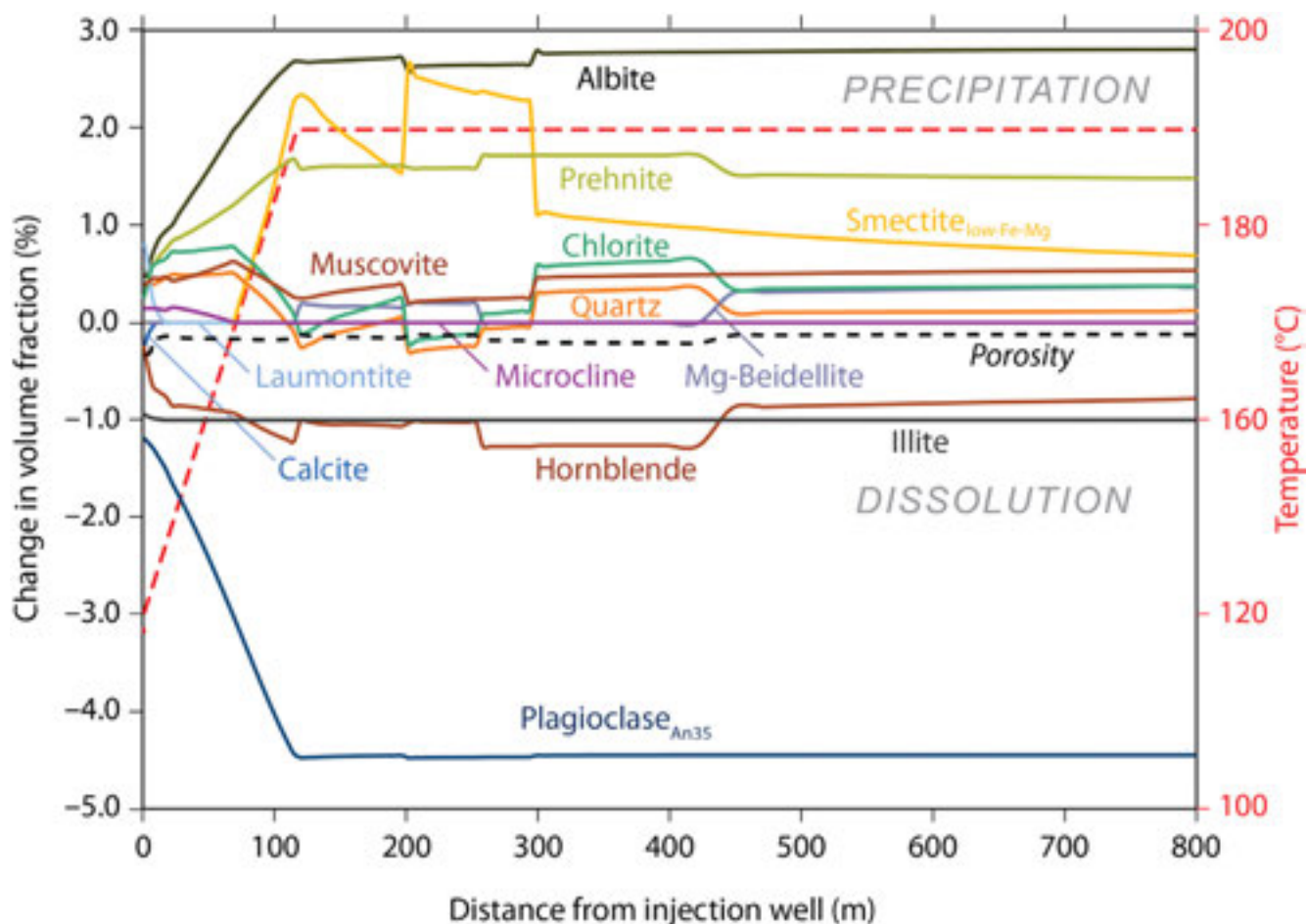


Figure 1. Changes in reservoir mineralogy during the first 15 years of closed-system doublet operation. Red dashed line: temperature profile. Time-integrated changes in volume fractions of minerals are plotted as a function of distance from the base of the injection well. Positive volume fractions indicate mineral precipitation; negative fractions indicate dissolution or porosity decrease (dashed curve). Minerals with very low changes in volume (e.g. biotite, and the ferric oxides and hydroxides formed during initial stimulation) are not shown.

## 12.7

### The effects of CO<sub>2</sub> injection in Muschelkalk: first laboratory results

Fabbri Stefano<sup>1</sup>, Zappone Alba<sup>1,2</sup>, Madonna Claudio<sup>1</sup>, Mazzotti Marco<sup>2</sup>

<sup>1</sup> Geological Institute, ETH Zurich, Sonneggstrasse 5, 8092 Zurich  
(alba.zappone@sed.ethz.ch)

<sup>2</sup> Institute for Process Engineering, ETH Zurich, Sonneggstrasse 5, 8092 Zurich

Anthropogenic emissions of Carbon Dioxide (CO<sub>2</sub>) are one of the key drivers regarding global climate change (IPCC, 2007). Carbon Dioxide Capture and Storage (CCS) is one valuable technology to mitigate current climate change with an immediate impact. Switzerland has started to investigate its potential for CO<sub>2</sub> storage and is currently performing research on the characterization of the most promising reservoir rocks for CO<sub>2</sub> sequestration. One aquifer of considerable large extent in the Swiss Molasse Basin is the Muschelkalk, a carbonate sequence of shallow marine limestones, with an estimated storage potential of 706 MtCO<sub>2</sub> (Chevalier et al., 2010). The uppermost part of the Muschelkalk unit, reveals favorable storage properties. The Gipskeuper, a thinly bedded alternation of clay-stones, anhydrite, gypsum and marls, overlies the Muschelkalk and acts as tight seal.

A series of laboratory measurements were carried out at the Rock Deformation Laboratory of ETH Zurich, on dolomite core samples recovered from a drill core from Benken, in the northeast of Switzerland (courtesy of Nagra). The transient step method (Brace et al., 1968) was used to measure the permeability, using argon and dry carbon dioxide, and employing an experimental setup developed in house (Pini et al., 2009). The rig is capable to simulate in situ pressure and temperatures conditions, and thus it allows an accurate evaluation of the reservoir's capacities for CO<sub>2</sub> sequestration. Recent implementations of the rig enable to perform permeability measurements and acoustic velocity measurements simultaneously (Fig. 1).

The minimal injection depth considered for CO<sub>2</sub> sequestration is 800 m, corresponding to a lithostatic pressure of 20 MPa and a temperature of 50°C (Chevalier et al., 2010; Nagra report, 2001). At such PT conditions, CO<sub>2</sub> changes its state of aggregation to supercritical and is significantly denser than in gaseous state. The experiments were performed under confining pressure of 6 MPa, 10 MPa, 14 MPa, 18 MPa and 20 MPa. The samples were heated in steps, together with the injected gas to temperatures of 23 °C, 35 °C and 50 °C. The two gas pressure reservoirs (see Fig. 1) were set to 2 MPa and 2.5 MPa. After the reservoirs equilibrated, a pore pressure of around 2.3 MPa was set and acoustic velocities were measured. Then the two reservoirs were set to 8 MPa and 8.5 MPa with a final pore pressure of 8.3 MPa after equilibration.

Our result indicate that the permeability crucially depends on confining pressure, temperature and pore pressure conditions of the sample. Especially at in situ conditions with CO<sub>2</sub> being at supercritical state, a substantial loss in permeability have to be taken into consideration when it comes to the calculation of potential injection rates.

These results are part of an on-going study and are very preliminary, up to now only cores perpendicular to bedding have been investigated, and we expect different physical properties behaviour in samples cut at different angles to bedding. Further investigations of more rock samples and in wet conditions, are required to support the results shown in this study.

#### REFERENCES

- Brace W. F., Walsh J. B. and Frangos W. T. 1968: Permeability of Granite Under High Pressure. *Journal of Geophysical Research*, 73, 2225-2236.
- Chevalier, G., Diamond, L. W., and Leu, W. 2010: Potential for deep geological sequestration of CO<sub>2</sub> in Switzerland: a first appraisal. *Swiss Journal of Geosciences*, 103, 427-455.
- IPCC, Working group III (Metz, B., O. Davidson, H. C. de Coninck, M. Loos, and L. A. Meyer (eds.) 2005: IPCC Special Report on Carbon Dioxide Capture and Storage. Cambridge University Press, Cambridge, United Kingdom and New York, 442 pp.
- Nagra, Inc. 2001: Sondierbohrung Benken, Untersuchungsbericht. Nagra Technical Report, NTB 00-01, 288 pp.
- Pini R., Ottiger S., Burlini L., Storti G. and Mazzotti M. 2009: Role of Adsorption and Swelling on the Dynamics of Gas Injection in Coal. *Journal of Geophysical Research*, 114, 14 pp.

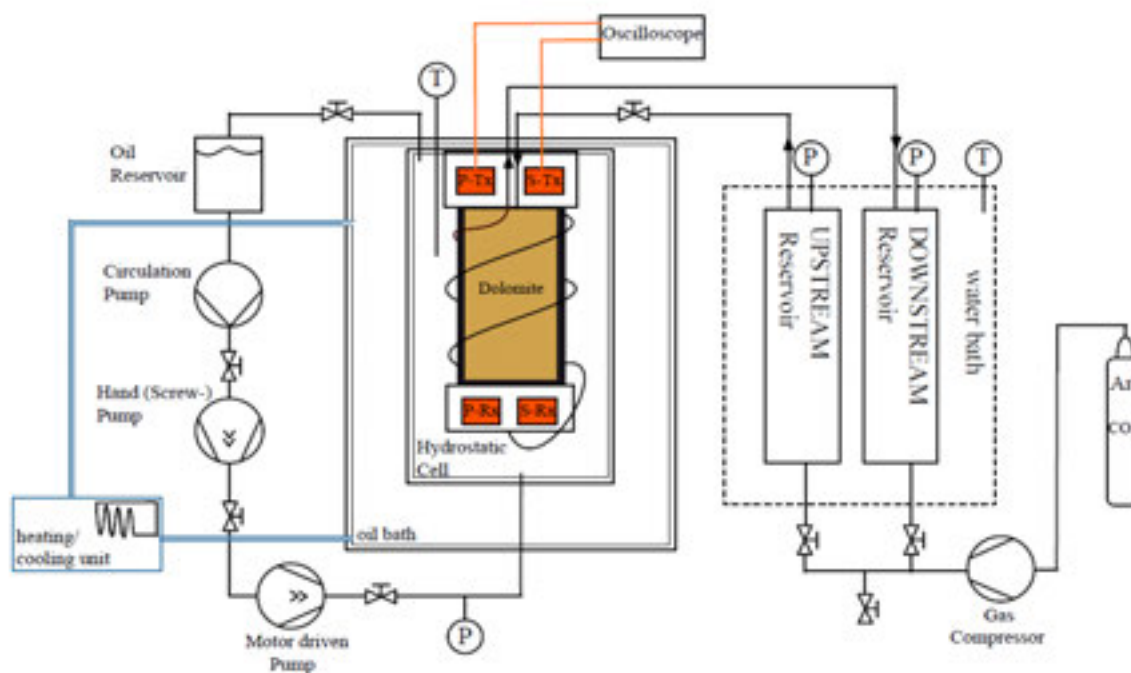


Figure 1. Setup of the modified Pini rig (redrawn from Pini et al., 2009 and updated) for permeability/velocities measurements. The transducers in the new sample holder emit at 0.5 MHz ultrasonic waves and enable the user to record acoustic wave velocities without any change on the set-up. Confining pressures up to 100 MPa and temperatures up to 100°C can be reached.

## 12.8

## Unconventional plays along the East European Craton – a review of E & P activities in Poland

Gawenda Piotr <sup>1</sup>

<sup>1</sup>IHS Global SA, 24 chemin de la Mairie, CH-1258 Perly-Geneva (piotr.gawenda@ihs.com)

The western limit of the Precambrian East European Craton (EEC) in Poland (Fig. 1) is being intensely explored for unconventional resource potential since a few years. The key tectonic units of interest are the Baltic Syncline, Danish-Polish Marginal Trough and Volhyno-Podolian Monocline, all within the EEC, as well as the Pomeranian and Kujawy highs, elements of the Northeast German-Polish Basin.

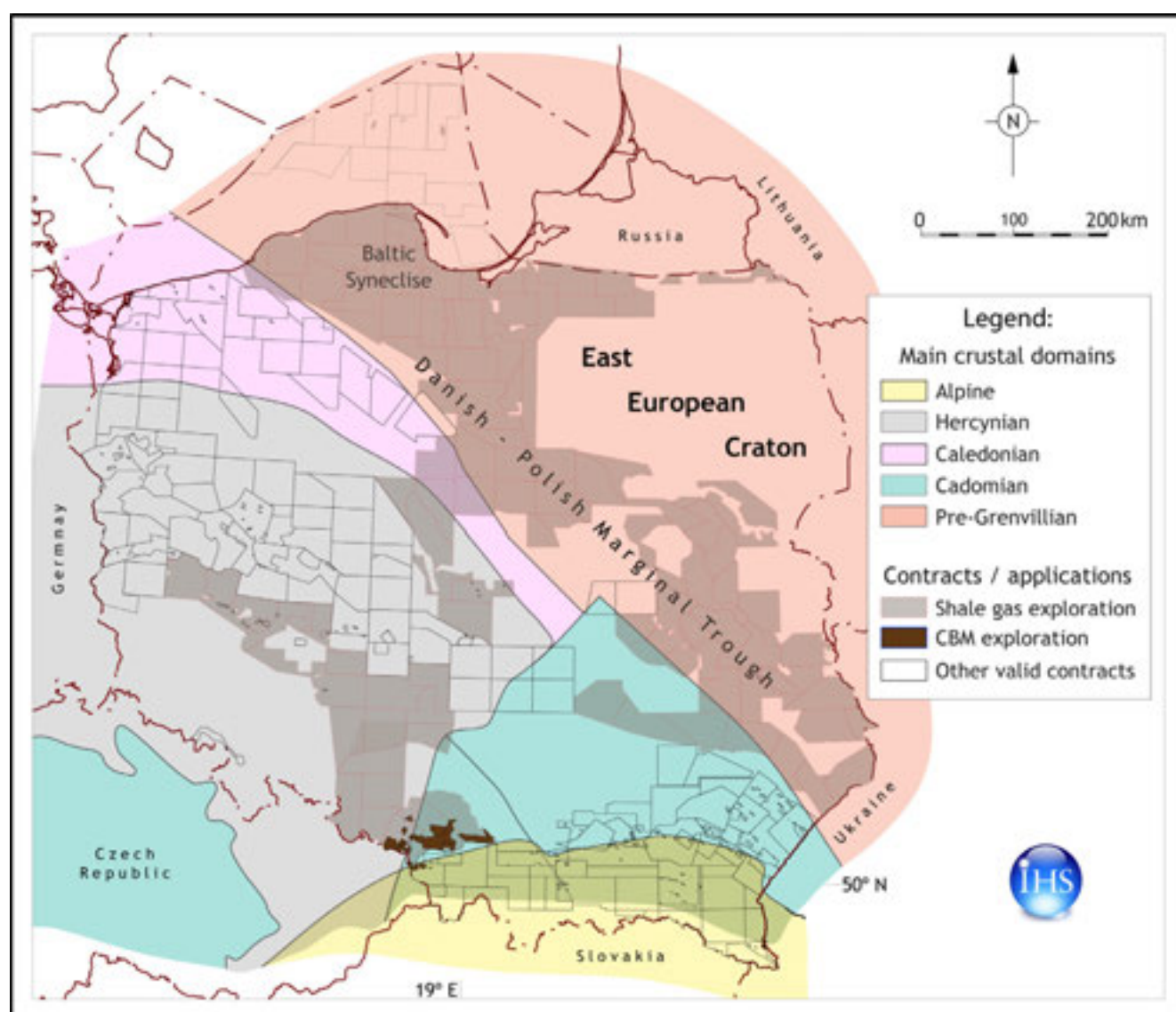


Figure 1. Map of Poland with location of the permits for unconventional exploration on the background of crustal terrains (after Karnkowski 2008).

The prime targets of exploration are found within the Upper Cambrian-Ordovician-Lower Silurian organic-rich sequences (Carboniferous series are also seen as a potential exploration target in places). The available seismic and well data indicate that the top of the Carboniferous series within the EEC limit can be traced at depths of 500-5,500 m, with the depth increasing to the west and southwest, towards the Teisseyre-Tornquist fault zone. Subsidence history reconstructed from well data shows that the Lower Palaeozoic formations in Poland were subject to rapid burial initiated during the Early Silurian and that the series attained hydrocarbon-generating maturity as early as in the Late Silurian/Ordovician, with the major pulse of thermal maturation associated with the Variscan orogeny.

Some 100 valid exploration contracts awarded in the sector since 2007 cover almost the entire acreage deemed prospective for hydrocarbon exploration. Following the initial period of land-grabbing, when operators of diverse sizes secured a significant acreage position, the late 2012/ 2013 period was epitomised by the withdrawal of a few players.

Over 40 shale wells have been drilled since mid-2010 to attest the potential of the area - majority of the wells is located within the Baltic basin (Fig. 2) – with some dozen of them flow-tested. The results of to-date drilling operations show that prospective series are gas-bearing over a few dozen metre-thick intervals. Tests conducted in the wells in northern Poland have proven that gas can be brought to surface, albeit not always at commercial rates.

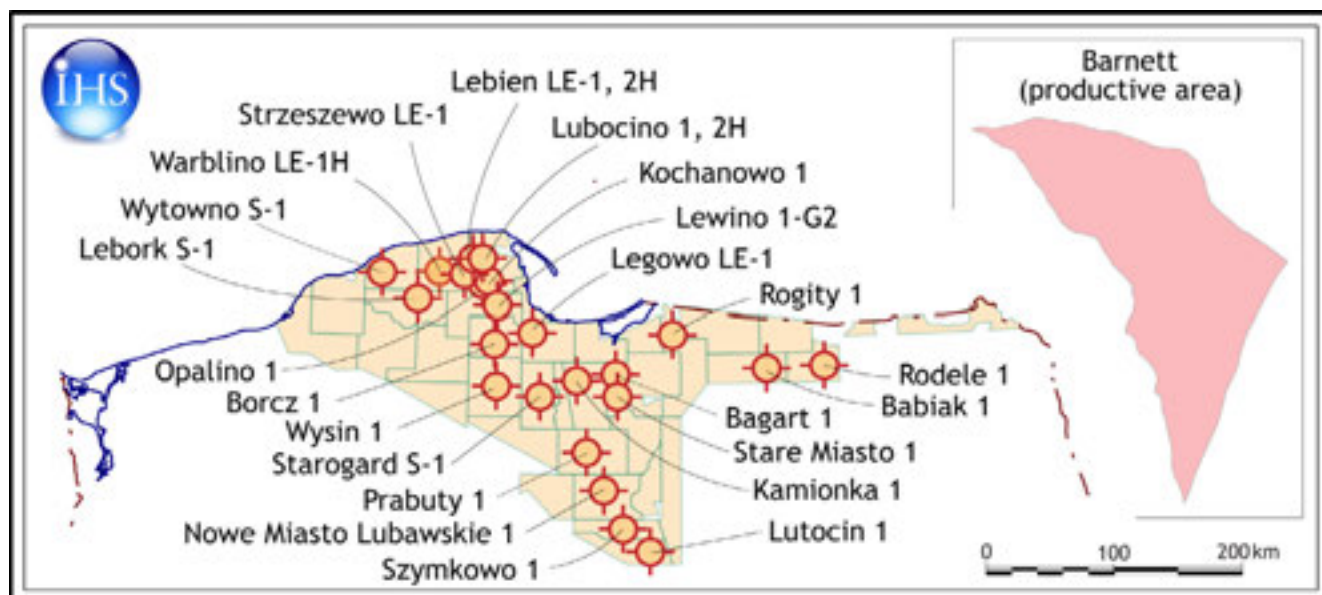


Figure 2. Map of northern Poland showing the wells drilled to-date for unconventional resources. Barnett (US) productive area is given for scale.

In spite of the initial exploration successes, unconventional exploration in Poland is still in its very early stage. The geological and technical features of the tested plays need further addressing; it has yet to be unequivocally determined if, and to what extent, a commercial production of hydrocarbons from the Palaeozoic series is feasible. The process requires more wells/tests than initially anticipated, consequently more time and investment to arrive at comprehensive conclusions.

## REFERENCES

Karnkowski, P.H. 2008. Tectonic subdivision of Poland: Polish Lowlands. *Przegląd Geologiczny*, vol. 56/10, 895–903.

## 12.9

### Internal structure of the Aar Massif: What can we learn in terms of exploration for deep geothermal energy?

Herwegh Marco<sup>1</sup>, Baumberger Roland<sup>1</sup>, Wehrens Philip<sup>1</sup>, Schubert Raphael<sup>1</sup>, Mock Samuel<sup>1</sup>, Berger Alfons<sup>1</sup>, Mäder Urs<sup>1</sup>, Spillmann Thomas<sup>2</sup>

<sup>1</sup> Institute of Geological Sciences, University of Bern, Baltzerstrasse 1+3, 3012 Bern ([marco.herwegh@geo.unibe.ch](mailto:marco.herwegh@geo.unibe.ch))

<sup>2</sup> Nagra, Hardstrasse 73, 5430 Wettingen

The successful use of deep geothermal energy requires 3D flow paths, which allow an efficient heat exchange between the surrounding host rocks and the circulating fluids. Recent attempts to exploit this energy resource clearly demonstrate that the new technology is facing severe problems. Some major problems are related to the prediction of permeability, the 3D structure of the flow paths and the mechanical responses during elevated fluid pressures at depths of several kilometers. Although seemingly new in a technical perspective, nature is facing and solving similar problems since the beginning of the Alpine orogeny.

Based on detailed studies in the Hasli Valley (Aar Massif) we can demonstrate that deformation and fluid flow are strongly localized along mechanical anisotropies (e.g. lithological variations, brittle and ductile faults). Some of them already evolved during Variscan and post-Variscan times. Interestingly, these inherited structures are reactivated over and over again during the Alpine orogeny. Their reactivation occurred at depths of ~13-15 km with elevated temperatures (400-475°C) and involved both ductile and brittle deformation processes. Brittle deformation in form of hydrofracking was always present due to the circulating fluids. It is this process, which was and still is responsible for seismic activity. With progressive uplift and exhumation of the Aar Massif, ductile deformation structures became replaced by brittle cataclasites and fault gouges during fault activity at shallower crustal levels. Existing hydrotest data from the Grimsel Test Site (Nagra's underground research laboratory) indicate that these brittle successors of the ductile shear zones are domains of enhanced recent fluid percolation. Note that although being exposed today, the continuation of these fault structures are still active at depth in both brittle and ductile deformation modes, a fact that can be inferred from recent uplift rates and the active seismicity.

On the scale of the Aar Massif, the aforementioned deformation sequence induced a complex and dense network of large-scale fault zones. The 3D structure of this network and the associated spacing between the individual faults strongly depends on the type of host rock, intensity of background strain and the location (kinematics) within the massif. Similar effects have to be expected in the crystalline rocks underneath the sedimentary cover in Northern Switzerland. However, based on the aforementioned findings, several facts might be in favor for future exploration of deep geothermal energy in the Aar Massif: (i) enhanced permeability in brittle fault rocks, (ii) dense 3D network auf brittle faults, (iii) weak vegetation allows a reliable projection of the structures to depth as well as tracking of their lateral continuation (crucial for estimates on seismic potential) and last but not least the existence of an elevated geothermal gradient.

## 12.10

## Hydromechanical coupling in carbon dioxide injection into a deep aquifer

Chao Li<sup>1</sup> & Lyesse Laloui<sup>1</sup>

<sup>1</sup> Laboratory of Soil Mechanics - Chair "Gaz Naturel" Petrosvibri, Swiss Federal Institute of Technology of Lausanne, EPFL - ENAC - LMS Station 18 CH-1015 Lausanne (chao.li@epfl.ch)

CO<sub>2</sub> storage in deep aquifer is considered as a compromising technology to reduce the impact of CO<sub>2</sub> on the greenhouse effect. Practically, large-volume (>1Mt/year) of CO<sub>2</sub> could be injected into a system which consists of a highly porous host aquifer covered by a very low permeable sealing caprock. High rate injection could result in an abrupt fluid pressures build-up, deforming the aquifer and compromising the integrity of caprock. The interaction between fluid flow and mechanical reaction of geomaterials gives rise to a complexly coupled system. It is crucial to understand such hydromechanical processes in order to secure the injection.

We investigate numerically the multiphase hydromechanical effects induced by CO<sub>2</sub> injection on the aquifer and the related interactions with the caprock. The proposed simulator incorporates real physical properties of supercritical CO<sub>2</sub> such as the density, the viscosity and the fugacity. A conceptual deep aquifer is modelled to investigate the state of stress and strain during the injection of CO<sub>2</sub>. Simulation responses show that significant geomechanical variations occur during the early period of injection where fluid pressures are increasing sharply (see Figure. 1). Overpressure leads to a decrease in the effective stress, which leads to volumetric expansion around the injection well. Because of this porosity and permeability increase via the hydromechanical coupling, which allows fluid flow more easily. As injection continues, the stress path moves away from the failure line and geomaterials return back to the elastic state. In this study, the safety of carbon dioxide injection is assessed mainly from a geomechanical point of view. Most influential parameters in the injection-induced responses are highlighted with the aid of a predefined security factor, which can be employed in the design of an industrial CO<sub>2</sub> storage project.

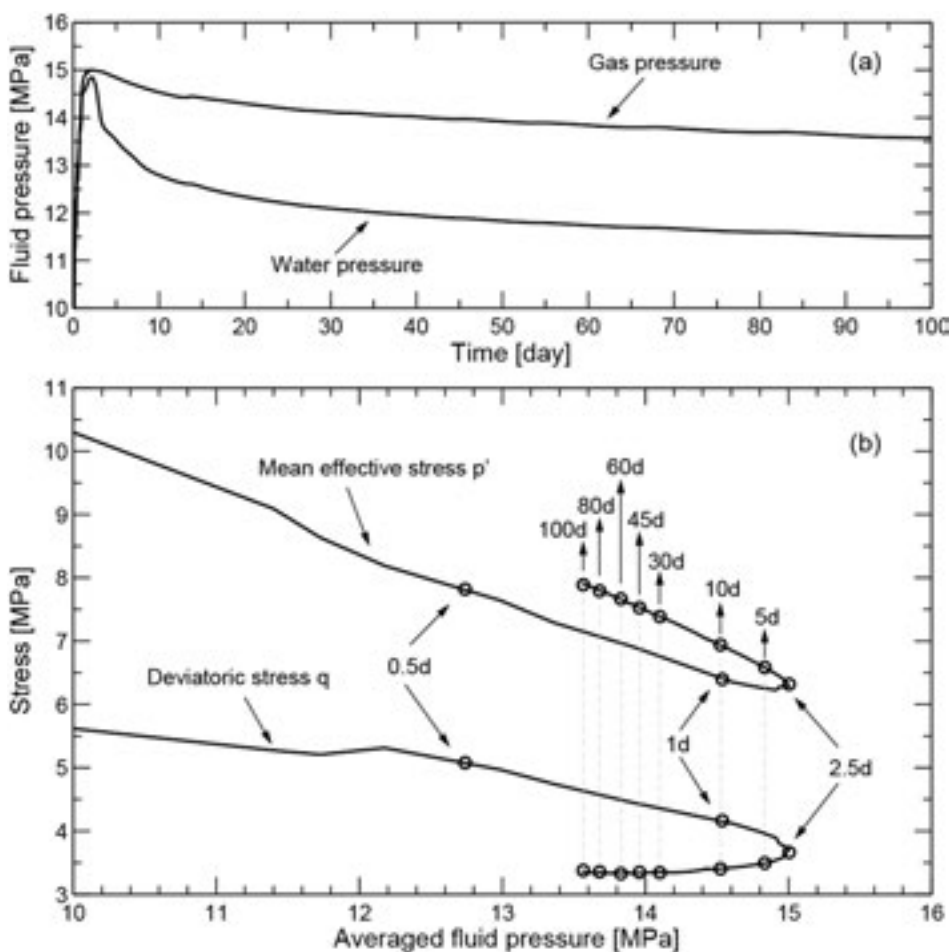


Figure 1. Temporal evolution of the water pressure and CO<sub>2</sub> pressure, (b) Temporal evolution of relationship between stress and fluid pressure on the top of the aquifer and next to the injection well.

## 12.11

### Field experiment in an underground rock laboratory to study the well integrity in the context of CO<sub>2</sub> geological storage

Manceau Jean-Charles<sup>1</sup>, Claret Francis<sup>1</sup>, Tremosa Joachim<sup>1</sup>, Audigane Pascal<sup>1</sup> & Nussbaum Christophe<sup>2</sup>

<sup>1</sup>BRGM, 3 avenue C. Guillemin 45060 Orléans Cedex 2 France (jc.manceau@brgm.fr)

<sup>2</sup>swisstopo, Seftigenstrasse 264, 3084 Wabern, Switzerland

Wells drilled through low-permeable caprock are potential connections between the CO<sub>2</sub> storage reservoir and overlying sensitive targets like aquifers and the surface environment. The long term well integrity is therefore essential for fluids confinement (brine with or without dissolved CO<sub>2</sub> or buoyant gaseous CO<sub>2</sub>). This integrity can be first affected by *in situ* operations (Zhang & Bachu, 2011): during the drilling, the caprock can be damaged leading to the formation of an excavation damaged zone; the quality and placement of the cement during the completion is also essential for a suitable bonding; the pressure and temperature changes during the life of the well as well as the conditions of its abandonment are additional factors that may impact the isolation capacity of the well. The well integrity can also be modified by geochemical reactions occurring between well compartments (cement, caprock, casing) and fluids (CO<sub>2</sub>-saturated water as well as wet CO<sub>2</sub>). Cement reactivity is of first concern and a significant amount of studies have already been carried out to characterize these interactions (for instance Kutchko et al., 2007; Duguid and Scherer, 2010).

Given the buoyant character of CO<sub>2</sub> associated with a potential overpressure due to the leakage (driving force), the hydraulic properties of the wellbore environment and their evolution over time appear to be the more influent variables for assessing the long term risks related to the wells. Some field studies have assessed the consequences of the contact between wellbores and CO<sub>2</sub> in an EOR field and in a natural CO<sub>2</sub> reservoir (Carey et al., 2007; Crow et al., 2010). They highlighted in particular the lack of integrity that may occur at the interfaces rather than through the cement matrix. Understanding the near well sealing integrity then requires studying the potential pathways and associated migration via altered well compartments but also along interfaces with deficient bonding: it implies the study of the well environment as a whole. To go beyond the state of the art, we present a new experiment, implemented in the Underground Rock Laboratory of Mont Terri (St-Ursanne, Switzerland), at an intermediate scale between the laboratory experiments (which offer the opportunity to assess specific phenomena over time) and field observations (which allow an assessment of the entire system in subsurface at a specific time). Our purpose is to follow the integrity evolution of the whole well system due to changes in well conditions (e.g. changes in temperature and in the geochemical environment with and without CO<sub>2</sub>).

To meet this purpose, the following steps are contemplated: 1/ the building of classical well elements to reproduce a part of the barrier system constituted of the low permeable formation, the cemented annulus, the casing and the cement plug; 2/ the characterization of the initial geochemical and hydraulic properties of the system; 3/ the increase in temperature of the system and the characterization of the potential geochemical and hydraulic changes; 4/ the injection of CO<sub>2</sub>-rich fluid in the experimental apparatus and the characterization of the potential geochemical and hydraulic changes; 5/ the retrieval of solid samples from the experimental apparatus for further analyses in laboratory.

The concept of the experiment is as follows: the system is divided in two parts, an internal part consisting of the casing and the cement plug inside the casing, and an external part consisting of the formation rock, the cemented annulus and the casing. A first interval, where fluids are injected, is located below the well elements. Over the cement plug, a second interval allows measuring the flow inside the casing. A third interval allows measuring the flow outside the casing.

The drilling of the borehole and well completion were performed in autumn 2012. The system was then saturated with synthetic pore water and relaxed. Some pulse and constant head tests have been run at the beginning of 2013 with the purpose of characterizing the initial hydraulic properties of the system (well and surrounding caprock). In addition to the constant head tests, the experimental set-up allows a continuous monitoring of the effective well permeability over time at steady state. The system was relaxed again to observe the evolution of the hydraulic properties under initial conditions. No major changes were observed in one month. The temperature was then increased in the system up to 50°C. The system was let at this temperature during several months in order to equilibrate the temperatures and then to characterize the changes in terms of hydraulic properties. Significant modifications in the hydraulic behavior of the system have been observed, showing clearly an increase of the well integrity. The next steps of the experiment plan are the injection of CO<sub>2</sub>-saturated water associated with tracers and the monitoring of the well hydraulic properties and fluids composition evolution over time.

In addition to that experiment, modeling work has been performed. The caprock and wellbore hydraulic properties have been retrieved from the hydro-tests using analytical and numerical modeling. In terms of geochemical modeling, predictive models have been built to understand the potential behavior of the well system in contact with CO<sub>2</sub>. These predictive

modeling are used to calibrate the experimental conditions. Predictive modeling also makes possible to link the measured changes in chemistry during the experiment to the interaction processes occurring at the casing/cement/clay interface.

#### Acknowledgements

This work is performed as part of the EU-funded FP7 project ULTimateCO<sub>2</sub>. The ULTimateCO<sub>2</sub> consortium would like to thank Swisstopo and Obayashi for funding a part of this experimentation.

#### REFERENCES

- Carey, J.W., Wigand, M., Chipera, S.J., WoldeGabriel, G., Pawar, R., Lichtner, P.C., Wehner, S.C., Raines, M.A., Guthrie Jr., G.D. Analysis and performance of oil well cement with 30 years of CO<sub>2</sub> exposure from the SACROC unit, west Texas, U.S.A. *International Journal of Greenhouse Gas Control* 2007; 1 (1), 75–85.
- Crow, W., Carey, J.W., Gasda, S., Williams, D.B., Celia, M., Wellbore integrity analysis of a natural CO<sub>2</sub> producer. *International Journal of Greenhouse Gas Control* 2010; 4 (2), 186–197.
- Duguid, A., Scherer, G.W. Degradation of oilwell cement due to exposure to carbonated brine. *International Journal of Greenhouse Gas Control* 2010; 4 (3), 546–560.
- Kutchko, B.G., Strazisar, B.R., Dzomback, D.A., Lowry, G.W., Thaulow, N. Degradation of well cement by CO<sub>2</sub> under geologic sequestration conditions. *Environmental Science & Technology* 2007; 41 (12), 4787–4792.
- Zhang, M., Bachu S. Review of integrity of existing wells in relation to CO<sub>2</sub> geological storage: What do we know? *International Journal of Greenhouse Gas Control* 2011; 5:826–840

## 12.12

# The geothermal site of Eclépens: new geological insights from an integrated seismic and satellite study.

Moscariello Andrea<sup>1</sup>, Mondino Fiammetta<sup>2</sup>, Vinard Pascal<sup>3</sup>

<sup>1</sup> *Earth and Environmental Sciences, University of Geneva, Rue de Maraîchère 13, CH-1205 Genève (andrea.moscariello@unige.ch)*

<sup>2</sup> *113 Chemin de la Scierie, Valleiry, France*

<sup>3</sup> *BKW Energie Ltd. Viktoriaplatz 2, 3000 Bern 25*

In response to the ever-increasing demand of energy supply in Switzerland, over the last 10 years a concerted effort to identify technically and economically viable deep geothermal projects has been promoted both by the public and private sector.

One of the most promising projects currently in the phase of the feasibility study is the EGS project of Eclépens (Canton of Vaud, Western Switzerland) promoted primarily by BKW and a group of industry partners.

The targeted site was discovered in 1981 by the hydrocarbon exploratory well Eclépens -1 which encountered the known stratigraphy of the region (from top to bottom Tertiary Molasse, Lower Cretaceous and Jurassic series) and reached the top of the Triassic at around 2200 m below surface where a temperature of ca.110°C was recorded.

This paper aims to present the preliminary results of the recent study carried out based on both the newly acquired and the reprocessed vintage 2D seismic lines (Fig. 1) integrated with the satellite image analysis of the area.

The Eclépens area has been investigated since mid 70s for hydrocarbon resulting on a relatively large number of cross cutting 2D seismic lines and the presence of few hydrocarbon exploration wells. The latter allow a good calibration of the stratigraphy imaged by seismic data. The newly reprocessed 2D seismic lines from the 70s (SAdH survey) using DMT's CRS technology (signal/noise improvement), have brought a remarkable improvement in the imaging. In particular, much sharper contrast between stacked reflectors with different amplitude and better definition and vertical extension of faulted/damage zones have been achieved.

The reprocessed data have been integrated with few newly acquired seismic lines (survey Geo2X in 2012) around the well Eclépens-1 and few others vintage lines re-examined by the recent comprehensive regional work carried by Paolacci (2013). The Eclépens area and its immediate western neighbouring Jura relief have been also examined using aerial photographs and satellite images with the aim to identify major structural lineaments which could be linked to subsurface features.

The examination of 2D lines seismic highlighted the occurrence of 0.5 to 2.5 km wide deformation zones interrupting the stratigraphical continuity of the subsurface. These deformation zones are predominantly vertical and sub vertical (5-15°) and often appear to have little or not associated vertical displacement.

Inverse faulting has been observed often associated with convex bending of stratigraphical seismic reflectors (Fig. 1). The latter are often deformed also in correspondence of vertical fault zones forming convex deformation interpreted as drag folds. Overall, the deformation style observed on seismic data, suggest a strike-slip system with transpressive component.

Moreover, the detailed seismic interpretation carried out in a 3D environment (Petrel software by Schlumberger) has allowed the identification of several discontinuous and segmented faults which can be grouped in 2 main clusters intersecting each other at an angle of ca 80°. These two systems have been interpreted as a Riedel/Anti-Riedel conjugate set likely associated with a NNW-SSE left-lateral strike slip system.

The identification of a Riedel and Anti Riedel conjugate set is key to understand better the influence of structural features and the working mechanisms of the Eclépens geothermal system.

These fault systems appear to be deeply rooted within the Permo-Carboniferous strata suggesting a possible link with original basement lineations. Moreover, considerable changes in stratigraphic thickness of Jurassic sequences across some of these fault zones, suggest that the latter may represent possibly vertical reactivation of Mesozoic lineaments during the subsequent Alpine deformation phases.

This proposed structural model will be used to build a realistic range of discrete fault and fracture network models for characterisation and quantification of water discharge and heat flow associated with a potential EGS development.

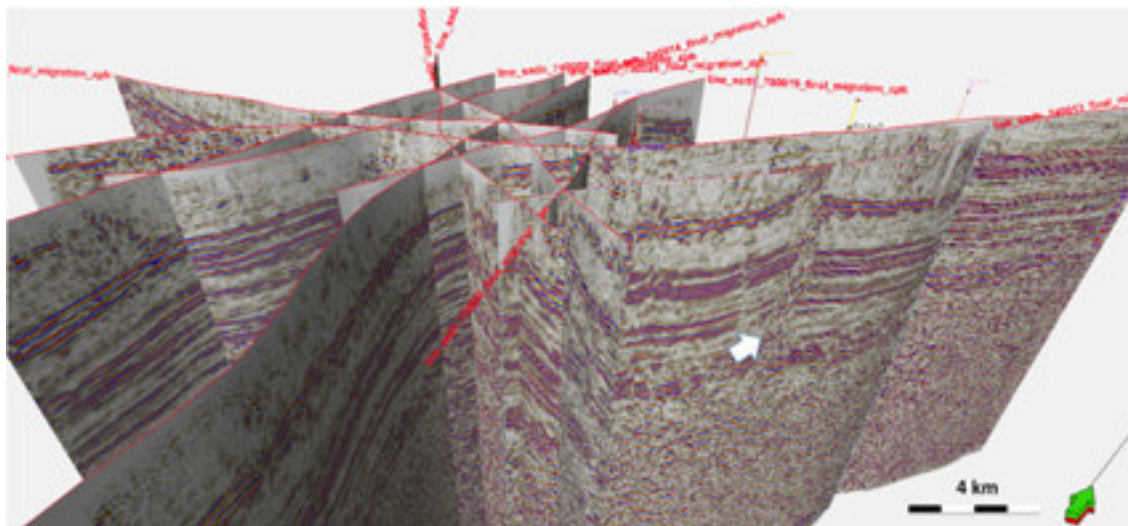


Figure 1. Three dimensional view of the newly reprocessed 2D seismic lines in the Eclépens area. Subvertical fault damage zone indicated with white arrow is ca. 1.2 km wide.

#### REFERENCES

- Paolacci (2013) Seismic facies and structural configuration of the western alpine Molasse Basin and its substratum (France and Switzerland). PhD thesis University of Geneva. Terre et Environnement Series, in press.
- SERIANEX 2009 - Deep Heat Mining Basel - Seismic Risk Analysis, 1-21 p. <http://www.wsu.bs.ch/geothermie>

## 12.13

### The subsurface geology of the Western Swiss Plateau and its French extension: state of the art and implications for geo-resources exploration.

Paolacci Sabrina<sup>1</sup>, Gorin Georges <sup>1</sup>, Moscariello Andrea<sup>1</sup>

<sup>1</sup> *Earth and Environmental Sciences, University of Geneva, Rue de Maraîchers 13, CH-1205 Geneva (andrea.moscariello@unige.ch)*

A large comprehensive study of the subsurface geology of the western part of the Swiss Molasse Basin, from its westernmost part in France up to the border between cantons Fribourg and Bern has been recently completed (Paolacci, 2012). This work is based on more than 1700 kilometers of vintage 2D seismic lines (early 70s through 90s) and some 27 wells with penetration ranging from the Tertiary down to the Palaeozoic, obtained during both hydrocarbon and geothermal exploration activities over the last 50 years.

Subsurface data from seismic, integrated with published outcrop data indicate that the Molasse Basin is affected by numerous strike-slip faults which cut the Jura arch in a radial way, and by SSW-NNE trending thrust faults. These structures have been analyzed at Mesozoic level, focusing on their possible interaction with underlying tectonic features affecting the Palaeozoic and basement.

Above the crystalline basement, the Intra-Permo-Carboniferous (IPC) seismic unit is defined by a group of high amplitude continuous reflections underlying a more transparent seismic facies, corresponding to the more homogeneous Permian siliciclastics. The IPC reflections are interpreted as coal rich sequences, possibly containing primary hydrocarbons as indicated by the frequent occurrence of amplitude anomalies (bright spots) likely associated both with stratigraphic and structural traps. Source rocks also may be contained in Early Permian shales overlaying the Carboniferous coal-bearing sequence.

In the Greater Geneva region, the detailed mapping of the IPC reflective sequence suggests the presence of basins with asymmetric geometry (i.e. half-grabens) and structural features mostly oriented NE-SW. These half-grabens extend below the Bornes Plateau Basin, at the front of the Salève ridge s.l. and close to the Jura Mountain. In the Vaud-Fribourg region, these basins have more variable orientations, varying between NW-SE (below the Pontarlier fault zone and at the front of the Prealps), E-W (in the Chamblon region) and NE-SW south of the Cuarny Anticline.

The thickness of the Triassic varies within the study region, partly for tectonic but also for depositional reasons. The Keuper evaporites represent the main ductile level in the major part of the study region, whereas the Anhydrite Group (Middle Muschelkalk) constitutes the detachment horizon in the eastern half of the Vaud-Fribourg region. Both these units may represent sealing intervals although their integrity may have been jeopardised by subsequent tectonic movements.

In the Greater Geneva area, the SSW-NNE trending Salève ridge s.l. is crosscut by numerous WNW-ESE trending left-lateral strike-slip fault zones. The basal detachment plane of these thrust anticlinal structures flattens within the Liassic marls and Keuper anhydrites, thereby determining characteristic flat-ramp geometry. Moreover, they all seem to have formed above a basement high delimited to the NW by a Permo-Carboniferous half-graben.

Compressive tectonics date back to the Late Cretaceous-Early Tertiary which in some cases reactivated Late Hercynian lineaments (Salève ridge s.l.). Possible structural traps such as anticlines and fault traps may have formed during this time. The majority of the NW-SE trending strike slip faults in the studied region affect the underlying Permo-Carboniferous at depth. Several of them (e.g. Vuache, Pontarlier, etc.) have been active at least from Triassic times, during Lower and Upper Jurassic and Lower Tertiary times. Considerable differences of thicknesses in the Mesozoic sequence (e.g. Vuache and Eclepens area) may suggest an active structuration during time of deposition. This will implies likely lateral facies changes and higher variability, especially during Triassic and Jurassic time of reservoir development (Keuper sandstone, Malm carbonates) and potential source rock represented by the Posidonia shales Formation.

The entire studied area is disseminated by both left-lateral and conjugate right-lateral strike-slip faults, forming complex-shaped, often transpressive, fault systems. Many of these (e.g. Pontarlier, Fribourg lineaments, etc.) are deeply rooted in Palaeozoic strata, and could be likely target for deep geothermal projects (e.g. la Côte, Eclépens) as suggested by some boreholes data (Eclépens-1, Moscariello et al., 2013).

Overall, this study (Paolacci, 2012) represents the first complete overview of the Western Switzerland subsurface based on almost all available data. However, further investigations are required to quantify the geo-resource potential of this large region. Seismic reprocessing, for instance, has been key to obtain better images although new 3D seismic will be necessary in order to map accurately complex structural features (see Moscariello et al., 2013) and thus generate predictive reservoir models (e.g. fracture network). Detailed petrophysical log evaluation, rock typing studies and seismic facies analysis are currently being carried out, to characterise the subsurface and assess quantitatively the possibility of geo-resources occurrence.

The research of S. Paolacci was funded by the FNSRS Project n. 20-53543.98.

#### REFERENCES

- Gorin, G.E., Signer, C. & Amberger, G. 1993: Structural configuration of the western Swiss Molasse Basin as defined by reflection seismic data, *Eclogae geol. Helv.*, 86/1, 693-716.
- Paolacci S. 2012: Seismic facies and structural configuration of the western alpine Molasse Basin and its substratum (France and Switzerland), PhD thesis University of Geneva. *Terre et Environnement Series*, in press.
- Moscariello A. Mondino F., Vinard P. 2013: The geothermal site of Eclépens: new geological insights from an integrated seismic and satellite study,

## 12.14

## Use of surface patches for hydraulic fracture monitoring

Schilke Sven<sup>1</sup>, Bradford Ian<sup>2</sup>, Probert Tony<sup>2</sup>, Özbek Ali<sup>2</sup> & Robertsson Johan<sup>1</sup>

<sup>1</sup>Institut of Geophysics, ETH Zurich, Sonnegstrasse 5, CH-8092 Zurich (sschilke@student.ethz.ch)

<sup>2</sup>Schlumberger Gould Research Center, High Cross, Madingley Road, UK-CB30EL Cambridge

In the last decade the exploration of unconventional reservoirs has increased significantly. To produce a conductive pathway to the producing well, additional stimulation referred to as hydraulic fracturing is necessary. One method of monitoring the fracturing process is the observation of microseismic events.

In 2011 Schlumberger and an independent operator (who are required to be anonymous) jointly acquired a comprehensive dataset of hydraulic fracturing operations which stimulated the Fayetteville shale in Arkansas in order to track signal and noise from the reservoir to the earth surface and then across the surface. The performance of alternative monitoring technologies such as surface and shallow borehole seismic arrays as well as a downhole seismic array are analyzed.

The level of noise on different seismic arrays is characterized and appropriate attenuation techniques are applied. Furthermore linear and non-linear stacking methods are successfully utilized to increase the signal-to-noise ratio (SNR). The application of the Source- Scanning-Algorithm (SSA) to locate microseismic events conclude that an accurate source location requires an accurate velocity model together with consistent and aligned signal. Coherent noise, insufficient signal or noise discrimination are key factors influencing location uncertainty.

Although surface line segments benefit from larger receiver apertures, SNRs of stacks were usually only slightly higher than from stacks of surface patches using linear stacking methods. However, source localization is more accurate using surface lines. Nevertheless, surface patches are easily deployable so provided sufficient signal is recorded and noise attenuation methods are applied prior to stacking and source scanning, they may ultimately become the preferred surface monitoring configuration.

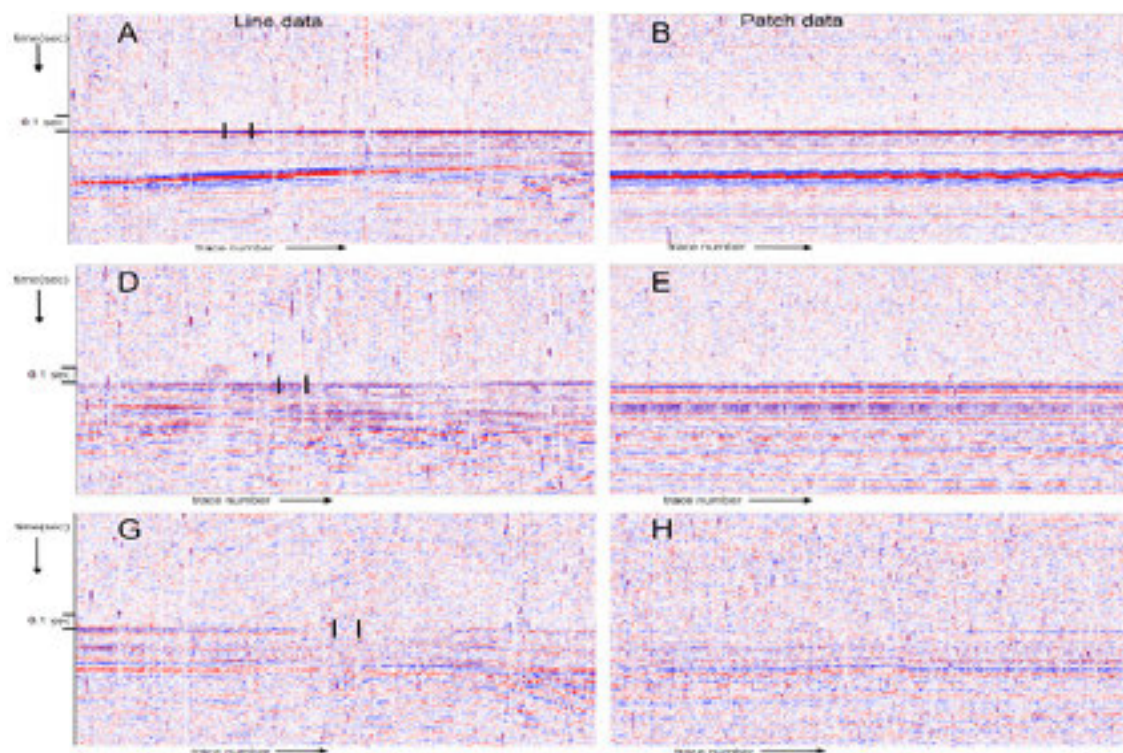


Figure 1. Comparison of static corrected surface line segment and surface patch data. The position of the surface patch on the line segment is indicated by vertical black lines.

## REFERENCES

- Drew, J., Primiero, P., Brook, K., Raymer, D., Probert, T., Kim, A. & Leslie, D. 2012: Microseismic monitoring field test using surface, shallow grid, and downhole arrays. 82nd Annual International Meeting, SEG, Expanded Abstracts.
- Kao, H. & Shan, S.-J. 2004: The Source-Scanning Algorithm: mapping the distribution of seismic sources in time and space. *Geophysics Journal International*, 157, 589-594.
- Maxwell, S.C., Raymer, D., Williams, M. & Primiero, P. 2012: Tracking microseismic signals from the reservoir to surface. *The Leading Edge*, 1, 1300-1308.
- Özbek, A., Probert, T., Raymer, D. & Drew, J. 2013: Nonlinear Processing Methods for Detection and Location of Microseismic Events. 75th Conference and Exhibition, EAGE.
- Peyret, O., Drew, J., Mack, M., Brook, K., Maxwell, S. & Cipolla, C. 2012: Subsurface To Surface Microseismic Monitoring for Hydraulic Fracturing, Annual Technical Conference and Exhibition, SPE.

## 12.15

### Multiphysics methods: a link between pore-scale and Darcy-scale models

Tomin Pavel<sup>1</sup>, Lunati Ivan<sup>1</sup>

<sup>1</sup>*Faculté des géosciences et de l'environnement, University of Lausanne, UNIL-Mouline, CH-1015 Lausanne (pavel.tomin@unil.ch)*

Modern energy-related applications require an increasing complexity in the physical processes that have to be considered in geological formations. In hydrocarbon recovery, Carbon Capture and Storage, or deep geothermal energy one has to deal with multiphase multicomponent flow, reactive transport, thermal and geomechanical coupling. Under these circumstances, traditional macroscopic models might be inadequate and new approaches are required that allow a more accurate description of pore-scale processes.

The Darcian approximation of momentum transfer, for instance, is well justified for simple linear problems (e.g., single-phase flow), but is not always applicable to nonlinear flow regimes, leading to a breakdown of Darcy's law and to a macroscopic solution that depends on the pore-scale details. However, the failure of Darcy's law is often local in space, such that a detailed, pore-scale description is required only in regions characterized by specific flow conditions, whereas Darcy's law remains sufficiently accurate in the rest of the domain. Multiphysics (or hybrid) numerical algorithms that couple different scales of description offer an effective tool to investigate this problem.

We present a multiphysics model that couples a Darcy coarse-scale description with a pore-scale description in which full Navier-Stokes equations are solved and the Volume Of Fluid (VOF) method is used to model the evolution of the fluid-fluid interface in presence of wetting and surface-tension effects. The Darcy coarse-scale description is constructed by using the Multiscale Finite Volume (MsFV) method as numerical volume averaging procedure and assuming that pressure is the only relevant degree of freedom at the coarse scale.

This framework allows great flexibility in the adaptive strategies that can be used to resolve the details of the flow process only where and when needed. Also, it offers a tool to numerically investigate the limits of validity of the Darcy assumption, as well as to test alternative models.

## 12.16

### Deep geothermal Energy in Switzerland – actual developments and perspectives for the future

Roland Wyss

*Geothermie.ch, Zürcherstrasse 105, 8500 Frauenfeld*

In the last decades, several geothermal projects for district heating or balneological use were realized in Switzerland. In contrast, «deep geothermal power» has not been produced yet. Through the enacted nuclear phaseout in 2011, the perspectives of deep geothermal energy have been distinctively improved and the development has accelerated. The expectations related to deep geothermal energy increased but the general acceptance is currently ambivalent. Deep geothermal energy is of high potential in Switzerland and could play an important role in Swiss energy supply in the future. However to achieve this goal, challenges of the most different kind must be tackled. One of the most important barriers in Switzerland is the still poorly known deep underground, as its unexpected response in St.Gallen illustrates.

## P 12.1

# Optimized layout of engineered geothermal systems and potential in Germany

Jain Charitra<sup>1</sup>, Clauser Christoph<sup>2</sup>, Vogt Christian<sup>2</sup>

<sup>1</sup>Institute of Geophysics, ETH Zürich, Sonneggstrasse 5, CH-8092 Zürich, Switzerland (charitra1989@gmail.com)

<sup>2</sup>Institute for Applied Geophysics and Geothermal Energy, E.ON Energy Research Center, RWTH Aachen University, Mathieustrasse 10, D-52056 Aachen, Germany

The forward modelling code SHEMAT can simulate operated Engineered Geothermal System (EGS) reservoirs by solving coupled partial differential equations governing fluid flow and heat transport. Building on EGS's strengths of inherent modularity and storage capability, it is possible to implement multiple wells in the reservoir to extend the rock volume accessible for circulating water in order to increase the heat yield. By varying parameters like flow rates and well-separations in the subsurface, we analyse their long-term impacts on the reservoir's development in time. This allows us to experiment with different placements of the engineered fractures and different EGS layouts for achieving optimized heat extraction. Considering the available crystalline area and accounting for competing land uses, we evaluate the overall EGS potential in Germany and compare it with those of other popular renewables: The area available in Germany suffices to support 13450 EGS plants each consisting of six reversed-triplets (18 wells), providing an average electric power of 35.3 MW<sub>e</sub> corresponding to a total capacity of 475 GW<sub>e</sub>. When operated at full capacity, these systems can collectively supply 4155 TW h of electric energy in one year, more than six times the electric energy produced in Germany in 2011. We conclude that Engineered Geothermal Systems make a compelling case for contributing towards national power production in a future powered by a sustainable and decentralized energy system, provided that suitable fracture systems can be engineered at depths.

## P 12.2

# Solving three-dimensional non-linearly coupled hydro-mechanical two-phase flow on GPUs

Räss Ludovic<sup>1</sup>, Omlin Samuel<sup>1</sup>, Podladchikov Yuri Y.<sup>1</sup>, & Simon Nina S. C.<sup>2</sup>

<sup>1</sup>*Institut des Sciences de la Terre (ISTE), University of Lausanne, Géopolis, CH-1015 Lausanne (ludovic.raess@unil.ch)*

<sup>2</sup>*IFE (Institutt for energiteknikk), Instituttveien 18, NO-2007 Kjeller, Norway*

Computational geodynamics benefit from the fast-growing computer industry, allowing to solve real-world complex problems at higher resolution and faster rates than in the past. An actual problem that requires codes that efficiently solve complex non-linear problems in three-dimensions (3D) is CO<sub>2</sub> underground storage. All over the world, large amounts of CO<sub>2</sub> and other waste fluids are being injected into reservoirs. One example is the injection of about one million tons of CO<sub>2</sub> per year since 1996 into the Utsira formation at Sleipner in the Norwegian North Sea. Conventional reservoir simulations fail to predict the formation of flow channels or chimneys, and the fast lateral and directional spreading of CO<sub>2</sub> underneath the caprock.

We developed a fully three-dimensional, non-linear mechanical model, utilizing the latest computing technologies, such as graphical processing units (GPU), high-performance computing parallel implementations with message passing interface (MPI), on our in-house mid-sized cluster (Räss 2013). A speed-up of more than 700 times was reached with the C-CUDA GPU implementation in comparison to the Matlab<sup>®</sup> CPU code.

In the mechanical part, Stokes equations with non-linear viscosity (Figure 1) are solved focusing on the vertical motion that results from non-linear coupling of gravitational and tectonic forces. A new vertical velocity analytical solution for non-linear and non-zero far-field stresses is proposed to fill the gap between the two existing analytical solutions.

The newly developed fully coupled two-phase flow code takes solid velocities obtained from the mechanical solver. We then study coupled deformation and fluid flow in large pre-stressed reservoirs, based on the porosity waves concept (Connolly & Podladchikov 1998, Simon et al. 2011, Simon et al. 2013), without prescribing pre-existing fractures.

The results of the mechanical part of our model set up a benchmark for future development. The fully coupled two-phase flow helps to understand and explain under which conditions localization of fluid will occur and is also applicable to the injection of other fluids (e.g. waste water).

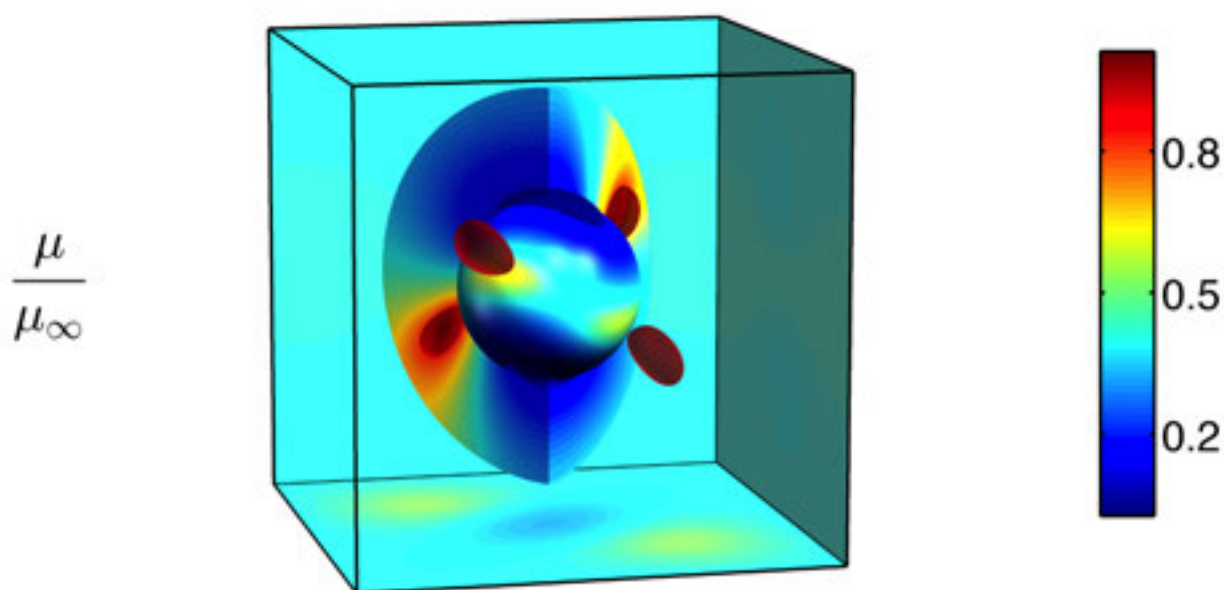


Figure 1. 3D surface plot of the viscosity reduction (viscous softening) of the surrounding media due to non-linear coupling in power-law rheology.

## REFERENCES

- Connolly, J. A. D. & Podladchikov, Y. Y. 1998 : Compaction-driven fluid flow in viscoelastic rock. *Geodinamica Acta* 11(2-3), 55-84.
- Räss, L. 2013: Three-Dimensional GPU-Accelerated modelling of Buoyancy-Driven Flow Under Horizontal Far-Field Stress. Master Thesis, University of Lausanne, Switzerland.
- Simon, N. S. C., Podladchikov, Y. Y. & Johansen, H. 2011 : Dynamic permeability due to physical coupling of reactive CO<sub>2</sub>-flow and deformation. *Sustainable Earth Sciences - SES*, extended abstract. EAGE, Valencia, Spain.
- Simon, N. S.C., Räss L., Podladchikov, Y. Y., Souche A., & Yarushina, Y. 2013 : Predicting dynamically evolving permeability, localization of fluid flow and breaching of low permeability barriers in waste storage operations. *Workshop on Geomechanics and Energy*, extended abstract. EAGE, Lausanne, Switzerland.

## P 12.3

## Geochemical and structural data for the evaluation of the geothermal potential

Linda Soma<sup>1,2</sup>, Christian Ambrosi<sup>1</sup>, Daniel Bernoulli<sup>3</sup>, Lorenzo Bonini<sup>2</sup>, Sebastian Pera<sup>1</sup> & Silvio Seno<sup>1,2</sup>

<sup>1</sup> *Institute of Earth Sciences, SUPSI, Campus Trevano, CH-6952 Canobbio*

<sup>2</sup> *Department of Earth and Environmental Sciences, University of Pavia, Via Ferrata 1, IT-27100 Pavia*

<sup>3</sup> *Geologisch-Paläontologisches Institut, University of Basel, Bernoullistrasse 32, CH-4056 Basel*

The aim of the research is to identify suitable areas for high-enthalpy geothermal exploitation in Tessin, Switzerland. The research is focused on the test site of Stabio, located in the southern part of the country, close to the border with Italy. The site is characterized by the presence of springs, with a different geochemistry and temperature from those in nearby areas. These waters could be related to existing geological structures like the Gonfolite backthrust. A coupled structural and hydrogeological model has been developed to check the feasibility for geothermal exploration.

The geological-structural model is based on all the available data: surface data (lithological information, dip data, maps), drillings and seismic reflection lines from the Swiss National Research Programme NRP-20. Detailed surveys were conducted to derive geological cross-sections. Moreover, these data, in association with the chemistry of waters (basic chemistry, isotopes and noble gases), allow the team to formulate hypothesis about the origin and the preferred flowpath of the springs, to understand whether these springs could have a deep origin.

To better constrain the geological-structural model it is necessary to know the precise depth of the bedrock top. Where this information is lacking, a passive seismic method (3D geophone) has been applied to improve information about the depth of bedrock. This permits to produce a geophysical monodimensional model of the subsoil. At the first stage, in the areas where there are stratigraphic data available, this method will be applied to understand the changes in the geophysical models in different points of the area, then it will be applied in the nearby areas, where the depth of bedrock is lacking.

Geological and geochemical data are integrated in a 3D data base through the use of Move™ software.

## REFERENCES

- Bernoulli, D. Bertotti, G. & Zingg, A. 1989: Northward thrusting of the Gonfolite Lombarda („South-Alpine Molasse“) onto the Mesozoic sequence of the Lombardian Alps: implications for the deformation history of the Southern Alps, *Eclogae Geologicae Helveticae*, 82, 841-856.

# 13. Atmospheric predictability, phenology and seasonality

Michael Sprenger & Tobias Grimbacher, This Rutishauser, Martine Rebetez

*Swiss Meteorological Society,  
Swiss Commission for Phenology and Seasonality*

## TALKS:

- 13.1 Eugster M.: Seasonal observations with automated camera (PhenoCam)
- 13.2 Giannakaki P., Rompainen-Martius O.: Forecast errors of Rossby waveguides
- 13.3 Grams C.: Forecast uncertainty for the midlatitude flow
- 13.4 Høye T.: Rapid phenological responses to arctic climate change across trophic levels
- 13.5 Hüsler F., Jonas T., Wunderle S.: Snow cover from satellite data: valuable information for phenological investigations
- 13.6 Kuszli C.-A., Goyette S., Beniston M.: Improvement of a windgust parametrization with an application using the Canadian Regional Climate Model over Switzerland
- 13.7 Sprenger M., Meyer D., Piaget N.: The interannual variability of Foehn - Linking the long Foehn timeseries at Altdorf with the 20th Century Reanalysis
- 13.8 Vitasse Y.: Seasonality of freezing resistance in temperate trees
- 13.9 Vogel R., Erdin R., Frei C.: Quantifying the uncertainty of spatial precipitation analyses with observation ensembles
- 13.10 Wartenburger R., Brönnimann S., Stickler A.: Observation errors in historical upper-air observations
- 13.11 Wheeler J., Wipf S., Hoch G., Cortes A., Sedlacek J., Rixen C.: Longer, warmer, less productive: the effects of early snowmelt and warming on Alpine shrub *Salix herbacea*

## POSTERS:

- P 13.1 Egli S., Büntgen U.: Linking long-term European mushroom productivity and phenology to climate variability
- P 13.2 Koch E., Jurkovic A., Lipa W.: [www.pep725.eu](http://www.pep725.eu) – the Pan European Phenological database
- P 13.3 Rutishauser T., Brönnimann S.: «OpenNature» for climate impact science with citizens

## 13.1

### Seasonal observations with automated camera (PhenoCam)

Markus Eugster<sup>1</sup>, Dr. Werner Eugster<sup>2</sup>, Simon Eugster<sup>3</sup>, Iris Huber<sup>2</sup>

<sup>1</sup> Sekundarschule, Schoentalstrasse 2, 9244 Niederuzwil (markus.eugster@schule-uzwil.ch)

<sup>2</sup> ETH Zurich, Institute of Agricultural Sciences, LFW C56, Universitaetsstrasse 2, 8092 Zurich, (werner.eugster@usys.ethz.ch / huberir@student.ethz.ch)

<sup>3</sup> ETH Zurich, Rämistrasse 101, 8092 Zurich (simon.eu@gmail.com)

#### Introduction

This project arose when GLOBE Switzerland collaborated with the ETH CCES@school project. I present you the result of collaboration between scientists and students. It also shows a way to connect science and education. Scientists are friendly invited to join in, use this project and give feedback.

#### Investigation

The original aim was to detect green-up with automated cameras which delivered a film that was analyzed by an existing software for green-fraction. As the project's target group was Sek I we decided to develop a borrowable box with all the material, a powerful and easy to use specific software and to use a modular structure for the different applications. As there is no official colour model for phenological phases we decided to choose among existing colour models and propose an interesting solution: the HSV colour model.

#### Solution

Short overview of what will be presented in detail:

1. Film: (Figure 1) Load all the pictures into a computer and choose the appropriate ones which are converted into a time lapse clip.

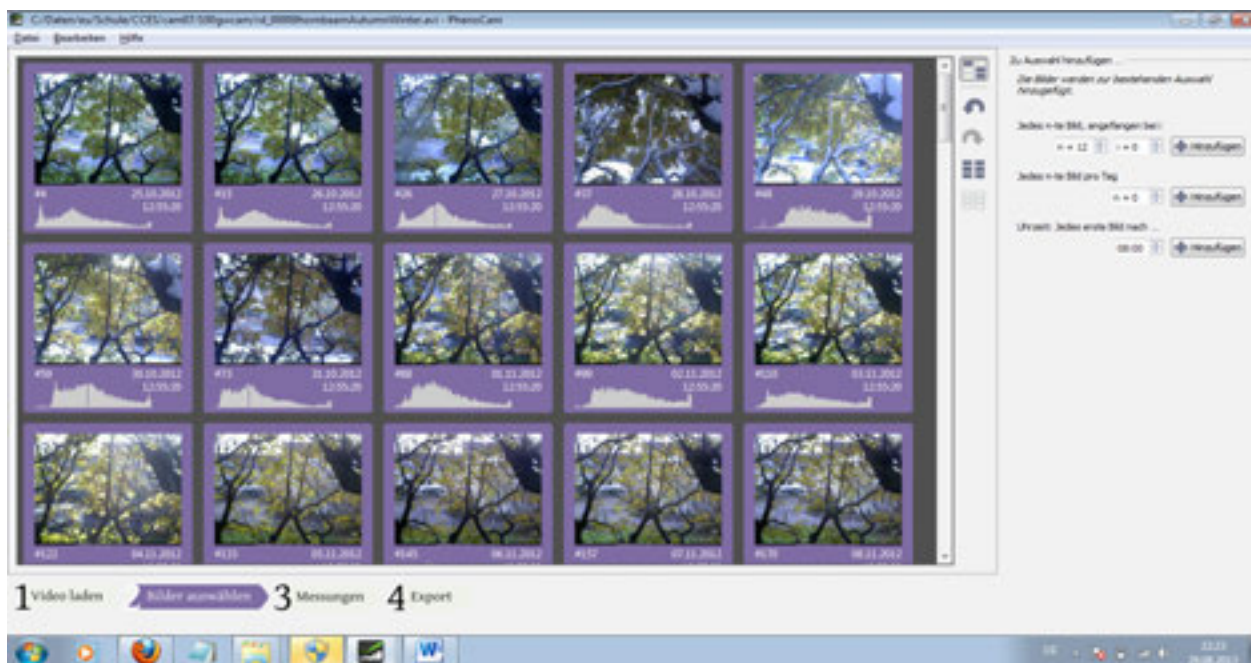


Figure 1: overview of the selected pictures

2. Analysis: (Figure 2) Define the area(s) and the method the colour analysis is conducted with.

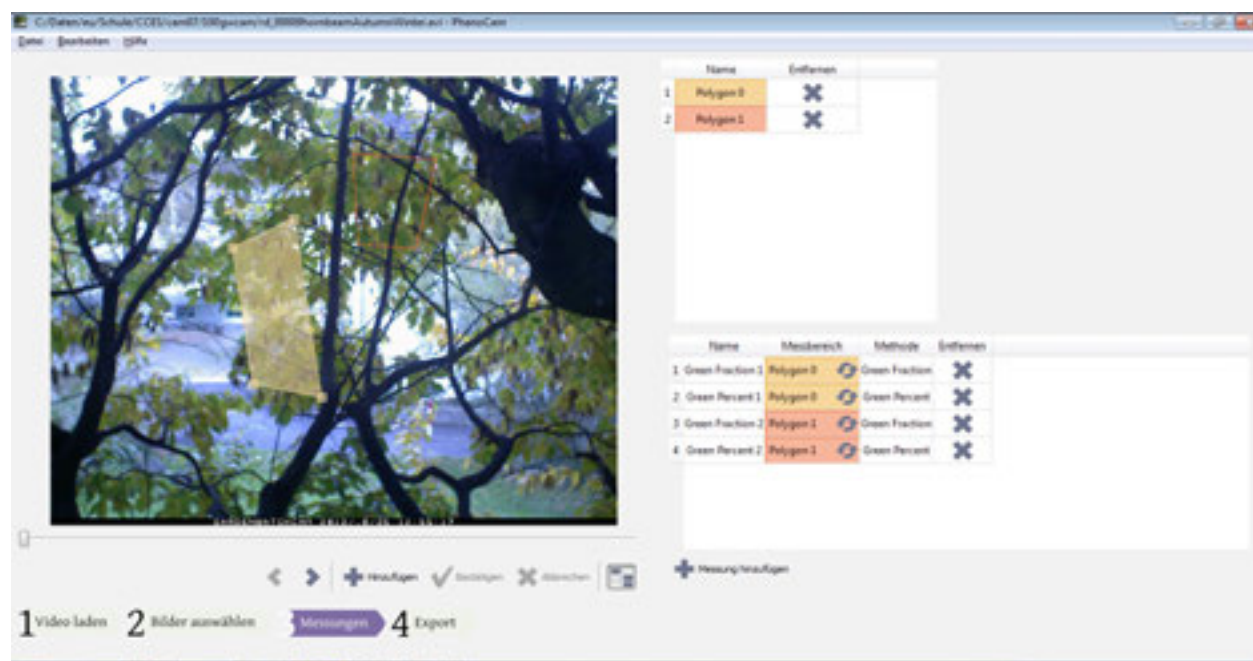


Figure 2: Definition of the areas to analyze and the methods

3. Export: Export the colour analysis results into tables.

4. Results: (Figure 3) Convert the data into graphics. Interpret the graphics.

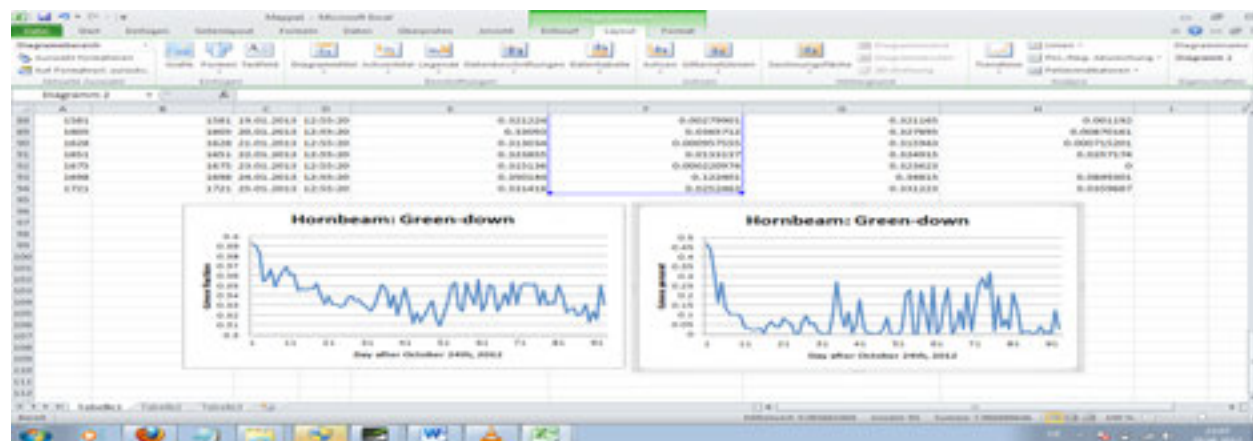


Figure 3: The diagrammed data of Polygon 0, analyzed with two different methods, shows the decreasing green in October 2012.

### Practice and references

There are many possible uses for this project as for example green-up, crystallization, cloud formation, green-down, snow and ice cover, blooming period, etc.

Download of the software: <http://phenocam.granjow.net/download.html>

The project's web page will be: <http://www.swissfluxnet.ch/phenocam>

## 13.2

### Forecast errors of Rossby waveguides

Giannakaki Paraskevi<sup>1</sup>, Romppainen-Martius Olivia

<sup>1</sup> *Institute of Geography, Oeschger Center for Climate Change Research, University of Bern, Hallerstrasse 12, 3012 Bern (paraskevi.giannakaki@giub.unibe.ch)*

The significance of upper level Rossby wave trains (RWTs) for weather forecasting has long been recognised. More recently Langland et al. (2002) found that RWTs originating over Western Pacific may play an important role for the middle and long range predictability of high impact weather events over North America and beyond. Dirren et al. (2003) analysed forecast errors from a PV perspective and they found that errors are concentrated along the waveguide of RWTs due to amplitude or phase errors of RWTs. However, our knowledge of the factors limiting the predictability of RWTs and the forecast skill of numerical weather prediction systems with respect to RWTs is still limited.

Our research is focused on the forecast errors of spatially localized areas of high PV gradients which act as waveguides for the RWTs (Schwierz et al. 2004). An object based spatial forecast verification tool has been developed which compares form, amplitude and location characteristics of waveguide objects in the analysis and in a forecast. As input ECMWF analysis and deterministic forecast data of ECMWF's Integrated Forecast System (<http://www.ecmwf.int/research/ifsdocs/>) were used. A short climatology of forecast errors is presented for the period 01/2008-12/2010 for short and medium range forecast lead times (1day-10days). These climatology is used to derive error statistics as a function of season and location and to identify time periods where large errors occur.

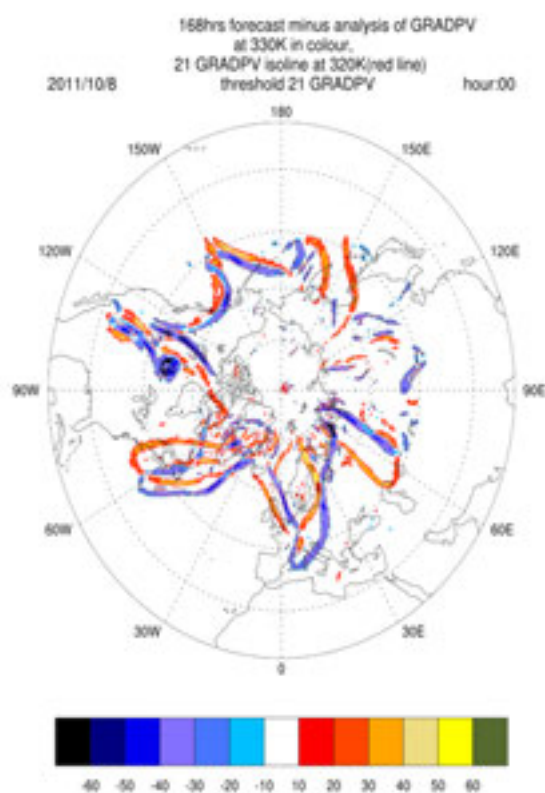


Figure 1. (08/10/2011,00UTC) 7days Forecast minus analysis of GRAD(PV) @ 330K in colour using a threshold of 18 pvu/1000km.

#### REFERENCES

- Dirren, S., M. Didone, & H.C.Davies, 2003: Diagnosis of forecast-analysis differences of a weather prediction system. *Geophys. Res. Lett.* 30 (20),2060.
- Langland, R., M. Shapiro, & R.Gelaro, 2002: Initial condition sensitivity and error growth in forecasts of the 25 January 2000 East Coast snowstorm. *Monthly Weather Review*, 130, 957-974.
- Schwierz, C., S.Dirren, and H.C.Davies. 2004: Forced waves on a zonally aligned jet stream. *J. Atmos. Sci.*,61,73-87.

## 13.3

### Forecast uncertainty for the midlatitude flow

Christian M. Grams<sup>1</sup>

<sup>1</sup> *Institute for Atmospheric and Climate Science, ETH Zürich, Universitätstrasse 16, 8092 Zürich, Switzerland  
(christian.grams@env.ethz.ch)*

The large-scale midlatitude flow is dominated by a strong horizontal temperature gradient that serves as the midlatitude wave guide and results in the upper-level midlatitude jet. Deflections of the midlatitude wave guide, so-called Rossby waves, trigger synoptic-scale weather systems, i.e. extratropical cyclones or anticyclones, which in turn are responsible for local surface weather. Despite the overall progress in numerical weather forecasting periods with poor forecast skill for the large-scale midlatitude flow still occur and the correct prediction of individual weather systems, their track, structure, intensity, and associated (high impact) weather remains a challenge for general circulation models. In this presentation forecast uncertainty for the midlatitude flow is discussed by elucidating interactions on various temporal and spatial scales based on examples from current research.

First, basic concepts for quantifying the forecast error of the large-scale midlatitude flow are introduced. A recent example of an Alpine flooding event reveals caveats of this approach and how also relatively small error in the representation of the Rossby wave pattern lead to significant forecast error of local surface weather. Then the interaction of tropical cyclones with the midlatitude flow during extratropical transition serves as an illustrative example on how individual weather systems can modify the upper-level flow. It is shown that during extratropical transition rapidly ascending air streams, so-called warm conveyor belts, are able to modify or trigger upper-level Rossby waves so that a Rossby wave train may emerge that significantly alters the weather in downstream regions. This interaction crucially depends upon the phasing of the tropical cyclone and the midlatitude flow which is an important source for forecast uncertainty. Finally extratropical cyclones linked to high impact weather and their forecast error in the deterministic ECMWF model is investigated based on a two-year climatology. The outlook emphasises the need for a better understanding of the basic physical and dynamical processes that govern the interactions on the various scales associated with the midlatitude flow.

## 13.4

### Rapid phenological responses to arctic climate change across trophic levels

Høye, T.<sup>1</sup>

<sup>1</sup> *Arctic Research Centre and Department of Bioscience, Aarhus University, Denmark (toh@dmu.dk)*

Advancing phenology in response to global warming has been reported across biomes raising concerns about the temporal uncoupling of trophic interactions. Phenological responses in the Arctic have been shown to outpace responses from lower latitudes and recent studies suggest that differences between such responses for e.g. plants and their flower visitors could be particularly pronounced in the Arctic. The evidence for phenological uncoupling is scant because relevant data sets are lacking or not available at a relevant spatial scale. One notable exception is the long-term monitoring program at Zackenberg in North-east Greenland, where detailed phenological observations have been carried out since 1996. North-east Greenland has experienced a dramatic rise in temperatures in the past two decades. In this talk, I present evidence of rapid phenological changes to recent dramatic warming at Zackenberg across plants, arthropods and birds. Our results demonstrate important landscape scale spatial variation in phenological responses. As an example, we found a climate-associated shortening of the flowering season and a concomitant decline in flower visitor abundance. The shortening of the flowering season arose through spatial variation in phenological responses to warming. Our results demonstrate that the dramatic climatic changes currently taking place in the Arctic are strongly affecting individual species and ecological communities, with implications for trophic interactions.

## 13.5

### Snow cover from satellite data: valuable information for phenological investigations

Hüsler Fabia<sup>1,2</sup>, Jonas Tobias<sup>3</sup>, Wunderle Stefan<sup>1,2</sup>

<sup>1</sup> Geografisches Institut der Universität Bern, Hallerstrasse 12, CH-3012 Bern (fabia.huesler@giub.unibe.ch)

<sup>2</sup> Oeschger Center for Climate Research, Universität Bern, Zähringerstrasse 25, CH-3012 Bern

<sup>3</sup> WSL Institute for Snow and Avalanche Research SLF, Flüelastrasse 11, CH-7260 Davos Dorf

Alpine plants may be very sensitive indicators of ecosystem response patterns to climatic changes. Therefore, they are considered to be particularly suitable for studies of a variety of phenomena on relatively small spatial scales as the complex topography results in highly variable climatic zones on short horizontal and vertical distances. Particularly in these regions snow cover duration is an important factor, which determines the timing of the flowering and limits the growing season length of plants. Hence, it is of great interest to consider knowledge of snow onset, snow duration as well as snow melt-out information in phenological investigations. Complementary to pointwise station data, snow cover parameters derived from optical satellite imagery offer an attractive option to gain comprehensive information even in complex terrain and remote areas.

The University of Bern receives and archives daily full resolution (1.1 km) satellite data over Europe acquired by the Advanced Very High Resolution Radiometer (AVHRR) since 1984. This historical dataset offers a unique source of information for understanding long-term changes and interannual variability in alpine snow cover extent and duration. Hence, we present the first comprehensive space-borne 1-km snow extent climatology for the Alpine region for the period 1985–2011 and demonstrate the potential of such data to be used in phenological applications. Parameters such as snow cover area percentage, snow onset day, snow cover duration, and melt-out date were calculated and employed to analyze the spatio-temporal variability and interannual differences in the seasonality of snow cover over the course of the last three decades. The dataset will be made available for research purposes upon request.

#### REFERENCES

Hüsler, F., Jonas, T., Riffler, M., Musial, J. P., and Wunderle, S.: A satellite-based snow cover climatology (1985–2011) for the European Alps derived from AVHRR data, *The Cryosphere Discuss.*, 7, 3001-3042, doi:10.5194/tcd-7-3001-2013, 2013.

## 13.6

### Improvement of a windgust parametrization with an application using the Canadian Regional Climate Model over Switzerland

Kuszli Charles-Antoine; Goyette Stéphane ; Martin Beniston

*Université de Genève*

Severe winds recorded during a number of winter storms are simulated over the period 1990 to 2011 with the Canadian Regional Climate Model (CRCM) at a high spatial resolution. Flow fields are first downscaled from NCEP-NCAR reanalyses and then down to 2-km grid spacing in the horizontal through a self-nesting technique. During this last step, different windgust schemes of different complexities were tested and their performances compared one to each other and to observations from MeteoSwiss national network. Simple schemes reproduced the surface observations in an overall realistic manner but differences are noticed in the hourly maximum values. In order to improve one of the simple schemes, an empirically fixed parameter in the formulation is now allowed to vary in the horizontal where values have been calibrated using the MeteoSwiss stations hourly wind maximum. Then, these unequally-spaced values are interpolated onto the model surface computational grid. The CRCM using this modified scheme is applied on the 2-km grid in order to qualify and quantify the changes of the hourly gust values. The improvements are noticeable where hourly differences between observed and simulated values are reduced at several stations. This modified simple gust scheme would be useful in numerical weather prediction modelling where an application is envisaged in the near future.

## 13.7

### The interannual variability of Foehn - Linking the long Foehn timeseries at Altdorf with the 20th Century Reanalysis

Sprenger M, Meyer D., Piaget N.

*ETH Zurich*

A long time series (1864-2010) of Foehn for Altdorf shows a pronounced interannual variability. In this study, the variability is analysed based on the twentieth century reanalysis dataset (20CR). The aim of the study is to see whether the Foehn variability is related to corresponding weather type variations in 20CR.

In a first approach, the Weusthoff classification, with 18 different classes, is used. For the whole 20CR period (1871-2010) the weather type is determined, and monthly probabilities  $P(\text{weather type})$  are calculated. Conditional probabilities  $P(\text{foehn}|\text{weather type})$  are established based on a training period from 1980-2010. Then, the 20CR data are used to reconstruct a model-based Foehn timeseries, which is compared to the observed one. It turns out that the two timeseries do not strongly correlate, i.e. that the interannual Foehn variability cannot be explained based on the Weusthoff weather classification.

The same methodology is repeated with a second weather classification which is specifically constructed based on relevant Foehn characteristics. The parameters extracted from the 20CR are: pressure difference across the Alps, wind speed and direction at 700 hPa and wind at 500 hPa. Weather types are defined based on the typical values during Foehn. The outcome justifies the special choice of a Foehn-related classification: The correlation between reconstructed and observed timeseries improves, although it still is not able to explain the strong interannual variability.

Based on the partly negative outcome of the reconstruction, the possible reasons for disagreement are discussed and further, more refined methodologies are presented.

## 13.8

### Seasonality of freezing resistance in temperate trees

Yann Vitasse, Armando Lenz, Günter Hoch, Christian Körner

*Institute of Botany, University of Basel, 4056 Basel, Switzerland.*

<sup>1</sup>Corresponding author: Yann Vitasse. Tel. +41 (0)61 267 35 06, Fax: ++41 (0)61 267 29 80, e-mail: [yann.vitasse@unibas.ch](mailto:yann.vitasse@unibas.ch)

Trees have evolved to optimize their phenology against the risk of freezing injuries in autumn, winter and early spring. Here we aim to give new insights about the relationship between phenology of various tree species, species-specific freezing resistance and the risk that trees encounter freezing damage in the Swiss Alps.

Specifically, we showed that (i) the level of freezing resistance of buds in winter during dormancy strongly depends on preceding temperatures, so that a cold spell in winter can substantially harden tree buds; (ii) the most critical period for temperate trees occurs during flushing in spring when the freezing resistance reaches the lowest value; (iii) the timing of leaf-out converges towards a similar risk of freeze damage within species among different sites and among species within a same site; (iv) young trees exhibit similar freezing resistance as adult trees during flushing, but are more prone to undergo freeze damage due to their earlier spring phenology.

## 13.9

# Quantifying the uncertainty of spatial precipitation analyses with observation ensembles

Vogel Raphaela<sup>1</sup>, Erdin Rebekka<sup>1</sup>, Frei Christoph<sup>1</sup>

<sup>1</sup> Federal Office of Meteorology and Climatology MeteoSwiss, Krähbühlstrasse 58, CH-8044 Zürich ([raphaela.vogel@meteoswiss.ch](mailto:raphaela.vogel@meteoswiss.ch))

It has become popular to call for precipitation analyses at higher and higher spatial resolution. Finer grid spacing may satisfy these requests from a purely technical viewpoint, but the scales effectively resolved in such “high-resolution” analyses are constrained by the resolution and accuracy of the underlying observations. As a result, there are large uncertainties, which may be relevant for the outcome of an application. However, there is little quantitative information about these uncertainties. We propose to frame knowledge about spatial precipitation distributions by ensembles of fields, randomly generated, but conditioned on measurements. They shall quantify uncertainties due to limited observation density. In this study, we develop an ensemble approach for a radar rain-gauge combination over Switzerland and present results of km-scale, daily precipitation ensembles for several cases.

The ensemble simulation is based on the stochastic concept of random Gaussian fields with a spatially varying mean and a second order stationary covariance. The concept is identical to that for kriging rain-gauge observations using radar as external drift. Our implementation involves a case dependent data transformation to better comply with the Gaussian model and the stationarity assumption. Uncertainty estimates obtained with this stochastic concept turned out to be reasonably reliable (in a statistical sense) as was verified by cross-validation. Our applications suggest that there can be considerable residual uncertainty in km-scale precipitation patterns, even when radar information is included. The degree of uncertainty, however, varies considerably from case to case with typically larger ensemble spread for convective cases. The ensembles bear plausible dependencies upon aggregation scale (mean over catchments of different size) and network density. Observation ensembles may be a promising alternative to “best estimate” grid datasets, especially when uncertainties are large and when it is desirable to propagate them into application models.

## 13.10

## Observation errors in historical upper-air observations

Wartenburger Richard<sup>1</sup>, Brönnimann Stefan<sup>1</sup>, Stickler Alexander<sup>1</sup><sup>1</sup>Oeschger Centre for Climate Change Research & Geographical Institute, University of Bern, Hallerstr. 12, CH-3012 Bern

Upper-air observations are a fundamental data source for global atmospheric data products, but uncertainties, particularly in the early years, are not well known. Most of the early observations, which have now been digitized, are prone to a large variety of undocumented uncertainties (errors) that need to be quantified, e.g. for their assimilation in reanalysis projects. We apply a novel approach to estimate errors in upper-air temperature, geopotential height and wind observations from the Comprehensive Historical Upper-Air Network (CHUAN (Stickler et al. 2010); 1904 – 1966). We distinguish between random errors, biases, and a term that quantifies the representativity of the observations. The method is based on a comparison of neighboring observations and is hence independent of metadata, making it applicable to a wide scope of observational datasets. The estimated mean random errors for all observations within the study period are 1.5K for air temperature, 1.3hPa for pressure, 3.0ms<sup>-1</sup> for wind speed and 21.4° for wind direction. The estimates are compared to results of previous studies and analyzed with respect to their spatial and temporal variability. Figure 1 shows the mean vertical error profiles.

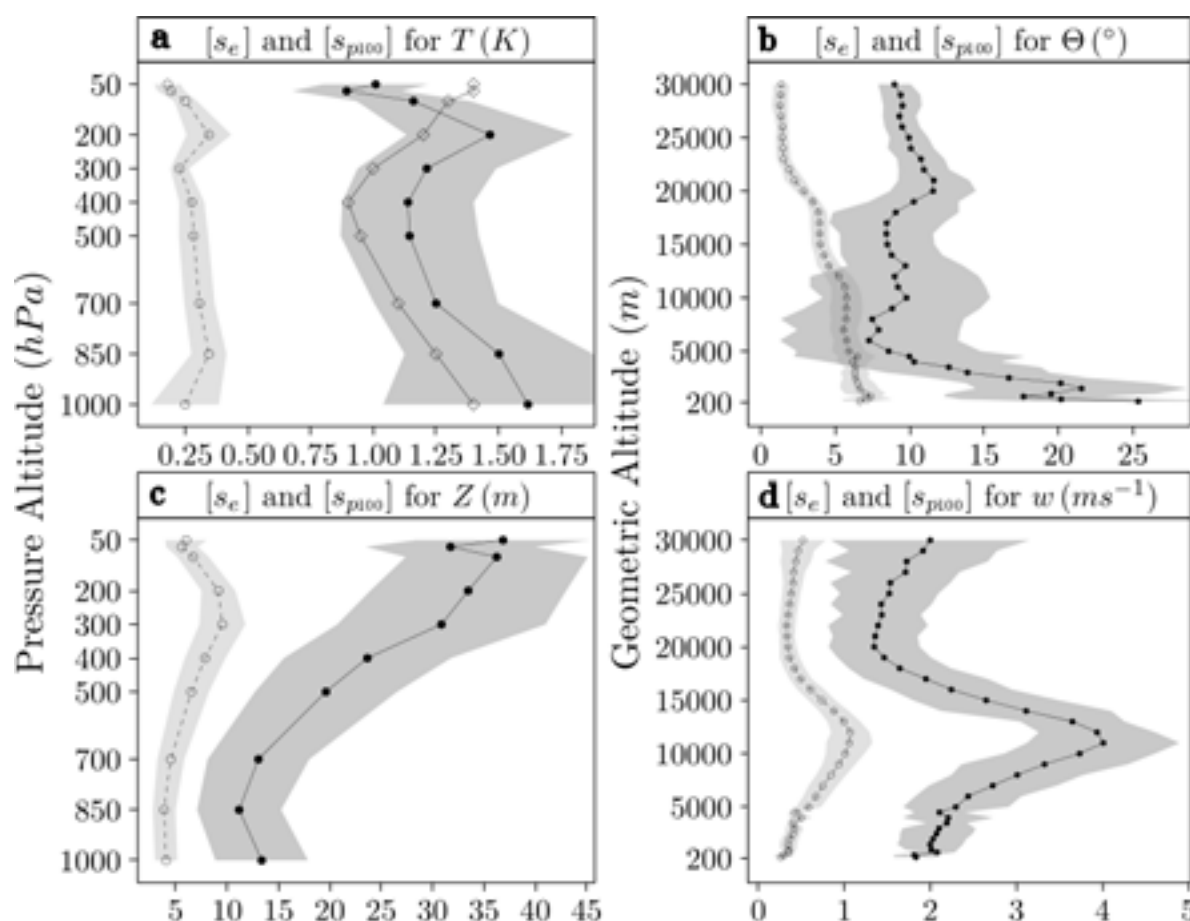


Figure 1: Profiles of estimates of mean random errors  $[s_e]$  (solid lines with filled circles) and representativity errors  $[s_{p100}]$  (dashed lines with open circles) for a) temperature, b) wind direction, c) geopotential height, and d) wind speed. Open diamonds correspond to observation errors assumed in the ERA-Interim reanalysis. Shaded bands indicate the standard deviations of the random errors (medium gray) and representativity errors (light gray) for all stations; their overlap is printed in dark gray. Levels with less than 30 error estimates were omitted.

## REFERENCES

Stickler, A., A. Grant, T. Ewen, T. Ross, R. Vose, J. Comeaux, P. Bessemoulin, K. Jylhä, W. Adam, P. Jeannet, A. Nagurny, A. Sterin, R. Allan, G. Compo, T. Griesser, and S. Brönnimann (2010), The Comprehensive Historical Upper-Air Network, *B. Am. Meteorol. Soc.*, 91, 741-751.

## 13.11

### Longer, warmer, less productive: the effects of early snowmelt and warming on alpine shrub *Salix herbacea*

Wheeler Julia<sup>1,2</sup>, Wipf Sonja<sup>1</sup>, Hoch Guenter<sup>2</sup>, Cortes Andres<sup>3</sup>, Sedlacek Janosch<sup>4</sup> & Rixen Christian<sup>1</sup>

<sup>1</sup> WSL Institute for Snow and Avalanche Research SLF, CH-7260 Davos, Switzerland (julia.wheeler@slf.ch)

<sup>2</sup> University of Basel, Institute of Botany, CH-4056 Basel, Switzerland

<sup>3</sup> University of Uppsala, Evolutionary Biology Centre, 752 36 Uppsala, Sweden

<sup>4</sup> University of Konstanz, Department of Biology, 78457 Konstanz, Germany

Growing seasons are beginning earlier in many alpine systems due to accelerating snowmelt. Currently, it is poorly understood whether longer growing seasons will benefit alpine shrubs. Determining species-specific responses, particularly in common and dominant species, is critical for understanding how alpine communities will alter or adapt to changing climates. We studied a wide range of fitness traits in *Salix herbacea*, a prostrate dwarf shrub, along elevational and snowmelt gradients for two seasons, in order to determine the overall response to an unmanipulated extended growing season and overall warmer temperatures.

We recorded phenology, reproductive capacity, growth and leaf damage for 480 *S. herbacea* shrubs. The shrubs were marked from 2100-2800 m asl, representing the core species range on three mountains, in two snow microhabitat types (early-exposure ridges and late snowbeds) and were monitored weekly for two seasons. Snowmelt date and soil temperatures were recorded.

From snowmelt to each phenophase (leaf open, flowering, fruiting), shrubs required fewer days to develop with later snowmelt and at lower elevations, suggesting temperature accumulation thresholds required for development. Percent stems flowering decreased with elevation and with later snowmelt, while percent stems fruiting decreased significantly with elevation but were consistent across the snowmelt gradient. Stem density, leaf area and fall wood NSCs all increased with later snowmelt. Likelihood of leaf herbivory and gall damage decreased with later snowmelt, while lower elevation shrubs were more likely to be damaged by fungi.

Although *S. herbacea* appears to allocate more energy to flower production under early snowmelt, fruit production is constant along the snowmelt gradient. Warmer temperatures at lower elevations lead to more fruit and larger leaves but this does not translate to increased local growth or competitive advantage. Increased likelihood of leaf damage during early snowmelt and at warmer temperatures could lead to long-term reductions in fitness. Longer development time to each phenophase under early snowmelt could lead to increased exposure to frost during vulnerable early development stages. Thus, we conclude an overall detrimental effect of a longer growing season and warmer temperatures for *S. herbacea*.

## P 3.1

# Linking long-term European mushroom productivity and phenology to climate variability

Egli Simon<sup>1</sup> & Büntgen Ulf<sup>1,2</sup>

<sup>1</sup> Swiss Federal Research Institute WSL, Birmensdorf, Switzerland (simon.egli@wsl)

<sup>2</sup> Oeschger Centre for Climate Change Research (OCCR), Bern, Switzerland (ulf.buentgen@wsl.ch)

Fruit-body production of wild forest mushrooms fluctuates considerably from year to year, mainly due to interannual meteorological variability. Water availability and temperature during summer are recognized to be the key factors for fruit-body formation (Büntgen et al. 2012a).

New findings reveal short-term weather fluctuations to be superimposed on long-term trends of climate change. An analysis of weekly fruit-body counts of 115,417 mushroom species from permanent Swiss inventories between 1975 and 2006 exhibit an average autumnal delay of 12 days after 1991 compared with before (Büntgen et al., 2013). Intra- and interannual coherency of symbiotic and saprotrophic mushroom fruiting, together with little agreement between mycorrhizal yield and tree growth suggests direct climate controls on fruit body formation of both nutritional modes.

These findings are in agreement with European-wide phenological observations (Kausserud et al. 2012). Mushroom records of 486 autumnal fruiting species from Austria, Norway, Switzerland, and the UK commonly describe an extended annual fruiting season during the 1970-2007 period.

These two examples are indicative for positive effects of climate change on ecosystem functioning and productivity. In contrast depicts the high-valued Périgord truffle, another mycorrhizal species, a negative example of how climate change can affect fungal yield. A continuous decline in Périgord truffle production has been reported for many Mediterranean habitats and the past four decades. Increasing summer temperatures and decreasing precipitation totals may cause fading harvests, which subsequently trigger local economic uncertainty and global prize inflation (Büntgen et al. 2012b).

If climate change will continue as predicted by climate model ensembles, the distribution range of European truffle species will be highly affected by increasing summer drying. *T. melanosporum* may be less productive in its traditional Mediterranean habitats, whereas *T. aestivum* could even benefit from a slightly warmer climate north of the Alpine arc. Even though only some edible mushrooms are among the world's most expensive delicacies, most of them are mycorrhizal and thus essential for forest ecosystem health.

A better understanding of growth-climate interactions therefore describes a direct ecological and economic interest, especially for populations in more rural areas of Europe.

## REFERENCES

- Büntgen, U., Peter, M., Kausserud, H. & Egli, S. 2013: Unraveling environmental drivers of a recent increase in Swiss fungi fruiting. *Global Change Biology* 19, 2785-2794.
- Büntgen, U., Kausserud H., Egli S. 2012a: Linking climate variability to mushroom productivity and phenology. *Frontiers in Ecology and the Environment* 10(1), 14-19.
- Büntgen, U., Egli, S., Camarero, J.J., Fischer, E.M., Stobbe U., Kausserud, H., Tegel, W., Sproll, L., Stenseth, N.C. 2012b: Drought-induced decline in Mediterranean truffle harvest. *Nature Climate Change* 2, 827-829.
- Kausserud, H., Heegaard, E., Ulf Büntgen, U., Halvorsen, R., Egli, S., Boddy, L., Senn-Irlet, B., Greilhuber, I., Dämon, W., Sparks, T., Nordén, J., Høiland, K., Kirk, P., Semenov, M., Stenseth, N.C. 2012: Warming-induced shift in European mushroom fruiting phenology. *PNAS* 109 (36), 14488-14493.

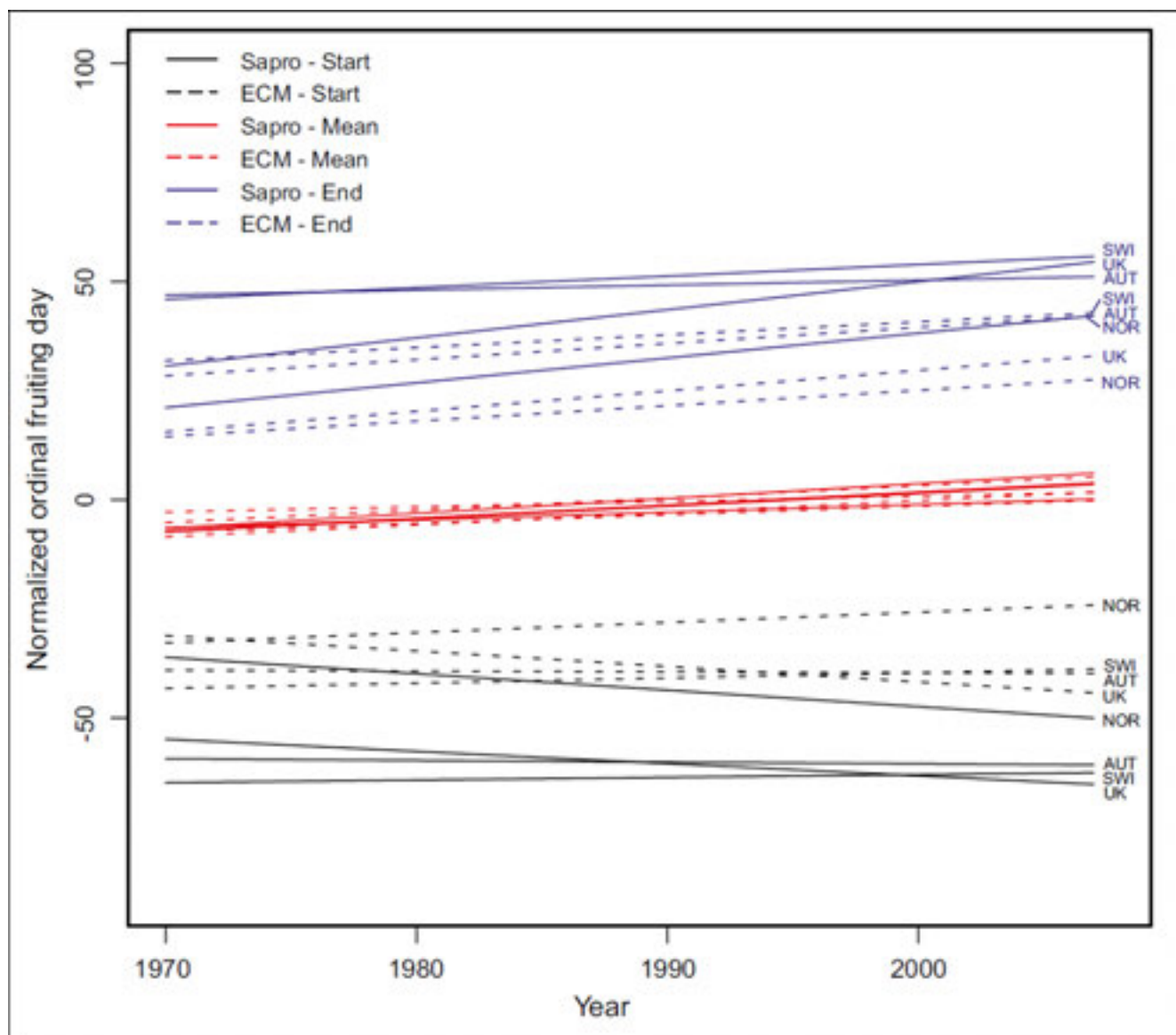


Figure 1. The number of days of change in start, mean, and end of fruiting season during the period 1970–2007, averaged over all species and split according to countries and nutritional mode (saprotrophic or ECM). The 2.5th percentiles reflect changes in season start and the 97.5th percentiles changes in season end. The sampling intensities are accounted for within the model, and the plots here illustrate the expected trends at average intensities,  $\ln(N + 1) = 2.2 - 10$  individuals per year. Abbreviations: AUT, Austria; ECM, ectomycorrhizal fungi; NOR, Norway; sapro, saprotrophic fungi; SWI, Switzerland (from Kauserud et al., 2012).

## P 13.2

### www.pep725.eu – the Pan European Phenological database

Koch Elisabeth<sup>1</sup>, Jurkovic Anna<sup>1</sup>, Lipa Wolfgang<sup>1</sup>, Ungersböck Markus<sup>1</sup>, Zach-Hermann Susanne<sup>1</sup>

<sup>1</sup> Zentralanstalt für Meteorologie und Geodynamik, 1190 Vienna, Austria ([pep725@zamg.ac.at](mailto:pep725@zamg.ac.at))

Modern phenology is the study of the timing of recurring biological events in the animal and plant world, the causes of their timing with regard to biotic and abiotic forces, and the interrelation among phases of the same or different species. Leaf unfolding, flowering of plants in spring, fruit ripening, colour changing and leaf fall in autumn as well as the appearance and departure of migrating birds and the timing of animal breeding are all examples of phenological events. And phenology is perhaps the simplest way to track ecological changes due to climate change.

PEP725 is a 5 years project with the main object to promote and facilitate phenological research by delivering a pan European phenological database with an open, unrestricted data access for science, research and education. PEP725 is funded by EUMETNET (the network of European meteorological services), ZAMG and the Austrian ministry for science & research [bm:w\\_f](http://bm.w_f).

So far 17 European national meteorological services and 7 partners from different national phenological network operators have joined PEP725. At present more than 8 500 000 phenological events are available in the PEP725 database coming from 31 European countries and from more than 15 000 observation sites. Most of them are in the UK and Germany. A huge number of reports came from the agriculture sector (e.g. Barley - *Hordeum vulgare* 8% of all observations, Potato - *Solanum tuberosum* 6% and Wheat - *Triticum aestivum* 5%) but there are also other plants common (Horse Chestnut - *Aesculus hippocastanum* with 7% or Oak - *Quercus robur*). The data set starts in 1868 with a fast development of the observation network in the 1950s. Until now most of interest for our users are Birch (*Betula*), Sweet Cherry (*Prunus avium*) and Oak (*Quercus robur*). On request of our users there is also a link to freely available meteorological datasets from the European Climate Assessment & Dataset project ([eca.knmi.nl](http://eca.knmi.nl)) over our map-based station browser. Quality checking is also a big issue. At the moment we study the literature to find some appropriate methods.

Another objective of PEP725 is to bring together network-operators and scientists by organizing workshops and symposia. So far three meetings were organized. Invited speakers gave presentations spanning the whole study area of phenology starting from observations to modeling. PEP725 is a co-convenor of the phenology session at EGU2014 in Vienna.

## P 13.3

### “OpenNature” for climate impact science with citizens

Rutishauser This<sup>1</sup>, Brönnimann Stefan<sup>1</sup>, Rebetez Martine<sup>2</sup>, Eugster Werner<sup>3</sup> & project collaborators

<sup>1</sup> Oeschger Centre for Climate Change Research and Institute of Geography, University of Bern, Hallerstrasse 12, CH-3012 Bern (rutis@giub.unibe.ch)

<sup>2</sup> University of Neuchâtel, Neuchâtel, and Swiss Federal Institute for Forest, Snow and Landscape Research WSL, Neuchâtel, Switzerland

<sup>3</sup> Institute of Agricultural Sciences, ETH Zurich, Zurich, Switzerland

With a changing climate, seasons shift, too. The Swiss National Science Foundation (SNF) AGORA science communication project “Open the Book of Nature” aims at collecting evidence seen in daily life, that can also be used to quantify climate change impacts. Data are collected using a “Citizen science” approach to climate change impact research. Interested laypersons engage in documenting shifts in seasonal timing of their environment. Citizen scientists collect geo-referenced and precisely dated field observations and photographs in one or more of the four topics plants, animals, landscapes, and climate extremes. These topics are considered chapters of the Book of Nature that shall be opened and filled with content by these laypersons. Scientists in return will provide observation guidelines (protocols), information from the science community and interpretation to the public.

The main goal of the project is the launch of the “OpenNature” website. In addition, “Open the Book of Nature” plans to deliver a collaboration concept to assure information exchange and technical compatibility, a website and strong links with social media sites for presenting information and fostering discussions. In this project a well-established network of climate change researchers is supported by communication experts in print and web-content journalism, as well as by internet graphics and technical designers. “Open the Book of Nature” builds on existing observations programs (e. g. phaeno.ethz.ch, ornitho.ch, ...) and partnerships in Switzerland under the auspices of the Swiss Academy of Natural Sciences SCNAT. The project is funded by the Swiss National Science Foundation via its AGORA program from 2012–2015. A possible continuation is envisaged in partnership with SCNAT, the educational GLOBE Swiss program, the Global Climate Observation System (GCOS), the phenological observation program by the Swiss Meteorological Office MeteoSwiss and environmental observation programs by Federal Office for the Environment FOEN.

# 14. Cryospheric Sciences

J. Alean, A. Bauder, B. Krummenacher, J. Nötzli, C. Lambiel,  
M. Lüthi, J. Schweizer, M. Schwikowski

*Swiss Snow, Ice and Permafrost Society*

## TALKS:

- 14.1 Finger D., Vis M., Seibert J.: Estimations of glacier-, snow-, and rainfall contribution to alpine streams in the Swiss headwaters
- 14.2 Fischer M., Huss M., Hoelzle M.: Changes in area and volume of all Swiss glaciers over the last 25 years
- 14.3 Haberkorn A., Phillips M., Hoelzle M., Kenner R.: Influences of the seasonal varying snow cover on thermal processes in steep Alpine permafrost rock walls
- 14.4 Kenner R., Phillips M.: Results from five years of ground surface monitoring in mountain permafrost regions using terrestrial laser scanning
- 14.5 Koenig S.J., Foppa N., Fontana F., Seiz G.: Monitoring the Cryosphere in Switzerland and Incentives for Extending Glacier Observations Worldwide
- 14.6 Leinß S., Parrella, G., Hajsek I.: Snow Height Determination by Polarimetric Phase Differences in X-Band SAR Data
- 14.7 Schmucki E., Marty C., Fierz C., Lehning M., Weingartner R.: Future trends of the alpine and ephemeral snowpack at selected sites across Switzerland
- 14.8 Walter F., Rösli C., Dalban Canassy P., Faillettaz J., Husen S., Clinton J. F., Deichmann N., Funk M.: Seismic Monitoring Deployments of the Swiss Institute of Technology (ETH Zurich)

## POSTERS:

- P 14.1 Spence R., Bavay M.: Precipitation Redistribution for Snow Models
- P 14.2 Reiweger, I., Schweizer, J.: Measuring acoustic emissions in an avalanche starting zone to monitor snow stability
- P 14.3 Naegeli K., Huss M., Hoelzle M., Hauck C.: State, changes and impact of glacier surface albedo in the Swiss Alps
- P 14.4 Pellet C., Scherler M., Hauck C.: Soil moisture quantification in mountain permafrost: A model-data comparison between Southern Norway and the Swiss Alps
- P 14.5 Sold L., Hoelzle M., Huss M., Eichler A., Schwikowski M.: Recent accumulation and firn compaction rates on Findelengletscher derived from airborne GPR and firn cores
- P 14.6 Linsbauer A., Haeberli W., Fischer U.H.: On the morphological characteristics of overdeepenings in high-mountain glacier beds
- P 14.7 Barboux C., Fischer M., Delaloye R., Huss M., Collet C.: Mapping of debris-covered ice using DInSAR and airborne photography: A pilot study in the Upper Valais (Swiss Alps)
- P 14.8 Luethi R., Gruber S.: Towards a better understanding of temperature conditions in rock fall detachment areas in permafrost: a computer-simulation approach
- P 14.9 Marmy A., Salzmann N., Scherler M., Hauck C.: Permafrost model sensitivity to seasonal climatic changes and extreme events in mountainous regions
- P 14.10 Haeberli W., Drenkhan F., Torres J., Cochachin A., Salazar C.: Google Earth-based rapid assessment of glacier evolution, lake formation and hazard change – the example of Artesonraju in the Cordillera Blanca, Peru
- P 14.11: Helfricht K., Schneider K., Sailer R., Kuhn M.: Lidar snow cover studies in the Ötztal Alps

## 14.1

# Estimations of glacier-, snow-, and rainfall contribution to alpine streams in the Swiss headwaters

Finger David<sup>1</sup>, Vis Marc<sup>1</sup> & Seibert Jan<sup>1</sup>

<sup>1</sup> Department of Geography, University of Zurich, Wintherturerstr 140, CH-8046 Zurich, Switzerland,

The contribution of glacier-, snow- and rainwater to runoff in mountain streams is of major importance for water resources managers as climate change is expected to distinct impacts on all three sources (e.g. Huss, 2012). While glaciers are retreating worldwide, the snow cover during winter becomes shorter and precipitations events become more intense (e.g. Finger et al., 2012). Besides field investigation such as chemical fingerprints in water samples and artificial tracer experiments (e.g. Finger et al., 2013), the contribution can also be estimated with hydrological models, given that the modeling accounts adequately for snow-, glacier and rainwater runoff (Finger et al., 2011).

We present a multi-variable calibration technique to estimate runoff composition using the conceptual HBV model (Seibert and Vis, 2012). The model code was updated in order to calibrated and validate simulation results with glacier mass balances, satellite derived snow cover area, observed snow heights and continuously measured discharge. We tested our method on two small scale study sites in Switzerland: i) Rhoneglacier and ii) Paradise glacier. Subsequently, we compared the results to similar studies performed with physically based, fully distributed hydrological models (Finger et al., 2011).

Preliminary results indicate that all four observational datasets are reproduced by the model adequately, allowing an accurate estimation of the runoff composition in the two mountain streams. However, the use of one dataset alone to calibrate the model leads to unrealistic snow- and glacier melt (Figure 1). These results are in line with previous studies carried out with a more complex, physically based fully distributed hydrological model (Finger et al. 2011).

Based on these results we conclude that it is essential to use various observational datasets in order to constrain model parameters and compute realistic discharge estimations. Finally, we postulate based on the comparison of model performance of HBV and the physically based, fully distributed model that the availability and use of different datasets to calibrate hydrological models might be more important that model complexity in regard to realistic predictions of runoff composition.

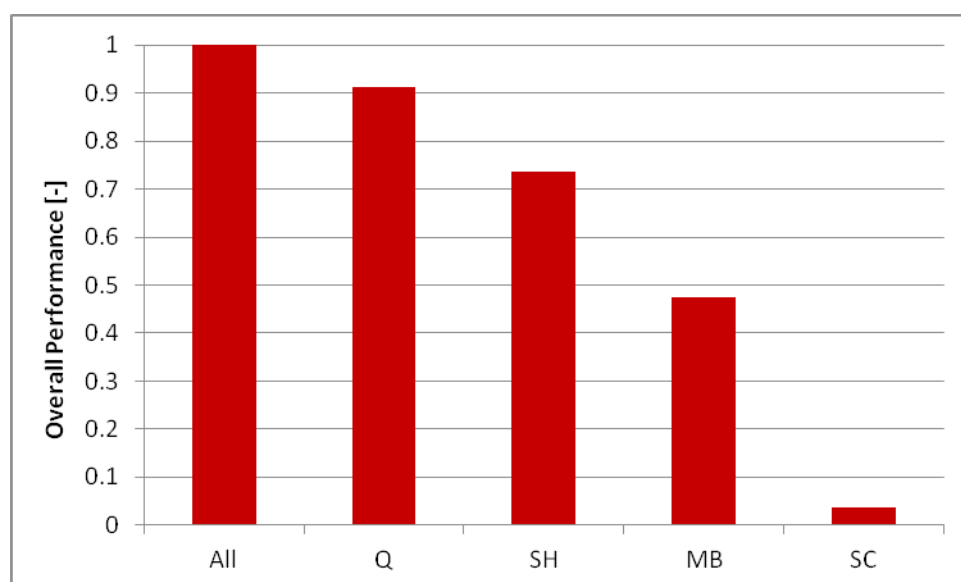


Figure 1. Mean overall performance,  $P_{OA,norm}$ , of the best runs selected with the observational data set indicated on the abscissa (Q: discharge; SH: snow heights; MB: Glacier mass balances; and SC: satellite derived snow cover).

## REFERENCES

- Finger, D., A. Hugentobler, M. Huss, A. Voinesco, H.R. Wernli, D. Fischer, E. Weber, P-Y. Jeannin, M. Kauzlaric, A. Wirz, T. Vennemann, F. Hüsler, B. Schädler, and R. Weingartner (2013). Identification of glacial melt water runoff in a karstic environment and its implication for present and future water availability. *Hydrol. Earth Syst. Sci. Discuss.* 10, 1-45, doi: 10.5194/hessd-10-1-2013.
- Finger, D., Heinrich, G., Gobiet, A., and Bauder, A.: Projections of future water resources and their uncertainty in a glacierized catchment in the Swiss Alps and the subsequent effects on hydropower production during the 21st century, *Water Resources Research*, 48, doi: 10.1029/2011wr010733, W02521, 2012.
- Finger, D., Pellicciotti, F., Konz, M., Rimkus, S., and Burlando, P.: The value of glacier mass balance, satellite snow cover images, and hourly discharge for improving the performance of a physically based distributed hydrological model, *Water Resources Research*, 47, doi: W07519, 10.1029/2010wr009824, 2011.
- Huss, M.: Present and future contribution of glacier storage change to runoff from macroscale drainage basins in Europe, *Water Resources Research*, 47, doi: W07511, 10.1029/2010wr010299, 2011.
- Seibert, J., and Vis, M. J. P.: Teaching hydrological modeling with a user-friendly catchment-runoff-model software package, *Hydrol. Earth Syst. Sci.*, 16, 3315-3325, doi: 10.5194/hess-16-3315-2012, 2012.

## 14.2

### Changes in area and volume of all Swiss glaciers over the last 25 years

Fischer Mauro<sup>1</sup>, Huss Matthias<sup>1</sup> & Martin Hoelzle<sup>1</sup>

<sup>1</sup>Department of Geosciences, University of Fribourg, Chemin du Musée 4, CH-1700 Fribourg, Switzerland (mauro.fischer@unifr.ch)

Since the mid-1980s, glaciers in the entire European Alps have shown widespread and accelerating mass losses. These glacier changes have been investigated in several studies both focusing on area and length changes as well as on volume losses (e.g. Carturan et al. 2013, Abermann et al. 2009). By comparing the DHM25 level1 Digital Elevation Models (DEMs) from Swisstopo with the coarse-resolution and moderately accurate Shuttle Radar Topography Mission (SRTM) DEM, Paul and Haeberli (2008) analyzed the spatial variability of glacier elevation changes in the Swiss Alps between the mid-1980s and 2000.

According to the latest Swiss Glacier Inventory INVGLAZ10MF derived by manual digitization from high-resolution (50cm) aerial orthophotographs acquired between 2009-2011 (Fischer et al. in prep.), the total area still glacierized in Switzerland by 2010 amounts to 944 km<sup>2</sup> (-28% or 366 km<sup>2</sup> since 1973 (1311 km<sup>2</sup> glacierized)). Together with this inventory and the new high-precision DEM swissALTI3D of the same dates it became possible to extend the dataset of elevation changes of individual glaciers in Switzerland by 10 years. Moreover, because the Alps are dominated by very small and thin glaciers, we argue that a sound analysis of glacier elevation changes can only satisfactorily be done now that source data of sufficient quality is available.

In the context of this ongoing work, we present a first analysis of measured volume changes and area-averaged geodetic mass balance of all glaciers in the Swiss Alps over the last 25 years (e.g. see Fig. 1). For the latter, the arithmetic mean of 1420 still existing glaciers amounts to -0.60 m w.e. a<sup>-1</sup>. The overall mass loss calculated over the analyzed period is -22.1 km<sup>3</sup>.

We discuss the uncertainties of our new dataset and compare it to available long-term mass balance time series (Huss et al. 2010). Moreover, we can reassess the issue of extrapolating measured mass balance to the entire Swiss Alps (cf. Huss 2012).

#### REFERENCES

- Abermann, J., Lambrecht, A., Fischer, A., & Kuhn, M. 2009: Quantifying changes and trends in glacier area and volume in the Austrian Ötztal Alps (1969-1997-2006). *The Cryosphere*, 3, 205-215.
- Carturan, L., et al. 2013. Area and volume loss of the glaciers in the Ortles-Cevedale group (Eastern Italian Alps): controls and imbalance of the remaining glaciers. *The Cryosphere Discussions*, 7, 267-319.
- Huss, M. 2012. Extrapolating glacier mass balance to the mountain-range scale: the European Alps 1900-2100. *The Cryosphere* 6, 713-727.
- Huss, M., Hock, R., Bauder, A., & Funk, M. 2010: 100-year mass changes in the Swiss Alps linked to the Atlantic Multidecadal Oscillation. *Geophysical Research Letters*, 37, L10501.
- Paul, F., & Haeberli, W. 2008: Spatial variability of glacier elevation changes in the Swiss Alps obtained from two digital elevation models. *Geophysical Research Letters*, 35, L21502.

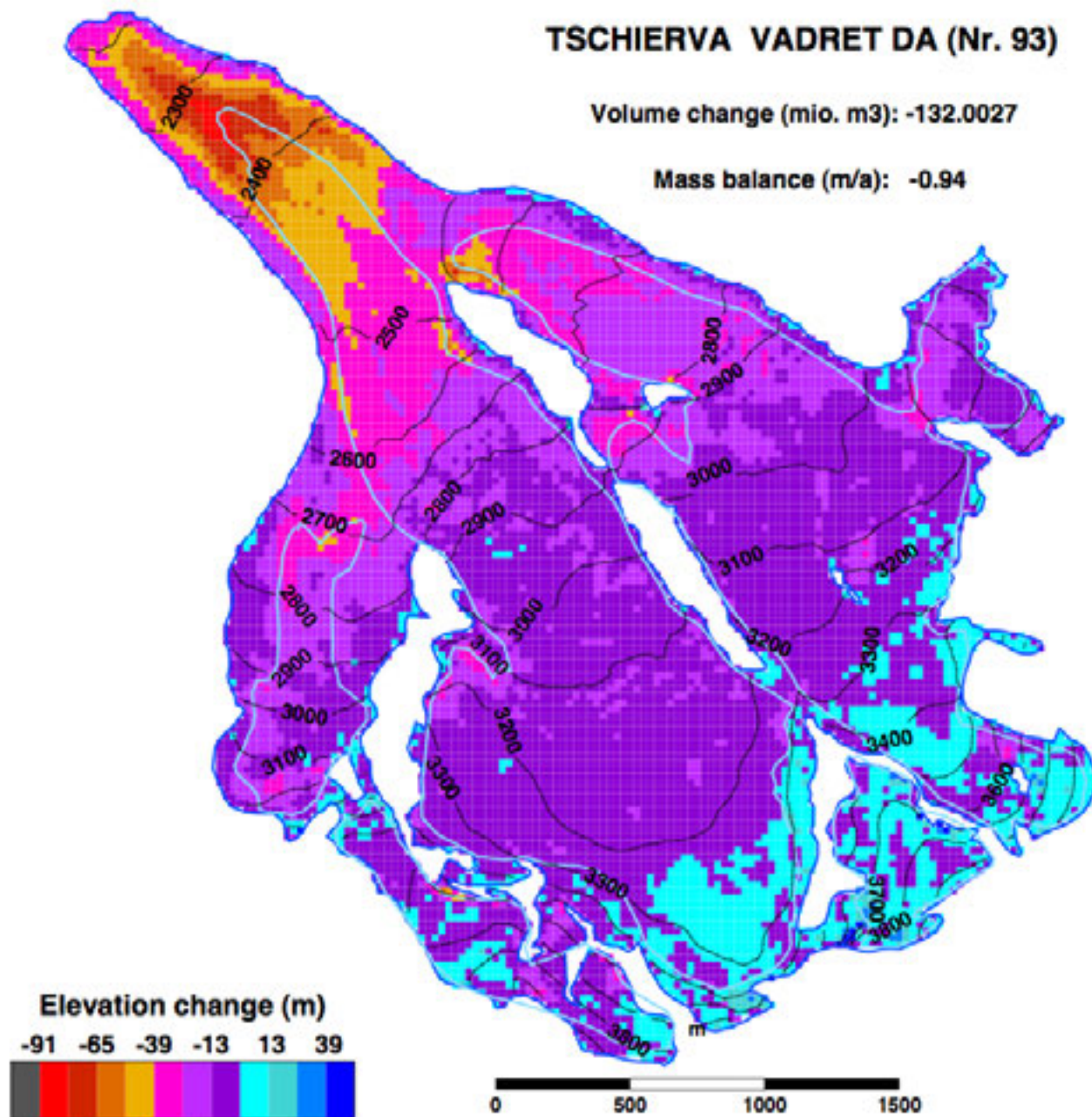


Figure 1. Spatial distribution of elevation changes for Vadret da Tschierva (GR) derived from the difference between the DEM25 level1 and the swissALTI3D DEM. Volume change (mio m<sup>3</sup>) and area-averaged geodetic mass balance (m a<sup>-1</sup>) was calculated by combining the DEMs with the digital glacier outlines from both the 1973 (dark blue) and the new 2010 (light blue) inventories.

## 14.3

### Influences of the seasonal varying snow cover on thermal processes in steep Alpine permafrost rock walls

Anna Haberkorn<sup>1,2</sup>, Marcia Phillips<sup>1</sup>, Martin Hoelzle<sup>2</sup>, Robert Kenner<sup>1</sup>

<sup>1</sup> WSL Institute for Snow and Avalanche Research SLF, Flüelastrasse 11, CH-7260 Davos Dorf, (haberkorn@slf.ch)

<sup>2</sup> Department of Geosciences, University of Fribourg, Chemin du Musée 4, CH-1700 Fribourg

In recent years rock fall events in high mountain permafrost have been more pronounced due to changes in rock temperatures or shifts in the ice and water content of the rock walls. Snow free conditions or a thin, uniformly distributed snow cover have been assumed for the modelling of the thermal regime in permafrost rock walls. However, in reality a heterogeneously distributed snow cover is mostly present in steep rock walls. Depending on the terrain, slope and surface roughness of the rock walls, either a considerable amount or just a thin layer of snow can accumulate. The impact of the varying snow cover on permafrost rock slopes is still not understood in detail and is often poorly implemented in some permafrost models. Nevertheless, the role of the snow, which affects the rock temperatures, the ice and water content and the energy balance of the rock walls, is most likely of central importance. Altered thermal properties and variations in ice and water content influence mechanical processes which lead to rock wall instabilities.

We investigate the role of the snow on the thermal regime and mechanical stability of steep permafrost rock walls. To assess the temporal and spatial evolution and influence of the snow, detailed measurement campaigns in summer and winter time have been carried out on several north and south facing permafrost rock walls in the Swiss Alps since 2012. Especially near-surface rock temperature measurements in the slopes provide substantial information about different snow cover conditions and snow cover duration, depending on local conditions, like aspect, slope and shading effects.

In order to run the 1 dimensional energy balance model SNOWPACK, a multi-method approach is applied, combining meteorological measurements in the near vicinity of the rock walls, borehole rock temperature measurements and rock properties, such as thermal conductivity. To validate the results of the ground thermal regime and the seasonal varying snowpack, the model output is compared to near-surface ground temperature measurements and remote (terrestrial laser scanning and time lapse photography), as well as in-situ (snow pit investigations) snow cover observations.

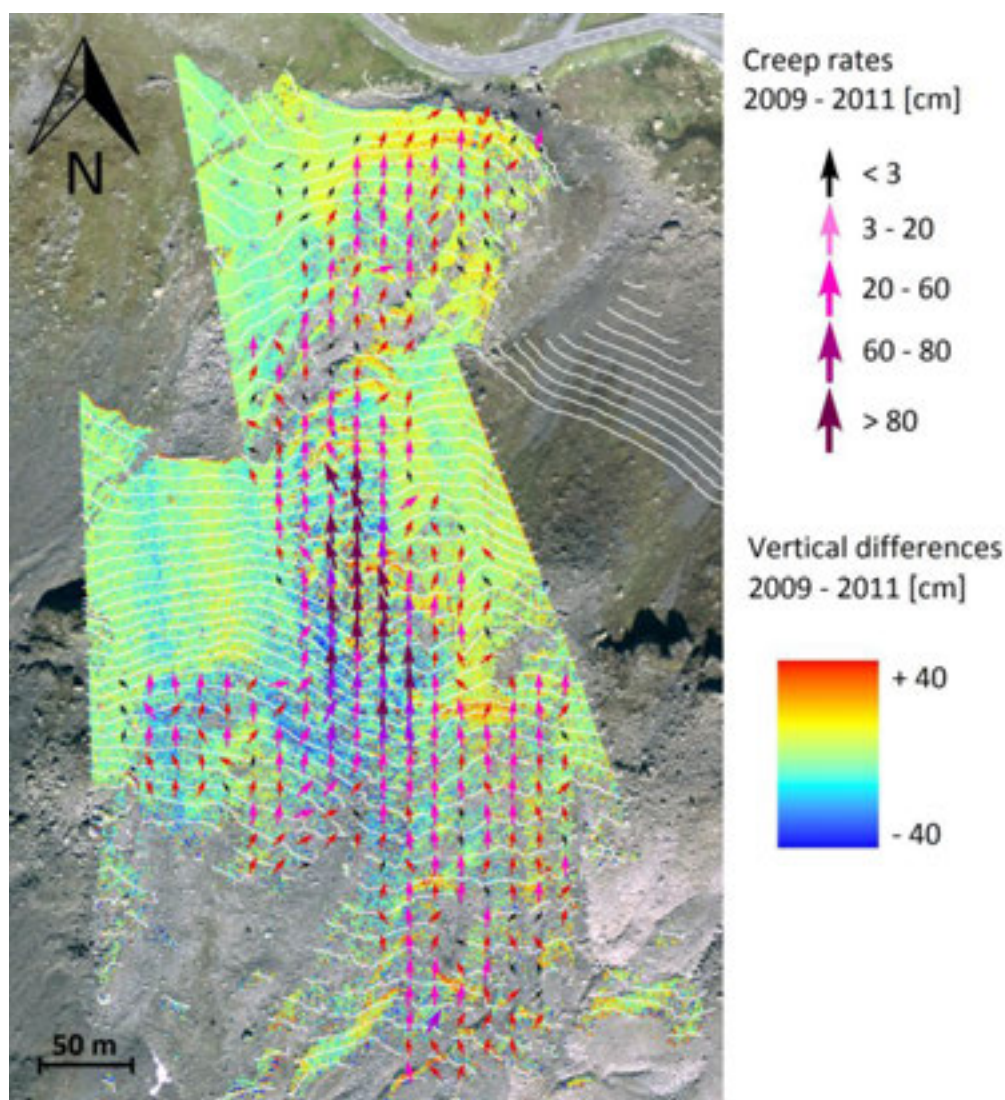
## 14.4

# Results from five years of ground surface monitoring in mountain permafrost regions using terrestrial laser scanning

Robert Kenner<sup>1</sup>, Marcia Phillips<sup>1</sup>

<sup>1</sup>WSL-Institut für Schnee und Lawinenforschung SLF, Flüelastrasse 11, 7260 Davos Dorf

Terrestrial laser scanning has become a commonly used method to monitor ground surface deformation in mountain permafrost regions. We have carried out terrestrial laser scanning since 2009 on active rock glaciers and permafrost rock walls in the Swiss Alps. At some of the sites additional data was obtained from borehole temperature measurements, weather stations or automatic photographs. The dataset provided some interesting observations regarding the dynamics of rock glaciers, rock fall events and surface changes related to snow distribution. We observed intermittent acceleration of rock glaciers in steeper terrain, leading to heave in the acceleration zone in steep terrain and subsidence in the root zone, thus finally contributing to the formation of ridges and furrows in the compression zone on flatter terrain. During the warm and wet summer 2012 rock glacier creep accelerated by a factor of ten in an ice-rich feature with ground temperatures just below 0°C. In addition, surface subsidence downslope from snow avalanche deposits was observed and numerous rock fall events and debris flows were registered and quantified at various sites. Terrestrial laser scanning proved to be a useful tool to distinguish annual fluctuations in surface dynamics.



Vertical movements and creep rates of the Schwarzhorn rock glacier between 2009 and 2011 (orthophoto © Swisstopo DV03349.2).

## 14.5

# Monitoring the Cryosphere in Switzerland and Incentives for Extending Glacier Observations Worldwide

Koenig Sebastian J.<sup>1</sup>, Foppa Nando<sup>1</sup>, Fontana Fabio<sup>1</sup>, & Seiz Gabriela<sup>1</sup>

<sup>1</sup> *Federal Office of Meteorology and Climatology MeteoSwiss, Swiss GCOS Office*  
([sebastian.koenig@meteoswiss.ch](mailto:sebastian.koenig@meteoswiss.ch))

Switzerland has a long tradition in the observation of cryospheric parameters, including more than 100 years of glacier and snow depth measurements, the longest Central European lake ice cover records, the permafrost monitoring network PERMOS, the world's longest snow water equivalent series for catchment areas, and is also hosting the World Glacier Monitoring Service WGMS. The National Climate Observing System (GCOS Switzerland) at the Federal Office of Meteorology and Climatology MeteoSwiss ensures the continuation of such climate relevant measurements and international data centres in Switzerland.

Here, we report on activities of the Swiss GCOS Office and its partners on monitoring cryospheric Essential Climate Variables (ECV) in Alpine Switzerland and provide an example on how systematic monitoring can be extended worldwide through means of a capacity building project.

We provide an overview of systematic observation of state and changes of mountain permafrost and ice in the Swiss Alps from Swiss GCOS partners as contributions to GCOS Switzerland. Complementing the network of snow cover data from the ground, we present results from a recent study demonstrating a 10-year spatiotemporal variability of snow cover days over Switzerland based on satellite data.

Whereas Switzerland features an established network of cryospheric information, globally, data is highly limited. In the framework of the GCOS Cooperation Mechanism the Swiss GCOS Office coordinates an international project to improve climate observation in developing and emerging countries where climate and terrestrial data is sparse. Financed by the Swiss Agency for Development and Cooperation (SDC), this project promotes among others in situ glacier mass-balance monitoring in alpine Central Asia and South America. The data obtained through field measurements are submitted to the WGMS. We present results from this capacity building project and show how the outcomes will contribute to extending glacier observations globally.

### REFERENCES

- Foppa, N. & Seiz, G. 2012. Inter-annual variations of snow days over Switzerland from 2000–2010 derived from MODIS satellite data. *The Cryosphere*, 6, 331–342, doi:10.5194/tc-6-331-2012.
- Seiz, G. & Foppa, N. 2011. National Climate Observing System of Switzerland (GCOS Switzerland). *Advances in Science Research*, 6, 95-102, doi:10.5194/qsr-6-95-2011.
- International CATCOS Project – Capacity Building and Twinning for Climate Observing Systems  
[www.meteoswiss.ch/catcos](http://www.meteoswiss.ch/catcos)

## 14.6

# Snow Height Determination by Polarimetric Phase Differences in X-Band SAR Data

Leinß Silvan<sup>1</sup>, Parrella Giuseppe<sup>2</sup>, Hajnsek Irena<sup>1,2</sup>

<sup>1</sup> Institute of Environmental Engineering (IfU), ETH Zürich, 8093 Zürich, Switzerland (leinss@ifu.baug.ethz.ch)

<sup>2</sup> Microwaves and Radar Institute, German Aerospace Center (DLR), Germany

Snow depth determination and the estimate of the main hydrological parameter, snow water equivalent (SWE) from remote sensing data are very tricky as the electromagnetic properties of snow change over orders of magnitude. In this talk I will give a short overview over current techniques and their limitations to determine snow properties from microwave remote sensing data and will present a new technique which is sensitive to freshly fallen snow.

Current techniques to retrieve snow-related parameters are based on optical, nuclear and microwave methods. The sensitivity of optical methods is limited to the top surface layer and can provide binary snow/no-snow maps, clear-sky conditions and daylight presupposed. Nuclear methods are available only as ground and air-borne instruments which provide accurate information about SWE, but are limited to point measurements or by a very coarse resolution. Microwave techniques, being weather independent, are able to penetrate the snow volume. Passive microwave instruments are able to cover very large area with the drawback of a very coarse resolution. Active radar instruments (SAR) are right choice to provide a high spatial resolution. However, the penetration depth and scattering properties of snow vary significantly with temperature and frequency. Optical frequencies are scattered very strong due to the refractive index of ice and water, causing the white color of snow. For microwave frequencies, the penetration depth depends on the frequency and ranges between several 10s of meters for frequencies around 1 GHz, a few meters at 10 GHz and some cm at 40 GHz, as long as the snow is cold and dry (Hallikainen, 1986). When the snow shows some liquid water content, the high dielectric constant of water at microwave frequencies, together with strong absorption, leads to a dramatic loss of penetration depth such that only the top few cm can be samples for wet snow.

Here I will present observations of early winter snow at a test site in northern Finland, close to the city of Sodankylä. Space-borne polarimetric SAR measurements (sensor: TanDEM-X, 9.56 GHz) show a strong phase delay between horizontal and vertical polarized microwaves (polarimetric phase difference,  $\phi_{HHVV}$ ) which is proportional to snow depth in early winter. A model, developed by (Parrella, 2013) explains the observed delay and links it to the orientation of snow crystals. Recent measurements of the Swiss snow and avalanche research institute (SLF) support the modeled anisotropy of snow and can explain the observed decay of the polarimetric phase difference by observing the structural changes of a snow samples under a temperature gradient, which is observed with computer-tomographical scans (Riche, 2013).

### REFERENCES

- Riche, F., Montagnat, M. & Schneebeli, M., 2013: "Evolution of crystal orientation in snow during temperature gradient metamorphism", *Journal of Glaciology*, vol. 59, P.47-55.
- Parrella, G., Papathanassiou, K. & Hajnsek, I., 2013 : " On the Interpretation of L- and P-band PolSAR Signatures of Polithermal Glaciers ", *POLinSAR 2013*, Frascati.
- Hallikainen, M., Ulaby, F., & Abdelrazik, M., 1986: „Dielectric properties of snow in the 3 to 37 GHz range“, *IEEE Transactions on Antennas and Propagation*, vol. 34, p. 1329 – 1340.

## 14.7

# Future trends of the alpine and ephemeral snowpack at selected sites across Switzerland

Schmucki Edgar<sup>1,2,3</sup>, Marty Christoph<sup>1</sup>, Fierz Charles<sup>1</sup>, Lehning Michael<sup>1,4</sup> & Weingartner Rolf<sup>2,3</sup>

<sup>1</sup>WSL Institute for Snow and Avalanche Research SLF, Flüelastrasse 11, CH-7260 Davos Dorf, Switzerland (schmucki@slf.ch)

<sup>2</sup>Institute of Geography and <sup>3</sup>Oeschger Centre for Climate Change Research, University of Bern, Switzerland

<sup>4</sup>CRYOS, School of Architecture, Civil and Environmental Engineering, EPFL, Lausanne, Switzerland

Snow is a key feature of mountainous environments because of its high implications for hydrology, vegetation and economics, such as winter tourism or hydropower (Beniston et al. 2003, Marty 2008). In particular, snow depth, the stored snow water equivalent, the snow load on a roof or the duration of the snow on the ground are all important parameters for services like road maintenance, avalanche warning, water management, hydro power, flood prevention or building code regulations. The measurement of these snow parameters is either not always possible or too expensive. To overcome this problem, snow models with input from meteorological stations are sometimes used.

In this study we apply the complex one-dimensional, physically based snow model SNOWPACK (Lehning et al. 2002). We first demonstrate the performance of SNOWPACK in modelling the seasonal evolution of snow characteristics such as snow depth or duration of snow cover for single years. The input data SNOWPACK requires includes air temperature, relative humidity, wind speed and direction, incoming short- and long-wave radiation, and precipitation intensity. As most stations do not measure incoming long-wave radiation, it needs to be parameterized. Moreover, due to wind-induced errors, it is not meaningful to use precipitation measurements directly as an input into SNOWPACK, so they need to be calibrated or corrected.

In a second step we show future trends of the Swiss snowpack at selected sites located at different elevations across Switzerland. Therefore we concentrate on the ability of SNOWPACK to model climatological mean values of seasonal snow depth, maximum snow depth and the length of snow season for example. For the assessment of future trends, scenario data from the recently released CH2011 report will be used in order to perturb the observed time series of temperature and precipitation.

### REFERENCES

- Beniston, M., Keller F., Koffi B. & Goyette S. 2003: Estimates of snow accumulation and volume in the Swiss Alps under changing climatic conditions. *Theor. Appl. Climatol.*, 76, 125-140.
- CH2011 2011: Swiss Climate Change Scenarios CH2011. published by C2SM, MeteoSwiss, ETH, NCCR Climate, and OcCC, Zurich, Switzerland, 88p. ISBN: 978-3-033-03065-7
- Lehning, M., Bartelt, P., Brown, B. & Fierz, C. 2002: A physical SNOWPACK model for the Swiss avalanche warning Part III: Meteorological forcing, thin layer formation and evaluation. *Cold Reg. Sci. Tech.*, 35, 169-184.
- Marty, C. 2008: Regime shift of snow days in Switzerland. *Geophys. Res. Lett.*, 35.

## 14.8

### Seismic Monitoring Deployments of the Swiss Institute of Technology (ETH Zurich)

Walter Fabian<sup>1,2,3</sup>, Rösli Claudia<sup>3</sup>, Dalban Canassy Pierre<sup>2</sup>, Faillettaz Jérôme<sup>4</sup>, Husen Stephan<sup>3</sup>, Clinton John F.<sup>3</sup>, Deichmann Nicholas<sup>3</sup> & Funk Martin<sup>2</sup>

<sup>1</sup>*Institute des Sciences de la Terre (ISTerre), Université de Grenoble I, F-38041 Grenoble (Fabian.Walter@ujf-grenoble.fr)*

<sup>2</sup>*Versuchsanstalt für Wasserbau, Hydrologie und Glaziologie (VAW), ETH Zürich, CH-8092 Zürich*

<sup>3</sup>*Swiss Seismological Service, ETH Zürich, CH-8092 Zürich*

<sup>4</sup>*Soil and Terrestrial Environmental Physics, ETH Zürich, CH-8092 Zürich*

Recent advances in seismic instrumentation have allowed for the deployment of seismic networks on glaciers and ice sheets. This has accelerated the development of cryo-seismology, an emerging field of glaciology benefitting from a large suite of well-established and sophisticated seismological techniques. Consequently, a large variety of glaciological phenomena have been scrutinized with seismic techniques, including englacial fracturing, basal sliding, glacier outburst floods, subglacial hydraulics and iceberg calving.

The Swiss Federal Institute of Technology (ETH Zurich) has made important contributions to our understanding of seismogenic processes in glaciated regions. Combining efforts and resources, the glaciological groups at the Laboratory of Hydraulics, Hydrology and Glaciology (VAW) and the Swiss Seismological Service (SED) have installed seismic instruments on Alpine glaciers, the Greenland ice sheet and various unstable ice masses. Resulting from these deployments were high precision locations of ice fracture processes as well as source characterization via waveform modeling techniques. Furthermore, seismic precursors to collapses of instable ice masses have expanded the toolbox for monitoring of glacier-related natural hazards.

Here we give an overview of ETH's seismic deployments during the last ten years focusing on high-density seismic networks in the Alps and on the Greenland ice sheet. We describe the challenges of seismometer installations, seismic analysis techniques and the glaciological phenomena, which they have targeted. Whereas earlier studies were mostly event-based and focused on the study of discrete 'icequakes', ongoing projects highlight the benefit of continuous data acquisition. This allows for monitoring of sustained signals related to englacial and subglacial processes. Processes at the glacier or ice sheet base, in particular, are inherently difficult to investigate due to their remoteness. In combination with other observations (e.g. surface motion, ice deformation, basal water pressure), seismic methods thus constitute valuable tools to study the subglacial environment.

## P 14.1

# Precipitation Redistribution for Snow Models

Robert Spence & Mathias Bavay

*WSL-Institut für Schnee- und Lawinenforschung SLF, Flüelastrasse 11, CH-7260 Davos Dorf, Schweiz  
(robert.spence@slf.ch, bavay@slf.ch)*

An approach has been developed to model the redistribution of precipitation falling on steep terrain, a progression of research performed by Huss et al. (2008) and Magnusson et al. (2011). This method involves modifying the solid precipitation distribution according to the local slope and curvature of the Digital Elevation Model (DEM). With models such as this, the precipitation fields must be tuned in order to maintain a constant global sum within the catchment area. A major weakness of this modeling technique is that precipitation is removed from the higher, steeper slopes and reintroduced elsewhere in the domain. This can lead to unrealistic results and means precipitation from a particular slope may be deposited anywhere in the domain, not necessarily nearby. This project aims to improve and redesign the way in which precipitation is redistributed by these models, such that the redistribution occurs in a more realistic and physically meaningful way.

Two additional algorithms have been developed and implemented into the simulation.

The first of the algorithms tests each cell to determine if redistribution is required and then, where required, removes precipitation from this cell, with the amount dependent on the slope angle. The function then uses an iterative minimisation to find the route of steepest descent (ROSD) and then systematically moves the precipitation along this route, gradually depositing it as it descends. In this way, the precipitation can be tracked and will accumulate at the bottom of the same slope from which it was removed. If the ROSD leads out of the domain, the precipitation is allowed to leave. This means that the global sum may not remain constant, but this is a much more natural and logical way to redistribute solid precipitation due to the terrain.

The second algorithm tests for cells that have accumulated an unnatural amount of precipitation during the redistribution. This is achieved by comparing the precipitation height from one cell with all adjacent cells. If the difference in heights is unreasonably large then the function equally distributes the excess precipitation until a more acceptable level is reached.

This new approach has been successful for data at a single time-step. An example output is shown in figure 1. Simulations have also been performed continuously over an entire winter, in order to investigate how the precipitation builds up over this period. After each interpolation, the DEM is updated in order to see how the constantly changing terrain - due to precipitation build-up - affects how the model redistributes the precipitation. Effects of melt and sublimation are ignored for the purposes of the investigation. The final output, which can be considered a reasonable estimate of the snow water equivalent, can then be validated using measured data.

## REFERENCES

- Magnusson, J et al. (2011), Quantitative evaluation of different hydrological modelling approaches in a partly glacierized Swiss watershed, *Hydrological Processes*, 25(13), 2071-2084.
- Huss, M et al. (2008), Modelling runoff from highly glacierized alpine catchments in a changing climate, *Hydrological Processes*, 22(19), 3888-3902.

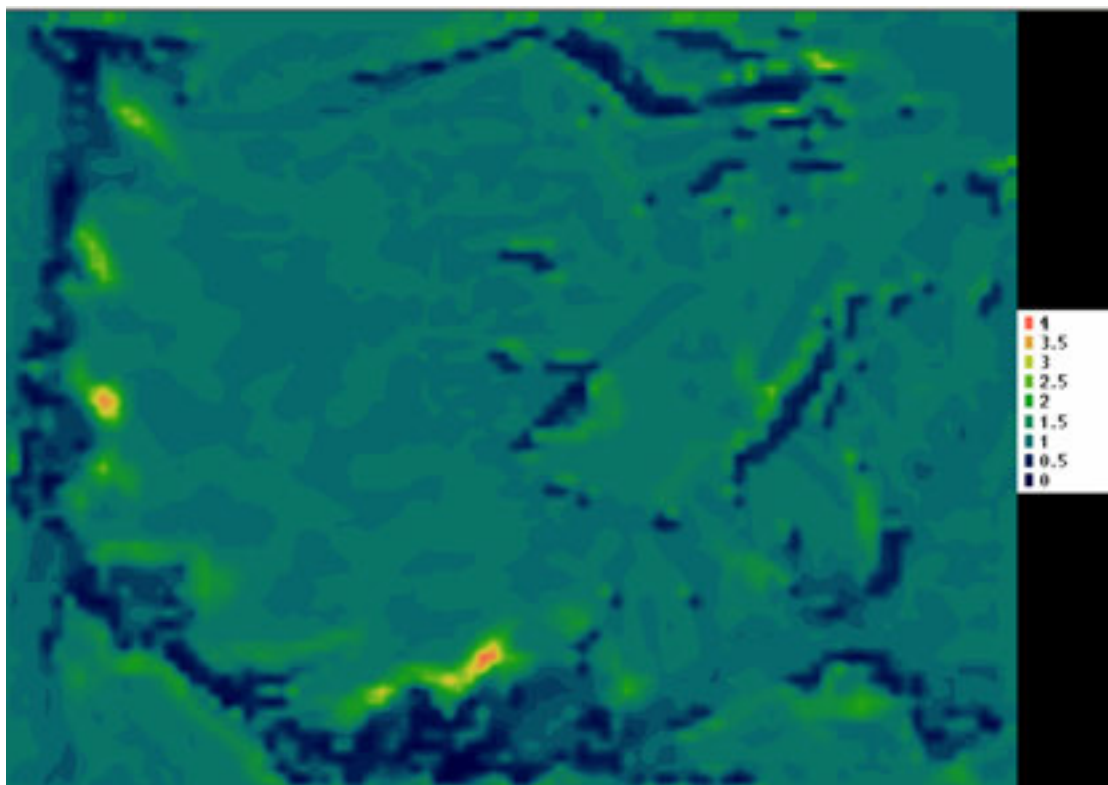


Figure 1. Simulated precipitation accumulation after interpolation of data from a single time-step of one hour. Two areas with particularly substantial build-up are indicated. The colour-coded key to the right is precipitation height in mm.

## P 14.2

### Measuring acoustic emissions in an avalanche starting zone to monitor snow stability

Ingrid Reiweger, Jürg Schweizer

*WSL Institute for Snow and Avalanche Research SLF*

Evaluating the stability of a specific snow slope still involves time-consuming and labour-intensive manual tests; in dangerous or remote areas it might not even be possible at all. In other natural, heterogeneous materials such as wood, limestone, or ice, monitoring the acoustic signals emitted by cracks forming and growing within the material has proven a valuable tool for stability estimation and fracture prediction. In a pioneer field study we tested the acoustic emission method for monitoring snow stability and possibly predicting avalanche release. We performed several preparatory laboratory studies in order to evaluate the optimal sensor frequencies and coupling of the sensors to the snow. The resonant (30 kHz) sensors, which were coupled to thin aluminium plates with silicone and protected by a plastic housing, were placed in a potential avalanche slope close to a weak interface (old snow – storm snow) within the snow cover. We then measured acoustic emissions and seismic signals and compared those to the slope stability which was assessed by the success of avalanche control by explosives. Preliminary results are shown and discussed with respect to their practical relevance for avalanche prediction.

## P 14.3

## State, changes and impact of glacier surface albedo in the Swiss Alps

Naegeli Kathrin<sup>1</sup>, Huss Matthias<sup>1</sup>, Hoelzle Martin<sup>1</sup>, Hauck Christian<sup>1</sup>

<sup>1</sup>Department of Geosciences, University of Fribourg, Switzerland, (kathrin.naegeli@unifr.ch)

The ice-albedo feedback plays a crucial role in various glacial processes, but especially influences glacier ablation. Furthermore, glacier surface albedo depends in a complicated way on many factors, such as cryoconite concentration, impurities due to mineral dust and organic matter or ice surface morphology, and is therefore difficult to model or parameterize. Nevertheless, albedo is one of the most important variables in the energy balance of snow and ice and glacier mass balance modelling, and hence is usually strongly simplified.

In the last two decades, several studies focused on glacier surface albedo using in-situ automatic weather stations (e.g. Oerlemans and Knap, 1998; Bühlmann, 2011) or satellite images (e.g. Klok et al., 2003; Paul et al., 2005). Nevertheless, still fairly little is known about the state, changes and impact of glacier surface albedo in the Swiss Alps, although there are obvious changes and variations in glacier surface characteristics on most alpine glaciers over the last years. The SEON (Swiss Earth Observatory Network) project therefore aims to undertake detailed investigations of glacier surface albedo using data from the hyperspectral sensor APEX (Airborne Prism Experiment) as well as from in-situ observations.

The 2013 field campaign on the Glacier de la Plaine Morte, VS, Switzerland includes a stake farm of 22 ablation stakes distributed randomly on the glacier surface, whereof 12 and 10 stakes are placed in a rather dark and bright area of the glacier, respectively. Additionally, measurements of spectral reflectance as well as albedo are conducted along a transect leading west to east on the glacier surface.

Here, we present first results of the measurements of the 2013 field campaign and discuss them in terms of recent changes in the dynamics and the spatial distribution of ice melt on Glacier de la Plaine Morte.

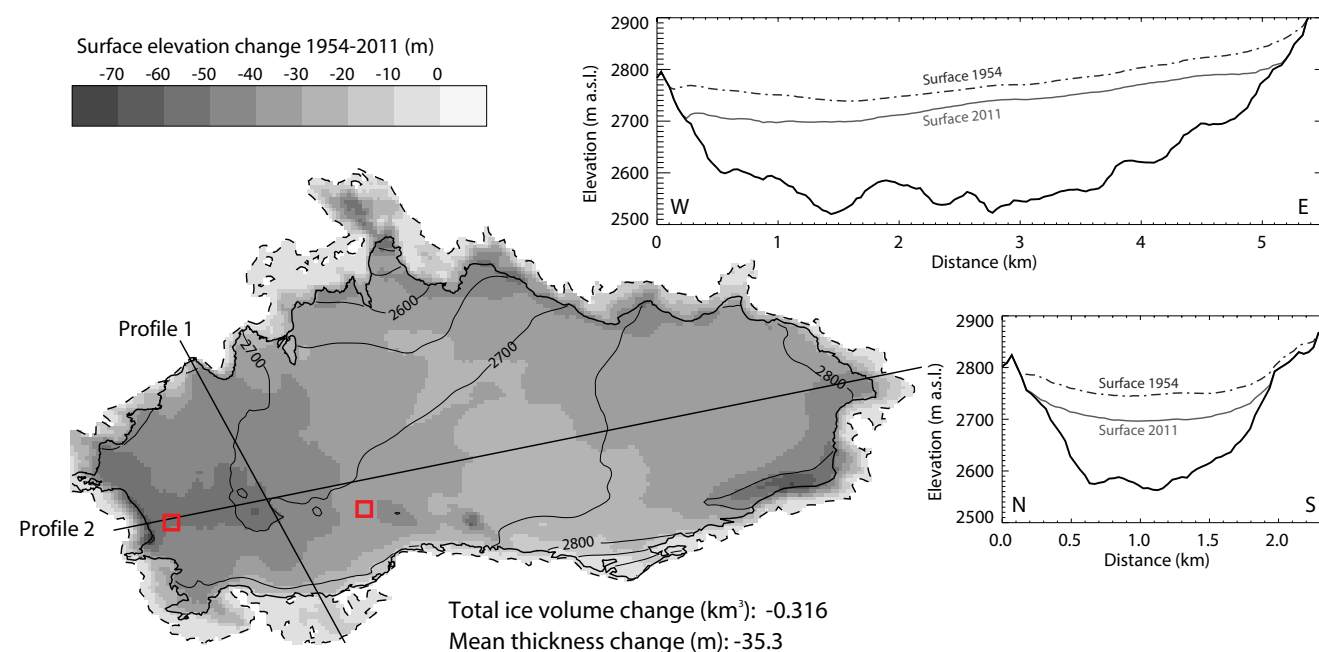


Figure 1. Observed glacier surface elevation changes between 1954 and 2011. Two cross-profiles are shown in the insets. Two red squares represent the two plots of the stake farm. (modified after Huss et al., *subm.*)

## REFERENCES

- Bühmann, E. (2011), Influence of particulate matter on observed albedo reductions on Plaine Morte glacier, Swiss Alps, 97 pp., University of Bern.
- Huss, M., A. Voinesco, and M. Hoelzle (subm.), Implications of climate change on Glacier de la Plaine Morte, *Geographica Helvetica*.
- Klok, E. J. L., W. Greuell, and J. Oerlemans (2003), Temporal and spatial variation of the surface albedo of Morteratschgletscher, Switzerland, as derived from 12 Landsat images, *Journal of Glaciology*, 49(167), 491–502, doi:10.3189/172756503781830395.
- Oerlemans, J., and W. H. Knap (1998), A 1 year record of global radiation and albedo in the ablation zone of Morteratschgletscher, Switzerland, *Journal of Glaciology*, 44(147), 231–238.
- Paul, F., H. Machguth, and A. Kääb (2005), On the impact of glacier albedo under conditions of extreme glacier melt: the summer of 2003 in the Alps, *EARSeL eProceedings*, 4(2), 139–149.

## P 14.4

# Soil moisture quantification in mountain permafrost: A model-data comparison between Southern Norway and the Swiss Alps

Pellet Cécile<sup>1</sup>, Scherler Martin<sup>1</sup> & Hauck Christian<sup>1</sup>

<sup>1</sup>Department of Geosciences, University of Fribourg, Chemin du Musée 4, CH-1700 Fribourg (cecile.pellet@unifr.ch)

Soil moisture is a key factor controlling the energy and water exchange processes at the soil-atmosphere interface as well as the physical properties of the subsurface such as heat capacity, thermal conductivity, etc. In mountain environments it is a particularly crucial factor since it can affect the stability of slopes and modify the characteristics and behaviour of periglacial landforms. In 2010 soil moisture was classified as an Essential Climate Variable (ECV) by the Global Climate Observing System (GCOS) and has thus to be continuously and globally monitored.

In spite of its importance, the technical challenges and its strong variability prevented the soil moisture from being measured operationally at high and/or middle altitudes. The newly launched SNF-project at the University Fribourg (SOMOMOUNT) intends to fill this data gap with the installation of soil moisture stations distributed along an altitudinal gradient between the Jura mountains and the Alps. In the mean time, quantification of soil moisture at high altitude remains possible through modelling approaches.

Here we present the analysis of data sets from two well-studied permafrost sites, Juvvasshøe (N) and Schilthorn (CH), where two different types of model were implemented in order to calculate soil moisture. At both locations soil temperature, geophysical profiles and meteorological data over more than 10 years are available. Moreover at Schilthorn a 6-years period of soil moisture measurements exists. In a first step the meteorological records and the soil temperature measurements were used to constrain one dimensional heat and mass transfer models, to generate long term predictions and reconstructions of the subsurface properties including soil moisture and temperature (Hipp et al., 2012 & Scherler et al., 2013). Then the available electrical resistivity tomography (ERT) and refraction seismic tomography (RST) data sets were combined through a simple physically based model to calculate the different phase contents (ice, air and water) in the ground (Hauck et al., 2011). Finally, the data from modelled long term point information and the one-time two-dimensional geophysical profiles were compared to each other, and between the study areas. Validation of both approaches could be performed at Schilthorn using the in-situ measurements.

## REFERENCES

- Hauck, C., Böttcher, M., & Maurer, H. 2011: A new model for estimating subsurface ice content based on combined electrical and seismic data sets, *The Cryosphere*, 5(2), 453–468
- Hipp, T., Etzelmüller, B., Farbrot, H., Schuler, T. V., & Westermann, S. 2012: Modelling borehole temperatures in Southern Norway - insights into permafrost dynamics during the 20th and 21st century, *The Cryosphere*, 6(3), 553–571.
- Scherler, M., Hauck, C., Hoelzle, M., & Salzmann, N. 2013: Modeled sensitivity of two alpine permafrost sites to RCM-based climate scenarios, *Journal of Geophysical Research: Earth Surface*, 118(2), 780–794.

## P 14.5

## Recent accumulation and firm compaction rates on Findelengletscher derived from airborne GPR and firm cores

Leo Sold<sup>1</sup>, Martin Hoelzle<sup>1</sup>, Matthias Huss<sup>1</sup>, Anja Eichler<sup>2</sup> & Margit Schwikowski<sup>2</sup>

<sup>1</sup> Department of Geosciences, University of Fribourg, Ch. du Musée 4, CH-1700 Fribourg (leo.sold@unifr.ch)

<sup>2</sup> Analytical Chemistry, Paul Scherrer Institute, OFLB/109, CH-5232 Villigen

The accumulation area of alpine glaciers contains a record of glacier mass balance in the past. By measuring thickness and density of annual firm layers, past accumulation rates can be retrieved. We discuss such measurements from 2012 on Findelengletscher, Switzerland, a large Alpine valley glacier, using several in-situ firm cores. The firm cores provide depth and dating of annual summer surfaces, i.e. ice lenses, from the density profile, ionic content, and Deuterium concentration (Eichler et al. 2000). Ground-penetrating radar (GPR) has previously been used for a non-destructive assessment of internal layers in snow, firm and ice (Plewes & Hubbard 2001). Signal reflections indicate changes in the dielectric properties of the material, e.g. density changes at former summer surfaces. Conversion to depth or water equivalent requires the radio-wave velocity that is obtained from the in-situ density-depth profiles. The depths of reflectors in the helicopter-borne single-offset GPR profiles are in line with the findings from the firm cores. A distributed data set of past accumulation rates can thus be obtained by tracking of the reflectors between the firm cores. Furthermore, we use GPR to reconstruct the annual accumulation on Findelengletscher since 2007 based on the measurements that have been conducted in 2010 – 2013. Overlapping GPR profiles in consecutive years allow tracking firm layers over time and thus provide firm compaction rates (Fig. 1). Results are compared with a firm densification model. We show that in remote areas helicopter-borne GPR is an effective method to derive several years of past accumulation rates. It benefits but does not depend exclusively on the time-matched availability of firm cores when overlapping profiles are mapped in subsequent years.

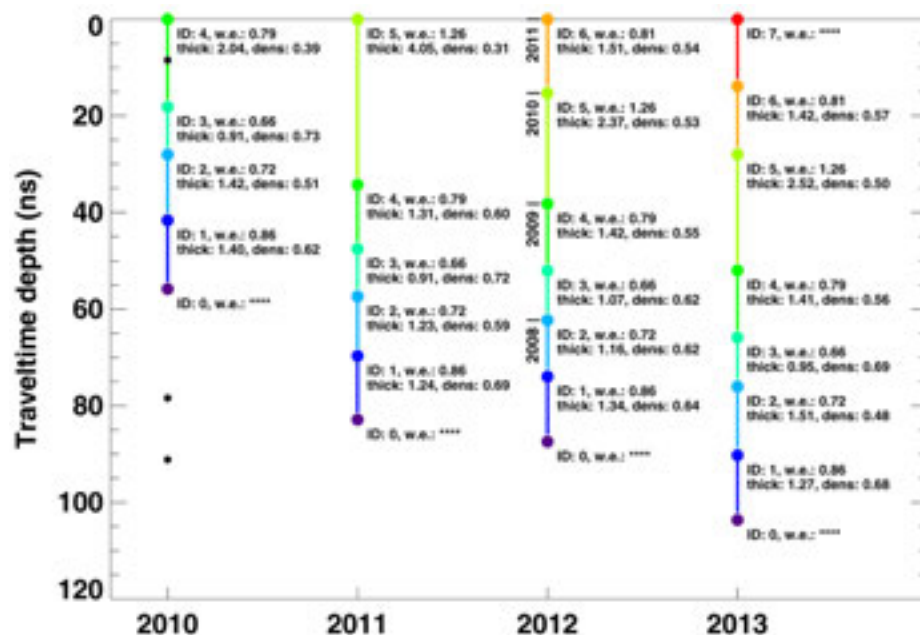


Figure 1. Water equivalent (w.e.), thickness and density of firm layers detected by GPR in 2010, 2011, 2012, and 2013 at drilling site A1. Black dots mark reflectors that were not detected in the following year. Dating of layers is taken from the 2012 firm core analysis.

## REFERENCES

- Eichler, A., Schwikowski, M., Gäggeler, H. W., Furrer, V., Synal, H.-A., Beer, J., Saurer, M., Funk, M. (2000). Glaciochemical dating of an ice core from upper Grenzletscher (4200 m a.s.l.). *Journal of Glaciology*, 46(154), 507–515.
- Plewes, L. A., & Hubbard, B. (2001). A review of the use of radio-echo sounding in glaciology. *Progress in Physical Geography*, 25(2), 203–236.

## P 14.6

# On the morphological characteristics of overdeepenings in high-mountain glacier beds

Linsbauer Andreas<sup>1</sup>, Haeberli Wilfried<sup>1</sup> & Fischer Urs H.<sup>2</sup>

<sup>1</sup> Department of Geography, University of Zurich, Winterthurerstrasse 190, CH-8057 Zurich, Switzerland  
(andreas.linsbauer@geo.uzh.ch)

<sup>2</sup> NAGRA, Hardstrasse 73, CH-5430 Wettingen, Switzerland

Overdeepenings, i.e. closed topographic depressions with adverse slopes in the flow direction, are characteristic for glacier beds and glacially sculpted landscapes. Besides their importance as geomorphological landforms, groundwater bodies and sedimentary archives, they are of increasing interest in relation to climate-induced lake formation in de-glaciating landscapes (Linsbauer et al., 2012) and depth erosion under ice age conditions in connection with the long-term safety of radioactive waste repositories in some mid-latitude countries (Fischer & Haeberli, 2010, 2012). Quantitative predictions of their shape, distribution and conditions of occurrence remain difficult. One major problem thereby relates to the still unsatisfactory treatment in glacier erosion theory of sediment evacuation at glacier beds, especially by subglacial meltwater. An alternative way of searching for realistic/empirical quantitative estimates is, therefore, to analyse the geometry of well-documented overdeepenings. The present study attempts to do this by combining statistical analyses of numerous bed overdeepenings below still existing glaciers of the Swiss Alps as modelled with a robust shear stress approximation linking surface slope to ice thickness at high resolution.

This data sample includes more than 500 modelled overdeepenings, locations of possible future lake formation in the Swiss Alps. For all these polygons, mean and maximum values of the parameters surface area, length, width, depth, volume, adverse slope and their statistical interrelations are determined with their corresponding uncertainty ranges (cf. Figure 1). The bathymetry of these overdeepenings reveals maximum depths ranging from 3 to 300 m and mean depths from 2 to 100 m, the overall average of mean depth being 15 m. The range of the values of the adverse slope is from 5° to 64°, with a mean of 22°. For the larger overdeepenings in the sample basal shear stress (as used in the model), thermal ice types, glacier size/type, relation to flow characteristics (position along flow, confined-unconfined, confluence-diffuence-channel-forefield) are also included. As a principal problem thereby remains the unsolved question of when (and if) the overdeepenings is going to be formed or exposed. Some results nevertheless remain safe. Marked overdeepenings can, for instance, exist under very small cirque glaciers flowing under low shear stresses and having low melt-water input. They can form at confluences but also often occur under conditions of confined flow in rather straight channel configurations. Corresponding lakes can be dammed by huge (terminal) moraines or may form in beautifully polished pure rock beds. The full results of the study are hoped to improve the knowledge basis for practical applications (unmeasured and future lakes, depth erosion by glaciers).

## REFERENCES

- Fischer U. & Haeberli W. 2010: Glacial erosion modelling – Results of a workshop held in Unterägeri, Switzerland, 29 April – 1 May 2010). Nagra Arbeitsbericht NAB-10-34.
- Fischer U. & Haeberli, W. 2012: Glacial overdeepening – Results of a workshop held in Zürich, Switzerland, 20-21 April 2012. Nagra Arbeitsbericht NAB-12-48.
- Linsbauer, A., Paul, F. & Haeberli, W. 2012. Modeling glacier thickness distribution and bed topography over entire mountain ranges with GlabTop: Application of a fast and robust approach. *Journal of Geophysical Research*, 117 (F03007). doi: 10.1029/2011JF002313.

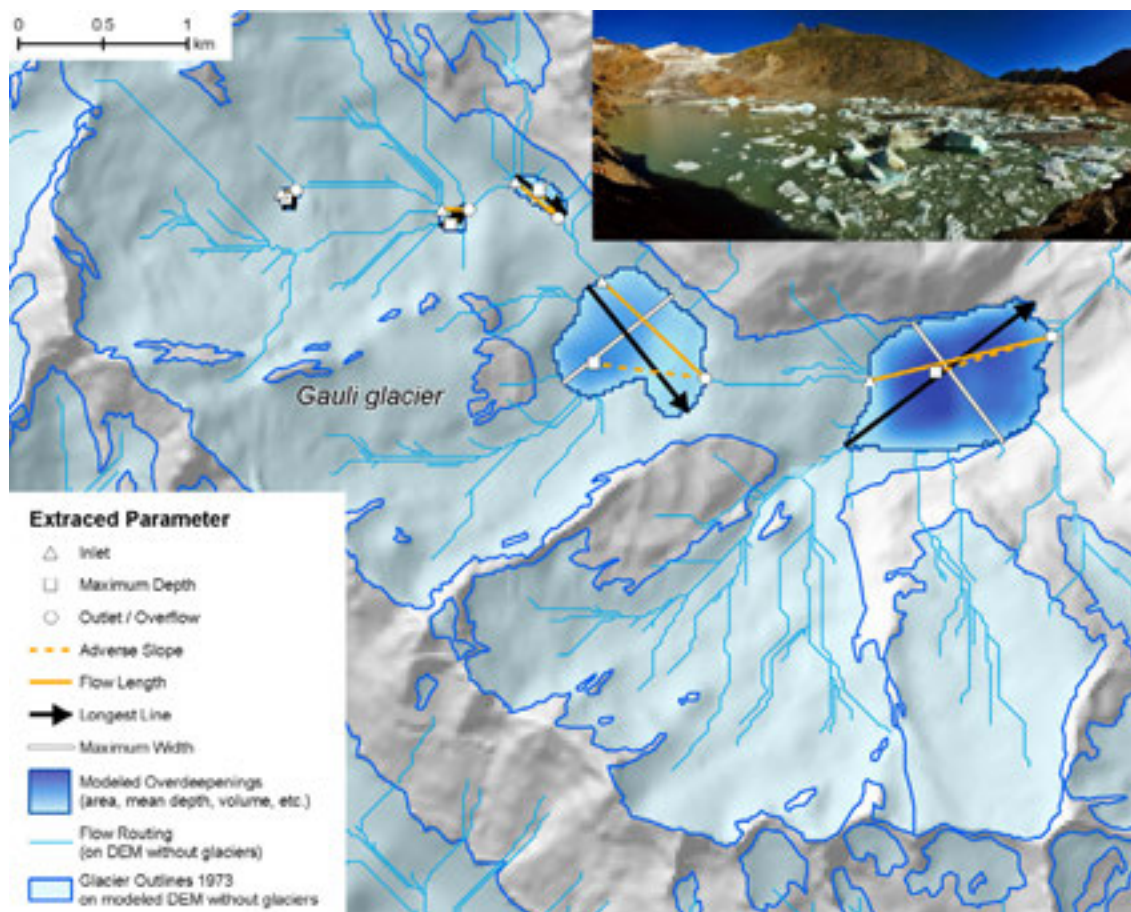


Figure 1. The photo on top right shows Gauli glacier with its recently forming lake in the fore field (the picture is taken from the south shore of the lake by Bruno Petroni in August 2009; source: swisseduc.ch). The map depicts the outlines of the glaciers in the Gauli region as from 1973, displayed on a relief of a modeled DEM without glaciers. Based on this (filled) DEM the potential overdeepenings in the glacier bed geometries are extracted and flow routing is derived, which leads to further parameters shown in the legend.

## P 14.7

## Mapping of debris-covered ice using DInSAR and airborne photography: A pilot study in the Upper Valais (Swiss Alps)

Barboux Chloé<sup>1</sup>, Fischer Mauro<sup>1</sup>, Delaloye Reynald<sup>1</sup>, Huss Matthias<sup>1</sup> & Collet Claude<sup>1</sup>

<sup>1</sup> University of Fribourg, Departement of Geosciences, Geography Unit; Ch. Du Musée 4, CH-1700 Fribourg  
(*firstname.lastname@unifr.ch*)

The extent of glaciers in the European Alps has been mapped and inventoried consistently. Most of them have been outlined using semi-automated remote-sensing techniques. A major problem when deriving the glacier outlines from satellite imagery is to detect debris-covered ice. Promising results using a semi-automatic method combining satellite multispectral images and a digital elevation model have been obtained in the Swiss Alps (Paul et al. 2011). However, even if manual delineation is very time-consuming and work-intensive for a large number of glaciers, it remains the best way to produce an accurate inventory of glacier ice bodies in the Alps, where outstanding data sources are available. Therefore, mapping of debris-covered glaciers using remote sensing techniques should only be used to assist in the development of an accurate inventory as an efficient starting point for manual delineation.

Differential SAR Interferometry (DInSAR) is a well-established technique for mapping surface displacement at mm to cm resolution over alpine areas, where dense vegetation is no longer present. Moreover the nature of passive microwave response of the signal reflected by natural scatters on the ground is related to a number of ground factors and depends on the composition and the surface roughness. Especially, water and vegetation have a dielectric constant different from other ground objects and can be clearly identified (Gupta 2003). Therefore, during snow-free periods, debris-covered glaciers are well delimited on shortest time lapse interferograms with a strongly decorrelated signal that can be caused by the exposure of the melting ice itself (thinner debris coverage), by the rapid settlement of the glacier surface and/or by a significant glacier motion (Delaloye et al. 2007).

This contribution proposes the use of DInSAR combined with airborne photography to outline debris-covered glacier ice in glacier inventories. Firstly, glacier outlines are digitized manually using high-resolution (25 cm) orthophotographs covering the entire Swiss Alps acquired twice for every scene (both in the early and late 2000s). In contrast to the known shortcomings of approaches based on satellite remote-sensing, the margins of very small glaciers are (with a few exceptions) clearly distinguishable on these orthophotos, even in shaded, snow- or debris-covered areas (Fischer et al. 2013). Then the inventory is compared to a terrain activity map derived from DInSAR scenes where decorrelated areas are detected (Barboux et al. 2013).

This method allows refining outlines of debris-covered glaciers where visual interpretation is difficult. Moreover, it allows the detection of debris-covered glacier ice bodies no more connected to any glacier source or no more fed by the glacier flow (dead ice). Current glacier inventories do not consider every type of debris-covered glacier ice as they are mainly used for climatic interpretation. The question is now: Is it necessary to take into account these (dead) ice bodies in glacier inventories if they are rather used to study runoff contribution, sediment transfer, slope dynamics, or natural hazards?

### REFERENCES

- Barboux, C., Delaloye, R., Lambiel, C., Strozzi, T., Raetzo H. & Collet C. 2013b: Semi-automated detection of terrain activity in the Swiss Alpine periglacial environment from DInSAR scenes. Proceedings of the Living Planet Symposium, 9-13 sept. 2013, Edinburgh – Scotland (in prep).
- Delaloye, R., Lambiel, C., Lugon, R., Raetzo & H., Strozzi, T. 2007: Typical ERS InSAR signature of slope movement in a periglacial mountain environment (Swiss Alps). Proceeding of ENVISAT Symposium 2007 (ESA SP-636, July 2007).
- Fischer, M., Huss, M., & Hoelzle, M. 2013: Recent changes of very small glaciers in the Swiss Alps 15, EGU2013-149.
- Gupta, R. P. 2003: Remote sensing geology. Chap. 12 Microwave Sensors. Ed. Berlin: Springer. ISBN: 3-540-43185-3.
- Paul, F., Fray, H. & Le Bris, R. 2011: A new glacier inventory for the European Alps from Landsat TM scenes of 2003: challenges and results. *Annals of Glaciology* 52(59): 144-152.

## P 14.8

# Towards a better understanding of temperature conditions in rock fall detachment areas in permafrost: a computer-simulation approach

Lüthi Rachel<sup>1,3</sup> & Gruber Stephan<sup>2,3</sup>

<sup>1</sup> WSL-Institut für Schnee- und Lawinenforschung SLF, Flüelastrasse 11, CH-7260 Davos Dorf ([rachel.luethi@slf.ch](mailto:rachel.luethi@slf.ch))

<sup>2</sup> Carleton University, 1125 Colonel By Drive, Ottawa ON K1S 5B6, Canada

<sup>3</sup> Department of Geography, University of Zurich, Winterthurerstrasse 190, CH-8057 Zürich

Although the interest in mountain permafrost and related processes increased during the past decade due to its high sensitivity to climate change, little is known about transient temperature conditions in rock fall detachment areas. Since (i) rock slopes are difficult to access, (ii) it is usually not known in advance where and when a rock fall will occur and (iii) not every single rock slope can be monitored. As a consequence, a modeling approach is chosen to determine the ground surface temperature conditions under which rock fall in permafrost occurs.

For each investigated rock fall event the conditions in the detachment area from the beginning of the meteorological series up to the rock fall event are modelled with a physically-based energy balance model including ground temperatures under freezing conditions.

To evaluate if ground temperatures in the detachment area are extreme it is determined in which percentile of all temperatures the temperature at the time of the rock fall event lies (Figure 1). The focus isn't on the singular rock fall event indeed the rock falls are investigated together. This approach allows investigating a huge number of rock fall events and so preconceived notions can be reduced. The evaluation of the methodological approach as well as its implications for application and some selected results are presented.

It can be shown that the chosen approach is suitable and the only major implications are given through the availability of long enough meteorological data and the selection of the meteorological stations for modeling.

Numerous rock fall events in locations where permafrost is likely and which have volumes of up to 50'000 m<sup>3</sup> occur at ground surface temperatures in high percentiles. It is more pronounced for daily and for weekly than for monthly temperatures. This and the seasonal distribution suggest that rock fall events in permafrost areas are advective controlled. Since other processes correlate with the height further investigations are necessary for a better understanding of the related processes. In a next step the influence of the snow could be investigated.

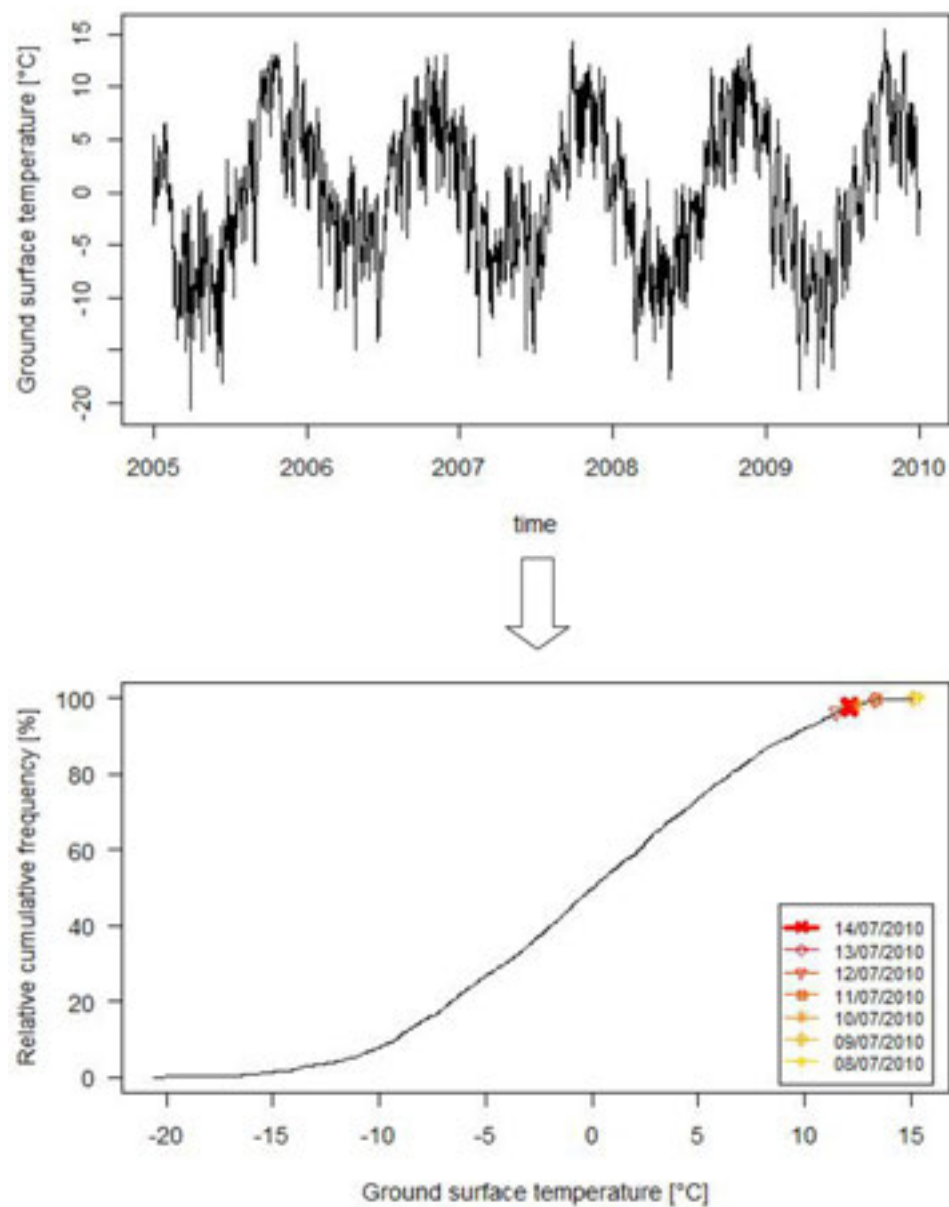


Figure 1 Modelled ground temperatures in a detachment area (top) are summed up in a cumulative frequency curve and the percentile of the ground temperature for a rock fall event on the 14th of July 2010 is determined (bottom).

## P 14.9

# Permafrost model sensitivity to seasonal climatic changes and extreme events in mountainous regions

Marmy Antoine, Salzmann Nadine, Scherler Martin, Hauck Christian

*Alpine Cryosphere and Geomorphology Group, Department of Geosciences, University of Fribourg.*

Modeling the evolution and the sensitivity of permafrost in the European Alps in the context of climate change is one of the most relevant and challenging task of the permafrost research in progress. Climate models project considerable ranges and uncertainties in future climatic changes. To assess the potential impacts of climatic changes on mountain permafrost within these ranges of uncertainty, this contribution presents a sensitivity analysis using a dimensional soil-snow-atmosphere model CoupModel (Jansson & Karlberg 2001) calibrated to the Schilthorn (Scherler et al, 2013) a typical low-ice content mountain permafrost location in the Swiss Alps. The model is combined with climate input based on delta change approaches.

Delta values comprise a multitude of coupled air temperature and precipitation changes to analyze long-term, seasonal and seasonal extremes changes. The results show that seasonal changes in autumn (SON) have the largest impact on the near-surface permafrost thermal regime in the model, and lowest impacts in winter (DJF) (Figure 1). For most of the variability, snow cover duration and timing is the important factor, whereas maximum snow height only plays a secondary role unless maximum snow heights are very small. At least for the low-ice content site of this study, extreme events have only short-term effects and have less impact on permafrost than long-term air temperature trends.

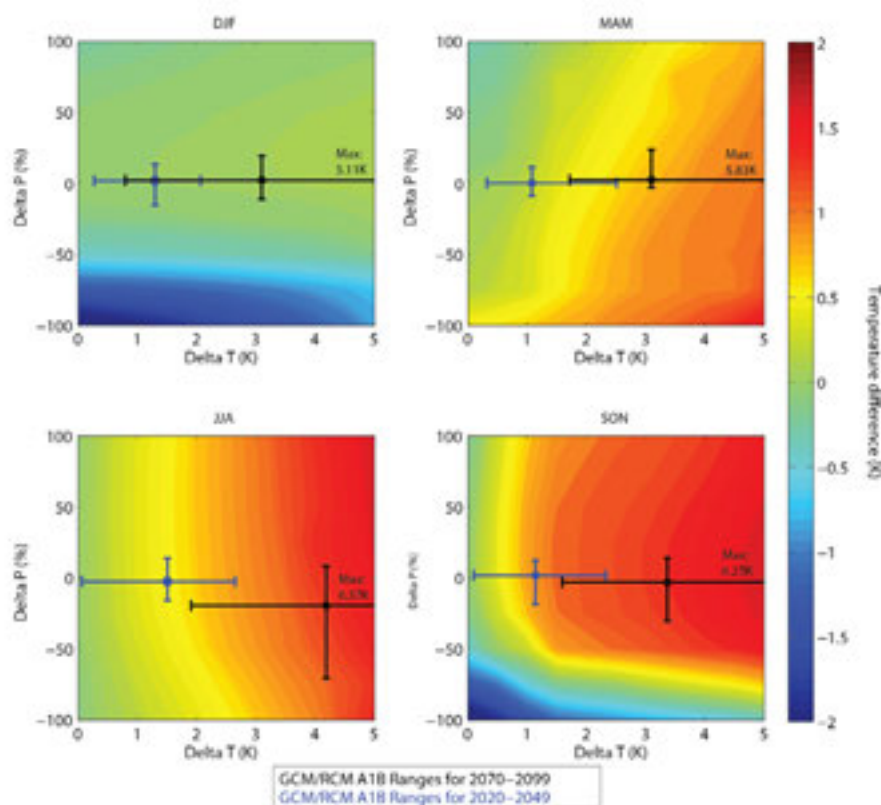


Figure 1 - Difference in mean annual soil temperature at 5m depth at the end of the century between SEA (i.e. the application of a  $\Delta T$  and a  $\Delta P$  during a given season: DJF, MAM, JJA and SON, for every year) compared to the reference run (SEA-REF). The bars indicate the range of 10 individual GCM/RCM model chains for A1B scenario for the period 2020-2049 (blue) and for the period 2070-2099 (black).

## REFERENCES

- Jansson P E 2012 CoupModel: Model use, calibration and validation, Transactions of the ASABE, 55, 1335–1344.  
 Scherler M, Hauck C, Hoelzle M and Salzmann N 2013 Modeled sensitivity of two alpine permafrost sites to RCM-based climate scenarios. Journal of Geophysical Research: Earth Surface, 118, 1–15, doi:10.1002/jgrf.20069.

## P 14.10

# Google Earth-based rapid assessment of glacier evolution, lake formation and hazard change – the example of Artesonraju in the Cordillera Blanca, Peru

Wilfried Haeberli<sup>1</sup>, Fabian Drenkhan<sup>1,2</sup>, Judith Torres<sup>3</sup>, Alejo Cochachin<sup>3</sup> & César Salazar<sup>3</sup>

<sup>1</sup> *Geography Department, University of Zurich, Winterthurerstrasse 190, CH-8057 Zürich (wilfried.haeberli@geo.uzh.ch)*

<sup>2</sup> *Pontifical Catholic University of Peru, Lima, Peru*

<sup>3</sup> *Glaciology and Water Resources Unit, Huaraz, Peru*

Digital high-resolution terrain information contained in Google Earth can be combined with a simple, fast, robust and transparent parameterization scheme for analyses of glacier inventory data (Haeberli and Hoelzle, 1995) to derive important quantitative information about the characteristics and evolution of mountain glaciers under conditions of climate change. This is demonstrated for the Artesonraju glacier, Cordillera Blanca, Peru.

We determined the maximum and minimum altitude of the glacier at 5420 m a.s.l. and 4720 m a.s.l., its vertical extent at some 700 m and the length at 3.2 km. With an average slope of 13° and an assumed average basal shear stress of 150 kPa, its mean thickness along the central flowline can be estimated at nearly 100 m with a maximum thickness of around 200 m at the upper and wider part of the flat tongue. Mid-range elevation as a good approximation for the ELA is near 5060 m a.s.l. With the glacier margin rising from about 4300 m a.s.l., the ELA shifted by some 200 m since the maximum extent of the LIA.

This corresponds to a warming of 1 to 1.5°C if only temperature change is considered. With additional atmospheric warming by 1°C, the lower glacier end would have to rise to about 5000 m a.s.l. at the upper end of the flat glacier tongue leaving a reduced vertical extension of approximately 400 m. The mass balance at today's terminus is nearly 6 m y<sup>-1</sup> and the dynamic response time of the glacier about 30 to 40 years. The flat tongue is therefore likely to be a left-over from the late 20<sup>th</sup> century as confirmed by observed negative mass balances in recent years (unpublished data of UGRH); its foreseeable vanishing will enable the formation of a medium-size lake (a few million m<sup>3</sup> volume) in a predominant rocky glacier bed. Ice avalanches with a runout distance 3 times the drop height can reach the upper parts of this lake. Corresponding floods can be retained in the regulated but conflict-related Lake Parón (Carey et al., 2012) if an adequate freeboard is maintained.

## REFERENCES

- Carey M., French A. & O'Brian E. 2012: Unintended effects of technology on climate change adaptation: an historical analysis of water conflicts below Andean Glaciers. *Journal of Historical Geography* 38, 181-191.
- Haeberli W. & Hoelzle M. 1995: Application of inventory data for estimating characteristics of and regional climate-change effects on mountain glaciers: a pilot study with the European Alps. *Annals of Glaciology*, 21, 206-212. Russian translation: *Data of Glaciological Studies*, Moscow, 82, 116-124.



Figure 1. Regulated Laguna Parón (lower left) and Glaciar Artesonraju at the foot of Nevado Artesonraju (6025 m a.s.l.; top, center) in the Cordillera Blanca, Peru.

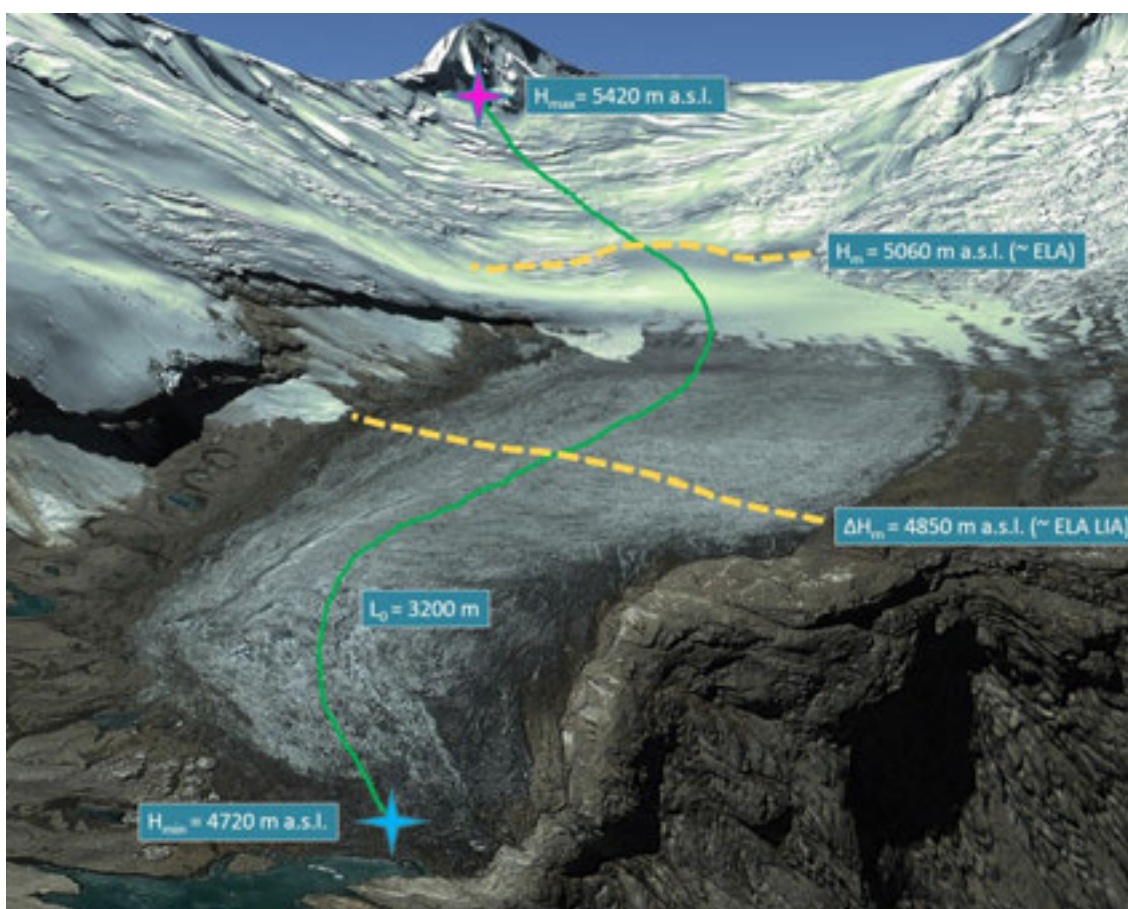


Figure 2. Glacier tongue of Artesonraju (cutout Figure 1, dashed rectangle) with maximum and minimum altitude, total horizontal length and past (LIA) and actual ELA.

## P 14.11

### Lidar snow cover studies in the Ötztal Alps

Kay Helfricht<sup>1,2</sup>, Katrin Schneider<sup>1</sup>, Rudolf Sailer<sup>3</sup>, Michael Kuhn<sup>2</sup>

<sup>1</sup> *alps Centre for Climate Change Adaptation, Grabenweg 68, A-6020 Innsbruck (helfricht@alps-gmbh.com)*

<sup>2</sup> *Institute of Meteorology and Geophysics, University of Innsbruck, Innrain 52, A-6020 Innsbruck*

<sup>3</sup> *Institute for Geography, University of Innsbruck, Innrain 52, A-6020 Innsbruck*

The storage of water within the seasonal snow cover is a substantial source for runoff generation in high mountain catchments. For hydrological modelling in these catchments, knowledge about the spatial distribution of the snow cover is an important requirement. However, data of snow depths is usually available only on the point scale. Lidar techniques provide spatially distributed records of the surface elevation. Information on snow depth distribution can be derived by airborne laser scanning (ALS) even in inaccessible terrain on the catchment scale.

However, in addition to the snow cover, densifications of snow and firn and ice flow contribute to surface elevation changes on glacier surfaces. To evaluate surface elevation changes derived from ALS ( $\Delta z_{\text{ALS}}$ ) on four glaciers in the upper Rofental (Ötztal Alps, Austria),  $\Delta z_{\text{ALS}}$  were compared to in-situ measurements of snow depth using ground penetrating radar ( $h_{\text{GPR}}$ ). In firn areas snow densification, firn densification and submergent ice flow cause an underestimation of actual snow depths by  $\Delta z_{\text{ALS}}$ . This underestimation is less than assumed errors of measuring precipitation with rain gauges in mountain catchments and less than the typical snow depths on the investigated glaciers.

On the major parts of the glacier surfaces, differences between  $\Delta z_{\text{ALS}}$  and  $h_{\text{GPR}}$  are less than uncertainties calculated for the combination of ALS and GPR techniques to derive snow depths. The results support the analysis of ALS data of seasonal surface elevation changes recorded in the Ötztal Alps since 2001

Inter-annual persistence of the spatial snow distribution is a requirement for the application of simple parameterizations of snow redistribution in hydro-meteorological models simulating the snow cover of high mountain catchments. Therefore, a set of  $\Delta z_{\text{ALS}}$  of five accumulation seasons was analysed regarding the inter-annual persistence of snow accumulation in a small glacierized catchment (approx. 36 km<sup>2</sup>) in the Ötztal Alps (10°50'E, 46°49.5'N). Obviously snow is redistributed from adjacent slopes towards the glacier (Fig. 1). While accumulation patterns on the glaciers are more persistent, a higher annual variability of surface elevation changes is found on ice-free slopes. In general, frequency distributions of snow depth were more similar when using snow depths relative to the annual mean snow depth rather than absolute values.

Inter-annually persistent maximum snow depths were found along glacier margins at the footslopes of rock walls caused by avalanches and snow slides.

The results are a basis for snow-hydrological modelling in this mountain area and comparable Alpine catchments.

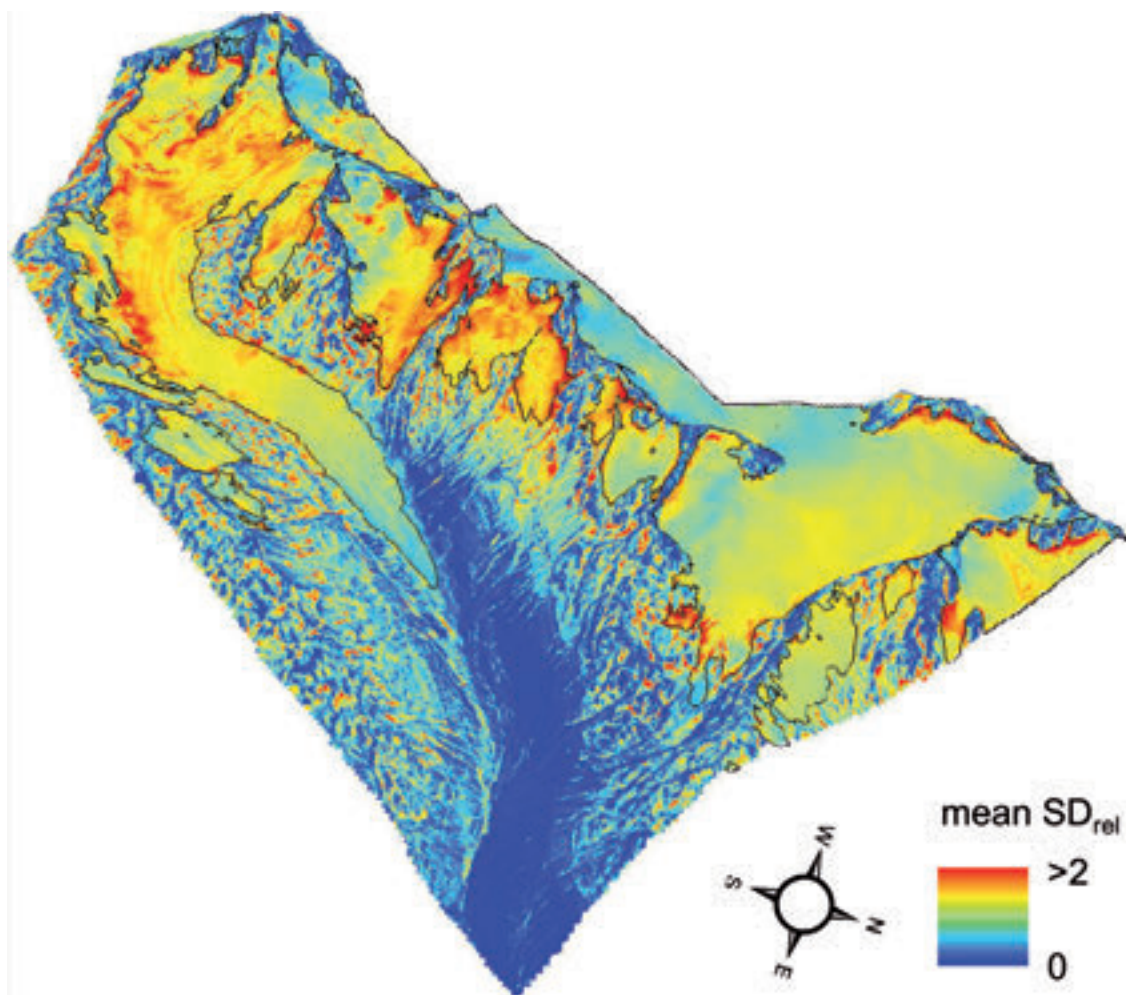


Figure 1. Mean relative snow depth of five accumulation seasons. Glacier outlines are shown in black.

# 17. Computational GIScience

M. Kanevski, Ch. Kaiser, F. Bavaud

## TALKS:

- 17.1 Bavaud, F.: Spatial autocorrelation and clustering: a minimal yet sufficient formalism
- 17.2 Emmanouilidis T.: GIS and urban planning: a new clustering algorithm for schools and students location-allocation
- 17.3 Grangier L., Kaiser C.: Touristic guides on smartphone – The Kalman filter for a smarter GPS localization in mountain area.
- 17.4 Guex G.: Mixing random walks and shortest paths to create new graph dissimilarities
- 17.5 Joost S., Stucki S., Leempoel K.: Geocomputational approaches for the analysis of Next-Generation Sequencing (NGS) and multi-scale data in landscape genomics
- 17.6 Josset L., Demyanov V., Ginsbourger D., Lunati I.: Uncertainty quantification in porous media using stochastic sampling algorithm and Functional Data Analysis
- 17.7 Kaiser C.: Searching geolocated databases with vague spatial objects
- 17.8 Kanevski M.: Geospatial data analysis and modelling using geostatistics and machine learning
- 17.9 Lochbühler T., Vrugt J.A., Linde N.: Realistic model constraints in probabilistic inversion of geophysical data: Summary statistics from training images
- 17.10 Price B., Kienast F., Seidl I., Verburg P., Ginzler C., Bolliger J.: Spatially explicit modelling of land-use suitability and future land-use pattern for Switzerland

## POSTERS:

- P 17.1 Calianno M., Gourley J. J., Ruin I.: Forecasting flash flood impacts utilizing anthropogenic exposure factors
- P 17.2 Demyanov V., Kanevski M.: Multi-scale spatial modelling of radioactive pollution with a kernel learning algorithm
- P 17.3 Golay J., Kanevski M., Vega Orozco C.: The multipoint Morisita index for the analysis of geodemographic data
- P 17.4 Leuenberger M., Kanevski M.: Extreme learning of environmental pollution
- P 17.5 Leuenberger M., Vega Orozco C., Tonini M., Kanevski M.: Random Forest for susceptibility mapping of natural hazards
- P 17.6 Ruggeri P., Irving J., Holliger K.: Evaluation of geostatistical resampling as a proposal mechanism in Bayesian MCMC solutions to hydrogeophysical problems
- P 17.7 Tonini M., Vega Orozco C., Kanevski M.: Wildfires spatio-temporal aggregation: from global cluster to local mapping
- P 17.8 Vega Orozco C., Tonini M., Kanevski M.: Analysis of the dynamic of urban areas and of their interaction with forest fires

## 17.1

# Spatial autocorrelation and clustering: a minimal yet sufficient formalism

Bavaud François

*Institute of Geography and Sustainability, Faculty of Geosciences and Environment, University of Lausanne, CH-1015 Lausanne*

One considers  $n$  topologically related, irregular regions, with differing multivariate profiles. Measuring and modeling spatial autocorrelation, as well as clustering the regions into  $m$  groups requires a minimal yet sufficient set of three non-negative matrices:

- a  $(n \times n)$  symmetric *exchange matrix*  $E$ , whose components, summing to unity, interpret as the probability of selecting a pair of regions, and whose margin defines the regional weights  $f$
- a  $(n \times n)$  *dissimilarity*  $D$  between regions, chosen as squared Euclidean
- a  $(n \times m)$  *soft membership matrix*  $Z$  giving the probability that region  $i=1, \dots, n$  belongs to group  $g=1, \dots, m$ .

For instance:

- *weighted multidimensional scaling* of  $(D, f)$  amounts in the *principal component analyses* routinely used in quantitative Geography
- pointwise Schoenberg transformations of  $D$  into new squared Euclidean distances produce the high-dimensional embedding of features encountered in Machine Learning
- the index  $1 - \text{trace}(ED)/(f'Df)$  provides a multivariate generalization of *Moran's I*, measuring spatial autocorrelation
- *spectral clustering* consists in partitioning the weighted undirected network described by  $E$  by considering the eigenvectors of (a standardized version of  $E$ ) as the regional features.
- minimizing over  $Z$  the free energy functional  $V[D, f, Z] + T H[Z]$  amounts in the *soft K-means clustering* procedure, where  $V$  is the within-groups dispersion,  $H$  the regions-groups mutual information and  $T > 0$  the temperature, controlling the softness of the resulting clustering.

We present a new algorithm, **landscape clustering**, favoring the grouping of regions with small dissimilarities *and* strong exchanges. It works for any positive semi-definite exchange matrix  $E$ , such as resulting from a continuous-time jump process whose infinitesimal generator is given by a binary adjacency matrix, with fixed weights. It contains two free parameters, namely the *temperature*  $T$ , as well as the *contiguity contribution*  $p$  in  $[0, 1]$ :  $p=1$  amounts to spectral clustering,  $p=0$  to K-means, and  $0 < p < 1$  to a clustering scheme taking into account *both proximity and similarity between regions*. Illustrations are provided by the clustering of French departments, taking into account their spatial contiguity as well as their political configurations in the first round of the French presidential 2012 election.

## 17.2

# GIS and urban planning: a new clustering algorithm for schools and students location-allocation

Emmanouilidis Théophile

*Institute of Geography and Sustainability, Faculty of Geosciences and Environment, University of Lausanne, CH-1015 Lausanne*

The use of GIS (for data visualisation or simulation) in the public administration has greatly increased in the past years. Since 2009, the school department of Lausanne has been able to answer political and public demands by leading two main GIS-projects. The first one was to give public transport subvention to schoolchildren by considering their age and shortest path distance from home to school. The second one, which will be exposed here, is about primary schools and students (from 4 to 10 years old) location-allocation. Due to major changes in the Swiss educational laws (HarmoS), the department was asked to reduce the population of each school establishment (group of schools) by creating new ones of similar size and taking into account the future growth of the city.

Conceptually the idea is to assign node (student home location)  $i=1,\dots,n$  to the nearest school  $g=1,\dots,m$  considering its location  $L^*(g)$  and capacity  $\rho^*(g)$ . This classical location-allocation problem is solved by a new soft constrained clustering algorithm defined as:

$$z_{ig} = \frac{\rho_g^* \epsilon_g \exp(-\beta F(d_{iL^*(g)}))}{\sum_h \rho_h^* \epsilon_h \exp(-\beta F(d_{iL^*(h)}))}$$

- $z_{ig}$  : probability to attribute node  $i$  to school  $g$
- $F(d_{iL^*(g)})$ : is an increasing non negative function of distance between  $i$  and  $g$ . In the present case, it corresponds to the shortest path distance computed through the pedestrian network of the city.
- $\beta$ : parameter controlling the sharpness of the groups.
- $\epsilon$ : is a parameter controlling the capacity constraints, iteratively determined as :

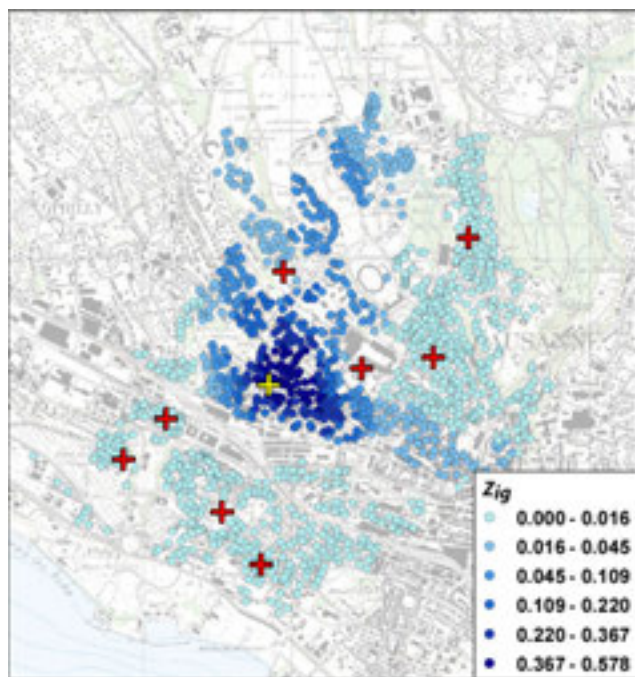
$$\frac{1}{\epsilon_g} = \sum_i \frac{f_i \exp(-\beta F(d_{iL^*(g)}))}{\sum_h \rho_h^* \epsilon_h \exp(-\beta F(d_{iL^*(h)}))}$$

- $f_i$  : proportion of student living in location  $i$  (relative weight)

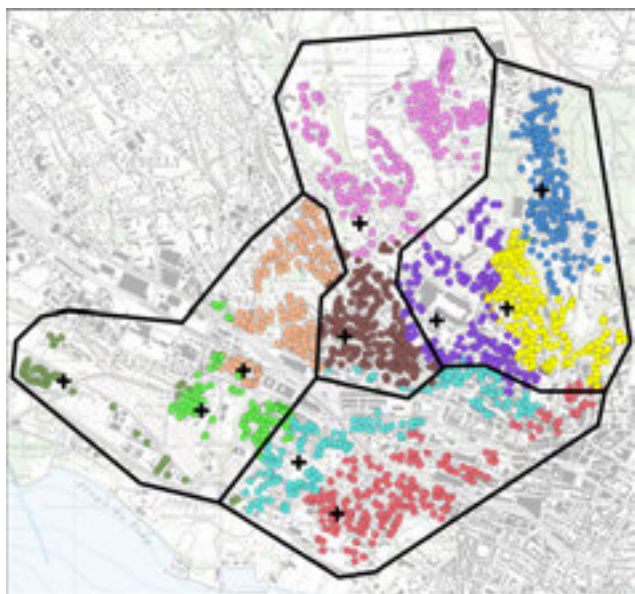
### REFERENCES

- A. Antunes, D. Peeters (2000) A dynamic optimization model for school network planning, *Socio-Economic Planning Sciences* 34, pp. 101-120
- F. Bavaud (2010) Aggregation invariance in general clustering approaches, *Advances in Data Analysis and Classification* 3, pp. 205-225
- T. Emmanouilidis and F. Bavaud (2012) Analysis of the pedestrian network of Lausanne : eccentricity, accessibility and partitionning, to be published
- Nock, R. and Nielsen, F. (2006) On weighting clustering in *Pattern Analysis and Machine Intelligence* Vol.28, n°8
- Wilson A G, (1971) A family of spatial interaction models, and associated developments *Environment and Planning* 3(1), pp. 1 – 32

## RESULTS:



Constrained fuzzy-clustering in the West of Lausanne ( $\beta=0.005$ ). Each dot represent a schoolchildren(s) building and the colour its probability to be assigned to the school of "Prélaz" (yellow cross) considering the 8 others schools.



"Hardened" soft constrained clustering of the West part of Lausanne: map depicts for each node the regions of highest membership. Contiguous regions can then be merged to create new school establishments.

## 17.3

### Touristic guides on smartphone – The Kalman filter for a smarter GPS localization in mountain area.

Grangier Lucien<sup>1</sup>, Kaiser Christian<sup>1</sup>

<sup>1</sup>*Institute of geography and sustainability, Mouline – Geopolis, University of Lausanne, 1015 Lausanne (Lucien.grangier@unil.ch)*

With the increasing ubiquity of smartphones and tablet computers, the number of available applications for mobile platforms is growing fast while their quality is highly variable. Nearly every brand, store, and municipality wants a smartphone application to be in the main stream. Many visitor/touristic guides are among this abundance of applications. Generally they permit to guide the user in a city or a museum, to share knowledge and information, to interact with other users and also increasingly with the environment through Augmented Reality (AR).

This kind of applications uses multiple device features such as the camera, Wireless, 3G connection or GPS, which are all voracious in energy. Usually the user is indoors or in an urban environment where it's easy to connect and charge the device. But what happens if we want to use an application in a mountain area? Often, no Internet connection is available, and generally no electricity to charge the battery. Applications designed for use in such an environment need to deal with a lot of constraints, and special care needs to be given to limited battery resources.

The Geographic Information Science Group of the Institute of Geography and Sustainability has developed in collaboration with the bureau "Relief" the application "Geoguide", which is a guide for a didactic walk in Lausanne (available on Android/iOS). Another application has been developed for the Vallon de Nant, which is in a mountain area. The concept of these applications is to offer a didactic trail through the region of interest, and at some precise locations, detailed information around a given theme is given using text, images and potentially videos. These applications provide the opportunity to develop and test new techniques in a real-world scenario.

In order to increase battery lifetime we want to optimise the localisation process. To display the current location on the screen, the device calculates its position every 10 seconds using GPS and cell tower locations. In this paper, we explore a technique to reduce usage of GPS and other location techniques while still providing an optimal user experience. The key idea is to vary the time between two requests to the device's location service. Around points of interest where the applications offers detailed information about the location, the frequency of locational requests is kept at 10 seconds, while in locations between points of interest, the frequency can be as low as one locational request each minute, or even less. In our approach, we use a Kalman filter to predict the user's future location, which is likely to be on the suggested trail. The application calculates the mean walking speed, and makes locational requests only occasionally to confirm and update the location prediction or before arriving at a point of interest.

The approach of using a Kalman filter for locational prediction can also be used for notifying the user when arriving at a point of interest. This is especially useful in a mountain environment where points of interest might be sparse and in some cases considerable physical effort is required between two points of interest. Especially in such an environment, the user of the smartphone application does not want to let the device switched on to permanently checking if detailed information about his current location is available. As a solution, the device calculates the approximate time of arrival at the next point of interest to confirm and update its position more frequently, and finally notifies the user through a sound or vibration notification that information is available. This feature allows for putting the device into standby mode for most of the time, further reducing the energy consumption and increasing battery lifetime.

Link

<http://igd.unil.ch/geoguide/>

## 17.4

# Mixing random walks and shortest paths to create new graph dissimilarities

Guex Guillaume

Institute of Geography and Sustainability, University of Lausanne, CH-1015 Lausanne

The analysis of geographical networks often requires to compute a dissimilarity between nodes and to use this dissimilarity to perform classifications and visualisation algorithm or to compute derived indices. The *shortest-path distance* is historically the most used dissimilarity, but it has been shown recently that the *commute-time distance* offer an interesting alternative (see e.g. Liu et al. 2013), as it is squared Euclidean for all graphs and gives very different and interesting results.

This contribution presents the properties of known graph dissimilarities in the first part and shows how to build more general *flow-based dissimilarities* in the second part. A flow  $\mathbf{X} = (x_{ij})$ , modelling agents moving on the edges of a graph, is computed to minimize a *free energy functional*  $F(\mathbf{X}) = U(\mathbf{X}) + T G(\mathbf{X})$ , where the *energy*  $U(\mathbf{X})$  encourages agents to follow routes of least cost, the *entropy*  $G(\mathbf{X})$  adds a random component to movements and the *temperature*  $T > 0$  arbitrates between the conflicting objectives of minimizing the costs and maximizing randomness (Saerens et al. 2009, Bavaud & Guex 2012). The properties of these new dissimilarities will be studied on different networks and various examples of applications on geographical and spatial networks will be exhibited.

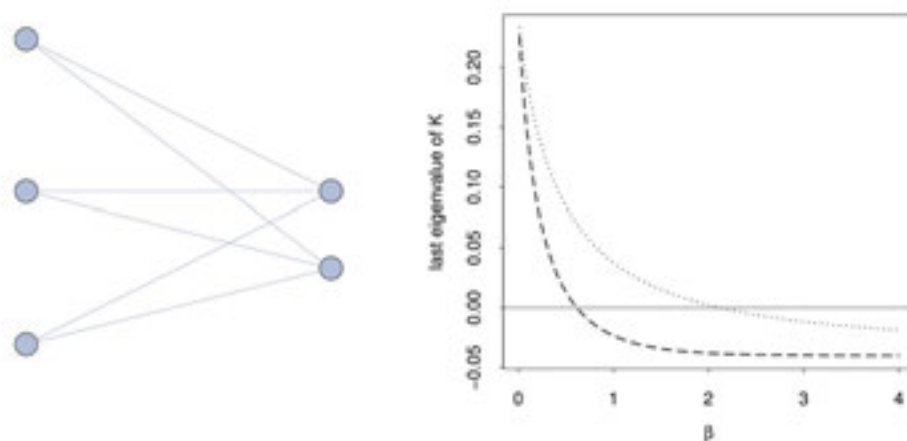


Figure 1. Evolution of the last eigenvalue of  $\mathbf{K}$ , the matrix of “scalar product” derived from two different flow-based dissimilarities built on the bipartite network shown left, regarding  $\mathbf{b} = 1/T$ , the inverse temperature. When  $\mathbf{b}$  is small, the dissimilarities tend to commute-time distances and are squared Euclidean as  $\mathbf{K}$  is positive semidefinite. As  $\mathbf{b}$  increases, they tend to shortest-path distances and negative eigenvalues occur, ruining the squared Euclidean nature of the dissimilarities.

## REFERENCES

- Bavaud, F. & Guex, G. 2012: Interpolating between random walks and shortest paths: a path functional approach. K. A. et al. (Ed.), SocInfo 2012, Vol. 7710 of Lecture Notes in Computer Science, pp. 68-81. Springer.
- Liu, S., Matzavinos, A., Sethuraman, S. 2013: Random walk distances in data clustering and applications. Adv. Data Analysis and Class.7, pp. 83-108.
- Saerens, M., Achabany, Y., Fouss, F., Yen, L. 2009: Randomized shortest-path problems: two related models. Neur. Comp. 21, pp. 2363-2404.

## 17.5

## Geocomputational approaches for the analysis of Next-Generation Sequencing (NGS) and multi-scale data in landscape genomics

Joost Stéphane<sup>1</sup>, Stucki Sylvie<sup>1</sup>, Leempoel Kevin<sup>1</sup>

<sup>1</sup> Laboratory of Geographic Information Systems (LASIG), School of Architecture, Civil and Environmental Engineering (ENAC), Ecole Polytechnique Fédérale de Lausanne (EPFL), Building GC, Station 18, CH-1015 Lausanne (stephane.joost@epfl.ch)

The application of geocomputation to the field of landscape genomics (Manel et al. 2010) permits to carry out demanding computational tasks that recently emerged because of the advent of large Next-Generation Sequencing data. When investigating the genetic mechanisms of evolution in spatially distributed plants or animals, geocomputation also proves to be useful to process many association models (gene x environment) in a multi-scale context.

One challenge for correlative approaches when detecting genomic regions possibly under natural selection is to distinguish the effect of environmental conditions from effects caused by the demographic history of investigated populations. Several methods have been developed in population genetics, the most promising being the analysis of patterns of linkage disequilibrium (LD) (Jensen et al. 2007). LD is the occurrence of combinations of alleles (variant forms of the same gene) in a population more often or less often than would be expected at random. Correlative approaches also offer a solution by means of the integration of measures of Local Indicators of Spatial Association (LISA). Indeed, Stucki et al. (2012) made it possible to process high-throughput geo-referenced molecular datasets and underlying environmental variables, and to simultaneously provide a list of genomic regions likely to be under selection with a measure of local spatial autocorrelation. The latter constitutes a useful indication as regards the possible kinship relationship between individuals. In the context of a research on local adaptation in 102 Ugandan cattle individuals, more than 2 million of binary markers have been compared to 73 WorldClim and SRTM-derived environmental variables (Stucki et al. 2013). The most interesting model included an interesting genetic marker that maps to a gene (CHST11) involved in cartilage make up (Figure 1).

Another challenge for landscape genomics is to address a fundamental issue often referred as to “at which spatial scale does adaptation act?” Most of the time, research is carried out at one single scale. However, Leempoel et al. (2013) developed a geocomputational framework based on a signal processing generalization technique to produce DEMs at multiple scales allowing for a continuous representation of the landscape. In order to better understand the way an Alpine plant named *Biscutella laevigata* L. adapts to the environment, the approach was used to investigate its adaptive response to environmental variables derived from these DEMs. For this purpose 266 genetic markers from 361 individuals sampled on the ridge of “Les Rochers-de-Naye” in the Swiss Prealps were used. Preliminary results show that resolution matters at a local scale (Figure 2), but that the use of very high resolution variables does not necessarily improve the significance of the results obtained. However, current investigations will show if their use combined with a multi-scale analysis system permits to detect relationships that would have gone unnoticed otherwise.

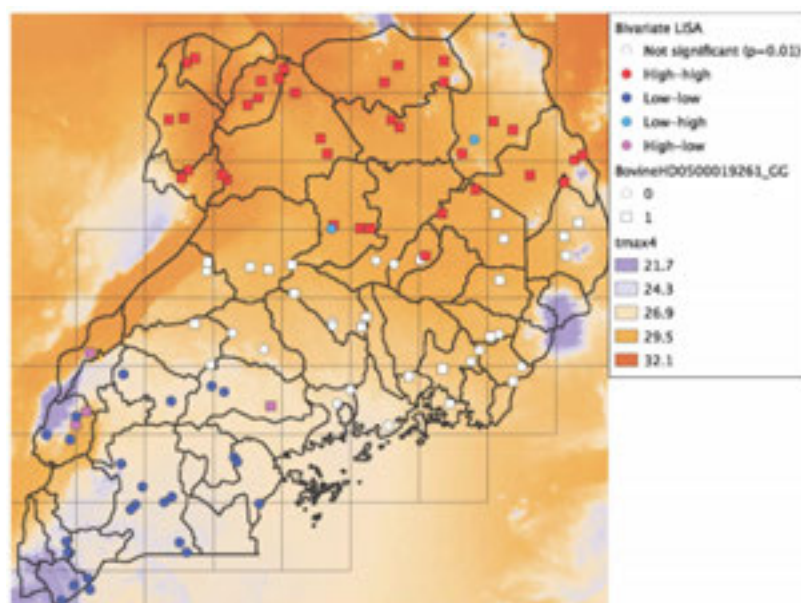


Figure 1. Bivariate LISA between marker BovineHD0500019261\_GG and mean temperature in April with corresponding clusters (weighting scheme is  $K = 20$  nearest neighbors). Dots indicate the presence (square) or absence (circle) of markers and their color shows the type of association.

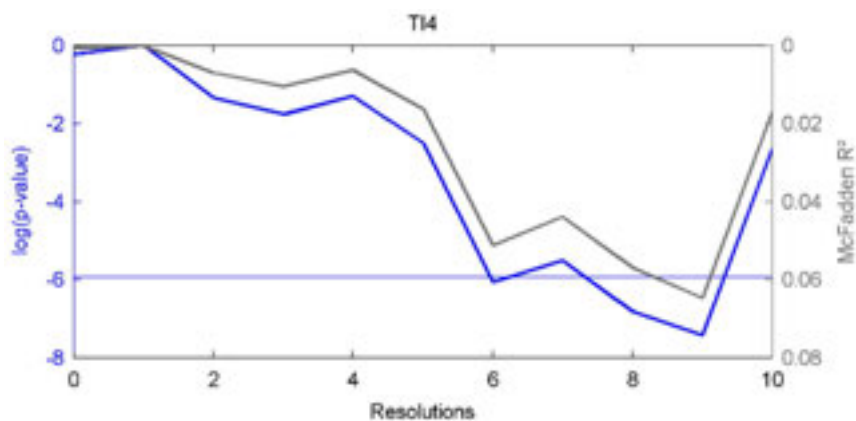


Figure 2. Variation of the log of the p-value in function of the spatial resolution (m) for the model involving genetic marker C1v242 and solar radiation.

## REFERENCES

- Jensen, J.D., Thornton, et al. 2007: On the utility of linkage disequilibrium as a statistic for identifying targets of positive selection in nonequilibrium populations. *Genetics*, 176, 2371–2379.
- Leempoel, K., Geiser, et al. 2013: A multiscale landscape genomics analytical framework to identify local adaptive variation in the Buckler Mustard, IALE 2013 European Congress, Manchester, September 2013.
- Manel, S., Joost, S., et al. 2010: Perspectives on the use of landscape genetics to detect genetic adaptive variation in the field. *Mol. Ecol.*, 19, 3760-3772.
- Stucki, S., Orozco-terWengel, et al. 2013: Sambada in Uganda: landscape genomics study of traditional cattle breeds with a large SNP dataset, IALE 2013 European Congress, Manchester 9-12 September 2013.
- Stucki, S. Agha, S., et al. 2012: Utilization of the Scythe C++ open source library for statistical geocomputation in livestock landscape genomics. Proc. OGRS Symposium, Yverdon-les-Bains, Switzerland, October 2012.

## 17.6

### Uncertainty quantification in porous media using stochastic sampling algorithm and Functional Data Analysis

Josset Laureline<sup>1</sup>, Demyanov Vasily<sup>2</sup>, Ginsbourger David<sup>3</sup> & Lunati Ivan<sup>1</sup>

<sup>1</sup> Centre de Recherche en Environnement Terrestre, University of Lausanne, Quartier UNIL-Mouline, Bâtiment Géopolis, CH-1015 Lausanne (laureline.josset@unil.ch)

<sup>2</sup> Institute of Petroleum Engineering, Heriot-Watt University, Energy Academy Building, Edinburgh EH14 4AS, UK

<sup>3</sup> Institute of Mathematical Statistics and Actuarial Science, University of Bern, Alpeneggstrasse 22, CH-3012 Bern

Predicting flow in aquifers and reservoirs is difficult due to the lack of information on flow and transport properties of the formation. Generation of multiple model realisations aims at quantifying the uncertainty of flow predictions. A pragmatic approach to uncertainty quantification in flow modelling is to determine the region of the model-parameter space where model results match observed dynamic flow responses (e.g. flow rates, contaminant concentration). However, due to the computational limitation, the systematic evaluation of the flow response for each model realization generated in a Monte Carlo implies prohibitive computational costs.

We propose two strategies to reduce the computational costs: on one hand, we employ an adaptive stochastic sampling algorithm (particle swarm optimization) to accelerate the exploration of the parameters space; on the other hand, to evaluate the flow response of the generated models, we use an approximate model coupled with an error model to predict the corresponding exact response. This error model is constructed using Functional Data Analysis (FDA) on a training set of model solutions for which both exact and approximate responses are known.

The proposed approach is tested on a synthetic test case: a layered aquifer divided by a fault, for which the permeabilities of the layers and the fault throw have to be determined. We evaluate the performance of this approach and present a comparison with concurrent methods that have been previously applied to this test case.

## 17.7

### Searching geolocated databases with vague spatial objects

Kaiser Christian

*Institute of geography and sustainability, University of Lausanne, CH-1015 Lausanne*

Geographic databases are increasingly available on the Web. For example, Viatimages ([www.unil.ch/viatimages](http://www.unil.ch/viatimages)) is an on-line database with geolocated historic images mainly with Alpine landscapes. Many other similar examples exist on the Web. Such a database frequently contains geographic features with vague boundaries or unknown extent. During the geolocalisation process, the exact location of an item might not be known, or the chosen location is wrong. Or the user of the database is interested in all items that are located «around the Lake of Geneva» or «along the Rhône river». The human representation of these locations is usually relatively vague. At the same time, the digital representation of the same concepts is frequently built around vector geometries, which have very precise boundaries. This paper shows a possible solution to this discrepancy, by introducing vague vector geometries and simple spatial query operators.

Geolocated items in a database, such as images with known location, are usually stored as simple points. Regions are mostly represented as polygons. For such vector geometries, efficient spatial operators such as intersection, membership (A within B) or union exist. Due to the precise boundary of vector geometries, they are unsuitable for spatial objects with vague extent or limits. Consequently, vague spatial objects are generally modelled using a raster representation with values varying between 0 (outside of the object) and 1 (inside the object). For big objects with high raster resolution, this approach leads to big datasets while still being limited in the spatial resolution. As an alternative, we use vector geometries enhanced with information on the vagueness of the boundary. Different types of transition from «inside the spatial object» to «outside the spatial object» can be defined. Such a transition is any function going from 1 (inside the object) to 0 (outside

the object). Figure 1 gives some possible transition functions. For each point on the boundary of a vector geometry, a transition function can be defined. A transition function usually needs at least one parameter defining the size of the vague boundary. In the case of a Gaussian function, this parameter is usually referred to as «bandwidth». Figure 2 shows a simple representation of an example polygon with a vague boundary. The small lines orthogonal to the polygon boundary are the definition of the transition function, where the length of the line represents the bandwidth of the Gaussian function. For points between two transition functions, a weighted average based on the proximity to the transition function is calculated. Such a representation also allows for simple editing of vague vector geometries. It is important to note that these vague vector geometries are a simple extension of traditional vector geometries with hard boundaries.

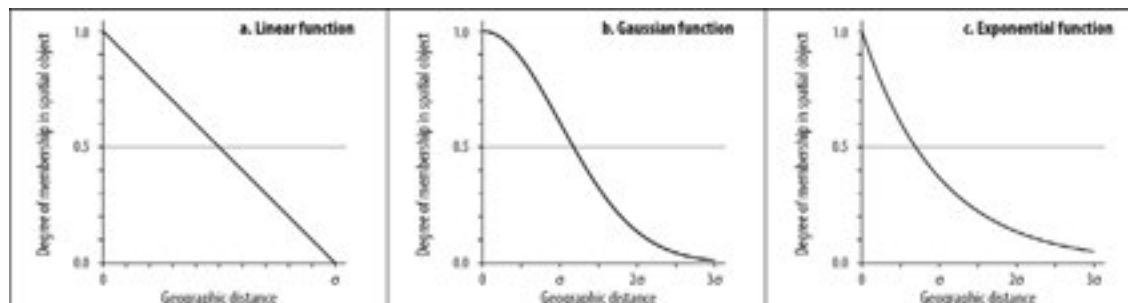


Figure 1. Different possible functions for defining vague boundaries on vector geometries.

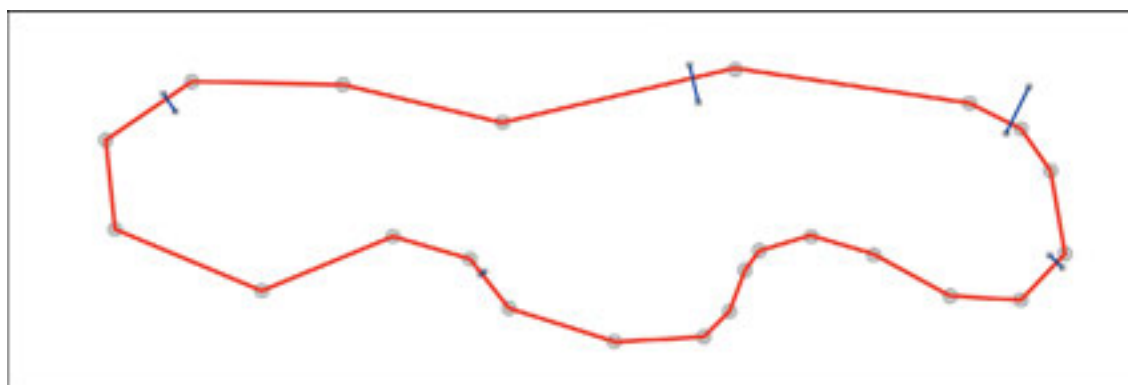


Figure 2. Definition of a polygon with vague boundary. The blue lines with small rectangle handles for manipulation allow for definition of the extent of the vague boundary.

Once the spatial objects with vague boundaries are defined, they can be used for spatial search using membership and intersection operators known from traditional GIS. Due to the imprecise boundary, these operators need to be modified. For example, a query of type «Does polygon A contain point B?» does not necessarily have an answer «true» (=1) or «false» (=0), but 0.9 indicating that there is a high chance that point B is inside polygon A. The search result can be sorted according to these membership operator values.

Membership and intersection operators are only in some special cases easy to define for geometries with vague boundaries. In most cases, a discrete approximation needs to be calculated, which can be done by creating a local raster image at locations with vague boundaries. The operators are well defined for the case of discrete raster images.

The presented approach to define vague spatial objects is a relatively simple extension of existing vector geometries, allowing at the same time for quite easy editing of the geometries. It gives the flexibility to deal with a wider range of spatial objects in a straightforward manner, and enabling spatial databases with more flexible search functionality.

## 17.8

# Geospatial data analysis and modelling using geostatistics and machine learning

Kanevski Mikhail

*Centre for Research on Terrestrial Environment, University of Lausanne, CH-1015 Lausanne (Mikhail.Kanevski@unil.ch)*

The presentation gives an overview of the research on geospatial data analysis, modeling and visualization carried out at the Faculty of Geosciences and Environment, University of Lausanne. The research covers both elaboration and adaptation of new methods and models, as well as algorithms and software tools developments. The main applications deal with geospatial environmental, natural hazards, socio-economic and demographic data. Some of the achievements were published in books and book chapters, see the references below.

The main approaches widely used for geospatial data include: geostatistics (variography, predictions and simulations, including risk mapping); machine learning (supervised, unsupervised, semi-supervised) algorithms (artificial neural networks of different architectures – multilayer perceptron, general regression neural networks, probabilistic neural networks, radial basis function networks, Gaussian mixtures, mixture density networks, random forest; and statistical learning theory - kernel-based methods, e.g. support vector machines, etc.), and visualization of multivariate and high dimensional data using, between many others, parallel coordinates, Andrews plots, Kohonen self-organizing maps.

It should be noted that, the most relevant and efficient methods and tools are selected depending on the quantity and quality of data, dimensionality of the problem and objectives of the study. In case of application of machine learning, an important problem is testing and justification of the quality of the results by characterizing the uncertainties and confidence intervals. An important part of the methodology is a comprehensive exploratory analysis of raw data and the modelling residuals.

In fact, many environmental, natural hazards and socio-economic phenomena should be considered and modeled in a high dimensional feature space ( $d \sim 10-100$ ). Therefore the problem of relevant features/characteristics extraction/selection becomes an important one, both for the understanding of the phenomena and the explanation of the results. For this reason, machine learning algorithms which have inherent capabilities to rank or select features (adaptive general regression neural networks, random forest, multiple kernel learning, and others) are very useful.

Some of the recent and representative results on the application of machine learning algorithms for geo- and environmental data (pollution and natural hazards) are presented and discussed within the framework of the developed self-consistent data modelling methodology. An important part of the methodology concerns the analysis and optimization of monitoring networks. The problem is quite difficult, especially when the phenomena are considered in a high dimensional space. Within the framework of machine learning an active learning approach was successfully applied for monitoring networks design/redesign both for low and high dimensional environmental data.

The most important future developments deal with better characterization of uncertainties, multiscale analysis of geospatial data, automatic feature selection, and better understanding and modelling of space-time phenomena.

The author would like to thank to many colleagues and coauthors for fruitful and interesting collaboration on the topics considered.

### REFERENCES

- Kanevski, M. & Maignan M. 2004: Analysis and Modelling of Spatial Environmental Data, EPFL Press, Lausanne.
- Kanevski M. (Editor). 2008: Advanced Mapping of Environmental Data, iSTE and Wiley.
- Kanevski M., Foresti L., Kaiser Ch., Pozdnoukhov A., Timonin V. & Tuia D. 2009: Machine Learning Models for Geospatial Data. In: F. Bavaud and C. Mager (Eds.), Handbook of Quantitative and Theoretical Geography, University of Lausanne, pp. 175-227
- Kanevski M., Pozdnoukhov A. & Timonin V. 2009: Machine Learning for Spatial Environmental Data. Theory, Applications and Software. EPFL Press, Lausanne.
- Tuia D., Pozdnoukhov A., Foresti L. & Kanevski M. 2013: Active learning for monitoring network optimization. In: Mateu J. & W. Muller, Spatio-temporal design. Wiley.

## 17.9

# Realistic model constraints in probabilistic inversion of geophysical data: Summary statistics from training images

Lochbühler Tobias<sup>1</sup>, Vrugt Jasper A.<sup>2</sup>, Linde Niklas<sup>1</sup>

<sup>1</sup> Applied and Environmental Geophysics Group, Faculty of Geosciences and Environment, University of Lausanne, Lausanne, Switzerland (tobias.lochbuehler@unil.ch)

<sup>2</sup> Department of Civil and Environmental Engineering, University of California Irvine, Irvine, CA, USA

Multiple-point statistics training images are conceptual geological models that feature the dominant lithological units and structural patterns of a site of interest. They provide strong *a priori* information on model morphology that is used to constrain models in probabilistic inversion. This is done by extracting summarizing statistical metrics from realizations of a training image and including the probability of each proposal state given the difference between the observed and simulated summary metrics in the calculation of the posterior probability of each proposal model. Realistic constraints are thus imposed on the inverse models avoiding expensive model updating of common geostatistical approaches. The inverse problem is solved in a Bayesian formulation by Markov chain Monte Carlo sampling with the MT-DREAM<sub>(ZS)</sub> algorithm. Additional to the summary metrics, the training image realizations are used to define case-dependent optimal parameterizations by compressed sensing analysis in the discrete cosine domain, which drastically reduces the dimensionality of the inverse problem but maintains the ability to recover realistic subsurface structures. The methodology is applied to crosshole ground-penetrating radar data for two synthetic case studies. The benefits of two different summary metrics are evaluated: the frequency of occurrence of different geological facies and the total sum of discrete cosine transform coefficients as a global measure of model variability. It is shown that using the model constraints helps to (1) steer the inversion towards geologically more realistic *a posteriori* models, (2) prevent inversion artifacts, and (3) decrease the deviation between the most probable model and the true subsurface, thus mitigating a common pitfall of high-dimensional inverse problems. The proposed approach is general and allows great flexibility in terms of the applied model constraints and the type of geophysical forward problem.

## 17.10

# Spatially explicit modelling of land-use suitability and future land-use pattern for Switzerland

Price Bronwyn<sup>1</sup>, Kienast Felix<sup>1</sup>, Seidl Irmi<sup>1</sup>, Verburg Peter<sup>2</sup>, Ginzler Christian<sup>1</sup> & Bolliger Janine<sup>2</sup>

<sup>1</sup> Swiss Federal Institute for Forest, Snow and Landscape Research WSL, Zürcherstrasse 111, CH-8903 Birmensdorf (bronwyn.price@wsl.ch)

<sup>2</sup> Institute for Environmental Studies (IVM), VU University Amsterdam, De Boelelaan 1087, 1081 HV Amsterdam, The Netherlands

Using three time steps of the high-resolution Swiss Land-Use/Land-Cover Statistics (1985, 1997 and 2009), we map and measure past land-use and land-use type transitions. We model the suitability for a given land-use and the probability of land-use transitions for the whole of Switzerland with respect to a suite of biophysical explanatory variables, comparing the predictive ability of various (geo)statistical and data-mining techniques such as regression kriging, random forests and logistic regression. The models of land-use suitability are a key input to land-use change models for Switzerland.

Socio-economic processes are strong drivers of land-use change across European landscapes. Land abandonment, relating to a decline of agricultural significance, has been a dominant process affecting European landscapes, and in particular mountainous regions such as in Switzerland since the mid 20th century. Urbanisation in Switzerland is increasing at a rapid rate as population increases and, in particular, with increasing demand in living-space per capita. Decrease in public support for nuclear power stations is driving a push towards increased production of renewable energy within Switzerland. These inter-related and sometimes competing processes have significant implications for land-use and patterns of land-use change within Switzerland, yet the extent and location of anticipated land-use changes remain unknown, as does the impact on landscape services.

This project defines 5 scenarios of future land-use demands for Switzerland under different projections for urban-sprawl, land abandonment and land use for renewable energy production.

Using the Dyna-CLUE land-use change modelling framework (Verburg and Overmars, 2009) we applied the 5 future scenarios to determine and visualize (map) future land-use patterns in a spatially explicit manner. Under a 'business-as-usual' scenario we evaluate the ability of the model to produce the 'current' land-use pattern (Swiss land-use statistics 2009), from the 1997 initial state.

The resulting spatially explicit land-use scenarios will be freely available for download by researchers and policy makers. These scenarios will provide key base information for future work including assessing conflicts and synergies in land-use planning or assessing impacts of land-use change on landscape services.

## REFERENCES

Verburg, P.H. & Overmars, K.P. 2009: Combining top-down and bottom-up dynamics in land use modeling: exploring the future of abandoned farmlands in Europe with the Dyna-CLUE model. *Landscape Ecology*, 24: 1167-1181. <http://dx.doi.org/10.1007/s10980-009-9355-7>

## P 17.1

# Forecasting flash flood impacts utilizing anthropogenic exposure factors

Calianno Martin<sup>1</sup>, Gourley Jonathan J.<sup>2</sup> & Ruin Isabelle<sup>3</sup>

<sup>1</sup>Institut de Géographie et Durabilité (IGD), University of Lausanne, Géopolis, CH-1015 Lausanne (martin.calianno@unil.ch)

<sup>2</sup>NOAA, National Severe Storm Laboratory (NSSL), Norman, USA

<sup>3</sup>Laboratoire d'étude des Transferts en Hydrologie et Environnement (LTHE), Université Joseph Fourier, Grenoble, France

If you've ever attempted to hand contour of map of damage from flash flooding, you will quickly discover the spatial character is strongly influenced by surface controls, which creates discontinuous and untidy contours. Low-water crossings, infrastructure built in close proximity to streams, normally dry riverbeds in populated zones, and roads in low-lying areas are all examples of anthropogenic factors that increase societal susceptibility to flash flooding.



Figure 1. Flash flood in Fort Worth, TX, June 27, 2007. © AP photograph/Fort Worth Star-Telegram, Ron Jenkin

Unfortunately, tools commonly used to monitor and predict flash flooding, including sophisticated distributed hydrologic models, rarely incorporate any information about these factors. In this study, we rely on a detailed impact classification and analysis of flash flood reports from the National Weather Service (NWS) Storm Data and Severe Hazards Analysis and Verification Experiment (SHAVE) conducted at the National Severe Storms Laboratory (NSSL) in Norman, Oklahoma (Gourley et al. 2010). The flash flood impact database is then used to derive static exposure indices using GIS layers of road networks, population density, stream locations, elevation, degree of imperviousness (urbanization), land use, etc (Calianno et al. 2013). The exposure indices are then used in conjunction with distributed hydrologic model simulations with forcing from radar quantitative precipitation estimations (QPE) to improve the specificity and accuracy of forecasts, with a focus on the particular impacts. Two extreme flash flooding events in Oklahoma are studied to demonstrate the new approach, highlighting improvements and shortcomings.

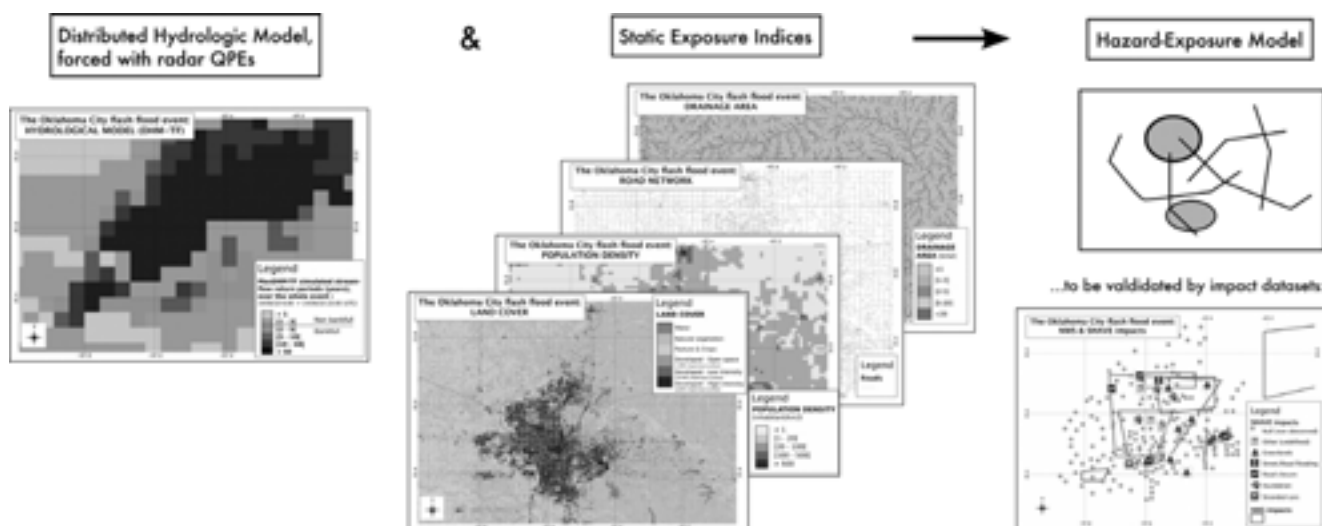


Figure 2. Conceptual scheme of the Hazard-Exposure model for flash flood impact forecasting.

## REFERENCES

- Calianno M., Ruin I. & Gourley J.J. 2013: Supplementing flash flood reports with impact classifications. *J. Hydrol.* 477, 1-16.
- Gourley, J.J., Erlingis, J.M., Smith, T.M., Ortega, K.L. & Hong, Y. 2010: Remote collection and analysis of witness reports on flash floods. *J. Hydrol.* 394, 53-62.

**P 17.2****Multi-scale spatial modelling of radioactive pollution with a kernel learning algorithm**

V. Demyanov<sup>1</sup>, M. Kanesvki<sup>2</sup>

<sup>1</sup> Heriot-Watt University, Erinbugh, UK, [vasily.demyanov@pet.hw.ac.uk](mailto:vasily.demyanov@pet.hw.ac.uk)

<sup>2</sup> University of Lausanne, Suisse

Modelling multi-scale spatial patterns originated from complex combination of sources and impact factors is a challenging problem. Many conventional spatial modelling algorithms (geostatistics) are limited by stationarity assumptions and are not flexible enough to cope with highly variable patterns correlated at multiple scales. Machine learning approach provides an effective alternative in modelling spatial patterns of different complexity at a range of spatial scales without the limitation of the stationarity assumption.

Multi-scale spatial structure can be modelled using kernel learning methods that fuse together in a non-linear model the information extracted from multiple input features, which represent a range spatial scales. The contribution of the input features is controlled by a set of kernel functions through Multiple Kernel Learning (MKL). The kernel learning model is subject to the kernel width choice as well as to a regularisation constant and the error threshold [Kanevski et.al. 2009]. The choice of these parameters can be routinely selected through cross-validation, training/testing or even ad-hoc trial and error approaches.

The present work proposes to use a modern stochastic optimisation technique to find multiple combinations of the MKL parameters that provide the best predictions. Adaptive stochastic sampling technique is good at searching effectively the multi-dimensional model parameter space to identify the subset of models with better prediction quality. Multi-criteria optimisation provides a way to minimise the objective function based on different components representing different aspects of the prediction quality: matching the test data, matching the target distribution, avoiding predictions outside the realistic range of values.

The proposed approach was applied to the Chernobyl radioactive fallout data, which are well known for their multi-scale character and are difficult to model with conventional stationary algorithms. The problem of multi-scale spatial mapping is tackled by extracting information from spatial features that represent different scales of the phenomenon. The features were derived with Gaussian kernel smoothing from the measurement data using different kernel sizes. This provides a range of input spatial features representing spatial scales from 1 to 50 km. Furthermore, the spatial features were processed to derive gradients and differences, which were also used as MKL inputs.

The methods resulted in multiple optimal prediction maps, which corresponds to a different balance of spatial multi-scale features contributing to the resulting prediction.

## REFERENCES

- Kanevski M., Pozdnoukhov A., and Timonin V. (2009) *Machine Learning Algorithms for Environmental. Spatial Data. Theory, Applications and Software.* EPFL Press.

## P 17.3

# The multipoint Morisita index for the analysis of geodemographic data

Golay Jean<sup>1</sup>, Kanevski Mikhail<sup>1</sup> & Vega Orozco Carmen<sup>1</sup>

<sup>1</sup> Center for Research on Terrestrial Environment, Faculty of Geosciences and Environment, University of Lausanne, CH-1015 Lausanne (jean.golay@unil.ch)

The present research deals with the application of the functional multipoint Morisita index (Hulbert, 1990; Golay et al., 2013) to geodemographic data. The main objective is to detect and characterize spatial structures in the distribution of the Swiss population at different scales. The population dataset of Year 2000, considered in this study, is based on a high resolution grid (100m x 100m). It can thus be treated as the realization of a point process where each point is associated with a spatial location and the number of inhabitants of the considered hectare.

The classical Morisita index is a global measure of clustering. It measures how many times more likely it is to randomly select two points belonging to the same quadrat (the spatial dataset is covered with a grid of varying cell size) than it would be if the points were distributed at random (i.e. Poisson process). It can be generalized through the multipoint Morisita index (k-Morisita) which takes into account k points with  $k \geq 2$ . Besides, the k-Morisita index is closely related to the concept of multifractality (Golay et al., 2013), which helps to gain a deeper understanding of its behavior when applied to complex point distributions.

In this study, the fundamental idea was to compare the raw data clustering (i.e. clustering of the considered grid nodes) with the clustering of reference random patterns (produced by shuffling the original one) at different thresholds of the measured function (i.e. the number of inhabitants). The levels of clustering were estimated with the k-Morisita index with  $k = 2,3,4,5$ ; one hundred shuffled datasets were generated and the decile thresholds were applied. It was shown that the k-Morisita index was a powerful tool for studying complex population distributions embedded in geographical spaces characterized by a highly irregular topography.

### ACKNOWLEDGEMENTS

The research was partly supported by the Swiss NSF project No. 200021-140658: "Analysis and modeling of space-time patterns in complex regions".

### REFERENCES

- Golay, J., Kanevski, M., Vega Orozco, C., & Leuenberger, M. 2013: The multipoint Morisita index for the analysis of spatial patterns, arxiv (<http://arxiv.org/pdf/1307.3756.pdf>).
- Hulbert, S. H. 1990: Spatial distribution of the Montane Unicorn, *Oikos*, 58, 257-271.

## P 17.4

# Extreme learning of environmental pollution

Leuenberger Michael<sup>1</sup>, Kanevski Mikhail<sup>1</sup>

<sup>1</sup>Center for Research on Terrestrial Environment, University of Lausanne, Géopolis, CH-1015 Lausanne (michael.leuenberger@unil.ch)

Extreme learning machine (ELM) is a fast and powerful algorithm being part of the machine learning algorithm category. Developed by G.-B. Huang et al.(2006), it follows the structure of a multilayer perceptron (MLP) with one single-hidden layer feedforward neural networks (SLFNs).

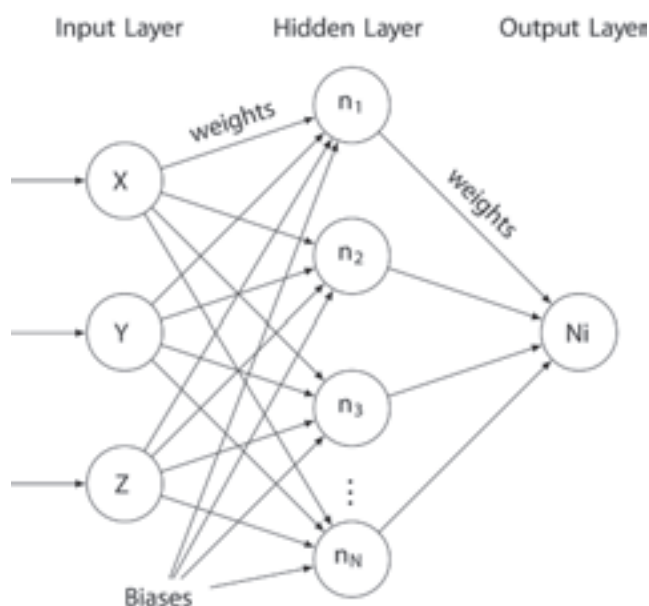


Figure 1. Structure of one single-hidden layer feedforward networks (SLFNs).

The learning step of classical artificial neural networks, like MLP, deals with the optimization of weights and biases by using gradient-based learning algorithm (e.g. back-propagation algorithm). Opposed to this optimization phase, which can fall in local minima, ELM generates randomly the weights between the input layer and the hidden layer and also the biases in the hidden layers. By this initialisation, it optimizes just the weight vector between the hidden layer and the output layer in a single way. The main advantage of this algorithm is the speed of the learning step. In a theoretical context and by growing the number of hidden node, the algorithm can learn any set of training data with zero error. To avoid overfitting, cross-validation method or “true validation” (by randomly splitting data in training, validation and testing subsets) are recommended in order to find the optimal number of neuron. Practically, the optimal number of neuron is catch when the minimum error on the validity set is reached. So with its universal propriety and its theoretical basis, ELM is a good machine learning algorithm which can push the field forward.

The main objective of this study is to: 1) highlight the concept and the theory underlying in this new algorithm, 2) use ELM for environmental pollution data, and 3) compare with geostatistical tools - variography and models – predictors – family of kriging models (Kanevski & Maignan, 2004).

The database used for this study is composed of 200 spatial measurement points in Lake Lemman. Each of them has information about the sediment pollution by heavy metals. Focused on the Nickel pollutant we optimize the ELM algorithm in order to draw a spatial prediction map. This process is controlled/verified by geostatistics and by scenario permutation based-model comparison. Although it is a benchmark case study, it allows us to validate the whole methodology from the data validation to the final results via the preprocessing of the data and the data mining.

Other related works in progress use ELM for multidimensional data, multitask learning, features selection and also risk assessment, in particular in natural hazards assessments.

## REFERENCES

- Huang G.-B., Zhu Q.-Y., & Siew C.-K. 2006: Extreme learning machine: theory and applications. *Neurocomputing* 70, 489-501.
- Kanevski M. & Maignan M. 2004: *Analysis and Modelling of Spatial Environmental Data*. EPFL Press.

## P 17.5

### Random Forest for susceptibility mapping of natural hazards

Leuenberger Michael<sup>1</sup>, Vega Orozco Carmen<sup>1</sup>, Tonini Marj<sup>1</sup>, Kanevski Mikhail<sup>1</sup>

<sup>1</sup>Center for Research on Terrestrial Environment, University of Lausanne, Géopolis, CH-1015 Lausanne (michael.leuenberger@unil.ch)

The present research deals with the application of the Random Forest algorithm (RF) to analyze and model natural hazards in a high dimensional input feature space. RF (Breiman 2001) is a type of recursive partitioning methods which involves different classification trees. By a pseudo-random variable selection for each split node, the algorithm grows a variety of classification/regression trees which return different results. A committee system votes (or averages) these results and assigns the predicted values to the unlabeled locations within the validity domain. Furthermore, the algorithm provides the measure of the contribution of each variable. This measure can be used to display the mainly factors affecting the occurrences of the natural hazard under study. In this way, RF allowed assessing the degree of predisposition to the hazard. We applied a binary approach for which the occurrences (i.e. the observations) are displayed against simulated event-locations, randomly distributed in the area where the hazard is highly unlikely to occur. This assumption let us to elaborate susceptibility maps which give an estimation of the probability that a hazard event occurs in a specific area without considering an absolute temporal scale.

This method was successfully applied in the Swiss territory to different study cases, such as landslides, forest fires and permafrost. As results of the application of RF algorithm we obtained an estimation of the importance of different environmental variables for predicting the specific natural hazard occurrence. Moreover, susceptibility maps were elaborated based on the selected variables. The list of the environmental variables influencing the occurrences includes topographic, geological and anthropogenic features, all available at high resolution.

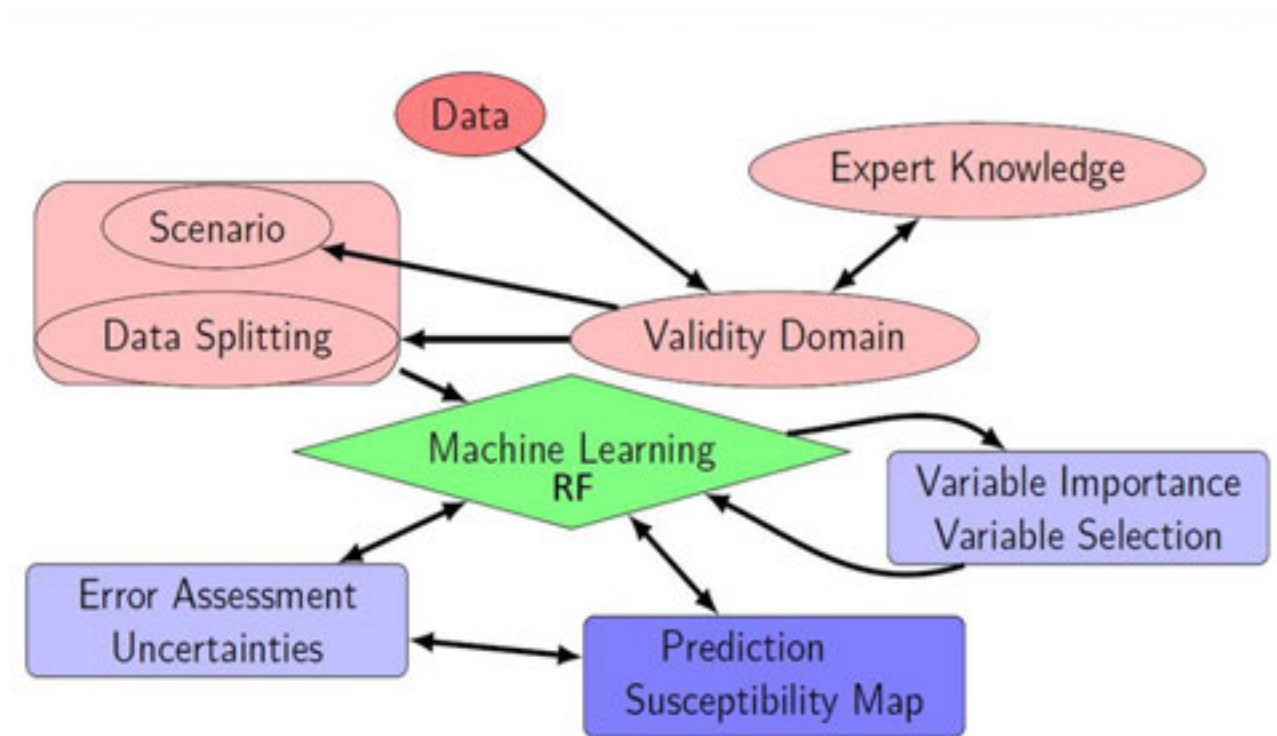


Figure 1. Mind map of the methodology.

#### REFERENCES

Breiman, L. 2001: Random Forest, Mach. Learn. 45, 5–32.

Liaw, A. & Wiener, M. 2002: Classification and Regression by randomForest. R News 2(3), 18–22.

## P 17.6

# Evaluation of geostatistical resampling as a proposal mechanism in Bayesian MCMC solutions to hydrogeophysical inverse problems

Ruggeri Paolo<sup>1</sup>, James Irving<sup>1</sup> & Klaus Holliger<sup>1</sup>

<sup>1</sup> Applied Geophysics Group, Center for Research of the Terrestrial Environment, University of Lausanne, Unil-Mouline, CH-1015 Lausanne (paolo.ruggeri@unil.ch)

Quantification of model parameter uncertainties is essential for hydrological risk assessment and the development of effective groundwater management and/or remediation strategies. While deterministic inverse theory offers a robust and proven framework for estimating spatially distributed subsurface parameters from geophysical and hydrological data, the corresponding parameter uncertainty estimates are well known to significantly underrepresent our lack of knowledge for many problems. To address this limitation, much interest has recently been expressed in the use of stochastic inverse methods for hydrogeophysical parameter estimation and uncertainty analysis. In particular, Markov-chain-Monte-Carlo (MCMC) sampling of the Bayesian posterior distribution has gained significant attention, as it offers the potential for full uncertainty quantification in a relatively straightforward manner. Bayesian-MCMC methods, however, are severely limited by their high computational cost, which results from the typically large size of the parameter space and the need for small model perturbations in order to ensure reasonable rates of proposal acceptance. One key aspect of reducing this computational cost is to incorporate as much prior information as possible into the proposals, such that the number of subsurface configurations tested is limited to a small subset of the total number of possibilities. In this regard, geostatistical simulation methods are attractive, and have gained much recent popularity, because of the inherent flexibility and ease with which they allow us to represent complex prior information as well as the fact that they can be conditioned to a wide variety of measured and previously simulated data. In this work, we evaluate in detail the viability of sequential geostatistical resampling as a proposal mechanism for MCMC methods applied to high-dimensional geophysical and hydrological inverse problems. Focusing on a wide range of realistic crosshole georadar tomographic examples characterized by different numbers of observed data, data error levels, and degrees of model parameter spatial correlation, we investigate the efficiency of different resampling strategies with regard to their ability to generate independent realizations from the Bayesian posterior distribution. We also investigate the potential of a resampling strategy based on a gradual deformation method to generate optimal proposals based on estimates of model parameter sensitivity.

## REFERENCES

- Cordua, K.S., Hansen, T.M. & Mosegaard, K., 2012: Monte Carlo full-waveform inversion of crosshole GPR data using multiple-point geostatistical a priori information, *Geophysics*, 77, H19-H31.
- Fu, J. & Gomez-Hernandez, J.J., 2009: A Blocking Markov Chain Monte Carlo Method for Inverse Stochastic Hydrogeological Modeling, *Mathematical Geoscience*, 41, 105-128.
- Hansen, T.M., Cordua, K.S. & Mosegaard, K., 2012: Inverse problems with non-trivial priors: Efficient Solution through sequential Gibbs sampling, *Computational Geosciences*, 1-19.
- Hu, L.Y., Blanc, G. & Noetinger, B., 2001: Gradual deformation and iterative calibration of sequential stochastic simulations, *Mathematical Geology*, 33, 475-489.
- Irving, J. & Singha, K., 2010. Stochastic inversion of tracer test and electrical geophysical data to estimate hydraulic conductivities., *Water Resources Research*, 46, W11514.
- Mariethoz, G., Renard, P. & Caers, J., 2010: Bayesian inverse problem and optimization with iterative spatial resampling, *Water Resources Research*, 46, W11530.

## P 17.7

# Spatio-temporal aggregation of wildfires: from global cluster to local mapping

Tonini Marj<sup>1</sup>, Vega Orozco Carmen<sup>1</sup>, Kanevski Mikhail<sup>1</sup>

<sup>1</sup> Centre for Research on Terrestrial Environment (CRET), University of Lausanne, Quartier UNIL-Mouline, Bâtiment Géopolis, CH-1015 Lausanne (Marj.Tonini@unil.ch)

Many natural hazards, such as wildfires, can be modelled as stochastic point processes where events are represented as sets of geographical coordinates and time indicating where and when events occurred. Stochastic point processes refer to as sets of random points (events) distributed within a space and/or a time. However, natural events are normally not randomly distributed; instead, they are grouped in clusters over a range of scales. Therefore, the analysis of their spatio-temporal aggregation is of paramount importance to understand predisposing factors, as well as, for prevention and forecasting purposes.

Space-time cluster analysis let us to identify whether groups of observed events are closer in time and in space than expected for a random distribution (absence of structure). The results of this exploratory data analysis allow in turn detecting more vulnerable areas and time-frame periods where hazardous events can more likely occur. Although numerous environmental studies aim at investigating the global spatial clustering behaviour, they often miss a comprehensive analysis of data aggregation both in space and in time.

In the present study authors attempt to detect whether space and time interact to generate clusters and, secondly, to map the results. The case study is represented by wildfire events inventoried in canton Ticino (Switzerland) over the last four decades (data delivered by the WSL Federal Institute). A global cluster indicator, the Ripley's space-time  $K$ -function, was applied to this purpose.

Computationally, the space-time  $K$ -function ( $K(s,t)$ ) is a bivariate function where space and time represent the two variables of the equation. It is defined as the number of further events occurring within a distance 's' and time 't' of an arbitrary event. The perspective plot of the difference ( $D$ ) between  $K(s,t)$  and the product of the purely space and purely temporal  $K$ -function ( $K(s)*K(t)$ ) provide a first diagnostic for space-time clustering. Namely, if there is no interaction between space and time,  $K(s,t)$  equals  $K(s)*K(t)$  and the difference is zero, while positive values of  $D$  indicate space-time interaction at a well detectable scale. Results of our analyses revealed annual clusters with a temporal maximum aggregation over 6 months and a spatial peak clustering around 3 km (Fig.1a). These results helped to setup the optimal bandwidth for the kernel density function which enabled to produce density maps of wildfires for different time periods (Fig.2b).

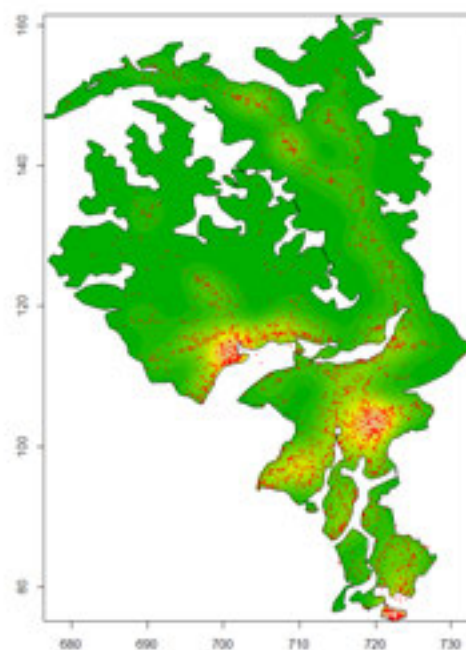
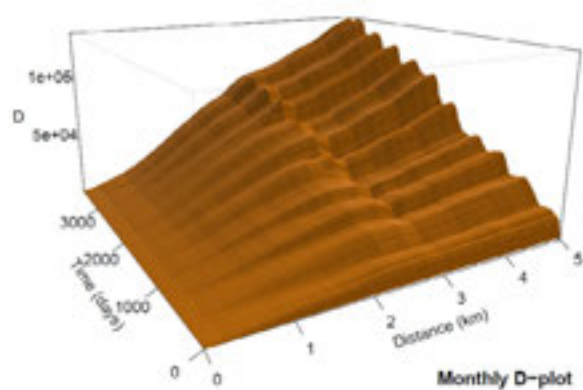


Figure 1. (Left) Perspective plot of the function  $D = K(s,t) - K(s)K(t)$  considering a monthly temporal aggregation. (Right) Density map of forest fires occurrences in Ticino from 1971 to 2010.

#### REFERENCES

- Bivand, R., Rowlingson, B. & Diggle, P. 2012: *splancs* package in R project.
- Diggle, P., Chetwynd, A., Haggkvist, R. & Morris, S. 1995: Second-order analysis of space-time clustering, *Statistical Methods in Medical Research*, 4(2), 124-136.
- Tonini, M., Pedrazzini, A., Penna, I. & Jaboyedoff, M. 2013: Spatial pattern of landslides in Swiss Rhone Valley, *Natural Hazard*, DOI: 10.1007/s11069-012-0522-9.
- Vega Orozco, C., Tonini, M., Conedera, M. & Kanveski, M. 2012: Cluster recognition in spatial-temporal sequences: the case of forest fires, *GeoInformatica*, 16(4), 653-673.

#### Acknowledgments

This work was partly supported by the SNFS projects No. 200021-140658: "Analysis and modelling of space-time patterns in complex regions"

## P 17.8

# Analysis of the dynamic of urban areas and of their interaction with forest fires

Vega Orozco Carmen<sup>1</sup>, Tonini Marj<sup>1</sup>, Kanevski Mikhail<sup>1</sup>

<sup>1</sup>Centre for Research on Terrestrial Environment, University of Lausanne, Géopolis, CH-1015 Lausanne (carmendelia.vegaorozco@unil.ch)

The delimitation of the urban area is an important issue for studies related to urban growth or urban interface. Its definition has to be carefully evaluated since it affects statistical analyses aiming to investigate the distribution of phenomena occurring inside the urban space or the neighbouring areas.

In the present study we applied the “City Clustering Algorithm” (CCA) as proposed by Rozenfeld et al. (2008) to define the urban area. This method is based on the spatial location of the population (e.g. zip code or aggregated grid) and defines the urban areas as the clusters of connected nonzero-populated cells of a defined size (Figure 1). The dynamic of the urban zones was carried out by changing the spatial scales at which the demographic cells were connected. We analysed the Swiss population census data in Canton Ticino for the years 1990, 2000 and 2010 delivered as a hectometric grid (100 x100 m resolution) issued by the Swiss Federal Statistical Office. Changing the cluster’s cell sizes (from 100 m up to 500 m) allowed us to aggregate connected clusters and to evaluate the dynamic of the urban space. A first result consisted of an analysis of the urban growth in Canton Ticino in the last three decades.

Additionally, we examined the spatial interaction between the defined urban areas and a natural hazard, namely the forest fires (Figure 2). These events are quite important in Canton Ticino and they are more likely to occur close to the urban spaces (Vega Orozco et al. 2012). Thus, the forest fire events falling inside the urban zones were easily selected and the frequency and spatio-temporal evolution of their occurrences inside the urban clusters were explored.

This method provides an innovative approach to investigate the dynamic of urban areas and the surrounding forest fire occurrences. Furthermore, this can be applied to study and assess complex phenomena delivered or enhanced by the co-existence of both human activities and natural hazards.

### Acknowledgments

This work was partly supported by the SNFS Project No. 200021-140658, “Analysis and Modelling of Space-Time Patterns in Complex Regions”.

### REFERENCES

- Rozenfeld, H.D., Rybski, D., Andrade, J.S., Batty, M., Stanley, E. & Makse, H.A. 2008: Laws of population growth. PNAS 105, 18702–18707.
- Vega Orozco, C., Tonini, M., Conedera, M. & Kanevski, M. 2012: Cluster recognition in spatial-temporal sequences: the case of forest fires. Geoinformatica 16, 653–673.

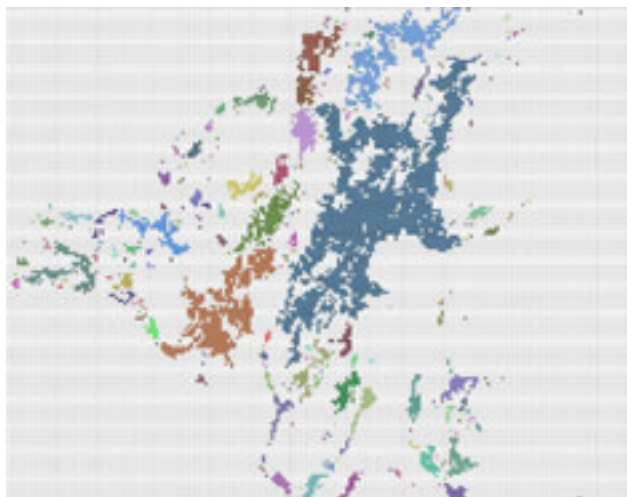


Figure 1. Urban clusters generated by CCA. Same-coloured cells belong to the same cluster.

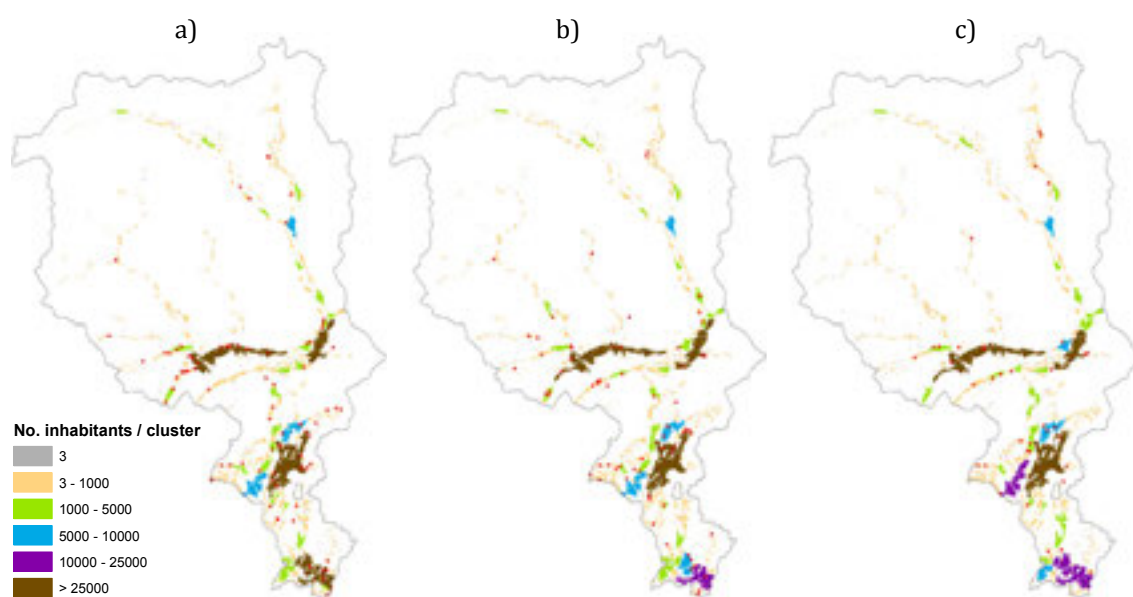


Figure 2. Urban clusters originated from CCA for the three periods in canton Ticino: a) 1981-1990, b) 1991-2000, and c) 2001-2010. Red dots represent the forest fire occurrence inside the urban clusters.



# 18. Geoscience and Geoinformation - From data acquisition to modelling and visualisation

Nils Oesterling, Adrian Wiget, Massimiliano Cannata

*Swiss Geodetic Commission,  
Swiss Geotechnical Commission,  
Swiss Geophysical Commission,  
Swiss Hydrogeological Society*

## TALKS:

- 18.1 Akhtman Y., Rehak M., Constantin D., Tarasov M., Lemmin U.: Remote sensing methodology for an ultralight plane
- 18.2 Anselmetti F., Hilbe M., Girardclos St., Kremer K., Niemann St., Wessels M., Wildi. W.: Under water landscapes - The last frontier of geomorphologic explorations (Keynote)
- 18.3 Aubert M., Kraiem A., Haeberlin Y., Zwahlen F.: From satellite imagery to hydrogeological survey maps of Chad
- 18.4 Baumberger R., Herwegh M., Kissling E., Wehrens P.: Towards the semi-automated analysis of lineaments in the Aar massif: uncertainty estimates for geological surface information – A combined remote sensing and field data approach
- 18.5 Cannata M., Antonovic M., Molinari M.: HELI-DEM: Helvetia-Italy Digital Elevation Model
- 18.6 Nussbaum M., Papritz A., Walther L.: Predicting soil density of Swiss forests by component wise gradient boosting
- 18.7 Papritz A., Grêt-Regamey A., Keller A.: NRP68 projects PMSoil, iMSoil, OPSOL: From legacy soil data and element cycles in agro-ecosystems to a land use decision support system for sustainable use of soils
- 18.8 Rickenbacher M.: Journeys through time with the Swiss national map series

## POSTERS:

- P 18.1 Franz M., Podladchikov Y., Jaboyedoff M.: Modelling landslide-generated tsunamis in alpine lakes
- P 18.2 Jaquet S., Schwab M., Yersin R., Ribeiro D.: Geographical information system for materials management in the canton Fribourg (Switzerland)
- P 18.3 Molinari M., Cannata M., Ambrosi C., Meisina C.: A new open-source simulation model for fast landslide runout assessment
- P 18.4 Neyer F., Limpach Ph., Geiger A.: Monitoring rock glaciers with GPS and high-resolution cameras
- P 18.5 Psimoulis P., Houlié N., Meindl M., Rothacher M., Clinton J., Dalguer L.: Estimation of maximum ground shaking for the Tohoku 2011 earthquake based on collocated GPS and strong-motion data
- P 18.6 Rogers S.R., Fischer M., Huss M.: GlaciArch: applying glaciological methods for gauging archaeological potential using GIS

## 18.1

### Remote sensing methodology for an ultralight plane

Yosef Akhtman<sup>1</sup>, Martin Rehak<sup>1</sup>, Dragos Constantin<sup>1</sup>, Michael Tarasov<sup>2</sup> and Ulrich Lemmin<sup>1</sup>

<sup>1</sup> Department of Environmental Engineering, École Polytechnique Fédérale de Lausanne, Lausanne, Switzerland (yosef.akhtman@epfl.ch)

<sup>2</sup> Faculty of Geography, Moscow State University, Moscow, Russian Federation

Over a short period of eight months starting in October 2012, we have developed and deployed a remote sensing platform optimised for the collection of multispectral and hyperspectral observations of both land and water surfaces from an ultralight aircraft. The platform is comprised of four cameras, auxiliary GNSS position and orientation sensors, as well as data recording equipment. The development was carried out as part of the international Leman-Baikal research project of the Limnology Research Centre of EPFL.

Our main instrument is constituted by an Alava ARS3 system, which is based on a Headwall Photonics Micro Hyperspec VNIR sensor. In addition, the platform includes two high-resolution RGB and near-infrared sensors based on consumer-grade Sony NEX-5r cameras, as well as a thermal infrared sensor based on the DIAS Pyroview 640L Compact camera. The resultant remote sensing platform is portrayed in Figure 1. As principal carrier we have utilised the Air Creation Tanarg 912S ultralight aircraft depicted in Figure 2.

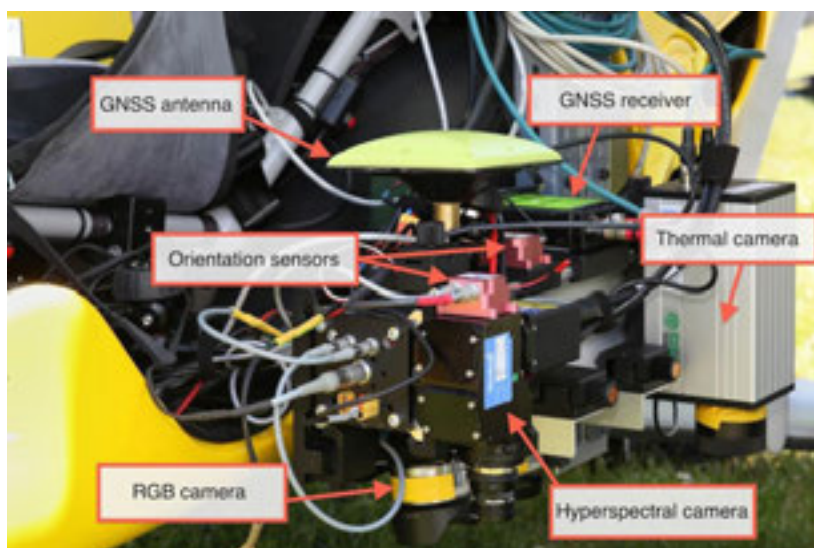


Figure 1: Multispectral and hyperspectral remote sensing platform installed on an ultralight aircraft.

The scientific objectives of the developed platform were centered on a series of limnological studies, in particular the exploration of remote sensing methodologies for the analysis of hydrological processes, such as the runoff dynamics of both natural and anthropogenic origins, as well as the study of processes pertaining to the land-water and air-water interfaces in lakes.

During the stage of the system development, as well as during the collection of the initial data, we have conducted a series of flights in the Lake Geneva area. Our initial points of interest included the plumes of rivers Venoge and Rhone in the lake, which exhibit a particularly wide range of visually observable hydrological phenomena.

In the consequent stage of the project, which took place during the months June and July of 2013, we have carried out a comprehensive field campaign in the area of delta of river Selenga in Southern Siberia region of the Russian Federation. The campaign was conducted in close collaboration with the Geography Faculty of the Moscow State University and the Institute of Nature Resource Management in Ulan Ude. Our airborne observations were complemented by extensive groundwork, which included the collection and analysis of *in situ* samples, as well as the recording of the corresponding spectral reflectance signatures of the water surface.



Figure 2: Air Creation Tanarg 912S ultralight aircraft with the remote sensing platform installed (left) and the flight trajectories for the Baikal 2013 phase of the Lemna-Baikal project (right).

The field campaign resulted in the collection of the total of around 7 Terabytes of airborne remote sensing data covering an area in excess of 1000 km<sup>2</sup>, including more than 100 in situ sampling sites indicated in Figure 2. We have conducted a range of methodological experiments, while collecting data from different altitudes between 500 and 2500 meters, resulting in the ground resolution for the high-resolution RGB/nIR imagery of approximately 16 to 80 cm per pixel, respectively.

The results of the preliminary analysis of the collected data demonstrate its suitability for the generation of a wide range of remote sensing products exemplified in Figure 4. A detailed analysis of the collected data is in progress and further field campaigns over both lakes are planned for the period of the next two years.

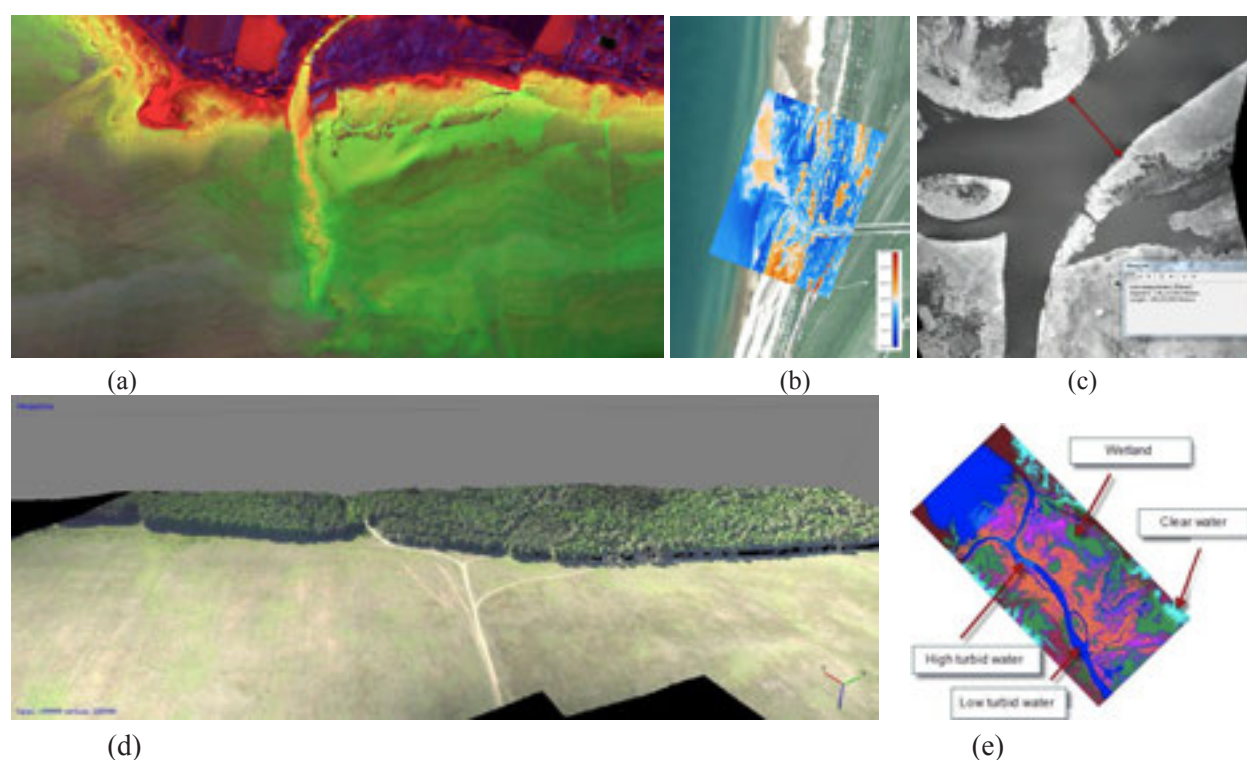


Figure 3: Examples of remote sensing products, including hyperspectral cubes (a), thermal maps (b), metric surface morphology analysis (c), DTMs (d), as well as various types of manual and automated land cover classification maps (e).

The financial support of this research by the Ferring Pharmaceuticals, St-Prex, Switzerland and the Metropol Group of Companies, Moscow, Russian Federation is thankfully acknowledged.

## 18.2

### Under water landscapes - The last frontier of geomorphologic explorations

Anselmetti, Flavio S.<sup>1</sup>, Hilbe, Michael<sup>1</sup>, Girardclos, Stéphanie<sup>2</sup>, Kremer, Katrina<sup>2</sup>, Niemann, Steffen<sup>3</sup>, Wessels, Martin<sup>3</sup>, Wildi, Walter<sup>2</sup>

<sup>1</sup> Institute of Geological Sciences and Oeschger Centre for Climate Change Research, University of Bern, Baltzerstrasse 1+3, 3012 Bern, Switzerland (flavio.anselmetti@geo.unibe.ch; michael.hilbe@geo.unibe.ch)

<sup>2</sup> Department of Earth sciences, Institut des Sciences de l'Environnement and Institut Forel, University of Geneva, Rue des Maraîchers 13, CH-1205 Geneva, Switzerland (stephanie.girardclos@unige.ch; katrina.kremer@unige.ch; walter.wildi@unige.ch)

<sup>3</sup> Landesanstalt für Umwelt, Messungen und Naturschutz Baden-Württemberg, Institut für Seenforschung, Argenweg 50/1 88085 Langenargen, Germany (Steffen.Niemann@lubw.bwl.de; Martin.Wessels@lubw.bwl.de)

Shaped by the interplay between the inherited geology of the substrate and the successions of multiple erosive glaciations, perialpine lakes represent major sediment sinks that gradually become infilled. These sediments provide the archive of environmental processes, which leave their characteristic traces on the lake floor. In turn, understanding and visualizing lake-floor processes thus sheds new light on past environmental states including environmental cycles and catastrophic events.

Not only environmental events may occur in cycles. Advances in acquisition techniques disclosing the lake-floor morphologies also occur in cycles, usually separated by decades during which application of the current technology explores and maps these morphologies. However, as the underwater bathymetry is hidden for the naked eye, the subaquatic domain received less attention than the subaerial counterparts. The newest vintages of high-resolution digital terrain models (DTMs) for the earth surface, generated by airborne laser scanning, have been well established in Switzerland for a few years. Providing a typical horizontal resolution of a few meters or less, they are used for a variety of tasks such as geomorphological mapping or the monitoring of earth surface processes related to natural hazards. Bathymetric data for the Swiss lakes, however, did not provide a comparable level of detail due to limitations of the traditional techniques such as single soundings or single-beam echo sounders. State-of-the-art acoustic hydrographic survey systems (multibeam echosounder, swath bathymetry systems) allow a significant improvement of the horizontal resolution of subaquatic DTMs to values comparable or better than high-resolution terrestrial data. Such equipment was used for the first time in Switzerland in the framework of a pilot project started in 2007. In the meanwhile, many lakes have been surveyed using these new technologies, and more are to come. This presentation introduces the methods, challenges, goals, possibilities and limitations of this technology, exploring and visualizing so far hidden morphologies at the lake bottom.

The presented examples indicate that the use of high-resolution bathymetric data is an appropriate and necessary approach to map otherwise invisible underwater morphologies. The data are the basis for subsequent investigations of the lake sediments and for other applications in coastal engineering and construction, natural hazard analysis and natural resource prospecting. Combining bathymetric data with Lidar data above the water line and from shallow waters permits analysis of a seamless landscape, i.e. without relevant processes stopping at the shore line. Periodic repetitions of the surveys will allow monitoring and quantifying alterations of the lake floors related to natural processes as well as to human impact.

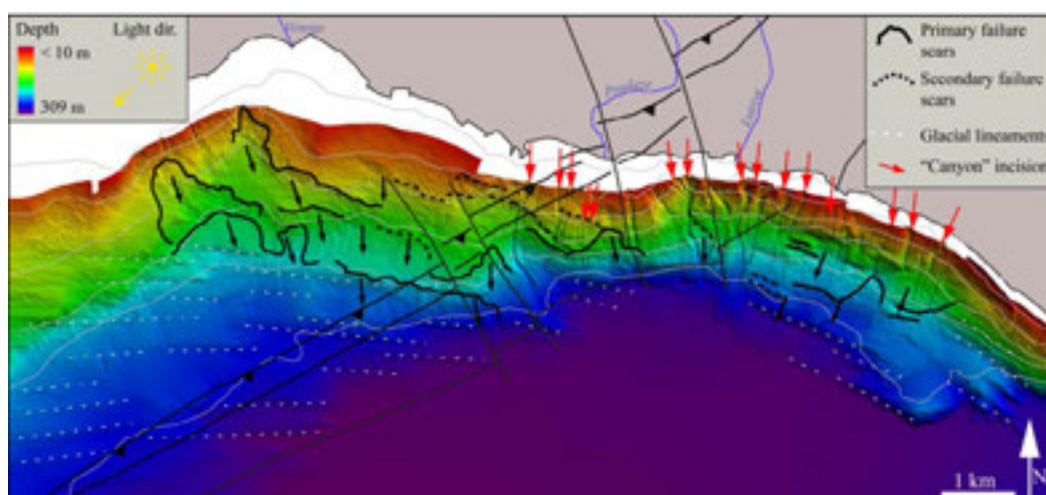


Figure 1. Newly acquired bathymetric data from Lac Léman near Lausanne. Note subaquatic canyons incisions, glacial lineaments and failure scars (Kremer et al, accepted; data courtesy Direction Générale de l'Environnement, State of Vaud)

## REFERENCES

- Hilbe, M., Anselmetti, F.S., Eilertsen, R.S., Hansen, L. and Wildi, W., 2011: Subaqueous morphology of Lake Lucerne (Central Switzerland): Implications for mass movements and glacial history, *Swiss Journal of Geosciences* 104, 425-443.
- Hilbe, M. and Anselmetti, F.S., subm.: Mass movement-induced tsunami hazard on perialpine Lake Lucerne (Switzerland): Scenarios and numerical experiments, subm. to *Pure and Applied Geophysics*.
- Kremer, K., Marillier, F., Hilbe, M., Simpson, G., Dupuy, D., Yrro, B.J.F., Rachoud-Schneider, A.-M., Corboud, P., Bellwald, B., Wildi, W. and Girardclos, S. accepted. Lake dwellers occupation gap in Lake Geneva (France-Switzerland) possibly explained by an earthquake – mass movement – tsunami event during Early Bronze Age. *Earth and Planetary Science Letters*.
- Sastre, V., Loizeau, J.-L., Greinert, J., Naudts, L., Arpagaus, P., Anselmetti, F., Wessels, M., Busmann, I., Schloemer, S., Schlüter, M. and Böder, V., 2010: Distribution, morphology, and formation of pockmarks in Lake Constance, Germany, *Limnology and Oceanography* 55, 2623-2633.
- Wildi, W., 2010: Morphology and recent history of the Rhone River Delta in Lake Geneva (Switzerland), *Swiss Journal of Geoscience* 103, 33-42.

## 18.3

## From satellite imagery to hydrogeological survey maps of Chad

Aubert Maëlle<sup>1</sup>, Kraiem Amira<sup>1</sup>, Haeberlin Yves<sup>1</sup>, Zwahlen François<sup>2</sup>

<sup>1</sup> UNOSAT, United Nations Institute for Training and Research (UNITAR), Palais des Nations, CH-1211 Genève (maelle.aubert@unitar.org)

<sup>2</sup> CHYN, University of Neuchâtel, Rue Emile-Argand 11, CH-2000 Neuchâtel

The RésEAU Chad project implemented by UNITAR on behalf of the Ministry of Rural and Urban Hydraulics aims to make available exhaustive, pertinent information about the nature, extent, and potential of the aquifers to all actors in the water resources management sector. To meet this objective, existing data must be consolidated concerning the geology, hydrology and soils in Chad, areas where information is lacking need to be identified and the gap need to be filled by generating additional data. Given Chad's surface area and the difficulties to access remote regions, it is highly improbable that full coverage can be achieved through field surveys. Given the context, optical and radar satellite sensors provide cost-effective data to support a geological, structural and hydrogeological interpretation of the territory.

A methodology has been developed to produce hydrogeological maps using satellite imagery and a limited amount of field data (Fig. 1). It can be applied to the areas of Chad with sparse vegetation cover, namely the North and the East.

- Step I - Geological regions are delimited by photointerpretation then subdivided into rock types based on various petrographic and contextual criteria.
- Step II - a hydrogeologist converts the rock types into hydrogeological units based on their nature and local knowledge, and then ranks them according to their potential productivity in aquifers, aquicludes or aquitards.
- Step III - The various units are represented on a base map with the water points to produce a hydrogeological map.

At map scales of 1:200,000 and 1:500,000, the most appropriate satellite images are LANDSAT-7 and ASTER scenes because of the variety of their spectral ranges. After calibrating the images, derivative products are calculated using band ratios (color compositions by Sultan et al., 1987, and Ninomiya et al., 2005) or as principal components (PCA). These products help convey the maximum amount of information about the geology and soils, more specifically on rock varnishes and surficial alterations. Photointerpretation of these color images was used to delimit alluvial deposits and to map bedrock/sandstone and bedrock/volcanic rock contacts. These correspond to the geological regions that make up the territory. A narrow subdivision of these regions is then completed, based on different criteria, such as morphology (slope, plateau, rupture), stratigraphic and cutting relationships, adjacent (neighbouring lithologies) and contextual (soils, vegetation cover) determinants and textures such as foliations and circular structures. Field samples, exogenous data (old maps) and background images from Bing and Google Earth are used to plug some holes in the interpretation process. Radar imagery

will also be used to help detect wet zones and faults. For topology reasons and to facilitate corrections and future updates, the decision was made to work with polylines in the GIS. To this end, ToolMap software (Schreiber et al., 2009) was used to model, vectorise and export geological information in the form of polygons.

The hydrogeological units are an interpretation of the lithologies based on their water potential, defined by:

- their nature (detrital, carbonate, volcanic, metamorphic, intrusive, regolith)
- their porosity (loose rock, consolidated),
- their grain size, and
- their permeability or capacity to let water circulate.

The rock's condition is also taken into account (altered, fissured, fractured or karstic), as is the layer's geometry, the hydraulic parameters and productivity, the piezometric levels of the wells/boreholes and their frequency within the unit. Using his synthetic skills and his experience, the hydrogeologist is able to attribute variable aquifer potentials to the units.

The survey maps obtained highlight groundwater followed by surface water and finally geology, using a standard base map. They offer a novel synthesis on a relatively large scale of the hydrogeology of the regions under investigation, the details of which were unknown until now. Despite their partly speculative content, they nevertheless allow for both a relatively precise measurement of the nature, extent and importance of water resources in these regions and for planning their use.

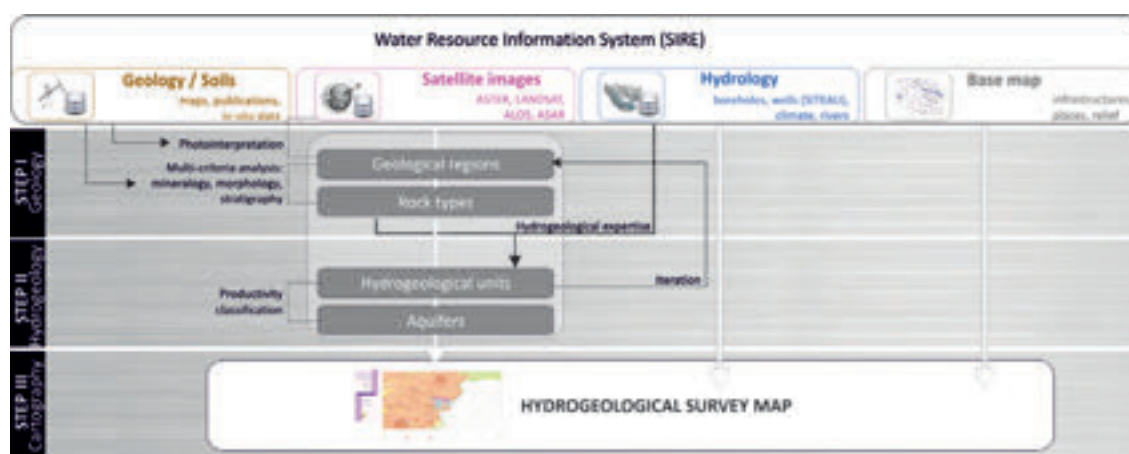


Figure 1. Methodological flowchart for developing hydrogeological units and survey map.

## REFERENCES

- Ninomiya, Y., Fu, B. & Cudahy T.J. 2005: Detecting lithology with Advanced Spaceborne Thermal Emission and Reflection Radiometer (ASTER) multispectral thermal infrared radiance-at-sensor data. *Remote Sens. Environ.* 99, 127-139.
- Schreiber, L., Ornstein, P., Sartori, M., & Kühni A. 2009. ToolMap – “Sion” method: development of a new GIS Framework for digital geological mapping. 6th EUREGEO, Munich 2009, Proceedings, I, 89–90. [www.toolmap.ch](http://www.toolmap.ch)
- Sultan, M., Arvidson, R.E., Sturchio, N.C. & Guinness E.A. 1987: Lithologic mapping in arid regions with Landsat TM data: Meatiq dome, Egypt. *Bull. Geol. Soc. Amer.* 99, 748-762.

## 18.4

### Towards the semi-automated analysis of lineaments in the Aar massif: uncertainty estimates for geological surface information – A combined remote sensing and field data approach

Roland Baumberger<sup>1,3</sup>, Marco Herwegh<sup>1</sup>, Edi Kissling<sup>2</sup>, Philip Wehrens<sup>1</sup>

<sup>1</sup> University of Bern, Institute of Geological Sciences, Baltzerstrasse 1+3, CH-3012 Bern

<sup>2</sup> ETH Zurich; Institute of Geophysics; Sonneggstrasse 5; CH-8092 Zurich

<sup>3</sup> Federal Office of Topography, Swiss Geological Survey, Seftigenstrasse 264, CH-3084 Wabern (roland.baumberger@swisstopo.ch)

The quality, consistency and density of geological surface information is of key importance for the development of geological three-dimensional (3D) models in areas, where underground data is lacking. One of the major problems with such models is the determination of their uncertainties, particularly with increasing distance from the surface. The intrinsic uncertainty of the surface information, therefore, needs to be accurately characterized, methodologically recorded, quantified, evaluated and described. Here, a methodology is presented that combines both semi-automated remote sensing data acquisition and subsequent evaluation in the field to allow consistent acquisition and uncertainty assessment for large data sets.

The basic idea consists on the fact that mechanical anisotropies, such as shear zones and faults, are prominently expressed in surface morphology. These surface geometries can be mapped by means of remote sensing based on a high resolution digital elevation model (DEM) and orthophotos providing information for 3D modeling of subsurface structures by depth projecting their surface intersections.

We investigate the Alpine 3D deformation of the crystalline rocks of the Aar massif (Haslital, Central Switzerland) by establishing a lineament map consisting of 32'000 features complemented by manual quality control. The data set subsequently underwent geostatistical verification, in order to obtain a valid basis for further analysis. As a final step, the lineament map was transformed into a shear zone map.

Lineament analysis reveals an increase in lineament density from N to S in the study area, which corresponds very well with the formation and deformation history of the lithological units present. Two main striking directions exist WSW-ENE and WNW-ESE, which are sub-parallel and perpendicular to the strike of the Aar massif, respectively. This finding mimics again the current geological setting.

Investigation of the shear zone map using 360 outcrop data shows that the quality of the remote sensing data very well fits field measurements. About 60% of the shear zones mapped in the field and those evaluated via remote sensing, show differences of less than 20° in strike directions. The remaining 40% are related to secondary structures not resolved on the digital data but visible at the outcrop scale. Hence, we note a scale-dependent effect in the automated remote sensing results and a reasonable and consistent observation error.

The orientation of lineaments of each of the four units within the plutonic rock complex of the Aar massif (Grimsel Granodiorite, Zentraler Aaregranite, Südlicher Aaregranite, Mittagfluh granite) is very heterogeneous. For these units, we can demonstrate that there exists a correlation between formation age, mineralogical composition, deformation history and the orientation of the lineaments. The main focus of future works will be laid on the projection of surface structures to depth and their verification in the various tunnels and caverns present in the study area.

## 18.5

### HELI-DEM: Helvetia-Italy Digital Elevation Model

Cannata Massimiliano<sup>1</sup>, Antonovic Milan<sup>1</sup>, Molinari Monia<sup>1</sup>

<sup>1</sup> Institute of Earth Sciences, University of Applied Sciences and Arts of Southern Switzerland, Campus Trevano, CH-6952, Canobbio (massimiliano.cannata@supsi.ch)

HELI-DEM (Helvetia-Italy Digital Elevation Model) is a project developed in the framework of Italy/Switzerland Operational Programme for Trans-frontier Cooperation 2007-2013 whose major aim is to create a unified digital terrain model that includes the alpine and subalpine areas between Italy and Switzerland. The partners of the project are: Lombardy Region, Piedmont Region, Polytechnic of Milan, Polytechnic of Turin and Fondazione Politecnico from Italy; Institute of Earth Sciences (SUPSI) from Switzerland.

The digital terrain model has been produced by integrating and validating the different elevation data available for the areas of interest, characterized by different reference frame, resolutions and accuracies: DHM at 25 m resolution from Swisstopo, DTM at 20 m resolution from Lombardy Region, DTM at 5 m resolution from Piedmont Region and DTM LiDAR PST-A at about 1 m resolution, that covers the main river bed areas and is produced by the Italian Ministry of the Environment. Further results of the project are: the generation of a unique Italian-Swiss geoid with an accuracy of few centimeters (Gilardoni et al. 2012); the establishment of a GNSS permanent network, prototype of a transnational positioning service; the development of a geo-portal, entirely based on open source technologies and open standards, which provides the cross-border DTM and offers some capabilities of analysis and processing through the Internet.

With this work, the authors want to present the main steps of the project with a focus on the geo-portal development carried out by the Institute of Earth Sciences; finally discussions about the experience in this project and general considerations about INTERREG projects will be proposed.



Figure 1. Geo-portal of HELI-DEM project

#### REFERENCES

- Helidem Consortium, 2013: HELI-DEM: integrazione dei dati di altezza transalpini tra Italia e Svizzera. SIFET Bulletin, special edition (in printing.)
- Gilardoni, M., Sampietro, D. & Reguzzoni M. 2012: Unione dei geoidi italiano e svizzero con l'utilizzo di dati GOCE: metodologia e risultati. Atti 16° Conferenza Nazionale ASITA - Fiera di Vicenza 6-9 novembre 2012

## 18.6

# Predicting soil density of Swiss forests by component wise gradient boosting

Nussbaum Madlene<sup>1</sup>, Papritz Andreas<sup>1</sup>, Walthert Lorenz<sup>2</sup>

<sup>1</sup>Institute of Terrestrial Ecosystems (ITES), ETH Zurich, Universitätstrasse 16, 8092 Zürich (madlene.nussbaum@env.ethz.ch)

<sup>2</sup>Swiss Federal Institute for Forest, Snow and Landscape Research (WSL), Zürcherstrasse 111, 8903 Birmensdorf

Soil density is an important characteristic to derive soil hydraulic properties, to characterize soil compaction or to calculate stocks of nutrients, trace elements or organic carbon. Measuring density is simple but laborious; hence, many soil surveys lack such measurements. Predictive models, so-called pedotransfer functions (PTF), have been developed to estimate density from soil properties that can be more easily measured. PTF relate density mostly to soil organic carbon (SOC) and/or soil texture and often show good predictive power for the study area where data was collected. However, applying a PTF to soils sampled in different regions commonly results in poor predictions, although prediction accuracy improves if the PTF is re-calibrated with density measurements taken in the target area. Besides SOC or texture, the use of additional soil data often leads to a further improvement of a PTF for soil density. Additionally, density depends on soil properties mostly in a nonlinear fashion. As a result, machine-learning techniques like neural networks or regression trees were used to model soil density, but the pedologic interpretation of such models remains usually difficult.

The present study derived a PTF for the density of the fine fraction (< 2 mm) of Swiss forest soils based on data from 134 soil profiles (559 sampled horizons). A wide range of covariates, most of them relating to the same horizons as the density measurements, were available for statistical modelling. We used a gradient boosting approach that included as base learners linear and smooth nonlinear terms. Gradient boosting of this flavor selects relevant covariates and inherently models nonlinear dependencies on covariates during the fitting process. The restriction to linear and smoothing spline base learners retains interpretability of the fitted predictive models. The number of boosting iterations is the main tuning parameter and was determined by tenfold cross validation.

We compared the results of boosting with a customary robustly fitted linear model. Furthermore, we evaluated the performance of the fitted models by predicting the density of 131 horizons of 34 forest soil profiles not used for fitting the model.

## 18.7

# NRP68 projects PMSoil, iMSoil, OPSOL: From legacy soil data and element cycles in agro-ecosystems to a land use decision support system for sustainable use of soils

Andreas Papritz<sup>1</sup>, Adrienne Grêt-Regamey<sup>2</sup>, Armin Keller<sup>3</sup>

<sup>1</sup> Institute of Terrestrial Ecosystems, ETH Zurich, Universitätstrasse 16, CH-8092 Zürich (papritz@env.ethz.ch)

<sup>2</sup> Planning of Landscape and Urban Systems, ETH Zurich, HIL, CH-8092 Zürich

<sup>3</sup> Agroscope Reckenholz-Tänikon ART, Reckenholzstrasse 191, CH-8046 Zürich

Soils play an essential role in ecosystems and provide important services for humans. Soils are the dominant basis for food and fodder production and are also needed for housing and infrastructure. But soils provide many more functions, for example, by retaining water after heavy rainfall and supplying water to plants from this storage during drought periods, providing habitats to organisms, storing carbon, preventing nutrients and pollutants from leaking into ground- and freshwaters, etc. Soil functions are often not noticed, let alone valued, except when soils fail to provide them. Soil sealing is just one of the uses that harm soil functions. In agroecosystems, soil functions are strongly influenced by land management. Besides soil compaction and erosion, the gradual accumulation of nutrients, trace elements or pesticides is a major threat for soil fertility and hence for the essential soil function of food production.

A sustainable use of the soil resources needs to balance human requirements with the capacity of the soils to provide the various services. Currently, land use decisions in spatial planning are largely taken without consideration of the potentials of the soils for the various functions. One important reason for this unfortunate situation in Switzerland is the widespread lack of accurate large-scale spatial information on soils. Spatial information on soil properties is available only for less than 30 % of the agricultural land in Switzerland. In addition, standardised evaluation methods for assessing soil functions in Switzerland are still lacking. Most soil functions cannot be measured directly but must be deduced from basic soil properties, site characteristics and pedotransfer functions by modelling.

The projects PMSoil, iMSoil and OPSOL, all funded by the National Research Programme “Sustainable Use of Soil as a Resource” (NRP68) for the period 2013–2015, jointly aim

- to develop digital soil mapping procedures for generating spatial soil information from legacy soil data and comprehensive covariate information on pedogenetic conditions and land management,
- to establish an inference system of pedotransfer functions to derive soil function potentials from basic soil properties,
- to map basic soil properties and the potentials for selected soil functions in three joint study regions in the Cantons of Zurich and Berne,
- to develop a regional soil monitoring tool for balanced element cycles on agricultural soils, which will provide indicators for sustainable management of agricultural soils in the study regions,
- to develop a decision support platform by which stakeholders can jointly develop strategies for sustainable use of soils. This interactive platform will link spatial information of soil properties and functions with anticipated economic, ecological and social effects of various soil uses and will visualises the results in a 3D virtual environment. The platform users can thereby assess and explore the effects of various soil uses on soil properties and functionalities in real-time.

The three projects will jointly strive to provide answers to the pressing question how the scarce resource “soil”, which is currently still lost at a very fast pace in Switzerland (about 3'000 ha each year), can be better preserved and more sustainably managed in the future. Built-up areas extended in the past nearly exclusively at the cost of agricultural land — approximately one third of the arable soils of Switzerland were lost in the last 30 years — because federal law protects forests quite rigorously. In spatial allocation of new infrastructure and housing areas, soil information was hardly ever considered, resulting in some cantons in a shortage of so-called “crop rotation areas”. Their conservation is the only legal instrument at federal level to prevent loss of agricultural soils for infrastructure and housing. Re-dimensioning and spatial reallocation of construction areas, protection of groundwater recharge areas in forests with acid soils against leaching of mobile heavy metals are other problems that found recently attention in public discussion. All these examples have in common that adequate tackling of the respective problem asks for spatial information about the capacity of the Swiss soils to function and to provide services to our society in the long-term. This is where the focus of our endeavours will lie.

## 18.8

# Journeys through time with the Swiss national map series

Rickenbacher Martin

Federal Office of Topography swisstopo, Topography division, Seftigenstrasse 264  
CH-3084 Wabern ( martin.rickenbacher@swisstopo.ch )

In 2013, the Swiss Federal Office of Topography swisstopo celebrates its 175th anniversary. Since its foundation as «Bureau topographique fédéral» by general Guillaume-Henri Dufour in 1838, swisstopo has produced three national map series (Topographische Karte der Schweiz 1:100.000, Topographischer Atlas der Schweiz 1:25.000/1:50.000, Landeskarten der Schweiz). They include approximately 7500 first and updated editions of maps in different scales. Therefore all these maps can be regarded as a cultural heritage of national significance. They are called the «topographical landscape memory of Switzerland». The Federal Act on Geoinformation (Geoinformation Act, 2008) commits the producers to make available their geodata in a sustainable way.

On this background, swisstopo launched its jubilee year on 17th of January 2013 by publishing the major part of its printed maps on the internet site [www.swisstopo.ch](http://www.swisstopo.ch). For users it is now possible to navigate at any place in Switzerland covered by the map series 1:25.000, 1:50.000 and 1:100.000. This enables to study very precisely the development of the actual National Map which was established by the «Map Law» of 1935. Since mid-2013, all the published maps in the scales mentioned above are online, which means, that also the establishment of the Dufour- and the Siegfried-Map can be visualized. Everybody can now undertake a journey through time from 1844 till 2011 across the complete territory of Switzerland. By links to the bibliographical metadata, the users can query the data status of the map shown on the screen. Printing facilities (A4 format) and further advanced functionalities (measure, draw) are supported as well.

The launch of this tool was very well accepted in the Swiss media, and within the first four days, the journey through time was visited by more than 70.000 users. In this short time, questions from the user side about the presented maps aroused, which required special historical knowledge to answer. As far as we know, such a web based publication of all printed maps in a georeferenced frame by a national mapping agency is unique in the world. Historically, this cartographic going public is the modern counterpart of the secrecy of maps which was maintained by the governments in former centuries.



Figures 1 – 3. Cartography in Cold War: In the last two editions of the Topographical Atlas of Switzerland 1:25.000 («Siegfried map»), the gunpowder factory of Wimmis is represented, even during World War II. From the first edition of the map sheet 1207 Thun of the Swiss National Map 1:25.000 (NM25) published 1958, it disappears – probably by secrecy reasons – until the edition of 1993, when it cartographically rose again like a phoenix (short link <http://s.geo.admin.ch/c87591b2>, click start button).

### REFERENCES

- Gerber, U. 2013: 175 Jahre swisstopo – Eine «Zeitreise». *Cartographica Helvetica* 48, 41–42.
- Rickenbacher, M. 2013: Zeitreihen bei swisstopo. Download from [http://www.swisstopo.admin.ch/internet/swisstopo/de/home/topics/geodata/historic\\_geodata/key\\_dat/tim\\_se.html](http://www.swisstopo.admin.ch/internet/swisstopo/de/home/topics/geodata/historic_geodata/key_dat/tim_se.html) (pdf file (3.6 MB) under “Dokumentation”).
- Rickenbacher, M. 2011: Zeitreihen – eine neue Herausforderung für das Bundesamt für Landestopografie swisstopo. *Cartographica Helvetica* 44, 34-41.

## P 18.1

### Modelling landslide-generated tsunamis in alpine lakes

Franz Martin<sup>1</sup>, Podladchikov Yury<sup>2</sup>, Jaboyedoff Michel<sup>1</sup>

<sup>1</sup> Center for Research on Terrestrial Environment (CRET), University of Lausanne, (martin.franz@unil.ch)

<sup>2</sup> Institute of Earth Sciences (ISTE), University of Lausanne

The Alps are the location of many mass movements (landslide, rockslide/fall, icefall), as well as numerous reservoirs and lakes. In addition, a high density of population is situated in the valleys. This situation could lead to potentially catastrophic tsunamis and associated downstream flows.

In order to assess the risk of tsunami in alpine regions, it is necessary to model the phenomenon as accurate as possible. However, the modelling of landslide generated tsunamis in closed and relatively small water bodies is confronted to various difficulties. The strong effects due to the bathymetry shape and the necessity of transition between wet to dry state, i.e. run-up and downstream flows modelling, leads to numerical instabilities.

Therefore, the goal of this study is the development of a numerical code that solves the aforementioned problems and that runs at high resolution.

To this end, several different codes based on the shallow water equations were verified with tests from Toro (2001) and some additional ones. The accuracy, the efficiency and the monotony are tested, in order to define the best code. The Lax-Friedrich and the Godunov Upwind schemes are selected and their combination allows the modelling of the wave propagation in the water body as well as the downstream flow.

## P 18.2

### Geographical information system for materials management in the canton Fribourg (Switzerland)

Jaquet Sylvain<sup>1</sup>, Schwab Marco<sup>1</sup>, Yersin Raphael<sup>1</sup>, Ribeiro Daniel<sup>2</sup>

<sup>1</sup> Service des Constructions et de l'Aménagement (SeCA), Etat de Fribourg, Rue des Chanoines 17, CH-1701 Fribourg (sylvain.jaquet@fr.ch)

<sup>2</sup> Topomat Technologies SA, 6 chemin Sus-la-Meule, CH-1297 Founex

The use of geographical information system (GIS) to provide quantitative data related to materials live cycle is implemented in the canton Fribourg in order to achieve the coordination between volume of extracted materials and volumes for disposal of clean materials. Due to new legal provisions, gravel-pit and dump operators have to plan operation (extraction, filling, reinstatement) in stages of maximum 5 years and to provide annual data about their activity: volumes, type of activity, material flux, environmental conditions...

A system in two parts has been developed: the Desktop side provides an ArcGIS 10 geodatabase and an ArcMap plugin associated with a content management system. This tool is devoted to the internal administrative management. The second part of the system is a cartographic Web-application designed for the gravel-pit and dump operators. The application provides the cartographic and attribute information needed to help the user in fulfilling the requested data and documents for the annual report. These data are then uploaded through the web to the Desktop side of the system, to the cantonal administration.

GIS techniques are useful for the administration to develop the required dataset in order to evaluate the needs for new gravel-pits and dumps or extension of existing sites. It also allows to allocate free volumes for clean materials disposal. The possibility given to explore site-specific data coupled with other general data (aerial photographs, digital elevation models...) allows the user to provide the accurate data to the administration. The tool is aimed at becoming the communication vector between gravel-pit and dump operators and cantonal administration.

## P 18.3

# A new open-source simulation model for fast landslide runout assessment

Molinari Monia<sup>1</sup>, Cannata Massimiliano<sup>1</sup>, Ambrosi Christian<sup>1</sup>, Meisina Claudia<sup>2</sup>

<sup>1</sup> Institute of Earth Sciences, University of Applied Sciences and Arts of Southern Switzerland, Campus Trevano, CH-6952, Canobbio (monia.molinari@supsi.ch)

<sup>2</sup> Department of Earth and Environmental Sciences, University of Pavia, Via Ferrata 1, 27100 Pavia, Italy

r.massmov is a new model for landslide runout simulation developed in the GRASS GIS open-source environment.

The model is the result of a series of enhancements ported to the original Massmov2D code (Begueria et al. 2009) in order to obtain a tool suitable for early warning monitoring system modeling services. To this purpose, the authors identified four model key requirements: i) low calculation times to perform simulations in timeframe consistent with early warning system real-time services; ii) GIS-embedded approach to access all the spatial analysis features including visualization and elaboration; iii) three-dimensional analysis capabilities to take account of complex topographies and iv) open source approach to reduce costs and guarantee sustainability in time.

With this work the authors want to illustrate the main features of the model (governing equations, input and output data and algorithms) and present its peculiarities with respect to the original code. Furthermore the results of the model application on a case study located in Tessin with a multi-spatial resolution analysis and validation are presented.

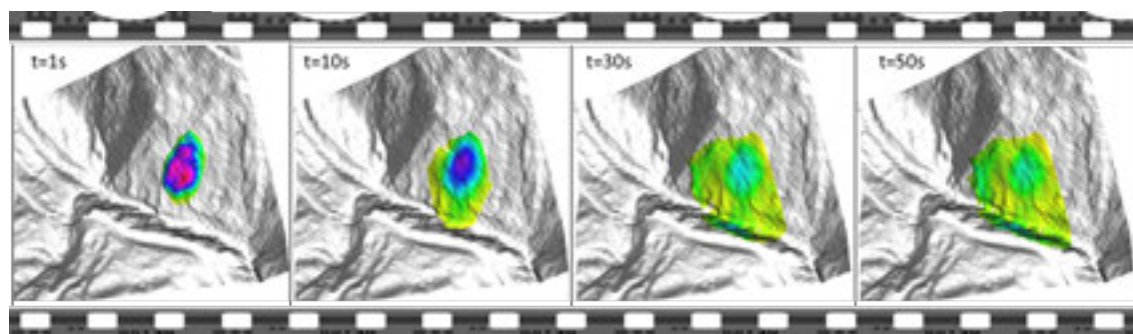


Figure 1. 3D timeline simulation of a fast landslide generated by r.massmov

## REFERENCES

Begueria, S., Van Asch, T.W.J., Malet, J.P. & Grondahl, S. 2009: A GIS based numerical model for simulating the kinematics of mud and debris flows over complex terrain. *Nat Hazards Earth Syst Sci*, 9, 1897-1909.

## P 18.4

### Monitoring rock glaciers with GPS and high-resolution cameras

Fabian Neyer, Philippe Limpach & Alain Geiger

*Geodesie und Photogrammetrie ETH Zürich, Schafmattstrasse 34, 8093 Zürich (fabian.neyer@geod.baug.ethz.ch)*

Rock glaciers are creeping accumulations of perennially-frozen debris. The response of rock glaciers to global warming and their driving physical processes are still relatively unknown. To construct accurate physical models and to understand the response to extrinsic forces (changing surface temperature, heavy precipitation, etc), accurate and reliable information about the observable surface displacement is necessary. Conventionally, such measurements (GPS, Radar, Laser-scan, etc) are taken by repeated and costly campaigns typically held a few times a year. The resulting displacement maps are usually well sampled in the spatial domain but suffer from resolution in time.

Recent work has shown that rock glaciers are affected by short-term velocity variations, typically occurring during the snow melt period. Because flow velocity can rapidly increase by up to a factor of 5 in certain areas, permanent monitoring is of major importance for any early warning systems in hazardous areas.

This work presents a pilot study where several rock glaciers in the Matter Valley (VS, Switzerland) are permanently monitored using low cost L1 GPS and optical cameras. A special focus will be given on the optical image data processing and validation. As first results show, optical image data can provide accurate, 2-dimensional displacement estimates within the pictured area.

## P 18.5

### Estimation of maximum ground shaking for the Tohoku 2011 earthquake based on collocated GPS and strong-motion data

Panos Psimoulis<sup>1</sup>, Nicolas Houlié<sup>1</sup>, Michael Meindl<sup>1</sup>, Markus Rothacher<sup>1</sup>, John Clinton<sup>2</sup>, Luis Dalguer<sup>2</sup>

<sup>1</sup> *Geodesy and Geodynamics Lab., Inst. of Geodesy and Photogrammetry, ETH Zurich, Schafmattstr. 34, 8093, Zurich (panospsimoulis@ethz.ch; nhoulie@ethz.ch; michael.meindl@ethz.ch; markus.rothacher@geod.baug.ethz.ch)*

<sup>2</sup> *Swiss Seismological Service (SED), ETH Zurich, Sonnegstr. 5, 8092 Zurich (jclinton@sed.ethz.ch; dalguer@sed.ethz.ch)*

Traditionally, GPS is known for applications in tectonics mainly for the reliable and accurate detection of surface ground motion due to dislocation, differences of material property and fault dip variations (Wright et al., 2012). However, the global rapid development of 1Hz GPS networks can provide information on deformation corresponding to seismic wave propagation and seismic rupture. The obtained information from GPS networks can be collocated with or supplement the seismometer network.

The Mw9.0 Tohoku-Oki 2011 earthquake is one of the best-observed megathrust seismic events, as it was recorded by the GNSS network of Japan, known as GEONET, and also by the seismometer networks. GPS records of 847 sites, the records of 700 and 525 sites of the KiK-net and the K-NET strong-motion networks, respectively, corresponding to the seismic event, are available. The aim of the current study is the evaluation of the estimated displacement, velocity and acceleration from collocated GPS and strong-motion stations, for certain periods of motion.

From the available stations, the GPS and strong-motion sites, whose distance did not exceed 1km, were considered as collocated, assuming that they recorded practically the same seismic motion. 124 collocated sites of GPS and strong-motion stations were found fulfilling this criterion (Fig. 1). The 1Hz GPS records were processed in PPP-mode with the Bernese GNSS Software Version 5.2 and the derived displacement time series were differentiated once and twice to obtain velocity and acceleration series, respectively. On the other hand the 100Hz strong-motion data from the collocated sites were corrected and synchronized with GPS time and the corresponding velocity and displacement time series were derived from the obtained acceleration time series by integrating once and twice, respectively.

The evaluation was done on the basis of the maximum values of displacement/velocity/acceleration of GPS and strong-motion time series for certain period bands. The latter ranged from 2.5 to 40sec for GPS and 0.025 to 40 sec for strong-motion data, respectively, due to the different recording frequency, by following a ½-octave wide distribution (Clinton and Heaton, 2002). The time series for each period band derived by filtering the corresponding GPS and strong-motion time series using a Chebyshev I band-pass filter and the evaluation was performed for the period bands common to GPS and strong-motion data.

By comparing the maximum displacements of GPS and strong-motion data, it becomes evident that GPS detects a larger long-period (>10sec) displacement, especially for the sites far from the epicenter, where the long-period seismic

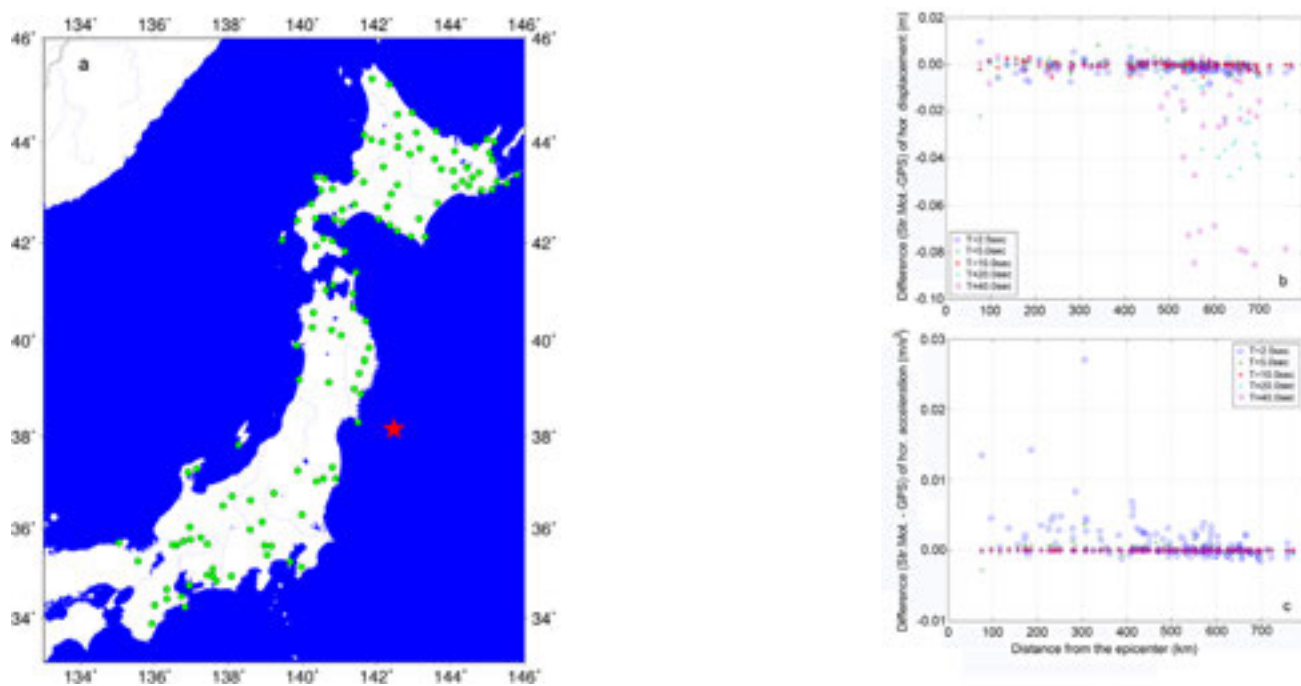


Figure 1. a) The 124 collocated sites of GPS network and strong motion KIK-net, K-NET networks. The difference of the maximum (a) displacement and (b) acceleration between strong-motion and GPS data for five period bands (2.5, 5, 10, 20 and 40sec) versus the distance of the site from the earthquake epicenter.

signal is relatively low and not detectable by the strong-motion sensors. The short-period estimations of GPS and strong-motion sensors seems to be consistent, considering also the GPS noise level of ~1cm. Regarding the acceleration, difference of the maximum estimations between GPS and strong-motion data are observed mainly for the short-period (2.5 sec) acceleration, probably due to the high noise of the GPS data in this short-period range. Regarding the velocity maximum estimation, it seems to follow a combination of the GPS and strong-motion sensor performance of displacement and acceleration; strong-motion data are more precise for short-period (2.5sec), while for long-period (>10sec) the GPS seems more accurate, especially far from the epicentre.

Based on the GPS and strong motion data of the Tohoku 2011 earthquake it can be shown that the consistency of the recovered displacement, velocity and acceleration from GPS and strong-motion data depends on the period and the distance from the epicenter. Thus, after a detailed assessment, the GPS and strong-motion sensors can be combined resulting in an improvement of the recovered displacement, velocity and acceleration.

## REFERENCES

- Clinton, J.F., Heaton, T.H., 2003: Potential advantages of a strong-motion velocity meter over a strong-motion accelerometer, *Seismological Research Letters*, 73(3), 332-342.
- Wright, T.J., Houlié, N., Hildyard, M., Iwabuchi, T., 2012: A comparison of GPS solutions for strain and SKS fast directions: Implications for modes of shear in the mantle of a plate boundary zone, *Earth and Planetary Science Letters*, 345-348, 117-125

## P 18.6

# GlaciArch: applying glaciological methods for gauging archaeological potential using GIS

Rogers Stephanie R.<sup>1</sup>, Fischer Mauro<sup>1</sup>, Huss Matthias<sup>1</sup>

<sup>1</sup> Department of Geosciences, Geography, University of Fribourg, Chemin de Musée 4, CH-1700 Fribourg  
(stephanie.rogers@unifr.ch, mauro.fischer@unifr.ch)

Recent climate changes have led to an increase in the exposure of archaeological remains in frozen environments due to the melting of glaciers, ice patches, and permafrost on a global scale. In the majority of cases, the discovery of glacial archaeological remains has occurred due to chance. In order to avoid the risk of losing exceptional, often organic, cultural remains due to decomposition, systematic and predictive methodologies should be employed to locate areas of high archaeological potential. In this paper, we merged existing glaciological knowledge and methodologies with archaeological and historical information in GIS to gain a better understanding about how people interacted with frozen environments in the recent past, as well as to create a model to determine areas of high archaeological potential for the future based on glacier melting rates. First, glacier outlines from the years 1850, 1973, and 2010, as well as topographic properties such as slope and aspect, were compared to archaeological and historical databases to validate the relationship between artifact discoveries and glacial extents over time. Next, a simple but robust, broad-scale hypsometric glacier recession model (Paul et al. 2007) was employed along with several climate change scenarios for the Pennine Alps region. This approach was based on the relationship between current glacier extents and changes in the balanced-budget equilibrium line altitude ( $ELA_0$ ) and was used to predict where glaciers will recede fastest. The results specify locations in which archaeological investigations should be conducted first. Ground Penetrating Radar (GPR) data and the spatial distribution of modeled mass balance was then used to calculate a high resolution glacier evolution model (Huss et al. 2008; Juvet et al. 2009) at two control sites, the Theodule glacier and the Haut glacier d'Arolla, in order to check the accuracy of the regional model (Linsbauer et al. 2013). The results of archaeological and historical database investigations increased understanding about the location and retrieval of artifacts in relation to glacier extents over time. The variations in glacier dynamics between sites makes it difficult to predict where archaeological remains might be located; however, we found that database investigation along with broad- and local-scale glacier modeling provided insight into patterns of artifact location and retrieval to aid in archaeological prospection and investigation in the future.

## REFERENCES

- Huss, M., Farinotti, D., Bauder, A., & Funk, M. 2008: Modelling Runoff from Highly Glacierized Alpine Drainage Basins in a Changing Climate. *Hydrological Processes* 22, 3888–3902.
- Juvet, G., Huss, M., Blatter, H., Picasso, M., & Rappaz, J. 2009: Numerical Simulation of Rhonegletscher from 1874 to 2100. *Journal of Computational Physics* 228, 6426–6439.
- Linsbauer, A., Paul, F., Machguth, H., & Haeberli, W. 2013: Comparing Three Different Methods to Model Scenarios of Future Glacier Change in the Swiss Alps. *Annals of Glaciology* 54, 241.
- Paul, F., Maisch, M., Rothenbühler, C., Hoelzle, M., & Haeberli, W. 2007: Calculation and Visualisation of Future Glacier Extent in the Swiss Alps by Means of Hypsographic Modelling. *Global and Planetary Change* 55, 343–357.

# 19. Earth System Science related Earth Observation

Michael E. Schaepman, Brigitte Buchmann, Alain Geiger

*Swiss Commission for Remote Sensing,  
Swiss Geodetic Commission*

## TALKS:

- 19.1 Garonna I., De Jong R., De Wit A., Múcher C.A., Schmid B., Schaepman, M.E.: Testing Land Surface Phenology (LSP) indicators in Europe
- 19.2 Matasci G., Volpi M., Kanevski M., Tuia D.: Hyperspectral and LiDAR data fusion for high resolution urban land cover/land use classification
- 19.3 Salvini D., Parada I., Jerik A. C.: Defining the geodetic datum for a tectonically active country
- 19.4 Schanz A., Studer S., Hocke K., Kämpfer N.: The Diurnal Cycle in Stratospheric Ozone: Observation, Simulation and Understanding
- 19.5 Torabzadeh H., Morsdorf F., Leiterer R., Schaepman M.: Determining forest species composition using imaging spectrometry and airborne laser scanner data
- 19.6 Zwieback S., Hajnsek I.: Soil Moisture Effects in Differential SAR Interferometry – Impact on estimated deformations and elevations

## POSTERS:

- P 19.1 Parkan M., Tuia D.: Modelling coastal atmospheric temperature in Greenland with support vector regression
- P 19.2 Volpi M., Matasci G., Kanevski M., Tuia D.: Interactive multisensor change detection in remote sensing images via kernel canonical correlation transformation

## 19.1

### Testing Land Surface Phenology (LSP) indicators in Europe

Garonna I.<sup>1</sup>, De Jong R.<sup>1</sup>, De Wit A.<sup>2</sup>, Mùcher C.A.<sup>2</sup>, Schmid B.<sup>3</sup> & Schaepman, M.E.<sup>1</sup>

<sup>1</sup> Remote Sensing Laboratories (RSL), Department of Geography, University of Zurich, Winterthurerstr. 190, 8057 Zurich, Switzerland

<sup>2</sup> Team Earth Observation and Environmental Informatics, Alterra, Wageningen University and Research Centre, P.O. Box 47, NL-6700 AA Wageningen, the Netherlands

<sup>3</sup> Institute of Evolutionary Biology and Environmental Studies, University of Zurich, Winterthurerstr. 190, 8057 Zurich, Switzerland

Significant recent increases in vegetation activity over time (i.e. *greening*) have been identified over Europe (e.g. *Stöckli and Vidale, 2004*), and associated both with climatic changes and with large-scale human interventions, including land-use change (*de Jong et al., 2013*). The long-standing human managing and shaping of the landscape make the European region a particularly challenging – and interesting – region of study for environmental change studies.

Land Surface Phenology (LSP) focuses on intra-annual dynamics of vegetation activity as observed from satellite observations. As such, this field plays a key role in understanding the terrestrial carbon budget, as well as the response of terrestrial ecosystems to environmental change.

In this study, we characterize LSP changes in Europe's eco-regions for the last 30 years. We use the latest version of the 8-km Global Inventory Modeling and Mapping Studies (GIMMS) Normalized Difference Vegetation Index dataset (third generation, or NDVI-3g) to retrieve LSP metrics for Pan-Europe for the last three decades (1982–2011). Each year of NDVI data is processed using the Harmonic Analysis of Time Series (HANTS) algorithm, producing smooth NDVI annual profiles on a pixel-by-pixel basis. We derive LSP metrics for each year, namely Start, End and Length of Growing Season, by applying the Midpoint<sub>pixel</sub> local threshold method, based on the White et al. (2009) inter-comparison.

A landscape-based stratification, using the European Landscape Classification (LANMAP) (*Mùcher et al., 2010*) allows us to examine LSP characteristics and trends for the different European eco-regions. We demonstrate statistically significant shifts in LSP metrics over the study period, with a general lengthening of the growing season in Europe of approximately 0.3 days year<sup>-1</sup>. LSP trends varied significantly between eco-regions, and we discuss potential reasons for these spatially diverse trends.

#### REFERENCES

- de Jong, R., et al. (2013), Spatial relationship between climatologies and changes in global vegetation activity, *Global Change Biology*, 19(6), 1953-1964.
- Mùcher, C. A., J. A. Klijn, D. M. Wascher, and J. H. J. Schaminée (2010), A new European Landscape Classification (LANMAP): A transparent, flexible and user-oriented methodology to distinguish landscapes, *Ecological Indicators*, 10(1), 87-103.
- Stöckli, R., and P. L. Vidale (2004), European plant phenology and climate as seen in a 20-year AVHRR land-surface parameter dataset, *International Journal of Remote Sensing*, 25(17), 3303-3330.
- White, M. A., et al. (2009), Intercomparison, interpretation, and assessment of spring phenology in North America estimated from remote sensing for 1982–2006, *Global Change Biology*, 15(10), 2335-2359.

## 19.2

## Hyperspectral and LiDAR data fusion for high resolution urban land cover/land use classification

Matasci Giona<sup>1</sup>, Volpi Michele<sup>1</sup>, Kanevski Mikhail<sup>1</sup> & Tuia Devis<sup>2</sup>

<sup>1</sup> Center for Research on Terrestrial Environment (CRET), University of Lausanne, Quartier UNIL-Mouline, CH-1015 Lausanne. (giona.matasci@unil.ch)

<sup>2</sup> Laboratory of Geographic Information Systems (LaSIG), Ecole Polytechnique Fédérale de Lausanne, EPFL Station 18, CH-1015 Lausanne.

In this study we investigated the possible synergies between hyperspectral and LiDAR-derived data for the detailed thematic classification of the land cover/land use in an urban environment (Dalponte et al. 2008; Priestnall et al. 2000). To this end, we could resort to two datasets available for the 2013 IEEE GRSS Data Fusion Contest describing a neighbourhood of the city of Houston, USA. The datasets consisted of a hyperspectral image with 144 VNIR spectral bands and a Digital Surface Model extracted from a LiDAR acquisition. The two layers were co-registered and presented a spatial resolution of 2.5 meters. The purpose was to discriminate 15 highly overlapping classes of interest related to the land cover/land use present in the considered urban scene.

First, we processed the remotely sensed image with a histogram matching procedure with the aim of removing the shadows cast by the clouds. Then, we extracted spatial features (morphological opening and closing filters and the associated top hat operators) at various scales both from the hyperspectral image (after PCA transformation) and from the raw LiDAR height map (Tuia et al. 2009; Benediktsson et al. 2003). Additionally, the set of features has been complemented with spectral indices, namely with variations of the NDVI based on different band combinations.

Subsequently, after having stacked all the extracted features into a single dataset, a Support Vector Machine classifier has been trained using the available labeled samples. A prediction over the entire extent of the image has been performed to obtain the final classification map. After a suitable post-processing involving a spatial majority vote filtering with a moving window, the resulting thematic map accurately delineates the various land cover/land use classes in the scene.



Figure 1. True color RGB visualization of the hyperspectral image.

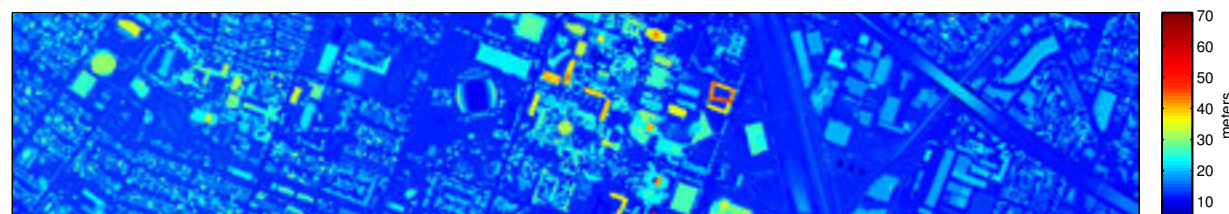


Figure 2. Digital Surface Model derived from the LiDAR acquisition.

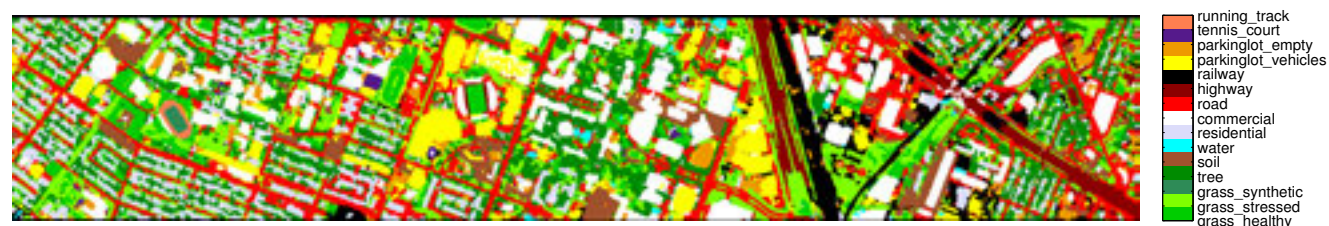


Figure 3. Final classification map with 15 classes (Kappa statistic = 0.945).

## REFERENCES

- Benediktsson, J. A., Pesaresi, M., & Amason, K. 2003. Classification and feature extraction for remote sensing images from urban areas based on morphological transformations. *IEEE Transactions on Geoscience and Remote Sensing*, 41(9), 1940-1949.
- Dalponte, M., Bruzzone, L., & Gianelle, D. 2008. Fusion of hyperspectral and LIDAR remote sensing data for classification of complex forest areas. *IEEE Transactions on Geoscience and Remote Sensing*, 46(5), 1416-1427.
- IEEE GRSS Data Fusion Contest 2013, Online: <http://www.grss-ieee.org/community/technical-committees/data-fusion/>
- Priestnall, G., Jaafar, J., & Duncan, A. 2000. Extracting urban features from LiDAR digital surface models. *Computers, Environment and Urban Systems*, 24(2), 65-78.
- Tuia, D., Pacifici, F., Kanevski, M., & Emery, W. J. 2009. Classification of very high spatial resolution imagery using mathematical morphology and support vector machines. *IEEE Transactions on Geoscience and Remote Sensing*, 47(11), 3866-3879.

## 19.3

### Defining the geodetic datum for a tectonically active country

Salvini Dante<sup>1</sup>, Parada Ivan<sup>2</sup>, Jerik Axpuc Calderas<sup>3</sup>

<sup>1</sup>BSF Swissphoto AG, Dorfstrasse 53, CH-8105 Regensdorf-Watt ([dante.salvini@bsf-swissphoto.com](mailto:dante.salvini@bsf-swissphoto.com))

<sup>2</sup>Instituto Geográfico Nacional, Avenida Las Américas 5-76, zona 13, GT-01013 Guatemala-City ([ivan.parada@ign.gob.gt](mailto:ivan.parada@ign.gob.gt))

<sup>3</sup>Registro de Información Catastral, 21 calle 10-58, zona 13, GT-01013, Guatemala-City ([jaxpuac@ric.gob.gt](mailto:jaxpuac@ric.gob.gt))

Guatemala is located between the Pacific Ocean and the Caribbean Sea at a latitude of 15° N. From a geological point of view, the country lies within an area of active plate convergence and transversal plate motion. The Motagua Fault, part of the boundary between the Caribbean and North American tectonic plates, transects Guatemala. In addition, the Middle America Trench is located along the southwest coast. Here, the Cocos Plate subducts beneath the Caribbean Plate. Due to this configuration, earthquakes occur frequently, many of them killing people and causing damages. The last major earthquake occurred in November 2012 near the Pacific coast and caused irreversible displacements of the ground in the order of several centimeters. The quantification of these displacements and the extension of the affected area were only possible because the country runs a continuously operating reference network (CORS). The network consists of 17 GNSS stations distributed over the entire country and was realized with funding and support of Switzerland (SECO, mixed credit project in Guatemala). The periodical computation of the coordinates of each station allows tracking of the displacements. In other words, the CORS acts as a monitoring system of the earth surface. The results over the last 12 years of the 3 longest-running stations show a continuous movement of the tectonic plates mentioned before (see fig. 1). In addition to the continuous movement, it is well known that earthquakes can produce abrupt shifts.

The primary scope of the installation and the operation of the CORS is to support surveying operations, notably land surveying and the cadastral land register. It is considered state of the art that countries base their local reference systems on CORS networks. Such a local reference system includes the official national coordinate and height systems with all their basic definitions (reference ellipsoid, geoid model and map projection). All surveying activities are then based on that one national reference system. When defining national reference systems, it is normally assumed that the country is geologically stable or at least that the displacement of the plate on which the country lies is homogeneous. These prerequisites are not given for Guatemala. This fact forces the surveyors to take into account the geological displacements when defining the reference system. In 2012, as the full CORS of Guatemala was brought into service, the Swiss consultants proposed a unique approach for a reference system, consisting of two phases. In a first step, the coordinates of the 17 sites have to be defined according to the global reference frame (ITRF). These coordinates can be obtained by international computing centers, in the case of Guatemala by SIRGAS (Geocentric Reference System for the Americas). These coordinates constitute the basis for every surveying activity. For a period of approx. 8 years, the coordinates of the sites maintain their validity regardless of the moving plates (estimated displacement in this time is 10 cm). After three to four years, the continuous computation of the station coordinates done by SIRGAS allows the derivation of a velocity model which approximates the movement of the plates. During the subsequent years, the model has to be kept up to date (e.g. including shifts due to earthquakes) and validated. Based on the discrete velocity model, a grid (so called NTV2) covering the entire country can be derived. In the second and final phase, this grid is used to switch between the current epoch in which surveying is done and the epoch in which the reference system was defined. This transformation is needed to keep every position (coordinate) regardless of its time of measurement in a unique and consistent reference frame.

The National Geographic Institute of Guatemala is now refining the Swiss proposal in order to implement the new reference system as soon as possible.

#### REFERENCES

Salvini D, Brockmann E. 2013, Marco de referencia y proyección para Guatemala, BSF Swissphoto 2013

Brockmann E. 2009: Coordinate Reference Frame Definition Guatemala, swisstopo 2009.

Sanchez L., Cruz O. 2012, SIRGAS and the earthquake of November 7th 2012 in Guatemala, SIRGAS 2012.

Department of Geological and Environmental Sciences 2005, Field Guide to Guatemala Geology, Stanford University 2005

<http://www.swisstopo.ch>, last visit 31.08.2013

<http://en.wikipedia.org>, last visit 31.08.2013

<http://www.sirgas.org>, last visit 31.08.2013

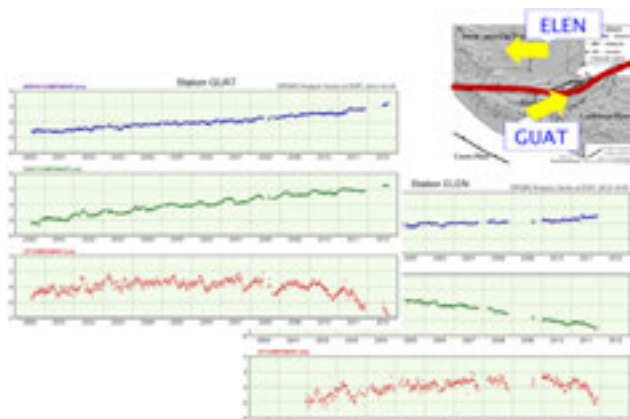


Figure 1. Plots of the continuous displacements monitored for the site GUAT (Caribbean plate) and ELEN (North American plate)

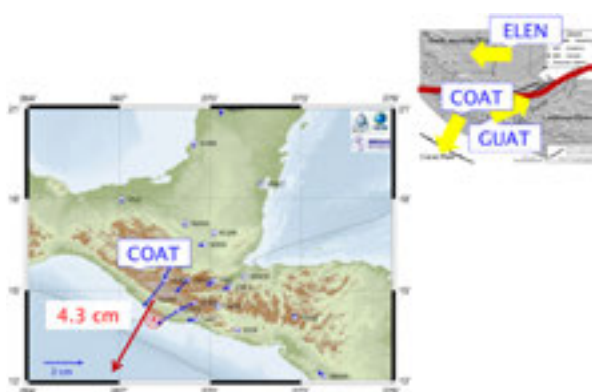


Figure 2. Earthquake of Nov. 2012 caused a displacement of 4.3 cm at the site COAT (near the Middle America Trench)

## 19.4

# The Diurnal Cycle in Stratospheric Ozone: Observation, Simulation and Understanding

Schanz Ansgar, Studer Simone, Hocke Klemens, Kämpfer Niklaus

*Institute of Applied Physics and Oeschger Centre for Climate Change Research, University of Bern, Sidlerstr. 5, CH-3012 Bern (ansgar.schanz@iap.unibe.ch)*

The diurnal cycle in stratospheric ozone only amounts a few percent. This small amplitude significantly affects trend estimates of the stratospheric ozone layer. The ozone layer is expected to recover by about +1% per decade until 2050. Since satellite orbits differ or slightly drift in local solar time, the diurnal cycle in stratospheric ozone will bias global ozone data sets from satellites.

For correction of the diurnal bias we have to observe, to simulate and to understand the diurnal cycle in stratospheric ozone at each geographic location. Seasonal and interannual variations of the diurnal ozone cycle also should be taken into account (Figure 1).

We present a climatology of the diurnal ozone cycle derived from 17 years of ozone microwave radiometry at University of Bern (Figure 2). We discuss the intercomparison between the observations and simulation results of the Whole Atmosphere Community Climate Model (WACCM). The simulation helps us to understand the chemical, radiative, dynamical and thermal forcings which are responsible for the diurnal cycle in stratospheric ozone.



Figure 1. Illustration of the versatility of the diurnal cycle in stratospheric ozone which depends on many other factors such as systematic instrument errors, thermal tides and diurnal variations in ozone depleting substances. The diurnal ozone cycle can be utilized as a benchmark for the accuracy of ozone measurement and retrieval techniques. A good knowledge of the diurnal ozone cycle is needed for the correction of diurnal biases in ozone data sets from satellites.

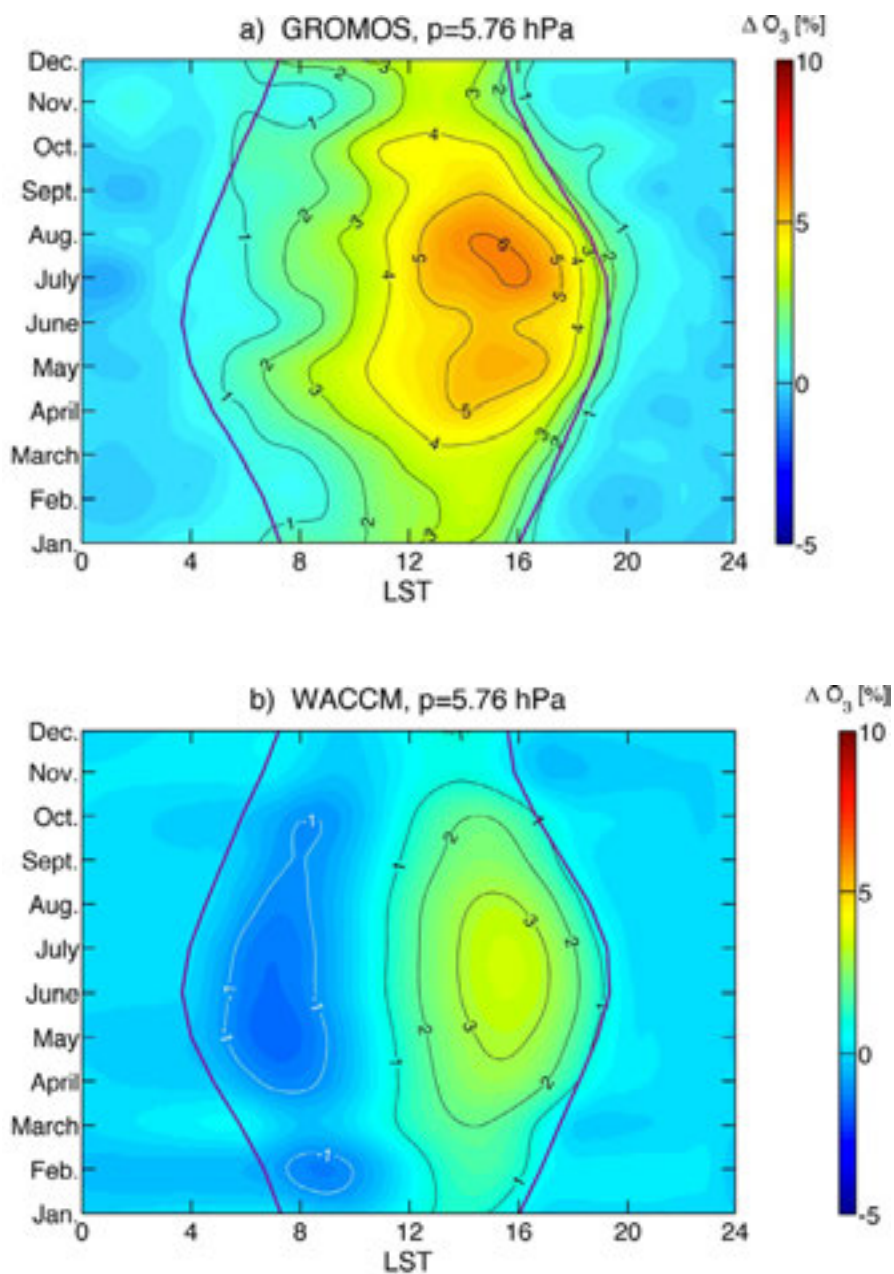


Figure 2. Climatology of the diurnal ozone variation at about 35 km altitude: a) derived from 17 years of ozone observations at Bern, b) simulated by the chemistry-climate model WACCM. The relative ozone variation with respect to midnight ozone is maximal in the afternoon during summer. The two black curves denote the Local Solar Time (LST) of a solar zenith angle of 90 deg. (Studer et al., 2013)

## REFERENCES

Studer S., K. Hocke, A. Schanz, H. Schmidt, N. Kämpfer: A climatology of the diurnal variation of stratospheric and mesospheric ozone over Bern, Switzerland, submitted to Atmos. Chem. Phys. Discuss., July 2013

## 19.5

# Determining forest species composition using imaging spectrometry and airborne laser scanner data

Torabzadeh Hossein, Morsdorf Felix, Leiterer Reik, Schaepman E. Michael

*Remote Sensing Laboratories, Department of Geography, University of Zurich, Winterthurerstrasse 190, 8057 Zurich, Switzerland,  
Email: hossein.torabzadeh@geo.uzh.ch*

Forests cover almost one third of the total land surface of the Earth and play an important role in the global energy- and matter fluxes between atmosphere and the land surface. Assessing and quantifying forest ecosystem goods and services (associated with water refinement, carbon sequestration, biodiversity, or wildlife habitats) and their underlying processes helps to develop sustainable management strategies and to project biogeochemical cycles under changing climate conditions (Fisher et al., 2009). Particularly the tree species composition is an important aspect of forest monitoring as well as for management planning. Assessing of tree species composition with traditional fieldwork is labor-intensive, time-consuming and mostly limited by spatial extent; accordingly, remote sensing data enables to overcome these limitations.

Although different tree species often have unique spectral signatures, mapping based on spectral reflectance properties alone is often an ill-posed problem, since the spectral signature is as well influenced by age, canopy gaps, shadows and background characteristics. Thus, reducing the unknown variation by knowing the structural parameters of different species (e.g. branching and foliage distribution) should improve determination procedures (Holmgren & Persson, 2004).

In this study we combine imaging spectrometry (IS) and airborne laser scanning (ALS) data in a broadleaf dominated forest in the Swiss Jura (latitude 47°28'N, longitude 8°21'E) to differentiate tree species more accurately as single-instrument data could do. Spectral information has been acquired by Airborne imaging spectrometry Prism Experiment (APEX) in 285 bands (400 - 2500 nm). A small footprint, full-waveform RIEGL light detection and ranging (LiDAR) system has been deployed to scan the study area under leaf-on conditions. To validate the results, tree location and species, crown dimensions, diameter in breast height (DBH) and understory condition were derived using a field map system. ALS and IS datasets was scrupulously co-registered so that miss-alignment differences remained less than half size of the IS data pixel size (approximately ±1 m). Minimum noise fractions were calculated from IS data, while, within each image pixel, structurally related statistics along the vertical (e.g. height percentiles) were derived from the full-waveform ALS data. Additionally, the full-waveform information (e.g. echo width and amplitude) was statistically evaluated for each pixel and at different heights.

Due to high dimensionality of multiple sources data that we have, support vector machine (SVM) classifier has been deployed for distinguishing the eight most prevalent tree species in our study area. The spatially explicit information layers containing both, the spectral and structural components from the IS and ALS datasets, were then combined together in the pixel-based image classification procedure.

The final map, improved on single system products, provides the distribution and fraction of each tree species throughout our forest site. A thorough accuracy analysis for each species reveals which species profit most from which variables from the exhaustive structural and/or spectral feature set for its discrimination. We conclude, that the combined use of multi-source ALS and IS data significantly improves the overall accuracy of the tree species classification but is still limited in dense forest areas with deciduous trees, where the individual crowns merged into each other and prevent an unambiguous assignment of a specific tree species.

### REFERENCES

- Fisher, Brendan, R. Kerry Turner & Paul Morling. Defining and Classifying Ecosystem Services for Decision Making. *Ecological Economics* 68.3 (2009): 643-53.
- Holmgren, Johan & Asa Persson. Identifying Species of Individual Trees Using Airborne Laser Scanner. *Remote Sensing of Environment* 90.4 (2004): 415-23

## 19.6

# Soil Moisture Effects in Differential SAR Interferometry – Impact on estimated deformations and elevations

Zwieback Simon<sup>1</sup> & Hajnsek Irena<sup>1,2</sup>

<sup>1</sup>*Institute of Environmental Engineering, ETH Zurich, Schafmattstr. 6, CH-8093 Zurich (zwieback@ifu.baug.ethz.ch)*

<sup>2</sup>*Microwaves and Radar Institute, German Aerospace Center, PO BOX 1116, D-82234 Wessling*

Repeat-pass Synthetic Aperture Radar (SAR) Interferometry (or Differential SAR Interferometry, DInSAR) is a valuable remote sensing technique as it is sensitive to deformations or the height of scattering objects (Gabriel et al. 1989). Due to the first sensitivity, it is a common tool for studying subsidence phenomena (e.g. due to groundwater extraction or soil freezing/thawing) or mass movements; due to the second, it allows for the estimation of digital surface models or maps of vegetation height.

This is done by combining two SAR images acquired at different times: during this time interval, the soil moisture (SM) content can change and this change is hypothesized to influence the phase  $\Phi$ , from which deformations or height are inferred. If this influence is indeed present, these retrieved deformations or heights will be erroneous.

Such an effect was first postulated 25 years ago by Gabriel et al. (1989) – since then a handful of dedicated experiments and observational studies have yielded inconclusive (and partially inconsistent) results (Rudant et al. 1996; Morrison et al. 2011). Thus the prevalence, sign and size of these influences remain poorly understood.

We propose to statistically analyze the observed phase (two L-band airborne campaigns) as a function of SM changes (measured in situ) using regression techniques; this allows us to i) determine whether these effects are significant; ii) estimate their size; iii) compare this to predictions of proposed models/ explanations; and iv) gauge their impact on retrieving deformations or heights.

The results reveal that soil moisture changes influence the observed phase in both campaigns. Optional figures 1 and 2 show the linear dependence of  $\Phi$  on SM changes: this slope term  $\beta$  is predominantly positive and significant. This pattern is consistent for both campaigns; there are, however, large inter- and intra-field variations present. The positive sign corresponds to a movement of the soil away from the antenna as the soil becomes moist.

The size of the linear slope term  $\beta$  is usually on the order of 5, but much larger sensitivities occur for certain fields in the CanEx campaign. For illustration: a slope of 5 corresponds to the following: if soil moisture changes by 10%, the phase changes by around 30°.

This size of the slope term as well as its sign can be compared to the predictions of possible origins of the soil moisture effect. Three such explanations have been advanced:

1. Penetration depth hypothesis: the phase is related to the absorption in the soil (Nolan 2003). The predicted sign is opposite to the observed one.
2. Clay swelling: certain soils swell as they become moist, corresponding to a movement towards the sensor and a negative (i.e. opposite to the observed) sign of the effect.
3. Dielectric volume scattering: inhomogeneities within the soil lead to scattering, their apparent distance (optical path) increases as the soil becomes wet (Rudant et al. 1996; de Zan et al. 2013). The sign and also the magnitude (which depends on the specific parameterizations) are compatible with the observations.

These results show that for the data sets studied these effects are significant and only consistent with volume scattering, but not with the other two explanations. This insight can prove beneficial for understanding and also predicting the impact of soil moisture changes, leading to the possibility to estimate soil moisture or provide corrections for the chief applications of the technique: deformation and elevation measurements. The latter would be necessary if these effects were larger than the random noise, and indeed this is the case in the present data sets. In these campaigns, soil moisture induced phases of 90° (and larger) have been observed: this corresponds to a deformation of 3 cm and is much larger than the noise and than typically studied subsidence phenomena considering the time scale of several days. Similar conclusions also apply to the estimation of elevations, where preprocessing assures that the random noise in the phase is much smaller than 90°. These influences thus have to be taken into consideration for a reliable estimation of deformations using DInSAR, e.g. for monitoring groundwater-related subsidence or tectonic movements.

## REFERENCES

- de Zan, F., Parizzi, A., Prats-Iraola, P. & Lopez-Dekker, P. 2013: A SAR Interferometric Model for Soil Moisture. IEEE Trans. Geosci. Remote Sens., in press.
- Gabriel, A., Goldstein, R. & Zebker, H. 1989: Mapping small elevation changes over large areas: Differential radar interferometry. J. Geophys. Res. 94, 9183-9191.
- Morrison, K., Bennett, J., Nolan, M. & Menon, R. 2011: Laboratory Measurement of the DInSAR Response to Spatiotemporal Variations in Soil Moisture. IEEE Trans. Geosci. Remote Sens. 49, 3815-3823.
- Nolan, M. 2003: Penetration depth as a DInSAR observable and proxy for soil moisture. IEEE Trans. Geosci. Remote Sens. 41, 532-537.
- Rudant, J., Bedidi, A., Calonne, R., Massonnet, D., Nesti, G. & Tarchi, D. 1996: Laboratory Experiment for the Interpretation of Phase Shift in SAR Interferograms. Proceedings of FRINGE.

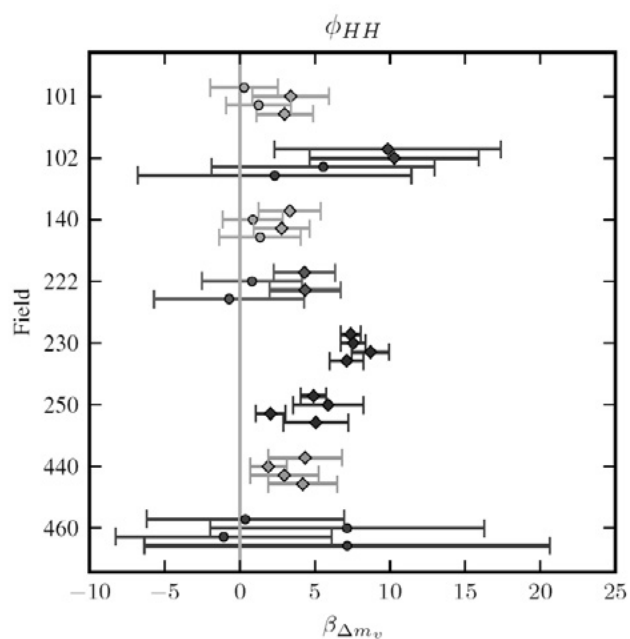


Fig. 1: Estimated linear dependence  $\beta$  of the HH phase on soil moisture for the AGRISAR campaign: the coefficients for each of the four samples within the fields are given by the markers, the error bars denote the 95% confidence intervals.

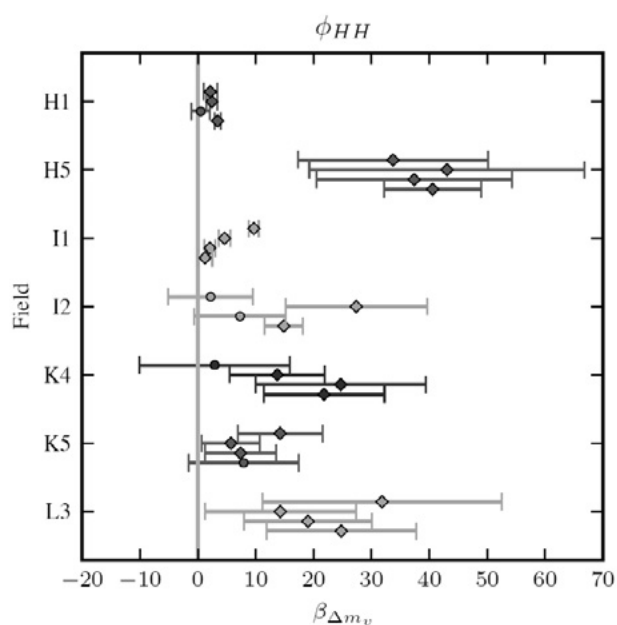


Fig. 2: Same as Fig. 1 but for the CanEx campaign.

## P 19.1

# Modelling coastal atmospheric temperature in Greenland with support vector regression

Matthew Parkan<sup>1</sup>, Devis Tuia<sup>1</sup>

<sup>1</sup>Laboratoire des Systèmes d'Information Géographique, Ecole Polytechnique Fédérale de Lausanne, Switzerland.  
{matthew.parkan,devis.tuia}@epfl.ch

In the recent years, global climate change has induced thinning of the Greenland ice sheet and an evergrowing loss of sea ice in the Arctic (Abdalati et al, 2001, Krabill et al., 2004). Various local and regional forcing mechanisms and feedback interactions between offshore and inshore variables in coastal areas are currently under scrutiny, but are not yet well understood. One of the key variables influencing the rate of ice disappearance is atmospheric temperature (Tedesco, 2007, Tedesco and Miller, 2007). In this paper, we present a statistically derived model that links coastal atmospheric temperature to offshore conditions, such as expanding open water areas (Rennermalm et al., 2009), sea level pressure or wind speed (Kobashi et al, 2011) at six weather stations on the Coast of Greenland. Our aim is to observe statistical relationships between variations in atmospheric temperatures and changes in offshore conditions. To study these relations, a machine learning approach based on a nonlinear model, support vector regression (SVR, Schölkopf and Smola, 2002), is considered.

Based on a combination of daily in situ (i.e., wind velocity, sea level pressure, cloud ceiling height) and remotely sensed (i.e. sea surface temperature, sea ice concentration) data, a series of daily predicting features are constructed for the years 1981-2012. Daily temperature averages are considered as dependent variables. Two experiments are conducted:

In the first experiment, temperatures predictions by the SVR are compared to a widely used linear model, a multivariate linear regression (LR) with the same independent variables. Results of the SVR indicate that prediction NRMSE of 10–15% are routinely achievable, which are between 2% and 4% lower than when using the linear model.

In the second experiment, individual models are built for each month of the year. Prediction errors are found to be smaller in summer months and/or at lower latitudes (Stations Prins Christian Sund or Aasiaat, 1.5 – 2°C, 9-10% error).

## REFERENCES

- Abdalati, W. and Steffen, K. 1992: Snowmelt on the Greenland ice sheet as derived from passive microwave satellite data, *Journal of Climate*, 10, 165–175.
- Kobashi, T., Kawamura, K., Severinghaus, J. P., Barnola, J., Nakae-gawa, T., Vinther, B. M., Johnsen, S. J., and E., B. J. 2011: High variability of Greenland surface temperature over the past 4000 years estimated from trapped air in an ice core, *Geophysical Research Letters*, 38, L21 501.
- Krabill, W., Hanna, E., Huybrechts, P., Abdalati, W., Cappelén, J., Csatho, B., Frederick, E., Manizade, S., Martin, C., Sonntag, J., et al. 2004: Greenland ice sheet: increased coastal thinning, *Geophysical Research Letters*, 31.
- Rennermalm, A. K., Smith, L. C., Stroeve, J. C., and Chu, V. W. 2009: Does sea ice influence Greenland ice sheet surface-melt?, *Environmental Research Letters*, 4, 024 011.
- Schölkopf, B. and Smola, A. 2002: *Learning with Kernels*, MIT press, Cambridge (MA).
- Tedesco, M. 2007: A New Record in 2007 for Melting in Greenland, in: *Eos, Transactions American Geophysical Union*, vol. 88, p. 383.
- Tedesco, M. and Miller, J. 2007: Observations and statistical analysis of combined active-passive microwave space-borne data and snow depth at large spatial scales, *Remote Sensing of Environment*, 111, 382–397.

## P 19.2

## Interactive multisensor change detection in remote sensing images via kernel canonical correlation transformation

Volpi Michele<sup>1</sup>, Matasci Giona<sup>1</sup>, Kanevski Mikhail<sup>1</sup>, Tuia Devis<sup>2</sup>

<sup>1</sup> Centre de Recherche en Environnement Terrestre (CRET), University of Lausanne, UNIL-Mouline, CH-1015 Lausanne. (michele.volpi@unil.ch)

<sup>2</sup> Laboratoire des Systèmes d'Information Géographique (LaSIG), École Polytechnique Fédérale de Lausanne, EPFL Station 18, CH-1015 Lausanne.

Multisensor change detection is defined as the process of identifying changes in two (or more) images of the same geographical area acquired by different instruments at different time instants (Bruzzone and Fernandez-Prieto, 2000; Mercier et al., 2008; Longbotham et al., 2012). In this study, we investigate the feasibility of multisensor change detection in remote sensing images by interactively exploiting the user knowledge in the process. Recently, a system able to make two images acquired by different sensors comparable has been proposed (Volpi et al., 2013). Such a system allows to perform accurate pixelwise spectral change detection relying on the difference image. The process exploits a nonlinear transformation, the kernel canonical correlation analysis (kCCA) (Bach and Jordan, 2002), to reproject both the involved images in a common space in which unchanged pixels are maximally correlated and thus comparable, making their difference the closest possible to zero. After this statistical image alignment step, standard change detection methods may be applied to obtain the change map.

However, a major issue was the choice of the samples used to compute the kernel-based alignment, that is, selecting appropriate examples from which to compute the transformation. In this contribution, we study the possible synergy with the user in selecting such samples. The user is asked to iteratively select from the transformed difference image a subset of samples representing either unchanged pixels and unwanted changes (e.g. phenological differences). To drive the process, two measures are used to provide information about the quality of the alignment: the correlation of the transformed components implicitly provided by the kCCA, and the distance of the bi-temporal samples in the transformed space.

Finally, after the alignment step, the change vector analysis (CVA) is applied to perform change detection from the transformed difference image (Bruzzone and Fernandez-Prieto, 2000). Furthermore, the samples that have been iteratively selected by the user are included in the automatic process. Those pixels help the system to choose a proper threshold discriminating whether a change has occurred or not at a given pixel location.

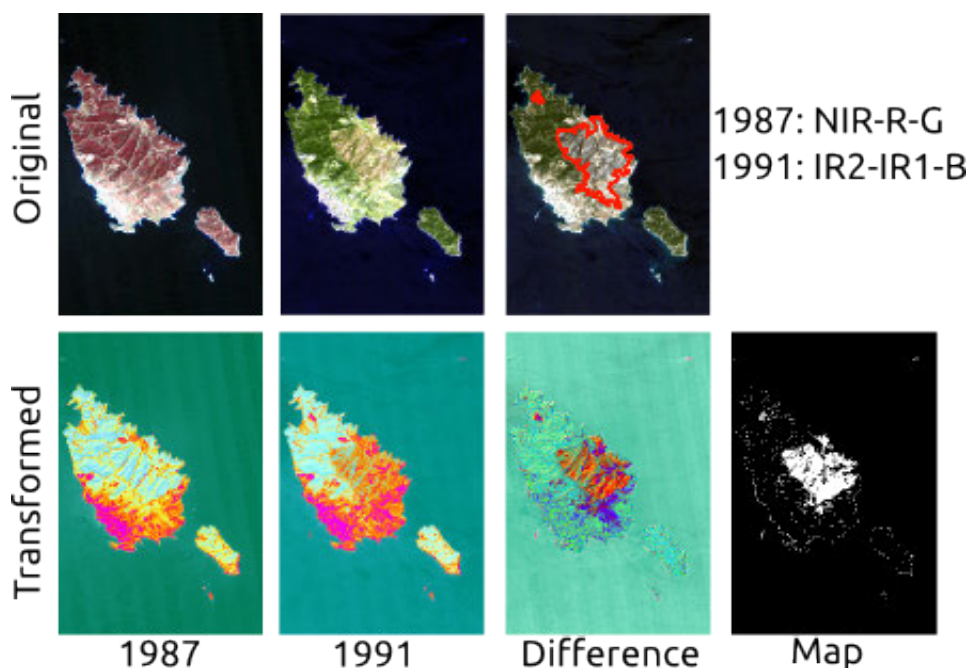


Figure 1: The multisensor change detection system. Original images (false colors) are aligned to obtain comparable, transformed images of equal dimensionality enhancing changed area in their difference.

## REFERENCES

- F. R. Bach and M. I. Jordan, "Kernel independent component analysis," *Journal of Machine Learning Research*, vol. 3, pp. 1–48, 2002.
- L. Bruzzone and D. Fernandez-Prieto, "Automatic analysis of the difference image for unsupervised change detection," *IEEE Transactions on Geoscience and Remote Sensing*, vol. 38, no. 3, pp. 1171–1182, 2000.
- N. Longbotham, F. Pacifici, T. Glenn, A. Zare, M. Volpi, D. Tuia, E. Christophe, J. Michel, J. Inglada, J. Chanus-sot, and Q. Du, "Multi-modal change detection, application to the detection of flooded areas: Outcome of the 2009-2010 data fusion contest," *IEEE Journal of Selected Topics on Applied Earth Observation*, vol. 9, no. 6, pp. 331–342, 2012.
- G. Mercier, G. Moser, and S. B. Serpico, "Conditional copulas for change detection in heterogeneous remote sensing images," *IEEE Transactions on Geoscience and Remote Sensing*, vol. 46, no. 5, pp. 1428–1441, 2008.
- Volpi, M.; de Morsier, F.; Camps-Valls, G.; Kanevski, M. and Tuia, D., "Multi-sensor change detection based on nonlinear canonical correlations", *IEEE International Geosciences and Remote Sensing Symposium IGARSS 2013, Melbourne (AUS), 2013*.

## 20. Quaternary environments: landscapes, climate, ecosystems, human activity during the past 2.6 million years

Naki Akçar, Luc Braillard, Gaudenz Deplazes, Hansruedi Graf,  
Irka Hajdas, Olivier Heiri, Susan Ivy Ochs, Christine Pümpin

*Swiss Society for Quaternary Research (CH-QUAT)*

### TALKS:

- 20.1 Akçar N., Tikhomirov D., Ivy-Ochs S., Graf A., Schlunegger F., Reber R., Claude A., Kubik P.W., Vockenhuber C., Hajdas I., Schlüchter C.: The Valais Glacier: its disappearance from the Alpine Foreland
- 20.2 Amann B., Lobsiger S., Tylmann W., Grosjean M.: Scanning reflectance spectroscopy (380-730 nm) for Paleo-environmental and climatic changes assessment
- 20.3 Claude A., Akçar N., Ivy-Ochs S., Graf H.R., Kubik P.W., Vockenhuber C., Dehnert A., Rahn M., Rentzel P., Pümpin C., Schlüchter C.: The challenge of dating Swiss Deckenschotter with cosmogenic nuclides
- 20.4 Herman F., Seward D., Valla P.G., Carter A., Kohn B., Willett S.D., Ehlers T.A.: Worldwide acceleration of mountain erosion under a cooling climate
- 20.5 Lombardo U.: Mid to late Holocene environmental change in the Bolivian Amazon reconstructed from paleosols and archaeological sites.
- 20.6 Luetscher M., Boch R., Cheng H., Edwards R.L., Sodemann H., Spötl C.: A speleothem record of the Last Glacial Maximum from the western Swiss Alps
- 20.7 Reber R., Tikhomirov D., Akçar N., Yesilyurt S., Yavuz V., Kubik P., Schlüchter C.: Late Quaternary Glacial History in northeastern Anatolia
- 20.8 Rodrigues L., Umberto L., Veit H.: An insight into the morphology of pre-Columbian raised fields in different landscapes in the Llanos de Moxos, Bolivia
- 20.9 Tikhomirov D., Akçar N., Ivy-Ochs S., Schlüchter C.: Advanced model for limestone fault scarp dating and paleoearthquake history reconstruction
- 20.10 Wirsig C., Ivy-Ochs S., Zasadni J., Akcar N., Christl M., Schlüchter C.: Towards a «true» age of LGM ice surface decay in Oberhaslital
- 20.11 Wüthrich L., Zech R., Haghypour N., Gnägi C., Christl M., Ivy-Ochs S.: Dating glacial deposits in the western Swiss lowlands using cosmogenic <sup>10</sup>Be

## POSTERS:

- P 20.1 Belfar D., Deguaechia A., Djerrab Ar., Bouhleb S., Fehdi Ce.: Sedimentological and paleoenvironmental study of quaternary alluvial formations Zeïet Oued, Ain Zerga W Tébessa. N-E Algeria.
- P 20.2 Buechi M.W., Lowick S. E., Anselmetti F. S.: Multiphase depositional and erosional history recorded in the infill of the glacially overdeepened Lower Glatt valley, Northern Switzerland
- P 20.3 Diaz N., Dietrich F., Cailleau C., Sebag D., Verrecchia E.: Origin of unexpected tropical carbonate mounds (TCM) in northern Cameroon – Carbonate accumulation context: hypotheses and challenges
- P 20.4 Hippe K., Hajdas I., Ivy-Ochs S., Maisch M.: Middle Würm radiocarbon chronologies in the Swiss Alpine foreland - first results from the TiMIS project
- P 20.5 King G., Herman F., Valla P.: The new luminescence laboratory at the University of Lausanne
- P 20.6 Lantos I., Spangenberg J.E., Giovannetti M.A., Maier, M., Ratto N.: Archaeometric evidence of foodways in the South-Central Andes: Prehispanic maize consumption in West Tinogasta (Catamarca, Argentina)
- P 20.7 Messerli, M. Maisch, M., Ivy-Ochs, S.: GIS-based geomorphological mapping, dating of selected landforms and landscape evolution during the Lateglacial and Holocene, in the region of Val Tuoi, Grisons, Switzerland
- P 20.8 Mozafari Amiri N., Tikhomirov D., Özkaymak Ç., Sümer Ö., Ivy-Ochs S., Vockenhuber Ch., Uzel B., Sözbilir H., Akçar N.: Using cosmogenic <sup>36</sup>Cl to determine periods of enhanced seismicity in western Anatolia, Turkey
- P 20.9 Scapozza C., Ambrosi C., Castelletti C., Soma L., Dall'agnolo S.: Timing of deglaciation on the Southern Swiss Alps
- P 20.10 Togni V., Adatte T., Foellmi K., Spangenberg J., Thevenon F., Wirth S.: Paleoenvironmental study of the Lago d'Alzasca (Ticino, Switzerland) during the last 10'000 years

## 20.1

## The Valais Glacier: its disappearance from the Alpine Foreland

Akçar Naki<sup>1</sup>, Tikhomirov Dmitry<sup>1</sup>, Ivy-Ochs Susan<sup>2</sup>, Graf Angela<sup>3</sup>, Schlunegger Fritz<sup>1</sup>, Reber Regina<sup>1</sup>, Claude Anne<sup>1</sup>, Kubik Peter W.<sup>2</sup>, Vockenhuber Christof<sup>2</sup>, Hajdas Irka<sup>2</sup> and Schlüchter Christian<sup>1</sup>

<sup>1</sup> Institut für Geologie, Universität Bern, Baltzerstrasse 1+3, CH-3012 Bern  
(akcar@geo.unibe.ch)

<sup>2</sup> Labor für Ionenstrahlphysik (LIP), ETH Zürich, Schafmattstrasse 20, CH-8093 Zürich

<sup>3</sup> Geologische Beratungen Schenker Korner + Partner GmbH, Büttenehalde 42, CH-6006 Luzern

The northern Alpine foreland was covered by the Piedmont glaciers for the last time during the Last Glacial Maximum (LGM; Bini et al., 2009). Among these lobes, the Valais Glacier left the Rhone Valley and extended across the Alpine Foreland to the Jura Mountains. This mountain belt obstructed the northward extension of the Piedmont glacier and the glacier was split into two lobes. One lobe flowed to the southwest and joined to the Arve glacier, which extended ca. 20 km to the east of Lyon. Another lobe was diverted towards northeast and terminated at its maximum ca. 10 km east of Solothurn (Figure 1; Ivy-Ochs et al. 2004; Graf, 2008; Bini et al. 2009). The advance of the Valais Glacier onto the foreland occurred after 30 cal yr BP (Schlüchter, 2004) and it reached its maximum position at around 22 ka. The timing of this maximum is constrained <sup>10</sup>Be exposure ages from erratic boulders in Steinhof, Möschberg and the Jura Mountains (Figure 1; Ivy-Ochs et al. 2004; Graf, 2008; Akçar et al., 2011). Although the advance of the Alpine glaciers has been reconstructed within a relatively detailed chronological framework, reconstructions of their demise have been rather vague mainly because of poor age constraints.

In this study, we complement the existing chronological dataset with new ages inferred from a depth profile at Finsterhennen where we analyzed depth-dependent variations of cosmogenic <sup>36</sup>Cl concentration for the LGM basal till of the Valais glacier (Figure 1). We use the concentration pattern to: (1) test the suitability of cosmogenic <sup>36</sup>Cl for age assessments; and to (2) improve the chronology of the ice retreat. Finally, we calculated a model age for its deposition. We also found a piece of wood at the bottom of this till and dated it with radiocarbon. Furthermore, we dated the exposure of three erratic boulders close to the left lateral ice margin in Martinsflue with cosmogenic <sup>10</sup>Be (Figure 1).

Our results indicate that the Valais glacier reached Finsterhennen after 29 cal kyr BP. Erratic boulders from the left lateral position yielded an age of ca. 22 ka, which is consistent with the existing exposure ages. Our model age from the cosmogenic <sup>36</sup>Cl depth-profile indicate that at around 18 ka the margin of the Valais glacier was still located to the northeast of Finsterhennen. Furthermore, because the earliest non-glacial deposits, which were encountered at the archeological site Rouges Terres at the border of Lake Neuchâtel ca. 15 km to the southwest of Finsterhennen, were dated to ca. 16 kyr cal BP (Hajdas et al., 2004), the demise of the Valais glacier in the foreland occurred within less than 2 ka, which is shorter than previously thought. Finally, a practical implication of this study is that ages ranging up to hundreds of thousands of years can be determined for the top-most layers (e.g. terraces) simply by measuring cosmogenic <sup>36</sup>Cl depth-profiles in cores or trenches of 2-4 m depth, independent of lithological composition of the sediment and sample size.

## REFERENCES

- Akçar, N., Ivy-Ochs, S., Kubik, P.W., Schlüchter, C., 2011. Post-depositional impacts on 'Findlinge' (erratic boulders) and their implications for surface-exposure dating. *Swiss Journal of Geosciences* 104, 445-453.
- Bini, A., Buonchristiani, J.-F., Couterand, S., Ellwanger, D., Felber, M., Florineth, D., Graf, H.R., Keller, O., Kelly, M., Schlüchter, C., Schöneich, P., 2009. Die Schweiz während des letzteiszeitlichen Maximums (LGM) 1:500 000. In: Burkhalter, R. (Ed.). Federal Office of Topography, swisstopo, CH-3084 Wabern, Bern.
- Graf, A., 2008. Surface exposure dating of LGM and pre-LGM Erratic Boulders: A comparison of paleoclimate records from both hemispheres. PhD dissertation, Institute of Geological Sciences, University of Bern, Bern, Switzerland, p. 215.
- Ivy-Ochs, S., Schafer, J., Kubik, P.W., Synal, H.A., Schlüchter, C., 2004. Timing of deglaciation on the northern Alpine foreland (Switzerland). *Eclogae Geologicae Helveticae* 97, 47-55.
- Hajdas I, Bonani G, Hadorn P, Thew N, Coope GR, and Lemdahl G. 2004. Radiocarbon and absolute chronology of the Late-Glacial record from Hauterive/Rouges-Terres, Lake Neuchatel (CH). *Nuclear Instruments and Methods in Physics Research Section B: Beam Interactions with Materials and Atoms* 223-224: 308-312.
- Schlüchter, C., 2004. The Swiss glacial record - a schematic summary, In: Ehlers, J., Gibbard, P.L. (Eds.), *Quaternary Glaciations - Extent and Chronology. Part I: Europe*. Elsevier, Amsterdam, pp. 413-418.

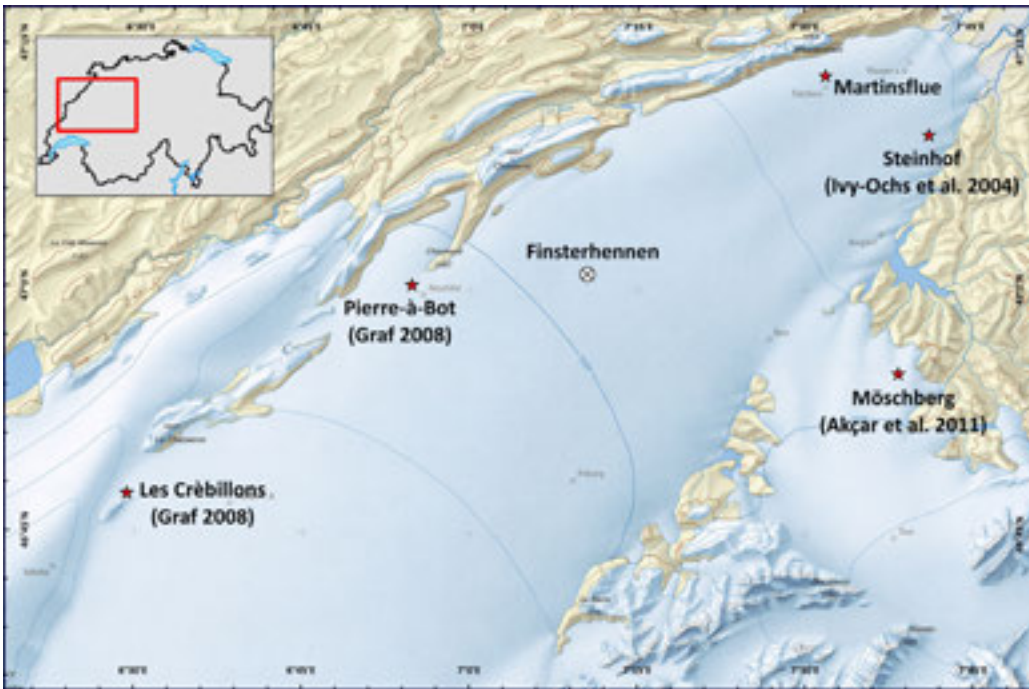


Figure 1. The LGM Valais Glacier and study sites (after Bini et al., 2009). Red stars indicate the locations of exposure dated erratic boulders, while crossed-circle show the gravel pit at Finsterhennen.

## 20.2

## Scanning reflectance spectroscopy (380-730 nm) for Paleo-environmental and climatic changes assessment

Amann Benjamin<sup>1</sup>, Lobsiger Simon<sup>2</sup>, Tylmann Wojciech<sup>3</sup> & Grosjean Martin<sup>1</sup>

<sup>1</sup>Institute of Geography and Oeschger Center for Climate Change Research, University of Bern, Switzerland (Benjamin.amanni@unibe.ch)

<sup>2</sup>Department of Chemistry, University of Virginia, Virginia

<sup>3</sup>Institute of Geography, University of Gdansk, Poland

High resolution quantitative reconstructions of climate variables for the last 2,000 years are recognized as one of the primary targets for current climate research (PAGES 2k 2013). Paleodata from natural paleoclimatic archives are one of the few means to obtain this information beyond the instrumental period.

In this context, varved (laminated) lake sediments are valuable paleoclimatic archives due to their potential to preserve past climate over long periods of time at very high resolution (annual) and with good chronological precision.

However, one of the fundamental methodological obstacles is that most of the analytical techniques for proxy data acquisition are very time consuming and expensive. This limits the number of data points generated and, in turn, restricts the temporal resolution and lengths of paleoclimate records (Ojala et al. 2012).

To avoid this problem, we present here the potential of scanning visible reflectance spectroscopy (VIS-RS, 380-730nm spectral range) using the portable device “Spectrolino” on biogeochemical varves. This tool provides a rapid, non-destructive high-resolution technique for data acquisition with direct measurement on the fresh sediment core surfaces.

We show that VIS-RS data may be used for relating primary productivity in biogeochemical lake sediments, thus providing a strategy for rapid exploratory assessments of paleoenvironmental changes.

Ideal sediments for this purpose were found in Lake Żabińskie (Masurian Lake District, NE Poland), a dimictic, 44-meter deep lake which is ice-covered from January to March (Tylmann et al. 2006). It exhibits biogeochemical varves with a high content of organic matter from different sources (terrestrial, aquatic plants, algae and bacteria), a simple inorganic composition (predominantly summer-precipitated autigenic calcite) and high annual sedimentation rates (5-8mm). We retrieved and analyzed a short sediment core (50-cm long) that covers the last 80 years. Pigments were extracted following standard protocols (Reuss et al. 2010) with freeze drying and extraction in acetone, followed by analysis of pigments by High Performance Liquid Chromatography (HPLC). Biogenic silica (BiSi) as well as loss on ignition and Carbon-Nitrogen-Sulfur elemental analyses were also analysed to provide additional information.

The combination of proxies first highlights a recent eutrophication of the Polish lake (Fig.1) detected notably by depth-constrained cluster analysis.

After deriving a series of spectral indices, we calibrated VIS-RS data with composition and concentration of pigments in Żabińskie's sediments. The results (Fig.2) revealed that VIS-RS data best reflect concentrations of *Chlorophyll a* and its diagenetic products (*Pheophytin a* and *Pyro-pheophytin a*).

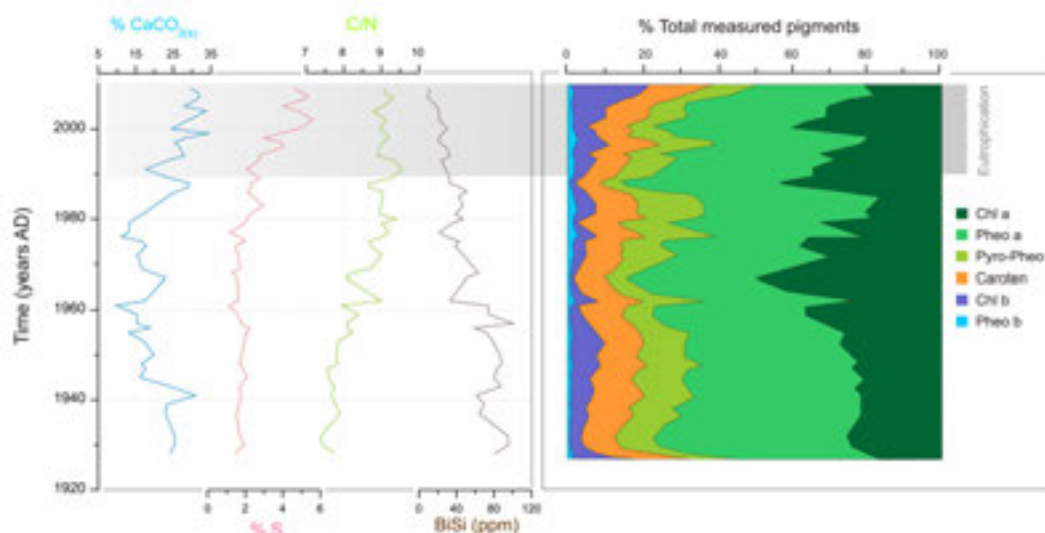


Figure 1. Time series of the proxy data. The recent (last 20 years) eutrophication of Lake Zabinskie is marked by the shaded grey area.

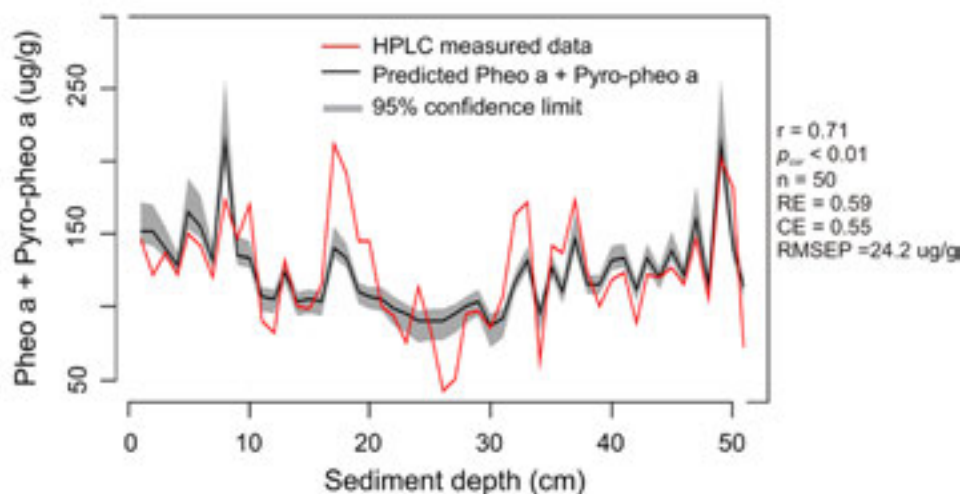


Figure 2. Proxy-proxy calibration. VIS-RS data is used as a predictor for *chlorophyll a* derivatives (*pheophytin a* and *Pyro-pheophytin a*).

## REFERENCES

- PAGES 2k Consortium Network 2013: Continental-scale temperature variability during the past two millennia. *Nature Geoscience*, 6, 339-346.
- Ojala A.E.K., Francus P., Zolitschka B., Besonen M., Lamoureux S. 2012: Characteristics of sedimentary varve chronologies: A review. *Quaternary Science Reviews*, 43, 45-60.
- Tylmann W., Wozniak P.P., Czarnecka K., Jazwiecka M. 2006: New sites with laminated lake sediments in north-eastern Poland: preliminary results of field survey. *Limnological Review*, 6, 283-288.
- Nina Reuss N., Leavitt P.R., Hall R.I., Bigler C., Hammarlund D. 2010: Development and application of sedimentary pigments for assessing effects of climatic and environmental changes on subarctic lakes in northern Sweden. *Journal of Paleolimnology*, 43, 149-169.

## 20.3

## The challenge of dating Swiss Deckenschotter with cosmogenic nuclides

Claude Anne<sup>1</sup>, Akçar Naki<sup>1</sup>, Ivy-Ochs Susan<sup>2</sup>, Graf Hans R.<sup>3</sup>, Kubik Peter W.<sup>2</sup>, Vockenhuber Christof<sup>2</sup>, Dehnert Andreas<sup>4</sup>, Rahn Meinert<sup>4</sup>, Rentzel Philip<sup>5</sup>, Pümpin Christine<sup>5</sup> and Schlüchter Christian<sup>1</sup>

<sup>1</sup> Institut für Geologie, Universität Bern, Baltzerstrasse 1+3, CH-3012 Bern (anne.claude@geo.unibe.ch)

<sup>2</sup> Labor f. Ionenstrahlphysik (LIP), ETH Zürich, Schafmattstrasse 20, CH-8093 Zürich

<sup>3</sup> Dorfstrasse 40, CH-8214 Gächlingen

<sup>4</sup> Eidgenössisches Nuklearsicherheitsinspektorat ENSI, Industriestrasse 19, CH-5200 Brugg

<sup>5</sup> Institut für Prähistorische und Naturwissenschaftliche Archäologie IPNA, Spalenring 145, CH-4055 Basel

Deckenschotter (cover gravels) are Quaternary sediments, which cover Tertiary Molasse or Mesozoic bedrock and are located beyond the limit of the Last Glacial Maximum. The Deckenschotter are a succession of proximal glaciofluvial gravels of the Northern Alpine Foreland, showing locally an intercalation with till and overbank deposits from (paleo-) valleys (Graf 1993). These deposits, which can be differentiated by their distinct topographical position, are divided into two main geomorphic units: Höhere (Higher) and Tiefere (Lower) Deckenschotter. Even though the Höhere Deckenschotter occupies a topographically higher position, it is older than the Tiefere Deckenschotter as the two are separated from each other by a phase of incision. Both Höhere and Tiefere Deckenschotter bear evidence of at least four glacial advances that reached the Alpine foreland and are, therefore, complex lithostratigraphic sequences.

The chronology of the Deckenschotter is poorly constrained. In the Höhere Deckenschotter at the Irchel site, mammalian faunal assemblages (MN17) were found which place the Deckenschotter between 2.5 and 1.8 Ma (Bolliger et al. 1996). This is the only age available until this study. They are therefore the oldest Quaternary units in the northern Swiss Alpine foreland known so far. Reconstruction of the chronology of these glaciofluvial units will provide fundamental information about the onset of Quaternary glaciation in the Alps as well as about the timing and magnitude of incision on the foreland.

In this study, we collected 54 samples from three sites: Pratteln (BL), Stadlerberg (ZH) and Irchel (ZH) for depth-profile dating with cosmogenic <sup>10</sup>Be and/or <sup>36</sup>Cl and for isochron-burial dating with <sup>10</sup>Be and <sup>26</sup>Al (Figure 1). Depth-profile dating uses the fact that cosmogenic nuclide build-up diminishes with depth following the known physical principles, while isochron-burial dating is based on the decay and on different pre-burial and same post-burial histories of the quartz clasts stemming from the same time-line. In addition to the cosmogenic nuclide dating, we are also determining the lithological composition of the Deckenschotter. We are doing detailed lithostratigraphy of several sites by examining the petrography of the pebbles.

## REFERENCES

- Bolliger, T., Fejar, O., Graf, H.R., Kälin, D. 1996. Vorläufige Mitteilung über Funde von pliozänen Kleinsäugern aus den höheren Deckenschottern des Irchels (Kt. Zürich). *Eclogae Geologicae Helveticae*, 89/3, 1043-1048.
- Bini, A., Buoncristiani, J.-F., Couterrand, S., Ellwanger, D., Fleber, M., Florienth, D., Graf, H.R., Keller, O., Kelly, M., Schlüchter, C., Schoeneich, P. 2009. Die Schweiz während des letzteiszeitlichen Maximums (LGM), 1:500'000. Bundesamt für Landestopographie, swisstopo, Wabern.
- Graf, H.R. 1993. Die Deckenschotter der zentralen Nordschweiz. Dissertation, ETH Zürich, 187 pp.

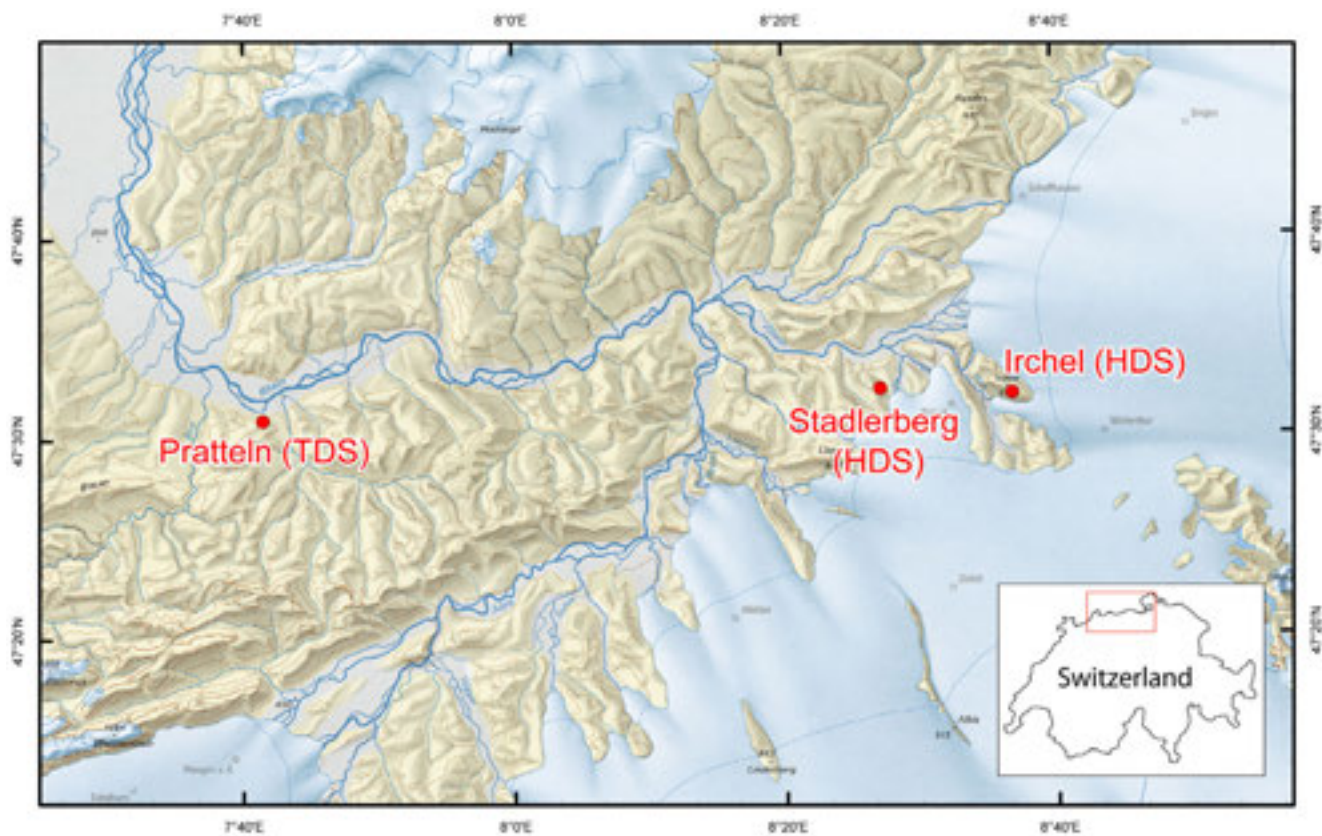


Figure 1. Location of the Prätteln, Stadlerberg and Irchel study sites in the map showing the extent of Last Glacial Maximum (Bini et al. 2009).

## 20.4

### Worldwide acceleration of mountain erosion under a cooling climate

Frédéric Herman<sup>1,2</sup>, Diane Seward<sup>3</sup>, Pierre G. Valla<sup>1,2</sup>, Andrew Carter<sup>4</sup>, Barry Kohn<sup>5</sup>, Sean D. Willett<sup>2</sup> & Todd A. Ehlers<sup>6</sup>

<sup>1</sup> *Institute of Earth Sciences, University of Lausanne, Switzerland*

<sup>2</sup> *Department of Earth Sciences, Swiss Federal Institute of Technology, Zürich, Switzerland*

<sup>3</sup> *School of Geography, Environment and Earth Sciences, Victoria University of Wellington, New Zealand*

<sup>4</sup> *Department of Earth and Planetary Science, Birbeck University of London, United Kingdom*

<sup>5</sup> *School of Earth Sciences, University of Melbourne, Australia*

<sup>6</sup> *Department of Geosciences, University of Tübingen, Germany*

Climate influences the erosion processes acting at the Earth surface. However, the impact of Late Cenozoic cooling, including the onset of Plio-Pleistocene Northern Hemisphere glaciation (~2-3 Ma), on global erosion rates remains elusive. The uncertainty mainly arises from a lack of consensus on the use of the sedimentary record as a proxy for erosion<sup>3,4</sup> and the difficulty of isolating the respective contributions of tectonics and climate to erosion. Here we show that mountain erosion rates have increased since ca. 6 Ma and most rapidly since ca. 2 Ma. To quantify erosion for the source areas that ultimately produce the sediment record at a Myr timescale, we have compiled about 18,000 bedrock thermochronometric data from around the world and use a formal inversion procedure to estimate temporal and spatial variations in erosion rates. The observed increase of erosion rates is expressed at all latitudes, but is most pronounced in glaciated mountain ranges, indicating that glacial processes played a significant role. Because mountains represent a significant fraction of the global production of sediments, our results imply an increase of sediment flux at a global scale that tightly coincides with enhanced cooling during the Late Plio-Pleistocene. These findings have important implications for potential feedbacks between global climate and erosion.

## 20.5

## Mid to late Holocene environmental change in the Bolivian Amazon reconstructed from paleosols and archaeological sites.

Umberto Lombardo<sup>1</sup><sup>1</sup> Geographisches Institut, Universität Bern, Hallerstrasse 12, CH-3012 Bern (lombardo@giub.unibe.ch)

The Llanos de Moxos (LM), in the Bolivian lowlands, is a seasonally flooded savannah (Mayle et al. 2007). The recent discovery of the oldest archaeological sites in the region shows that the LM has been inhabited since the beginning of the Holocene (Lombardo et al. 2013). These sites have long remained unnoticed because they were buried by fluvial sediments, together with several paleo surfaces, mostly paleosols, in the southern part of the LM. Linking together paleo-ecological reconstructions and archaeology, this research hopes to shed new light on the large scale environmental changes that took place in south-western Amazonia during the Holocene, the nature of human-environment interactions at the time and the potential value of these archaeological sites as paleo-environmental proxies.

Despite their similar aspect, early Holocene archaeological sites are often located in very different geomorphological and stratigraphic settings.

Preliminary results of geo-archaeological research on these sites in south-eastern LM will be presented, together with new stratigraphic data from 3 outcrops and 10 cores taken along a 230 km transect crossing the south-western LM.

The data from the archaeological sites suggests that the early Holocene landscape, in which the first hunter-gatherers settled, was significantly different from what we see today. One of the sites, associated with an early to mid-Holocene paleosol, has been almost totally buried by fluvial sediments and only its topmost 30-40 cm has remained above the alluvium that forms the current savannah (Fig. 1). The second site, currently outcropping in the middle of a flat swamp, was actually located on a sandy fluvial levee and subsequently flooded and partially buried by peat-like sediments. There is evidence suggesting that during the mid to late Holocene, the Río Grande entered a highly active avulsive phase which led to the deposition of a sedimentary lobe which covered the south-eastern LM (Lombardo et al. 2012). However, the causes behind the mid to late Holocene activation of Río Grande are still unclear. The 230 km long stratigraphic transect shows an extensive presence of buried organic horizons, probably paleosols, in the south-western LM, suggesting that the avulsive phase of the Río Grande was not an isolated event but part of a wider change in environmental conditions that took place at a regional scale. The activation of the fluvial network during this period reshaped the whole southern LM, covered most of the early Holocene landscapes and archaeological sites and created a new landscape which remained stable at least for the past 2500 years.

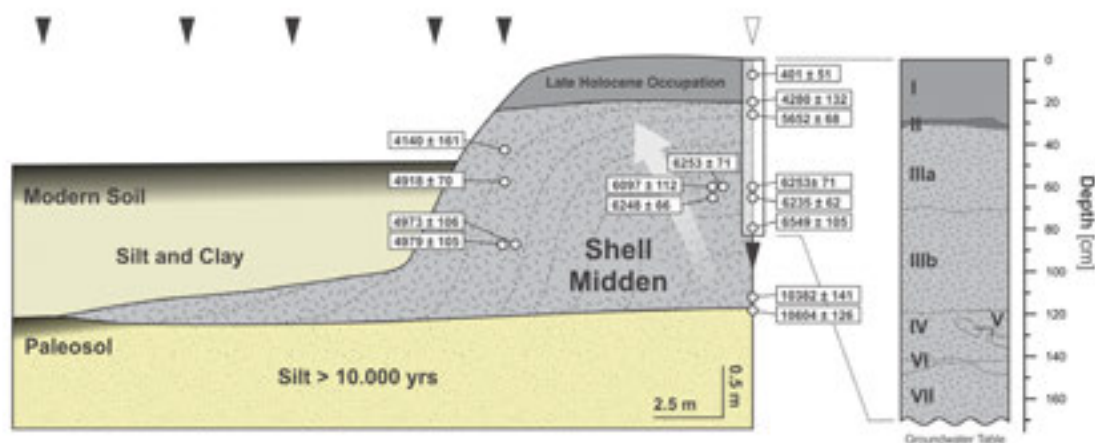


Figure 1. Cross-section transect of the shell midden SM1. Dashed lines and grey arrow highlight the onion-like growth of the midden reflected in the <sup>14</sup>C dates. The black triangles above mark the coring locations and the white triangle the excavation site.

## REFERENCES

- Lombardo, U., Szabo, K., Capriles, J.M., May, J.-H., Amelung, W., Hutterer, R., Lehndorff, E., Plotzki, A., Veit, H., 2013. Early and Middle Holocene Hunter-Gatherer Occupations in Western Amazonia: The Hidden Shell Middens. *PLoS ONE*, 8(8), e72746.
- Lombardo, U., May, J.-H., Veit, H., 2012. Mid- to late-Holocene fluvial activity behind pre-Columbian social complexity in the southwestern Amazon basin. *The Holocene*, 22(9), 1035-1045.
- Mayle, F.E., Langstroth, R.P., Fisher, R.A., Meir, P., 2007. Long-term forest-savannah dynamics in the Bolivian Amazon: implications for conservation. *Philosophical Transactions of the Royal Society B: Biological Sciences*, 362(1478), 291-307.

## 20.6

### A speleothem record of the Last Glacial Maximum from the western Swiss Alps

Luetscher Marc<sup>1</sup>, Boch Ronny<sup>1</sup>, Cheng Hai<sup>2</sup>, Edwards R. Lawrence<sup>2</sup>, Sodemann Harald<sup>3</sup>, Spötl Christoph<sup>1</sup>

<sup>1</sup> Institute of Geology, University of Innsbruck, Innrain 52, A-6020 Innsbruck (marc.luetscher@uibk.ac.at)

<sup>2</sup> Geology and Geophysics, University of Minnesota, Minneapolis, USA

<sup>3</sup> Institute for Atmospheric and Climate Science, ETH, Zurich, Switzerland

Several lines of evidence from alpine cave environments suggest that karstification is not solely restricted to warm interglacial periods. Indeed, dissolution of carbonate rock may also arise without the intervention of biogenic (soil-derived) CO<sub>2</sub>, e.g. by the oxidation of pyrite present in the aquifer hostrock (Atkinson, 1983). Providing there is sufficient water available speleothem deposition may therefore also occur under temperate glacier cover (Spötl and Mangini, 2007; Luetscher et al. 2011). Here we present a speleothem record from the Sieben-Hengste cave system (Swiss Alps) covering the Last Glacial Maximum (LGM), the first of its kind from Central Europe.

Two coeval stalagmites were sampled at approximately 160 m below the modern ground surface (i.e. 1540 m a.s.l.), in an alcove at the base of a vadose shaft. 49 high-precision uranium-series ages reveal a continuous deposition between 30 and 14.7 ka b2k. Both stalagmite time series correlate fairly well in the overlapping segments and, therefore, likely responded to a same hydrological forcing. While the δ<sup>13</sup>C stays remarkably constant at +4.4±0.4 ‰ supporting the absence of biogenic CO<sub>2</sub> contribution, δ<sup>18</sup>O values vary between -10.5 and -13.5 ‰ and show a remarkable similarity to other Northern Hemisphere isotope records, both on orbital and millennial timescales. However, in marked contrast e.g. to NGRIP, the Sieben-Hengste record shows a δ<sup>18</sup>O minimum centred on 25.3 ka synchronous with the maximum Alpine glacier advance. We propose that the first-order variance in our δ<sup>18</sup>O values primarily records changes in the trajectories of the storm tracks reaching the Swiss Alps which is consistent with the build-up of large ice domes south of the present weather divide (Florineth and Schlüchter, 2000). This hypothesis is currently being tested by modelling oxygen isotopes along different trajectories.

#### REFERENCES

- Atkinson T.C., 1983: Growth mechanisms of speleothems in Castleguard Cave, Columbia Icefields, Alberta, Canada. *Arctic Alpine Res.*, 15, 523-536.
- Florineth D., Schlüchter C., 2000. Alpine evidence for atmospheric circulation patterns in Europe during the Last Glacial Maximum. *Quaternary Research*, 54, 295-308.
- Luetscher M., Hoffmann D., Frisia S., Spötl C., 2011: Holocene glacier history from alpine speleothems, Milchbach cave, Switzerland. *Earth and Planetary Science Letters*, 302, 95–106.
- Spötl C., Mangini A., 2007: Speleothems and paleoglaciers. *Earth and Planetary Science Letters*, 254, 323-331.

## 20.7

## Late Quaternary Glacial History in northeastern Anatolia

Reber Regina<sup>1</sup>, Tikhomirov Dmitry<sup>1</sup>, Akçar Naki<sup>1</sup>, Yesilyurt Serdar<sup>2</sup>, Yavuz Vural<sup>3</sup>, Kubik Peter<sup>4</sup>, Schlüchter Christian<sup>1</sup>

<sup>1</sup> Institute of Geological Sciences, University of Bern, Baltzerstrasse 1+3, CH-3012 Bern (rreber@geo.unibe.ch)

<sup>2</sup> Department of Geography, Çankırı Karatekin University, TR-18100, Çankiri

<sup>3</sup> Faculty of Mines, Istanbul Technical University, TR-80626 Maslak, Istanbul

<sup>4</sup> Laboratory of Ion Beam Physics, ETH Zürich, CH- 8093 Zürich

The reconstruction of paleoglaciers is a terrestrial climate approximation for cold and wet periods but also a sensitive archive for rapid warming. Then the rates of deglaciation can correspondingly be used in determining the loss of ice volume and this will help to better understand feedback mechanisms and rates of climate changes (e.g. Schlüchter 2004). Paleoglacier reconstructions in the circum-Black Sea area are incomplete, mainly due to the lack of absolute chronology. In this study, we mapped the glacial deposits in the Başyayla Valley in north eastern Anatolia in detail and reconstructed the chronology of glacier advances with surface exposure dating with cosmogenic nuclides (Figure 1).

The Başyayla Valley is a ca. 6 km long east-west oriented tributary valley in the northern side of the Eastern Black Sea Mountains. Based on the detailed mapping, three glacier advances, which are constrained with terminal moraines, were identified in the field. The inner and outer terminal moraines are geomorphologically well constrained, whereas the middle one is poorly preserved because the mountain village was built on this moraine. 40 samples from the glacially transported boulders and one from the bedrock outcrop on the crest line of the north-western valley flank were sampled for cosmogenic <sup>10</sup>Be and <sup>26</sup>Al analysis.

Our results show that the Başyayla glacier advanced ca. 40 ka down to an altitude of 2350 m a.s.l., but it did not reach the main valley system. The next advance extended down to an altitude of 2440 m a.s.l. and its timing is attributed to the Early Last Glacial Maximum (LGM) based on the exposure ages of the boulders from the left lateral moraine. The last advance of the Başyayla glacier was down to 2480 m a.s.l. and at ca. 22 ka during the global LGM (Shakun and Carlson 2010). In the upper part of the valley, exposure ages from boulders on a retreat position at an altitude of ca. 3050 m a.s.l. indicate that the valley was ice-free since around 17 ka. Hence, the terminus of the glacier must have been restricted to the cirque in the upper most part of the valley during the Lateglacial.

Our study presents the first evidence for a pre-LGM advance in the Anatolian mountains, which is more extensive than the LGM advance. Pre-LGM glaciations are still to be explored in Anatolia. The global-LGM advance of the Başyayla paleoglacier ca. 22 ka and its retreat at around 17 ka is comparable with the paleoglacier reconstructions in the neighbouring Kavron and the Verçenik Valley systems (Akçar et al. 2007; 2008), as well as the other Anatolian mountains (Zahno et al. 2009). Finally, glacier advances in the Başyayla Valley indicate similar climatic conditions between around 40 ka and 22 ka, which resulted in the ice build-up and oscillations, whereas almost the deglaciation of the valley at around 17 ka may imply rapid change in these conditions.

## REFERENCES

- Akçar, N., Yavuz, V., Ivy-Ochs, S., Kubik, P.W., Vardar, M., Schlüchter, C., 2007. Paleoglacial records from Kavron Valley, NE Turkey: Field and cosmogenic exposure dating evidence. *Quaternary International* 164-65, 170-183.
- Akçar, N., Yavuz, V., Ivy-Ochs, S., Kubik, P.W., Vardar, M., Schlüchter, C., 2008. A Case for a down wasting Mountain Glacier during the Termination-I, Verçenik Valley, NE Turkey. *Journal of Quaternary Sciences* 23, 273-285.
- Reber R., Akçar N., Tikhomirov D., Yesilyurt S., Yavuz V., Kubik P.W., and Schlüchter C.. (in prep.) re Global LGM Glaciation in the eastern Mediterranean: Field evidence from north eastern Turkey. *Quaternary Science Review*.
- Schlüchter, C., 2004. The Swiss glacial record - a schematic summary, In: Ehlers, J., Gibbard, P.L. (Eds.), *Quaternary Glaciations - Extent and Chronology. Part I: Europe*. Elsevier, Amsterdam, pp. 413-418.
- Shakun, J. D., & Carlson, A. E., 2010. A global perspective on Last Glacial Maximum to Holocene climate change. *Quaternary Science Reviews* 29, 1801-1816.
- Zahno, C., Akçar, N., Yavuz, V., Kubik, P.W., Schlüchter, C., 2009. Surface exposure dating of Late Pleistocene glaciations at the Dedegöl Mountains (Lake Beyşehir, SW Turkey). *Journal of Quaternary Science* 24, 1016-1028.



Figure 1. Location map of studied valley systems in north eastern Anatolia (Reber et al. *in prep.*).

## 20.8

# An insight into the morphology of pre-Columbian raised fields in different landscapes in the Llanos de Moxos, Bolivia

Rodrigues Leonor<sup>1</sup>, Lombardo Umberto <sup>1</sup>, Veit Heinz<sup>1</sup>

<sup>1</sup> *Geographisches Institut, University of Bern, Hallerstrasse 12, CH-3012 Bern (leonor.rodrigues@giub.unibe.ch)*

Since the beginning of the 1960s, research in the Amazon has revealed that in pre-Columbian times, landscapes that were regarded as hostile living environments were nevertheless altered and settled in several ways. In South-eastern Amazonia, one of the most impressive way pre-Columbians altered the landscape was through the construction of raised fields.

Pre-Columbian raised fields are earth platforms of differing shape and dimension that are elevated above the landscapes natural surface. The Llanos de Moxos (LM), situated in the Bolivian Lowlands is one of the areas with the highest density of raised fields.

The LM itself hosts an enormous variety of distinct landscapes and soils where numerous types of raised fields have been described (Denevan 2002; Erickson 1995; Lombardo 2011; Walker 2004)

Theories about raised fields have given rise to interesting debates on the function of these cultivation systems. The opinion is greatly divided in matters concerning their productivity and management. Some have proposed that raised fields are a very productive cultivation method, able to generate high yields without the need of fallow periods (Erickson 2006) others have suggested that the construction of raised fields have mostly served as a prevention method for protecting their harvests against severe flood events (Lombardo 2011).

In spite of the high interest in raised field agriculture, very few field-based investigations have been performed. As a result, there is still little explanation concerning their construction, management or for what time frame they were in use.

We studied five different sites with raised fields of the LM having in mind their specific landscape, soils and hydrology. Laboratory tests concerning fertility parameters were carried out in 2012 and suggest rather unfertile conditions for productive agriculture.

Recently, more detailed investigations have been performed on raised fields located in the vicinity of San Borja situated in the south-east of the Andes in the Beni department of Bolivia. It turned out that this site is of special interest because fields were built on different types of sediments ranging from clay to sand. For this study we have applied a virtual grid onto an area of 450x64m consisting of 90 rectangles (~16x20m) (see Fig 1). In each rectangle we carried out sampling for grain size every 20cm up to 100cm depth. The area could be divided into seven different land use types within or away from raised fields. To understand the construction history of the different raised fields, five trenches were excavated extending from the elevated part of the bed to the lowest point in the canal. For comparison three reference profiles outside raised fields were dug. Description and standard soil horizon/layer identification procedures were carried out followed by sampling every 10 cm for particle size distribution and standard soil lab analysis. Additionally samples for thin section preparation were taken.

The findings derived from the field description of the profiles seem to challenge the assumption that raised fields were managed through continuous transport of sediments from the canal to the field. By contrast, our results suggest that these raised fields were more likely built during single episodes as large construction events. Furthermore raised fields could have allowed the pre-Columbian population to extend the cultivation ground and also its time frame for example during the wet season when unraised land is flooded.

## REFERENCES

- Denevan, W.M., 2002. *Cultivated landscapes of native Amazonia and the Andes*, Oxford; New York: Oxford University Press.
- Erickson, C., 1995. *Archaeological methods for the study of ancient landscapes of the Llanos de Mojos in the Bolivian Amazon*. In: P. Stahl, (editors). *Archaeology in the lowland American tropics : current analytical methods and applications*. Cambridge; New York: Cambridge University Press, S. 66-95.
- Erickson, C., 2006. *El valor actual de los Camellones de cultivo precolombinos: Experiencias del Perú y Bolivia*. In *Agricultura ancestral. Camellones y albarradas: Contexto social, usos y retos del pasado y del presente*, edited by Francisco Valdez, pp. 315-339. Ediciones Abya-Yala, Quito.

Lombardo, U. et al., 2011. Raised fields in the Bolivian Amazonia: a prehistoric green revolution or a flood risk mitigation strategy? *Journal of Archaeological Science*, 38 (3), 502-512.

Walker, J., 2004. *Agricultural change in the Bolivian Amazon / Cambio agrícola en la Amazonia boliviana*, Pittsburgh: University of Pittsburgh Dept. of Anthropology.

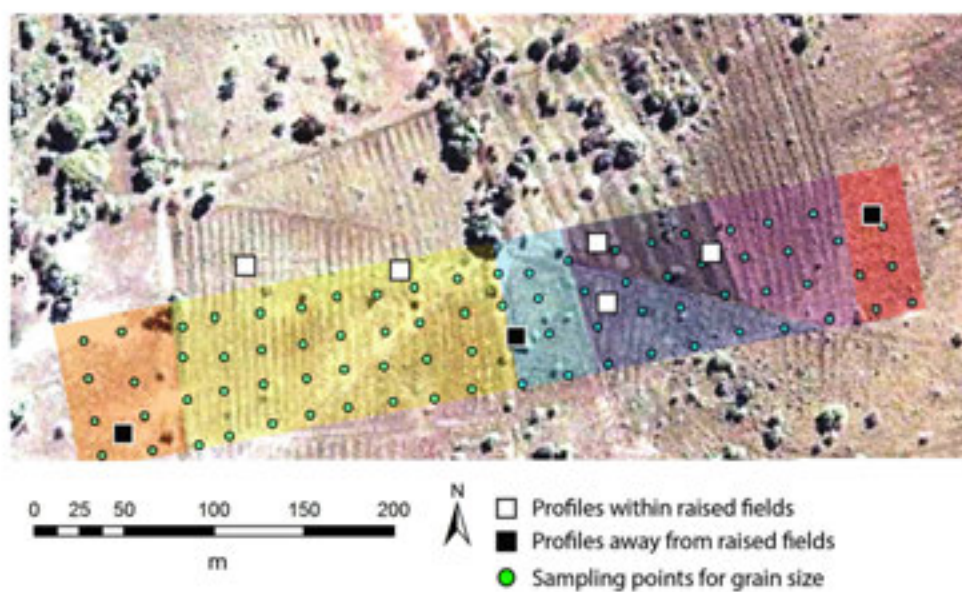


Figure 1. Land use-map with raised fields in San Borja, Bolivia. Each color represents a specific land use.

## 20.9

## Advanced model for limestone fault scarp dating and paleoearthquake history reconstruction

Tikhomirov Dmitry<sup>1</sup>, Akçar Naki<sup>1</sup>, Ivy-Ochs Susan<sup>2,3</sup> & Schlüchter Christan<sup>1</sup>

<sup>1</sup>Institut für Geologie, Universität Bern, Baltzerstrasse 1+3, 3012 Bern, Switzerland

<sup>2</sup>Labor für Ionenstrahlphysik, ETH Zürich

<sup>3</sup>Geographisches Institut, Uni Zürich

One of the most challenging applications of terrestrial cosmogenic nucleides is the reconstruction of paleoearthquake histories. In this method, <sup>36</sup>Cl accumulated by exposed footwall of normal fault scarp is used to date past seismic events and to estimate their magnitude. Time span of the method is about a few tens of kiloyears; precision is about 0.5 kiloyear. Modern earthquake chronologies are based on instrumental data and historical observations during the last 2500 years, therefore methods operative beyond this limit are essential for producing long-term earthquake models.

The fault scarp dating method shares the same general principles with surface exposure dating. In the simplest case, there is a footwall of infinite height and accumulated colluvium that covers the lower part of the footwall. During an earthquake footwall is moving upwards and exposing a new segment. Complex geometrical shielding and periodical displacements of footwall during active history of the fault scarp complicate interpretation of accumulated concentration profile. Hereupon, previous researches on fault scarp dating were supplied with special models and calculation codes (Schlagenhauf et al., 2010).

We present an advanced model for limestone fault scarp dating and paleoearthquake history reconstruction. The model is realized in practice as a MATLAB® code with user-friendly interface (Figure 1). The code uses state-of-the-art model of <sup>36</sup>Cl production and special model for fault scarp shielding factors calculation (Tikhomirov et al., 2013). Monte-Carlo method is finally applied to achieve best fit between measured and modeled concentration profiles, as well as to find ages of seismic events and displacements caused by them. Reanalysis of two fault scarp data sets (Schlagenhauf et al., 2010, Akçar et al., 2012) give comparison with previously published models and example of code application.

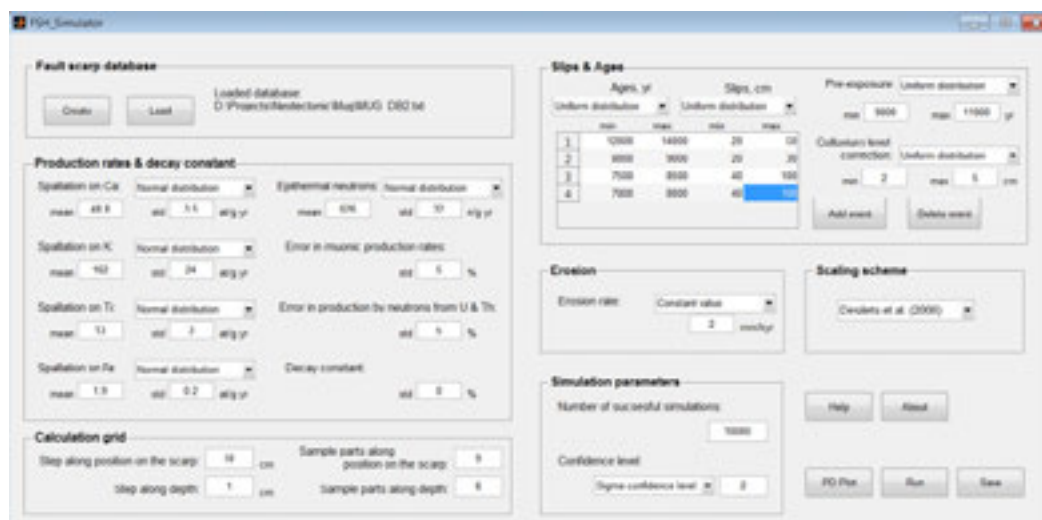


Figure 1. Screen shot of program interface

### REFERENCES

- Akçar N., Tikhomirov D., Özkaymak Ç., Alfimov V., Ivy-Ochs S., Sözbilir H., Uzel B., Schlüchter C., 2012. <sup>36</sup>Cl Exposure dating of paleoearthquakes in the Eastern Mediterranean: First results from Western Anatolian Extensional Province, Manisa Fault Zone, Turkey. *Geological Society of America Bulletin*, 124 (11-12), 1724–1735.
- Schlagenhauf A., Gaudemer Y., Benedetti L., Manighetti I., Palumbo L., Schimmelpfennig I., Finkel R., Pou K., 2010. Using in situ Chlorine-36 cosmogenic nuclide to recover past earthquake histories on limestone normal fault scarps: a reappraisal of methodology and interpretations. *Geophysical Journal International*, 182 (1), 36-72.
- Tikhomirov D., Akçar N., Ivy-Ochs S., Alfimov V., Schlüchter C., 2012. Calculation of shielding factors for production of cosmogenic nuclides in fault scarps. *Quaternary Geochronology*, (in press).

## 20.10

## Towards a 'true' age of LGM ice surface decay in Oberhaslital

Christian Wirsig<sup>1</sup>, Susan Ivy-Ochs<sup>1</sup>, Jerzy Zasadni<sup>2</sup>, Naki Akcar<sup>3</sup>, Marcus Christl<sup>1</sup> & Christian Schlüchter<sup>3</sup>

<sup>1</sup>Laboratory of Ion Beam Physics, ETH Zürich, Switzerland (wirsig@phys.ethz.ch)

<sup>2</sup>AGH University of Science and Technology, Krakow, Poland

<sup>3</sup>University of Bern, Bern, Switzerland

During the Last Glacial Maximum (LGM) the Alps were nearly completely covered by ice. In Switzerland, geomorphological mapping in the previous century allowed to reconstruct a system of ice domes located in the high Alps that fed enormous piedmont lobes extending far into the foreland (Florineth & Schlüchter, 1998). Concerning the understanding of the chronology of events, surface exposure ages of the end moraines of these piedmont lobes as well as radiocarbon ages of lake sediments indicate an ice free alpine foreland no later than 18-19 ka BP (e.g. Ivy-Ochs et al., 2004). In contrast, attempts to date the lowering of the ice surface so far yield maximum ages of only around 17 ka (e.g. Kelly et al., 2006). Here we will discuss possible explanations of this apparent discrepancy. In addition, we will present a model suitable to test our hypotheses at the specific case of our study site at Gelmersee in Oberhaslital.

Grimsel Pass, ice transfluence -> sensitive location

Ice cover – set of low altitude boulders -> model

Inheritance – Cl/Be ratio

'true age'? ice surface decay likely synchronous to retreat from foreland. But possibly non-erosive ice masses remain until lateglacial in flat high-altitude settings.

## REFERENCES

- Florineth, D. & Schlüchter, C. 1998: Reconstructing the Last Glacial Maximum (LGM) ice surface geometry and flowlines in the Central Swiss Alps. *Eclogae geologicae Helvetiae*, 9, 391-407.
- Ivy-Ochs, S., Schaefer, J., Kubik, P., Synal, H.-A. & Schlüchter, C. 2004: Timing of deglaciation on the northern Alpine foreland (Switzerland). *Eclogae Geologicae Helvetiae*, 97, 47-55.
- Kelly, M., Ivy-Ochs, S., Kubik, P., von Blanckenburg, F. & Schlüchter, C. 2006: Chronology of deglaciation based on 10Be dates of glacial erosional features in the Grimsel Pass region, central Swiss Alps. *Boreas*, 35, 634-643.

## 20.11

## Dating glacial deposits in the western Swiss lowlands using cosmogenic $^{10}\text{Be}$

Wüthrich Lorenz <sup>1</sup>, Zech Roland<sup>1</sup>, Haghipour Negar<sup>1</sup>, Gnägi Christian<sup>2</sup>, Christl Marcus<sup>3</sup>, Ivy-Ochs Susan<sup>3</sup>

<sup>1</sup> Geological Institute, Swiss Federal Institute of Technology Zürich, Sonneggstrasse 5, CH-8092 Zürich (lorenz@student.ethz.ch)

<sup>2</sup> Weg>punkt, Länggasse 7, CH- 3360 Herzogenbuchsee

<sup>3</sup> Laboratory of Ion Beam Physics, Swiss Federal Institute of Technology Zürich, Schafmattstrasse 20, CH-8093 Zürich

During the Pleistocene, glaciers advanced repeatedly from the Alps into the Swiss Molasse basin. The exact extent and timing are still under debate, even for the last glacial advances. Decalcification depths, for example, increase from west to east in the western Swiss lowlands and have been interpreted to indicate that the Valais (Rhône) glacier might have been most extensive not synchronous with the global Last Glacial Maximum (LGM) at 20 ka, but early during the last glacial cycle (Bitterli et al. 2011).

In an attempt to provide more quantitative age control, we applied  $^{10}\text{Be}$  depth profile dating (Hidy et al. 2011) on moraines at two locations. First, a gravel pit near Niederbuchsiten, which presumably lies outside the last glacial ice extent (Bitterli et al. 2011). The second location, Steinhof, is located south of Herzogenbuchsee. Here, two boulders have been dated to the global LGM (Ivy-Ochs et al. 2004), but the decalcification depth is unexpectedly high with 3.9 m.

The results show that depth profile dating using  $^{10}\text{Be}$  at our sites can only be applied successfully, when erosion is sufficiently constrained independently. Assuming no erosion would yield unrealistic, too young ages of 12.2 (+2.4/- 2.0) and 10.6 (+1.4/- 1.3) for Niederbuchsiten and Steinhof, respectively. A recent, anthropogenically induced loss of the uppermost 40 cm of sediments would yield ages of 19.4 (+ 5.3 /- 1.2) ka for Steinhof and 23.5 (+ 1.0/- 3.4) ka for Niederbuchsiten. Several meters of sediment must have been eroded to obtain a penultimate (marine isotope stage 6) age for Niederbuchsiten.

We conclude that deposition of the tills at both our research locations was likely during the global LGM (marine isotope stage 2) and that the Rhône Glacier might have been more extensive at that time than hitherto assumed. Further research is necessary to independently constrain erosion and to evaluate, to which degree decalcification depths are influenced by different original carbonate contents in the till.

### REFERENCES

- Bitterli, T., Jordi, H., Gerber, M., Gnaegi, C. & Graf, H.R. 2011: Blatt 1108: Murgenthal. Geologischer Atlas der Schweiz 1:25'000. Schweizerische Geologische Kommission, Bern.
- Hidy, A.J., Gosse, J.C., Pederson, J.L., Mattern, J.P. & Finkel, R.C. 2010: "A geologically constrained Monte Carlo approach to modeling exposure ages from profiles of cosmogenic nuclides: An example from Lees Ferry, Arizona". *Geochemistry Geophysics Geosystems*, 11.
- Ivy-Ochs, S., Schäfer, J., Kubik, P.W., Synal, H.A. & Schlüchter, C. 2004: Timing of deglaciation on the northern Alpine foreland". *Eclogae geologicae Helveticae*, 97, 47-55.

## P 20.1

## Sedimentological and paleoenvironmental study of quaternary alluvial formations Zeïet Oued, Ain Zerga W Tébessa. N-E Algeria.

Belfar Dalila <sup>1</sup>, Deguaechia Amor <sup>2</sup>, Djerrab Abdel Razzak <sup>3</sup>, Bouhleb Saleh <sup>4</sup>, &Fehdi Chemci Edin <sup>5</sup>.

<sup>1</sup> Department of earth science and the universe, University of Tébessa, Route de Constantine 12002 (dalilabelfar@yahoo.fr)

<sup>2</sup> Department of earth science and the universe, University of Tébessa, Route de Constantine 12002 (dalilabelfar@yahoo.fr)

<sup>3</sup> Department of history and archeology, University of Guelma, (djerrab@yahoo.fr)

<sup>4</sup> Department of Earth Sciences, University of El Mannar, (salah.bouhleb@fst.rnu.tn)

<sup>5</sup> Department of earth science and the universe, University of Tébessa, Route de Constantine 12002 (fehdi@yahoo.fr).

The Quaternary deposits in Tébessa regions (Algeria) have been studied extensively. This study of these deposits especially on river terraces. The objective of this work is the study of processes and environmental change through their recent sedimentary records in the fluvial terrace located along the Zeïet Valley that is localized in Ain Zerga catchment's area. We preferred methods to obtain information on the depositional environment and the chronology of events such as sedimentological analysis (grain size analysis and determination of sedimentological parameters, morphoscopy, exoscopy, calcimetry, mineralogical (X-ray diffraction for clay fraction). The exoscopy helped differentiate the depositional history of quartz (weathering, transport continental water, ice and sometimes back) The tests carried out using a scanning electron microscope on the surfaces of these grains have led to the identification of various figures that can be connected either with the original crystal lattice of quartz or with actions specific corrosive medium of alteration. the study of clay minerals in sediments allowed us to conclude for both units, the origin of sediments of smectite, Kaolinite and Illite must be sought within the catchment area of this study. in conclusion, we proposed a reconstruction of environmental conditions during the formation of the terrace.

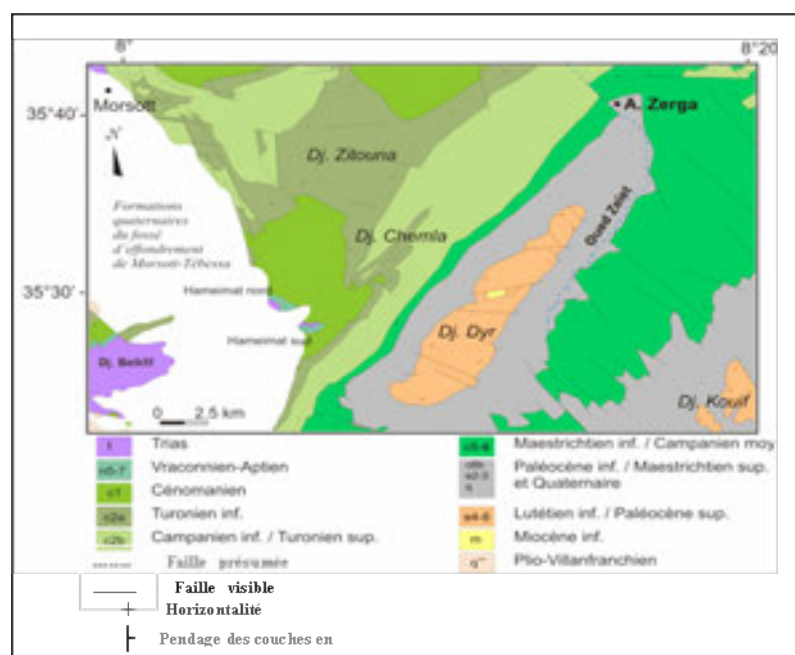


Figure 1. geological and Structural diagram of the study area (from the geological map of Morsot scale 1:50,000).

### REFERENCES

- Djerrab. A., 2001 : Etude des propriétés magnétiques du remplissage de sites préhistoriques. Contribution à l'étude stratigraphique de leurs dépôts et à leur évolution géochimique post-dépositionnelle », Thèse de Doctorat de l'Université de Perpignan, 667.
- Damnati. B., Maatouk. M., Meco. J. et Petit-Maire. N., (2005) : Sédimentologie et minéralogie de la séquence Sédimentaire « mala » située a Lanzarote (iles canaries, Espagne) : les significations paléoclimatiques. pp179-185.
- Le Ribault. L., (1977) : l'exoscopy des quartz Edition Masson. 141 p
- Leneuf. N., (1972) : Aspects microscopiques de la surface de grains de quartz Du continental terminal de cote d'ivoire. pp. 53-65.
- Millot G., 1964 : géologie des argiles .Edition Masson, Paris, 1964,499p.

## P 20.2

# Multiphase depositional and erosional history recorded in the infill of the glacially overdeepened Lower Glatt valley, Northern Switzerland

M. W. Buechi<sup>1</sup>, S. E. Lowick<sup>1</sup>, F. S. Anselmetti<sup>1</sup>

<sup>1</sup> *Institute of Geological Sciences & Oeschger Centre for Climate Change Research, University of Bern, Switzerland*

Glacially overdeepened valley fills are a direct record of glacier presence and absence in the Northern Alpine foreland for the Middle and Late Pleistocene. As such, they provide an important archive reflecting environmental processes during the Middle and Late Pleistocene. While the formation of these overdeepened valleys (tunnel valleys) by subglacial processes of warm based glaciations is undisputed (Cook & Swift 2012), the timing of erosional and subsequent infilling phases are poorly constrained. It is known that many of these unconsolidated valley fills contain a nested sedimentary architecture reflecting the multiphase erosion and deposition history (e.g. Preusser et al. 2010, Dehnert et al. 2012).

We are currently investigating the overdeepened valley fill of the Lower Glatt valley, Northern Switzerland, by integrating existing drilling and outcrop data with five recently drilled cores (65-190 m long) that are being investigated in detail. There is evidence for preservation of sediments from several glaciations, due to the shifting magnitude and focus of subglacial erosion. Our project aims to develop i) a model for sedimentary processes in glacial overdeepenings and ii) a chronology based on luminescence dating. Our contribution will present first results of the detailed sedimentary analysis and dating of glaciolacustrine sediments.

This project is a pilot-study in the context of the international drilling initiative “Drilling overdeepened Alpine valleys” (DOVE) that aims to drill overdeepened valleys all around the Alps involving all Alpine countries (ICDP proposal status). More information is available here:

[http://www.icdp-online.org/front\\_content.php?idcat=1739](http://www.icdp-online.org/front_content.php?idcat=1739)

## REFERENCES

- Cook, S. J. & Swift, D. A. 2012: Subglacial basins: Their origin and importance in glacial systems and landscapes, *Earth-Science Reviews*, 115, 332-372.
- Dehnert, A., Lowick, S. E., Preusser, F., Anselmetti, F. S., Drescher-Schneider, R., Graf, H. R., Heller, F., Horstmeyer, H., Kemna, H. A., Nowaczyk, N. R., Züger, A. & Furrer, H. 2012: Evolution of an overdeepened trough in the northern Alpine Foreland at Niederweningen, Switzerland. *Quaternary Science Reviews*, 34, 127-145.
- Preusser, F., Reitner, J. & Schlüchter, C. 2010: Distribution, geometry, age and origin of overdeepened valleys and basins in the Alps and their foreland. *Swiss Journal of Geosciences*, 103, 407-426.

## P 20.3

# Origin of unexpected tropical carbonate mounds (TCM) in northern Cameroon – Carbonate accumulation context: hypotheses and challenges.

Nathalie Diaz<sup>1</sup>, Fabienne Dietrich<sup>1</sup>, Guillaume Cailleau<sup>1</sup>, David Sebag<sup>2</sup>, Eric Verrecchia<sup>1</sup>

<sup>1</sup> Institute of Earth Sciences, University of Lausanne, Geopolis, CH-1015 Lausanne, Switzerland.

<sup>2</sup> UMR CNRS 6143, Université de Rouen, F-76821 Mont Saint Aignan Cedex and UMR CNRS/IRD 5569, Université de Montpellier 2, F-34095 Montpellier Cedex 5

Carbonate accumulations are observed in the area of Maroua (northern Cameroon). Their presence is unexpected as the catchment basin geology is strictly carbonate-free. At the landscape scale, accumulations have a metric mound shape when they are exhumed from the surrounding pediment red sediments. When they are still partially buried, they display a dark circle section on the ground. What could be the hypotheses to explain such carbonate accumulations?

During the Holocene, climatic conditions varied from wetter to drier conditions. It is assumed that carbonates could be deposited during a wetter period. Three hypotheses of carbonate production can be proposed (fig. 1).

First hypothesis refers to a “Vertisol context”. Vertisols are characterized by heavy clay content with high proportion of swelling clay (FAO, 2006). Their colour generally is dark and pH can be very alkaline, generally > 9. Carbonate nodules are commonly observed in Vertisols, particularly into those from northern Cameroon (Nguetnkam et al., 2008). At the landscape scale, Vertisols can display metric mound shapes known as “gilgai landscape” (Kovda et al., 1996).

The second hypothesis refers to a “Termite system”. Soil feeding termites are known to modify soil properties. Clay proportions, pH, and elements such Ca, Mg, and K are generally in higher amounts than in surrounding soil (Mujinya et al., 2011). Furthermore, although carbonate nodules are observed, it is still unclear if carbonates come directly from termite guts (implication of oxalotrophy?), where pH is alkaline, or if they are inherited carbonate brought during soil bioturbation (upward movements).

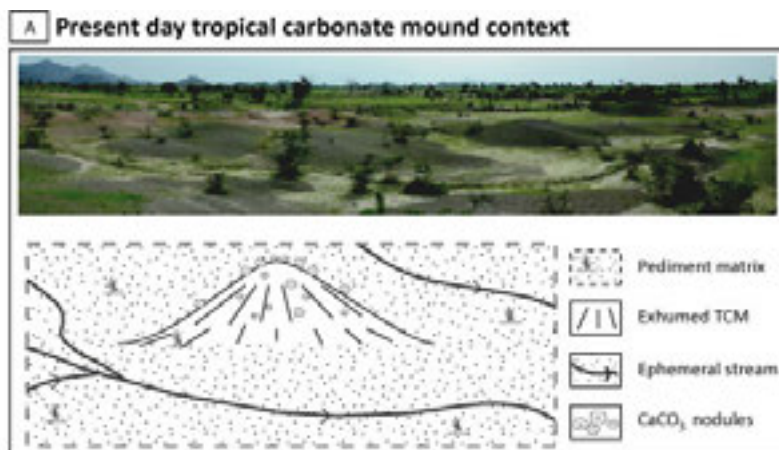
Third hypothesis refers to an “Oxalogenic-oxalotrophic system”. In tropical forests, unexpected carbonate accumulations, resulting from the oxalate-carbonate pathway (or OCP), are observed in soils surrounding oxalogenic trees, e.g. *Milicia excelsa* (Cailleau et al., 2011). OCP leads to the transformation of atmospheric CO<sub>2</sub> into pedogenic CaCO<sub>3</sub>. Oxalate is released from plant tissues during litter decay, and then oxidized by soil oxalotrophic bacteria. This process induces a pH increase, which can reach values beyond the stability pH for calcite. As a consequence, calcium carbonate can precipitate in originally acidic soils associated with oxalogenic trees.

In order to explain tropical carbonate mounds (TCM) formation a two steps approach is planned. After deciphering diagenetic and post-carbonate sedimentary settings, the aim is to characterize the primary accumulation process. How did TCM formed over time in such a carbonate-free environment? What are the timing and the nature of processes causing carbonate accumulations?

Figure 1 shows the general framework and geomorphological context in which TCM are observed. To take up the challenges raised by the various hypotheses, two TCM (one exhumed and one buried) are investigated using a combined geomorphological, petrographic, and biogeochemical approach.

## REFERENCES

- Cailleau, G., Braissant, O., Verrecchia, E.P. 2011: Turning sunlight into stone: the oxalate-carbonate pathway in a tropical tree ecosystem. *Biogeosciences* 8, 1755-1767.
- FAO, 2006: World reference base for soil resources. World soil resources report. Rome.
- Kodova, I., Morgun, E., Tessier, D. 1996: Étude de Vertisols à gilgai du Nord-Caucase: mécanismes de différenciation et aspects pédogéochimiques. *Étude et gestion des sols*, 3, 1, 41-52
- Nguetnkam, J.-P., Kamga, R., Villiéras, F., Ekodeck, G. E., Yvon J. 2008: Altération différentielle du granite en zone tropicale. Exemple de deux séquences étudiées au Cameroun (Afrique Centrale). *Geoscience* 340, 451-461.
- Mujinya, B.B., Mees, F., Boeckx, P., Bodé, S., Baert, G., Erens, H., Delefortrie, S., Verdoodt, A., Ngongo, M., Van Ranst, E. 2011: The origin of carbonates in termite mounds of the Lubumbashi area, D.R. Congo. *Geoderma* 165, 95-105.



Time ? ↑ ? Diagenesis and pediment matrix deposit

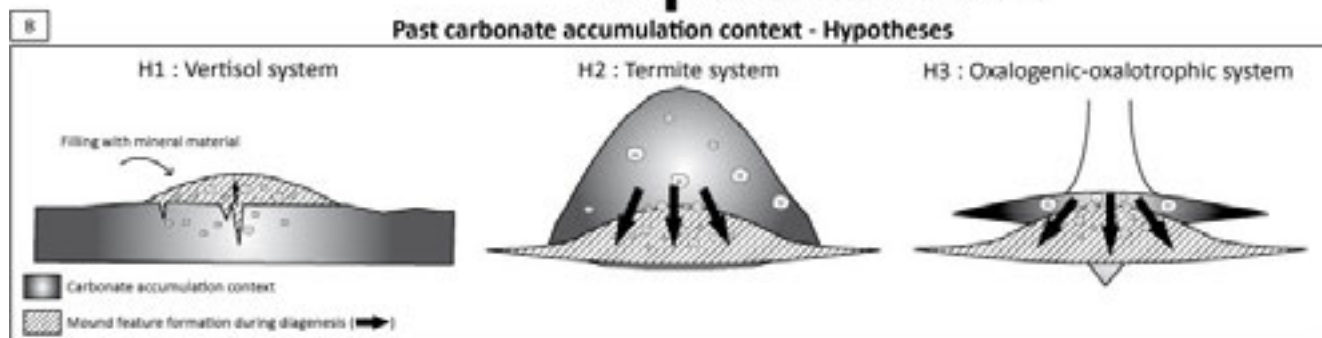


Figure 1: A- Present-day geomorphological context of TCM near Maroua (northern Cameroun). B- Hypotheses for carbonate accumulations: H1- Desiccation processes in Vertisols with mineral material in cracks, forming a gilgai landscape (Kovda et al., 1996). Accumulation of carbonate in termite mounds (H2) or carbonate formation through a oxalogenic-oxalotrophic system (H3) undergoing diagenetic processes leading to observed present-day mounds.

## P 20.4

# Middle Würm radiocarbon chronologies in the Swiss Alpine foreland - first results from the TiMIS project

Hippe Kristina<sup>1</sup>, Hajdas Irka<sup>1</sup>, Ivy-Ochs Susan<sup>1</sup> & Maisch Max<sup>2</sup>

<sup>1</sup> *Laboratory of Ion Beam Physics, ETH Zürich, Schafmattstrasse 20, CH-8093 Zürich (hippe@phys.ethz.ch)*

<sup>2</sup> *Department of Geography, University of Zürich, Winterthurerstrasse 190, CH-8057 Zürich*

The COST funded TiMIS project aims at refining the radiocarbon chronology of the middle part of the last glacial cycle (middle Würm: 50 to 25 ka) focussing on the records preserved in the Swiss Alpine forelands where huge piedmont glaciers expanded during the Last Glacial Maximum (LGM). We perform radiocarbon dating of selected key sites in the Alpine foreland to add high-resolution chronological information crucial for understanding the phase of ice build-up just prior to the LGM and to provide important links to other records of Marine Isotope Stage 3 (MIS 3). TiMIS results are integrated into the COST Action ES0907 INITMATE, which is centered on integrating ice, marine and terrestrial records for paleoclimate reconstructions between 60-8 ka.

The Swiss foreland fossil peat deposits are one of the best records available for the ca. 25 ka just before the LGM. Although many peat sections have already been described by the Swiss Quaternary scientists of the 1960s and 70s, reliable age data are not widely available. One important peat deposit, which has been largely exploited throughout the 19<sup>th</sup> century, is situated at Dürnten, SE of Zürich. Based on detailed pollen analysis in three drill cores, Welten (1982) has reconstructed climate variability since the Riss glacial stage and proposed several stadial-interstadial cycles throughout the Würm. Here, we present first radiocarbon ages from two outcrops of fossil peat deposits at Dürnten. Preliminary ages from peat and wood samples range from 40-45 ka BP and agree very well with <sup>14</sup>C ages of ~45 ka reported from peat layers of the Gossau and Niederweningen sites (Schlüchter et al. 1987; Hajdas et al. 2007). Gossau and Dürnten are both located within the LGM extent of the Linth/Rhein glacier and clearly document a phase of moderate climate and glacier absence during the early middle Würm.

## REFERENCES

- Welten, M. 1982: Pollenanalytische Untersuchungen im Jüngeren Quartär des nördlichen Alpenvorlandes der Schweiz. Beiträge zur Geologischen Karte der Schweiz, N.F. 156. Stämpfli & Co., Bern, 174 pp.
- Schlüchter, C., Maisch, M., Suter, J., Fitze, P., Keller, W.A., Burga, C.A. & Wynistorf, E. 1987: Das Schieferkohlenprofil von Gossau (Kanton Zürich) und seine stratigraphische Stellung innerhalb der letzten Eiszeit. Vierteljahrsschrift der Naturforschenden Gesellschaft in Zürich 132, 135–174.
- Hajdas, I., Bonani, G., Furrer, H., Mader, A. & Schoch, W. 2007: Radiocarbon chronology of the mammoth site at Niederweningen, Switzerland: Results from dating bones, teeth, wood, and peat. Quaternary International 164-165, 98-105.

## P 20.5

### The new luminescence laboratory at the University of Lausanne

King Georgina, Herman Frédéric, Valla Pierre

*Institute of Earth Sciences, University of Lausanne*

Luminescence dating is a Quaternary dating method which is widely utilised to constrain the timing of Quaternary events. The technique exploits the time-dependent accumulation of charge within certain minerals, when they are exposed to naturally occurring radiation. Quartz and K-feldspar are the most commonly used minerals, and ages can be generated over timescales of  $10^1$  to  $10^6$  years.

Optically stimulated luminescence dating can be used to date a wide variety of landforms in different depositional settings, including glacial, marine, aeolian and fluvial sediments as well as human artefacts. In addition to its conventional applications, luminescence dating has also recently been proposed as a low-temperature thermochronometer (Herman et al., 2010). This is because in addition to being light-sensitive, the luminescence signal is also sensitive to temperature.

The new luminescence laboratory at UNIL has been established by the Earth Surface Dynamics group led by Professor Frédéric Herman. In addition to sedimentary and rock sample preparation facilities the laboratory is equipped with a Risø luminescence TL/OSL reader, which has capacity for time-resolved and single photon counting experiments. A second reader, with the facility for single-grain quartz and feldspar analyses has been ordered and will be available from Spring 2014.

For further information on OSL dating and the new OSL facilities available at UNIL and to discuss potential collaborations, please contact Dr Georgina King ([georgina.king@unil.ch](mailto:georgina.king@unil.ch)).

#### REFERENCES

Herman, F., Rhodes, E.J., Braun, J. & Heiniger, L., 2010. Uniform erosion rates and relief amplitude during glacial cycles in the Southern Alps of New Zealand, as revealed from OSL-thermochronology. *Earth and Planetary Science Letters* 297, 183-189.

## P 20.6

## Archaeometric evidence of foodways in the South-Central Andes: Prehispanic maize consumption in West Tinogasta (Catamarca, Argentina)

Lantos Irene<sup>1</sup>, Spangenberg Jorge E.<sup>2</sup>, Giovannetti Marco A.<sup>3</sup>, Maier Marta<sup>4</sup> & Ratto Norma<sup>1</sup>

<sup>1</sup> Museo Etnográfico, Universidad de Buenos Aires, Argentina

<sup>2</sup> Institute of Earth Sciences, University of Lausanne, Geopolis, CH-1015 Lausanne (jorge.spangenberg@unil.ch)

<sup>3</sup> Museo de Ciencias Naturales, Universidad Nacional de la Plata, Argentina

<sup>4</sup> Departamento de Química Orgánica, Universidad de Buenos Aires, Argentina

Pre-Hispanic Andean societies depended economically to a large degree on the extensive horticultural production of maize (*Zea mays*), the main staple food crop in the region. Carbonized maize and maize-based food residues can be identified in archaeological ceramics by a combination of chemical and stable carbon isotope analyses of preserved lipids by the use of bulk and molecular isotopic techniques combining gas chromatography and mass spectrometry (GC-MS, GC-C-IRMS; e.g. Reber & Evershed 2004, Seinfeld et al. 2009).

Archaeological finds at the West Tinogasta area in the Catamarca Province, NW Argentina record a long and discontinuous history of pre-Columbian human occupation from early hunter-gatherers to the highly developed Inka civilization in the south-central Andes. Here we report the results of the first chemical and isotopic analyses of organic residues in ceramic potsherds recovered from sites at Tinogasta covering two distinct periods, the Formative Period (450-1020 cal. AD) and the Inka State Period (1400-1550 cal. AD) that overlaps with the first Hispanic contact. The results were compared with reference samples derived from i) typical Andean food products including local maize landraces, beans (*Phaseolus vulgaris*), algarrobo (*Prosopis* sp.), and animal fat obtained from native llama (*Lama glama*) and introduced cattle (*Bos taurus*), and ii) three replicate test pots used each for cooking traditional Andean maize-based recipes, such as *locro*, *mazamorra* and *pochoclo*. The extracted lipids were analysed by TLC, GC-FID, GC-MS and GC-C-IRMS. The reference food products showed a high concentration of triacylglycerols (TAG), low concentrations of diacylglycerols (DAG), monoacylglycerols (MAG) and free fatty acids (FFA), and significant amount of sterols. Relatively high amount of lipids were recovered from the test pots (up to 18 mg/g) and the Tinogasta potsherds (0.5 mg/g). The test pots had higher concentration of DAG, MAG and FFA than the food products, due to degradation during cooking. The archaeological samples had mainly FFA and sterols, with low amounts of partially hydrolysed acylglycerols, most probably due to degradation at the burial site. Andean maize landraces have similar fatty acid methyl ester (FAME) profiles to those of commercial maize species, with high levels of oleic (18:1) and linoleic (18:2) acids. The FA distributions in the archaeological samples compare favourably to test pots, and are typical of degraded mixtures of vegetable oils (18:2) and animal fats (myristic and stearic acids; 14:0, 18:0). Polyunsaturated acids tend to disappear in more degraded samples. Differences in the FA profiles within the archaeological samples set suggest that various types of food products were stored/cooked in the pots. The  $\delta^{13}\text{C}$  values of the main fatty acids in 22 archaeological samples were compared with those of the references samples (symbols and fields in Figure 1). The Tinogasta samples plot between the fields for  $\text{C}_3$  plants and maize, clearly indicating a mixed  $\text{C}_3$ - $\text{C}_4$  ecosystem. Principal component analysis and cluster analysis of the FAME concentrations and  $\delta^{13}\text{C}$  values permit to define the compositional associations and group the archaeological samples. Most archaeological samples are close to the pre-industrial composition of llama fat. They were mostly cooking pots where meat and/or grease were stewed with  $\text{C}_3$  (beans and American algarrobo) and  $\text{C}_4$  (maize) vegetables. Further evidence for such mixtures provides the microscopic identification of *Zea mays*, *Phaseolus vulgaris* and *Prosopis* sp. starch grains in the organic crust covering the inner wall of several potsherds. For the first time combined microscopic, molecular and isotopic direct evidences indicate that Pre-Columbian societies in the south-central Andes had maize and maize-based food as an important part of their daily foodway.

### REFERENCES

- Reber E.A. & Evershed R.P. 2004: How did Mississippians prepare maize? The application of compound-specific carbon isotope analysis to absorbed pottery residues from several Mississippi Valley sites. *Archaeometry*, 46, 19-33.
- Seinfeld D.M., Von Nagy C. & Pohl, M.D. 2009: Determining Olmec maize use through bulk stable carbon isotope analysis. *Journal of Archaeological Science*, 36, 2560-2565.

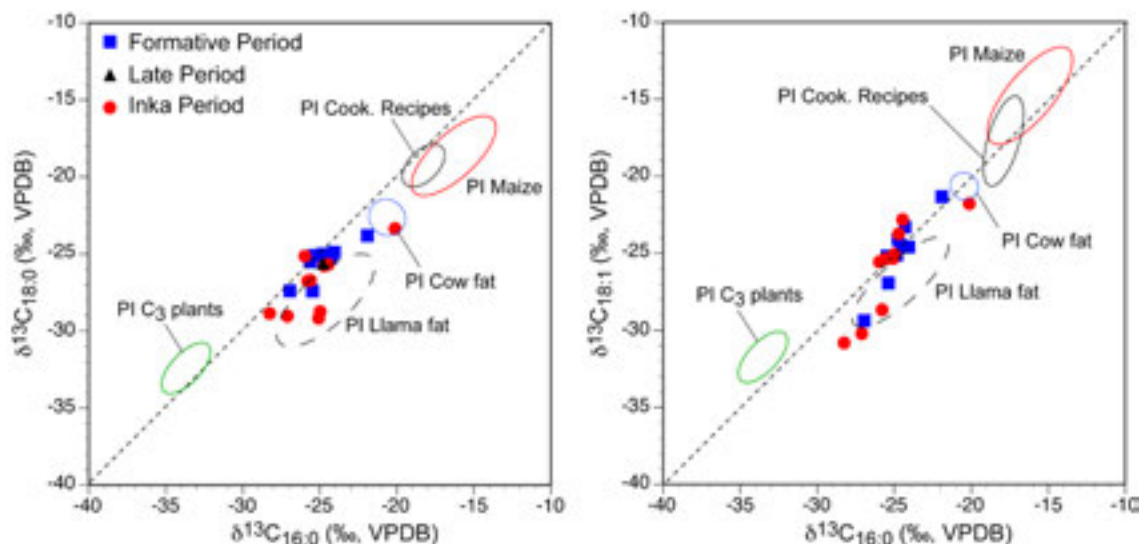


Figure 1. Comparison of the carbon isotope composition of stearic acid ( $\delta^{13}\text{C}_{18:0}$ ) and oleic acid ( $\delta^{13}\text{C}_{18:1}$ ) acid versus palmitic acid ( $\delta^{13}\text{C}_{16:0}$ ) of the organic residues in Tinogasta potsherds and pre-industrial animal and plant foodstuffs. The isotopic fields for pre-industrial (PI) animal and plant fats were determined assuming an atmospheric  $\text{CO}_2$  enriched in  $^{13}\text{C}$  by  $\sim 1.6\text{‰}$  than in present time.

## P 20.7

### GIS-based geomorphological mapping, dating of selected landforms and landscape evolution during the Lateglacial and Holocene, in the region of Val Tuoi, Grisons, Switzerland

Maja Messerli<sup>1</sup>, Max Maisch<sup>1</sup>, Susan Ivy Ochs<sup>2</sup>

<sup>1</sup> Department of Geography, University of Zurich

<sup>2</sup> Laboratory of Ion Beam Physics, ETH Zurich

The study of glacial and periglacial landforms provides important information about the climate and glacier history of the region and the related processes. Since the Last Glacial Maximum (LGM) glaciers in the Alps have left distinct traces of their activities. The Val Tuoi, Grisons, Switzerland offers a wide range of glacial and periglacial landforms. In order to reconstruct the landscape evolution and the regional climate history during the Lateglacial and the Holocene a detailed understanding of the geomorphological settings and an optimally designed application of the corresponding relative and absolute dating methods are compulsory. Based on current and former topographic maps, vector data, orthophotos, digital elevation models (DEM) and fieldwork, a detailed geomorphological map (1:25'000) was produced and digitalized with ArcGIS. Geochronological investigation with Schmidt-hammer was applied on debris cones, moraines, as well as relictic and inactive rock glaciers. To obtain absolute ages, rock surface samples on moraines and other striking features (rockslide deposits) have been collected and examined with the  $^{10}\text{Be}$  exposure dating method. Furthermore, five former stadials of the Val Tuoi glacier were reconstructed based on the Accumulation Area Ratio (AAR) method. For each stadial the equilibrium line altitude (ELA) and the ELA-depressions with reference to the Little Ice Age (LIA) are calculated and compared with the sequence of Lateglacial re-advances of the Eastern Alps. Combining the new dating results with ELA estimations, a critically reviewed synthesis is worked out to show the correlations with the known stratigraphy and the related climate history (Lateglacial and Holocene). It includes a tentative morphostratigraphic system of the selected glacial and periglacial features in the Val Tuoi with promising new results on the chronology of the stadials that are older than the Younger Dryas (Daun, Clavadel).

## P 20.8

### Using cosmogenic $^{36}\text{Cl}$ to determine periods of enhanced seismicity in western Anatolia, Turkey

Mozafari Amiri Nasim<sup>1</sup>, Tikhomirov Dmitry<sup>1</sup>, Özkaymak Çağlar<sup>2</sup>, Sümer Ökmen<sup>3</sup>, Ivy-Ochs Susan<sup>4</sup>, Vockenhuber Christof<sup>4</sup>, Uzel Bora<sup>3</sup>, Sözbilir Hasan<sup>3</sup>, Akçar Naki<sup>1</sup>

<sup>1</sup> Institute of Geological Sciences, University of Bern, Baltzerstrasse 1-3, 3012 Bern, Switzerland

<sup>2</sup> Department of Geological Engineering, Afyon Kocatepe University, Ahmet Necdet Sezer Kampusü, 03200 Afyonkarahisar, Turkey

<sup>3</sup> Department of Geological Engineering, Dokuz Eylül University, 35160 İzmir, Turkey

<sup>4</sup> Institut für Teilchenphysik, Eidgenössische Technische Hochschule, Zürich, Switzerland

The West Anatolian Extensional Province, one of the seismically most active and rapidly extending regions in the world, is dominated by three major E-W trending graben systems, namely Gediz, Küçük Menderes and Büyük Menderes. These are formed in response to approximately N-S continental extension and geomorphologically characterized by well exposed limestone normal fault scarps.

Because seismicity and thus rupture along these high angle normal faults is sporadic, periods of marked uplift of the footwall block alternate with periods of quiescence. During period of quiescence, cosmogenic  $^{36}\text{Cl}$  builds up in the exposed limestone scarps. Consequently periods of seismic activity and inactivity can be examined based on the distribution of measured  $^{36}\text{Cl}$  concentrations.

The aforesaid fault systems are the main structures in the West Anatolian Extensional Province representing extensional activity along with evidences of surface faulting during the Pleistocene and Holocene. Consequently, we apply surface exposure dating with cosmogenic  $^{36}\text{Cl}$  to better understand the tectonic outline of this seismically active province by revealing patterns of past seismic activities.

In this study, we collected more than 300 limestone samples from well-exposed sections of bedrock fault scarps along the Manisa Fault (the main segment of the Gediz graben), the Yavansu and the Kalafat Faults (related to Küçük Menderes graben) as well as the Priene-Sazlı Fault (related to Büyük Menderes graben) to measure  $^{36}\text{Cl}$  concentrations. In order to reconstruct the chronology of the seismic events, a new Matlab code will be run to identify the timing of periods of significant ruptures. Then the average slip rates for each event will be estimated. Our first results reveal enhanced seismic activity during the early Holocene in the Gediz Graben.

## P 20.9

### Timing of deglaciation on the Southern Swiss Alps

Scapozza Cristian<sup>1</sup>, Ambrosi Christian<sup>1</sup>, Castelletti Claudio<sup>1</sup>, Soma Linda<sup>1</sup> & Dall'Agnolo Stephan<sup>2</sup>

<sup>1</sup> Istituto scienze della Terra, Scuola Universitaria Professionale della Svizzera Italiana (SUPSI), Campus Trevano, CH-6952 Canobbio (cristian.scapozza@supsi.ch)

<sup>2</sup> Swiss Geological Survey, Federal Office of Topography swisstopo, Seftigenstrasse 264, CH-3084 Wabern.

The detailed Quaternary geological mapping of Southern Switzerland (Mendrisiotto and neighbouring regions in Italy) and the compilation of several radiocarbon dating data allow the reconstruction of the geometry and chronology of the Last Glacial Maximum (LGM) in the Southern Swiss Alps (Episodio Cantù). Moreover, they allow obtaining a detailed chronostratigraphy of the main recessional stadials during the Lateglacial and the beginning of the Holocene. The defined glacial stadials were correlated with the Greenland isotopic record of the borehole NGRIP.

For the LGM and the Pleniglacial, data are not exclusively from the Ticino glacier (Verbano lobe and a part of the Ceresio lobe), but also from the Adda glacier, which came from Valtellina (Lombardy, Italy) and occupied the Mendrisiotto by the Lario and Ceresio lobes. The analysis of calibrated maximal and minimal ages of the LGM allow proposing an age of the Episodio Cantù (the LGM extent equivalent in the Southern Swiss Alps, as defined by Bini 1997) comprised between ca. 25'500 and 18'000 14C BP ( $\approx$  30'200–21'250 cal BP). The Episodio Cantù was then correlated with the Greenland stadial GS-3, comprised between 27'400 and 22'700 cal BP (Scapozza et al. 2012).

For the Pleniglacial and the transition Pleniglacial/Lateglacial, the first recessional phases after the LGM were placed between ca. 22'500 and 21'000 cal BP, and correspond probably with the two first cold events of the Greenland stadial GS-2c.

The first Lateglacial stadial was the Melide phase, and may match with one of the two cold events of 20'450 and 19'850 cal BP. Then, five glacial stadials (defined for the first time by Hantke 1983 and Renner 1982) were highlighted for the Oldest Dryas (Biasca, Faido, Airolo, Fontana and All'Acqua), two for the Younger Dryas (Maniò and Alpe di Cruina) and one (Val Corno) in correspondence with the Greenland Holocene event GH-11.2. Thanks to the correlation with the Greenland isotopic record, it was also possible to propose a relationship between the stadials defined in the Southern Swiss Alps and the "classical" glacial stadials defined in the Eastern Alps.

#### REFERENCES

- Bini, A. 1997: Stratigraphy, chronology and paleogeography of Quaternary deposits of the area between the Ticino and Olona rivers (Italy – Switzerland). *Geologia Insubrica*, 2(2), 21-46.
- Hantke, R. 1983: *Eiszeitalter. Die jüngste Erdgeschichte der Schweiz und ihrer Nachbargebiete. Band 3: Westliche Ostalpen mit ihrem bayerischen Vorland bis zum Inn-Durchbruch und Südalpen zwischen Dolomiten und Mont-Blanc*. Thun, Ott Verlag, 730 pp.
- NGRIP–Members, 2004: North Greenland Ice Core Project Oxygen Isotope Data. IGBP PAGES/World Data Center for Paleoclimatology Data Contribution Series n. 2004-059. Boulder (CO), NOAA/NGDC Paleoclimatology Program.
- Renner, F. 1982: Beiträge zur Gletscher-Geschichte des Gotthardgebietes und Dendroklimatologische Analysen an Fossilen Hölzern. *Physische Geographie*, 8, 180 pp.
- Scapozza, C., Antognini, M., Oppizzi, P. & Patocchi, N. 2012: Stratigrafia, morfodinamica, paleoambienti della piana fluvio-deltizia del Ticino dall'Ultimo Massimo Glaciale a oggi: proposta di sintesi. *Bollettino della Società ticinese di Scienze naturali*, 100, 89-106.



## P 20.10

# Paleoenvironmental study of the Lago d'Alzasca (Ticino, Switzerland) during the last 10'000 years

Valentina Togni<sup>1</sup>, Thierry Adatte<sup>1</sup>, Karl Föllmi<sup>1</sup>, Jorge Spangenberg, Florian Thevenon<sup>2</sup>, Stefanie Wirth<sup>3</sup>

<sup>1</sup> ISTE, University of Lausanne, Géopolis, 1015 Lausanne, Switzerland, [valentina.togni@unil.ch](mailto:valentina.togni@unil.ch)

<sup>2</sup> Institute F.-A. Forel, University of Geneva, Versoix, Switzerland

<sup>3</sup> Geological Institute, Climate Geology, ETH Zürich, Switzerland

This research is mainly based on the study and the analysis of a 10 meters thick lacustrine sediment cores with good age control and covering a period of almost 10'000 years. 300 samples were collected from cores drilled in the alpine Alzasca lake, located at 1855m in the Soladino Valley, a lateral valley of the Maggia Valley (Ticino, Southern Switzerland). The main goal of this study is to decipher Holocene paleoenvironmental and paleoclimatic changes that characterized the southern swiss Alps using a multiproxy approach including sedimentology, mineralogy and geochemistry. Overall, TOC and HI/OI index Rock data as well as C/N ratio and  $\delta^{13}\text{C}$  results revealed a mixed source of organic mater, of predominant lacustrine origin. Granulometry and bulk mineralogy have also been carried out, qualifying sediments as sandy-silt dominated by detrital components such as that quartz, K-feldspaths, Na-plagioclases and phyllosilicates. Phosphorus concentrations are sometimes very high particularly in the first 2m of the core, with values ranging between 2'000 and 20'000 ppm, suggesting that glacial erosion may be an important P source, which may subsequently boost lake productivity.

Warm and cool periods with similar and distinct sedimentary characteristics were therefore identified. In warmer periods, the data are consistent with stable conditions indicated by a relatively constant composition of sediments (elevated HI values, low phosphorus concentrations and relatively high TOC content). Moreover, framboidal pyrite has been observed in sediments deposited during the Holocene thermal optimum (between 8'000 and 6'000 cal yr. BP), meaning that bottom waters were anoxic. In contrast, sediment composition appears to be more unstable during colder periods with high variability in HI-OI, TOC and phosphorus trends). Interestingly, trace elements data highlight the beginning of human impact on the environment. Lead, in particular, shows a gradual increase from the Roman epoch, and a maximum near the top of the core (almost 500 ppm) that corresponds to the intensive use of lead in gasoline.

## 21. Scientific challenges for geoheritage conservation and promotion in Switzerland

Emmanuel Reynard, Heinz Furrer, Pierre-Yves Jeannin, Philippe Häuselmann

*Working group for Geotopes in Switzerland,  
Swiss Geomorphological Society,  
Swiss Paleontological Society,  
Swiss Speleological Society*

### TALKS:

- 21.1 Biot V., Caze B.: La valorisation du patrimoine paléontologique : la réalisation de la maison de site du gisement Lagerstätte de La Voulte.
- 21.2 Perret A., Martin S., Guyomard A., Kramar N., Marthaler M.: A simplified geological map of the Chablais Geopark
- 21.3 Perret A., Reynard E., Delannoy J.-J., Nugue N., Guyomard A.: Itinerant exhibition in the Chablais area. Association of “objective knowledge” and “interpretation method” to elaborate a geotourism product.
- 21.4 Regolini-Bissig G., Martin S., Reynard E., Kaiser Ch.: Promotion of geosciences through non-personal interpretation: the Lausanne Geoguide application

### POSTERS:

- P 21.1 Buchmann M.: Geoheritage in the Moesano region – between nature protection and landscape enhancement
- P 21.2 Bussard J.: Protection and promotion of geomorphological heritage in the Gruyère – Pays-d’Enhaut Regional Nature Park. Assessment and perspectives
- P 21.3 Fanguin P.: Geoheritage promotion of Thonon-les-Bains (Fr) region by the development of a geotourism product
- P 21.4 Maret H.: Cartography of the geomorphological diversity in Derborence (Valais, Swiss Alps)
- P 21.5 Reynard E., †Berger J.-P., Constandache M., Dumas J., Felber M., Grangier L., Häuselmann P., Jeannin P.-Y., Martin S., Regolini G.: The revision of the Swiss Inventory of Geosites (2006-2012)

## 21.1

### La valorisation du patrimoine paléontologique : la réalisation de la maison de site du gisement Lagerstätte de La Voulte.

Biot Vincent<sup>1,2</sup> et Caze Bruno<sup>1</sup>

<sup>1</sup> Mairie de La Voulte-sur-Rhône, 07800 La Voulte-sur-Rhône, France

<sup>2</sup> Laboratoire EDYTEM, UMR 5204, Université de Savoie, 73376 La Bourget-du-Lac cedex, France

La paléontologie est une des disciplines scientifiques rattachée à la géologie. Si les dinosaures sont les « stars » du grand public, les fossiles ne se réduisent pas simplement à ce groupe de vertébrés aujourd'hui disparu. Ainsi, différents musées de paléontologie ou d'espaces exposition dédiés aux fossiles traitent des sciences de la terre et de la géologie. La valorisation du patrimoine géologique devient alors moteur du développement économique d'un territoire. L'initiative de la réserve naturelle géologique de Haute Provence, en est un exemple avec, à partir de 1994, l'aménagement et la valorisation de sites géologiques, la création de routes thématiques et de sentiers, l'édition d'ouvrages présentant le territoire et l'ouverture d'un musée permettant de remonter l'histoire de la terre sur 300 millions d'années.

Un projet est actuellement en cours de réalisation à La Voulte-sur-Rhône en Ardèche. Le territoire de la commune abrite un gisement fossilifère à conservation exceptionnelle appelé Lagerstätte de La Voulte situé sur le site de La Boissine. Les scientifiques dénombrent une cinquantaine de Lagerstätte dans le monde dont 6 en France. Celui de La Voulte-sur-Rhône constitue un patrimoine remarquable de part la qualité de préservation des parties molles de ces fossiles. Afin de préserver le périmètre où se situe le gisement fossilifère, le Conseil général de l'Ardèche a fait l'acquisition du site de La Boissine et l'a classé espace naturel sensible (ENS). La commune a signé un bail emphytéotique avec le département pour réaliser une maison de site et un espace d'exposition sur l'ENS.

Ce projet prend place dans un contexte local marqué par une activité industrielle importante dans les années 1970 avec la présence de Rhône-Poulenc textile. La crise du textile entrainera la fermeture de l'usine en 1981 impactant la vie économique locale. Aujourd'hui, le géotourisme est un des leviers à actionner pour assurer le passage vers un nouveau modèle économique.

Le Lagerstätte de La Voulte étant connu essentiellement des scientifiques, la commune de La Voulte-sur-Rhône a souhaité faire découvrir ce patrimoine au grand public. Si un musée privé de paléontologie fonctionna de 1989 à 2006, il dû fermer ses portes car les locaux devenaient vétuste et exiguë. Le projet actuellement conduit par la commune, en lien avec le conseil général de l'Ardèche et en partenariat avec le Museum national d'Histoire naturelle, est la réalisation d'une maison de site présentant les collections du gisement de La Voulte mais également d'autres Lagerstätten. Cette maison est construite directement sur le site de la Boissine de façon à se situer sur les lieux mêmes des découvertes et des fouilles. En ce sens, ce projet se distingue de nombreux autres musées de paléontologie de par cette proximité entre « musée » et « terrain ».

Les fouilles qui vont reprendre pourront également être valorisés à travers des animations et une sensibilisation auprès du grand public. Sur le même lieu touristique, les visiteurs pourront ainsi s'immerger dans l'histoire géologique et de la vie sur la terre.

Dans un contexte d'ouverture prochaine de l'espace de restitution de la grotte Chauvet et de la réouverture de la Cité de la Préhistoire en Sud Ardèche, mais également de réflexion de création d'un Géopark par le Parc naturel régional des monts d'Ardèche, le projet de maison de site, dont l'ouverture est prévue à l'été 2014, prend place dans une dynamique territoriale de valorisation du patrimoine culturelle et géologique.

#### REFERENCES

- Charbonnier S., 2009, Le Lagerstätte de La Voulte : un environnement bathyal au jurassique, Mémoires du Museum national d'Histoire naturelle, T.199, 272 p.
- Reynard, E. et Panizza M., 2005, Géomorphosites : définition, évaluation et cartographie, Géomorphologie : relief, processus, environnement, n° 3, p. 177-180.
- Riou B., 2009, Le Domaine Départemental de Nature de La Boissine et le site paléontologique de La Voulte Sur Rhône, Actes du colloque 7èmes Rencontres du Patrimoine scientifique en Rhône-Alpes - Patrimoine naturel : le patrimoine géologique, p. 113-119
- Sabouraud C., 2008, Guide de la géologie en France, édition Belin, 816 p.

## 21.2

### A simplified geological map of the Chablais Geopark

Perret Amandine<sup>1,2</sup>, Martin Simon<sup>2</sup>, Guyomard Anne<sup>3</sup>, Kramar Nicolas<sup>4</sup> & Marthaler Michel<sup>1</sup>

<sup>1</sup> Institute of Geography and Sustainability, University of Lausanne, Mouline - Géopolis, CH-1015 Lausanne (amandine.perret@unil.ch)

<sup>2</sup> Bureau d'étude Relief, Chemin des Oisillons 9, CH-1860 Aigle

<sup>3</sup> Syndicat Intercommunal d'Aménagement du Chablais, Square Voltaire, 2 rue des Allobroges - BP 33, F-74201 Thonon-Les-Bains

<sup>4</sup> Route d'Evian, F-74500 Champagnes

The Chablais area is member of the European Geopark Network (EGN) since 2012. Among other geotourist products the elaboration of a simplified geological map has been initiated in 2013 by the Chablais Geopark. For this project, the geopark associate specialists in quaternary research, geology research, geological education and geotourism.

Only official BRGM maps now present the Chablais area. Four of them are needed to cover the perimeter of the geopark. These maps are relatively complex as they address to specialists. The staff of the Chablais Geopark wish to propose a map which integrate latest knowledge on the regional quaternary deposits and which could be used by non specialists, in particular the local guides. The map should also encourage the visit of less-known geosites by presenting sixteen of them. The elaboration of the map is based on the method developed by Martin and al. (2010), which propose, after a first analysis of context and the definition of communication objectives to take into account four aspects to build geotourism products : the site and objects; the message and content of the product; the media; and the audience (fig.1). In the case of the simplified geological map of the Chablais Geopark, we have to deal with predefined aspects: the media (a map) and the audience (principally guides with a basic training in geosciences). The main objectives are also fixed: (1) the geological map has to be adapted to the level of knowledge of guides; (2) geosites have to be accessible and understandable by the widest audience; (3) the map should also be usable by the guide to support direct interpretation (to the general public).

The sites (or objects) have been selected in order to represent the geodiversity of the Chablais: sites have to cover the various kind of rocks and sediments of the area, as shown on the simplified map. Concerning the message, all the content is organized upon the three-stage story of structural landscape (rock formation, folding, erosion) developed by Kramar (2003, 2005, 2012) and Marthaler and Kramar (2003). The legend of the map and structural schemes, as well as the presentation of the (geo)sites are based on this concept. For instance, the legend of the simplified map regroupes in only ten colors all the rocks of the Chablais pile of nappes.

With the use of these methods and concepts (Martin et al. and Kramar) we try to develop a geointerpretive product especially efficient to communicate scientific knowledge to the public.

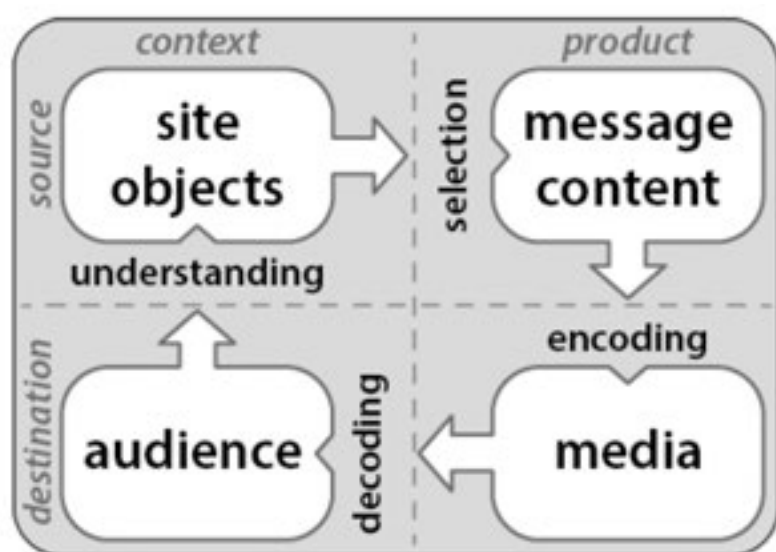


Figure 1. Four aspects to consider when elaborating non personal interpretation products.

#### REFERENCES

Martin, S., Regolini-Bissig, G., Perret, A. & Kozlik, L. 2010: Élaboration et évaluation de produits géotouristiques.

- Propositions méthodologiques. *Téoros*. 29(2), 55-66.
- Kramar, N. 2003 : Le cycle orogénique comme outil didactique. Colloque Quartz sur « l'enseignement et la vulgarisation des Sciences de la Terre », Nice.
- Kramar, N. 2005 : Enjeux didactiques et épistémiques liés à l'utilisation d'un modèle historique en Sciences de la Terre, XIXe Journées Internationales sur la communication, l'éducation et la culture scientifique et industrielle, 19th International Workshop on Communication, Education and Scientific and Industrial Culture. Editors: A. Giordan, J.-L. Martinand and D. Raichvarg.
- Kramar, N. 2012 : Le tourisme scientifique en question vers de nouvelles potentialités, G. Brougère et G.Fabbiano (dir.), *Tourisme et apprentissages*, Actes du colloque de Villeteuse (16-17mai 2011), Villeteuse, EXPERICE – Université Paris 13, 2012, p. 95-100
- Marthaler, M. & N. Kramar 2003 : Les paysages valorisés par leur histoire géodynamique, Quelques exemples où la mémoire de la terre est révélée par les panoramas, Quartz sur « l'enseignement et la vulgarisation des Sciences de la Terre », Nice.

## 21.2

### Itinerant exhibition in the Chablais area. Association of "objective knowledge" and "interpretation method" to elaborate a geotourism product.

Perret Amandine<sup>1,2</sup>, Reynard Emmanuel<sup>1</sup>, Delannoy Jean-Jacques<sup>2</sup>, Nugue Natacha <sup>3</sup>, Guyomard Anne<sup>3</sup>

<sup>1</sup>Institute of Geography and Sustainability, University of Lausanne, Mouline - Géopolis, CH-1015 Lausanne (amandine.perret@unil.ch)

<sup>2</sup>EDYTEM Laboratoire UMR5204, University of Savoie, Bâtiment « Pôle Montagne » F-73376 Le Bourget du Lac

<sup>3</sup>Syndicat Intercommunal d'Aménagement du Chablais, Square Voltaire, 2 rue des Allobroges - BP 33, F-74201 Thonon-Les-Bains

The Chablais area (French and Swiss Prealps) is considered as one of the cradles of glacial theory after the work of several researchers at the end of the 19<sup>th</sup> century (de Charpentier, 1841; Morlot, 1859). The association between glacial witnesses well preserved (moraines, erratics blocks, quaternary outcrops), the activity of scientists and a large use of glacial material by local populations in the area makes that the Chablais has an interesting potential to develop mediation tools based on glacial heritage.

Nevertheless, several problems must be solved before researchers and territory actors can be able to communicate on this "heritage" (glacial witnesses with high geocultural and scientific value and a strong link with quotidian life). First, the knowledge of glacial witnesses (deposits and landforms) is still incomplete and several questions remain unresolved, especially in zones where studies are rare or inexistent. Even to a larger scale, researchers do not agree, for example, on glacial retreat chronology. This situation requires a preliminary study in order to improve scientific knowledge of glacial deposits. In effect, it is difficult to communicate about obscure objects, in terms of age or formation (Gauchon 2010). To try to complete quaternary knowledge we undertook two kinds of studies: 1) geomorphological maps to establish a relative chronology and 2) cosmogenic dating to obtain ages.

The second problem is that glacial witnesses are relatively little-known by the population (Perret et al. 2010) even if these deposits and landforms are greatly used in building, tourism, leisure and strongly linked with resources as mineral water, for example.

Chablais actors' wish was to elaborate an itinerant exhibition to present glacial heritage. This work is a small part of an Interreg project ([www.123chablais.com](http://www.123chablais.com)) dealing with the promotion of different types of natural and cultural heritage in the area. In order to elaborate an interpretative tool efficient to communicate the scientific knowledge to the public, we defined a specific audience for this exhibition: local population. The aim of the exhibition was not to propose a course on glaciers but to arouse awareness on Chablais glaciers and their witnesses. Then we defined a "scenario" in three steps: 1) glacial theory history 2) glacial retreat 3) link with daily life. A special work was to eliminate scientific vocabulary of texts and we used as often as possible pictures or sketches. A special care was made to illustrate maps and texts by local examples.

The exhibition is now shown since more than one year and we begin to collect impressions of the public. Several points can be improved: texts are too long, sites could be best situated (some people want to visit sites after the exhibition) and the conception of the three experiment posts is too fragile. The next step to finish the process of elaboration of a new geotourism product should be to analyse conceptions of public before and after visiting this exhibition, to control if visitors are better informed on glacial heritage.



Figure 1. Three thematics of the exhibition (1) glacial theory history 2) glacial retreat 3) link with daily life.

## REFERENCES

- de Charpentier, J. 1841 : Essai sur les glaciers et sur le terrain erratique du bassin du Rhône. M. Ducloux, Lausanne.
- Gauchon, C. 2010 : Tourisme et patrimoines : un creuset pour les territoires? (Thèse de HDR). Université de Savoie, Chambéry.
- Morlot, A. 1859 : Sur le terrain quaternaire du bassin du Léman. Bulletin de la société vaudoise des sciences naturelles, 6, 101-108.
- Perret, A, Reynard, E & J-J. Delannoy, 2010: Reconstitution des principaux stades glaciaires du Chablais : base scientifique pour la valorisation d'un patrimoine glaciaire régional. In Reynard E., Laigre L. et Kramar N. (Eds) (2011). Les géosciences au service de la société. Actes du colloque en l'honneur du Professeur Michel Marthaler, 24-26 juin 2010, Lausanne (Géovisions n° 37). Institut de géographie, Université de Lausanne.

## 21.4

### Promotion of geosciences through non-personal interpretation: the Lausanne Geoguide application

Géraldine Regolini-Bissig<sup>1</sup>, Simon Martin<sup>1</sup>, Emmanuel Reynard<sup>2</sup> & Christian Kaiser<sup>2</sup>

<sup>1</sup> Bureau d'étude RELIEF, Ch. des Oisillons 9, CH-1860 Aigle (geraldine.regolini@bureau-relief.ch, simon.martin@bureau-relief.ch)

<sup>2</sup> University of Lausanne, Institute of Geography and Sustainability, CH-1015 Lausanne (emmanuel.reynard@unil.ch, christian.kaiser@unil.ch)

According to Dowling & Newsome (2006) geotourism products communicate geoscientific knowledge and ideas to the public. The objectives of geotourism – promotion and conservation of geosites and objects – request effective communication and education of the public. It is therefore essential to guarantee this efficiency in interpretive products, personal (e.g. guided tour) or non-personal (e.g. media-based).

The proposed global approach for the elaboration of non-personal interpretation products considers four fundamental aspects and their interplay: the site and objects; the message and content of the product; the media; the audience (Martin et al., 2010). Each of the aspects should be carefully analyzed before decision making about the products characteristics. This conceptual framework was applied i) to produce geotourism products like brochures, maps or trails and ii) to elaborate a method for the assessment of natural heritage trails (Regolini & Martin 2010).

The *Geoguide Lausanne* is an application for mobile platforms such as smartphones and tablets that aims at the communication of geosciences in an urban context (Reynard et al., 2014). In 30 stops evenly distributed in the city of Lausanne, interesting for its natural framework, the *Geoguide* focuses on research topics of the Faculty of Geosciences and Environment of the University of Lausanne. It was the Faculty's desire to communicate its findings in occasion of its 10<sup>th</sup> anniversary.

The application is an innovative interpretation tool addressed to local population and tourists interested to learn more about the urban landscape and its sometimes hidden mysteries (e.g. canalized watercourses or the origin of the steep streets of the town). The content focuses on the relationships existing between three spheres: A. the climate, water and atmosphere; B. the town and human activities; C. the substratum, rocks and landscape. Each stop focuses, therefore, on one specific relationship (e.g. alteration of the molassic rocks (relationship AC); urban development of a fluvial valley (BC); derivation of a watercourse for reducing rainwater volumes reaching wastewater treatment plants (AB), etc.

There are different possibilities to access the content: i) by tapping on the corresponding marker on the map where all stops are displayed, ii) by selecting a place of interest in a simple list, iii) by structuring the stops according to one of the three relationships mentioned above (fig. 1). Therefore, the application can be used as a fieldtrip guide following the proposed track, as a punctual interpretation device when visiting a given site or as thematic access to geosciences. Furthermore, the application offers two levels of complexity: a first level with short texts that attracts the users attention and raises its curiosity and pictures that not only illustrate the message (e.g. photo) but provide further explanation (e.g. maps or graphs) and a second level where more technical information and further reading is proposed (e.g. scientific papers in pdf format, etc.).



Figure 1. *Geoguide Application* with toolbar (below in blue) offering multiple entrance to the content and excerpt of the content of the stop 29 (<http://igd.unil.ch/geoguide/>).

As the application can be considered a trail when being used as fieldtrip guide, its quality was evaluated by the assessment method for heritage trails. The results give us an indication about the robustness of the model for non-personal interpretation to generate products that archive communication, educational and tourism objectives.

#### Acknowledgments

Lausanne Geoguide was financially and technically supported by the Faculty of Geosciences and Environment of the University of Lausanne for the 10 years of the Faculty.

#### REFERENCES

- Newsome, D. & Dowling, R. K. 2006: The scope and nature of geotourism. In: *Geotourism. Sustainability, impacts and management* (Eds. by Dowling, R. K. & Newsome, D.), Amsterdam, Elsevier, 3-25.
- Martin, S., Regolini-Bissig, G., Perret, A. & Kozlik, L. 2010: Élaboration et évaluation de produits géotouristiques. Propositions méthodologiques. *Téoros*. 29(2), 55-66.
- Regolini-Bissig, G. & Martin, S. 2010: Quality assessment of natural heritage trails. Abstract Volume 8<sup>th</sup> Swiss Geoscience Meeting, Fribourg 19<sup>th</sup>-20<sup>th</sup> November 2010, 20. *Geotopes and Geoparks*, 352-353.
- Reynard, E., Kaiser, C., Martin, S. & Regolini, G. 2014: Urban Geotourism: an application for communicating on geosciences by smartphone. Proceedings Conference of the International Associations for Engineering Geology and the Environment, Torino, 15-19 September 2014, submitted.
- <http://igd.unil.ch/geoguide/> (consulted 28.08.2013)

## P 21.1

# Geoheritage in the Moesano region – between nature protection and landscape enhancement

Marco Buchmann,

*University of Lausanne*

This work consists in the realisation of a geo(morpho)sites inventory (in a large sense of their definition) for the Moesano region (Mesolcina and Calanca valleys), which is situated in the south-eastern part of the Graubünden canton in Switzerland. It is partly situated in the perimeter of the National Park candidate – Parc'Adula, which presents both central and peripheral designed zones of the project.

An evolution of the assessment method developed by Reynard et al., 2007 will be applied. It will permit us to highlight and evaluate the characteristics of each selected geo(morpho)logical site, providing so a scientific basis for proposing a management strategy, including protection and/or enhancement measures.

The geoheritage approach is used by integrating it to an emergent kind of tourism called geotourism, which wants to promote geosciences to a broader public on a sustainable development basis. In fact the Moesano is a marginal and financially disadvantaged region, but it presents a great territorial richness on the cultural and the natural level, which if well promoted, can bring a certain regional development.

The ascertainment is that the abiotical part of the natural heritage is neglected compared to the biological and the cultural heritage as well as not well known by society as well as by the actors having an influence on the territorial development. One of the goals of the work is so to show the importance by taking it into account and to show the links that exist between the different nature and human spheres.

The reflexions of the work deal also with the apparent paradox between nature protection and landscape enhancement through tourism and/or educational promotion of a given site: how is it possible to promote geo(morpho)logical features which compose the landscape, without having a negative impact or pressure on the nature? What is the relation between nature protection and landscape promotion? Do we have first to protect nature before promoting landscape or is it possible to ensure nature protection by promoting the educational value of the landscape? In the case of the study area, we want to explore how it is possible to promote geo(morpho)sites inside the central zone of the National Park (if the project will be accepted). According to the new Suisse law this zone is in fact really restrictive. However, it is central that knowledge should be accessible to everybody if we want to promote a region in a sustainable way.

For responding to these questions it is necessary to document in detail each selected site and assess the more objectively as possible in order to show their overall characteristics. In a second step, protection measures are proposed for the sites which present high sensibility.

## REFERENCES

Reynard, E., Fontana, G., Kozlik, L. Scapozza, C., (2007). A method for assessing « scientific » and « additional values » of geomorphosites. *Geographica Helvetica*, 62/3, 148-158.

## P 21.2

# Protection and promotion of geomorphological heritage in the Gruyère – Pays-d'Enhaut Regional Nature Park. Assessment and perspectives

Bussard Jonathan<sup>1</sup>

<sup>1</sup> *Institute of Geography and Sustainability, University of Lausanne, Mouline – Géopolis, CH-1015 Lausanne (jonathan.bussard@unil.ch)*

This Master thesis deals with two main issues: the protection of the abiotic nature and the promotion of geotourism in a protected area, the Gruyère – Pays-d'Enhaut Regional Nature Park in Switzerland. Regarding the protection of non-living nature (especially its geomorphological part), an identification and assessment of the geomorphological heritage is conducted, with special attention given to the degree of protection of the sites under the various laws existing at different administrative levels. The assessment is carried out using a method developed by the Institute of Geography and Sustainability of the University of Lausanne (Reynard et al., 2007), which aims to reduce the subjectivity of the evaluation using different defined criteria (such as the scientific value, additional values, etc.). Some modifications of the existing method and the addition of new criteria concerning the present use and management of the sites are proposed and tested by the author. Concerning the promotion of geotourism, we try to understand how Earth sciences, and especially geomorphological sites, are taken into account by the main stakeholders of tourism in the region. The final goal is to give some perspectives for a suitable protection and a better promotion of the geomorphosites according to the hypothesis that their promotion allows their social recognition as a heritage that has to be preserved.

The assessment method (see fig. 1) is separated in two distinct parts. First, the intrinsic value gives information about the scientific value (integrity, representativeness, rareness and paleogeographical value) and additional values (ecological, cultural and aesthetic value) of the geomorphosites. The scientific value is quantitatively assessed in order to classify the sites according to their scientific interest. Secondly, the present use and management of the sites are documented by different criteria related to the protection of the sites (sensibility, protection status) and their promotion. The visit conditions (accessibility, security and environment of the site, presence of tourism equipments), the educational value (readability of the site) and the economic value are criteria that inform about the possibilities to develop geotouristic activities.

33 sites are inventoried in the Gruyère – Pays-d'Enhaut Regional Nature Park area. Most of them (27 sites) are related to three main geomorphological processes: karst formations (karren fields, dolines, cavities and underground networks, etc.), relicts of glacial and periglacial processes (relict moraines or former rock glaciers) and fluvial landforms (terraces, waterfalls, canyons, etc.). The other sites are due to gravity processes (landslides, rockfalls), to organic processes (marshlands) and to structural processes (perched synclines).

The first results of the inventory show that the study area has a high diversity of landforms and presents a large set of geomorphosites with an important scientific value. The majority of the sites (but not all) have a good protection status. This protection is however more related to their ecological or landscape value than to their geomorphological characteristics. An improved knowledge of this geomorphological value and a better recognition by scientists and by the society are important in order to improve the protection of geomorphosites.

## REFERENCES

Reynard, E., Fontana, G., Kozlik, L. & Scapozza, C. 2007: A method for assessing «scientific» and «additional values» of geomorphosites, *Geographica Helvetica*, 62(3), 148-158.

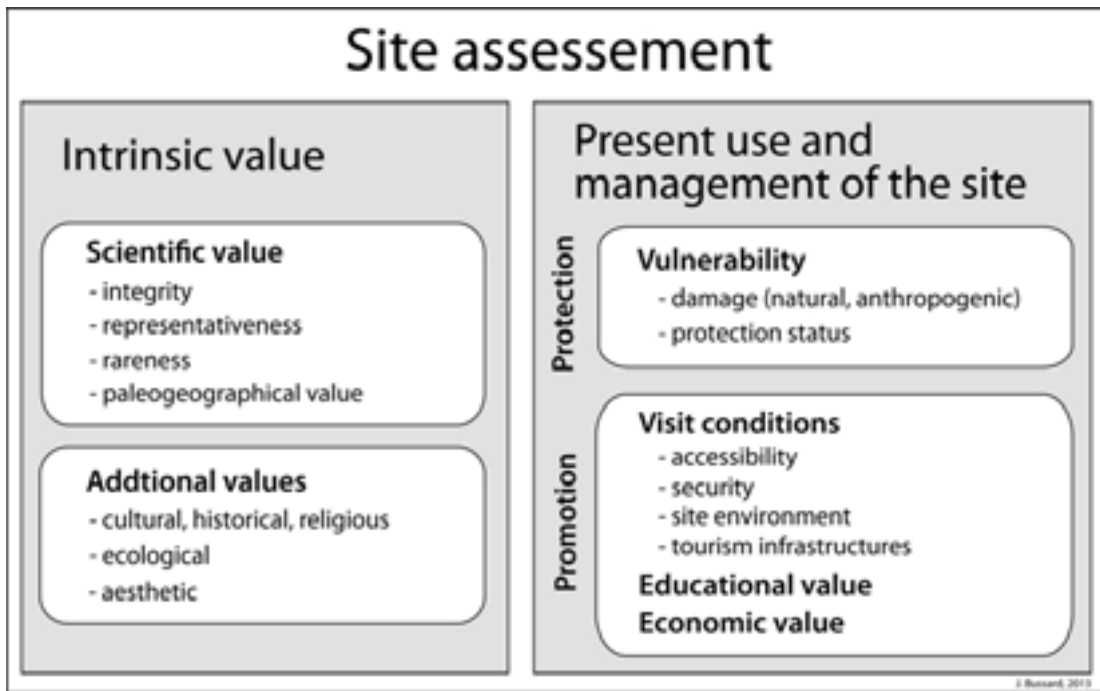


Figure 1. Summary of the assessment method.

## P 21.3

# Geoheritage promotion of Thonon-les-Bains (Fr) region by the development of a geotourism product

Fanguin Pauline<sup>1</sup>

<sup>1</sup>Institut de Géographie et durabilité, University of Lausanne, Quartier Mouline, CH-1015 Lausanne (pauline.fanguin@unil.ch)

Since 2012, the Chablais region (only in France) has acquired the Geopark label. This Geopark contributes to sustainable economic development of the region through geotourism. Moreover, the three Chablais (figure 1) are concerned by an Interreg IV program since 2009 (program of cooperation between European countries). The main objective of this program is to enhance the heritage resources (nature, culture and lifestyle of the region) (www.interreg-francesuisse.org). Therefore, the geotourism offer in this area just waiting to expand.

The geodidactics models like the simplification of the scientific content are essential for geoheritage promotion, because this content must be available to a wide audience, allowing thereby the geoheritage recognition. The geotourism permits to apply different models (Cayla et al. 2010, Sellier, 2009) through a wide range of geotourism products, like guide, educational panels, thematic hikes and recently developed, new medias (website, smartphone applications).

A geotourism product is based on four areas of questioning and was developed by Martin et al. (2010): (1) site (choice of sites to be valued), (2) public (a family public, good example of heterogeneous public), (3) contents (reasoning on geodidactics models) and (4) support (smartphone application). These four areas are very fundamental before the creation of any geotourism product. These reflexions aim to obtain a mediation product that integrates into geotourism offer of a region and contributes to its development and meets public expectations.

New media, such as digital media – smartphone, tablets, website – become geotourism products more and more attractive. In addition, the necessary technologies to develop new media help to integrate a high interactivity potential with the public and thus get their attention. The architecture of this geotourism product is based on the new application developed by the Institute of Geography and sustainability, and the Bureau Relief. One of the thematic itineraries is focused on the discovery of different natural resources by explaining their formation and their use by society, allowing to enhance a selection of geoheritage. The itinerary is entitled: In the footsteps of the exploitation of natural resources... a history of water and rock.

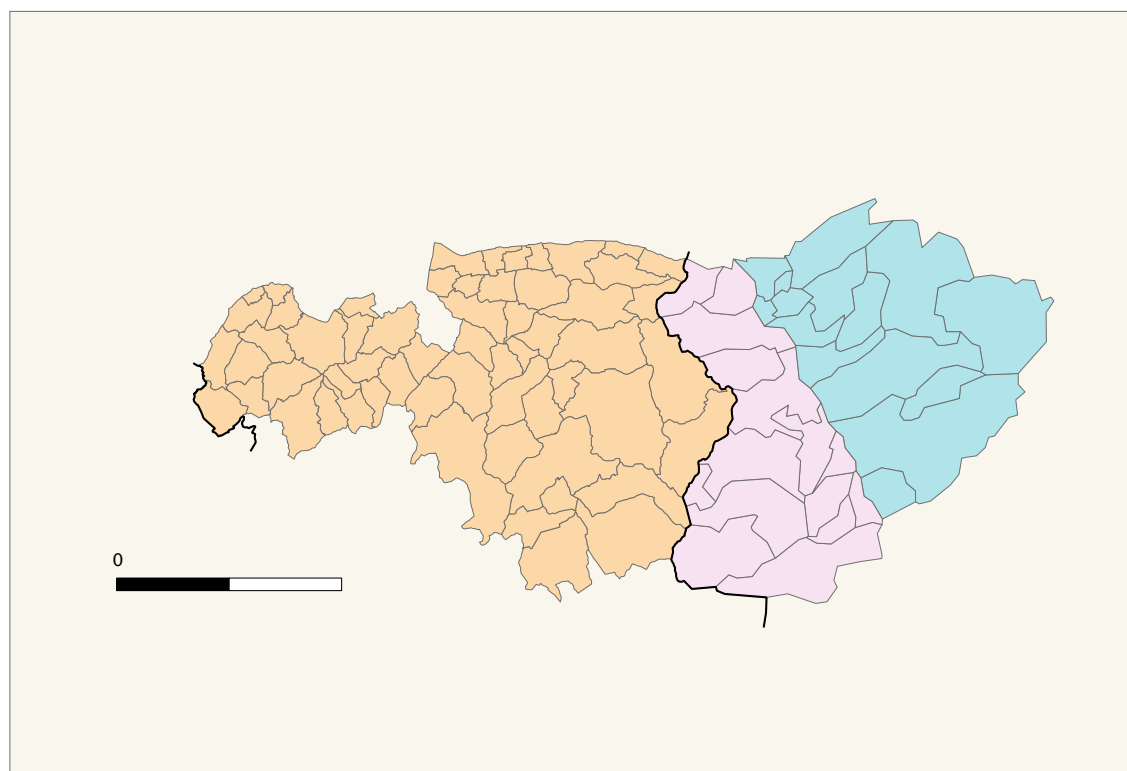


Figure 1. The limits of the three Chablais

## REFERENCES

- Cayla, N., Hobléa, F., & Gasquet, D. (2010). Guide des bonnes pratiques de médiation des géosciences sur le terrain. *Géologie de la France* (1), pp. 47-55. Disponible sur : <http://geolfrance.brgm.fr/article.asp?annee=2010&revue=1&article=8> (consulté le 4.02.2013).
- Martin, S., Regolini-Bissig, G., Perret, A., & Kozlik, L. (2010). Elaboration et évaluation des produits géotouristiques. *Téoros*, 29-2/2010. Disponible sur : <http://teoros.revues.org/898> (consulted the 13.12.2012).
- Sellier D. (2009). La vulgarisation du patrimoine géomorphologique. Objets, moyens et perspectives. *Bulletin de l'Association des Géographes Français*, 1, pp. 67-81.

## P 21.4

# Cartography of the geomorphological diversity in Derborence (Valais, Swiss Alps)

Hélène Maret

Institute of Geography and Durability, University of Lausanne (helene.maret@unil.ch)

Valuing diversity of Earth features is a quite new topic in Switzerland. A lot of studies have been conducted about geomorphosites and geoconservation but the quantification of geodiversity has almost never been studied in Lausanne. "Geodiversity is the natural range (diversity) of geological (rocks, minerals, fossils), geomorphological (landform, processes) and soils features. It includes their assemblages, relationships, properties, interpretations and systems." (Gray, 2004: 6). In other words, "geodiversity refers to the heterogeneity of abiotic nature i.e. variability of earth surface materials, forms and processes at global, regional and local scales" (Hjort and Luoto, 2012). As geodiversity has a strong spatial component, cartography is a very good way to figure it.

This study tries to assess the geomorphological diversity from the basis of a geomorphological map. The diversity is not a value but an intrinsic characteristic of geomorphological features. It means that we do not consider geomorphosites in the cartographic process. The aim of this master thesis is to assess the geomorphological diversity by finding a methodology that permits to transform a geomorphological map into a map of the geomorphological diversity. The three stages of the study are: (1) to draw a geomorphological map of the area, (2) to find an index of the geomorphological diversity and, finally, (3) to draw a map of the geomorphological diversity and find a methodology for transforming the geomorphological map into a map of geomorphological diversity.

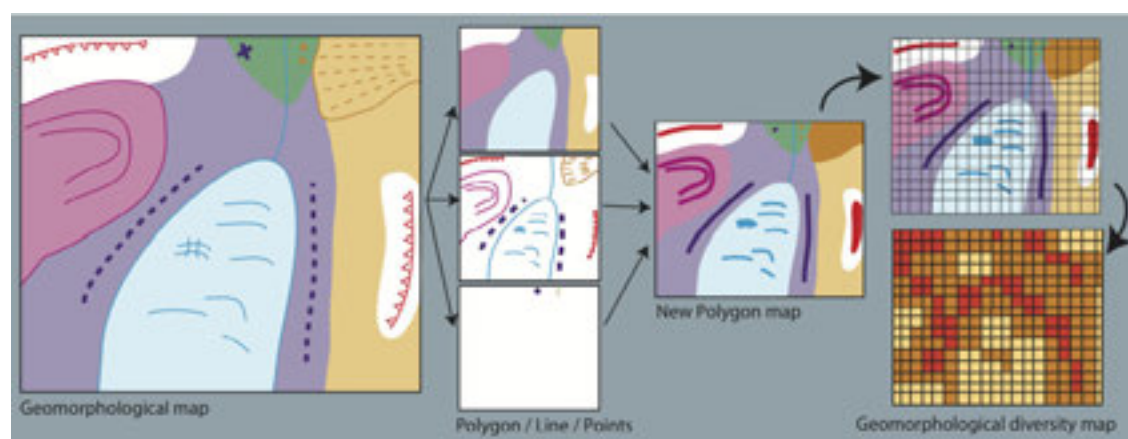


Figure 1. From a geomorphological map to the geomorphological diversity map

As represented in figure 1, geomorphological maps permit us to represent the main processes and the forms. This vector map is subdivided in three layers: points, lines and surfaces. The surfaces represent the processes: one colour per processes and no colour (white) for erosional processes. The lines and points can represent real forms (like moraines or rivers) or only be graphic (the direction of the debris fans for example). The next stage is to transform the three layers in one new polygon layer. Lines and points have to be transformed in polygons if they represent a form. New colors will appear: The debris fan in the upper right for example. From this new map, we will have to put a grid on it and calculate the geomorphological diversity index for each pixel.

Mapping geodiversity is a quite new topic in Switzerland. Although the diversity is meant here as the "intrinsic" diversity of geomorphological features without considering their value, this study could initiate a new value to consider when assessing geomorphosites. On the other hand, geodiversity assessment can also be very helpful for geoconservation.

## REFERENCES

- Gray, M. 2004: Geodiversity: valuing and conserving abiotic nature. Chichester : John Wiley et Sons Ltd.  
 Hjort, J., et Luoto, M. 2012: Can geodiversity be predicted from space? *Geomorphology*, 153, 74-80.

## P 21.5

### The revision of the Swiss Inventory of Geosites (2006-2012)

Emmanuel Reynard<sup>1</sup>, †Jean-Pierre Berger<sup>2</sup>, Monica Constandache<sup>1,2</sup>, Joëlle Dumas<sup>2</sup>, Markus Felber<sup>3</sup>, Lucien Grangier<sup>1</sup>, Philipp Häuselmann<sup>4</sup>, Pierre-Yves Jeannin<sup>4</sup>, Simon Martin<sup>1</sup>, Géraldine Regolini<sup>1</sup>

<sup>1</sup> University of Lausanne, Institute of Geography and Sustainability, CH-1015 Lausanne (emmanuel.reynard@unil.ch)

<sup>2</sup> University of Fribourg, Department of Geosciences, CH-1700 Fribourg

<sup>3</sup> Consulenze geologiche e ambientali, CH-6834 Morbio Inferiore

<sup>4</sup> Swiss Institute for Speleology and Karst Studies, CH-2301 La-Chaux-de-Fonds

Switzerland has a long history of geoconservation but it is only during the last two decades that a growing attention has been given to geoheritage protection and promotion (Reynard, 2012). In order to disseminate knowledge of Swiss geoheritage and to encourage the Swiss Confederation and the cantons to protect this heritage accordingly, the Swiss Academy of Sciences (SCNAT) created a working group on Geotopes in 1993. The working group undertook the compilation of a list of geosites of national importance. This work was not a real inventory, based on a common methodology, but rather a list of proposals made by experts from various parts of the country, various fields (palaeontology, mineralogy, geomorphology, etc.), and various institutions (cantonal administrations, nature historical museums, universities, etc.). More than 800 proposals were received from which the working group retained 401 geosites.

This list suffered several problems. One of them was its heterogeneity both in terms of content (regional discrepancy, differences between the various fields of Earth sciences) and of form (some proposals were very well documented in spite of others which were limited to the name of the site without any details of perimeter and description). Moreover, there was no information in digital form.

As a result, a revision of the inventory was carried out in 2006 by the working group, with the financial support of the SCNAT and the Federal Office for the Environment (FOEN). The revision was both formal and digital. A relational database was created and hosted on the SCNAT server. It allowed project contributors to introduce information in the system by completing a form from their office. In parallel, all the geographical information – especially the perimeters – was managed within a Geographical Information System (GIS) in order to simplify use by the public administrations. At the end of the project, the list was published on the mapviewer of the Swiss Confederation (<http://map.geo.admin.ch/>) and on the SCNAT website (<http://www.geosciences.scnat.ch>). Finally, a book, containing the list of Swiss geosites and a selection of the most emblematic sites, described in more detail, will be published in 2014.

In terms of content, the revision of the inventory needed a huge amount of homogenization work. A lot of data was added mainly because most of the geosites were poorly detailed in the 1999 inventory. Several sites were merged, others were abandoned because their national relevance was debatable. Moreover, a large survey was carried out to add new sites, especially for regions as well as fields of Earth sciences that were missing in the 1999 inventory. Also, some sites, which were not known in the 1990s, could be added. A good example is the Courtedoux geosite where numerous dinosaur tracks were discovered in 2000 during the construction of the A16 highway and that has gained international recognition today. The Glarner Hauptüberschiebung / Sardona Tektonic Arena, in the Cantons of Glarus, St. Gallen and Graubünden, is another good example. As a matter of fact, though the Glarus overthrust had already been recognized since the mid-19th century as one of the prominent examples of alpine tectonic history, it was curiously not proposed in the 1999 inventory. In the meantime, the site has been inscribed as a World Heritage Site by the UNESCO in 2008 and was added to the Swiss inventory of geosites.

An initial list of 248 geosites was published in 2008, while the final list (322 sites) was published in 2012 (Reynard et al., 2012). This inventory stimulated an interesting debate around the generic name that should be given to it. According to the FOEN, the terms “inventory” and “national importance” as used in 1999 (SCNAT,) – should be avoided today because such references could create a confusion with the official inventories carried out based on the Nature Protection Act. Finally, it was decided to call it the “Swiss Inventory of Geosites”. The next steps will be to distribute the inventory to Swiss cantonal administrations – in order to include its results in their land planning strategies – as well as to the managers of the new natural parks currently being created in Switzerland.

#### Acknowledgments

The inventory was financed by the Swiss Academy of Natural Sciences (SCNAT) and by the Federal Office for the Environment (FOEN). It received technical support from the Faculty of Geosciences and Environment of Lausanne University.

## REFERENCES

- Reynard, E., †Berger, J.-P., Constandache, M., Felber, M., Grangier, L., Häuselmann, P., Jeannin, P.-Y. & Martin, S. 2012: Révision de l'inventaire des géotopes suisses : rapport final. Lausanne, Groupe de travail pour les géotopes en Suisse. 45 p.
- Reynard E. 2012: Geoheritage protection and promotion in Switzerland. *European Geologist*. 34, 44-47.



## 23. Symposium in Human Geography

Olivier Graefe & Martin Müller

*Swiss Geography Association (ASG)*

### TALKS:

- 23.1 Berndt C.: Behavioral economics, experimentalism and the marketization of development
- 23.2 Forêt P.: Cycles and Events in Environmental History: The Return of Greenness in Victoria Harbour
- 23.3 Guelat J., Kaenzig R., Piguet E.: Environmental change and human migration: state of the art and new research results
- 23.4 Haisch, T.: Individual versus regional economic resilience: Perceptions of crises and resilience in resource-dependent communities
- 23.5 Kern A.: Manpower agencies in Nepal and their contested function of facilitation
- 23.6 Laketa S.: Youth and Affective Geopolitics of Everyday Life in Bosnia and Herzegovina
- 23.7 Mayer H., Baumgartner D.: The federal strategy for rural and mountain areas in Switzerland: Finding ways to embed endogenous territorial development into a coherent national framework
- 23.8 Mayer H., Bürcher S., Habersetzer A.: Entrepreneurship in peripheral regions: Conceptual approaches to studying entrepreneurial heritage and embeddedness from an evolutionary perspective
- 23.9 Militz E.: Europe as identifier - empirical insights from Azerbaijan
- 23.10 Raeymaekers T., Vogel C.: The geography of property: a case study from the Democratic Republic of Congo (DRC)
- 23.11 Rattu P.: Gouvernamentalité néolibérale de l'eau en Suisse: dynamiques en évolution, entre centralisation et renforcement des administrations locales
- 23.12 Sontowski S.: Biometric border control in the making
- 23.13 Sudmeier-Rieux K., Penna I., Jaquet S., Kaenzig R., Schwilch G., Jaboyedoff M., Liniger H.: Understanding migration impacts on sustainable land management. Case studies from Bolivian and Nepalese mountain populations.

## 23.1

# Behavioral economics, experimentalism and the marketization of development

Berndt Christian

*Department of Geography, University of Zurich, Winterthurerstrasse 190, CH-8057 Zürich (christian.berndt@geo.uzh.ch)*

For quite some time now, the market has been considered as the panacea for development in the global south. A heterogeneous development community is actively implicated in the extension of capitalist market relations and/or the reconfiguration of the ways in which people and places in the global south are articulated with global commodity circuits (*marketization*). Aiming at the mobilization of the poorest segments of the population, policies travel under catchy slogans such as “markets for the poor” (M4P) and connect to established academic models such as the global value chain. What is promised in this context is the improvement of individual livelihoods by overcoming perceived obstacles to market-integration. In this paper I engage with the “marketization of development” from a perspective that draws inspiration from performativity and governmentality studies, developing my argument in three steps:

*First*, although the drive towards a marketization of development is already well documented in the academic literature, it is often overlooked that underlying this drive is a profound shift in the way the market is conceptualized. This is connected to the ongoing transformation of development economics and economics more generally and, as a result of this, economic policy intervention and formulation. Just as in other economic sub-disciplines the old neoclassical orthodoxy has been challenged by behavioral and experimental approaches. Development programs and policies are increasingly legitimated in opposition to the neoclassical market, the implementation of the GVC concept, for instance, rationalized with an apparently more realistic treatment of market integration. In sum, in this emergent new orthodoxy it seems that the rational market centered on the *homo economicus* ceases to be the model for human action.

*Second*, the emergence of this new orthodoxy is accompanied by a reorientation with regard to the target of market-oriented development policies. It is no longer the failing market as an institution to which policy interventions are directed but the failing market subject. Rather than focusing on institutions that may resolve problems between people, emphasis is put on problems “within a person” (Mullainathan 2005: 33). As a result of this, market-based development has turned to behavioral engineering, actively formulated to address the bounded rationality or “irrationality” of the subject of development (e.g. World Bank 2010). In the typical discourse of economic behavioralism attention is directed to “self-control problems”, “loss aversion”, and “hyperbolic discounting”, and concrete policies are formulated with the help of well-known prompts such as the ones provided by Richard Thaler (e.g. Thaler/Sunstein 2008). Not surprisingly given the self-proclaimed birth of “libertarian paternalism” as a new movement (Thaler/Sunstein 2008: 5), in its developmentalist cloth behavioral engineering comes with only thinly disguised paternalistic undertones, “short-termism” and “impatience” being blamed for suboptimal development outcomes and behavioral anomalies regarded as being particularly wide-spread in the global south (Anderson/Stamoulis 2006: 12, 17).

The third section of the paper turns to the question of how exactly the new orthodoxy works on the subject. In order to reconstruct the practical constitution of emerging market subjects I direct my attention to concrete market experiments designed to identify the best way to change suboptimal individual behavior in a development context. To this end a confusing array of technical tools and instruments is mobilized, so-called “commitment devices” designed to force individuals to voluntarily modify their behavior in the desired direction. To this end, peer pressure and competitive benchmarking play a crucial role, often actively utilizing and thereby (re)producing various registers of social difference (e.g. gender).

Heeding Mitchell’s (2007: 245) advice to focus on what economists do rather than on what they say, I conclude my paper with second thoughts on the apparent retreat of neoliberal market-thinking in the development context. For the explicit distancing from market fundamentalism notwithstanding, policy interventions at a second glance are in fact also a means to (re)stabilize the belief in the perfect, competitive market and the rational economic subject. This is for two reasons: First, there still is an unfettered belief in the inherently positive nature of the market. Applications of choice architecture and design economics to the “problem of development” are full of positive references to diversity, freedom and morality as integral parts of perfect markets. Second and relatedly, protagonists of behavioral developmentalism are at pains to stress that social engineering is only a means to achieve the perfect market as an ultimate goal. “Markets can be learnt” – this is the message. By reducing development to a technical problem of social engineering and paying little more than lip service to issues of redistribution and recognition, policy interventions designed in the name of marketization are unlikely to live up to the expectations raised by their protagonists.

## REFERENCES:

- Anderson, C.L. and Stamoulis, K. (2006): *Applying behavioural economics to international development policy*. United Nations University, World Institute for Development Economics Research (UNU-WIDER), Research Paper No. 2006/24.
- Mitchell, T. (2007): The properties of markets. In: MacKenzie D., Muniesa, F. and Siu, L. (eds), *Do Economists Make Markets? On the Performativity of Economics*, Princeton University Press, Princeton: 244-275.
- Mullainathan, S. (2005): Development economics through the lens of psychology. In: Bourguignon F. and Pleskovic, B. (eds), *Annual World Bank Conference in Development Economics 2005: Lessons of Experience*, The World Bank / Oxford University Press, New York: 45-70.
- Thaler, R.H. and Sunstein, C.R. (2008): *Nudge: Improving Decisions About Health, Wealth, And Happiness*. Yale University Press, New Haven.
- World Bank (2010): *World Development Report 2010: Development and Climate Change*. Washington.

## 23.2

## Cycles and Events in Environmental History: The Return of Greenness in Victoria Harbour

Forêt, Philippe,

*Chair of Chinese culture and Society, School of Humanities and Social Sciences, University of St. Gallen, Girtannerstrasse 6, CH-9010 St. Gallen (pforet@bluewin.ch)*

This paper will discuss circularity in the perception of the environment by using recurrence as a leading theme in the rewriting of the historical geography of Hong Kong. I will criticize the ‘artifice of good policy’ that has benefited the colonial and postcolonial administrations of Hong Kong (Ngo 1999). Impatient with the government’s uncritical approach toward history and with its heavy hand toward geography, scholars have reassessed positive clichés about Hong Kong (Tsang 2004). They have questioned why a ‘miraculous development model’ would have let the government decide alone ‘what kind of place Hong Kong had been and will be’ (Carroll 2006). They concur on the significance of place in any investigation of this terrain, where global dynamism, ruptures and connections have met the creativity of local cultures and a challenging physical environment.

Geographers may regret that the notion of ‘subjectivity in a space of disappearance’ (Abbas 1997) says little on the environmental history of that ‘space’ and on the many formulations of reality and representation allowed by the conflation of the local and global scales. As I review the research done on the politics of geographical disappearance, I will seek to answer several questions. How have official and alternative narratives of remembrance influenced public memory, urban planning, nature preservation, heritage policy, and debates about the city’s environment? How do we comprehend the environmental values and attitudes of a Chinese metropolis that experts and officials have repeatedly robbed of its past, culture, identity and sense of place?

My sources of information come mostly from fiction by writers like Dung Kai-Cheung and from the comparison of historical records to today’s advertising campaigns that promote environmental awareness.

## REFERENCES

- Abbas, A. 1997. *Hong Kong. Culture and the Politics of Disappearance*. Minneapolis MN: University of Minnesota Press, 1997.
- Carroll, J.M. 2006. “Colonial Hong Kong as a Cultural-Historical Place.” *Modern Asian Studies*, 40-2, 517-543.
- Dung, K.C. 2012. *Atlas. The Archaeology of an Imaginary City [Ditujij]*. New York NY: Columbia University press.
- Forêt P. 2007. “Kartographie der Kontinuität: Vom vormodernen Ostasien zum postmodernen Hong Kong.” In Jürg Glauser and Christian Kiening, eds. *Text-Bild-Karte. Kartographien der Vormoderne*. Freiburg: Rombach, 131-145.
- Ngo, T.W. 1999. “Industrial History and the Artifice of Laissez-faire Colonialism.” In T.W. Ngo, ed. *Hong Kong's History: State and Society under Colonial Rule*. London: Routledge, 119-140.
- Tsang, S. 2004. *A Modern History of Hong Kong*. London: I.B. Tauris.

無論身處任何一個角落...  
我們都希望  
有好的**環境**



香港特別行政區政府 環境局  
Environment Bureau Hong Kong SAR Government

Figure 1. "I Love Hong Kong. I love GREEN" poster. Environment Bureau, Hong Kong SAR Government

## 23.3

### Environmental change and human migration: state of the art and new research results

Jérémie Guélat<sup>1</sup>, Raoul Kaenzig<sup>1</sup>, Etienne Piguet<sup>1</sup>

<sup>1</sup> Institut de géographie, Université de Neuchâtel, FLSH, CH-2000 Neuchâtel  
 Jeremie.guelat@unine.ch, Raoul.kaenzig@unine.ch, Etienne.piguet@unine.ch.

The impact of environmental change on migration and the way migration can act as a response to environmental change are attracting an increasing attention from both policy-makers and researchers worldwide (Piguet 2012; Swiss Academies of Arts and Sciences 2013). Yet, knowledge in this field remains limited and fragmented (Piguet and Laczko forthcoming 2013). This paper therefore provides an overview of the environmental change – migration nexus and investigates the key issues at stake. The concepts and methods most adequate to address these relationships will also be questioned (Warner et al. 2013; Piguet 2013).

In the second part of the paper, recent field research results from Bolivia and the Philippines will focus on the differentiate impact of glacial retreat (slow onset) and hurricanes (sudden onset) on population displacements including the social and political context in which the topic emerged, states' policy responses and the views of different institutional actors. Different types of human (im-)mobility linked to environmental degradation will be addressed, such as rural-urban migration and circular movements between Bolivian highlands and La Paz/El Alto, as well as urban forced displacements, immobility and flood-induced resettlement in Metro Manila's vulnerable riverways.

Whereas most empirical studies focus on the rural areas only, this paper also addresses the emerging issue of urban areas. In both case studies, migration flows are going towards major cities even if these areas are themselves characterized by a high environmental vulnerability and in some cases internal displacements of populations.

#### REFERENCES

- Piguet, E. 2012. Migration: The drivers of human migration. *Nature Clim. Change* 2 (6):400-401.
- . 2013. From "primitive migration" to "climate refugees" - The curious fate of the natural environment in migration studies. *Annals of the Association of American Geographers* 103 (1):148-162.
- Piguet, E., and F. Laczko eds. forthcoming 2013. *People on the move in a changing climate: Comparing the impact of environmental change in different regions of the world*: Springer.
- Swiss Academies of Arts and Sciences. 2013. Environmental change and migration in developing countries. *FactSheet* - [www.akademien-schweiz.ch/de/factsheets](http://www.akademien-schweiz.ch/de/factsheets).
- Warner, K., T. Afifi, W. Kälin, S. Leckie, B. Ferris, S. F. Martin, and D. J. Wrathall. 2013. Changing climate, moving people: framing migration displacement and planned relocation. *UNU-EHS Policy Brief* (81).

## 23.4

# Individual versus regional economic resilience: Perceptions of crises and resilience in resource-dependent communities

Tina Haisch<sup>1</sup>

<sup>1</sup>*Institute of Geography & Center for Regional Economic Development (CRED), University of Bern, Switzerland*

The current economic crisis not only challenges national economies across Europe but also stresses regional resilience, i.e. the adaptive capacity or shock resistance of regions, which at the moment is discussed in academic literature (Davies, 2011; Simmie & Martin, 2010).

From an evolutionary perspective it is argued, that recessionary shocks in the past strengthen a region's resistance and recovery to future economic shocks for example through restructuring processes from production oriented towards a more diversified economy (Martin, 2011), leading in the end to a more balanced regional incidence. This phenomenon can also be observed for the Swiss economy, which in times of the "Great Moderation" in the years after 1970, experienced a decline in volatility of growth rates compared to the period 1920-1950. Nevertheless, the resistance and recovery to economic shocks differs widely between different regions and is linked to the sectoral composition of a region's production activity (Martin 2011), trade linkages and institutions. While some studies deal with the overall economic reaction to or after economic shocks by making use of secondary data analysis across Europe (e.g. Davies 2012), only few studies investigate the interplay between different processes and perceptions of actors within a region in regard to economic resilience in detail.

In contrast to the 'adaptive cycle model' (Pendall, Foster, & Cowell, 2009; Simmie & Martin, 2010) of regional economies, in this paper it is argued that different actors (firms, organisations, associations, land owners etc.) have a very different perception and thus a different adaptive capacity with their own position within the "regional adaptive cycle". Consequently the argument, that a region as such can be classified according to the "adaptive cycle model", is challenged. Instead it is proposed that groups of similar actors (like companies in one specific industry) face the same problems and crises over time and thus have a similar adaptive capacity.

The aim of this paper is therefore to investigate the perception and the resulting behaviour and strategies of firms and other regional actors in a resource dependent community (Grindelwald, Jungfrauregion), which at the moment has to deal with several shocks and slow burns (Zweitwohnungsinitiative, strong Swiss Franc, sectoral change etc.)

For that purpose, a statistical analysis is conducted to answer the questions how have population and employment structure, GDP, number and structure of hotels, tourism infrastructure etc. changed in the last 10-20 years? Second, in-depth interviews with experts (e.g. from tourism associations or industry organisations) provide an understanding of the complex processes and different actor groups, which are coping with different problems in regard and other slow burns. Third, in a semi-structured inquiry, the different actor groups are asked directly to get insights into their actual strategies to overcome the crisis and the manifold slow burns, past problems and resulting learning processes, interaction patterns and support from public sector.

Preliminary results of the analyses are first, that indeed past 'shocks' and slow burns, lessons learned and established social and economic ties help the region now to deal with the actual insecurities. Second, different actors have a very different perception of the actual shock, in the sense that for some it is rather a chance, e.g. the "Zweitwohnungsinitiative" for the tourism industry and for others, e.g. the construction industry, it's a real shock with expected negative long-term effects. Thus, the effects of the shock are perceived very differently and the strategies developed on basis of the individual perceptions differ widely. Furthermore, the strategies are not only limited to overcome the actual disturbance but also to face on-going slow burns like e.g. the strong Swiss Franc.

## REFERENCES

- Davies, S. (2011). Regional resilience in the 2008-2010 downturn: comparative evidence from European countries. *Cambridge Journal of Regions, Economy and Society*, 4(3), 369–382. doi:10.1093/cjres/rsr019
- Martin, R. (2011). Regional economic resilience, hysteresis and recessionary shocks. *Journal of Economic Geography*, 12(1), 1–32. doi:10.1093/jeg/lbr019
- Pendall, R., Foster, K. a., & Cowell, M. (2009). Resilience and regions: building understanding of the metaphor. *Cambridge Journal of Regions, Economy and Society*, 3(1), 71–84. doi:10.1093/cjres/rsp028
- Simmie, J., & Martin, R. (2010). The economic resilience of regions: towards an evolutionary approach. *Cambridge Journal of Regions, Economy and Society*, 3(1), 27–43. doi:10.1093/cjres/rsp029

## 23.5

## Manpower agencies in Nepal and their contested function of facilitation

Kern Alice<sup>1</sup><sup>1</sup>Human Geography, Department of Geography, University of Zurich, Winterthurerstr. 190, CH-8057 Zürich (alice.kern@uzh.ch)

As the International Organization for Migration states, “facilitating migration for work can be a win-win proposition” (IOM 2013). However, Nepali manpower agents facilitating labour migration suffer from a very negative reputation. Recently, the *Neue Zürcher Zeitung* published an article about the “fraudulent job agents” in Nepal who “shamelessly” exploit the poor population (Spalinger 2013). Also the Nepali newspapers enforce this negative image. For example, the *Kathmandu Post* (2013) regularly reports fraud cases, highlighting how “unscrupulous manpower agencies have long taken advantage of the desperation of Nepali citizens.” This research project looks behind the commonplace and explores the every day practice of labour brokerage in Nepal.

The dimension of international labour migration in Nepal has become immense. Every day, almost 1500 Nepalese leave their country in order to work abroad. Currently, the number of Nepali labour migrants has reached 3 million, not including the Nepali workers in India. The number of registered recruitment companies in Nepal has reached almost 800 today. The remittances represent almost a quarter of Nepal’s GDP, presenting an integral part of the national economy. International labour migration has also significant social and political impacts on Nepal’s development. Furthermore, the destination countries, especially the Gulf States, experience diverse consequences of migration, and benefit from the availability of cheap labour. Thus, migration has become big business.

While the motivation for, as well as the consequences of, migration has been topics of intensive research, many aspects of the migration industry (Gammeltoft-Hansen & Nyberg Sorensen 2013) have remained a black box. This research project aims at opening the black box of brokering migration (Lindquist et al 2012) and analyses the important role of migrant brokers and manpower agencies. Taking Nepal as a case study, we aim at answering the following research questions: Who facilitates international labour migration in Nepal? How do migrant brokers and manpower agencies function? What role do agents and agencies play in the emerging migration industry? Considering the tension between the negative reputation and the important practice of labour brokerage in Nepal, this project is also an example of doing research in a contested field.



Figure 1. People waiting for the approval of their emigration documents at the Department of Foreign Employment (DoFE), Kathmandu, August 2013. Source: Photograph by Alice Kern.

## REFERENCES

- Gammeltoft-Hansen, T. & Nyberg Sorensen, N. (Eds.) 2013: *The Migration Industry and the Commercialization of International Migration*. Oxon: Routledge.
- International Organization for Migration (IOM) 2013: *Nepal - Facilitating Migration*. <http://www.iom.int/cms/en/sites/iom/home/where-we-work/asia-and-the-pacific/nepal.default.html?displayTab=latest-news> (25.8.2013)
- Kathmandu Post 2013: *Troubled travellers*. <http://www.ekantipur.com/the-kathmandu-post/2013/08/25/editorial/troubled-travellers/252823.html> (26.08.2013)
- Lindquist, J., Xiang, B., & Yeoh, B.S.A. 2012: *Opening the Black Box of Migration: Brokers, the Organization of Transnational Mobility and the Changing Political Economy in Asia*. *Pacific Affairs* 85 (1), 7-19.
- Spalinger, A. 2013: *Exodus junger Männer aus Nepal*. *Neue Zürcher Zeitung* 187, International, 9, 15.08.2013.

## 23.6

# Youth and Affective Geopolitics of Everyday Life in Bosnia and Herzegovina

Sunčana Laketa

*School of Geography and Development, University of Arizona, Harvill Bldg, PO Box 210076, Tucson, AZ 85721, slaketa@email.arizona.edu*

Recent years have seen a proliferation of work concerning emotions and affect throughout social sciences, and geographers as well seem to follow the trend on bringing emotions back at the focus of research. This paper is a response to the emerging literature on emotion in politics (Ó Tuathail 2003; Pain 2009; Smith 2011; Thrift 2004) and an acknowledgment of their central relevance to critical and feminist geopolitics.

Drawing from my work in the ethnically-divided country of Bosnia and Herzegovina, I investigate the mundane practices of what has been called the “geopolitics of everyday life” (Smith 2011) in order to learn how ethnic identity is embodied through a diverse range of affective and emotional socio-spatial practices. Specifically, this study is an examination of the relationship between emotions, space and identity in Mostar, a city divided between two ethnic groups – Bosniaks and Croats. I focus in particular on Mostar’s high school students where effects of the volatile political climate are most acutely felt. Namely, the specific circumstances of young people in Mostar have made them one of the most vulnerable, yet highly politically charged, citizens. Being brought up in an extremely poignant post-war atmosphere has had significant influence on this generation’s perception of the city and its spaces, as well as their different notions of identity, belonging, difference and equality. In many ways, youth in Mostar have become significant geopolitical subjects where struggles over identity, territory and domination are being waged.

The findings point to the ways the human body, with its rich sensual and sensing world, is deeply implicated in geopolitical tensions and conflicts. In this paper I open a discussion on the role of visceral experiences of identity, belonging and exclusion in geopolitics, and on the ways we need to rethink and deepen our understanding of the body in order to account for these often automatic and unconscious “gut feelings”. Specifically, this research points to a complex and intertwined relationship among the psychic, sensual and social dimensions of identity, as well as between the discourses and materialities of the body and social space. In Mostar, geopolitical subjectivities emerge through an intricate process where the social and psychic intertwine in ways that make the inside and the outside overlap.

### REFERENCES

- Ó Tuathail, G. 2003. “Just out looking for a fight”: American affect and the invasion of Iraq. *Antipode*, 35(5), 856-870.
- Pain, R. 2009. Globalized fear? Towards an emotional geopolitics. *Progress in Human Geography*, 33 (4), 466–486.
- Smith, S. 2011. ‘She says herself, “I have no future”’: love, fate and territory in Leh District, India. *Gender, Place and Culture*, 18 (4), 455–476.
- Thrift, N. 2004. Intensities of feeling: towards a spatial politics of affect. *Geografiska Annaler*, 86, 57–78.

## 23.7

### The federal strategy for rural and mountain areas in Switzerland: Finding ways to embed endogenous territorial development into a coherent national framework

Heike Mayer<sup>1</sup> & Daniel Baumgartner<sup>2</sup>

<sup>1</sup>*Institute of Geography, Economic Geography Group, University of Bern, Hallerstrasse 12, 3012 Bern*

<sup>2</sup>*Ernst Basler & Partner, Zurich*

Switzerland is a country with a long-standing tradition of balanced territorial development and strategies aimed at reducing disparities between urban and rural areas. However, federal strategies have shifted away from such a balanced perspective towards fostering regional economic growth. Such a shift towards a growth-oriented model of regional policy is in line with general trends in Europe (Pike et al. 2006). As a consequence, there is a need for strategies in support of economic growth in urban centres, while at the same time fostering sustainable, endogenous development in mountain and rural regions.

In this paper, we present the current state of development of a coherent federal framework for an endogenous development strategy for mountain and rural areas in Switzerland. In recent years, these regions were exposed to substantial economic and demographic challenges. At the same time, there has been a reappraisal of the economic relevance of some of the natural resources these regions offer. These developments have been framed by changing policy paradigms, in which policy shifted from a centralized, top-down donor-recipient model to a decentralized, bottom-up growth-oriented model (Ward & Brown 2009).

In order to cope with these challenges and changes, the Swiss parliament called for a strategy for mountain and rural areas at the federal level, which aims at fostering endogenous economic development within one single coherent framework. Yet, mountain and rural areas have heterogeneous characteristics, ranging from peri-urban towns to remote villages in the Alps. This makes the design of a coherent framework at the federal level a substantial challenge for policymakers. The paper focusses on questions about the integration of endogenous development theory into a coherent strategic governance framework at the national scale and examines the ways in which the new strategy aims at finding new solutions to managing territorial inequalities in Switzerland.

#### REFERENCES

- Pike, A., Rodriguez-Pose, A. & Thomaney, J., 2006. *Local and regional development* 1st edition., New York: Routledge.
- Ward, N., & Brown, D. L. (2009). Placing the rural in regional development. *Regional Studies*, 43(10), pp. 1237–1244.

## 23.8

## Entrepreneurship in peripheral regions: Conceptual approaches to studying entrepreneurial heritage and embeddedness from an evolutionary perspective

Heike Mayer<sup>1</sup>, Sandra Bürcher<sup>1</sup> & Antoine Habersetzer<sup>1</sup>

<sup>1</sup> Institute of Geography, Economic Geography Group, University of Bern, Hallerstrasse 12, CH-3012 Bern

Regions outside the main metropolitan areas of a nation are often characterized as periphery not only in a geographical sense: lower labor productivity, higher factor cost not only for labor, but also for capital and knowledge, lower shares of innovative activities, fragmented or 'thin' institutions and dense networks of mutual social control make them to 'entrepreneurial laggards' compared to urban growth centers (Tödtling & Trippel 2005; Karlsen et al. 2011; Lagendijk & Lorenzen 2007). Yet, some non-metropolitan areas can be very dynamic and entrepreneurial. Some areas in the periphery even host highly entrepreneurial firms, often referred to as hidden champions (Domhardt et al. 2009), which substantially contribute to a region's successful economic evolution despite its peripheral location. Such dynamic examples are of high relevance for regional policy in most Western countries including Switzerland (OECD 2009, 2011) which favor growth-oriented approaches and aim to tap endogenous entrepreneurial potential.

Yet, research in economic geography is unclear about the factors that contribute to long-term growth of a peripheral region. Is it the entrepreneur who makes the periphery successful? Or is it the particular social and economic environment, which fosters the growth of entrepreneurship? To answer these questions, the paper will conceptualize two approaches: the embeddedness and the heritage approach. Under the former, entrepreneurship is seen as an outcome (*effect*) of economic vitality of a region (Porter 1990, 1998). Thus, entrepreneurship may be a consequence of a social environment which favored entrepreneurial initiatives over time and eventually created a conducive climate for new firm creation and entrepreneurial business activity in the present. Under the heritage approach, in contrast, entrepreneurship is conceptualized as a direct driver (*cause*) of economic evolution over time. Sources of entrepreneurship are rooted in the professional and biographical traits of particular entrepreneurs and their organizations (Klepper 2001; Klepper & Buenstorf 2010). In considering a mixed methods approach to studying peripheral regions in Switzerland, the paper provides a basis for a study that is currently underway.

### REFERENCES

- Domhardt, H.-J., Hemesath, A., Kaltenecker, C., Scheck, C., & Troeger-Weiß, G., 2009. Erfolgsbedingungen von Wachstumsmotoren außerhalb der Metropolen. In G. Troeger-Weiß & H.-J. Domhardt (Eds.), *Arbeitspapiere zur Regionalentwicklung, Elektronische Schriftenreihe des Lehrstuhls Regionalentwicklung und Raumordnung* (Vol. 3). Kaiserslautern: Technische Universität Kaiserslautern.
- Karlsen, J., Isaksen, A., & Spilling, O. R., 2011. The challenge of constructing regional advantages in peripheral areas: The case of marine biotechnology in Tromsø, Norway. *Entrepreneurship & Regional Development*, 23(3-4), pp. 235–257.
- Klepper, S., & Buenstorf, G., 2010. Why does entry cluster geographically? Evidence from the US tire industry. *Journal of Urban Economics*, 68(2), pp. 103-114.
- Klepper, S., 2001. Employee startups in high-tech industries. *Industrial and Corporate Change*, 10(3), pp. 639-673.
- Lagendijk, A., & Lorenzen, A. 2007. Proximity, knowledge and innovation in peripheral regions. On the intersection between geographical and organizational proximity. *European Planning Studies*, 15(4), pp. 457-466.
- Organisation for Economic Co-Operation and Development (OECD), 2011. *OECD Territorial Reviews: Switzerland 2011*. Paris: Organisation for Economic Co-Operation and Development.
- Organisation for Economic Co-operation and Development (OECD), 2009. *Regions matter. Economic recovery, innovation and sustainable growth*, Paris: Organisation for Economic Co-Operation and Development.
- Tödtling, F. & Trippel, M., 2005: One size fits all? Towards a differentiated regional innovation policy approach. *Re-search Policy*, 34(8), pp. 1203-1219.

## 23.9

**“Europe” as identifier – empirical insights from Azerbaijan**Militz Elisabeth<sup>1</sup><sup>1</sup>*Department of Geography, University of Zurich, Winterthurerstrasse 190, CH-8057 Zurich (elisabeth.militz@geo.uzh.ch)*

Since 1996 Azerbaijan and the European Union (EU) maintain growing institutional relations under the framework of the EU-Azerbaijani Partnership and Cooperation Agreement (PCA), the European Neighbourhood Policy (ENP), as well as the Council of Europe and the Eastern Partnership (EaP) initiative. Agreements are signed between the government and the EU and most of the measures implied in them are established on institutional levels in the political, social, economic and cultural spheres. Furthermore Azerbaijan is member of a variety of “European” organisations which supposedly aim to increase cooperation on a people-to-people level by producing a defined territorial container of “Europe” within which the integrated sovereign states participate in events like the Football European Championship or the Eurovision Song Contest. For certain groups of people “Europe” seems to be a core element of identification and includes the affiliation with certain perspectives, social groups and values and a strong and distinguished differentiation from others at the same time. The “European” part of individual identification is often described as desirable and superior to identification as the national cultural Self (cf. Ismayilov 2012). But why is it so desirable to identify with “Europe” and oneself as “European”? Which meanings ascribed to this “Europe” is it that people refer to within their everyday identification? What are people’s understandings and imaginations of “Europe” and “European” values?

Regional studies literature explaining the “South Caucasus” and its “European way” often follow macro-economic and macro-political approaches to interpret state building and identity formation. By focusing on elite perspectives, models of linear development and interpreting “realities” as being mainly driven by external, political and economic forces they lack critical discussion of hegemonic power relations and often miss a reflection of the evident influences on and impacts of their research and interpretation. This paper aims to let the people in Azerbaijan talk and suggests an ethnography-based methodological procedure in order to alternatively analyse and view identification processes. The empirical material presented in this paper helps to exemplarily discuss and criticize ways of explaining the production of identity markers like “Europe” and the process of identification with those markers. Based on qualitative empirical material gathered during a field research in May 2013, I would like to point out two aspects. On the one hand I am analysing people’s understanding of “Europe” and “European” values. Local politicians and civil society activists for instance often perceive “Europe” as role model for a democratic society. Other citizens equalise “Europe” with supposedly positive connotations like “open-mindedness” and a society integrating all classes. On the other hand I am interested in the mechanisms of identification with “Europe”. By referring to the interdependency of “lack and desire” in the process of identification (cf. Lacan 1977, Stavrakakis 2008), I intend to discuss why people to some extent identify very strong with what they define as “Europe”. This question seems to be especially interesting to discuss since Stavrakakis (2007: 212) remarks that “[...] [the construction of a] European identity as a collectively appealing object of identification [...]” is not self-evident at all.

Therewith the process of identification with “Europe” is twofold. On the material side that is to discuss, “Europe” can be perceived as constituted by social practices. This materiality of “Europe” appears in the lifestyle of people, the way they dress, their choice of haircuts and clothes and the books they read. It comes to the fore when youth groups celebrate the “European Day” on May 9th or civil society initiatives include a “European” in their self-description and/or their social movement’s name as a standard procedure. The social practices, which express affiliation and differentiation as well as unification and separation, are rather embedded, influenced and shaped by social discourse and the semiotic markers of everyday life. The symbolism of “Europe”, “European” values, democracy and liberty on the one side and its opposing equivalent Other - the “Azerbaijan” produced via differentiation with its national values, conservatism and isolation - on the other side are inscribed in discursively constituted subject positions, which are in return the driving force for materially expressed everyday identification.

Based on the empirical material and the suggested theoretical perspective the paper intends to stimulate critical discussions on interpretations of identity and identification processes, which could also be enriching for a broader discussion of methods and concepts in Political Geography and regional studies. Questions of who identifies with what, how and why, who is mirroring and producing whom and how and where does this alleged identification with “Europe” come from have not been finally answered yet and the analytical approach I propose provides an opportunity to discuss possible answers.

## REFERENCES

- Ismayilov, M. 2012: State, identity, and the politics of music: Eurovision and nation-building in Azerbaijan, *Nationalities Papers*, 40 (6), 833-851.
- Lacan, J. 1977: *Écrits: A selection*. London: Tavistock.
- Stavrakakis, Y. 2007: *The Lacanian left. Psychoanalysis, theory, politics*. Edinburgh: Edinburgh University Press.
- Stavrakakis, Y. 2008: Subjectivity and the Organized Other: Between Symbolic Authority and Fantasmatic Enjoyment, *Organization Studies*, 29(07), 1037-1059.

## 23.10

## The geography of property: a case study from the Democratic Republic of Congo (DRC)

Raeymaekers Timothy and Vogel Christoph<sup>1</sup>

<sup>1</sup>*Political Geography Unit, Department of Geography, University of Zurich*

The project presented here aims to test the validity of the ‘resource curse’ paradigm through a comparative geography of transnational mineral governance in the Democratic Republic of Congo (DRC). Concentrating on the transformation of the rights of use and access to natural resources in selected mining enclaves in Katanga and South Kivu (Eastern DRC), it seeks to understand how different participants in the mining economy react to formalization incentives and how these reactions influence the regulation of the mining economy as a whole. Through this study we seek to reveal the stratified integration of Congolese minerals into the global resource industry, i.e.: how different regimes of (global) access to natural resources generate a stratified, or multi-levelled, system of production, distribution and exchange, rather than running simply “from mine to market”. To do this, we start from a more networked and interconnected understanding of the DRC’s mining economy, contrarily to the global commodity chain analysis, which dominates the current drive towards formalization (Bair 2005).

In the context of DRC’s post-war reconstruction, a range of transnational organizations currently promote radical property rights reforms in the natural resources sector. These reforms are based on the assumption that private property, or “full legal and transferable mining titles”, will ultimately benefit both user and government rights (Barry 1995:2, Geenen 2012). A constellation of (trans) national agencies promotes the full-scale privatization of property rights, particularly in artisan and small scale mining, through a three-step process of (1) *classification* (the categorization of access regimes into typologies of ‘formal’ and ‘informal’, conflict-sensitive and conflict-free frameworks), (2) *standardization* (the transformation of multiple access regimes into standardized instruments of exchange); and (3) *formalization* (the integration of these access regimes into legal categories).

The main problem with such reform programmes is that they generally misread the high degree of institutional pluralism, which typically characterizes the regulation of mineral trade and exploitation in such post-war environments (Hilson and Potter 2005, Mazalto 2009). International agencies do not usually jump into an institutional void when proposing their reforms of privatization and enhancement of formal property rights, but they typically formulate in *competition* with other systems of regulation, be they defined as ‘traditional’, ‘informal’ or ‘military’ rules of the game (Esselbein 2007, Garrett et al. 2009, see also Blomley 2003, 2010). How and in what specific institutional constellations such alternative systems of ‘power, profit and protection’ (Ballentine and Sherman 2003) currently take shape will be the particular interest of this study.

The focus of the project will be on one specific set of minerals (tantalite, tin ore and tungsten – „the three T’s“ in reform jargon) and their regulation through the ITRI Tin Supply Chain Initiative (iTSCi). In doing so the project assesses the way this reform process impacts on the performance of mineral markets in both mining areas, and which wider ramifications this reform process has for the institutional choice patterns of mine workers. In sum the study aims to provide more insights into the political ecology of natural resource markets in countries emerging from protracted armed conflict, specifically detailing (1) the transnational dimension of economic regulation and (2) its impact on the institutional choice patterns of direct natural users of natural resources in the specific case of the DRC.

### REFERENCES

- Bair, J. (2005) Global capitalism and commodity chains: looking back, going forward, in: *Competition and Change*, 9/2 (June), pp. 153-180.
- Ballentine, K. and Sherman, J. eds. (2003) *The political economy of armed conflict. Beyond greed and grievance*, Boulder & London, Lynne Rienner.
- Barry, M., ed. (1995) Regularizing informal mining: a summary of the proceedings of the international roundtable on artisanal mining organized by the World Bank, The World Bank, Industry and Energy Department, Washington, DC.
- Blomley (2003) Law, property, and the geography of violence: The frontier, the survey, and the grid, in: *Annals of the Association of American Geographers*, 93/1, pp. 121-141.
- Blomley, N. (2010) Cuts, Flows, and the Geographies of Property, in: *Law, Culture and the Humanities*, 7/2, pp. 203–216.
- Esselbein, G. (2007) *The rise and decline of the Congolese state: an analytical narrative of state-making*, Crisis States Research Centre Working Paper, London: LSE.
- Garrett, N., Sergiou, S. and Vlassenroot, K. (2009) Negotiated peace for extortion: the case of Walikale territory in eastern DR Congo, in: *Journal of Eastern African Studies*, 3/1, pp. 1-21.

- Geenen, S. (2012) A dangerous bet: The challenges of formalizing artisanal mining in the Democratic Republic of Congo, in: *Resources Policy*, 37/3 (September), pp. 322–330.
- Hilson, G., Potter, C. (2005) Structural adjustment and subsistence industry: artisanal gold mining in Ghana, in: *Development and Change*, 36 (1), 103–131.
- Mazalto, M. (2009) Governance, human rights and mining in the Democratic Republic of Congo, in: Campbell, B. (ed.), *Mining in Africa. Regulation and Development*, Pluto Press, London and New York, pp. 187–242.

## 23.11

## Gouvernementalité néolibérale de l'eau en Suisse: dynamiques en évolution, entre centralisation et renforcement des administrations locales

Rattu Paola<sup>1</sup>

<sup>1</sup> *Institut de Géographie et Durabilité, Université de Lausanne, Bâtiment Géopolis, Quartier Mouline, CH-1015 Lausanne (paola.rattu@unil.ch)*

L'eau en réseau peut être considérée comme une marchandise non coopérative (Bakker, 2005) insérée dans des cycles hydro-sociaux (Swyngedouw, 2009).

En Suisse, l'eau a historiquement été gérée à travers une forme particulière de gouvernementalité néolibérale (Foucault, 1991): les actions socialement les plus désirables apparaissent comme les seules à être rationnelles et moralement acceptables, et ainsi les individus sont encouragés à les accomplir.

Cette contribution est centrée sur un des défis auxquels cette forme de gouvernementalité a fait face au cours des dernières années, à savoir une certaine concentration (et polarisation) de la production discursive auprès de la Société Suisse de l'Industrie du Gaz et de l'Eau (SSIGE). En particulier, l'objectif de cette contribution est de comprendre les dynamiques de cette production discursive centralisée et polarisée, et comment elles interagissent avec la forme de gouvernementalité préexistante et décentralisée.

Les résultats montrent que cette production discursive concentrée et polarisée ne met pas en danger la gouvernementalité néolibérale décentralisée caractéristique de la gestion de l'eau en Suisse. Au contraire, la SSIGE semble fournir des économies d'échelle et des mécanismes de redistribution, permettant la production de campagnes de communication plus efficaces qui sont ensuite adaptées au niveau local. Ainsi, la SSIGE apparaît comme un acteur rendant possible la continuité et le renforcement d'une gouvernementalité néolibérale et de technologies de pouvoir ayant des bases locales.

Les résultats confirment aussi que la néolibéralisation est un phénomène varié et présentant une path dependence (Brenner and Theodore, 2002).

### REFERENCES

- Bakker, K. 2005: Neoliberalizing Nature? Market Environmentalism in Water Supply in England and Wales. *Annals of the Association of American Geographers*, 95(3), 542–565.
- Brenner, N., & Theodore, N. 2002: Cities and the Geographies of "Actually Existing Neoliberalism." *Antipode*, 34(3), 349–379. doi:10.1111/1467-8330.00246
- Foucault, M. 1991: Governmentality. In G. Burchell, C. Gordon, & P. Miller (Eds.), *The Foucault Effect: Studies in Governmentality* (pp. 87–104). Harvester Wheatsheaf: Hemenl Hempstead.
- Swyngedouw, E. 2009: The Political Economy and Political Ecology of Hydro-Social cycle. *Journal of Contemporary Water Research and Education*, 142(1), 56–60.

## 23.12

### Biometric border control in the making.

Sontowski Simon<sup>1</sup>

<sup>1</sup>*Department of Geography, University of Zurich, Winterthurerstrasse 190, CH-8057 Zurich (simon.sontowski@geo.uzh.ch)*

Biometric recognition technology has become an outstanding signifier of current changes in the governing of people on the move. Against the background of recent attempts to frame border control as a problem of management, government agencies and private manufacturers alike promote biometrics as a promising technological tool to facilitate and accelerate desirable cross-border travel while impeding movements deemed risky, illegitimate or undesirable. These actors portray biometrics as being able to reconcile security and speed, to transform borders into intelligent and semipermeable filters, and hence to make the international circulation of people possible.

But despite their apparent sophistication, biometric applications are by no means ready-made systems that function by default once they are implemented. Quite to the contrary, they are perpetually in the making and depend on constant socio-material practices of assembling, aligning, and adjustment. Taking their functioning for granted from the outset would overstate their coherence and reify their power. Thus, would it not make sense to turn the take on biometrics upside down and start with assuming its malfunction in order to reveal how it is set into motion? In my talk I argue that biometric technologies should not be understood as omnipotent instruments of control, but as unstable attempts to order a diffuse world in motion. Seen from this perspective, biometric innovations no longer appear as self-evident solutions, but as precarious and always contested accomplishments that remain fragile and prone to failure and need constant technological work in order to be realized, stabilized and maintained.

Against this background, in my talk I will give an insight in my current research on the European Union's border management, taking the development and intended deployment of biometric e-gates at the Schengen borders as an example. These fully automated sorting machines shall accelerate the border crossing process for pre-screened and trustworthy third-country nationals and will be part of the EU's proposed Registered Traveler Program. By tracing the emergence and preparation of this new biometric border control system, I will illustrate four main aspects: first, the geoeconomic rationality that underlies recent attempts to manage borders more efficiently; second, the role corporate actors play in providing the technological infrastructure necessary to this end; third, the interplay of technical devices and mobile bodies that e-gates perform; and fourth, the socio-material practices of assembling and aligning heterogeneous elements that make biometric border control possible in the first place.

## 23.13

## Understanding migration impacts on sustainable land management. Case studies from Bolivian and Nepalese mountain populations.

Sudmeier-Rieux, Karen<sup>1</sup>, Penna, Ivanna<sup>1</sup>, Jaquet, Stéphanie<sup>2</sup>, Kaenzig, Raoul<sup>3</sup>, Schwilch, Gudrun<sup>2</sup>, Jaboyedoff, Michel<sup>1</sup>, Liniger, Hanspeter<sup>2</sup>

<sup>1</sup> University of Lausanne, Centre for Research on Terrestrial Environment. Geopolis 3156. karen.sudmeier@unil.ch

<sup>2</sup> University of Berne, Centre for Development and Environment.

<sup>3</sup> University of Neuchâtel, Institute of Geography.

Disaster risk management, climate change and development are central current themes in understanding human-nature interactions. The 2012 IPCC Special Report on Extreme Events highlights how extreme hazard events and chronic everyday hazards (i.e. water shortages and shallow landslides) hinder sustainable development goals. A majority of disasters are thus caused by poor development and governance: people living in dangerous places, lack of disaster preparedness, unsustainable land management practices, poorly constructed roads, lack of sustainable economic activities (UNISDR 2011; IPCC 2012). Populations living in harsh environmental conditions have always adapted their living conditions through both short term coping and long term adaptation strategies. This includes choices about housing, cropping and grazing practices, economic activities as well as migration, which has been intensifying in many areas of the world in recent years (Piguet 2010).

The aim of this contribution is to analyse the complex human-environmental dynamics using the Cochabamba region of Bolivia and Panchase region of Western Nepal as examples within on-going trans-disciplinary study about out-migration of mountain populations. Bolivia and Nepal are home to some of the world's largest and poorest mountain populations, with low food and water security, where high rural-urban and foreign out-migration at time is leaving behind women and elderly to manage daily life tasks such as maintaining terraces, irrigation canals, roads, and stabilizing slopes. Although many studies have focused on the consequences of migration on destination areas, few studies have analyzed the consequences of changing demographics on land and risk management in the area of origin. By combining qualitative and quantitative methods from both physical and social sciences, this study intends to contribute to the knowledge about changes on land management in mountains being affected by changing on human and natural dynamics. The hypothesis is that both changing factors are leading to more vulnerable mountain populations, by adding stress on the adaptation capacity of agricultural practices, and the management of water, landslides, fluvial erosion and flooding.

Preliminary results point to loss of labor capacity, family and community fragmentation, impacts on education, and specially in the case of Nepal a widespread land abandonment. Income sources are also changing. In Nepal, remittance revenues are replacing traditional sources of income, whereas in Bolivia seasonal migration of mountain populations toward cash crop areas is more dominant. In Nepal, traditional caste relations are changing as lower social status groups are able to rent abandoned lands, to which they would not have had access to in the past. Likewise, the increase in road construction, closely linked to migration is a major conditioning factor for landslide occurrence, which at the same time is increasing the sediment charge in rivers. In Bolivia, mobility exacerbates the loss of knowledge transfer between generations. This loss of traditional knowledge about weather predictability and agricultural practices, and the decrease of labor force is weakening the sustainable management of the lands and leading to potential degradation. The processes of erosion may be accelerated by the change of management of lands, an issue which is still being explored by this study.

While exploring key human-nature dynamics, the findings from this study will have broad policy and practical relevance for policies and decisions related to climate change adaptation funds, disaster risk, water management, migration policies and practices of mountain populations.

### REFERENCES

- IPCC. 2012: Managing the Risks of Extreme Events and Disasters to Advance Climate Change Adaptation. A Special Report of Working Groups I and II of the Intergovernmental Panel on Climate Change eds. C. B. Field, V. Barros, T. F. Stocker, D. Qin, D. J. Dokken, K. L. Ebi, M. D. Mastrandrea, K. J. Mach, G.-K. Plattner, S. K. Allen, M. Tignor & M. P.M., 582 pp. Cambridge, UK, and New York, NY, USA.
- Piguet, E. 2010: Linking Climate Change, Environmental Degradation and Migration: a Methodological Overview. *Wiley Interdisciplinary Change*, 1, 517-524.
- UNISDR. 2011: Global Assessment Report. 178. Geneva: United Nations International Strategy for Disaster Reduction.

## 24. Sustainable Water Management – Scientific Findings from recent research

Bruno Schädler, Tobias Jonas, Massimiliano Zappa,  
Sandro Peduzzi, Daniel Hunkeler, Christian Leibundgut

*Swiss Hydrological Commission CH,  
Swiss Society for Hydrology and Limnology SGHL,  
Swiss Hydrogeological Society SGH,  
Steering Committee NRP 61*

### TALKS:

- 24.1 Fischer B., Seibert J., Stähli M.: Runoff Generation Mechanisms In A Swiss Pre Alpine Catchment By Spatial Intercomparison
- 24.2 Künze R., Lunati I.: Multiscale Methods: Tools to Balance Accuracy and Efficiency
- 24.3 Marlard A., Vouillamoz J., Weber E., Jeannin P.-Y.: Geometric and hydrological characterization of karst-system combining KARSYS approach and simulation tools - Application to Beuchire/Creugenat and Bonnefontaine/Voyeboeuf karst systems (JU, Switzerland)
- 24.4 Milano M., Ruelland D., Dezetter A., Fabre J., Servat E.: Assessing the impacts of climate change and human activities on water allocation in the Ebro catchment (Spain)
- 24.5 Rey E., Schneider F., Liniger HP., Herweg K., Weingartner R.: Climate change and socio-economic scenarios, land use modelling and water resources in an inner alpine area, Switzerland
- 24.6 Rezaeian Langeroudi S., Karimi Y.: Mashhad Plain Groundwater Quality Assessment for Drinking and Irrigation Suitability, Iran
- 24.7 Ryffel A., Celio E., Grêt-Regamey A.: HydroServ – Vulnerability of Hydrological Ecosystem Services: linking land use, hydrology and ecosystem services for sustainable water management
- 24.8 Schweizer R., Rodewald R., Liechti K., Knoefel P.: Cooperative irrigation governance in Valais: a model of sustainable water resource management?
- 24.9 Vogt M.-L., Pera S., Hamit A., Haeberlin Y., Bünzli M.-A.: Hydrochemical exploration of Ennedi, Northern Chad
- 24.10 Weijs S., Mutzner R., Parlange M.: Could electrical conductivity replace water depth in rating curves for alpine streams?

## POSTERS:

- P 24.1 Aelvoet P., Bullinger-Weber G., Le Bayon R.-C., Guenat C.: Impact Of River Restoration On Alluvial Soils
- P 24.2 Brauchli T., Weijs S., Lehning M., Huwald H.: WeSenseIt: A citizen-based observatory of water
- P 24.3 Buchs A.: The dark side of the blueprint. A reflexive analysis of watershed management in Switzerland
- P 24.4 Finger F., Bertuzzo E., Mari L., Knox A., Gatto M., Rinaldo A.: Rainfall driven cholera outbreak modelling
- P 24.5 Heimann F., Böckli M., Rickenmann D., Turowski J., Badoux A.: Bedload transport dynamics in mountain rivers – Development and application of the model sedFlow
- P 24.6 Kauzlaric M., Schädler B., Weingartner R.: Customization of a hydrological model for the estimation of water resources in an alpine karstified catchment with sparse data
- P 24.7 Gasperini G., Amadori M., Pera S., Bronzini S., Toscani A.: Geochemical characterization of Chiasso aquifer

## 24.1

# Runoff generation mechanisms in a Swiss pre alpine catchment by spatial intercomparison

Fischer, Benjamin, M. C.<sup>1</sup>, Seibert, Jan<sup>1,2</sup>, Manfred Stähli<sup>3</sup>

<sup>1</sup> University of Zurich, Department of Geography - Hydrology and Climate, Winterthurerstrasse 190, 8057 Zürich, Switzerland  
(benjamin.fischer@geo.uzh.ch)

<sup>2</sup> Uppsala University, Department of Earth Sciences, Uppsala, Sweden

<sup>3</sup> Swiss Federal Institute for Forest, Snow and Landscape Research WSL, Birmensdorf Switzerland

Mountainous headwaters are dynamic, complex and heterogeneous hydrological systems of different landscape elements in terms of topography, geology, wetlands, land use and land cover which are spatially arranged and connected. Only few catchments have been studied and long-term detailed data are sparse. This makes it difficult to identify runoff generation processes in space and time and understand the event dynamics of a region. Here we present results from a data set collected in the Zwäckentobel a 4.3 km<sup>2</sup> Swiss pre-alpine catchment with high annual precipitation input, steep and flashy character of streams and dominant wet conditions. Characteristic for mountainous catchments, the contribution and response of the Zwäckentobel to storm flow in space and time is largely unknown. This study tried to address this issue by comparing several sub-catchments. The aim was to learn from differences, similarities and to put each catchment into perspective at different scales. The basic question was whether there is a difference in response to rainfall and if so are the runoff contribution processes different? Can this be linked to catchment characteristics? For the ungauged Zwäckentobel and six sub-catchment, rainfall, runoff and isotope concentrations of the snow free season 2010 and 2011 were measured and compared with a sub-catchment with long-term observations as reference. Here we present results of this study, which show the difference in rainfall runoff response and stable isotopes. From both hydrometric and stable isotope we could identify for all streams their dominant runoff generating mechanisms. Antecedent conditions and storm size have influence on the stream response; all streams are fast responding where big rainfall events tend to have larger event water contribution while smaller events have larger pre-event contribution to stream flow. Small catchment are generally expected to react similar to storm flow, while from this study it emerges that mountainous headwaters have spatial and temporal difference in input as well as in the response of the different streams streams. The mixture of hydrometric short and the indispensable long-term observations in combination with stable isotope were valuable to increase our knowledge of hydrological processes of pre alpine headwater catchments with high precipitation input and a dynamic character. This can serve as base for a better water management in these hydrological complex regions.

## 24.2

### Multiscale Methods: Tools to Balance Accuracy and Efficiency

Künze Rouven<sup>1</sup>, Lunati Ivan<sup>1</sup>

<sup>1</sup>*Faculté des géosciences et de l'environnement, Université de Lausanne, UNIL-Mouline, CH-1015 Lausanne (rouven.kunze@unil.ch)*

Groundwater is the most important drinking water reserve worldwide. Multiple natural and anthropogenic pollution sources can affect the groundwater quality and threaten a sustainable use of this important resource. To assess risks of contamination and avoid environmental and public-health hazards, reliable predictions of flow and transport processes in the aquifer are needed.

Groundwater aquifer systems can extend horizontally over tens of kilometers with a vertical depth of more than hundred meters, but flow and transport properties vary at much smaller scale. The resolution necessary to explicitly describe this heterogeneity structure would yield to prohibitive computational costs. To overcome this limitation, approximate solutions based on upscaling procedures have been widely employed to efficiently solve large-scale field models.

In this context multiscale models gained popularity over the last decade because they allow combining upscaled with local solutions that are used to interpolate the coarse solution to the scale of interest. The major strength of these methods is the high level of flexibility towards adaptive formulations, which permit different resolution in different regions and at different times.

With the new advances recently achieved, adaptive multiscale techniques offer a general framework to balance accuracy and efficiency of the solution. However, an optimal balance depends on the specific application and on the corresponding quantities of interest. We demonstrate the potential of these methods (and in particular of the Multiscale Finite Volume (MsFV) method (Jenny et al., 2003)) by considering density-driven problems.

#### REFERENCES

- P. Jenny, S. H. Lee, and H. Tchelepi. Multi-scale finite-volume method for elliptic problems in subsurface flow simulation. *J. Comp. Phys*, 187(1):47–67, 2003.

## 24.3

### Geometric and hydrological characterization of karst-system combining KARSYS approach and simulation tools - Application to Beuchire/Creugenat and Bonnefontaine/Voyeboeuf karst systems (JU, Switzerland)

Malard Arnaud<sup>1</sup>, Vouillamoz Jonathan<sup>1</sup>, Weber Eric<sup>1</sup> & Jeannin Pierre-Yves<sup>1</sup>

<sup>1</sup>ISSKA - Swiss Institute for Speleology and Karst Studies, CH/2300 La Chaux-de-Fonds

In the frame of the Swisskarst project (part of the NRP61) and thanks to additional subsidies from the Jura Canton; karst flood hazards have been assessed in the region of Porrentruy. The well-known Beuchire/Creugenat karst system which display a discharge rate of 20 m<sup>3</sup>/s during usual flood event may represent a flood risk for the city as evidenced by strong inundation events in the past (1804, 1910, etc.).

The hydrological functioning of the system (nearly 100 km<sup>2</sup>) is quite complex as it is controlled by the activation of underground thresholds and emerging overflows which depend on the evolution of the hydraulic gradient in the conduits system (Vouillamoz et al. 2013). Hydraulic gradient rises in the upstream part of the system up to 30-40 m which significantly enlarges the underground catchment. Divergence mechanisms do occur and lead to an interconnection of adjacent karst systems. This may significantly enhance the flood risk.

The communication relates the application of the KARSYS approach (Jeannin et al. 2013) to characterize the systems of Beuchire/Creugenat and Voyeboeuf/Bonnefontaine and to implement a combined-hydrogeological simulation according to the hydraulic parameters resulting of the approach (position and geometry of the drainage axes, geometry of the catchment and sub-catchments). The simulation aims to assess the respective recharge and hydraulic functioning of the systems in order to:

- Reproduce the outlets discharge rates (permanent base springs);
- Explain the evolution of the hydraulic gradient and the activation of the overflow springs (i.e. Creugenat);
- Confirm and quantify the modalities of the diffluent mechanism between these two regional systems according to flow conditions.

The workflow includes a geometric 3d modeling of the karst aquifers and the hydraulic gradients (KARSYS approach) and a combination of two simulation tools to reproduce (i) the hydrological and (ii) the hydraulic behavior of the systems. The recharge simulation of the systems is performed using a semi-distributed routing system model RS.3.0 (e-dric 2012). This type of model focuses on refining recharge and runoff processes on the ground of the catchment -subdivided in sub-catchments. This type of model reveals particularly adapted in karst media and numerous simulation have been succeed (Weber et al. 2011, Weber et al. 2012).

In the second work-step - as the recharge, catchment and sub-catchments have been validated - a hydraulic SWMM model is established to conceive the probable geometry of the karst conduits-network based on the parameters inferred from the KARSYS approach and existing speleological surveys (conduits diameter, connection, storage, thresholds...). Thanks to valuable head measurements (borehole, pit, etc.) the consistency of the model could be checked on various location of the karst-network.

The respective discharges of the permanent springs, the activation and the discharge rate of the overflow springs as well as the oscillation of the boreholes water table have been relevantly reproduced. Exchange thresholds have been identified as well as the respective exchanged flows.

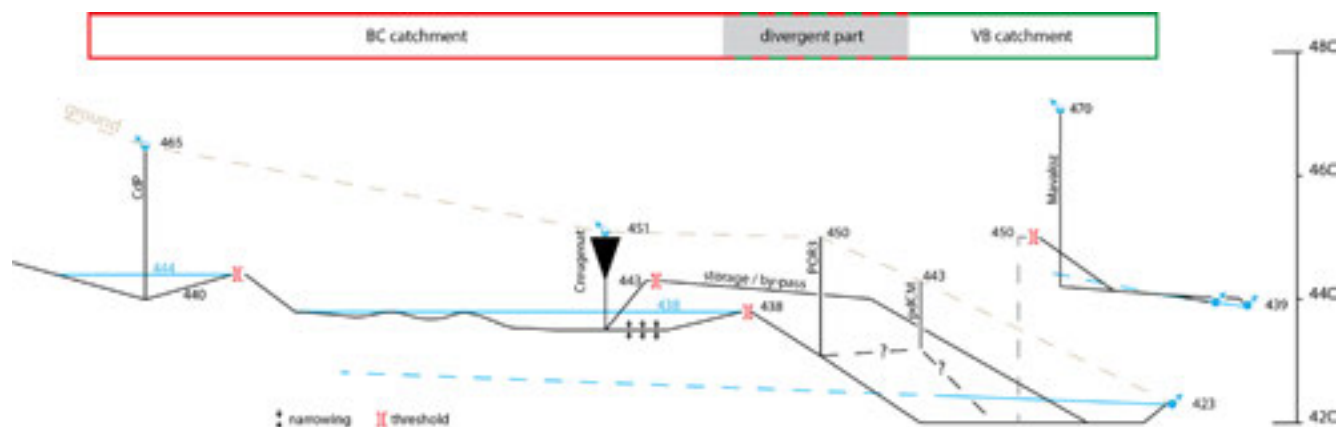


Figure 1. Construction of a probable karst conduits-network of the Beuchire/Creugenat and Voyeboeuf/Bonnefontaine karst system as inferred from the KARSYS approach, observations and measurements. These results prove the efficiency of the combination of the KARSYS approach with an appropriate simulation tools to characterize the geometry of karst systems (i.e. the conduits network), their respective functioning as well as their interaction according to hydrological conditions.

## REFERENCES

- Jeannin, P.-Y., Eichenberger, U., Sinreich, M., Vouillamoz, J., Malard, A. et al. 2013: KARSYS: a pragmatic approach to karst hydrogeological system conceptualisation. Assessment of groundwater reserves and resources in Switzerland, *Environmental Earth Sciences*, 69(3), 999-1013.
- Vouillamoz, J., Malard, A., Schwab-Rouge, G., Weber, E., Jeannin, P.-Y. 2013: Mapping flood related hazards in karst using KARSYS approach. Application to the Beuchire-Creugenat karst system (JU, Switzerland), *Proceedings of the 13th Multidisciplinary Conference on Sinkholes and the Engineering and Environmental Impacts of Karst*, held in Carlsbad, New Mexico, May 06-10, 2013. 333-342.
- Weber, E., Jeannin, P.-Y., Malard, A., Vouillamoz, J., Jordan, F. 2012: A pragmatic simulation of karst spring discharge with semidistributed models. Advantages and limits for assessing the effect of climate change, *Actes des 13. Nationalen Kongresses für Höhlenforschung*, 220-224.
- Weber, E., Jordan, F., Jeannin, P.-Y., Vouillamoz, J., Eichenberger, U. et al. 2011: Swisskarst project (NRP61): Towards a pragmatic simulation of karst spring discharge with conceptual semi-distributed model. The Flims case study (Eastern Swiss Alps), *Proceeding H2Karst, 9th Conference on Limestone Hydrogeology*, Besançon (France) 1-4 sep. 2011. 483-486.
- e-dric 2012: Manuel d'utilisation de RS3.0, unpubl. rep e-dric.ch – Ch du Rionzi 54, CH-1052 Le Mont-sur-Lausanne, Suisse.

## 24.4

### Assessing the impacts of climate change and human activities on water allocation in the Ebro catchment (Spain)

Marianne Milano<sup>1,2</sup>, Denis Ruelland<sup>3</sup>, Alain Dezetter<sup>4</sup>, Julie Fabre<sup>3</sup>, Eric Servat<sup>4</sup>

<sup>1</sup>*Institut de Géographie et Durabilité, Université de Lausanne, Batiment Géopolis, CH-1015 Lausanne (marianne.milano@unil.ch)*

<sup>2</sup>UM2, <sup>3</sup>CNRS, <sup>4</sup>IRD, UMR HydroSciences Montpellier, Place E. Bataillon, 34095 Montpellier Cedex 5, France

The Mediterranean basin has been identified as one of the world's most vulnerable regions to climatic and anthropogenic changes and constitutes a water crisis' hot spot. By the 2050 horizon, climate change will most likely contribute to the depletion of freshwater resources in already arid to semi-arid catchments. Furthermore, if domestic and agricultural water demands follow past trends, 80% of the Mediterranean basin would have to deal with severe water stress (Milano et al., 2013). The Ebro catchment, third largest Mediterranean basin, is very representative of this context. Since the late 1970s, a negative trend in river discharge has been observed at the outlet of the Ebro catchment and at several gauging stations. This can be attributed to a decrease in mean precipitation, a rise in temperature and a water consumption increase (Milano et al. 2013). Indeed, the Ebro catchment is a key element in the Spanish agricultural production with respectively 30% and 60% of the meat and fruit production of the country. Moreover, population has increased by 20% over the catchment since 1970. Finally, more than 250 storage dams have been built over the Ebro River for hydropower production and irrigation water supply purposes, hence regulating river discharge. If global changes follow past trends, the question arises whether future water needs will still be satisfied in the Ebro catchment. In order to better understand the respective influence of climatic and anthropogenic pressures on the Ebro hydrological regime, an integrated water resources modeling framework was developed. This approach confronts water supplies, generated by a conceptual rainfall-runoff model and by a storage dam module, and water demands and environmental flow requirements. Water demands were evaluated for the most water-demanding sector, i.e. irrigated agriculture (5 670 Hm<sup>3</sup>/year), and the domestic sector (252 Hm<sup>3</sup>/year), often defined as being of prior importance for water supply. The capacity of water resources to meet water demands is assessed through a water allocation index. This index depends on site priorities and supply preferences. This modeling framework was applied to 9 sub-catchments to which 11 water demand sites were attributed, in order to take into account the different hydro-climatic regimes. Results define the current pressures applied to water resources and show growing competition among users by 2050. Environmental and domestic water demands should be fully met but agricultural water demands could have to face severe water shortages during the summer season. This study identifies sub-catchments most vulnerable to climate change and anthropogenic pressures as well as those where water use tensions could occur. It also highlights the interest of integrated modeling to better sustain water management policies and to support the co-construction of scenarios between users, policy-makers and scientists.

#### REFERENCES

- Milano, M., Ruelland, D., Fernandez, S., Dezetter, A., Fabre, J., Servat, E., Fritsch, J-M., Ardoin-Bardin, S. & Thivet, G. (2013) Current state of Mediterranean water resources and future trends under climatic and anthropogenic changes. *Hydrol. Sc. J.* 58:3, 498-518.
- Milano, M., Ruelland, D., Dezetter, A., Fabre, J., Ardoin-Bardin, S. & Servat, E. (2013) Modeling the current and future capacity of water resources to meet water demands in the Ebro basin. *J. Hydrol.* In press.

## 24.5

# Climate change and socio-economic scenarios, land use modelling and water resources in an inner alpine area, Switzerland

Rey Emmanuel<sup>1</sup>, Schneider Flurina<sup>1,2</sup>, Liniger Hanspeter<sup>2</sup>, Herweg Karl<sup>2</sup> & Weingartner Rolf<sup>1</sup>

<sup>1</sup> Hydrology group, Institute of geography, University of Bern, Hallerstrasse 12, CH-3012 Bern (Emmanuel.rey@giub.unibe.ch)

<sup>2</sup> Center for development and environment, Institute of geography, University of Bern, Hallerstrasse 10, CH-3012 Bern

The MontanAqua project aims to study the water resources management in the region Sierre-Montana (Valais, Switzerland). Land use is known to have an influence on the water resources (soil moisture dynamic, soil sealing, surface runoff and deep percolation). Thus land use modelling is of importance for the water resources management.

Some land use type are more important than other regarding the water resource management, irrigated or not irrigated grassland does not exist as GIS data. Thus an actual land use map was produced using infrared imagery (Niklaus 2012, Fig.1). Land use changes are known to be mainly driven by socio-economic factors as well as climatic factors (Dolman et al. 2003). Potential future Land uses was predicted according to 1-. socio-economic and 2-. climatic/abiotic drivers :

- 4 socio-economic scenarios were developed with stakeholders (Schneider et al. 2013) between 2010 and 2012. We modeled those socio-economic scenarios into a GIS application using Python programming (ModelBuilder in ArcGIS 10) to get a cartographic transcription of the wishes of the stakeholders for their region in 2050.
- Uncorrelated climatic and abiotic drivers were used in a BIOMOD2 (Georges et al. 2013) framework. 4 models were used: Maximum Entropy (MAXENT), Multiple Adaptive Regression Splines (MARS), Classification Tree Analysis (CTA) and the Flexible Discriminant Analysis (FDA) to predict the actual grassland in our study region. Climatic scenarios were then introduced into the models to predict potential land use in 2050 driven only by climatic and abiotic factors

Future work will be to cross the different land use maps obtained by the two models and to use them to implement soil moisture and evaporation data for the near-future in the region Sierre-Montana.

### REFERENCES

- Rey E., Kauzlaric M., Herweg K., Weingartner R., Liniger H & Schädler B., 2013. Approching water stress in the alps – water management options in the Crans-Montana-Sierre region, Valais, Switzerland (MontanAqua). Submitted. La Houille Blanche.
- Niklaus M., 2012. An Object-oriented Approach for Mapping Current Land Use/Land Cover in the Study Area Crans-Montana-Sierre, Valais. MSc, Geography Institute, University of Bern
- Dolman A.J., Verhagen A. & Rovers C.A., 2003. Global environmental change and land use. Kluwer Academic Publisher. Dordrecht.
- Schneider F. & Rist S. 2013. Co-constructing development scenarios for sustainable water governance by stakeholders and scientists. Journal Water resource management, submitted.
- Georges D. & Thuiller W., 2012. An example of species distribution modelling with biomod2. biomod2 version : 2.0.17

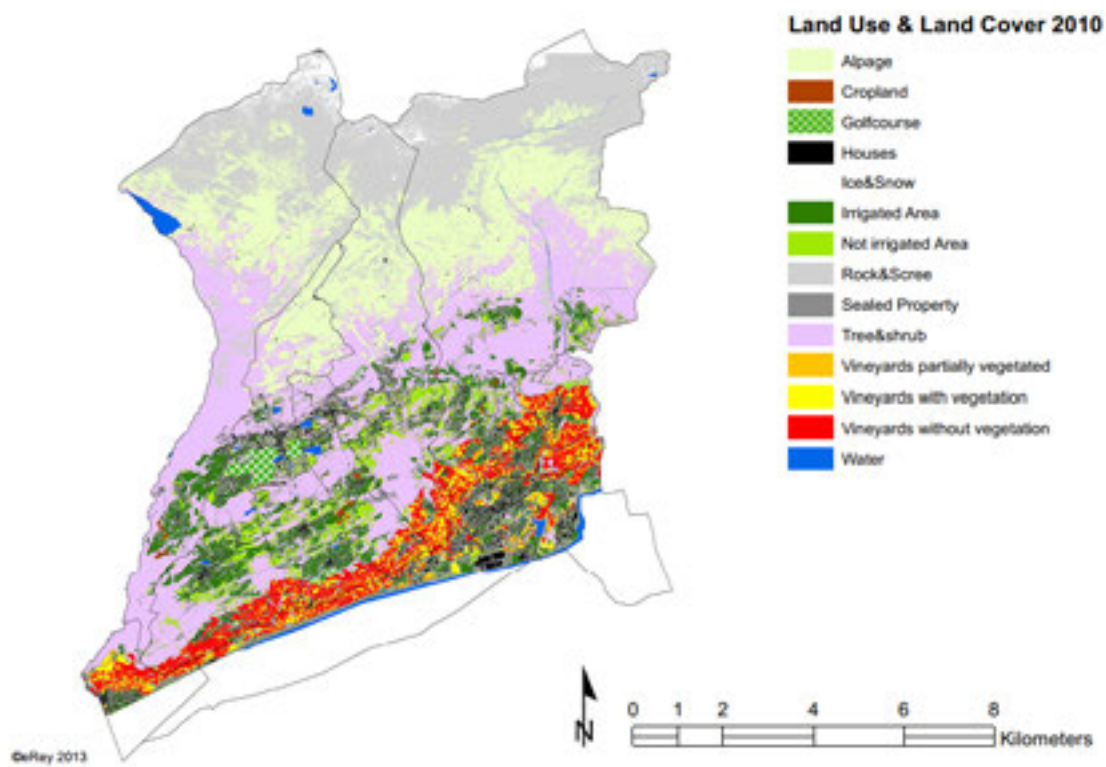


Figure 1: Actual land use in the Sierre-Crans-Montana region (Niklaus 2012)

## 24.6

# Mashhad Plain Groundwater Quality Assessment for Drinking and Irrigation Suitability, Iran

Rezaeian Langeroudi Saeed <sup>1</sup>, Karimi Yavar <sup>2</sup>

<sup>1</sup> M.Sc. of sedimentology, geology group, Teacher-training University

<sup>2</sup> M.Sc. of hydrology, geology group, Teacher- training University

Mashhad plain which belongs to the Kashafrud catchment with area more than 16500 Km<sup>2</sup>, located between Binaloud and Hezarmasjed mountains (Fig. 1). In order to investigation of groundwater quality characteristics in Mashhad plain, 42 data from water of well belong to 2012 selected to processing and interpretation. All data were processed for determination of groundwater quality such as magnesium adsorption rate (MAR), solution sodium percent (SSP), residual sodium bicarbonate (RSBC), permeability index (PI), Kelly ratio (KR) and sodium adsorption ratio (SAR) after editing of data. According to Piper diagram the groundwater type of the study area is currently Na+Cl-SO<sub>4</sub><sup>2-</sup> (Piper, 1994). Assessment of the suitability for drinking and domestic consumption was evaluated using Schoeller diagram as well as comparing the hydrogeochemical parameters of groundwater in the study area with the prescribed specification of World Health Organization (WHO, 2004). On the basis of Schoeller diagram, the water is unsuitable for drinking and domestic uses (Schoeller, 1955). According to the electric conductivity (EC) and SAR calculation the most dominant classes (C4-S4, C4-S2, C4-S3 and C3-S2) were found. The salinity hazard for water samples in Mashhad Plain is classified as high (50%) and very high (50%). Sodium content in above 85% of water samples collected is regarded as high and is not suitable for irrigation purposes. Thus, high salinity, SAR and Na% in most water samples have restricted the water quality for irrigation uses. Investigation and interpretation of hydrogeochemistry data indicated that SAR and total dissolved solid (TDS) amounts from northwest to southeast of the plain increase because of huge amount of marl and evaporate sediments in the north-eastern part of the study area (Fig. 2). On the other hand, topography map and curves of water table changes indicate that the plain recharge from NW and discharge to SE.

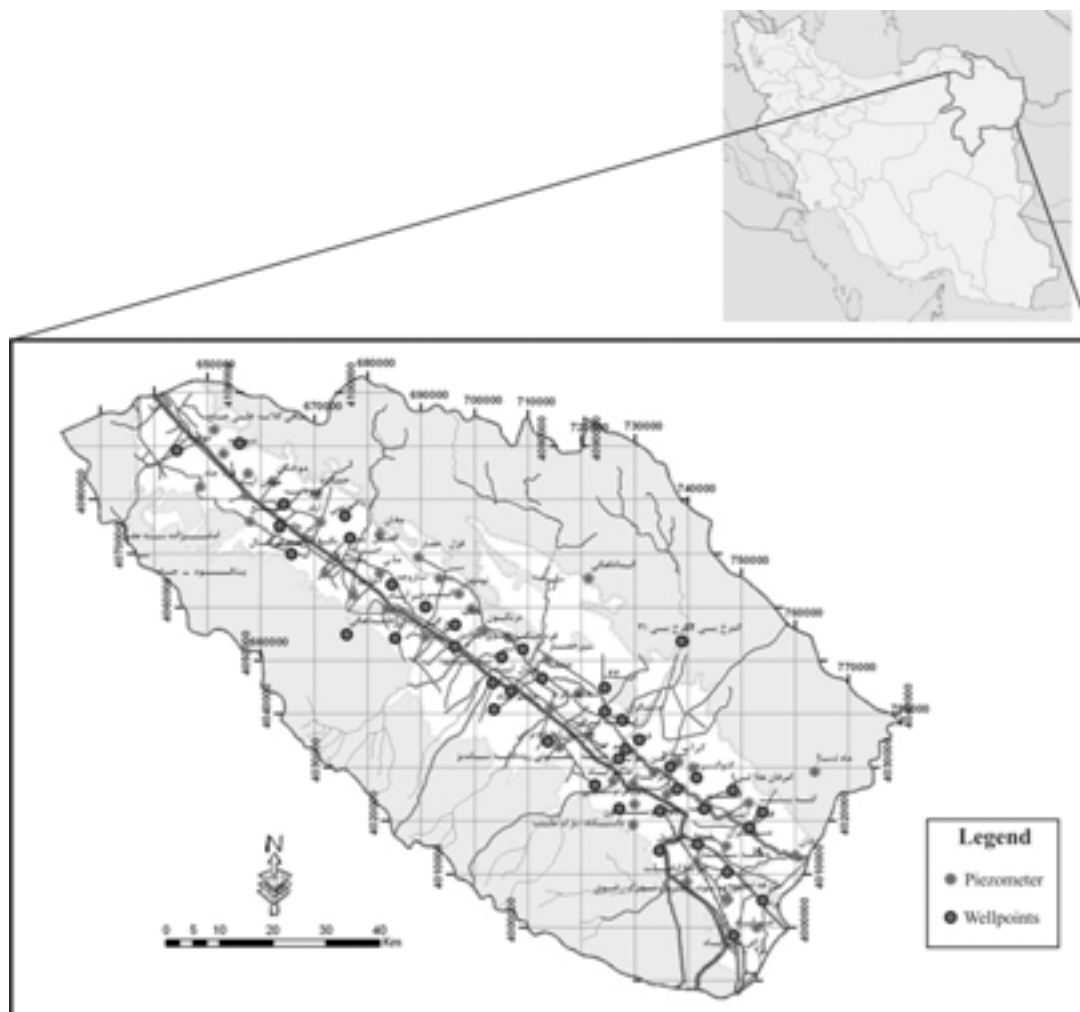


Figure 1. Location of Mashhad Plain (Geological Survey of Iran, 2006).

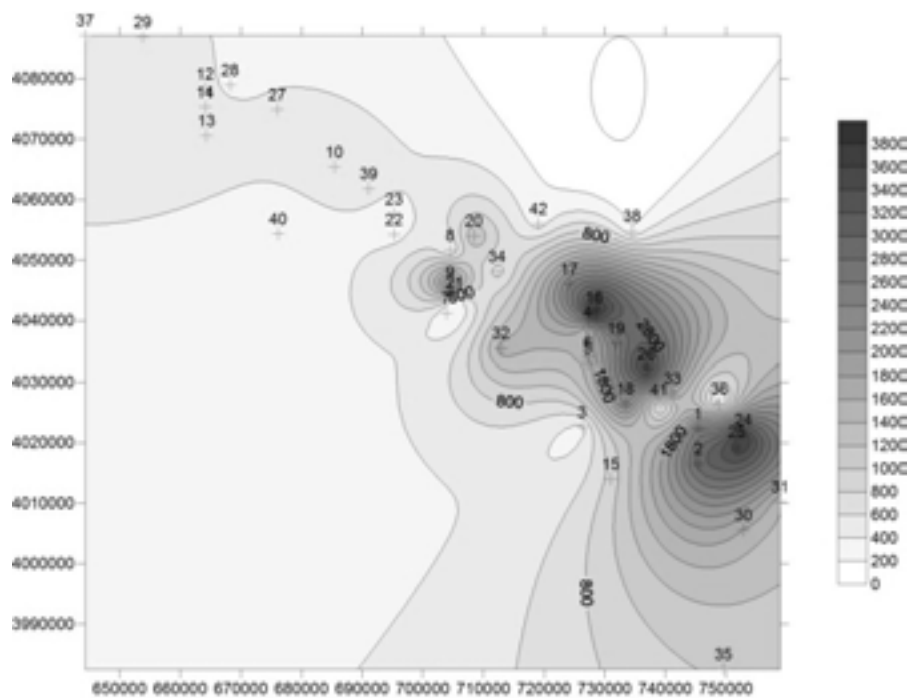


Figure 2. Distribution map of TDS parameter in the study area.

#### REFERENCES

- Piper, A.M., 1994: A graphical procedure in the geochemical interpretation of water analysis. *Am. Geophys. Union Trans.*, 25, 914-928.
- Schoeller, H., 1955: *Geochimie des eaux souterrains*. Rev. Inst. Franc. Petrole. Paris, (10) 3, p. 181-213.
- World Health Organization, 2004: „Guidelines for Drinking Water Quality“, 1, Recommendations (3rd ed.), WHO, Geneva.
- Geological Survey of Iran, 2006: Engineering geological map of Khorasan-Razavi.

## 24.7

### HydroServ – Vulnerability of Hydrological Ecosystem Services: linking land use, hydrology and ecosystem services for sustainable water management

Ryffel Andrea<sup>1</sup>, Celio Enrico<sup>2</sup> & Grêt-Regamey Adrienne<sup>1</sup>

<sup>1</sup>Planning of Landscape and Urban Systems, ETH Zurich, Wolfgang-Pauli-Str. 15, CH-8093 Zurich (ryffel@nsl.ethz.ch)

<sup>2</sup>Planning of Landscape and Urban Systems, ETH Zurich, Wolfgang-Pauli-Str. 15, CH-8093 Zurich

Sustainable water management implies addressing both human needs for natural resources delivery and the state of the natural system. In order to support decision-making, a thorough understanding on how to link the human and the natural spheres is required. The NRP 61 project 'HydroServ' deals with the vulnerability of hydrological ecosystem services (HES) resulting from societal changes to the natural system. The interdisciplinary project links land use, hydrology and ecosystem service valuation for fostering the understanding of the value chain of HES under uncertain changes of climate and land use, using flood protection HES as an example.

We present an integrative framework that links results from a land use model, a hydrological model and of HES valuation in a Bayesian Network (BN). The key root nodes include precipitation and land use changes. These states of the natural system are transformed into monetary values by adding a cost factor and stated preferences. The BN is developed in two directions to model (1) potential flood damage costs and (2) willingness to pay for flood protection HES.

The resulting monetary values are compared to see whether land management can serve as a partial substitution to technical flood protection measures. The results allow for (1) a comparison of the monetary values of flood damage costs and willingness to pay for flood protection HES, and (2) a comparison of the uncertainties inherent in the modeling of damage costs and the willingness to pay.

Finally, we reflect trade-offs between technical measures and land use management in terms of monetary efficacy in order to reduce flood hazards. The same integrative approach can be applied to quantify other HES and may therefore support sustainable water management.

## 24.8

## Cooperative irrigation governance in Valais: a model of sustainable water resource management?

Rémi Schweizer <sup>1</sup>, Raimund Rodewald <sup>2</sup>, Karina Liechti <sup>2</sup>, Peter Knoepfel <sup>1</sup>

<sup>1</sup> Swiss Graduate School of Public Administration (IDHEAP, Lausanne University), Quartier UNIL Mouline, CH-1015 Lausanne (remi.schweizer@unil.ch, peter.knoepfel@unil.ch)

<sup>2</sup> Swiss Foundation for Landscape Conservation (SL), Schwarzenburgstrasse 11, CH-3007 Bern (r.rodewald@sl-fp.ch, k.liechti@sl-fp.ch)

As in other mountain regions, meadows in dry Alpine valleys have been irrigated from time immemorial. The Swiss canton of Valais, characterised by spectacular and century-old water channels (FR: *bisses* / DE: *Suonen*), makes no exception. Showing long trajectories of historical continuity, these *bisses* constitute what the literature often refers to as *common-pool resources* (CPR, Ostrom 1990). Far from representing the relics of a bygone agro-pastoral age, they still provide a wide range of services that are crucial not only to the mountain communities, but also to the people living downhill: water provision for the irrigation of agricultural land (meadows, vineyards, orchards), biodiversity support and landscape formation (ecoservices), regulation of floods, socio-cultural and touristic services. Constructed, maintained, and regulated by local communities or users' groups (*consortages* / *Geteiltschaften*), *bisses* have been traditionally characterised by cooperative governance structures the robust, enduring and sustainable nature of which has been highlighted many times (e.g., Ostrom 1990, Crook 1997). Long before concepts such as "participation" and "integration" became matters of concern and begun being advocated for in the literature (e.g., Ansell & Gash 2008, Bäckstrand et al. 2010), the Valaisan irrigation systems thus offered examples of cooperative and participative water management. Hence, they provide rare empirical settings to study such forms of governance on the long-term, in a context that has experienced major changes during the last century, (diversification of water and land uses, arrival of new actors in previously enclosed arenas, etc.).

Against this background, the NRP 61 project *Water channels – a model for sustainable management* aimed at offering a holistic appraisal of these cooperative models of governance, with specific *foci* on the analysis of the alterations they have experienced in the last decades, their capacity to integrate new actors, and their impacts in terms of sustainability. Relying on a qualitative (participant observations, semi-structured interviews) and interdisciplinary (at the crossroad of political sciences, human geography, and institutional resource economics) approach, the project applied a resource-based and actor-centred perspective to five in-depth case studies (*bisse Vieux* in Nendaz, *bisse de Tsa Crêta* in Mont-Noble, *Torrent-Neuf* in Savièse, *Grossa* in Birgisch, *Niwärch* in Ausserberg).

The goal of this contribution is to present the main results of this three-year research project (to be published in a collective book, Schweizer et al. *in press*). Characterized by a diachronic approach (comparison of two periods throughout the 20<sup>th</sup> century), the five case studies proved to be rich in theoretical and empirical findings. Our results highlighted, first, the changing nature of the traditional cooperative models of governance. Today's *bisses* are not managed as they were yesterday, and politico-administrative as well as touristic actors appeared to play a critical role in their evolution and survival. Second, our analysis showed that the sustainable character of the cooperative models of governance does not go without saying. Those models had strengths as well as weaknesses, notably on a social level. *Bisses* and *consortages* were, in particular, characterized by a strong exclusivity of access that tends to reproduce rather than reduce social inequalities within the community, and to bring them closer to *clubs* rather than to *common-pool resources*. All in all, these results challenge the rosy picture generally associated with cooperative models of governance in the literature, and demonstrate that the path towards sustainability is a complex one, in which a multitude of actors, interests, and strategies interact.

### REFERENCES

- Ansell C. & Gash A. 2008: Collaborative governance in theory and practice. *Journal of public administration research and theory* 18, 543-571.
- Bäckstrand K., Khan J., Kronsell A., Lövbrand E. (Eds) 2010: *Environmental Politics and Deliberative Democracy. Examining the Promise of New Modes of Governance*. Edward Edgar, Cheltenham.
- Crook D. 1997: *Sustainable mountain irrigation ? The bisses of the Valais, Switzerland : a holistic appraisal*. University of Huddersfield.
- Ostrom E. 1990: *Governing the Commons: the Evolution of Institutions for Collective Action*. Cambridge University Press, Cambridge.
- Schweizer R., Rodewald R., Liechti K. & Knoepfel P. *in press*: *Des systèmes d'irrigation alpins entre gouvernance communautaire et étatique - Alpine Bewässerungssysteme zwischen Genossenschaft und Staat*. Rüegger Verlag, Zurich.

## 24.9

### Hydrochemical exploration of Ennedi, Northern Chad

Marie-Louise Vogt<sup>1</sup>, Sebastian Pera<sup>2</sup>, Abderamane Hamit<sup>3</sup>, Yves Haeberlin<sup>1</sup>, Marc-André Bünzli<sup>4</sup>

<sup>1</sup> UNOSAT, United Nations Institute for Training and Research (UNITAR), Palais des Nations, CH-1211 Genève (marie-louise.vogt@unitar.org)

<sup>2</sup> Institute of Earth Sciences, Scuola Universitaria Professionale della Svizzera Italiana (SUPSI), CH-6952 Lugano

<sup>3</sup> Département de Géologie, Faculté des Sciences Exactes et Appliquées, Université de N'Djaména, Tchad

<sup>4</sup> Humanitarian Aid and SHA, Swiss Agency for Development and Cooperation (SDC), Federal Department of Foreign Affairs, CH-3003 Bern

The Ennedi is a vast region of northern Chad, at the southern edge of the northern middle of the Sahara desert. A remarkable hydrological and hydrogeological regime characterizes the area, despite the aridity that prevails in most of the region: the Ounianga lakes (Ounianga Kébir and Ounianga Seghir), and the Archéï and Bachiquélé springs are some examples of groundwater occurrence indicating that significant resources may be present underground.

The Nubian Sandstone Aquifer System (NSAS) is believed to represent a thousand meter aquifer, with water having last being recharged during the Holocene. Referring to the current coupe geologic profile for the area (Mahamoud, 1986), mesozoic rocks are laying onto the palaeozoic sedimentary rocks that outcrop in the Ennedi region and in the area of Faya Largeau, south of Erdis plateau and Tibesti massif. Although NSAS is commonly considered to be composed only by Mesozoic formations, an increasing consensus (REF) consider that it should also comprise the Palaeozoic formations. In the cited regions, springs and artesian phenomena occur frequently.

The Ennedi Plateau is a thousand meters sedimentary pile of Palaeozoic sedimentary rocks, mainly sandstones (Boeuf et al., 1971, Mahamoud, 1986). At its southern edge, coarse sandstones of Cambrian age are in discordance onto the granitic Precambrian basement. They are locally overlain by Ordovician periglacial sediments. The series continues with fine-grained and argillaceous (Devonian) sandstone. North of the Ennedi massif, the E-W trending Mourdi depression, composed of marine Carboniferous sediments (Klitzsch et al., 1993), separates the range from the Erdis Bassin, composed of various Mesozoic sandstone. The Ennedi massif is an important hydrological divide: a complex network of ouadis conveys runoff water from the Ennedi to the Mortcha depression, to the West, to the Nile basin to the East and to the Mourdi depression, to the North.

In the framework of the RésEau I-Chad project, a scientific mission has been held early 2013 in the Ennedi, coupling geological works and a hydrochemical investigation. A total of 31 water points, mainly wells and springs were sampled for chemical (major and traces elements), stable (<sup>18</sup>O, <sup>2</sup>H) and radiogenic (<sup>3</sup>H) isotopes.

Plateau is a thousand meters sedimentary pile of Palaeozoic sedimentary rocks, mainly sandstones (Mahamoud, 1986). Its coarse of Cambrian age are granitic. There are locally overlain by Ordovician periglacial sediments. The series continues with fine-grained Devonian sandstones and argillaceous sandstones, in particular in the Fada region and on the top of the Plateau. To the north, the E-W trending is composed by C sediments. The northern side of the depression is the so-called Erdis Bassin and is composed of various Mesozoic sandstone units., mainly

Preliminary results indicate that the Ennedi water supply is currently relying entirely on juvenile water, the fossil water being deeper or eventually absent; water conductivity suggests that to some extent modern recharge in the area may be present. A hydrochemical divide is observable, with water having a pH of 6-7 and conductivity values of 300-500 µS/cm on the southern part of the range, and pH of 8-9 and conductivity values of 800-900 µS/cm on the northern part of the range.

A differential GPS survey was carried out near Fada to dress a piezometric map and to propose a simple hydrogeological model. The measured water table shows that groundwater flow is to NW, with a hydraulic gradient of 3 ‰. Electrical conductivity of water along flowpath indicates that some modern recharge is present near discharge areas probably due to the position of the phreatic layer close to ground surface.

#### Acknowledgments

This research work has been performed in the frame of the "RésEau Tchad" project. The project was born as a result of a request by the Ministry of Rural and Urban Hydraulics MHRU) in Chad to the Swiss Development and Cooperation (SDC). The United Nations Institute for Training and Research (UNITAR) and in particular its operational satellite applications programme, UNOSAT, has been mandated from SDC to implement the project together with Chadian government. The project's aims are to increase the knowledge of water resources in Chad, reinforce national capacities, and diffuse a Geographical Information System on Water Resources as well as survey hydrogeological maps. Chemical and isotopic measurements have been possible thanks to KFH funding.

## REFERENCES

- Beuf, S., Biju-Duval, B., de Charpal, O., Rognon, P., Gariel, O., Bennacef, A., 1971. Les grès du paléozoïque inférieur au Sahara: sédimentation et discontinuités, évolution structurale d'un craton. Editions Technip, Paris, 464p.
- Klitzsch, E., Reynolds, P.-O., & Barazi, N. 1993. Geologische Erkundungsfahrt zum Ostteil des Ennedi gebirges und der Mourdi Depression (NE Sudan) in Januar 1992. Würzburger Geographische Arbeiten, 87, 49-61 pp.
- Mahamoud, A.H., 1986. Geologie und Hydrogeologie des Erdis-Beckens, NE-Tschad. Berliner Geowissensch. Abh., A76, 67p.

## 24.10

## Could electrical conductivity replace water depth in rating curves for alpine streams?

Weijs Steven<sup>1</sup>, Mutzner Raphael<sup>1</sup> & Parlange Marc<sup>1,2</sup>

<sup>1</sup>ENAC, IIE, EPFL, Station 2, CH-1015 Lausanne ([steven.weijs@epfl.ch](mailto:steven.weijs@epfl.ch))

<sup>2</sup>Faculty of applied Sciences, University of British Columbia, Vancouver, Canada

Note: adapted from (Weijs et al. 2013).

Time series of streamflow are an important source of information for inference and understanding of the hydrological processes in alpine watersheds. Streamflow is expensive to continuously measure directly, hence it is usually derived from measured water levels, using a rating curve that models the stage-discharge relationship. In alpine streams, this practice is complicated by the fact that the streambed constantly changes due to erosion and sedimentation by the turbulent mountain streams, which never lie quietly in their beds. This makes the stage-discharge relationship dynamic, requiring frequent discharge gaugings to have reliable streamflow estimates. The remaining uncertainty, which is considerable, needs to be accounted for in model calibration, for example by using information-theoretical measures for model-data comparisons (Weijs et al 2011).

During an ongoing field study in the Val Ferret watershed in the Swiss Alps, 93 streamflow values were measured in the period 2009–2011 using salt dilution gauging with the gulp injection method. The natural background electrical conductivity in the stream, which was measured as by-product of these gaugings, was shown to be a strong predictor for the streamflow, which even marginally outperformed water level over the 3 year period. Simultaneous analysis of the residuals of both predictive relations revealed errors in the gauged streamflows. These could be corrected by filtering disinformation from erroneous calibration coefficients. In total, by extracting information from the auxiliary data, we were able to reduce the uncertainty in the rating curve, as measured by the root-mean-square error in log-transformed streamflow relative to that of the original stage-discharge relationship, by 43.7% (Weijs et al 2013).

## REFERENCES

- Weijs, S. V. & Van de Giesen, N. 2011: Accounting for observational uncertainty in forecast verification: an information-theoretical view on forecasts, observations and truth Monthly Weather Review, 139, 2156-2162
- Weijs, S. V.; Mutzner, R. & Parlange, M. B. 2013: Could electrical conductivity replace water level in rating curves for alpine streams? Water Resources Research, 49, 343-351

# P 24.1

## Impact Of River Restoration On Alluvial Soils

Aelvoet Pauline<sup>1, 2</sup>, Bullinger-Weber Géraldine<sup>1</sup>, Le Bayon Renée-Claire<sup>2</sup>, Guenat Claire<sup>1</sup>

<sup>1</sup>Laboratoire ECOS, École polytechnique de Lausanne (EPFL), bâtiment GR, station 2, CH-1050 Lausanne

<sup>2</sup>Laboratoire Sol & Végétation, Université de Neuchâtel, Rue Emile-Argand 11, CH-2000, pauline.aelvoet@unine.ch

Floodplains provide environmental functions (flood protection, recreation areas, biodiversity reservoir, nutrients cycling). These ecosystems have been intensively altered, but are now being restored. Our aim is to assess the post-restoration changes in alluvial soils and the success of river restoration.

A successful river restoration re-creates a panel of i) habitats (soil types), ii) pedological functions (carbon storage) and iii) faunal biodiversity (earthworm communities) similar to those of near-natural floodplains.

We make a comparison of pre-restored stretches, restored stretches and near-natural stretches using complementary criteria: soil type, earthworm communities, carbon storage. Soil diversity increases from embanked to near-natural stretches, but varies according to floodplain characteristics (fig 1). Earthworm diversity is higher in the restored stretch than in the embanked one with presence of colonizer species (*Lombriacus. rubellus*, *Aporectodea ripicola*) (fig 2). Carbon storage is different in near-natural and in restored stretches and varies according to soil type within each stretch (fig 3).

River restoration has increased i) soil type and earthworm diversity and ii) the variability of carbon storage within floodplain. As earthworms rapidly colonize habitats created by river restoration, they can thus be used as bioindicators of early stages of river restoration. The restored stretches remain different from the near-natural ones could be interpreted as a partial success of river restoration projects.

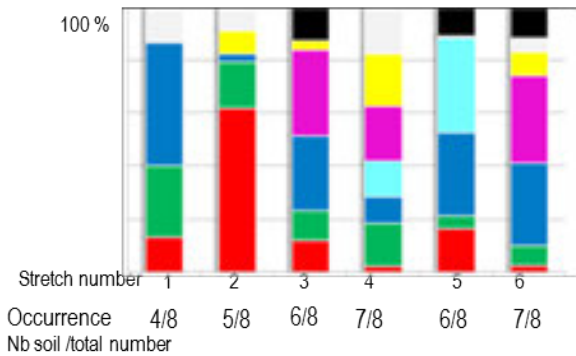


Figure 1. Frequency and occurrence of soil types in six river stretches. Emme River: embanked stretch (1) and restored stretch (3). Thur River : embanked stretch (2) and restored stretch (4). Rhine River : near-natural stretch (5). Sense River : near-natural stretch (6) (from P. Aelvoet, Master thesis)

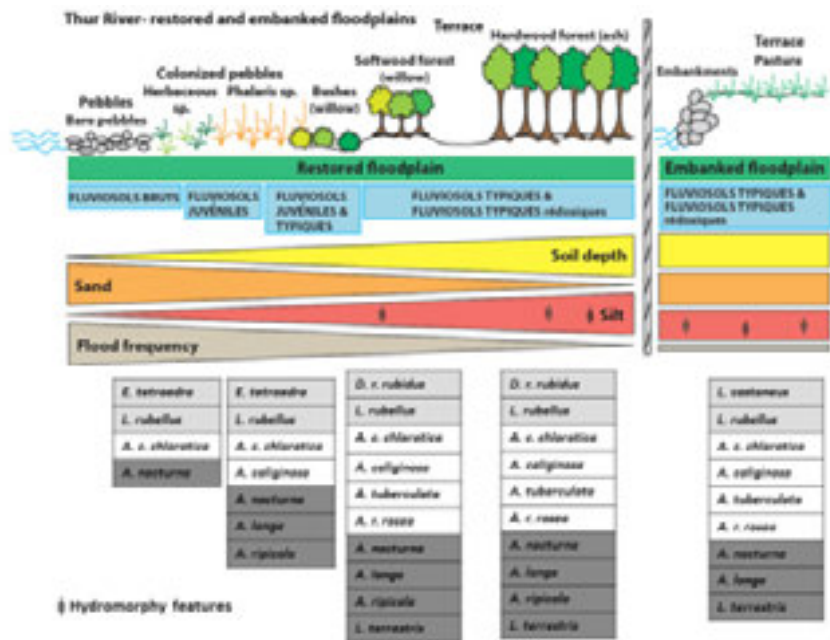


Figure 2: Vegetation, soil, floods and earthworm communities at Thur floodplain. Earthworm species and ecological categories: epigeic, (white), endogeic (grey) and anecic (black) (from Le Bayon et al , 2013, in press).

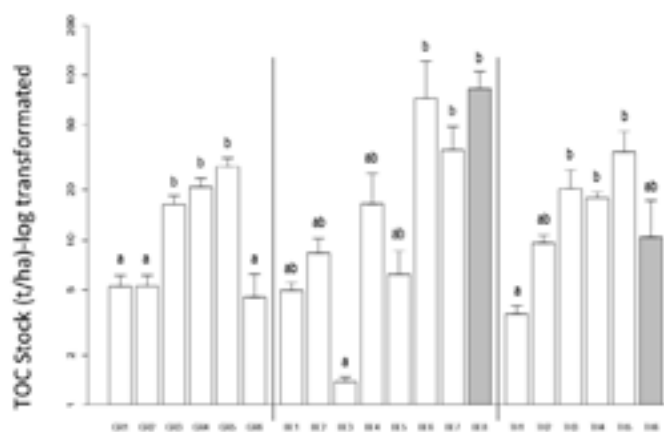


Figure 3: Total Organic Carbon stock in the different topsoils  
 Grey bars correspond to embanked topsoil groups (from Bullinger et al, in revision)

#### REFERENCE:

Le Bayon R-C. & Bullinger-Weber G. & Gobat J-M. & Guenat C. 2013 : Earthworm communities

## P 24.2

### WeSenseIt – a citizen-based observatory of water

Tristan Brauchli<sup>1</sup>, Steven Weijs<sup>1</sup>, Michael Lehning<sup>1</sup>, Hendrik Huwald<sup>1</sup>

<sup>1</sup> School of Architecture, Civil and Environmental Engineering, Ecole Polytechnique Fédérale de Lausanne (EPFL), Lausanne, Switzerland  
 (tristan.brauchli@epfl.ch)

For detailed understanding and forecast of water resources and components of the water cycle spatially and temporally resolved observations of numerous water-related variables are required. Such observations are typically obtained from wireless networks of automated weather stations. The WeSenseIt project develops a citizen- and community-based observatory of water to improve the water and risk management at the catchment scale and support decision-making of stakeholders. Each citizen becomes a potential observer and transmits intentionally or not water-related variables. Recent technologies (wireless communication, internet, smartphone) enable to use smartphones or create innovative low cost sensors that may be less accurate but accessible to a large community; these sensors will be combined with traditional sensing techniques. The goal is to increase the spatial and temporal coverage of observations, which results in the acquisition of large amounts of data. In three specific case studies citizen observatories are being implemented addressing questions related to flood, drought, water resource management, and water quality and pollution. Acquired data ranges from quantitative physical data to qualitative 'social' data extracted from data streams and social media/networks. This study presents the most recent progress and developments of the project related to the measurement of water conditions and fluxes.

## P 24.3

# The dark side of the blueprint. A reflexive analysis of watershed management in Switzerland

Buchs Arnaud

*Institute of Geography and Sustainability, Faculty of Geosciences and Environment, University of Lausanne, Geopolis building, CH-1015 Lausanne (arnaud.buchs.1@unil.ch)*

This poster summarizes the scope and first results of a new research project conducted within the Institute of Geography and Sustainability that aims at questioning present Swiss water policies that globally target the implementation of integrated water resources management (IWRM) in the catchment area, i.e. at the watershed level. More precisely, this research questions the common idea that the watershed, as a supposedly “neutral” scale, should be seen as the panacea to solve coordination problems.

This reflexive analysis is based on two corpora. On the one hand, we focus on recent research that empirically reveals that many attempts to implement IWRM since two decades have not been as successful as expected (Biswas 2008); and theoretically shows that considering the watershed as the sole relevant scale is, at least, biased, or even instrumented (Graefe 2013). On the other hand, blueprint documents produced by the Federal Office for the Environment (FOEN), which pertain to the goal of “shaping evidence”, are analysed.

The notion of IWRM appeared in the middle of the twentieth century and then fell into disuse until the Conference in Mar del Plata in 1977. From 1992 on, it has become the flagship concept of effective and sustainable water policy particularly via the Agenda 21 (or Action 21) adopted at the Earth Summit in Rio de Janeiro and via the Dublin Conference whose first principle states that: “effective management links land and water uses across the whole of a catchment area or groundwater aquifer”.

In Switzerland, the notion explicitly appeared in policy documents in 2003 (during the International year of freshwater) as an “imperative” (FOWG 2003), and the attention paid to the notion has intensified since 2007, when the FOEN mandated several reports on this topic and when the Federal Council mandated the Swiss National Fund to launch the “Sustainable Water Management” National Research Programme (NRP 61). Since then, the Swiss water policy has truly been oriented toward watershed management. FOEN states that “with the watershed as reference area, the integrated management of water is primarily based on the natural system. The area in which the interactions occur and the decision-making scope coincide. The problems are solved where they are caused” (2011: 14). Thanks to IWRM at the watershed level, water management is supposed to be “efficient”, “customised”, “future oriented” and “durable”.

If several attempts to implement integrated water management in Switzerland can be mentioned (Fribourg, Neuchâtel, Geneva, etc.), to consider the watershed as the most relevant “functional regulatory space” (Varone et al.: 2013) does not seem so obvious. More fundamentally, the reference to the basin should also be discussed from the perspective of its supposed “axiomatic neutrality”. For example, for Graefe (2013: 15): “the river basin fetishism, the domination of the IWRM and governance concepts are symptoms of the depoliticisation of water management. They should be seen as being part of a process creating new instances of environmental management dominated by scientific and technocratic expertise void of political interests, political representations and politics overall”.

## REFERENCES

- Biswas, A.K. 2008: Integrated Water Resources Management: Is It Working?. *International Journal of Water Resources Development*, 24:1, 5-22.
- Federal Office for the Environment (FOEN), 2011: *Watershed Management Guiding Principles for Integrated Management of Water in Switzerland*, FOEN, Bern.
- Federal Office for Water and Geology (FOWG), 2003: *Plongée dans l'économie des eaux. Découvrez le monde fascinant de l'économie des eaux en Suisse*, FOWG, Bern.
- Graefe, O. 2013: The River Basin as a Territorial Water Management Unit. *Towards Post-political Water Management*. In: *European Continental Hydrosystems under Changing Water Policy* (Ed. by Arnaud-Fassetta, G., Masson, E. & Reynard, E.), Pfeil, München, 11-16.
- Varone, F., Nahrath, S., Aubin, D. & Gerber, J.D. 2013: Functional Regulatory Spaces. *Policy Sciences*, 46, 1-23.

## P 24.4

### Rainfall driven cholera outbreak modelling

Finger Flavio<sup>1</sup>, Bertuzzo Enrico<sup>1</sup>, Mari Lorenzo<sup>1,2</sup>, Knox Allyn<sup>1</sup>, Gatto Marino<sup>2</sup> & Rinaldo Andrea<sup>1,3</sup>

<sup>1</sup> *Laboratory of Ecohydrology (ECHO), School of Architecture, Civil and Environmental Engineering, École Polytechnique Fédérale de Lausanne (EPFL), Lausanne, Switzerland*

<sup>2</sup> *Dipartimento di Elettronica e Informazione, Politecnico di Milano, Milano, Italy*

<sup>3</sup> *Dipartimento di Ingegneria Civile, Edile ed Ambientale, Università di Padova, Padova, Italy*

Epidemiological models can provide crucial understanding about the dynamics of infectious diseases. Possible applications range from real-time forecasting and allocation of health care resources to testing alternative intervention mechanisms such as vaccines, antibiotics or the improvement of sanitary conditions. We apply a spatially explicit model to the cholera epidemic that struck Haiti in October 2010 and is still ongoing. The dynamics of susceptibles, infectives and recovered are modelled at the scale of local human communities. Dissemination of *Vibrio cholerae* through hydrological transport and human mobility along the road network is explicitly taken into account, as well as the effect of rainfall as a driver of increasing disease incidence. Rainfall data was obtained from remotely sensed satellite measurements. The model is calibrated using a dataset of reported cholera cases. The model allows us to draw predictions on longer-term epidemic cholera in Haiti from multiseason Monte Carlo runs, using rainfall fields forecasts.

#### REFERENCES

- Gatto, M., Mari, L., Bertuzzo, E., Casagrandi, R., Righetto, L., Rodriguez-Iturbe, I., and Rinaldo, A. (2012). Generalized reproduction numbers and the prediction of patterns in waterborne disease. *PNAS* 109, 19703–19708.
- Mari, L., Bertuzzo, E., Righetto, L., Casagrandi, R., Gatto, M., Rodriguez-Iturbe, I., and Rinaldo, A. (2012). Modelling cholera epidemics: the role of waterways, human mobility and sanitation. *J. R. Soc. Interface* 9, 376–388.
- Rinaldo, A., Bertuzzo, E., Mari, L., Righetto, L., Blokesch, M., Gatto, M., Casagrandi, R., Murray, M., Vesenbeckh, S.M., and Rodriguez-Iturbe, I. (2012). Reassessment of the 2010–2011 Haiti cholera outbreak and rainfall-driven multiseason projections. *PNAS* 109, 6602–6607.

## P 24.5

# Bedload transport dynamics in mountain rivers – Development and application of the model *sedFlow*

Heimann Florian U. M.<sup>1</sup>, Böckli Martin<sup>1</sup>, Rickenmann Dieter<sup>1</sup>, Turowski Jens M.<sup>2,1</sup> & Badoux Alexandre<sup>1</sup>

<sup>1</sup> WSL Swiss Federal Institute for Forest, Snow and Landscape Research, Zürcherstr. 111, CH-8903 Birmensdorf (florian.heimann@wsl.ch)

<sup>2</sup> Helmholtz Centre Potsdam, GFZ German Research Centre for Geosciences, Albert-Einstein-Str. 48, D-14473 Potsdam

In alpine environments the hazard potential of a stream, its ecologic relevance and the sustainability of civil engineering measures is influenced by bedload transport dynamics. In numerous contexts this entails the need for the numeric simulation of the bedload transport process. Within the framework of the NRP 61, the model *sedFlow* has been developed, which accounts for the different requirements of such simulations.

Bedload transport in steep mountain channels shows different characteristics compared to flatter channel gradients and thus requires modified calculation procedures (e.g. Rickenmann 2001; Rickenmann & Recking 2011; Nitsche et al. 2011). Feedbacks between hydraulics and sediment dynamics accounting for the evolution of channel gradient and grain size distribution are considered in the *sedFlow* model as well.

Despite more detailed results and process interactions, *sedFlow* facilitates simulations, which are two to three orders of magnitude faster as with the comparable modelling software. For data input, xml and other special formats have been largely renounced in favour of intuitive spread sheet representations. Thus, a quick and easy pre-processing of input data with regular spread sheet software such as Excel™ is possible.

As an example, observations concerning bedload transport and morphodynamics of the Brenno river in southern Switzerland have been reproduced with *sedFlow* simulations using a reasonable parameter set-up. The Brenno sediment transport system is found to be more sensitive to variations of discharge and grain size distributions compared to variations of the threshold for initiation of transport and of channel width. Simulations with variable sediment input by tributaries show that the downstream effect is more pronounced regarding transported bedload volumes whereas variable sediment inputs have a spatially much more limited impact on the morphodynamics.

## REFERENCES

- Nitsche, M., Rickenmann, D., Turowski, J. M., Badoux, A., & Kirchner, J. W. 2011: Evaluation of bedload transport predictions using flow resistance equations to account for macro-roughness in steep mountain streams, *Water Resour. Res.*, 47, W08513.
- Rickenmann, D. 2001: Comparison of bed load transport in torrents and gravel bed streams. *Water Resources Research*, 37(12), 3295–3305.
- Rickenmann, D., & Recking A. 2011: Evaluation of flow resistance in gravel-bed rivers through a large field data set. *Water Resources Research*, 47, W07538.

## P 24.6

# Customization of a hydrological model for the estimation of water resources in an alpine karstified catchment with sparse data

Kauzlaric Martina<sup>1,2</sup>, Schädler Bruno<sup>1,2</sup>, Weingartner Rolf<sup>1,2</sup>

<sup>1</sup>*Geographisches Institut, Universität Bern, Hallerstrasse 12, CH-3012 Bern (martina.kauzlaric@giub.unibe.ch)*

<sup>2</sup>*Oeschger Center for Climate Change Research, University of Bern*

The main objective of the MontanAqua transdisciplinary project is to develop strategies moving towards a more sustainable water resources management in the Crans-Montana-Sierre region (Valais) in view of global change. Therefore a detailed assessment of the available water resources in the study area today and in the future is needed.

The study region is situated in the inner alpine zone, with strong altitudinal precipitation gradients: from the precipitation rich alpine ridge down to the dry Rhône plain. A typical plateau glacier at the top of it is partly drained through the karstic underground formations and linked to various springs. The main anthropogenic influences on the system are reservoirs and diversions to the irrigation channels. Thus the study area does not cover a classical hydrological basin as the water flows frequently across natural hydrographic boundaries. This is a big challenge from a hydrological point of view, as we cannot easily achieve a closed, measured water balance.

A representative climatological measurement network covering altitudinal belts as well as the main land cover types has been recently installed, but the calibration and validation of a hydrological model require longer time series. The general lack of comprehensive historical data in the catchment reduces the degree of process conceptualization possible, as well as prohibits usual parameter estimation procedures.

Besides the need for a physically based hydrological model, a flexible discretization is essential. It minimizes the resolution of spatial discretization (fewest number of elements to preserve the essential physics) while still capturing the local heterogeneities in parameters and process dynamics.

The Penn State Integrated Hydrologic Model (PIHM) (Kumar, 2009) has been selected to estimate the available natural water resource for the whole study area. It is a semi-discrete, physically-based model which includes: channel routing, overland flow, subsurface saturated and unsaturated flow, rainfall interception, snow melting and evapotranspiration. Its unstructured mesh decomposition offers a flexible domain decomposition strategy for efficient and accurate integration of the physiographic, climatic and hydrographic watershed.

The model was modified in order to be more suitable for a karstified mountainous catchment: it now includes the possibility to punctually add external sources, and the temperature-index approach for estimating melt was adjusted to include the influence of solar radiation.

Parameters are estimated with values obtained from the literature, catchment boundaries were determined basing on tracer experiments, as well as the relationship between precipitation, spring- and river-discharge.

Historical data such as river discharge, infiltration experiments and snow measurements were used to validate simulations, and are here presented in case studies.

## REFERENCES

Kumar, M. 2009: Toward a hydrologic modeling system. PhD Thesis, Department of civil and Environmental engineering, Pennsylvania State University, USA.

## P 24.7

## Geochemical characterization of Chiasso aquifer

Gasperini Greta<sup>1</sup>, Amadori Michele<sup>1</sup>, Pera Sebastian<sup>2</sup>, Bronzini Simona<sup>2</sup>, Toscani Alessandro<sup>3</sup>

<sup>1</sup> Dipartimento di Scienza della Terra, Università di Pisa, Via Santa Maria 53, 56126 Pisa, Italy

<sup>2</sup> Istituto Scienze della Terra, Scuola Universitaria Professionale della Svizzera Italiana, Via Trevano CH6952 Canobbio, Switzerland (sebastian.pera@supsi.ch)

<sup>3</sup> Sezione per la protezione dell'aria dell'acqua e del suolo – SPAAS, Via Carlo Salvioni 2a, CH6500 Bellinzona, Switzerland

The aim of this work is to determine the geochemical characterization of Chiasso aquifer (Switzerland), and to investigate the behavior of dissolved nitrogen related compounds ( $\text{NO}_2^-$ ,  $\text{NO}_3^-$ ,  $\text{NH}_4^+$ ).

A monitoring survey including groundwater and surface water sampling, and piezometric measurements was carried out in 2012 and 2013. (figure 1) Sampling was completed in collaboration with SPAAS and the Environmental monitoring office, which performed the chemical analysis.

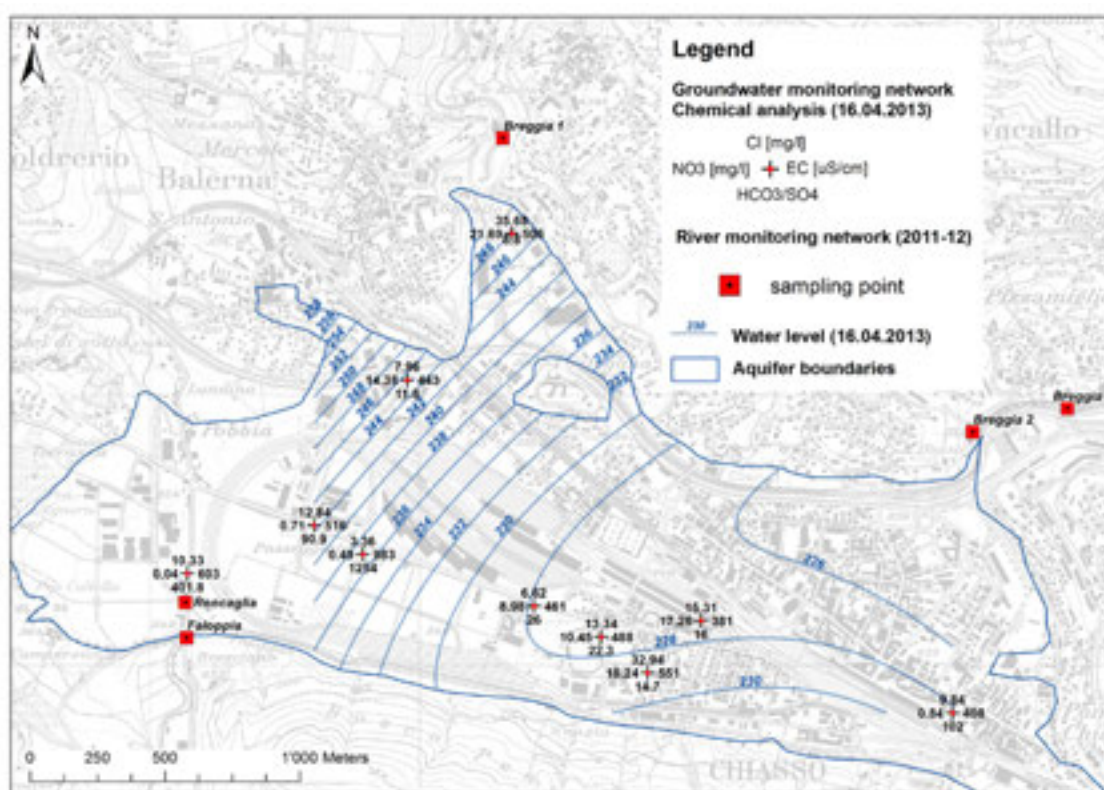


Figure 1 sampling network, piezometric map and selected results

The results from chemical analysis were treated with Statistica 6 software to analyze correlation among elements and the presence of clusters. Based on the results and the observed spatial geochemical variation, two different models were tested with PHREEQC to investigate processes that control geochemical evolution of water within the aquifer. According with the results waters are classified as alkaline-earth bicarbonate in Ludwig-Langelier diagram being bicarbonate the main anion. Along the flowpath  $\text{HCO}_3^-$  ratios to the other main anions generally tends to decrease (figure 1), especially downstream urban areas where the amount of chlorides and sulphates augments. The bicarbonate remains the predominant species due to atmospheric  $\text{CO}_2$  dissolution and water interaction with the aquifer's matrix which is partially derived from limestone. Temporal variations of conductivity and bicarbonates follow the same pattern reflecting recharge effects during fall and late spring diluting the salts concentrations, and therefore lowering water conductivity. Most nitrate and potassium have natural origin, from interaction of water with the organic matter in the aquifer matrix (Istituto Geologico Cantonale, 1990). However, spatial distribution of N related compounds also suggests that other sources, like wastewaters treatment facilities, overflow sewage discharge, fertilizers may be also present. The statistical analysis emphasizes that the calcium represents the dominants cation and it is closely related with bicarbonate as both have the same origin. Chlorides and sulphates seem to have different sources, one geologic probably enrichment from gypsum present in limestone of the area, and the other from evaporites dissolution from the aquifer's matrix, as the area was originally a swamp.

Principal Component Analysis applied to major anions, cations and nitrogen compounds highlighted that the origin of nitrogen, chlorine, probably due to the weathering of organic matter contained in the aquifer matrix. Results from Phreeqc modeling shows that Na – K exchange and calcite precipitation occur along flow- path. Geochemical evolution of water proceeds controlled by increasing  $\text{CO}_2$  and  $\text{NO}_3^-$  derived from organic matter oxidation, and water - rock interaction within the aquifer.

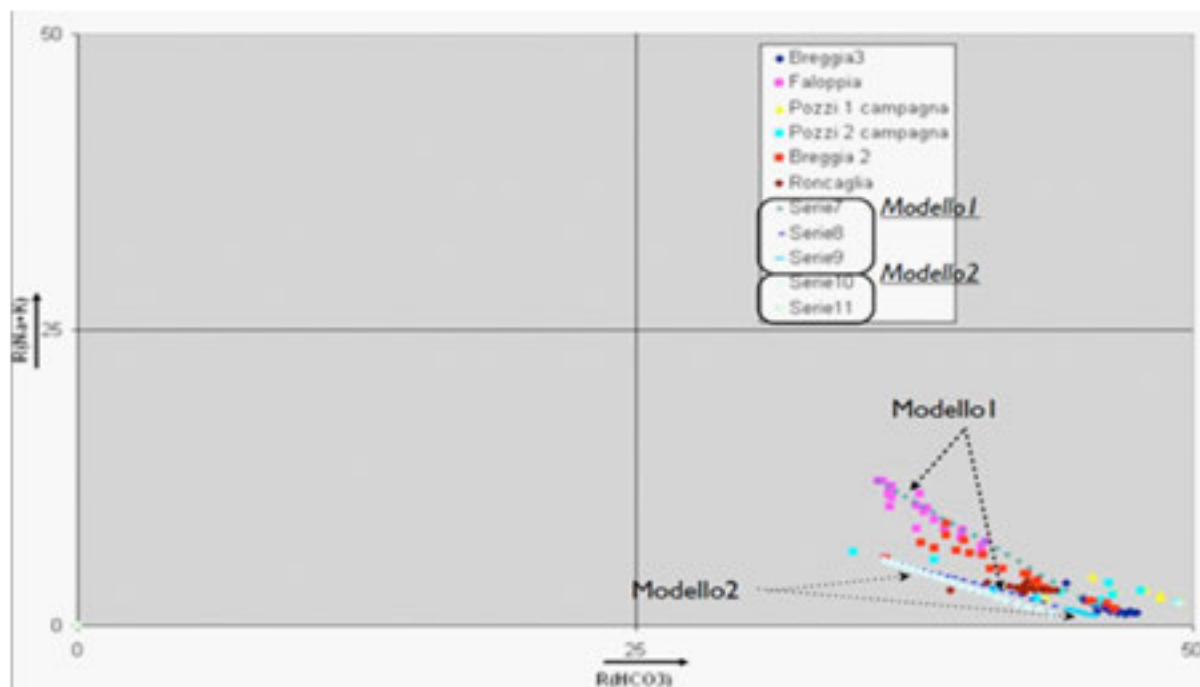


Figure 2 Langelier Ludwig diagram with tested Phreeqc models

#### REFERENCES

- Istituto Geologico Cantonale 1990: Idrogeologia del bacino di Chiasso rapporto interno nro 20, Bellinzona.  
 Appelo C.A.J., Postma D., 2005: Geochemistry Groundwater And Pollution, 2nd edition, A.A. Balkema Publishers, Leiden, The Netherlands a member of Taylor and Francis Group plc.



## 25. Limnological and hydro(geo)logical advances for mid-sized lakes as a water resource for the next century

Nathalie Chèvre, Jean-Luc Loizeau, Hans-Rudolf Pfeifer, Torsten Vennemann

*ProDoc project Leman21,  
Swiss Commission for Oceanography and Limnology (COL)*

### TALKS:

- 25.1 Bonvin F., Razmi A.M., Barry D.A., Kohn T.: Micropollutant dynamics in Vidy Bay- a coupled hydrodynamic-photolysis model to assess the spatial extent of ecotoxicological risk
- 25.2 Dang D. H., Lenoble V., Durrieu G., Omanovic D. François D., Mounier S., Garnier C.: Coastal sediments: sink or source of pollution? A case study (Toulon bay, SE France)
- 25.3 Daouk S., Copin P.-J., Chèvre N., Rossi L., De Alencastro L.F., Pfeifer H.-R.: Diffuse transfer of the herbicide glyphosate from the Lavaux vineyards to the Lake of Geneva: Dynamics and environmental risk assessment.
- 25.4 Finger D., Wüest A., Bossard P.: Effects of oligotrophication on primary production in peri-alpine lakes
- 25.5 Garnier C., Oursel B., Syakti A.H., Durrieu G., Mounier S., Doumenq P., Lucas Y.: Evaluation of pollutants inputs from large agglomeration to the coastal zone: the case of Marseille (France)
- 25.6 Gascon Diez E., Cosio C., Loizeau J.-L. : Mercury and Methylmercury resuspension in Vidy Bay, Lake Geneva (Switzerland)
- 25.7 Girardclos S., Faessler J., Zehring M.: Radionuclide fluxes in Lake Biel sediments (1955-2010) and Mühleberg NPP <sup>137</sup>Cs liquid emissions
- 25.8 Gregorio V., Chèvre N.: Assessing the risk of mixture of micropollutants in Geneva lake: from the theoretical approach to “in-situ” ecological effects
- 25.9 Razmi A.M., Barry D.A., Lemmin U.: Current variability in a wide lacustrine embayment (Vidy Bay, Switzerland)
- 25.10 Rodríguez-Murillo J.C., Filella M.: Trends in organic carbon concentrations in Swiss lakes
- 25.11 Rossi L., Chesaux L., Chèvre N. : Diffuse sources of micropollutants in a mid-size-lake: how to handle them?

## POSTERS:

- P 25.1 Borgatta M., Waridel P., Decosterd L-A., Buclin T., Chèvre N.: Chronic tests of two anticancer drug metabolites on *Daphnia pulex*
- P 25.2 Bouffard D., Boegman L., Ackerman Jda.: Physical process and hypoxia in Lake Erie
- P 25.3 Chevrolet A., Fischer B., Seibert J.: Spatial runoff estimations based on the deuterium-excess due to the isotopic evaporation effect in an upstream lake
- P 25.4 Copin P-J., Chèvre N.: Enhancement of the representativeness of herbicide effect modelling in watercourses.
- P 25.5 Darvishi Khatooni J., Lak R., Mohammadi A.: Calculation of Physical Chemistry Parameters (Amount and Rate of Salt Precipitation) from Brines Urmia Lake
- P 25.6 Darvishi Khatuoni J., Mohammadi A., Salehipuor Milani A., Lak R.: The History of Sedimentation and the Risk of Falling Urmia lake level in Iran
- P 25.7 Lak R., Fayazi Sh.: Evolution of Lake Maharlou brine during 4 years monitoring
- P 25.8 Lak R., Rezaeian Langeroudi S.: Sedimentology, Sedimentary Sub-environments and Mineralogy of Holocene Sediments of Maharlou Lake, Southwest of Iran
- P 25.9 Margot J., Kienle C., Magnet A., Weil M., Rossi L., De Alencastro L.F., Abegglen C., Thonney D., Chèvre N., Schärer M., Barry D.A.: Treatment of micropollutants in municipal wastewater: Ozone or powdered activated carbon?
- P 25.10 Niel T., Coutu S., Margot J. & Faust A-K.: Economical comparison of three water treatment projects in Vidy Bay (Geneva Lake, CH)
- P 25.11 Queloz P., Bertuzzo E., Botter G., Rao P.S., Rinaldo A.: Herbicides export dynamics of a mid-sized lake tributary: lessons from observations and modelling
- P 25.12 Rezaeian Langeroudi S., Lak R.: Verification of Holocene Sediments in Hoz-e-Soltan Lake (Qom) through Sedimentary Cores

## 25.1

# Micropollutant dynamics in Vidy Bay- a coupled hydrodynamic-photolysis model to assess the spatial extent of ecotoxicological risk

Bonvin Florence<sup>1</sup>, Razmi Amir M.<sup>2</sup>, Barry David Andrew<sup>2</sup> & Kohn Tamar<sup>1</sup>

<sup>1</sup> Environmental Chemistry Laboratory (LCE), Ecole Polytechnique Fédérale de Lausanne (EPFL), IIE-ENAC, Station 2, CH-1015 Lausanne (florence.bonvin@epfl.ch)

<sup>2</sup> Ecological Engineering Laboratory (ECOL), Ecole Polytechnique Fédérale de Lausanne (EPFL), IIE-ENAC, Station 2, CH-1015 Lausanne

The direct discharge of wastewater (WW) effluent into the Vidy Bay of Lake Geneva results in the seasonal formation of an effluent plume containing locally high concentrations of wastewater-derived micropollutants. A 10-month sampling campaign showed that the plume depth followed the thermocline, which moved to greater depths over the course of the warm seasons. In absence of thermal stratification, between November and January, the plume surfaced or was not detected due to enhanced mixing of the water column. The high concentrations of micropollutants near the wastewater treatment plant (WWTP) outfall present a potential ecotoxicological risk, yet the spatial extent of the risk zone remains unclear.

This work couples the two main processes affecting the spreading of the plume, namely water hydrodynamics and photolysis. The concentration of micropollutants around the wastewater outfall was predicted for typical wind scenarios and seasons relevant in Vidy Bay using a coupled hydrodynamic-photolysis model. Specifically, we experimentally determined the photolysis quantum yields and indirect photolysis rate constants for 24 wastewater-derived micropollutants (mainly pharmaceuticals), and implemented this data into a hydrodynamic particle tracking model, which tracked the movement of water parcels (“particles”) from the WWTP outfall through the Vidy Bay. Modeling results were validated with monthly field measurements collected in 2010.

Model results showed that the zone of potential ecotoxicological risk was generally larger under stratified (summer) conditions than under well-mixed (winter) conditions. This could be attributed to slower dilution, as well as decreased photodegradation due to the entrapment of the WW plume below the thermocline. The largest extent of the risk zone was observed under conditions of Bise (north-easterly wind) during the summer season, with a westward expansion of > 300m. Under Vent (south-westerly wind) conditions, the area of risk was generally smaller and extended mainly to the east (upstream) of the WWTP. As expected, photodegradation was an important removal mechanism for many compounds and thus contributed to a reduction in the ecotoxicological risk over time and distance from the WW outfall. The mixture toxicity near the outfall was dominated by five substances, mainly antibiotics. The coupled photolysis-hydrodynamic model revealed that the risk zone may affect a stretch of up to 600 m in proximity to the shore (ca. 300 m in east and west direction of the WW outfall). This zone should be targeted in future studies of the ecotoxicological effects of WW effluent in Vidy Bay.

## 25.2

### Coastal sediments: sink or source of pollution? A case study (Toulon bay, SE France)

Duc Huy Dang<sup>1</sup>, Véronique Lenoble<sup>1</sup>, Gaël Durrieu<sup>1</sup>, Dario Omanovic<sup>2</sup>, David François<sup>3</sup>, Stéphane Mounier<sup>1</sup> and Cédric Garnier<sup>1</sup>

<sup>1</sup> Laboratoire PROTEE, Université du Sud Toulon Var, BP20132, 83957 La Garde, France, duc-huy.dang@univ-tln.fr

<sup>2</sup> Center for Marine and Environmental Research, Ruđer Bošković Institute, P.O. Box 180, 10002 Zagreb, Croatia

<sup>3</sup> LASEM-Toulon, Base Navale de Toulon, BP 61, 83800 Toulon, France

The highly contaminated sediments from Toulon bay (France, NW Mediterranean Sea, Tessier et al., 2011) were deeply studied to investigate their potential threat toward the seawater quality. In such context, analytical and modelling approaches were used to better understand the dynamic and fate of diagenesis tracers and inorganic contaminants in coastal sediments. Core sediments were sampled through the bay every 2 months, for 1.5 years to characterize porewater (physical/chemical parameters, diagenesis tracers and major/trace concentrations ...) and solid sediments (major/trace contents, selective extractions and carrier phase identification). A 1D steady-state modelling approach (PROFILE, Berg et al., 1998) was used to fit the elements' profiles, estimating depth reaction intervals and reaction rates. Thermodynamic simulation (PHREEQC, Parkhurst & Appelo, 1999) was also performed to calculate elements' chemical speciation. Laboratory simulations of sediments resuspension were carried out at various solid/liquid ratios of surface and anoxic sediments (0-2 cm and 20-22 cm, respectively), aiming at considering the risk of contaminant mobilization through events of various magnitudes.

The element dissolved profiles showed significant seasonal variations. The highest diagenesis activity was recorded in November and March, suggesting a link with the varying input of "fresh" organic matter (e.g. plankton bloom). Otherwise, the coupling of experimental (selective extractions) and modelling approaches demonstrated the strong link between contaminants and the diagenesis-sensitive phases in subsurface sediments. The most recurrent examples were the coupling of As/Fe oxides and Co/Mn oxides. Precisely, the estimation of the Fe and As quantity lost or gained through different diagenetic processes (mineral dissolution/precipitation or adsorption...) demonstrated a correlation with a Fe/As ratio of 230. Selective extractions have also underlined that As was mainly linked to amorphous iron oxyhydroxide. The relationship between As and this diagenetic-sensible mineral explained the important As remobilization in subsurface sediment. The estimated As diffusive flux from sediments is then significant (i.e.  $\sim 1.6 \text{ ng}_{\text{As}} \text{ cm}^{-2} \text{ d}^{-1}$  in July 2009).

The simulations experiments of sediments resuspension showed a high risk of pollutants remobilization. The mechanisms of these phenomena (oxidation and/or formation of new carrier phases, adsorption/desorption of pollutants...) seemed to be element-dependant while the sediments characteristics appear to control the remobilization amplitude. For all cases, the trace element concentrations reached at the maximum of remobilization exceeded the toxicity levels for microorganisms (e.g. plankton).

The monitoring of the diagenetic activity showed a significant seasonal modification of the behaviour of numerous elements, either diagenetic tracers or inorganic contaminants. A high mobilization of such contaminants in subsurface sediments, resulting in a significant diffusive flux toward seawater, could turn the sediments a potential pollution source. In parallel, sediments suspension events (storm, nautical traffic, dredging operations...) were also demonstrated to be active pollution incidents. Being not only an ultimate sink of contamination in a surrounding ecosystem, sediments must be also considered as a passive/active source of pollution.

#### REFERENCES

- Tessier, E., Garnier, C., Mullot, J.-U., Lenoble, V., Arnaud, M., Raynaud, M. & Mounier, S. 2011: Study of the spatial and historical distribution of sediment inorganic contamination in the Toulon bay (France). *Mar. Pollut. Bull.* 62, 2075–2086.
- Berg, P., Risgaard-Petersen N. & Risgaard S. 1998: Interpretation of measured concentration profiles in sediment pore water. *Limnol. Oceanogr.* 43, 1500–1510.
- Parkhurst D. & Appelo C.A.J. 1999: User's guide to PHREEQC (Version 2) – A program for speciation, batch-reaction, one-dimensional transport, and inverse geochemical calculations. *US Geol. Surv. Water Resour. Inv. Rep.*, 99–4259.

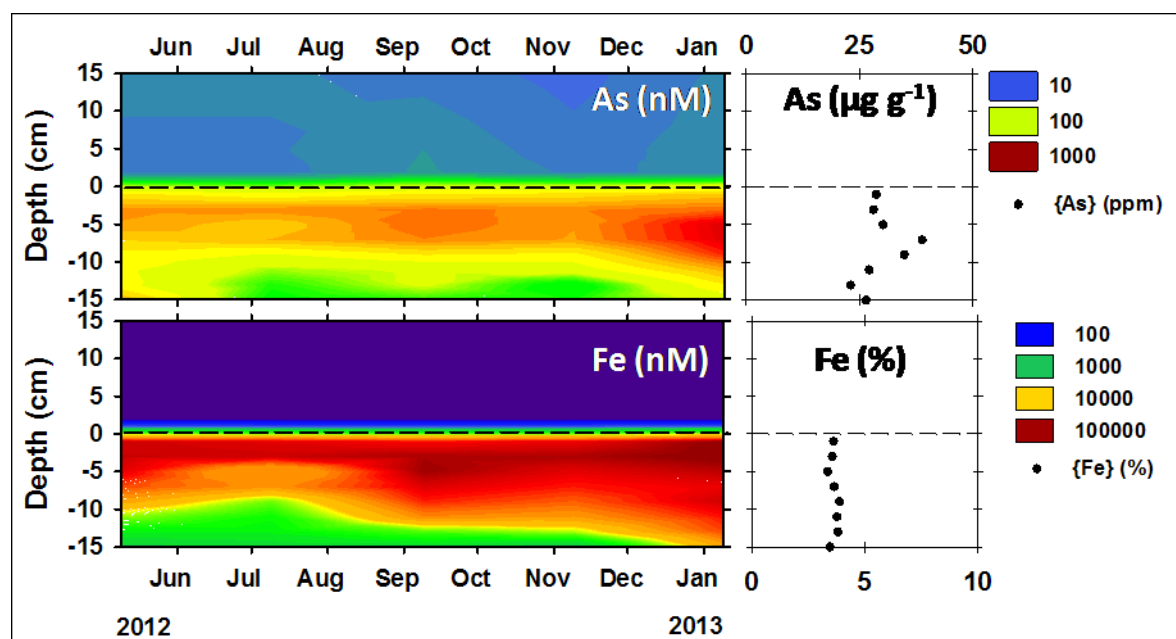


Figure 1: Monitoring of As and Fe concentration in sea/pore water and sediments.

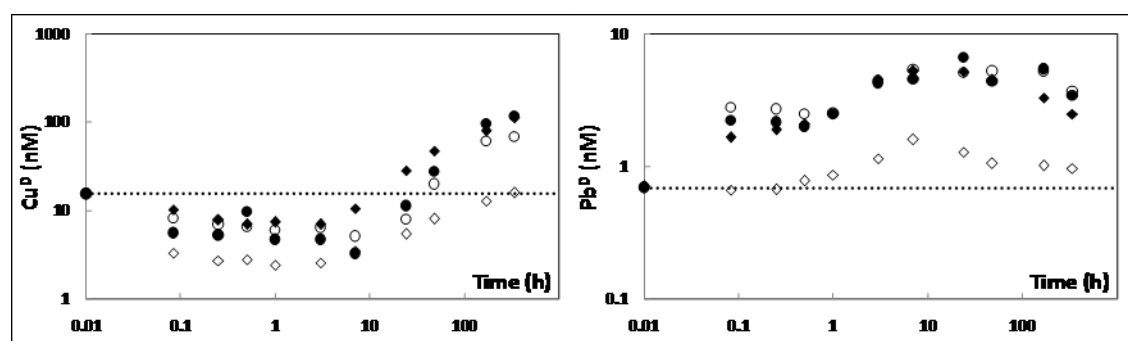


Figure 2: Dissolved Cu (left) and Pb (right) concentration remobilized during resuspension experiments of surface (diamond symbol) and anoxic (circle symbol) sediments. The solid/liquid ratio was close to 0.1 (open symbol) and 1 (full symbol)  $\text{g L}^{-1}$ .

## 25.3

# Diffuse transfer of the herbicide glyphosate from the Lavaux vineyards to the Lake of Geneva: Dynamics and environmental risk assessment.

Daouk Silwan<sup>1</sup>, Copin Pierre-Jean<sup>1</sup>, Chèvre Nathalie<sup>1</sup>, Rossi Luca<sup>2</sup>, De Alencastro Luiz Felipe<sup>3</sup> & Pfeifer Hans-Rudolf<sup>1</sup>

<sup>1</sup> Institute of Earth Science, University of Lausanne, CH-1015 Lausanne (Silwan.Daouk@unil.ch)

<sup>2</sup> Ecological Engineering Institute, Ecole Polytechnique Fédérale de Lausanne, CH-1015 Lausanne

<sup>3</sup> Central Environmental Laboratory, Ecole Polytechnique Fédérale de Lausanne, CH-1015 Lausanne

The use of herbicides in agriculture may lead to environmental problems, such as surface water pollution, with a potential risk for aquatic organisms. The herbicide glyphosate is the most used active ingredient in the world and in Switzerland. In the Lavaux vineyards it is nearly the only molecule applied. This work aimed at studying its fate in soils and its transfer to surface waters.

First of all, an analytical method using ultra performance liquid chromatography coupled with tandem mass spectrometry (UPLC-MS/MS) was developed for the trace level quantification of this widely used herbicide and its main by-product, aminomethylphosphonic acid (AMPA). The method was validated for the matrix effect correction in relevant environmental samples, with limits of detection and quantification as low as 5 and 10ng/l respectively.

In the field, two parcels of the Lavaux vineyard area, located near the Lutrive River at 6km to the east of Lausanne, were monitored to assess to which extent glyphosate and AMPA were retained in the soil or exported to surface waters. They were equipped at their bottom with porous ceramic cups and runoff collectors, which allowed retrieving water samples for the growing seasons 2010 and 2011. Results revealed that the mobility of glyphosate and AMPA in the unsaturated zone was likely driven by the precipitation regime and the soil characteristics, such as slope, porosity structure and layer permeability discrepancy. Elevated glyphosate and AMPA concentrations were measured at 60 and 80 cm depth at parcel bottoms, suggesting their infiltration in the upper parts of the parcels and the presence of preferential flow in the studied parcels. Indeed, the succession of rainy days induced the gradual saturation of the soil porosity, leading to rapid infiltration through macropores, as well as surface runoff formation. Furthermore, the presence of more impervious weathered marls at 100 cm depth induced throughflows, the importance of which for the lateral transport of the herbicide molecules was determined by the slope steepness. Important rainfall events (>10 mm/day) were clearly exporting molecules from the soil top layer, as indicated by important concentrations in runoff samples. A mass balance showed that total loss (10-20%) mainly occurred through surface runoff (96%) and, to a minor extent, by throughflows in soils (4%), with subsequent exfiltration to surface waters (Fig.1).

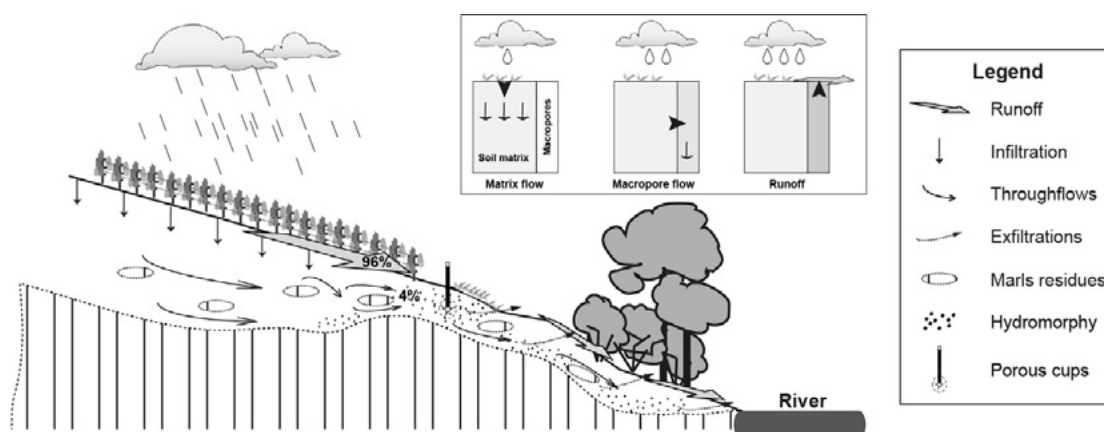


Figure 1. Synthesis of water pathways in vineyard parcels responsible for the diffuse export of glyphosate and AMPA molecules in the river direction.

Observations made in the Lutrive River revealed glyphosate and AMPA dynamics at the catchment level, which strongly depend on application rates, precipitation regime, land use and also on the presence of drains or constructed channels. Elevated concentrations, up to 4970 ng/l, observed just after the application, confirmed the diffuse export of these compounds from the vineyard area by surface runoff during main rain events (Fig.2A). From April to September 2011, a total

load of 7.1 kg was calculated, with 85% coming from vineyards and minor urban sources and 15% from arable crops. Small vineyard surfaces could generate high concentrations of herbicides and contribute considerably to the total load calculated at the outlet, due to their steep slopes (~10%). The extrapolated total amount transferred yearly from the Lavaux vineyards to the Lake of Geneva was of 190kg. Lastly, based on maximum concentrations measured in the river, an environmental risk for these compounds was assessed, using laboratory tests and ecotoxicity data from the literature (Fig.2B). In our case and with the methodology applied, the risk towards aquatic species was found negligible ( $RF < 1$ ).

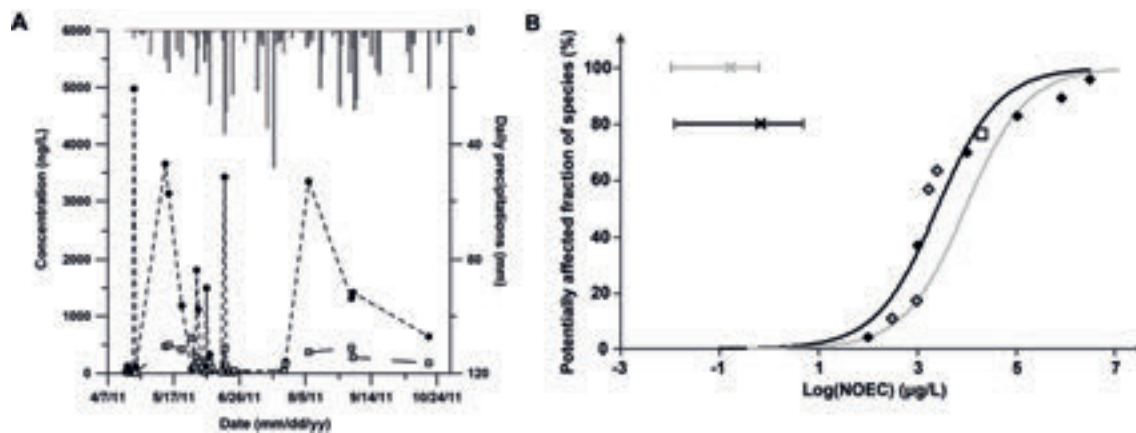


Figure 2. A: Glyphosate (●) and AMPA (□) concentrations at the Lutrive River outlet from April to October 2011 and daily precipitations; B: Species Sensitivity Distribution (SSD) curves for glyphosate (black line) and for AMPA (grey line). Their minimum, maximum and mean concentrations measured in the Lutrive River are represented on the top left of the figure.

## 25.4

## Effects of oligotrophication on primary production in peri-alpine lakes

Finger David<sup>1</sup>, Wüest Alfred<sup>2,3</sup> & Bossard Peter<sup>2</sup><sup>1</sup> Department of Geography, University of Zurich, Wintherturerstr 140, CH-8046 Zurich, Switzerland,<sup>2</sup> Eawag: Swiss Federal Institute of Aquatic Science and Technology, Kastanienbaum, Switzerland<sup>3</sup> Physics of Aquatic Systems Laboratory - Margaretha Kamprad Chair, ENAC, EPFL, Lausanne, Switzerland

During the second half of the 20th century untreated sewage released from housing and industry into natural waters led to a degradation of many freshwater lakes and reservoirs worldwide. In order to mitigate eutrophication, wastewater treatment plants, including Fe-induced phosphorus precipitation, were implemented throughout the industrialized world, leading to reoligotrophication in many freshwater lakes. To understand and assess the effects of reoligotrophication on primary productivity, we analyzed 28 years of <sup>14</sup>C assimilation rates, as well as other biotic and abiotic parameters, such as global radiation, nutrient concentrations and plankton densities in peri-alpine Lake Lucerne, Switzerland. Using a simple productivity-light relationship, we estimated continuous primary production and discussed the relation between productivity and observed limnological parameters. Furthermore, we assessed the uncertainty of our modeling approach based on monthly <sup>14</sup>C assimilation measurements using Monte Carlo simulations. Results confirm that monthly sampling of productivity is sufficient for identifying long-term trends in productivity and that conservation management has successfully improved water quality during the past three decades via reducing nutrients and primary production in the lake. However, even though nutrient concentrations have remained constant in recent years, annual primary production varies significantly from year to year. Despite the fact that nutrient concentrations have decreased by more than an order of magnitude, primary production has decreased only slightly. These results suggest that primary production correlates well to nutrients availability but meteorological conditions lead to interannual variability regardless of the trophic status of the lake. Accordingly, in oligotrophic freshwaters meteorological forcing may reduce productivity impacting on the entire food chain of the ecosystem.

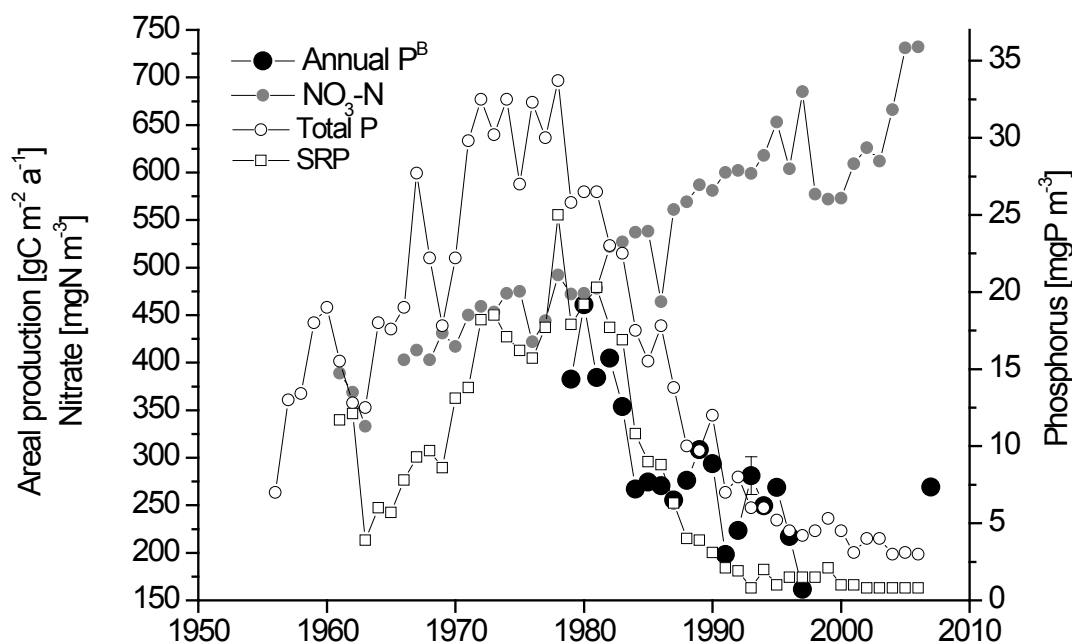


Figure 1. Long-term development of nutrients concentrations and annual productivity in Lake Lucerne. The legend in the top left corner describes the symbols. (Figure from Finger et al., 2013)

## REFERENCES

Finger, D., A. Wüest, and P. Bossard (2013), Effects of oligotrophication on primary production in peri-alpine lakes, *Water Resour. Res.*, 49, doi:10.1002/wrcr.20355.

## 25.5

## Evaluation of pollutants inputs from large agglomeration to the coastal zone: the case of Marseille (France)

Garnier Cédric<sup>1</sup>, Oursel Benjamin<sup>1</sup>, Syakti Agung Dhamar<sup>2,3</sup>, Durrieu Gaël<sup>1</sup>, Mounier Stéphane<sup>1</sup>, Doumenq Pierre<sup>2</sup>, Lucas Yves<sup>1</sup>

<sup>1</sup> Laboratoire PROTEE, Université du Sud Toulon Var, BP20132, 83957 La Garde, France

<sup>2</sup> LCE, Aix-Marseille Université, Europôle Environnement de l'Arbois, 13545 Aix en Provence, France

<sup>3</sup> Fisheries and Marine Science Department, Faculty of Sciences and Techniques-University of Jenderal Soedirman, Jl. HR. Boenyamin 708-Purwokerto, Indonesia

Only a few studies have dealt with the Mediterranean area despite its rapid anthropization due to present-day heliotropism from Northern Europe and despite its climate specificities. Among all the possible sources of marine pollution, large coastal cities are among the most worrying, especially in the Mediterranean Sea. A typical example is Marseille, the largest Mediterranean French city, with over 1.7 million inhabitants. Two small rivers, the Huveaune and the Jarret, run through the agglomeration and join before their outlet to the sea. The uniqueness of this system is that the river waters are mixed with the city waste water treatment plants (WWTP) effluents and then rapidly discharged into the open sea without passing through an estuary, so that the WWTPs' contribution to the water characteristics at the outlet is most likely predominant during baseflow periods. These inputs have a certain impact on the local coastal ecosystem, however, a high number of such anthropized sources along the coast is likely to impact the whole Mediterranean Sea.

During baseflow conditions, dissolved and total organic carbon and metal concentrations in the rivers considered were comparable to values observed for other small coastal Mediterranean rivers, surpassing the world average river values. Concerning the trace metal dynamics in the plume salinity gradient (Fig. 1), Cu, Cd, Co, Pb and Zn are desorbed from the SPM, increasing the potentially bioavailable fraction of these metals. It was clearly demonstrated that the release of metal ions can occur at low salinity with fast kinetics followed by partial re-adsorption onto SPM; a behavior especially observed for Cu. Other metals (e.g. Ni) can undergo a fast adsorption onto SPM followed by slower desorption. Such unusual behaviors make mandatory the practice of filtration immediately after sampling to avoid under- or over-estimation of dissolved metal concentrations (Oursel et al., 2013).

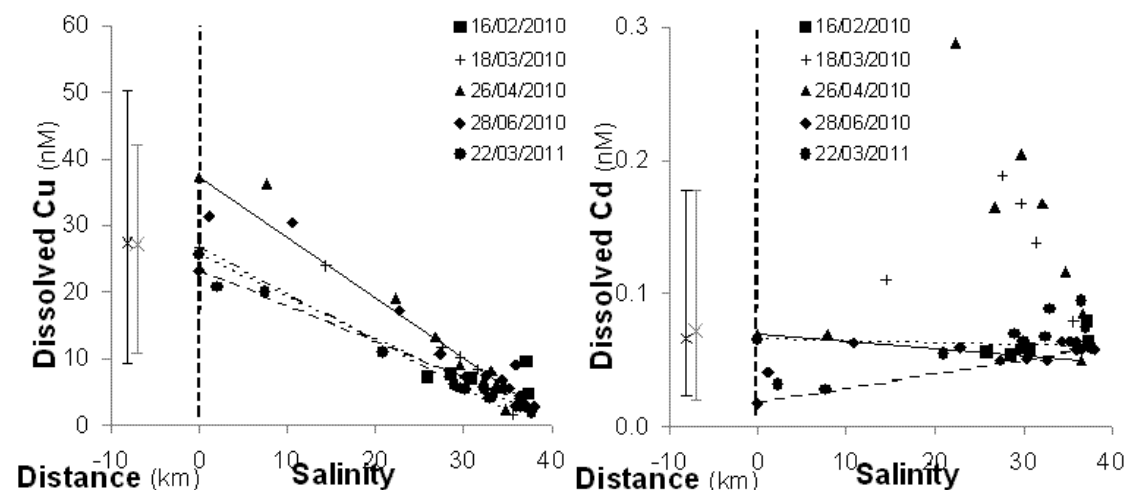


Figure 1. Variation of dissolved Cu (left) and Cd (right) concentrations, during dry season, in rivers (as a function of the distance until the outlet) and from outlet to seawater (as a function of the salinity).

A second important point of this study is that, at the outlet, the river signatures were hidden by the WWTP anthropogenic input for most elements or compounds. The anthropogenic input was higher than 90% of the total input to the sea for particulate Cd, Pb and Cu and higher than 65% for particulate Zn, Co and dissolved Zn and Pb. The daily variation of these inputs followed the fluctuations of the TWW issued from WWTP. Although most likely not frequent, the observed abnormal event linked to a WWTP malfunction or bypass can temporally strongly enhance the impact of an urbanized area on the coastal zone. Similar phenomena all around the Mediterranean are more than probable, especially in countries without wastewater treatment plants. This underlines the need for such treatment facilities for an improvement of local coastal water quality, but most likely also at a more global scale. Such chronic fluxes of pollutants require better study in

comparison to other main sources (large rivers, aerosols, etc.). During wet conditions, trace metals fluxes increased, with a main contribution from rivers (compared to WWTP). Considering the high anthropogenic organic matter and trace element contents of the output to the sea, a detailed study of their chemical speciations, which are known to be strongly influenced by dissolved organic ligands, must be performed to evaluate their bioavailability for marine biota.

Surface sediments were also collected along a coastal-offshore transect (up to 800m from the outlet), and analyzed for major/minor/trace inorganic elements and organic pollutants (hydrocarbons, PAH, PCB) (Syakti et al., 2012). For most of the studied inorganic and organic contaminants, the obtained values significantly overpassed background levels and limits defined by the French authorities in the context of dredging, which attests the past and present contamination of this area and so the strong impact of such urban inputs.

## REFERENCES

- Oursel, B., Garnier, C., Durrieu, G., Mounier, S., Omanović, D. & Lucas, Y. 2013: Dynamic and fate of trace metals in coastal zone impacted by large urban area diffusive inputs: the case of Marseille (France), *Marine Pollution Bulletin*, 69, 137-149.
- Syakti, A.D., Asia, L., Kanzari, F., Umasangadji, H., Malleret, L., Ternois, Y., Mille, G. & Doumenq, P. 2012: Distribution of organochlorine pesticides and polychlorinated biphenyls (PCBs) in marine sediments directly exposed to wastewater from Cortiou, Marseille, *Environmental Science Pollution Research*, 19, 1524-1535.

## 25.6

### Mercury and Methylmercury resuspension in Vidy Bay, Lake Geneva (Switzerland)

Gascon Diez Elena<sup>1</sup>, Cosio Claudia<sup>1</sup> & Loizeau Jean-Luc<sup>1</sup>

<sup>1</sup> F.-A. Forel Institute, Earth and Environmental Sciences Section, Faculty of Sciences, Route de Suisse 10, 1290 Versoix, Switzerland and Institute for Environmental Sciences, University of Geneva, 1211 Geneva, Switzerland (Elena.Gascon@unige.ch)

Mercury (Hg) is an element that accumulates in sediments. Hg can then be transformed into methylmercury (MeHg) by the activity of some bacteria. This form of Hg is known to bioaccumulate in organisms and bioamplifies along the food web. MeHg is highly toxic because it affects the nervous system of organisms.

Lake sediments in Vidy Bay (Lake Geneva) have been shown to be highly contaminated by Inorganic Mercury (IHg) and MeHg. This amount of Hg has been related to the effluent of a Waste Water Treatment Plant (WWTP) that releases into the bay treated wastewaters and combined sewer overflows, loaded with elevated content of organic matter and contaminants, making Vidy Bay rich in heterotrophic bacteria.

The aim of this study was to assess the sources and fate of Total Mercury (THg) and MeHg in the lake. The closest sampling sites to the WWTP reach 1.32 mg/kg of THg and 5.2 µg/kg of MeHg. Further away from the WWTP influence, THg and MeHg concentrations were 0.17 mg/kg and 0.56 µg/kg respectively. In parallel, settling particles have been collected by sediment traps during a one-year period at two sites and two depths. MeHg concentrations on settling particles varied between 1 and 16 µg/kg in the upper sediment trap locations (Figure 1).

As mentioned above, MeHg concentration can be five times higher on settling particles than in the surface sediments. In order to evaluate the hypothesis of an artificial methylation on settling particles during the one-month period collection, sediment traps were exposed to an antibiotic mixture to inhibit the growth of bacteria on the collected particles. MeHg was measured and DNA and RNA were extracted to assess bacterial community structure and functions. MeHg concentrations were lower on settling particles treated with antibiotics than on untreated ones. Therefore, an artefact resulting from a confined environment that promotes anoxia and development of a methylating bacteria community could explain the high MeHg observed in the sediment traps.

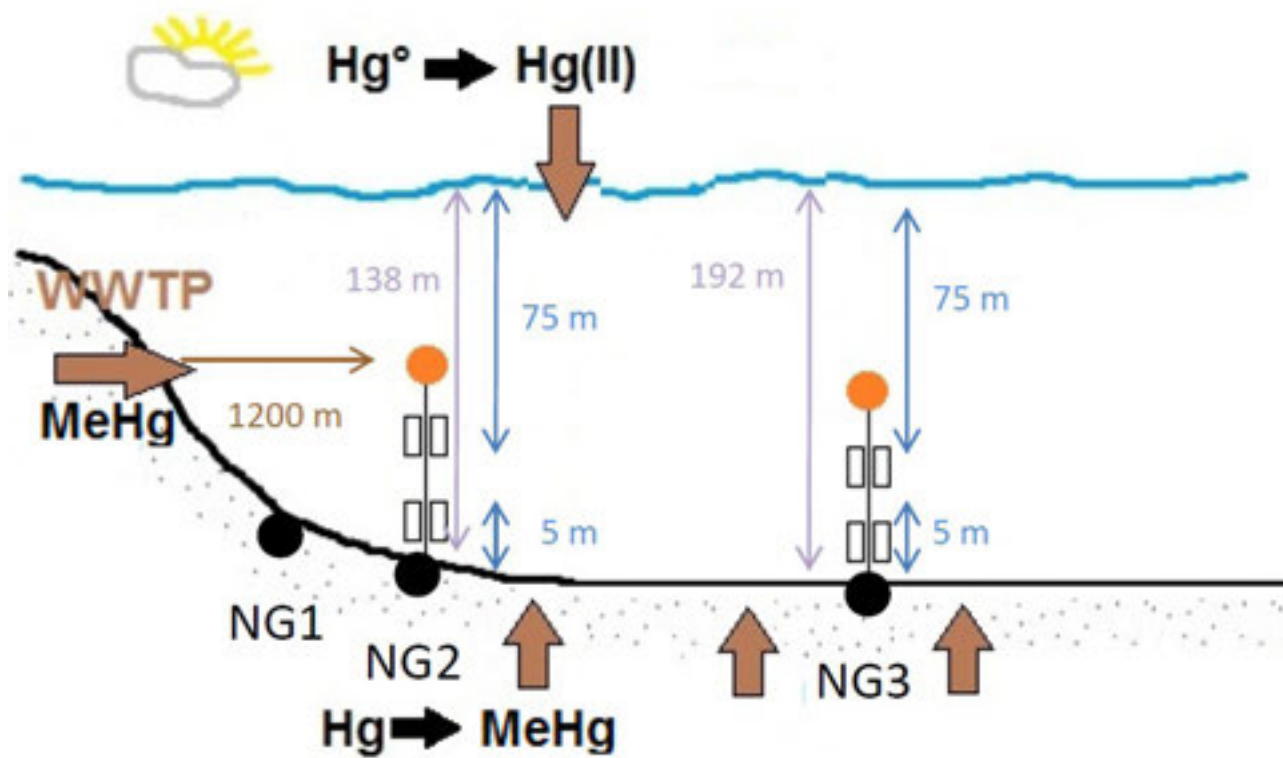


Figure 1. Diagram of the sediment traps catchment system into the lake.

## 25.7

### Radionuclide fluxes in Lake Biel sediments (1955-2010) and Mühleberg NPP <sup>137</sup>Cs liquid emissions

Girardclos Stéphanie<sup>1,2</sup>, Faessler Jérôme<sup>2</sup> & Zehringer Markus<sup>3</sup>

<sup>1</sup> Dept of Earth Sciences, University of Geneva, Rue des Maraîchers 13, CH-1205 Genève (stephanie.girardclos@unige.ch)

<sup>2</sup> Environmental Sciences Institute (ISE), University of Geneva, Route de Drize 7, CH-1227 Carouge/ GE

<sup>3</sup> State Laboratory Basel-City, Kannenfeldstrasse 2, CH-4055 Basel

Lake sediments are good archives of changes happening in their upstream river catchment and environment. Since the second half of the 20th century, they record the history of artificial radionuclides emissions deriving from human activities. <sup>137</sup>Cs emissions started in the early 1950's and peaked in 1963-64 due to high atmosphere nuclear bomb tests. A second activity peak, due to the Chernobyl accident in 1986, can also be detected in central Europe. These two events serve routinely as time markers for recent lake records.

Lake Biel, a mid-sized lake of the Swiss Plateau, lies on the Aare river course and serves as drinking water reservoir for the town of Biel (60'000 inhab.). Its outflowing water is further used by downstream cities lying on the Aare-Rhine course such as Basel (200'000 inhab.). In Switzerland, Nuclear Power Plants (NPPs) were constructed along the Aare river course for cooling purposes. Since 1972, Mühleberg NPP lies 18 km upstream Lake Biel and releases radioactive liquid emissions into the Aare which adds to the diffuse - above mentioned - radioactive pollution, as revealed by Albrecht et al. (1995; 1998) from Lake Biel sediments and recently confirmed by Thevenon et al. (2013).

In this study, the <sup>137</sup>Cs activity curve of a 90-cm-long sediment core (BIE10-8), retrieved in April 2010 from the central Lake Biel basin at ca. 50 m depth, and measured by gamma ray spectrometry using high resolution germanium detectors, confirms previous work and reveals a new peak for the year 1998-2000, as observed by Thevenon et al. (2013). This peak is most certainly due to Mühleberg NPP as shown by the good correlation with declared <sup>137</sup>Cs liquid emissions indicating a significant increase in 1998-99. Comparison with previous data confirms that the central part of Lake Biel, being in the main pathway of Aare underwater inflow, shows a clearer recording of the <sup>137</sup>Cs river input than other sites (Albrecht et al. 1999). Decay corrected activity data, converted into <sup>137</sup>Cs fluxes, point to water pollution by Mühleberg NPP in 1975-1985 as being similar to those linked to the catastrophic events in 1963-64 and 1986 (about 75%). As Lake Biel sediments scavenge only a portion of the total radionuclide in water (30-55%; Albrecht et al. 1999), the present results raise concerns on the past radioactivity of water along the Aare and Rhine course, as the non-scavenged radionuclide emissions add-up in the same river system until Basel (and beyond in Germany). Out of the scope of this work, questions arise on the effects of >35-years-long exposure to low but repeated radioactivity in drinking water over human health and aquatic environments.

This work was financed by SNF projects on Lake Biel nr. 121666 and 146889 and gamma ray analysis by the State Laboratory of Basel-City.

#### REFERENCES

- Albrecht, A., Groudsmid, G. & Zeh M. 1999: Importance of lacustrine physical factors for the distribution of anthropogenic <sup>60</sup>Co in Lake Biel. *Limnol. Oceanogr.*, 44, 196-206.
- Albrecht, A., Reichert, P., Beer, J. & Lück A. 1995: Evaluation of the importance of reservoir sediments as sinks for reactor-derived radionuclides in riverine systems. *Journal of Environmental Radioactivity*, 28, 239-269.
- Albrecht, A., Reiser, R., Lück, A., Stoll, J.-M.A. & Giger W. 1998. Radiocesium dating of sediments from lakes and reservoirs of different hydrological regimes. *Environmental Science & Technology*, 1882-1887.
- Thevenon, F., Wirth, S.B., Fujak, M., Poté, J. & Girardclos S. 2013. Human impact on the transport of terrigenous and anthropogenic elements to peri-alpine lakes (Switzerland) over the last decades. *Aquatic Sciences*, 75, 413-424.

## 25.8

### Assessing the risk of mixture of micropollutants in Geneva lake: from the theoretical approach to “in-situ” ecological effects.

Gregorio V., Chèvre N.

Geneva lake is essential as ecosystem, but it is also used as recreational area, for fishing, and as source of drinking water for more than 600'000 inhabitants. The control of the lake water quality is therefore crucial and a long-term survey is organised by the Commission pour la protection des eaux du Léman (CIPEL, [www.cipel.org](http://www.cipel.org)). This survey provides data on the broad range of chemicals detected at the middle of the lake and in catchment for several years. However, the environmental risk posed by these chemicals is still often assessed substance-by-substance, neglecting mixture effects. In this poster, we present the strategy we used to assess the risk of these chemicals as a “cocktail”. The approach is based on two models called “concentration addition” and “response addition”. The environmental risk assessment of mixture has to deal with the lack of ecological toxicity data for several compounds, which leads to use simplified methodologies and mathematical extrapolations. Indeed, the above models are usually used to calculate a prediction of affected species according to a simplified mathematical methodology but that has the advantage to overcome the lack of data. Therefore, in a first step, our study aimed in validating the use of this mathematical methodology for risk assessment by comparing predictions with a more stringent procedure. Ours results confirmed the validity of this methodology but showed that great uncertainties appeared above some mathematical limits. Then, we assessed the risk of the herbicides detected in Geneva lake for several years and estimated their potential impact on phytoplankton community. The results highlighted a correlation between some algae species and the calculated mixture effect gradient, taking into account the other potential stressors, i.e. the physic-chemical changes. The potential influence of herbicide mixture on some specific populations of micro-algae species is a first step in the understanding of the impact of herbicides on ecological functions of the ecosystem of Geneva lake.

## 25.9

## Current variability in a wide lacustrine embayment (Vidy Bay, Switzerland)

Amir M. Razmi<sup>1</sup>, D. Andrew Barry<sup>1</sup>, Ulrich Lemmin<sup>1</sup>

<sup>1</sup> *Faculté de l'environnement naturel, architectural et construit (ENAC), Ecole polytechnique fédérale de Lausanne (EPFL), Station 2, 1015 Lausanne, Switzerland. E-mails: amir.razmi@epfl.ch, andrew.barry@epfl.ch, ulrich.lemmin@epfl.ch.*

Field measurements and numerical simulations were carried out to examine the effects of meteorological conditions on the hydrodynamics in Vidy Bay. To simulate the flow field, a 3D finite difference hydrodynamic model (Delft3D-FLOW) was employed that simulate whole of Lake Geneva. The Lake hydrodynamics were computed using the Navier-Stokes equations combined with a k- $\epsilon$  turbulence closure model. High-resolution bathymetry and a non-uniform grid system were applied. Detailed over-lake maps of wind, temperature and humidity were used as input to drive the model. An accompanying Lagrangian experiment, using drifters, was conducted in the bay to capture the current patterns and local meteorological data. Acoustic Doppler Current Profiler (ADCP) data and Lagrangian drifter studies in Vidy Bay were compared with numerical results and a reasonable agreement was achieved. Meteorological conditions were categorized in a limited set of typical events and then several numerical scenarios based on typical conditions were simulated. Markedly different circulation patterns were measured within the embayment, with the transition from one pattern to another occurring abruptly for small changes in wind direction. These distinct patterns resulted from relatively small changes in the large gyre of Lake Geneva's main basin, especially the angle between the current in front of the embayment and the embayment shoreline. The model is able to reproduce the velocity profiles and the temperature structures during events.

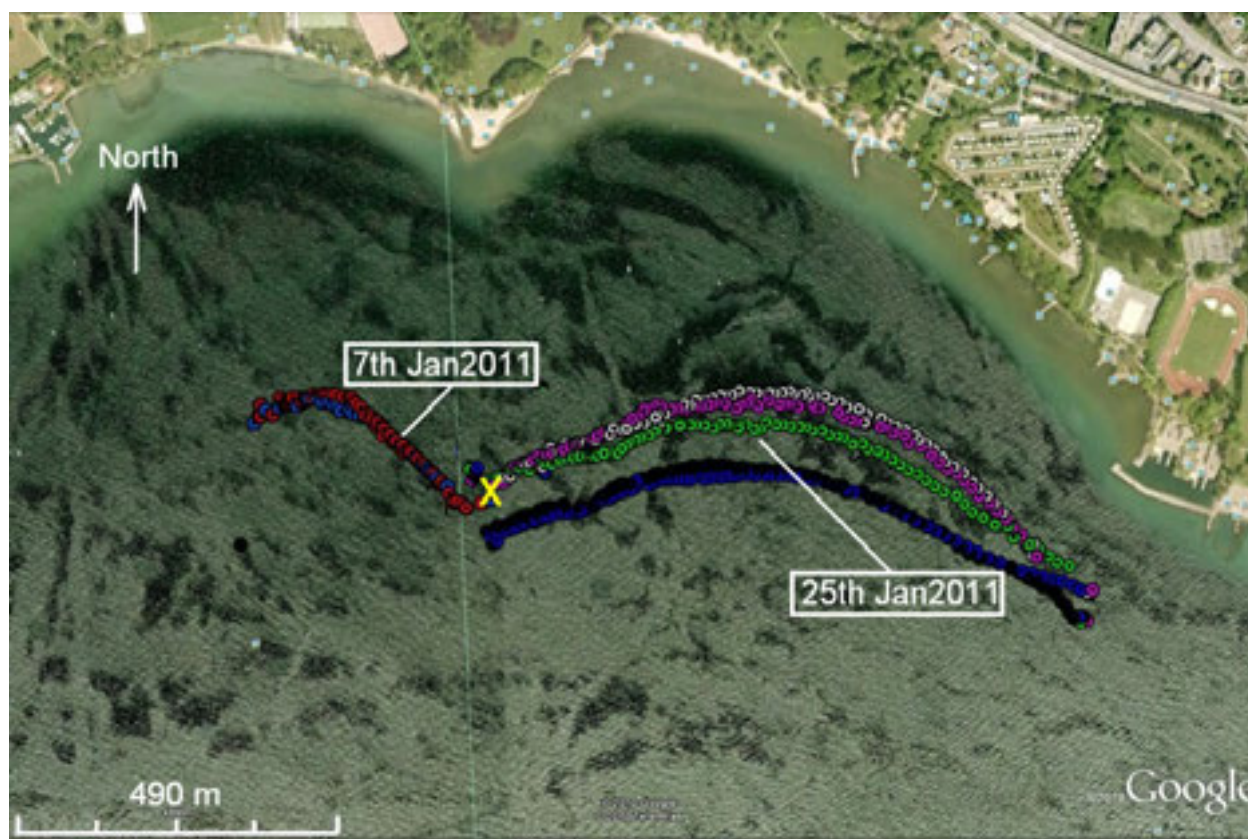


Figure 1. Drifter studies in Vidy Bay (Lake Geneva) showing that there are different current patterns after the similar wind event (Bise) in the embayment.

## REFERENCE

Razmi, AM, Barry, DA, Bakhtyar, R, Le Dantec, N, Dastgheib, A, Lemmin, U, Wüest, A (2013) Current variability in a wide open lacustrine embayment in Lake Geneva (Switzerland). *J Great Lakes Res.* In press. Doi:10.1016/j.jglr.2013.06.011.

## 25.10

### Trends in organic carbon concentrations in Swiss lakes

Juan Carlos Rodríguez-Murillo<sup>1</sup>, Montserrat Filella<sup>2</sup>

<sup>1</sup> Museo Nacional de Ciencias Naturales, CSIC, Serrano 115 dpdo., E-28006 Madrid, Spain (jcmurillo@ccma.csic.es)

<sup>2</sup> Institute F.-A. Forel, University of Geneva, Route de Suisse 10, CH-1290 Versoix, Switzerland (montserrat.filella@unige.ch)

It is generally accepted that organic carbon (OC) concentrations have increased in rivers and lakes of Northern Europe and North America over the last 20-30 years but numerous exceptions to this trend exist. As part of our on-going study on long-term OC dynamics in freshwaters (Rodríguez-Murillo et al. 2013), we have studied OC concentration trends in 34 lakes in Switzerland using data from the Swiss Federal Office for the Environment (FOEN). The set of lakes studied includes large Swiss lakes (7 lakes, 9 time series) as well as 27 smaller lakes (30 time series). All OC concentration time series are longer than 10 years and include at least one value per year (sampling frequency from 1 to 26 per year). Time trends have been studied with LOWESS (LOcally, WEighted Scatterplot Smoothing) regression; long term trends have been obtained with the non-parametric Mann-Kendall and Seasonal Kendall methods. There is no common temporal trend in the OC of the Swiss lakes studied. Large lakes generally show a small (<1% mean OC concentration per year) increase in OC concentrations (increase in 6 series, of which in 4 significantly, and decreases in 3 but none significantly). Small and medium-sized lakes display different trends and levels of significance. These results will be presented together with the discussion of the weight of allochthonous OC versus primary production in the trends observed as well as of the relationship between OC concentration trends in Swiss lakes and rivers.

#### REFERENCES

Rodríguez-Murillo, J.C., Zobrist, J. & Filella, M. 2013: Temporal trends in organic carbon content in the main Swiss rivers, 1974-2010. Submitted.

## 25.11

### Diffuse sources of micropollutants in a mid-size-lake: how to handle them?

Rossi Luca<sup>1</sup>, Chesaux Lydie<sup>1</sup>, Chèvre N<sup>2</sup>

<sup>1</sup> Ecological engineering laboratory, Architecture, Civil and Environmental engineering, EPFL, CH-1015 Lausanne (luca.rossi@epfl.ch, lydie.chesaux@ebiox.ch)

<sup>2</sup> Faculté des géosciences et environnement, Université de Lausanne, CH-1015 Lausanne (Nathalie.chevre@unil.ch)

Diffuse sources of micropollutants in Lake Geneva are regularly identified through monitoring and research activities, including the LEMAN21 ([www.leman21.ch](http://www.leman21.ch)) project. However, several questions remain open regarding the origin of the pollution, its importance and how to handle it. These micropollutants may represent a risk for the ecosystem of Lake Geneva and for the population around the lake, through drinking water. The goals of this study are:

- to identify and quantify diffuse sources of micropollutants in Lake Geneva through sampling and analysis of three tributaries of the lake
- to develop a methodological approach for the sampling of diffuse sources of micropollutants;
- to propose a conceptual approach for the diffuse inputs into Lake Geneva

To reach this goal, three watersheds were equipped with flow measurement systems and auto-samplers to measure the concentrations of 19 substances during rain events and dry weather periods. They are the Rhône watershed (Porte-du-Scex) Chamberonne and Venoge [Rossi and Chesaux, 2013]. On the Rhône river, three sampling campaigns of 14 days (daily samples) were conducted. Three average 14 days samples were also analyzed following the screening methodology developed by Eawag on the Rhine River [Krauss et al 2010]. The results show relatively low concentrations in the Rhone, with the presence of some industrial substances. The concentration ranges are similar to those measured in the Rhine. The screening methodology allowed identifying a molecule not commonly measured in the Rhone River.

The results obtained in rivers Chamberonne and Venoge are representative of the tributaries of Lake Geneva in terms of pesticide concentrations. The results of our measurements show relatively low concentrations during dry weather period and high pollutant dynamic during rain weather period, leading to concentrations sometimes exceeding standards environmental quality standards (EQS).

For each watershed, the quantities of substances used in agriculture were estimated on the basis of the PESTIBASE tool developed by CIPEL [Klein et al 2007]. For the Rhone basin, the comparison between the theoretical quantities applied and the measured concentrations is satisfactory. A detailed survey of part of the Chamberonne watershed was also performed. The study of the reliability of the results was performed using tools based on the sampling theory [Rossi et al, 2010]. For the Rhone, the uncertainties on the annual mass discharged to Lake Geneva are estimated at 35% for dissolved compounds. For the adsorbed compounds, a change in the sampling procedure is needed to reduce the level of uncertainties. In the case of other rivers, taking average samples over 24 hours during the year cannot estimate the annual load in a satisfying way (uncertainty of about 60% even with 40 samples per year). The study of sampling scenarios is strongly recommended before embarking monitoring programs. The establishment of a guideline or a directive on diffuse pollutant sampling is also highly recommended.

A concept leading to the development of indicators of diffuse pollution from agricultural sources for the classification of watersheds is also proposed, based on the agricultural activities and on the watershed vulnerability. A test was conducted on Chamberonne and Venoge watersheds, demonstrating the feasibility of this approach using the tools and the data available in the Geneva Lake context. The criteria and the assigned weights to the different selected indicators still need to be discussed by an expert group.

As a conclusion, we find that the measurement of micropollutants in different rivers is now considered as a goal in itself. But the real goal is to supply information for management tools dedicated to the preservation of the natural environment. These tools are, at present, lacking. Better planning of measurement campaigns based on specific goals and scenarios defined thanks to these tools is essential to avoid accumulating little or no representative information. Prioritization of watersheds, in terms of diffuse pollution contamination and risk is a need to better target actions to preserve the environment of Lake Geneva

## REFERENCES

- Rossi, L., Chesaux L. 2013 : Sources diffuses de micropolluants dans le Léman : Etude de bassins versants spécifiques et définition d'outils d'extrapolation. Rapport d'étude de l'EPFL, laboratoire de technologie écologique (ECOL), sur mandat de l'Office fédéral de l'environnement (OFEV). EPF Lausanne, 101 p + Annexes.
- Krauss, M., H. Singer, and J. Hollender, 2010: LC-high resolution MS in environmental analysis: from target screening to the identification of unknowns. *Analytical and Bioanalytical Chemistry* 397(3): 943-951.
- Klein, A., F. Manco, and R. Charles, 2007: Pesticides d'origine agricole dans le bassin versant suisse du Léman. *Rapp. Comm. int. prot. eaux Léman contre pollut., Campagne 2006*: p. 187-201.
- Rossi L., Rumley L., Ort C., Minkinen P., Barry D.A, Chèvre, N: 2011. Samplinghelper a web-based tool to assess the reliability of sampling strategies in sewers and receiving waters, *Water Science and Technology* 63(12): 2975-2982.

## P 25.1

Chronic tests of two anticancer drug metabolites on *Daphnia pulex*

Borgatta Myriam<sup>1</sup>, Waridel Patrice<sup>2</sup>, Decosterd Laurent-Arthur<sup>3</sup>, Buclin Thierry<sup>3</sup>, Chèvre Nathalie<sup>1</sup>

<sup>1</sup> Institute of Earth Sciences, Faculty of Earth Sciences and Environment, University of Lausanne, Switzerland (myriam.borgatta(a)unil.ch)

<sup>2</sup> Protein Analysis Facility, Center for Integrative Genomics, Faculty of the Faculty of Biology and Medicine, University of Lausanne, Switzerland (patrice.waridel(a)unil.ch)

<sup>3</sup> Division of Clinical Pharmacology and Toxicology, Faculty of Biology and Medicine, Centre Hospitalier Universitaire Vaudois (CHUV), Switzerland (thierry.buclin(a)chuv.ch)

Pharmaceuticals taken by humans are eliminated through the excreta in either intact or transformed form (i.e. metabolites). In developed countries, drug residues follow urban sewage water networks to a sewage treatment plant (STP), which has originally been intended for organic matters, but not such chemicals. Therefore, pharmaceuticals and derivatives that still have some pharmacological activities may escape STP processes and reach the aquatic ecosystem (Williams, 2005). Such bioactive molecules are susceptible to interact with biological processes of aquatic species, even at low concentrations.

Among other pharmaceuticals, anticancer agents are of particular concern because of their potential side effects on human body (Daughton and Ternes, 1999). Tamoxifen is a chemotherapeutic anti-estrogen compound that is prescribed worldwide for the prevention and treatment of hormone receptor-positive breast cancer. It is known to escape degradation process by STPs and was measured in both STPs effluents and natural waters at concentrations up to 0.31.8 µg/L and 0.22 µg/L respectively (López-Serna et al., 2012). In a previous study (manuscript in progress), we showed that tamoxifen induces neonatal abnormalities in *Daphnia pulex*, a freshwater microcrustacean, exposed over 21-days to concentrations ranging from 0.2 to 1 µg/L.

Tamoxifen is considered nearly as a prodrug (Rautio et al., 2008), which release active molecules after enzymatic and/or chemical transformation *in vivo*. Although tamoxifen is already an active molecule, two of its metabolites namely 4-hydroxy-tamoxifen (4OHTam) and endoxifen are pharmacologically more potent in vertebrates. These metabolites as well as their parent compound are body-excreted, mainly through feces. Tamoxifen and both metabolites continuously reaching the aquatic environment may induce long-term effects on aquatic organisms. However, to the best of our knowledge, no data have been reported addressing actual concentration of endoxifen and 4OHTam in the aquatic environment and their long-term effects on aquatic organisms. In this work, we assessed the long-term effects of 4OHTam and endoxifen on *D. pulex* over two generations (F0 and F1). The objective was to observe whether these anticancer drug metabolites affect the survival, reproduction and size of daphnids.

The results showed that the metabolites 4OHTam and endoxifen induced effects on reproduction, survival and body-length at relatively low concentrations. The mortality was 100% in the F0 generations exposed to 99 µg/L of 4OHTam or 202 µg/L of endoxifen. The reproduction decreased significantly in the F0 and F1 exposed to 6.8 and 23.8 µg/L of 4OHTam. In addition to mortality and disturbed reproduction, differences of body-length were observed. At the two highest concentrations tested, the F0 generation did not grow up and kept a size similar to control < 24-h neonates. The offspring from reduced-size parents were also smaller at the end of their respective test period.

In spite of their high pharmacological potency and their extensive release in the environment, endoxifen and 4OHTam had never been tested on aquatic species. While we could show detrimental effects of these tamoxifen metabolites on *D. pulex*, additional long-duration experiments should be carried out on daphnids and other aquatic species to confirm the results and better characterize their effects on the aquatic fauna. In general, pharmaceutical metabolites are insufficiently studied in ecotoxicology and the question of prodrugs and active derivatives receives too little consideration in this field. The issue of active metabolites should be fully integrated into the environmental toxicology assessment of pharmaceuticals, as currently required by the European Medicine Agency. We hope that our observations contribute to promote a better integrated assessment of pharmaceutical ecotoxicity of both novel and ancient medicines.

## REFERENCES

- Daughton, C.G., and Ternes, T.A. (1999). Pharmaceuticals and personal care products in the environment: agents of subtle change? *Environ Health Perspect* 107, 907–938.
- Lien, E.A., Solheim, E., Lea, O.A., Lundgren, S., Kvinnsland, S., and Ueland, P.M. (1989). Distribution of 4-hydroxy-N-desmethyltamoxifen and other tamoxifen metabolites in human biological fluids during tamoxifen treatment. *Cancer Res.* 49, 2175–2183.
- López-Serna, R., Petrović, M., and Barceló, D. (2012). Occurrence and distribution of multi-class pharmaceuticals and their active metabolites and transformation products in the Ebro River basin (NE Spain). *Sci. Total Environ.* 440, 280–289.

- Rautio, J., Kumpulainen, H., Heimbach, T., Oliyai, R., Oh, D., Järvinen, T., and Savolainen, J. (2008). Prodrugs: design and clinical applications. *Nat Rev Drug Discov* 7, 255–270.
- Williams, R.T. (2005). *Human Pharmaceuticals: Assessing the Impacts on Aquatic Ecosystems* (Pensacola: Society of Environmental Toxicology and Chemistry, SETAC Press).

## P 25.2

### Physical process and hypoxia in Lake Erie

Bouffard D., Boegman L., Ackerman JDA.

EPFL, ENAC IIE APHYS, Station 2, 1015 Lausanne

Hypoxia in the hypolimnion of Lake Erie has been examined by assessing (i) the spatial and temporal extent of the hypoxia (e.g., July to October in the central basin,  $>10^4$  km<sup>2</sup>) and (ii) linking the rate of oxygen (DO) depletion to the hypolimnion thickness. However, assessing the processes driving inter-annual variability in oxygen and the small-scale temporal and spatial patchiness in DO depletion ( $-0.7$  to  $+0.3$  mg L<sup>-1</sup> d<sup>-1</sup>) remain unknown. Data from the summers of 2008 and 2009 in central Lake Erie (13 moorings) enabled us to quantify how much of the DO variability is controlled by physical processes, relative to biological processes and the sediment oxygen demand (SOD). The flux of oxygen through the thermocline to the hypolimnion was equivalent to ~18% of the total oxygen depletion in the hypolimnion over the stratified period. The total oxygen depletion in the hypolimnion was due to equivalent amounts of *HOD* and *SOD*. This latter finding was strongly dependent on hypolimnion thickness, which appears to control the vertical volumetric fluxes and hence the competition between vertical flux and community respiration in the hypolimnion of other shallow lakes.

## P 25.3

### Spatial runoff estimations based on the deuterium-excess due to the isotopic evaporation effect in an upstream lake

Chevrolet Alexandra, Fischer Benjamin, Seibert Jan

Geographisches Institut, University of Zürich, Winterthurerstrasse 190, CH-8057 Zürich (alexandra.chevrolet@uzh.ch)

Where does the water in a stream come from? We asked this question for the stream *Reppisch* close to Zürich. With a growing urbanisation and possible changes in the water regime there is an increasing need to obtain better information about the *Reppisch*-catchment (25 km<sup>2</sup>). As a tracer we used the stable water-isotopes  $\delta^{18}\text{O}$  and  $\delta\text{D}$ , which are a proven tool to understand the different flow paths of water and help to quantify the groundwater contributions along the *Reppisch*. The *Türlersee* at the top of the long narrow *Reppisch*-valley and the absence of bigger inflows to the stream make this an ideal location for examining the contribution of a lake to downstream discharge by tracing the isotopic evaporation signal of the lake. We compared isotopic and hydrometric data of the summers 2010, 2011 and 2013 for the *Türlersee* with that at different locations downstream along the *Reppisch* and at some inflows as well as that of precipitation in the area. First results show that the isotopic evaporation signal of the *Türlersee* is clearly traceable downstream the *Reppisch*. The deuterium-excess curve of the *Reppisch* approaches closer to the Global Meteoric Waterline (GMWL) the further the distance from the lake. We conclude that this alteration occurs mainly through groundwater and the small inflows from the hills aside the *Reppisch*. The inflows' deuterium-excess signal is lying in the range of 7.5 to 10 ‰. This is up to 8 ‰ closer to the GMWL than the *Türlersees* and *Reppischs* signals. We reason that the further away from the lake the bigger becomes the portion of the little streams and groundwater in the *Reppischs* discharges. In the case of an event, the immediate reaction of the little streams and their isotopic signal being close to the isotopic signal of the current rain, show that the dynamics of the *Reppisch*-system leads the precipitation to a quick runoff. The obtained results can serve as a basis for an improved hydrological model of the *Reppisch*-catchment by allowing calibration and testing of spatially distributed simulations.

## P 25.4

### Enhancement of the representativeness of herbicide effect modelling in watercourses.

Copin Pierre-Jean<sup>1</sup>, Chèvre Nathalie<sup>1</sup>

<sup>1</sup> *Faculté des géosciences et de l'environnement, Institut des Sciences de la Terre, Université de Lausanne, Quartier UNIL-Mouline, Bâtiment Géopolis, CH-1015 Lausanne.*

These last years, many herbicides were detected in Swiss watercourses. The concentrations of some of these herbicides were higher than the criteria of 0.1 µg/l defined in the Swiss legislation. Moreover, these herbicides are discharged non-continuously in watercourses or streams after crop applications and during rain events. It is therefore important to determine the effects of these non-continuous exposures on aquatic species. Algae species are specifically interesting as they are commonly very sensitive to herbicides. Furthermore, they are at the base of the food chain. Consequently, if they are damaged, the whole fauna may be affected. In this context, a model was developed to assess the growth inhibition of the green alga *Scenedesmus vacuolatus* caused by non-continuous exposure scenarios to the herbicide isoproturon. The uncertainties of the predictions were also estimated. This model was validated with laboratory experiments. Non-continuous exposure is characterized by periods of exposure (with the herbicide) and recovery (without the herbicide). The effects on algae species will therefore depend on the length of these 2 types of periods but also on the herbicide concentration during the pulse exposure. Indeed, even if the pulse duration is short, a high concentration can inhibit the growth of the algae. To improve the environmental representativeness of this model, it was adapted to predict the effects of non-continuous exposure to mixture of herbicides. Finally, the model was also evaluated by testing pulse exposure scenario of isoproturon on two algae species growing in the same medium: a circular one (*Scenedesmus vacuolatus*) and a rangy one (*Pseudokirchneriella subcapitata*). The model validity is discussed for each case studied.

## P 25.5

### Calculation of Physical Chemistry Parameters (Amount and Rate of Salt Precipitation) from Brines Urmia Lake

Javad Darvishi khatuoni<sup>1</sup>, RaziyeH lak<sup>2</sup>, Ali Mohammadi<sup>3</sup>

<sup>1</sup> *Geological survey of Iran, Iran*

<sup>2</sup> *Research Institute for earth sciences, geological survey of Iran, Iran*

<sup>3</sup> *Geological Institute, ETH Zuerich*

Urmia Lake as the largest hypersaline lake in the world located Azerbaijan area(NW of Iran). Considering the international importance of saving Urmia lake from the drying crisis and attention to the problem of thick masses of salt accumulation in the lake bottom,in the present study,we intend to show that how, where, and at what rate a hypersaline brine as a case the Urmia lake gets rid of one of its components, the common sodium chloride.

The actual density-salinity relation  $\beta^* = \Delta\rho/\Delta S$  is a combination of two different thermodynamic constants. One of them,  $\beta_{NaCl}$ , is the brine's expansion coefficient to sodium chloride and relates to the process of halite precipitation; and the other  $\beta$ , is the brine's expansion coefficient to total salts and relates to the dilution-evaporatiqn process. For every particular period under study, the actual density-salinity relation  $\beta^*$  must be evaluated separately. The approximate salinity value and the observed rate of change of density and with estimations of salt balance of the lake, yield an evaluation of the rate of salt precipitation from the Urmia lake. The existing estimations for the salt balance of the lake are widely variable, reflecting the unknown subsurface water inflow, the rate of evaporation, and the rate of salt accumulation at the lake bottom. To estimate these we calculate the mass balances for the Urmia lake utilizing measured meteorological and hydrographical data from 1999 to 2011.

## P 25.6

# The History of Sedimentation and the Risk of Falling Urmia lake level in Iran

Javad Darvishi khatuoni<sup>1</sup>, Ali Mohammadi<sup>1</sup>, Alireza salehipuor Milani<sup>3</sup>, RaziyeH lak<sup>3</sup>

<sup>1</sup> Geological survey of Iran, Iran

<sup>2</sup> Geological Institute, ETH Zuerich

<sup>3</sup> Geological survey of Iran, Iran

**Background and Aims:** Urmia Lake is one of the biggest and salt over-saturated Lakes in the world. It is located at the northwestern part of Iran. Today, it has been endangered by drying up processes. This environmental hazard is one of the most significant geological problems of Iran. Verification of evolutionary history of Holocene and understanding the reasons for sudden downfall of Urmia Lake water level is the main subject for current study.

**Objectives:** In this research, remote sensing examinations for a period of 35 years, 55-year climatic data processing and their relationship with Lake Water fluctuations were implemented, and undisturbed sedimentary cores of western Lake sediments were prepared by Auger coring method (eg. Piovano et al., 2002). 16 cores having a maximum depth of 9 meters, and totally 98m of the Lake sub-floor sediments were verified.

**Methods:** Sedimentary facies were separated by color, grain size, mineralogy specifications, sedimentary fabrics and evaporative minerals (Li et al., 1996; Valeo- Garces et al., 1999; Benison, K. C., and Goldstein, R. H., 2001). With regard to vertical sedimentary facies (from surface to sub-surface areas) changes, geography, climatic conditions and Lake water level fluctuation were re-constructed. Results indicated 17 separable types of sedimentary facies in cores. Facies are from Lacustrine, Playa, Swamp, fluvial and terrestrial environments. Coring and verification of Lake Sub-environment sedimentary facies indicate that sequential drying up tracks are visible in the coastal areas of Urmia Lake

**Results:** However, the main part of the Lake has had Lacustrine environment (6.5m of the Lake floor sediments) for 13000 years. Sedimentation was continuous during the mentioned period and seismic data confirm this issue. Climate change and particularly evaporation increment are significant agents in downfall of Lake water. But these are not the main causes for drought in Urmia Lake region. Iran has experienced a long-term drought since 13000 years ago up to now. Hence, shallow Lakes, such as Maharloo, Mirabad and Zarivar were frequently dried (Lak et al., 2007). It is important to note that Urmia Lake has never experienced dryness except in coastal areas. The main stage of Urmia Lake region drought commenced about 13000 years ago. This event indicated coincidence with the last Ice Age. Regarding the Ice Age, downfall of moisture and Lakes' water levels of North Africa and southern Asia was pointed out (Cohen, 2003).

**Conclusions:** Based on assessment of age in Urmia lake sediments (Kelts and Shahrabi, 1986) sedimentation rate varies from 0.1 to 1 mm per year. But the core near the core study area sedimentation rate is about 0.5 mm per year. The facies sequence of the great drought in the lake at a depth of 650 cm with an approximate age is 13,000 years since there is continuous deposition of supersaturated salt in a lake. But now not only at the core of the harvest, but up to 4 km of the lake has become a dandruff dry prairie and desert, which indicates the influence of anthropogenic factors (water structures such as dams, Bridge, indiscriminate use of water resources underground) present in the lake is drying. Therefore, today, the important agent in downfall of the Urmia Lake water is anthropogenic factor.

## REFERENCES

- Benison KC and Goldstein RH (2001) Evaporites and siliciclastics of the Permian Nippewalla group of Kansas, USA: a case for non-marine deposition in saline lakes and saline pans, *Sedimentology*, 48, p.165-188.
- Cohen AS (2003) *Paleolimnology. The history and evolution of lake systems*, Oxford university press, 500p.
- Kelts K and Shahrabi M (1986) Holocene sedimentology of hypersaline Lake Urmia, Northwestern Iran, *Palaeogeography, Palaeoclimatology, Palaeoecology*, 54:pp. 105-130.
- Lak R, Fayazi F, Nakhaei M (2007) Sedimentological evidences of a major drought in the Mid - Late Holocene of the Lake Maharloo, SW Iran, 4th International Limnogeology Congress, Abstract book.
- Li J, Lowenstein TK, Brown CB, Ku TL, Luo S (1996). A 100 ka record of water tables and paleoclimates from salt cores, Death Valley, California, *Paleogeography, Paleoclimatology, Paleoecology*, v:123, p:179-203.
- Piovano EL, Ariztegui D and Moreiras SD (2002). Recent changes in Laguna Mar Chiquita (central Argentina): a sedimentary model for a highly variable saline lake, *Sedimentology*, no. 49, p: 1371-1384
- Valero Garces, BL, Grosjean M, Kelts K, Schreier H, Messerli B (1999). Holocene lacustrine deposition in the Atacama Altiplano. facies models, climate and tectonic forcing, *Paleogeography, Paleoclimatology, Paleoecology*, no.151, p:101-125.

## P 25.7

# Evolution of Lake Maharlou brine during 4 years monitoring

Lak Razyeh<sup>1</sup>, Fayazi, Shahrzad <sup>2</sup>

<sup>1</sup> Research Institute for Earth Sciences, Geological Survey of Iran, Tehran, Iran, [lal\\_ir@yahoo.com](mailto:lal_ir@yahoo.com)

<sup>2</sup> Department of Mathematics, Shahid Beheshti University, Tehran, Iran, [shahrzadfayazi@yahoo.com](mailto:shahrzadfayazi@yahoo.com)

Maharlou Lake is located southeast of Shiraz, Iran (Fig. 1). In wet seasons, the Lake in its largest size is 26 km long and 12 km wide covering an area of 280km<sup>2</sup>. The Maharlou basin is situated in a relatively elevated depression (1455 m above sea level) with a northwest-southeast trend. Maharlou Lake is an intra-continental sedimentary basin. The water level in the lake is controlled by several factors, including runoff from Maharlou catchments, groundwater seepage, and direct rainfall over the lake and the evaporation rate. Hydrochemistry of the catchments water resources showed mainly chloride and sulfate waters due to the geology of the surrounding areas and its variable lithology. Hydrochemical investigations were carried out over a time period from 1975 to 2002 using previously published analysis, together with newly collected water samples. Two hundred thirty samples were collected during summer 2002, 2003, 2004 and spring 2005. The new types of waters flowing into the lake were also determined. Hydrochemical analyses of these waters showed that the difference of cations and anions is a cause for the different geological features (e.g Jones and Deocampo 2004). The amount of calcium and magnesium cations and sulfate and chloride anions are dominant. It should be noted that in all the input waters, the total amount of Ca and Mg exceeds the amount of HCO<sub>3</sub>; HCO<sub>3</sub> << Ca + Mg. This means that evolution path II of the brine evolution flowchart (Eugster and Hardie 1978) eventually create a Na-SO<sub>4</sub>-Cl or Ca-Na-Cl brine type, whereas the current brine is Na-Mg-Cl-(SO<sub>4</sub>) which belonged to the path III<sub>2b</sub> of the mentioned flowchart. The current Maharlou Lake brine type is similar to Great Salt Lake in the USA (Spencer et al. 1985). Relative amounts of ions in dry and wet seasons are as follows: Na> Mg> K>Ca and Cl> SO<sub>4</sub>>HCO<sub>3</sub>> CO<sub>3</sub> (Fig. 7). Due to high concentrations of sodium and chloride, on the surface of the lake, salt crusts are developed during the dry season. In the wet season, dissolution of salt crusts increases lake water concentration. In the summer, large amounts of evaporite minerals precipitate to the lake floor (Sonnenfeld 1984). The largest amount of salty crust precipitated in the summer of 2002, when it reached a thickness of 60 cm. During wet seasons, diluted waters entering the lake dissolve a major portion or even the whole salty crust. Mineralogy composition of the salty crust, in the dry condition is only Halite whereas in wet conditions a variety of evaporite and carbonate minerals are precipitated; among which Halite, Gypsum and Calcite are the most abundant.

Results showed distinct changes in the brine type over time; from Mg-SO<sub>4</sub>-Cl type reported by Krinsley (1970) to a recent Na-Mg-Cl-(SO<sub>4</sub>) type, which is comparable with Great Salt Lake in the USA. A Change in diluted water composition going from HCO<sub>3</sub> ≥ Ca + Mg to HCO<sub>3</sub> << Ca + Mg has taken place. That is, the path of brine composition on the Eugster & Hardie (1978) flow diagram has changed from row III<sub>2b</sub> to the path II, and may finally result in a Ca-Na-Cl or Na-SO<sub>4</sub>-Cl brine type in the future. In this study, two mixed zones of fresh and saline waters were recognized in the northwest and center of the lake, with the lowest ionic concentrations, located where there is significant river and ground water supply.

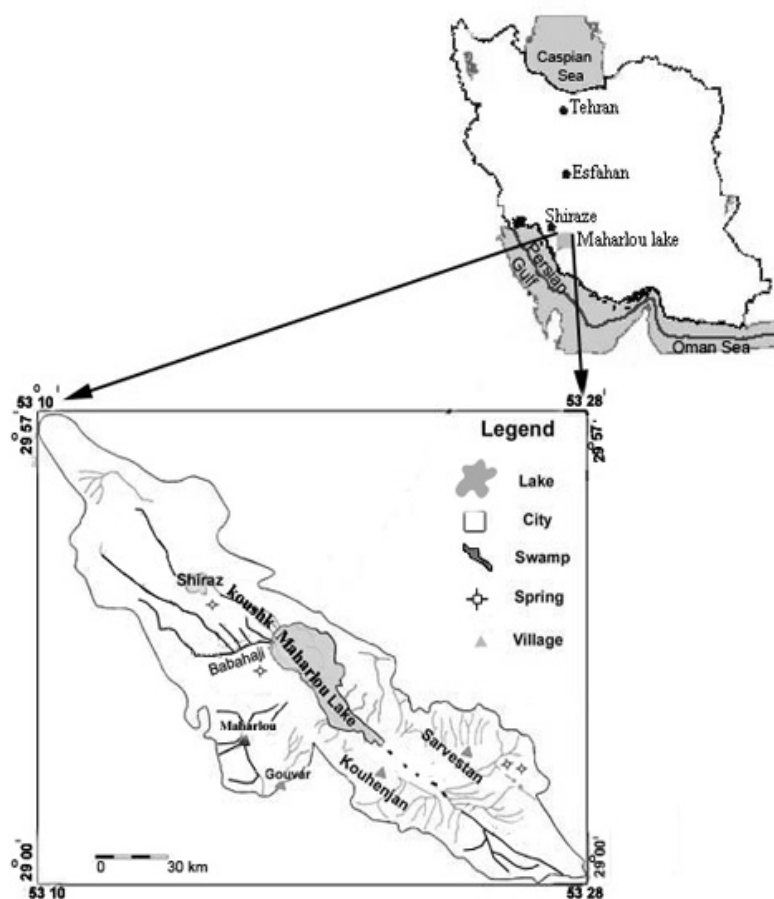


Figure 1. Hydrographic map of the Maharlou Basin. Nahr-e-Azam (Khoshk) and Chenar Rahdar Rivers are more important than others.

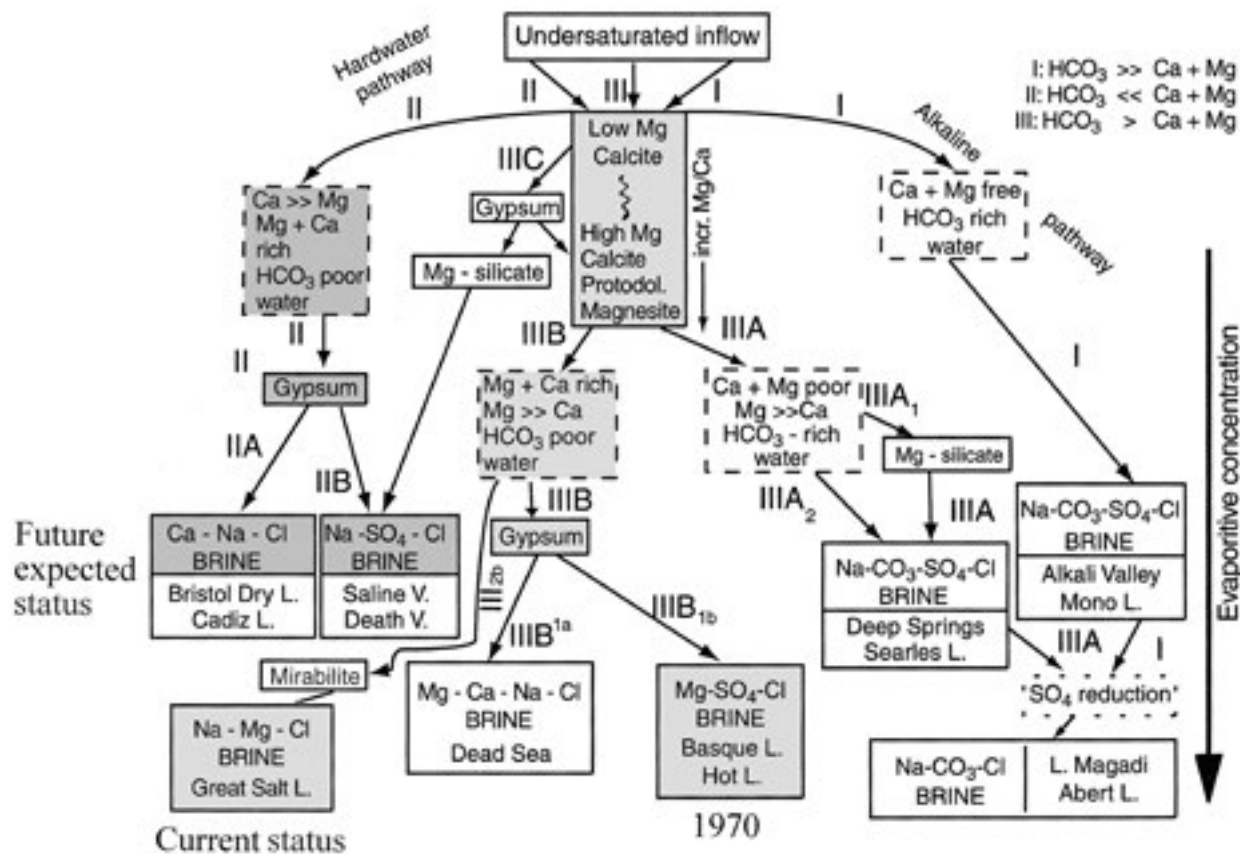


Fig. 2: Flow diagram for the geochemical evolution of closed basin brines from Eugster and Hardie (1978). The brine type changed from Mg-SO<sub>4</sub>-Cl type reported in 1970 to a recent Na-Mg-Cl(SO<sub>4</sub>) type (highlighted in light gray).

## REFERENCES

- Eugester, H.P. and Hardie, L.A., 1978, Saline Lakes, in Lerman, A., (ed.), Lakes, Chemistry, Geology and Physics. Springer – Verlag, p. 237-293.
- Jones, B.F. and Deocampo, D.M., 2004, Geochemistry of Saline Lake, in Treatise on Geochemistry, US Geological Survey, p. 393-424.
- Krinsley, D.B., 1970, Geomorphological and Paleoclimatological Studies of the Playa of Iran, US Government Printing Office Washington D.C., v. 20, 402 p.
- Sonnenfeld, P., 1984, Brines and Evaporites, Academic Press, INC. 613p.
- Spencer, J., Eugster, H.P., Jones B.F., and Rettig S.L., 1985, Geochemistry of Great Salt Lake, Utah: Hydrochemistry since 1850. Geochimica Cosmochimica Acta, v. 49, p. 727-737

## P 25.8

## Sedimentology, Sedimentary Sub-environments and Mineralogy of Holocene Sediments of Maharlou Lake, Southwest of Iran

Lak Razyeh <sup>1</sup>, Rezaeian Langeroudi Saeed <sup>2</sup>

<sup>1</sup> Research Institute for Earth Sciences, Geological Survey of Iran, Tehran, Iran, (lak\_ir@yahoo.com)

<sup>2</sup> M.Sc. student of teacher-training University, Tehran, Iran, (saeedsediment@yahoo.com)

Maharlou Lake with 280km<sup>2</sup> catchment area in wet seasons is located southeast of Shiraz, Iran (Fig. 1) and according to the Sonnenfeld classification Scheme (1991), is regarded as an intra-continental basin. This research was conducted with the aim to determine sedimentary facies and identify evaporate minerals as well as the change in the type of mineral composition within the sediments that were formed during the Holocene period reflecting the balance in water input and output in the studied basin. In this study, thirteen core samples (max length 180 cm) were selected from the intact bottom of the Lake using a gravity core sampler (Mudroch and MacKnight, 1994). The core samples were then dissected in halves longitudinally, underneath the sediments, Playa environment was detected. In total, 85 sub-samples were prepared from various core samples of sedimentary facies, which were then analyzed using grain and mineral analytical methods such as granulometry and XRD (Fig. 2). In addition, details of sediment samples were examined with binocular and electronic microscopes. The results of these analysis showed that the Lake sediments are composed of three types of sediments: Detrital sediments, Carbonated sediments (chemical and biochemical sources), and evaporate sediments. Minerals that formed detrital sediments were: quartz, feldspar, clay minerals such as illite, palygorskite, flugopite. Carbonated minerals were calcite, dolomite, aragonite, magnesite, natron. Biochemical sediments were composed of artemia pallet dominated by aragonite. Evaporate minerals were gypsum, halite, basanite, polyhalite, glauberite, sudoite. The bottom of the Lake was mainly formed by sandy clay silt. A few gravel was found in some of the samples which originate from larger gypsum crystals.

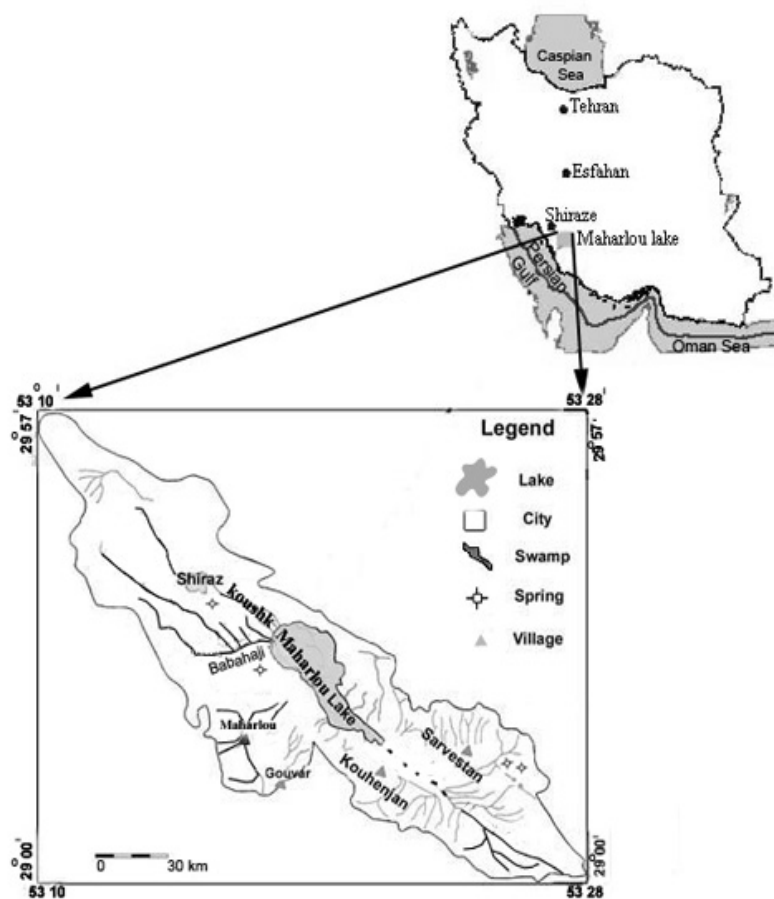


Figure 1. Hydrographic map of the Maharlou Basin. Nahr-e-Azam (Khoshk) and Chendar Rahdar Rivers are more important than others.

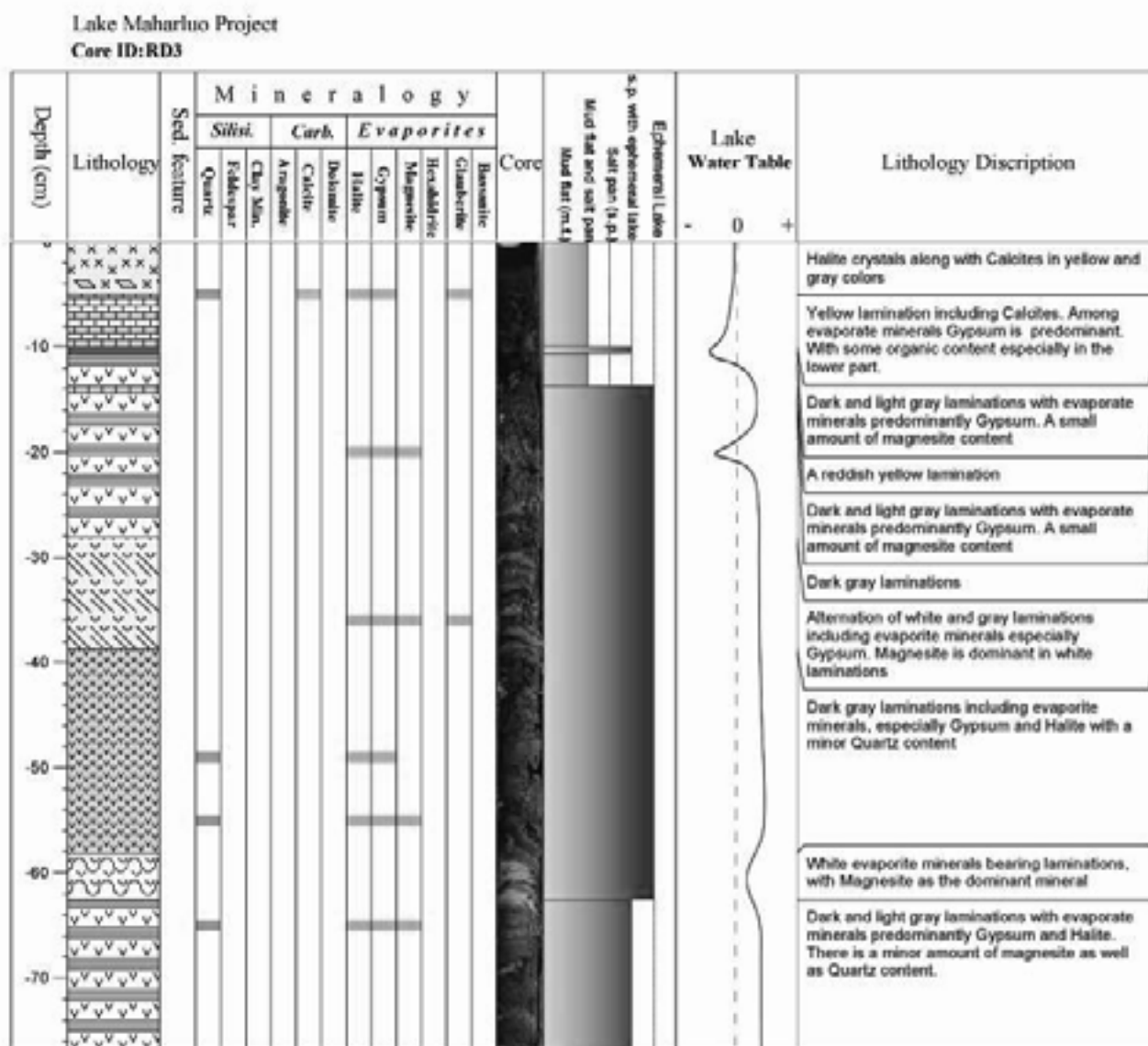


Figure 2. Description of stratigraphical, mineralogical, macroscopic image, sedimentary sub-environment, water table fluctuation column of RD3 core.

#### REFERENCES

- Sonnenfeld, P., 1991: Evaporite basin analysis. In E.R. Force (ed.), Sedimentary and Diagenetic Mineral Deposits: A basin analysis approach to exploration, 159-169.
- Mudroch, A. & MacKnight, S.D. 1994: Techniques for aquatic sediments sampling, CRC Press, 236p.

## P 25.9

# Treatment of micropollutants in municipal wastewater: Ozone or powdered activated carbon?

Margot Jonas<sup>1</sup>, Kienle Cornelia<sup>2</sup>, Magnet Anoy<sup>3</sup>, Weil Mirco<sup>4</sup>, Rossi Luca<sup>1</sup>, de Alencastro Luiz Felipe<sup>1</sup>, Abegglen Christian<sup>5</sup>, Thonney Denis<sup>3</sup>, Chèvre Nathalie<sup>6</sup>, Schärer Michael<sup>7</sup>, Barry D. Andrew<sup>1</sup>

<sup>1</sup> School of Architecture, Civil and Environmental Engineering (ENAC), Ecole Polytechnique Fédérale de Lausanne (EPFL), Station 2, 1015 Lausanne, Switzerland (jonas.margot@epfl.ch)

<sup>2</sup> Swiss Centre for Applied Ecotoxicology, Eawag/EPFL, Überlandstrasse 133, 8600 Dübendorf, Switzerland

<sup>3</sup> Sanitation Service, City of Lausanne, Rue des terreaux 33, 1002 Lausanne, Switzerland

<sup>4</sup> ECT Oekotoxikologie GmbH, Boettgerstrasse 2-14, 65439 Floersheim/Main, Germany

<sup>5</sup> Swiss Federal Institute of Aquatic Science and Technology (Eawag), Überlandstrasse 133, 8600 Dübendorf, Switzerland

<sup>6</sup> Faculty of Geosciences and the Environment, University of Lausanne, 1015 Lausanne, Switzerland

<sup>7</sup> Federal Office for the Environment (FOEN), Water Division, 3003 Bern, Switzerland

Many organic micropollutants present in wastewater, such as pharmaceuticals and pesticides, are poorly removed in conventional wastewater treatment plants (WWTPs). To reduce the release of these substances into the aquatic environment, advanced wastewater treatments are necessary. In this context, two large-scale pilot advanced treatments were tested in parallel over more than one year at the municipal WWTP of Lausanne, Switzerland. The treatments were: i) oxidation by ozone followed by sand filtration (SF) and ii) powdered activated carbon (PAC) adsorption followed by either ultrafiltration (UF) or sand filtration. More than 70 potentially problematic substances (pharmaceuticals, pesticides, endocrine disruptors, drugs metabolites and other common chemicals) were regularly measured at different stages of treatment.

Additionally, several ecotoxicological tests such as the yeast estrogen screen, a combined algae bioassay and a fish early life stage test were performed to evaluate effluent toxicity. Both treatments significantly improved the effluent quality. Micropollutants were removed on average over 80% compared with raw wastewater, with an average ozone dose of 5.7 mg O<sub>3</sub> l<sup>-1</sup> or a PAC dose between 10 and 20 mg l<sup>-1</sup> (Figure 1). Depending on the chemical properties of the substances (presence of electron-rich moieties, charge and hydrophobicity), either ozone or PAC performed better. Both advanced treatments led to a clear reduction in toxicity of the effluents, with PAC-UF performing slightly better overall. As both treatments had, on average, relatively similar efficiency, further criteria relevant to their implementation were considered, including local constraints (e.g., safety, sludge disposal, disinfection), operational feasibility and cost. For sensitive receiving waters (drinking water resources or recreational waters), the PAC-UF treatment, despite its current higher cost, was considered to be the most suitable option, enabling good removal of most micropollutants and macropollutants without forming problematic by-products, the strongest decrease in toxicity and a total disinfection of the effluent.

## REFERENCES

Margot, J., Kienle, C., Magnet, A., Weil, M., Rossi, L., de Alencastro, L.F., Abegglen, C., Thonney, D., Chèvre, N., Schärer, M., Barry, D.A. 2013: Treatment of micropollutants in municipal wastewater: Ozone or powdered activated carbon? *Sci. Total Environ.* 461–462(0), 480-498.

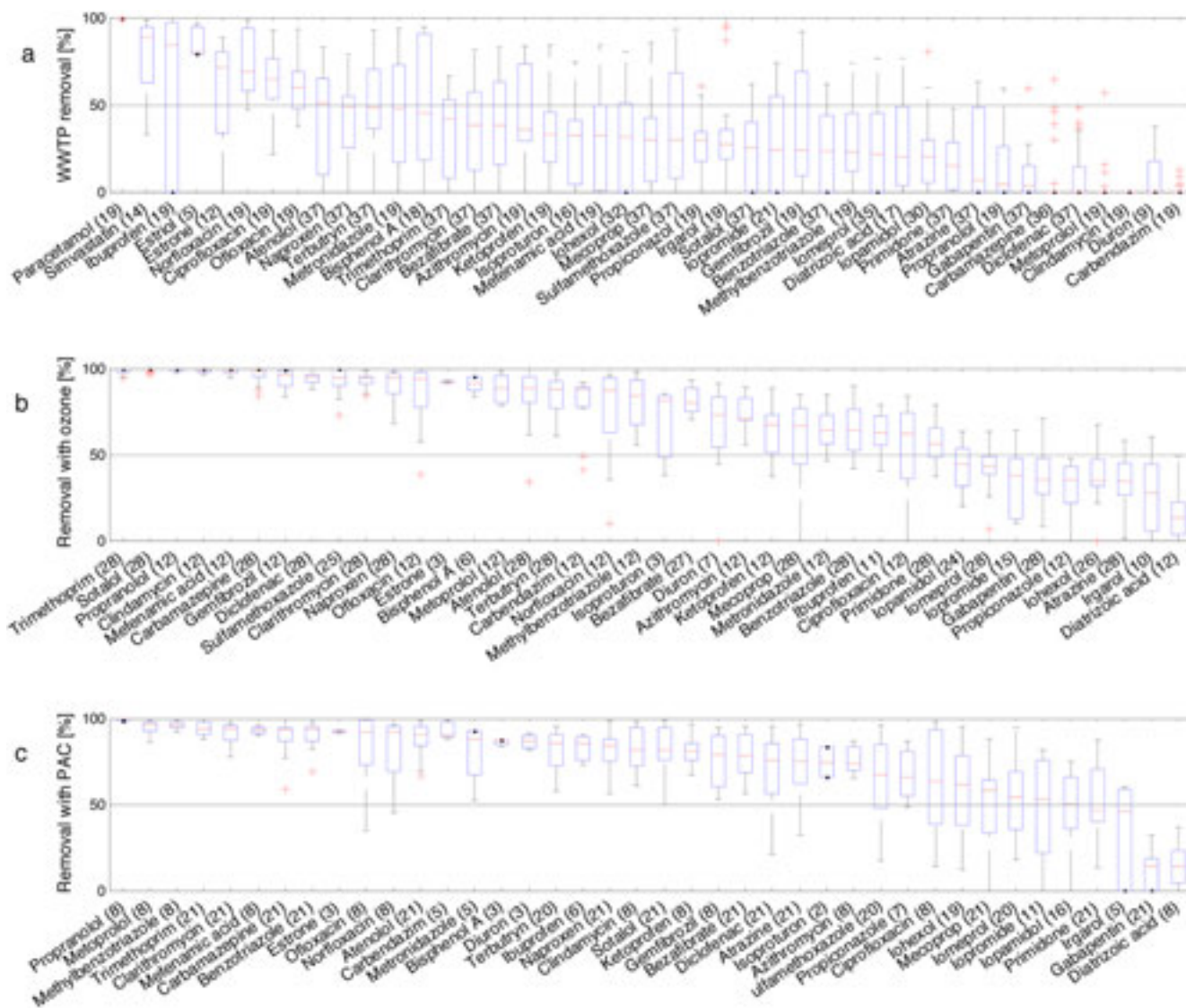


Figure 1. Removal efficiency of 40 to 43 micropollutants during (a) the conventional biological wastewater treatment with partial to complete nitrification (average removal of 35%), (b) the ozonation (ozone dose between 2.3 to 9.1 mg O<sub>3</sub> l<sup>-1</sup>, median 5.9 mg O<sub>3</sub> l<sup>-1</sup> or 0.83 g O<sub>3</sub> g<sup>-1</sup> DOC, average removal of 71%) and (c) the PAC-UF treatment (PAC dose between 10 to 20 mg PAC l<sup>-1</sup>, median 12 mg l<sup>-1</sup>, average removal of 73%). Results of (n) analyses (24 h to 72 h composite samples) conducted between June 2009 and October 2010. Representation of the median removal, the quartiles 25-75 %, the minimum and maximum values and the outliers (after Margot et al., 2013).

## P 25.10

## Economical comparison of three water treatment projects in Vidy Bay (Geneva Lake, CH)

Niel Thibaud<sup>1</sup>, Coutu Sylvain<sup>2</sup>, Margot Jonas<sup>2</sup> & Faust Anne-Kathrin<sup>3</sup>

<sup>1</sup> *École des mines de Saint-Étienne, cours Fauriel 158, CH-42023 Saint-Étienne (thibaud.niel@etu.emse.fr)*

<sup>2</sup> *Laboratoire de Technologie Écologique, EPFL, Station 2, CH-1015 Lausanne*

<sup>3</sup> *Economics and Environmental Management Laboratory, EPFL, Station , CH-1015 Lausanne*

Wastewater Treatment Plants (WWTP) as we know them nowadays were developed in the middle of the past century. Their first objective was to treat organic materials, nitrogen and phosphorus (Lofrano and Brown 2010). Recent progresses in analytical chemistry (High-Performance Liquid Chromatography, Mass spectrometry, Pressurized Liquid Extraction) have allowed pushing further the detection limit for pollutants into water, sludge and soils. As a consequence, many scientific studies of field measurement have reported the occurrence of non expected traces of new micropollutants in the environment, that widen the already long list of chemical substances present in open waters (Zoppou 2001; Verlicchi, Al Aukidy et al. 2012).

In Europe and in the USA, environmental agencies are increasing the pressure on water quality of wastewater treatment plants. Advanced treatment techniques such as ozonation will soon be required for the biggest of them, to prevent from the occurrence of human xenobiotics into the natural environment (OFEV 2009). As a result, water quality of WWTP effluents will get closer to World Health Organization standards for drinkable water (WHO 2008). This fact raises the social and economical question of direct water reuse (DPR) i.e., the transformation of raw wastewater into drinkable water. A better assessment of wastewater pollution dynamics at high time resolution, will help in the optimization of removal strategies and reduce the costs of DPR (Coutu, Wyrsh et al. 2013). The economical benefit of DPR is of major importance, as it could be the next source of water for countries suffering from water scarcity.

The objective of this study was to investigate the potential benefits of advanced water treatment techniques, including DPR, for the city of Lausanne, Switzerland. In this perspective, we compared different water treatment chains for wastewater and potable water. Comparison was made in terms of environmental performances and economical viability. The different treatment chain investigated are: (i) addition of ozonation at the end of the local (Vidy) WWTP (Micropoll 1), (ii) ozonation at the end of the local WWTP plus addition of powdered activated carbon to the potable water treatment chain process (Micropoll 2) and (iii), DPR i.e., the use of treated wastewater directly as input to the potable water network.

The results show that the use of DPR would lead to a significant increase of water price in the Lausanne area for a non significant water quality increase (Table 1). Thus, the application of this technique in a region not suffering from water scarcity is not recommended. Yet, the improvement of the water treatment process with techniques allowing micropollutants removal, for both wastewater and potable water chains (Micropoll 2), are advised to match future environmental regulations.

	New project supplementary cost (CHF/Year)	Consumer cost augmentation (%)
Micropoll 1	4.41E+06	12
Micropoll 2	9.74E+06	27
DPR	2.18E+07	60

Table 1. Supplementary costs to implement each of the three projects considered.

### REFERENCES

- Coutu, S., V. Wyrsh, et al. (2013). "Temporal dynamics of antibiotics in wastewater treatment plant influent." *Science of The Total Environment* 458: 20-26.
- Lofrano, G. and J. Brown (2010). "Wastewater management through the ages: A history of mankind." *Science of The Total Environment* 408(22): 5254-5264.
- OFEV (2009). *Rapport explicatif relatif à la modification de l'ordonnance sur la protection des eaux (OEaux)*. C. Suisse. Berne.
- Verlicchi, P., M. Al Aukidy, et al. (2012). "Occurrence of pharmaceutical compounds in urban wastewater: removal, mass load and environmental risk after a secondary treatment – a review." *Science of The Total Environment* 429: 123-155.
- WHO (2008). *Guideline for drinking waer quality: Vol.1 Recommendations*. 1.
- Zoppou, C. (2001). "Review of urban storm water models." *Environmental Modelling & Software* 16(3): 195-231.

## P 25.11

# Herbicides export dynamics of a mid-sized lake tributary: lessons from observations and modelling

Queloz Pierre<sup>1</sup>, Bertuzzo Enrico<sup>1</sup>, Botter Gianluca<sup>2</sup>, Rao P. Suresh<sup>3</sup>, Rinaldo Andrea<sup>1</sup>

<sup>1</sup> Laboratory of Ecohydrology, Ecole polytechnique fédérale de Lausanne, Station 2, CH-1015 Lausanne (pierre.queloz@epfl.ch)

<sup>2</sup> ICEA, University of Padova, via Marzolo 9, I-35131 Padova

<sup>3</sup> School of Civil Engineering, Purdue University, 550 Stadium Mall Drive, West Lafayette, IN 47907-2051, USA

We present here a model which couples the hydrologic component and the transport of herbicides within a catchment. The model used takes into account the age structure of the stream water in order to characterize short and long term fluctuations of herbicide flux concentrations. The highly dynamic behavior of herbicides concentrations may lead to the exceedance of specific toxic threshold and is therefore key to exposure risk assessment of aquatic ecosystems.

The model is based on a travel time formulation of transport embedding a source zone that describes near surface dynamics. Travel time distributions are analytically derived for the case of solutes subject to partial intake from vegetation and chemical degradation. The framework developed is evaluated by comparing modeled hydrographs and atrazine chemographs with those measured in the Aabach agricultural catchment (Switzerland). The model proves reliable at representing the specific transport features shaped by the interplay of long term processes (persistence of solute compounds in soils), short and long term hydrological transport related to the temporal structure of rainfall. It also allows evaluating the effects of the stochasticity of rainfall patterns and application dates on the export dynamics of herbicides.

This exercise is further confronted to recent data obtained during three spring storm events in a tributary of Lac Léman. Nineteen herbicide compounds were analyzed at four sampling stations dispatched along the stream network. The occurrence of the substances, their specific release dynamics during storms are further discussed in regards to the atrazine data in the Aabach catchment and the model capability.

## REFERENCES

Bertuzzo E., Thomet M., Botter G., Rinaldo A. 2012: Catchment-scale herbicides transport: Theory and application. *Advances in Water Resources*, 52, 232-242

## P 25.12

# Verification of Holocene Sediments in Hoz-e-Soltan Lake (Qom) through Sedimentary Cores

Rezaeian Langeroudi Saeed<sup>1</sup>, Lak Razyeh<sup>2</sup>

<sup>1</sup> M.Sc. student of teacher-training University, Tehran, Iran, (saeedsediment@yahoo.com)

<sup>2</sup> Research Institute for Earth Sciences, Geological Survey of Iran, Tehran, Iran, (lak\_ir@yahoo.com)

Hoz-e-Soltan Lake is an ephemeral saline lake and according to the Sonnenfeld classification Scheme (1991), is regarded as an intra-continental basin. The studied Lake having 195km<sup>2</sup> catchment area, 25-50cm depth, located at 85 km of southwest of Tehran, in Central Part of Iran (Fig. 1). It is located between 43°56' and 35°31' north and 50°53' and 51°20' east at western-north of Hoz-e-Masileh (Fayazi 1991). The maximum superficial relief is about 1940m to the north and 1150m to the south. On the basis of, Aqanabati classification (2006), the study area is located in Central Part of Iran. The objective of this research was to determine the paleoclimate and former water table fluctuations in Holocene through sedimentary facies studies. In this research, 9 cores were taken having a maximum length of 700 centimeters from the Lake substrate, and then facies investigations, such as sediment's characteristics, organic matter contents, colors, crystals of evaporative minerals and sedimentary sub-environment were determined. 213 subsamples were prepared from different sedimentary facies, and then granulometry analysis and mineralogy XRD were carried out. Results indicated that there are 5 sedimentary sub-environments, including sand flat, mud flat, saline mud flat, salt pan and ephemeral lake in the 9 studied cores (Fig. 2). On the basis of granulometry results, 5 sedimentary types were recognized in the subsurface sediments which are as follows; slight gravel-bearing sandy mud, slight gravel-bearing muddy sand, mud, sandy mud and muddy sand.

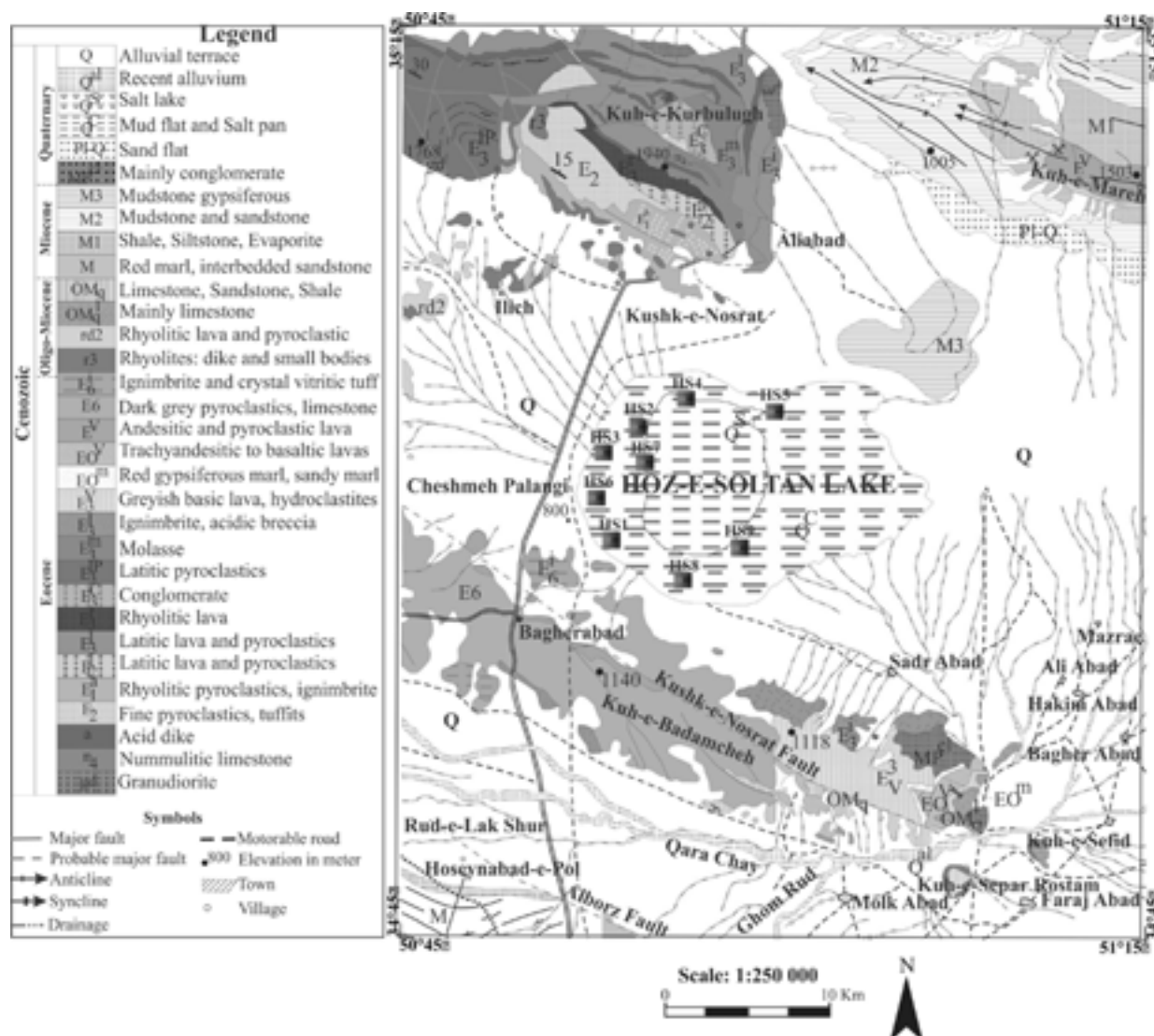


Figure 1. Geological map of Hoz-e-Soltan Lake (after Qalamqash, 2000).

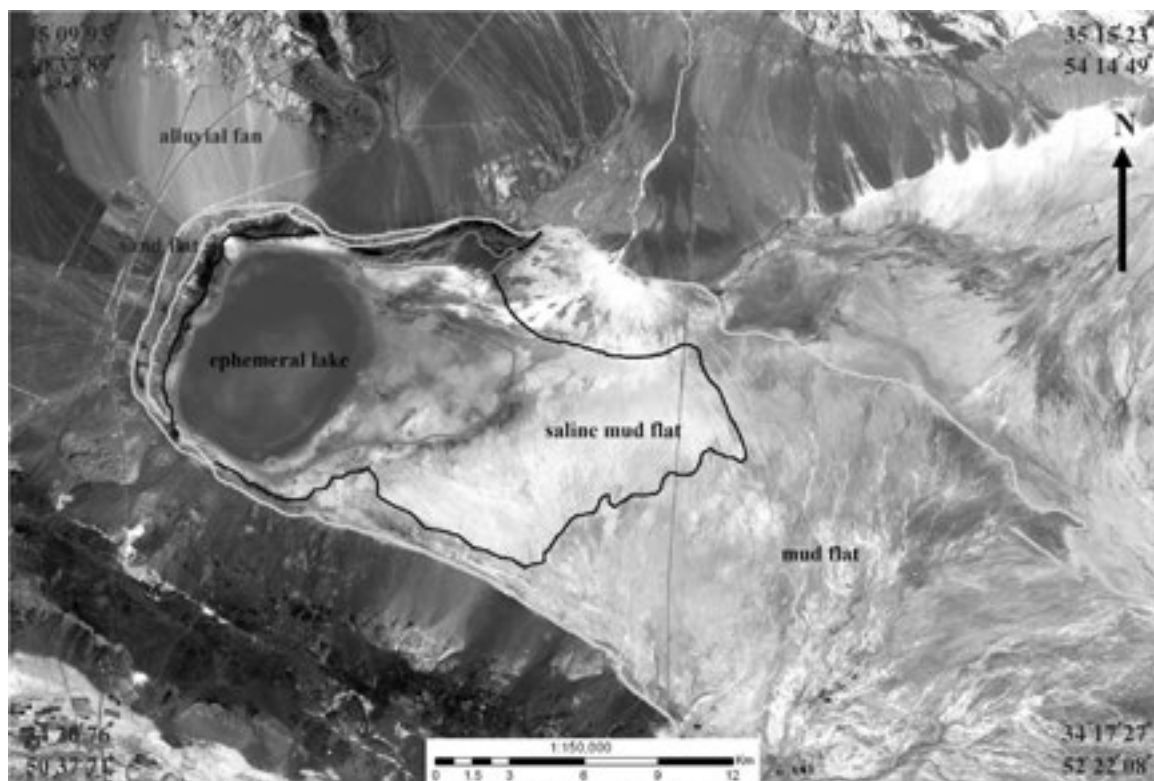


Figure 2. Sub-environments of Hoz-e-Soltan Lake

#### REFERENCES

- Aqanabati, S.A., 2006: Geology of Iran, Geological Survey of Iran, 586p.
- Fayazi, F., 1991: Sedimentological studies in the Qom area, PhD. Thesis, Unpublished UEA U.K., 145p.
- Sonnenfeld, P., 1991: Evaporite basin analysis. In E.R.Force (ed.), *Sedimentary and Diagenetic Mineral Deposits: A basin analysis approach to exploration*, 159-169.
- Qalamqash, J., 2000: Geological map of Iran (Scale: 1:250000), Geological Survey of Iran, Tehran.

## 26. Geomorphology

I. Gärtner-Roer, R. Delaloye, C. Graf, M. Keiler, N. Kuhn, S. Lane, B. Staub

*Swiss Geomorphological Society*

### TALKS:

- 26.1 Bosson J.-B., Capt M., Lambiel C.: Internal structure and geomorphic processes of a high mountain small glacier system: the case of Tsarmin Glacier (Arolla, Valais)
- 26.2 Champagnac J.-D., Valla P., Herman F.: Late-Cenozoic relief evolution under evolving climate: a global review
- 26.3 Frehner M., Gärtner-Roer I., Ling A.H.M.: Furrow-and-ridge structures on active rockglaciers explained by gravity-driven buckle folding: A finite-element study applied to the Murtèl rockglacier
- 26.4 Keiler M., Fuchs S.: The challenge of frequency-magnitude relationship for mountain hazard management
- 26.5 Scapozza C., Conedera M., Bozzini C., Mari S., Lambiel C.: Multi-temporal rock glacier kinematics in the Southern Swiss Alps
- 26.6 Schoeneich P.: The glacial trough – an attempt at theoretical geomorphology

### POSTERS:

- P 26.1 Ambrosi C., Scapozza C.: Multi-method assessment of slope tectonics activity in Val Bedretto (Ticino)
- P 26.2 Bätz N., Lane S., Verrecchia E.: The Fluvial Critical Zone – a co-evolving geomorphic-vegetation-soil system
- P 26.3 Bayrakdar C., Görüm T., Durmus M., Ivy-Ochs S., Akçar N.: Reconstruction of the evolution and chronology of the Akdag rockslide (SW Turkey)
- P 26.4 Borgeaud, L., Lane, S., Vittoz, P.: Interactions between hydrogeomorphology and vegetation on an Alpine alluvial fan: the case of Larzettes, Vallon de Nant (VD, Switzerland)
- P 26.5 Castelletti C., Scapozza C., Ambrosi C.: Multi-methods assessment of shallow landslide evolution in the Cassarate watershed (Valcolla, Ticino)
- P 26.6 Cuomo A., Sartori M., Manzella I., Bonadonna C.: Evaluation of landslide hazard on the Vulcano Island
- P 26.7 Deluigi N., Lambiel C.: The permafrost distribution map of the Bagnes valley (VS)
- P 26.8 Fischer B.: Risk evolution in debris flow prone regions of Lai-Ji (來吉村), Taiwan
- P 26.9 Giraldez C., Choquevilca W., Drenkhan F., Fernandez F., Frey H., Garcia J., Haeberli W., Huggel C., Price K.: "Proyecto Glaciares 513": an integrated assessment of high mountain hazards and related risk reduction in the Peruvian Andes.
- P 26.10 Grischott R., Kober F., Hippe K., Lupker M., Christl M., Hajdas I., Willett S.: Paleodenudation rates and possible links with climate and sediment flux variations in the Engadine, Eastern Swiss Alps

- P 26.11 Haghypour N., Burg J-P: Geomorphological analysis of the drainage system on the growing Makran Accretionary Wedge in SE Iran
- P 26.12 Keiler M., Zischg A., Papathoma-Köhle M., Fuchs S.: A tool for vulnerability assessment to mountain hazards
- P 26.13 Kummert M., Delaloye R.: The sediment yield at the front of active rock glaciers, results from the first summer of investigations at Gugla-Bielzug rock glacier, Mattertal (VS)
- P 26.14 Lambiel C., Maillard B., Regamey B., Martin S., Kummert M., Schoeneich P., Pellitero Ondicol R., Reynard E.: Adaptation of the geomorphological mapping system of the University of Lausanne for ArcGIS
- P 26.15 Maillard B., Regamey B., Kummert M., Reynard E., Lambiel C., Theler D.: The geomorphological map of the Hérens valley
- P 26.16 Mandal, S.K., Lupker M., Burg, J-P., Haghypour, N., Christl, M.: Low denudation recorded by  $^{10}\text{Be}$  in river sands from Southern Peninsular India
- P 26.17 Mölg, N., Haeberli, W., Zemp, M., Linsbauer, A.: Changing glacial sediment balance - a GIS-based model approach for the Swiss Alps
- P 26.18 Najafiha B., Boynagryan V., Diseh J.: Evolutions of coastal lines of Gorgan Lagoon (East of Caspian Sea) by using satellite images
- P 26.19 Yamani M., Moghimi E., Lak R., Salehipour Milani A., Tajik R.: Investigation and Elevation leveling of terraces as Indicator of Pleistocene Lake Levels (Urmia South west of Iran)
- P 26.20 Schoeneich P., Lambiel C., Bosson J.-M.: Geomorphological map of the Diablerets massif – Swiss Alps
- P 26.21 Utz S., Lambiel C.: Typology of solifluction landforms in the south-western Swiss Alps (Valais)

## 26.1

### Internal structure and geomorphic processes of a high mountain small glacier system: the case of Tsarmine Glacier (Arolla, Valais)

Bosson Jean-Baptiste <sup>1</sup>, Capt Maxime <sup>1</sup> & Lambiel Christophe <sup>1</sup>

<sup>1</sup>Institut de géographie et durabilité, Université de Lausanne, Mouline, CH-1015 Lausanne (jean-baptiste.bosson@unil.ch)

High-mountain glacier systems (HMGS) are among the most active part of mountain geomorphic systems in relation to the current global warming and the related para(periglacial) crisis. In HMGS, glacier-permafrost interactions are frequent. When massive ice, frozen and unfrozen sediments coexist, a complex influence on sediment cohesion and fluxes takes place. However, the present knowledge on internal structure (in particular ice content, thickness and depth), as well as sediment storage and fluxes still need improvements.

In this purpose, the internal structure, the ground surface kinematic and thermal state of Tsarmine glacier system - located in the right side of the Arolla valley (Valais) between 2500-3100m a.s.l. - was studied between summers 2011 and 2013. ERT profiles were carried out in addition to dGPS and temperature measurements. Results suggest a complex system where area with different internal structure (in term of ground ice distribution), morphogenesis and current geomorphic dynamic coexist. A debris-covered glacier composes most of the system. It dominates a thick unfrozen morainic bastion and a rock glacier. In response to climate forcing, we concluded that the ground ice melting is the most important process in the sediment stores reworking.

## 26.2

### Late-Cenozoic relief evolution under evolving climate: a global review

Champagnac J.-D., Valla P., Herman F.

ETH

The review paper is an attempt to globally gather quantitative evidences of topographic relief change over the Late Cenozoic, as reported in the literature. We first define different acceptations of the word "relief", as it is commonly used, and detail the metrics used to quantify relief. We then specify methodological tools used to quantify relief change (mostly low-temperature thermochronometry and terrestrial cosmogenic nuclides), and critically analyse published evidence by regions.

We first show that relief changes and rate of change rate are more important at mid latitudes, and appears to be insensitive to mean precipitation rates. We also show that relief change is positive (relief increases) in most of the reported cases (~80%). We subsequently define two functional relationships between relief and erosion, depending on how relief has been defined and propose a conceptual model of landscape memory that is independent of intrinsic damping time. We conclude, following others, that there is a non-linear dependency of erosion change to relief evolution. This implies that the relief increases documented in this review may have subsequently led to erosion rate increases during the same timescales. Last, we discuss the importance of glacial and periglacial processes on the Late Cenozoic relief and erosion rate changes, and stress the importance of frost shattering and glacial erosion at mid- and high latitude.

## 26.3

## Furrow-and-ridge structures on active rockglaciers explained by gravity-driven buckle folding: A finite-element study applied to the Murtèl rockglacier

Frehner Marcel<sup>1</sup>, Isabelle Gärtner-Roer<sup>2</sup>, Anna Hui Mee Ling<sup>1,2</sup>

<sup>1</sup> Geological Institute, ETH Zurich ([marcel.frehner@erdw.ethz.ch](mailto:marcel.frehner@erdw.ethz.ch))

<sup>2</sup> Department of Geography, University of Zurich

Rockglaciers, typical permafrost landforms, often feature a prominent furrow-and-ridge topography. The Murtèl rockglacier in the Upper Engadin valley is a very spectacular example for such morphology, with amplitudes and wavelengths in the order of 5 m and 20 m, respectively (Figure 1). Previous studies have suggested that these structures develop under the influence of a longitudinal compressive flow regime in the lower part of a rockglacier (Haeberli et al., 1998; Käab and Weber, 2004). However, these hypotheses have mostly been based on descriptive observations and therefore remained speculative.

Buckle folding is the mechanical response of a layered viscous material to compression if the mechanical contrast between the layers is significant. The resulting buckle folds are common structures in rocks and have been studied extensively in field outcrops, experimentally, numerically, and analytically (see Hudleston and Treagus, 2010 for a review). We believe that buckle folding is also the main responsible process for the formation of the transverse furrow-and-ridge topography on rockglacier surfaces. In this cross-disciplinary study we use the buckle folding theory, which is well-established in the field of structural geology, and apply it to the field of rockglacier geomorphology.

The Murtèl rockglacier is an ideal case study due to its well-studied internal structure (Arenson et al., 2002), which can be approximated with two layers: an upper mixed rock-ice layer and a lower pure ice layer, both exhibiting a viscous rheology. Such a simple structure is a prerequisite for the analytical buckle folding expressions, which assume a single layer embedded in a weaker material. A 1 m-resolution digital elevation model (DEM; Figure 1), based on low-altitude aerial photographs of the Swiss Permafrost Monitoring Network, is analyzed using the Fold Geometry Toolbox (FGT; Adamuszek et al., 2011). This software uses analytical buckle folding expressions and as such provides a quantitative relationship between the observed wavelength, layer thickness, and the effective viscosity ratio between the folded layer and the underlying ice.

We developed a numerical finite element (FE) algorithm to simulate dynamical 2D buckle folding of a layered viscous medium (Frehner et al., 2012) and apply it to the gravitational flow of a two-layer rockglacier (Figure 2). For the lower pure ice layer we use standard density and viscosity values for glacier ice; for the upper mixed rock-ice layer we use material parameters obtained from the previous FGT-analysis of the Murtèl rockglacier DEM. The initial setup is inspired by the Murtèl rockglacier geometry. The simulated gravitational flow leads to a buckling instability of the upper layer due to the mechanical contrast to the underlying pure ice layer (Figure 2). The resulting wavelengths and amplitudes are similar to the Murtèl rockglacier. In addition, the modeled strain rate field highlights the basal shear zone, which is also observed in boreholes.

Our study promotes buckle folding as the dominant process for the formation of transverse furrow-and-ridge structures on rockglacier surfaces.

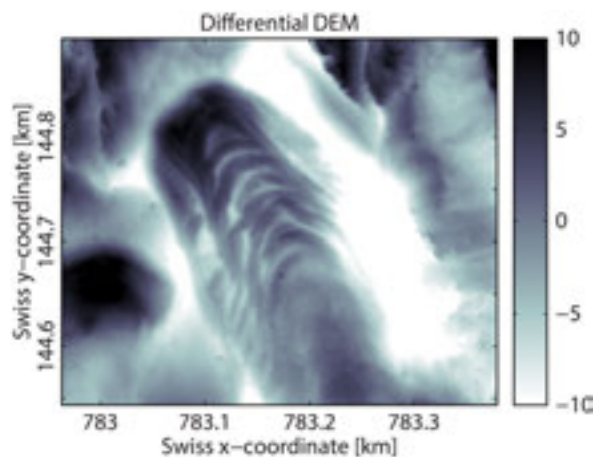


Figure 1: Difference between the Murtèl rockglacier DEM and the moving average of the same DEM. The latter is calculated at each pixel as the mean within a 200 m radius circular area.

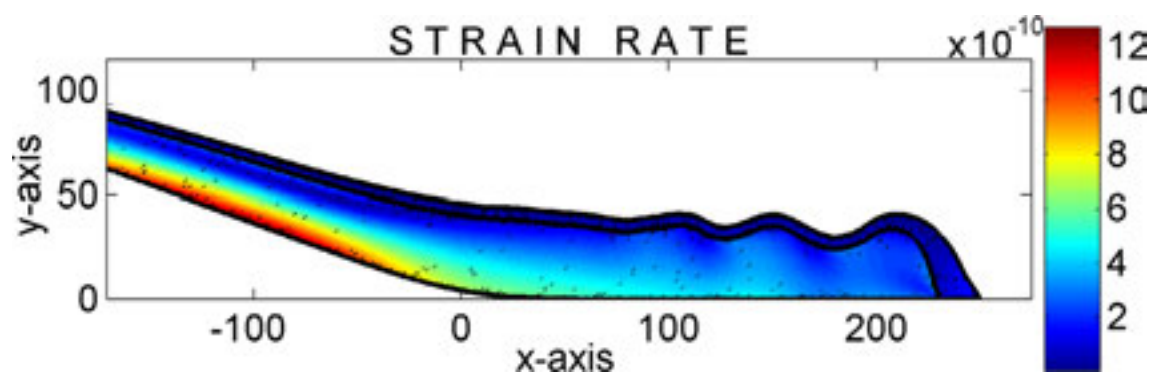


Figure 2: 2D FE-simulation snapshot of a rockglacier flowing downslope due to gravity. The upper mixed rock-ice layer exhibits a higher effective viscosity than the underlying pure ice layer. Colors represent the second invariant of the strain rate tensor; short black lines indicate the long axis of the strain rate ellipse. The bottom boundary is fixed in accordance with borehole measurements.

## REFERENCES

- Adamuszek, M., Schmid, D. W. and Dabrowski, M. 2011. Fold Geometry Toolbox – Automated determination of fold shape, shortening, and material properties. *Journal of Structural Geology*, 33, 1406–1416.
- Arenson, L., Hoelzle, M. and Springman, S. 2002. Borehole deformation measurements and internal structure of some rock glaciers in Switzerland. *Permafrost and Periglacial Processes*, 13, 117–135.
- Frehner, M., Reif, D. and Grasemann, B. 2012. Mechanical versus kinematical shortening reconstructions of the Zagros High Folded Zone (Kurdistan Region of Iraq). *Tectonics* 31, TC3002.
- Haerberli, W., Hoelzle, M., Käab, A., Keller, F., Vonder Mühl, D. and Wagner, S. 1998. Ten years after drilling through the permafrost of the active rock glacier Murtèl, Eastern Swiss Alps: Answered questions and new perspectives. *Permafrost 7th International Conference*, 403–410.
- Hudleston, P. J. and Treagus, S. H. 2010. Information from folds: A review. *Journal of Structural Geology*, 32, 2042–2071.
- Käab, A. and Weber, M. 2004. Development of transverse ridges on rock glaciers: Field measurements and laboratory experiments. *Permafrost and Periglacial Processes*, 15, 379–391.

## 26.4

### The challenge of frequency-magnitude relationship for mountain hazard management

Keiler Margreth<sup>1</sup> & Fuchs Sven<sup>2</sup>,

<sup>1</sup> *Institute of Geography, University of Bern, Hallerstrasse 12, CH-3012 Bern (margreth.keiler@giub.unibe.ch)*

<sup>2</sup> *Institute of Mountain Risk Engineering, University of Natural Resources and Life Sciences, Peter-Jordan-Strasse 82, A-1190 Wien*

Torrent processes pose a threat to elements at risk exposed. In order to assess the hazardousness of such phenomena, firstly information on the probability of occurrence of the process is necessary, usually with respect to a defined design event. Secondly, this design event is characterised by a certain process magnitude. As a consequence, frequency-magnitude relationships are developed and used for hazard assessment and the subsequent management options considering natural hazard risk.

Traditional approaches are based on discrete hydrological events and a magnitude by measures of volume or mass of water and sediment associated with those events. They assume a direct relationship between the hydrological processes and the geomorphic response, such as the capacity of the water body to entrain and transport a certain amount of sediment in dependence of the shear stress and the grain size. However, such an assumption cannot be made considering torrent processes as once a major event has occurred in a catchment; time is required before sufficient material available for further events can accumulate. With respect to torrent events, internal system dynamics are responsible for a major limitation of frequency-magnitude relationships. Moreover, the relation between the trigger of torrent processes (e.g., precipitation intensity) and the system response of the catchment is nonlinear, therefore, even if empirical relationships propose a certain statistic relation they do not mirror the different system behaviour accordingly.

By analysing system loading and response scenarios, the challenge of system dynamics is treated in this paper and alternative concepts to express the frequency and magnitude of torrent processes are discussed. It is argued that such an approach can contribute to the discussion on an enhanced hazard assessment procedure which is targeted under the umbrella of the risk concept at a sustainable use of mountain environments for human settlement.

## 26.5

### Multi-temporal rock glacier kinematics in the Southern Swiss Alps

Scapozza Cristian<sup>1</sup>, Conedera Marco<sup>2</sup>, Bozzini Claudio<sup>2</sup>, Mari Stefano<sup>3</sup> & Lambiel Christophe<sup>4</sup>

<sup>1</sup> *Istituto scienze della Terra, Scuola Universitaria Professionale della Svizzera Italiana (SUPSI), Campus Trevano, CH-6952 Canobbio (cristian.scapozza@supsi.ch)*

<sup>2</sup> *Istituto federale di ricerca WSL, Via Belsoggiorno 22, CH-6500 Bellinzona*

<sup>3</sup> *Département des Géosciences, Unité de Géographie, Université de Fribourg, Chemin du Musée 4, CH-1700 Fribourg*

<sup>4</sup> *Institut de géographie et durabilité, Université de Lausanne, Géopolis, CH-1015 Lausanne*

The multi-temporal assessment of the dynamics of the Stabbio di Largario rock glacier, located in the Southern Swiss Alps, was performed by the combination of three different methods, focusing on three different time periods (Scapozza et al., submitted to *Earth Surface Processes and Landforms*). Schmidt hammer exposure-age dating (SHD) was applied to study long-term kinematics of the rock glacier since the beginning of its development, digital monophotogrammetry allowed the definition of horizontal surface velocities evolution since the end of the Little Ice Age and differential GPS monitoring provided information about recent variations of rock glacier creep.

SHD allowed obtaining calibrated numerical ages of the surface of the rock glacier, which decrease linearly from the front to the rooting zone, where Late Holocene moraines are present (Scapozza 2013). Thanks to SHD, it was also possible to extrapolate the age of formation of the rock glacier ( $5.05 \pm 0.57$  ka cal BP), which may have starting its development after the Mid-Holocene climate optimum, and to define a possible first acceleration in horizontal surface velocities during the Medieval Warm Period (MWP). The MWP was characterised in the Southern Swiss Alps by summer temperatures as much as 1.2°C higher than in 1950 and which caused also important changes in dynamics, rheological properties and thermal conditions of the neighbouring Piancabella rock glacier (Scapozza et al. 2010).

Digital monophotogrammetry performed thanks to the WSL-Monoplotting-tool (Bozzini et al. 2012; Conedera et al. 2013) allowed the georeferentiation and orthorectification of six historical photographs of the rock glacier taken between 1910 and today. By the creation of a smoothed digital elevation model of the rock glacier surface, it was possible to define the variations of the position of the rock glacier front in the last century. In combination with differential GPS monitoring data available since 2009, digital monophotogrammetry allowed defining two other accelerations of creeping rates after the end of the Little Ice Age and at the end of the 1990s.

The first one occurred after the end of the LIA as a reaction of a warming of MAAT and an increase in MAP during the first half of the 20<sup>th</sup> century (regional parameter), and probably also as a consequence of the melting of the glacier that occupies its rooting zone (local parameter). The more recent important acceleration take place since the end of the 1990s as the consequence of the severe recent warming, causing a partial destabilization of the Stabbio di Largario rock glacier (creating crevasses on the rock glacier tongue).

Considering the surface velocities behavior since the development of the rock glacier, it was possible to link phases of rock glacier acceleration with climate warming periods.

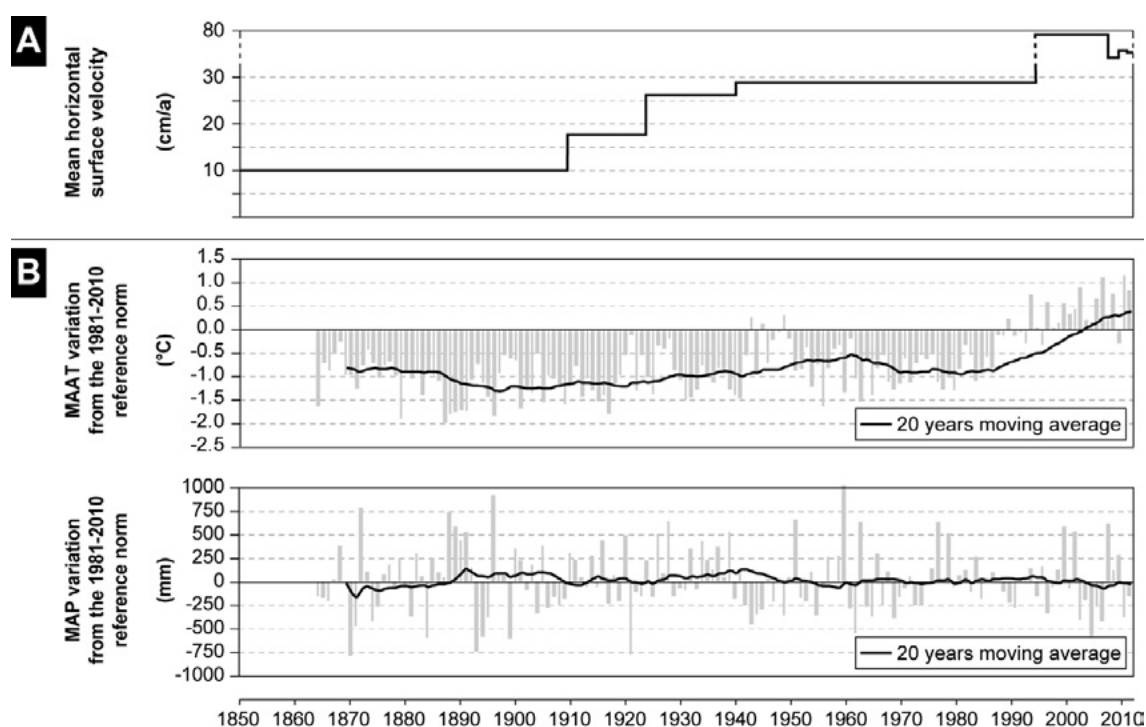


Figure 1. Comparison between the multi-temporal kinematics of the Stabbio di Largario rock glacier and climate parameters since 1850. (A) Compilation of the mean horizontal surface velocities obtained from the WSL-Monoplotting-tool and DGPS monitoring. (B) Homogenised mean annual air temperature (MAAT) and mean annual precipitations (MAP) of the MeteoSwiss station of Lugano from 1864 to 2012. Data from MeteoSwiss.

## REFERENCES

- Bozzini, C., Conedera, M. & Krebs, P. 2012: A new monoplotting tool to extract georeferenced vector data and orthorectified raster data from oblique non-metric photographs. *International Journal of Heritage in the Digital Era*, 1, 499-518. DOI: 10.1260/2047-4970.1.3.499
- Conedera, M., Bozzini, C., Scapozza, C., Rè, L., Ryter, U. & Krebs, P. 2013: Anwendungspotenzial des WSL-Monoplotting-Tools im Naturgefahrenmanagement. *Schweizerische Zeitschrift für Forstwesen*, 164, 173-180. DOI: 10.3188/szf.2013.0173
- Scapozza, C. 2013: Stratigraphie, morphodynamique, paléoenvironnements des terrains sédimentaires meubles à forte déclivité du domaine périglaciaire alpin. Institut de géographie et durabilité de l'Université de Lausanne: Lausanne. *Géovisions* 40, 1-551 [<http://www.unil.ch/igul/page96426.html>].
- Scapozza, C., Lambiel, C., Reynard, E., Fallot, J.-M., Antognini, M. & Schoeneich, P. 2010: Radiocarbon dating of fossil wood remains buried by the Piancabella rock glacier, Blenio Valley (Ticino, Southern Swiss Alps): implications for rock glacier, treeline and climate history. *Permafrost and Periglacial Processes*, 21, 90-96. DOI: 10.1002/ppp.673

## 26.6

### The glacial trough – an attempt at theoretical geomorphology

Schoeneich Philippe<sup>1</sup>

<sup>1</sup> *Institut de Géographie Alpine – PACTE/Territoires, Université de Grenoble Alpes, 14 bis av. Marie-Reynoard, 38100 Grenoble, France (Philippe.Schoeneich@ujf-grenoble.fr)*

In the late 19th century, geomorphology was part of geology and an almost empirical science. It is the theoretical synthesis of the « normal » erosion system by Davis which both established geomorphology as an independent science and separated it from the still empirical geology. Davis' erosional cycle theory provided not only an explicative framework, but also a predictive model, allowing geomorphological predictions to be searched in the field. In its beginning, geomorphology was a theoretically based science! If the history and fate of Davis' theories are well known, the most excessive tentative of theoretical approach in geomorphology remains largely unknown, mainly because it was almost confined to German-speaking geography: the glacial trough theory. Its main propagator was Hans Hess with his paper *Der Taltrog* in 1903. According to this theory, successive glaciations carve narrower and deeper troughs, which leave remnants in the form of embedded glacial troughs. In the early 20th century many geomorphologists searched for benches and examined slope profiles in order to find embedded troughs, four of them if possible, corresponding to the four Alpine glaciations defined by Penck and Brückner. Other authors tried to define troughs corresponding to the last deglaciation phases. Associated concepts like tongue basins and stepped glacial cirques were also used and led sometimes to opposite interpretations of the same features. Almost all studies based only on a topographical analysis – the most excessive relied even only on analysis of maps, without any field work. Criticisms arose from the beginning and developed in the 1920's. The interest for glacial troughs, and debate around it, disappeared after the 1930's. Today with the development of cosmonuclide exposure dating, the question whether glacial troughs, like trimlines, could enjoy a revival arises.

We will expose a brief history of the concepts, and develop some examples mainly from the Swiss Alps..

## P 26.1

# Multi-method assessment of slope tectonics activity in Val Bedretto (Ticino)

Ambrosi Christian<sup>1</sup> & Scapozza Cristian<sup>1</sup>

<sup>1</sup> Istituto scienze della Terra, Scuola Universitaria Professionale della Svizzera Italiana (SUPSI), Campus Trevano, CH-6952 Canobbio (christian.ambrosi@supsi.ch)

The right flank of the Val Bedretto is characterized by a series of large scarps and counterscarps referred to Deep-seated gravitational slope deformations (*Sackung*, DSGSD) formed by the interplay of (neo)tectonics, gravitation and postglacial rebound (Ustaszewski et al. 2008). These DSGSD are the visible expression of slope tectonics processes (e.g. Jaboyedoff et al. 2011).

Several field studies have focus on the neotectonic faulting, postglacial uplift and numerical modeling of postglacial rebound (e.g. Ustaszewski & Pfiffner 2008; Ustaszewski et al. 2008), whereas Renner (1982) has determined the main stadials of glacier retreat during the Lateglacial, highlighting the displacement of several moraines in the area.

By means of new instabilities and geomorphological maps obtained by 3D digital stereoscopic photogrammetry (Castelletti et al. 2012), and Schmidt hammer exposure-age dating (SHD) of the glacial and periglacial landforms, a re-evaluation of the genetical processes and of the activity of the DSGS since 20'000 BP is proposed.

## REFERENCES

- Castelletti, C., Soma, L., Scapozza, C. & Ambrosi, C. 2012. Quaternary geological map of Sheet Reichenau (Canton Graubünden): improvement of several GIS tools. Abstract volume 10th Swiss Geoscience Meeting, Bern, Switzerland, 16–17 November 2012, Abstract P 10.5: 254-255.
- Jaboyedoff, M., Crosta, G.B. & Stead, D. 2011. Slope tectonics: a short introduction. In: Slope tectonics (Ed. by Jaboyedoff, M.). Geological Society, London, Special Publications, 351, 1-10.
- Renner, F. 1982. Beiträge zur Gletscher-Geschichte des Gotthardgebietes und Dendroklimatologische Analysen an fossilen Hölzern. Thesis, Universität Zürich, Physische Geographie, 8, 182 p.
- Ustaszewski, M. & Pfiffner, O.A. 2008. Neotectonic faulting, uplift and seismicity in the central and western Swiss Alps. In: Tectonic Aspects of the Alpine-Dinaride-Carpathian System (Ed. by Siegesmund, S., Fügenschuh, B. & Froitzheim, N.). Geological Society, London, Special Publications, 298, 231-249.
- Ustaszewski, M., Hampel, A. & Pfiffner, O.A. 2008. Composite faults in the Swiss Alps formed by the interplay of tectonics, gravitation and postglacial rebound: an integrated field and modeling study. Swiss Journal of Geosciences, 101, 223-235.

## P 26.2

## The Fluvial Critical Zone – a co-evolving geomorphic-vegetation-soil system

Nico Bätz<sup>1</sup>, Stuart Lane<sup>1</sup>, Eric Verrecchia<sup>2</sup>

<sup>1</sup> Institute of Geography and Sustainability - University of Lausanne, Quartier UNIL-Mouline, CH-1015 Lausanne (nico.baetz@unil.ch)

<sup>2</sup> Institute of Earth Sciences - University of Lausanne, Quartier UNIL-Mouline, CH-1015 Lausanne

Conventional geomorphological studies have largely considered sediment transport processes and its link to river planform development (e.g. Leopold and Wolman, 1957). More recently the impacts of vegetation and biogeomorphic succession (e.g. Corenblit et al., 2011), through notions such as ‘ecosystem engineers’ (e.g. Gurnell, 2013), have been recognised to play a key role in determining riverine processes and landform development. However, the main remaining question is where does soil fit into these accounts?

In more stable fluvial systems, such as meandering terrace systems (e.g. Cierjacks et al., 2010) or embanked systems (Gueux et al., 2003), alluvial soils have been widely described and quantified. Nevertheless, the role of pedogenesis in transforming fresh alluvial sediment deposits into (initial) soil, and its impact on biogeomorphic succession in more dynamic systems has been largely overlooked. Thus, what role does embryonic soil development play? Is it simply passive, or, as vegetation studies have shown, actively implicated in these dynamics?

In braided rivers, we know that the initial stratification of sediments and topography modulate habitat properties for initial vegetation colonisation. In theory, soil forming processes, such as organic matter accumulation and transformation, should then influence succession speed and pathways. These are likely to be sustained so long as the site does not switch to being erosional (i.e. destroyed) or too depositional (i.e. buried by fresh sediment), and also influenced by the ameliorated habitat properties due to soil development (e.g. moisture retention capacity). This will feed back into vegetation dynamics and potentially topography, notably as soil organic matter accumulation builds up the soil surface. In time, the surface may become independent of fluvial material influx. Still, these processes are strongly linked to river dynamics due to erosion and deposition processes and due to the connections to the ground water table.

The above mentioned feedbacks are crucial for understanding the morphological evolution of rivers over the timescales of years to decades. We conceptualised these links in a model that we label the ‘Fluvial Critical Zone’ (Figure 1). We test this model in the Allondon River, a protected nature reserve in the west of Canton Geneva, Switzerland, which comprises a braided river – terrace system, including active braiding processes, rapid vegetation colonisation, stabilisation of braid bar deposits, and development of soil profiles.

We have tested this conceptual model and set the time frame for the co-evolution of the fluvial critical zone.

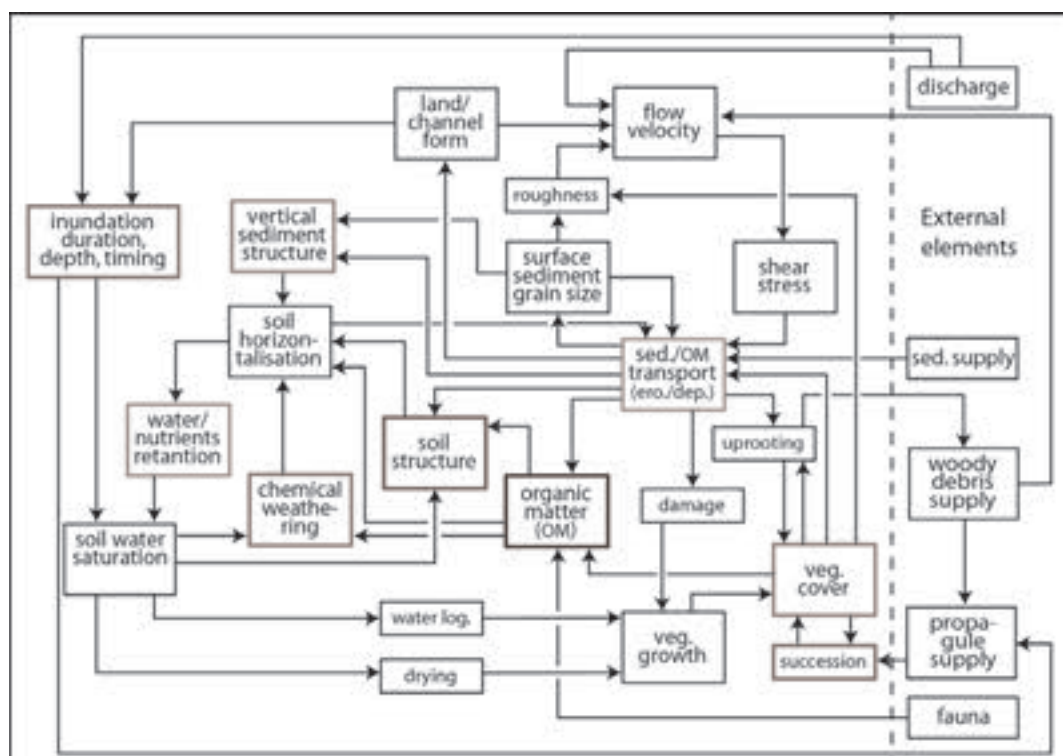


Figure 1: Conceptual model of the Fluvial Critical Zone, showing the feedback between soil, vegetation and geomorphology.

## REFERENCES

- Cierjacks A, Kleinschmit B, Babinsky M, Kleinschroth F, Markert A, Menzel M, Ziechmann U, Schiller T, Graf M, Lang F. 2010. Carbon stocks of soil and vegetation on Danubian floodplains. *Journal of Plant Nutrition and Soil Science* 173: 644–653.
- Corenblit D, Baas ACW, Bornette G, Darrozes J, Delmotte S, Francis RA, Gurnell AM, Julien F, Naiman RJ, Steiger J. 2011. Feedbacks between geomorphology and biota controlling Earth surface processes and landforms: A review of foundation concepts and current understandings. *Earth-Science Reviews*.
- Guex D, Weber G, Musy A, Gobat J-M. 2003. Evolution of a swiss alpine floodplain over the last 150 years: hydrological and pedological considerations. presented at the International conference “Towards natural flood reduction strategies”, 6-13 September 2003. Warsaw.
- Gurnell A. 2013. Plants as river system engineers. *Earth Surface Processes and Landforms*: n/a–n/a.
- Leopold L, Wolman M. 1957. River Channel Patterns-braided, Meandering and Straight. US Geological Survey Professional Paper 282B: 39–85.

## P 26.3

## Reconstruction of the evolution and chronology of the Akdağ rockslide (SW Turkey).

Bayraktar Cihan<sup>1</sup>, Görüm Tolga<sup>2</sup>, Durmuş Mücahit<sup>1</sup>, Ivy-Ochs Susan<sup>3</sup> and Akçar Naki<sup>4</sup>

<sup>1</sup> Department of Geography, Istanbul University, Istanbul, 34452 Beyazıt/Fatih-Istanbul.

<sup>2</sup> Natural Sciences Research Center, Yıldız Technical University, Davutpaşa Cad. B-Blok Z-59 34220 Esenler-Istanbul, Turkey.

<sup>3</sup> Labor für Ionenstrahlphysik (LIP), ETH Zürich, Schafmattstrasse 20, CH-8093 Zürich

<sup>4</sup> Institut für Geologie, Universität Bern, Baltzerstrasse 1+3, CH-3012 Bern .

Akdağ rockslide is a very large, active slope failure in carbonate rocks and flysch deposits located in the southern slopes of paleo-glaciated Akdağ Massif, SW Turkey (Figure 1). The landslide resulted in the collapse of a 5 km segment of the Akdağ Mount, and covers an area of 15 km<sup>2</sup> and has a volume of about 7 km<sup>3</sup>. It is one of 108 known very large (10<sup>6</sup> - 10<sup>7</sup> m<sup>3</sup>) landslides in Turkey, and possibly the largest landslide of its type in the Western and Central Taurides (Bayraktar, 2012). At least, three distinct phases of evolution can be distinguished in the field: (1) avalanche of carbonate rocks onto the flysch; (2) successive slumps of the flysch; and (3) planar sliding and disintegration of the latter. Shattered and weak material from the large slide has recently been subjected to intensive denudation by numerous shallow secondary landslides, gully erosion and subsequent aggradation of debris on valley floors. Due to the landslide activity, settlement areas and infrastructure has been severely damaged. The timing of the landslide is generally attributed to the post-Last Glacial period. In this study, we employ geographic information systems and remote sensing methods, spatial and morphometric analysis, and cosmogenic nuclide dating with <sup>36</sup>Cl in order to reconstruct the evolution and the chronology of the landslide.

Cosmogenic nuclides such as <sup>3</sup>He, <sup>10</sup>Be, <sup>14</sup>C, <sup>21</sup>Ne, <sup>26</sup>Al and <sup>36</sup>Cl are produced within the crystal lattices of minerals (as sediment and/or mineral in the rock) at or near the earth's surface (Ivy-Ochs et al., 2013). These nuclides are most often used for surface exposure dating, which depends on the build-up of the nuclides (Dunai, 2010). Boulders which are deposited by mass movements have already been exposure-dated in the Alps (Ivy-Ochs et al., 2009, Akçar et al., 2012 among others). In this study, we collected 21 samples from the carbonaceous boulders within the Akdağ active landslide in order to build the timing of the different phases, which are already identified in the field.

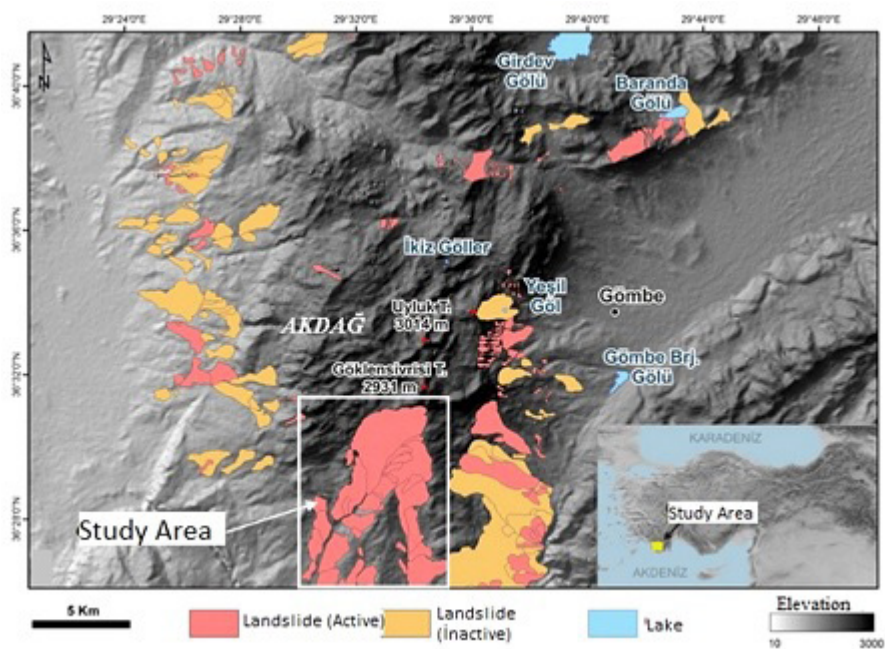


Figure 1. Distribution of the landslides in the Akdağ Massif, SW Turkey.

## REFERENCES

- Akçar, N., Deline, P., Ivy-Ochs, S., Alifimov, V., Hajdas, I., Kubik, P.W., Christl, M., Schlüchter, C. 2012: The 1717 AD rock avalanche deposits in the upper Ferret Valley (Italy): A dating approach with cosmogenic  $^{10}\text{Be}$ . *Journal of Quaternary Science* 27, 383-392.
- Bayrakdar, C. 2012: Geomorphological Analysis of Karstification-Glacier Relation in Akdağ Massif (Western Taurus Mountains). Istanbul University Institute of Social Sciences. unpublished PhD thesis. Istanbul.
- Dunai, T. 2010: *Cosmogenic Nuclides: Principles, concepts and applications in the Earth surface sciences* book p. 198. Cambridge: Cambridge University Press.
- Ivy-Ochs, S., Poschinger, A.V., Synal, H.A., Maisch, M. 2009: Surface exposure dating of the Flims landslide, Graubunden, Switzerland. *Geomorphology* 103, 104-112.
- Ivy-Ochs, S., Dühnforth, M., Densmore, A. L., & Alifimov, V. 2013: Dating fan deposits with cosmogenic nuclides. In: *Dating Torrential Processes on Fans and Cones*, 243-263. Springer Netherlands.

## P 26.4

## Interactions between hydrogeomorphology and vegetation on an Alpine alluvial fan: the case of Larzettes, Vallon de Nant (VD, Switzerland)

Borgeaud Laure<sup>1</sup>, Lane Stuart<sup>1</sup> & Vittoz Pascal<sup>2</sup>

<sup>1</sup>*Institute of Geography and Sustainability, University of Lausanne, Géopolis, Unil – Mouline, CH-1015 Lausanne (laure.borgeaud@unil.ch)*

<sup>2</sup>*Department of Ecology and Evolution, University of Lausanne, Biophore, Unil – Sorge, CH-1015 Lausanne*

Recent research has recognised that there is a critical co-evolution between geomorphic systems and ecosystems in which vegetation exerts a crucial role as an ‘engineer’ of geomorphic response (Corenblit et al., 2008), whilst the nature of that geomorphic response has profound impacts upon ecosystem dynamics (e.g. Pfeffer et al., 2003 ; Dickerson et al., 2012 ; Landolt, 1986, Garcia-Aguire et al., 2007).

Here, we present results based on field studies of an active fan system in the Vallon de Nant, Canton Vaud, Switzerland. The work focuses on the measurement of a combination of biotic and abiotic components. In 100 quadrats, plants were identified and recorded to species level, environmental parameters (e.g. soil, hydrologic, topographic characteristics) were measured and age was estimated by dendrochronology and aerial imagery analysis.

Statistical ordination was used to identify the spatial structure of the plant communities. Fractal type approaches were used to identify the spatial scale dependence of diversity. These two sets of data were then tied back into the geomorphologic history of fan development. The work showed that distinctive spatial and temporal patterns emerge in fan vegetation communities that can be related to both spatial and temporal properties of fan dynamics, and notably the accommodation space available to fan surface channels. The latter sets the magnitude and frequency characteristics of channel occupancy and causes a down fan shift in community organisation biodiversity from being discrete ‘on-off’ driven in the more constrained fan head to being more spatially continuous where accommodation space is greater.

## REFERENCES

- Corenblit, D., Gurnell, A. M., Steiger, J. and Tabacchi, E. 2008: Reciprocal adjustments between landforms and living organisms: Extended geomorphic evolutionary insights, *Catena*, 73, 261-273.
- Dickerson, R. P., Forman, A. and Liu, T. 2012: Co-development of alluvial fan surfaces and arid botanical communities, Stonewall Flat, Nevada, USA, *Earth Surface Processes and Landforms*. ARTICLE PUBLISHED ONLINE 30 OCT 2012 (<http://onlinelibrary.wiley.com/doi/10.1002/esp.3336/full>)
- Garcia-Aguire, M. C., Ortiz, M. A., Zamorano, J. J. and Reyes, Y. 2007: Vegetation and landform relationships at Ajusto volcano Mexico, using a geographic information system (GIS), *Forest Ecology and management*, 239, 1-12.
- Landolt, E. 1986: *Notre flore alpine*, 3e édition d’après la 5e édition allemande, entièrement remaniée. Addaptation française par D. Aeschimann. Brugg, Club Alpin Suisse.
- Pfeffer, K., Pebesma, E. J. and Burrough, P. A. 2003: Mapping alpine vegetation using vegetation observations and topographic attributes, *Landscape Ecology*, 18, 759-776.

## P 26.5

# Multi-methods assessment of shallow landslide evolution in the Cassarate watershed (Valcolla, Ticino)

Castelletti Claudio, Scapozza Cristian & Ambrosi Christian

*Institute of Earth Sciences, University of Applied Sciences and Arts of Southern Switzerland (SUPSI), Campus Trevano, CH-6952 Canobbio (claudio.castelletti@supsi.ch)*

The upper watershed of the Cassarate River is affected by shallow instabilities whose occupies the whole slope and often extends to the valley floor by mass transport phenomena (debris flows, earth flows, etc.) in ravines.

To contain these effects, the upper part of the watershed has been the subject, between 1880 and 2000, of major reforestation programs causing positive effects in the reduction of the total area affected by shallow landslides (Mariotta 2011). However, there are some areas where an important slope erosion persist, even have a tendency to worsen.

In this framework, the Consortium “Valle del Cassarate e golfo di Lugano” has mandated the Institute of Earth Sciences SUPSI of evaluate the evolution of shallow landslides and regressive erosion in the upper part of the watershed. The aim of this study is then to provide essential basic data for an assessment of the present situation and an evaluation of the future evolution, with the goal of provide scenarios for works of prevention and mitigation.

For the realization of this project, it was decided to follow a plan of work that crosses multiple methods:

- historical analysis of events;
- landslide mapping by 3D digital stereoscopic photogrammetry (Castelletti et al. 2012),
- geological structures mapping (upgrade of Reinhard & Bernoulli 1964);
- analysis of the thickness of surface deposits through passive seismic (Dal Moro 2012);
- land use mapping;
- analysis thanks to the WSL-Monoplotting-Tool (Conedera et al. 2013) for assess the spatial evolution of the shallow landslides (fig. 1);
- analysis of the landslide triggering processes (precipitation, avalanches, forest fires, etc.);
- definition of the geotechnical characteristics of surface deposits.

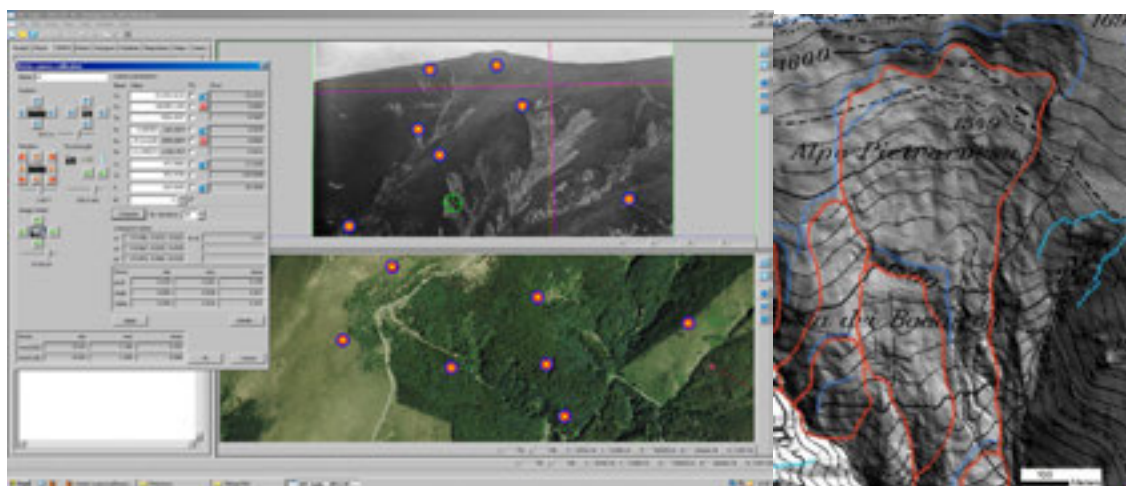


Figure 1. Overview of two cartographic methods used in the study of instabilities; on the left, screen shot of the WSL-Monoplotting-tool, used to extract georeferenced vector data and orthorectified raster data from oblique non-metric photographs; on the right, shallow landslides mapping in ESRI ArcMap® GIS environment.

## REFERENCES

- Castelletti, C., Soma, L., Scapozza, C. & Ambrosi, C. 2012. Quaternary geological map of Sheet Reichenau (Canton Graubünden): improvement of several GIS tools. Abstract volume 10th Swiss Geoscience Meeting, Bern, Switzerland, 16–17 November 2012, Abstract P 10.5: 254-255.
- Conedera, M., Bozzini, C., Scapozza, C., Rè, L., Ryter, U. & Krebs P. 2013: Anwendungspotenzial des WLS-Monoplotting-Tool im Naturgefahrenmanagement. Schweizerische Zeitschrift für Forstwesen, 164, 173–180.
- Dal Moro, G. 2012. Onde di superficie in geofisica applicata. Acquisizione e analisi di dati secondo tecniche MASW e HVSR. Palermo, Dario Flaccovio Editore, 191 p.
- Mariotta S. 2011: Il bacino del Cassarate 1880-2000, 120 anni di interventi forestali per la sicurezza del territorio. Lugano, Edizioni universitarie della Svizzera italiana, 167 p.
- Reinhard, M. & Bernoulli, D. 1964: Erläuterungen der Blatt 1333/Tesserete. Blatt 39 der Geologischer Atlas der Schweiz 1:25'000. Bern, Schweizerische Geologische Kommission, 53 p.

## P 26.6

## Evaluation of landslide hazard on the Vulcano Island

Cuomo Aline<sup>1</sup>, Sartori Mario<sup>1</sup>, Manzella Irene<sup>1</sup> & Bonadonna Costanza<sup>1</sup>

<sup>1</sup> Earth Sciences Department, University of Geneva, Rue des Maraîchers 13, CH-1205 Geneva, Aline.Cuomo@etu.unige.ch

The island of Vulcano (Aeolian Islands, Italy) is exposed to many natural hazards, including landslides. Several phenomena such as volcanic eruptions, earthquakes, fumarolic activity and intense rainfall can generate landslides. As an example, a rockslide occurred in 1988 on the NE side of la Fossa cone, which generated a small tsunami and was probably triggered by the increase of fumarolic and seismic activity. The northern and eastern parts of la Fossa cone are the most prone to landslide hazard. The potential mobilization mechanism and the run out process are better described in terms of rock mechanics than soil mechanics. Two main unstable zones have been identified.

In the eastern flank of La Fossa cone, the volume of rocks involved in the 1988's landslide has been estimated around 200'000 m<sup>3</sup> by pre- and post- event modeling studies (Tinti et al., 1999; Tommasi et al., 2007; Olivares & Tommasi, 2008). New investigations on the field lead to an estimation of the volume of the landslide closer to 100'000 m<sup>3</sup>. The scar comprises a residual unstable rock volume of around 39'000 m<sup>3</sup> that could be mobilized as rockslide. No current fumarolic activity was observed near the unstable volume.

The northern edge of the la Fossa cone, which is located above a populated area, is characterized by strongly altered zones, with open fractures and rock masses where toppling could occur. After the assessment of the unstable volumes we carried out some numerical simulation with a 2D discrete element code WinMimes developed at the Massachusetts Institute of Technology (MIT). This allowed us to draw the hazard map related to this unstable zone of around 8'000 m<sup>3</sup>.

## REFERENCES

- Manzella, I., Einstein, H., & Grasselli, G. : 2013 (in press): DEM and FEM/DEM modelling of granular flows to investigate large debris avalanche propagation, *Landslide Science and Practice, Volume 3: Spatial Analysis and Modelling*. Margottini, Claudio; Canuti, Paolo; Sassa, Kyoji (Eds.), Springer-Verlag
- Olivares, L. & Tommasi, P. 2008: The role of suction and its changes on stability of steep slopes in unsaturated granular soils, *Landslides Engineerer Slopes*, 203-215.
- Tinti, S., Bortolucci, E. & Armigliato, A. 1999: Numerical simulation of the landslide-induced tsunami of 1988 on Vulcano Island, Italy, *Bull Volcanol*, 61, no. 1-2, 121–137.
- Tommasi, P., Graziani, A., Rotonda, T., & Bevivino, C. 2007: Preliminary analysis of instability phenomena at Vulcano Island, Italy, in *Volcanic Rocks/Proceedings of the International Workshop on Volcanic Rocks, Workshop W2, 11th Congress ISRM, Ponta Delgada, Azores, Portugal, 14-15 July, 2007*, Taylor & Francis Group, London, 147–154.

## P 26.7

### The permafrost distribution map of the Bagnes valley (VS)

Deluigi Nicola<sup>1</sup>, Lambiel Christophe<sup>1</sup>

<sup>1</sup> *Institut de Géographie et Durabilité, University of Lausanne, Bâtiment Géopolis, CH-1015 Lausanne (nicola.deluigi@unil.ch)*

One of the major concerns on periglacial research is the sensitivity of permafrost to climate change. In the context of current global warming, an increase of instabilities at high elevations has already been observed. Thus, a precise knowledge of the permafrost distribution at the local scale may interest the public administrations responsible for natural hazard assessments, because the impact of the permafrost degradation on slope stabilities is one of the common questions when dealing with infrastructures or sites located in high mountain regions.

High-resolution permafrost maps can be created using machine learning algorithms. Support Vector Machines (SVMs) showed to be accurate for the prediction of the permafrost occurrence (Deluigi & Lambiel, 2013). This methodology has aroused the interest of the municipality of Bagnes (VS), for which a permafrost map of the corresponding valley has been elaborated. A dataset composed by 15 variables was used. Some were simply calculated and extrapolated from a 25m resolution DEM, whereas others were extracted from the swisstopo primary surface map and two rock glacier inventories (Lambiel & Reynard, 2001; Delaloye & Morand, 1997). The dataset was completed by empirical measurements obtained during field campaigns. The resulting map revealed to be rather in accordance with field observations. In particular, the high discontinuity of mountain permafrost could be reflected with a relatively good success. A further sectorial analysis highlighted the elements of the landscape potentially sensitive to hazards related to periglacial processes.

#### REFERENCES

- Delaloye, R., Morand, S. (1997). Du Val Ferret au Grand-Combin (Alpes valaisannes): inventaire des glaciers rocheux et analyse spatiale du pergélisol à l'aide d'un système d'information géographique (IDRISI). Travail de Diplôme, Institut de Géographie de l'Université de Fribourg [unpublished].
- Deluigi N., Lambiel C. (2013). PERMAL: a machine learning approach for alpine permafrost distribution modeling. In: Graf, C. (ed) Mattertal - ein Tal in Bewegung. Jahrestagung der Schweizerischen Geomorphologischen Gesellschaft 29. Juni - 1. Juli 2011, St. Niklaus, Birmensdorf, Eidg. Forschungsanstalt WSL. 47-62.
- Lambiel, C., Reynard, E. (2001). Regional modelling of present, past and future potential distribution of discontinuous permafrost based on a rock glacier inventory in the Bagnes-Héréme area (Western Swiss Alps). *Norsk Geografisk Tidsskrift*, 55, 219-223.

## P 26.8

### Risk evolution in debris flow prone regions of Lai-Ji (來吉村), Taiwan

Benjamin Fischer<sup>1</sup>

<sup>1</sup>*Geographisches Institut, University of Bern, Hallerstrasse 12, CH-3012 Bern (beni.fischer@students.unibe.ch)*

In the last decades the numbers of hazard events and associated losses have increased worldwide. This increase cannot be solely explained by climate change and it is widely accepted that human activity plays also a key role for increased losses (IPCC 2012). The concept of risk analysis was applied in various areas because it includes the three parameters hazard, exposure and vulnerability and therefore offers a broader approach than hazard assessment, especially if facing the problem of increasing monetary losses. Currently, only few studies focus on detailed analysis of natural hazard risk evolution (Keiler et al. 2006, Schwendtner et al. [in Press]). In this study, risk evolution is studied for a debris flow endangered area in Lai-Ji (來吉村), Taiwan. The main objective is to assess the current natural hazard risk situation, to identify main drivers of risk evolution and to gain a broader understanding of risk trajectories and the connectivity between the different risk parameter. For that reason, different hazard scenarios were generated and for three time intervals exposure and vulnerability were analysed in Lai-Ji (來吉村): The first time slot mirrors the situation before the occurrence of the first known debris flow in the 1970s. The second pictures the situation of the devastating debris flow event during typhoon Morakot in 2009 which resulted in 20 destroyed and another 20 damaged buildings including an elementary school and a church (Sinotech 2010). The third time slot re-presents the current situation (field investigation in 2012). First results indicate that risk evolution in Lai-Ji (來吉村) is dominated by increase of the hazard level and a non-adaptive risk management. Hazard is high when heavy rainfalls of typhoons hit the destabilized soil after high earthquake activity as it happened several times since the Chi-Chi earthquake in 1999 (e.g. typhoon Mindulle in 2004 and Morakot in 2009). But also the rain intensity and the frequency of extreme events increased from 1960-2010 as a result of climate change (Central Weather Bureau 2013). The second main driver for risk evolution in Lai-Ji (來吉村) is risk management, as no local protection measures were undertaken after the both events. Furthermore, most buildings were rebuilt in the same place after the event or elsewhere within the endangered area. In the next steps, risk maps for Lai-Ji (來吉村) will be generated, another case study in Switzerland (Sörenberg) will be conducted.

#### REFERENCES

- Central Weather Bureau 2013 : Precipitation data from Alishan rain gauge from 1960-2010. Taiwan.
- Keiler, M., Sailer, R., Jörg, P., Weber, C., Fuchs, S., Zischg, A., Sauermoser, S., 2006: Avalanche risk assessment – a multi-temporal approach , results from Galtür, Austria. In : Natural Hazards and Earth System Sciences 2006 (6) : 637-651.
- Intergovernmental Panel on Climate Change (IPCC) 2012: Managing the risks of extreme events and disasters to advance climate change adaptation. Special report of the intergovernmental panel on climate change. Cambridge University Press.
- Schwendtner, B., Papatoma-Köhle, M., Glade, T., [in Press]: Risk evolution: How can changes in the built environment influence the potential loss of natural hazards?
- Sinotech, 2010: Risk analysis for Lai-Ji village [in Chinese]. 嘉義縣阿里山鄉來吉村 土石流潛勢地區風險分析.

## P 26.9

**“Proyecto Glaciares 513”: an integrated assessment of high mountain hazards and related risk reduction in the Peruvian Andes.**

Giraldez Claudia<sup>1</sup>, Choquevilca Walter<sup>2</sup>, Drenkhan Fabian<sup>1</sup>, Fernandez Felipe<sup>2</sup>, Frey Holger<sup>1</sup>, García Javier<sup>3</sup>, Haerberli Wilfried<sup>1</sup>, Huggel Christian<sup>1</sup> & Price Karen<sup>2</sup>

<sup>1</sup> Department of Geography, University of Zurich, Winterthurerstrasse 190, CH-8057 Zurich (claudia.giraldez@geo.uzh.ch)

<sup>2</sup> CARE Peru, Av. General Santa Cruz 659, PE-Lima 11

<sup>3</sup> Centre de recherche sur l'environnement alpin, CREALP, Rue de l'Industrie 45, CH-1951 Sion

The ice covered Peruvian Cordilleras are often seriously affected by high mountain hazards such as ice and rock avalanches, glacier lake outbursts, floods and debris flows. In the past, thousands of people have been killed in such disasters (Carey, 2005). More recently in 2010, massive floods in the Cusco Region and an outburst flood from glacier lake “Laguna 513” in the Cordillera Blanca (Ancash Region) drew the attention of the public, policy and science (Carey et al., 2012).

As a follow up of the Laguna 513 event in 2010 and corresponding to assessments by international experts (Haerberli et al., 2010), an integrative and international project was initiated in 2011, funded by the Swiss Agency for Development and Cooperation (SDC) and executed by the University of Zurich (UZH) and CARE-Perú. This project, “Proyecto Glaciares 513”, aims at sustainably enhance climate change adaptation and to reduce high-mountain risks in the Peruvian Cordilleras. Thus it combines three components. First, a local level with detailed case studies including the implementation of a monitoring and early warning system for ice/rock avalanches and glacier lake outburst floods downstream from Laguna 513 (Ancash), and a risk management system for rain-triggered mass movements in the region of Santa Teresa, Cusco. Secondly, an academic level to strengthen local capacities in glaciology, high-mountain processes, climate change and risk management. Finally, an institutional level to strengthen glaciology in Peru on a national and international level.

Here we focus on the risk management system for rain-triggered mass movements in the region of Santa Teresa, Department of Cusco, close to the Machu Picchu Inca City. Research about glacier and high-mountain hazards in the southern Peruvian Cordilleras of Cusco is still sparse although some of the largest debris flows worldwide affected this region in recent years (Frey et al. 2012, Huggel et al., 2003). In fact, very little is known about the nature, origin and dimensions of mass movements in this area, and long-term climatic records are neither available. In the framework of the “Proyecto Glaciares 513” a risk management system is being designed for the Distrito de Santa Teresa and its subcatchments. This system is structured through three components: technical, institutional, and social. Within the technical component (i.e. monitoring and communication) the origin, trigger and characteristics of potential hazards (Fig. 1) are analyzed with the final goal of generating a risk map for each community. This work is based on satellite images, field work, available meteorological data, and numerical modelling. A radio-communication system is currently being implemented to allow communication and interaction amongst the communities in case of an event. Furthermore a climatic and hydrological monitoring network is also being established and led by locals, with the support of the Local Water Authority (ALA) and the National Meteorological and Hydrological Service (SENAMHI). It includes both manual and automatic instruments to measure precipitation, temperature and relative humidity, as well as water levels in rivers.

In summary, the risk management system for the Distrito de Santa Teresa is already in a preliminary phase and takes into account not only the complex geomorphodynamics of such high-mountain environment under climate change but also the socio-economic and institutional characteristics of the region.

## REFERENCES

- Carey, M. 2005: Living and dying with glaciers: people's historical vulnerability to avalanches and outburst floods in Peru. *Global and Planetary Change*, 47 (2-4), 122-134
- Carey, M., Huggel, C., Bury, J., Portocarrero, C. & Haerberli, W. 2012: An integrated socio-environmental framework for glacier hazard management and climate change adaptation: lessons from Lake 513, Cordillera Blanca, Peru. *Climatic Change*, 112 (3), 733–767.
- Frey, H., Schneider, D. & Huggel, C. 2012: Satellite based analysis of the hazard situation of Santa Teresa, Perú. Baseline report, University of Zurich, Department of Geography. 21pp.
- Haerberli, W., Portocarrero, C. & Evans, S. 2010: Nevado Hualcán, Laguna 513 y Carhuaz 2010 -Observaciones, evaluación y recomendaciones (short technical report after meetings and field visit in July 2010). Huaraz.
- Huggel, C., Käab, A. & Haerberli, W. 2003: Vulnerability study of the Central Hidroeléctrica Machupicchu – Glacial assessment and modeling based on satellite imagery. Final Report. University of Zurich, Department of Geography. 24pp.

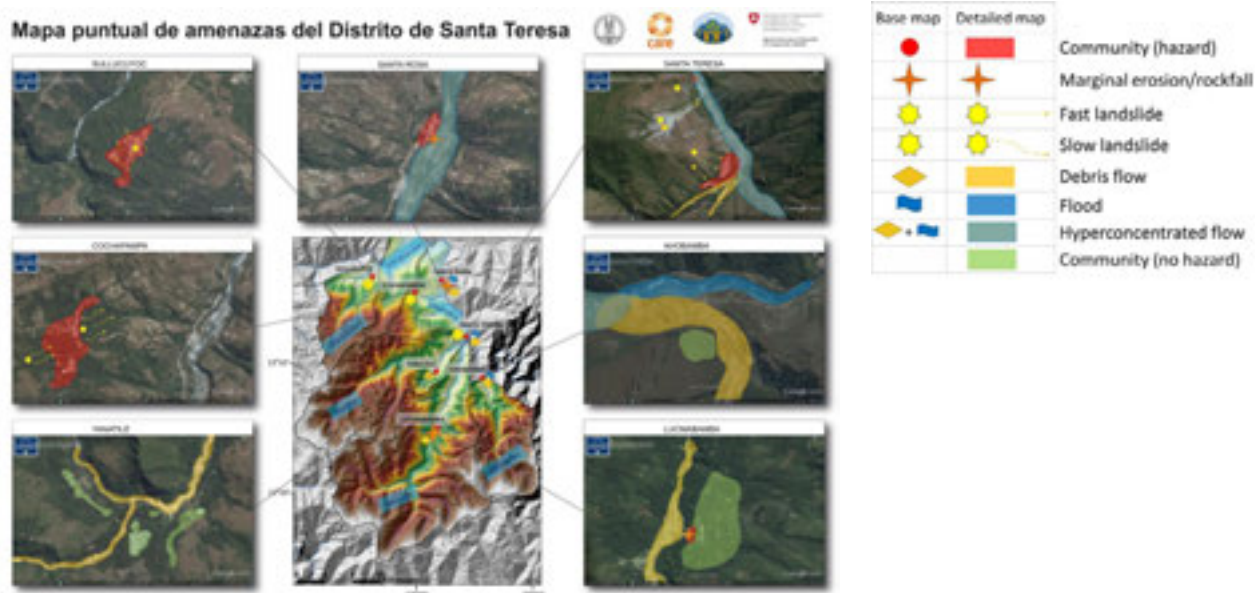


Figure 1. Hazard map for Santa Teresa, Cusco. It identifies the most significant geomorphodynamic processes that constitute a potential hazard for the most populated communities.

## P 26.10

# Paleodenudation rates and possible links with climate and sediment flux variations in the Engadine, Eastern Swiss Alps

Reto Grischott, Florian Kober, Kristina Hippe, Maarten Lupker, Marcus Christl, Irka Hajdas & Sean Willett

Modern estimates of denudation rates using cosmogenic nuclides and correlations with various geomorphic parameters have been established for several regions of the Alps (Wittmann et al. 2007; Norton et al. 2011; Kober et al. 2012). Cosmogenic denudation rates and mean denudation based on valley and lake fillings integrated since the Last Glacial Maximum suggest an 12 to 14-fold higher denudation rate compared to modern estimates (Hinderer 2001). Due to the lack of knowledge on paraglacial processes and response times as well as the influence of late Pleistocene to Holocene climate changes, empirical paleodenudation rates are needed. In an attempt to overcome this missing link, an alpine sediment archive was selected where significant changes in vegetation cover, glacier fluctuations, periglacial activity have been reported.

In the Eastern Swiss Alps one cold phase and two warm phases were reported for the Late Holocene based on stratigraphical and palynological data (Burga et al. 1997). We aim to quantify the effect of climate variation on erosion and sediment flux in the Fedoz river that drains a small high alpine valley (currently 10% glaciated) to Lake Sils, Eastern Switzerland. The major part of fluvial sediments is archived in the subaerial parts of the Isola delta. Radiocarbon-dated sediment cores provide the opportunity to determine  $^{10}\text{Be}$ -catchment wide denudation rates for distinct time intervals since the Middle Holocene.

Sediment cores on the fan were retrieved which range back to 4000 years. A detailed radiocarbon age model was established based on terrestrial organic macro fossils (seeds, wood and leafs), due to eroding Holocene peat layers in the catchment that dominate organic matter in the sediment. Sand layers in the sediment core between those dated peat layers were sampled and measured for  $^{10}\text{Be}$  nuclides. The same sediment intervals were tested – if correlation was possible - in different cores to test the homogeneity of the signal. Additionally, estimates of present-day nuclide concentrations were performed in modern stream samples. A postdepositional  $^{10}\text{Be}$  correction after Schaller et al. (2004) does not exceed 20-30% of the measured signal.

The data provide high resolution denudation rates in the time range from 4000 to 2000 years BP (from 2000 y BP to present soil formation). Calculated paleodenudation rates are slightly increased compared to the modern signal  $\sim 0.7$  mm/yr. Due to the high altitude, the landscape is sensitive to permafrost and glacier fluctuations which are supposed to dominate the response of landscape evolution. However, the influence of these changes in the erosional regime to the measured  $^{10}\text{Be}$ -signal has not yet been clarified. The relative proximity to the glacier might bias the  $^{10}\text{Be}$ -signal due to remobilization of glacial deposits.

### REFERENCES:

- Burga, C. A., R. Perret, S. Gehrig, H.-H. Vogel, B. Maggetti, P. Fitze, M. Maisch and K. Graf (1997). Geoökologische und klimamorphologische Untersuchungen im Alpenraum: Isola-Delta, Val Fedoz und Val Fex, Oberengadin, Kanton Graubünden; [Projektschlussbericht im Rahmen des nationalen Forschungsprogrammes „Klimaänderungen und Naturkatastrophen in der Schweiz“ NFP 31]. Zürich, vdf, Hochschulverlag.
- Hinderer, M. (2001). „Late Quaternary denudation of the Alps, valley and lake fillings and modern river loads.“ *Geodinamica Acta* 14(4): 231-263.
- Kober, F., K. Hippe, B. Salcher, S. Ivy-Ochs, P. W. Kubik, L. Wacker and N. Hählen (2012). „Debris-flow-dependent variation of cosmogenically derived catchment-wide denudation rates.“ *Geology* 40(10): 935-938.
- Norton, K. P., F. von Blanckenburg, R. DiBiase, F. Schlunegger and P. W. Kubik (2011). „Cosmogenic  $^{10}\text{Be}$ -derived denudation rates of the Eastern and Southern European Alps.“ *International Journal of Earth Sciences* 100(5): 1163-1179.
- Schaller, M., F. von Blanckenburg, N. Hovius, A. Veldkamp, M. W. van den Berg and P. W. Kubik (2004). „Paleoerosion rates from cosmogenic Be-10 in a 1.3 Ma terrace sequence: Response of the river meuse to changes in climate and rock uplift.“ *Journal of Geology* 112(2): 127-144.
- Wittmann, H., F. von Blanckenburg, T. Kruesmann, K. P. Norton and P. W. Kubik (2007). „Relation between rock uplift and denudation from cosmogenic nuclides in river sediment in the Central Alps of Switzerland.“ *Journal of Geophysical Research-Earth Surface* 112(F4).

**P 26.11****Geomorphological analysis of the drainage system on the growing Makran Accretionary Wedge in SE Iran**Haghipour Negar<sup>1</sup>, Burg Jean-Pierre<sup>1</sup><sup>1</sup> *Department of Earth Sciences, ETH-Zurich, Sonneggstrasse 5, 8092 Zurich, Switzerland*

The morphology of six adjacent major catchments draining the onshore Makran Accretionary Wedge in southeast Iran and southwest Pakistan was studied to examine how the channel pattern and the length profiles may reflect the recent and active growth of the wedge. Qualitative field surveys were combined with the quantitative analysis of channel steepness and concavity measured from digital elevation models. These profiles were compared with modelled profiles using a stream power approach and assuming homogeneously uplifting, uniform rock substratum. Results show a distinct difference between the studied western and eastern catchments. The westernmost river is disturbed by the Minab-Zendan Transform Fault, which separates the Makran Accretionary Wedge from the collided Zagros Fold Belt; for this reason, this river has been omitted from further interpretation of accretionary processes. The three western rivers are in morphological equilibrium whereas the two eastern rivers exhibit profiles with prominent convexities and knickpoints, thus notably diverging from equilibrium concave-up shapes. All the studied catchments share the same base level, flow on similar lithologies and developed under uniform climate conditions. Therefore, the morphometric differences are interpreted in terms of differential rock uplift rate as a response to local tectonic activity. This interpretation is consistent with both uplift rates of marine terraces along the coast of Makran and the recorded seismicity. The geomorphological work extends coastal information to wide inland areas and documents longer term tectonic behaviour than the seismo-tectonic record. Hence, the steeper surface slope and faster surface uplift rates recorded by the eastern catchments compared to equilibrium of the western catchments are regional, long term signals relevant for a wide part of the Makran Accretionary Wedge. The regional geomorphic difference is attributed to Quaternary variations in tectonic regimes that forced differential uplift rates of the wedge surface. The different tectonic regimes are tentatively related to different subduction rates.

**P 26.12****A tool for vulnerability assessment to mountain hazards**Keiler Margreth<sup>1</sup>, Zischg Andreas<sup>2</sup>, Papathoma-Köhle Maria<sup>3</sup> & Fuchs Sven<sup>4</sup>,<sup>1</sup> *Institute of Geography, University of Bern, Hallerstrasse 12, CH-3012 Bern (margreth.keiler@giub.unibe.ch)*<sup>2</sup> *ABENIS AG, Quaderstrasse 7, CH-7000 Chur*<sup>3</sup> *Department of Geography and Regional Research, Universitätsstrasse 7, A-1010 Wien*<sup>4</sup> *Institute of Mountain Risk Engineering, University of Natural Resources and Life Sciences, Peter-Jordan-Strasse 82, A-1190 Wien*

Torrents prone to debris flows regularly cause extensive destruction of the built environment, loss of life stock, agricultural land and loss of life in mountain areas. Climate change may increase the frequency and intensity of such events. On the other hand, extensive development of mountain areas is expected to change the spatial pattern of elements at risk exposed and their vulnerability. Consequently, the costs of debris flow events are likely to increase in the coming years. Local authorities responsible for disaster risk reduction are in need of tools that may enable them to assess the future consequences of debris flow events, in particular with respect to the vulnerability of elements at risk.

An integrated tool for loss estimation is presented here which is based on a newly developed vulnerability curve and which is applied in test sites in the Province of South Tyrol, Italy. The tool has a dual function: 1) continuous updating of the database regarding damages and process intensities that will eventually improve the existing vulnerability curve and 2) loss estimation of future events and hypothetical events or built environment scenarios by using the existing curve. The tool integrates the vulnerability curve together with new user friendly forms of damage documentation. The integrated tool presented here can be used by local authorities not only for the recording of damage caused by debris flows and the allocation of compensation to the owners of damaged buildings but also for land use planning, cost benefit analysis of structural protection measures and emergency planning.

## P 26.13

# The sediment yield at the front of active rock glaciers, results from the first summer of investigations at Gugla-Bielzug rock glacier, Matternal (VS)

Kummert Mario<sup>1</sup> & Delaloye Reynald<sup>1</sup>

<sup>1</sup>Department of Geosciences/Geography, University of Fribourg, Chemin du Musée 4, CH-1700 Fribourg (name.surname@unifr.ch)

In the current context of global warming, different studies suggest that the amount of sediment available for intense transfer processes will grow during the upcoming decades in the Alps (e.g. Zimmermann & Haeberli 1992). It is mainly due to the melting of glacier and permafrost ice, which is assumed to induce an important release of rock debris. In that perspective, the particular case of rock glaciers is interesting because the warming process of the permafrost ice and the presence of liquid water usually generate creep acceleration (Kääb et al. 2007, Roer et al. 2008). Thereby, if we consider that the sediment yield at the front of active rock glaciers is related to their velocity, this creep acceleration observed recently by several research (e.g. Roer et al. 2008, Delaloye et al. 2013) will probably participate in the increase of easily transferable sediment stored in alpine hillslopes. In some situation, where there is a direct or partial connection with torrential channels, the possibility of developing debris flow events will be reinforced (Delaloye et al. 2010). Therefore, sedimentary connectivity in periglacial slopes represents an important aspect in the assessment of natural hazards in mountain areas.

This research project aims to study the characteristics of the sediment yield at the front of active rock glaciers, both qualitatively and quantitatively. The goal is to reach a better understanding of the processes involved, but also to assess the connectivity between rock glaciers and torrential channels, and the link between the sediment yield and the creep velocity. To achieve this, a combination between field measurement (Terrestrial Laser Scanning, DGPS, ...) and visual information (observations, webcam images) is used.

This contribution presents the results from measurements and observations conducted during the summer 2013 at the Gugla-Bielzug rock glacier. This rock glacier is located on the orographic right side of Matter Valley (Valais, Switzerland) and is characterized by a direct connectivity with the torrential network. Particularly high velocity (up to more than 25 m/y for some parts of the form) have been measured during the snowmelt period in June and several debris flow events occurred at that time, spreading downhill from the front of the rock glacier to the main valley. The webcam images provide a rich source of visual information that has allowed identifying the different processes responsible for the sediment yield. In this particular case, the presence of water in the system has played a key role by inducing small sliding events and regressive erosion in the unfrozen sediment laying at the rock glacier snout. Terrestrial laser scans were also performed at different dates after the June debris flow events. Those scans bring helping information to locate and quantify the sediment recharge at the rock glacier front and in the subjacent gully.

## REFERENCES

- Delaloye, R., Lambiel, C. & Gärtner-Roer, I. (2010). Overview of rock glacier kinematics research in the Swiss Alps. Seasonal rhythm, interannual variations and trends over several decades. *Geogr. Helv.*, 65: 2, 135-145.
- Delaloye, R., Morard, S., Barboux, C., Abbet, D., Gruber, V., Riedo, M. & Gachet, S. (2013). Rapidly moving rock glaciers in Matternal. In : Graf, C. (eds). *Matternal - ein Tal in Bewegung*. Publikation für Jahrestagung der Schweizerischen Geomorphologischen Gesellschaft 29. Juni - 1. Juli 2011, St. Niklaus, Birmensdorf, Eidg. Forschungsanstalt WSL. 21-31.
- Kääb, A., Frauenfelder R. & Roer, I. (2007). On the response of rockglacier creep to surface temperature increase. *Global and Planetary Change*, 56, 172-187.
- Roer, I., Haeberli, W., Avian, M., Kaufmann, V., Delaloye, R., Lambiel, C. & A. Kääb. (2008). Observations and considerations on destabilizing active rockglaciers in the European Alps. In : Kane, D.L. & Hinkel, K.M. (eds). *Proceedings of the 9th International Conference on Permafrost*, June 29-July 3 2008, Fairbanks, Alaska, 2, 1505-1510.
- Zimmermann, M. & Haeberli, W. (1992). Climatic change and debris flow activity in high-mountain areas. A case study in the Swiss Alps. *Greenhouse Impact on Cold Climate Ecosystems and Landscapes*, Catena, Suppl. Vol. 22, 59-72.

## P 26.14

# Adaptation of the geomorphological mapping system of the University of Lausanne for ArcGIS

Lambiel Christophe<sup>1</sup>, Maillard Benoît<sup>1</sup>, Regamey Benoît<sup>1</sup>, Martin Simon<sup>1</sup>, Kummert Mario<sup>1</sup>, Schoeneich Philippe<sup>2</sup>, Pellitero Ondicol Ramon<sup>3</sup>, and Reynard Emmanuel<sup>1</sup>

<sup>1</sup>*Institute of geography and sustainability, University of Lausanne, Geopolis, 1015 Lausanne, Switzerland*

<sup>2</sup>*Institut de Géographie Alpine, PACTE/Territoires, Université Joseph Fourier, 38100 Grenoble, France*

<sup>3</sup>*Departamento de Geografía, Universidad de Valladolid, Espana*

The geomorphological mapping legend of the University of Lausanne has been used for more than 20 years for detailed mapping especially in high and middle mountain regions. It is a morphogenetic mapping system built on the following principles:

- The colours represent process categories;
- The signatures have a genetic significance and are drawn in the colour of the related process;
- The morphodynamic differentiation of erosion and accumulation areas is achieved by white and coloured surfaces respectively.
- The morphography, the slope gradient and the lithology are not represented.

The legend was developed first for mapping by hand with colour pencils in the field. In the 1990s, several attempts were made for developing computer-assisted maps, especially by using Adobe Illustrator software. The improvement of the graphical performance of GIS in the last years permitted the adaptation of the legend for GIS to be considered. Through various geomorphological mapping projects, a new version could be developed in ArcGIS 10.0. It consists in a geodatabase containing three Feature Datasets containing respectively the Features Classes “points”, “lines” and “surfaces”. Specific symbols were developed using the Representation tool in ArcGIS 10.0. For some landforms (e.g. alluvial fans, rockglaciers, deltas), it was necessary to combine two or three point, line or surface symbols. Thanks to the ArcGIS version of the legend, it is now possible to map the geomorphology in a GIS environment from the combination of orthophotos, topographical maps and high resolution DEM, that is with reduced field survey.

This poster will present the concept of the legend, the geodatabase and some illustrative examples.

## P 26.15

### The geomorphological map of the Hérens valley

Maillard Benoît<sup>1,2</sup>, Regamey Benoît<sup>1</sup>, Kummert Mario<sup>1</sup>, Reynard Emmanuel<sup>1</sup>, Lambiel Christophe<sup>1</sup> & Theler David<sup>2</sup>

<sup>1</sup> *Institute of geography and sustainability, University of Lausanne, Geopolis, 1015 Lausanne, Switzerland*

<sup>2</sup> *Ecotec Environnement SA, CH-Sierre*

Within a project dealing with debris flow hazards in the Hérens valley (Switzerland) a geomorphological map of the whole valley has been produced. The map is based on a legend developed in the 1980s at the Institute of geography of the University of Lausanne. The morphogenetic legend classifies the landforms according to the process(es) responsible of their formation (green for fluvial processes, pink for periglacial processes, etc.) and according to erosional (graphics on white background) or depositional (graphics on coloured background) character. The map has been produced in ArcGIS with the new adapted version of the legend for this software.

The glacial processes have had the main influence of the morphogenesis of the valley. If large glaciers are still modelling the morphology in the head of the valleys, Lateglacial landforms are present in the entire valley. Periglacial processes and landforms are widespread in the numerous secondary valleys and in the steep slopes, as for instance the east side of Arolla valley. They are often associated with an active gravitational activity, resulting in large talus slopes and some deep-seated gravitational deformations. Finally, the torrential activity is important and has led to the formation of numerous fans in the valley bottom.

## P 26.16

### Low denudation recorded by <sup>10</sup>Be in river sands from Southern Peninsular India

Mandal Sanjay Kumar<sup>1</sup>, Lupker Maarten<sup>2</sup>, Burg Jean-Pierre<sup>1</sup>, Haghypour Negar<sup>1</sup>, Christl Marcus<sup>3</sup>

<sup>1</sup> *Geological Institute, ETH Zurich, Sonneggstrasse 5, CH -8092 Zurich (sanjay.mandal@erdw.ethz.ch)*

<sup>2</sup> *Institute of Geochemistry and Petrology, ETH Zurich, Clausiusstrasse 25, CH-8092 Zurich*

<sup>3</sup> *Laboratory of Ion Beam Physics, ETH Zurich, Schafmattstrasse 20, CH-8093 Zurich*

The persistence of high elevation topography observed along many passive margins remains one of the outstanding problems in landscape evolution. In Southern Peninsular India, this question revolves around the understanding of whether the observed high relief and pronounced topography results from equilibrium with contemporaneous external forcing or whether the relief was acquired during the late Cenozoic and conserved over several tens of millions years. Modern denudation rates dictating the current landscape evolution are ruled by the interactions between climate, tectonics and rock strength. We used detrital cosmogenic <sup>10</sup>Be from 43 drainage basins ranging in size from 4 to 68768 km<sup>2</sup>, to infer millennial basin averaged denudation rates along and across the Western Ghat Mountains in Southern India and to understand if the present landscape is still actively evolving or not.

The Western Ghat is characterized by a W-E gradient in relief and rainfall with only minor variations in lithology allowing us to isolate the relationship between erosion rates and topographic indices. Cosmogenic-derived erosion rates are spatially variable, ranging from ~8 to 77 mm/ka on the western side and 8 to 51 mm/ka on the eastern side. The rugged topography of Western Ghats and Nilgiri Mountains exhibit pronounced topography in conjunction with low denudation rates. This represents an exception to the often-cited coupling of topography and denudation rates and suggests that steep slopes and high relief in passive margin settings are not associated to high denudation. Nevertheless, the differences in denudation rates along and across the Western Ghats are well correlated with local relief, which suggests that the inherited topography still controls on current denudation rates. Even though the catchments in Western Ghats receive a mean annual precipitation ~ 5 m, due to the SW Indian monsoon, precipitation shows only a minor control on denudation rates. This suggests that in the absence of significant tectonic forcing, climate is not an active driver of landscape evolution in passive margins such as the Western Ghats.

## P 26.17

# Changing glacial sediment balance - a GIS-based model approach for the Swiss Alps

Mölg Nico<sup>1</sup>, Haerberli Wilfried<sup>1</sup>, Zemp Michael<sup>1/2</sup>, Linsbauer Andreas<sup>1</sup>

<sup>1</sup>Institute of Geography, University of Zurich, Winterthurerstrasse 196, CH-8057 Zürich (nico.moelg@geo.uzh.ch)

<sup>2</sup>World Glacier Monitoring Service, Winterthurerstrasse 196, CH-8057 Zürich

Continuing atmospheric warming and consequently strong retreat of alpine glaciers will strongly change high-alpine landscapes, as we know them. The aim of the present study was to estimate whether glaciers would leave behind rocky or sedimentary beds during certain timeframes of their future retreat. This is crucial to know, as changes in sediment availability may have impacts on water reservoirs or might determine whether (new) lakes will fill up with sediments.

The presented investigation is based on an erosion-sedimentation index ( $I_{es}$ ) developed by Haerberli (1986) and its application on Swiss glaciers (Zemp, 2002). The index allows estimating the sediment characteristics of the exposed glacier bed after the glaciers' retreat. The study was performed with the Swiss glacier inventory from 1973 (Müller et al., 1976). Due to the fact of extensive and consistent glacial retreat in the Swiss Alps since then the ice-covered areas of 1973 have changed considerably, almost one third of it has got lost until 2000 (Paul et al., 2011).

Recently developed models exist that calculate future glacier retreat and distributed DEM information on glacier beds getting exposed in the future (Linsbauer et al., 2009). The basic inputs necessary for the calculation of the  $I_{es}$  can thereof be extracted and the index can thus be calculated for future landscape scenarios, taking into account changing glacier surface area and changing topography in regions that are presently ice-covered. The present study expands the former way of applying the index to one set of glaciers at one point in time to all Swiss glaciers at predicted extents in the future until the disappearance of all Alpine glaciers. Additionally, the GIS-based models have been modified to take into account future changes of alpine conditions that alter the input parameters of the index, p.e. equilibrium line altitude, glacier mass balance or slope of the glacial stream.

Results indicate varying and changing glacier bed characteristics in response to changing climatic conditions, even within the bed of the same glacier. Message and limitations of the index are discussed and its validity is being estimated by comparing the index results with newly exposed glacier forefields. Further the suitability of the results to be coupled with other characteristics of the new landscapes such as simultaneously developing glacial lakes, which might lead to potential hazard situations, will be discussed.

## REFERENCES

- Müller, F., T. Caflisch and Müller, G. 1976. Firn und Eis der Schweizer Alpen: Gletscherinventar. Zürich, Eidgenössische Technische Hochschule. (Geographisches Institut Publ. 57.)
- Haerberli, W. (1986): Factors influencing the distribution of rocky and sedimentary glacier beds. Hydraulic effects at the glacier bed and related phenomena. Mitteilung der Versuchsanstalt für Wasserbau, Hydrologie und Glaziologie, Nr. 90, S. 48f.
- Zemp, M., Käab, A., Hoelzle, M. and Haerberli, W. 2005. GIS-based modelling of glacial sediment balance. *Zeitschrift für Geomorphologie*, 138:113-129.
- Paul, F; Frey, H; Le Bris, R (2011). A new glacier inventory for the European Alps from Landsat TM scenes of 2003: challenges and results. *Annals of Glaciology*, 52(59):144-152.
- Linsbauer, A., Paul, F., Hoelzle, M., Frey, H., and Haerberli, W.: The Swiss Alps Without Glaciers – A GIS-based Modelling Approach for Reconstruction of Glacier Beds. *Geomorphometry 2009 Conference Proceedings*, edited by: Purves, R., Gruber, S., Straumann, R., and Hengl, T., University of Zurich, 243–247.

## P 26.18

# Evolutions of coastal lines of Gorgan Lagoon (East of Caspian Sea) by using satellite images

Babak Najafiha<sup>1</sup>, Vladimir r. Boynagryan<sup>2</sup>, Jahanigir Disedh<sup>3</sup>

<sup>1</sup> Senior Expert Marine Geomorphology department Geology Management, Geological Survey of Iran, Meraj St, Azadi Sq. Tehran, Iran (Njafiha@yahoo.com)

<sup>2</sup> Head of chair of Geomorphology and cartography, Yerevan state University, Yerevan, Armenia

<sup>3</sup> Head of Coastal Geomorphology department Geology Management, Geological Survey of Iran, Meraj St, Azadi Sq. Tehran, Iran

The caspian sea is the largest lake in the world and GORGAN lagoon is considered as largest lagoon on the south coast of this lake

Coastal environments are the most important forms which are continuously changing in short term or long term durations. The boundary between the land and sea is not only under different amounts of energy by atmospheric and ocean forces, but also it is severing from human use of the coastal regions.

Gorgan Lagoon is located at east Caspian Sea and by use of aerial pictures and satellite images of the years 1975, 2000 and 2004 the pictures for evolutions of these lines are surveyed. By sampling the old coast which is located in lowlands, it is observed that the sediments are in fine grains. These deposits are observable in flood area. Longitudinal sand hills exist along the sea in the land and after aggregation of samples it was specified that the sand is from fine grains. Coastal dunes provide important ecosystem services and are susceptible to human disturbance such as vehicle traffic and human trampling these hills which are the result of wind processes in the region play important role in protection of the coast during years. Their orientation is along the dominant wind in the region (west to east). Some parts of longitudinal sand hills have grass and tree vegetation due to good climate and some other parts lack vegetation and they indicate complicated relations between vegetation and sand transfer. These hills have about 7 meters height that a ground is located between them which is showing marine environment in the long past. Seasonal swings and changes of Caspian Sea water level bring the water near these hills and they act as a natural obstacle against water approaching in the land. Investigation of aerial pictures of 1955 and their periodic comparing with new pictures indicates that the area of hills has decreased due to human activities for leveling the coasts for construction of coastal structures, ports, breakwaters, touristic complexes and removal of sands for constructional aims and these actions have caused water approaching in the beach and decreasing coastal area and as a result bringing serious risk for coastal installations.



Fig. 1 .Location of Gorgan Lagoon in South East of Caspian Sea

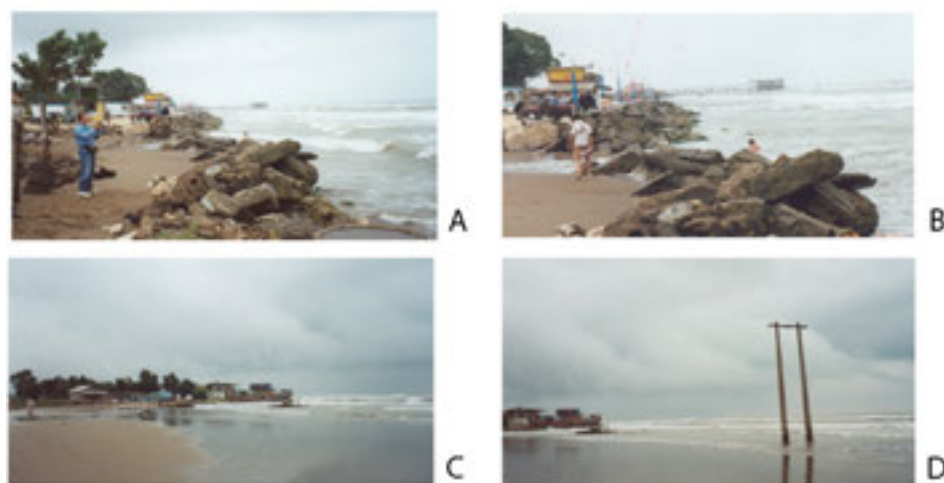


Fig. 2. Attack of sea as result of level's rise: a, b - abrasion of coast to west from mouth of river Tajan; c, d -retreat of coast by Farahabad

## REFERENCES

- Thomas A. Schlacher, a, , Rudolf de Jagera and Tara Nielsena,2010,Vegetation and ghost crabs in coastal dunes as indicators of putative stressors from tourism Indicators, Volume, March 2011, Pages 284–294
- Najafiha babak-Salehipor milani 2011, investigation of effective processes in forming of deltas in Gorgan Lagoon (Caspian sea)Geomed the 2nd international Geography symposium

## P 26.19

### Investigation and Elevation leveling of terraces as Indicator of Pleistocene Lake Levels (Urmia South west of Iran)

Mojtaba Yamani<sup>1</sup>, Ebrahim Moghimi<sup>2</sup>, Razyeh Lak<sup>3</sup>, Alireza Salehipour Milani<sup>4</sup>, Reza Tajik<sup>5</sup>

<sup>1</sup> Faculty of Geography, University of Tehran, Azin Allay, Vesal-e-Shirazi St. Enghelab St. Tehran, Iran (myamani@ut.ac.ir)

<sup>2</sup> Faculty of Geography, University of Tehran, Azin Allay, Vesal-e-Shirazi St. Enghelab St. Tehran, Iran (emoghimi@ut.ac.ir)

<sup>3</sup> Research Institute for Earth Science, Geological Survey of Iran, Meraj St. AzadiSq. Tehran, Iran (lak\_ir@yahoo.com)

<sup>4</sup> Faculty of Geography, University of Tehran, Azin Allay, Vesal-e-Shirazi St. Enghelab St. Tehran, Iran, Senior Expert of Geomorphology at Geological Survey of Iran, Meraj St. AzadiSq. Tehran, (Ar.salehipour@gmail.com)

<sup>5</sup> Geological Survey of Iran, Meraj St. AzadiSq. Tehran, Iran (tajik.re@gmail.com)

Lake Urmia in the northwestern corner of Iran is one of the largest permanent hypersaline lakes in the world and the largest lake in the Middle East (1, 2, and 3). It extends as much as 140 km from north to south and is as wide as 85 km east to west during high water periods (4). The lake's surface area has been estimated to have been as large as 6 100 km<sup>2</sup> but since 1995 it has generally been declining (7.5 Meter) and reach to 1270 (9) and was estimated from satellite data to be only 2 366 km<sup>2</sup> in August of 2011 (Landsat data). The decline is generally blamed on a combination of drought, increased water diversion for irrigated agriculture within the lake's watershed and mismanagement (2, 9,10,and1). Using extensive field trip along 3000km around Urmia Lake we can find 26 terraces. The ancient Terrace in Zanbil Daghi Island, Tasuj,Salmas, Gharabagh,Golaman Khnaeh, Eslami Island, Naghade, Mahabad, Miandoab, Bookan, Shahindezh, Malekan and Elkhchi(Fig.1). The elevations of 26 terraces and Plaeo lake level were measured with a differential global positioning system and ranged between 1298 to 1369. Sedimentological and geomorphological studies of terraces around Urmia Lake provided a preliminary framework for lake-level variations and paleoclimatology and Paleogeomorphology during Late Pleistocene. Benthic foraminifera and Ostracoda and Gastropoda assemblages were studied from 26 terraces.



Fig.1- Distribution of Pleistocene lake terrace around Urmia Lake



Fig.2- Naghadeh Lake Terrace Bedding

## REFERENCES

1. Zarghami, M. (2011). Effective watershed management; Case study of Urmia Lake, Iran. *Lake and Reservoir Management*, 27(1), 87-94. doi: 10.1080/07438141.2010.541327.
2. Hassanzadeh, E., Zarghami, M., Hassanzadeh, Y. (2011). Determining the Main Factors in Declining the Urmia Lake Level by Using System Dynamics Modeling. *Water Resources Management*, 26(1), 129-145. doi: 10.1007/s11269-011-9909-8.10
3. Karbassi, A., Bidhendi, G., Pejman, A., Bidhendi, M. (2010). Environmental impacts of desalination on the ecology of Lake Urmia. *Journal of Great Lakes Research*, 36(3), 419-424. doi: 10.1016/j.jglr.2010.06.004.
4. Jalili, S., Kirchner, I., Livingstone, D., Morid, S. (2011). The influence of large-scale atmospheric circulation weather types on variations in the water level of Lake Urmia, Iran. [10.1002/joc.2422]. *International Journal of Climatology*, n/a-n/a.

**P 26.20****Geomorphological map of the Diablerets massif – Swiss Alps**

Schoeneich Philippe<sup>1</sup>, Lambiel Christophe<sup>2</sup>, Bosson Jean-Baptiste<sup>2</sup>

<sup>1</sup> *Institut de Géographie Alpine – PACTE/Territoires, Université de Grenoble Alpes, 14 bis av. Marie-Reynoard, 38100 Grenoble, France (Philippe.Schoeneich@ujf-grenoble.fr)*

<sup>2</sup> *Institut de Géographie et Durabilité, Université de Lausanne, Geopolis, 1015 Lausanne, Suisse*

The Diablerets massif is part of the frontal limestone ranges of the Western Swiss Alps, and culminates at 3200 m asl. Geomorphological processes range from glacial and periglacial in its upper part to gravitational, torrential and fluvial processes in the lower parts, and it is concerned by huge powder avalanches. The area includes a very well preserved lateglacial moraine complex, a fluvial terrace system, as well as limestone and gypsum karst.

A detailed geomorphological map at 1:10'000 of its northern slope has been established, using the legend of the University of Lausanne. The field surveys were digitized using orthophotos and a 1 m resolution laser DTM. The map has been edited with GIS and CAD softwares.

The geomorphological survey has been used for lateglacial paleoglaciological reconstructions, for reconstruction of historical and recent glacier fluctuations, and for the assessment of hazards related to permafrost and of torrential hazard. The map covers several registered geomorphosites and will serve for public education as well.

The poster will present the geomorphological map, as well as maps of lateglacial and recent glacier fluctuations.

**P 26.21****Typology of solifluction landforms in the south-western Swiss Alps (Valais)**

Utz Stephan<sup>1</sup>, Lambiel Christophe<sup>1</sup>

<sup>1</sup> *Institute of geography and sustainability, Mouline – Geopolis, University of Lausanne, 1015 Lausanne (Stephan.utz@unil.ch)*

The slopes of alpine reliefs are subject to various phenomena of mass movements that all participate to sediment transfer. Among them, solifluction processes are widespread, and although transfer rates are low in comparison with phenomena such as debris flows or rock glaciers, they clearly contribute to the evolution of mountain landscapes. Solifluction is mainly considered as being a superficial mass-movement initiated by water saturation, which operates a slow downslope movement with yearly rates generally comprised between centimetric and metric scale. This process depends mainly on climate, hydrology, geology and topography, and the resulting landforms are generally lobate. However, some confusion still remains around the term solifluction because of the various definitions proposed in literature and the many different landforms that can be associated with.

This study focused especially on the morphology of alpine landforms. Based on field observations carried out in the western Swiss Alps during summers 2011 and 2012, this study mainly proposes a typology of the different landforms resulting from solifluction. Four different types could be defined, based on morphological criterions such as the dimensions of the landforms, the front characteristics and their layout on slopes. This typology permits to distinguish the most frequent solifluction landforms in the study area without requiring any heavy field measurements and can be used for geomorphological mapping. The influence of various environmental parameters such as vegetal cover, water supply or permafrost on the process and the landforms were also tackled by comparing field observations with the literature, in order to show the specificity of solifluction in alpine environment.



## 27. Fluxes of water, sediment and dissolved substances in geomorphologically active/changing environments

Nikolaus Kuhn, Stuart Lane

*Swiss Geomorphological Society*

### TALKS:

- 27.1 Fister Wolfgang, Heckrath Goswin, Greenwood Philip, Kuhn Nikolaus J.: Biochar erosion: A potential threat to its suitability for carbon sequestration?
- 27.2 Greenwood Philip, Kuhn Nikolaus J.: Does the invasive plant, *Impatiens glandulifera*, influence soil flux from riparian zones? An investigation on a small watercourse in northwest Switzerland
- 27.3 Haeberli Wilfried, Schaub Yvonne, Huggel Christian, Böckli Lorenz: Vanishing glaciers, degrading permafrost, new lakes and increasing probability of extreme floods from impact waves in cold mountain chains
- 27.4 Hu Yaxian, Xiao Liangang, Fister Wolfgang, Kuhn J Nikolaus: The effect of aggregation onto the fate of eroded carbon
- 27.5 Lane Stuart N., Balin D., Lovis B., Micheletti Natan: The impacts of climatically-driven hydrological flux upon coarse sediment flux in Alpine river basins
- 27.6 Micheletti Natan, Lane Stuart N.: Investigation of mass movement and sediment flux at the decadal scale for Alpine mountain basins using archival digital photogrammetry

### POSTERS:

- P 27.1 Delunel Romain et al.: Transient sediment supply in a high-altitude Alpine environment evidenced through a  $^{10}\text{Be}$  budget of the Etages catchment (French Western Alps)
- P 27.2 Gallice Aurélien, Mutzner Raphael, Parlange Marc B., Huwald Hendrik: Experimental Investigation of the Energy-Balance of an Alpine Catchment
- P 27.3 Kuhn Nikolaus J.: Sediment on Mars: settling faster, moving slower
- P 27.4 Schaub Yvonne, Schneider Demian, Guillén Ludeña Sebastián, Huggel Christian: Modeling process chains: rock/ice-avalanche induced outburst floods at Laguna 513, Cordillera Blanca, Peru
- P 27.5 Alissa Zuijdgheest, Timothy Eglinton, Francien Peterse, Bernhard Wehrli: Can soil biomarkers trace floodplain contributions to organic carbon export in a pristine, tropical river system?

## 27.1

### Biochar erosion: A potential threat to its suitability for carbon sequestration?

Fister Wolfgang<sup>1</sup>, Heckrath Goswin<sup>2</sup>, Greenwood Philip<sup>1</sup> & Kuhn Nikolaus J.<sup>1</sup>

<sup>1</sup> *Physical Geography and Environmental Change, University of Basel, Klingelbergstr. 27, CH-4056 Basel (Wolfgang.Fister@unibas.ch)*

<sup>2</sup> *Department of Agroecology, Aarhus University, Aarhus Denmark*

Biochar is often considered to be a 'soft' geo-engineering option, with the potential to encourage soils to sequester more carbon (C) from the atmospheric C pool, and so increase both medium- and long-term soil C stocks. Similar to soil organic carbon (SOC), biochar has a lower bulk density than typical agricultural soils. Therefore, the question about its preferential mobilization and redistribution in the landscape has been raised in recent years. This is especially relevant on soils, which are regularly cultivated and are vulnerable to soil erosion themselves. However, so far few studies about the erodibility and fate of biochar in the landscape exist and the answer to this question is still unknown. Since the efficacy of biochar for sequestering carbon and improving soil quality depends on its amount and residential time in the upper soil matrix, it is important to further our knowledge about mobilization and transport behaviour of biochar. Moreover, such knowledge could have profound economic implications for farmers committed to its use, as a high net annual loss of biochar by erosion could exceed any net annual economic gain. The overall objective of this study was, therefore, to investigate the erodibility of biochar, when erosion events occur directly or soon after its application. The estimation of the financial value of the eroded biochar and its cost-effectiveness were scaled up from plot to field scale.

In this investigation, the biochar was applied to the soil surface of three plots on a recently cultivated sandy field near Viborg in northern Jutland, Denmark at concentrations equivalent to 1.5-2.0 kg m<sup>-2</sup>. After application, the biochar was manually incorporated into the till-zone (20cm). Three consecutive erosion events (each lasted for 30 min. with rainfall intensity of approx. 90 mm h<sup>-1</sup>) were conducted on both biochar and reference plots. The erosion events were generated by the 2.2 m<sup>2</sup> Portable Wind and Rainfall Simulator.

The preliminary results of this study show that the sediment from plots with biochar application contains more carbon than sediment eroded from reference plots. Results based on floating biochar particles indicate that a considerable amount of biochar can be eroded from the fields within the first rainfall events after biochar application to the soil, most likely causing a reduction in the capability to sequester carbon. The economic loss of the floating biochar particles from a single event account for 3-32 €/ha, depending on the carbon content of the biochar and the erodibility of the soil. This seems to be negligible, but considering that the amount of applied biochar was very low and that erosion events occur more often than once in Denmark and most probably even more frequently under future climate conditions, the economic losses to landowners could be severe.

## 27.2

### Does the invasive plant, *Impatiens glandulifera*, influence soil flux from riparian zones? An investigation on a small watercourse in northwest Switzerland

Philip Greenwood & Nikolaus J. Kuhn

*Physical Geography & Environmental Change Research Group, Department of Environmental Sciences, University of Basel, Switzerland.*

*Impatiens glandulifera* (common English name: Himalayan Balsam) was introduced into Europe in the mid-19th century. Its invasive tendency has facilitated its expansion throughout much of mainland Europe due to certain lifecycle traits that have facilitated its rapid establishment and have allowed it to out-compete most native floral species. Its favoured habitat includes damp, nutrient-rich soils which experience frequent natural disturbance, such as riparian zones. Once present, watercourses then inadvertently act as conduits that facilitate the downstream movement of seeds into un-contaminated parts of the catchment. Deposited seeds then germinate and form discrete mono-cultural stands of plants. These can typically range from a few m<sup>2</sup> to > 400 m<sup>2</sup>. *Impatiens glandulifera* is cold-intolerant, however, and in temperate countries is rapidly killed by the first frosts. When die-back occurs, the dense vegetation canopy previously affording protection to the underlying soil surface from erosion processes is reduced. This can potentially increase the susceptibility of those areas to soil erosion, particularly by impacting raindrops. This paper reports the preliminary findings from on-going work conducted in a contaminated sub-catchment of the Birs River in northwest Switzerland. The investigation sought to quantify soil loss from a number of discrete riparian areas occupied by *I. glandulifera* before, during and after the die-back period. A technique using erosion pins and a profile bridge was employed to measure changes in the soil surface over a ca. 5-month period. Initial soil surface profiles were established at six contaminated sites before die-back occurred, as well as at six nearby uncontaminated reference sites. Soil surface profiles at all 12 sites were then re-measured at regular intervals. The average change in the soil surface profile was quantified for each transect and the results from both sets of transects were statistically compared. Significantly more sediment was lost from contaminated sites than from comparable reference sites. This is attributed to the presence of *I. glandulifera* and its role in promoting soil erosion along riparian zones. This finding could have important implications for water quality and for future river management strategies in all affected catchments in Europe, and be of particular relevance to European Union (EU) member states, since those countries are committed by the Water Framework Directive (WFD) to having their waterways in good ecological and chemical condition by the 2015 implementation date.

## 27.6

# Vanishing glaciers, degrading permafrost, new lakes and increasing probability of extreme floods from impact waves in cold mountain chains

Wilfried Haeberli<sup>1</sup>, Yvonne Schaub<sup>1</sup>, Christian Huggel<sup>1</sup> & Lorenz Böckli<sup>1</sup>

<sup>1</sup> *Geography Department, University of Zurich, Winterthurerstrasse 190, CH-8057 Zürich (wilfried.haeberli@geo.uzh.ch)*

As a consequence of continued global warming, rapid and fundamental changes are taking place in high-mountain regions. Within decades only, many still existing glacier landscapes will probably transform into new and strongly different landscapes of bare bedrock, loose debris, numerous lakes and sparse vegetation. These new landscapes are then likely to persist for centuries if not millennia to come. During variable but mostly extended parts of this future time period, they will be characterized by pronounced disequilibria within their geo- and ecosystems. Such disequilibria include a long-term stability reduction of steep/icy mountain slopes as a slow and delayed reaction to stress redistribution following de-butching by vanishing glaciers and to changes in strength and hydraulic permeability caused by permafrost warming and degradation. With the formation of many new lakes in close neighborhood to, or even directly at the foot of, so-affected slopes, the probability of far-reaching flood waves from large rock falls into lakes is likely to increase over extended time periods.

Quantitative information for anticipating possible developments exists in the European Alps. The present (2013) glacier cover is some 1700 km<sup>2</sup> with an average annual loss rate in area of about 40 km<sup>2</sup>; the still existing total ice volume can be estimated at 80 ± 20 km<sup>3</sup> with an average loss rate of about 2 km<sup>3</sup> ice per year (updated from Haeberli et al., 2013). The permafrost area has recently been estimated at some 3000 km<sup>2</sup> with a total subsurface ice volume of 25 ± 2 km<sup>3</sup> (Böckli, 2013); loss rates are hardly known but are certainly much smaller than for glaciers – probably by at least a factor of 10. Based on a detailed study for the Swiss Alps, total future lake volume may be assumed to be a few percent of the presently remaining glacier volume, i.e. a few km<sup>3</sup> for the entire Alps (Linsbauer et al., 2012). Forward projection of such numbers into the future indicates that glacier volumes tend to vanish much more rapidly than volumes of subsurface ice in permafrost, and lake volumes are likely to steadily increase. Already during the second half of the 21st century, more subsurface ice in permafrost may remain than surface ice in glaciers. The new lakes will then coexist with, or even be surrounded by, largely de-glaciated/de-butching over-steepened slopes and mountain peaks with thermally disturbed and degrading permafrost (Haeberli, 2013).

Similar scenarios are likely to take place in many cold mountain chains. Using integrated spatial information on glacier/permafrost evolution and lake formation together with models for rapid mass movements, impact waves and flood propagation in connection with vulnerability considerations related to settlements and infrastructure, hot spots of future hazards from flood waves caused by large rock falls into lakes can already now be recognized in possibly affected regions. This enables in-time planning of risk reduction options, which may include adapted spatial planning, early-warning systems, improved preparedness of local people and institutions, artificial lake drainage or lake-level lowering (Fig. 1), and flood retention optimally in connection with multipurpose structures for hydropower production and/or irrigation.



Figure 1. Laguna Llaca near Huaraz in 2013. Since the 1960s, the level of this lake at the foot of Nevado Ranrapalca (6162 m; background) was artificially lowered by about 30 m, greatly reducing the lake volume and the potential for large impact waves

#### REFERENCES

- Carey, M., Huggel, C., Bury, J., Portocarrero, C. and Haeberli, W. 2012. An integrated socio-environmental framework for glacier hazard management and climate change adaptation: lessons from Lake 513, Cordillera Blanca, Peru. *Climatic Change* 112, 3, 733-767.
- Böckli, L. 2013. Characterizing permafrost in the entire European Alps : Spatial distribution and ice content. PhD thesis, University of Zurich.
- Haeberli, W. 2013. Mountain permafrost – research frontiers and a special long-term challenge. *Cold Regions Science and Technology* (2013). <http://dx.doi.org/10.1016/j.coldregions.2013.02.004>
- Haeberli, W., Paul, F. and Zemp, M. (2013): Vanishing glaciers in the European Alps. In: *Fate of Mountain Glaciers in the Anthropocene*. Pontifical Academy of Sciences, *Scripta Varia* 118, 1-9.
- Linsbauer, A., Paul, F. and Haeberli, W. 2012. Modeling glacier thickness distribution and bed topography over entire mountain ranges with GlabTop: Application of a fast and robust approach. *Journal of Geophysical Research* 117, F03007, doi:10.1029/2011JF002313

## 27.4

### The effect of aggregation onto the fate of eroded carbon

Hu Yaxian<sup>1</sup>, Xiao Liangang<sup>1</sup>, Fister Wolfgang<sup>1</sup>, Kuhn J Nikolaus<sup>1</sup>

<sup>1</sup> *Physical Geography and Environmental Changes, University of Basel, Klingelbergstrasse 27, CH-4056 Basel (yaxian.hu@unibas.ch)*

The effect of soil erosion on the global Carbon (C) cycle is subject of an intense debate. The controversy is mostly due to the lack of understanding of the fate of transported C from the source of erosion to the eventual site of deposition. The fate of eroded carbon is strongly influenced by the settling velocities of the eroded fractions and the corresponding transport distance and environment at the site of deposition. Some erosion/deposition models already include the settling velocity of particles to evaluate the sediment transport distance and selective redistribution after erosion. However, the settling velocities in these models are either based on grain size (e.g. the EUROSEM model) or an arbitrary number of size classes (e.g. the WEPP model and the Hairsine-Rose model). In reality, most soil is eroded as aggregates, or at least aggregates are present in the sediment, which affects settling velocity and C content of the eroded soil. Without considering the effects of aggregation on sediment movement and C content, the extent of mineralization of deposited C as well as the transfer of organic C to aquatic systems is likely to be incorrect.

To identify the effect of aggregation on the fate of eroded C, a rainfall simulation was carried out on two soils of distinct texture and structure. The eroded sediments were then fractionated by a settling tube apparatus according to their likely transport distance after erosion. The sediment of each class was incubated for 50 days to monitor the respiration rate.

Weight, total organic carbon (TOC) of the sediment in each class were also measured. The distribution of C across our settling velocity classes indicates that most of the eroded C was incorporated in coarse aggregates that would have been deposited after short transport distances. This portion likely to be deposited across the landscape carried 58.8 to 88.2% of the total organic C stock in the eroded sediment and released about 55.4 to 81.9% of the total sediment CO<sub>2</sub> emission. The fine sediment likely transferred into rivers contained 3.6 to 7.4% of the total organic C stock and produced about 6.1 to 17.3% of the total CO<sub>2</sub> emission. As a consequence, if C erosion and mineralization had been solely based on grain size and associated C, the potential release of CO<sub>2</sub> during transport would have been underestimated. Future research should account for the effects of transport processes in a real field environment.

## 27.5

### The impacts of climatically-driven hydrological flux upon coarse sediment flux in Alpine river basins

Lane S.N., Balin D., Lovis B., Micheletti N.

*IGD, Université de Lausanne, LAUSANNE, SWITZERLAND*

Both future temperature and precipitation changes could have a dramatic impact upon the geomorphic response of high mountain river basins. The availability of historical climate records and aerial image archives since the 1940s now provides the opportunity to investigate over the recent past the forcing of geomorphic systems by rapid climate change, of importance because very few studies have disentangles the signature of such change in geomorphic records. Here we consider an Alpine river basin (altitude c. 1,200 m to 3,005 m), with very little direct human impact, but where there is excellent archival imagery. The imagery reveals three distinct phases of river basin change each period corresponding almost exactly to periods of known climatic warming/cooling in the last 5 decades of the 20th Century. To evaluate this climate forcing, we test a set of plausible hypotheses using mathematical modelling. To assess possible changes in sediment production activity, we apply the 1D heat diffusion equation to the basin scale, driven using historical temperature records. This shows that one plausible explanation remains decreases/increases in the percentage of the sediment supply zone that is frozen during warming/cooling periods. To assess changes in sediment transport capacity, we apply a multi-fraction sediment transport model to the predictions from a reconstruction of basin hydrological response that begins in 1940. This reveals systematic changes in hydrological response which, notably because of non-linearities in the transport equations, translates into dramatic changes in sediment transport capacity that mirror those of possible temperature driven changes in sediment production. Thus, both of these hypotheses remain plausible and it is possible that they act synergistically to cause rapid and dramatic changes in basin sediment state. Thus, understanding climate impacts on geomorphic response requires coupled temperature-precipitation effects to be considered.

## 27.6

# Investigation of mass movement and sediment flux at the decadal scale for Alpine mountain basins using archival digital photogrammetry

Micheletti Natan<sup>1</sup>, Lane Stuart N.<sup>1</sup>

<sup>1</sup> *Institut de Géographie et Durabilité, Université de Lausanne, 1015 Lausanne (Natan.Micheletti@unil.ch)*

Geomorphologists developed a good level of knowledge about mass movement and sediment flux at both the event scale (through direct measurement) and over longer timescales (through erosion measurement techniques such as those based upon cosmogenic methods). However, our understanding of sediment flux at the timescale of decades to centuries is still showing a deficit, especially when we try to establish a link between anthropological influence and climate change and their impacts upon geomorphic systems. Extensive coverage of mountain environments by aerial imagery begins in the 1940s, before the period of most rapid climate warming linked to human activity, and is essential to fill this gap of knowledge. The information contained in such imagery can be unlocked applying archival digital photogrammetry and producing high precision digital elevation models (DEMs) over large spatial scales. Using the appropriate data management and error propagation methods, we are able to perform quantitative comparisons of successive DEMs to build DEMs of Differences (DoD), to reconstruct histories of mass movement and sediment flux over the timescales of decades. Interpret these results with the help of geomorphological maps unveils the different ways in which climate change impacts individual landforms. Further, a proxy for mass movement behavior can be computed using multiple flow direction and flow accumulation algorithms considering sediment budget by the use of the aforementioned DoD. By doing so, we are able to investigate how the spatial arrangement of sediment system elements determines the diffusion of climate impacts through hillslopes.

Results demonstrate how, while particular elements of the sediment flux system prove to have been much more sensitive to climatic change than others, variations in high sediment production areas do not necessarily propagate throughout the hillslope because of the presence of disconnections and sediment trapping zones. As a consequence, despite a notable sediment production at the top of the sediment cascade, alluvial fans at the valley bottom seem to be stabilized and are mostly vegetation-covered. Accordingly, we suggest that warming-driven sediment dynamics on high mountain hillslopes are highly location specific and may depend more on sediment connectivity than sediment production process themselves.

## P 27.1

### Transient sediment supply in a high-altitude Alpine environment evidenced through a $^{10}\text{Be}$ budget of the Etages catchment (French Western Alps)

Delunel R., van der Beek P.A., Bourlès D.L., Carcaillet J., Schlunegger F.

Although  $^{10}\text{Be}$  concentrations in stream sediments provide useful synoptic views of catchment-wide erosion rates, little is known on the relative contributions of different sediment supply mechanisms to the acquisition of their initial signature in the headwaters. Here we address this issue by conducting a  $^{10}\text{Be}$ -budget of detrital materials originated from the morphogenetic domains representative of high-altitude environments of the European Alps (i.e. glacial system, high-elevation periglacial domain, intermediate rock-slope of valley walls, polygenic talus and cones at the valley bottom). We focus on the Etages catchment, located in the Ecrins-Pelvoux massif (SE France), and illustrate how in situ  $^{10}\text{Be}$  concentrations can be used for tracing the origin of the sand fraction from the bedload in the trunk stream. The  $^{10}\text{Be}$ -budget approach conducted here reveals that  $^{10}\text{Be}$  concentrations vary by a factor of ca. 50 within the Etages catchment while they display consistent distributions within each of the identified morphogenetic domain. We show in this small glaciated basin  $^{10}\text{Be}$  cannot be used to constrain erosion rates, as the different morphogenetic units supply sediment with a specific  $^{10}\text{Be}$  concentration and do not mix with each other within the alluvial network. The averaging principle needed to calculate erosion rates is thus not fulfilled. However, we suggest that the  $^{10}\text{Be}$  signature measured in different morphogenetic domains using this budget approach serve as a detrital tracer and help illustrating the origin of bedload in dynamic and changing high-altitude alpine environments.

## P 27.2

### Experimental Investigation of the Energy-Balance of an Alpine Catchment

Aurélien Gallice<sup>1</sup>, Raphael Mutzner<sup>1</sup>, Marc B. Parlange<sup>1</sup>, Hendrik Huwald<sup>1</sup>

<sup>1</sup> School of Architecture, Civil and Environmental Engineering, Ecole Polytechnique Fédérale de Lausanne (EPFL), Lausanne, Switzerland (aurelien.gallice@epfl.ch)

Water temperature is an important environmental factor, which affects the habitat suitability of many fish species and is of central interest for many ecohydrological studies. Over the past 30 years, the scientific community has focused on the understanding and modeling of the mechanisms controlling in-stream temperature. However, the thermal regime of water in the unchanneled state has been poorly studied so far, so that the mechanisms linking precipitation temperature to the water temperature in the stream channel are still unresolved. In particular, existing stream temperature models either rely on direct measurements or on simple correlations with the air temperature to estimate the temperature of stream sources and tributaries. The present study is seen as a first step towards a more physically based computation of such temperatures. The energy balance of a small alpine catchment (20 km<sup>2</sup>) is investigated in detail using a set of meteorological and hydrological observations. Particular attention is given to the physical quantities, in particular ground temperature, which affects water temperature in the unchanneled state. The database used for this study was collected over the past six years and contains meteorological data from a high-density network of wireless weather stations, as well as river stage, discharge and temperature measurements. The present work lays the foundations for the future development of an energy balance model at the catchment scale, which will be able to compute the temperature of surface, interflow, and baseflow runoffs – and therefore provide some boundary conditions to the actual stream temperature models.

## P 27.3

### Sediment on Mars: settling faster, moving slower

Kuhn Nikolaus J.<sup>1</sup>

<sup>1</sup> *Physical Geography and Environmental Change, University of Basel, Klingelbergstr. 27, CH-4056 Basel (Nikolaus.Kuhn@unibas.ch)*

Using empirical approaches developed on Earth to assess Martian hydrology based on conglomerates such as those found at Gale crater may deliver false results because Martian gravity potentially alters flow-sediment interaction compared to Earth. In this study, we report the results of our Mars Sedimentation Experiments (MarsSedEx I and II) which used settling tubes during reduced gravity flights in November 2012 (and scheduled for November 2013) on board Zero g's G-Force 1. The settling velocity data collected during the flights are compared to several models for terrestrial settling velocities. The results indicate that settling velocities on Mars are underestimated by up to 30 to 50%, depending on the selected model. As a consequence, transport distances of sediment particles increase by a similar proportion in a given flow. We suspect that the underestimation of settling velocity is caused by poor capture of flow hydraulics under reduced gravity. While MarsSedEx I (and II) results are only very preliminary, they indicate that applying empirically derived models for Earth to conglomerates such as those found at Gale crater to derive properties of surface runoff carries the risk of significantly misjudging flow depth and velocities. In the light of the potentially strong influence of topography on runoff generation on Mars, we may therefore end up looking for water in the wrong place.

## P 27.4

# Modeling process chains: rock/ice-avalanche induced outburst floods at Laguna 513, Cordillera Blanca, Peru

Schaub Yvonne<sup>1</sup>, Schneider Demian<sup>1</sup>, Guillén Ludeña Sebastián<sup>2</sup> & Huggel Christian<sup>1</sup>

<sup>1</sup> Department of Geography, University of Zurich, Winterthurerstrasse 190, 8057-Zurich, Switzerland (yvonne.schaub@geo.uzh.ch)

<sup>2</sup> Laboratoire de Constructions Hydrauliques, École Polytechnique Fédérale de Lausanne, Station 18, 1015 Lausanne, Switzerland

Changes in the cryosphere induce as much general changes in the high-alpine environment as they induce changes in specific hazard processes. One feature are new lakes that are forming in recently deglaciated glacier beds (Linsbauer et al., 2012) underneath destabilized, oversteepened slopes and that are therewith subject to impacts from rock-/ice-avalanches (Schaub et al., in press). In Switzerland many new lakes are to form in the near to middle-term future, nevertheless several new glacier lakes have already stressed attention (Grindelwald, Plaine Morte, Trift, amongst others). In other areas of the world (such as Cordillera Blanca, Peru) several outburst floods have happened (e.g. Laguna 513, (Carey et al., 2012)) and also caused extreme damage. In 1941, an outburst flood from the lake Palcacocha caused 4000 fatalities in the town of Huaraz (Vilímek et al, 2005). Similarly to the Peruvian setting, in Switzerland the valley bottoms are also densely populated and possible hazardous glacier lake outburst floods threaten huge damage potential.

Natural hazard processes are typically assessed as single hazards. Multi-hazard assessments of entire process chains are rarely done but are important in view of the potentially devastating effects of such events. However, in order to generate intensity or hazard maps of process chains such as a rock-/ice-avalanche triggering an impact wave in a lake, which leads to a lake outburst flood, the entire process chain has to be modeled. We here present an approach on how to connect numerical process models (RAMMS and IBER) in order to reproduce the entire process chain. As a case study, the Hualcán-south face in the Cordillera Blanca, Peru, is considered. The models were calibrated with help of the 2010 outburst event (Schneider et al, in press) and then scenarios were modeled based on estimations of future ice-avalanche detachment zones and volumes. The influence of scenario definition on hazard intensities (flood inundation, flow velocity) was evaluated to better understand the importance for hazard mapping and risk reduction measures. Results indicate, that zones of high hazard are primarily located in the vicinity of the river channel. However, large or extreme events have the potential to reach the center of Carhuaz.

## REFERENCES

- Carey, M., Huggel, C., Bury, J., Portocarrero, C. & Haeberli, W. 2012: An Integrated Socio-Environmental Framework for Climate Change Adaptation and Glacier Hazard Management: Lessons from Lake 513, Cordillera Blanca, Peru. *Climatic Change*, 112 (3–4), 733–767.
- Linsbauer, A., Paul, F. & Haeberli, W. 2012: Modeling glacier thickness distribution and bed topography over entire mountain ranges with GlabTop: Application of a fast and robust approach. *Journal of Geophysical Research*, 117, p. F03007.
- Schaub, Y., Haeberli, W., Huggel, C., Künzler, M. & Bründl, M. in press: Landslides and new lakes in deglaciating areas: a risk management framework. *Proceedings of the Second World Landslide Forum – October 2011, Rome, Italy*.
- Schneider, D., Huggel, C., Cochachin, A., Guillén, S. & García, J. submitted: Mapping hazards from glacier lake outburst floods based on modelling of process cascades at Lake 513, Carhuaz, Peru. *Advances in Geosciences*.
- Vilímek, V., Zapata, M.L., Klimes, J., Patzelt, Z. & Santillán, N. 2005: Influence of glacial retreat on natural hazards of the Palcacocha Lake area, Peru. *Landslides*, 2, 107-115.

## P 27.5

# Can soil biomarkers trace floodplain contributions to organic carbon export in a pristine, tropical river system?

Alissa Zuijdgeest<sup>1,2</sup>, Timothy Eglinton<sup>3</sup>, Francien Peterse<sup>3</sup>, Bernhard Wehrli<sup>1,2</sup>

<sup>1</sup> *Eawag: Swiss Federal Institute of Aquatic Science and Technology, Kastanienbaum*

<sup>2</sup> *Institute of Biogeochemistry and Pollutant Dynamics, ETH Zürich*

<sup>3</sup> *Geological Institute, ETH Zürich*

Floodplains represent important biogeochemical reactors for organic matter during fluvial transport. While in temperate systems most floodplains only become inundated as part of management schemes or in extreme-weather situations, some tropical floodplains still experience natural, seasonal flooding. One such floodplain can be found in the Zambezi River Basin, the fourth largest river on the African continent. Due to its location within the Inter Tropical Convergence Zone, this system is characterized by distinct dry (April-November) and wet seasons (December-March). This seasonality has marked influence on the export of organic matter and nutrients from floodplains. Since the Zambezi is the largest African river draining into the Indian Ocean, the export of organic matter and nutrients is important for understanding elemental cycles in the western part of this ocean.

With a bigger aim to reconstruct past flooding patterns, and indirectly thus organic carbon dynamics, we present here a present-day study to investigate to what extent lipid biomarkers (specifically, glycerol dialkyl glycerol tetraethers, GDGTs), which are commonly associated with soil material, can be used to trace the contribution of floodplain-derived organic material to particulate organic carbon carried by the river mainstem. The hypothesis is that during inundation soil organic matter (including the GDGT lipids) are mobilized and entrained in the suspended load. We will describe GDGT concentrations and distributions in particulate organic matter collected immediately upstream and downstream of the Barotse Plains (Zambia), one of Africa's major wetlands that is located in the upper reach of the Zambezi River.